

Regd. No. C-90

INDIAN JOURNAL OF PHYSICS

VOL. 43

AND

PROCEEDINGS

OF THE

INDIAN ASSOCIATION FOR THE CULTIVATION OF SCIENCE

VOL. 52

(Edited in collaboration with the Indian Physical Society).

(With Eleven Plates)

Published by the Registrar, Indian Association for the Cultivation of Science,
Jadavpur, Calcutta-32, and printed by Art Engravers,
2-B, Garcha 1st Lane, Calcutta-19.

1969

BOARD OF EDITORS

F. C. AULUCK	D. N. KUNDU
K. BANERJEE	B. D. NAG CHOUDHURI
D. BASU	R. RAMANNA
D. M. BOSE	K. R. RAO
S. N. BOSE	S. C. SIRKAR
S. D. CHATTERJEE	B. N. SRIVASTAVA
S. R. KHASTGIR	A. R. VERMA
D. S. KOTHARI	A. BOSE (<i>Hon. Secretary</i>)

EDITORIAL COLLABORATORS

R. K. ASUNDI	S. R. PALIT
G. N. BHATTACHARYA	T. PRADHAN
J. N. BHAR	B. RAMACHANDRA RAO
V. G. BHIDE	H. RAKSHIT
H. N. BOSE	A. K. RAY CHOUDHURY
S. K. CHAKRABORTY	A. K. SAHA
J. S. CHATTERJEE	N. K. SAHA
N. N. DAS GUPTA	N. N. SAHA
J. DHAR	D. SHARMA
A. K. DUTTA	VIKRAM A. SARABHAI
S. DUTTA MAZUMDAR	R. K. SEN
S. N. GHOSH	A. K. SEN GUPTA
S. GUPTA	NAND LAL SINGH
G. S. KASTHA	N. R. TAWDE
R. C. MAZUMDAR	B. V. THOSAR
Y. G. NAIK	P. VENKATESWARLU

R. VIJAYRAGHAVAN

INDIAN JOURNAL OF PHYSICS VOL. 43, 1969

C O N T E N T S

No. 1. January

	Page
1. On deformations of a rotating disk of electrostrictive material characterized by a viscoelasticity of Voigt type—B. Chaudhuri	1
2. On longitudinal disturbances in a semi-infinite piezo-electric rod with a body-force in a magnetic field—B. Chaudhuri ...	10
3. A new method for the determination of molecular and inter-molecular relaxation times—G. S. Kastha, B. Dutt, J. Bhattacharyya & S. B. Roy	14
4. Test of current viscosity theories for dilute polymer solutions in solvent-nonsolvent mixtures—Dilip K. Sarker & Santi R. Palit	23
5. A note on the spin of the 1970 keV level in Ba ¹³⁴ —S. P. Sud, V. K. S. Shante, & P. N. Trehan	40

LETTERS TO THE EDITOR—

1. X-ray crystallographic data on homophthalic acid—M. P. Gupte & S. Bose	45
2. Molecular packing in some dicarboxylic acids—M. P. Gupta & N. P. Gupta	47
Book Review	50

No. 2. February

6. Application of time-dependent suction to free convection laminar flow—Krishna Lal	51
7. On mechanical reponse in a piezoelectric transducer carrying a time-decaying space-charge—Hari Sankar Chakraborty ...	67
8. Hydromagnetic waves in an ideally conducting medium with a two-dimensional inhomogeneous magnetic field—G. S. Bajwa & K. M. Srivastava	72
9. Impedance bridge network problem as solved by relaxation method—S. N. Dutta	76
10. $^2\Sigma^+ - ^2\Pi$ band system in CP molecule [PLATE 1]—A. K. Chaudhury & K. N. Upadhyaya	83

	PAGE
11. Wave equation of charged particle of spin 1—the Kemmer equation—S. Gupta ...	92
12. Recording instrument for measurement of thermal expansion—P. D. Pathak, M. C. Gupta & J. M. Trivedi ...	104
LETTERS TO THE EDITOR—	
3. Optical absorption spectra of diluted $\text{Ni}(\text{KSO}_4)_2 \cdot 6\text{H}_2\text{O}$ single crystals—S. Banerji ...	108
Book Review ...	110

No. 3. March

13. Matrix elements of the 1.492 Mev beta transition in ^{153}Eu —K. B. Applacharyulu, D. L. Sastri & Swami Jnanananda ...	113
14. A new phase-meter using a thyratron—S. Roy ...	123
15. On elastic morse Scattering—K. D. Krori & Krishna Sen Gupta ...	128
16. Reduction of wave function which transform as a complex antisymmetric tensor to the irreducible representation of Lorentz group—B. S. Rajput ...	135
17. Differential thermal analyses of some complexes of montmorillonite—Sabita Ghosh ...	147
18. The Cherenkov radiation in a wave-guide loaded with a moving medium—R. M. Khan ...	156

LETTERS TO THE EDITOR—

4. On the structure of hydroxylamine uranium (iv) fluoride T. Ratho, T. Patel & B. Sahu ...	164
5. On the structure of dithiocyanato tetrakis γ -picoline zinc (ii) T. Ratho & T. Patel ...	166
6. Electrical properties of molybdenite—S. R. Guhathakurta ...	169
Book Reviews ...	173

No. 4. April

19. Molecular constants of a few group (iv) tetra hydrides and their deuterium substituents—K. Ramaswamy & V. Ranganathan ...	177
20. Sunrise effect in the intensity of atmospherics at low frequencies—A. K. Sen & M. K. Das Gupta ...	184

Contents

iii

PAGE

21. On the unsteady hydromagnetic free convection flow past a vertical infinite flat plate—Ioan Pop ... 196
22. Infrared eigen frequency and characteristic Debye temperature of a few heavier halides—D. C. Gupta & M. N. Sharma ... 201
23. Emission spectra of E-X & F-X systems of CaF (PLATE 2)—S. C. Prasad & M. K. Narayan ... 205
24. Thermal and electrical conductivities of alloys at low temperatures—B. N. Srivastava, S. Chatterjee & S. K. Sen ... 213

LETTERS TO THE EDITOR—

7. The crystal structure of cresotic acid—M. P. Gupta & S. M. Prasad ... 223
8. Crystal structure of dipotassium fumarate dihydrate, $K_2C_4H_2O_4 \cdot 2H_2O$ —M. P. Gupta & B. N. Shahu ... 225
9. Ultrasonic absorption in binary mixtures of CS_2 —K. Samal & S. C. Misra ... 227
10. Electric and thermoelectric properties of specular hematite—A. K. Mukherjee ... 230
11. Crystal structure of Cu (II) bis-morpholine biguanide—Sankarananda Guha ... 232
- Book Reviews ... 234
- Obituary ... 236

No. 5. May

25. A study of electrode glow during electrolysis (PLATES 3A, 3B & 4A, 4B)—R. G. Edkie, & Mande, Chintamani ... 239
26. On a non-homogeneous cylindrically aeolotropic, magnetostrictive rotating long cylinder—B. Chaudhuri, ... 252
27. Zone refining of silver iodide—Iqbal Singh ... 259
28. Relaxation solution of transit problem of Marx surge generator circuit—S. N. Dutta ... 265
29. On the unsteady flow of a viscous incompressible fluid in a channel bounded by two parallel flat plates—S. N. Dube ... 274
30. On magnetic stability of some Hamiltonians—Dipan K. Ghosh, Chanchal K. Majumdar, & A. K. Rajagopal ... 282

LETTERS TO THE EDITOR—

12. Effect of lattice vibration on the exchange-interaction in ferro- and anti-ferromagnetic crystals—A. T. Maitra	...	289
13. Electric and thermoelectric properties of ilmenite— A. K. Mukherjee	293
14. K-conversion coefficient of the 412 KeV transition in Hg^{198} — H. S. Sahota & B. S. Sood	296
15. Attenuation of low energy gamma rays in alloys—J. Rama Rao, K. Parthasaradhi, A. Lakshmana Rao, & P. V. Ramana Rao	298
16. Absolute photoelectric cross-section of 800 keV gamma rays— M Raja Rao, K. Parthasaradhi & Swami Jnanananda	300
Book Reviews	301

No. 6. June

31. Circular regions under uniform pressures in second order elasticity—D. Pande & G. S. Dube	303
32. New bands in the A-X system of CaF (PLATE-5)—K. V. Subbaram & D. Ramachandra Rao	312
33. Excitation of atomic hydrogen in the Vainshtein approximation— B. N. Roy	315
34. Note on the torsional vibration of a finite circular cylinder of non-homogeneous material by a particular type of twist on one of the plane surfaces—S. K. Biswas	320
35. A note on the rotating inhomogeneous piezoelectric thick disc— M. Bhattacharya	324
36. Thermal conductivity of CO_2-N_2 gas mixture—R. S. Gambhir	...	330
37. Elastic scattering of neutrons by deuterons—Gita Purkayastha & N. C. Sil	335
38. Coherent generation and reception of frequency shift keyed signals—A. K. Dutta	344

LETTERS TO THE EDITOR—

17. Lattice energies and thermal expansions of some heavier halides—M. N. Sharma	358
18. Normal coordinate analysis of tungsten hexachloride (WCl_6)— Nitish K. Sanyal, H. S. Singh & A. N. Pandey	361
Book Reviews	365
Books Recently Received for Reviews	366

No. 7. July

39. Thermal expansion of some Cu-and Ag-base alloys at high temperatures—M. De	367
40. Velocity of sound and an equation of state for liquids—R. V. Gopala Rao & V. Venkata Seshaiah	377
41. Acoustic amplification in semi-conductors in the presence of external electric and magnetic fields—A. Singh	385
42. The stability of a gravitating fluid layer of infinite extent but finite thickness with a force-free magnetic field—K. P. Das	391
43. Temperature distribution in generalized plane Couette flow between two parallel flat plates—S. N. Dube	399
44. Unsteady flow through a circular tube—Krishna Lal	409
45. Field theoretic treatment of ionization of H-atom by protons—A. Roy Chowdhury	415

LETTERS TO THE EDITOR—

19. Angular distribution of K-shell photoelectrons—K. Parthasaradhi & J. Rama Rao	419
20. A furnace with uniform temperature region for a horizontal X-ray diffractometer—P. D. Pathak & N. G. Vasudeva	421
21. The δ -parameter of liquid state evaluation of molecular diameter—R. V. Gopala Rao & V. Venkata Seshiah	424
22. X-ray study of the orthorhombic modification of the paracetotoluidide crystals—S. N. Mitra	426
23. On second harmonic generation in a two level system—B. K. Mohanty & G. P. Sastri	427
Book Reviews	430
Books recently received for review	430

No. 8. August

46. Studies on some microstructures on octahedral faces of natural diamonds—A. R. Patel & M. K. Agarwal	431
47. Reduction of wavefunction which transforms as complex antisymmetric tensor to irreducible representation of Lorentz group (zero mass system)—B. S. Rajput	439
48. Molecular force fields for germanium compounds—K. Ramaswamy & V. Balasubramanian	454

	PAGE
49. A field theoretic view of atom-atom collision—A. Roy Chowdhury	464
50. Variation of modulus of elasticity with frequency of vibration—B. R. Pradhan, S. S. Kakkar & A. P. Saxena ...	468
51. On the vibrational spectra of benzyl benzoate [PLATE 6]—S. Chattopadhyay	474
52. Setting up of a double beam recording spectrophotometer—R. K. Mukherjee, S. C. Bera & M. Chowdhury ...	482
LETTERS TO THE EDITOR—	
24. The crystal structure of calcium fumarate, trihydrate $\text{CaC}_4\text{H}_2\text{O}_4 \cdot 3\text{H}_2\text{O}$ —M. P. Gupta & B. N. Sahu ...	487
25. $1s-2s$ excitation in e-H collision by Glauber approximation—A. S. Ghosh & N. C. Sil	490
26. Incoherent scattering of gamma rays by K-shell electrons—Surya N. Chintalapudi & K. Parthasaradhi	492
Book Reviews	494
Errata	497
Statement	498
Mahendra Lal Sircar Memorial Lecture, 1968—B.D. Nag Choudhuri (Proc. I.A.C.S.)	1-9

No. 9. September

53. Theoretical design of the experiment to study scattering of electrons and positrons by electrons—M. R. Bhiday, V. M. Bhise & A. G. Shastri	499
54. Flow of a viscous incompressible fluid between two co-axial unsteadily rotating porous cylinders—S. N. Dube & S. R. Mukherjee	507
55. Mechanical response of a free piezoelectric plate—D. K. Sinha ...	516
56. Propagation of shock waves in earth's atmosphere—V. P. Singh	519
57. Free convection oscillatory flow along an infinite vertical plate with constant suction—Krishna Lal	528
58. Waves in metals at low temperature—P. Mishra & S.K. Ray... ..	534
59. Temperature effect on resistance of Tl_2Se and Tl_2Te films—A. M. Dighe & A. Goswami	538

Contents

vii

PAGE

60. Diffusion of macromolecules by high frequency technique—J. N. Chakravorty & K. Sengupta ... 543
61. Note on the pure bending of thin non-isotropic plates in the presence of couple stresses—Rathindra Nath Das ... 546
62. A note on the linear flow of a viscous incompressible conducting fluid past an infinite flat plate with constant suction in the presence of a transverse magnetic field —S. N. Dube ... 550

LETTER TO THE EDITORS—

27. X-ray crystallographic data on metha pyrilene fumarate—M. P. Gupta & S. M. Prasad ... 555
28. Electron paramagnetic resonance study of calcium copper acetate hexahydrate—D. Majumdar & P. K. Biswas ... 557
29. Comment on the results on ultraviolet absorption spectra of ortho- and meta-bromoanilines —G. N. R. Tripathi ... 559
- Book Review ... 561

No. 10. October

63. Electrical properties of tin-chalcogenide films—A. Goswami & R. H. Jog ... 563
64. A fast high voltage spark gap pulser—Gurmej Singh ... 575
65. Laminar flow of two incompressible immiscible fluids between two parallel plates with suction and injection—D. S. Rawat ... 580
66. $1^1S \rightarrow 2^1P$ excitation of helium-like ions by electron impact—D. P. Sural & N. C. Sil ... 589
67. A note on the molecular and intramolecular relaxation times of anisole and phenetole in carbon tetrachloride solution—B. Dutta, (Neé Sinha) ... 595
68. Reduction of three-dimensional vector fields to the irreducible representation of inhomogeneous Lorentz group —B. S. Rajput ... 602

LETTERS TO THE EDITOR—

30. Excited state Zeeman splitting of $K_2Cr(CN)_6$ —R. K. Mukherjee, S. C. Bera, A. Bose & M. Chowdhury, ... 621
31. Internal conversion coefficients—M. Raja Rao & K. Parthasaradhi ... 623

	PAGE
32. Radiation damping of electromagnetic waves in plasmas— R. Burman	625
Book Reviews	628
Books Recently Received for Review	629

No. 11. November

69. Chemiluminescent reaction between sodium and oxygen atoms (PLATES 7A, 7B, 8A, 8B)—S. N. Ghosh, A. N. Srivastava & R. V. Shukla	631
70. The study of magnetic anisotropy and susceptibility of ruthenium acetylacetonate—Madhusudan Saha	646
71. Properties of ionic crystals on Born-Mayer theory—C. M. Kachhava & S. C. Saxena	654
72. Surface conductivity of freshly cleaved mica—R. N. Dhar	660
73. On the ultraviolet band system of silicon monoxide (Plate 9)— Jagadish Singh, K. N. Upadhy & K. P. R. Nair	665
74. On the variational states and the ground state energy—N. D. Sen Gupta	674
75. On initial development of axisymmetric waves due to sources —L. Debnath	680
76. Green's function analysis of NF_3 and $NOCl_2$ —K. Ramaswamy & N. Mohan	693

LETTERS TO THE EDITOR—

33. Probability-operator of a quantum system for thermodynamics —M. Dutta	700
34. Some observations on dynamic vibrations of homogeneous incompressible elastic shells—M. Dutta	703
35. Decay characteristics of CaS (Zr. Di) phosphors—B. R. Malhotra	705
Book Reviews	708
Books Recently Received for Review	710
Statement	711

Contents

ix

PAGE

No. 12. December

77. Angular correlation studies in Tc^{99} —P. Jagam & V. Lakshminarayana	713
78. E. S. R. study of copper dipyrindine sulphate dihydrate—P. V. Gopalakrishna Murthy	725
79. Mean scattering cross-section of radiation during diffusion—R. C. Mohanty	730
80. Force field for germylacetylene—K. Ramaswamy & V. Balasubramanian	735
81. Vibrational transition probabilities of the bands of BO_2 system—A. P. Walvekar	742
82. Negative pion capture in closed shell nuclei—B. Banerjee	746
83. Fluid flow through a channel bounded by parallel flat walls—Ram Charitra Tripathi	754
84. On Kelvin-Helmholtz instability in the presence of a uniform electric field—S. Narasimha Murthy	762
85. On the longitudinal vibration in a thin visco-elastic rod of variable cross-section—Satyanarayan Mandal	767

LETTERS TO THE EDITOR—

36. Polarised absorption spectrum of Co^{2+} doped in $CsCdCl_3$ at 77°K and 20°K—Ranjit Kumar Shaha, Ranjit Kumar Mukherjee, A. Bose & M. Chowdhary	775
37. The crystal structure of potassium salt of homophthalic acid—M. P. Gupta & D. S. Dubey	777
Books Recently Received for Review	780
Mahendra Lal Sircar Memorial Lecture, 1969—J. C. Roy (Proc. I. A. C. S.)	1

AUTHOR INDEX

(L) indicates Letter to the Editor

AUTHOR	SUBJECT	PAGE
A		
Agarwal M. K.	See Patel A. R.	431
Appalacharyulu K. B., Sastri D. L. & Swami Jnanananda	Matrix elements of the 1.492 Mev betatransition in ^{189}Eu	113
B		
Bajwa G. S. & Srivastava K. M.	Hydromagnetic waves in an indally conducting medium with a two dimensional inhomoge- neous magnetic field	72
Balasubramaniam V.	See Ramaswamy K.	454
" "	" " "	735
Banerjee B.	Negative pion capture in closed shell nuclei	746
Banerjee S.	Optical absorption spectra of diluted $\text{Ni}(\text{KSO}_4)_2 \cdot 6\text{H}_2\text{O}$ single crystals (L)	108
Bera S. C.	See Mukherjee R. K.	482
" "	See Mukherjee R. K.	621
Bhattacharyya J.	See Kastha G. S.	14
Bhattacharya M.	A note on the deformation of a rotating inhomogeneous piezo- electric thick disc	324
Bhiday M. R., Bhise V. M. & Shastri A. G.	Theoretical design of the experi- ment to study scattering of electrons and positrons by electrons	499
Bhise V. M.	See Bhiday M. R.	499
Biswas P. K.	See Majumdar D.	557
Biswas S. K.	Note on the torsional vibration of finite circular cylinder of nonho- mogeneous material by a parti- cular type of twist on one of the plane surfaces	320

Author Index

xi

AUTHOR	SUBJECT	PAGE
Bose A.	See Mukherjee R. K.	621
" "	See Shaha Ranjit Kr.	775
Bose S.	See Gupta M. P.	45
Burman R.	Radiation damping of electro-magnetic waves in plasmas (<i>L</i>)	625
C		
Chakraborty Hari Sankar	On mechanical response in a piezo-electric transducer carrying a time decaying space charge	67
Chakraborty J. N. & Sen Gupta K.	Diffusion of macromolecules by high frequency technique	543
Chatterjee S.	See Srivastava B. N.	213
Chattopadhyay S.	On the vibrational spectra of benzyl benzoate (Plate 6)	474
Chaudhury A. K. & Upadhyay K. N.	$^2\Sigma^+ - ^2\Pi$ band system in CP molecule (Plate 1)	83
Chaudhuri B.	On deformations of a rotating disc of electrostrictive material characterized by a viscoelasticity of Voigt type	1
" "	On longitudinal disturbances in a semi infinite piezo-electric rod with a body force in a magnetic field	10
" "	On a nonhomogeneous cylindrically anisotropic magnetostrictive rotating long cylinder	252
Chintalapudi Surya N. & Parthasaradhi K.	Incoherent scattering of gamma rays by <i>K</i> -shell electrons	492
Chowdhury M.	See Mukherjee R. K.	482
" "	" "	621
" "	See Shaha Ranjit Kr.	775
D		
Das K. P.	The stability of a gravitating fluid layer of infinite extent but finite thickness with a force free magnetic field	391

AUTHOR	SUBJECT	PAGE
Das Rathindra Nath	Note on the pure bending of thin non-isotropic plates in the presence of couple stresses	546
Das Gupta M. K.	See Sen A. K.	184
Datta A. K.	Coherent generation and reception of frequency shift keyed signals	344
De M.	Thermal expansion of some Cu and Ag-base alloys at high temperatures	367
Debnath L.	On initial development of axisymmetric waves due to sources	680
Dhar R. N.	Surface conductivity of freshly cleaved mica	660
Dighe A. M. & Goswami A.	Temperature effect on resistance of Tl_2Se and Tl_2Te films	538
Dube G. S.	See Pande D.	303
Dube S. N.	On the unsteady flow of a viscous incompressible fluid in a channel bounded by two parallel flat plates	274
" "	Temperature distribution in generalized plane Couette flow between two parallel flat plates	399
Dube S. N.	A note on the linear flow of a viscous incompressible conducting fluid past infinite flat plate with constant suction in the presence of a transverse magnetic field	550
Dube S. N. & Mukherjee S. R.	Flow of a viscous incompressible fluid between two coaxial unsteadily rotating porous cylinders	507
Dubey D. S.	See Gupta M. P.	777

AUTHOR	SUBJECT	PAGE
Dutta B.	A note on the molecular and intramolecular relation times of anisole and phenetole in carbon tetrachloride solution	595
Dutta B.	See Kastha G. S.	14
Dutta M.	Probability operator of a quantum system for thermodynamics (<i>L</i>)	700
" "	Some observations on dynamic vibrations of homogeneous incompressible elastic shells (<i>L</i>)	703
Dutta S. N.	Impedance bridge network problem as solved by relaxation method	76
" "	Relaxation solution of transit problem of Mark surge generator circuit	265
E		
Edkie R. G. & Mande Chintamani	A study of electrode glow during electrolysis (Plates 3A, 3B, 4A, 4B)	239
G		
Gambhir R. S.	Thermal conductivity of $\text{CO}_2\text{-N}_2$ gas mixture	330
Ghosh A. S. & Sil N. C.	$1s\text{-}2s$ excitation in e-H collision by Glauber approximation (<i>L</i>)	490
Ghosh Dipan K., Majumder Chanchal K. & Raja Gopal A. K.	On magnetic stability of some Hamiltonians	282
Ghosh Sabita	Differential thermal analysis of some complexes of montmorillonite	147
Ghosh S. N., Srivastava A. K. & Shukla R. V.	Chemiluminiscent reaction between sodium and oxygen atoms (Plates 7A, 7B, 8A, 8B)	631
Goswami A.	See Dighe A. M.	538

AUTHOR	SUBJECT	PAGE
Goswami A. & Jog R. H.	Electrical properties of tin-chalcogenide films	563
Guha Sankarananda	Crystal structure of Cu (II) bis-morpholine biguanide (L)	232
Guhathakurta S. R.	Electrical properties of molybdenite (L)	169
Gupta D. C. & Sharma M. N.	Infrared eigen-frequency and characteristic Debye temperature of a few heavier halides	201
Gupta M. C.	See Pathak P. D.	104
Gupta M. P. & Bose S.	X-ray crystallographic data on homophthallic acid (L)	45
Gupta M. P. & Dubey D. S.	The crystal structure of potassium salt of homophthallic acid (L)	777
Gupta M. P. & Gupta N. P.	On the coefficient of molecular packing in some dicarboxylic acids (L)	47
Gupta M. P. & Prasad S. M.	Crystal structure of cresotic acid (L)	223
" " "	X-ray crystallographic data on metha pyrilene fumarate, $2C_{14}H_{18}N_3S \cdot 3C_4H_4O_4$ (L)	555
Gupta M. P. & Sahu B. N.	The crystal structure of dipotassium fumarate dihydrate, $K_2C_4H_2O_4 \cdot 2H_2O$ (L)	225
" " " "	The crystal structure of calcium fumarate trihydrate, $CaC_4H_2O_4 \cdot 3H_2O$ (L)	487
Gupta N. P.	See Gupta M. P.	47
Gupta S.	Wave equation of charged particle of spin 1—the Kemmer equation	92

AUTHOR	SUBJECT	PAGE
J		
Jagam P. & Lakshminarayana V.	Angular correlation studies in Tc ⁹⁹	713
Jog R. H.	See Goswami A	563
K		
Kachhava C. M. & Saxena S. C.	Properties of ionic crystals on Born-Mayer theory	654
Kakkar S. S.	See Pradhan B. R.	468
Kastha G. S., Dutta B., Bhattacharyya J. & Roy S. B.	A new method for the determination of molecular and inter-molecular relaxation time	14
Khan R. M.	The Cherenkov radiation in a waveguide loaded with a moving medium	156
Krori K. D. & Sen Gupta Krishna	On elastic Morse scattering	128
L		
Lakshminarayana V.	See Jagam P.	713
Lal Krishna	Application of time dependent suction to free convection laminar flow	51
" "	Unsteady flow through a circular tube	409
" "	Free convection oscillatory flow along an infinite vertical plate with constant suction	528
M		
Maitra A. T.	Effect of lattice vibration on the exchange interaction in ferro-and antiferromagnetic crystal (L)	289
Majumder Chanchal K.	See Ghosh Dipan K.	282
Majumdar D. & Biswas P. K.	Electron paramagnetic resonance study of calcium copper acetate (L)	557

AUTHOR	SUBJECT	PAGE
Malhotra B. R.	Decay characteristics of CaS (Zr, Di) phosphors (L)	705
Mandal Satyanarayan	Note on the longitudinal vibration in a thin visco-elastic rod of variable cross-section	767
Mande Chintamani	See Edkie R. G.	239
Mishra P. & Ray S. K.	Waves in metals at low temperature	534
Misra S. C.	See Samal K.	227
Mitra S. N.	X-ray study of the orthorhombic modification of the para-acetotoluidide crystals (L)	426
Mohan N.	See Ramaswamy K.	693
Mahanty B. K. & Sastri G. P.	On second harmonic generation in a two level system	427
Mohanty R. C.	Mean scattering cross-section of radiation during diffusion	730
Mukherjee A. K.	Electric and thermoelectric properties of specular hematite (L)	230
" "	Electric and thermoelectric properties of ilmenite (L)	293
Mukherjee R. K., Bera S. C., Bose A. & Chowdhury M.	Excited state Zeeman splitting of $K_3Cr(CN)_6$ (L)	621
Mukherjee R. K., Bera S. C. & Chowdhury M.	Setting up of a double beam recording spectrophotometer	482
Mukherjee R. K.	See Saha Ranjit Kr.	775
Mukherjee S. R.	See Dube S. N.	507
Murthy P. V. Gopalkrishna	E. S. R. study of copper dipyrindine sulphate dihydrate	725
Murthy S. Narasimha	On Kelvin-Helmholtz instability in the presence of a uniform electric field	762

AUTHOR	SUBJECT	PAGE
<i>N</i>		
Nag Chowdhuri B. D.	Plasma acceleration : Mahendra Lal Sircar Memorial Lecture, 1968 (Proc. I.A.C.S.)	1—9
Nair K. P. R.	See Singh Jagadish	665
Narayan M. K.	See Prasad S. C.	205
<i>P</i>		
Palit Santi R.	See Sarkar Dilip K.	23
Pande D. & Dube G. S.	Circular regions under uniform pressures in second order elasticity	303
Pandey A. N.	See Sanyal Nitish K.	361
Parthasaradhi K.	See Chintalapudi Surya N.	492
" "	See Rao J. Rama	298
" "	See Rao M. Raja	300
" "	" " " "	623
Parthasaradhi K. & Rao J. Rama	Angular distribution of K -shell photoelectrons (L)	419
Patel A. R. & Agarwal M. K.	Studies on some microstructures on octahedral faces of natural diamonds	431
Patel T.	See Ratho T.	164
" "	" " "	166
Pathak P. D., Gupta M. C. & Trivedi J. M.	Recording instrument for measurement of thermal expansion	104
Pathak P. D. & Vasudeva N. G.	A furnace with uniform temperature region for a horizontal X-ray diffractometer (L)	422
Pop Ioan	On the unsteady hydromagnetic free convection flow past a vertical infinite flat plate	196

AUTHOR	SUBJECT	PAGE
Pradhan B. R., Kakkar S. S. & Saxena A. P.	Variation of modulus of elasticity with frequency of vibration	468
Prasad S. M.	See Gupta M. P.	223
" "	" "	555
Prasad S. S. & Narayan M. K.	Emission spectra of $E-X$ and $F-X$ systems of CaF (Plate 2)	205
Purkayastha Gita & Sil N. C.	Elastic scattering of neutrons by deuterons	335
R		
Rajagopal A. K.	See Ghosh Dipan K.	282
Rajput B. S.	Reduction of wave function which transforms as a complex antisymmetric tensor to the irreducible representation of Lorentz group	135
" "	Reduction of wave function which transforms as complex antisymmetric tensor to irreducible representation of Lorentz group (zero mass system)	439
" "	Reduction of three dimensional vector fields to the irreducible representation of inhomogeneous Lorentz group	602
Ramaswamy K. & Balasubramanian V.	Molecular force fields for germanium compounds	454
" " " "	Force field for germylacetylene	735
Ramaswamy K. & Mohan N.	Green function analysis of NF_3 and NCI_3	693
Ramaswamy K. & Ranganathan V.	Molecular constants of a few group IV tetrahydrides and their deuterium substituents	177

Author Index

xix

AUTHOR	SUBJECT	PAGE
Ranganathan V.	See Ramaswamy K.	177
Rao A. Lakshmana	See Rao J. Rama	298
Rao D. Ramachandra	See Subbaram K. V.	312
Rao J. Rama	See Parthasaradhi K.	419
Rao J. Rama, Parthasaradhi K., Rao A. Lakshmana & Rao P. V. Ramana	Attenuation of low energy gamma rays in alloys (L)	298
Rao M. Raja, Parthasaradhi K. & Swami Jnanananda	Absolute photoelectric cross-section of 800 kev gamma rays (L)	300
Rao M. Raja & Parthasaradhi K.	Internal conversion coefficients (L)	623
Rao P. V. Ramana	See Rao J. Rama	298
Rao R. V. Gopala & Seshaiah V. Venkata	Velocity of sound and an equation of state for liquids	377
" " " " " "	The δ -parameter of liquid state evaluation of molecular diameter (L)	424
Ratho T. & Patel T.	On the structure of dithiocyanatotetrakis γ -picoline zinc (II) (L)	166
Ratho T., Patel T. & Sahu B.	On the structure of hydroxylamine uranium (IV) fluoride (L)	164
Rawat D. S.	Laminar flow of two incompressible immiscible fluids between two parallel plates with suction and injection	580
Ray S. K.	See Mishra P.	534
Roy B. N.	Excitation of atomic hydrogen in the Vainshtein approximation	315
Roy Chowdhury A.	Field theoretic treatment of ionization of H-atom by protons	415
" " "	A field theoretic view of atom-atom collision	464

AUTHOR	SUBJECT	PAGE
Roy J. C.	Mahendra Lal Sircar Memorial Lecture, 1969 (Proc. I.A.C.S.)	1-14
Roy S.	A new phase-meter using a thy- ratron	123
Roy S. B.	See Kastha G. S.	14
S		
Saha Madhusudan	The study of magnetic anisotropy and susceptibility of ruthenium acetyl acetate	646
Sahota H. S. & Sood B. S.	K-conversion coefficient of the 412 KeV transition in Hg^{198} (L)	296
Sahu B.	See Ratho T.	164
Sahu B. N.	See Gupta M. P.	225
" "	" " "	487
Samal K. & Misra S. C.	Ultrasonic absorption in binary mixtures of CS_2 (L)	227
Sanyal Nitish K., Singh H. S. & Pandey A. N.	Normal coordinate analysis of tungsten hexachloride (WCl_6) (L)	361
Sarkar Dilip K. & Palit Santi R.	Test of current viscosity theories for dilute polymer solutions in solvent-nonsolvent mixtures	23
Sastri D. L.	See Appalacharyulu K. B.	113
Sastri G. P.	See Mohanty B. K.	427
Saxena A. P.	See Pradhan B. R.	468
Saxena S. C.	See Kacchava C. M.	654
Sen A. K. & Das Gupta M. K.	Sunrise effect in the intensity of atomspherics at low frequencies	184
Sen S. K.	See Srivastava B. N.	213
Sen Gupta K.	See Chakravorty J. N.	543
Sen Gupta Krishna	See Krori K. D.	128
Sen Gupta N. D.	On the variational states and the ground state energy	674

AUTHOR	SUBJECT	PAGE
Seshaiah V. Venkata	See Rao R. V. Gopala	377
" " "	" " "	424
Shaha Ranjit Kr., Mukherjee Ranjit Kr., Bose A. & Chowdhury M.	Polarised absorption spectrum of Co^{2+} doped in CsCdCl_3 at 77°K and 20°K (L)	775
Shante V. K. S.	See Sud S. P.	40
Sharma M. N.	Lattice energies and thermal ex- pansions of some heavier halides (L)	358
" "	See Gupta D. C.	201
Shastri A. G.	See Bhiday M. R.	499
Shukla R. V.	See Ghosh S. N.	631
Sil N. C.	See Ghosh A. S.	490
" "	See Purkayastha Gita	335
" "	See Sural D. P.	589
Singh A.	Acoustic amplification in semi- conductors in the presence of external electric and magnetic fields	385
Singh Gurmej	A fast high voltage spark gap pulser	575
Singh H. S.	See Sanyal Nitish K.	361
Singh Iqbal	Zone refining of silver iodide	259
Singh Jagadish, Upadhya K. N. & Nair K. P. R.	On the ultraviolet band system of silicon monoxide (Plate 9)	665
Singh V. P.	Propagation of shock waves in earth's atmosphere	519
Sinha (Neé) B.	See Dutta B.	595
Sinha D. K.	Mechanical response of a free piezoelectric plate	516
Sood B. S.	See Sahota H. S.	296
Srivastava A. N.	See Ghosh S. N.	631

AUTHOR	SUBJECT	PAGE
Srivastava B. N., Chatterjee S. & Sen S. K.	Thermal and electrical conductivities of alloys at low temperatures	213
Srivastava K. M.	See Bajwa G. S.	72
Subbaram K. V. & Rao D. Ramachandra	New bands in the Δ -X system of CaF (Plate 5)	312
Sud S. P., Shante V. K. S. & Trehan P. N.	A note on the spin of the 1970 keV level in Ba ¹³⁴	40
Sural D. P. & Sil N. C.	$1^1S \rightarrow 2^1P$ excitation of helium-like ions by electron impact	589
Swami Jnanananda	See Appalacharyulu K. B.	113
" "	See Rao M. Raja	300
T		
Trehan P. N.	See Sud S. P.	40
Tripathi G. N. R.	Comment on the results on ultraviolet absorption spectra of ortho- and meta-bromoanilines (L)	559
Tripathi Ram Charitra	Fluid flow through a channel bounded by parallel flat walls	754
Trivedi J. M.	See Pathak P. D.	104
U		
Upadhyaya K. N.	See Chaudhry A. K.	83
" "	See Singh Jagadish	665
V		
Vasudeva N. G.	See Pathak P. D.	421
W		
Walvekar A. P.	Vibrational transition probabilities of the bands of BO- α system	742

SUBJECT INDEX

(L) indicates Letter to the Letter

SUBJECT	AUTHOR	PAGE
A		
Acoustic amplification in semi-conductors in the presence of external electric and magnetic fields	A. Singh	385
Angular correlation studies of Tc^{99}	P. Jagam & V. Lakshminarayana	713
Atom-atom collision — A field theoretic view of	A. Roy Chowdhury	464
Atomic hydrogen in the Vainshtein approximation—Excitation of	B. N. Roy	315
Axisymmetric waves due to sources— On initial development of	L. Debnath	680
A-X system of CaF—New bands in the (Plate 5)	K. V. Subbaram & D. Ramachandra Rao	312
B		
Beta transition in ^{152}Eu —Matrix elements of the 1.492 MeV	K. B. Appalacharyulu, D. L. Sastri & Swami Jnanananda	113
Book reviews	50, 110, 173, 236, 301, 365, 430, 494, 561, 628, 708.	
Books recently received for review	366, 430, 629, 710, 780.	
C		
Charged particle of spin 1-Wave equation—the Kemmer equation	S. Gupta	92
Chemiluminescent reaction between sodium and oxygen atoms (Plates 7A, 7B, 8A, 8B)	S. N. Ghosh, A. N. Srivastava & R. V. Shukla	631
Cherenkov radiation in a wave-guide loaded with a moving medium—The	R. M. Khan	156

SUBJECT	AUTHOR	PAGE
CP molecule— $^2\Sigma^+ - ^2\Pi$ band system in (Plate 1)	A. K. Chaudhry & K. N. Upadhyaya	83
Crystal structure of calcium fumarate trihydrate $\text{CaC}_4\text{H}_2\text{O}_4 \cdot 3\text{H}_2\text{O}$ —The (<i>L</i>)	M. P. Gupta & B. N. Sahu	487
Crystal structure of cresotic acid (<i>L</i>) —The	M. P. Gupta & S. M. Prasad	223
Crystal structure of Cu (II) -bis- morpholine biguanide (<i>L</i>)	Sankarananda Guha	232
Crystal structure of dipotassium fumarate dihydrate, $\text{K}_2\text{C}_4\text{H}_2\text{O}_4 \cdot 2\text{H}_2\text{O}$ —The (<i>L</i>)	M. P. Gupta & B. N. Sahu	225
Crystal structure of potassium salt of homophthalic acid (<i>L</i>)	M. P. Gupta & D. S. Dubey	777
D		
Decay characteristics of $\text{CaS}(\text{Zr.Di})$ phosphors (<i>L</i>)	B. R. Malhotra	705
δ -parameter of liquid state evaluation of molecular diameter—The (<i>L</i>)	R. V. Gopala Rao & V. Venkata Seshaiah	424
Differential thermal analyses of some complexes of montmorillonite	Sabita Ghosh	147
Diffusion of macromolecules by high frequency technique	J. N. Chakravorty & K. Sen Gupta	543
Double beam recording spectrophoto- meter—Setting up of a	R. K. Mukherjee, S. C. Bera & M. Chowdhury	482
Dynamic vibrations of homogeneous incompressible elastic shells—Some observations on (<i>L</i>)	M. Dutta	703
E		
e-H collision by Glauber approxima- tion— $1s-2s$ excitation in (<i>L</i>)	A. S. Ghosh & N. C. Şil	490

Subject Index

xxv

SUBJECT	AUTHOR	PAGE
Elastic scattering of neutrons by deuterons	Gita Purkayastha & N. C. Sil	335
Electrical properties of molybdenite (L)	S. R. Guha Thakurta	169
Electrical properties of tin-chalcogenide films	A. Goswami & R. H. Jog	563
Electric and thermoelectric properties of ilmenite (L)	A. K. Mukerjee	293
Electric and thermoelectric properties of specular hematite (L)	A. K. Mukerjee	230
Electrode glow during electrolysis—A study of (Plates 3A, 3B, 4A, 4B)	R. G. Edkie & Chintamani Mande	239
Electromagnetic waves in plasmas—Radiation damping of (L)	R. Burman	625
Electron paramagnetic resonance study of calcium copper acetate hexahydrate (L)	D. Majumdar & P. K. Biswas	557
Electrostrictive material characterized by a viscoelasticity of Voigt type—On deformation of a rotating disc of	B. Chaudhuri	1
Emission spectra of E -X and F -X systems of CaF (Plate 2)	S. C. Prasad & M. K. Narayan	205
Errata 497		
E. S. R. study of copper dipyrindine sulphate dihydrate	P. V. Gopalakrishna Murthy	725
Excited state Zeeman splitting of $K_2Cr(CN)_6$ (L)	R. Mukherjee, S. C. Bera, A. Bose & M. Chowdhury	621
F		
Fast high voltage spark gap pulser—A	Gurmej Singh	515
Fluid flow through a channel bounded by parallel flat walls	Ram Charitra Tripathi	754
Force field for germylacetylene	K. Ramaswamy & V. Balasubramanian	735

SUBJECT	AUTHOR	PAGE
Free convection laminar flow—Application of time-dependent suction to	Krishna Lal	51
Free convection oscillatory flow along an infinite vertical plate with constant suction	Krishna Lal	528
Free piezoelectric plate—Mechanical response of a	D. K. Sinha	516
Frequency shift keyed signals—Coherent generation and reception of	A. K. Datta	344
Furnace with uniform temperature region for a horizontal X-ray diffractometer—A (<i>L</i>)	P. D. Pathak & N. G. Vasudeva	421
G		
Gamma rays by K-shell electrons—Incoherent scattering of (<i>L</i>)	Surya N. Chintalapudi & K. Parthasaradhi	492
Generalized plane Couette flow between two parallel flat plates—Temperature distribution in	S. N. Dube	399
Gravitating fluid layer of infinite extent but finite thickness with a force-free magnetic field—The stability of a	K. P. Das	391
Green's function analysis of NF_3 and NCl_3	K. Ramaswami & N. Mohan	693
H		
Helium-like ions by electron impact— $1^1S \rightarrow 2^1P$ excitation of	D. P. Sural & N. C. Sil	589
Hydromagnetic waves in an ideally conducting medium with a two-dimensional inhomogeneous magnetic field	G. S. Bajwa & K. M. Srivastava	72

SUBJECT	AUTHOR	PAGE
<i>I</i>		
Impedance bridge network problem as solved by relaxation method	S. N. Dutta	76
Infrared eigen-frequency and characteristic Debye temperature of a few heavier halides	D. C. Gupta & M. N. Sharma	201
Internal conversion coefficients (<i>L</i>)	M. Raja Rao & P. Parthasaradhi	623
Ionic crystals on Born-Mayer theory—Properties of	C. M. Kachhava & S. C. Saxena	654
Ionization of H-atom by protons—Field theoretic treatment of	A. Roy Chowdhury	415
<i>K</i>		
K-conversion coefficient of the 412 KeV transition in Hg ¹⁰⁰ (<i>L</i>)	H. S. Sahota & B. S. Sood	296
K-shell photoelectrons—Angular distribution of (<i>L</i>)	K. Parthasaradhi & J. Ram Rao	419
Kelvin-Helmholtz instability in the presence of a uniform electric field—On	S. Narasimha Murthy	762
<i>L</i>		
Laminar flow of two incompressible immiscible fluids between two parallel plates with suction and injection	D. S. Rawat	580
Lattice energies and thermal expansions of some heavier halides (<i>L</i>)	M. N. Sharma	358
Lattice vibration on the exchange-interaction in ferro- & antiferromagnetic crystals—Effect of (<i>L</i>)	A. T. Maitra	289
Longitudinal vibration in a thin viscoelastic rod of variable cross-section—Note on the	Satyanarayan Mandal	767

SUBJECT	AUTHOR	PAGE
Low energy gamma rays in alloys— Attenuation of (<i>L</i>)	J. Rama Rao, K. Parthasaradhi, A. Lakshmana Rao & P. V. Ramana Rao	298
M		
Mahendra Lal Sircar Memorial Lecture 1968	B. D. Nag Choudhuri Proc. I. A. C. S. August	1-9
Mahendra Lal Sircar Memorial Lecture 1969	J. C. Roy Proc. I. A. C. S. December	1-14
Magnetic anisotropy and susceptibility of ruthenium acetylacetonate—The study of	Madhusudan Saha	646
Magnetic stability of some Hamil- tonians—On	Dipan K. Ghosh, Chanchal K. Majumder & A. K. Rajagopal	282
Marx surge generator circuit—Relaxa- tion solution of transit problem of	S. N. Dutta	265
Mean scattering cross-section of radiation during diffusion	R. C. Mohanty	730
Microstructures on octahedral faces of natural diamonds—Studies on some	A. R. Patel & M. K. Agarwal	431
Modulus of elasticity with frequency of vibration—Variation of	B. R. Pradhan, S. S. Kakkar & A. P. Saxena	468
Molecular and intermolecular relaxa- tion times—A new method for the determinations of	G. S. Kastha, B. Dutta, J. Bhatta- charyya & S. B. Roy	14
Molecular and intramolecular relaxa- tion times of anisole and phenetole in carbon tetrachloride solution— A note on the	B. Dutta (née Sinha)	595

Subject Index

xxix

SUBJECT	AUTHOR	PAGE
Molecular constants of a few Groups-IV tetrahydrides and their deuterium substituents	K. Ramaswamy & V. Ranganathan	177
Molecular force fields for germanium compounds	K. Ramaswamy & V. Balasubramanian	454
Molecular packing in some dicarboxylic acids—On the coefficient of (<i>L</i>)	M. P. Gupta & N. P. Gupta	47
Morse scattering—On elastic	K. D. Krori & Krishna Sen Gupta	128
Negative pion capture in closed shell nuclei	B. Banerjee	746
Non-homogeneous cylindrically aelotropic, magnetostrictive rotating long cylinder—On a	B. Chaudhuri	252
Normal coordinate analysis of tungsten hexachloride (WCl_6) (<i>L</i>)	Nitish K. Sanyal, H. S. Singh & A. N. Pandey	361
O		
Obituary		236
Optical absorption spectra of diluted $Ni(KSO_4)_2 \cdot 6H_2O$ single crystals (<i>L</i>)	S. Banerji	108
P		
Phase-meter using a thyratron—A new	S. Roy	123
Photoelectric cross-section of 800 KeV gamma rays—Absolute (<i>L</i>)	M. Raja Rao, K. Parthasaradhi & Swami Jnanananda	300
Piezoelectric rod with a body-force in a magnetic field—On longitudinal disturbances in a semi-infinite	B. Chaudhuri	10
Piezoelectric transducer carrying a time-decaying space-charge—On mechanical response in a	Hari Sankar Chakraborty	67

SUBJECT	AUTHOR	PAGE
Polarised absorption spectrum of Co ²⁺ doped in CsCdCl ₃ at 77°K and 20°K (L)	Ranajit Kr. Shaha, Ranajit Kr. Mukherjee, A. Bose & Mihir Chowdhury	775
Polymer solutions in solvent-nonsol- vent mixtures—Test of current viscosity theories for dilute	Dilip K. Sarkar & Santi R. Palit	23
Probability-operator of a quantum system for thermodynamics (L)	M. Dutta	700
R		
Resistance of Tl ₂ Se and Tl ₂ Te films— Temperature effect on	A. M. Dight & A. Goswami	538
Rotating inhomogeneous deformation of a thick disc—A note on the	M. Bhattacharya	324
S		
Scattering of electrons and positrons by electrons—Theretical design of the experiment to study	M. R. Bhiday, V. M. Bhise & A. G. Shastri	499
Second harmonic generation in a two level system—On (L)	B. K. Mohanty & G. P. Sastri	427
Second order elasticity—Circular regions under uniform pressures in	D. Pande & G. S. Dube	303
Shock waves in earth's atmosphere— Propagation of	V. P. Singh	519
Spin of the 1970 keV level in Ba ¹³⁴ — A note on the	S. P. Sud, V. K. S. Shante & P. N. Trehan	40
Statement		498, 711
Structure of dithiocyanato-tetrakis γ-picoline zinc (II)—On the (L)	T. Ratho & T. Patel	166

Subject Index

xxxi

SUBJECT	AUTHOR	PAGE
Structure of hydroxylamine uranium (IV) fluoride—On the (L)	T. Ratho, T. Patel & B. Sahu	164
Sunrise effect in the intensity of atmospherics at low frequencies	A. K. Sen & M. K. Das Gupta	184
Surface conductivity of freshly cleaved mica	R. N. Dhar	660

T

Thermal and electric conductivities of alloys at low temperatures	B. N. Srivastava, S. Chatterjee & S. K. Sen	213
Thermal conductivity of CO ₂ —N ₂ gas mixture	R. S. Gambhir	330
Thermal expansion—Recording instrument for measurement of	P. D. Pathak, M. C. Gupta & J. M. Trivedi	104
Thermal expansion of some Cu- and Ag- base alloys at high temperatures	M. De	367
Thin non-isotropic plates in the presence of couple stresses—Note on the pure bending of	Rathindra Nath Das	546
Three-dimensional vector fields to the irreducible representation of inhomogeneous Lorentz group—Reduction of	B. S. Rajput	602
Torsional vibration of a finite circular cylinder of non-homogeneous material by a particular type of twist on one of the plane surfaces—Note on the	S. K. Biswas	320

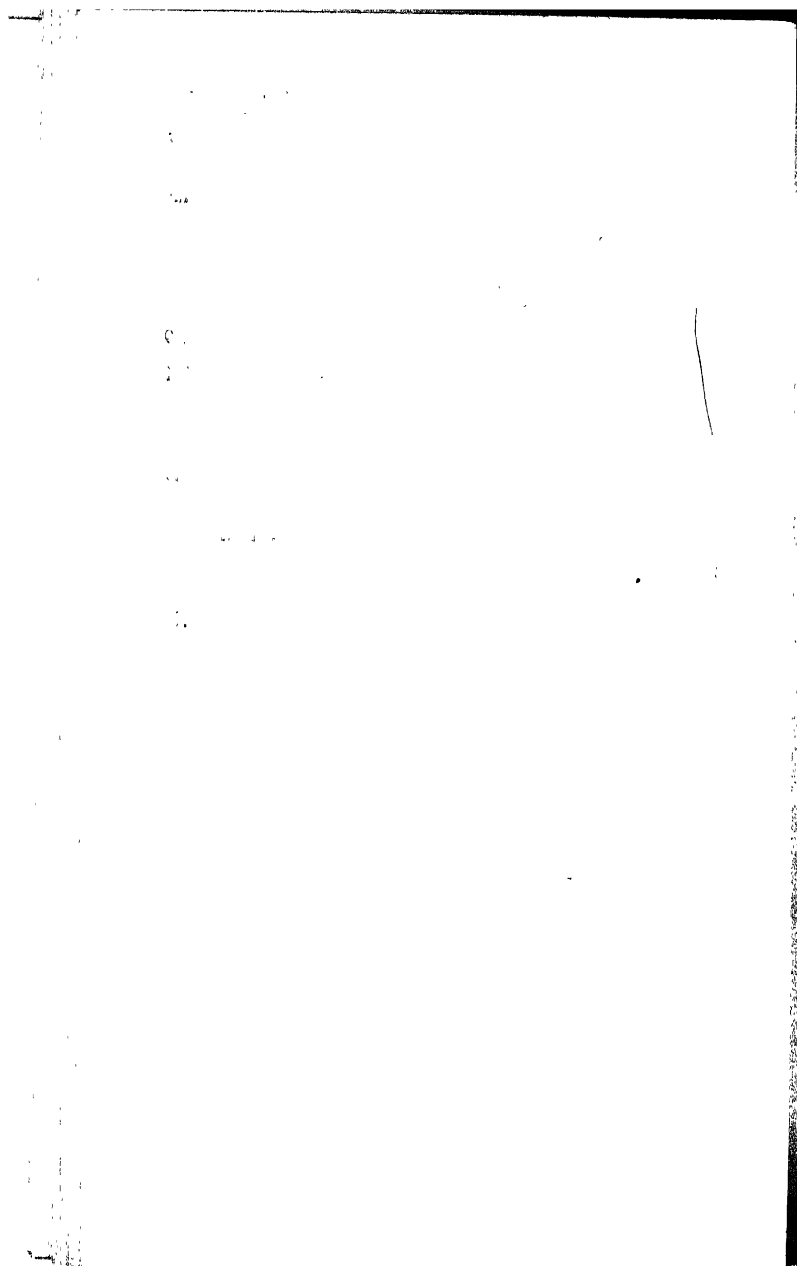
U

Ultrasonic absorption in binary mixtures of CS ₂ (L)	K. Samal & S. C. Misra	227
Ultraviolet absorption of ortho- and meta-bromoanilines—Comments on the results on (L)	G. N. R. Tripathi	559

SUBJECT	AUTHOR	PAGE
Ultraviolet band system of silicon monoxide—On the (Plate 9)	Jagadish Singh, K. N. Upadhyaya & K. P. R. Nair	665
Unsteady flow through a circular tube	Krishna Lal	409
Unsteady hydromagnetic free convection flow past a vertical infinite flat plate—On the	Ioan Pop	196
V		
Variational states and the ground state energy—On the	N. D. Sen Gupta	674
Velocity of sound and an equation of state for liquids	R. V. Gopala Rao & V. Venkata Seshiah	377
Vibrational spectra of benzyl benzoate (Plate 6)—On the	S. Chattopadhyay	474
Vibrational transition probabilities of the bands BO- α system	A. P. Walvekar	742
Viscous incompressible conducting fluid past an infinite flat plate with constant suction in the presence of a transverse magnetic field—A note on the linear flow of a	S. N. Dube	550
Viscous incompressible fluid between two co-axial unsteady rotating porous cylinders—Flow of a	S. N. Dube & S. R. Mukherjee	507
Viscous incompressible fluid in a channel bounded by two parallel flat plates—On the unsteady flow of a	S. N. Dube	274
W		
Wavefunction which transforms as a complex antisymmetric tensor to the irreducible representation of Lorentz group—Reduction of	B. S. Rajput	135

*Subject Index**xxviii*

SUBJECT	AUTHOR	PAGE
Wavefunction which transforms as complex antisymmetric tensor to irreducible representation of Lorentz group (zero mass system)—Reduction of	B. S. Rajput	439
Waves in metals at low temperatures	P. Mishra and S. K. Ray	534
X		
X-ray crystallographic data on homophthalic acid (<i>L</i>)	M. P. Gupta and S. Bose	45
X-ray crystallographic data on meta-pyrilene fumarate (<i>L</i>)	M. P. Gupta and S. M. Prasad	555
X-ray study of the orthorhombic modification of the para-acetotoluidide crystals (<i>L</i>)	S. N. Mitra	426
Z		
Zone refining on silver iodide	Iqbal Singh	259



On deformations of a rotating disk of electrostrictive material characterized by a viscoelasticity of Voigt type

By B. CHAUDHURI

Department of Mathematics, Jadavpur University, Calcutta, India.

(Received 26 December 1967)

The object of the present paper is to investigate the nature of the deformations of a rotating disk of electrostrictive material characterized by a viscoelasticity of Voigt type. The method of Laplace-transforms has been found effective in making the problem amenable to solution.

1. INTRODUCTION

The phenomenon of electrostriction; as is well-known, is the outcome of the interaction of two fields i.e. mechanical and electrical. The problems on dielectrics, subjected to suitable electric fields, can be extended to electro-strictive problems when appropriate elastic fields are accommodated in the former type of problems. The electrostrictive problems have been investigated by several authors in recent years. The recent paper of Sinha (1969) may be mentioned in this context. The present paper sets out to consider the nature of the deformations in a rotating disk of electrostrictive material having the property of visco-elasticity of Voigt type. The solution of this problem has been facilitated by the use of Laplace transforms. Finally the displacement at a point on the boundary has been evaluated completely. The nature of the expression for the displacement brings out the fact it is composed of two parts, one which is time-dependent and the other which remains steady.

2. PROBLEM AND BASIC EQUATIONS

Let us consider a thin rotating electrostrictive disk of radius a and of length $2l$, having the property of viscosity of Voigt type. The disk is rotating with the given angular velocity Ω . Our purpose is to find out the deformations due to the interaction of two fields, i. e. mechanical and electrical. To work out the expressions for deformations, we have to fall back upon the equations of equilibrium, expressed in terms of displacements. These equations of equilibrium can be solved only when the relevant constitutive relations are made use of. The constitutive relations of an electrostrictive material as in Knops (1963) have been modified for the viscoelastic problem and they are given by, when referred to coordinates (r, θ, z) ,

$$\begin{aligned}
\sigma_{rr} &= \left(\lambda + \lambda' \frac{\partial}{\partial t} \right) (S_{rr} + S_{\theta\theta} + S_{zz}) + 2 \left(\mu + \mu' \frac{\partial}{\partial t} \right) S_{rr} \\
&\quad + (a_1 + b_1) E_r^2 + a_1 E_\theta^2 + a_1 E_z^2 \\
\sigma_{\theta\theta} &= \left(\lambda + \lambda' \frac{\partial}{\partial t} \right) (S_{rr} + S_{\theta\theta} + S_{zz}) + 2 \left(\mu + \mu' \frac{\partial}{\partial t} \right) S_{\theta\theta} \\
&\quad + a_1 E_r^2 + (a_1 + b_1) E_\theta^2 + a_1 E_z^2 \\
\sigma_{zz} &= \left(\lambda + \lambda' \frac{\partial}{\partial t} \right) (S_{rr} + S_{\theta\theta} + S_{zz}) + 2 \left(\mu + \mu' \frac{\partial}{\partial t} \right) S_{zz} \\
&\quad + a_1 E_r^2 + a_1 E_\theta^2 + (a_1 + b_1) E_z^2 \\
\sigma_{\theta z} &= 2 \left(\mu + \mu' \frac{\partial}{\partial t} \right) S_{\theta z} + b_1 E_\theta E_z \\
\sigma_{rz} &= 2 \left(\mu + \mu' \frac{\partial}{\partial t} \right) S_{rz} + b_1 E_r E_z \\
\sigma_{r\theta} &= 2 \left(\mu + \mu' \frac{\partial}{\partial t} \right) S_{r\theta} + b_1 E_r E_\theta
\end{aligned}$$

where σ_{rr} , etc. are stress components, S_{rr} , etc. are strain components, E_r , E_θ , E_z are components of electric intensity, λ , λ' , μ , μ' are the material parameters while a_1 , b_1 are electrostrictive constants.

Referred to coordinates (r, θ, z) the stress equation of equilibrium for a rotating disk, as suggested by Timoshenko & Goodier (1934) is

$$\frac{\partial \sigma_{rr}}{\partial r} + \frac{\sigma_{rr} - \sigma_{\theta\theta}}{r} + \sigma \Omega^2 r = 0 \quad \dots (1)$$

where ρ is the mass per unit volume of the material of the disk.

The electric field is governed by the equations

$$\text{rot} \vec{E} = 0, \quad \dots (2)$$

$$\text{div} \vec{D} = 0, \quad \dots (3)$$

$$\vec{D} = K \vec{E} \quad \dots (4)$$

where \vec{D} and \vec{E} are the electric displacement vector and the electric intensity vector respectively, K is the specific inductive capacity.

The solution of the equation of equilibrium is subject to the usual Boundary conditions, the most important of which is

$$\int_{-l}^{+l} \sigma_{rr} dz = 0 \quad \text{on } r=a$$

3. SOLUTION OF THE PROBLEMS :

The corresponding problem for the purely elastic case has been solved in the treatise of Love (1927) and the present solution broadly conforms to this procedure. Therefore, we consider the problem as one of plane stress in order to obtain an approximate solution of the problem so that

$$\sigma_{zz} = 0, \quad \sigma_{rz} = 0,$$

throughout the disk.

Let u and w be the respective radial and longitudinal displacements, then

$$\left. \begin{aligned} S_{rr} &= \frac{\partial u}{\partial r}, \quad S_{\theta\theta} = \frac{u}{r}, \quad S_{zz} = \frac{\partial w}{\partial z} \\ S_{rz} &= \frac{\partial u}{\partial z} + \frac{\partial w}{\partial r}, \quad S_{r\theta} = 0, \quad S_{\theta z} = 0. \end{aligned} \right\} \quad \dots (5)$$

when u and w are functions of both r and z .

Let V be the electric potential. Then from (2) $\vec{E} = -\text{grad } V \quad \dots (6)$

From (3) and (4)

$$\text{div } (K \text{ grad } V) = 0. \quad \dots (7)$$

Since K is a constant and V is a function of Z , we get from (7)

$$\frac{d^2 V}{dz^2} = 0.$$

The solution of this equation is given by

$$V = Az + B$$

where A and B are constants to be determined from the potentials at the ends of the disk. Therefore $B = \frac{V_l - V_{-l}}{2}$ and $A = \frac{V_l - V_{-l}}{2} = E_0$ (say)

Thus, the components of the electric field are given by

$$\left. \begin{aligned} E_r &= -\frac{\partial V}{\partial r} = 0 \\ E_\theta &= -\frac{\partial V}{r \partial \theta} = 0 \\ E_z &= -\frac{\partial V}{\partial z} = -A = -E_0. \end{aligned} \right\} \quad \dots (8)$$

Considering the equations (5) and (8) we have

$$\sigma_{rr} = \left(\lambda + \lambda' \frac{\partial}{\partial t} + 2\mu + 2\mu' \frac{\partial}{\partial t} \right) \frac{\partial u}{\partial r} + \left(\lambda + \lambda' \frac{\partial}{\partial t} \right) \frac{u}{r} + \left(\lambda + \lambda' \frac{\partial}{\partial t} \right) \frac{\partial w}{\partial z} + a_1 E_0^2 \dots (9)$$

$$\sigma_{\theta\theta} = \left(\lambda + \lambda' \frac{\partial}{\partial t} \right) \frac{\partial u}{\partial r} + \left(\lambda + \lambda' \frac{\partial}{\partial t} + 2\mu + 2\mu' \frac{\partial}{\partial t} \right) \frac{u}{r} + \left(\lambda + \lambda' \frac{\partial}{\partial t} \right) \frac{\partial w}{\partial z} + a_1 E_0^2 \dots (10)$$

$$0 = \sigma_{zz} = \left(\lambda + \lambda' \frac{\partial}{\partial t} \right) \frac{\partial u}{\partial r} + \left(\lambda + \lambda' \frac{\partial}{\partial t} \right) \frac{u}{r} + \left(\lambda + \lambda' \frac{\partial}{\partial t} + 2\mu + 2\mu' \frac{\partial}{\partial t} \right) \frac{\partial w}{\partial z} + (a_1 + b_1) E_0^2 \dots (11)$$

$$\sigma_{\theta z} = 0 \dots (12)$$

$$0 = \sigma_{rz} = \left(2\mu + 2\mu' \frac{\partial}{\partial t} \right) \left(\frac{\partial u}{\partial z} + \frac{\partial w}{\partial r} \right) \dots (13)$$

$$\sigma_{r\theta} = 0 \dots (14)$$

Let \bar{u} and \bar{w} denote Laplace transforms of u and w respectively.

Thus

$$\bar{u} = \int_0^\infty u \exp(-pt) dt.$$

$$\bar{w} = \int_0^\infty w \exp(-pt) dt.$$

Let the system be stressed by sudden application of forces so that initially all the unknown quantities are zero.

$$\text{Then } \int_0^\infty \left(\lambda + \lambda' \frac{\partial}{\partial t} \right) u \exp(-pt) dt = \lambda_1 \bar{u}$$

where $\lambda_1 = \lambda + \lambda' p$

$$\text{Similarly, } \int_0^\infty \left(\mu + \mu' \frac{\partial}{\partial t} \right) u \exp(-pt) dt = \mu_1 \bar{u}$$

where $\mu_1 = \mu + \mu' p$

From (13),

$$\frac{\partial u}{\partial z} = - \frac{\partial w}{\partial r}$$

Therefore

$$\frac{\partial \bar{u}}{\partial z} = - \frac{\partial \bar{w}}{\partial r} \quad \dots (15)$$

From (11), we have

$$\frac{\partial \bar{w}}{\partial z} = - \frac{\lambda_1}{(\lambda_1 + 2\mu_1)} \left(\frac{\partial \bar{u}}{\partial r} + \frac{\bar{u}}{r} \right) - \frac{(a_1 + b_1) E_0^2}{(\lambda_1 + 2\mu_1) \rho} \quad \dots (16)$$

Using (9), (10) and $\lambda_1 = \lambda + \lambda' p$, $\mu_1 = \mu + \mu' p$ in (1) we have

$$(\lambda_1 + 2\mu_1) \left(\frac{\partial^2 \bar{u}}{\partial r^2} + \frac{1}{r} \frac{\partial \bar{u}}{\partial r} - \frac{\bar{u}}{r^2} \right) + \lambda_1 \frac{\partial^2 \bar{w}}{\partial z \partial r} = - \frac{\rho \Omega^2 r}{p}$$

From (16)

$$\frac{\partial^2 \bar{w}}{\partial r \partial z} = - \frac{\lambda_1}{(\lambda_1 + 2\mu_1)} \frac{\partial}{\partial r} \left(\frac{\partial \bar{u}}{\partial r} + \frac{\bar{u}}{r} \right) \quad \dots (17)$$

Therefore,

$$\begin{aligned} (\lambda_1 + 2\mu_1) \left(\frac{\partial^2 \bar{u}}{\partial r^2} + \frac{1}{r} \frac{\partial \bar{u}}{\partial r} - \frac{\bar{u}}{r^2} \right) + \frac{\lambda_1^2}{(\lambda_1 + 2\mu_1)} \frac{\partial}{\partial r} \left(\frac{\partial \bar{u}}{\partial r} + \frac{\bar{u}}{r} \right) \\ = - \frac{\rho \Omega^2 r}{p} \\ \text{or } 4\mu_1(\lambda_1 + \mu_1) \frac{\partial}{\partial r} \left(\frac{\partial \bar{u}}{\partial r} + \frac{\bar{u}}{r} \right) = - \frac{(\lambda_1 + 2\mu_1)}{p} (\rho \Omega^2 r). \end{aligned} \quad \dots (18)$$

Again from (15), (17) and (18)

$$\frac{\partial^2 \bar{u}}{\partial z^2} = - \alpha r \quad \dots (19)$$

where

$$\alpha = \frac{\lambda_1 \rho \Omega^2}{4\mu_1(\lambda_1 + \mu_1)p}$$

The solution of (19) is

$$\bar{u} = - \frac{1}{4} \alpha r z^2 + f_1(r) + f_2(r) \quad \dots (20)$$

where $f_1(r)$ and $f_2(r)$ are functions of r to be determined. To find $f_1(r)$ and $f_2(r)$ we substitute this value of \bar{u} in (18). Thus we have

$$\left[f_1''(r) + \frac{f_1'(r)}{r} - \frac{f_1(r)}{r^2} \right] z + \left[f_2''(r) + \frac{f_2'(r)}{r} - \frac{f_2(r)}{r^2} + \delta r \right] = 0 \quad \dots (21)$$

$$\text{where } \delta = \frac{(\lambda_1 + 2\mu_1)\rho\Omega^2}{4\mu_1(\lambda_1 + \mu_1)\beta}$$

If this equation (21) is to hold for all values of z , we must have

$$f_1''(r) + \frac{f_1'(r)}{r} - \frac{f_1(r)}{r^2} = 0$$

$$f_2''(r) + \frac{f_2'(r)}{r} - \frac{f_2(r)}{r^2} + \delta r = 0$$

$$\text{Thus } f_1(r) = A_1 r + \frac{A_2}{r} \quad \dots (22)$$

$$f_2(r) = A_3 r + \frac{A_4}{r} - \frac{1}{8} \delta r^3 \quad \dots (23)$$

where A_1, A_2, A_3, A_4 are arbitrary constants of integration to be determined from the boundary conditions.

We now impose the condition (Love 1927) that $u=0$ at $r=0, z=0$, i.e. $\bar{u}=0$ at $r=0, z=0$. With these values of $f_1(r)$ and $f_2(r)$ we get from (20),

$$\bar{u} = -\frac{1}{2} \alpha r z^2 + A_1 r z + \frac{A_2 z}{r} + A_3 r + \frac{A_4}{r} - \frac{1}{8} \delta r^3$$

Putting $\bar{u} = 0$ at $r = 0, z = 0$, we have $A_2 = A_4 = 0$. Imposing now the condition as in (4) that $\frac{\partial u}{\partial z} - \frac{\partial w}{\partial r} = 0$ at $r = 0, z = 0$ which

means from (15), $\frac{\partial \bar{u}}{\partial z} = 0$

Applying this condition to the expression for \bar{u} , we have $A_1 = 0$.

$$\therefore \bar{u} = -\frac{1}{2} \alpha r z^2 + A_3 r - \frac{1}{8} \delta r^3$$

To evaluate the constant A_3 , we shall use the boundary condition

$$\int_{-l}^{+l} \sigma_{rr} dz = 0 \text{ on } r = a.$$

That is, $\int_{-l}^{+l} \sigma_{rr} dz = 0$ on $r = a$.

Now from (9)

$$\bar{\sigma}_{rr} = -\frac{(3\lambda_1 + 2\mu_1)\mu_1}{(\lambda_1 + 2\mu_1)} \alpha z^2 + \frac{2(3\lambda_1 + 2\mu_1)\mu_1}{(\lambda_1 + 2\mu_1)} A_3 - \frac{(7\lambda_1 + 6\mu_1)\mu_1}{4(\lambda_1 + 2\mu_1)} \delta r^2 \\ - \frac{(\lambda_1 b_1 - 2\mu_1 a_1)E_0^2}{p(\lambda_1 + 2\mu_1)}$$

Therefore $\int_{-l}^{+l} \bar{\sigma}_{rr} dz = 0$ on $r=a$ gives on simplification

$$A_3 = -\frac{\alpha l^2}{6} + \frac{7\lambda_1 + 6\mu_1}{8(3\lambda_1 + 2\mu_1)} \delta a^2 + \frac{(b_1 \lambda_1 - 2\mu_1 a_1)E_0^2}{2\mu_1(3\lambda_1 + 2\mu_1)p} \quad \dots (25)$$

Hence \bar{u} is completely known from (24) and (25). By taking its inverse transform, we can determine u . In particular, to obtain the value of u , at the point ($r=a, z=l$), we have from (24) and (25),

$$u \Big|_{r=a, z=l} = -\frac{\alpha \alpha l^2}{3} + \frac{(7\lambda_1 + 6\mu_1)\alpha \delta}{8(3\lambda_1 + 2\mu_1)} + \frac{(b_1 \lambda_1 - 2\mu_1 a_1)\alpha E_0^2}{2\mu_1(3\lambda_1 + 2\mu_1)p} - \frac{1}{8} \delta a^3. \quad \dots (26)$$

Now inverse transform of α is

$$\frac{\lambda' \rho \Omega^2}{4\mu'(\lambda' + \mu')} \left[\frac{L}{MN} + \frac{L-M}{M(M-N)} e^{-Mt} + \frac{L-N}{N(N-M)} e^{-Nt} \right] \quad \dots (27)$$

Inverse transform of δ is

$$\frac{(\lambda' + 2\mu')\rho \Omega^2}{4\mu'(\lambda' + \mu')} \left[\frac{L_1}{MN} + \frac{L_1-M}{M(M-N)} e^{-Mt} + \frac{L_1-N}{N(N-M)} e^{-Nt} \right] \quad \dots (28)$$

Inverse transform of $\frac{(7\lambda_1 + 6\mu_1)\delta}{(3\lambda_1 + 2\mu_1)}$ is

$$\frac{(7\lambda' + 6\mu')(\lambda' + 2\mu')\rho \Omega^2}{4\mu'(\lambda' + \mu')3\lambda' + 2\mu'} \left[\frac{L_1 L_0}{MNW} H(t) + \frac{L_1 L_0 - M(L_1 + L_0) + M}{M(M-N)(W-M)} e^{-Mt} \right. \\ \left. + \frac{L_1 L_0 - (L_1 + L_0)N + N}{N(W-N)(N-M)} e^{-Nt} + \frac{L_1 L_0 - (L_1 + L_0)W + W}{W(M-W)(W-N)} e^{-Wt} \right] \quad \dots (29)$$

Inverse transform of $\frac{(b_1 \lambda_1 - 2\mu_1 a_1)}{2\mu_1(3\lambda_1 + 2\mu_1)p}$ is

$$\frac{(b_1 \lambda' - 2\mu' a_1)}{2\mu'(\lambda' + 2\mu')} \left[\frac{K}{MW} + \frac{K-M}{M(M-W)} e^{-Mt} + \frac{K-W}{W(W-M)} e^{-Wt} \right] \quad \dots (30)$$

where

$$L = \frac{\lambda}{\lambda'}, \quad M = \frac{\mu}{\mu'}, \quad N = \frac{\lambda + \mu}{\lambda' + \mu'}, \quad L_1 = \frac{\lambda + 2\mu}{\lambda' + 2\mu'},$$

$$L_2 = \frac{7\lambda + 6\mu}{7\lambda' + 6\mu'}, \quad K = \frac{b_1 \lambda - 2\mu a_1}{b_1 \lambda' - 2\mu' a_1}, \quad W = \frac{3\lambda + 2\mu}{3\lambda' + 2\mu'},$$

$$H(t) = \begin{cases} 1, & t > 0 \\ 0, & t < 0 \end{cases}$$

Now considering all the results (27), (28), (29), and (30), we have from (26), at $(r=a, z=l)$ in the form given by

$$\begin{aligned} u \Big|_{r=a, z=l} = & \left[-\frac{\lambda' \rho \Omega^2 a l^2 L}{12\mu'(\lambda' + \mu')MN} - \frac{(\lambda' + 2\mu')\rho \Omega^2 a^3 L_1}{32\mu'(\lambda' + \mu')MN} \right. \\ & \left. + \frac{(b_1 \lambda' - 2\mu' a_1) a \rho a E_0^2 K}{2\mu'(3\lambda' + 2\mu')MW} \right] + \\ & + \left[-\frac{\lambda' \rho \Omega^2 a l^2 (L-M)}{12\mu'(\lambda' + \mu')M(M-N)} - \frac{(\lambda' + 2\mu')\rho \Omega^2 a^3 (L_1-M)}{32\mu'(\lambda' + \mu')M(M-N)} + \right. \\ & + \frac{(7\lambda' + 6\mu')(\lambda' + 2\mu')\rho \Omega^2 a^3 \{L_1 L_2 M(L_1 + L_2) + M\}}{32\mu'(\lambda' + \mu') + 3\mu' + 2\mu'(M(N-N))(W-M)} + \\ & + \left. \frac{(b_1 \lambda' - 2\mu' a_1) a E_0^2 (K-M)}{2\mu'(3\lambda' + 2\mu')M(M-W)} \right] e^{-Ml} + \\ & + \left[-\frac{\lambda' \rho \Omega^2 a l^2 (L-N)}{12\mu'(\lambda' + \mu')N(N-M)} - \frac{(\lambda' + 2\mu')\rho \Omega^2 a^3 (L_1-N)}{32\mu'(\lambda' + \mu')N(N-M)} + \right. \\ & + \left. \frac{(7\lambda' + 6\mu')(\lambda' + 2\mu')\rho \Omega^2 a^3 \{L_1 L_2 - (L_1 + L_2)N + N\}}{32\mu'(\lambda' + \mu')(3\lambda' + 2\mu')N(W-N)(N-M)} \right] e^{-Nl} \\ & + \left[-\frac{(7\lambda' + 6\mu')(\lambda' + 2\mu')\rho \Omega^2 a^3 \{L_1 L_2 - (L_1 + L_2)W + W\}}{32\mu'(\lambda' + \mu')(3\lambda' + 2\mu')W(M-W)(W-N)} \right. \\ & + \left. \frac{(b_1 \lambda' - 2\mu' a_1) a E_0^2 (K-W)}{2\mu'(3\lambda' + 2\mu')W(W-M)} \right] e^{-Wl} + \\ & + \frac{(7\lambda' + 6\mu')(\lambda' + 2\mu')\rho \Omega^2 L_1 L_2}{4\mu'(\lambda' + \mu')(3\lambda' + 2\mu')MNW} H(l), \end{aligned}$$

Thus the expression for the displacement shows that it consists of two parts, namely, the time-independent part and the time-dependent part. The first part, being time-independent, remains unaffected with the increase of time and therefore represents the steady state solution.

Having determined \bar{u} we can similarly determine the longitudinal deformation w from (16) by a simple integration, the constant of integration being zero when we impose the condition $r=0$ when $z=0$

I am grateful to Dr. R. R. Giri of the Department Mathematics, Jadavpur University, Calcutta, for his kind help and active guidance.

REFERENCES

- Knops, R. J. 1963 *Z. A. M. P.* **14**, 148-155.
Love, A. E. H. 1927 *A treatise on the Mathematical Theory of Elasticity*, Dover Publication (4th Edition), New York.
Sinha, D. K. 1965 *I. J. M. M.* **III**, 57-64.
Timoshenko, S. & Goodier, J. N. 1934 *Theory of Elasticity*, McGraw Hill Book Company, Kogakusha Int. Student Edition, P. 58-69.

On longitudinal disturbances in a semi-infinite piezoelectric rod with a body-force in a magnetic field.

By B. CHAUDHURI

Department of Mathematics

Jadavpur University, Calcutta, India,

(Received 19 April 1968)

This article presents the solution of the problem of longitudinal disturbances in a semi-infinite piezoelectric rod being acted by a magnetic field in presence of a body-force.

1. INTRODUCTION

The elastic problems on piezoelectric bodies have been thoroughly discussed in the recent papers of Paria (1960), Paul (1961), Sinha (1963, 1965), Giri (1966) and of Das (1967). A few of these papers have been mentioned here as references. This kind of discussion can be conveniently extended to the corresponding cases in a magnetic field. Banerjee & Sosa (1964) have, perhaps for the first time, studied the effect of a magnetic field on the disturbances in a piezoelectric material in their recent paper (1964). Recently, Sinha (1967) has considered the problem of similar nature. The object of the present paper is to deal with the simple problem of longitudinal disturbances in a semi-infinite piezoelectric bar caused by a body-force and a magnetic field. Body-force dependent on the dimension as well as time has been assumed here. The method of Laplace transform has been found effective in making the problem amenable to solution.

2. PROBLEM, EQUATIONS AND BOUNDARY CONDITIONS

Let a magnetic field represented by the magnetic induction B run in a direction perpendicular to the direction of a semi-infinite piezoelectric bar $0 \leq x < \infty$. Let a time-dependent displacement be applied at the finite end of the bar $x=0$. The problem is to investigate the longitudinal displacement $u(x,t)$ of the bar that stems from the interaction of mechanical and electromagnetic fields with a body force F .

The basic equations are, therefore, given by Banerjee & Sosa (1964) as follows,

$$C_{ijk} \frac{\partial u_{kl}}{\partial x_j} + e_{ijr} \left[e_{jrs} \left(\frac{\partial u_r}{\partial t} + \frac{\partial u_r}{\partial x_m} \cdot \frac{\partial x_m}{\partial t} \right) + \epsilon_{0} k_{jm} \frac{\partial E_m}{\partial t} \right] = \rho \frac{\partial^2 u_i}{\partial t^2} \quad (1)$$

$$2u_{kl} = \frac{\partial u_k}{\partial x_l} + \frac{\partial u_l}{\partial x_k} \quad \dots(2)$$

Where the symbols have their usual meanings as in Benes & Soska's (1964) For present discussion, the equation of motion is given by

$$C_{22} \frac{\partial^2 u}{\partial x^2} - e_{1,2} B \frac{\partial^2 u}{\partial x \partial t} + \rho F = \rho \frac{\partial^2 u}{\partial t^2} \quad \dots(3)$$

where F , being the body-force which is assumed to be $H(t)e^{-\lambda x}$, λ , being a constant and $H(t)$ being Heaviside's unit function equal to unity when $t > 0$ and equal to zero then $t > 0$.

Therefore (3) becomes

$$C_{22} \frac{\partial^2 u}{\partial x^2} - e_{1,2} B \frac{\partial^2 u}{\partial x \partial t} - \rho \frac{\partial^2 u}{\partial t^2} = -\rho H(t)e^{-\lambda x} \quad \dots(4)$$

The boundary conditions are

$$u \rightarrow 0 \text{ as } x \rightarrow \infty \quad \dots(5)$$

$$u = P_0 \left(1 - e^{-kx} \right); k > 0 \text{ and } P_0 \text{ a constant, at } x=0 \quad \dots(6)$$

3. SOLUTION OF THE PROBLEM

The present problem, being one of the boundary value problems encountered in partial differential equations, the principles of Laplace transform can be used effectively to obtain $u(x, t)$ from the equation (4). Defining

$$\bar{u}(x, p) = \int_0^\infty e^{-pt} u(x, t) dt, \quad \operatorname{Re}(p) > 0, t > 0$$

as the Laplace transform of $u(x, t)$, the equation (4) is transformed to

$$C_{22} \frac{\partial^2 \bar{u}}{\partial x^2} - e_{1,2} B, p \frac{\partial \bar{u}}{\partial x} - \rho p^2 \bar{u} = -\frac{\rho e^{-\lambda x}}{p} \quad \dots(7)$$

Its solution is given by

$$\bar{u} = C_1 e^{m_1 x} + C_2 e^{m_2 x} - \frac{\rho e^{-\lambda x}}{p(C_{22}\lambda^2 - e_{1,2} B p \lambda - \rho p^2)} \quad \dots (8)$$

where m_1 , and m_2 are the roots of

$$C_{22}m^2 - e_{1,2} B p m - \rho p^2 = 0 \quad \dots (9)$$

The conditions (5) and (6) give

$$\bar{u} \rightarrow 0 \text{ as } x \rightarrow \infty \quad \dots (10)$$

$$\bar{u} = -\frac{P_0 K}{p(p+K)} \text{ at } x = 0 \quad \dots (11)$$

Because of (10), (8) is given by

$$\bar{u} = C_2 e^{-px[\sqrt{e_{1,2}^2 B^2 + 4\rho C_{22}} + e_{1,2} B]/2C_{22}} - \frac{\rho e^{-\lambda x}}{p(C_{22}\lambda^2 - e_{1,2} B p \lambda - \rho p^2)} \quad \dots (12)$$

using (11), we have

$$C_2 = \frac{P_0 K}{p(p+K)} + \frac{\rho}{p(C_{22}\lambda^2 - e_{1,2} B p \lambda - \rho p^2)}$$

Therefore

$$\begin{aligned} \bar{u} = & \left[-\frac{P_0 K}{p(p+K)} + \frac{\rho}{p(C_{22}\lambda^2 - e_{1,2} B p \lambda - \rho p^2)} \right] \\ & \times e^{-\frac{px}{2} [\sqrt{e_{1,2}^2 B^2 + 4\rho C_{22}} - e_{1,2} B]/2C_{22}} \\ & - \frac{\rho e^{-\lambda x}}{p(C_{22}\lambda^2 - e_{1,2} B p \lambda - \rho p^2)} \quad \dots (13) \end{aligned}$$

Taking the inverse transform of (13), we obtain

$$u = \frac{e^{-\lambda x}}{-2\beta(\beta^2 - \delta^2)} \left[2\beta - (\beta + \delta)e^{-(\beta - \delta)t} + (\beta - \delta)e^{+(\beta + \delta)t} \right]$$

$$\text{when } 0 < t < x[\sqrt{e_{1,2}^2 B^2 + 4\rho C_{22}} + e_{1,2} B]/2C_{22}$$

and

$$u = P_0 \left[\frac{-k \{ t - (\sqrt{e_{11}^2 B^2 + 4\rho C_{22}} + e_{11} B) / 2C_{22} \}}{1 - e^{-\lambda x}} \right] +$$

$$+ \frac{i}{2\beta(\beta^2 - \delta^2)} \left[\frac{2\beta - (\beta + \delta)e^{-(\beta - \delta)t} x(\sqrt{e_{11}^2 B^2 + 4\rho C_{22}} + e_{11} B) / 2C_{22}}{2\beta - (\beta + \delta)e^{-(\beta + \delta)t} x(\sqrt{e_{11}^2 B^2 + 4\rho C_{22}} + e_{11} B) / 2C_{22}} \right]$$

$$- \frac{e^{-\lambda x}}{2\beta(\beta^2 - \delta^2)} \left[\frac{2\beta - (\beta + \delta)e^{-(\beta - \delta)t}}{2\beta - (\beta + \delta)e^{-(\beta + \delta)t}} + (\beta - \delta)e^{-(\beta + \delta)t} \right]$$

when

$$t > x[\sqrt{e_{11}^2 B^2 + 4\rho C_{22}} + e_{11} B] / 2C_{22}$$

where

$$\beta = \frac{\lambda}{2\rho} \sqrt{e_{11}^2 B^2 + 4\rho C_{22}}, \quad \delta = \frac{e_{11} B \lambda}{2\rho}$$

Thus we find that the displacement is partly transient in nature for a certain period of time and is partly constant and partly transient after it exceeds a certain period.

In conclusion, I would like to express my respectful thanks to Dr. R. R. Giri of the department of Mathematics, Jadavpur University, Calcutta, for his kind help and active guidance.

REFERENCES

- Benes, F & Soska, F. 1964 *Czech. Jour. Phys.* **14**, 188.
 Das, N. C. 1967 *Indian J. Phys.* **41**, 611.
 Giti, R. R. 1966 *Indian J. Theor. Phys.* **14**, 65-72.
 Giri, R. R. 1966 *Rev. Roum. Sci. Techn.—Mec. Appl.* **11**, 253-260.
 Paris, G. 1960 *Jour. Sci. Engg. Res.* **4**, 381.
 Paul H. S. 1961 *Jour. Sci. Engg. Res.* **5**, 233.
 Sinha, D. K. 1967 *Indian J. Phys.* **42**, 784-786.
 Sinha, 1963, *Indian J. Theor. Phys.* **11**, 93-99.
 Sinha, D. K. 1965 a, *Zeits. Ang. Math. Phys.* **1**, 411.
 Sinha, D. K. 1965 b, *Proc. Nat. Inst. Sci.* **31**, 395;

A new method for the determination of molecular and intramolecular relaxation times.

By G. S. KASTHA, B. DUTTA, J. BHATTACHARYA AND S. B. ROY

Optics Department,

Indian Association for the Cultivation of Science,

Calcutta-32, India.

(Received 10 January 1969)

A new method for analysing the data on dielectric constant (ϵ') and dielectric loss factor (ϵ'') measured at different microwave frequencies in the case of dilute solutions of anisole and *o*-nitrophenol in non polar solvents and anisole in the liquid state in terms of two Debye terms for determining the relaxation times of the whole molecule (τ_1) and of the rotatable polar group (τ_2) and their relative contribution factors C_1 and C_2 has been described. It is pointed out that the present analytical method is more straightforward compared to the generally adopted trial and error method of analysis.

1. INTRODUCTION

The dielectric constant (ϵ') and dielectric loss (ϵ'') of anisole in different microwave frequency regions and at different temperatures have been investigated by many workers in solutions in non-polar solvents (Hase 1953, Klages & Zentek 1961, Grubb & Smyth 1961, Forrest & Smyth, 1964, Farmer, Holt & Walker 1966, Kastha, Dutta & Roy 1967) and in the pure liquid state (Roberti & Smyth 1960, Vaughan, Bergmann & Smyth 1961; Vaughan & Smyth 1961). Similar investigations in the case of ortho nitrophenol and a number of other phenolic compounds in dilute solutions in non-polar solvents have recently been reported by Magee & Walker (1966). The results have been interpreted in terms of two Debye relaxation mechanisms with the help of the following equations,

$$\frac{\epsilon' - \epsilon_\infty}{\epsilon_0 - \epsilon_\infty} = \frac{C_1}{1 + \omega^2 \tau_1^2} + \frac{C_2}{1 + \omega^2 \tau_2^2} \quad \dots 1 (a)$$

$$\text{and} \quad \frac{\epsilon''}{\epsilon_0 - \epsilon_\infty} = \frac{C_1 \omega \tau_1}{1 + \omega^2 \tau_1^2} + \frac{C_2 \omega \tau_2}{1 + \omega^2 \tau_2^2} \quad \dots 1 (b)$$

with $C_1 + C_2 = 1$; where τ_1 is the time of relaxation for the orientation of the whole molecule and τ_2 is the time of relaxation of the rotating polar group, C_1 and C_2 are the relative contributions to overall dielectric constant and loss-values due respectively to the two relaxation mechanisms and all other symbols have their usual significance,

The analysis of the results have usually been made by assuming reasonable values of τ_1 , τ_2 and C_2 (sometimes the value of ϵ_∞ is also slightly varied) and then comparing the values of ϵ' and ϵ'' calculated with the help of equation (1) with those of the respective experimental values at different microwave frequencies. Though there is fair agreement in the results obtained in any particular investigation, the values of τ_2 and C_2 obtained by different workers vary considerably. For example, in the case of dilute solutions of anisole in benzene the value of τ_2 reported by various workers varies between 6.5×10^{-12} sec (Forrest & Smyth, 1964) to 0.8×10^{-12} sec (Klages & Zentek 1961) and the corresponding values of C_2 are 0.8 and 0.2 respectively.

In the case of pure liquid the data are fewer. Vaughan & Smyth (1961) have analysed the dielectric constant and loss data at the microwave frequencies measured by Roberti & Smyth (1960) in the pure liquid state at 20°C with help of equations (1) and have obtained the value of τ_2 as 3.7×10^{-12} sec and C_2 as 0.2.

Recently, Kastha (1968) has pointed out that though the equation (1) are approximately valid in the case of very dilute solutions of polar molecules e. g. anisole, in non-polar solvents, in the case of the pure liquids, these equations are not applicable and hence the values of τ_1 , τ_2 and C_2 obtained with their help will not be the true ones. In the present paper the results reported in the existing literature have been examined critically and a method by which the trial and error method of determining the τ_1 , τ_2 and C_2 values is avoided has been outlined.

2. THEORY OF THE METHOD

Kastha (1968) has given the following functional relations between ϵ' , ϵ'' , τ_1 and τ_2 in the case of polar liquids consisting of molecules, like anisole, or solutions of such polar compounds in non polar solvents :

$$\frac{(\epsilon_0 + 2)[(\epsilon' - \epsilon_\infty)(\epsilon' + 2) + \epsilon''^2]}{(\epsilon_0 - \epsilon_\infty)[(\epsilon' + 2)^2 + \epsilon''^2]} = \frac{C_1}{1 + \omega^2 \tau_1^2} + \frac{C_2}{1 + \omega^2 \tau_2^2} \quad \dots 2 (a)$$

$$\text{and} \quad \frac{(\epsilon_\infty + 2)(\epsilon_0 + 2)\epsilon''}{(\epsilon_0 - \epsilon_\infty)[(\epsilon' + 2)^2 + \epsilon''^2]} = \frac{C_1 \omega \tau_1}{1 + \omega^2 \tau_1^2} + \frac{C_2 \omega \tau_2}{1 + \omega^2 \tau_2^2} \quad \dots 2 (b)$$

with $C_1 + C_2 = 1$.

In the case of very dilute solutions in non polar solvents for which $\epsilon' \approx \epsilon_0 \approx \epsilon_\infty$ and ϵ'' is very small these equations reduce to those given in equations 1 (a) and 1 (b). Denoting the expressions on the left hand side of equation 1 (a) or 2 (a) by a and those of equations 1(b) or 2 (b) by b and

putting $\omega\tau_1 = X_1$ and $\omega\tau_2 = X_2$ we get,

$$a = \frac{C_1}{1+X_1^2} + \frac{C_2}{1+X_2^2}$$

$$\text{and } b = \frac{C_1 X_1}{1+X_1^2} + \frac{C_2 X_2}{1+X_2^2}$$

From these relations we obtain

$$C_1 = \frac{(b-aX_2)(1+X_1^2)}{X_1-X_2}; \quad C_2 = \frac{(a-bX_1)(1+X_2^2)}{X_1-X_2} \quad \dots 3 \text{ (a)}$$

$$\text{and } a(1-a)-b^2 = \frac{C_1 C_2 (X_1-X_2)^2}{(1+X_1^2)(1+X_2^2)} \quad \dots 3 \text{ (b)}$$

Equation 3 (b) takes care of the fact that for the existence of two relaxation times the condition $a(1-a)-b^2 > 0$ must be satisfied. Using the relation $\frac{C_1+C_2}{C_1+C_2} = 1$, the following equation is obtained from 3 (a),

$$\frac{1-a}{b} = X_1 + X_2 - \frac{a}{b} X_1 X_2; \text{ when dividing by } \omega \text{ we get}$$

$$\frac{1-a}{b\omega} = \tau_1 + \tau_2 - \frac{a\omega}{b} \tau_1 \tau_2 \quad \dots (4)$$

So if the values of $\frac{1-a}{b\omega}$ and $\frac{a\omega}{b}$ obtained from the experimental values of ϵ' , ϵ'' , ϵ_0 and ϵ_∞ at a certain temperature for different microwave frequencies are plotted as ordinate and abscissa respectively, a straight line graph will result from whose intercept and inclination the values of $\tau_1 + \tau_2$ and $\tau_1 \tau_2$ respectively are obtained. From these values the values of τ_1 and τ_2 are determined. The values of C_1 or C_2 are then obtained from the corresponding expressions on equation 3(a). If the C_1 or C_2 values obtained for the different microwave frequencies are the same then the values of τ_1 , τ_2 , C_1 or C_2 are uniquely determined.

The method outlined above has been applied to a number of cases and short descriptions of the procedure adapted for the analysis of the experimental data and the results of the analysis are given in the following paragraphs.

3. RESULTS

(a) *Solution of anisole in cyclohexane*: Farmer et al (1966) have measured the values of ϵ' and ϵ'' of solution of anisole in cyclohexane of

two different strengths at five microwave frequencies at 25°C and also the ϵ_0 and ϵ_∞ values of the solutions at the same temperature. The a and b values calculated with the help of these data from the L. H. S. expressions of equation (1) are given in table 1 (a). It is seen that the a or b value for the two solutions at any microwave frequency are different though according to the R. H. S. expression of equation (1) they should be the same for both the solutions. Accordingly, the mean values of a and b have been used to obtain the values of $\frac{1-a}{b\omega}$ and $\frac{a\omega}{b}$ which are entered in table 1(b).

Instead of a graphical evaluation of equation (4) the method of least squares for the best fit of the experimental data with the linear relation of equation (4) has been used to obtain the values of $\tau_1 + \tau_2$ and $\tau_1\tau_2$ and hence of τ_1 and τ_2 . The C_2 values obtained for different microwave frequencies are also shown in table 1(b). The values of τ_1 , τ_2 and the most probable C_2 value obtained in this way are shown in table 1(c) along with those reported by Farmer, Holt and walker, (1966) for comparison.

TABLE 1 (a)
ANISOLE IN SOLUTION IN CYCLOHEXANE TEMP. 25°C
VALUE OF a AND b CALCULATED BY DIFFERENT METHODS

λ cm.		L.H.S. expressions of equation (1) using ϵ' , ϵ'' , ϵ_0 and ϵ_∞ values of		R.H.S. expression of equation (1) using	
		Farmer <i>et al</i> (1966) .05976 wt fraction	.0792 wt fraction	τ_1 , τ_2 , C_1 and C_2 values of this work	τ_1 , τ_2 , C_1 and C_2 values of Farmer <i>et al</i> (1966)
0.428	a	.143	.111	.117	.112
	b	.286	.289	.288	.291
0.860	a	.286	.333	.315	.314
	b	.372	.400	.400	.422
1.249	a	.428	.444	.453	.462
	b	.414	.444	.429	.447
1.850	a	.428	.555	.599	.616
	b	.414	.422	.420	.431
3.220	a	.857	.888	.778	.797
	b	.376	.344	.356	.354

TABLE 1 (b)
ANISOLE IN SOLUTION IN CYCLOHEXANE TEMP. 25°C
 $\frac{1-a}{b\omega}$ AND $\frac{a\omega}{b}$ VALUES OBTAINED FROM MEAN a AND b
VALUES OF COLUMNS (2) AND (3) OF TABLE 1 (a)

λ cm.	0.428	0.860	1.249	1.850	3.220
$1-a/b\omega \times 10^{12}$	6.91	8.17	8.71	11.93	6.63
$a\omega/b \times 10^{-12}$.1949	1755	.1516	.1199	.1546
C_2	0.65	0.59	0.61	0.40	0.90

TABLE 1 (c)
ANISOLE IN SOLUTION IN CYCLOHEXANE TEMP. 25°C

Method	$\tau_1 \times 10^{12}$ sec.	$\tau_2 \times 10^{12}$ sec.	C_2
Present analytical method	15.4	4.77	0.59
Trial and error method Farmer <i>et al</i> (1966)	14.6	5.20	0.65

In order to find out how far the values of τ_1 , τ_2 , and C_2 obtained by the present method reproduce the experimentally observed ϵ' and ϵ'' at different microwave frequencies, the values of a and b have been calculated with the R. H. S. expressions of equation (1) using these values and they have been compared with the a and b values obtained from the L. H. S. expressions of equation (1) using the experimental values of ϵ' , ϵ'' , ϵ_0 and ϵ_∞ . These are shown in table 1 (a). In the same table are also included for comparison the values of a and b calculated from the R. H. S. expressions of equation (1) using the τ_1 , τ_2 , C_1 , C_2 values reported by Farmer, Holt and Walker (1966). The agreement seems to be slightly better in the case of a and b values calculated with the data of the present work.

(b) *Ortho nitrophenol in solution in paraxylene :*

The ϵ' and ϵ'' values at four microwave frequencies in the case of .02056 M solution of *o*-nitrophenol in *p*-xylene at 25°C along with the value of ϵ_0 and ϵ_∞ have been reported by Magee and Walker (1966). The a and b values calculated from the L. H. S. expressions of equation (1) using the experimental values of ϵ' , ϵ'' , ϵ_0 and ϵ_∞ are given in Table 2(a) and values of $\frac{1-a}{b\omega}$ and $\frac{a\omega}{b}$ are entered in table 2(b). The τ_1 , τ_2 and the most probable C_2 values determined in the same way as described in the

case of solution of anisole in cyclohexane are presented in Tables 2(c) and 2(b) and in the former table the values of τ_1 , τ_2 and C_2 obtained by Magee and Walker are shown for comparison.

TABLE 2 (a)
o-NITROPHENOL IN SOLUTION IN *p*-XYLENE TEMP. 25°C
VALUES OF a AND b CALCULATED BY DIFFERENT METHODS

λ cm.		L.H.S. expressions of equation (1) using ϵ' , ϵ'' , ϵ_0 and ϵ_∞ values of Magee & Walker (1966)	R.H.S. expressions of equation (1) using	
		.02056 M	τ_1 , τ_2 , C_1 and C_2 values of this work	τ_1 , τ_2 , C_1 and C_2 values of Magee & Walker (1966)
0.86	a	.1487	.1555	.1750
	b	.3120	.3134	.3137
1.25	a	.2477	.2503	.2665
	b	.3814	.3809	.3789
1.85	a	.3467	.3840	.3988
	b	.4309	.4382	.4353
3.22	a	.6439	.6170	.6315
	b	.4556	.4514	.4457

TABLE 2 (b)
o-NITROPHENOL IN SOLUTION IN *p*-XYLENE TEMP. 25°C
 $\frac{1-a}{b\omega}$ AND $\frac{a\omega}{b}$ VALUES OBTAINED FROM a AND b

VALUES OF COLUMN (2) OF TABLE 2 (a)				
λ cm.	0.86	1.25	1.85	3.22
$1-a/b\omega \times 10^{12}$	12.46	13.09	15.24	13.37
$a\omega/b \times 10^{-12}$.1043	.0979	.0859	.0827
C_1	0.18	0.20	0.17	0.24

TABLE 2 (c)
o-NITROPHENOL IN SOLUTION IN *p*-XYLENE TEMP. 25°C

Method	$\tau_1 \times 10^{12}$ sec.	$\tau_2 \times 10^{12}$ sec.	C_2
Present analytical method	15.8	4.87	0.20
Trial and error method (Magee & Walker 1966)	15.0	3.60	0.17

A comparison of the a and b values calculated from the R.H.S. of equation (1) with the a and b values determined from experimental data, which are all given in table 2(a), shows the true values of τ_1 , τ_2 and C_2 are possibly closer to those obtained in the present investigation than those reported by Magee & Walker (1966).

(c) *Anisole in the pure liquid state :*

The ϵ' and ϵ'' values of liquid anisole at three microwave frequencies at 20°C and two other temperatures and the ϵ_0 and ϵ_∞ values have been measured by Roberti & Smyth 1960. These results have been analysed with the help of equation (1) by Vaughan & Smyth (1961) using $\epsilon_\infty = 2.38$ (in place of the value of $n_D^2 = \epsilon_\infty = 2.30$). They reported that the values $\tau_1 = 13.3 \times 10^{-12}$ sec, $\tau_2 = 3.7 \times 10^{-12}$ sec and $C_2 = 0.20$ satisfactorily reproduces from the R.H.S. expressions of equations (1) the experimental values of ϵ' and ϵ'' measured at three microwave frequencies.

Kastha (1968) pointed out that equations (1) are not applicable to the case of polar liquids like anisole and therefore, the experimental results have been analysed by the present method (outlined in the case of solution of anisole in cyclohexane) using a and b values calculated from the experimental ϵ' , ϵ'' and ϵ_0 values and $\epsilon_\infty = 2.30$ with the help of the L.H.S. expressions of equations (2). The relevant data are given in tables 3 (a) and 3 (b).

TABLE 3 (a)

ANISOLE—PURE LIQUID
VALUES a and b CALCULATED BY DIFFERENT METHODS

A.cm.		L.H.S. expression of eqn. (2) using ϵ' , ϵ'' , ϵ_0 and $\epsilon_\infty = 2.3$ values of Roberti & Smyth (1960)	R.H.S. expression of eqn. (2) using τ_1 , τ_2 , C_1 and C_2 values of this work
1.25	a	.5024	.5519
	b	.3612	.3551
3.22	a	.8153	.8128
	b	.3107	.3056
10.00	a	.9712	.9717
	b	.1336	.1362

TABLE 3 (b)

ANISOLE—PURE LIQUID			TEMP. 20°C
$\frac{1-a}{b\omega}$	AND	$\frac{a\omega}{b}$	VALUES OBTAINED FROM a AND b
VALUES OF COLUMN (2) OF TABLE 3 (a)			
λ cm.	1.25	3.22	10.00
$I-a/b\omega \times 10^{12}$	9.137	10.160	11.440
$a\omega/b \times 10^{-12}$.2097	.1536	.1371
C_2	0.42	0.52	0.53

TABLE 3 (c)

ANISOLE—PURE LIQUID			TEMP. 20°C
Method	$\tau_1 \times 10^{12}$ sec	$\tau_2 \times 10^{12}$ sec	C_2
Present analytical method	12.65	2.18	0.49
Trial and error method	13.30	3.75	0.20
Vaughan & Smyth (1961)			

The values of τ_1 , τ_2 and the mean C_2 value obtained from these calculations together with those given by Vaughan & Smyth (1961) are tabulated in table 3(c).

From table 3(a) it is seen that the agreement between the a and b values calculated from the experimental data (column 1) with those obtained from the R.H.S. expressions of equations (2) using the τ_1 , τ_2 , C_1 and C_2 values obtained in the present investigation are satisfactory. It is also noted from table 3 (c) that though the present values of τ_1 and τ_2 are somewhat smaller than those given by Vaughan & Smyth, the value of C_2 obtained in this investigation is much higher than that obtained by the latter authors. This difference in the evaluation of the relative contribution made by the relaxation mechanism of the methoxy group to overall dielectric constant and dielectric loss factor in the case of liquid anisole is due to the exact two terms Debye dispersion relations derived by Kastha (1968),

5. CONCLUSION

From the considerations presented above it may fairly be concluded that the present method of analysis yields values of τ_1 , τ_2 and C_2 which closely satisfy the two term Debye dispersion relation used to describe the functional dependence of the dielectric constant and dielectric loss factor values at different microwave frequencies in the case of polar molecules with one rotatable polar group in different states of aggregation. Moreover, the method is straightforward and does not involve any guess work associated with the hitherto adopted trial and error method of analysis.

Finally, it need be pointed out that the calculated value of C_2 at some microwave frequencies in some cases indicates large relative errors in the values of a and b corresponding to the ϵ' and ϵ'' values measured at these microwave frequencies for the particular case in consideration.

REFERENCES

- Farmer, O. B., Holt, A. & Walker, S. 1966 *J. Chem. Phys.* 44, 4116.
Forrest, E. & Smyth, C. P. 1964 *J. Am. Chem. Soc.* 86, 3475.
Grubb, E. L. & Smyth, C. P. 1961 *J. Am. Chem. Soc.* 83, 4873.
Hase, H. 1953, *Z. Naturf.* 8a, 695.
Kastha, G. S. 1968 *Ind. J. Phys.* 42, 223.
Kastha, G. S. Dutta, B. & Roy, S. B. 1967 *Indian J. Phys.* 41, 725.
Klages, G. & Zentek, A. 1961 *Z. Naturf.* 16a, 1016.
Magee, M. D. & Walker, S. 1966 *Molecular Relaxation Process*.
Chemical Society Publication No. 20, 89.
Robert, M. D. & Smyth, C. P. 1960 *J. Am. Chem. Soc.* 82, 2160.
Vaughan, W. E., Bergmand, K. & Smyth, C. P. 1961 *J. Phys. Chem.*, 65, 94.
Vaughan, W. E. & Smyth, C. P. 1961 *J. Phys. Chem.* 65, 98.

Test of current viscosity theories for dilute polymer solutions in solvent-nonsolvent mixtures

By DILIP K. SARKAR AND SANTI R. PALIT

Department of Physical Chemistry,

Indian Association for the Cultivation of Science, Jadavpur,

Calcutta-32, India,

(Received 10, January 1969)

The linear expansion factor α_η for the fractions of a number of polymers in various solvent-nonsolvent mixtures has been determined using Stockmayer-Fixman's relationship. The validity of the Flory, Kurata and Ptitsyn theories has been tested in terms of the dependence of the function α_η on molecular weight using our data on poly m-methyl styrene and from available literature data. It has been found that Kurata theory (and in a few cases Ptitsyn theory) are in better agreement than that of Flory or Ptitsyn. Palit's viscosity-molecular weight relationship has been found to be satisfactory in almost all cases.

1. INTRODUCTION

Of the equations describing volume effects on the dimensions of macromolecules in a good solvent, the best known are Flory's (1948, 1949, 1951),

$$\alpha_\eta^3 - \alpha_\eta^2 = CM^{\frac{1}{2}} \quad \dots (1)$$

Kurata, Stockmayer and Roig's (1960),

$$\left(\alpha_\eta^3 - \alpha_\eta \right) \left(1 + \frac{1}{3\alpha_\eta^2} \right)^{\frac{3}{2}} = C' M^{\frac{1}{2}} \quad \dots (2)$$

and Ptitsyn' (1962)

$$[(4.68 \alpha_\eta^3 - 3.68)^{3/2} - 1] = C' M^{\frac{1}{2}} \quad \dots (3)$$

Palit's (1955) equation which correlates intrinsic viscosity and molecular weight of polymers reads as follows

$$100\rho_0[\eta] = K_1 M^{\frac{1}{2}} - \ln M + K_2 \quad \dots (4)$$

where $K_1 = 1.09 N^{\frac{1}{2}} \gamma v_p^{2/3} / RT \simeq$ order of 10^{-2} and K_2 are constants.

The validity of equations (1), (2) (3) and (4) is tested in this paper in terms of α_η values obtained from new unpublished data and from available literature values calculated for solutions of several fractions of a number of polymers in different solvent-nonsolvent mixtures at different temperatures. The validity of these equations in case of single

solvents has been tested in earlier communications (Sarkar & Palit 1967 ; Chaudhury, Sarkar & Palit 1968) where the method of computation of K and α_η (Stockmayer-Fixman) has been discussed.

2. EXPERIMENTAL RESULTS AND DISCUSSION

1. Poly m-methyl styrene

Our method of treatment of the experimental data is illustrated in table I in some details. Our \bar{M}_n and $[\eta]$ values at various temperatures are utilised to calculate K and α_η values. The \bar{M}_n values are taken from a previous communication (Chaudhury, Sarkar & Palit 1968)

The values of α_η are found to increase with increase of molecular weight, indicating increased expansion of the molecule.

Graphical Test of the Four Equations

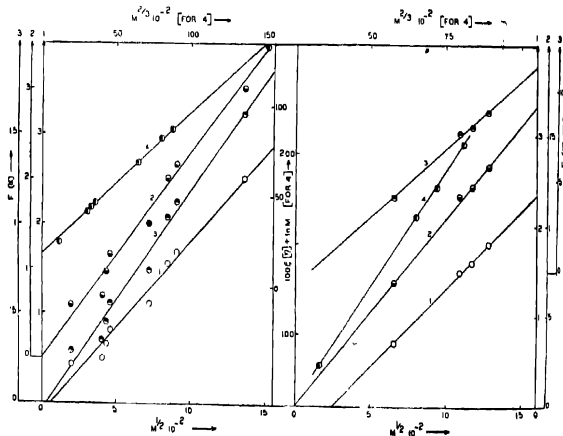


Figure 1. Poly m-methyl styrene in ethyl acetate-methanol mixture (9:1 V/V) at 30°C. Figure 2. Poly m-methyl styrene in benzene-methanol mixture (9:1 V/V) at 30°C.

Analysis of Flory Relation : According to equation (1) plots of $\alpha_\eta - \alpha_\eta^0$ against $M^{1/2}$ are expected to give a straight line passing through the origin. In mixture I the Flory plot shows a fairly good linear monotonic increase but it does not pass through the origin (figure 1 marked 1) ; abscissa intercept being at $M \approx 4100$. In mixture II (figure 2), good linearity is obtained but again an abscissa intercept at $M \approx 26,800$

is observed. In mixture III (figure 3), at 30°C linearity is poor and abscissa intercept is at $M \approx 16,3000$. At 40°C (figure 4), the linearity is again poor and abscissa intercept is at $M \approx 7,100$. At 50°C (figure 5), the linearity is very good with an abscissa intercept of $M \approx 6600$. So Flory theory is adequate with respect to linearity of the Flory plot but the latter does not conform to the theoretical necessity of passing through the origin.

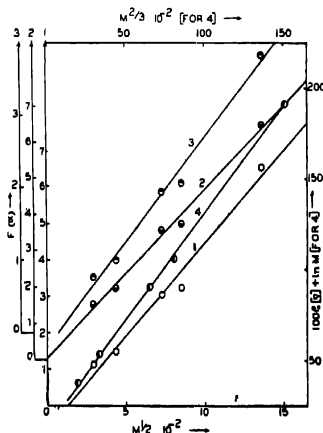


Figure 3. Poly m-methyl styrene in benzene-methanol mixture (3:1 V/V) at 30°C.

Analysis of Kurata et al relation : According to equation (2) plots of $(\alpha_n^2 - \alpha_n) (1 + 1/3 \alpha_n^2)^{3/2}$ versus $M^{1/2}$ should be linear passing through the origin. In mixture I, such a plot is slightly scattered about a straight line passing through the origin (figure-1, marked 2). In mixture II, fairly good linearity is obtained and it passes through the origin. In mixture III at 30°C, the plot is good linear and passes through the origin. At 40°C, the linearity is fairly good and it passes through the origin. At 50°C, the linearity is good and it passes through the origin. This suggests that the data fit in excellently with the Kurata-Stockmayer-Roig (K-S-R) equation.

Analysis of Pitsyn Relation : According to equation (3) plots of $[(4.68\alpha_n^2 - 3.68)\alpha_n^{1/2} - 1]$ against $M^{1/2}$ are expected to give a straight line passing through the origin. In mixture 1, such a plot is found to be scattered and does not pass through the origin but gives an abscissa inter-

TABLE 1. EXPERIMENTAL VALUES OF INTRINSIC VISCOSITIES $[\eta]$ IN VARIOUS SOLVENTS AT DIFFERENT TEMPERATURES

Fr. No.	$\bar{M}_n \times 10^{-3}$	Mixture I $\text{CH}_2\text{COC}_2\text{H}_5(90) : \text{CH}_3\text{OH}(10)$			Mixture II $\text{C}_6\text{H}_6(90) : \text{CH}_3\text{OH}(10)$			Mixture III $\text{C}_6\text{H}_6(75) : \text{CH}_3\text{OH}(25)$		
		$\text{K} \cdot 10^4 = 6.73$ 30°C			$\text{K} \cdot 10^4 = 9.59$ 30°C			$\text{K} \cdot 10^4 = 7.87$ 30°C		
		$[\eta]$	a_η	$[\eta]$	$[\eta]$	a_η	$[\eta]$	$[\eta]$	a_η	$[\eta]$
T ₁	18.5200	1.195	1.092	—	—	1.769	1.182	—	—	—
I	8.2480	.742	1.067	—	—	—	—	—	—	—
2	7.2350	.688	1.063	1.920	1.329	.920	1.112	—	—	—
8	6.1090	—	—	1.680	1.308	—	—	—	1.004	1.153
5	5.2550	.560	1.047	1.520	1.298	.773	1.107	0.810	1.163	1.141
7	2.6605	—	—	—	—	—	—	0.535	1.134	0.585
4 _s	2.1430	.347	1.036	—	—	—	—	—	—	—
5A	1.9050	.321	1.030	.707	1.191	0.410	1.060	0.416	1.103	—
5B	1.6790	.295	1.023	—	—	—	—	—	—	—
5D	0.8356	—	—	—	—	0.262	1.048	0.252	1.070	0.289
5E	0.3964	.142	1.020	—	—	—	—	—	—	—

cept, as obtained by the least square method, corresponding to $M \approx 1300$ (figure 1, marked 3). In benzene containing 10% methanol, good linearity is obtained but it gives an abscissa intercept corresponding to $M \approx 5700$. In benzene containing 25% methanol at 30°C, the plot is poorly linear and gives an abscissa intercept corresponding to $M \approx 5000$. At 40°C, the linearity is poor and the abscissa intercept corresponds to $M \approx 2000$. At 50°C, the linearity is good but it gives an abscissa intercept corresponding to $M \approx 2000$. This indicates that like Flory equation, Pitsyn equation has got limited applicability in this case but in a sense it is better as its range of applicability is greater.

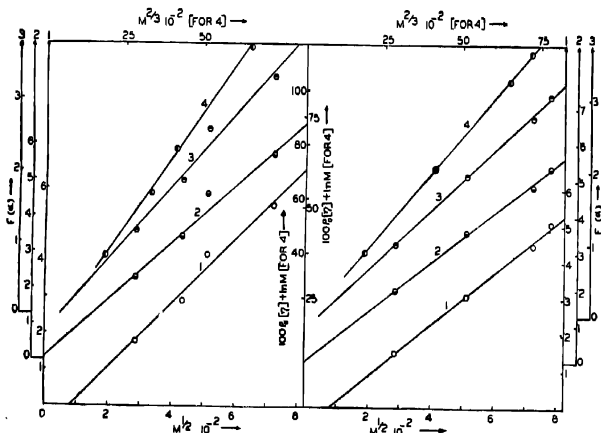


Figure 4. Poly m-methyl styrene in benzene-methanol mixture (3:1 V/V) at 40°C. Figure 5. Poly m-methyl styrene in benzene-methanol mixture (3:1 V/V) at 50°C.

Analysis of Palit Relation : According to equation (4) plots of $100\rho_0[\eta] + \ln M$ against $M^{1/2}$ are expected to give a straight line with a slope of the order of 10^{-3} . Very good linearity is obtained in all the cases with slopes of 0.79×10^{-3} (figure 1, marked 4), 2.57×10^{-3} (figure 2), 1.18×10^{-3} at 30° (figure 3), 1.28×10^{-3} at 40° (figure 4) and 1.38×10^{-3} at 50°C (figure 5) respectively.

2. Polystyrene

The \bar{M}_n and $[\eta]$ data of Rossi *et al* (1965) in M.E.K-cyclohexane (1:1 in volume) mixture at 34°C are utilised. The Flory plot is highly scattered and gives a least square intercept corresponding to $M \approx 11200$ (figure 6). The K-S-R plot is fairly good linear and it passes through the origin. The Pitsyn plot is fairly good linear but gives an abscissa intercept at $M \approx 2100$.

Very good linear plot according to Palit equation is obtained with a slope of 1.93×10^{-2} .

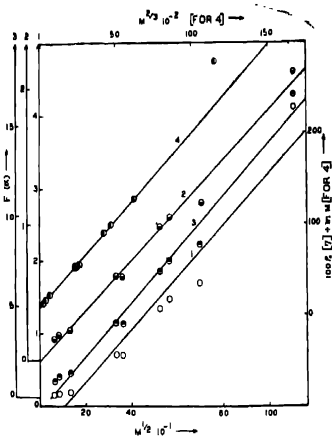


Figure 6. Polystyrene in MEK-cyclohexane (1:1 V/V) mixture at 34°C.

The \bar{M}_n and $[\eta]$ data of Bawn *et al* (1950) in toluene-heptane mixtures and in toluene-methyl alcohol mixtures at 25°C are utilised.

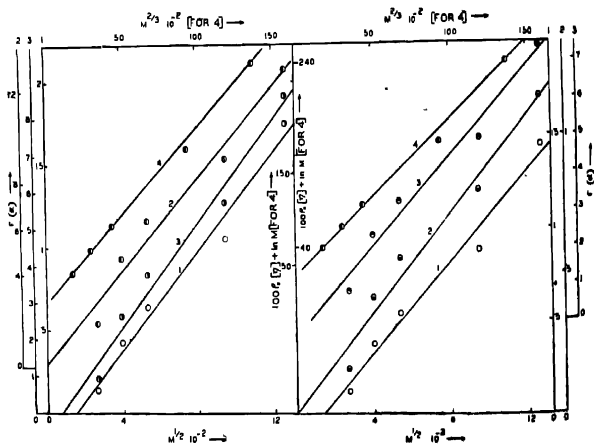


Figure 7. Polystyrene in toluene containing 10% heptane at 25°C.

Figure 8. Polystyrene in toluene containing 20% heptane at 25°C.

In 10% heptane (figure 7), all the first three plots are scattered but while the K-S-R plot passes through the origin, the Flory and Ptitsyn plots give abscissa intercepts corresponding to $M \approx 21600$ and 5100 . Very good linear Palit plot is obtained with a slope of 1.91×10^{-2} . In 20% heptane (Fig. 8) exactly similar results are obtained — the abscissa intercepts in case of Flory and Ptitsyn plots are at $M \approx 19400$ and 4900 respectively and the value of K_1 in the case of Palit equation is 1.67×10^{-2} .

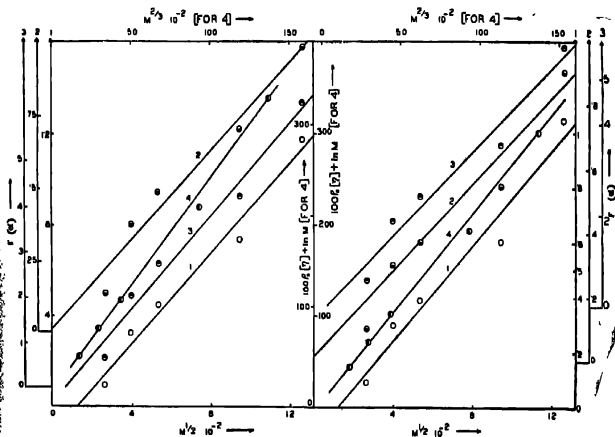


Figure 9. Polystyrene in toluene containing 30% heptane at 25°C.

Figure 10. Polystyrene in toluene containing 40% heptane at 25°C.

In 30% heptane (figure 9), the observation is the same — the Flory and Ptitsyn equations are valid above $M \approx 16400$ and 4500 and the value of slope in case of Palit equation is 2.38×10^{-2} . In 40% heptane (figure 10), the Flory plot is scattered and gives an abscissa intercept at $M \approx 14800$. Very poor linearity is observed in case of K-S-R equation but it passes through the origin. The Ptitsyn plot is scattered and gives an abscissa intercept at $M \approx 4100$. Very good linearity is obtained in case of Palit plot with a slope of 2.16×10^{-2} .

In 5% methanol (figure 11), poor linearity is observed in case of Flory and Ptitsyn equations with abscissa intercepts at $M \approx 19700$ and 4600 respectively. The K-S-R plot, though scattered, passes through the origin. Very good linear Palit plot is obtained with a slope of 2.35×10^{-2} . In 10% methanol (figure 12), all the three plots are scattered but while the K-S-R

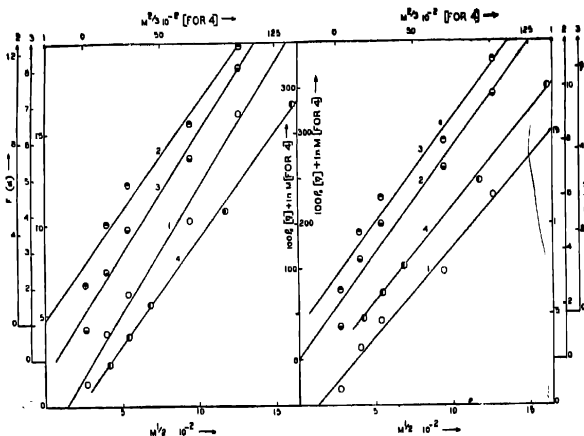


Figure 11. Polystyrene in toluene containing 5% heptane at 25°C. Figure 12. Polystyrene in toluene containing 10% heptane at 25°C.

plot passes through the origin, the Flory and Pritsyn plots give abscissa intercepts at $M \approx 14900$ and 3600 respectively. Very good linear plot according to Palit equation is obtained with a slope of 2.08×10^{-2} .

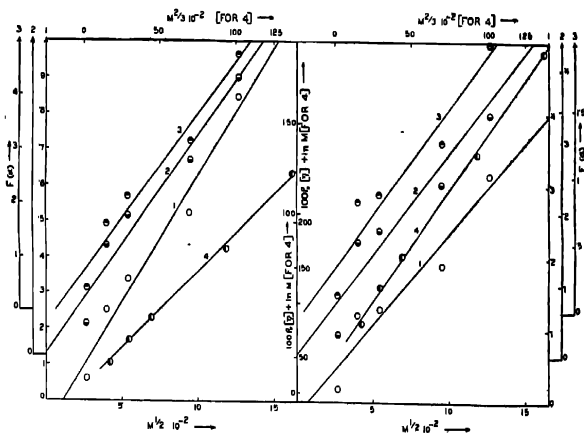


Figure 13. Polystyrene in toluene containing 15% heptane at 25°C. Figure 14. Polystyrene in toluene containing 20% heptane at 25°C.

In 15% methanol (figure 13), more or less similar results are obtained—the Flory and K-S-R Plots are valid above $M \simeq 13100$ and 4100 respectively. Good linear plot according to Palit equation is obtained with a slope of 1.71×10^{-2} . In 20% methanol (figure 14), the Flory and Ptitsyn plots are scattered and give abscissa intercepts at $M \simeq 4600$ and 1700 respectively. The K-S-R plot, though highly scattered, passes through the origin. Very good linearity is obtained in case of Palit equation and it has a slope of 1.23×10^{-2} .

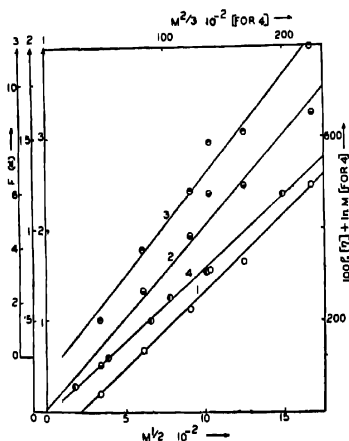


Figure 15. Polystyrene in chloroform containing 10% methanol at 25°C.

The \bar{M}_w and $[\eta]$ data of Oth & Desreux (1954) are utilised. In chloroform containing 10% methanol (figure 15), good linearity is obtained in case of Flory equation, but it gives an abscissa intercept at $M \simeq 44000$. Very poor linearity is obtained in case of K-S-R equation but it passes through the origin. Ptitsyn plot is poorly linear and it gives an abscissa intercept at $M \simeq 9000$. Very good linear plot according to Palit equation is obtained with a slope of 2.40×10^{-2} .

In 20% methanol (figure 16), good linearity is obtained both in case of Flory equation and Ptitsyn equation, but they give abscissa intercepts at $M \simeq 30400$ and 7400 respectively. The K-S-R plot, although poor, passes through the origin. Very good linearity is obtained in case of Palit plot with a slope of 1.47×10^{-2} .

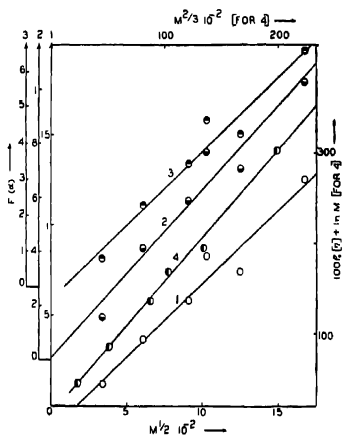


Figure 16. Polystyrene in chloroform containing 20% methanol at 25°C.

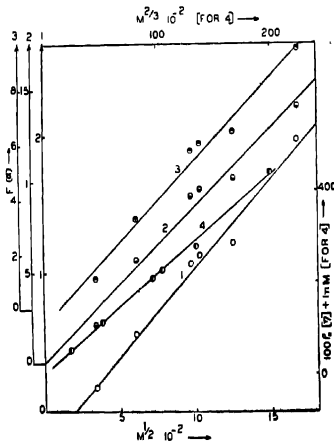


Figure 17. Polystyrene in toluene containing 10% methanol at 25°C.

In toluene-methanol mixture containing 10% methanol (figure 17), both the Flory and Pitsyn plots are very poor and give abscissa intercepts at $M \approx 38,00$ and 7900 respectively. The K-S-R plot, although scattered,

passes through the origin. Very good linear plot according to Palit equation is obtained with a slope of 2.17×10^{-2} .

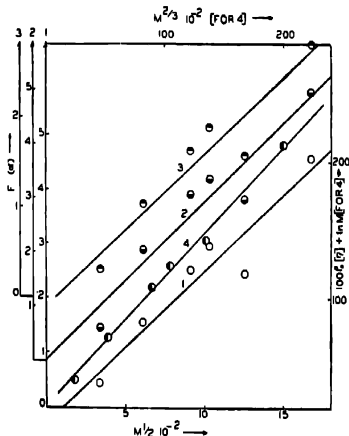


Figure 18. Polystyrene in MEK containing 5% methanol at 25°C.

In MEK-methanol mixture containing 5 % methanol (figure 18), all the first three plots are highly scattered and while the K-S-R plot passes through the origin, the Flory and Pitsyn plots give abscissa intercepts at $M \approx 11600$ and 3400 respectively. Good linear plot according to Palit equation is obtained with a slope of 0.95×10^{-2} .

3. AMYLOSE ACETATE

The \bar{M}_w and $[\eta]$ data of Patel et al (1965) are utilised. In case of 65/35% chloroform-cyclohexane mixture at 15°C (figure 19), good linear Flory plot is obtained with an abscissa intercept at $M \approx 53700$. Very good linearity is obtained in case of K-S-R plot and it passes through the origin. Pitsyn plot is very good linear with abscissa intercept at $M \approx 7800$. Plot according to Palit equation is good linear with a slope of 6.54×10^{-2} .

In 50/50% chloroform-cyclohexane mixture at 15°C (figure 20), the Flory plot is scattered and gives an abscissa intercept at $M \approx 51700$. Fairly good

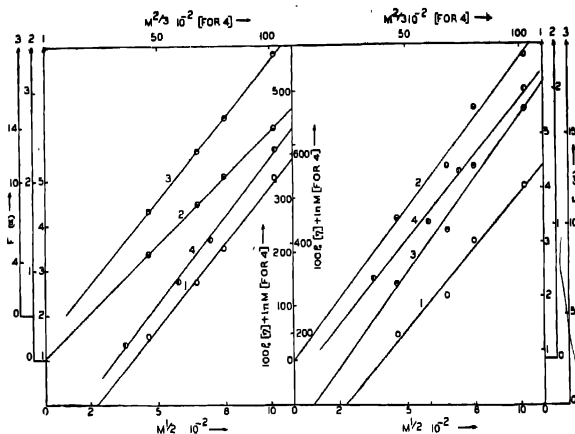


Figure 19. Amylose acetate in 65/35% chloroform-cyclohexane mixture at 15°C.

Figure 20. Amylose acetate in 50/50% chloroform-cyclohexane mixture at 15°C.

linearity is obtained in case of K-S-R equation and it passes through the origin. Pitsyn plot is fairly good linear with an abscissa intercept at $M = 8300$. Good linear plot according to Palit equation is obtained with a slope of 5.24×10^{-2} .

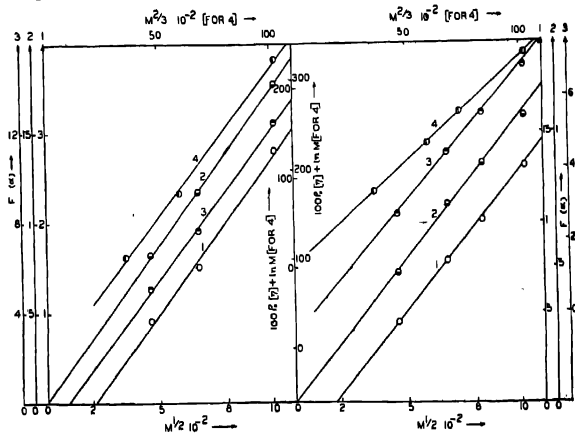


Figure 21. Amylose acetate in 50/50% nitromethane-methanol mixture at 40°C.

Figure 22. Amylose acetate in 35/65% nitromethane-methanol mixture at 40°C.

In 50/50% nitromethane-methanol mixture at 40°C (figure 21), fairly good linear Flory plot is obtained with an abscissa intercept at $M \approx 45200$. Very good linearity is obtained in case of K-S-R equation and it passes through the origin. Pitsyn plot is good linear with an abscissa intercept at $M \approx 8400$. Good linear plot according to Palit equation is obtained with a slope of 3.31×10^{-2} .

In 35/65% nitromethane-methanol mixture at 40°C (figure 22), Flory plot is good linear but it has an abscissa intercept at $M \approx 30100$. K-S-R plot is fairly good linear and it passes through the origin. Good linear plot is obtained in case of Pitsyn equation but it has an abscissa intercept corresponding to $M \approx 7100$. Very good linear plot according to Palit equation is obtained with a slope of 2.32×10^{-2} .

DISCUSSION

In the 22 different polymer-solvent-nonsolvent systems studied, it is observed (table 2) that as regards linearity of the $F(\alpha_1)$ vs. $M^{\frac{1}{2}}$ plot, Flory plot is found to be best in 12 cases while K-S-R equation is best in 6 cases and Pitsyn equation is best in 4 cases only. It is evident that from the stand-point of linearity Flory equation is the best. However, as regards the criteria of passing through the origin, the K-S-R equation is satisfactory in almost all cases while the Flory and the Pitsyn equations are not satisfactory even in a single case; they always give abscissa intercepts, Pitsyn shows a lower intercept than Flory. Palit plot is very good linear in 20 cases and good in the remaining 2 cases; the theoretical slope of the order of 10^{-2} is obtained in all cases.

It is therefore concluded that considering the two criteria together viz., the linearity and the passing through origin, the K-S-R plot is somewhat better than the Pitsyn or Flory plot. Hence the K-S-R equation, based on an equivalent ellipsoid model, is best suited to interpret the molecular expansion of the polymers discussed. Palit's equation excellently correlates intrinsic viscosity and molecular weight of polymers.

Thanks are due to C. S. I. R. (India) for the award of a Junior Research Fellowship to D. K. S.

TABLE 2. TABULAR SUMMARY OF RESULTS

Polymer	Solvent-Nonsolvent (Volume ratio)	Temp °C	Linearity and Abscissa Intercepts in terms of M				General Remarks	
			Flory plot	K-S-R plot	Pitayn plot	Palit plot	Best linear	Eq. that passes through the origin among 1, 2 & 3
			Eq. 1	Eq. 2	Eq. 3	Eq. 4, K ₁ 10 ³	Eq.	
Poly m-me thyl styrene	Ethyl Acetate-Methanol (9 : 1)	30	fairly good 4050	very poor 0	scattered 1340	very good .79	4.1	2
			good 26,800	good 0	good 5690	very good 2.57	4.1	2
	Benzene-Methanol (3 : 1)	30	poor 16,300	good 0	poor 5,000	very good 1.18	4.2	2
		40	poor 7100	fairly good 0	poor 203	very good 1.28	4.2	2
Polystyrene	MEK-Cyclohexane (1 : 1)	50	very good 6600	good 0	good 2000	very good 1.38	4.1	2
			highly scattered 11,200	fairly good 0	fairly good 2100	very good 1.93	4.2	2
		34	scattered 21600	scattered 0	scattered 5070	very good 1.91	4.1	2
		25	scattered 19400	scattered 0	scattered 4920	very good 1.67	4.1	2
	Toluene-Heptane (9 : 1)	25	scattered 16400	scattered 0	scattered 4510	very good 2.38	4.1	2
			scattered 14800	very poor 0	scattered 408	very good 2.16	4.1	2
		25						

TABLE 2.—(Contd.)

Polymer	Solvent:Nonsolvent (Volume ratio)	Temp °C	Linearity and Abscissa Intercepts in terms of M				General Remarks	
			Flory plot Eq. 1	K-S-R plot Eq. 2	Pittslyn plot Eq. 3	Palit plot Eq. 4, K ₁ -10 ³	Best linear Eq.	Eq. that passes through the origin among 1, 2 & 3
Polystyrene	Toluene-Methanol (9.5:0.5)	25	poor 19700	scattered 0	poor 4580	very good 2.35	4.1	2
	(9:1)	25	scattered 14900	scattered 0	scattered 3630	very good 2.08	4.1	2
	(8.5:1.5)	25	scattered 13100	scattered 0	scattered 4070	good 1.71	4.3	2
	(8:2)	25	scattered	highly scattered 0	scattered	very good		
			4650	scattered 0	1720	1.23	4. None	2
Chloroform-Methanol	(9:1)	25	good 44000	very poor 0	poor 8960	very good 2.40	4.1	2
	(8:2)	25	good 30400	poor 0	good 7380	very good 1.47	4.1	2
	Toluene-Methanol (9:1)	25	very poor 38700	scattered 0	very poor 7940	very good 2.17	4.1	2
	MEK-Methanol (9.5:0.5)	25	highly scattered 11600	highly scattered 0	highly scattered 3430	good 0.95	4.2	2
Amylose Acetate	Chloroform- Cyclohexane (9.5:1.5)	15	good 53700	very good 0	very good 7770	good	2 & 3	2
	(1:1)	15	scattered 51700	fairly good 0	fairly good 8330	good 5.24	4.3	2

TABLE 2.—(Contd.)

Polymer	Solvent:Nonsolvent (Volume ratio)	Temp °C	Linearity and Abscissa Intercepts in terms of M				General Remarks	
			Flory plot Eq. 1	K-S-R plot Eq. 2	Pitsyn plot Eq. 3	Falke plot Eq. 4, K ₁ ·10 ³	Best linear Eq.	Eq. that passes through the data among 1, 2 & 3
Amylose Acetate	Nitromethane: Methanol (1 : 1)	40	fairly good 45200	very good 0	good 8420	good 3,31	2	2
	(3.5 : 6.5)	40	good 30100	fairly good 0	good 7050	very good 2,32	4,1	2

REFERENCES

- Bawn C. E. M., Grimley T. B. & Wajid M. A. 1950 *Trans Faraday Soc.* 45, 1112.
Chaudhury A. K., Sarkar D. K. & Palit S. R. 1968 *Macromol Chem.* 111, 36.
Flory P. J. 1949, *J. Chem. Phys.* 17, 303.
Fox T. G. & Flory P. J. 1951, *J. Am. Chem. Soc.* 73, 1904.
Kurata M., Stockmayer W. H. & Roig A. 1960, *J. Chem. Phys.* 33, 151.
Oth J. & Desreux (Liege) V. 1954 *Bull Soc. Chim Belg.* 63, 285.
Palit S. R. 1955 *Indian J. Phys.* 29, 65
Patel R. S. & Patel R. D. 1965, *J. Polym. Sci.*, 3, 2123.
Ptitsyn O. B. 1962 *Polymer Sci U. S. S. R.*, 3, 1061.
Rossi C., Bianchi E. & Pedemonte E 1965 *Macromol Chem.* 89, 95
Sarkar D. K. & Palit S. R. 1967, *Indian J. Phys.* 41, 389.
Schaeffgen J. R. & Flory P. J. 1948 *J. Am Chem. Soc.* 70, 2709.
-

A note on the spin of the 1970 keV level in Ba^{134} *

S. P. SUD, V. K. S. SHANTE AND P. N. TREHAN

Physics Department, Panjab University, Chandigarh-14, India.

(Received 16 December 1968)

The directional correlation of the 802-1168 keV gamma ray cascade in the decay of Cs^{134} to Ba^{134} has been measured by sum-peak coincidence spectrometer to check the recently proposed (Rama Mohan *et al* 1967) spin assignment 3 to the 1970 keV level of Ba^{134} . The present investigations favour a spin 4 to this level. The 802 keV gamma transition has been found to be pure E2.

1. INTRODUCTION

In a recent study of the directional correlation of some cascades in Ba^{134} (Rama Mohan *et al* 1967), a spin 3 has been proposed for the 1970 keV level of Ba^{134} (figure 1a) on the basis of results for the 802-1168 keV cascade. These authors observed a negative asymmetry, whereas previous investigators (Everett & Glaubman 1955, Segal *et al* 1963) had observed a positive asymmetry for this cascade. A spin assignment 3 to the 1970 keV level is in contradiction with the hereto-fore accepted spin 4 for this level. Hence it was considered worthwhile to reinvestigate the directional correlation of the 802-1168 keV cascade so as to verify the spin assignment to the 1970 keV level of Ba^{134} .

The measurement of the directional correlation of the 802-1168 keV cascade is complicated by the presence of a strong 563-605 keV cascade de-exciting the 1168 keV level in competition with the weak 1168 keV cross-over transition. Therefore, it is desirable to use large source-to-crystal distance for the detector selecting the 1168 keV transition so as to reduce the detection of the cascade sum (563+605 keV) compared to the cross-over gamma ray.

An increase in the source-to-crystal distance, however, also reduces the detection efficiency for 1168 keV gamma ray, making it very time consuming to measure the directional correlation of 802-1168 keV cascade with conventional slow-fast coincidence spectrometer. The sum-peak coincidence spectrometer (Kantele & Fink 1962) has more than twice the coincidence detection efficiency compared to a conventional slow-fast coincidence

* Work supported by National Bureau of Standards, Washington D. C., U. S. A. and Department of Atomic Energy, Government of India, India.

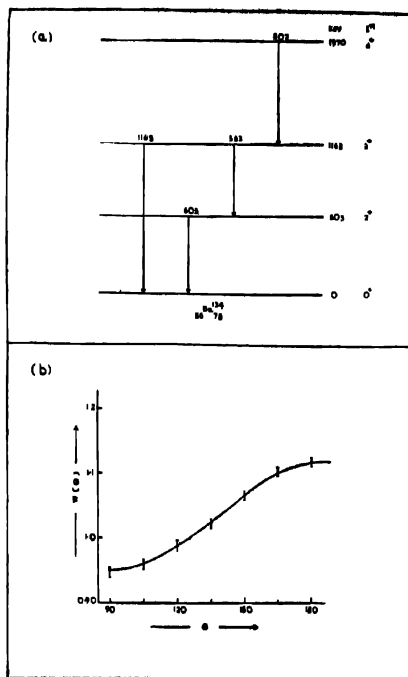


Figure 1. (a) Partial Level Scheme of Ba^{134} populated in the decay of Cs^{138} .

(b) Plot of angular correlation function $W(\theta)$ Vs θ for the 802-1168 KeV cascade of Ba^{134} .

spectrometer and has proved useful in the measurement of angular correlation of weak gamma ray cascades (Sud *et al* 1968). Therefore a sum peak coincidence spectrometer has been utilized in the present study.

2. MEASUREMENTS AND RESULTS

The experimental arrangement was the same as described elsewhere (Sud *et al* 1968) except the detectors which were a matched pair of Harshaw integral line assemblies with 3" dia and 3" thick NaI (Tl) crystals. These detectors have a resolution of 7.6% for 662 keV gamma rays. A

moderately strong liquid source of radioisotope Cs^{134} was prepared in a cylindrical perspex holder with a vertical cavity of 1.5 mm dia \times 4 mm depth. This source was mounted vertically at the inter-section of the axes of the two detectors at a distance of 14 cm from each crystal. The face of either crystal was covered with 7 mm of lead. This geometry reduced the detection of cascade sum (563-605 keV) compared to the 1168 keV crossover gamma ray to less than 2%. Compton graded lead cylinders and lead cones were used to eliminate crystal-to-crystal scattering. The source could be centred to within less than 0.5% variation in the singles rate of movable detector. The integral biases of the two single channel analysers were set at 700 keV to completely bias out the 605 keV gamma ray. The sum-peak coincidence spectrum was recorded on a 256-channel pulse height analyser at seven angles from 90° to 180° at intervals of 15° each. This spectrum after subtraction of random coincidences shows a peak at 1970 keV corresponding to the sum of 802 and 1168 keV cascade. The area under this peak directly gave the coincidences between the 8020 and 1168 keV gamma rays. After a least squares fit of the data (Rose 1953) the correlation coefficients were corrected for finite angular resolution of the detectors (Yates 1965). The corrected correlation coefficients (an average of two independent measurements) are given in table 1 along with the results of previous investigators. The present results are in good agreement with the results of Everett and Glaubman (1955) and Segaert *et al* (1963) but do not agree with the results of Rama Mohan *et al* (1967).

3. DISCUSSION

The spin and parity of ground state of even-even nucleus Ba^{134} is 0^+ . The experimental K-conversion coefficient for the 1168 keV gamma ray (Brown & Ewan 1965) assigns a character 2^+ to the 1168 keV level of Ba^{134} . The 86 keV beta group from the 4^+ ground state of Cs^{134} feeding the 1970 keV level of Ba^{134} is an allowed transition (Nuclear data sheets). This suggests a character 3^+ , 4^+ or 5^+ to the 1970 keV level. The lifetime consideration for this level, however, rules out the 5^+ assignment, leaving only two possibilities 3^+ or 4^+ . A spin assignment 3 requires $A_4 \leq 0$ for all values of mixing ratio (δ) for the 802 keV transition. The definite positive value of A_4 , from the present measurements favours a 4^+ assignment for the 1970 keV level. Therefore the spin sequence for the 802-1168 keV cascade is $4 (2,3) 2(2) 0$. Figure 2 shows a graphical analysis of the present results in terms of the above spin sequence for determining the mixing ratio (δ) for the 802 keV transition. This analysis gives $\delta \leq -0.01$ i.e. 802 keV transition is pure E2. This conclusion is in agreement with

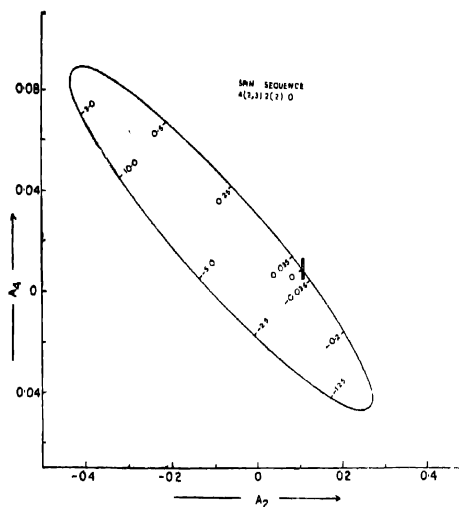


Figure 2. Parametric plot of A_2 Vs A_4 for the spin sequence 4-2-0 for determining the mixing ratio in the 802 keV transition. The shaded area corresponds to the experimental values of A_4 and A_2 .

the results based on internal conversion coefficient for the 802 keV gamma ray (Brown & Ewan 1965) which shows this transition to be pure E2.

TABLE 1. A SUMMARY OF THE RESULTS OF DIRECTIONAL CORRELATION MEASUREMENTS ON THE 802-1168 keV CASCADE IN Ba^{134} .

Reference	A_2	A_4
Everett & Glaubman, 1955	0.095	0.006
Segaert <i>et al</i> 1963	0.15 ± 0.01	-0.019 ± 0.001
Rama Mohan <i>et al</i> 1967	-0.1235 ± 0.0015	0.0009 ± 0.001
Present measurements	0.1081 ± 0.0025	0.0091 ± 0.0040

REFERENCES

- Brown, R.A. & Ewan, G.T. 1965 *Nucl. Phys.* 68, 325-36.
- Everett, A.E. & Glaubman, M.J. 1955 *Phys. Rev.* 100, 955A.
- Kantele, J. & Fink, R.W. 1962 *Nucl. Instr. and Meth.* 15, 69-73.
- Rama Mohan, R. V., Reddy, K.V., Raju, B.B.V., & Jnnananda, S. 1967 *Indian J. Phys.* 41, 30-8.
- Rose, M.E. 1953 *Phys. Rev.* 91, 610-15.
- Segaert, O. J., Demuyne, J. L., Dorikens-Vanpraet, L. V., Dorikens, M. 1963 *Nucl. Phys.* 43, 76-91.
- Sud, S. P., Mangal, P. C., Suri, K. K., & Trehan, P. N. 1968 *Indian J. Phys.* 42 167-176.
- Way, K. 1961 *Nuclear Data Sheets*, Nat. Acad. Sci., Nat. Research Council Washington D. C., NRB-61-2-97.
- Yates, M. J. L. 1965 *Alpha, Beta and Gamma Ray Spectroscopy* Ed. by K. Siegbahn North Holland Publishing Co. Amsterdam North Holland p. 1691-1703.

Letters to the Editor

X-ray crystallographic data on homophthalic acid

By M. P. GUPTA AND S. BOSE

Department of Physics, Ranchi University, India.

(Received 20 February 1967)

As part of a programme of determining the crystal structure of simple organic molecules, we have examined homophthalic acid (α -2-toluene dicarboxylic acid), $C_8H_8(CH_2COOH) \cdot COOH$, using X-ray diffraction techniques.

Colourless, platy crystals of homophthalic acid were grown out of water solution. The platy face is designated as (010) and the bounding edges as [101], [001] and [100]. The angles between [100] and [101] is $\sim 37^\circ$ and between [001] and [100] $\sim 65^\circ$. In some crystals only the [101] and [100] directions appear as the bounding edges of the face [010], the crystal resembling an elongated rhombus.

Examined under the polarizing microscope, with the [010] face horizontal, the extinction direction makes an angle of $\sim 12^\circ$ with the [100] axis of the crystal. Laue photographs with [010] face perpendicular to the X-ray beam showed two well defined zone directions which were taken to be [001] and [100]. The average value of the measurements on these laue photographs gave β or $(180-\beta)$ as $115^\circ 35'$. Rotation photographs along [001] and [100] gave the identity periods to be 5.23 Å and 8.45 Å. Normal beam Weissenberg zero layer photographs along [00] and [100] gave A or $180-\alpha^*$ and C or $180-\gamma^*$ as 97.4° and 92° respectively. The values of A, C and β or $180-\beta$ gave rise to two possibilities for the interaxial angles α, β and γ i. e.

$$\alpha = 80^\circ 54' \quad \beta = 115^\circ 35', \quad \gamma = 95^\circ 45' \quad \dots (1)$$

$$\text{and } \alpha = 82^\circ 46' \quad \beta = 64^\circ 25' \quad \gamma = 88^\circ 40' \quad \dots (2)$$

Laue and oscillation photographs along the perpendicular directions of the (100) and (008) faces gave evidence of the first possibility of the angles α, β and γ .

Finally from the combined evidence of normal beam zero layer Weissenberg photographs along [010], [100], [001], [101] and [101] axes, rotation photographs along [100], [001], [021] and [012] axes and Laue photographs along [001], [100] and [010] axes the following unit cell constant were obtained, i. e.

$$\begin{aligned} a &= 8.45 \pm 0.02 & \alpha &= 80^{\circ}3' \\ b &= 10.87 \pm 0.03 & \beta &= 116^{\circ}10' \\ c &= 5.23 \pm 0.01 & \gamma &= 96^{\circ}44' \end{aligned}$$

which tallies with the first possibility of the angles α , β and γ . Index powder data using the above unit cell constants for homophthalic acid will be found in table 1 below. Powder photograph with the powdered sample sealed in Lindemann glass capillary with internal diameter 0.3 mm, was taken in a 9 cm. unicum powder camera with Van-Arkel arrangement. Copper (Ni-filtered) radiation was used for photographing the powder lines.

TABLE I

I/I_0 Relative Intensity.	Index h k l	d obs (\AA°)	d cal (\AA°)	I/I_0 Relative Intensity	Index h k l	d obs (\AA°)	d cal (\AA°)
64	110	6.08	6.05	4	$\begin{Bmatrix} 3\bar{1}0 \\ 041 \\ \bar{1}22 \end{Bmatrix}$	2.47	$\begin{Bmatrix} 2.48 \\ 2.47 \\ 2.47 \end{Bmatrix}$
2	020	5.36	5.35				
100	$10\bar{1}$	5.10	5.12	1	212	2.36	2.36
4	001	4.70	4.65	5	221	2.28	2.27
36	011	4.50	4.49	2	$\begin{Bmatrix} 022 \\ 320 \end{Bmatrix}$	2.25	$\begin{Bmatrix} 2.25 \\ 2.24 \end{Bmatrix}$
45	$\begin{Bmatrix} 120 \\ 111 \end{Bmatrix}$	4.27	$\begin{Bmatrix} 4.28 \\ 4.28 \end{Bmatrix}$	3	$12\bar{2}$	2.18	2.17
73	$01\bar{1}$	4.08	4.07	1	$\begin{Bmatrix} 240 \\ 330 \end{Bmatrix}$	2.12	$\begin{Bmatrix} 2.14 \\ 2.11 \end{Bmatrix}$
13	$\begin{Bmatrix} 200 \\ 021 \end{Bmatrix}$	3.79	$\begin{Bmatrix} 3.79 \\ 3.78 \end{Bmatrix}$	1	032	2.09	2.08
6	210	3.53	3.52	3	022	2.04	2.03
3	$\bar{1}21$	3.38	3.38	3	$11\bar{2}$	1.92	1.92
73	$\begin{Bmatrix} 02\bar{1} \\ 111 \\ \bar{1}30 \end{Bmatrix}$	3.29	$\begin{Bmatrix} 3.29 \\ 3.29 \\ 3.28 \end{Bmatrix}$	2	032	1.84	1.84
8	$22\bar{0}$	3.16	3.16	2	$\begin{Bmatrix} 340 \\ 060 \end{Bmatrix}$	1.79	$\begin{Bmatrix} 1.80 \\ 1.78 \end{Bmatrix}$
13	031	3.05	3.04	2	$\bar{1}60$	1.75	1.75
2	$22\bar{1}$	2.91	2.92	3	$\bar{1}13$	1.69	1.69
5	$\begin{Bmatrix} 301 \\ 311 \end{Bmatrix}$	2.77	$\begin{Bmatrix} 2.77 \\ 2.78 \end{Bmatrix}$	4	$\begin{Bmatrix} 042 \\ 212 \\ 222 \end{Bmatrix}$	1.65	$\begin{Bmatrix} 1.65 \\ 1.65 \\ 1.64 \end{Bmatrix}$
8	$\begin{Bmatrix} 03\bar{1} \\ 230 \end{Bmatrix}$	2.66	$\begin{Bmatrix} 2.66 \\ 2.66 \end{Bmatrix}$	V.V.W.	$\begin{Bmatrix} 440 \\ 500 \end{Bmatrix}$	1.51	$\begin{Bmatrix} 1.51 \\ 1.52 \end{Bmatrix}$
11	230	2.54	2.54	V.V.W.	$\begin{Bmatrix} 302 \\ 043 \end{Bmatrix}$	1.43	$\begin{Bmatrix} 1.43 \\ 1.43 \end{Bmatrix}$

The density of the crystal measured by floatation method was 1.41 gm/cc and that calculated with 2 molecules per unit cell was 1.423 gms/cc.

Evidences from the morphology of the crystal, intensity, statistics (Howells *et al* 1950) as well as the number of molecules per unit cell suggest the space group to be P $\bar{1}$. Pyroelectric tests on the crystal gave negative results.

A full investigation of the crystal structure using Fourier techniques and partial three-dimensional data is in progress, the details of which will be published later.

The authors wish to acknowledge with thanks the gift of the sample of homophthalic acid by Dr J. N. Chatterjee of the chemical laboratories, Science College, Patna. One of us (S. B.) is indebted to the University Grants Commission of India, New Delhi, for the award of a Junior Fellowship during the tenure of which this work is being pursued. The authors also thank Prof. K. Lonsdale, F. R. S. of the University College, London in whose laboratory pyroelectric tests on the crystal were carried out.

REFERENCE

Howells, E. R. Phillips, D. C. Rogers, D. 1950, *Acta Cryst.* 3, 210.

On the co-efficient of molecular packing in some dicarboxylic acids.

M. P. GUPTA AND N. P. GUPTA

Department of Physics, Ranchi University, Ranchi, India.

(Received 20 February 1967)

Kitaigorodski (1961) has put forward the theory that "a crystal of an organic compound can be considered as a system of closely packed layers, the molecules within a layer are also very closely packed, having coordination numbers of six and being so arranged that no polarities appear perpendicular to the layer". He has also suggested that "the intermolecular radii elements found in organic compounds are universal and reasonably constant i. e. applicable to all molecules. They can be used to assign definite shapes to molecules. If, after the molecules have been built up from intermolecular radii, we consider the molecular posi-

tioning found by experiment, it appears that all the molecules are in contact none are suspended in empty space and none interpenetrate". According to this view, the crystal structures of organic molecules were governed solely by the close-packing principles and one could predict the organic crystal structures in the various space groups by regarding the molecules in them as being built up from the close packing of atoms with rigid spherical shapes, where rigid spherical contact radii could be specified to within 0.1 Å. Kitaigorodskii defines a quantity $K = Z \frac{V_0}{V}$ which he calls the packing density "co-efficient of molecular packing", where Z = number of the molecules in the cell, V_0 = molecular volume calculated from the contacts of rigid sphere (truncated for chemical bonding, where necessary), V = volume of the unit cell.

The value of ' K ' ranges from 0.68 to 0.887 (Graphite) whereas the theoretical value for closed-packed spheres is 0.74. K increases from values below 0.70 to theoretical value of 0.74 for closed packed spheres as the molecular shape tends to become more spherical or ellipsoidal.

In course of testing Kitaigorodskii's theory, the authors have calculated (table 1) the coefficients of molecular packing in some simple dicarboxylic acids whose crystal structures are well known or have been established very recently by X-ray Fourier analysis. In calculating these coefficients, Kitaigorodskii's empirical rule has been followed that "while calculating volumes and constructing models, the H-atoms participating in hydrogen bonds should be neglected, while the X-atoms to which they are valence-bonded should be taken as spherical in the X-H direction."

TABLE 1 INTERMOLECULAR RADII $C=1.90$ Å, $O=1.35$ Å

Molecule	Molecular volume V (Å ³)	Molecular packing co-efficient K	Reference
α -oxalic acid	57.73	0.751	Cox <i>et al</i> (1952)
β -oxalic acid	57.73	0.731	Hendricks (1935)
Oxalic acid dihydrate	57.73	0.618	Ahmed and Cruickshank (1953)
Acetylene dicarboxylic acid dihydrate	113.17	0.671	Robertson (1947)
Dihydroxyfumaric acid dihydrate	111.0	0.620	Gupta (1964)

However, if one assumes a value for the intermolecular radius as actually found in the crystal structure (*e. g.* determined from the shortest carbon-carbon or carbon-oxygen contact distances), the values for the coefficient of molecular packing changes significantly as may be seen from comparison of table 1 and table 2 (given below).

TABLE 2

Molecule	Molecular volume V_0 (Å)	K Molecular packing coefficient	Shortest distances calculated Å	Assumed value of intermolecular radius	
				C (Å)	O (Å)
α -oxalic acid	63.40	0.811	C—C 3.93 C—O 3.37	1.97	1.40
β -oxalic acid	56.19	0.700	C—C 3.71 C—O 3.35	1.86	1.49
oxalic acid dihydrate	71.07	0.556	C—C 3.60 C—O 3.16	1.80	1.36
Acetylene dicarboxylic acid dihydrate	116.9	0.693	C—C 3.86 C—O 3.29	1.93	1.36
Dihydroxyfumaric acid dihydrate	118.87	0.664	C—C 3.97 C—O 3.40	1.98	1.42

As tables 1 and 2 above show, the values of intermolecular radii for the atoms are not universal constants as Kitaigorodskii claims but vary somewhat from crystal structure to crystal structure. This is admitted even by Kitaigorodskii (*ibid*) to be due to second order effects depending on relative orientation of the contact with respect to the chemical bonds near it (steric hindrances) and on the anisotropy of thermal vibrations.

It would, therefore, appear that packing consideration is not the only criterion determining the crystal structure of organic molecules as Kitaigorodskii suggests but secondary effects also play an important role.

REFERENCES

- Carpenter, G. B. & Donohue, 1950 *J. Am. Chem. Soc.* **72**, 2315
 Cox, E. G. Dougill, M.W. & Jeffery, G. A. 1952 *J. Chem. Soc.* 4854
 Dunitz, J. D. & Robertson, J. M. 1947 *J. Chem. Soc.* 148
 Gupta, N. P. 1964 *Ph. D. thesis*, Ranchi University.
 Hendricks, S. B. 1935 *Z. Krist.* **91**, 48
 Kitaigorodskii, A. I. 1961 *Organic Chemical crystallography*, Consultants Bureau, New York.
 Whitney, J. Corvin, J. & Macrone, W. C. 1949 *Anal. Chem.* **21**, 191

BOOK REVIEWS

GENERAL PHYSICS-MECHANICS AND MOLECULAR PHYSICS—by Landau,
Akhiezer and Lifshitz (English translation by Sykes, Petford and Petford).
Pergamon Press 1967 Price-50sh, pp 372

The book covers a very wide area of physics in what the authors call an attempt "to acquaint the reader with the principal phenomena and most important laws of physics". However this acquaintance can hardly be deep or critical for the book of 372 pages has something to say about a rather wide variety of topics. Naturally enough one misses very often a discussion or mathematical treatment which can in any sense be called complete. Yet if anybody likes to have an idea of say classical mechanics, classical field theory, the crystalline symmetry and lattices, the kinetic theory, the laws and approach of thermodynamics, the electrolytes, chemical reactions and surface phenomena, transport properties, plasticity and elasticity, and viscosity (well, here there are a few pages on superfluidity even) in one single small volume then here is that unique combination and he will also have a flavour of the lucidity, and originality which has characterised the now famous series of texts by Landau and Lifshitz. This book will not serve as a text book for any course in our universities but will be a pleasant reading outstudy book for undergraduate students in Physics and Chemistry and will help in clarifying their ideas.

A.K.R.C.

A SHORT TEXT BOOK OF PHYSICS—by Wilhelm H. Westphal Springer-Verlag,
Berlin Price 97s.

This book is meant for students for whom Physics is a secondary subject and whose mathematical equipment is rather poor. Use of even elementary calculus and complex quantities has been avoided. This book explains mainly elementary principles of Physics without going into details of apparatus and experimental techniques. The coverage, on the other hand, is quite good. Every aspect of physics, from Newton's law to nuclear fission and pair production has received its due emphasis. Serious students of Physics at high school level will find in this book plenty of things to ponder over and learn. One, however, feels disappointed that microscopic interpretation of properties of matter has been severely left out of consideration. An elementary discussion on kinetic theory of matter and of the free electron theory of electrical conductivity would surely not be out of place in this book which, otherwise, deals with sophistications regarding inertial and gravitational mass (p.12), origin of tides (p.53), electron microscopes, (p 197) mass defects (p. 316), the betatron (p. 322) and the like. Description of structure of matter (p. 58-60) has been too short and too sketchy. Since this topic has been introduced in the chapter on Mechanics of substances, a discussion on dislocations would be welcome. I hope that, in the next edition, these points will be attended to. The get up of the book is pleasing and it is well illustrated. The net effect is a very good elementary text book of Physics.

G.B.M.

Application of time-dependent suction to free
convection laminar flow

By KRISHNA LAL

BANARAS HINDU UNIVERSITY, BANARAS, INDIA.

(Received 6 January 1969)

The boundary layer equations for the laminar flow past a porous vertical wall has been discussed for the free convection when the suction velocity is an oscillatory function of time. Expressions for the velocity and temperature distributions have been calculated in the non-dimensional forms. From these equations, the rate of heat transfer from the wall to the fluid, Nusselt number and skin-friction have been calculated. It is found that the rate of heat transfer from the wall to the fluid, decreases as the suction velocity increases. The phase angle of the skinfriction is also found to decrease with increasing the unsteady part of the suction velocity. Graphically the variations for phase angle, steady part of velocity distribution the skin friction have been shown in some cases when the frequency of fluctuations are small or large. For large frequency of oscillations, the skin friction is found to lag behind the wall velocity fluctuations. This phase angle is found to decrease as the suction velocity increases.

1. INTRODUCTION

The unsteady two-dimensional laminar flow was considered by Lighthill (1954) for the velocity and thermal boundary layers. He has analyzed mathematically the equations of motion and energy when the velocity of the on-coming flow relative to the body oscillates in magnitude but not in direction. (Messiha, 1966) has considered unsteady oscillatory flow past an infinite flat plate and calculated the expressions for the velocity, temperature and skin-friction for small and large frequency of oscillations. It has been assumed (Messiha, 1966) that the suction velocity and free stream velocity and free stream velocity are both functions of time. It has been concluded there that the effect of increasing the suction velocity is that the amplitude of skin friction is increased and the phase is decreased. For small value of the frequency of fluctuation, it is given (Messiha, 1966) that the wall temperature decreases for increasing the suction velocity. Lal (1966) has considered the free convection problem when the suction velocity depends on time and expressions for skin and rate of heat transfer are deduced.

In the present paper, the author has considered the problem of Messiha (1966) for free convection laminar flow when the dissipation term is

neglected. The suction velocity is taken as $V_0[1 + \epsilon A e^{i\omega t}]$ where V_0 is constant mean velocity and $\epsilon A \ll 1$. For $A=0$, the problem is reduced to steady suction velocity. Expressions for $u(y, t)$, temperature, rate of heat transfer from the wall to the liquid, skin-friction have been calculated and interesting results are obtained regarding the dependence of the skin-friction and the rate of heat transfer from the boundary to fluid, on the fluctuating part of the suction velocity. The expressions are expanded for large and small frequency of oscillations and graphically some variations are represented.

2. FUNDAMENTAL EQUATIONS

Let \bar{x} -axis be taken along the vertical plate and \bar{y} -axis perpendicular to it. The equations which describe the unsteady free convection flow of a viscous incompressible fluid for the present problem are

$$\frac{\partial \bar{u}}{\partial t} + \bar{v} \frac{\partial \bar{u}}{\partial \bar{y}} = g\beta (\bar{T} - \bar{T}_\infty) + \nu \frac{\partial^2 \bar{u}}{\partial \bar{y}^2} \quad \dots 1.1$$

$$\frac{\partial \bar{v}}{\partial \bar{y}} = 0 \quad \dots 1.2$$

$$\frac{\partial \bar{p}}{\partial \bar{y}} = - \frac{1}{\rho} \frac{\partial \bar{p}}{\partial \bar{y}} \quad \dots 1.3$$

$$\frac{\partial \bar{T}}{\partial t} + \bar{v} \frac{\partial \bar{T}}{\partial \bar{y}} = K \frac{\partial^2 \bar{T}}{\partial \bar{y}^2} \quad \dots 1.4$$

where \bar{u} , \bar{v} are velocity components, ρ the density, g the acceleration due to gravity, β the coefficient of volume expansion, t time, \bar{p} the pressure; ν the kinematic coefficient of viscosity, \bar{T} the temperature, \bar{T}_∞ the temperature at infinity, K the thermal diffusivity. From (1.2), it is clear that \bar{v} is a function \bar{t} only. In a thin boundary layer, $\frac{\partial \bar{p}}{\partial \bar{y}}$ is very small and so if $-v_0$ be the steady suction velocity, we replace \bar{v} by

$$\bar{v} = v_0 [1 + \epsilon A e^{i\omega \bar{t}}] \quad \dots 1.5$$

where

$$\epsilon A \ll 1,$$

The above equations are reduced into non-dimensional forms by the substitutions of

$$\left. \begin{aligned} y &= \frac{y}{L}, \quad t = \frac{vt}{L^2}, \quad u = \frac{\bar{u}L}{|v_o| \nu}, \quad v = \frac{\bar{v}L}{\nu} \\ T &= g\beta L^3 (\bar{T} - \bar{T}_\infty) / |v_o| \nu^2, \quad p = \bar{p}L^2 / \rho \nu^2 |v_o|, \quad \omega = \frac{L\bar{\omega}}{\nu} \end{aligned} \right\} \dots 1.6$$

where \bar{T}_∞ is reference temperature and L is characteristic length. Equations 1.1 and 1.4 are replaced by

$$\frac{\delta u}{\delta t} - [1 + \epsilon A e^{i\omega t}] \frac{\delta u}{\delta y} = T + \frac{\delta^2 u}{\delta y^2} \dots 1.7$$

$$\frac{\delta T}{\delta t} - [1 + \epsilon A e^{i\omega t}] \frac{\delta T}{\delta y} = \frac{1}{\sigma} \frac{\delta^2 T}{\delta y^2} \dots 1.8$$

where σ is the Prandtl number. The boundary conditions are

$$\left. \begin{aligned} t < 0 : u = v = T = 0 \text{ for } y \geq 0 \\ t \geq 0 : u = 0, v = -v_o(t), T = \theta(t) \text{ for } y = 0 \\ y = \infty : u(\infty, t) = 1, T = 0 \end{aligned} \right\} \dots 1.9$$

2. SOLUTIONS OF EQUATIONS

To solve the equations 1.7 and 1.8, with above boundary conditions, we assume

$$u(y, t) = F_0(y) + F_1(y)\epsilon e^{i\omega t} + F_2(y)\epsilon^2 e^{2i\omega t} + \dots + F_n(y)\epsilon^n e^{in\omega t} \dots 2.1$$

$$T(y, t) = T_0(y) + T_1(y)\epsilon e^{i\omega t} + T_2(y)\epsilon^2 e^{2i\omega t} + \dots + T_n(y)\epsilon^n e^{in\omega t} \dots 2.2$$

where ϵ is small parameter such that $\epsilon^3, \epsilon^4, \epsilon^5, \dots, \epsilon^n$ are negligibly small quantities. If, we give the wall temperature as $\cos \omega t, \cos 2\omega t, \dots$ we consider real parts of equations 2.1 and 2.2.

Substituting 2.2 into 1.8 and equating the coefficient of ϵ^n and harmonic terms, we have

$$in \omega T_n - A T'_{n-1} = \frac{T''_n}{\sigma} \dots 2.3$$

where

$$n = 0, 1, 2, \dots$$

The boundary conditions for T_n are reduced to

$$\left. \begin{aligned} y=0 : T_0 = T_0(0) = \theta_0 \text{ (say)}, T_1(0) = \theta_1, \dots, T_n(0) = \theta_n \\ y=\infty : T_0 = T_1 = T_2 = \dots = T_n = 0 \end{aligned} \right\} \dots 2.4$$

Solving 2.3 with the boundary conditions from the set 2.4, we have

$$T_0(y) = \theta_0 \exp(-\sigma y) \dots 2.5$$

$$T_1(y) = \theta_1 e^{-hy} + \frac{i\theta_0 \sigma A}{\omega} [e^{-\sigma y} - e^{-hy}] \dots 2.6$$

$$T_2(y) = \theta_2 e^{-my} + \frac{Ah\sigma}{h^2 - h\sigma - \frac{i\theta_0 \sigma A}{\omega}} \left[e^{-hy} - e^{-my} \right] - \frac{\theta_0 \sigma^2 A^2}{2\omega^2} [e^{-\sigma y} - e^{-my}] \dots 2.7$$

$$\text{where, } h = \frac{\sigma}{2} \left[1 + \sqrt{1 + 4i\omega/\sigma} \right], m = \frac{\sigma}{2} \left[1 + \sqrt{1 + 8i\omega/\sigma} \right] \dots 2.8$$

Using equations 2.1 and 2.2 into 1.7, we have following relation from equating the coefficients of e^n and harmonic terms,

$$i\omega n - F_n F'_n - AF'_{n-1} = T_n + F_n'' \dots 2.9$$

where $n = 0, 1, 2, \dots$

Solving above equation and the following boundary conditions for F_n

$$\left. \begin{aligned} y=0 : F_0 = F_1 = F_2 = \dots = F_n = 0 \\ y=\infty : F_0 = 1, F_1 = F_2 = \dots = F_n = 0 \end{aligned} \right\} \dots 2.10$$

we have for F_0, F_1 and F_2

$$F_0(y) = 1 - e^{-y} + a(e^{-\sigma y} - e^{-y}) \dots 2.11$$

$$F_1(y) = \frac{A(1+a)}{i\omega} [e^{-y} - e^{-my}] + b[e^{-\sigma y} - e^{-my}] + c[e^{-hy} - e^{-my}] \dots 2.12$$

$$\begin{aligned}
F_2(y) = & \frac{e^{-m_1 y}}{m_1^2 - m_1 - 2i\omega} \left[-\theta_2 + \frac{A h \sigma \left(\theta_1 - \frac{i \theta_0 \sigma A}{\omega} \right)}{h^2 - h \sigma - 2i\omega \sigma} - \frac{\theta_0 \sigma^2 A^2}{2\omega^2} \right] \\
& - \frac{e^{-m_1 y}}{m_1^2 - m_1 - 2i\omega} \left[\frac{m_1 A^2 (1+a)}{i\omega} + m_1 A b + m_1 A c \right] + \frac{\sigma A e^{-\sigma y}}{\sigma^2 - \sigma - 2i\omega} \left(-b + \frac{\theta_0 \sigma A}{2\omega^2} \right) \\
& + \frac{A h e^{-h y}}{h^2 - h - 2i\omega} \left[c - \frac{a \left(\theta_1 - \frac{i \theta_0 \sigma A}{\omega} \right)}{h^2 - h \sigma - 2i\omega \sigma} \right] + \frac{A^2 (1+a)}{2\omega^2} e^{-y} + c_1 e^{-D y} \quad \dots 2.13
\end{aligned}$$

where the constant of integration C_1 , is easily obtained by using the boundary condition at $y=0$. The values of the constants D , a , b and c are

$$\left. \begin{aligned}
D &= \frac{1}{2} [1 + \sqrt{1 + 4i\omega}], \quad a = \frac{\theta_0}{\sigma - \sigma^2}, \\
b &= \frac{A \sigma \left(a - \frac{i \theta_0}{\omega} \right)}{\sigma^2 - \sigma - i\omega}, \quad c = \left(\frac{i \theta_0 \sigma A}{\omega} - \theta_1 \right) / (h^2 - h - i\omega) \\
m_1 &= \frac{1}{2} [1 + \sqrt{1 + 4i\omega}]
\end{aligned} \right\} \quad \dots 2.14$$

3. DISCUSSIONS

If q , be the rate of heat addition from the plate to the fluid, we have

$$\begin{aligned}
q &= -k \left[\frac{\partial T}{\partial y} \right]_{y=0} \\
&= \frac{k v_\infty^2}{g \beta L^4} \left\{ \theta_0 \sigma + \epsilon e^{i\omega t} \left[\theta_1 h + \frac{i \theta_0 \sigma A}{\omega} (\sigma - h) \right] + \dots \right\} \quad \dots 3.1
\end{aligned}$$

after substitutions and simplifications.

And if N be the Nusselt number, we have

$$N = \frac{L q}{k (\bar{T}_w - \bar{T}_\infty)} = \frac{\theta_0 \sigma + \epsilon e^{i\omega t} \left\{ \theta_1 h + \frac{i \theta_0 \sigma A}{\omega} (\sigma - h) \right\} + \dots}{\theta_0 + \theta_1 \epsilon e^{i\omega t} + \theta_2 \epsilon^2 e^{2i\omega t} + \dots} \quad \dots 3.2$$

where \bar{T}_w is the wall temperature. Since $h > \sigma$, we see that q and N decrease as A increases or the suction velocity increases.

If T_o be the skin-friction, we have

$$T_o = \mu \left[\frac{\partial \bar{u}}{\partial y} \right]_{y=0}$$

$$= \frac{\mu^2 v_o}{L^2 \rho} \left[1 + \alpha(1 - \sigma) + \epsilon e^{i\omega t} \left\{ b(m_1 - \sigma) + c(m_1 - h) - \frac{iA(1 + a)}{w}(m_1 - 1) \right\} + \dots \right] \quad 3.3$$

if the terms having ϵ^2 , ϵ^3 are not considered.

The skin-friction is obtained in terms of b and c which are complex quantities. Hence to combine ωt with phase angle, we have to separate real and imaginary part.

Case (i) if ω is small

From the expressions for F_o and T_o , we see that these are independent of ω . Hence we have deduced the expressions of F_1 and T_1 for small or large frequency of oscillations. For small values of ω , we have

$$m \simeq \left(\sigma + \frac{4\omega^2}{\sigma} \right) + i \left(2\omega - \frac{16\omega^3}{\sigma^2} \right) + 0(\omega^4) \quad 3.4$$

$$h \simeq \left(\sigma + \frac{\omega^2}{\sigma} \right) + i \left(\omega - \frac{2\omega^3}{\sigma^2} \right) + 0(\omega^4) \quad 3.5$$

which may be written as for example

$$m = m_r + i m_i \quad 3.6$$

where $m_r = \left(\sigma + \frac{4\omega^2}{\sigma} \right)$, $m_i = \left(2\omega - \frac{16\omega^3}{\sigma^2} \right)$ if terms of order

ω^4 are neglected. Similarly, we use

$$h = h_r + i h_i \quad \dots 3.7$$

where h_r and h_i obtained as in the case of m , and m_i . In the same manner, we have

$$b = b_r + i b_i$$

$$= \left[\left(\frac{A}{\sigma-1} + \frac{A \theta_o}{\sigma(\sigma-1)^2} \right) + \omega^2 \left(\frac{A \theta_o}{\sigma^3(\sigma-1)^2} - \frac{A}{\sigma^2(\sigma-1)^3} \right) \right] \\ + i \left[-\frac{A \theta_o}{\omega(\sigma-1)} + \frac{A \omega}{\sigma(\sigma-1)^2} \left(1 + \frac{\theta_o}{\sigma(\sigma-1)} \right) \right] \quad 3.8$$

$$h^2 - h - i\omega = \left[\sigma(\sigma-1) + \frac{\sigma-1}{\sigma} \omega^2 \right] + i \left[2\omega(\sigma-1) - \frac{2\omega^3}{\sigma^2}(\sigma-1) \right] \quad 3.9$$

and

$$C = Cr + iC_i$$

$$= \frac{1}{\sigma(\sigma-1)} \left\{ \left[2\theta_o A - \theta_1 + \omega^2 \left(\frac{5\theta_1}{\sigma^2} - \frac{6\theta_o A}{\sigma^2} \right) \right] \right. \\ \left. + i \left[\frac{\theta_o \sigma A}{\omega} + \omega \left(\frac{2\theta_1}{\sigma} - \frac{5\theta_o A}{\sigma} \right) + \omega^3 \left(-\frac{6\theta_1}{\sigma^3} \right) \right] \right\} \quad \dots 3.10$$

If ω^2 and higher products of ω are neglected, we have

$$u(y, t) = 1 - e^{-y} + \frac{\theta_o}{\sigma(1-\sigma)} \left[e^{-\frac{\sigma y}{1-\sigma}} \right] + \epsilon e^{i\omega t} \left[F_{1r} + iF_{1i} \right] \quad \dots 3.11$$

where

$$F_{1r} = \frac{A e^{-\sigma y}}{\sigma(\sigma-1)} \left[y(\theta_o \sigma - \theta_o + \sigma^2 - \sigma) \right] \quad \dots 3.12$$

and

$$F_{1i} = \frac{A \omega \theta_o (2\sigma-1) e^{-\sigma y}}{\sigma(\sigma-1)^2} \left[y + \frac{y^2(\sigma-1)}{2(2\sigma-1)} \left\{ 2 + \frac{2(\sigma-\sigma^2)}{\theta_o} - \sigma \right\} \right] \\ + \frac{A}{\omega} \left[\frac{\theta_o}{\sigma} + \frac{\sigma - \sigma^2}{\sigma} \left(\frac{-y}{e} - e^{-\sigma y} \right) \right] \quad \dots 3.13$$

Thus if only real parts are considered, we have from above equations,

$$u(y, t) = 1 - e^{-y} + \frac{\theta_o}{\sigma(\sigma-1)} \left(e^{-\frac{\sigma y}{1-\sigma}} \right) + \epsilon |F_1| \cos(\omega t + \alpha) \quad \dots 3.14$$

where

$$\left. \begin{aligned} |F| &= \sqrt{F_{1r}^2 + F_{1i}^2} \\ \alpha &= \tan^{-1} \left(\frac{F_{1i}}{F_{1r}} \right) \end{aligned} \right\} \quad \dots 3.15$$

Thus the phase angle of the velocity distribution inside the boundary layer leads by an angle α .

The motion becomes independent of time if

$$\alpha = \pi \left(n + \frac{1}{2} \right) - \omega t, \quad n = 0, 1, 2, \quad \dots 3.16$$

Also, we have $\alpha = \pi/2$ for $\theta_0 = -\sigma$. From above equations, we see that the unsteady part of $u(y, t)$ increases by increasing the value of A , on which the suction velocity depends. Thus increasing the suction velocity, we see that the unsteady part of the velocity distribution inside the boundary layer increases. The variations of steady part of $u(y, t)$ with y , have been shown in figure 1.

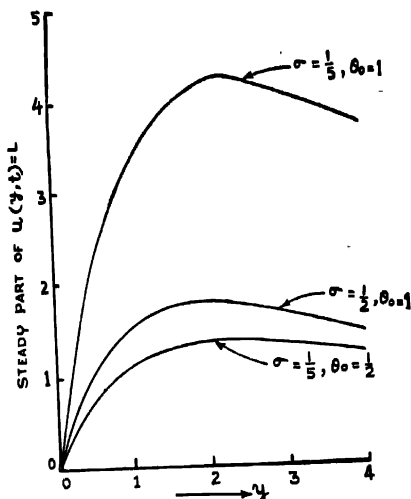


Figure 1. Graph between $1 - e^{-y} + \theta_0 (\sigma - 1) (e^{-y} - e^{-\sigma y})$ and y for given θ_0 and σ ,

The variations of other parameters such as F_{1r} , F_{1i} , F_1 and α may also similarly be represented graphically. The graphical representations in such cases are done in other cases.

Using the expansions for h from equation 3.5 into 2.2,

$$T(y, t) = \theta_0 \exp(-\sigma y) + \epsilon e^{i\omega t} [T_{1r} + i T_{1i}] \quad \dots 3.17$$

when ϵ^2 and other small terms are neglected. The expressions for T_{1r} and T_{1i} are given by

$$\left. \begin{aligned} T_{1r} &= e^{-\sigma y} (\theta_1 - \theta_0 \sigma A y) \\ T_{1i} &= \omega e^{-\sigma y} \left[\frac{\theta_0 \sigma A y^2}{2} - y \theta_1 \right] \end{aligned} \right\} \quad \dots 3.18$$

Thus we may easily write

$$T(y, t) = \theta_0 e^{-\sigma y} + \epsilon |T_1| \cos(\omega t + \gamma) \quad \dots 3.19$$

where,

$$\left. \begin{aligned} |T_1| &= \sqrt{T_{1r}^2 + T_{1i}^2} \\ \gamma &= \tan^{-1} \frac{T_{1i}}{T_{1r}} \end{aligned} \right\} \quad \dots 3.20$$

The variation of angle γ with y has been shown graphically in figure 2 for given σ , A , θ_0 , θ_1 , ω . The value of γ on the wall is $\pi/2$ if $\theta_1 = 0$. From the figure (when $A = \theta_0 = \frac{1}{2}$, $\sigma = 1$, $\theta_1 = \frac{1}{4}$) we see that if ω increases, the value of phase angle, γ also increases with respect to y . The angle γ becomes negative between $y = 0$ and $y = 1$ which implies that temperature distribution inside the boundary layer lags behind the wall fluctuations between $y = 0$ and $y = 1$. Between $y = 1$ and $y = 2$, this angle is positive and then temperature distribution leads by an angle γ for $1 \leq y \leq 2$.

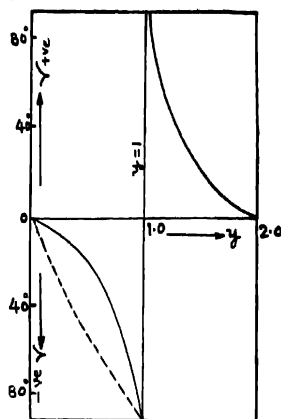


Figure 2. —————, $\omega = 0.5$; -----, $\omega = 2.0$

From equations 3.5 and 3.1, we have

$$q = \frac{K v_0 v^2}{g \beta L^4} \left\{ \theta_0 \sigma + \epsilon e^{i \omega t} \left[\theta_1 \sigma + \theta_0 \sigma A + i \omega \theta_1 \right] + \dots \right\} \quad \dots 3.21$$

which considering the real parts may be written as

$$q = \frac{K v_0 v^2}{g \beta L^4} \left\{ \theta_0 \sigma + \epsilon |B| \cos(\omega t + \phi) + \dots \right\} \quad \dots 3.22$$

$$\left. \begin{aligned} \text{where } B = B_r + i B_i = \sigma (\theta_1 + \theta_0 A) + i (\omega \theta_1) \\ \text{and } \phi = \tan^{-1} \frac{B_i}{B_r} \end{aligned} \right\} \quad \dots 3.23$$

By an inspection of equations of set 3.23, we see that angle ϕ will be positive and thus the rate of heat transfer has a lead over the surface temperature fluctuations. The variations of angle ϕ with ω has been drawn in figure 3 for various values of A when $\theta_0 = \theta_1 = \frac{1}{2}$, $\sigma = 2$. From figure 3, we see that this angle ϕ is positive and increases as ω increases. The increment in ϕ is large upto $\omega = 1.5$ and from $\omega = 1.5$ to 3.5 slow and for $\omega > 3.5$ it is very slow. As A increases, the angle ϕ is found to decrease. If A increases, we see that the suction velocity increases.

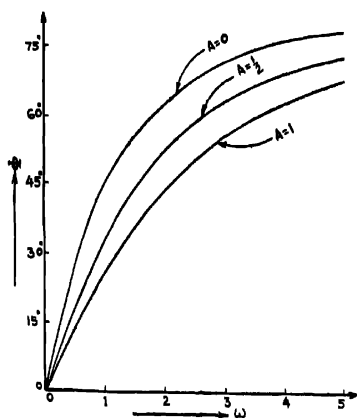


Figure 3. Curves showing $\phi = \tan^{-1} B_i/B_r^* V_s, \omega$ for $A = 0, \frac{1}{2}, 1$

To find the expression for the skin friction, we put the expansions for m , h , b and c into equation 3.3 and get

$$\begin{aligned}
 T_o &= \frac{\mu^2 v_o}{L^2 \sigma} \left[\left(1 + \frac{\theta_o}{\sigma} \right) + \epsilon e^{i\omega t} \left\{ \left[b_i (m_i - \sigma) - b_i m_i + C_i (m_i - h_i) \right. \right. \right. \\
 &\quad \left. \left. - C_i (m_i - h_i) + \frac{A}{\omega} m_i \left(\frac{\theta_o}{\sigma - \sigma^2} \right) \right] + i \left[b_i (m_i - \sigma) + b_i m_i \right. \right. \\
 &\quad \left. \left. + C_i (m_i - h_i) + C_i (m_i - h_i) - \frac{A}{\omega} (m_i - 1) \left(1 + \frac{\theta_o}{\sigma - \sigma^2} \right) \right] + \dots \right] \quad \dots 3.24 \\
 &= \frac{\mu^2 v_o}{L^2 \rho} \left[\left(1 + \frac{\theta_o}{\sigma} \right) + \epsilon e^{i\omega t} \left\{ M_i + i M_i \right\} + \dots \right] \quad \dots 3.25
 \end{aligned}$$

where m , σm_i and other terms are known from equations 3.4 to 3.10 and M_i and M_i are easily known from equations 3.24 and 3.25.

Using the values of m_r , m_i etc. and simplifying, we have

$$M_r = A \left(2 - \frac{\theta_0}{\sigma-1} \right) + \omega^2 \left[-\frac{5\theta_1}{\sigma^2(\sigma-1)} + \frac{A}{\sigma} \left\{ \theta_0 \frac{25\sigma^2-46\sigma+19}{\sigma(\sigma-1)^2} - \frac{(4\sigma+2)(3\sigma-8)}{\sigma(\sigma-1)^2} \right\} \right] \quad \dots 3.26$$

$$M_i = \frac{A}{\omega\sigma} (\theta_0 - \sigma^2 + \sigma) + \frac{\omega}{\sigma(\sigma-1)} \left[A \left\{ \frac{\theta_0(\sigma^2+5\sigma-4)}{\sigma(\sigma-1)} - 2(\sigma-2) \right\} - \theta_1 \right] \quad \dots 3.27$$

Thus from above equations 3.26 and 3.27, we observe, that for sufficiently small values of ω , M_r and M_i are approximately given by first terms of the equations. Equation 3.25 may be written approximately by considering real parts alone,

$$T_0 = \frac{\mu^2 v_0}{L^2 \rho} \left\{ \left(1 + \frac{\theta_0}{\sigma} \right) + \epsilon |M| \cos \left(\omega t + \tan^{-1} \frac{M_i}{M_r} \right) \right\} \quad \dots 3.28$$

where $M = \sqrt{M_r^2 + M_i^2}$

$$= \frac{A}{\omega\sigma(\sigma-1)} \sqrt{\sigma^2\omega^2(2\sigma-2-\theta_0)^2 + (\sigma-1)^2(\theta_0-\sigma^2+\sigma)^2} \quad 3.29$$

and the sign of $\tan^{-1} \frac{M_i}{M_r}$ depends upon the values of ω , θ_0 , σ and A .

The variations of M with A for given values of ω has been shown graphically in figure 4 when $\sigma = 3/2$, $\theta_0 = 1$. This has been selected for simplicity of calculations and then a linear relation exists between M and A when ω is given certain value. It is found from the graph that M and A increases together and thus the skin friction increases as the suction velocity increases.

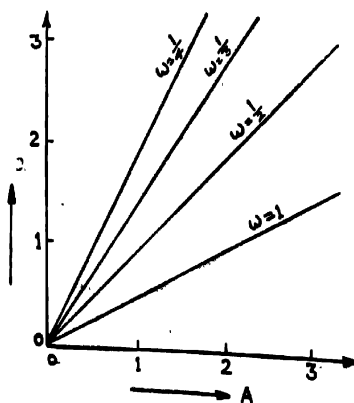


Figure 4. Graph between M and A for $\omega = \frac{1}{2}, \frac{1}{4}, \frac{1}{2}, 1$.

Case (ii) if ω is large

If ω^{-2} and higher negative powers of ω are omitted, we have in this case

$$\left. \begin{aligned} h &\simeq \sqrt{\frac{\omega \sigma}{2}} (1+i) \\ m &\simeq \sqrt{\omega \sigma} (1+i) \\ b &\simeq \frac{1}{\omega^2} \left[A \sigma^2 (\sigma-1) + A \sigma \theta_0 \right] + \frac{i A \sigma}{\omega} \\ h^2 - h - i \omega &\simeq (\sigma-1) \left[\left(\frac{\sigma}{2} + \sqrt{\frac{\omega \sigma}{2}} + i \left(\omega + \sqrt{\frac{\omega \sigma}{2}} \right) \right) \right] \\ c &\simeq \frac{\theta_0 \sigma A}{\omega^2 (\sigma-1)} + \frac{i \theta_1}{\omega (\sigma-1)} \end{aligned} \right\} \quad \dots 3.30$$

Thus we have

$$\begin{aligned} F_1 = & \frac{A}{\sigma-1} \left[e^{-\sigma y} - e^{-y \sqrt{2 i \omega \sigma}} \right] + \frac{i}{\omega} \left[e^{-y \sqrt{2 i \omega \sigma}} \left\{ A \left(1 + \frac{\theta_0}{(1-\sigma)} \right) \right. \right. \\ & \left. \left. - A \left(1 + \frac{\theta_0}{\sigma-\sigma^2} \right) e^{-y} + \frac{\theta_1}{\sigma-1} e^{-y \sqrt{i \omega \sigma}} \right\} \right] \quad \dots 3.31 \end{aligned}$$

$$T_1 = \theta_1 e^{-\gamma \sqrt{i\omega\sigma}} + \frac{i\theta_0\sigma A}{\omega} \left[e^{-\sigma\gamma} - e^{-\gamma \sqrt{i\omega\sigma}} \right] \quad \dots 3.32$$

$$\text{and } q = \frac{K\nu_0\nu^2}{g\beta L} \left\{ \theta_0\sigma + \epsilon e^{i\omega t} \left[\theta_1 \sqrt{i\omega\sigma} + \frac{i\theta_0\sigma A}{\omega} \left(\sigma - \sqrt{i\omega\sigma} \right) + \dots \dots \right] \right\} \quad \dots 3.33$$

where, we easily find that q decreases as A increases. However if the real and imaginary parts are separated, we have

$$q = \frac{K\nu_0\nu^2}{g\beta L^2} \left[\theta_0 + \sigma + \epsilon \left\{ \theta_1 \sqrt{\omega\sigma} \cos \left(\omega t + \frac{\pi}{4} \right) + \frac{\theta_0\sigma^2 A}{\omega} \cos \left(\omega t + \frac{\pi}{2} \right) - \theta_0\sigma A \sqrt{\frac{\sigma}{\omega}} \cos \left(\omega t + \frac{3\pi}{4} \right) \right\} + \dots \right] \quad 3.34$$

from which looking at various terms, it is clear that the wall temperature leads by certain angles. The values of F_0 and T_0 are unaffected by changes in ω . If we substitute the equations 3.32 and 3.31 into 2.1 and 2.2, we have expressions for $u(y,t)$ and $T(y,t)$ with the help of equations 2.5 and 2.11.

Now using the equations of set 3.30 into 3.3, we have

$$T_0 = \frac{\mu^2\nu_0}{L^2\rho} \left[1 + \frac{\theta_0}{\sigma} + \epsilon e^{i\omega t} \left\{ L_1 + iL_2 \right\} + \dots \right] \quad \dots 3.35$$

$$\text{where, } L_1 = i\omega^{1/2} \left[A \left\{ \sigma^{1/2} \left(1 - \frac{\theta_0}{\sigma(\sigma-1)} \right) - \sigma^{3/2} \right. \right.$$

$$\left. - \frac{0.3\theta_1\sigma^{1/2}}{\sigma-1} \right] + \omega^{-3/2} A \left[\sigma^{3/2}(\sigma-1) + \sigma^{3/2} \theta_0 \left(1 + \frac{0.3}{\sigma-1} \right) \right]$$

$$- \omega^{-2} [A\sigma^2(\sigma-1) + A\sigma^2\theta_0] \quad \dots 3.36$$

$$\begin{aligned}
 \text{and } L_i = \omega^{-1/2} \left[A \left\{ \sigma^{3/2} + \frac{\theta_0 \sigma^{-1/2}}{\sigma-1} - \sigma^{-1/2} \right\} + \frac{0.3 \theta_1 \sigma^{1/2}}{\sigma-1} \right] \\
 + \omega^{-1} \left[A \left(1 - \sigma^2 - \frac{\theta_0}{\sigma(\sigma-1)} \right) \right] + \omega^{-3/2} \left[A \sigma^{3/2} \left\{ \frac{0.3 \theta_0}{\sigma-1} \right. \right. \\
 \left. \left. + \sigma(\sigma-1) + \theta_0 \right\} \right] \quad \dots 3.37
 \end{aligned}$$

Thus as in previous cases, the phase angle $\tan^{-1} L_i/L_r$ may easily be calculated for given values of parameters. Dividing equations 3.37 and 3.36, we easily see that L_i/L_r becomes -45° when ω is very large. Thus for very large frequency of oscillations, the skin friction lags behind the wall fluctuations by 45° . If $A = 0$, i. e. steady suction we also have the same conclusions.

We see that L_r and L_i are important factors and thus its variations with ω has been shown graphically in figure 5 when $\sigma=0.64$ $\theta_0 = \theta_1 = 1$ and $A = 0, \frac{1}{2}, 1$.

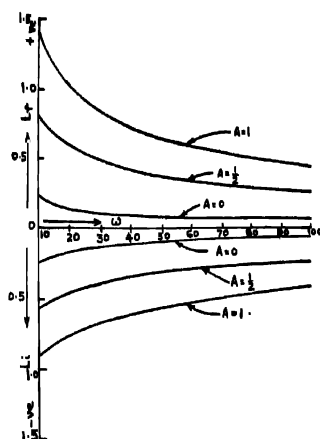


Figure 5. Curves showing L_r and L_i against ω for $A = 0, \frac{1}{2}, 1$.

From the graph, we find that L_i is always negative and thus the skin-friction lags behind the wall fluctuations. The value of the ratio of L_i and L_r may easily be calculated from the figure for given A at various values of ω . As an example for $\omega = 10$, we have from figure 5, that $|L_i/L_r| \leq 1$ if $A \geq 0$. Thus the phase angle becomes less than 45° .

REFERENCES

- Lighthill, M. J. 1954 *Proc. Roy. Soc., A* **224** 1-33
- Messiha, S. A. S. 1966 *Camb. Phil. Soc.*, **62** 329-337
- Lal, K. 1969, *J. Appl. Mech.*, A. S. M. E., U. S. A. (in course of publication)

On mechanical response in a piezoelectric transducer
carrying a time-decaying space-charge

By HARI SANKAR CHAKRABORTY

Kanyapur Polytechnic, Asansol.

(Received 12, February 1968 ; Resubmitted 8, December 1968)

The transform calculus is used to determine the mechanical response in a piezoelectric transducer carrying a time-decaying space-charge. The response is found to be partly linear, partly constant and partly transient in character to a first order of approximation.

1. INTRODUCTION

The studies on piezoelectric transducers are very important in view of their applications in manifold branches of physics, engineering and technology, particularly in ultrasonics, for they provide the methods for detecting ultrasonic waves, vide, Redwood (1961a). The piezoelectric materials used for ultrasonic purposes can emit mechanical responses due to electrical excitations and vice-versa. Mason (1948) has carried out this analysis by pursuing the principles of circuit theory. The methods of continuous media were introduced by Redwood (1961a), (1968b) and some papers have been contributed by Sinha (1965), (1967a), (1963), (1967b), Giri (1966), Roy (1967), Das (1967). The author here attempts to determine the mechanical response in a piezoelectric transducer carrying a time-decaying space-charge. The response is found to be partly transient, partly constant and partly linear in character to a first order of approximation.

2. FUNDAMENTAL EQUATIONS AND BOUNDARY CONDITIONS

We consider a piezoelectric transducer in the form of a bar executing vibration in the thickness direction which we take to be the x-axis. To obtain the mechanical response we are to couple the equations connecting the two fields mechanical and electrical.

The piezoelectric equations of state in one-dimensional strain is

$$T = cS - hD \qquad \dots(1)$$

$$E = -hS + \frac{D}{\epsilon} \quad \dots(2)$$

where T is the stress, S the strain, E the electric field strength, D the electric displacement, ϵ the elastic stiffness for constant E , h the piezo-electric constant measured with D constant and ϵ the permittivity for constant S .

$$\text{From Newton's second law, } \rho \frac{\delta^2 \xi}{\delta t^2} = \frac{\delta T}{\delta x} = c \frac{\delta^2 \xi}{\delta x^2} - h \frac{\delta D}{\delta x} \quad \dots(3)$$

by (1), where ρ is the density of the material, ξ the mechanical displacement.

We assume the variation of space-charge ρ_1 with time in the form given by $\rho_1 = \rho_0 e^{-\alpha t}$, $\alpha (> 0)$, ρ_0 are constants.

$$\text{so that we can write } \frac{\delta D}{\delta x} = \rho_0 e^{-\alpha t}. \quad \dots(4)$$

$$\text{Then (3) becomes } \rho \frac{\delta^2 \xi}{\delta t^2} = c \frac{\delta^2 \xi}{\delta x^2} - h \rho_0 e^{-\alpha t}.$$

The Laplace's transform of this equation gives

$$\frac{\delta^2 \bar{\xi}}{\delta x^2} - \frac{\rho p^2 \bar{\xi}}{c} = \frac{h \rho_0}{c(p + \alpha)}$$

The solution of this equation gives

$$\bar{\xi} = A e^{-\frac{p x}{v}} + B e^{\frac{p x}{v}} - \frac{h \rho_0}{\rho p^2 (p + \alpha)} \quad \dots(5)$$

where $v^2 = \frac{c}{\rho}$, A and B are amplitude factors to be determined from the boundary conditions.

Also from the equation (4), $D = x \rho_0 e^{-\alpha t}$, D being assumed to be zero at $x = 0$.

$$\text{Taking Laplace's transform, we have } \bar{D} = \frac{x \rho_0}{p + \alpha}. \quad \dots(6)$$

From (1) we get

$$T_{yz} = cYZ \left(\frac{\delta \xi}{\delta x} \right) - h \bar{D}YZ$$

$$\therefore \bar{F} = cYZ \frac{\delta \xi}{\delta x} - \frac{h x \rho_0 YZ}{p + \alpha} \quad \dots(7)$$

where F is the force exerted over an area L normal to x — axis.

The boundary equations are given by the conditions of continuity of force and displacement at its two extremities where two mechanical systems may be attached. Let the entities of the corresponding systems at the two extremities $x = 0$ and $x = X$ be denoted by the suffixes 1 and 2 respectively. Thus we have

$$(\xi)_0 = (\xi_1)_0 \quad \dots (8)$$

$$(\bar{F})_0 = (\bar{F}_1)_0 \quad \dots(9)$$

$$(\bar{F})_X = 0 \quad \dots (10)$$

3. SOLUTION OF THE PROBLEM

To achieve the solution of the problem, in a general way we associate with the transducer with two mechanical systems. We assume the disturbance to proceed from the system 1, and assume the transducer to be rigidly backed at $x=X$.

These give from (5) and (8),

$$A + B = B_1 \quad \dots(11)$$

From (7) and (9),

$$v (-A + B) = v_1 B_1 \quad \dots (12)$$

From (10),

$$-\frac{hX\rho_0YZ}{p+\alpha} + \rho v YZ p \left(-A \frac{bX}{v} + B \frac{bX}{e^v} \right) = 0 \quad \dots(13)$$

Eliminating B_1 from (11), (12) and (13) we get

$$\begin{aligned}
 A &= \frac{\hbar X \rho_o (v - v_1)}{\rho p v (p + \alpha) \left\{ (v + v_1) e^v - (v - v_1) e^v \right\}} \\
 B &= \frac{\hbar X \rho_o (v + v_1)}{\rho p v (p + \alpha) \left\{ (v + v_1) e^v - (v - v_1) e^v \right\}} \\
 (\xi)_o &= \frac{\hbar X \rho_o}{\rho p v (p + \alpha)} \left\{ \frac{2v}{(v + v_1) e^v - (v - v_1) e^v} \right\} - \frac{\hbar \rho_o}{\rho p^2 (p + \alpha)} \\
 &= -\frac{2\hbar X \rho_o}{\rho p (p + \alpha)} \frac{e^v}{v + v_1} \left\{ 1 - \frac{v - v_1}{v + v_1} e^v \right\}^{-1} - \frac{\hbar \rho_o}{\rho p^2 (p + \alpha)}
 \end{aligned}$$

The inversion of it being too complicated, we proceed as in Redwood (1961), to obtain it for small values of time, and expanding as in Redwood (1961), we get

$$(\xi)_o = \frac{2\hbar X \rho_o}{\rho p (v + v_1) (p + \alpha)} e^{\frac{pX}{v}} - \frac{\hbar \rho_o}{\rho p^2 (p + \alpha)} = \frac{\theta_1 e^{\frac{pX}{v}}}{p(p + \alpha)} + \frac{\theta_2}{p^2} + \frac{\theta_3}{p} + \frac{\theta_4}{p + \alpha}$$

where $\theta_1, \theta_2, \theta_3, \theta_4$ are constants containing material parameters of the problem.

Taking inverse transform, $\xi = \theta_3 + \theta_4 t + (\theta_1 e^{-\alpha t})$

$$+ \frac{\theta_2}{\alpha} \left\{ 1 - e^{-\alpha t} \right\} u \left(t - \frac{x}{v} \right) \text{ where } t > \frac{x}{v}$$

$$\text{where } u \left(t - \frac{x}{v} \right) = 0 \text{ for } t < \frac{x}{v}$$

$$= 1 \text{ for } t > \frac{x}{v}$$

This shows that the mechanical response in a piezoelectric transducer carrying time-decaying space-charge is partly linear, partly constant and partly transient in character.

The author is deeply indebted to Dr. D. K. Sinha, Reader in Mathematics, Jadavpur University, for his constant guidance in the preparation of this paper.

REFERENCES

- Das N. C., 1967 *Ind. Jour. Phys.*, **11**, 611.
Giri R. R., 1966 *Roum. Techn. Sci.*, **11**, 253.
Mason, W.P., 1948 *Electromechanical Transducers & Wave Filters*, D. Van Nostrand Co., New Jersey, 2nd edition.
Redwood M., 1961, *Jour. Acoust. Soc. Amer.*, **33**, 527.
Redwood M., 1961b *Jour. Acoust. Soc. Amer.* **33**, 1386.
Roy P., 1967 *Ind. Jour. Pure Appl. Phys.* **5**, 152.
Sinha D. K., 1965 *Proc. Natl. Inst. Sci.* **31**, 4.
Sinha D. K. 1967a *Proc. Ind. Acad. Sci.* LXV 136.
Sinha D. K., 1963 *Ind. Jour. Theor. Phys.*, **11**, 93.
Sinha D. K., 1967b *Ind. Jour. Pure. Appl. Phys.* **5**, 375.

Hydromagnetic waves in an ideally conducting medium with
a two-dimensional inhomogeneous magnetic field.

By G. S. BAJWA AND K. M. SRIVASTAVA

Department of Mathematics, University of Jodhpur, India

(Received 26 December 1968)

Possibility of the propagation of hydromagnetic waves is explored in an ideally conducting incompressible fluid mass immersed in a two-dimensional inhomogeneous magnetic field. The magnetic field lies in a plane perpendicular to the surface of the fluid and varies along the normal to the above plane. Because of the absence of the boundary conditions, it is not possible to get a dispersion relation. If the components of the magnetic field are linearly related and its pressure decays exponentially, it is found that the hydromagnetic waves propagate for all values of the wave number and frequency.

1. INTRODUCTION

Gajewski & Winterberg (1963), have discussed the propagation of the small amplitude hydromagnetic waves in an ideally conducting uniform medium embedded in an inhomogeneous magnetic field of constant direction. Uberoi (1964), has reconsidered the problem by taking into account the perturbation in pressure and established that the medium is non-dispersive. We have considered the case of a two-dimensional inhomogeneous magnetic field lying in a plane perpendicular to the surface of the fluid and varying in a direction normal to its own plane. It is again found that the medium is non-dispersive and waves can propagate for all wave numbers and frequencies in a direction orthogonal to the direction of inhomogeneity of the magnetic field.

LINEARISED EQUATIONS

Consider, in the state of equilibrium, an ideally conducting incompressible fluid mass of uniform density ρ and pressure p immersed in a time-independent magnetic field \vec{H} . We choose a Cartesian coordinate system and its coordinate axes are oriented in such a way that its xy -plane coincides with the surface of the fluid mass and yz -plane contains the inhomogeneous magnetic field \vec{H} . The magnetic field varies as a function of x alone and is independent of y , z and t .

Taking perturbations in velocity, magnetic field, pressure and gravitational potential as \vec{v} , \vec{h} , δp and δU respectively, the linearised equations are

$$(a) \text{ Equation of continuity : } \operatorname{div} \vec{v} = 0, \quad (1)$$

$$(b) \text{ Equation of motion : } \rho \frac{\delta \vec{v}}{\delta t} = -\nabla \delta p - \rho \nabla \delta U \\ + \frac{\mu}{4\pi} \{ (\operatorname{curl} \vec{H}) \times \vec{h} + (\operatorname{curl} \vec{h}) \times \vec{H} \}, \quad (2)$$

and

$$\text{Maxwell's equations : } \frac{\delta \vec{h}}{\delta t} = \operatorname{curl} (\vec{v} \times \vec{H}), \quad (3)$$

$$\operatorname{div} \vec{h} = 0. \quad (4)$$

COMPONENT EQUATIONS

Choosing the dependence of the perturbed quantities on y , z and t as

$$f(x) \exp i(\omega t + k_1 y + k_2 z), \quad (5)$$

equation (1) becomes (omitting the exponential factor)

$$Dv_x = -i(k_1 v_y + k_2 v_z). \quad (6)$$

In view of relation (5) and using equation (6), the components of equation (2) and equation (3) can be written as

$$\rho \omega v_x = iD(\delta p + \rho \delta U) - \frac{\mu}{4\pi} \{ Lh_x + i(H_y h_y + H_z h_z) \}, \quad (7)$$

$$\rho \omega v_y = k_1(\delta p + \rho \delta U) - \frac{\mu}{4\pi} \{ i(DH_y)h_x - k_2 H_z h_y - (M - k_1 H_z)h_z \}, \quad (8)$$

$$\rho \omega v_z = -k_2(\delta p + \rho \delta U) - \frac{\mu}{4\pi} \{ i(DH_z)h_x + (M + k_2 H_y)h_y - k_1 H_y h_z \}, \quad (9)$$

$$\vec{h} = [Lv_x, i(DH_y)v_x + Lv_y, i(DH_z)v_x + Lv_z]; \quad (10)$$

where

$$L = k_1 H_y + k_2 H_z, \quad M = k_2 H_y - k_1 H_z. \quad (11)$$

Eliminating \vec{h} from equations (7)–(9) with the help of equation (10), we get

$$2(\omega^2 - \alpha) \{ (\omega^2 - \alpha)^2 + \alpha\beta \} D^2 v_x - \{ (2\alpha' - \beta') (\omega^2 - \alpha)^3 - (\alpha'\beta + 2\alpha\beta') (\omega^2 - \alpha) - 2\omega^2 \alpha'\beta \} Dv_x - \{ 2(k_1^2 + k_2^2) (\omega^2 - \alpha)^3 - \beta' (\omega^2 - \alpha)^2 - (\alpha'\beta) (\omega^2 - \alpha) - (\alpha')^2 \beta \} v_x = 0, \quad (12)$$

$$v_x = \frac{2i \{ k_1 (\omega^2 - \alpha) + k_2 (\alpha\beta)^{1/2} \} Dv_x + ik_2 \alpha' (\beta/\alpha)^{1/2} v_x}{2(k_1^2 + k_2^2) (\omega^2 - \alpha)}, \quad (13)$$

$$v_z = \frac{2i \{ k_2 (\omega^2 - \alpha) - k_1 (\alpha\beta)^{1/2} \} Dv_x - ik_1 \alpha' (\beta/\alpha)^{1/2} v_x}{2(k_1^2 + k_2^2) (\omega^2 - \alpha)}, \quad (14)$$

where

$$\alpha = (\mu/4\pi\rho) L^2, \quad \beta = (\mu/4\pi\rho) M^2, \quad (15)$$

and the quantities L and M are given by equation (11). The prime and D stand for differentiation with respect to x .

DISCUSSION

Since there are no boundary conditions to be satisfied it is not possible to get a dispersion relation. But the amplitude of the waves if propagate may be determined from equations (12) to (14).

If the components of the magnetic field are linearly related by

$$H_y = (k_1/k_2) H_z, \quad (16)$$

then in view of assumption (16), equation (15) becomes

$$\alpha = (Q/k_2^2) (k_1^2 + k_2^2)^2, \quad \beta = 0, \quad (17)$$

where

$$Q = (\mu/4\pi\rho) H_z^2. \quad (18)$$

With the help of equation (17), equations (12) – (14) are reduced to

$$D^2 v_x - \frac{(k_1^2 + k_2^2)^2 Q'}{k_2^2 \omega^2 - (k_1^2 + k_2^2)^2 Q} Dv_x - (k_1^2 + k_2^2) v_x = 0, \quad (19)$$

$$v_x = [ik_1/(k_1^2 + k_2^2)] Dv_x, \quad (20)$$

$$v_z = [ik_2/(k_1^2 + k_2^2)] Dv_x. \quad (21)$$

From equation (18) it follows that Q is proportional to the magnetic pressure ($\mu H^2/8\pi$). Assuming the dependence of the magnetic pressure on x , of the form

$$Q = [k_1^2 \omega^2 / (k_1^2 + k_2^2)^2] + K e^{-A|x|}, \quad (22)$$

where K and A are arbitrary constants, equation (19) takes the form

$$D^2 v_x - A D v_x - (k_1^2 + k_2^2) v_x = 0,$$

and it admits a solution of the form

$$v_x = B \exp [A - \{A^2 + 4(k_1^2 + k_2^2)\}^{1/2}] |x| / 2, \quad (23)$$

where B is an arbitrary constant and other constant becomes zero as $v_x \rightarrow 0$ for large values of x .

Equation (23), (20) and (21) establish that the hydromagnetic waves can propagate in a direction orthogonal to the direction of the inhomogeneity of the magnetic field for all values of ω , k_1 and k_2 under the assumptions (16) and (22).

REFERENCES

- Gajewski, R., & Winterberg, F., 1963 *Ap. J.* 137, 1203.
 Uberoi, C., 1964 *J. App. Phys.* 2, 4, 133, 134.

Impedance bridge network problem as solved by relaxation method

By S. N. DUTTA

Department of Applied Physics, Calcutta University,

(Received 27 December 1968)

Here it is shown how the relaxation method can be advantageously used to solve the problems of A. C. networks containing complex circuit constants. This has been done in the solution of impedance bridge network problem, in which many useful information are obtained at a time. The results so obtained are compared with those calculated by the conventional method.

1. INTRODUCTION

Impedance bridges are commonly used to measure the circuit constants such as A. C. resistance, inductance etc. In this paper a network problem of unbalanced impedance bridge (figure 1) has been considered and the currents flowing in all the branches including the detector have been found out. This bridge circuit in a slightly unbalanced condition has great importance in having delicate sensing device. The methods

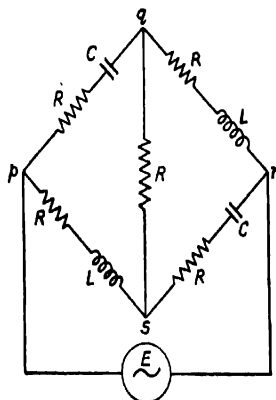


Figure 1. Impedance bridge.

which are generally used for analysis of this bridge configuration consisting of three meshes are a bit complicated due to the presence of complex circuit constants. It is described here how it can be solved easily and quickly by relaxation method when the equivalent circuit diagram (figure 2a) of the said network (figure 1) is considered.

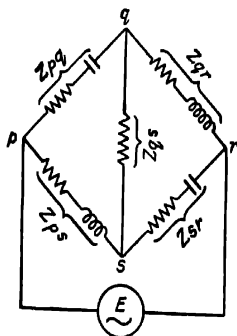


Figure 2a. Equivalent impedance network diagram of figure 1.

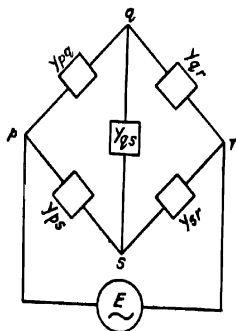


Figure 2b. Equivalent admittance network diagram of figure 1.

First of all Southwell & Black (1938) and later on Dutta (1966), and Basu & Dutta (1967) showed that the relaxation method can be suitably applied to solve the A. C. network problem without having much difficulty due to the presence of complex circuit constants. The method itself speaks of its advantage in getting many useful information simultaneously.

THE METHOD

Let Y_{pq}, Y_{qs}, \dots etc., be the reciprocals of the impedances Z_{pq}, Z_{qs}, \dots etc., of the branches 'pq', 'qs' etc., of the network shown in figure 2b.

Then the admittances of any branch for example 'qs' can be written as,

$$Y_{qs} = g_{qs} + jb_{qs} \quad \dots (1)$$

Let the potentials at the nodal points 'q' and 's' be

$$\left. \begin{aligned} V_q &= v_{x(q)} + jv_{y(q)} \\ V_s &= v_{x(s)} + jv_{y(s)} \end{aligned} \right\} \quad \dots (2)$$

So a current which flows from 'q' to 's' in branch 'qs' is given by,

$$\begin{aligned} I_{qs} &= Y_{qs} (V_q - V_s) \\ &= g_{qs} \{v_{x(q)} - v_{x(s)}\} - b_{qs} \{v_{y(q)} - v_{y(s)}\} \\ &\quad + j [g_{qs} \{v_{y(q)} - v_{y(s)}\} + b_{qs} \{v_{x(q)} - v_{x(s)}\}] \end{aligned}$$

If the total current flowing into 'q' from all the branches linked with it be,

$$-\Sigma I_{qs} = I_{q1} = (i_{x(q)1} + j i_{y(q)1})$$

then,

$$-i_{x(q)1} = \Sigma_q [g_{qs} \{v_{x(q)} - v_{x(s)}\} - b_{qs} \{v_{y(q)} - v_{y(s)}\}] \quad \dots(3)$$

and

$$-i_{y(q)1} = \Sigma_q [g_{qs} \{v_{y(q)} - v_{y(s)}\} + b_{qs} \{v_{x(q)} - v_{x(s)}\}]$$

Also, if the current supplied to 'q' from outside be,

$$I_{q2} = i_{x(q)2} + j i_{y(q)2}$$

then by Kirchhoff's law,

$$\begin{aligned} i_{x(q)} &= i_{x(q)1} + i_{x(q)2} = 0 \\ \text{and } i_{y(q)} &= i_{y(q)1} + i_{y(q)2} = 0 \end{aligned} \quad \dots(4)$$

Let the vector potential of the point 'p' be unity and those of the points 'q' and 's' be zero. Then the currents flowing in the branches 'pq' and 'ps' are given by,

$$\begin{aligned} I_{pq} &= Y_{qp} = g_{qp} + j b_{qp} \\ \text{and } I_{ps} &= Y_{sp} = g_{sp} + j b_{sp} \end{aligned} \quad \dots(5)$$

and no current will flow in any other branch of the circuit. But in order to have the assumed potential correct, a current,

$$-I_{p2} = I_{pq} + I_{ps} = i_{x(p)2} + j i_{y(p)2},$$

is to be supplied to the point 'p' from outside. Under that condition the currents I_{pq} and I_{ps} leave the network at the points 'q' and 's' respectively. But actually no current enters into or leaves the network at the points 'q' and 's'. So on the assumed potentials those are to be superposed which would result if the currents $I_{qs} = I_{pq}$, and $I_{rs} = I_{ps}$ were supplied at points 'q' and 's' and allowed to leave the network at the points 'p' and 'r', the latter points being maintained at zero potential.

Thereafter it is obtained initially as follows :

$$\begin{aligned} i_{x(q)} &= i_{x(q)2} = g_{pq} ; & i_{x(r)} &= i_{x(r)2} = g_{rp} ; \\ i_{y(q)} &= i_{y(q)2} = b_{qp} ; & i_{y(r)} &= i_{y(r)2} = b_{rp} ; \\ i_{x(p)} &= i_{x(p)2} = -(g_{qp} + g_{rp}) ; \\ i_{y(p)} &= i_{y(p)2} = -(b_{qp} + b_{rp}) ; \end{aligned}$$

and

$$i_{x(r)} = i_{y(r)} = 0.$$

The standard operation table required for liquidation of the residuals that is, the initial values $i_{x(q)}$, $i_{y(q)}$, $i_{x(r)}$ and $i_{y(r)}$, by giving suitable vector potentials at the points 'q' and 'r' only can be obtained using the following expression developed from the relations (3) :

$$\left. \begin{aligned} \frac{\delta i_{x(r)}}{\delta v_{x(q)}} &= g_{qr} = \frac{\delta i_{y(r)}}{\delta v_{y(q)}} ; \\ - \frac{\delta i_{x(r)}}{\delta v_{y(q)}} &= b_{qr} = \frac{\delta i_{y(r)}}{\delta v_{x(q)}} ; \\ \frac{\delta i_{x(q)}}{\delta v_{x(q)}} &= \frac{\delta i_{y(q)}}{\delta v_{y(q)}} = - \sum_q (g_{qs}) ; \\ - \frac{\delta i_{x(q)}}{\delta v_{y(q)}} &= \frac{\delta i_{y(q)}}{\delta v_{x(q)}} = - \sum_q (b_{qs}) ; \end{aligned} \right\} \quad \dots (6)$$

The vector currents at the points 'p' and 'r' and the vector potentials at the points 'q' and 's' corresponding to unit potential difference between the points 'p' and 'r' are obtained after liquidation of the residuals. The following illustration will show the advantage of the method.

ILLUSTRATION

This example (figure 1) worked out by Kerchner & Corcoran (1960) is taken, up for illustration in which,

$$\begin{aligned} V_{pr} &= 100 \angle 0^\circ \text{ volts, } R_{pq} = 1 \text{ ohm, } X_{pq} = 12 \text{ ohms, } R_{pq} = 4 \text{ ohms,} \\ X_{pq} &= 6 \text{ ohms, } R_{rr} = 0.6 \text{ ohms, } X_{rr} = 6.7 \text{ ohms, } R_{qr} = 6.12 \text{ ohms, } X_{qr} \\ &= 10.16 \text{ ohms} \end{aligned}$$

The currents delivered by the source and those flowing in the four arms and the detector of the bridge network are to be found out.

Considering the different branches of the network shown in figure 2b, the corresponding admittances for the problem are calculated to be,

$$Y_{pg} = (7.6923 + j 11.5385) \times 10^{-2} \text{ mho,}$$

$$Y_{gr} = (4.3503 - j 7.2221) \times 10^{-2} \text{ ,, ,}$$

$$Y_{pr} = (0.6897 - j 8.2758) \times 10^{-2} \text{ ,, ,}$$

$$Y_{rr} = (1.3260 + j 14.8066) \times 10^{-2} \text{ ,, ,}$$

$$Y_{qr} = (33.3333 + 0) \times 10^{-2} \text{ ,, ,}$$

The above admittances are multiplied by 10^2 to have a simplified calculation and higher accuracy of results. This multiplying factor 10^2 and the potential difference V_{pr} have to be taken into account in calculating the currents.

Thus the currents which flow in the branches ' pq ' and ' pr ' are written as,

$$I_{pq} = 7.6923 + j 11.5385 \text{ amps,}$$

$$I_{pr} = 0.6897 - j 8.2758 \text{ ,,}$$

So the current to be flown from outside at the point ' p ' is found out to be,

$$-I_{p2} = 8.3820 + j 3.2627 \text{ amps.}$$

Thereafter the following initial values are obtained :

$$i_{x(q)} = 7.6923 ; i_{x(r)} = 0.6897 ; i_{x(p)} = -8.3820 ;$$

$$i_{y(q)} = 11.5385 ; i_{y(r)} = -8.2758 ; i_{y(p)} = -3.2627 ;$$

$$\text{and } i_{x(r)} = i_{y(r)} = 0.$$

In liquidating the residuals the unit operation table (table 1) is obtained using the relations (6) in which the ' g ' and ' b ' values are multiplied by 10^2 for the above mentioned reason. Afterwards the group operations (Allen, 1954 ; Dutta, 1966), are performed as shown in table 2. Finally the residuals are liquidated in four steps only shown in the relaxation table (table 3) obtained by using tables 1 and 2.

The following values of the currents as wanted in the problem are found out by relaxation method and those obtained by the conventional one are shown side by side within the square brackets and they are seen to be in good agreement.

TABLE 1. UNIT OPERATION TABLE

Operation Steps	$\delta v_{x(q)}$	$\delta v_{x(s)}$	$\delta v_{y(q)}$	$\delta v_{y(s)}$	$\delta i_{x(p)}$	$\delta i_{x(q)}$	$\delta i_{x(s)}$	$\delta i_{x(r)}$	$\delta i_{y(p)}$	$\delta i_{y(q)}$	$\delta i_{y(s)}$	$\delta i_{y(r)}$
1	1	—	—	—	7.6923	-45.3759	33.3333	4.3503	11.5385	-4.3164	0	-7.2221
2	—	1	—	—	0.6897	33.3333	-35.3490	1.3260	-8.2758	0	-6.5308	14.8066
3	—	—	1	—	111.5385	4.3164	0	7.2221	7.6923	-45.3759	33.3333	4.3503
4	—	—	—	1	-8.2758	0	6.5308	-14.8066	0.6897	33.3333	-35.3490	1.3260

TABLE 2. GROUP OPERATION TABLE

Operation Steps	$\delta v_{x(q)}$	$\delta v_{x(s)}$	$\delta v_{y(q)}$	$\delta v_{y(s)}$	$\delta i_{x(p)}$	$\delta i_{x(q)}$	$\delta i_{x(s)}$	$\delta i_{x(r)}$	$\delta i_{y(p)}$	$\delta i_{y(q)}$	$\delta i_{y(s)}$	$\delta i_{y(r)}$
1	1	0	10.5124	-5.1040	-155.8447	0	0	155.8447	88.8828	-651.4592	530.8343	31.7421
2	0	1	-7.7225	5.4127	134.5902	0	0	-134.5903	-63.9464	530.8385	-448.7499	-11.6113
3	1	1.2272	1.0353	1.5385	10.3353	0	0	-9.3253	10.4074	0	-27.8891	17.4925

TABLE 3. RELAXATION TABLE

Liquidation Steps	$\delta v_{x(q)}$	$\delta v_{x(s)}$	$\delta v_{y(q)}$	$\delta v_{y(s)}$	$\delta i_{x(p)}$	$\delta i_{x(q)}$	$\delta i_{x(s)}$	$\delta i_{x(r)}$	$\delta i_{y(p)}$	$\delta i_{y(q)}$	$\delta i_{y(s)}$	$\delta i_{y(r)}$
	Initial Values											
1	0	0	-1.7821	0	-8.3820	7.6923	0.6897	0	-3.2627	11.5385	-8.2758	0
2	0	0	0	-0.1056	11.3069	0	0	-11.3069	-17.0439	88.8829	-63.9462	-7.8927
3	0.1364	0	1.4339	-0.6962	-9.9506	0	0	9.9506	-4.9202	0	8.4604	-3.5631
4	0.3034	0.3723	0.3141	0.4668	-7.1211	0	0	7.1209	-1.7624	0	0	1.7436
	0.4398	0.3723	-0.0341	-0.3350	-7.1211	0	0	7.1209	-1.7624	0	0	1.7436

The current delivered by the source is,

$$I_s = I_r = 7.121 + j1.753 [7.140 + j1.760] \text{ amps.}$$

the currents in the four arms are,

$$I_{p1} = 3.205 - j4.963 [3.190 - j4.960] \text{ amps,}$$

$$I_{p2} = 3.916 + j6.726 [3.930 + j6.726] \text{ ,, ,}$$

$$I_{r1} = 5.454 + j5.068 [5.444 + j5.090] \text{ ,, ,}$$

$$I_{q1} = 1.670 - j3.320 [1.680 - j3.320] \text{ ,, ,}$$

and the detector current is,

$$I_{q2} = -2.250 - j10.030 [-2.254 - j10.050] \text{ amps.}$$

DISCUSSION

The solution of impedance bridge network, particularly, when it is unbalanced becomes laborious by the conventional method, whereas, the discussed one is seen to yield easily the values of the detector voltages (vector) viz., V_q and V_r , and the current I_r at a time. Thereafter, other required quantities can be calculated quickly. Also the number of residuals to be liquidated being four the labour involved in it is further reduced. Herein lies the advantage of the method over those followed normally.

The author is highly indebted to Prof. A. K. Sengupta, D. Sc., M. I. E. E. (London), Head of the Department of Applied Physics, Calcutta University, for his help and guidance throughout the progress of this work.

REFERENCES

- Allen, D. N. deG., 1954 *Relaxation Methods* McGraw-Hill Book Co., Inc., New York 17.
 Basu, R. N. & Dutta, S. N. 1967 *Indian J. Phys* 41, 382.
 Black, A. N., & Southwell, R. V. 1938 *Proc. Roy. Soc. (A)*, 164, 447.
 Dutta, S. N., 1966 *Indian J. Phys*, 40, 581.
 Kerchner, R. M., & Corcoran, G. F. 1960 *Alternating Current Circuits*,
 John Wiley & Sons, Inc., New York 207.
 Southwell, R. V., 1951 *Relaxation Methods in Engineering Science*,
 Oxford University Press, London 114.

Indian J. Phys. **43**, 83-91 (1969)

$^2\Sigma^+ - ^2\Pi$ band system in CP molecule

By A. K. CHAUDHRY AND K. N. UPADHYA

Department of Spectroscopy,

Banaras Hindu University, Varanasi-5.

(Received January 9, 1969)

[PLATE 1]

Rotational structure of 0,0 band of *B-A* system of CP molecule has been examined. Molecular constants for both the states have been determined. The electronic transition is found to be $^2\Sigma^+ - ^2\Pi$ type which is in confirmation of the previous prediction.

1. INTRODUCTION

The band spectra of CP molecule was first studied by Barwald *et al* (1934) by exciting it in a discharge tube containing organic vapour and white phosphorus in a flow of argon gas. These authors obtained two band systems having common upper electronic state. One of these the *B-X* system lies in the near ultraviolet region and consists of red degraded bands. Barwald *et al* (1934) also analysed the rotational structure of (3, 0), (2, 0), (0, 1) and (0, 3), bands of this system and found the transition to be of $^2\Sigma^+ - ^2\Sigma^+$ type.

The other system *B-A* lies in the visible region (4390-4660 Å). The earlier workers (1934) predicted rotational constants of this system on the basis of head-origin separation. They pointed out the transition of this system to be of $^2\Sigma^+ - ^2\Pi_i$ type. No further work seems to be available on this molecule.

In order to gain more informations regarding the electronic states of *B-A* system, we photographed some bands of this system in the second order of a 10.6 metre grating spectrograph (0.33 Å/mm dispersion). In spite of all attempts, only the (0, 0) band with its two sub-bands could be photographed with sufficient intensity. Rotational analysis of two sub (0, 0) bands has been done and the respective rotational constants are reported.

EXPERIMENTAL

A Π -type discharge tube has been used for this purpose having one replaceable container filled with white phosphorus in its middle. By

operating discharge tube with a 1 KV transformer a typical greenish white colour was obtained in the presence of continuous controlled flow of argon gas. Ten hours exposure was found sufficient to record the bands on blue rapid plates. A low current iron arc was used as source for standard spectrum superimposed on the main spectrum. The plates were measured against these iron lines and the estimated accuracy for such measurement is $\pm 0.03 \text{ cm}^{-1}$.

ROTATIONAL ANALYSIS

The rotational analysis was started assuming the transition of the type ${}^2\Sigma^+ - {}^2\Pi$. Figure 1 shows the energy level diagram for such transi-

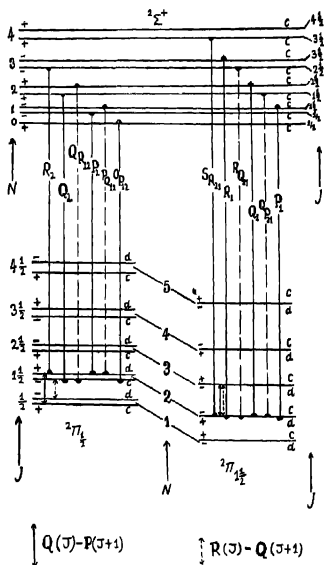


Figure 1. Energy level diagram for ${}^2\Sigma^+ - {}^2\Pi$ transition showing all the twelve branches for the bands of B-A system of CP molecule.

tion, and twelve branches are predicted by theory for this transition. These branches are designated $P_1, Q_1, R_1, {}^oP_{11}, {}^oQ_{11}, {}^sR_{11}$ for ${}^2\Sigma^+ - {}^2\Pi_{1/2}$ sub-band and $P_2, Q_2, R_2, {}^oP_{12}, {}^oQ_{12}, {}^sR_{12}$ for ${}^2\Sigma^+ - {}^2\Pi_{3/2}$ sub-band. The

head forming branches are $^sR_{11}$ and R_1 for the first and R_2 and Q_2 for the second transition, respectively. In the present analysis all the 12 branches have been identified for (0,0) band and are marked in figure 2. The respective wavenumbers of lines of each branch are given in table 1(a) and 1(b). Rotational constants for the two molecular states have

TABLE 1(a)
VACUUM WAVENUMBER AND ASSIGNMENTS OF THE ROTATIONAL
LINES OF THE $^3\Sigma-^3\Pi_{1/2}$ SUB-BAND

J	$R_1(J)$	$Q_2(J)$	$P_1(J)$	$^O P_{11}(J)$	$^O R_{11}$	$^P Q_{11}$
0.5	21936.42	21933.69				
1.5	38.26	34.10	21931.42			
2.5	40.06	34.62	30.54			
3.5	41.87	35.11	29.63			
4.5	43.53	35.46	28.57			
5.5	45.20	35.63	27.49			
6.5	46.75	36.00	26.35			
7.5	48.28	—	25.16	21915.62		
8.5	49.71	—	23.87	12.99		
9.5	51.13	—	22.57	10.34		
10.5	52.60	—	21.28	07.69		
11.5	53.90	36.30	19.90	04.86		
12.5	55.12	36.10	18.40	02.07		
13.5	56.26	35.92	16.82	21899.15		
14.5	57.30	35.63	15.14	96.15		
15.5	58.32	35.30	13.44	93.15	21935.46	
16.5	59.30	34.83	11.69	90.15	—	
17.5	60.38	34.48	09.89	86.95	34.62	
18.5	61.15	33.96	07.94		34.10	21908.10
19.5	61.90	33.49	05.99		—	06.14
20.5	62.60	32.76	04.02		32.92	04.17
21.5	63.25	32.05	01.95		32.23	02.07
22.5	63.77	31.18	21899.78		31.42	21899.95
23.5	64.29	30.31	97.56		30.54	97.75
24.5	64.74	29.44	95.23		29.63	95.48
25.5		21928.40	21892.92		21928.57	21893.15
26.5		27.49	90.45		27.69	90.65
27.5		26.35	87.91		—	88.11
28.5		25.16	85.37		25.30	85.60
29.5		23.87	82.72		24.05	82.99
30.5		22.57	79.94		—	80.22
31.5		20.99	77.12		21.18	77.35
32.5		19.68	74.28		19.90	74.52
33.5		17.98	71.33		18.20	71.60

TABLE 1(b)
VACUUM WAVENUMBERS AND ASSIGNMENTS ROTATIONAL
LINES OF THE ${}^2\Sigma-{}^2\Pi_{3/2}$ SUB-BAND

J	$R_1(J)$	$Q_1(J)$	$P_1(J)$	${}^R Q_{21}(J)$	${}^Q P_{21}(J)$	${}^S R_{21}(J)$
1.5	22092.10	22099.00				
2.5	92.54	88.28				
3.5	93.05	87.40				22101.58
4.5	93.45	86.47				03.32
5.5	93.80	85.42				04.94
6.5	94.07	84.40				06.43
7.5	94.25	83.40	22073.76			08.06
8.5	94.53	82.18	71.35			09.63
9.5	94.70	81.07	68.72			11.12
10.5	—	79.70	66.08			12.57
11.5	—	78.54	63.47			13.91
12.5	—	77.21	60.81			15.28
13.5	94.85	75.70	58.00			16.53
14.5	94.70	74.27	52.36			17.71
15.5	94.53	72.82	52.36			18.91
16.5	94.25	71.23	49.48			20.10
17.5	94.07	69.63	46.56			21.20
18.5	93.62	67.98	43.50	22093.45		22.18
19.5	93.24	66.08	40.42	93.05		23.11
20.5	92.77	64.40	37.20	92.54		24.03
21.5	92.30	62.35	33.96	92.10		24.81
22.5	91.82	60.68	30.72	91.60		25.60
23.5	91.17	58.48	27.35	90.98		26.33
24.5	90.42	56.52	23.83	90.17		26.94
25.5	89.67	54.40		89.47		22127.51
26.5	22088.88	22052.36		22088.70	—	28.90
27.5	88.01	50.30		87.75	—	28.56
28.5	87.10	48.10		86.90	—	28.87
29.5	86.06	46.00		85.85	—	29.26
30.5	85.05	43.72		84.81	22043.50	
31.5	83.98	41.37		83.70	41.09	
32.5	82.78	38.86		82.55	38.57	
33.5	81.62	36.27		81.30	36.00	
34.5	80.40	33.58		80.20	33.30	
35.5	79.15	30.88		78.88	30.60	

been evaluated as follows :

The $B {}^2\Sigma^+$ initial state : The rotational term values for a ${}^2\Sigma$ state are given by (Mulliken 1930)

$$F_1(N) = Bv' N(N+1) - Dv' N^2(N+1)^2 + \frac{1}{2} \gamma N \quad \dots (1)$$

$$F_2(N) = Bv' N(N+1) - Dv' N^2(N+1)^2 - \frac{1}{2} \gamma(N+1) \dots (2)$$

where, $F_1(N)$ and $F_2(N)$ refer to the components with $J = N + \frac{1}{2}$ and $F_3(N)$ refers to those with $J = N - \frac{1}{2}$. Bv' and Dv' are effective rotational constants and γ is the spin doubling constant.

(a) *Determination of Bv' and Dv'* : From equations (1) and (2) the following relations are found.

$$\Delta_2 F_1'(N) = 4 Bv' (N + \frac{1}{2}) - 8 Dv' (N + \frac{1}{2})^2 + \gamma \quad \dots(3)$$

$$\Delta_2 F_2'(N) = 4 Bv' (N + \frac{1}{2})^2 - 8 Dv' (N + \frac{1}{2})^3 - \gamma \quad \dots(4)$$

by taking mean value of (3) and (4) we have

$$\frac{1}{2} [\Delta_2 F_1'(N) + \Delta_2 F_2'(N)] = 4 Bv' (N + \frac{1}{2}) - 8 Dv' (N + \frac{1}{2})^2 \quad \dots(5)$$

Now $\Delta_2 F_1'(N)$ and $\Delta_2 F_2'(N)$ are obtained as follows :

$$\Delta_2 F_1'(N) = R_1(N) - P_1(N) \quad \dots(6)$$

$$\Delta_2 F_2'(N) = R_2(N) - P_2(N) \quad \dots(7)$$

The $^2\Sigma^+$ state seems to be common for both the transitions since there is a good agreement of upper state combination differences with common vibrational levels of the B state of B-X system. An equality of combination differences with (0, 1) band of B-X system is shown in table 2. From (5) we have

$$\frac{1}{2} \left[\frac{\Delta_2 F_1'(N) + \Delta_2 F_2'(N)}{N + \frac{1}{2}} \right] = 4 Bv' - 8 Dv' (N + \frac{1}{2})^2 \quad \dots(8)$$

If L. H. S. is plotted against $(N + \frac{1}{2})^2$, the intercept of the straight line will give $4 Bv'$ and slope will give $8 Dv'$.

(b) *Determination of γ* : The spin doubling in the $^2\Sigma^+$ state was determined from the combination relations :—

$$\begin{aligned} R_1(J) - {}^RQ_{21}(J) &= Q_1(J+1) - {}^RQ_{21}(J+1) = {}^RQ_{12}(J) - Q_2(J) \\ &= {}^RQ_{12}(J+1) - P_2(J+1) = \gamma(J+1). \end{aligned} \quad \dots(9)$$

By plotting the differences of main lines and their corresponding satellite lines against 'J' a straight line will be obtained whose slope will give the value of γ . The magnitude of γ agrees well with that reported by previous workers Barwald *et al* (1934).

TABLE 2
COMPARISON OF $\Delta_2 F' (N)$ VALUES

N	$F'_1 (N)$ of (0,0) band for sub-band	$F'_2 (N)$ of (0,0) band for sub-band	$F' (N)$ values of (0,1) band from reference (1)	
			$F'_1 (N)$	$F'_2 (N)$
2	6.84			
3	9.52			
4	12.24			
5	14.96			
9	17.71			
7	20.40	20.49		
8	23.12	23.18		
9	25.84	25.98		
10	28.56	—		28.59
11	31.32	—	31.22	31.20
12	34.00	—	34.00	33.97
13	36.72	36.85	36.72	36.72
14	39.44	39.55	39.49	39.38
15	42.16	42.17	42.18	42.05
16	44.88	44.77	44.80	44.75
17	47.61	47.51	47.49	47.47
18	50.49	50.12	50.20	50.17
19	53.21	52.82	52.89	52.95
20	55.91	55.57	55.62	55.55
21	58.58	58.34	58.34	58.31
22	61.30	61.10	61.00	61.00
23	63.99	63.82	63.69	63.67
24	66.73	66.59	66.45	66.39
25	69.51	—	—	69.12

Final $A {}^2\Pi_1$ state: The ${}^2\Pi$ separation of the lower state is of the order of 158 cm^{-1} , so this state belongs to Hund case (a). This fact is also evident from the rotational structure of (0,0) band shown in figure 2. All the four heads belonging to the two sub-bands are well separated from each other and are treated as two independent bands.

For ${}^3\Pi_1$ state belonging to case (a) the rotational term values are given by (Mulliken 1930)

$$F(J) = B_{eff} J(J+1) - D_0 J^3(J+1)^3 \quad \dots(10)$$

where effective rotational constant is somewhat different for the two multiplet components.

(a) *Determination of rotational constants for two components*:

From (10) we have

$$\text{for } {}^2\Pi_{3/2}, \Delta_2 F_1''(J) = 4 Bv''^{(1)}(J + \frac{1}{2}) - 8 Dv''^{(1)}(J + \frac{1}{2})^2 \dots (11)$$

$$\text{for } {}^2\Pi_{1/2}, \Delta_2 F_2''(J) = 4 Bv''^{(2)}(J + \frac{1}{2}) - 8 Dv''^{(2)}(J + \frac{1}{2})^2 \dots (12)$$

Now $\Delta_2 F_1''(J)$ and $\Delta_2 F_2''(J)$ are obtained as follows :

$$\left. \begin{aligned} \Delta_2 F_1''(J) &= R_1(J-1) - P_1(J+1) \\ \Delta_2 F_2''(J) &= R_2(J-1) - P_2(J+1) \end{aligned} \right\} \dots (13)$$

So by the help of (13) plotting $\Delta_2 F_1''(J)/(J+\frac{1}{2})$ and $\Delta_2 F_2''(J)/(J+\frac{1}{2})$ against $(J + \frac{1}{2})^2$ the values of $B_0''^{(1)}, D_0''^{(1)}, B_0''^{(2)}, D_0''^{(2)}$ for $(0, 0)$ band have been obtained.

(b) Λ Type Doubling : The $2\pi_{1/2}$ sub-state which forms the $F_2(J)$ series shows appreciable Λ type doubling. As a result of this the combination relations $R_2(J) - Q_2(J+1)$ and $Q_2(J) - P_2(J+1)$ are no longer found to be equal as shown in table 3 and a combination defect is obtained whose values will give the magnitude of Λ type doubling for different rotational levels of $2\pi_{1/2}$ state. The following expression show the magnitude of Λ doubling coefficient.

TABLE 3
COMBINATION DEFECT SHOWING Λ DOUBLING IN ${}^2\Sigma - {}^2\Pi_{3/2}$ AND
 ${}^2\Sigma - {}^2\Pi_{1/2}$ COMPONENTS

J	${}^2\Sigma - 2\Pi_{3/2}$		${}^2\Sigma - 2\Pi_{1/2}$	
	$R_2(J) - Q_2(J+1)$	$Q_2(J) - P_2(J+1)$	$R_2(J) - Q_2(J+1)$	$Q_2(J) - P_2(J+1)$
1.5	3.82		3.64	3.66
2.5	5.14		4.95	4.99
3.5	6.58		6.41	6.54
4.5	8.03		7.90	7.97
5.5	9.40		9.20	9.28
6.5	10.67	10.64	---	10.84
7.5	12.07	12.05	---	---
8.5	13.46	13.46	---	---
9.5	15.00	14.99	---	---
10.5	---	16.32	16.30	---
11.5	---	17.73	17.80	17.90
12.5	---	19.21	19.20	19.28
13.5	20.58	20.55	20.63	20.78
14.5	21.88	21.91	22.00	22.19
15.5	23.30	23.34	23.49	23.61
16.5	24.62	24.67	24.82	24.94
17.5	26.09	26.13	26.42	26.54
18.5	27.54	27.56	27.76	27.97
19.5	28.84	28.88	29.14	29.37
20.5	30.42	30.44	30.55	30.81
21.5	31.62	31.63	32.07	32.27
22.5	33.34	33.33	33.46	33.62
23.5	34.65	34.65	34.85	34.08
24.5	---	---	36.34	36.52

$$[Q_2(J) - P_2(J+1)] - [R_2(J) - Q_2(J+1)] = P(J+\frac{1}{2}) \quad \dots(14)$$

where p is Δ doubling coefficient for the $2\Pi_{1/2}$ state. By plotting L.H.S. of (14) against $(J+\frac{1}{2})$ the slope of the straight line will give the magnitude of P .

Corresponding differences for the sub-band involving $2\Pi_{3/2}$ state, however, agree within the accuracy of the measurements (shown in table 3) indicating negligible Δ doubling, as expected from the theory.

(c) *Determination of B_o'' and spin coupling constant 'A'*: The value of the effective rotational constant Bv'' and whole band origin is determined graphically from the relation :

$$Q_1(J) + Q_2(J) = 2\nu_{010} + 2B''_{eff} + 2(B' - B''_{eff})(J+1)^2 \quad \dots(15)$$

Also B''_{eff} will be the mean value of $B_o''^{(1)}$ and $B_o''^{(2)}$. The spin doubling of the $2\Pi_i(a)$ has been determined from the relation :

$${}^2R_{21}(J) - R_2(J) = Bv''_{eff} [4(J+\frac{1}{2})^2 + Y(Y-4)]^{1/2} \quad \dots(16)$$

where $Y = A/Bv''_{eff}$.

So by plotting $[L.H.S.]^2/Bv''^2$ against $(J+\frac{1}{2})^2$ gives an intercept of $Y(Y-4)$ from which the value of 'A' has been obtained. For inverted state this value will be negative.

Determination of band origins of ${}^2\Sigma^+ - {}^2\Pi_{3/2}$ and ${}^2\Sigma^+ - {}^2\Pi_{1/2}$ sub-bands: The band origins for the two sub-bands are related to the wave-numbers of the rotational lines in the following manner :

$$\text{for } {}^2\Sigma - {}^2\Pi_{1/2}; Q_2(J) + P_2(J) = 2\nu_o^{(2)} + \frac{1}{2}B_v' + 2(B_v' - B_v'')J(J+1) \quad \dots(17)$$

$$\text{for } {}^2\Sigma - {}^2\Pi_{3/2}; Q_1(J) + R_1(J) = 2\nu_o^{(1)} + \frac{1}{2}B_v' + 2(B_v' - B_v'')J(J+1) \quad \dots(18)$$

Thus by plotting L.H.S. of above equations against $J(J+1)$, the intercept of these straight lines will be $2\nu_o^{(2)}$, $2\nu_o^{(1)}$ and slopes will give $2(B_v' - B_o''^{(2)})$ and $2(B_v' - B_o''^{(1)})$ respectively. The values of B_o' , $B_o''^{(2)}$ and $B_o''^{(1)}$ can be corrected by the values of these slopes choosing B_o' value most accurate as suggested by Herzberg (1950).

The molecular constants for ${}^2\Sigma^+$ and $A {}^2\Pi_i(a)$ states are given in table 4.

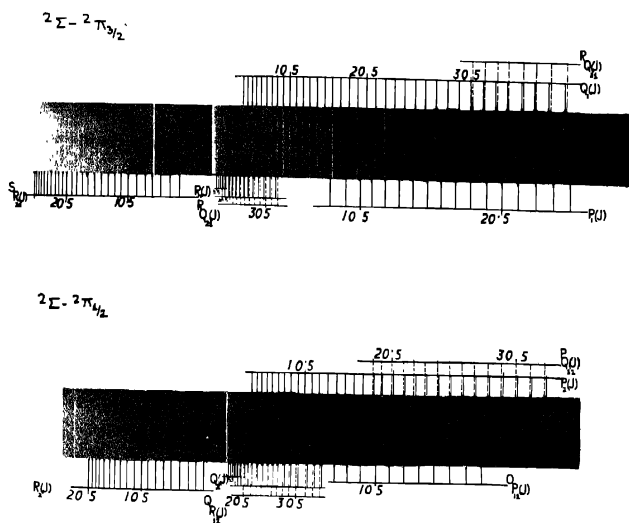


Figure 2. Rotational structures of two sub-bands of ${}^2\Sigma^+ - {}^2\Pi_{3/2}$ and ${}^2\Sigma^+ - {}^2\Pi_{1/2}$.

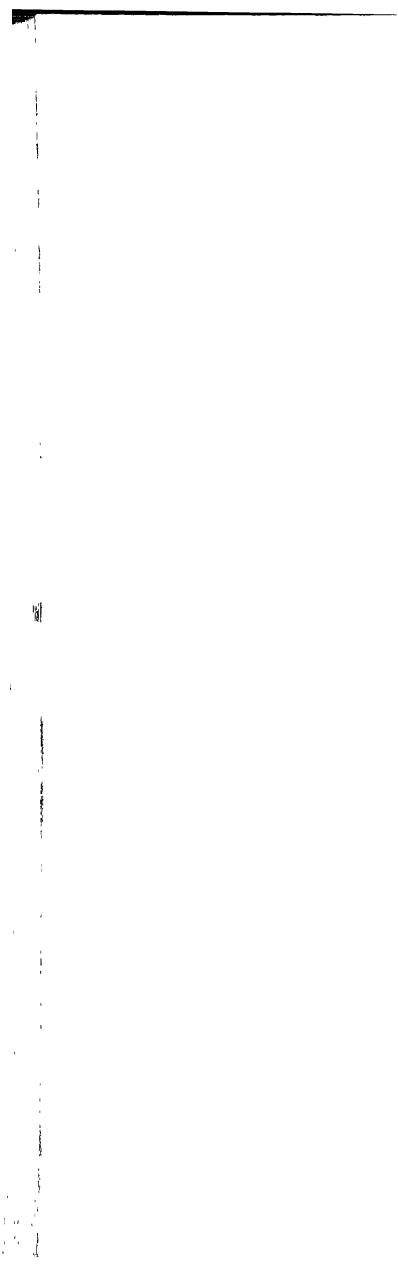


TABLE 4
MOLECULAR ROTATIONAL CONSTANTS FOR $B^2\Sigma^+ - A^2\Pi$ (a) BAND SYSTEM
OF CP MOLECULE

$B_0' = 0.67995 \text{ cm}^{-1}$	$\nu_0^{(1)} = 22090.43 \text{ cm}^{-1}$
$B_0''^{(1)} = 0.70731 \text{ cm}^{-1}$	$\nu_0^{(2)} = 21932.68 \text{ cm}^{-1}$
$B_0''^{(2)} = 0.71288 \text{ cm}^{-1}$	$\nu_0, 0 = 22010.94 \text{ cm}^{-1}$
$B_0'' = 0.71000 \text{ cm}^{-1}$	$A = -157.87 \text{ cm}^{-1}$
$D_0''^{(1)} = 1.51 \times 10^{-6} \text{ cm}^{-1}$	$\gamma = +0.0065 \text{ cm}^{-1}$
$D_0''^{(2)} = 0.40 \times 10^{-6} \text{ cm}^{-1}$	$p = 0.0042 \text{ cm}^{-1}$
$D_0' = 0.60 \times 10^{-6} \text{ cm}^{-1}$	

DISCUSSION

The present rotational analysis shows that the transition is $\delta^2\Sigma^+ - ^2\Pi_1$ type. The equality of upper state combination differences with $B-X$ system shows that the upper state is $^2\Sigma^+$. Moreover the presence of satellite branches prove that the upper state is one in which splitting is not due to Δ type doubling but is due to spin doubling. The inverted character of $2\Pi_1$ state is confirmed from three facts. The one that in $^2\Sigma - ^2\Pi_{1/2}$ transition the first line of Q branch is one with $J = 1/2$ and in $^2\Sigma - \Pi_{3/2}$ it is $J = 3/1$. The second support comes from Δ doubling constant. The table 3 shows that combination defect is large for the $^2\Pi_{1/2}$ state hence this state involves lesser energy. The third support comes from the sign of $[R(J) - Q(J-1)] - [Q(J) - P(J+1)]$. Energy level diagram (figure 1) for inverted state shows well that the sign of combination defect for inverted $^2\Pi_1$ state favours the present argument. A comparison with the respective state in isoelectronic molecules has been made by Barwald *et al* (1934). Their prediction of $^2\Pi$ as inverted state is confirmed in the light of above mentioned reasonings.

Authors thank Dr. D. K. Rai for his helpful discussions. Thanks are also due to Prof. N. L. Singh for his kind interest in the work. One of us (A. K. C.) is grateful to C. S. I. R., India for financial assistance.

REFERENCES

- Barwald, H., Herzberg, G. & Herzberg, L. 1934 *Ann der Physic*, 20 569-593
 Herzberg, G. 1950 *Spectra of diatomic molecule* 187 D. Von. Nostrand and Company, New York.
 Mulliken, R. S., 1930 *Rev. Mod. Phys.* 2 60

Wave equation of charged particle of spin 1 — the Kemmer equation

By S. GUPTA

*Department of Physics, University of Calcutta.**

(Received 18 December 1968)

The Kemmer relativistic wave equation of a particle of spin one or zero and particularly the commutation relations of Duffin-Kemmer β -matrices have been obtained by the generalization of the corresponding non-relativistic wave equation. This covariant formulation is achieved by making a Lorentz-transformation to a reference frame in which the velocity of the particle is relatively high from a reference frame in which the velocity is small and also by generalizing the concept of spin and spin space.

Feshback & Villars (1958) derived the Dirac equation by the generalization of the non-relativistic Pauli equation in a unique manner. They started with the particle in the reference frame in which the Pauli theory applies and the wave function, ϕ , has two components corresponding to two orientations of the spin. The relativistic description is then obtained by making a Lorentz transformation to a reference frame in which the velocity of the particle is relatively high. For this purpose they generalized the concept of spin and spin space, and sought for covariant equation in that space. The purpose of this paper is to show that by following their procedure a similar derivation can also be made of the Kemmer (1939) wave equation of a particle of spin one or zero, particularly in obtaining the commutation relations of Duffin-Kemmer (Duffin, 1939) β -matrices.

The non-relativistic Hamiltonian of a particle of charge e and the intrinsic magnetic moment μ in a given electromagnetic field defined by the vector potential \mathbf{A} and the scalar potential A_0 is given by

$$H = \frac{1}{2m} \left(\mathbf{p} - \frac{e}{c} \mathbf{A} \right)^2 + eA_0 - (\mu \cdot \mathbf{h}).$$

The wave equation is then

$$i\hbar \frac{\partial \phi}{\partial t} = \frac{1}{2m} \left(-i\hbar \text{grad} - \frac{e}{c} \mathbf{A} \right)^2 \phi + eA_0 \phi - (\mu \cdot \mathbf{h}) \phi, \quad (1)$$

where

$$\mu = \frac{e\hbar}{mc} \mathbf{S}, \quad (2)$$

*Present address : 86, Beltala Road, Calcutta-26.

S being the infinitesimal rotation operator in the spin space. We assume the commutation rules for the components of S as

$$S_i S_j - S_j S_i = i S_k, \quad (3)$$

where i, j, k are cyclic permutations of 1, 2, 3, which one expects for components of any angular momentum. When expressed in covariant form, (3) becomes

$$S_i S_j - S_j S_i = i \epsilon_{ijk} S_k. \quad (4)$$

Further we assume that

$$S_i^3 = S_i, \quad (i=1, 2, 3), \quad (5)$$

so that the eigenvalues of S_i are $-1, 0, 1$, which means that the particle has spin 1. The wave function ϕ in (1) then has three components corresponding to the three independent orientations of the spin.

In the irreducible representation in which S_3 is diagonal (3) and (5) are satisfied by (Powell & Crasemann, 1963)

$$S_1 = \frac{1}{\sqrt{2}} \begin{pmatrix} 0 & 1 & 0 \\ 1 & 0 & 1 \\ 0 & 1 & 0 \end{pmatrix}, \quad S_2 = \frac{i}{\sqrt{2}} \begin{pmatrix} 0 & -1 & 0 \\ 1 & 0 & -1 \\ 0 & 1 & 0 \end{pmatrix}, \quad S_3 = \begin{pmatrix} 1 & 0 & 0 \\ 0 & 0 & 0 \\ 0 & 0 & -1 \end{pmatrix} \quad (6)$$

One can show, as a consequence of (4) and (5), that S_i ($i=1, 2, 3$) satisfy the commutation relations

$$S_i S_j S_k + S_k S_j S_i = S_i \delta_{jk} + S_k \delta_{ji}, \quad (7)$$

which when written in details are equivalent to

$$S_i^3 = S_i \quad (8a)$$

$$S_i^2 S_j + S_j S_i^2 = S_i, \quad (i \neq j) \quad (8b)$$

$$S_i S_j S_i = 0, \quad (i \neq j) \quad (8c)$$

$$S_i S_j S_k + S_k S_j S_i = 0, \quad (i \neq j \neq k). \quad (8d)$$

To see this, multiply (3) on the left by S_i and on the right also by S_i and on subtraction one obtains

$$S_i^3 S_j + S_j S_i^3 - 2 S_i S_j S_i = -i(S_k S_i - S_i S_k) = S_j \quad (9)$$

Multiply this equation on both sides by S_i and using (5), one gets

$$S_i S_j S_i = 2 S_i^2 S_j S_i^2$$

Again multiplying on both sides by S_i

$$S_i^2 S_j S_i^2 = 2 S_i S_j S_i$$

Thus one derives (8c) and hence (8b) from (9). To obtain (8d) multiply (3) on both sides by S_i and S_j , again reverse this order of multiplication and add deriving

$$S_i^2 S_j^2 - S_j^2 S_i^2 = i(S_i S_k S_j + S_j S_k S_i), \quad (i \neq j \neq k),$$

where (8c) has been used. Now by repeated application of (8b) one proves that

$$S_i^2 S_j^2 = S_j^2 S_i^2$$

whence (8d) is verified.

The invariance of the commutation relation (7) or of (4) and (5) under an orthogonal transformation

$$S_k' = a_{ki} S_i, \quad a_{ki} a_{kj} = \delta_{ij}, \quad (k, i, j = 1, 2, 3), \quad (10)$$

a_{ik} being the transformation matrix relating the two coordinate systems, is evident. Clearly the transformation (10) changes the representation of the S matrices.

The relativistic description is now obtained by making a Lorentz transformation to the reference system in which the velocity is large. For this purpose we identify that S is the space-part of an antisymmetrical tensor $\Sigma_{\mu\nu}$ — that is the rotation operator S , whose components have the properties (8a)–(8d), is a pseudovector constructed from the spatial components of $\Sigma_{\mu\nu}$. Thus

$$\Sigma_{\mu\nu} = -\Sigma_{\nu\mu}, \quad S = (\Sigma_{23}, \Sigma_{31}, \Sigma_{12}). \quad (11)$$

The space-time part we denote by the vector operator

$$T = (\Sigma_{14}, \Sigma_{24}, \Sigma_{34}) \quad (12)$$

We must regard T as unknown for the present. Our first problem is to find the relations between T and S and also the commutation rules of T . Under a Lorentz transformation, $\Sigma_{\mu\nu}$ is transformed to

$$\Sigma_{\mu\nu}' = a_{\mu\rho} a_{\nu\sigma} \Sigma_{\rho\sigma}.$$

For instance, under a Lorentz transformation for a motion of the primed reference system relative to an unprimed one, in which the velocity of the particle is small, with velocity v in the x_1 -direction, we obtain

$$S_1' = S_1, S_2' = \xi \left(S_2 + i \frac{v}{c} T_3 \right), S_3' = \xi \left(S_3 - i \frac{v}{c} T_2 \right), \quad (13a)$$

and

$$T_1' = T_1, T_2' = \xi \left(T_2 + i \frac{v}{c} S_3 \right), T_3' = \xi \left(T_3 - i \frac{v}{c} S_2 \right) \quad (13b)$$

where $\xi = \left(1 - \frac{v^2}{c^2}\right)^{-\frac{1}{2}}$. Similar relations follow for motions in the x_2 -

and x_3 -directions, which can be obtained from (13a) and (13b) by cyclic permutations of 1, 2, 3.

The relations (8a) — (8d) should be valid for any inertial system of reference, and hence in the primed system also. Then from $S_1'^3 = S_1'$ and $S_1'^3 = S_1'$, we have

$$\left. \begin{aligned} S_1'^2 T_3 + T_3 S_1'^2 + S_2' T_3 S_1' &= T_3 \\ T_3^2 S_1' + S_2' T_3^2 + T_3 S_2' T_3 &= S_2' \\ T_3^3 &= T_3 \end{aligned} \right\} \quad (14)$$

with similar relations obtained by the interchange of 2 and 3.

Similar relations are obtained for motions along x_2 - and x_3 -directions, by cyclic permutations of 1, 2, 3.

To see (14) we substitute S_1' from (13a) in $S_1'^3 = S_1'$ and get

$$\begin{aligned} S_1'^3 + i \frac{v}{c} \left(S_1'^2 T_3 + T_3 S_1'^2 + S_2' T_3 S_1' \right) - \frac{v^2}{c^2} \left(T_3^2 S_1' + S_2' T_3^2 + T_3 S_2' T_3 \right) \\ - i \frac{v^3}{c^3} T_3^3 = \left(1 - \frac{v^2}{c^2} \right) \left(S_2 + i \frac{v}{c} T_3 \right) \end{aligned}$$

Equating the co-efficients of each power of $\frac{y}{c}$ on both sides of this equation we obtain the set (14). Similarly from $S_3'^2 = S_3'$.

In a similar way, $S_i'^2 S_j' + S_i' S_j'^2 = S_j'$, ($i \neq j$), gives for $i, j = (2,1), (3,1), (1,2), (1,3), (2,3), (3,2)$

$$\left. \begin{aligned} T_3^2 S_1 + S_1 T_3^2 &= S_1, \\ (S_1 T_3 S_2 + S_2 T_3 S_1) + (S_1 S_2 T_3 + T_3 S_2 S_1) &= 0, \\ \text{(with the interchange of 2 and 3)} \end{aligned} \right\} \quad \dots(15)$$

$$S_1^2 T_3 + T_3 S_1^2 = T_3, \quad S_1^2 T_2 + T_2 S_1^2 = T_2, \quad \dots(16)$$

$$\left. \begin{aligned} (S_2 T_3 S_3 + S_3 T_3 S_2) + (T_3 S_2 S_3 + S_3 S_2 T_3) - (S_2^2 T_3 + T_3 S_2^2) &= -T_2, \\ (T_3 S_2 T_2 + T_2 S_2 T_3) + (S_2 T_3 T_2 + T_2 T_3 S_2) - (T_3^2 S_3 + S_3 T_3^2) &= -S_2, \\ T_3^2 T_2 + T_2 T_3^2 &= T_2, \\ \text{(with the interchange of 2 and 3)} \end{aligned} \right\} \quad (17)$$

Further $S_i' S_j' S_k' = 0$, ($i \neq j$), contributes for $i, j = (2,1), (3,1), (1,2), (1,3), (2,3), (3,2)$

$$\left. \begin{aligned} S_2 S_1 T_3 + T_3 S_1 S_2 &= 0, \\ T_3 S_1 T_3 &= 0, \\ \text{(with the interchange of 2 and 3)} \end{aligned} \right\} \quad \dots(18)$$

$$S_1 T_3 S_1 = 0, \quad S_1 T_2 S_1 = 0, \quad \dots(19)$$

$$\left. \begin{aligned} S_2 T_3 S_2 &= T_3 S_3 S_2 + S_2 S_3 T_3, \\ T_3 S_2 T_3 &= S_2 T_2 T_3 + T_2 T_3 S_2, \\ T_3 T_2 T_3 &= 0, \\ \text{(with the interchange of 2 and 3)} \end{aligned} \right\} \quad \dots(20)$$

Finally $S_i' S_j' S_k' + S_k' S_j' S_i' = 0$, ($i \neq j \neq k$), gives for $i, j, k = (1,2,3), (1,3,2)$ and $(2,1,3)$

$$\left. \begin{aligned} (S_1 T_3 S_3 + S_3 T_3 S_1) - (S_1 S_2 T_2 + T_2 S_2 S_1) &= 0, \\ S_1 T_3 T_3 + T_2 T_3 S_1 &= 0, \\ \text{(with the interchange of 2 and 3)} \end{aligned} \right\} \quad \dots(21)$$

$$\left. \begin{aligned} (T_2 S_1 S_3 + S_3 S_1 T_2) - (S_2 S_1 T_2 + T_2 S_1 S_2) &= 0, \\ T_2 S_1 S_2 + T_2 S_1 T_3 &= 0, \end{aligned} \right\} \quad \dots(22)$$

The relations similar to (15)–(22) are obtained for transformations in the x_1 – x_2 and x_2 – x_3 plane by the cyclic permutations of 1, 2, 3.

Collecting the results one has the following relations between T_k :

$$\left. \begin{aligned} T_i^2 T_j + T_j T_i^2 &= T_{ij}, (i \neq j), \\ T_i T_j T_i &= 0, (i \neq j), \\ T_i^3 &= T_i, \end{aligned} \right\} \dots (23)$$

and the relations between S_k and T_k are given by

$$S_i^2 T_j + T_j S_i^2 = T_{ij}, (i \neq j), \dots (24a)$$

$$T_i^2 S_j + S_j T_i^2 = S_{ij}, (i \neq j), \dots (24b)$$

$$S_i T_j S_i = 0, (i \neq j), \dots (25a)$$

$$T_i S_j T_i = 0, (i \neq j), \dots (25b)$$

$$S_i T_i S_i = T_j S_j S_i + S_j S_j T_i, (i \neq j), \dots (26a)$$

$$T_i S_i T_i = S_j T_j T_i + T_j T_j S_i, (i \neq j), \dots (26b)$$

$$S_i S_j T_k + T_k S_j S_i = 0, (i \neq j \neq k), \dots (27a)$$

$$T_i T_j S_k + S_k T_j T_i = 0, (i \neq j \neq k), \dots (27b)$$

$$T_i S_j T_k + T_k S_j T_i = 0, (i \neq j \neq k), \dots (27c)$$

$$S_i T_j S_k + S_k T_j S_i = 0, (i \neq j \neq k), \dots (27d)$$

$$S_i T_j S_i + S_j T_j S_i + T_j S_i S_j + S_j S_i T_j - (S_i^2 T_i + T_i S_i^2) = -T_i, (i \neq j), \dots (28a)$$

$$T_i S_j T_j + T_j S_j T_i + S_j T_i T_j + T_j T_i S_j - (T_i^2 S_i + S_i T_i^2) = -S_i, (i \neq j), \dots (28b)$$

$$(S_i T_j S_j + S_j T_j S_i) - (S_i S_k T_k + T_k S_k S_i) = 0, (i \neq j \neq k), \dots (29a)$$

$$(T_j S_i S_j + S_j S_i T_j) - (S_k S_i T_k + T_k S_i S_k) = 0, (i \neq j \neq k), \dots (29b)$$

The relation (27d) has been obtained from the second set of (15) and (27a). The first set of (14) is satisfied by (24a) and (25a), and the second set by (24b) and (25b). It should be noticed that the relations between three T 's with different indices are absent in (23). This is caused by our restriction to Lorentz transformation for motion in the direction of coordinate axes only, in which case only two of the components of S are transformed and one remains unchanged.

For further discussion we use the following result:—Any vector V in spin-space satisfies the commutations relations (Powell & Crasemann, 1963)

$$[S_i, V_i]=0, [S_i, V_j] = -[S_j, V_i] = iV_k, \quad (i, j, k = \text{cyclic})$$

an equation, which in terms of the Σ_{ik} ($i, k = 1, 2, 3$) may be written as

$$[V_i, \Sigma_{jk}] = -i(\delta_{ij}V_k - \delta_{ik}V_j) \quad \dots (30)$$

Identifying T with V , we have the relations

$$[S_i, T_i] = 0, [S_i, T_j] = -[S_j, T_i] = iT_k, \quad (i, j, k = \text{cyclic}) \quad \dots (31)$$

The simplest solution of this equation for S_k in terms of T_j may be expressed as a product of two T -matrices. The detail working of the method, that we have followed here, is the same as has been used later for the derivation of the commutation relations for β -matrices. To avoid repetition of calculations we give here only the main results. Since $S_k = \Sigma_{ij}$ is an antisymmetrical tensor of rank two, we obtain

$$i S_k = (T_i T_j - T_j T_i), \quad (i, j, k = \text{cyclic}) \quad \dots (32)$$

with the three commutation relations (23) for T_i and in addition

$$T_i T_j T_k + T_k T_j T_i = 0, \quad (i \neq j \neq k), \quad \dots (33)$$

The relations (23) and (33) between T 's can then be expressed in co-variant form as

$$T_i T_j T_k + T_k T_j T_i = T_i \delta_{jk} + T_k \delta_{ji} \quad \dots (34)$$

With the use of $[S_i, T_i] = 0$, (26a) and (26b), the relations (28a) and (28b) can be simplified to

$$T_i S_j S_i + S_j S_i T_j - S_i T_j S_i = -T_i, \quad (i \neq j), \quad \dots (28a')$$

$$S_i T_i T_j + T_j T_i S_j - T_i S_i T_j = -S_i, \quad (i \neq j) \quad \dots (28b')$$

and (29a) and (29b) are identically satisfied.

The relations (24a)–(27d), (28a') and (28b') give all possible relations between two S 's and one T , and between two T 's and one S . By a simple but tedious calculations it can be shown that they are all identically satisfied by (32), which has been obtained from (31). Thus these relations together

with (34) are consistent with (31) and can also be obtained directly from it (See the Appendix).

We have thus obtained the properties of the rotation operator $\Sigma_{\mu\nu}$ in spin space. One should notice that the relations (7) and (34) are the commutation relations for the Duffin-Kemmer β -matrices. But there is one difference, the fundamental Duffin-Kemmer matrices are four, whereas we have here only three S -matrices and three T -matrices. We shall now prove that there exists a four-vector β_μ in spin space having the algebraic properties.

$$\beta_\mu \beta_\nu \beta_\lambda + \beta_\lambda \beta_\nu \beta_\mu \beta_\mu \delta_{\nu\lambda} + \beta_\lambda \delta_{\nu\mu} \quad \dots (35)$$

or

$$\beta_\mu \beta_\nu - \beta_\nu \beta_\mu = i \Sigma_{\mu\nu}, \quad \beta_\mu^3 = \beta_\mu^2 \quad \dots (36)$$

For this purpose, a general infinitesimal Lorentz transformation is performed on β_μ , such that

$$\exp \left(\frac{1}{2} i \Sigma_{\alpha\beta} \omega_{\alpha\beta} \right) \beta_\mu \exp \left(-\frac{1}{2} i \Sigma_{\alpha\beta} \omega_{\alpha\beta} \right) = a_{\mu\nu}(\omega_{\alpha\beta}) \beta_\nu \quad \dots (37)$$

where $a_{\mu\nu} = \delta_{\mu\nu} + \omega_{\mu\nu}$, $\omega_{\mu\nu} = -\omega_{\nu\mu}$, are the co-efficients in Lorentz transformation and the Einstein summation rule has been followed. The commutation relations between $\Sigma_{\alpha\beta}$ and β_μ are then obtained from (37) and the result will be a covariant generalization of (30) which is given by

$$[\beta_\mu, \Sigma_{\lambda\nu}] = -i[\delta_{\mu\lambda}\beta_\nu - \delta_{\mu\nu}\beta_\lambda], \quad (\mu, \nu, \lambda = 1, 2, 3, 4.) \quad \dots (38)$$

If we put $\Sigma_{23}, \Sigma_{31}, \Sigma_{12} = S_1, S_2, S_3$ and $\Sigma_{14}, \Sigma_{24}, \Sigma_{34} = T_1, T_2, T_3$, we have from (38)

$$\left. \begin{aligned} [\beta_1, S_1] &= 0, & [\beta_1, S_2] &= i\beta_3, & [\beta_1, S_3] &= -i\beta_2, \\ [\beta_2, S_1] &= -i\beta_3, & [\beta_2, S_2] &= 0, & [\beta_2, S_3] &= i\beta_1, \\ [\beta_3, S_1] &= i\beta_2, & [\beta_3, S_2] &= -i\beta_1, & [\beta_3, S_3] &= 0, \\ [\beta_4, S_1] &= 0, & [\beta_4, S_2] &= 0, & [\beta_4, S_3] &= 0, \\ [\beta_1, T_1] &= -i\beta_4, & [\beta_1, T_2] &= 0, & [\beta_1, T_3] &= 0, \\ [\beta_2, T_1] &= 0, & [\beta_2, T_2] &= -i\beta_4, & [\beta_2, T_3] &= 0, \\ [\beta_3, T_1] &= 0, & [\beta_3, T_2] &= 0, & [\beta_3, T_3] &= -i\beta_4, \\ [\beta_4, T_1] &= i\beta_1, & [\beta_4, T_2] &= i\beta_2, & [\beta_4, T_3] &= i\beta_3, \end{aligned} \right\} \quad \dots (39)$$

whence we have

$$[\beta_k, S_l] = i\beta_m, [S_k, \beta_l] = i\beta_m, \text{ for } k, l, m = \text{cycl. } (1, 2, 3), \quad \dots(40a)$$

$$[\beta_k, T_k] = i\beta_k, [T_k, \beta_k] = i\beta_k, k=1, 2, 3. \quad \dots(41a)$$

The solutions of (38) for $\Sigma_{\mu\nu}$ are evidently functions of the matrices β_μ . Following Bhabha (1945, 1949) the simplest assumption that can be made is that $\Sigma_{\mu\nu}$ contain no term that is a product of more than two β -matrices. Hence, since $\Sigma_{\mu\nu}$ is an antisymmetric tensor, it should have the form

$$i\Sigma_{\mu\nu} = q^2 (\beta_\mu \beta_\nu - \beta_\nu \beta_\mu) \quad \dots(42)$$

where q^2 is a constant c-number. The commutation relations for β_μ can now be obtained directly using the relations (40a) and (41a) and following the method given in the Appendix. Rather than work out this in detail we adopt the following method.

(42) can also be written in terms of S_k and T_k as

$$q^2[\beta_k, \beta_l] = iS_m, \text{ for } k, l, m = \text{cycl. } (1, 2, 3), \quad \dots(40b)$$

$$q^2[\beta_k, \beta_k] = iT_k, k=1, 2, 3 \quad \dots(41b)$$

The commutation relations (40a), (40b), (41a) and (41b) show that T_k and $q\beta_\mu$ will have the same eigen values as S_k (Hepner, 1951). Since for spin one the eigenvalues of S_k are $-1, 0, 1$, these are also the eigenvalues of the matrices $q\beta_\mu$ and T_k . Thus

$$q^2\beta_\mu^3 = \beta_\mu, T_k^3 = T_k. \quad \dots(43)$$

The second relation has already been obtained in (23). Since by (41b), T_k are expressed in terms of β_k , hence in order that the expression (32) for S_k may be consistent with the expression (40b), we should have

$$q^2 = 1. \quad \dots(44)$$

Hence we obtain

$$\beta_\mu^3 = \beta_\mu, \quad \dots(45)$$

$$i\Sigma_{\mu\nu} = (\beta_\mu \beta_\nu - \beta_\nu \beta_\mu) \quad \dots(46)$$

By the substitution of (46) in (38), we get

$$\beta_\mu \beta_\lambda \beta_\nu - \beta_\mu \beta_\nu \beta_\lambda - \beta_\lambda \beta_\nu \beta_\mu + \beta_\nu \beta_\lambda \beta_\mu = \delta_{\mu\lambda} \beta_\nu - \delta_{\mu\nu} \beta_\lambda, \quad \dots(47)$$

For $\mu \neq \nu \neq \lambda$, in particular,

$$2\beta_\mu\beta_\lambda\beta_\mu - \beta_\mu^3\beta_\lambda - \beta_\lambda\beta_\mu^3 = -\beta_\lambda^3, \quad (\mu \neq \lambda), \quad \dots(48)$$

Multiplying on both sides by β_μ and using (45), we have

$$2\beta_\mu^3\beta_\lambda\beta_\mu^3 = \beta_\mu\beta_\lambda\beta_\mu, \quad (\mu \neq \lambda)$$

Again multiplying on both sides by β_μ , we obtain

$$2\beta_\mu\beta_\lambda\beta_\mu = \beta_\mu^3\beta_\lambda\beta_\mu^2$$

Hence

$$\beta_\mu\beta_\lambda\beta_\mu = 0, \quad \dots(49)$$

Consequently (48) reduces to

$$\beta_\mu^3\beta_\lambda + \beta_\lambda\beta_\mu^3 = \beta_\lambda^3, \quad (\mu \neq \lambda), \quad \dots(50)$$

Further for $\mu \neq \nu \neq \lambda$, (47) becomes

$$\beta_\mu\beta_\lambda\beta_\nu + \beta_\nu\beta_\lambda\beta_\mu = \beta_\mu\beta_\nu\beta_\lambda + \beta_\lambda\beta_\nu\beta_\mu$$

Multiplying by β_ν^3 from the left and using (45) and (49)

$$\beta_\nu^3\beta_\mu\beta_\lambda\beta_\nu + \beta_\nu\beta_\lambda\beta_\mu = 0$$

We then obtain using (50) and (49)

$$\beta_\mu\beta_\lambda\beta_\nu + \beta_\nu\beta_\lambda\beta_\mu = 0, \quad (\mu \neq \nu \neq \lambda) \quad \dots(51)$$

Hence $\beta_\mu\beta_\lambda\beta_\nu + \beta_\nu\beta_\lambda\beta_\mu$ which is symmetric in μ and ν should have the form

$$\beta_\mu\beta_\lambda\beta_\nu + \beta_\nu\beta_\lambda\beta_\mu = \beta_\mu\delta_{\lambda\nu} + \beta_\nu\delta_{\mu\lambda}, \quad \dots(35)$$

which includes (45), (49), (50) and (51). These are the well-known Duffin-Kemmer commutation relations of β -matrices in the theory of spin one.

A four-vector β_μ , which is the Duffin-Kemmer representation, thus exists in spin-space, and has been obtained via Lorentz transformation from the non-relativistic representation of the spin. A scalar can then be formed by contracting β_μ with the four-vector $D_\mu = \frac{\partial}{\partial x_\mu} - \frac{ie}{\hbar c} A_\mu$, where

A_μ is the four-potential. This provides us the possibility of constructing a first order covariant wave equation for a particle of spin one.

$$(\beta_\mu D_\mu + \kappa\psi) = 0 \quad \dots(52)$$

where κ is to be so identified that one obtains in the field free case the Klein-Gordon equation as a second order equation. It is well known that on identification κ is found to be mc/\hbar .

APPENDIX

We have from (31)

$$S_i T_j - T_j S_i = iT_k, \quad i, j, k = \text{cycl}(1, 2, 3). \quad \dots(A1)$$

By multiplication of (A1) on the left with S_i and on the right also with S_i and on subtraction

$$S_i^2 T_j + T_j S_i^2 - 2 S_i T_j S_i = i (S_i T_k - T_k S_i) = T_j \quad \dots(A2)$$

and by multiplication of this on both sides by S_i and with the use of $S_i^2 = S_i$

$$S_i T_j S_i = 2 S_i^2 T_j S_i$$

Again multiplying on both sides by S_i

$$S_i^2 T_j S_i^2 = 2 S_i T_j S_i^2$$

Therefore

$$S_i T_j S_i = 0, \quad (i \neq j), \quad \dots(A3)$$

and, by (A2)

$$S_i^2 T_j + T_j S_i^2 = T_j, \quad (i \neq j) \quad \dots(A4)$$

By multiplication of (A1) on the right with $T_k S_i$ and on the left with $S_i T_k$ and on addition

$$S_i (T_i T_k - T_k T_i) S_i = i (T_k^2 S_i + S_i T_k^2)$$

with the use of (A3). Therefore, since $S_i^2 = S_i$,

$$T_k^2 S_i + S_i T_k^2 = S_i, \quad (i \neq k), \quad \dots(A5)$$

if

$$iS_i = (T_j T_k - T_k T_j), \quad i, j, k = \text{cycl} (1, 2, 3) \quad \dots (A6)$$

When (A1) is multiplied on the left with T_j and on the right also with T_j and subtracted

$$2T_j S_i T_j - (T_j^2 S_i + S_i T_j^2) = i(T_j T_k - T_k T_j) = -S_i$$

Therefore, by (A5)

$$T_j S_i T_j = 0, \quad (i \neq j) \quad \dots (A7)$$

Multiplying (A1) on both sides by T_j and using (A7)

$$T_j T_k T_j = 0, \quad (i \neq j), \quad \dots (A8)$$

By the substitution of (A6) in (A1) and with the use of (A8)

$$T_j^2 T_k + T_k T_j^2 = T_k, \quad (j \neq k), \quad \dots (A9)$$

By multiplication of (A1) on both sides by T_k

$$iT_k^3 = T_k S_i T_j T_k - T_k T_j S_i T_k$$

Hence, since $S_i T_k - T_k S_i = -iT_j$, with the use of (A8) and (A9)

$$T_k^3 = T_j^2 T_k + T_k T_j^2 = T_k \quad \dots (A10)$$

Finally multiplying (A1) on the left and on the right with T_i and T_j respectively and reversing the order of multiplication, and on addition

$$T_i T_k T_j + T_j T_k T_i = 0, \quad \dots (A11)$$

where (A7), (A5), (A9) and $T_i S_i = S_i T_i$ have been used.

By substitution of S_i given by (A6) in (26a)–(27b), (28a') and (28b'), we find that these are identically satisfied. Thus all the relations between T 's and between T 's and S 's are direct consequence of (31). Further S_i in (A6) satisfy all the commutation relations (8a)–(8d) if the commutation relations (34) for T_k are utilized.

REFERENCES

- Bhabha, H. J. 1945 *Rev. Mod. Physics*, **17**, 300.
 — — 1949 *Rev. Mod. Physics*, **21**, 451.
 Duffin, R. J. 1938 *Phys. Rev.*, **54**, 114.
 Feshbach, H. & Villars, F. 1958 *Rev. Mod. Physics*, **30**, 24.
 Hefner, W. A. 1951 *Phys. Rev.*, **84**, 744.
 Kemmer, N. 1939 *Proc. Roy. Soc. A*, **173**, 91.
 Powell, J. I., & Crasemann, B. 1963 *Quantum Mechanics*, 345, 369.

Recording Instrument for measurement of thermal expansion

P. D. PATHAK, M. C. GUPTA AND J. M. TRIVEDI

Physics Dept., University School of Sciences,

Gujarat University, Ahmedabad.

(Received 30, July 1968 ; Resubmitted 27, December 1968)

A recording instrument for the measurement of thermal expansion of solids is described in this article. The expansion of the specimen pushes mercury in a capillary tube in which a thin nichrome wire is placed. The potential difference across the wire changes when mercury moves in the tube. The changes in the potential difference are fed to a chart recorder. The sensitivity of the instrument can be varied within wide limits by employing capillary tubes of different bores or by changing the inclination of the tube to the horizontal. With suitable modifications, the instrument can be used for liquids and gases.

INTRODUCTION

Considerable attention has recently been devoted to the measurement of thermal expansion of solids not only from the point of view of obtaining accurate and reliable data on different solids but as a means of studying other properties of far-reaching importance. For example, the measurement of thermal expansion can give useful information about the lattice vibrations in crystals, the energy of formation and role of lattice defects in thermal properties, the mechanism of phase transition, the release or absorption of energy in transitions of ferromagnetic materials etc.

Various optical, electrical, mechanical and other devices are employed in order to measure small changes in length. For large specimens, simple optical lever may give good results while for small specimens interferometric methods are more common. Various other ingenious devices are also employed (Shapiro *et al* 1964, Cook 1964, Bottom 1964).

On examining the literature we hardly come across methods in which the expansion of a solid on heating can be transferred to a chart and hence obtain a permanent record which would be available at any time for the study of the internal processes occurring in solids.

In this paper, a simple instrument is described which can be built up from materials available in any common laboratory, so that a permanent record showing the relation between temperature and expansion of a solid can be obtained.

With the present instrument the thermal expansion of 99.99% pure aluminium is measured from room temperature to about 400°C to illustrate the accuracy of the instrument. The thermal expansion of 99.99% pure nickel is also measured from room temperature to about 500°C to show how the study of phase changes can be undertaken with the help of the instrument.

THE INSTRUMENT

The present instrument is shown schematically in figure 1. It consists of a fused silica tube T of about 22 cm. in length and 0.8 cm. in diameter. It is surrounded by nichrome heating coil HH . It is placed horizontally in a wooden box A which is then filled with magnesia powder. P_1 and P_2 are fused silica rods. The length of P_1 is such that the specimen rod S , whose expansion is to be measured, remains in the centre of the tube T .

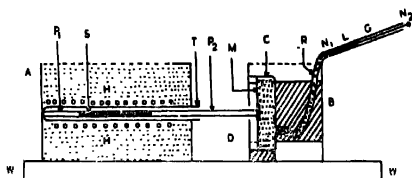


Figure 1

The other box B contains a small metal box C whose front surface M consists of a thin rubber membrane. A small thin circular metal piece was fixed at the centre of the membrane. The rod P_2 is in contact with this rubber membrane and when it expands it pushes the membrane inward.

The box C contains pure mercury and is connected to a glass capillary G , of about 50 cm. length, by a rubber tube R . When the specimen S expands the rod P_2 pushes the rubber membrane M inward and the mercury level L in the capillary moves forward. A millimeter scale placed behind the capillary tube enables the movement of the mercury level to be measured.

A thin nichrome wire $N_1 N_2$ of about 12 ohms resistance is placed inside the capillary tube so that a part of it remains within the mercury column. The points N_1 , N_2 (i. e. C and N_2) are joined in series to a

battery and a resistance so that a potential difference of about 20 mV is obtained across the wire. The movement of the mercury level L , as the specimen expands, increases or decreases the potential difference. The points N_1 N_2 are also connected to a chart recorder.

The box A is fixed to a rigid wooden plank WW . The box B can slide on WW and can be fixed at any desired position. It is moved to a position in which the push rod $P2$ touches the front rubber membrane M . It is then pushed a little forward so that the mercury level L moves by about 0.5 cm. This ensures that the push rod is firmly in contact with the membrane. The box B is then fixed firmly on WW by clamping screws.

One of the great advantages of this instrument is that its sensitivity can be altered by (i) employing capillary tubes of different bores and (ii) changing the inclination of the glass tube G to the horizontal. Thus specimens with low as well as high thermal expansion can be investigated by the same instrument. With a specimen of about 10 cm. in length an accuracy of about $\pm 1\%$ can be easily obtained. With suitable modifications, the instrument can be used for measuring the expansion of liquids and gases. Since the viscosity of mercury is a factor to be considered, the temperature of the specimen should be increased very slowly especially when studying the phase changes *e. g.* ferromagnetic transition in nickel or iron.

The observations were taken on aluminium and nickel rods of 10 cm. length and 0.5 cm. diameter. The purity of aluminium and nickel was 99.99% and were obtained from Messrs Johnson Mathey and Co. Ltd., London. The results on aluminium agreed very well with those of other workers.

Since the results obtained by different workers on the thermal expansion of nickel vary widely (Owen & Yates 1936, Nix & MacNair 1941, Mikryukov and Kamilov 1962), the results obtained in the present investigation are of importance. They are presented in the following table. The temperature of transition was found to be 357°C.

Temp. °C	$\alpha \times 10^6$	Temp. °C	$\alpha \times 10^6$
0	12.5	350	22.6
100	13.7	357	23.5
200	14.9		
250	15.5	400	16.1
300	17.4	450	17.0
320	19.1	500	17.6

REFERENCES

- Bottom, V. E. 1964 *Rev. Sci. Instrum.*, **35**, 374.
Cook, L. M. 1964 *Rev. Sci. Instrum.*, **35**, 758.
Mikryukov, V. E. & Kamilov, I. K. 1962 *Instrum. Exper Tech.* (U. S. A.), **3**, 581.
Nix, F. F. & MacNair, D. 1941 *Phys. Rev.*, **60**, 597.
Owen, E. A. & Yates, 1936 *Phil. Mag.*, **21**, 809.
Shapiro, J. M. Taylor, D. R. & Graham, G. M. 1964 *Canad. J. Phys.*, **42**, 835.

Letters to the Editor

Optical absorption spectra of diluted Ni (KSO₄)₂·6H₂O
single crystals.

By S. BANERJI

Physics Laboratory, Burdwan University, India.

(Received 24, April 1969)

Optical absorption studies (Mookherji & Chhonkar 1960) of about twenty salts of Ni⁺⁺ ion in aqueous solution showed that the red band consists of two maxima at about 13,900 cm⁻¹ and 15200 cm⁻¹. Absorption spectra of single crystals of NiSO₄·7H₂O and (Ni, Zn) (KSO₄)₂·6H₂O (Owen *et al* 1957) showed also that the red band has two peaks. Hartmann & Muller's study (1958) with improved technique, however, revealed that in case of NiSO₄·7H₂O single crystal the red band consists of three peaks. Bose & Chatterjee (1963) explained the results of Mookherji & Chhonkar (1960) and that of Hartmann & Muller (1958) by subjecting the Ni⁺⁺ ion to a field of orthorhombic symmetry superimposed on predominantly cubic field. A cubic field breaks the ground state of Ni⁺⁺ ion (⁶F) into Γ_4 , Γ_2 and Γ_3 in Bethe's notation. Superimposition of an orthorhombic field splits Γ_4 and Γ_3 each into three levels. In ordinary octahedral salts of Ni⁺⁺ ion Γ_2 which is a singlet, lies lowest while Γ_4 lies highest and Γ_3 lies intermediate in the stark pattern. Consequently one expects that the red band should have three peaks. Recent measurements (Mookherji & Chhonkar 1968) on the three undiluted tutton salts did not reveal this orthorhombic splitting.

In course of our ligand field calculations based on temperature variation of magnetic anisotropy of diluted crystals a knowledge of the optical absorption peaks was found to be helpful. Hence optical absorption study of tutton salts in crystalline state of iron group ions were undertaken. While recording the absorption spectra by a Hilger UVISPEC spectrophotometer it was observed that large mass absorption makes the absorption bands very broad even with very thin crystals so that the details of the fine structure of the anisotropic field hardly appears. Hence we have studied the absorption spectra of (Ni, Zn) (KSO₄)₂·6H₂O having varying proportions Zn⁺⁺ and Ni⁺⁺ ions in order to avoid the heavy mass absorption,

Our studies on undiluted salt of $Ni(KSO_4)_2 \cdot 6H_2O$ confirm the results of Mookherji & Chhonkar (1968). With the diluted salt, however, we find that for a crystal having 0.521% of Ni^{++} ion the red band splits into three, appearing at 14700 cm^{-1} , 15040 cm^{-1} , 15620 cm^{-1} . For the undiluted salt the overall splitting of this band was found to be 1390 cm^{-1} , while in this case it is 920 cm^{-1} , and the rhombic splittings are 340 cm^{-1} and 580 cm^{-1} . A shift in the peak positions was also observed with progressive dilution.

It may be mentioned here that following the same procedure it was possible to resolve Γ_5 into three levels in the case of $(Cu,Zn)(KSO_4)_2 \cdot 6H_2O$. This orthorhombic splitting has been reported recently by Mathur and Suri (1969) in case of $Cu(KSO_4)_2 \cdot 6H_2O$ diluted with corresponding zinc salt.

Details will be published later.

REFERENCES

- Bose, A. & Chatterji, R. 1963 *Proc. Phys. Soc. (London)* **82**, 23
Hartmann, H. & Muller, H. 1958 *Disc. Faraday Soc.* **26**, 49.
Mathur, S. C. & Suri, P. R. 1969 *J. Phys. Solids*, **29**, 2068.
Mookherji, A. & Chhonkar, N. S. 1960 *Indian J. Phys.* **34**, 363.
Mookherji, A. & Chhonkar, N. S. 1968 *Indian J. Phys.* **41**, 260.
Owen, G., Holmes, O. G., & Mc. Clure, D. B. 1957 *J. Chem. Phys.* **26**, 1686.

BOOK REVIEWS

STATISTICAL MECHANICS—By K. M. Khanna, Asia Publishing House, Bombay, 1968, pp. 283, Rs. 18.00

The contents of the book may be briefly described in the following: Chapter 1 on 'Statistical Thermodynamics' is a short introduction to important basic notions of the subject. Chapter 2 on 'Quantum Mechanics and Statistical Mechanics' discusses briefly important notions of quantum statistics after a statement of basic postulates of quantum mechanics. Chapters 3 and 4 are devoted to the 'Ideal Bose Gas' and the 'Ideal Fermi Gas' respectively. Chapter 5 deals with gases in which interactions become significant. Chapter 6 reports briefly different theories of Liquid Helium after a short note on distinctive physical properties of Liquid Helium. Chapter 7 is on applications of Second Quantization Methods to Boson and Fermion systems. In Chapter 8, expressions for fluctuations of several thermodynamic quantities are calculated. Chapter 9 contains a short account on uses of Green's Functions in the subject. Some special problems are considered in Chapter 10. Besides these, nine appendices on (i) Definite integrals, (ii) Natural constants (iii) Negative temperatures (iv) Quantum mechanical postulates on symmetries of wave functions for a system of identical particles, (v) Transition from quantum to classical statistics, (vi) Bose Einstein phase transition in an interacting system (vii) Creation and annihilation operators, (viii) Theory of Fermi liquid, (ix) Young and Lee theory of condensation.

From the above, it is clear that the book covers a good number of topics in the subject and also describes different modern techniques. Thus, the book will be considered as a useful text-book by the students of physics. As within a small compass a very long range of vast subject is covered, many important basic points could not be dealt properly. Even the basic question of the necessity of the subject has not been fully stressed. Though the book deals with a good deal of mathematical methods and notions used in the subject, yet due care has not been taken to avoid confusing lapses even in simple mathematical arguments as it will be clear from the following samples from the lot occurring in the book:

(1) 'none of the zeroes of G (i.e., roots of $G=0$) is real and positive. Therefore, Z_k the roots of G are complex'. But for the above inference the non-existence of negative real roots is to be demonstrated.

(2) $\rho(V, Z) = \frac{\bar{N}}{V}$ and $\frac{\bar{N}}{V}$ is a constant $< \infty$. Hence changes continuously with Z for any V . Unfortunately boundedness and continuity are not identical concepts in function theory.

(3) $\frac{P(T, Z)}{kT} = \lim_{V \rightarrow \infty} G$. " $\frac{P}{kT}$ in equation (7) is a continuous and monotonically increasing function of the activity Z . This means that G is an analytic function of Z for all Z in the complex plane and $\frac{1}{V} \log G$ is an analytic function". What is precisely meant by 'analytic function' here is not clear. In ordinary mathematics, a continuous, monotonically increasing function is not necessarily analytic.

Many topics have been reported without due care to explaining the important modern concepts and the working with them. So the book will be useful as a source of some information but will not help one to acquire the mastery in the subject. Of course, the references of some original works given in the book may be helpful to those who really want to learn the subject.

However, the author and the publisher deserve congratulation for making a book on higher physics like this available to our students.

M. D.

ADVANCES IN PLASMA PHYSICS. VOL. I—Edited by A. Simon and W. B. Thompson, Interscience Publishers, 1968, pp. 340, Price \$ 14.95.

Plasma physics has developed in a number of fields, viz., controlled thermonuclear research, astrophysics, space science, direct conversion, ion propulsion, solid state etc., which are apparently quite distinct and unrelated. There is, however, a connecting link in the common plasma phenomena, and one would agree with the editors that more of inter-field communication than existing at present is very desirable. The book, prepared in this context, contains three review articles on plasma instability and one each on radiation from plasma, magnetosphere and magnetohydrodynamics.

In the first article entitled 'Radiation from Plasma' J. M. Dawson discusses the emission and absorption of radiation by a plasma in the absence of a magnetic field. An interesting feature is provided by the section on the scattering and coupling of waves by density fluctuations.

An article by H. P. Furth deals with the minimum-average-B stabilization for eliminating hydromagnetic flute instabilities and other flutelike modes. It gives the advantages of the stabilizing process, describes the main configurations having the minimum-average-B property, presents some experimental results and discusses the possibility of using the stabilization in controlled fusion research. Drift waves and drift instabilities are covered by N. A. Krall. The derivation of the dispersion relation for an inhomogeneous plasma is followed by a discussion of drift modes as well as uniform plasma modes modified by drifts. The effect of collisions on drift motions in producing instability is considered. A thermodynamic approach to plasma instability is treated by T. K. Fowler. The concept of free energy (i. e., the energy in a plasma, which can be transferred to fluctuations) is developed with regard to both unbounded and bounded plasmas, and the usefulness of the concept in making intuitional assumptions for experimental data is illustrated.

F. L. Scarf describes the structure of the magnetosphere and discusses the presence of thermal plasma, energetic particles and waves in it, a considerable portion of the material being collected from the Journal of Geophysical Research; a number of data obtained by artificial satellites are furnished.

The longest article in the book is by T. R. Brogan on the plasma MHD power generator. It starts with a broad and informative introduction, describes the electrical properties of seeded working fluids, and gives the design and performance of different kinds of MHD generators. Due emphasis is placed on certain topics such as superconducting field coils and rocket-driven MHD generators.

While congratulating the editors of the book for presenting the developments of plasma physics in several different contexts in one volume, one feels that the purpose of the book would have been better served if it could, through the articles, give exposition to the interconnections between the various types of plasma study and the possibility of their cross-fertilization.

J. B.

ELECTRON WAVES AND RESONANCES IN BOUNDED PLASMAS—by P. E. Vandenplas. John Wiley & Sons, Inc., New York, 1968. Pp. xiv+222. Price \$ 11.50.

The development of plasma physics has, up to now, been characterised by a greater emphasis on theory than on experiments. In this context the book by Prof. Vandenplas on the interaction of bounded plasmas and electromagnetic radiation is of special significance in the sense that it deals with an aspect of plasma physics, in which both theoretical and experimental investigations have been carried out and detailed comparison between theoretical derivations and observational data is possible. The treatment is restricted to the cases for which the motion of ions is neglected and the Poynting vector of the incident electromagnetic wave is perpendicular to the axis of the system.

The book starts with a brief review of the basic concepts and general experimental techniques. The discussion is highlighted by a critical assessment of the moments method. However, the review is not quite comprehensive, for example, the microwave bridge technique is not at all mentioned.

The model of a condenser with infinite plates and with its vacuum dielectric partially replaced by a uniform plasma slab is studied, using fluid theory, in the cold and hot plasma limits. Some relevant experiments are described and the behaviour of high frequency plasmons is explained. The linearized Vlasov's equation is solved to give the impedance of a plasma slab. Next, the hollow cylindrical plasma is investigated and it is shown that average plasma densities can be obtained by the main resonances of cylindrical structures. The effects of asymmetry in the hollow structures are also discussed.

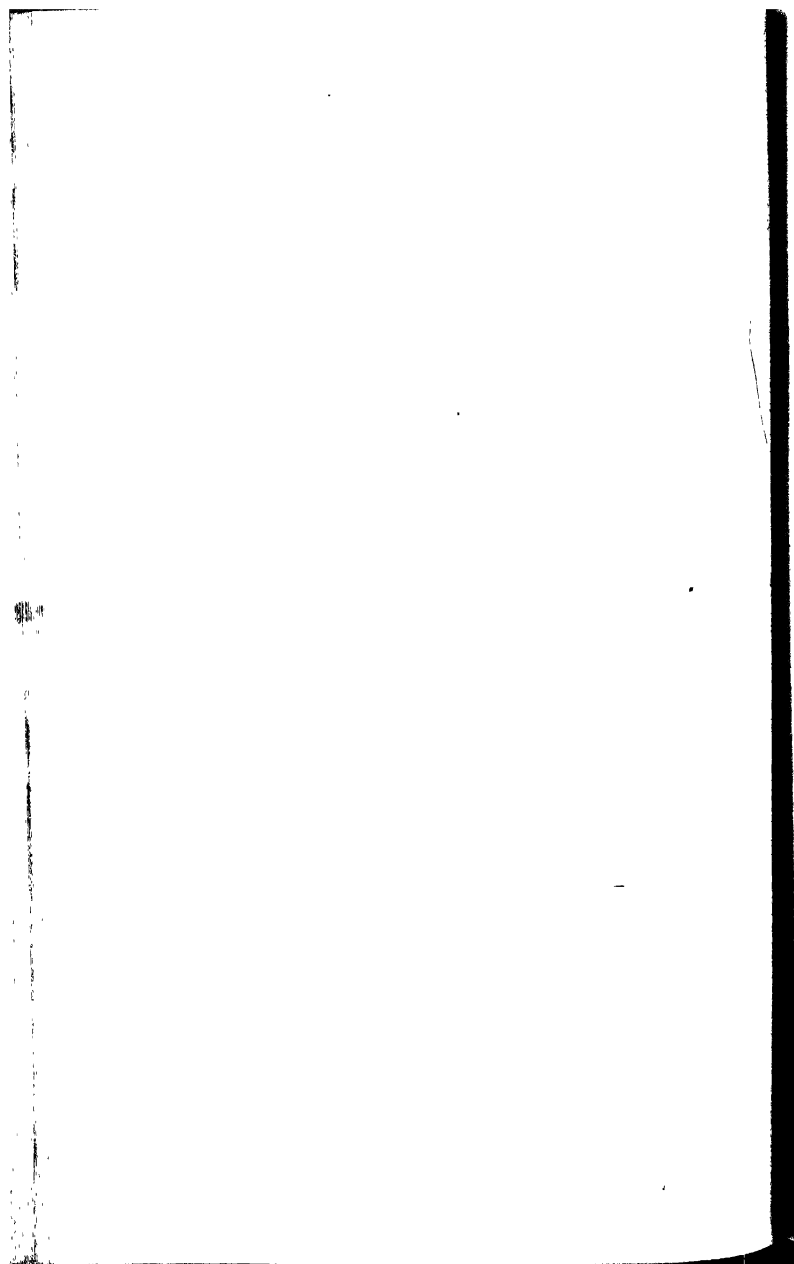
The scattering of a plane electromagnetic wave by a magnetized cold plasma column is studied, particular reference being made to the configurations in which the magnetic field is either parallel or perpendicular to the axis. It is worth noting that the high frequency effect due to axial velocity of the plasma column is also covered. This is followed by an investigation on the hot non-uniform plasma column, which reveals the temperature or secondary resonance spectrum. The influence of a steady magnetic field is mentioned. Non-linear effects connected with temperature resonances as well as resonances of a cold plasma are discussed.

Finally, it is shown how the resonance properties of plasma systems are used in plasma diagnostic techniques, namely the metallic and dielectric resonance probes, and in the study of resonant radiation by plasma-dielectric coated antennas. There is an interesting section on general considerations relating to resonances and anti-resonances of cold plasma systems.

The monograph serving as an introduction to an important branch of plasma physics would be of considerable help to research workers intending to enter this field.

J. B.

$$\begin{array}{r} 112 \\ 51 \\ \hline 61 \\ \hline \end{array}$$



Matrix elements of the 1.492 MeV beta transition in ^{140}Eu .

By K. B. APPALACHARYULU*, D. L. SASTRY AND S. JNANANANDA

The Laboratories for Nuclear Research, Andhra University, Waltair, India,

(Received December 23, 1968)

The angular correlation of the $3^- \xrightarrow[1.492\text{MeV}]{\beta} 2^+ \xrightarrow[0.343\text{MeV}]{\gamma} 0^+$ cascade in ^{140}Eu decay was measured as a function of beta energy in the region 950-1400 keV. The present angular correlation results were combined with those on spectrum shape factor and beta-gamma circular polarization available from previous works to determine nuclear matrix elements governing the 1.492 MeV beta transition in ^{140}Eu . The analysis was conducted on a CDC 3600 type computer employing the exact electron radial wavefunctions and taking into account the finite nuclear size effects. A comparison of the matrix elements obtained here with those determined by earlier workers who used the approximate formulae of

Kotani, has shown that the present value of $\int \frac{\vec{r}}{\rho}$ is enhanced considerably, while the

values of the other vector matrix elements are in agreement with the previous results

within experimental errors. Experimentally determined ratio of the $\int \frac{\vec{r}}{\rho}$ to $\int \frac{\vec{r}}{r}$ matrix

elements is found to be 16.0 ± 5.0 , which is not in agreement with the CVC prediction. The energy dependence of the circular polarization of the 343 keV gamma radiation is also predicted at an angle of 157° consistent with the matrix elements reported here.

1. INTRODUCTION

Nuclear matrix elements governing the non-unique first forbidden beta transitions have been determined from a knowledge of the various experimental observables using the approximate formulae due to Kotani, 1959. The formalism of Kotani was based on the point size nucleus assumption and thus higher order terms were neglected so as to facilitate an easy analysis. It has been, however, pointed out (Bühning 1963a, 1963b, 1965) that one cannot neglect the higher order terms in the multipole expansion if the usual first forbidden matrix elements are unusually small. In recent years, the availability of Bhalla and Rose tables (Bhalla & Rose 1962) for the parameters of the exact electron radial wavefunctions and the beta decay formalism due to Bühning including the higher order terms, have enabled an accurate analysis of the experimental data for finding the matrix elements. Such an attempt was made to analyze some $3^- \rightarrow 2^+$ beta transitions in Ga^{78} and La^{140} (Newsome & Fischbeck 1964) and La^{140} (Singru *et al* 1966). Simms, (1964,) has arranged the various theoretical expressions for beta decay observables in a convenient form for the analysis of $2^- \rightarrow 2^+$

*Present address : Research & Development Division, Sindri (Bihar) India,

beta transitions in ^{84}Rb and ^{86}Rb . Singru *et al* 1966 have adopted the same procedure in the case of ^{140}La . The findings of the various authors appear to justify the importance of finite nuclear size effects and the usage of exact expressions for the evaluation of matrix elements.

The decay scheme of ^{152}Eu is well established and is shown in figure 1. The 1.492 MeV beta transition ($3^- \rightarrow 2^+$) in ^{152}Eu decay has been the subject of study by various authors. The features of this transition are a high log ft value 12.2 (Nathan & Hultberg 1959, Schneider 1960), a large spectrum shape deviation (Langer & Smith 1960) and a large beta-gamma anisotropy (Feschbeck & Wilkinson 1960, Bhattacharjee & Mitra 1960,

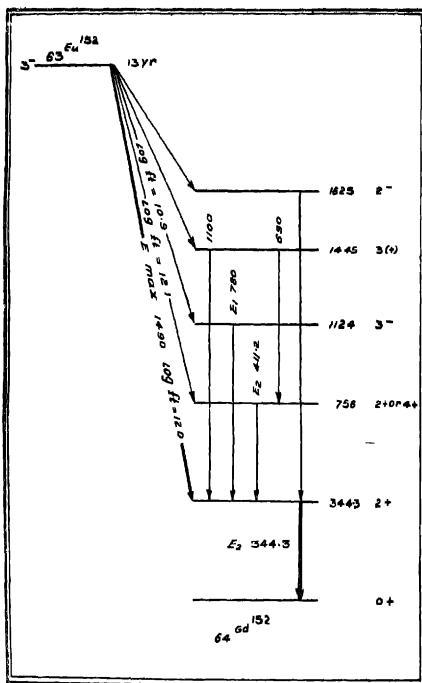


Figure 1 : Decay scheme of ^{152}Eu .

Dulaney *et al* 1960 and Alexander & Steffen 1962). Many authors (Bhattacharjee & Mitra 1960, Alexander 1962, Dulaney *et al* 1964 Lipnik & Sunier 1964) have extracted matrix elements that characterize the 1.492 beta transition of ^{152}Eu from a knowledge of the experimental observables and using the approximate expressions of Kotani. The present work is undertaken to investigate the matrix elements governing the same beta transition in ^{152}Eu , employing the electron radial wave functions of Bhalla and Rose and taking into account the finite nuclear size effects. The procedure adopted for the extraction of matrix elements was due to Simms (1965). We have also, incidentally, measured the energy dependence of angular correlation of 1.492 (β) — 0.343 MeV (γ) cascade in ^{152}Eu (figure 1) with our correlation set-up. The present data on angular correlation were combined with the data on spectrum shapefactor (Langer 1960) and beta-gamma circular polarization correlation (Alexander 1962) for finding the matrix elements. The analysis for the matrix elements was carried out on the CDC 3600 computer at Tata Institute of Fundamental Research, Bombay. The present results are compared with those of earlier workers who followed Kotani's formalism. The energy dependence of the circular polarization of the 0.343 MeV gamma following the beta at 157° is also predicted consistent with the present values of matrix elements, so as to facilitate a comparison as and when the experimental data on this function are available.

2. EXPERIMENTAL

The europium-152 source was obtained as liquid EuCl_3 in HCl from the Atomic Energy Establishment, Harwell (U. K.). A drop of liquid was deposited on a mylar film of thickness 0.6 mg/cm² for the present experimentation. The angular correlation of the $3^- \xrightarrow{\beta} 1^-_{1.492\text{MeV}} 2^+ \xrightarrow{\gamma} 0^+_{0.343\text{MeV}}$ cascade was measured with a fast-slow scintillation spectrometer described earlier (Rao *et al* 1965, Rao *et al* 1966) as a function of beta energy in the range 950-1400 keV. All the usual corrections were applied to the observed data and the differential correlation coefficients $\epsilon(\omega)$ in their final form are shown in figure 2 as a function of beta energy. These results are in substantial agreement with those reported by Alexander (1962).

3. ANALYSIS

The experimental data used for the determination of matrix elements are shown in figures 2, 3 and 4. The shape-factor $C(W)$ and the beta-gamma circular polarization $P_\gamma(\theta)$ functions shown in figures 3 and 4 were

taken from Langer (1960) and Alexander (1962) respectively. The search for the matrix elements which gave the best fit to all the experimental data, simultaneously, was made on the CDC 3600 computer.

One finds the relevant details concerning the extraction of matrix elements in several earlier papers (Newsome & Fischbeck 1964, Simms 1965) and so these are not given here again. The $3^- \rightarrow 2^+$ beta transition is caused by three matrix elements of rank 1 and one matrix element of rank 2. The matrix element parameters in Kotani's notation are given below :

$$\left. \begin{aligned} z &= C_A \int B_{ij}, & \rightarrow \lambda=2 \\ y &= \frac{-C_V \int \vec{\alpha}}{C_A \int B_{ij}} \\ x &= \frac{-C_V \int \vec{r}}{C_A \int B_{ij}} \\ u &= \frac{C_A \int \vec{\alpha} \times \vec{r}}{C_A \int B_{ij}} \end{aligned} \right\} = 1$$

The rank 1 matrix elements expressed above are relative to z .

$Y = \xi' y - \xi(x+u)$, a linear combination of rank 1 matrix elements. ξ' distinguishes the relativistic matrix elements from the nonrelativistic ones. And $\xi' \approx \xi$. The computer analysis was made for x , u and Y using the data shown in figures 2, 3 and 4. The standard matrix element can be known from the logft value of the beta transition and hence the absolute values of the rank 1 matrix elements can be calculated.

The parameters of the electron radial wave function that would occur in the expressions for $\epsilon(W)$, $C(W)$ and $P_\gamma(\theta)$ were determined using the Bhalla and Rose tables. In the first instance a coarse search was made for x , u and Y to know the approximate range of each parameter that explained all the experimental data, simultaneously. Afterwards a fine search was made in steps of 0.01 to get well defined solutions. The criterion for the acceptance of each solution was decided by the χ^2 test of the experimental data. The computer was instructed to print out only these sets of matrix element parameters yielding values of $\epsilon(W)$, $C(W)$ and $P_\gamma(\theta)$ that agreed with the experimental results with a more than 30% probability. Thus finally the following ranges consistent with the

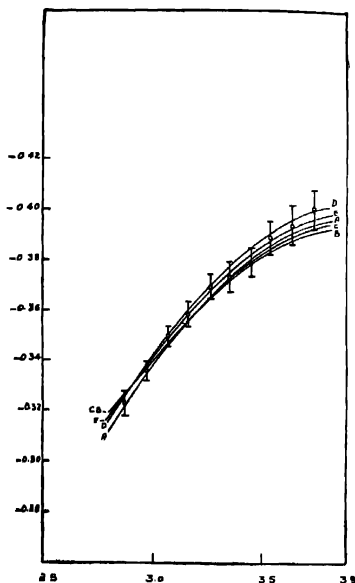


Figure 2: β - γ angular correlation function $e(W)$ as a function of beta energy (m_0c^2 units). The points with vertical flags represent the experimental values. The curves are the theoretically predicted functions for the sets of matrix element parameters given in table 1.

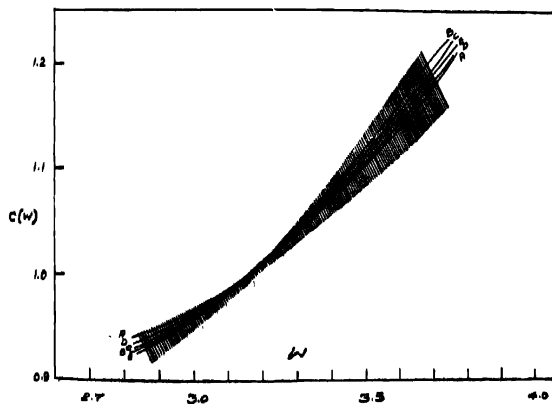


Figure 3: The experimental shape of $C(W)$ function taken from Langer (1960). The shading indicates the errors while solid lines are the energy dependence generated by the matrix element parameter sets given in table 1.

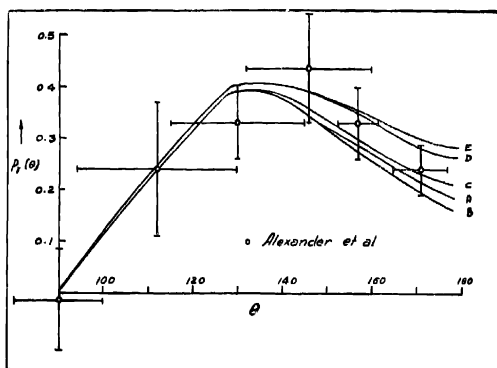


Figure 4 : The experimental data on β - γ circular polarization correlation taken from Alexander (1962), at E_β (average) = $3.2 (m_0 c^2)$ units. The solid lines are the theoretical $P_\gamma(\theta)$ generated by the matrix element parameter sets given in table 1.

experimental data shown in figures 2, 3 and 4 were obtained.

$$z = 1.00$$

$$0.47 \leq x \leq 0.58$$

$$0.08 \leq u \leq 0.00$$

$$0.60 \leq Y \leq 0.85.$$

Some sets of matrix element parameters are given in table 1 and the corresponding theoretical functions $\epsilon(W)$, $C(W)$ and $P_\gamma(\theta)$ are shown in figures 2, 3 and 4, respectively. From these figures one finds a good agreement between the theoretical and experimental values.

The prediction of the energy dependence of the 1.492 MeV beta - 0.343 MeV gamma circular polarization correlation was also included as a part of the computer programme, for each satisfactory set of parameters. In figure 5, the behaviour of $P_\gamma(W)$ at $\theta=157^\circ$ is shown as a function of beta energy for each of the sets given in table 1. An experiment of this kind may be helpful to obtain more well defined ranges for x , u and Y .

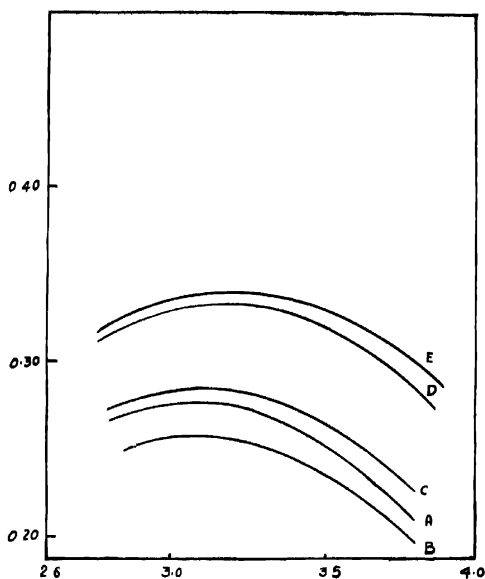


Figure 5: The theoretically predicted energy dependence of $\beta\gamma$ circular polarization $P_\gamma(W)$ at $\theta = 157^\circ$ shown as a function of beta energy for different sets of matrix element parameters given in table 1.

TABLE 1. SOME SETS OF MATRIX ELEMENT PARAMETERS WHICH GIVE THE BEST FIT TO THE EXPERIMENTAL DATA. $Z = 1.0$

Designation.	γ	x	u
A	0.65	0.55	0.08
B	0.66	0.56	0.04
C	0.70	0.56	0.05
D	0.74	0.53	0.04
E	0.79	0.52	0.01

TABLE 2. ABSOLUTE VALUES OF MATRIX ELEMENTS GOVERNING THE
1.492 MEV BETA TRANSITION OF ^{162}Eu

Reference.	$\frac{ \int B_{17} }{\rho}$ ($\times 10^3$)	$\frac{ \int \uparrow }{\rho}$ ($\times 10^3$)	$\frac{ \int \vec{\sigma} \times \uparrow }{\rho}$ ($\times 10^3$)	$ \int \vec{\sigma} $ ($\times 10^3$)
Present results.	3.1 ± 0.4	2 ± 0.2	0.13 ± 0.13	0.51 ± 0.17
Alexander, 1962.	2.9 ± 0.4	0.43 ± 0.25	0.36 ± 0.19	0.25 ± 0.11

The theoretical ratio Λ_{CVC} of the vector matrix elements $i\vec{\sigma}$ to \uparrow based on the conserved vector current hypothesis as derived by Fugita (1962), is

$$\Lambda_{CVC} = \frac{1.2\alpha Z}{\rho} + (W_0 - 2.5)$$

$$= 2.4\frac{\alpha}{\rho} + (W_0 - 2.5)$$

(α is the fine structure constant, Z is the charge of the daughter nucleus and ρ is the nuclear radius); for ^{162}Eu $\xi = 13.53$ and $\rho = 1.7 \times 10^{-2}$ natural units. Thus one gets Λ_{CVC} (theoretical) = 33.0 for the present beta transition.

Λ_{CVC} (experimental) obtained from the values of x , u and Y is 16.0 ± 5 . Thus one sees no agreement between the experimental and theoretical values of Λ_{CVC} . The experimental value of Λ that follows from Kotani's expressions was found to be in agreement with the theoretical one within experimental errors as reported by Alexander (1962). However, the error limits of this work are very wide. The experimental value of Λ for a similar transition in ^{140}La is also reported to be not in agreement with the theoretical prediction (Singru *et al* 1966). The inclusion of third forbidden matrix elements in the analysis might bring the experimental OVC ratio into agreement with the theoretical one. However, the analysis of beta transitions including the third forbidden matrix elements is rather a difficult task as they introduce a separate energy dependence of the observables. Further, it is doubtful how far the present experimental accuracies warrant the inclusion of third forbidden matrix elements in the beta decay theory.

4. ABSOLUTE VALUES OF THE MATRIX ELEMENTS.

The standard matrix element $C_A \int B_{ij}$ can be evaluated using the log f value of the 1.492 MeV beta transition of ^{153}Eu , from the relation

$$|C_A \int B_{ij}|^2 = \frac{\pi^2 \ln 2}{f_0 t}$$

where $f_0 t$ is the corrected value for the non-statistical shape of the beta spectrum. $f_0 t = 10^{11.9}$ for the present beta transition. Thus one gets $\int B_{ij} = 5.2 \pm 0.7 \times 10^{-5}$ natural units. Finally, one gets the absolute values of the vector matrix elements from a knowledge of x , u , Y and $\int B_{ij}$. In order to have a more significant comparison, the matrix elements containing r were divided by the nuclear radius ρ and are given in table 2 along with those of Alexander & Steffen (1962), whose values, in a way, represent all the earlier works.

5. DISCUSSION.

From table (2) it can be seen that the present value of \vec{r}/ρ is considerably enhanced while $\vec{\sigma}$ and $\vec{\sigma} \times \vec{r}/\rho$ values agree within experimental errors with the previous results. However the large uncertainties in the values of matrix elements do not allow a significant comparison. It also shows the masking of higher order effects by the large experimental errors in different observables. For the present case an experiment on the energy dependence of $\beta\gamma$ circular polarization will be helpful to narrow down the limits of matrix elements reported here. For this the theoretical energy dependence of $\beta\gamma$ circular polarization correlation functions given in this work will be helpful for a future experimenter to compare the experimental results with the theoretical predictions.

The values of rank one matrix elements suggest that one cannot apply the modified B_{ij} approximation (Kotani 1959) to the 1.492 MeV beta transition of ^{153}Eu , which requires x and u to vanish. The B_{ij} value characterizing the present beta transition has of course suffered less reduction in size than the rank one matrix elements. The same conclusion follows from the previous values of the matrix elements also. Finally it may be concluded from the present value of $\int \frac{\vec{r}}{\rho}$ that it is important

to take into account the finite nuclear size effects in beta decay theory for the determination of matrix elements. However, the full advantage of the inclusion of higher order effects in the theory may not be derived unless the experimental accuracies improve.

REFERENCES

- Alexandar, P. & Steffen, R. M. 1962 *Phys. Rev.* **128**, 1783.
Bhalla, C. P. & Rose, M. E. *Oakridge National Laboratory, Report No. ORNL-3207*.
Bhattacharjee, S. K. & Mitra, S. K. 1960 *Nuovo Cimento*, **16**, 175.
Bühring, W. 1963a *Nucl. Phys.* **40**, 472.
Bühring, W. 1963b *Nucl. Phys.* **49**, 190.
Bühring, W. 1965 *Nucl. Phys.* **61**, 110.
Dulaney, H., Braden, C. H. & Wyly, L. D., 1960 *Phys. Rev.*, **117**, 1092
Dulaney, H., Braden, C. H. & Wyly, L. D., 1964 *Nucl. Phys.*, **52**, 79.
Fischbeck, H. J., & Wilkinson, R. G. 1960 *Phys. Rev.*, **120**, 1762.
Fujita, J. J. 1962 *Phys. Rev.* **126**, 202.
Kotani, T., 1959 *Phys. Rev.*, **114**, 795.
Langer, L. M., & Smith, D. R., 1960 *Phys. Rev.*, **119**, 1308.
Lipnik, P. & Sunier, J. W., 1964 *Nucl. Phys.* **53**, 305.
Nathan, O. & Hultberg S, 1959 *Nucl. Phys.* **10**, 118.
Newsome, R. W., & Fischbeck, H. J., 1964 *Phys. Rev.* **133 B**, 273.
Rao, W. V. S., Rao, V. S., Sastry, D. L. & Jnanananda, S, 1965 *Phys. Rev.* **140**,
B 1193.
Rao, W. V. S, Rao, K. S. Sastry, D. L. & Jnanananda, S. 1966 *Proc. Phys. Soc.*,
87, 917.
Schneider, W. 1960 *Nucl. Phys.* **21**, 55.
Simms, P. C., 1965 *Phys. Rev.* **138 B**, 784.
Singru, R. M., Simms, P. C. & Steffen, R. M. 1966 *Phys. Rev.* **141**, B 107.

A new phase-meter using a thyatron,

By S. Roy

Physics Department, K. M. College, Delhi University, Delhi-7.

(Received December 18, 1968)

A thyatron tube which is used as a phasemeter shows a fair possibility of measuring varying phase difference between two constant voltages, although the instrument can be adapted for other measurements. An approximate analytical expression relating the average rectified current (I) and the phase difference (θ) has been obtained. The limitations of the instrument have been pointed out.

1. THEORY

Let us suppose that an alternating voltage of considerable magnitude is applied to the plate and a relatively smaller alternating voltage is applied to the grid of the thyatron.

The plate current (i) can only flow, if at all, during a fraction of the positive half-cycle of the plate voltage and it starts when the instantaneous grid voltage (e_g) goes just more positive than the critical (cut-off) value corresponding to the instantaneous plate voltage (e_p). Once started the plate current (i) is independent of the grid voltage and tends to jump to the full emission of the cathode even with a very low plate voltage of the order of 15 volts. i is however, limited by the resistance (R) in the plate circuit and remains substantially constant during the conducting period of the tube. It stops only when e_p falls below the value at which the ionisation can no longer be maintained in the tube.

To understand the dependence of I , the average rectified current, on the phase relation between the plate and grid voltages, let us suppose at first that the phase-difference (θ) between the two voltages is zero. Under this condition the grid and the plate go positive simultaneously and conduction starts almost at the start of the positive half cycle. On the other hand, if

$\theta = \pi$, the grid goes negative as the plate goes positive, and the conduction starts, if at all, rather late in the cycle. It is so because e_p must attain a certain magnitude before it can start the conduction overcoming the biasing effect of e_g .

With proper adjustment of the relative magnitudes of the two voltages ($E_g > E_p/\mu$) the tube may not conduct at all. This can be done with the help of a potentiometer P_1 in the grid circuit (figure 2).

It is obvious that although the starting point ϕ of the conduction period depends on θ , the extinction point does not. Therefore, the conduction period depends on θ , being greater as θ becomes smaller. An ammeter included in the plate circuit reads I which increases with decreasing θ .

A rough estimation of I can be done by assuming i to remain substantially constant and that conduction starts only when e_g is more positive than the cut-off bias for e_p (as in the case of high-vacuum tube).

Let $e_p = E_p \sin \omega t$ and $e_g = E_g \sin (\omega t - \theta)$, then $e_p/\mu + e_g$ must be zero for the initiation of i , where μ is the amplification factor of the tube. Then,

$$E_p \sin \omega t + \mu E_g \sin (\omega t - \theta) = 0$$

$$\text{or } \sin \omega t (E_p + \mu E_g \cos \theta) - \cos \omega t (\mu E_g \sin \theta) = 0.$$

Putting $E_p + \mu E_g \cos \theta = R \cos \phi$; and $\mu E_g \sin \theta = R \sin \phi$ the equation reduces to $R \sin (\omega t - \phi) = 0$... (1).

Therefore, either $R=0$ or $\sin (\omega t - \phi) = 0$.

$$\text{where, } \phi = \tan^{-1} \frac{\mu E_g \sin \theta}{E_p + \mu E_g \cos \theta} \text{ and } R = \{E_p^2 + \mu^2 E_g^2 + 2\mu E_p E_g \cos \theta\}^{1/2}$$

But $R=0$, only when $E_p = \mu E_g$ and $\theta = \pi, 3\pi \dots$;

whereas, $\sin (\omega t - \phi) = 0$, when $(\omega t - \phi) = 0, \pi, 2\pi \dots$

If E_g is adjusted with the help of P_1 so that $\mu E_g = E_p$,

$$\text{we get, } \phi = \tan^{-1} \tan \frac{\theta}{2} \quad \text{or } \phi = \frac{\theta}{2}. \quad (2)$$

This shows that the initiation of the current takes place when $\omega t = \phi = \theta/2$. If the extinction takes place, for the given tube, at $\omega t = \alpha$, this can be determined from the knowledge of extinction potential and E_p . Therefore I is given by

$$I = \int idt/T = i \int_{\phi/\omega}^{\alpha/\omega} \left| \frac{dt}{dt} \right| 2\pi/\omega = i(2\alpha - \theta)/4\pi \quad (3)$$

(provided i is constant)

The equation 3 shows that I varies linearly with θ . The maximum theoretical limit of θ are given by 2α and the minimum by 0. Actually, however, these are of theoretical interest as there is no point in measuring the phase difference which is greater than π . This will be equivalent to interchanging the leading phase into lagging phase and vice-versa.

2. DISCUSSIONS

The equation 3 holds only under the condition $E_p/\mu = E_g$ and therefore, the relative magnitudes of E_p and E_g must be maintained. The plate current also depends to a small extent on the absolute value of E_p , therefore E_p should be constant. Both the voltages may be made constant with the help of suitable potential dividers.

It is, however, possible to calibrate the instrument with any particular ratio (greater than 1) of E_p to E_g and to maintain the relative and absolute values of the voltages constant thereafter.

For $\theta = \pi$, if E_g is slightly smaller than E_p/μ then the conduction will start at $\omega t = \pi/2$ and I is given by $i(2\alpha - \theta)/4\pi$ (equation 3).

With this value of θ , if E_g is increased and just crosses E_p/μ no conduction is possible and I reduces to zero. Under this condition equation 2 is only approximately valid and ϕ will be greater than $\theta/2$. $I - \theta$ graph is again nearly linear but equation 3 no longer represents it accurately. At $\theta = \pi$ there is sharp fall to zero. This fall is not so much due to ϕ approaching and becoming equal to α (i.e. smaller conduction period) but due to no conduction at all, at this relative magnitudes of E_g and E_p . The relation between $I - \theta$ is shown by graph I in figure 1.

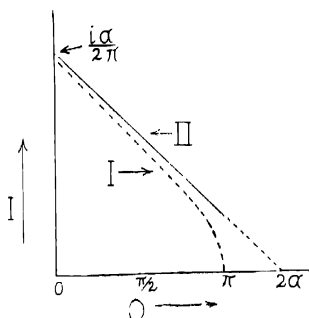


Figure 1. The graphs showing $I-\theta$ relationship.

Graph I E_g just greater than E_p/μ .

Graph II E_g just smaller than E_p/μ .

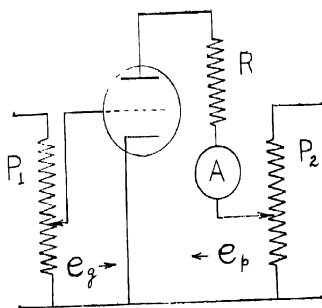


Figure 2. A thyratron phasemeter.

It would appear from above that $E_g = E_p/\mu$ is a critical condition.

It is to be noted that if the voltage applied to the grid is leading in phase (θ leading) then equation 1 ceases to have any meaning and $\sin(\omega t + \phi) = 0$, if both ωt and ϕ are equal to zero. Physically it is clear that as there cannot be any conduction during the negative half cycle of the plate voltage (i. e., ϕ cannot be negative), the discharge can only start at $\phi = 0$, whatever be the value of θ . Therefore I has the same magnitude for almost all leading angles. This is a major defect of the instrument. It is also to be noted that no consideration of R has been taken in the above treatment.

3. EXPERIMENTAL

The phasemeter is shown in figure 2. It has two potentiometers P_1 and P_2 in the grid and the plate circuit respectively, to control the relative values of the plate and grid voltages. In the preliminary test a gastube 885 was used with approximately 110 volts at the plate and 22 volts on the grid. With E_g just smaller than E_p/μ , θ (lagging) could be measured quite elegantly from 10° to about 180° . The range could be probably extended beyond 180° as the equation 3 predicts, but this could not be verified as a proper phase-shifter was not available. Within the range mentioned the $I-\theta$ relation follows closely the graph II in figure 1, which is the graph for the equation 3. Although only power-frequency was tried with, it is obvious that the frequency range can be extended from below the power frequency to about 10 kc/s for Hg. vapour tubes and to 50 kc/s for light-gas tubes, the maximum frequency being limited by the recombination period of the gas ions after the voltage fall.

4. CONCLUSION

The author has investigated the possibility of using a thyatron as a phasemeter. The preliminary test justifies the attempt. The instrument is however not perfect and there is a lot of scope for improvement and modification. Certain modifications are being contemplated.

The author is thankful to Prof. R. C. Majumdar, Ph.D., F.N.I., Pro-Vice-Chancellor, Delhi University for constant encouragement.

On elastic morse scattering

By K. D. KRORI

Mathematical Physics Forum Cotton College, Gauhati-1

Assam, India

AND

KRISHNA SEN GUPTA*

Pandu College, Pandu, Assam

(Received November 8, 1966, Resubmitted April 9, 1968)

Some calculations have been presented here on elastic scattering by Morse potential by some well-known methods. The influence of Coulomb field on Morse scattering has been discussed in the first approximation and the Schrodinger equation for S-wave scattering also solved rigorously.

1. INTRODUCTION

We propose to present here some calculations on elastic scattering by Morse potential by some well-known methods. In order to explain the spectra produced by diatomic molecules, Morse (1929) introduced the atomic potential

$$V(r) = V_0 \{1 - e^{-\alpha(r-r_0)}\}^2 \quad \dots(1)$$

We shall not, however, adopt this form in our discussions. The following equivalent form (Landau & Lifshitz, 1958) will be used,

$$V(r) = V_0 \{e^{-2\alpha(r-r_0)} - 2e^{-\alpha(r-r_0)}\} \quad \dots(2)$$

Here r_0 is the distance where the potential is minimum, $-V_0$. α gives a measure of the range of the potential. Evidently, Morse potential is a short-range potential.

2. SCATTERING AMPLITUDE

In the first Born approximation, the scattering amplitude is given (Kursunoglu 1962, Mott & Massey 1949) by,

$$\begin{aligned} f(\theta) &= -\frac{2m}{K^2} \int_0^\infty r \sin Kr \cdot V_0 \left(e^{-2\alpha(r-r_0)} - 2e^{-\alpha(r-r_0)} \right) \\ &= -\frac{8mV_0\alpha}{K^2} \left[\frac{e^{2\alpha r_0}}{(K^2 + 4\alpha^2)^2} - \frac{e^{\alpha r_0}}{(K^2 + \alpha^2)^2} \right] \quad \dots(3) \end{aligned}$$

* Present address : Department of Theoretical Physics, University of Delhi Delhi (India).

where m is the reduced mass and $K = 2k \sin \theta/2$, k being the momentum and θ the angle of scattering.

Now we consider two extreme cases (subject to the validity discussed in the next section) :

(a) For $K/\alpha \gg 1$

$$f(\theta) = - \frac{8mV_0\alpha}{\hbar^2 K^4} \left[e^{2\alpha r_0} - e^{\alpha r_0} \right] \quad \dots(4)$$

$$\text{i.e. } f(\theta) \propto \frac{1}{k^4 \sin^4 \theta/2} \quad \dots(5)$$

It appears that in this case, $f(\theta)$ diminishes very rapidly with k and $\sin \theta/2$.

(b) For $K/\alpha \ll 1$

$$f(\theta) = \text{constant.} \quad \dots(6)$$

This means that scattering is isotropic under this condition.

Finally, we consider Morse scattering in presence of Coulomb field. Replacing the incident plane wave function by Coulomb wave function in the first Born approximation (Messiah, 1961), we obtain for the scattering of an ion by an ion,

$$F(\theta) = - \frac{2m}{4\pi\hbar^2} \int_0^\infty e^{-ikr} V(r) e^{i[kr + \gamma \log k(1-z)]} d^3r$$

$$\text{where, } \gamma = \frac{mZZ'e^2}{\hbar k} ; Z, Z'e \text{ being the charges of the ions.} \quad \dots(7)$$

On calculation (Copson 1955), it appears that due to the presence of Coulomb field, phase changes and that we obtain for the intensity of scattering,

$$|F(\theta)|^2 = \left(\frac{2mV_0}{\hbar^2} \right)^2 (1+\gamma^2) \left(\frac{2\pi\gamma e^{\pi\gamma}}{e^{2\pi\gamma}-1} \right) [A^2+B^2] \quad \dots(8)$$

where, $A = e^{2\alpha r_0} (\cos \rho \sin 2\phi \cosh \gamma\phi + \sin \rho \cos 2\phi \sinh \gamma\phi)$

$$- 2e^{\alpha r_0} (\cos \sigma \sin 2\psi \cosh \gamma\psi + \sin \sigma \cos 2\psi \sinh \gamma\psi),$$

$$B = e^{2\alpha r_0} (\cos \rho \sin 2\phi \cosh \gamma\phi - \sin \rho \cos 2\phi \sinh \gamma\phi)$$

$$- 2e^{\alpha r_0} (\cos \sigma \sin 2\psi \cosh \gamma\psi - \sin \sigma \cos 2\psi \sinh \gamma\psi),$$

with $\phi = \tan^{-1} (K/2\alpha)$, $\psi = \tan^{-1} (K/\alpha)$

$$\rho = \frac{\gamma}{2} \log (4\alpha^2 + K^2), \sigma = \frac{\gamma}{2} \log (\alpha^2 + K^2). \quad \dots(9)$$

In the absence of Coulomb field, (8) is reduced to the corresponding form given by (3). This also happens for large values of k , i. e. for $\alpha \ll 1$.

3. VALIDITY OF BORN APPROXIMATION

The validity of the above calculations is conditioned (Merzbacher, 1961) by,

$$1 \gg \frac{2m}{\hbar^2 k^2} \left| \int_0^\infty e^{ikr} \sin kr \cdot V(r) \cdot dr \right| \\ = \frac{m}{\hbar^2 k^2} \left| V_0 \right| \left[\left\{ \frac{e^{2\alpha r_0}}{2} \left(\frac{-\alpha}{\alpha^2 + k^2} + \frac{1}{\alpha} \right) - 2e^{\alpha r_0} \left(\frac{-\alpha}{\alpha^2 + 4k^2} + \frac{1}{\alpha} \right) \right\}^2 \right. \\ \left. + \left\{ \frac{e^{2\alpha r_0}}{2} \left(\frac{k}{\alpha^2 + k^2} \right) - 2e^{\alpha r_0} \left(\frac{2k}{\alpha^2 + 4k^2} \right) \right\}^2 \right]^{1/2} \quad \dots(10)$$

For $k/\alpha \gg 1$, from (10) we have

$$1 \gg \frac{m}{\hbar^2 k^2 \alpha} \left\{ \frac{e^{2\alpha r_0}}{2} - 2e^{\alpha r_0} \right\} \quad \dots(11)$$

On the other hand, for $k/\alpha \ll 1$ we have

$$1 \gg \frac{m}{\hbar^2 \alpha^2} \left\{ \frac{e^{2\alpha r_0}}{2} - 4e^{\alpha r_0} \right\} \quad \dots(12)$$

The condition seems to be independent of velocity.

4. PHASE SHIFTS

In the first approximation, we now proceed to compute phase-shifts for S - and P -waves (Roman 1964). For the S -wave, we have

$$\tan \delta_0 \approx -k \int_0^\infty \{j_0(kr)\}^2 V(r) r^2 dr \\ = -\frac{V_0}{2k} \left[\left\{ \frac{e^{2\alpha r_0}}{2\alpha} - \frac{2e^{\alpha r_0}}{\alpha} \right\} \right. \\ \left. - \left\{ e^{2\alpha r_0} \cdot \frac{\alpha}{2(\alpha^2 + k^2)} - 2e^{\alpha r_0} \cdot \frac{\alpha}{\alpha^2 + 4k^2} \right\} \right] \quad \dots(13)$$

Taking k large compared to α ,

$$\tan \delta_0 \approx -\frac{V_0}{4k\alpha} \left\{ e^{2\alpha r_0} - 4e^{\alpha r_0} \right\} \\ \text{i.e., } \tan \delta_0 \propto \frac{1}{k} \quad \dots(14)$$

For the P -wave, we have

$$\begin{aligned}\tan \delta_1 &\approx -k \int_0^\infty \{j_1(kr)\}^2 V(r) r^2 dr \\ &= -\frac{V_0}{k} \left[\frac{1}{2k^2} \left\{ e^{2\alpha r_0} \left(2k \tan^{-1}(k/\alpha) - \alpha \log(4\alpha^2 + 4k^2) \right) \right. \right. \\ &\quad \left. \left. - 2e^{\alpha r_0} (2k \tan^{-1}(2k/\alpha) - \alpha \log(\alpha^2 + 4k^2)) \right\} \right. \\ &\quad \left. - \frac{1}{k} \left\{ e^{2\alpha r_0} \tan^{-1}(k/\alpha) - 2e^{\alpha r_0} \tan^{-1}(2k/\alpha) \right\} \right. \\ &\quad \left. + \frac{1}{2} \left\{ \left(\frac{e^{2\alpha r_0}}{2\alpha} - \frac{2e^{\alpha r_0}}{\alpha} \right) + \left(e^{2\alpha r_0} \cdot \frac{\alpha}{2(\alpha^2 + k^2)} \right. \right. \right. \\ &\quad \left. \left. \left. - 2e^{\alpha r_0} \frac{\alpha}{\alpha^2 + 4k^2} \right) \right\} \right]. \quad \dots(15)\end{aligned}$$

For k very large compared to α , it is found from (15) that δ_1 becomes almost equal to δ_0 .

On the other hand, for low-energy scattering under the condition (Roman 1964), $l > k/\alpha$ we have,

$$\begin{aligned}\tan \delta_l &\approx -\frac{2^{2l}(l!)^2}{[(2l+1)!]^2} k^{2l+1} \int_0^\infty V(r) r^{2l+2} dr \\ &= -\frac{(l!)^2}{(2l+1)} k^{2l+1} \frac{V_0}{\alpha^{2l+3}} \left[\frac{e^{2\alpha r_0}}{8} - 2^{2l+1} e^{\alpha r_0} \right]. \quad \dots(16)\end{aligned}$$

Lastly, we consider Morse scattering in presence of Coulomb field as before. Replacing the spherical Bessel function by spherical Coulomb function in the first approximation (Tiezt, 1965; Messiah 1961), we have for the S -wave phase-shift in this case,

$$\tan \Delta_0 \approx -\frac{V_0}{k} \int_0^\infty \left\{ \sin(kr - \gamma \log 2kr + \xi_0) \right\}^2 V(r) dr$$

where ξ_0 = Coulomb phase-shift

$$\begin{aligned}&= -\frac{V_0}{2k} \left[\left(e^{2\alpha r_0} \frac{1}{2\alpha} - 2e^{\alpha r_0} \cdot \frac{1}{\alpha} \right) \right. \\ &\quad \left. - \left\{ 2 \sqrt{\frac{\pi\gamma}{2 \sinh \pi\gamma}} \cdot \left[\frac{e^{2\alpha r_0 + 2\gamma\eta} \cos(A+x+\eta)}{(4k^2 + 4\alpha^2)^{1/2}} \right. \right. \right. \\ &\quad \left. \left. \left. - 2 \cdot \frac{e^{\alpha r_0 + 2\gamma\xi} \cos(A+y+\xi)}{(4k^2 + \alpha^2)^{1/2}} \right] \right\} \right]\end{aligned}$$

with,

$$\begin{aligned}\eta &= \tan^{-1} (k/\alpha), \quad \zeta = \tan^{-1} (2k/\alpha) \\ x &= \gamma \log (4k^2 + 4\alpha^2), \quad y = \gamma \log (4k^2 + \alpha^2) \\ A &= 2\xi_0 - 2\gamma \log 2k.\end{aligned}\quad \dots(19)$$

In the absence of Coulomb field, the formula assumes the form of (13). Also the same result is obtained for large values of k , i. e., for $\gamma \ll 1$.

5. SCATTERING LENGTH AND CROSS-SECTION

The scattering length is defined (Wu & Ohmura 1962) as

$$\begin{aligned}a &= -\lim_{k \rightarrow 0} \frac{Ll}{k} \approx V_0 \lim_{r \rightarrow \infty} \frac{Ll}{r} = \int_0^{\infty} \{j_0(kr)\}^2 V(r) r^2 dr \\ &= \frac{V_0}{4\alpha^3} e^{2\alpha r_0} \left[1 - 16 e^{-\alpha r_0} \right].\end{aligned}\quad \dots(20)$$

For bound states to be possible, a must be positive (Roman 1964). This means that $16e^{-\alpha r_0}$ must be < 1 . For Cl_2 , for example, this is satisfied. For this case, $r_0 = 1.988 \times 10^{-8}$ cm., $V_0 = 2.475$ ev, $\alpha = 4.048/(1.988 \times 10^{-8})$ so that $16e^{-\alpha r_0}$ is < 1 (Herzberg 1961). For the hydrogen molecule, however, this is not found to be satisfied (Messiah 1961). In this case, $r_0 = 0.74 \times 10^{-8}$ cm, $V = 4.72$ ev, $\alpha = 10^8/(0.68 \times 0.74)$ so that evidently $16e^{-\alpha r_0}$ is > 1 . Because, (20) holds only for weak potentials (Roman 1964).

The zero-energy limit of the total cross-section (Roman 1964) may be obtained from (20) :

$$\lim_{k \rightarrow 0} \sigma = 4\pi a^2 \frac{\pi}{4} \frac{V_0^2}{\alpha^6} e^{4\alpha r_0} \left[1 - 16 e^{-\alpha r_0} \right]^2 \quad \dots(21)$$

For very large α , this becomes

$$= \frac{\pi V_0^2}{4\alpha^6} e^{4\alpha r_0} \quad \dots(22)$$

6. S-WAVE SCATTERING

Lastly we solve the radial wave equation for the S -wave scattering. We write the equation in the form :

$$\frac{d^2\psi}{dr^2} + (k^2 - V(r))\psi = 0 \quad \dots (23)$$

Making the following substitutions

$$\begin{aligned} e^{-\alpha r} &= Z \\ C &= V_0 e^{2\alpha r_0/\alpha^2}, \quad D = 2V_0 e^{\alpha r_0/\alpha^2} \\ \psi &= A e^{-ikr/\alpha} \log z e^{-\beta z/2\alpha} \phi(z) \end{aligned} \quad \dots(24)$$

where β is yet undetermined, we obtain from (23)

$$\begin{aligned} z \frac{d^2\phi}{dz^2} + \left\{ \left(1 - \frac{2ik}{\alpha} \right) - \frac{\beta}{\alpha} z \right\} \frac{d\phi}{dz} + \left[\frac{\beta^2}{4\alpha^2} z - \frac{\beta}{2\alpha} \left(1 - \frac{2ik}{\alpha} \right) \right. \\ \left. - (Cz - D) \right] \phi = 0. \end{aligned} \quad \dots(25)$$

This equation may be taken in the confluent hypergeometric form (Morse & Feshbach 1953) by adjusting the value of β such that

$$\beta^2/4\alpha^2 = C. \quad \dots(26)$$

In that case, (25) has the solution

$$\psi = A e^{ikr} e^{-\beta/2\alpha}(e^{-\alpha r}) \phi \left[\frac{1}{2} \left(1 - \frac{2ik}{\alpha} - \frac{2\alpha D}{\beta} \right) \middle| \left(1 - \frac{2ik}{\alpha} \right) \middle| \frac{\beta}{\alpha} e^{-\alpha r} \right] \quad \dots(27)$$

The most general solution therefore takes the form :

$$\begin{aligned} \psi = e^{-\beta/2\alpha}(e^{-\alpha r}) \left\{ A e^{ikr} \phi_1 \left[\frac{1}{2} \left(1 - \frac{2ik}{\alpha} - \frac{2\alpha D}{\beta} \right) \middle| \left(1 - \frac{2ik}{\alpha} \right) \middle| \frac{\beta}{\alpha} e^{-\alpha r} \right] \right. \\ \left. + B e^{-ikr} \phi_2 \left[\frac{1}{2} \left(1 + \frac{2ik}{\alpha} - \frac{2\alpha D}{\beta} \right) \middle| \left(1 + \frac{2ik}{\alpha} \right) \middle| \frac{\beta}{\alpha} e^{-\alpha r} \right] \right\} \quad \dots(28) \end{aligned}$$

A similar solution for the radial S -wave equation has been obtained by Bhattacharjee & Sudarsan (1962) by a different method for a potential slightly different from (2).

One of the authors (K. D. K.) wishes to express his profound gratitude to the Government of Assam for all facilities provided at Cotton College, Gauhati, Assam and to the University Grants Commission, New Delhi, for all sorts of encouragement in working out this paper.

REFERENCES

- Bhattacharjee, A & Sudarsan, E. C. G. 1962 *Nuovo Cimento*, XXV, N. 4, 16 873-75.
- Copson, E. T. 1935 *Theory of Functions of A Complex Variable*, Oxford University Press, Pp 211-12.
- Herzberg, G. 1961 *Molecular Spectra & Molecular Structure*, Van Nostrand Co., Pp 519.
- Kursunoglu, B. 1962 *Modern Quantum Theory*, Freeman & Co. Pp 449-52.
- Landau, L. D. & Lifshitz, E. M. 1958 *Quantum Mechanics (Non-relativistic Theory)*, Pergamon Press, Pp 68-69.
- Menzelbacher, E., 1961 *Quantum Mechanics*, John Wiley & Sons, Pp 227-29.
- Messiah, A. 1961 *Quantum Mechanics*, Vol-I & II, North-Holland Co., Pp 421-23, 484-87, 787-98, 831-32.
- Morse, P. M. 1929 *Phys. Rev.*, 34, 57.
- Morse, P. M. & Feshbach, H. 1953 *Methods of Theoretical Physics*, McGraw-Hill Book Co. Pp 551-52.
- Mott, N. F. & Massey, H. S. W. 1949 *Theory of Atomic Collisions*, Oxford University Press, Pp 116-18.
- Roman, P., 1964 *Advanced Quantum Theory*, Addison-Wesley, Pp 165-66, 175-78.
- Tietz, T., 1965 *Nuovo Cimento*, XXXV, 1 Pp 308-9.
- Wu, T. & Ohmura, T. 1962 *Quantum Theory of Scattering*, Prentice-Hall, Pp 70-71.

Reduction of wave functions which transform as a complex antisymmetric tensor to the Irreducible representation of Lorentz group

By B. S. RAJPUT

Department of Physics

Kurukshetra University, India

(Received 23 December, 1968)

The reduction of the wavefunction which transforms as a complex antisymmetric tensor to the irreducible representation of proper orthochronous inhomogeneous Lorentz group, has been discussed by giving the proof of essential theorem which is used for the reduction. The effects of reality condition and wave equation are also discussed where the former reduces the expression to that of real wave function which transforms as a real antisymmetric tensor while the latter restricts the number of independent irreducible representations. By assuming the total energy to be positive, the constants of the expansion of wavefunction which satisfies wave equation, have been calculated to give the energies for our cases corresponding to positive and negative values of Hamiltonian density.

LIST OF SYMBOLS

- $\vec{\Psi}(x, t)$ for wavefunction
- i for imaginary quantity $(-1)^{1/2}$
- $i, j, k, \alpha, \beta, \gamma$ for integers (1, 2, 3)
- $\vec{\beta}$ for pure Lorentz transformation.
- $\vec{\theta}$ for rotation.
- \vec{a} for translation.
- F^{ij} for components of complex tensor.
- O for null matrix.
- $\epsilon_{\alpha\beta\gamma}$ for antisymmetric three index symbol.
- ∇ for Laplace operator.
- r for index denoting real and complex parts of wavefunction.
- μ for eigen values of mass operator.
- ϵ for eigen values of operator H (± 1)
- λ for integer which lies between 1 and 2
- s for spin corresponding to S_i

S'_i for spin matrix

I for unit matrix

ξ for collective representation of the variables upon which the function in given representation depends.

$\omega(\mu p)$ for $(\mu^2 + p^2)^{1/2}$

Σ for summation

$M(\mu, \epsilon)$ for measure function

C, D for constants

δ_{ij} for Kronecker symbol.

$\delta(\mu-m)$ for Dirac Delta function.

1. INTRODUCTION

All the relativistic particles were classified corresponding to the irreducible representations of the proper, orthochronous inhomogeneous Lorentz group by Wigner (1939) who showed how the wavefunctions for these particles in the momentum representation transform under the transformation of the group. Moses (1966) showed how electromagnetic vector potential can be reduced to photon wave function in a linear momentum basis. Here photon is defined as corresponding to a massless particle of spin 1 in Wigner's classification. Using the result of Moses (1965, 1967 a) reduction in linear momentum basis can be transformed to that in angular momentum basis. Moses (1966) showed how the wavefunction of photon is contained in the vector potential while in other paper by Moses (1959) the way that Maxwell's equations contain the photon wave-function is given. As discussed by Moses (1967b) the recipe of Lomont and Moses (1967) enables one to reduce any unitary ray representation of the proper, orthochronous, inhomogeneous Lorentz group. The methods of reduction have been discussed for both non-zero and zero-mass systems where for the former one obtains the Foldy (1956)—Shirokov (1958, 1959) relations and for the latter one is led to the Lomont-Moses (1964) realization. These methods are applied by Moses (1967b) to reduce the wavefunctions $\Psi(\vec{x}, t)$ which transform by means of unitary transformations to another function $\Psi(\vec{x}, t)$ when the space time coordinates undergo any transformation of the proper orthochronous homogeneous Lorentz group, to the irreducible representation of the group with the restriction to the cases where only nonzero-mass irreducible representation appear. It is shown in those discussions that to reduce the wavefunctions only the transformation properties are necessary while the requirement that $\Psi(\vec{x})$

satisfies the wave equation, restricts the number of independent irreducible representations which appear. The reduction of the wavefunction which transforms as a real antisymmetric tensor has been discussed by Moses (1967b). We reduce here the wavefunction which transforms as a complex antisymmetric tensor by giving the proof of the essential theorem which is used in this case. The effects of reality condition and wave equation are also discussed.

2. TRANSFORMATIONS OF WAVEFUNCTIONS

We consider a complex antisymmetric tensor ;

$$F^{ij} = F_R^{ij} + F_I^{ij} \quad \dots(2.1).$$

Where F_R^{ij} and F_I^{ij} are real and imaginary parts of the tensor F^{ij} with $F^{ij} = -F^{ji}$ (antisymmetric) which transform as a tensor under the transformation of proper homogeneous Lorentz group. It is proper to introduce the wavefunction field description of this tensor. For this we define :

$$\left. \begin{aligned} E_{iR} &= F^{0i} & E_{iI} &= F_I^{0i} \\ H_{1R} &= F_R^{23} & H_{2R} &= F_R^{31} \\ H_{3R} &= F_R^{12} & H_{1I} &= F_I^{23} \\ H_{2I} &= F_I^{31} & H_{3I} &= F_I^{12} \end{aligned} \right\} \quad \dots(2.2)$$

We then construct the two 3-components column vectors $\Psi_R(\vec{x})$ and $\Psi_I(\vec{x})$ from F_R^{ij} and F_I^{ij} respectively as :

$$\left. \begin{aligned} \Psi_R(\vec{x}, t, r) &= E_{rR}(\vec{x}, t) - i H_{rR}(\vec{x}, t) \\ \Psi_I(\vec{x}, t, r) &= E_{rI}(\vec{x}, t) - i H_{rI}(\vec{x}, t) \end{aligned} \right\} r=1, 2, 3. \quad \dots(2.3).$$

The wavefunction here is the six components column vector formed by placing the three components column vectors Ψ_R and Ψ_I

$$\Psi = \begin{bmatrix} \Psi_R \\ \Psi_I \end{bmatrix} \quad \dots(2.4).$$

where

$$\Psi_R = \Psi_R(\vec{x}, t) = \begin{bmatrix} F_R^{01} \\ F_R^{02} \\ F_R^{03} \end{bmatrix} - i \begin{bmatrix} F_R^{23} \\ F_R^{31} \\ F_R^{12} \end{bmatrix} \quad \dots(2.5).$$

$$\Psi_I = \Psi_I(\vec{x}, t) = \begin{bmatrix} F_I^{01} \\ F_I^{02} \\ F_I^{03} \end{bmatrix} - i \begin{bmatrix} F_I^{23} \\ F_I^{31} \\ F_I^{12} \end{bmatrix}.$$

Generally we consider the set of the functions $\Psi(x, t, r)$ given by

$$\Psi(x, t, r) = \Psi_R(\vec{x}, t, r) + i\Psi_I(\vec{x}, t, r) \quad \dots(2.6)$$

where the variable r runs through the set of discrete or continuous values. It is also useful sometimes to regard $\Psi(\vec{x}, t)$ as being a column vector with components $\Psi(\vec{x}, t, r)$ where every value of r has two signs one for real components and the other for imaginary components.

Here \vec{x} denotes the space vector : $\vec{x} = x_1 + x_2 + x_3$.

Let $x^\alpha (\alpha=0, 1, 2, 3)$ denotes the components of the space-time four component vector with $x^0 = -x^0 = t$, $x^1 = x_1$, $x^2 = x_2$ and $x^3 = x_3$ with the units $\hbar = c = 1$ then

$$\Psi(x^\alpha) = \Psi(\vec{x}, t)$$

Any transformation of the proper, orthochronous, inhomogeneous Lorentz group can be regarded as the product of three particular transformations, i. e. translation $\tau(a^\alpha)$, rotation $R(\vec{\theta})$ and pure Lorentz transformation $L(\vec{\beta})$, where the direction of $\vec{\beta}$ is in the opposite direction of moving frame of reference and the magnitude $\beta = |\vec{\beta}|$ is given by $\cosh \beta = (1 - v^2)^{-1/2}$. Under these transformations the components of x^α in the new frames are given (Moses 1967) by

$$\left. \begin{aligned} \vec{x}' &= T(a) \vec{x} = \vec{x} - a, \\ \vec{x}' &= R(\vec{\theta}) \vec{x} = \vec{x} \cos \theta + \frac{1 - \cos \theta}{\theta^2} (\vec{\theta} \cdot \vec{x}) \vec{\theta} - \frac{\sin \theta}{\theta} (\vec{\theta} \times \vec{x}) = \exp(i\vec{\theta} \cdot \vec{M}') \vec{x}, \\ \vec{x}' &= L(\vec{\beta}) \vec{x} = \vec{x} + \vec{\beta} (\vec{\beta} \cdot \vec{x}) \left(\frac{\cosh \beta - 1}{\beta^2} \right) + \vec{\beta} x^0 \left(\frac{\sinh \beta}{\beta} \right) = \exp(i\vec{\beta} \cdot \vec{N}') \vec{x}. \end{aligned} \right\} \quad (2.7)$$

Where M' and N' are introduced by Moses (1966) and they satisfy the commutation rules of the infinitesimal generators of the proper orthochronous, homogeneous Lorentz group :

$$\begin{aligned} [M'_\alpha, M'_\beta] &= i \sum_\gamma \epsilon_{\alpha\beta\gamma} M'_\gamma, \\ [M'_\alpha, N'_\beta] &= i \sum_\gamma \epsilon_{\alpha\beta\gamma} N'_\gamma, \\ [N'_\alpha, N'_\beta] &= i \sum_\gamma \epsilon_{\alpha\beta\gamma} M'_\gamma. \end{aligned} \quad \dots(2.8)$$

The matrices M' appear in reduced form and can be written as,

$$M'_i = \begin{bmatrix} S_i & 0 \\ 0 & S'_i \end{bmatrix}, \quad \dots(2.9)$$

where, $\vec{S}=0$ and matrices S'_i constitute the irreducible representations of the generators of rotation group corresponding to the vector rotations (Moses 1967b). Under these transformations the wavefunction $\Psi(\vec{x})$ transforms as follows,

$$\begin{aligned} \Psi'(\vec{x}) &= \psi(\vec{x} + \vec{\alpha}) \\ \Psi'(\vec{x}) &= \exp(i\vec{\theta} \cdot \vec{M}) \Psi[R(-\vec{\theta})\vec{x}] \\ \Psi'(\vec{x}) &= \exp(i\vec{\beta} \cdot \vec{N}) \Psi[L(-\vec{\beta})\vec{x}]. \end{aligned} \quad \dots(2.10)$$

Here the matrices M'_i and N'_i satisfy the commutation rules for the infinitesimal generators of the Lorentz group and can be used to generate a ray representation of homogeneous Lorentz group. For this case these matrices are given by $M_i = S_i$ and $N_i = -iS'_i$ where S'_i , which are used here in equation (2.9), are given by :

$$S'_1 = \begin{pmatrix} 0 & 0 & 0 \\ 0 & 0 & -i \\ 0 & i & 0 \end{pmatrix}, S'_2 = \begin{pmatrix} 0 & 0 & i \\ 0 & 0 & 0 \\ -i & 0 & 0 \end{pmatrix}, S'_3 = \begin{pmatrix} 0 & -i & 0 \\ i & 0 & 0 \\ 0 & 0 & 0 \end{pmatrix} \dots(2.11)$$

If,

$$(\vec{\theta}, S')^3 = \theta^2 (\vec{\theta}, S'),$$

then,

$$\exp(i\vec{\theta} \cdot S') = 1 + i(\vec{\theta} \cdot S') \left(\frac{\sin \theta}{\theta} \right) + (\vec{\theta} \cdot S')^2 \times \left(\frac{\cos \theta - 1}{\theta^2} \right) = \hat{R}(\vec{\theta})$$

where, 1 is unit matrix. Hence matrix elements of $\hat{R}(\vec{\theta})$ are given by,

$$[\hat{R}(\vec{\theta})]_{\alpha\beta} = \delta_{\alpha\beta} \cos \theta + \frac{\theta_\alpha \theta_\beta}{\theta^2} (\cos \theta - 1) + \sum_\gamma \epsilon_{\beta\alpha\gamma} \theta_\gamma \left(\frac{\sin \theta}{\theta} \right). \quad (2.12)$$

Similarly, if :

$$\begin{aligned} L(\vec{\beta}) &= \exp(i\vec{\beta} \cdot \vec{N}) \\ &= 1 + i(\vec{\beta} \cdot \vec{N}) \left(\frac{\sinh \beta}{\beta} \right) + (\vec{\beta} \cdot \vec{N})^2 \left(\frac{1 - \cosh \beta}{\beta^2} \right), \end{aligned}$$

where $(\beta, N)^2 = -\beta^2 (\beta, N)$.

Then the matrix elements of $\hat{L}(\vec{\beta})$ are given by,

$$[L(\vec{\beta})]_{\alpha\beta} = \delta_{\alpha\beta} \cosh \beta - \frac{\beta_\alpha \beta_\beta}{\beta^2} (\cosh \beta - 1) + i \sum_\gamma \epsilon_{\alpha\beta\gamma} \beta_\gamma \frac{\sinh \beta}{\beta}. \quad \dots(2.13)$$

3. REDUCTION OF WAVEFUNCTIONS

The ten infinitesimal generators of the proper, orthochronous, inhomogeneous Lorentz groups are the energy H , components of momentum P_i ($i = 1, 2, 3$), the three components of angular momentum K_i , and the three generators corresponding to space-time relations Z_i . As operators they are defined as,

$$\left. \begin{aligned} P_i &= P^i, \quad i=1, 2, 3, \\ P^0 &= -P_0 = H, = -i \frac{\partial}{\partial t} 1, \\ P_j &= -i \nabla_j, \quad I = -i \frac{\partial}{\partial x_j} 1, \\ K_j &= M_j - i [x \times \nabla]_j 1, \\ Z_j &= N_j + i [x_j \frac{\partial}{\partial t} + t \nabla_j] 1. \end{aligned} \right\} \quad \dots(3.1)$$

These generators satisfy the following commutation relations :

$$\left. \begin{aligned} [P^\alpha, P^\beta] &= 0, \\ [K_\alpha, K_\beta] &= i \sum_\gamma \epsilon_{\alpha\beta\gamma} K_\gamma, \\ [K_\alpha, P_\beta] &= i \sum_\gamma \epsilon_{\alpha\beta\gamma} P_\gamma, \\ [Z_\alpha, Z_\beta] &= i \sum_\gamma \epsilon_{\alpha\beta\gamma} K_\gamma, \\ [Z_\alpha, P^\beta] &= i P_\alpha, \\ [Z_\alpha, P_\beta] &= i \delta_{\alpha\beta} P_0. \end{aligned} \right\} \quad \dots(3.2)$$

Hence equations (2.10) can now be written as :

$$\left. \begin{aligned} \vec{\Psi}'(x) &= \exp [i \sum_\alpha a^\alpha P_\alpha] \vec{\Psi}(x), \\ \vec{\Psi}'(x) &= \exp [i \theta_\alpha K_\alpha] \vec{\Psi}(x), \\ \vec{\Psi}'(x) &= \exp [i \beta_\alpha Z_\alpha] \vec{\Psi}(x). \end{aligned} \right\} \quad \dots(3.3)$$

We introduce a complex function $f(\mu, \epsilon, p, i)$, where, the vector p has components p_i ($i = 1, 2, 3$) each of which takes on every value from $-\infty$ to ∞ . The variable μ takes on all the eigenvalues of the mass operator M , where,

$$M = [H^2 - P^2], \quad \text{with} \quad P^2 = \sum_i P_i^2,$$

The variable ϵ takes on the values which occur in the spectrum of the operator H . λ may have any value from 1 to $2s+1$ where s is the spin corresponding to matrices S'_i .

If $\hat{P}_\alpha, \hat{K}_i, \hat{S}_i$ are the infinitesimal generators of the unitary ray representation of Lorentz group then the function $f(\mu, \epsilon, p, \lambda)$ transforms under these operators as,

$$\left. \begin{aligned} \hat{P}^\alpha f(\mu, \epsilon, p, \lambda) &= \hat{H} f(\mu, \epsilon, p, \lambda) = \epsilon \omega(\mu, p) f(\mu, \epsilon, p, \lambda). \\ \hat{P}^i f(\mu, \epsilon, p, \lambda) &= p^i f(\mu, \epsilon, p, \lambda) \\ \hat{K}^i f(\mu, \epsilon, p, \lambda) &= \left[-i \sum_{j,k} \epsilon_{ijk} p_j \frac{\partial}{\partial p_k} + S_i \right] f(\mu, \epsilon, p, \lambda). \\ \hat{S}_i f(\mu, \epsilon, p, \lambda) &= \left[i \omega(\mu, p) \frac{\partial}{\partial p_i} + \frac{1}{\omega(\mu, p)} \sum_{j,k} \epsilon_{ijk} p_j S_k \right] f(\mu, \epsilon, p, \lambda). \end{aligned} \right\} \quad \dots(3.4)$$

$$\text{where,} \quad \omega(\mu, p) = [\mu^2 + p^2]^{1/2}. \quad \dots(3.5)$$

These generators satisfy the commutation rules as those of the generators P^α, K, S given by equations (3.2). Hence the required reduction of the wavefunction $\Psi(x, t)$ is done if we express it in terms of $f(\mu, \epsilon, p, \lambda)$. This can be done by using following theorem.

"The expansion of the function $\Psi(\vec{x})$ which transforms as complex tensor, in terms of irreducible unitary ray representation of the proper, orthochronous inhomogeneous Lorentz group is given by,

$$\begin{aligned} \Psi(\vec{x}) &= \sum_r \int dM(\mu, \epsilon) \int \frac{d^3p}{\omega(\mu, p)} \exp[i\{\vec{p} \cdot \vec{x} - \epsilon \omega(\mu, p) t\}] \\ &\times [\omega(\mu, p) f(\mu, \epsilon, p) - \frac{\vec{p} \cdot \{\vec{p} \cdot f(\mu, \epsilon, p)\}}{w(\mu, p) + \mu} - i \epsilon \{\vec{p} \times f(\mu, \epsilon, p)\}] \end{aligned} \quad \dots(3.6)$$

where, r has two values, one for Ψ_R wavefunction and the other for Ψ_L wavefunction. $dM(\mu, \epsilon)$ is the measure function of masses and energies which appear. It is an arbitrary measure in Stieltzes sense."

Proof: As discussed by Lomont & Moses (1967) we have,

$$f(\xi) = \Psi(\vec{x}) = \sum_\epsilon \int d\mu \int \frac{d^3p}{\omega(\mu, p)} \times \langle \xi | \mu, p, \lambda \rangle f(\mu, \epsilon, p, \lambda), \quad (3.7)$$

where, $f(\xi)$ is the representation of vector Ψ in the basis, being characterised by the space of wavefunctions in Hilbert space upon which the generators operate. ξ , collectively denotes all the variables upon which the functions in the given representation depend. The transformation function

$\langle \xi | \mu, \epsilon, p, \lambda \rangle$ may be considered to be the inner product of the bra $\langle \xi |$ and the ket $| \mu, \epsilon, p, \lambda \rangle$ and it is given by,

$$\langle \xi | \mu, \epsilon, p, \lambda \rangle = \exp [-i\beta \cdot Z] g(\xi, \mu, \epsilon, \lambda), \quad \dots(3.8)$$

where $g(\xi, \mu, \epsilon, \lambda)$ is the solution of the equations :

$$\begin{aligned} P_i g(\xi, \mu, \epsilon, \lambda) &= 0 \\ H g(\xi, \mu, \epsilon, \lambda) &= \epsilon \omega(\xi, \mu, \epsilon, \lambda). \end{aligned} \quad \dots(3.9)$$

This may also be written as :

$$g(\xi, \mu, \epsilon, \lambda) = \langle \xi | \mu, \epsilon, 0, \lambda \rangle$$

with,

$$P_i | \mu, \epsilon, p, \lambda \rangle = p_i | \mu, \epsilon, p, \lambda \rangle, \quad \dots(3.10)$$

$$H | \mu, \epsilon, p, \lambda \rangle = \epsilon \omega(\mu, p) | \mu, \epsilon, p, \lambda \rangle.$$

Using equations (3.1) we can write (3.8) as,

$$\xi | \mu, \epsilon, p, \lambda \rangle = \exp \left[-i\vec{\beta} \cdot \vec{N} + \left(\vec{\beta} \cdot \vec{x} \frac{\partial}{\partial \vec{t}} + \vec{\beta} \cdot \nabla \right) t \right] g(\xi, \mu, \epsilon, \lambda) \quad \dots(3.11)$$

where,

$$\left. \begin{aligned} \vec{p} &= -\epsilon \mu \frac{\vec{p}}{\beta} \sinh \beta, \\ \omega(\mu, p) &= \mu \cosh \beta, \\ p &= |\vec{p}| = \mu \sinh \beta. \end{aligned} \right\} \quad \dots(3.12)$$

If we define a column vector $\chi(\mu, \epsilon, p, \lambda)$ with components $\chi(r, \mu, \epsilon, p, \lambda)$ given by :

$$\chi(r | \mu, \epsilon, p, \lambda) = \exp [-i\vec{\beta} \cdot \vec{N}]_{r, \lambda} \quad \dots(3.13)$$

then using the equations (3.9), (3.10), (3.11) and (3.1) and introducing an arbitrarily chosen measure function $M'(\mu, \epsilon)$ equation (3.7) can be written as :

$$\begin{aligned} \Psi(\vec{x}) &= \sum_{\epsilon} \sum_{\lambda} \int dM'(\mu, \epsilon) \int \frac{d\vec{p}}{\omega(\mu, p)} \chi(\mu, \epsilon, p, \lambda) f'(\mu, \epsilon, p, \lambda) \\ &\quad \times \exp [i\{\vec{p} \cdot \vec{x} - \epsilon \omega(\mu, p)t\}]. \end{aligned} \quad \dots(3.14)$$

Using equations (2.13), (3.11) into (3.12) and then putting the values of components of vector $\chi(\mu, \epsilon, p, \lambda)$ after labeling over λ calculated in this way, in equation (3.13) gives the required result (on absorbing $\frac{1}{\mu}$ into the measure function). Four irreducible representations of the

inhomogeneous Lorentz group appear in the expansion (3.6) because index γ can take two values with two signs for both the values of r separately. In equation (3.6) ϵ has two values, i. e., $+1$ and -1 .

If we construct the vectors :

$$\begin{aligned} f'(\mu, p) &= f'(\mu, +1, p) \\ h'(\mu, p) &= f^{*'}(\mu, -1, p) \\ M'(\mu) &= M'(\mu, +1) \\ N'(\mu) &= M'(\mu, -1) \end{aligned}$$

where, $*$ denotes the complex conjugate, then equation (3.6) is written as :

$$\begin{aligned} \Psi(\vec{x}) &= \sum_r \int dM'(\mu) \int \frac{dp}{\omega(\mu, p)} \exp[i\{\vec{p} \cdot \vec{x} - \omega(\mu, p)t\}] \\ &\times [\omega(\mu, p)f'(\mu, p) - \frac{\vec{p} \cdot \vec{p} f'(\mu, p)}{\omega(\mu, p) + \mu} - i\{\vec{p} \times f'(\mu, p)\}] \\ &+ \sum_r \int dN'(\mu) \int \frac{dp}{\omega(\mu, p)} \exp[-i\{\vec{p} \cdot \vec{x} - \omega(\mu, p)t\}] \\ &\times [\omega(\mu, p)h^{*'}(\mu, p) - \frac{\vec{p} \cdot \vec{p} h^{*'}(\mu, p)}{\omega(\mu, p) + \mu} \\ &- i\{\vec{p} \times h^{*'}(\mu, p)\}]. \end{aligned} \quad \dots(3.14)$$

Hence if we denote the arbitrary measures and functions by dashes as superfix for imaginary wavefunction, then,

$$\begin{aligned} \Psi(\vec{x}) &= \int dM(\mu) \int \frac{dp}{\omega(\mu, p)} \exp[i\{\vec{p} \cdot \vec{x} - \omega(\mu, p)t\}] \times [\omega(\mu, p) \\ &f(\mu, p) - \frac{\vec{p} \cdot \vec{p} f(\mu, p)}{\omega(\mu, p) + \mu} - i\{\vec{p} \times f(\mu, p)\}] \\ &+ \int dM'(\mu) \int \frac{dp}{\omega(\mu, p)} \exp[i\{\vec{p} \cdot \vec{x} - \omega(\mu, p)t\}] \times [\omega(\mu, p)f'(\mu, p) \\ &- \frac{\vec{p} \cdot \vec{p} f'(\mu, p)}{\omega(\mu, p) + \mu} - i\{\vec{p} \times f'(\mu, p)\}] \\ &+ \int dN(\mu) \int \frac{dp}{\omega(\mu, p)} \exp[-i\{\vec{p} \cdot \vec{x} - \omega(\mu, p)t\}] \\ &\times [\omega(\mu, p)h^*(\mu, p) - \frac{\vec{p} \cdot \vec{p} h^*(\mu, p)}{\omega(\mu, p) + \mu} - i\{\vec{p} \times h^*(\mu, p)\}] \\ &+ \int dN'(\mu) \int \frac{dp}{\omega(\mu, p)} \exp[-i\{\vec{p} \cdot \vec{x} - \omega(\mu, p)t\}] \times [\omega(\mu, p)h^{*'}(\mu, p) \\ &- \frac{\vec{p} \cdot \vec{p} h^{*'}(\mu, p)}{\omega(\mu, p) + \mu} - i\{\vec{p} \times h^{*'}(\mu, p)\}]. \end{aligned} \quad \dots(3.15)$$

4. REALITY CONDITION

If the wavefunction contains only the real part then the measure function M need not be labeled by the index r ,

$$\begin{aligned} \psi(x) = \int dM(\mu) \int \frac{d\vec{p}}{\omega(\mu, \vec{p})} \exp[i\{\vec{p}, \vec{x} - \omega(\mu, \vec{p})t\}] \times [\omega(\mu, \vec{p})f(\mu, \vec{p}) - \frac{\vec{p}\{\vec{p}, f(\mu, \vec{p})\}}{\omega(\mu, \vec{p}) + \mu} \\ [-i\{\vec{p} \times f(\mu, \vec{p})\}] + \int dN(\mu) \int \frac{d\vec{p}}{\omega(\mu, \vec{p})} \exp[-i\{\vec{p}, \vec{x} + \omega(\mu, \vec{p})t\}] \times [\omega(\mu, \vec{p})h^*(\mu, \vec{p}) \\ - \frac{\vec{p}\{\vec{p}, h^*(\mu, \vec{p})\}}{\omega(\mu, \vec{p}) + \mu} - i\{\vec{p} \times h^*(\mu, \vec{p})\}] \end{aligned} \quad \dots(4.1)$$

Moreover, $\psi^* = \psi$, so

$$dM(\mu) [\omega(\mu, \vec{p})f(\mu, \vec{p}) - \frac{\vec{p}\{\vec{p}, f(\mu, \vec{p})\}}{\omega(\mu, \vec{p}) + \mu}] = dN(\mu) [\omega(\mu, \vec{p})h(\mu, \vec{p}) - \frac{\vec{p}\{\vec{p}, h(\mu, \vec{p})\}}{\omega(\mu, \vec{p}) + \mu}] \quad \dots(4.2)$$

$$\text{and} \quad dM(\mu) \{\vec{p}f(\mu, \vec{p})\} = dN(\mu) \{\vec{p} \times h(\mu, \vec{p})\}. \quad \dots(4.3)$$

Putting these values in (4.1) we get the expansion for real wavefunction Ψ which transforms as a real antisymmetric tensor given by Moses (1967b).

5. WAVE EQUATION

Let us assume that the wavefunction which transforms as a complex tensor satisfy the wave equation,

$$\left(\frac{\partial^2}{\partial t^2} - \nabla^2 + m^2 \right) \Psi(\vec{x}) = 0 \quad \dots(5.1)$$

where, m is the mass of the complex tensor particle. In terms of the infinitesimal generator equation (5.1) can be written as,

$$[H^2 - P^2] \Psi(x) = m^2 \Psi(x) \quad \dots(5.2)$$

For any infinitesimal generator M , $M\Psi(x)$ is obtained from equation (3.15) by replacing $f(\mu, p)$ and $h(\mu, p)$ by $Mf(\mu, p)$ and $Mh(\mu, p)$, where M 's are used in equations (3.4). Then equation (3.15) can be written as,

$$\begin{aligned} & \int dM(\mu) \int \frac{dp}{\omega(\mu, p)} (\mu^2 - m^2) [\omega(\mu, p) f(\mu, p) - \frac{\vec{p} \cdot \vec{p} f(\mu, p)}{\omega(\mu, p) + \mu} - i \{ \vec{p} \times \vec{f}(\mu, p) \}] \\ & \times \exp[i \{ \vec{p} \cdot \vec{x} - \omega(\mu, p) t \}] + \int dM'(\mu) \int \frac{dp}{\omega(\mu, p)} (\mu^2 - m^2) [\omega(\mu, p) f'(\mu, p) \\ & - \frac{\vec{p} \cdot \vec{p} f'(\mu, p)}{\omega(\mu, p) + \mu} - i \{ \vec{p} \times \vec{f}'(\mu, p) \}] \times \exp[i \{ \vec{p} \cdot \vec{x} - \omega(\mu, p) t \}] \\ & + \int dN(\mu) \int \frac{dp}{\omega(\mu, p)} (\mu^2 - m^2) [\omega(\mu, p) h^*(\mu, p) - \frac{\vec{p} \cdot \vec{p} h^*(\mu, p)}{\omega(\mu, p) + \mu} - i \{ \vec{p} \times \vec{h}^*(\mu, p) \}] \\ & \times \exp[-i \{ \vec{p} \cdot \vec{x} - \omega(\mu, p) t \}] + \int dN'(\mu) \int \frac{dp}{\omega(\mu, p)} (\mu^2 - m^2) [\omega(\mu, p) h^{*'}(\mu, p) \\ & - \frac{\vec{p} \cdot \vec{p} h^{*'}(\mu, p)}{\omega(\mu, p) + \mu} - i \{ \vec{p} \cdot \vec{p} h^{*'}(\mu, p) \}] \times \exp[i \{ \vec{p} \cdot \vec{x} - \omega(\mu, p) t \}]. \end{aligned} \quad (5.3)$$

Hence for $f(\mu, p)$ and $h(\mu, p)$ not to be identically zero, $M(\mu)$ and $N(\mu)$ are constants for all the values of $\mu \neq m$. For $\mu = m$, they have a jump,

$$dN^i = D^i \delta(\mu - m) d\mu, \quad dM^i = C^i \delta(\mu - m) d\mu. \quad (5.4)$$

Where C^i and D^i are real positive constants. Then equation (3.15) can be written as :

$$\begin{aligned} \Psi(\vec{x}) = & C \int \frac{dp}{\omega(p)} \exp[i \{ \vec{p} \cdot \vec{x} - \omega(p) t \}] [\omega(p) f(p) - \frac{\vec{p} \cdot \vec{p} f(p)}{\omega(p) + \mu} - i \{ \vec{p} \times \vec{f}(p) \}] \\ & + C' \int \frac{dp}{\omega(p)} \exp[i \{ \vec{p} \cdot \vec{x} - \omega(p) t \}] [\omega(p) f'(p) - \frac{\vec{p} \cdot \vec{p} f'(p)}{\omega(p) + \mu} - i \{ \vec{p} \times \vec{f}'(p) \}] \\ & + D \int \frac{dp}{\omega(p)} \exp[-i \{ \vec{p} \cdot \vec{x} - \omega(p) t \}] [\omega(p) h^*(p) - \frac{\vec{p} \cdot \vec{p} h^*(p)}{\omega(p) + \mu} - i \{ \vec{p} \times \vec{h}^*(p) \}] \\ & + D' \int \frac{dp}{\omega(p)} \exp[-i \{ \vec{p} \cdot \vec{x} - \omega(p) t \}] [\omega(p) h^{*'}(p) - \frac{\vec{p} \cdot \vec{p} h^{*'}(p)}{\omega(p) + \mu} - i \{ \vec{p} \times \vec{h}^{*'}(p) \}] \end{aligned} \quad (5.5)$$

where $f(p) = f(m, p)$, $h(p) = h(m, p)$, $\omega(p) = \omega(m, p)$. Equation (5.5) gives general solution of the equation (5.2).

6. CALCULATION OF THE CONSTANTS

If $H(x)$ is the Hamiltonian density of the field which leads to the wavefunction (5.2) then $H'(x) = -H(x)$ is also the Hamiltonian density which leads to the same wavefunction, and then the energy E of the field is given by $E = \int H(x) dx$. We choose the constants of the equation (5.5) in such a manner that E is always positive. We choose Hamiltonian density $H(x)$ for the cases,

$$(1) f(p) = h(p) = h'(p) = 0$$

$$(2) f(p) = h(p) = f'(p) = 0$$

$$(3) f'(p) = h(p) = h'(p) = 0$$

$$(4) f(p) = f'(p) = h'(p) = 0$$

$H(x)$ is defined as usual,

$$H(x) = \Psi^* \Psi + \nabla \Psi^* \nabla \Psi + m^2 \Psi \Psi^* \dots \dots \dots (5.6)$$

Then for the requirement that E is always positive we have,

$$C^* = D^* = (2)^{-1/2} [2\pi]^{-3/2}$$

Then energies for all the four cases above are given respectively as follows,

$$(1) E_f' = \int f^{*'}(p) f'(p) dp$$

$$(2) E_h' = \int h^{*'}(p) h'(p) dp$$

$$(3) E_f = \int f^*(p) f(p) dp$$

$$(4) E_h = \int h^*(p) h(p) dp$$

When the state is the superposition of all the four modes then the total energy E of the field is given by :

$$E = E_f + E_h + E_h' + E_f' \dots \dots \dots (5.8)$$

REFERENCES

- Foldy, L., 1956 *Phys. Rev.* 102, 568.
 Lomont, J. S. & Moses, H. E. 1964 *Journ. Math. Phys.* 5, 294.
 Lomont, J. S. & Moses, H. E. 1967 *Journ. Math. Phys.* 8, 837.
 Moses, H. E. 1966 *Nuovo Cimento*. 42, 757.
 Moses, H. E. 1965 *Journ. Math. Phys.* 6, 928.
 Moses, H. E. 1959 *Phys. Rev.* 113, 1670.
 Moses, H. E. 1967a *Nuovo Cimento*. 48, 43.
 Moses, H. E. 1967b *Journ. Math. Phys.* 8, 1134.
 Moses, H. E. 1967c *Ann. Phys.* 41, 158.
 Wigner, E. P. 1939 *Ann. Math.* 40, 149.

Differential thermal analysis of some complexes of montmorillonite

By SABITA GHOSH

Khaira Laboratory of Physics, University of Calcutta.

(Received June 28, 1968; Resubmitted December 14, 1968)

The heats of reaction for desorption of interlayer water, from montmorillonites in different cationic forms and equilibrated at different relative humidities, have been determined. The results favour a close correlation of desorption process between the divalent and the monovalent cationic forms within the observed range of relative humidities. The areas of the dehydroxylation loops have been measured, which supports the existing idea that the exchange cations have no influence on this process. It seems probable that the exothermic peak-temperature is dependent on the size of the exchange cations having the same charge.

1. INTRODUCTION

Montmorillonite is a three-layer lattice type of clay mineral having a high cation-exchange capacity due to its unbalanced charge distribution in the silicate layers. When heated to continuously elevated temperatures, a variety of reactions takes place in the montmorillonite lattices. At the initial stage, it loses the absorbed interlayer water within a range of temperatures, 100°C — 300°C. This water, influenced greatly by the exchange cations present, requires, however, a definite amount of energy for its complete elimination. Next, it is deprived of its structural water, i.e., (OH)-lattice water in the temperature range, 500°C, and finally the breakdown of the original structure takes place near the region of 900°C with the appearance of a new phase at higher temperatures. All these thermal reactions are generally registered by the differential thermal analysis technique. The first endothermic peak system corresponding to the loss of inter-layer water from different cationic forms of the montmorillonite samples shows a fine structure which was investigated by Hendricks *et al* (1940). Mackenzie (1950) correlated the peak temperature of the high temperature component of this endothermic peak system and the hydration energy of the cations in montmorillonite. Mackenzie (1957) also gave a summary of the discussion on the loss of inter-layer water from various cationic forms of montmorillonite, by different authors. Also, it was reported by R. A. Rowland (1955) that the exothermic loop accompanied by the formation of new phases is largely controlled by the isomorphic substitution within the lattice and the nature of the exchange cation present in it.

In the present paper, the results obtained from the differential thermal analyses (d. t. a.) for the different complexes equilibrated at some specific relative humidities, are given in the tables. Again, the heats of reaction for the loss of interlayer water, which are proportional to the areas under the peaks (Kerr & Kulp 1948), have been determined. For this purpose, a heat of reaction scale was established for the differential thermal analyser. Also the areas of the second endothermic loops (dehydroxylation loops) for the different samples have been measured and they seem to be nearly constant. It is also noted, that when the chemical composition, i.e., the isomorphic substitution of the mineral, remains the same, the peak temperatures of the exothermic reactions, for the different complexes of a particular sample, are dependent on the size of the exchange cation present.

2. DESCRIPTION OF THE SAMPLES AND EXPERIMENTAL PROCEDURE

It may be expected that the behaviour of montmorillonite is dependent upon its origin. The samples were, therefore, obtained from different deposits, which were bentonites originating from (i) England, (ii) Hanover, (iii) Assam, (iv) Kashmir (pink variety) and (v) Rajasthan. The different complexes of the minerals saturated with H^+ , Li^+ , Na^+ , K^+ , Mg^{2+} , Ca^{2+} and Ba^{2+} ions were obtained by the same method as used by the author (1965). The samples in the above mentioned cationic forms derived from a particular bentonite were equilibrated under the same relative humidity as indicated by a Hair-hygrometer and at the same temperature for a period of three to four weeks.

The cation exchange capacity of the different bentonites were determined by the half saturated KCl-KOH method (Ganguli 1951).

The differential thermal analyses were performed with an unit consisting of a bell-type furnace which could be envelopingly placed on the refractory stand fitted with blocks of pure nickel having two holes, in which the samples were packed. The unit is also provided with a set of chromel-alumel thermocouples for the connection of the pyrometer indicator and the galvanometer. The pyrometer indicator shows the temperature of the furnace which can be regulated by adjusting the energy regulation device from outside.

The sensitivity of the apparatus in the lower region of temperatures was measured by using 7 mgm. of NH_4NO_3 with $\alpha-Al_2O_3$ in one of the sample holes and 40 mgm. of AgI with 75 mgm. of Ca-bentonite in the other hole (Barshad 1952). The corresponding thermal breaks registered by the apparatus are shown in figure 1 with the necessary calculation for the sensitivity.

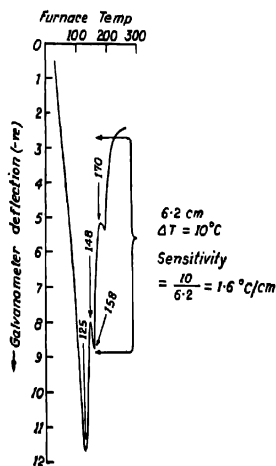


Figure 1. Sensitivity of the differential thermal analyser.

Also, the differential thermal analyser was calibrated to establish a heat of reaction scale following the method of Barshad (1952). The substances used for this purpose were $\text{CaSO}_4 \cdot 2\text{H}_2\text{O}$, $\text{SrCl}_2 \cdot 6\text{H}_2\text{O}$ and $\text{Na}_2\text{S}_2\text{O}_8 \cdot 5\text{H}_2\text{O}$ (hypo). In order to obtain the *d. t. a.* results of these hydrated salts and as well as the bentonite complexes, 250 mgms. of each sample were dispersed in calcined alumina ($\alpha\text{-Al}_2\text{O}_3$) around the thermocouple in a volume of 0.465 cc. and was heated to continuously elevated temperatures. The rate of heating was $10^\circ\text{C}/\text{minute}$ and was maintained approximately constant throughout the range. The temperature of the furnace was recorded by the pyrometer indicator, and the temperature difference between the sample and the inert material ($\alpha\text{-Al}_2\text{O}_3$) was recorded by a sensitive galvanometer connected in series with the differential thermocouple. The thermal reactions of the samples were then noted for different furnace temperatures and the results obtained for the various complexes of bentonites are given in tables 3-7.

The areas of the first and second endothermic peaks, as described by the contour of the peak and a line joining the two points of inflexion at the beginning and end of each peak, was measured by a planimeter (Rowland *et al* 1952) for different samples. The heats of reaction, for desorption of interlayer water from different samples of bentonites, were then calculated.

EXPERIMENTAL RESULTS AND CONCLUSIONS

The cation exchange capacities of the different bentonites expressed in me/100 gm. are tabulated below.

TABLE 1

Sample	England	Hanover	Assam	Kashmir (pink variety)	Rajasthan
Cation exchange capacity.	100	86	90	100	80

The heat of reaction data for the calibration of the differential thermal analyser are given in table below.

TABLE 2

Sample	Calculated value of heat of reaction (cal/gm).	Peak area for 250 mgm. of sample (sq. mm.)	Heat of desorption per 250 mgm. of sample per sq. mm.	Average heat of desorption per gm. of sample per sq. mm.
$\text{CaSO}_4 \cdot 2\text{H}_2\text{O}$	164	128	0.32 cal	
$\text{BaCl}_2 \cdot 2\text{H}_2\text{O}$	127	96	0.34 cal	
$\text{Na}_2\text{S}_2\text{O}_3 \cdot 5\text{H}_2\text{O}$ (hypo)	296	220	0.33 cal	1.28 cal
$\text{SrCl}_2 \cdot 6\text{H}_2\text{O}$	343	283	0.31 cal	

The values of the cation exchange capacities for the different samples of bentonite, shown in table 1, agree with the generally accepted values (Grim 1953) for the montmorillonite group.

The d. t. a. curves drawn for the different complexes and the nature of the thermal reactions agree with the standard curves for montmorillonite (Kerr *et al* 1949). They also show a loss by the mineral, of the adsorbed interlayer water within the range of temperatures, 100°C—300°C. Beyond this it has been found that the mineral loses the structural water in the temperature range—500°C—800°C. Also, the exothermic peaks for the different complexes appear within a range of temperatures 900°C—1000°C depending on the nature of the exchange cations present.

The differential thermal analyses data for different samples of bentonite are given in the following tables 3-7 showing the values of the

TABLE 3. RELATIVE HUMIDITY=20%, TEMPERATURE=30°C.

Complexes of bentonite from England.	Desorption temperature in d.t.a. (centigrade)	Heat of desorption (ΔH) (cal/gm.)	Dehydroxylation temperature in d. t. a (centigrade)	Peak area of dehydroxylation. (sq. mm.)	Peak temperature of exothermic reaction (centigrade)
H-bentonite	70-210	96.00	650-750	24	940
Li- „	60-215	51.20	600-720	25	945
Na- „	70-170	35.64	620-760	24	970
K- „	70-150	19.20	650-770	25	975
Mg- „	70-300	93.44	650-750	22	960
Ca- „	60-210	76.80	650-760	22	970
Ba- „	70-200	44.80	600-750	22	980

TABLE 4. RELATIVE HUMIDITY=25%, TEMPERATURE=31°C.

Complexes of bentonite from Kashmir (pink variety)	Desorption temperature in d.t.a (centigrade)	Heat of desorption (ΔH) (cal/gm.)	Dehydroxylation temperature in d. t. a. (centigrade)	Peak area of dehydroxylation (sq. mm.)	Peak temperature of exothermic reaction. (centigrade)*
H-bentonite	70-260	94.72	600-750	22	
Li- „	80-230	51.42	600-720	18	
Na- „	90-190	40.59	600-750	18	
K- „	70-180	32.00	600-720	20	*
Mg- „	80-270	97.28	600-740	22	
Ca- „	60-230	85.78	600-740	21	
Ba- „	70-220	55.04	600-760	18	

*As the peaks are not well defined the peak temperatures are not given.

beats of reaction for the desorption of interlayer water from the different complexes, the areas of the dehydroxylation peaks and also the peak temperatures of the exothermic reactions.

TABLE 5. RELATIVE HUMIDITY=25%, TEMPERATURE=23°C.

Complexes of bentonite from Hanover.	Desorption temperature in d.t.a. (centigrade)	Heats of desorption (ΔH) (cal/gm).	Dehydroxylation temperature in d. t. a. (centigrade)	Peak area of dehydroxylation (sq. mm.)	Peak temperature of exothermic reaction. (centigrade)
H-bentonite	43-233	107.52	613-733	18	933
Li- "	43-233	74.24	613-723	22	939
Na- "	53-213	66.56	623-753	22	948
K- "	53-203	58.88	613-753	26	953
Mg- "	53-253	120.32	653-773	20	949
Ca- "	43-253	96.00	613-753	20	953
Ba- "	43-223	73.75	623-763	26	961

TABLE 6. RELATIVE HUMIDITY=30%, TEMPERATURE=28°C. .

Complexes of bentonite from Assam	Desorption temperature in d.t.a. (centigrade)	Heats of desorption (ΔH) (cal/gm)	Dehydroxylation temperature in d. t. a. (centigrade)	Peak area of dehydroxylation (sq. mm.)	Peak temperature of exothermic reaction. (centigrade)
H-bentonite	60-200	51.20	500-650	45	960
Li- "	55-220	28.16	500-630	44	968
Na- "	70-170	19.20	500-640	45	983
K- "	70-150	14.08	500-630	43	996
Mg- "	60-330	76.80	500-640	44	983
Ca- "	60-330	51.20	500-630	46	988
Ba- "	60-200	28.16	500-640	44	993

The determined values of the heats of reaction in Kcal/equivalent are plotted against the heats of hydration* of the monovalent and the divalent cations in figures 2-6. The relation obtained in the graphs is linear and the slopes of the straight lines are nearly the same in each group for

* The values are taken from *Electrochemical Data* by B. E. Conway Ph. D., D. I. C., Elsevier Publishing Co., 1952.

TABLE 7

Complexes of bentonite from Rajasthan.	Desorption temperature in d.t.a. (centigrade)	Heats of desorption. (ΔH) (cal/gm.)	Dehydroxylation temperature in d. t. a. (centigrade)	Peak area of dehydroxylation (sq. mm.)	Peak temperature of exothermic reaction. (centigrade)
H-bentonite	38-218	81.92	428-578	16	928
Li- "	68-258	61.44	500-618	18	*
Na- "	58-218	51.20	518-628	16	933
K- "	68-208	44.80	508-628	16	*
Mg- "	38-298	76.80	478-588	16	918
Ca- "	48-228	67.84	508-628	18	925
Ba- "	58-228	43.52	500-618	17	960

*As the peaks are not well defined the peak temperatures are not given.

all the samples over the observed range of relative humidity. Thus, it may be said, that the mechanism of desorption of water from both divalent and monovalent cation saturated bentonites appears to be closely similar.

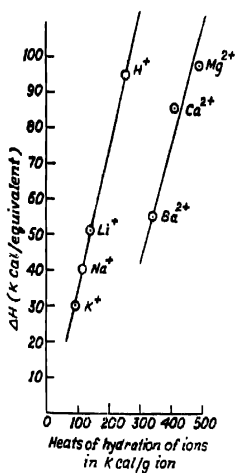


Figure 2. Variation of ΔH for salts of bentonite from England with heats of hydration of cations.

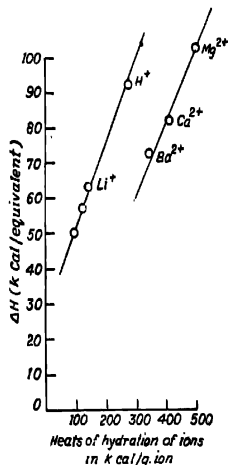


Figure 3. Variation of ΔH for salts of bentonite from Hanover with heats of hydration of cations.

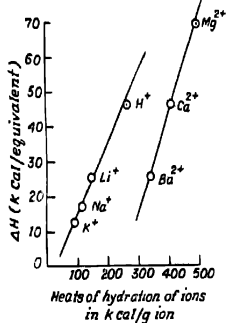


Figure 4. Variation of ΔH for salts of bentonite from Assam with heats of hydration of cations.

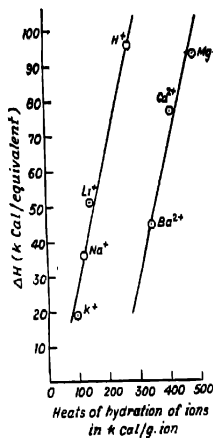


Figure 5. Variation of ΔH for salts of bentonite from Kashmir (pink variety) with heats of hydration of cations.

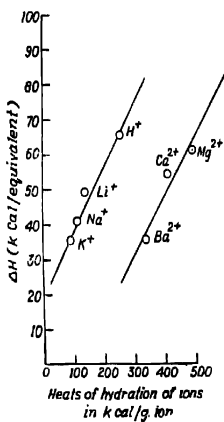


Figure 6. Variation of ΔH for salts of bentonite from Rajasthan with heats of hydration of cations.

The areas of the dehydroxylation peaks, shown in tables 3-7, are found to be nearly constant for a group of complexes derived from a particular bentonite, suggesting that the exchangeable cations have little or no influence on the dehydroxylation process. This is consistent with the idea that the OH-binding capacity is a characteristic physical constant of the material depending on the composition of the silicate layer and not on the exchangeable cations.

The peak temperatures of the exothermic reactions, given in tables 3-7, increase with the size of the cations having the same charge. The peak temperatures may also indicate the order of the energy associated with the rearrangement of the atoms as they shift to their new positions in the corresponding crystalline phases formed.

The author expresses her gratitude to Prof. S. R. Khastgir, Head of the Department of Physics, Bose Institute for his kind interest in the present work. She is indebted to Prof. S. K. Mukherjee, Department of Agricultural Chemistry, University of Calcutta for helpful discussions.

REFERENCES

- Barshad, I. 1949 *Am. Min.*, 34, 675.
1950 *Am. Min.*, 35, 225.
1952 *Am. Min.*, 37, 667.
- Ganguli, A. K. 1951 *Jr. Phys. & Coll. Chem.*, 55, 1417.
- Ghosh, S. 1965 *Indian J. Phys.*, 39, 352.
- Grim, R. 1953 *Clay Mineralogy*, McGraw Hill Book Co., New York.
- Hendricks, S. B. Nelson, R. A. & Alexander, L. T. 1940 *Jr. Am. Chem. Soc.*, 62, 1457
- Kerr, F. Paul & Kulp, J. L. 1948 *Am. Min.*, 33, 387.
- Kerr, F. Paul, Kulp, J. L. & Hamilton, P. K. 1949 *Am. Petrol. Inst.*, Project 49, Report No. 3.
- Mackenzie, C. R. 1950 *Clay Min. Bull.*, 1, 115.
- Mackenzie, C. R. 1957 *The Differential Thermal Investigation of clays Mineralogical Society*, London Ch. V. P. 146-147.
- Rowland, R. A. & Call W. Beck 1952 *Am. Min.*, 37, 76.
- Rowland, R. A. 1955 *Clays and Clay Technology*, Bull. 169, pp. 150.

The Cherenkov radiation in a wave-guide loaded with a moving medium

By R. M. KHAN

Department of Mathematics,

City College, Amherst Street, Calcutta, India

(Received May 29, 1968 ; Re-submitted September 23, 1968 and

January 21, 1969)

The field of a charge moving along the axis of a cylindrical wave-guide, which is filled with a moving dielectric, is obtained. Simple expressions are derived for the total energy loss due to the Cherenkov radiation and the excitation of plasma waves. The energy of the continuous spectrum is found to be concentrated at certain discrete frequencies, as usual in a waveguide.

1. INTRODUCTION

Abele (1952), Akhiezer (1956), Bogdankevich & Bolotovskii (1957), Bouch-Osmolovskii (1963), Lomize & Kurbanov (1961) and many others have studied the waveguide problem in relation to the Cherenkov radiation. In each case the medium within the waveguide is stationary and a point charge or a beam of electrons or a dipole is moving within it. So it is natural that one will be tempted to think of a waveguide loaded with a moving dielectric. Here we consider a dielectric medium moving within an infinite metallic cylinder of radius a and a point charge is also moving along the axis of the cylinder. To write down the fundamental equations we have borrowed some idea of Bolotovskii & Rukhadze (1959) who have discussed certain properties of the field and the energy loss due to the Cherenkov radiation for a moving charge in a moving medium.

Electro-magnetic field intensities have been investigated in section 3; they are consistent with the usual boundary conditions. In section 4 the total energy loss due to the Cherenkov radiation has been derived and as it is usual in waveguide problem the modes of frequencies are obtained in a very simple form. By a little modification it is shown in section 5 that energy loss due to plasma oscillations may be obtained. The energy loss of a charge in a waveguide is generally determined by the retardation force exerted on the charge by the field produced by the charge. We have calculated the total energy loss by the general technique of the Poynting vector. As a consequence the result obtained is not exactly identical with those of others.

2. PHENOMENOLOGICAL EQUATIONS

Let us consider the phenomenological equations of classical electrodynamics for a moving medium which have been used by Ryazanov (1957) and Bolotovskii & Rukhadze (1959). Let $\epsilon(\omega)$ and μ be the dielectric constant and the permeability of the medium in the rest system and

$$\chi = \epsilon\mu - 1 \quad \dots(1)$$

If the medium moves with the 4-velocity u_i ,

$u_{1,2,3} = \sqrt{\left(1 - \frac{u^2}{c^2}\right)}, u_4 = \sqrt{\left(1 - \frac{u^2}{c^2}\right)}$ (c is the velocity of light in vacuum and " u " is the three dimensional velocity of the medium) then dielectric-magnetic permeability tensor is written in the form

$$\epsilon_{ik,11} = \frac{1}{\mu} \left(\delta_{ik} + \frac{\chi}{c^2} u_i u_k \right) \left(\delta_{ik} + \frac{\chi}{c^2} u_i u_k \right). \quad \dots(2)$$

Maxwell's equations assume the form

$$\left. \begin{aligned} \delta_i F_{k,1} + \delta_k F_{i,1} + \delta_1 F_{ik} &= 0 \\ \delta_k H_{ik} &= -\frac{4\pi}{c} j_i \\ H_{ik} &= \epsilon_{ik,11} F_{ik} \end{aligned} \right\} \quad \dots(3)$$

where $\delta_i \left(-\nabla, \frac{1}{c} \frac{\partial}{\partial t} \right)$ is the four dimensional gradient. F_{ik} is a field tensor (electric field and magnetic induction field) and H_{ik} is a field tensor (magnetic field and electric induction field).

Let us introduce the 4-potentials A_i in accordance with the relation

$$F_{ik} = \delta_i A_k - \delta_k A_i. \quad \dots(4)$$

A supplementary condition about connection of the 4-potentials is

$$\delta_i \left(A_i + \frac{\chi}{c^2} u_i u_k A_k \right) = 0. \quad \dots(5)$$

Under these conditions the equations for potentials are

$$\left[\delta_k^2 + \frac{\chi}{c^2} (u_k \delta_k)^2 \right] \left(\delta_{ii} + \frac{\chi}{c^2} u_i u_i \right) A_i = -\frac{4\pi}{c} \mu j_i. \quad \dots(6)$$

These equations are in good agreement with those in a medium at rest ($u = 0$).

In our case we consider the axis of the cylinder as z -axis and the medium is moving with a velocity u in the direction of z -axis. Therefore

$$u_1 = 0 = u_2, u_3 = \frac{u}{\sqrt{1 - \frac{u^2}{c^2}}}, u_4 = \frac{c}{\sqrt{1 - \frac{u^2}{c^2}}}.$$

Further we assume that a point charge q moves along the z -axis with a velocity v inside the medium which is itself moving with a velocity u .

The components of 4-density vector are

$$\left. \begin{aligned} j_1 = 0, j_3 &= vq\delta(x)\delta(y)\delta(z-vt) \\ \text{and } j_4 &= -cq\delta(x)\delta(y)\delta(z-vt). \end{aligned} \right\} \quad (7)$$

Taking $A_1 = 0 = A_2$ and the Fourier transform of A_3 and A_4 in the form $A_3 = \int_{-\infty}^{\infty} A_3(\omega) e^{i\omega t} d\omega$, $A_4 = \int_{-\infty}^{\infty} A_4(\omega) e^{i\omega t} d\omega$, we have from (6) and (7)

$$\left. \begin{aligned} &\left[\frac{\partial^2}{\partial x^2} + \frac{\partial^2}{\partial y^2} + \frac{\partial^2}{\partial z^2} + \frac{\omega^2}{c^2} - \frac{\chi}{c^2 - u^2} \left(i\omega - u \frac{\partial}{\partial z} \right)^2 \right] \times \\ &\quad \left\{ \left(1 + \frac{\chi u^2}{c^2 - u^2} \right) A_3(\omega) + \frac{\chi c u}{c^2 - u^2} A_4(\omega) \right\} = -\frac{2\mu q}{c} \delta(x)\delta(y) e^{-i\omega z/v} \\ &\left[\frac{\partial^2}{\partial x^2} + \frac{\partial^2}{\partial y^2} + \frac{\partial^2}{\partial z^2} + \frac{\omega^2}{c^2} - \frac{\chi}{c^2 - u^2} \left(i\omega - u \frac{\partial}{\partial z} \right)^2 \right] \times \\ &\quad \left\{ \frac{\chi c u}{c^2 - u^2} A_3(\omega) + \left(1 + \frac{\chi c^2}{c^2 - u^2} \right) A_4(\omega) \right\} = \frac{2\mu q}{v} \delta(x)\delta(y) e^{-i\omega z/v} \end{aligned} \right\} \quad \dots(8)$$

Putting $A_3(\omega) = -\eta_1(x, y) e^{-i\omega z/v}$, $A_4(\omega) = \eta_2(x, y) e^{-i\omega z/v}$ in (5) and (8) we obtain

$$-\frac{M}{v} \eta_1 + \frac{N}{c} \eta_2 = 0, \quad \dots(9)$$

$$\left. \begin{aligned} \left(\frac{\partial^2}{\partial x^2} + \frac{\partial^2}{\partial y^2} + s^2 \right) \eta_1 &= \frac{2\mu q}{cP} \delta(x)\delta(y) \\ \left(\frac{\partial^2}{\partial x^2} + \frac{\partial^2}{\partial y^2} + s^2 \right) \eta_2 &= \frac{2\mu q}{vQ} \delta(x)\delta(y) \end{aligned} \right\} \quad \dots(10)$$

$$\left. \begin{aligned} \text{where, } M &= 1 + \chi \frac{u(u+v)}{c^2 - u^2}, \quad N = 1 + \frac{\chi}{v} \frac{c^2(u+v)}{c^2 - u^2}, \\ P &= \frac{K}{N}, \quad Q = \frac{K}{M}, \quad K = 1 + \chi \frac{c^2 + u^2}{c^2 - u^2} \\ \text{and } s^2 &= \frac{\omega^2}{c^2} + \chi \frac{\omega^2}{v^2} \frac{(u+v)^2}{c^2 - u^2} - \frac{\omega^2}{v^2} \end{aligned} \right\} \quad \dots(11)$$

Let,

$$\left. \begin{aligned} \eta_1 &= L_1 J_0(s\rho) + \frac{\mu Q}{2cP} N_0(s\rho) \\ \eta_2 &= L_2 J_0(s\rho) + \frac{\mu Q}{2vQ} N_0(s\rho) \end{aligned} \right\} \quad \dots(12)$$

where, $\rho = \sqrt{x^2 + y^2}$.

$$\text{By (9) and (12)} \quad \frac{M}{v} L_1 - \frac{N}{c} L_2 = 0. \quad \dots(13)$$

Now

$$\left. \begin{aligned} A_3 &= - \int \eta_1 e^{i\omega(t-z/v)} d\omega \\ A_4 &= \int \eta_2 e^{i\omega(t-z/v)} d\omega \end{aligned} \right\} \quad \dots(14)$$

3. FIELD COMPONENTS

By the help of (3), (4) and (14)

$$\left. \begin{aligned} E_x(\omega) &= \frac{\partial x}{\rho} \left[L_2 J_1(s\rho) + \frac{\mu Q}{2vQ} N_1(s\rho) \right] e^{i\omega(t-z/v)} \\ E_y(\omega) &= \frac{\partial y}{\rho} \left[L_2 J_1(s\rho) + \frac{\mu Q}{2vQ} N_1(s\rho) \right] e^{i\omega(t-z/v)} \\ E_z(\omega) &= i\omega \left(\frac{\eta_1}{c} - \frac{\eta_2}{v} \right) e^{i\omega(t-z/v)} \\ H_x(\omega) &= - \frac{\partial y}{\mu\rho} \left[\left(1 + \chi \frac{u^2}{c^2 - u^2} \right) \left\{ L_1 J_1(s\rho) + \frac{\mu Q}{2cP} N_1(s\rho) \right\} \right. \\ &\quad \left. - \frac{\chi\omega u}{v^2 - u^2} \left\{ L_2 J_1(s\rho) + \frac{\mu Q}{2vQ} N_1(s\rho) \right\} \right] e^{i\omega(t-z/v)} \\ H_y(\omega) &= \frac{\partial x}{\mu\rho} \left[\left(1 + \chi \frac{u^2}{c^2 - u^2} \right) \left\{ L_1 J_1(s\rho) + \frac{\mu Q}{2cP} N_1(s\rho) \right\} \right. \\ &\quad \left. - \frac{\chi\omega u}{c^2 - u^2} \left\{ L_2 J_1(s\rho) + \frac{\mu Q}{2vQ} N_1(s\rho) \right\} \right] e^{i\omega(t-z/v)} \\ H_z(\omega) &= 0, \end{aligned} \right\} \quad \dots(15)$$

In cylindrical co-ordinates (ρ, θ, z)

$$\left. \begin{aligned} E_{\rho}(\omega) &= s \left[L_0 J_1(s\rho) + \frac{\mu q}{2vQ} N_1(s\rho) \right] e^{i\omega(t-z/v)} \\ H_{\theta}(\omega) &= \frac{s}{\mu} \left[\left(1 + \kappa \frac{v^2}{c^2 - v^2} \right) \left\{ L_1 J_1(s\rho) + \frac{\mu q}{2cQ} N_1(s\rho) \right\} \right. \\ &\quad \left. + \kappa \frac{cu}{c^2 - v^2} \left\{ L_0 J_1(s\rho) + \frac{\mu q}{2vQ} N_1(s\rho) \right\} \right] e^{i\omega(t-z/v)} \end{aligned} \right\} \dots(16)$$

On the surface of the cylinder (i.e. $\rho = a$) $E_z = 0$.

For this

$$\left(\frac{L_1}{c} - \frac{L_0}{v} \right) J_0(sa) + \frac{\mu q}{2} \left(\frac{1}{c^2 P} + \frac{1}{v^2 Q} \right) N_0(sa) = 0. \dots(17)$$

By (13) and (17)

$$\left. \begin{aligned} L_1 &= - \frac{\mu q}{2c} \frac{N}{K} \frac{N_0(sa)}{J_0(sa)} \\ L_0 &= - \frac{\mu q}{2v} \frac{M}{K} \frac{N_0(sa)}{J_0(sa)} \end{aligned} \right\} \dots(18)$$

$$\text{Now } Re E_{\rho} = - \frac{q}{v} \int_0^{\infty} \frac{\mu s M}{K} \left\{ \frac{N_0(sa)}{J_0(sa)} J_1(s\rho) - N_1(s\rho) \right\} \cos \omega(t-z/v) d\omega$$

$$Re H_{\theta} = - \frac{q}{c} \int_0^{\infty} s \left\{ \frac{N_0(sa)}{J_0(sa)} J_1(s\rho) - N_1(s\rho) \right\} \cos \omega(t-z/v) d\omega$$

$$E_z = - i q \int_0^{\infty} \frac{\mu \omega}{K} \left(\frac{N}{c^2} - \frac{M}{v^2} \right) \left\{ \frac{N_0(sa)}{J_0(sa)} J_0(s\rho) - N_0(s\rho) \right\} e^{i\omega(t-z/v)} d\omega \dots(19)$$

4. THE RADIATION ENERGY LOSS

Total energy radiated by the particle inside the cylinder per unit time

$$\text{is } \frac{dW_1}{dt} = \frac{c}{4\pi} \int_{z=-\infty}^{\infty} \int_{\rho=0}^a (Re E_{\rho} Re H_{\theta}) 2\pi \rho d\rho dz.$$

Taking the values of $Re E_{\rho}$ and $Re H_{\theta}$ from (19) and using the formula

$$\int_{-\infty}^{\infty} \cos \omega(t-z/v) \cos \omega(t-z/v) dz = \pi v \delta(\omega - \omega')$$

we have
$$\frac{dW_1}{dt} = \frac{\pi q^2}{2} \int_{\omega=0}^{\infty} \int_{\rho=0}^a \mu s^2 \frac{M}{K} \left\{ \frac{N_0(sa)}{J_0(sa)} J_1(s\rho) - N_1(s\rho) \right\}^2 \rho d\rho d\omega$$

$$= \frac{q^2}{\pi} \int_{\omega=0}^{\infty} \frac{1 + \chi \frac{u(u+v)}{c^2 - u^2}}{1 + \chi \frac{c^2 + u^2}{c^2 - u^2}} \cdot \frac{1}{J_0^2(sa)} d\omega \quad \dots(20)$$

This integral can be determined by the residues at the poles of the expression under the integrand. Because of the poles the integral becomes a series and the continuous spectrum is replaced by a discrete spectrum characteristic of a waveguide.

Poles are obtained at the zeroes of $J_0(sa)=0$. If $J_0(sa)=0$ for $\omega=\omega_k$ and we write $sa=\alpha_k$ for this value of ω , then,

$$\frac{dW_1}{dt} = \frac{2q^2}{a^2} \sum \mu(\omega_k) \frac{1 + \chi(\omega_k) \frac{u(u+v)}{c^2 - u^2}}{1 + \chi(\omega_k) \frac{c^2 + u^2}{c^2 - u^2}} \cdot \frac{1}{J_1^2(\alpha_k)} \left\{ \frac{1}{d\omega} - \frac{\frac{d^2 s}{d\omega^2}}{2 \frac{ds}{d\omega}} \right\}_{\omega=\omega_k} \quad \dots(21)$$

The summation is taken over all harmonics for which the radiation condition $s^2 > 0$ is satisfied.

If the medium is stationary then $u=0$. In this case the total energy loss by the particle within the waveguide per unit time is

$$\frac{dW_2}{dt} = \frac{2q^2}{a^2} \sum_k \frac{1}{\epsilon(\omega'_k)} - \frac{1}{J_1^2(\alpha'_k)} \left\{ \frac{1}{\frac{ds'}{d\omega}} - \frac{\frac{d^2 s'}{d\omega^2}}{2 \frac{ds'}{d\omega}} \right\}_{\omega=\omega_k} \quad \dots(22)$$

where $s'^2 = \frac{\omega^2}{v^2} (\epsilon\mu\beta^2 - 1)$, $\beta = \frac{v}{c}$, $\alpha'_k = (s'a)_{\omega=\omega'_k}$ and $J_0(s'a)=0$ for $\omega=\omega'_k$.

For dispersionless medium ϵ and μ are independent of frequency and then from (22)

$$\frac{dW_3}{dt} = \frac{2q^2}{a^2 \epsilon} \sum_k \frac{1}{J_1^2(\alpha''_k)} \left(\frac{1}{\frac{ds''}{d\omega}} \right)_{\omega=\omega_k''} \quad \dots(23)$$

where $s''^2 = \frac{\omega^2}{v^2} (\epsilon\mu\beta^2 - 1)$, $\alpha''_k = (s''a)_{\omega=\omega_k''}$ and $J_0(s''a)=0$ for $\omega=\omega_k''$.

The summations of (22) and (23) are restricted by the conditions $s'^2 > 0$ and $s''^2 > 0$.

Following Bolotovskii (1959) and others the energy loss of the charge per unit length of the path is

$$\frac{dW}{dz} = q \cdot E_z \Big|_{\rho \rightarrow 0}^{\infty} = -q \cdot Re \int_0^\infty \frac{\mu}{K} \left(\frac{N}{c^2} - \frac{M}{v^2} \right) \frac{N_o(s'a)}{J_o(s'a)} i\omega d\omega \text{ by (19).}$$

For stationary medium $u=0$ and

$$\frac{dW}{dz} = -q \cdot Re \int_0^\infty \frac{i s'^2}{\epsilon \omega} \frac{N_o(s'a)}{J_o(s'a)} d\omega = -\frac{2q^2}{a^2} \sum_k \left[\frac{s'}{\epsilon \omega} \frac{1}{J_1^2(s'a)} \frac{1}{d\omega} \right]_{\omega=\omega'_k}$$

when $s'^2 > 0$ and $J_o(s'a) = 0$ for $\omega = \omega'_k$.

For dispersionless medium, $\frac{dW}{dz} = -\frac{2q^2}{\epsilon a^2} \sum_k \frac{1}{J_1^2(\kappa'_k)}$. It is identical with Akhiezer's result (1956).

5. ENERGY LOSS DUE TO EXCITATION OF PLASMA WAVES :

If the medium moves with a large velocity ($1 - \frac{u^2}{c^2} \ll 1$) then we may put $\mu=1$, $\epsilon = 1 - \frac{\omega_o^2}{\omega^2}$. In this case the propagation relation is the same as for an electron plasma (Bolotovskii & Rukhadze 1959) and the equations (10) convert to

$$\left. \begin{aligned} \left(\frac{\partial^2}{\partial x^2} + \frac{\partial^2}{\partial y^2} - \kappa^2 \right) \eta_1 &= \frac{2q}{cP'} \delta(x) \delta(y) \\ \left(\frac{\partial^2}{\partial x^2} + \frac{\partial^2}{\partial y^2} - \kappa^2 \right) \eta_2 &= \frac{2q}{vQ'} \delta(x) \delta(y) \end{aligned} \right\} \dots (24)$$

where $P' = \frac{K'}{N'}$, $Q' = \frac{K'}{M'}$, $K' = 1 - \frac{\omega_o^2}{\omega^2} \frac{c^2 + u^2}{c^2 - u^2}$, $M' = 1 - \frac{\omega_o^2}{\omega^2} \frac{u(u+v)}{c^2 - u^2}$,

$$N' = 1 - \frac{\omega_o^2}{\omega^2} \frac{c^2(u+v)}{v(c^2 - u^2)}, \quad \kappa^2 = \omega^2 \left[\frac{1}{v^2} + \frac{\omega_o^2}{\omega^2} \frac{(u+v)^2}{v^2(c^2 - u^2)} - \frac{1}{c^2} \right].$$

Taking $\eta_1 = I_s I_o(\kappa\rho) - \frac{q}{\pi c P'} K_o(\kappa\rho)$, $\eta_2 = I_s I_o(\kappa\rho) - \frac{q}{\pi v Q'} K_o(\kappa\rho)$

and proceeding as section 2 and 3 we have

$$\left. \begin{aligned} ReE_p &= -\frac{2\omega}{\pi v} \int_0^\infty \frac{\alpha M'}{K'} \left[\frac{K_0(\alpha a)}{I_0(\alpha a)} I_1(\alpha \rho) + K_1(\alpha \rho) \right] \cos \omega \left(t - \frac{z}{v} \right) d\omega \\ ReH_\theta &= -\frac{2q}{\pi c} \int_0^\infty \alpha \left[\frac{K_0(\alpha a)}{I_0(\alpha a)} I_1(\alpha \rho) + K_1(\alpha \rho) \right] \cos \omega \left(t - \frac{z}{v} \right) d\omega \end{aligned} \right\} (25)$$

Energy loss per unit time is

$$\begin{aligned} \frac{dW_3}{dt} &= \frac{c}{4\pi} \int_{z=-\infty}^\infty \int_{\rho=0}^a (ReE_p ReH_\theta) 2\pi \rho d\rho dz \\ &= \frac{q^2}{\pi} \int_{\omega=0}^\infty \frac{\omega^2 (c^2 - u^2) - \omega_0^2 u (u+v)}{\omega^2 (c^2 - u^2) - \omega_0^2 (c^2 + u^2)} \cdot \frac{1}{I_0^2(\alpha a)} d\omega. \end{aligned} \quad \dots (26)$$

The integration can be determined by residue method and the poles are obtained from $\omega^2(c^2 - u^2) - \omega_0^2(c^2 + u^2) = 0$

since $\omega > 0$, $\omega_k = \omega_0 \sqrt{\frac{c^2 + u^2}{c^2 - u^2}}$.

$$\text{Thus, } \frac{dW_3}{dt} = q^2 \frac{\sqrt{(c^2 - u^2) - u(u+v)}}{\sqrt{(c^2 - u^2) + c^2 + u^2}} \cdot \frac{1}{I_0^2 \left(\frac{a\omega_0 \sqrt{c^2 - u^2 v^2}}{cv} \right)}. \quad \dots (27)$$

This investigation may provide some information about the nature of the electron plasma as the state of ionization.

The author thanks Dr. T. C. Roy of Jadavpur University, Calcutta for constant guidance throughout the progress of this work.

REFERENCES

- Abele, M. 1952 *Nuovo Cim., Series, 9, 9*, Suppl. (3), 207.
 Akhiezer, A. I. 1956 *Nuovo Cim., Series, 10, 3*, Suppl. (4), 591.
 Bogdankevich, L. S. Bolotovskii, B. M. (1957) *Sov. Phys. JETP*, 5, 1157.
 Bouch-Osmolovskii, A. G. 1963 *Sov. Phys. Tech. (USA)*, 8 (3), 217.
 Lomize, L. G. Kurbanov, O.M. 1961 *Zh. Tekh. Fiz. USSR*, 31 (6), 657.
 Bolotovskii, B. M. Rukhadze, A. A. 1959 *Sov. Phys. JETP*, 37 (10), 695.
 Ryazanov, M.L. 1957 *Sov. Phys. JETP*, 5, 1013.
 Bolotovskii, B. M. 1961 *Sov. Phys. Uspekhi*, 4, 781.

Letters to the Editor

On the structure of hydroxylamine uranium (IV) flouride

By T. RATHO, T. PATEL AND B. SAHU*

Department of Physics, Regional Engineering College, Rourkela, India,

(Received September 5, 1968 ; Resubmitted April 13, 1969)

Hydroxylamine uranium (IV) flouride ($\text{UF}_4 \cdot \text{NH}_2 \cdot \text{OH} \cdot \text{HF}$) is obtainable in the form of micro-crystals, green in colour. As the substance did not show the possibility of yielding any suitable single crystal, the powder method of study was undertaken. In our previous paper (Ratho *et al* 1968), we have found out the unit cell dimensions, number of molecules per unit cell and space group of hydrazine uranium (IV) flouride ($\text{N}_2\text{H}_4\text{UF}_6$). Such study will throw light on how the different groups are rearranging themselves with uranium.

The chemically pure substance was taken and filtered $\text{CuK}\alpha$ ($\lambda=1.54\text{\AA}$) radiation, obtained from a Machlett A-2 X-ray Diffraction tube operated at 30 KV and 20 mA, was used to irradiate the sample in a 9 cm diameter Rigaku camera for 16 hours to record a suitable powder pattern. The rings on the photograph were measured and the corresponding $\sin^2\theta$ values and inter-planar spacings d were recorded in the table. Failing to fit the data to cubic, tetragonal and hexagonal systems the Lipson's (Lipson 1949) method was worked out. The difference diagram and the appearance of good number of constant differences forecasted that the crystal may be orthorhombic.

For orthorhombic crystal, we know,

$$\sin^2\theta = Ah^2 + Bk^2 + Cl^2$$

$$\text{where } A = \lambda^2/4a^2, B = \lambda^2/4b^2 \text{ and } C = \lambda^2/4c^2.$$

* Dept. of applied chemistry, I.I.T., Kharagpur.

TABLE 1.

Spacings 'd' and intensity	sin ² θ		Indices	Spacings 'd' and intensity	sin ² θ		Indices
	obs.	cal.			obs.	cal.	
3.65420 vvw	0.04442	0.04446 0.04379	300 230	1.51651 vvw	0.25785	0.25779 0.25792 0.25818	292 084 721
3.46227 m	0.04946	0.04990 0.04896	301 003			0.25832 0.25776	246 445
3.27860 m	0.05516	0.05514	320	1.48351 vvw	0.26937	0.26952	643
3.00434 w	0.06569	0.06622 0.06555	302 232	1.43830 vvw	0.28658	0.28676 0.28659 0.28632	2,10,0 275 207
2.84559 vvw	0.07322	0.07299 0.07393	033 331	1.38922 vw	0.30732	0.30688 0.30760	085 644
2.60890 vvw	0.08710	0.08704 0.08715 0.08651 0.08718	004 411 250 340			0.30666 0.30705	564 356
				1.37573 vvw	0.31326	0.31369	317
2.34326 vvw	0.10797	0.10827 0.10851	252 431	1.35443 vw	0.32218	0.32160 0.32170 0.32201	801 327 516
2.12810 m	0.13096	0.13083 0.13161 0.13150 0.13067	070 511 304 413	1.24103 vw	0.38497	0.38448 0.38436	0,12,0 626
				1.22243 vvw	0.39577	0.39594	5,10,1
2.05994 w	0.13973	0.13962	521			0.39529 0.39585	318 754
2.02960 vvw	0.14391	0.14361 0.14352	115 442	1.16791 vw	0.43473	0.43438 0.43404	3,12,1 862
1.84500 w	0.17417	0.17355 0.17422	254 344			0.43470	782
				1.07350 vvw	0.51454	0.51450	7,10,1
1.82424 m	0.17817	0.17784 0.17812	600 045			0.51467 0.51438	816 548
1.74780 vvw	0.19429	0.19396 0.19475	621 453	1.02760 vw	0.56210	0.56232 0.56222 0.56187	6,12,0 449 497
1.66852 vvw	0.21297	0.21240 0.21321	282 514				
1.56420 vvw	0.24223	0.24206 0.24232	700 642				

With the help of the above equation all the lines on the powder pattern could be easily indexed, and the constants obtained are $A = 0.00494 \pm 0.00006$, $B = 0.00267 \pm 0.000035$ and $C = 0.005444 \pm 0.000065$. Thus the cell dimensions obtained are $a = 10.9630 \pm 0.0660 \text{ \AA}$, $b = 14.9024 \pm 0.0890 \text{ \AA}$ and $c = 10.4391 \pm 0.0630 \text{ \AA}$.

The experimental value of the density of the crystal was found out to be 4.3501 gm/cc and the calculated density is 4.2909 gm/cc. The number of molecules per unit cell comes out to be 12. The study of indices shows, hkl, hk0, h0l, 0kl, h00, 0k0, and 00l to have no condition. Therefore the probable space group assigned to the crystal is $P222$ or $Pmm2$ or $Pmmm$.

REFERENCES

- Azaroff, L. V. & Buerger, M. J. 1958 *Powder Method*, The Maple Press Company, York, PA. McGraw Hill Book Co.
 D'eye, R. W. M. & Wait, E. 1960 *X-ray Powder Photography in Inorganic Chemistry*, London, Butterworths Scientific Publications, printed in Northern Ireland, at the University Press, Belfast.
 Henry, N. F. M., Lipson, H. & Wooster, W. A. 1951 *The Interpretation of X-ray Diffraction Photographs*, London, Mcmillan & Co. Ltd., New York, St. Martins Press.
 Lipson, H. 1949 *Acta Cryst.* **2**, 43.
 Ratho, T. & Patel, T. 1968 *Indian J. Phys.* **42**, 140.

Indian J. Phys. **43**, 166–168 (1969)

On the structure of dithiocyanato-tetrakis γ -picoline zinc (II)

By T. RATHO AND T. PATEL

Department of Physics, Regional Engineering College, Rourkela, India

(Received April 8, 1968 ; Resubmitted April 18, 1969)

Dithiocyanato-tetrakis γ -picoline zinc (II) $[\text{Zn}(\gamma\text{-C}_6\text{H}_7\text{N})_4(\text{CNS})_2]$ is white in colour and obtainable in the form of microcrystals. As it was not possible to develop single crystals out of it, the powder method of analysis was followed for identification. The Debye-Scherrer powder pattern was obtained in six hours by a 9 cm diameter Rigaku camera using filtered $\text{CuK}\alpha$ radiation obtained from a Machlett A-2 X-ray diffraction tube running at 30 KV and 15 mA.

Measuring the line positions on the film, Q_{hkl} values for the lines were computed accurately (table 1). A systematic analysis of the data after Azaroff *et al* (1958) and Henry *et al* (1951) eliminated the possibility for the crystal belonging to any higher symmetry.

Then the most general procedure due to Ito (1950) was adopted. We know that

$$Q_{hkl} = \frac{1}{d_{hkl}^2} = h^2 a^{*2} + k^2 b^{*2} + l^2 c^{*2} + 2hkb^*c^* \cos \alpha^* + 2lhc^*a^* \cos \beta^* + 2hka^*b^* \cos \gamma^*$$

where a^*, b^*, c^* and $\alpha^*, \beta^*, \gamma^*$ are reciprocal axes and cell angles respectively.

TABLE 1

Spacings 'd' and intensity	Q_{hkl}		Indices	Spacings 'd' and intensity	Q_{hkl}		Indices
	Obs.	Com.			Obs.	Com.	
9.23380 m	0.0117	0.01192	100	1.92458 vw	0.2700	0.27042	125
8.21992 s	0.0148	0.01460	010	1.85554 vvw	0.2905	0.29008	240
5.17910 m	0.0373	0.03720	002	1.75442 vvw	0.3249	0.32435	510
4.57762 m	0.0477	0.04768	200			0.32582	725
4.15377 w	0.0580	0.05798	201	1.48674 vvw	0.4524	0.45292	533
		0.05758	210	1.11118 vvw	0.8100	0.80980	822
		0.05840	020			0.80928	355
3.89852 s	0.0658	0.06562	120			0.80932	465
				1.02941 m	0.9441	0.94402	409
3.64670 vs	0.0752	0.07502	120			0.94448	280
3.44900 s	0.0841	0.08488	202	0.92066 m	1.1808	1.18068	2510
		0.08452	022			1.18137	675
		0.08370	003	0.86760 s	1.3285	1.32862	566
3.17819 vw	0.0990	0.09864	212			1.32781	4317
3.02753 vvw	0.1091	0.10875	221			1.32781	738
2.87830 vvw	0.1207	0.12088	113	0.86521 s	1.3358	1.33563	855
2.74888 m	0.1323	0.13239	031			1.33552	384
		0.13270	123	0.85073 s	1.3849	1.38509	673
						1.38513	855
						1.38548	359
2.59168 m	0.1489	0.14901	031			1.38421	4317
		0.14959	213				
		0.14880	004	0.84744 s	1.3925	1.39203	857
2.43144 vvw	0.1692	0.16798	131	0.78947 vvw	1.6050	1.60480	1133
2.23530 vw	0.2001	0.20002	401			1.60411	974
		0.19988	214	0.786646 vvw	1.6168	1.61652	864
2.18505 vw	0.2094	0.20899	411			1.61641	493
		0.20914	133			1.61626	3411
2.09844 vvw	0.2271	0.22758	412				
		0.22779	411				

After thorough search the first three lines in the table were selected as reasonable choice for Q_{100} , Q_{010} and Q_{001} . The corresponding reciprocal cell dimensions, as calculated, are

$$a^* = 0.10918, b^* = 0.12083 \text{ and } c^* = 0.096436.$$

The theoretical reciprocal inter-axial angles are given by

$$\cos \alpha^* = (Q_{0kl} - Q_{0k\bar{l}}) / 4klb^*c^*$$

$$\cos \beta^* = (Q_{hol} - Q_{h\bar{o}l}) / 4lhc^*a^*$$

$$\cos \gamma^* = (Q_{hko} - Q_{h\bar{k}o}) / 4hka^*b^*$$

The calculated values are $\alpha^* = 83^\circ 11'$, $\beta^* = 90^\circ$ and $\gamma^* = 8^\circ 54'$.

The dimensions of direct cell thus calculated are,

$$a = 9.19600 \pm 0.055 \text{ \AA} \quad \alpha = 96^\circ 51'$$

$$b = 8.36979 \pm 0.050 \text{ \AA} \quad \beta = 89^\circ 23'$$

$$c = 10.44370 \pm 0.063 \text{ \AA} \quad \gamma = 95^\circ 9'.$$

The Buerger test established the cell dimension to be reduced ones.

The indices show the following condition :

hkl , $hk0$, $h0l$, $h00$, $0k0$, $00l$ = no condition $0kl$, $k+l$ even present.

Therefore, the space group assigned is $P1$ or $P\bar{1}$. The experimental density is 1.2127 gm/cc and the calculated density is 1.15695 gm/cc. Thus the crystal was established to be triclinic.

REFERENCE

- Azaroff, L. V. & Buerger, M. J. 1958 *Powder Method*, The Maple Press Company, New York, PA. McGraw Hill Book Co.
- D'eye, R. W. M. & Wait, E. 1960 *X-ray powder Photography in Inorganic Chemistry*, London Butterworths Scientific Publications printed in Northern Ireland, at the University Press, Belfast.
- Henry, N. F. M., Lipson, H & Wooster, W. A. 1951 *The Interpretation of X-ray. Diffraction Photographs*, London, Mcmillan & Co. Ltd., New York, St. Martins Press.
- Ito, T., 1950, *X-ray Studies in Polymorphism*. Maruzen, Tokyo.

Electrical properties of molybdenite

By S. R. GUHA THAKURTA

*Department of Magnetism, Indian Association for the Cultivation of Science,
Jadavpur, Calcutta-32, India*

(Received April 30, 1969)

Of the investigations carried out to study the electrical properties of natural single crystals of molybdenite (MoS_2) special mention may be made of those by Gottstein (1914), Dey (1944), Dutta (1947), Mansfield & Salam (1953) and Evans & Young (1965). But none of these measurements is complete in the sense that both the principal values of all the required electrical properties have not been determined over the necessary temperature range. Further, these workers do not agree as to the sign of the carriers, as also to some extent the values and the nature of the temperature variations of the different electrical properties (table 1). We have, therefore, undertaken to measure in vacuum and in dark the principal values of electrical conductivities and of thermoelectric powers. The Hall effect could, however, be measured only for currents in the basal plane, measurement with current in the other direction not being possible, due to the peculiar flaky nature of the crystal. A number of natural molybdenite crystals used obtained from Ceylon, was used for these measurements extending over the temperature range from 90°K to about 840°K. Results of these measurements on a typical crystal are shown in table 1 and figures 1, 2 and 3.

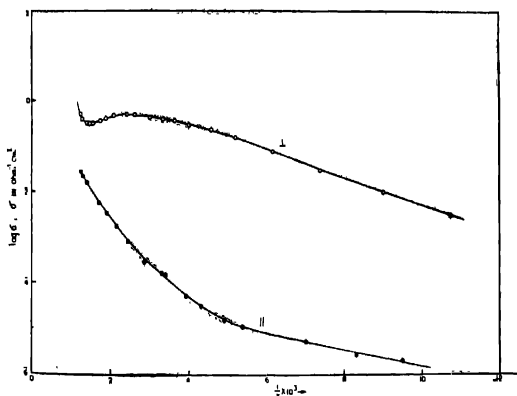


Figure 1. Variation of principal conductivities with temperatures.

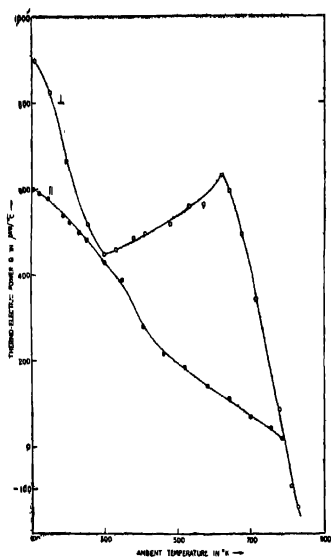


Figure 2. Variation of principal thermoelectric powers with temperatures.

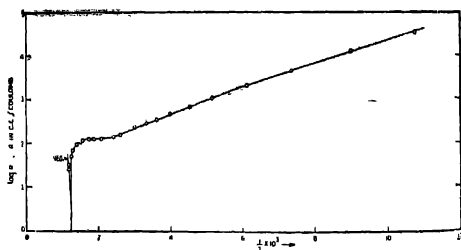


Figure 3. Variation of Hall coefficient with temperatures.

For directions in the basal plane molybdenite has been found to be a *p*-type semiconductor at lower temperatures changing to *n*-type in the

TABLE 1

Authors	Conductivities in $\text{Ohm}^{-1} \text{Cm}^{-1}$		Activation energy E_L in ev. in the range of		Activation energy $E_{ }$ in ev. in the range of	Hall coeff. in c.g.s. e m.u.	Thermoelectric power Q in $\mu\text{V}/^\circ\text{C}$ at 300°K	
	σ_L	$\sigma_{ }$	impurity	intrinsic			Q_L	$Q_{ }$
Gottstein	0.61 at 300°K	—	0.145	—	—	—1500 at 291°K	463 to 739	—
Dey	1.03 at 300°K	3.69×10^{-4}	0.09	—	0.12	—	—	—
Dutta	1.09 at 300°K	3.0×10^{-4}	0.0022	—	0.001	—	—	—
Mansfield & Salam	0.009 to 4.2 at room temperatures	—	0.09	—	—	350 to 30,000 at room temperatures	520 to 580	—
Evans & Young	0.078 at 290°K	4.6×10^{-4}	0.08	0.87	0.08	—2850 at 250°K	—	—
Present Author	0.79	3.88×10^{-4}	0.10	1.1	0.07	2880 at 300°K	450	430

intrinsic region at high temperature (about 800°K) as revealed by the reversal of sign of Hall coefficient and of thermoelectric power. But along the *c*-axis, though the actual reversal of sign of the thermoelectric power did not take place even upto 790°K, the value diminished in such a manner that an actual reversal at higher temperatures might be expected.

From a study of the conductivity curves (figure 1) and also in view of the above finding it may be inferred that at ordinary temperatures the σ_1 , conductivity along the basal plane, is mainly due to the presence of an acceptor type of impurity level in the forbidden region (*P*-type conduction) which owing to a large band gap gets exhausted at higher temperatures and after that, till a temperature sufficient to overcome the energy gap between the valence and conduction band is attained, and then the number of carriers remains steady (shown by the usual type of fall of conductivity with rise of temperature due to lattice scattering). After that conductivity begins to rise again due to excitation of electrons from valence band to the conduction band. But the absence of a similar behaviour along the *c*-axis appears to be due to the electrons being excited to the conduction band simultaneously with the exhaustion of the impurity level indicating a smaller energy gap (in this direction). Such view is also supported from the consideration of the structure of the Brillouin zone in molybdenite.

Author wishes to express his best thanks to Shri A. K. Dutta for suggestion and guidance and to Prof. A. Bose for his interest in the work. Thanks are also due to Mr. L. J. D. Fernando, Government Mineralogist, Ceylon for presenting us with the samples of molybdenite crystals and to late Dr. D. N. Wadia, F. R. S., for kindly helping us in obtaining some specimens of molybdenite.

REFERENCES

- Dey, A. P. 1944 *Proc. Nat. Acad. Sc. India*, **14**, 47.
Dutta, A. K. 1947 *Nature* **159**, 477.
Evans, B. L. & Young, P. A. 1965 *Proc. Roy. Soc. A* **284**, 402.
Gottstein, G. 1914, *Ann. Phys.* **43** 1079
Manfield. R. & Salam, S. A. 1953 *Proc. Roy. Soc. B* **66**, 377.

BOOK REVIEWS

Satyendra Nath Bose 70th Birthday Commemoration Part I and Part II.

Published by Prof. S. N. Bose 70th Birthday Celebration Committee,
92, Acharya Prafulla Chandra Road, Calcutta-9. Prices Part I-Rs. 10/- (India) \$ 3.00
or £ 1 (abroad), Part II Rs. 25/- (India) \$ 7.50 or £ 2-10sh (abroad)

It is in the fitness of things that the 70th Birthday of one of the greatest personalities and a top scientist not only of India but of the world was celebrated and the publication of two substantial volumes to commemorate this were undertaken. The latter task undertaken by the organisers has been a stupendous and delicate one on account of the mansided activities of Professor S. N. Bose and the eagerness of the very large number of his admirers to contribute papers to the volumes. It is highly gratifying that the long expected commemoration volumes have at last come out.

In Part I, the first two articles are the life sketches of Professor Bose. The first article depicts him as a scientist and the second his great personality. The former, though brief, touches upon in a very lucid way his principal scientific activities and brings out the great importance of Bose Statistics, in particular. One aspect of his scientific activities has unfortunately been left out, namely, the great impetus he gave to the construction of sophisticated apparatus for scientific research in our own laboratories. In the other sketch the emotional aspects of his life have been described. The great effect upon him of the renaissance in India including the political and educational fields as well as his own important contributions to the renaissance have been described. Although, it gives an insight into his great talents, one seriously misses one of the outstanding aspects of his character which makes him so near and dear to all who have the good fortune of knowing him, namely, his great love and sympathy for not only those near and around him but for his countrymen and humanity in general. His unstinting help to students and political workers in difficulties, whether financial or otherwise, has been proverbial. By plunging himself wholeheartedly into relief works particularly in the riot devastated areas of Dacca district he became a source of inspiration to social service workers. Inclusion of these aspects would have made the life sketch more complete.

Reproduction of his valuable and widely scattered publications in one volume has served a great purpose. Four of his papers have not, however, been reproduced and one expected a statement about the reason for their omission by the editor.

In Part II of the commemoration volumes, the organizers have to be highly congratulated for the collection of a large number of articles of high standard from leaders of scientific thoughts from all over the world. It is particularly befitting the occasion that contributions in widely divergent fields of his activity could be collected.

As a matter of minor criticism it may be mentioned that two of the articles do not properly fit in here as they are really subjects for short notes in scientific journal. The authors of these two publications are likely to suffer the disadvantage that these may not be abstracted in abstracting journals.

We are confident that these two volumes will be hailed by the scientists and all the admirers of Professor Satyen Bose all over the world.

K. B.

Indian J. Phys. **43**, 174 (1969)

International Conference on Spectroscopy, Bombay 1967.

Dept. of Atomic Energy, Govt. of India, Bombay.

Price Rs. 75'00, \$ 12'50

The book is a collection of invited talks presented at the symposium by some well-known spectroscopists. Most of the authors have reviewed the current developments in their special fields, while others have preferred to confine themselves to the discussion of their own work. The papers are classified into the following categories: a) Electronic spectrum, 1) Atoms and diatomic molecules 2) Polyatomic molecules; b) Infra-red and Raman vibration-rotation spectra c) NMR and Microwave spectra d) Miscellaneous (including solid state). The book is stimulating and succeeds in giving a fairly good idea of the recent activities in spectroscopy. However, topics like laser spectroscopy, luminescence and energy transfer, Zeeman splitting of molecular levels, crystal field transitions etc. have not received much attention. It would have been better to include the relevant 'discussions' along with paper. The printing is very good. The book will be a good addition to the library of any research organisation.

M. C.

Indian J. Phys. **43**, 174 (1969)

Erwin Schrödinger. An Introduction to his Writings.

by William T. Scott, University of Massachusetts Press 1967,

V & Bibliography Pp 175 Price \$6.50.

Erwin Schrödinger's contributions to Physics have been so great and their impact on philosophy so profound that his name is to-day familiar to anyone with a good general education. Yet as one goes through this book, one learns that Schrödinger was not merely a physicist, who besides making original researches, was troubled by the interpretations of his own work and not only did he ponder deeply of the basic problems of biology but his mind soared to such thoughts as 'Whence came I and whither go I?' and his analysis led him to the philosophy of 'Advaita' as propounded in the Vedanta. "We are all in reality sides or aspects of one single being, which may be called God while in the Upanishads its name is Brahman." The rather unusual book by Scott which proposes to give the reader an insight into the thoughts of this rich mind will naturally be welcome to the enlightened amongst the Physicists, but the reviewer feels afraid that there are not many who will be able to follow Schrödinger in this long and varied journey from physics to biology and then to philosophy and poetry.

A. K. B.

Particles and Fields

by David Lurie, New York, John Wiley, 1968 pp xii + 506. Price \$ 15.00

The interest in the quantum field theory is revived in recent years. Considerable attention is now being given to an examination of basic field theory by analyzing afresh some of the older problems. Field variables like currents and fields are being assigned important place as fundamental dynamical variables. At this juncture the appearance of this elegant representation of the orthodox quantum field theory by Dr. David Lurie is welcomed; and this is a new addition to a few books already available on this subject by well-known authors.

The first half of the book, consisting of six chapters, contains a graceful simple treatment of the elements of field quantization and the covariant perturbation theory—the traditional domain in the field. The opening chapter deals with relativistic one-particle theories of Klein-Gordon field, Dirac field, massive vector field of spin 1 and Rarita-Schwinger field of spin $3/2$ as well as the Maxwell field. Chapter 2 is devoted to emphasise the field aspect of these theories and for the formulation of Lagrangian formalism. The connection between field and quantum particle aspects are then discussed by means of field quantization in Chapters 3 and 4. The canonical quantization of spin 0 and spin $1/2$ fields, and on introductory discussion of Schwinger's quantum action principle are included in Chapter 3; whereas Chapter 4 is devoted to the quantization of electromagnetic field and massive fields of spin 1 and spin $3/2$. The explicit discussion of spin 1 and spin $3/2$ massive fields is an innovation in this book, which is seldom discussed in others. The present reviewer prefers the quantization of massive vector field retaining the β -formalism of Kemmer, which would have been just on the same line as Dirac field, instead of the method followed by the author.

Chapter 5 treats interacting quantum fields. The electromagnetic and non-electromagnetic couplings for elementary particle interactions have been formulated giving sufficient weight to the symmetry principles and conservation laws. Chapter 6 introduces the reader to the perturbation theory. The first half of this chapter is concerned with Feynman rules for calculating the transition matrix elements with simple applications to electromagnetic and weak processes and the second half is devoted to renormalization theory. The treatment of the renormalization theory, reduction formulae and spectral representation brings out the essential ideas without being too much entangled in mathematical details. Coupling constants and sum rules have been discussed in a quite fascinating manner.

The second half of the book, which constitutes the last four chapters, is devoted to introducing the reader to advanced quantum field theory. S-matrix and the link between transition amplitudes and the vacuum expectation values of products of field operators are developed in Chapter 7. Particular stress is made on the abstract nonperturbative reformulation of field theory based on the use of the asymptotic condition. Chapter 8 deals with a few applications of field theoretic techniques to particle physics topics include the Goldberger-Treiman relation, the Adler-Weisberger sum rule and the universality of the vector coupling constant in the theory of weak interactions. Chapter 9 is devoted to a number of topics relating to bound states, which include the Bethe-Salpeter equation and the assignment of field operators to composite particles. The final chapter is concerned with the powerful functional approach to quantum field theory developed by Schwinger. Application of this functional technique is made to the Gold-

stone theory and to one-dimensional quantum electrodynamics. A short discussion on the functional integration technique is also included. The treatment of the Bethe-Salpeter equation, of bound state and of the functional method, which are generally discussed only briefly in the most of the existing books on the field theory, is praiseworthy.

The dispersion relations and the axiomatic field theory—two major topics have been completely omitted in the book. On the inclusion of these topics the book would have been more or less complete. The author could not treat every aspect of many problems in the same detail, and one may differ from him in the appreciation of relative importance of such aspects. The book is mainly intended for theoretical physicists. Those with some experience in this field will find it extremely valuable both for consecutive reading and for reference purpose. A new comer would enjoy this book if he is well-acquainted with the ordinary non-relativistic quantum mechanics, including the formal theory of scattering, relativistic quantum mechanics, and with the basic phenomenology of elementary particles. He would derive a great deal of benefit by reading this book and supplementing it with other readings.

In summary, this book should prove very helpful to those who want to specialize in quantum field theory,

S. G.

Molecular constants of a few Group IV tetra hydrides and their deuterium substituents

By K. RAMASWAMY AND V. RANGANATHAN

Department of Physics, Annamalai University, Annamalaiagar.

(Received October 22, 1968 ; Resubmitted January 15, 1969)

The potential energy constants of a few Group IV tetrahydrides belonging to the tetrahedral XY_4 type were obtained by the method of "Characteristic set" of vibrational symmetry co-ordinates. The values were determined without any assumption regarding any specific force field. The mean amplitudes of vibration for the various characteristic bonds were determined by Cyvin's method. The Coriolis coupling constants and the rotational distortion constants were also obtained, which verify the validity of the symmetry force constants obtained by this method.

INTRODUCTION

Several attempts have been made earlier, to calculate the potential energy constants which help in the thorough understanding of the molecular dynamics. But it is not always possible to calculate the force constants from the vibrational spectral data alone, since the number of force constants exceed the number of fundamental frequencies. So one is forced to assume some specific force field as in the case of UBFF (Urey & Bradley 1931), HBFF (King 1962) and OVFF (Heath & Linnett 1948) or turn to other data regarding other molecular constants, and such attempts have been made previously by several workers (Aldous & Mills 1962, 1964; Krishna Pillai & Perumal 1964; Duncan & Mills, 1964). One such attempt in this direction has been made by Herranz & Castano (1966). This method does not make any specific assumption regarding force fields. Herranz & Castano (1966) have already applied this method to calculate the potential constants of silane and deuterio-silane. In the present study we have applied their method for the calculation of all the molecular constants of Group IV tetrahydrides and their deuterium substituents.

POTENTIAL ENERGY CONSTANTS.

A set of orthogonal, normalised internal symmetry co-ordinates (Cyvin 1960) was used in the normal co-ordinate analysis. As suggested by Herranz & Castano (1966), "a characteristic set" of symmetry co-ordinates is the one for which the trace of the matrix of transformation between symmetry and normal co-ordinate (l), is maximum. Such a matrix provides the most, or one close to the most, physically significant set of valence symmetry co-ordinates for use in assigning all the normal co-ordinates of the molecule.

It is well known that (Wilson *et al* 1965),

$$F = \tilde{L}^{-1} \Lambda L^{-1} \quad \dots(1)$$

$$\text{and} \quad G = \tilde{L} L \quad \dots(2)$$

where F and G are Wilson's potential and inverse kinetic energy matrices and Λ is the diagonal matrix whose elements,

$$\Lambda_k = 4\pi^2 C^2 \nu_k^2 \quad \dots(3)$$

are arranged according to the frequency assignments previously made (ν_k is the vibrational frequency in cm^{-1} of the k^{th} mode and C is the velocity of light).

The orthogonal matrix B , which diagonalizes G was constructed as suggested by Herranz & Castano (1966) from which,

$$L^{-1} = B M^{1/2} \tilde{B} \quad \dots(4)$$

where $M^{1/2}$ is the diagonal matrix of the reciprocal of the positive square root of the eigenvalues of G . The asterisk denotes the transposition of a matrix.

It is seen from the above relations, that by choosing a set of co-ordinates which will be characteristic of the normal modes of vibration, it is possible to compute L^{-1} directly from G matrix which depends on the geometry of the molecule alone.

Hence one can determine the symmetry force constants (F) without any ambiguity. To check the exactness of the choice of the characteristic set of symmetry co-ordinates, the potential energy distribution for the various normal modes in the different cases are calculated from the relation of Morino & Kuchitsu (1952),

$$X_{ik} = F_{ii} \frac{L_{ik}^2}{\lambda_k} \quad \dots(5)$$

where X_{ik} is the potential energy distribution of the i^{th} symmetry co-ordinate to the k^{th} normal mode and L_{ik} is the ik^{th} element of the L matrix.

The set of the orthonormalised internal symmetry co-ordinates chosen for the tetrahedral XY_4 type molecules are the same as those used by Cyvin (1960). The G matrix elements were obtained by the usual procedure and the symmetry force constants were obtained from (1) and (4). The computed F elements along with the values reported by Herranz & Castano (1966) for silane and deuterio-silane are given in table 1,

TABLE 1. SYMMETRY FORCE CONSTANTS† OF A FEW GROUP IV TETRAHYDRIDES AND THEIR DEUTERATED DERIVATIVES

F elements.	CH_4	SiH_4	GeH_4	CD_4	SiD_4	GeD_4
F_{11}	5.0045*	2.7999	2.3323	5.1268	2.8190	2.6645
F_{22}	0.5586	0.4052	0.3176	0.5665	0.4088	0.4049
F_{33}	4.6098	2.6994 (2.729)	2.6210	5.1685	2.7608 (2.796)	2.4358
F_{44}	0.5162	0.5025 (0.500)	0.4370	0.5599	0.5112 (0.521)	0.5004
F_{44}	0.2886	0.0759 (-0.117)	0.0254	0.5859	0.1444 (-0.223)	0.0799

†Unit used mdyn/Å.

*This number of significant figures are retained for internal consistency in the calculations.

Note: Data used in these calculations are the same as those used in a previous paper by the authors (Ramaswamy & Ranganathan, 1968).

The values in parenthesis are those reported by Herranz & Castano (1966).

The potential energy distributions for the various modes evaluated using equation (5) are presented in table 2.

TABLE 2. POTENTIAL ENERGY DISTRIBUTION FOR THE GROUP IV TETRAHYDRIDES AND THEIR DEUTERIDES FOR THE f_2 SPECIES

Sym. coord.	CH_4		SiH_4		GeH_4	
	Q_2	Q_4	Q_2	Q_4	Q_2	Q_4
S_2	1.008499*	0.003114	1.001205	0.003101	1.000141	0.000420
S_4	0.005205	1.035658	0.000101	1.018959	0.000011	1.000552
	CD_4		SiD_4		GeD_4	
	Q_2	Q_4	Q_2	Q_4	Q_2	Q_4
S_2	1.030543*	0.104057	1.004237	0.010728	0.995848	0.003757
S_4	0.002191	1.132408	0.000361	1.014664	0.000118	1.005141

*This number of significant figures are retained for internal consistency in the calculations.

MEAN SQUARE AMPLITUDES OF VIBRATION

The elements of the mean square amplitude matrix were evaluated by the method suggested by Cyvin (1959). The relation is given by,

$$\Sigma = L \Delta L^* \quad \dots (6)$$

where Δ is a diagonal matrix whose elements are defined as,

$$\Delta_k = \frac{h}{8\pi^2 \nu_k C} \coth \left(\frac{h \nu_k C}{2kT} \right) \quad \dots (7)$$

where h is Planck's constant, k Boltzmann's constant, T is absolute temperature and C is the velocity of light in vacuum. All the calculations were made for 298.16°K and the results are presented in table 3.

TABLE 3. SYMMETRIZED MATRIX ELEMENTS FOR GROUP IV TETRAHYDRIDES AND THEIR DEUTERIDES

Σ Elements.	CH ₄	SiH ₄	GeH ₄	CD ₄	SiD ₄	GeD ₄
Σ_{11}	0.005735*	0.007669	0.008402	0.004013	0.005343*	0.005496
Σ_{22}	0.027263	0.024206	0.026980	0.019304	0.017980	0.017658
Σ_{33}	0.006633	0.008184	0.008000	0.004672	0.005840	0.006190
Σ_{44}	0.026125	0.018944	0.019344	0.021171	0.014736	0.013298
Σ_{24}	-0.001902	0.000639	-0.000225	-0.002646	-0.000908	-0.000517

*This number of significant figures are retained for internal consistency in the calculations.

TABLE 4. CORIOLIS COUPLING CONSTANTS OF GROUP IV TETRAHYDRIDES AND THEIR DEUTERIUM ANALOGUES

Coriolis constants	CH ₄			SiH ₄			CD ₄	SiD ₄	GeD ₄
	Cal. Present	Shimanouchi <i>et al</i> (1966) Obs.	Cal present	Shimanouchi <i>et al</i> (1966) Obs.	Cal. Present	Present	Present	Present	Present
ζ_2	0.081	0.056 0.036 0.071	0.027	0.046 0.033	0.002	(0.222)	(0.109)	(0.050)	
ζ_1	0.419	0.450 0.464 0.429	0.454	0.454 0.467	0.498	(0.279)	(0.391)	(0.450)	

The values in parentheses are those obtained using the force constants of their hydrogenated molecule.

CORIOLIS COUPLING CONSTANTS

The Coriolis coupling constants are determined from the two equations:

$$Tr[F(G-C)] = Tr[\lambda(E-Z)] \quad \dots (8)$$

$$\text{and} \quad \zeta_3 + \zeta_4 = 0.5 \quad \dots (9)$$

where C is a matrix as defined by Shimanouchi *et al* (1966). The ζ values have been tabulated.

ROTATIONAL DISTORTION CONSTANTS

Following the procedure of Kivelson & Wilson (1952, 1953), the derivatives of the moments of inertia tensor with respect to the various internal co-ordinates defined as J 's were constructed and the different $\tau_{\alpha\beta\gamma\delta}$ elements were determined which are defined as,

$$\tau_{\alpha\beta\gamma\delta} = -\frac{1}{2} I_{\alpha\alpha}^0 I_{\beta\beta}^0 I_{\gamma\gamma}^0 I_{\delta\delta}^0 \sum_{ij} J_{\alpha\beta}^i (F^{-1})_{ij} J_{\gamma\delta}^j \quad \dots (10)$$

where $\alpha, \beta, \gamma, \delta$ can take in turn x, y , or z , I^i are the components of the moment of inertia tensor and i refers to the internal co-ordinate. The rotational distortion constants D_J and D_{JK} for the various Group IV tetrahydrides and deuterides are given in table 5.

TABLE 5. ROTATIONAL DISTORTION CONSTANTS OF GROUP IV TETRAHYDRIDES AND THEIR DEUTERIUM SUBSTITUTENTS
(in mc/sec.)

Rotational distortion constants.	CH ₄	SiH ₄	GeH ₄	CD ₄	SiD ₄	GeD ₄
D_J	3 420	1.203	1.116	0.812	0.281	0.229
D_{JK}	0.657	0.459	0.638	0.363	0.160	0.196

DISCUSSION OF RESULTS

The method suggested by Herranz has been successfully applied to the case of Group IV tetrahydrides and their deuterium substituted derivatives. The $X-H$ stretching force constants obtained as 4.945 md/Å for C-H, 2.725 md/Å for Si-H and 2.549 md/Å for Ge-H are in good agreement with the values obtained by Mills (Mansel Davies, 1963). The increase in the C-D and Si-D stretching force constants can be attributed to some shrinkage effect of the $X-D$ bond. The variation of the interaction constants obtained here are consistent with the results obtained earlier.

(Linnett & Wheatley 1949) and (Mills 1960). The bending force constants are also in agreement with the expected results. The symmetry force constants of silane and deuteriosilane obtained by the present calculations are compared with the calculated values of Herranz & Castano (1966). The differences in the interaction constants may be due to the differences in the choice of the characteristic set of symmetry coordinates by the present authors and by Herranz & Castano (1966).

The C-H and H-H mean amplitudes of vibration obtained as 0.08005\AA and 0.11984\AA and the corresponding C-D values of 0.06714\AA and 0.09348\AA are in good agreement with the electron diffraction results of Bartell *et al.* (1961). The values of Si-H, Ge-H, Si-D and Ge-D mean amplitudes obtained as 0.08975\AA for Si-H, 0.09000\AA for Ge-H, 0.07560\AA for Si-D and 0.07757\AA for Ge-D agree well with the earlier calculations of Venkateswarlu & Rajalakshmi (1965). The non bonded interaction of H-H and D-D values of 0.126448\AA in SiH_4 , 0.130769\AA in GeH_4 , 0.106320\AA in SiD_4 and 0.107815\AA in GeD_4 also agree with the results of the earlier workers (Venkateswarlu & Rajalakshmi 1966). All the above reported values are in good agreement with the values obtained using Green's Function procedure also (Ramaswamy & Ranganathan 1968).

The nature of the potential energy distribution between the two triply degenerate modes suggests the purity of the modes chosen and that the mixing between them is very negligible.

The individual values of the Coriolis coupling constants have been determined assuming the Coriolis sum rule which has been readily verified by the authors elsewhere (Ramaswamy & Ranganathan 1968). The values of the Coriolis coupling constants agree well with the values reported by earlier workers (Shimanouchi *et al.* 1966). The rotational distortion constants are also very close to the values of the earlier calculation (Shumanouchi *et al.* 1966, Thyagarajan & Herranz 1961 and Ramaswamy & Ranganathan 1968).

CONCLUSION

The determination of an unambiguous set of potential constants and other molecular constants have been well facilitated by the method suggested by Herranz & Castano. This has been successfully applied in the case of a few Group IV tetrahydrides and their deuterated derivatives which proves the applicability of the method here.

One of the authors (V. R.) is thankful to the Council of Scientific and Industrial Research, Government of India, New Delhi for the award of a Junior Research Fellowship.

REFERENCES

- Aldous J. & Mills I. M. 1962 *Spect. Chim. Acta*, **18**, 1073.
1964 *Spect. Chim. Acta*, **19**, 641.
- Bartell L. S., Kuchitsu K. & de Neuvi R. J. 1961 *J. Chem. Phys.* **31**, 1211.
- Cyvin S. J. 1959 *Spect. Chim. Acta*, **15**, 828.
1960 *J. Mol. Spectry*, **5**, 38.
- Duncan J. L. & Mills I. M. 1964 *Spect. Chim. Acta*, **20**, 523.
- Heath D. F. & Linnett J. W. 1948 *Trans. Faraday Soc.* **44**, 873.
- Herranz J. & Castano F. 1966 *Spect. Chim. Acta*, **22**, 1965.
1966 *Anales de la Real Sociedad Espanola de Fisica Y Quimica* **62A**, 199.
- King W. T. 1962 *J. Chem. Phys.* **36**, 165.
- Krishna Pillai M. C. & Perumal A. 1964 *Bull. Soc. Chim. Fr.* **73**, 641
- Kivelson D. & Wilson E. B. Jr. 1952 *J. Chem. Phys.* **20**, 1975.
- Kivelson D. & Wilson E. B. Jr. 1953 *J. Chem. Phys.* **21**, 1229.
- Linnett J. W. & Wheatley R. J. 1949 *Trans. Faraday Soc.* **45**, 33
- Mansel Davies, 1963 *Infrared Spectroscopy & Molecular Structure* Elsevier Publishing Company, Amsterdam.
- Mills I. M. 1960 *Spect. Chim. Acta*, **16**, 35.
- Morino Y. & Kuchitsu K. 1952 *J. Chem. Phys.* **20**, 1809.
- Ramaswamy K. & Ranganathan V. 1968a *Ind. J. Pure and Applied Phys.* **6**, 651.
1968b *Ind. J. Pure and Applied Phys.* (to be published)
- Thyagarajan G. & Herranz J. 1961 *J. Mol. Spectry*, **7**, 154.
- Shimanouchi T., Nakagawa I., Hiraishi J. & Ishii M. 1966 *J. Mol. Spectry*, **19**, 78.
- Urey H. C. & Bradley C. A. 1931 *Phys. Rev.* **38**, 1969.
- Venkateswarlu K. & Rajalakshmi K. V. 1965 *Proc. Ind. Acad. Sci.* **A61**, 255
- Wilson E. B. Jr., Decius J. C. & Cross D. C. 1955 *Molecular Vibrations* McGraw Hill, New York.

Sunrise effect in the intensity of atmospherics at low frequencies

By A. K. SEN AND M. K. DAS GUPTA

Institute of Radio Physics and Electronics, University of Calcutta

(Received January 22, 1969 Resubmitted May 15, 1969)

Round the clock observations of the integrated field intensity of atmospherics (IFIA) at the low frequencies, 30, 120 and 210 Kc/s, recorded in Calcutta, exhibit a remarkable sunrise effect. The results of a detailed study of the effect are presented. The duration of the effect, the frequency dependence of the duration as also the times of start and end of the effect are critically examined in relation to the location of the source and the existing knowledge of radio wave propagation at low frequencies.

INTRODUCTION

Important changes occur in the ionospheric structure during the periods of sunrise and sunset. The field intensity of distant atmospherics received at a place through ionospheric propagation, therefore, exhibit changes both during sunrise and sunset. Extensive studies have been made in different countries on the so called sunrise and sunset effects in the level of atmospherics observed at various frequencies and the results obtained have been reported in the literature (Thomas & Burgess 1947). Namba (1933) gave an explanation of the sunrise and sunset effects observed on very long waves in terms of a "metallic" and "dielectric" type of ionospheric reflection occurring in the day and night-sides of the ionosphere, respectively. Observations by Potter (1931) in the high frequencies and by Khastgir & Ali (1942) at medium frequencies indicated that a sharp single or sometimes a double peak in the radio noise level occurs just before and just after sunset and sunrise, respectively. They have given similar explanations of the peaks of noise level. During sunset, with the gradual disappearance of the solar ionizing radiations, the electron density of the *D*-layer as well as that of the *E*-layer decreases. As a result non-deviative absorption in the *E*-layer increases, while at the same time deviative absorption in the *E*-layer increases. At the beginning, the increasing *E*-layer absorption is predominant thereby decreasing the intensity, while after sunset the decreasing *D*-layer absorption becomes more effective causing an increase of intensity. The single peaks near sunrise have also been explained by a similar reasoning. The double peaks sometimes observed can be explained in terms of a sudden "jumping" of the reflection point from the *E*- to the *F*-layer. Investigation in later years by Khastgir, *et al* (1947) on 1000 meters, during sunset times led to similar conclusions. During the International Geophysical

Year the studies of sunrises and sunsets effect were continued with special emphasis on observations of the integrated field intensity of atmospherics (Horner 1962, 1964 ; Sen 1965). These studies revealed certain general features of the effects, observed at low and very low frequencies. However, the nature of the duration of the effects and, in particular, that of their frequency dependence is not clearly understood (Whitson 1961). Some of the interesting results obtained from an analysis of the integrated field intensity of atmospherics recorded in Calcutta (lat. $22^{\circ}34'N$, long. $88^{\circ}24'E$) on 30, 120 and 210 Kc/s have been presented in this paper.

EQUIPMENT

The receiving and the recording equipments used for the observations of IFIA were based upon designs adopted during the International Geophysical Year for solar flare patrolling by the s. e. a. (sudden enhancement of atmospherics) technique (Ellison 1955), with slight modifications required for handling a wide range of field intensities due to local thunderstorms. The overall time constant of the equipment is 8 seconds for a sudden increase of input level, while, it is 1 minute for a decrease.

OBSERVATIONS

A typical record of the integrated field intensity of atmospherics (IFIA) observed at each of the three frequencies, 30, 120 and 210 Kc/s, is reproduced in figure 1, which shows the usual diurnal variations. These are : sunrise effect (A), morning minimum (D), afternoon maximum (E), late minimum (F), and night maximum (G) (WMO 1957). The gradual fall in intensity between A and D, and a gradual rise between F and G indicate sunrise and sunset effects, respectively, in the propagation path. The sunset rise, on the majority of days is, however, obscured by meteorological activity in and around Calcutta. The sunrise fall, on the other hand, was discernible on about 80% of the days in a year thus offering a reasonable volume of data for a statistical analysis.

Statistical Characteristics of Duration

The duration of the sunrise effect at 30 Kc/s, 120 Kc/s and 210 Kc/s for each day was found out. Monthly average values as also the yearly average values of the duration were calculated. It was observed that both the monthly and the yearly average values of the duration of the sunrise effect were frequency dependent. In general, the duration decreases with increasing frequency. Moreover, the duration is a minimum, in January and in June. A similar trend as described above is, in fact, also exhibited by a typical record as shown in figure 1. To examine the nature of the frequency dependence in greater detail the logarithm of the monthly average duration, normalized at 30 Kc/s with respect to the yearly average

duration at that frequency, is plotted against the frequency on a scale as shown in figure 2, which indicates that the rate of decrease of duration with frequency for a particular month is higher between 120 and 210 Kc/s than between 30 and 120 Kc/s. The seasonal variation of the rates as indicated

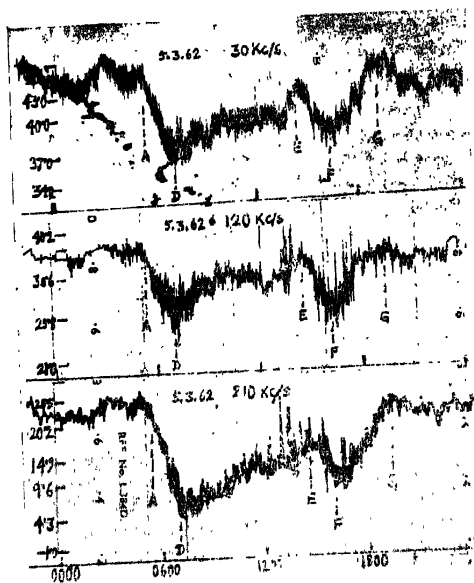


Figure 1. Photograph of a typical record of the integrated field intensity of atmospherics showing the usual diurnal variations observed on 30, 120 and 210 Kc/s at Calcutta (A : sunrise effect ; D : morning minimum ; E : afternoon maximum ; F : late minimum ; and G : night maximum). The ordinate shows the r. m. s. field strength for a 1 Kc/s bandwidth in decibels above $1 \mu\text{V/m}$.

by the slope of a line drawn in figure 2 is shown in figure 3, in which the slope is expressed in terms of a ratio of durations at frequencies differing by one octave. The figure exhibits a remarkable seasonal dependence of the slope particularly between 120-210Kc/s for which the slope is a maximum in January and a minimum in June. The yearly average of the

slopes are 1.028 and 1.065 per octave for the ranges 30-120 and 120-210 Kc/s, respectively.

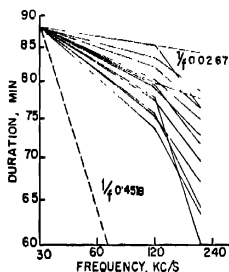


Figure 2. Frequency dependence of duration of the sunrise fall.

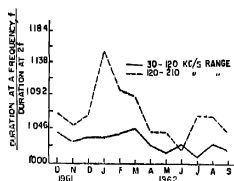


Figure 3. Seasonal variation of the ratio of durations at frequencies differing by one octave.

Upper and Lower Limits of Duration :

Table 1 shows the distribution of durations, observed at each of the frequencies over the one year period, beyond certain upper and lower limits.

TABLE 1. DISTRIBUTION OF DURATIONS BEYOND CERTAIN LIMITS.

Frequency Kc/s.	Percentage of days with durations				
	Less than 30 min	Less than 60 min	Greater than 120 min	Greater than 150 min	Greater than 180 min
30	0	7.6	13.8	2.9	0
120	0	19.3	8.4	0.7	0
210	1.3	30.1	5.7	0.3	0

The table indicates that the durations of the sunrise effect are mostly in the range 60-120 minutes. Moreover, both the lower and upper limits of the duration show marked frequency dependence.

Statistical Characteristics of the Time of Start and That of End of the Sunrise Fall :

In order to study the origin of the sunrise fall, two scatter diagrams showing the times of start and that of the end of the sunrise fall, observed at 30 Kc/s, in relation to the time of ground sunrise at the station, were drawn as shown in figure 4. It is found that the start and the end in a great majority of cases occur before and after, respectively, of the time of local ground sunrise. The diagrams also exhibit a tendency for the times of start to cluster about a line parallel to the line of local ground sunrise. A similar trend is also exhibited by the times of end. Histograms of the time advance of the start before the time of ground sunrise and that of the

time delay of the end after ground sunrise for each of the three frequencies are shown in figure 5. The histograms also indicate the yearly average values of the time differences. The average of the time advance of start are 29.30, 30.06 and 31.01 minutes at 30, 120 and 210 Kc/s, respectively, while that of the respective time delay of end are 60.37, 50.46 and 40.37 minutes. From these figures, it appears that the time advance of start is very slightly dependent on frequency, tending to increase with frequency, while the time delay of end is, on the other hand, fairly frequency dependent, showing a decrease with increasing frequencies. The same general nature of the frequency dependence is, in fact, exhibited by a typical record as shown in figure 1, reproduced in the preceding section.

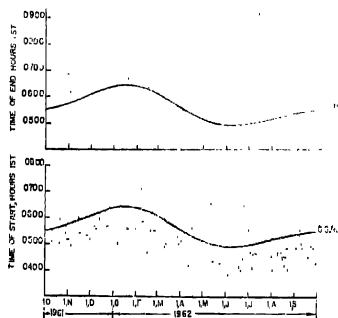


Figure 4. Scatter diagram of the time of start and the time of end of sunrise fall on 30 Kc/s against the day.

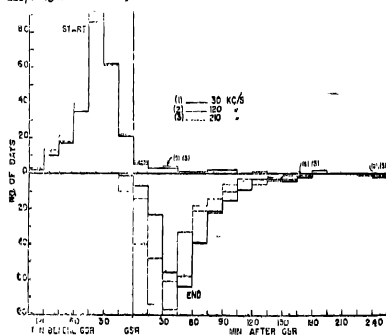


Figure 5. Histogram of the time difference between ground sun rise and start or end of sunrise fall.

Upper and Lower Limits of the Time Differences :

Table 2 shows the distribution of the time advance of start as well that of the time delay of end beyond certain upper and lower limits.

TABLE 2. DISTRIBUTION OF TIME DIFFERENCES BETWEEN GSR AND THE START OR END OF SUNRISE FALL, BEYOND CERTAIN LIMITS

Frequency Kc/s.	Percentage of days with time advance of start			Percentage of days with time delay of end	
	Less than 0 min.	Less than 15 min	Greater than 75 min.	Less than 0 min.	Greater than 90 min.
30	7.9	5.9	4.3	0.4	11.2
120	8.2	6.0	6.0	0.4	10.1
210	8.5	5.9	6.3	3.7	7.7

The table indicates that the time advance of start beyond the range—15 to 75 min is of the order of 6%, while those less than 0 minute is about 8%. The delay of end less than 0 minute is under 4% while that greater than 90 minute is about 10%.

DISCUSSION

Various authors observed the sunrise and sunset effects and tried to explain the phenomena in terms of source distribution and changes in the state of ionisation in the propagation path due to the impact of solar ionising radiations. Lugeon (1929) first reported that the start of sunrise effect always occurs before the local ground sunrise. Lauter (1958) observed from measurements of 27 Kc/s and 40 Kc/s atmospherics that the main drop in intensity occurred when the sun's zenith angle was about $99^{\circ}40'$. Reiker (1960) explained the latest time of start in his observations of the sunrise effect at 27 Kc/s as due to the most distant western sources. Chipionkar & Karekar (1963) tried to explain the times of start and end of the sunrise fall observed at 27 Kc/s in Poona, in terms of a single hop reception from eastern and western sources lying within the geometrical optical horizon. It was, however, felt that some of their assumptions required a modification in the light of the present knowledge of radio wave propagation at low frequencies (Aikin 1962; Belrose 1964a, 1964b; Davies 1965; Deeks 1965). Such a modified approach will be tried in order to explain our observations at 30, 120 and 210 Kc/s.

The geometry of the problem is illustrated in figure 6, which shows an east-west section through the station and the centre of the earth.

For any position of the receiver, R , there exist two farthest sources, S_1 and S_2 , from each of which radio waves can be received by a single hop

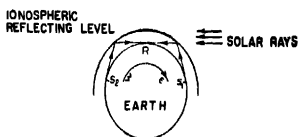


Figure 6. An east-west section through the station and centre of the earth

transmission. For such sources, the path of propagation will be tangential to the earth's surface at R .

Recent measurements of the phase of the sky wave at low frequencies at a range of 1900-2400 km indicated that the "phase height" of reflection begins to decrease about an hour before ground sunrise at the path midpoint, corresponding to a solar zenith angle of 101° , when visible light from the sun impinge on the ionosphere at a height of 85 km after grazing the ground (Belrose 1964a). In our case as the propagation paths are tangential to the earth's surface, the times of impingement of solar rays at the path midpoints for the sources at S_1 and S_2 will be the same as the times of ground sunrise at S_1 and R , respectively, and if we assume the absorption of the wave to start when the solar rays strike the night-time reflecting layer at the path midpoints, the earliest and latest start of the sunrise fall would occur at these times of ground sunrise at S_1 and R , respectively. If the earth's radius be taken as 6378 km then for a height of reflection equal to 85 km the earliest start would occur about 75 minutes before ground sunrise at R . Our observations at each of the three frequencies indicate that there are only about 6% of cases, in which the start is earlier than 75 minutes before ground sunrise at R . The results are thus in fairly good agreement with those expected for a one-hop model discussed above. The observed lack of frequency dependence for the number of cases occurring beyond 75 minutes suggests that the time of the earliest start is not frequency dependent in the range 30-210Kc/s. This implies that the height of reflection at night for such an oblique path does not vary over the frequency range involved. So far as the time of the latest start is concerned, our observations at each of the frequencies indicate that there are only 8% of the cases in which the start occurs after ground sunrise at R , when the latest start is expected. Of these cases in which the occurrence of the latest start is delayed, about 6% occur with delays greater than 15 minutes. The time of the earliest and the latest ends of the sunrise fall would be the same as the time of the end of sunrise fall for the paths RS_1 and RS_2 , respectively. Our

observations at each of the three frequencies show that in less than 4% of the cases ends occur immediately after ground sunrise at R , while in about 10% of the cases the ends occur 90 minutes after ground sunrise at R .

It is interesting to note that of cases with their ends occurring 90 after ground sunrise at R do not exhibit any significant frequency dependence. This suggests that the absorbing regions of the lower ionosphere behave in the same way to radio waves of frequencies in the range 30-210 Kc/s, when propagation to distances of the order of 2000 km are considered.

In the foregoing discussions, we have assumed the sources to be distributed along a east-west line through the station. However, the sources are, in general, widely scattered in various directions and one should take into account the role of a source in any direction on the observed time of start and end of the sunrise fall. As an approximation, if the height of the night-time reflecting layer be assumed to be constant all around the station, the farthest sources will lie on a circle of radius about 2000 km with the station at the centre (Sen 1968). The corresponding path midpoints will lie on a second circle of half the radius, 2000 km, for the farthest sources. Interruption of reception would occur earliest for an eastern source, which is situated at the point of contact of the line of sunrise with the second circle. The point of contact is farthest in the east in some parts of the year when the line of sunrise is oriented north-south at the point of contact. The start is, therefore, the earliest for the farthest eastern sources, at such times. A similar reasoning will show that the start would be the latest for the farthest western sources. In case, the sources are absent in the farthest eastern and western positions, the earliest start of the sunrise fall will obviously occur later, while the latest start will occur earlier than those expected from the above explanation. In fact, if the sources are distributed purely in the north-south directions the times of the earliest and latest start would be the same and equal to the time of sunrise at the reflection point just above the station.

The time-advance of start as well as that of the time-delay of end were also examined in greater details. A plot of the monthly average values of the time differences against the corresponding month is shown in figure 7. From the figure it is evident that the frequency dependence of the duration of sunrise fall arises mainly from the dependence of the time of end on frequency, the contribution arising from any dependence of the time of start being negligible. In contrast to this, both the times of the earliest and latest end of the sunrise fall exhibit no marked frequency dependence (table 2). The above results could, however, be reconciled

if one assumes a frequency-distance dependence of reflection coefficient of the ionospheric region involved, of the type observed by Belrose (1964b),

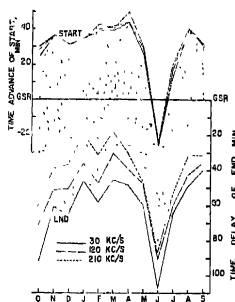


Figure 7. Seasonal variation of the monthly average time difference between ground sunrise G. S. R. and start or end of sunrise fall.

His results indicated that the absorption of a wave of frequency f , incident at an angle i , to the reflecting layer would be the same as that of a wave of 'effective frequency' f_e , incident vertically such that $f_e = f \cos i$ (Alcock 1955; Belrose 1964). Considering, first, the case for the earliest and latest end, it could be observed that the sources corresponding to these cases are on the geometrical optical horizon for a one hop ray, i. e., about 2000 km from the observing centre. The angle of incidence for this range is $80^\circ 40'$, which gives an effective frequency of about 5, 20 and 35 Kc/s corresponding to the observing frequencies 30, 120 and 210 Kc/s, respectively. The reflection coefficient in this range of 5-35 Kc/s, however, does not exhibit any marked frequency dependence and as such it is not surprising that a similar lack of frequency dependence is observed for the times of the earliest and latest ends. As regards the observed dependence of the monthly average time of end on frequency, our analysis indicates that the sources contributing towards this average result, are located somewhere between the observing station and the geometrical optical horizon for a one hop ray. If the great majority of the sources be located midway between the two extremes, as is also apparent from the monthly average time of end, their distances from the observing centre would certainly be less than 2000 km, which implies that the effective frequencies would be more widely spaced in the $f \cos i$ -axis, thus leading to a significant frequency dependence of reflection coefficient. This appears to explain why the frequency dependency, although insignificant for the earliest and latest ends could be appreciable for the monthly average time of end.

It may be noted that the role of any multihop ray within the geometrical optical horizon has not been considered in the present analysis. However, such rays are, in fact, always present as is evident from a study of the waveform of propagated atmospherics where they appear in the form of a succession of weaker pulses following a primary atmospheric pulse due to the one-hop ray. Nevertheless, such secondary pulses are of rapidly diminishing magnitudes and their contribution in the integrated field intensity of atmospherics, if any, are only of secondary importance.

In the above discussion it has been assumed that the solar rays grazing the ground is responsible for the earliest and latest start of a sunrise fall. Such ground-grazing rays are, however, devoid of the usual ionizing radiations as they would be absorbed in passing through the atmosphere producing the ozonosphere (Mitra 1938). Naturally some alternative mechanism of ionization must be sought, in which only the visible radiation of wavelengths longer than the upper limit of the Hartley band of ozone is involved. Such a mechanism has, in fact, been suggested to explain the formation of a so called "Cosmic-ray layer" developing below the *E*-region immediately after sunrise (Reid 1961; Whitten & Poppoff 1965). At low frequencies reflection from this layer occurs when propagation to distances of the order of 2000 km or greater are involved (Belrose 1964). Ionization in the layer has a basic component produced by cosmic rays incident equally by day and night. But when the sun's light impinges on the layer, a predominance of photodetachment of negative ions relative to that of attachment causes the free electrons to be more numerous (Aikin 1962). Consequently, the sunrise effect is expected to occur immediately after the impingement of a ground grazing visible light from the sun at the appropriate height. In support of the above discussion, reference may be made to a recent review of *D*-region processes in non-polar latitudes by Mitra (1968), who indicated the importance of high affinity negative ions in explaining the sunrise-sunset effects in the LF and VLF bands and the "twilight" anomaly of polar-cap absorption events (Reid 1961). It may be mentioned here that for propagation to distances less than about 1500 km, the cosmic-ray layer is penetrable and the sunrise fall would then occur due to the absorption by the normal *D*-region formed by the ionizing radiations grazing the ozonosphere. It is now believed that x-rays and ultraviolet rays from the sun are the important ionizing agents for the normal *D*-region (Whitten & Poppoff 1965).

CONCLUSION

Summarising what we have said, it may be concluded that the duration, times of start and end of a sunrise fall, as also their frequency dependence could be explained approximately in terms of a single hop propagation of radio waves at low frequencies, from sources lying within the geometrical optical horizon. For a more accurate interpretation additional propagation due to multihop rays, which become important particularly at great ranges, must also be taken into account. Recent measurements by Hargreaves' Roberts (1962) of the field strength of a c. w. transmission at 19.6 Kc/s have, in fact, revealed that a two hop component is not negligible, particularly in winter, for a range of the order of 1000 km. The multihop propagation becomes more and more important with increasing ranges until beyond about 1500-2000 km, the number of multihop paths becomes large.

Studies of sunrise effect by employing a radio transmission at low frequencies are handicapped by interference from atmospherics, which tend to obscure the end of sunrise fall, when the absorption is a maximum. Studies using atmospherics, on the other hand, effectively harnesses the powerful electromagnetic radiation from lightning discharges. Such studies, if supplemented by directional observation might prove to be useful in providing us with a better understanding of the phenomena occurring near sunrise. It must, however, be admitted that both the location and activity of a source of atmospherics exhibit a high variability and great care must, therefore, be taken in separating out any propagation effect from an observation of atmospherics.

The authors are grateful to Prof. J. N. Bhar, D. Sc., F. N. I., Director, Centre of Advanced Study in Radio Physics and Electronics, University of Calcutta, for his constant encouragement.

REFERENCES

- Aikin, A. C. 1962 *Radio Wave Absorption in the Ionosphere*, AGARDograph 53, (ed. N. C. Gereon), Pergamon Press, 287.
- Alcock, G. Mck. 1955 *Physics of the Ionosphere*, Physic Society, London, 14.
- Belrose, J. S. 1964a *Propagation of Radio Waves at Frequencies below 300 kc/s*, AGARDograph 74, (ed. W. T. Blackband), Pergamon Press 3.
- Belrose, J. S. 1964b *Propagation of Radio Waves at Frequencies below 300 kc/s*, AGARDograph 74, (ed. W. T. Blackband), Pergamon Press, 149.
- Chiplonkar, M. W. & Karckar, R. N. 1963 *J. Atmosph. Terr. Phys.*, 25, 23.
- Deeks, D. G. 1965 *D-region Electron Distributions in Middle Latitudes deduced from the Reflectivity of Long Radio Waves* Science Research Council, Radio and Space Research Station Slough, England, Internal Memoranda No. 219.
- Ellison, M. A. 1955 *URSI Information Bulletin* No. 92.

- Hargreaves, J. K. & Roberts, R. 1962 *J. Atmosph. Terr. Phys.*, **24**, 435.
- Horner, F. 1962 *Radio Noise of Terrestrial Origin*, (ed. F. Horner), Elsevier Publishing Co., N. Y. 40.
- Horner, F. 1964 *Advances in Radio Research* (ed. J. A. Saxton), Academic Press, N. F. **2**, 121.
- Khastgir, S. R. & Ali, M. I. 1942 *Indian J. Phys.*, **15**, 399.
- Khastgir S. R., Das Gupta, M. K. & Ganguli, D. K., 1947 *Indian J. Phys.*, **21**, 169.
- Lauter, E. A. & Schmelovsky, K. H. 1958 *Gerlands Beiträge Geophys.*, **67**, 218.
- Lugeon, J., 1929 *C. R. Acad. Sci. Paris*, **188**, 1690
- Mitra, A. P., 1968 *J. Atmosph. Terr. Phys.*, **30**, 1065.
- Namba, 1933 *Proc. IRE*, **21**, 238.
- Potter, R. K. 1931 *Proc. IRE*, **19**, 1731.
- Reid, G. C., 1961 *J. Geophys. Res.*, **66**, 4071.
- Ricker, J. 1960 *J. Geophys. Pure Appl.*, **46** 241.
- Sen, A. K. 1965 *J. Sci. & Industr. Res.* **24**, 571.
- Sen, A. K. 1968 *Studies on the Integrated Field Intensity of Atmospheric at Calcutta*,
Doctoral Thesis Calcutta University.
- Thomas, H. A. & Burgeses, R. E. 1947 *Radio Research Special, Report No. 15, Department of Scientific and Industrial Research, London.*
- Whitten, R. C. & Poppoff, I. G. 1965 *Physics of the Lower Ionosphere*, Prentice Hall, Inc.
- Whitson, A. L. 1961 *Report . SRI Project No. 3171, Stanford Research Institute, California.*
- WMO, 1957 *Final Report of the Working Group of Atmospheric, World Meteorological Organization.*

On the unsteady hydromagnetic free convection flow past a vertical infinite flat plate

By IOAN POP

University of Cluj, Cluj Roumania

(Received November 15, 1968)

This paper considers the unsteady laminar free convection flow of viscous incompressible and conducting fluid past a vertical infinite flat plate whose temperature varies as some powers of time in the presence of a constant horizontal magnetic field.

INTRODUCTION

Gupta (1960) using the method of characteristic has studied the effect of a constant horizontal magnetic field on two dimensional unsteady laminar free convection flow past a vertical infinite flat plate for a stepwise change in the surface temperature. The purpose of this paper is to present analytical solutions for the same problem when the wall temperature varies as some powers of time.

BASIC EQUATIONS

Let us assume that the origin of the coordinate system is at the lowest point of a flat plate, the \bar{x} -axis being along the plate vertically upwards and the \bar{y} -axis perpendicular to it. A uniform magnetic field of strength \bar{H}_0 is applied perpendicular to the plate. Under this condition considering an infinite vertical plate, the unsteady hydromagnetic laminar free convection boundary-layer equations may be written as :

$$\frac{\partial u}{\partial t} - \frac{\partial^2 u}{\partial y^2} = \theta - mu, \quad \dots(1)$$

$$\frac{\partial \theta}{\partial t} = \frac{1}{Pr} \frac{\partial^2 \theta}{\partial y^2}, \quad \dots(2)$$

where

$$\left. \begin{aligned} y &= \bar{y}/L, \quad t = \bar{t}/L^2, \quad u = \bar{u}L/\nu, \\ \theta &= \beta g L^3 (\bar{T} - \bar{T}_\infty)/\nu^2, \quad m = \sigma \bar{B}_0^2 L^2/\rho\nu, \end{aligned} \right\} \quad \dots(3)$$

where \bar{t} is the time variable, \bar{u} , the velocity component along the plate, \bar{T} , the temperature variable, \bar{T}_∞ , the ambient temperature, L , the characteristic length, $\bar{B}_0 = \mu_0 \bar{H}_0$, the magnetic induction, ν , the kinematic viscosity μ/ρ , the magnetic permeability, ρ , the density, g , the acceleration due to gravity, σ , the electrical conductivity, Pr , the Prandtl number, β , the coefficient of volumetric expansion and m , the hydromagnetic parameter.

Equations (1) and (2) are to be solved with the following initial and boundary conditions :

$$\left. \begin{aligned} u(y,0) &= \theta(y,0) = 0, \\ u(0,t) &= u(\infty,t) = \theta(\infty,t) = 0, \\ \theta(0,t) &= \theta_w(t) = u t^a, \end{aligned} \right\} \quad \dots (4)$$

where θ_w is the prescribed value of θ at the surface, a , an arbitrary constant and ∞ , any positive integer.

In (1) it is assumed that the magnetic Reynolds number is small, so that the induced magnetic field is negligible in comparison to the imposed magnetic field. Further, since no external electric field is applied, and the effect of polarization of ionized fluid is negligible, it can be assumed that the induced electric field is zero.

SOLUTION OF THE GOVERNING EQUATIONS

For small values of mt and for $Pr=1$ (it is a case frequently encountered in practical problems) we assume that the solution of the equations (1) and (2) is (Singh 1964) :

$$\theta = at^a \zeta(\eta), \quad u = ag\beta t^{a+1} \sum_{n=0}^{\infty} f_n(\eta) (mt)^n, \quad \dots (5)$$

where $\eta = y/2t^{1/2}$. Substituting (5) into (1) and (2) we get the equations :

$$\zeta'' + 2\eta\zeta' - 4a\zeta = 0, \quad \dots (6)$$

$$f_0'' + 2\eta f_0' - 4(a+1)f_0 = -4\zeta_0, \quad \dots (7)$$

$$f_1'' + 2\eta f_1' - 4(a+2)f_1 = 4f_0, \quad \dots (8)$$

$$f_2'' + 2\eta f_2' - 4(a+3)f_2 = 4f_1; \quad \dots (9)$$

where primes denote differentiation with respect to η . The corresponding boundary conditions of (6) - (9) are :

$$\left. \begin{aligned} \zeta(0) &= 1, \quad \zeta(\infty) = 0, \\ f_n(0) &= f_n(\infty) = 0 \quad (n \geq 0). \end{aligned} \right\} \quad \dots (10)$$

Case (i) : $a = 0$ (step change in the surface temperature). The equation (6) becomes :

$$\zeta'' + 2\eta\zeta' = 0. \quad \dots (11)$$

Solution of (11) satisfying the boundary conditions (10) is given by (Carslaw & Jaeger 1948) :

$$\zeta(\eta) = 1 - \frac{2}{V\pi} \int_0^\eta e^{-s^2} ds = \text{erf } \eta \quad \dots (12)$$

Now, the equation (7) becomes :

$$f_0'' + 2\eta f_0' - 4f_0 = -\text{erf } \eta. \quad \dots (13)$$

We now focus attention upon equation (13). We shall seek a particular solution of equation (13) by writing :

$$f_{op}(\eta) = X(\eta) \operatorname{erf}_e \eta + Y(\eta), \quad \dots(14)$$

where the functions $X(\eta)$ and $Y(\eta)$ defined by equations :

$$\left. \begin{aligned} X'' + 2\eta X' - 4X &= -4, \\ Y'' + 2\eta Y' - 4Y &= \frac{4}{\pi} X' e^{-\eta^2}, \end{aligned} \right\} \quad \dots(15)$$

are :

$$X(\eta) = -2\eta^2, \quad Y(\eta) = \frac{2}{\sqrt{\pi}} \eta e^{-\eta^2}. \quad \dots(16)$$

Two particular solutions of homogeneous equation (13) are :

$$f_{oh}(\eta) = 1 + 2\eta^2, \quad f_{oh}(\eta) = \frac{1}{4} (1 + 2\eta^2) \operatorname{erf}_e \eta - \frac{2}{\sqrt{\pi}} \eta e^{-\eta^2}. \quad \dots(17)$$

The general solution of (13) is :

$$\begin{aligned} f_o(\eta) = & C_1(1 + 2\eta^2) + C_2 \left[\frac{1}{4} (1 + 2\eta^2) \operatorname{erf}_e \eta - \frac{2}{\sqrt{\pi}} \eta e^{-\eta^2} \right] \\ & - 2\eta^2 \operatorname{erf}_e \eta + \frac{2}{\sqrt{\pi}} \eta e^{-\eta^2}. \end{aligned} \quad \dots(18)$$

To determine the constants C_1 and C_2 we shall make use of the boundary conditions (10). We have $C_1 = C_2 = 0$ and therefore (18) becomes :

$$f_o(\eta) = -2\eta^2 \operatorname{erf}_e \eta + \frac{2}{\sqrt{\pi}} \eta e^{-\eta^2}. \quad \dots(19)$$

The solutions of the equations (8) and (9) will be determined in the same way as the solution of equation (13) and have the following form :

$$\left. \begin{aligned} f_1(\eta) &= -\frac{2}{3} \eta^4 \operatorname{erf}_e \eta + \frac{1}{3\sqrt{\pi}} (2\eta^3 - \eta) e^{-\eta^2}, \\ f_2(\eta) &= -\frac{4}{45} \eta^6 \operatorname{erf}_e \eta + \frac{2}{45\sqrt{\pi}} \left(2\eta^5 - \eta^3 + \frac{3}{2} \eta \right) e^{-\eta^2} \end{aligned} \right\} \quad \dots(20)$$

Case (ii) : α is any positive integer. In this case the solutions of the equations (6) - (9) satisfying the boundary conditions (10) are (Pop 1967, 1968) :

$$\left. \begin{aligned} \zeta(\eta) &= 2^{2\alpha} \Gamma(\alpha+1) g_\alpha(\eta), \\ f_o(\eta) &= 2^{2\alpha} \Gamma(\alpha+1) g_\alpha(\eta) - 2^{2(\alpha+1)} \Gamma(\alpha+2) g_{\alpha+1}(\eta), \\ f_1(\eta) &= 2^{2(\alpha+1)} \Gamma(\alpha+2) g_{\alpha+1}(\eta) - 2^{2\alpha-1} \Gamma(\alpha+1) g_\alpha(\eta) \\ &\quad - 2^{2\alpha+3} \Gamma(\alpha+3) g_{\alpha+2}(\eta), \\ f_2(\eta) &= 1/3 [2^{2\alpha-1} \Gamma(\alpha+1) g_\alpha(\eta) - 2^{2\alpha+2} \Gamma(\alpha+4) g_{\alpha+3}(\eta)] \\ &\quad + 2^{2\alpha+3} \Gamma(\alpha+3) g_{\alpha+2}(\eta) - 2^{2\alpha+1} \Gamma(\alpha+2) g_{\alpha+1}(\eta), \end{aligned} \right\} \quad \dots(21)$$

where Γ is the symbol of the gamma function and

$$g_{\alpha}(\eta) = \frac{2^{1/2-\alpha}}{\sqrt{\pi}} e^{-1/2\eta^2} D_{-1-2\alpha}(\eta\sqrt{2}), \quad \dots(22)$$

$D_{-1-2\alpha}(\eta\sqrt{2})$ being the parabolic-cylinder function of order $-1-2\alpha$, for $\alpha \geq 0$ (Whittaker & Watson 1927). The properties of the function $g_{\alpha}(\eta)$ have already been discussed in detail by Watson (1955).

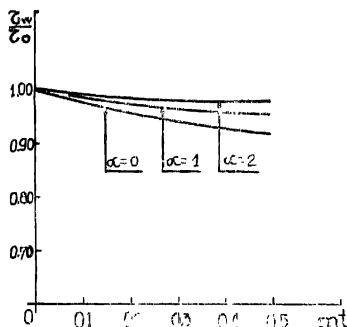


Figure 1. The variation of the ratio τ_w/τ_0 with mt .

Now, we can calculate the skin friction at the plate. Thus,

$$\tau_w = \mu \left(\frac{\partial u}{\partial y} \right)_{y=0} = \frac{ag\beta\rho}{2} t^{\alpha+1/2} y^{1/2} \left[f_0'(0) + f_1'(0) (mt) + f_2'(0) (mt)^2 + \dots \right] \quad \dots(23)$$

In the absence of magnetic field the local skin friction at the plate is given by :

$$\tau_0 = \frac{ag\beta\rho}{2} t^{\alpha+1/2} y^{1/2} f_0'(0). \quad \dots(24)$$

Considering (21) the ratio of the skin friction with and without the hydromagnetic interactions is given by :

$$\frac{\tau_w}{\tau_0} = 1 - \frac{1}{2(\alpha+3/2)} \left(\frac{mt}{2} \right) + \frac{1}{2(\alpha+3/2)(\alpha+5/2)} \left(\frac{mt}{2} \right)^2 + \dots \quad \dots(25)$$

The skin friction ratio τ_w/τ_0 is plotted against mt in figure 1 for $\alpha=0$, 1 and 2. It is clear that the effect of magnetic field is to decrease the skin friction. It is further noted that the skin friction increases when α increases.

REFERENCES

- Carslaw H. S. & Jaeger J. C. 1948 *Conduction of Heat in Solids*, Oxford.
- Gupta A. S. 1960 *Appl. Sci. Res.*, A 9, 319.
- Pop I. 1967 *Rev. Roum. Phys.* 12, 865.
- 1968 *ZAMM*, 48, 69.
- Singh D., 1964 *J. Phys. Soc. Japan*, 19, 751.
- Watson E. J. 1955 *Proc. Roy. Soc. (London)*, A231, 104.
- Whittaker T. E. & Watson N. G. 1927 *A Course of Modern Analysis*, Cambridge Univ. Press.

Infrared eigen frequency and characteristic Debye temperature of a few heavier halides.

By D. C. GUPTA AND M. N. SHARMA

Physics Department, Lucknow University, Lucknow-7 India.

(Received September 26, 1967 ; Resubmitted February, 13, 1969)

Using the Lennard-Jones (12:6) potential energy function the necessary equation for the force constant and infrared eigen frequency ν_0 have been derived. The calculated values of ν_0 and Debye Θ_D have been compared with the experimental data. The calculated results reveal the appropriateness of the Lennard-Jones potential model for heavier salts.

INTRODUCTION

The interatomic forces play a important role in predicting the various properties of matter. The behaviour of the forces for ionic crystals was studied in the early stage by Mie (1903), Gruneisen (1912, 1926), Born (1923), Born & Mayer (1932), and in the later stage by Cubicciotti (1959, 1951) Sharma & Madan (1961, 1962), Chatterjee (1963), Kachhava & Saxena (1965, 1966), Gohel & Trivedi (1967) and others and has been summarised by Kittel (1956) and by Born & Huang (1954). In an ionic crystal the degree of ionisation of the constituent atoms is often such that the electronic configuration of all ions corresponds to closed electronic shells, as in the case of inert gas atoms. Assuming this, Sharma and Madan (1964a, 1964b) have computed the various properties of alkali and metal halides. In the present paper we have extended the use of the Lennard-Jones (12:6) potential model in calculating some other properties, viz., infrared eigen frequency ν_0 and characteristic Debye temperature Θ_D of a few heavier halides.

COMPUTATION OF CRYSTAL PROPERTIES

Using the Lennard-Jones (12:6) potential model in conjunction with the Coulomb term, the expression for the energy per unit cell can be written as :

$$\phi(r) = - \frac{\alpha Z^2 e^2}{r} + \frac{B}{r^{12}} - \frac{C}{r^8} - \frac{D}{r^6} + \epsilon_0 \quad \dots(1)$$

where α is the Madelung constant, Ze is the charge on an ion, r is the interionic distance, B is the repulsive parameter, $\frac{C}{r^8}$ is the dipole-dipole interaction term, $\frac{D}{r^6}$ is the dipole-quadrupole interaction term, and ϵ_0 is the zero-point energy.

The experimental values of r , $\phi(r)$ and ϵ_0 can be substituted in equation (1) to determine B if we have a knowledge of C and D from other means. Estimates of C and D obtained from an analysis of optical data were employed to determine B (Mayer 1933; Mayer & Levy 1933; Bleich 1934). The values of B are given in table 1.

The force constant f is given by

$$f = \frac{1}{3} \left[\frac{2\phi'(r)}{r} + \phi''(r) \right] \quad \dots(2)$$

in which $\phi'(r)$ and $\phi''(r)$ are the first and second derivatives, respectively, of the overlap potential between a positive and a negative ion. Substituting for $\phi'(r)$ and $\phi''(r)$ in equation (3) we at once get

$$f = 44 \cdot \frac{B}{r^{14}} - 10 \cdot \frac{C}{r^8} - \frac{56}{3} \cdot \frac{D}{r^{10}} \quad \dots(3)$$

Using C and D from optical data and B from equation (1) we can compute the force constant which is tabulated in table 1.

(A) Infrared absorption frequency

The characteristic infrared eigen frequency ν_0 of the ionic crystals is the frequency of the lattice of positive ions moving as a unit relative to the lattice of negative ions. Taking polarisation into consideration, ν_0 can be calculated from

$$\nu_0 = \frac{1}{2\pi} \sqrt{\frac{f}{\mu} \left(\frac{\epsilon_\infty + 2}{\epsilon_0 + 2} \right)} \quad \dots(4)$$

where μ is the reduced mass of the ions, ϵ_0 is the static dielectric constant and ϵ_∞ is the high frequency dielectric constant.

Substituting for, f , we get

$$\nu_0 = \frac{1}{2\pi} \sqrt{\frac{\left(44 \cdot \frac{B}{r^{14}} - 10 \cdot \frac{C}{r^8} - \frac{56}{3} \cdot \frac{D}{r^{10}} \right) \left(\epsilon_\infty + 2 \right)}{\mu(\epsilon_0 + 2)}} \quad \dots(5)$$

Here C and D can again be taken from optical data of Mayer (1933), Mayer & Levy (1933) and Bleich (1934) and B from equation (1).

The values of ν_0 calculated from equation (5) are presented in table 1. The experimental values of ν_0 for the considered halides are also included in table 1 for comparison. It is interesting to note that ν_0 calculated from force constant compares well with the observed values of ν_0 . Specially in the case of TiCl and TiBr , the agreement is very good and this clearly indicates the adequacy of the Lennard-Jones potential model for the heavier ionic crystals,

TABLE 1. REPULSIVE PARAMETER B , FORCE CONSTANT f AND INFRARED EIGEN FREQUENCY ν_0 OF SOME HEAVIER HALIDES

Substance	$B \times 10^{104}$ (from equation 1)	$f \times 10^{-4}$ (from equation 3)	$\nu_0 \times 10^{-12}(\text{sec}^{-1})$	
			Exp. (Born & Housing (1954)).	Cal. (Using equation 5)
CuCl	4.660	11.730	5.67	6.037
CuBr	6.772	8.071	5.27	4.597
CuI	8.056	—	—	—
AgCl	45.290	9.610	(3.09)	4.812
AgBr	59.940	6.998	(2.29)	3.192
AgI	41.300	—	—	—
TlCl	419.700	7.068	2.58	2.732
TlBr	604.700	6.522	(1.85)	1.966

Gohel & Trivedi (1967) have also calculated the lattice energies of some heavier ions using the Lennard-Jones potential energy function which clearly supports the adequacy of Lennard-Jones (12:6) model for a heavier salts.

TABLE 2. CALCULATED AND EXPERIMENTAL VALUES OF DEBYE φ_D FOR SOME HEAVIER HALIDES

Substance	φ_D experi- mental**	φ_D Theoretical (Using Eq. 6)	φ_D refl.* (Infrared)	φ_D abs.* (Infrared)	φ_D elastic*	φ_D Black- mann* & Joshi*	φ_D Mitra
CuCl		289.80					
CuBr	183	220.70					
AgCl	144	231.10					
AgBr		153.20					
TlCl		131.10	157	123	125	100	164
TlBr		94.39	123	—	114	71	117

* Mitra & Joshi (1960 b)

** Reddy (1963)

(B) Characteristic Debye temperature φ_D

A number of relations have been given connecting the Debye characteristic temperature φ_D and the compressibility by Blackman (1942),

Mitra & Joshi (1960a) and by others. Once the value of γ_0 is calculated, ϕ_D can be computed from the relation

$$\phi_D = \frac{h\nu_0}{k} \quad \dots(6)$$

where h is the Planck's constant and k is the Boltzmann's constant.

The calculated values of ϕ_D using equation (6) are given in table 2 for a few heavier halides along with the values determined by various other methods for the sake of comparison. The agreement between the calculated and observed values of ϕ_D is quite satisfactory considering the approximations involved in the theory.

Authors are indebted to Prof. B. N. Srivastava, F. N. I. for helpful suggestions and going through the manuscript. Authors are also grateful to Prof. B. G. Gokhale, Head of the Physics Department, Lucknow University, for the continued interest and encouragement in the problem. One of us (D. C. G.) is grateful to State C. S. I. R., U. P. for financial assistance.

REFERENCES

- Blackmann, M. 1942 *Proc. Roy. Soc.*, **181A** 58.
 Bleick W. E. 1934 *J. Chem. Phys.* **2**, 160.
 Born, M. 1923 *Atomtheorie des festen Zustandes*, Teubner, Leipzig.
 Born, M. & Huang, K. 1954 *Dynamical Theory of Crystal Lattices*, (Clarendon Press Ltd., Oxford).
 Born, M. & Mayer, J. E. *Zeit. f. Physik*, **1**, 75.
 Chatterjee, S. 1963 *Indian J. Phys.* **37**, 105.
 Cubicciotti, D. 1959 *J. Chem. Phys.* **31**, 1646.
 1961 *J. Chem. Phys.* **34**, 2189.
 Gohel V. B. & Trivedi, M. D. 1967 *Indian J. Pure Appl. Phys.* **5**, 265.
 Gruneisen E. 1912 *Ann Physik*, **39**, 257.
 1926 *Handbuch der Physik*, Verlag Julius Springer, Berlin Vol. 10, Part I.
 Kachhava, C. M. & Saxena, S. C. 1965 *Indian J. Physics* **39**, 145.
 1966a, b, c *Indian J. Phys.* **40**, 225, 273, 567.
 Kittel C. 1956 *Introduction to Solid State Physics*, John Wiley & Sons Inc., N. Y.
 Mayer J. E., 1933 *J. Chem. Phys.* **1**, 327.
 Mayer J. E. & Levy, R. B. 1933 *J. Chem. Phys.* **1**, 647.
 Mitra S. S. & Joshi, S. K. 1960a, *Physica*, **26**, 284.
 1960b *Physica*, **26**, 825.
 Sharma M. N. & Madan, M. P. 1961 *Indian J. Phys.* **35**, 596.
 1962 *Current Science*, **31**, 54.
 1964a, *Indian J. Phys.* **38**, 231.
 1964b, *Indian J. Phys.* **38**, 305.
 Reddy P. Jayarama 1963 *Physica*, **29**, 63.

Emission spectra of E—X and F—X systems of CaF

By S. C. PRASAD AND M. K. NARAYAN

Department of Physics, University of Bihar,

L. S. College, Muzaffarpur.

(Received August 28, 1968)

PLATE 2

Bands of $E^2\Sigma - X^2\Sigma$ and $F^2\Pi - X^2\Sigma$ system of CaF lying in the region 3000-2600 Å have been observed for the first time in emission at a dispersion of about 12 Å/mm at 2800 Å, using the flame of C-arc fed with CaF₂ suitably mixed with Na₂CO₃ and operated at 220 V D.C. mains and 5 to 6 amp. current. In all, 12 bands of $\Delta V=0, +1$ and $+2$ sequences of E-X and 10 bands of $\Delta V = -1, 0$ and $+1$ sequences of F-X systems have been observed. Most of these bands were reported earlier in absorption. New vibrational constants for both E-X and F-X systems have been obtained and the reported mean vibrational constants of the ground state of the molecule have been accordingly modified. Transitions for both E-X and F-X systems reported in absorption have been supported and we feel that in E-X system, there is predominance of P_1 -heads in emission compared to the P_1 -heads reported in absorption. Predominance of P -heads both in in emission and absorption, reasonably indicates that the reported $F^2\Pi$ state cannot belong strictly to Hund case (b). Comparing the observed bands in emission with those reported in absorption, an attempt has been made to give the qualitative estimate of the rotational constants for both E-X and F-X systems.

INTRODUCTION

Six band systems of CaF arising due to the transitions from the excited $A^2\Pi$, $B^2\Sigma$, $C^2\Pi$, $D^2\Sigma$, $E^2\Sigma$ and $F^2\Pi$ states to the ground $X^2\Sigma$ state in each case, are known and no intercombination system has been reported to this date. The systems A-X and B-X are known both in emission (Dutta, 1921) and absorption (Walters & Barrett 1928; Fowler 1941) and have also been studied in details by different investigators (Johnson 1929; Harvey 1931; Mohanty & Upadhyaya 1967). The system C-X which was first reported by Datta (1921) in emission and reinvestigated by Johnson (1929) has been extended by Fowler (1941) in absorption. The systems D-X, E-X and F-X were reported by Fowler (1941) in absorption at a furnace-temperature of about 2000°C and the vibrational analysis of them was also carried out by him, but no further work on these systems has ever been reported.

In the present investigation, the bands of E-X and F-X systems reported in absorption by Fowler (1941) have been observed for the first time in emission, using the technique similar to that employed by Datta (1921) with some modifications.

EXPERIMENTAL

The usual C-arc with electrodes in vertical position was employed at 220 V, D. C. mains and 5 to 6 amp. current. The arc was fed with CaF_2 mixed with Na_2CO_3 . The addition of Na_2CO_3 was found suitable for increasing the separation between the electrodes in order to have the wider flame of the arc purposely required and also to reduce the possibility of occurrence of unwanted atomic lines. But it was necessary to mix Na_2CO_3 with CaF_2 in such a proportion that the flame formed in the gap of widely separated electrodes, was sufficiently rich in greenish colour for, with the flame of such colour the bands under investigation could be satisfactorily observed. The image of this flame was allowed to fall on the slit of a spectrograph through a suitable quartz-lens and its spectrum was photographed on a Hilger-Medium-Quartz-Spectrograph. The bands of $E-X$ and $F-X$ systems appeared in the region 3000-2600 Å at a dispersion of about 12 Å/mm at 2800 Å. An exposure of about 8 minutes on Ilford N-30 plate was found suitable for the purpose. Iron-arc lines were used as standard.

RESULTS

The enlarged reprint (plate 2) shows the observed emission bands with their vibrational assignments for both $E-X$ and $F-X$ systems. Table 1 gives the Deslandres scheme for the observed emission bands of $E-X$ system while table 2 shows that for $F-X$ system. Table 3 contains the new vibrational constants for both $E-X$ and $F-X$ systems obtained by us and for the sake of comparison, the constants reported by Fowler (1941) in absorption, are also given in it. This table further includes the reported (Herzberg 1950) mean vibrational constants of the ground state of the molecule, which have been modified by us in the light of new constants for the common lower state of $E-X$ and $F-X$ systems. These modified constants of the ground state, similar to those reported by Herzberg (1950), also represent the average of the constants (Johnson 1929, Harvey 1931, Herzberg 1950) of the lower states of all the known systems except those of the $B-X$ system. The constants of the lower state of the $B-X$ system have been excluded for the same reasons as suggested by Herzberg (1950). Table 4 gives the details of our measurements for the observed emission bands of both $E-X$ and $F-X$ systems including the eye-estimate of their relative intensities in the scale of 10 for each of the two systems. The wavenumbers calculated from the newly derived (table 3) and the reported (Fowler 1941) constants (since the latter values are not mentioned in the published paper (Fowler 1941) are also given in this table and the agreements of the observed emission bands both with respect to the newly derived (table 3) and the reported (Fowler 1941) constants, are, for the sake of comparison, included

in it. Table 5 shows the comparative agreements of the modified (table 3) and the reported (Herzberg 1950) mean vibrational constants of the ground state of the molecule with respect to the (0,0) bands of the different known systems and for the reasons stated above, the *B-X* system has been excluded. For calculating the wavenumbers of the (0,0) bands of the different systems (table 5), the corresponding constants of the upper state of the respective system reported by Herzberg (1950), have been used.

TABLE 1. (*E-X* SYSTEM OF CaF)

v'	v''	0	1	2	3	4	
0		34165.2	—				
		639.9					$\Delta G_{v''+1}$ 639.9
1		34805.1	583.8	34221.3			$2W_e'X_e'$ 7.2
		632.9		632.4		632.7	
2		35438.0	584.3	34853.7	—		6.4
				628.3		628.3	
3			35482.0	577.2	34904.8	—	6.9
				621.4		621.4	
4				35526.2	571.4	34954.8	—
					615.6		615.6
5					35570.4	563.0	35007.4
						608.6	608.6
6						35616.0	
	$\Delta G_{v''+1}$	584.1		577.2	571.4	563.0	
	$2W_e''X_e''$		6.9		5.8	8.4	

TABLE 2. (*F-X* SYSTEM OF CaF)

v'	v''	0	1	2	3	
0		37597.0	581.9	37015.1		
		675.0		674.0		$\Delta G_{v''+1}$ 674.5
1		38272.0	582.9	37689.1	573.7	37114.0
				668.0		667.7
						667.9
2			38357.1	575.4	37781.7	569.6
					659.5	37212.1
						658.3
						658.9
3					38441.2	570.8
						37870.4
	$\Delta G_{v''+1}$	582.4		574.6		570.2
	$2W_e''X_e''$		7.8		4.4	

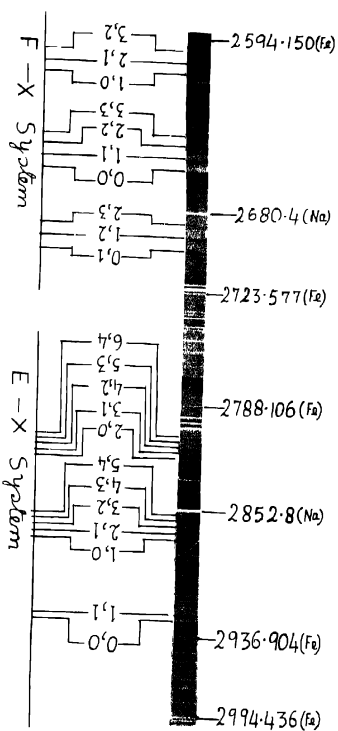
TABLE 3. COMPARISON OF NEWLY DERIVED AND REPORTED
CONSTANT OF CAF

System	New constants (Present Authors) cm ⁻¹	Reported constants (Fowler 1941) cm ⁻¹	N-R cm ⁻¹
X - F	$W_e' = 645.52$	$W_e' = 646.3$	-0.78
	$W_e'X_e' = 3.12$	$W_e'X_e' = 3.24$	-0.12
	$W_e'' = 587.86$	$W_e'' = 587.8$	+0.06
	$W_e''X_e'' = 2.94$	$W_e''X_e'' = 2.90$	+0.04
	$T_e = 34136.2$	$T_e = 34135.2$	+1.00
X - F	$W_e' = 682.2$	$W_e' = 681.7$	+0.50
	$W_e'X_e' = 3.68$	$W_e'X_e' = 3.55$	+0.13
	$W_e'' = 587.86$	$W_e'' = 586.9$	+0.96
	$W_e''X_e'' = 2.94$	$W_e''X_e'' = 2.82$	+0.11
	$T_e = 37549.7$	$T_e = 37547.9$	+1.80
	Modified (Present Authors)	Herzberg (1950)	Mo-R
Mean constants of ground state.	$W_e'' = 587.3$	$W_e'' = 587.1$	+0.2
	$W_e''X_e'' = 2.77$	$W_e''X_e'' = 2.74$	+0.03

Notes :—The letters N, R and Mo stand respectively for the words : New, Reported and Modified.

DISCUSSION

It can be seen from tables 1 and 2 that the observed bands in emission are represented quite satisfactorily in separate Deslandres schemes. The new vibrational constants (table 3) derived from these tables (1 & 2) and which have been modified in order to get the best fit to represent (table 4) the observed emission bands for the two systems, agree (table 3) fairly with those reported for *E-X* and *F-X* systems by Fowler (1941) in absorption. Moreover, the nature of the observed emission bands of both the systems, particularly with regard to their degradation to shorter wavelengths (plate 2), is quite similar to those of *E-X* and *F-X* system



Emission spectrum of CaF

of Fowler (1941). These facts taken together conclusively confirm that the observed emission bands of table 1 belong to the E-X system and those of table 2 belong to the F-X system of CaF.

TABLE 4 DETAILS OF THE MEASUREMENT OF E-X AND F-X SYSTEM OF CaF

System	V, V''	Bands observed in emission			ν -calculated with (cm^{-1})		$\nu_0 - \nu_0$ with (cm^{-1})	
		λ_{air} Å	Int.	ν_0 cm^{-1}	New const. (Pr. Auth.)	Reported const. (Fowler 1941)	New const. (Pr. Auth.)	Reported const. (Fowler 1941)
E → X	0,0	2926.1	10	34165.2	34165.0	34164.6	+0.2	+0.8
	1,1	2921.3	3	34221.0	34222.0	34222.2	-1.0	-0.9
	1,0	2872.3	6	34805.1	34804.3	34804.2	+0.8	+0.9
	2,1	2868.3	7	34853.7	34854.3	34855.5	-0.6	-1.8
	3,2	2864.1	8	34904.8	34906.0	34906.2	-1.2	-1.4
	4,3	2860.0	5	34954.8	34956.4	34956.2	-1.6	-1.4
	5,4	2855.7	2	35007.4	35006.3	35005.5	+1.1	+1.9
	2,0	2821.0	5	35438.0	35437.3	35437.5	+0.7	+0.5
	3,1	2817.5	7	35482.0	35482.1	35482.4	-0.1	-0.4
	4,2	2814.0	7	35526.2	35526.6	35526.6	-0.4	-0.4
	5,3	2810.4	5	35570.4	35570.7	35570.1	-0.3	+0.3
	6,4	2806.9	3	35616.0	35614.4	35612.9	+1.6	+3.1
F → X	0,1	2700.8	5	37015.1	37014.7	37013.9	+0.4	+1.2
	1,2	2693.6	6	37114.0	37113.4	37112.8	+0.6	+1.2
	2,3	2686.5	3	37212.1	37210.7	37210.4	+1.4	+1.7
	0,0	2659.0	10	37597.0	37596.7	37595.1	+0.3	+1.9
	1,1	2652.5	7	37689.1	37689.5	37688.5	-0.4	+0.6
	2,2	2646.0	3	37781.7	37780.9	37780.4	+0.8	+1.3
	3,3	2639.0	1	37870.4	37870.8	37870.8	-0.4	-0.4
	1,0	2612.1	5	38272.0	38271.5	38269.7	+0.5	+2.3
	2,1	2606.3	5	38357.1	38357.0	38356.0	+0.1	+1.1
	3,2	2600.6	2	38441.2	38441.0	38440.7	+0.2	+0.5

TABLE 5 COMPARATIVE AGREEMENT OF MODIFIED AND REPORTED
MEAN CONSTANT OF GROUND STATE OF CaF

System	V', V''	ν -reported cm^{-1}	ν -calculated with (cm^{-1})		$\nu_0 - \nu_c$ with (cm^{-1})		Remarks
			R.M.G.S.C.	Mo. M.G.S.C.	R.M.G.S.C.	Mo. M.G.S.C.	
A-X	0,0 (Q_{10})	16485.1 (3)	16484.4	16484.3	+0.7	-0.8	
	0,0 (Q_2)	16560.2 (3)	16560.3	16560.2	-0.1	0.0	
O-X	0,0 (Q_1)	30202.8 (5)	30203.4	30203.3	-0.6	-0.5	
D-X	0,0	30803.9 (5)	30804.1	30804.0	-0.2	-0.1	
	0,0	34164.4 (5)	34164.7	34164.6	-0.3	-0.2	With R.U.S.C.
E-X	0,0	34165.2 (A)	34165.3	34165.2	-0.1	0.0	With N.U.S.C.
	0,0	37595.1 (5)	37595.0	37594.9	+0.1	+0.2	With R.U.S.C.
F-X	0,0	37597.0 (A)	37597.1	37597.0	-0.1	0.0	With N.U.S.C.

Note :—The letters A, R, M, Mo, G, U, S and C stand respectively for the words :
Authors, Reported, Mead, Modified, New, Ground, Upper, State and Constants.

Table 3 shows that the new constants for the common lower state of E-X and F-X systems, unlike those reported by Fowler (1941) in absorption, are just the same as theoretically expected.

For E-X system the observed bands in emission are found to be of single-headed nature (plate 2) and support the reported view (Fowler 1941) that the system belongs to the $E^2\Sigma - X^2\Sigma$ transitions. The relative intensity-distribution of the observed bands in emission is approximately the same as that reported (Fowler 1941) in absorption. Moreover, particularly in the region of this system, there are a number of unaccounted bands and band-like features (plate 2) and are most likely those unclassified bands of Fowler (measurements not given by him) which were found by him also to lie in the region of E-X system.

For F-X system reported to belong to a $^2\Pi - ^2\Sigma$ transition, it can be seen (table 4) that the agreement of the observed heads in emission with new constants (table 3) compared to the constants reported by Fowler (1941) in absorption is not of the same order as found in the case of E-X system indicating that the observed heads in emission and those reported in absorption may not be just the same. The values of $\nu_0 - \nu_c$ with the constants of Fowler (1941) (reported by him for P_1 - heads), for all the heads

observed in emission except that for the weakest (3,3) band, are positive and it appears that the heads observed in emission are shifted, in general, slightly to the higher wave number (shorter λ) side of the corresponding P_1 -heads reported (Fowler 1941) in absorption. We consequently, feel that there is predominance of P_2 -heads in emission compared to the P_1 -heads reported (Fowler 1941) in absorption, for, comparing the observed value ($\nu_e=37597.0$ cm^{-1}) for the (0,0) band with that ($\nu_r = 37595.1$ cm^{-1}) reported (1941) in absorption, the $\nu_e - \nu_r = 1.9$ cm^{-1} also agrees with the separation (≈ 2.0 cm^{-1}) estimated by Fowler (1941) in absorption between P_1 - and P_2 -heads for the same (0,0) band. The Q_0 -heads indicated by Fowler (1941) in absorption (measurements not given by him) whose separation in the case of (0,0) band from P_1 -head has been estimated by him of the order of 11.7 cm^{-1} are, however, not observed in emission. Predominance of P -heads observed in emission in the present case and also reported earlier in absorption by Fowler (1941), quite reasonably show that the reported (1941) $F^2\Pi$ state cannot belong strictly to the Hund case (b), for, in that case Q -heads should be the strongest (Herzberg (1950), page 257) and like the most cases (Herzberg (1950), page 261), the $F^2\Pi$ state appears to belong to a case intermediate between (a) and (b). Moreover, the relative intensity-distribution of bands observed in emission is nearly the same as that reported (Fowler 1941) in absorption.

A further comparison of the observed bands in emission with those reported (Fowler 1941) in absorption for both *E-X* and *F-X* systems, shows that the (0,0) band (plate 2) of each of the two systems is the strongest member of the system, indicating quite reasonably that r_e -values and consequently the B_e -values of the upper and lower states for both *E-X* and *F-X* systems, are not very unequal. Using to relation (Herzberg (1950) page 179),

$$B_v = B_0 + \alpha_v \left(V + \frac{1}{2} \right) + \dots\dots\dots,$$

we get for the (0,0) band,

$$B_v' = B_0' + \frac{1}{2}\alpha_v',$$

and

$$B_v'' = B_0'' + \frac{1}{2}\alpha_v'',$$

Hence,

$$B_v' + \frac{1}{2}\alpha_v' \approx B_v'' + \frac{1}{2}\alpha_v'' \text{ for } B_v' \approx B_v''.$$

Since for both systems bands are degraded to shorter wavelengths, $B_v' > B_v''$ and the above relation clearly indicates that α_v' of each of *E-X* and *F-X* systems must be less than α_v'' . We thus get the qualitative estimate of the rotational constants for both *E-X* and *F-X* systems. However, a rotational analysis is essential for the confirmation of the conclusions arrived at.

One of the authors. (M. K. N.) is indebted to C. S. I. R, New Delhi for the award of a senior fellowship to him for the period of this research.

REFERENCES

- Datta S. 1921, *Proc. Roy. Soc.* **99**, 436.
Walters O. H. & Barratt S. 1928, *Proc. Roy. Soc.* **118**, 120.
Johnson R. C. 1929, *Proc. Roy. Soc.* **122**, 161.
Harvey A. 1931, *Proc. Roy. Soc.* **133**, 336.
Fowler Jr. C. A. 1941, *Phys. Rev.* **59**, 645.
Mahanty B. S. & Upadhy K. S. 1967, *Indian J. Pure. & Appl. Phys.* **5**, 523.
Herzberg G. 1950, *Spectra of Diatomic Molecules* (table 39), D. Van Nostrand Co.,
New York.

Thermal and electrical conductivities of alloys at low temperatures.

By B. N. SRIVASTAVA, S. CHATTERJEE AND S. K. SEN.

Indian Association for the Cultivation of Science, Calcutta-32

(Received April 26, 1969)

An apparatus for the simultaneous measurement of the electrical and thermal conductivities of metals and alloys at low temperatures has been described. A combined differential and absolute manometer has been designed for the measurement of the temperature gradient along a rod of the substance and also the absolute temperature at a point of the rod. The temperature of the bath is controlled by pumping liquid hydrogen, liquid nitrogen or liquid oxygen under controlled pressure through a Cartesian manostat.

Experiments have been made with two samples of copper alloys containing 1.96% Zn and 4.76% Zn respectively and the thermal conductivity data have been utilised to calculate separately the lattice and electronic parts with the help of electrical resistivity data, simultaneously taken on the same sample. The lattice thermal conductivity values thus obtained have been interpreted in terms of modern theories.

1. INTRODUCTION

The study of electrical and thermal conductivities of alloys at low temperatures has been the subject of many investigations (Hulm 1951; Berman 1951; Estermann & Zimmerman 1952; Kemp *et al* 1957; Lomer & Rosenberg 1959; Backlund 1961; Lindenfeld *et al* 1962; Garber *et al* 1963 and Charsley 1968). In the earlier investigations of the thermal conductivities at low temperatures the attention was mainly confined to metals (Rosenberg 1954, 1956, 1957; White 1953; White & Woods 1959) where the electronic part of the thermal conductivity was so predominant that the thermal conductivity due to lattice vibration could be neglected.

Recently, however, theoretical studies by Klemens and others (Klemens 1958) have shown that the thermal conductivity due to lattice vibrations is quite interesting because it gives different T -variations in different ranges of temperature on account of the different types of interaction of the phonons with the electrons, grain boundary, point defect, dislocation, etc. In fact, the lattice thermal conductivity K_g can be represented (Mendelssohn & Rosenberg, 1961) by the relation

$$\frac{1}{K_g} = W_e = W_{e_s} + W_B + W_P + W_U + W_{di}$$
$$= ET^{-3} + BT^{-3} + PT + gT^n e^{-g/10T} + DT^{-2} \quad \dots(1)$$

where the subscripts refer to the scattering of phonons by electrons, specimen and grain boundaries, point defects and isotopes, Umklapp process, and dislocations respectively. The equation shows that the

lattice thermal conductivity due to different interaction processes have, in general, widely different T -variations and therefore, it becomes possible to separate the ranges in which a particular interaction becomes predominant. Therefore, the study of the lattice thermal conductivity becomes a powerful method for studying the various types of interactions of phonons from which it is possible to have a knowledge of the imperfections in that particular substance.

However, since the experimental measurement of thermal conductivity has yet attained only limited accuracy, the separation of the contribution due to lattice thermal conductivity is almost impossible in pure metals because of the large values of electronic thermal conductivities. Hence it is desirable to reduce the electronic part to such an extent that it becomes comparable to the lattice thermal conductivity. This can be done by various methods (Klemens 1958) of which the alloying of the metal by some other impurities has been the most successful. The electronic thermal conductivity of the alloy is found out from the simultaneous measurement of the electrical resistivity of the sample and making use of the Wiedemann-Franz law to calculate the electronic thermal resistivity due to impurities.

In this work we have measured the thermal conductivity of two alloys of copper containing 1.96% Zn and 4.76% Zn respectively. Copper-zinc alloys have been previously investigated by Kemp, Klemens & Tainsh (1957) and Klemens, Klemens, Tainsh and White (1957) and the data have been analysed by White (1960) to explain the observed variation of W_g with temperature in terms of W_u and W_p , but the explanation is hardly satisfactory.

2. DESCRIPTION OF THE APPARATUS

The design of the cryostat is essentially similar to that of White & Woods (1955). The schematic diagram of the cryostat is shown in figure 1. The outer cylindrical can of brass, having a diameter of 8.5 cm., is suspended from the top plate by means of stainless steel pumping tubes. These tubes are soft soldered through bushes of brass which are hard soldered into the plates. The outer can is joined with Wood's metal at X so that it can be easily removed and replaced after mounting the specimen. The inner copper shield (chromium plated) is attached to the heat sink by screwing the shield at the joint marked Y . The electrical leads and the thermometer capillary tubes are taken out through the slot Z . The refrigerating liquid can enter the copper chamber through the inlet valve V which consists of a stainless steel needle of 10° total taper seating in a brass shoulder and is operated by turning the knurled head above the main top plate.

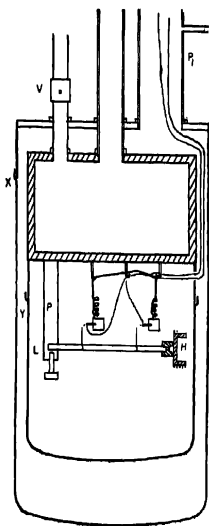


Figure 1. Schematic diagram of the cryostat for the measurement of thermal conductivity.

The specimen is mounted horizontally by screwing and soldering one end into a hole *L* drilled in the copper pillar *P*, the latter being hard soldered to the heat sink. A heater *H* is fixed at the other end of the specimen by Wood's metal. The heater is made of silko-ribbon constantan resistance which is fixed to a copper performer by glyptal. It is properly baked and dried to ensure good thermal contact and at the same time good electrical insulation. For potential leads, which serve also as thermometer leads, two short lengths of copper wire are tightly wrapped round the specimen at two points, and then soldered to it. This gas thermometer bulbs of copper are gold plated to prevent tarnishing and also to keep the radiation correction small and constant. They are connected by cupro-nickel capillary tubing to the external manometer system. To avoid electrical short-circuit through these thermometers and their supporting capillaries both the thermometers are electrically insulated from the specimen but thermally well-connected. This is done by covering the copper strip (1/16 in. x 1/64 in.) attached to the thermometer bulbs with a layer of glyptal and cigarette paper, baking the varnish, adding fresh varnish and then wrapping this layer with copper foil and finally baking it to harden

the varnish (figure 2). The copper potential leads from the specimen are then attached by Wood's metal to this foil. For simultaneous measurement of electrical conductivity current leads are also soldered at the two ends of the specimen.

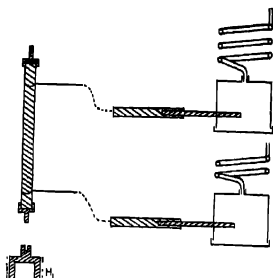


Figure 2. Method of mounting thermal conductivity specimens.

The inner and outer containers are evacuated during the thermal and electrical conductivity measurements through a common pumping line P_1 as shown in figure 1. All electrical and thermal leads are brought through the pumping line P_1 and araldite is used to seal the top of the tube from where the leads are taken out. The electrical resistivity is measured with the help of an accurate potentiometer reading upto 10^{-8} volt in conjunction with a photocell galvanometer amplifier (type 5214) supplied by M/s. H. Tinsley & Co. Ltd., London.

(n) *Measurement of temperature and the thermal gradient.*

Helium gas thermometers have been used to measure the absolute temperatures as well as temperature gradient along the specimen. For the measurement of temperature gradient a butyl phthalate manometer similar to the one described by Hulm (1950) has been employed (figure 3). In the present arrangement however, the sensitivity of the differential thermometer has been increased by using mercury for total pressure measurement and oil for differential measurement. This is a modification of the arrangement described by Mendelssohn and Pontius (1937) in which mercury manometer and differential manometer were separated. In our set up, both are connected whereby compactness has been achieved although at the cost of a slight error in the measurement of the absolute temperature.

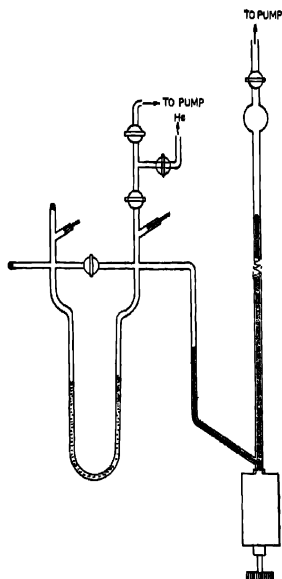


Figure 3. Combined differential and absolute manometer for temperature measurements.

(b) *Temperature control.*

The temperature control of the sink is usually done by (a) vapour pressure control and (b) electrical heating. In the present work, we have only employed vapour pressure control.

The vapour pressure has been controlled by means of a Cartesian manostat discussed in detail by Gilmont (1946, 1951). The design shown in the figure 4 is convenient to construct and handle. It consists of a glass dewar *D* of about 1 in. diameter. This is $\frac{1}{4}$ in. smaller in outside diameter than the internal diameter of the main tube. The diver has several glass pips suitably attached for centering. A valve is formed by a glass orifice *P* (1 mm. dia) seating and unseating against a rubber pad attached to the diver. During operation, the desired pressure above the liquid is attained by pumping through a bypass valve and keeping the glass stopcock *G* open. Then the bypass valve and *G* are both closed and the pressure remains steady.

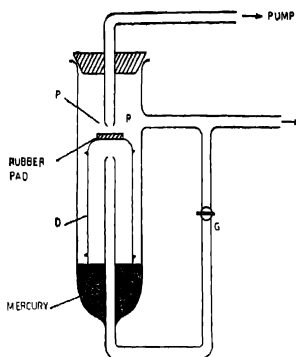


Figure 4. Cartesian manostat of glass for temperature control.

(c) Preparation of the alloys.

The alloys were prepared from spectrographically pure rods of copper and zinc, supplied by Messrs. Johnson, Matthey & Co., Ltd., London. The metals in appropriate proportions were sealed in an evacuated quartz tube and placed in a furnace and the temperature was raised to 1100°C. The mixture was melted and thoroughly shaken. The temperature of the furnace was then brought down to 900°C and kept at that temperature for five days to facilitate complete mixing of the two components. The alloy was then rolled in rod form and annealed in evacuated sealed glass tubes at about 500°C for six hours. The samples were then ready for mounting in position.

3. RESULTS AND DISCUSSION.

Measurements of the thermal conductivity of the specimens were taken in the temperature regions of 16°K to 20°K and 60°K to 90°K. These results are plotted in figure 5 and the best curves have been drawn through these observed points. The gaps between the two temperature ranges were bridged by interpolation. The electronic thermal conductivity K_e is given by

$$\frac{1}{K_e} = W_e = W_i + W_r, \quad \dots(2)$$

where W_i and W_r are ideal and residual thermal resistivities respectively. W_e is calculated with the help of Wiedemann-Franz law

$$W_e = \rho_0 / L_0 T, \quad \dots(3)$$

where ρ_0 is the residual electrical resistivity, and L_0 , the Lorentz number ρ_0 is determined from the measurement of electrical resistivity of the alloys at several temperatures down to 16°K and subtracting the electrical resistivity of pure metal at the corresponding temperatures. The values of ρ_0 thus obtained were found to be constant within the limits of experimental error. The value of W_i was assumed to be unaltered by alloying and was taken from the measurements on pure metals by Po-well *et al* (1961). In tables 1 and 2, Ke and Kg values are given for different temperatures for the two alloys.

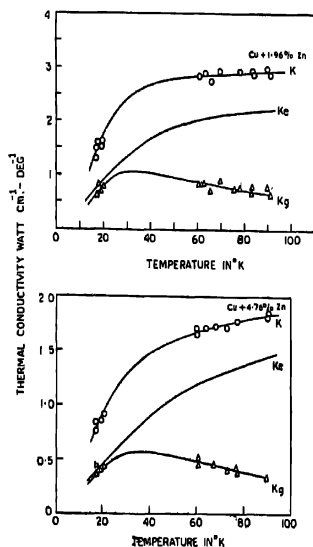


Figure 5. Thermal conductivities of Cu + 1.96% Zn and Cu + 4.76% Zn

The total thermal conductivity values are also listed in the tables from the smoothed experimental curves of figure 5. From these tables it can be seen that W_g/T in the temperature range of 60°K to 90°K is almost constant for particular alloy. In this region W_{gi} , W_i and W_{dis} become negligible, hence from eq. (1), $W_g = W_p + W_u$. But this expression does not take into account the effect of the three phonon anharmonic interaction conserving quasi-momentum (N-process) as pointed out by Ziman (1956). The role of N-process is to maintain the equilibrium of the phonon spectrum by feeding energy from the low frequency

TABLE 1. Cu + 1.96% Zn, $\rho_0 = 5.49 \times 10^{-7}$ OHM. CM.

Temp. in °K T'	Total conductivity K	Ideal resistivity W_i	Residual resistivity W_e	Electronic conductivity K_e	Lattice conductivity K_g	Lattice resistivity/Temp. W_g/T
20	1.67	.0114	1.120	.889	.786	
30	2.25	.0250	.747	1.295	.955	
40	2.55	.0503	.560	1.639	.911	
50	2.70	.0847	.448	1.576	.824	
60	2.80	.125	.373	2.008	.792	.0210
70	2.83	.164	.320	2.006	.764	.0187
80	2.87	.189	.280	2.137	.733	.0171
90	2.89	.213	.249	2.165	.725	.0171

K is in watt $\text{cm}^{-1} \text{ deg}^{-1}$, W is in watt $^{-1}$ cm. deg and W_g/T in watt $^{-1}$ cm.
Mean $W_g/T = .0176$ watt $^{-1}$ cm.

TABLE 2 : Cu + 4.76% Zn ; $\rho_0 = 1.043 \times 10^{-6}$ OHM. CM.

Temp. in °K T	Total conductivity K	Ideal resistivity W_i	Residual resistivity W_o	Electronic conductivity K_e	Lattice conductivity K_g	Lattice resistivity/Temp. W_g/T
20	.90	.0114	2.128	.467	.433	
30	1.24	.0250	1.419	.693	.547	
40	1.45	.0503	1.064	.897	.553	
50	1.57	.0847	.851	1.068	.502	
60	1.72	.125	.710	1.198	.522	.0320
70	1.76	.164	.608	1.295	.465	.0310
80	1.80	.189	.532	1.387	.413	.030
90	1.84	.213	.473	1.458	.382	.029

K is in watt. $\text{cm}^{-1} \text{ deg}^{-1}$; W is in watt $^{-1}$ cm deg and W_g/T in watt $^{-1}$ cm.
Mean $W_g/T = 0.031$ watt $^{-1}$ cm.

modes, which are not scattered strongly by U-processes or point defects, into the higher frequency modes. Assuming as a general case, the effective relaxation time σ for N-processes as $\sigma = n \tau_u$ where τ_u is the relaxation time due to Umklapp processes, we obtain, following the same procedure as Klemens *et al.* (1962)

$$\frac{K_g}{K_e} = \sqrt{\frac{n}{n+1}} \frac{\omega_o}{\omega_d} \tan^{-1} \left(\sqrt{\frac{n}{n+1}} \frac{\omega_d}{\omega_o} \right) \quad \dots(4)$$

Here ω_d is the Debye frequency and ω_o is defined by

$$\frac{\omega_o}{\omega_d} = \left[\frac{2}{\pi} \frac{k v}{a^3 q_D \epsilon K_U} \right]^{1/2} \quad \dots(5)$$

Here k is the Boltzman constant, q_D , the radius of the Debye sphere, u , the velocity of sound and $\epsilon = \Sigma C_i \left(\frac{\Delta M_i}{M} \right)^2$ where C_i denotes mass defect concentration, M , the weighted mean of the atomic masses and ΔM_i , deviation of mass of each component from M .

For Cu-Zn alloy ΔM , being very small, the expression $\frac{\omega_d}{\omega_o}$ becomes very small and eq. (4) can be approximated to

$$\frac{K_s}{K_u} = \frac{n}{n+1} \quad \dots(6)$$

Now from our experimental data

$$\begin{aligned} \frac{W_s}{T} &= .018 \pm .002 \text{ for Cu} + 1.96\% \text{ Zn} \\ &= .030 \pm .003 \text{ for Cu} + 4.76\% \text{ Zn.} \end{aligned}$$

Since the effect of point imperfection scattering due to mass difference is negligible in this case, W_s is mainly due to Unklapp processes and normal interactions, which are practically independent of the compositions for dilute alloys of the same parent metal. Hence we can assume for W_s/T the average value $.024 \pm .006$ with an experimental error of $\pm .005$. Now, the theoretical expression of W_u given by Leibfried and Schlomann (1954) is

$$\frac{1}{W_u} = 3.61 a A \theta_D^3 / \gamma^2 T \text{ watt Cm}^{-1} \text{ deg}^{-1} \quad \dots(7)$$

where a is the lattice constant, A , the atomic weight, θ_D , the Debye temperature and γ , the Gruneisen parameter. For copper White (1960) has assumed γ to be 2.6 where as Gruneisen's value is 2.0. The corresponding values of W_u/T are .0285 and .017 respectively. But it is clear from the expression (6) that White's value of W_u/T does not give any positive value n . We therefore select Gruneisen's value of γ and the corresponding W_u/T . Hence from (6)

$$\frac{n}{n+1} = \frac{K_s}{K_u} = \frac{W_u/T}{W_s/T} = \frac{.017}{.024}$$

giving $n=2.4$, which appears to be quite reasonable in view of the results obtained by Klemens (1962) and Garber et al (1963).

REFERENCES

- Backlund, N. G. 1961 *J. Phys. Chem. Solids*, **20**, 1.
 Berman, R. 1951 *Phil. Mag.* (7), **42**, 642.
 Charsley, P. Salter, J. A. M. Leaver, A. D. W. 1968 *Phys. Stat. Sol.* **25**, 531.
 Estermann, I. & Zimmerman, J. E. 1952, *J. Appl. Phys.* **23** 578.
 Garber, M. Scott, B. W. & Blatt, F. J. 1963 *Phys. Rev.* **130**, 2188.
 Gilmont R. 1946 *Industr. Engng. Chem. Anal. Ed.* **18**, 633.
 Gilmont R., 1951 *Anal. Chem.*, **23**, 157.
 Hulm, J. K. 1950 *Proc. Roy. Soc. A* **204**, 98.
 Hulm, J. K. 1951 *Proc. Phys. Soc. B* **64**, 207.
 Kemp, W. R. G. Klemens, P. G. & Tainsh, R. J. 1957 *Austr. J. Phys.*, **10**, 454.
 Kemp, W. R. G. Klemens, P. G. Tainsh, R. J. & White, G. K. 1957, *Acta Met.* **5**, 303.
 Klemens, P. G. 1958, *Solid State Physics*, **7**, 1.
 Klemens, P. G. White G. K. & Tainsh R. J. 1962 *Phil. Mag.* **7**, 1323.
 Leibfried, G. & Schlomann, F. 1954 *Nachr. Akad. Wiss. Göttingen*, **IIa**, 71.
 Lindenfeld, P. & Pennabaker, W. B. 1962 *Phys. Rev.* **127**, 1881.
 Lomer, J. L. & Rosenberg, H. M. 1959 *Phil. Mag.*, (8) **4**, 467.
 Mendelssohn, K. & Pontius, R. B. 1937 *Phil. Mag.* (7), **24**, 777.
 Mendelssohn, K. & Rosenberg, H. M. 1961 *Solid State Physics*, **12**, 234.
 Powell, R. L. 1961 *Properties of materials at low temperature (Phase I)*, A compendium,
 NBS, Pergamon Press.
 Rosenberg, H. M. 1954 *Phil. Mag.* (7), **45**, 73.
 1956 *Phil. Mag.* (8), **1**, 738.
 1957 *Phil. Mag.* (8), **2**, 541.
 White, G. K. 1953 *Proc. Phys. Soc. A* **66**, 844.
 White, G. K. 1953 *Austr. J. Phys.* **6**, 397.
 White, G. K. 1960 *Austr. J. Phys.* **13**, 255.
 White, G. K. & Woods S. B. 1955 *Canad. J. Phys.* **33**, 58.
 White, G. K. & Woods, S. B. 1959 *Phil. Trans. Roy. Soc. A* **251**, 273.
 Ziman, J. M. 1956 *Canad. J. Phys.* **34**, 1256.

Letters to the Editor

The crystal structure of cresotic acid

M. P. GUPTA AND S. M. PRASAD

Department of Physics, University of Ranchi, Ranchi-8

(Received January 20, 1969)

Cresotic acid ($C_8H_8O_3$) is a monocarboxylic acid with a hydroxyl group attached to it



and the scheme of hydrogen bonding in the crystal is likely to be of great interest as, like many other carboxylic acid structures, the molecules are likely to form dimers in the crystal structure and in addition, there is the possibility of intramolecular hydrogen bonds being formed between the oxygen atoms of the carboxyl (COOH) and hydroxyl (OH) groups, or there is also the possibility of same oxygen atoms being linked by two hydrogen bonds, one through dimerization (COOH groups) and the other through linkages with the hydroxyl groups (OH). We have, therefore, studied the crystal structure of this acid and this note presents a preliminary report on it.

The compound (white powder) was crystallized as long needles from an alcoholic solution. The unit cell dimensions were determined using rotation and Weissenberg photography. The crystallographic data are as follows :—

$a = 10.83 \text{ \AA}$	$\rho \text{ calc.} = 1.408 \text{ g/ml.}$
$b = 4.105 \text{ \AA}$	$\rho \text{ measured} = 1.397 \text{ g/ml.}$
$c = 16.15 \text{ \AA}$	$\mu = (\text{linear absorption co-efficient for X-rays})$
	for CuK_{α} radn. $= 9.597 \text{ cm}^{-1}$
$\beta = 91^{\circ} 47'$	$Z = 4.$

Diffraction spectra give : hkl no condition,

$h0l$ present only when $l = 2n$,

$0k0$ present only when $k = 2n$,

This gives the space group uniquely as $P2_1/c$. Intensity data collected, using CuK unfiltered radiation from Weissenberg photography with the crystal mounted along the $[010]$ axis, were $(h01, h11, h21)$. Other reflexions collected were $(hk0)$.

Determination of the structure :

As the $[010]$ axis is a short axis, a Patterson projection (unsharpened) was calculated. A theoretical vector map for the benzene ring along with the attached carboxyl group was superimposed on the Patterson function and this gave the orientation of the molecule. Packing considerations

(dimerization across a centre of symmetry and linkages through the COOH groups) led to a reasonable model and trial coordinates. Reiterative Fourier refinements and least squares refinements yield good x and z coordinates giving $R(h01) = 0.166$. The $[010]$ electron density projection is shown in figure 1. The y -coordinates were determined using generalized Fourier projections ($h11$ and $h12$ data) and Fourier projection down the $[001]$ axis. The overall R factor for the $hk0$ reflexions is 11.7%.

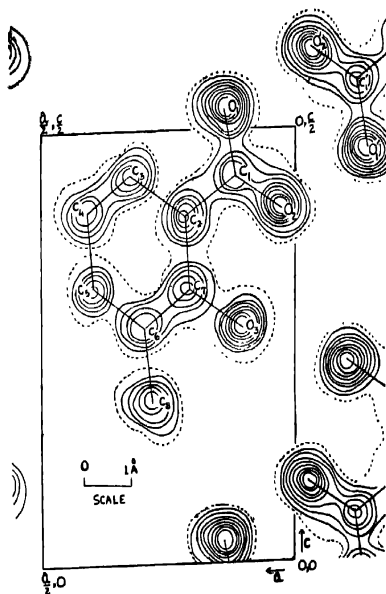


Figure 1. Electron density projection down the $[010]$ axis.

Description of the structure :

As expected the COOH groups of the molecules are linked across centres of symmetry by hydrogen bonds of 2.61\AA . This is a feature present in all carboxylic acids. The oxygen atoms of the hydroxyl groups are linked with the oxygen atoms of the COOH groups by 2.56\AA bonds which are intramolecular in nature. Other distances are normal Van der Waals distances (3\AA upwards). As considerable interest lies in an accurate location of the hydrogen atoms, we are now doing a complete three dimensional analysis of the structure and the results will be reported later. The molecular geometry is normal.

The crystal structure of dipotassium fumarate dihydrate,
 $K_2C_4H_4O_4 \cdot 2H_2O$

By M. P. GUPTA AND B. N. SAHU

Department of Physics, University of Ranchi, Ranchi-8

(Received January 20, 1969)

As part of a programme for determining the crystal structures of simple organic molecules with hydrated structures involving hydrogen bonds, we have determined the crystal structure of dipotassium fumarate dihydrate, $K_2C_4H_4O_4 \cdot 2H_2O$, by X-ray diffraction methods. This compound is interesting, apart from its scheme of hydrogen bonding, from another point of view. The accurate dimensions of the dipotassium fumarate 'molecule' are likely to settle the question of composition of another salt of fumaric acid, namely, acid potassium fumarate (Gupta 1956).

Crystal data :

The compound crystallizes from water solution with pH value about 8, with a platy habit, the (100) face being the pronounced platy face. The crystallographic data are the same as reported earlier by Gupta & Barnes (1961) and are given below :

$a = 6.35_A$	ρ measured = 1.819 g/ml
$b = 18.22_A$	ρ calculated = 1.817 g/ml
$c = 7.27_A$	μ = (linear absorption co-efficient for X-rays) with
$\beta = 98^\circ 20'$	$CuK_\alpha = 100.89 \text{ cm}^{-1}$
$Z = 4$	$MoK_\alpha = 10.59 \text{ cm}^{-1}$
Sp. group : $P2_1/c$	

Intensity data were collected using small single crystals and precession photographs using Mo unfiltered radiation ($hk0$, $0kl$, $h0l$, hkh , hkh). Equi-inclination photographs with Weissenberg goniometer and CuK_α radiation permitted some more reflexions ($hk1$, $hk2$, $hk3$, $hk4$) to be collected and all these were put on an absolute scale using statistical methods.

Determination of the structure :

Patterson projections failed to give any clue about the positions of the potassium atoms. Inequality relations were tried but proved fruitless. A three-dimensional Patterson function (unsharpened and without the origin peak removed) gave rough indications of the potassium atoms. Two dimensional Fourier projections and several cycles of least squares refinements have now given the details of the structure with $R(hk0)$ 0.155,

$R(0k1)$ 0.220, $R(h01)$ 0.251. Figure 1 below shows the electron density projection down the $[001]$ axis and as can be seen, there is overlap in this projection, the picture being even worse in the other projections.

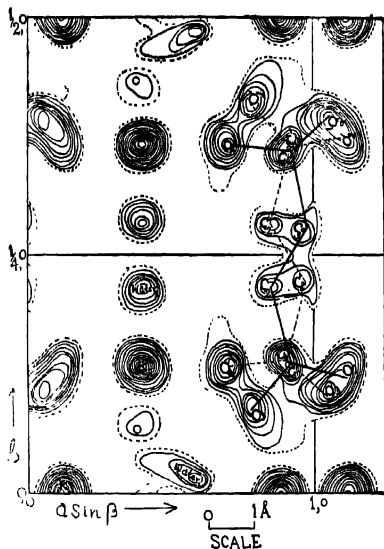


Figure 2. Electron density projection down the $[001]$ axis.

Description of the structure :

In the crystal structure fumarate groups are aligned roughly parallel to the $[010]$ axis at heights approximately zero and $\frac{1}{2}c$. The water molecules provide the binding links with hydrogen bonds linking the chains of the fumarate groups. The K^+-O distances are similar to those normally found in other structures (2.72 to 2.91 Å)

As the overlap is serious in the projections, a full three-dimensional refinement of the data is in progress, the results of which will be reported later. The basic features of the crystal structure, however, are not likely to be changed from being reported here.

REFERENCES

- Gupta M. P. 1956 *Acta Cryst.* **9**, 263.
Gupta M. P. & Barnes W. H. 1961 *Can. J. Chem.* **39**, 1739.

Ultrasonic absorption in binary mixtures of CS₂

K. SAMAL AND S. C. MISRA

Post Graduate Physics Department, Utkal University, Vani-Vihar,

Bhubaneswar-4, India,

(Received December 2, 1968)

It has been reported by Samal & Das (1967) that the coefficient of ultrasonic absorption of CS₂ decreases more when mixed with xylene ($\alpha/f^2=78 \times 10^{-17}$ c.g.s.) than with kerosine ($\alpha/f^2=110 \times 10^{-17}$ c.g.s.). This gives an impression that the lower the absorption coefficient of an impurity the more effective it is in reducing the absorption coefficient of CS₂. A calculation from Bauer's theory (1949) gives also similar indication when tried with benzene-toluene and benzene-carbon tetrachloride mixtures. But the theory does not fit well to the experimental findings of Samal & Das (1967) in case of binary mixtures of xylene and kerosene with CS₂ as one of the components in each.

TABLE 1.

C ₆ H ₆ (0.878 gm/cc) in CS ₂ mole frac- tion $\times 10^3$	$\alpha/f^2 \times 10^{17}$ c.g.s.	CCl ₄ (1.596 gm/cc) in CS ₂ mole frac- tion $\times 10^3$	$\alpha/f^2 \times 10^{17}$ c.g.s.	CH ₃ I (2.285 gm/cc) in CS ₂ mole fraction $\times 10_4$	$\alpha/f^2 \times 10^{17}$ c.g.s.
0.63	5533	0.63	5379	0.972	4906
1.36	5187	1.251	5272	2.908	4599
2.04	4256	1.876	5169	4.827	4260
4.73	3773	3.124	4793	8.674	3881
8.43	3457	4.367	4383	12.000	3493
11.80	3320	5.608	4150	16.730	3119
16.70	3074	10.870	3473	23.730	2882
20.00	2863	15.420	3391	28.340	2569
26.50	2636	18.450	3259	37.430	2460
32.80	2558	25.060	2870	46.360	2184
39.20	2442	31.320	2643	55.120	2079
45.40	2305	36.230	2468	63.720	1902
51.60	2243	42.020	2219	—	—
57.60	2102	47.730	2050	—	—
63.40	2948	53.390	1916	—	—
—	—	58.950	1601	—	—

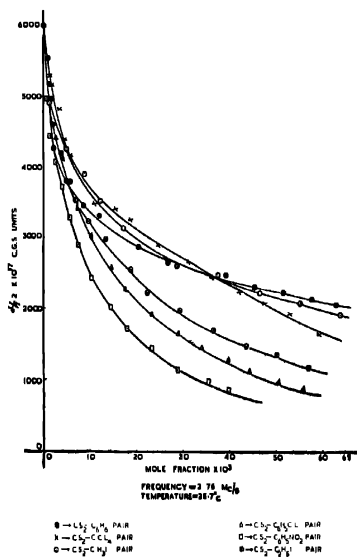
In order to test the theory further, a number of unassociated liquids like C_6H_6 , CCl_4 , CH_3I , C_6H_5Cl , $C_6H_5NO_2$ and C_6H_5I with their α/f^2 values (α -amplitude abs. coeff. and f -frequency) ranging from 900×10^{-17} c.g.s. to 40×10^{-17} c.g.s., are added separately as impurities to CS_2 and the variation of α/f^2 of the mixture with the concentration of the impurity in each case is shown graphically on a common scale for contrast.

TABLE 2

C_6H_5Cl (1.107 gm/cc m) CS_2 mole fraction $\times 10^2$	$\frac{\alpha}{f^2} \times 10^{17}$ c.g.s.	$C_6H_5NO_2$ (1.197 gm/cc) in CS_2 mole fraction $\times 10^2$	$\frac{\alpha}{f^2} \times 10^{17}$ c.g.s.	C_6H_5I (1.943 gm/cc) in CS_2 mole fraction $\times 10^2$	$\frac{\alpha}{f^2} \times 10^{17}$ c.g.s.
0.591	5284	0.588	5458	0.753	5318
1.181	4931	1.116	4968	1.503	4986
1.770	4613	1.750	4475	2.253	4603
2.947	4439	2.912	4068	3.750	4199
4.121	4110	4.065	3724	5.242	3799
7.334	3414	5.254	3292	6.730	3520
10.238	3040	7.300	2906	9.324	3234
14.563	2551	10.100	2432	13.000	2992
17.394	2219	14.400	2016	18.480	2546
23.100	1881	17.320	1708	22.090	2216
28.622	1632	22.850	1454	29.230	1917
33.616	1451	28.360	1124	26.280	1685
44.159	1088	35.040	982	43.220	1468
50.430	957	39.280	823	50.060	1337
55.810	872	—	—	56.800	1185

The coefficients of ultrasonic absorption of the mixtures of the liquids supplied by E. Merck were determined at a fairly constant temperature of $25.7^\circ C$ with the optical arrangement reported by Samal (1956). The ultrasonic transducer being a rectangular quartz of natural frequency 1 mc/s, was made to vibrate at 2.76 mc/s inside the mixtures of CS_2 . The density of CS_2 is taken to be 1.26 gm/cc and the values for other liquids are given in the tables, by the sides of the liquids.

One can easily note from the graphs of $CS_2-C_6H_6$ and CS_2-CCl_4 that benzene with higher absorption coefficient has reduced the absorptions coefficient of CS_2 more effectively than CCl_4 of relatively lower



absorption coefficient. But in the case of liquids of similar structures (C_6H_6 , $\text{C}_6\text{H}_5\text{Cl}$, and $\text{C}_6\text{H}_5\text{NO}_2$) the fall in the absorption coefficient is more rapid the lower the value of α/f^2 of the impurity. This needs more critical analysis of the experimental finding as well as the theory.

The authors are indebted to Board of Scientific and Industrial Research, Orissa for financial help.

REFERENCES

- Bauer, E. 1949 *Proc. Phys. Soc. (Lond)* **62A**, 141
 Samal, K., & Das, S. C. 1967 *Curr. Sci.* **36**, 316
 Samal, K. 1956 *Acoustica (Switzerland)* **7**, 251

Electric and thermoelectric properties of specular hematite

By A. K. MUKERJEE

Magnetism Department, Indian Association for the Cultivation

of Science, Calcutta-32, India.

(Received August, 2, 1969)

In some recent communications the results of measurements of magnetic properties (Mukerjee 1967 a, b) of single crystals of naturally occurring hematite of purities 95.5% and 99.1% and the electric and thermoelectric properties of the former variety (Mukerjee 1968) were reported. The principal electrical conductivities (σ_{\parallel} and σ_{\perp}) and Seebeck voltages (θ_{\parallel} and θ_{\perp} with respect to Pt.) of the latter variety have been recently studied in air in the temperature range 200°K to 1000°K for the fresh sample as also repeated for the same in this whole temperature range (figures 1 and 2). Due to heat treatment no permanent change* was produced and the results were reproducible.

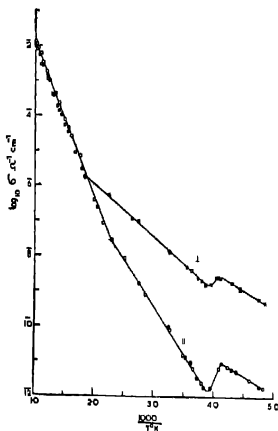


Figure 1. The conductivity of hematite. Open and solid points indicate measurements on fresh and heated samples respectively.

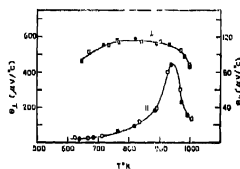


Figure 2. Seebeck effect of hematite. Open and solid points indicate measurements on fresh and heated samples respectively.

The temperature variation of principal conductivities could be given by a formula of the type

$$\sigma = \sigma_0 \exp \frac{-\Delta E}{kT}$$

where the symbols have their usual meaning (Smith 1959), but with different sets of values for σ_0 and ΔE for different temperature ranges which are given in table 1 for different crystallographic directions.

The changes in conductivities in both the directions round about 250°K are quite marked (figure 1). The magnetic properties of these samples were also found to undergo sharp changes near this temperature (Mukerjee 1967b). Neutron diffraction also shows a spin flip about this temperature (Shull *et al* 1951). It is further observed from figure 1 that anisotropy in electrical conductivity practically vanishes at high temperature. Due to very high resistances of the samples the Seebeck voltages could be measured only at high temperatures (figure 2). The signs of both the principal Seebeck voltages were found to be negative indicating that the electrons are the major charge carriers. Unlike the electrical conductivities, appreciable anisotropy in Seebeck voltages remains throughout the entire temperature region. Details of the work will be published soon elsewhere.

TABLE 1. ΔE AND σ_0 IN DIFFERENT TEMPERATURE REGIONS

Crystal direction	ΔE in ev	$\sigma_0 \Omega^{-1} \text{cm}^{-1}$	Temperature region °K
Basal plane	.20	5.0×10^{-8}	$T < 240$
	.30	1.1×10^{-8}	$255 < T < 540$
	1.00	5.6×10^4	$540 < T$
c-axis	.20	2.0×10^{-7}	$T < 240$
	.55	6.3×10^{-8}	$255 < T < 385$
	1.00	5.6×10^3	$385 < T$

The author is thankful to Shri A. K. Dutta for guidance and Prof. A. Bose for his kind interest in the work. He also wishes to thank Prof. S. D. Chatterjee for his kind help in devising the vacuum tube electrometer for some of the measurements.

REFERENCES

- Mukerjee, A. K. 1967 a *Indian J. Phys.* **41**, 466.
 b *Indian J. Phys.* **41**, 781.
 1968 *Indian J. Phys.* **42**, 673.
 Shull, C. G., Strauser, W. A. & Wollan, E. O. 1951 *Phys. Rev.* **83**, 333
 Smith, R. A. 1959 *Semiconductors*, Cambridge University Press.

Crystal structure of Cu(II)-bis-morpholine biguanide

By SANKARANANDA GUHA

Indian Association for the Cultivation of Science, Calcutta-32

(Received August 7, 1969)

Copper (II)-bis-morpholine biguanide (Poddar 1968) crystallizes as deep red plates. Rotation and Weissenberg photograph show that the crystal belongs to the monoclinic system with cell dimensions

$$a=8.68\text{\AA}, b=12.74\text{\AA}, c=7.75\text{\AA}, \text{ and } \beta=93.5^\circ.$$

The only systematic absences were for $0k0$ with k odd and for $h0l$ with l odd, indicating that the space group is $P2_1$. Density determination by flotation method showed that there are two formula units of $\text{Cu}(\text{C}_6\text{H}_8\text{N}_6\text{O}_2)_2$ per unit cell.

Three dimensional data were collected using multiple-film equi-inclination Weissenberg technique and CuK_α radiation. The intensities were estimated visually and corrected for Lorentz polarization and spot-size effects. The data were then brought to the absolute scale.

A three-dimensional Patterson synthesis showed that the copper atoms are placed at $(0.0.0)$ and $(0.\frac{1}{2}.\frac{1}{2})$ and the two ligands attached to copper have a trans- configuration. Due to their special positions, the copper contribute to the structure factors of $(k+1)$ even group of reflections only. Therefore, the three-dimensional Fourier synthesis calculated with the signs of the copper atoms showed a pseudosymmetry. The spurious mirrors at $y=0$ and $y=\frac{1}{2}$ made the correct identification of the lighter atoms very difficult, though it became evident that the four nitrogens around copper had a square planar configuration.

To avoid this difficulty symbolic addition procedure (Karle & Karle 1963, 1964; Karle *et al* 1964) of direct sign determination was applied with some modifications. For the $(k+1)$ even reflections the contribution of the copper atoms were subtracted from the F_0 's, assuming that their signs are the same as those due to the copper atoms only. The new F 's are thus due only to the lighter atoms of the structure. To these structure factors the Σ_2 formula

$$SE_{hkl} \simeq \sum_{h'k'l'} SE_{h'k'l'} SE_{h-h', k-k', l-l'} \quad \dots(1)$$

was applied, where S means 'sign of'. The E values for all the reflections were calculated with the expression

$$E_{hkl}^2 = |F_{hkl}|^2 / \epsilon \sum_1^N f_i^2 \quad \dots(2)$$

where f_i is the scattering factor of the i th atom, ϵ is an integer, which in the case of group $P2_{1/2}$ is 2 for $h0l$ and $0k0$ reflections and 1 for all others. The origin was fixed by assigning positive sign to three reflections (210, 021 and $\bar{2}1$) with very large E values. Starting from these initial signs the signs of many other reflections were generated by using equation (1). The probability of the sign of a particular E_{hkl} being positive was calculated with the formula,

$$P_+(E_{hkl}) = \frac{1}{2} + \frac{1}{2} \tanh \left(\frac{1}{\sqrt{N}} |E_{hkl}| \sum_{h'k'l'} E_{h'k'l'} E_{h-h', k-k', l-l'} \right) \quad (3)$$

where N is the total number of atoms in the unit cell.

The $(k+1)$ odd group of reflections to which signs could be assigned by the above method have now been added in the next three-dimensional Fourier synthesis. This synthesis clearly shows that the spurious mirror is broken partially, so that the location of the light atom peaks is no longer a formidable task. The refinement of the structure is now in progress.

I am grateful to the Director of Saha Institute of Nuclear Physics and to Professor N. N. Saha for providing me with the facilities for the work and a Research fellowship of the Institute. My sincere thanks are due to Dr. N. G. Poddar for providing me with the crystals for study.

REFERENCES

- Karle, I.L. & Karle, J. 1963 *Acta Cryst.* **16**, 969.
- Karle, I.L. & Karle, J. 1964 *Acta Cryst.* **17**, 1356.
- Karle, I.L. Britts, K. & Gum, P. 1964 *Acta Cryst.* **17**, 496.
- Poddar, N. G., 1968 D. Phil. Thesis, Calcutta University.

BOOK REVIEW

Fundamental University Physics, by Marcelo Alonso &
Edward J. Finn, Addison-Wesley Publishing Co. 1967. Vols. 1 & 2.
Price Vol. 1. \$8.75, Vol. 2. \$8.75

This is a new addition to the growing list of U. S. publications on integrated Physics Course for undergraduate students. However, there is a distinct departure from the conventional approach to Physics text book writing. During the past two decades or so, most authors of undergraduate Physics text books have tended to emphasize on the basic principles, rather than on details (which, unfortunately, is not so much the practice with Indian publication). The present volumes not only conform to this practice, but go further in trying to present the various physical principles from a unified point of view. According to the authors, the traditional division of physics into subjects like mechanics, heat, sound etc. no longer has any justification. Instead they have followed "a logical and unified presentation, emphasizing the conservation laws, the concepts of fields and the atomic view of matter".

The first volume deals with Mechanics (Part I) which includes the usual fundamental topics upto Dynamics of Rigid Bodies. This is followed by relativistic dynamics and a chapter on oscillatory motion. In all the chapters, the discussion of the fundamental principles is accompanied by illustrations from as diverse fields of Physics as possible. Thus, while dealing with the dynamics of a particle such topics as the momentum conservation in the collision between an α -particle and a proton, terminal velocity attained in falling through a viscous medium (useful in analysing Millikan's oil drop experiment), of the scattering of a particle under the action of a central field, are discussed. Again in the chapter on the dynamics of a system of particles, the basic concepts of the kinetic theory of gases are introduced by way of illustrating a many particle system. These are few of the many attempts made by the authors throughout the book in emphasising the applicability of the fundamental laws of nature in widely diverse fields of Physics.

The last Chapter in Vol. 1 deals with gravitational interaction which is actually the prelude to a comprehensive discussion on Interactions and Fields (Part 2) carried through in Vol. 2, the later half of which (Part 3) deals with waves. After presenting the fundamental ideas of electric and magnetic interactions, a useful discussion on the Lorentz transformation of the electromagnetic field and a revision of the principle of conservation of momentum is included. Atomic structure is also introduced at this stage. Finally Maxwell's equations are formulated in the last chapter. Some of the more advanced concepts, such as the electromagnetic interactions between moving charges are introduced only in passing.

In Part 3, after deducing the differential equation of wave motion, different types of wave motion such as elastic waves in solids transverse waves in strings, surface waves in liquids, pressure in gases and finally electromagnetic waves are separately discussed. Much of the material usually covered under the headings of acoustics and optics are also included. The last chapter is on Transport Phenomena, the inclusion of which at this stage can probably be justified only by reference to the topics intended to be discussed in next volume which is not yet published.

So far as the Indian students are concerned, these two volumes will be very useful addition to their reference library, specially for undergraduate honours students. They do not however cover the entire syllabi of the undergraduate curriculum of most Indian Universities, which unfortunately abounds in absurd details even now.

The volumes are full of many highly interesting illustrative examples. Besides, large numbers of problems are included at the end of each chapter. An useful appendix of common mathematical relations and tables is included at the end of the first volume.

The authors have succeeded to a large extent in the difficult job of presenting a comprehensive and unified view of the physical world to the undergraduate students. Not only would the serious undergraduate students in this country derive considerable benefit from these volumes, but the teachers in undergraduate Institutions will have the opportunity of looking at their subject from a considerably different and novel angle.

S. N. G.

OBITUARY

Prof. Ashutosh Mookherji :

Professor Ashutosh Mookherji, D. Sc., passed away on the 3rd October, 1969 at the age of 64 years, leaving behind his wife, one son and a daughter, many relatives, friends and students to mourn his untimely death. To the present writer the death has come as a great shock and sense of deepest personal loss, as Dr. Mookherji was not only a life long colleague of the writer in the field of Crystal Magnetism, but more than a staunch friend in adversity and prosperity.

Coming from a middle-class family of Paschimpara, Vikrampur, Dacca (now in East Pakistan) he graduated with Chemistry honours from the Daulatpur Hindu Academy and passed the M. Sc., examination in Physics of the Dacca University in 1931. Thereafter, he undertook research work in Crystal Magnetism, until 1933 at the Dacca University under late Professor K. S. Krishnan, then Reader in Physics at that University, and was associated with Dr. S. Banerjee (Recently retired from the Central Water and Power Station, Poona), N. C. Chakravorty (retired from Govt. of India, Ministry of Education Dr. B. C. Guha (retired from Education Service, Govt. of West Bengal) and the present writer, forming the first nucleus for the growth of the study of Crystal Magnetism in this country. When in 1933 Prof. Krishnan as the first Mahendralal Sircar Professor of Physics, joined the Indian Association for the Cultivation of Science at the "historic" 210, Bowbazar Street, Calcutta, already hallowed by the discovery of Raman Effect, a small batch of his students from Dacca, including Dr. Mookherji, Dr. Banerjee and the present writer accompanied him there and the nucleus grew up at last into a school of Magnetism, which carried out extensive and intensive investigations in the field of dia- and para-magnetism of single crystals, to win international fame in future years, with the help of the most simple and rudimentary, home-made equipments, housed in the old, dilapidated premier shrine of scientific learning in India. Amongst the foremost students of Krishnan Dr. S. Banerjee's name is associated with the pioneer magnetic anisotropy work on a large number of aromatic organic crystals and on the feebly anisotropic S-state ions of transition elements. On the other hand, Dr. Mookherji initiated the pioneer work on a vast number of anisotropic salts of the iron group establishing Van Vleck's "Theory of Crystalline Electric Fields", on a firm experimental basis, and achieved the crowning success of his career by the first ever measurements of the anisotropy of rare earth salts, which property was admitted, for a long time to come, as a puzzle by even Prof. Van Vleck. As is well known, the rare-earth ions are chemically so very alike that it is a specialized job to separate them. On the other hand, their magnetic behaviours are very different and any small admixtures between them would totally vitiate the results. Moreover, only two or three laboratories in the world at that time (1933-38) were experimentally preparing spectroscopic quality of rare-earth oxides, so that these were practically unavailable to others. With the ideal of self-help learnt at the feet of the sage-scientist Prof. S. N. Bose (his professor at the Dacca University), Dr. Mookherji brushed up his knowledge of B. Sc. course of analytical chemistry and launched upon the ambitious task of purifying the rare-earth salts available in the market. Starting with only a gram or two each, of oxides of cerium, praseodymium, neodymium and samarium, all that the very limited means of the laboratory at that time could purchase, he made for the first time a complete study of the magnetic

anisotropy and susceptibility of ethylsulphates, sulphates, chlorides and nitrates of each of the said ions, recovering the material after each measurement, for the preparation of the next salt. At a later time, he was able to get small quantities of the spectroscopically pure samples as a gift from Prof. Trombe of Paris, which confirmed fully his earlier results. This achievement alone will show how painstaking, exact and meticulous experimenter he was. Before this work was complete he had to pass through many family vicissitudes and in 1938 had to join the Rangoon University as the Professor of Physics, where he miraculously escaped death during the bombing of Rangoon in 1941, and somehow returned to Calcutta, to be faced on arrival with a great family disaster. On rejoining the Association in 1941, he took up with calmness and fortitude his original line of work and when in the middle of 1942 Prof. Krishnan left for Allahabad, he was put in sole charge of the Association Laboratories and Library, and with a small sincere band of colleagues, continued bravely to uphold his sacred trust in the face of bombing and imminent danger of aggression to Calcutta. When in 1943 Dr. K. Banerjee joined the Association as the M.L.S. Professor of Physics, Dr. Mookherji left for Pilani as the Professor of Physics, where again, as in Rangoon University, he built up the Physics Department virtually from scratch and also a research laboratory in Magnetism. All these ups and downs caused considerable delay in submitting his thesis but at last in 1947 he was awarded a well merited D. Sc. degree of the Dacca University, for his work of Paramagnetism of Crystals of iron and rare-earth group salts. It was perhaps destined that Dr. Mookherji could never settle down at one place. He had already migrated from Rangoon to this Association and from Association to Pilani but again he shifted from Pilani to Agra College in 1955 and from Agra finally to Burdwan in 1963. At each of the places he had made his name as a first rate organizer, teacher and research worker and held up before his students and admirers an ideal of simplicity, honesty, industry and gentlemanly behavior, at home and in the laboratory, and added to this a hearty and bluff attitude towards life. He started his research career as a research scholar of this Association from 1933-37, became later on a research fellow in 1941 on his return from Rangoon and was made successively the Assistant Secretary and a Research Assistant then the highest post in the Association after M.L.S. Professor. He was an ordinary member of this Association until his death, a member of the Council of the Association for a number of years, a member of the Board of Editorial Collaborators of Indian Journal of Physics and had the best interest of the Association always foremost in his heart.

Ashutosh was, as his name in Bengali implies, soon pleased with very little and though could never tolerate evil, could be appeased easily with a little effort. It was hoped that with his apparently vigorous health he would continue for quite a number of years to inspire his students and collaborators to achieve a lasting fame for the Dept. of Physics, Burdwan University. But, an insidious lurking disease has suddenly robbed us of a friend and the country of a true physicist. We pray to God for the eternal peace of his soul and for consolation to his bereaved relatives and friends,

A. Bose

OBITUARY

Prof. C. S. Ghosh.

Chandra Sekhar Ghosh graduated with honours in Physics in 1928 and obtained a first class M.Sc. degree in Applied Physics from the University of Calcutta in 1930 standing second in order of merit. He was awarded Sir Rashbehari Scholarship and in 1934 he joined the University of Calcutta as an Assistant Lecturer. After serving the University for a number of years he went to the United States of America and joined the Massachusetts Institute of Technology and obtained from there his Master's degree in Electrical Engineering. He then joined the Indian Institute of Science, Bangalore, as a Professor and later became Professor and Head of the Department of Electrical Engineering at Roorkee University. He also acted as its Vice-Chancellor for sometime before his retirement in 1968. During this period he had won a good name as a teacher and an administrator. After his retirement he came back to Calcutta and joined the University Department of Applied Physics as a retired scientist; but unfortunately within a very short time—on the 19th December, 1968, a sudden heart-stroke cut short his valuable life. Professor Ghosh was connected with many institutions and learned societies of this country and abroad. He was a member of the Indian Association for the Cultivation of Science also member of its Council for some time a Fellow of the National Institute of Sciences of India and a Senior Member of the Institute of Electrical and Electronics Engineers, New York. For a number of years he acted as the Outstation-Secretary of the Indian Science Congress Association and was also the Editor-in-Chief of *Everyman's Science*, a quarterly journal published by this Association. He was a member of the Board of Collaborators of the Indian Journal Physics. A man of hearty and jovial temperament, he was liked by all who came in contact with him, and his loss therefore was felt by a large number of friends and admirers throughout the country.

(G. N. Bhattacharya)

A study of electrode glow during electrolysis

By R. G. EDKIE AND CHINTAMANI MANDE

Department of Physics, Nagpur University, Nagpur

(Received April 9, 1969)

[PLATES—3A-3B AND 4A-4B]

Electrode glows during the electrolysis of aqueous alkali solutions at wire electrodes of different materials and dimensions have been studied using spectroscopic and oscillographic techniques. It has been shown that the glow does not depend upon the electrolyte but is governed mainly by the electrode geometry. The glow spectrum consists of the atomic lines of the electrode material and the metal ions in the electrolyte along with some band structures in the case of the cathode glows. The anode glow spectrum exhibits a few atomic lines of the alkali metal ions, superimposed on a continuum. It is proposed that these glows are due to corona discharges through an insulating thermal layer surrounding the electrode. The nature of this layer is essentially similar to the thermal boundary layer encountered in the electro-hydro-dynamic (EHD) techniques. The onset of the glow is primarily governed by the dimensions of the insulating layer, the temperature of the electrolyte and the field distribution around the layer. The oscillographic studies have revealed corona discharge pulses in the insulating layer surrounding the electrodes.

INTRODUCTION

Following the interesting work on electrode glow during electrolysis, recently reported by Palit (1967), the authors have undertaken detailed investigation of this phenomenon in order to study the conditions under which this glow appears and to understand the basic mechanism of the glow process. Preliminary results of this work have already been reported earlier (Mande & Edkie 1961).

According to Hickling & Ingram (1964) this phenomenon was probably first observed at a platinum electrode during the electrolysis of water by Fizeau & Foucault as early as in the year 1884. These authors, who observed that the glow was particularly intense at the cathode, considered it to be an arc discharge through hydrogen. In the year 1950, Kellogg, using higher current densities in aqueous solutions observed intense glows at wire electrodes and attributed them to local heating. He also pointed out the similarity between this phenomenon and the well known anode effect observed in the electrolysis of fused salts. More recently, Hickling & Ingram (1964) have studied this phenomenon in detail, particularly the reactions at the anode and the corresponding power requirement for the production of a continuous glow. According to Ivey (1963) the glow in aqueous solutions can be termed as 'galvano-luminescence'. Kuwana (1966) has recently given an historical account of this type of work with particular reference to organic electrolytes. Very recently Palit (1968) has studied the liberation

of hydrogen and oxygen together on the electrodes during electrolysis accompanied by electrode glow in a number of electrolytes. As no spectroscopic and oscilloscopic investigations of this phenomenon in alkali solution appear to have been reported so far, it was thought worthwhile to undertake this study.

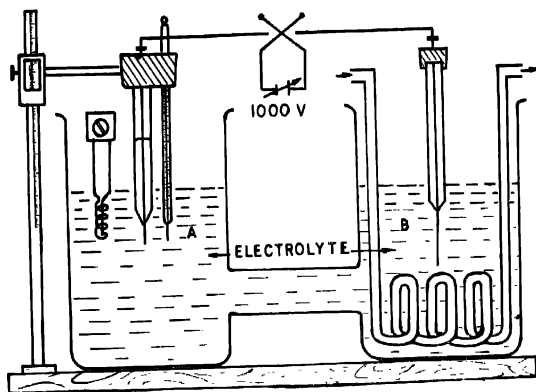


Figure 1. Basic experimental set up.

EXPERIMENTAL

The main experimental arrangement used in this investigation is shown in figure 1. It essentially consists of two beakers, each of 500 c. c. capacity, joined together by a glass tube of 1.5 cm internal diameter. The region A of the electrolyte could be heated by using an immersion heater and the region B could be cooled by using a water-cooled copper coil. A sufficient temperature difference between the two regions A and B surrounding the electrodes could be maintained by using this arrangement. Different types of electrodes, such as, platinum and tungsten wires fused in glass and thin copper and aluminium rods, introduced through suitable glass tubes into the electrolyte, were tried. The power for the electrolysis was obtained from a D. C. power supply unit, fabricated in this laboratory, giving up to 1000 volts at 2 amps. The depth of immersion of the electrodes in the electrolyte could be adjusted with the adjustable stands for the electrodes. This was necessary in order to compensate for the changes in the electrolyte level caused by heating effects.

Spectroscopic investigations of glow at low dispersion, were carried out on a constant deviation glass prism spectrograph manufactured

by the Andhra Scientific Co., India. In order to obtain more details, the spectra were also photographed on Hilger medium quartz spectrograph. Since the glows were flickering it became necessary to use rather wide slits to record the glow spectra. Iron arc and hydrogen discharge tube spectra were recorded for comparison, using Hartmann 3-aperture diaphragm. The slit width, exposure time and the power supply for the production of the glow were suitably adjusted in each case.

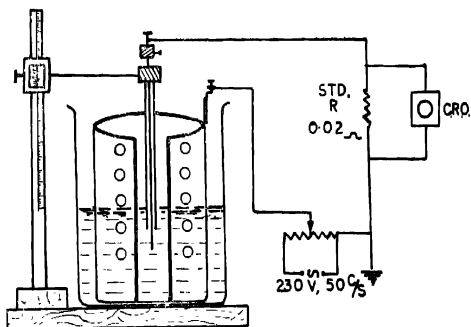


Figure 2. Experimental set up for oscillographic studies.

It was found difficult to lock-up the random pulse pattern causing the glow on a cathode ray oscillograph under purely D. C. conditions. These difficulties were minimized by using a modified experimental arrangement as shown in figure 2. A hollow, slotted, stainless steel cylinder of diameter 6 cm and height 8 cm and a thin axially placed wire within the cylinder served as electrodes. The power for the electrolysis was obtained from A. C. mains through a variac. A Hewlett-Packard C. R. O. was connected across a standard low resistance, R . The oscillographic traces were photographed using the camera attachment of the C. R. O.

RESULTS

The results obtained in this investigation are described in the following three sections :—

- I. Effects of the concentration and temperature of the electrolyte and the geometry of the electrodes on the glow.
- II. Spectroscopic studies of the glow.
- III. Oscillographic studies of the glow.

I(a). *Effect of concentration of the electrolyte*

In this investigation platinum wires were used as electrodes ; one of them was of diameter 0.5mm and length 2.0 cm and the other was of diameter 0.15mm and length 0.72cm. CaCl_2 and NaOH solutions of different concentrations, in the range 0.0027 to 0.20 molar, were used as electrolytes. The depth of immersion of the thinner electrode in the electrolyte was maintained at 3.0cm from the free surface.

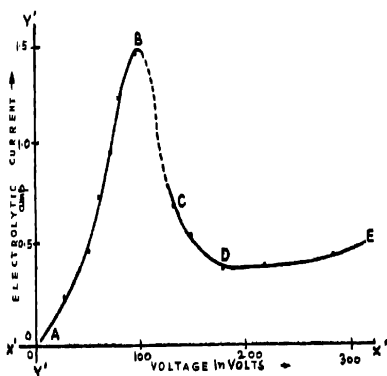


Figure 3. Variation of current with applied voltage in the cell circuit.

It was observed that as the potential difference between the electrodes is gradually increased, at a certain critical voltage the current suddenly decreases with fluctuations. A large number of bubbles are then seen to surround the electrodes and a spectacular glow, surrounding the thinner electrode, appears. By changing the polarity of the electrodes, it was found that the glow always appears at the thinner electrode, irrespective of its being either the cathode or the anode. By changing the concentration of the electrolyte it was observed that the concentration has very little effect upon the input power required to produce a continuous glow. A curve showing the variation of the electrolytic current with the applied voltage for 0.1M CaCl_2 solution is shown in figure 3. The general nature of the curves for different concentrations of the electrolytes is essentially similar. The point D on the curve, shown in figure 3, indicates the onset of the continuous glow at the thinner electrode. Table 1 gives the power requirement for the onset of the continuous glow during the electrolysis of CaCl_2 and NaOH solutions of different concentrations.

TABLE 1. POWER REQUIREMENT FOR A CONTINUOUS GLOW, CORRESPONDING TO THE POINT 'D' ON THE CURVE IN FIGURE 3, AT A PLATINUM CATHODE OF DIAMETER 0.15mm AND LENGTH 0.72cm.

Concentration	Volts	Amps	Watts	Volts	Amps	Watts
	(for CaCl_2)			(for NaOH)		
0.0027M	250	0.29	72.5	150	0.47	70.5
0.004M	235	0.30	68.9	145	0.48	69.6
0.010M	215	0.32	68.8	135	0.51	68.9
0.050M	205	0.34	69.7	128	0.53	67.8
0.100M	190	0.37	70.3	120	0.57	68.4
0.200M	170	0.40	68.0	108	0.62	66.9

I(b). *Effect of temperature*

Using the same electrode system as described in the earlier section, it was found that as the temperature of the region *A* surrounding the thinner electrode is gradually increased, keeping the temperature of the region *B* constant at about 35°C, the input power required for the appearance of the continuous glow goes on decreasing. When the temperature of the region *A* approaches about 99°C, the input power required for the glow is found to be almost negligible.

I(c). *Effect of the geometry of the electrodes*

In this investigation three sets of platinum wire electrodes were used. The first set consisted of one wire of diameter 0.5 mm and length 2.0 cm and the other of diameter 0.15 mm and length 0.72 cm; the second set consisted of one wire of diameter 0.3 mm and length 1.0 cm and the other of diameter 0.15 mm and length 0.59 cm; the third set consisted of both the wires of diameter 0.15 mm and length 1.5 cm. It was found that the glow always appears at the thinner electrode, irrespective of its polarity as mentioned earlier. With the third set in which both electrodes are thin and have the same dimensions, the glow phenomenon was observed at both the electrodes simultaneously at higher current densities. If the regions *A* and *B* are preheated, the glows at both the electrodes appear at relatively lower current densities. Similar conclusions were obtained by arranging the electrodes in the end-on positions in a single beaker cell. However, at no time a complete break down of the electrolytic medium was observed.

In order to study the polarizing effects at the electrode surface, platinum wires, one of diameter 0.3mm and length 0.85cm and the other of diameter 0.3mm and length 1.58 cm were used as electrodes. These electrodes were

immersed in NaOH solution of 0.5M strength. Power input for the onset of a continuous glow was found to be about 108 watts when the electrodes were clean. After platinizing them the input power required was found to be increased to 300 watts.

II. *Spectroscopic studies*

Platinum and tungsten wires of diameter 0.5 mm and copper and aluminium rods of diameter 0.56 cm were used as electrodes in this investigation. The experimental procedure for the excitation of the glow was the same as described earlier in section I(a). The colour of the glow was found to be yellowish in NaOH solutions and reddish in CaCl_2 solutions. The glow at the cathode was more intense and characterized by sputtering and hissing. A vapour sheath was seen to surround the glowing electrode and at higher input voltages it exhibited a sort of vortex motion. The intensity of the glow at the anode was found to be weak as compared to that at the cathode. The region surrounding the anode was also found to be comparatively quiet.

Typical spectra of the anode and cathode glows are shown in figures 4a to 4g (plates 3A—3B and 4A—4B). Figure 4a shows the anode glow spectrum which occurs in the form of a continuum in the region $\lambda 4870\text{\AA}$ to $\lambda 3990\text{\AA}$ along with superimposed atomic lines of calcium. The spectrum was recorded on the medium quartz spectrograph. Iron arc spectrum as well as hydrogen discharge tube spectrum were also recorded for comparison and identification of the glow lines. No atomic hydrogen lines are seen in this glow spectrum.

The spectra of cathode glows, displayed in figures 4b and 4c, were recorded on a low dispersion, constant deviation glass prism spectrograph. In figure 4b, the central spectrum is due to a hydrogen discharge tube for comparison. While one of the spectrum is due to cathode glow at a platinum electrode in NaOH solution the other is in CaCl_2 solution. These two glow spectra clearly exhibit persistent atomic lines of the metal ions present in the electrolyte. A faint atomic line of the electrode is also visible in one spectrum. Again the atomic hydrogen lines are not seen in both the glow spectra. Figure 4c exhibits two cathode glow spectra in NaOH solution, one at an aluminium electrode and the other at a copper electrode. It is observed that along with prominent sodium lines, the atomic lines of the metal electrodes are visible and some impurity lines have also appeared.

The cathode glow spectra exhibited in figures 4d to 4g have been recorded on the medium quartz spectrograph. Figure 4d clearly exhibits the existence of the OH bands along with the atomic lines of sodium

and copper in the case of the cathode glow at a copper electrode in NaOH solution. In figure 4e are seen the NaH bands in the region $\lambda 3380\text{\AA}$ to $\lambda 4670\text{\AA}$ in addition to the OH bands. In figure 4f is seen the general luminescence intensity distribution in the form of a structureless broad band in the region $\lambda 3700\text{\AA}$ to $\lambda 4700\text{\AA}$ at a copper cathode in CaCl_2 solution, in addition to the OH bands. Figure 4g clearly exhibits OH bands in cathode glows in both, CaCl_2 and NaOH solutions along with prominent atomic lines.

III. Oscillographic studies

The development of the random pulses, during the glow phenomenon, as superimposed on the A.C. cycle, is shown in the oscillographic traces in figures 5a to 5e. The voltage scale for the C.R.O. screen used for these traces was 0.2 volts/cm. The A.C. input voltage for the electrolytic cell was adjusted, consecutively at 2, 10, 18, 38 and 40 volts for these traces; the electrode in these studies was a copper wire of diameter 1.5 mm. In figure 5f is seen the fully developed pulse pattern when a continuous glow was visible at a copper wire electrode of diameter 0.5 mm at 40 volts A.C. input. Figure 5g depicts a similar situation at a platinum wire electrode of diameter 0.3 mm at 45 volts A.C. input.

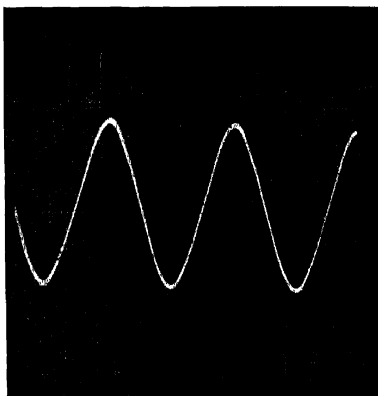


Figure 5a Oscillographic trace

DISCUSSION

The electrolytic process leading to a luminescent glow at a wire electrode in aqueous solution is best depicted by the curve shown in

figure 3. A similar curve has been previously obtained by Hickling & Ingram (1964) also. The region *AB* of the curve indicates conven-

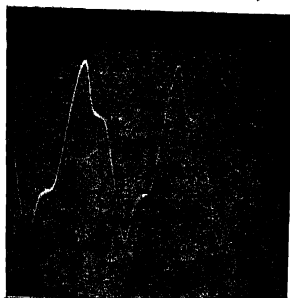


Figure 5b

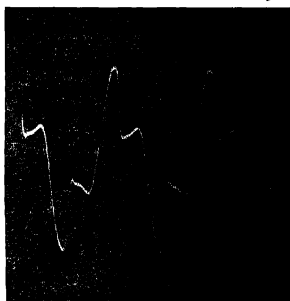
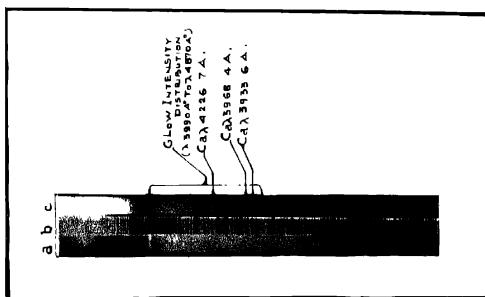


Figure 5c

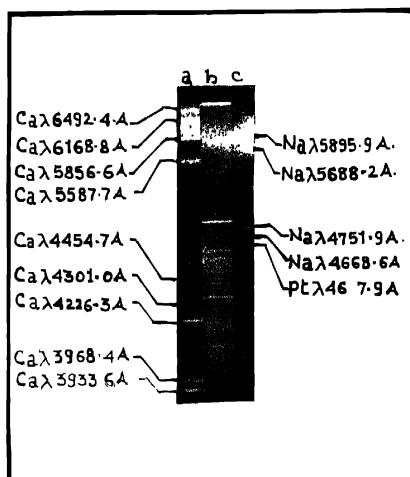
tional faradaic electrolysis. Due to the increase in the applied voltage the rate of gas evolution exceeds the rate of migration of the ions and the charge transfer processes at the electrodes are obstructed. At this stage, as mentioned earlier, the ammeter and the voltmeter pointer fluctuate within wide limits and then the current through the cell circuit falls, as indicated by the broken line *BC*. Further increase in the supply voltage results in the formation of a very thin and mobile vapour film around the thinner wire electrode. This film periodically collapses at some points, permitting the electrolyte to touch the electrode



Anode glow
 Solution : CaCl_2
 Anode : Platinum.

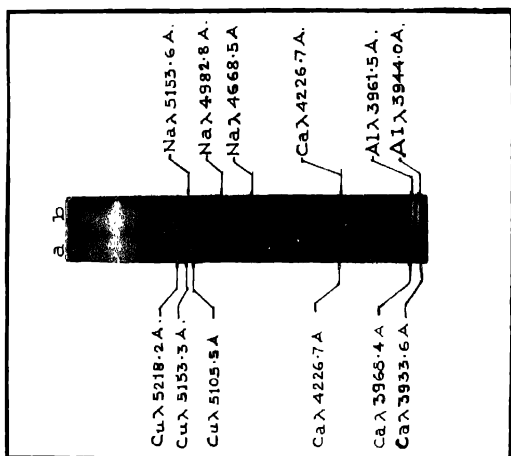
a :- Hydrogen spectra
 b :- Iron spectra
 c :- CaCl_2 Sol. spectra

Figure. 4a



Solution: CaCl_2 (b) Hydrogen
 (a) Cathode Tube spectra
 Platinum (c) Cathode :
 Platinum

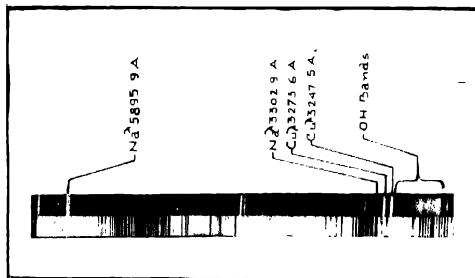
Figure. 4b



Solution :- NaOH

Cathode: - (a) Copper
(b) Aluminium

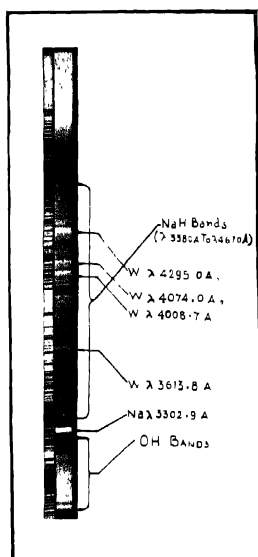
Figure. 4c



Solution:- NaOH

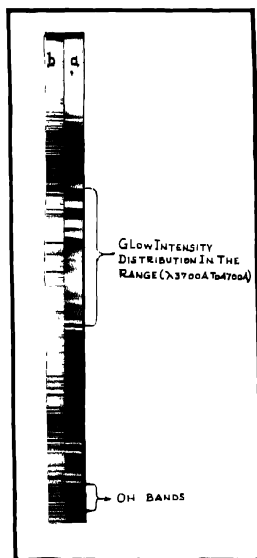
Cathode : Copper rod.

Figure. 4d



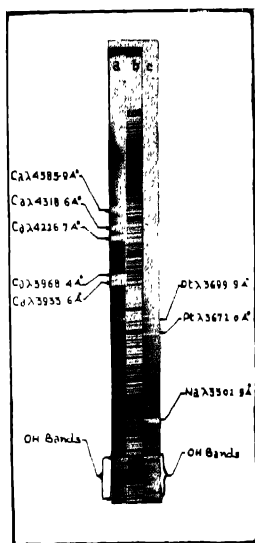
Solution: NaOH Cathode, Tungsten

Figure. 4e



a. Solution: CaCl_2 Cathode, Copper
b: Iron Arc

Figure. 4f



a. Solution : CaCl_2

Cathode : Platinum

b. Iron Arc

c. Solution : NaOH

Cathode : Platinum

Figure 4g

surface at those points. This results in a surge of current which produces local heating at the electrode surface and also visible spark-over. The local



Figure 5d

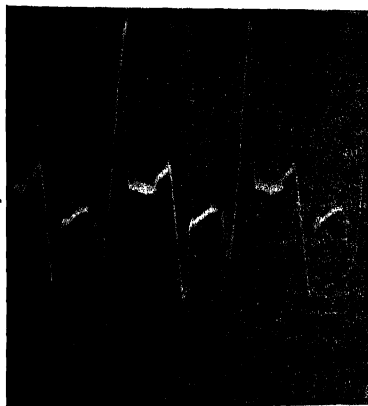


Figure 5e

heating process then forces out a vapour jet and the neighbouring liquid molecules rush there to take its place. The corresponding voltage-current

relation, representing this situation, is depicted by the region OD of the curve. At the point D the violent gas evolution ceases. The voltage-current

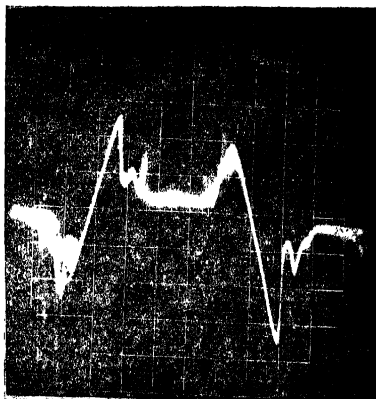


Figure 5f

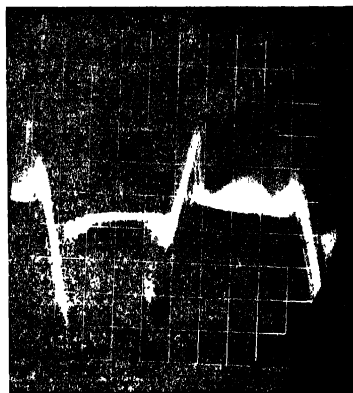


Figure 6g

readings are then stabilized. This situation is indicative of the formation of a stable superheated insulating layer around the electrode. It is at this stage that a continuous glow at the electrode appears. As the supply voltage is still further increased, the intensity of the glow increases monotonously with the current. The discharge of accumulated ions through the insulating layer, resulting into a visible glow, can be pictured as corona discharge.

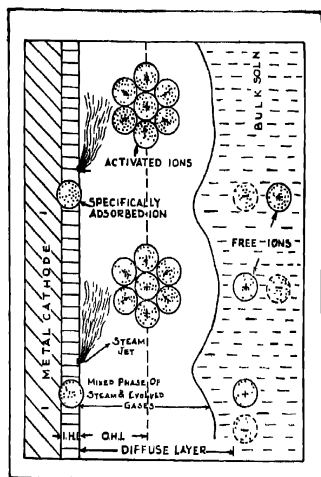


Figure 6. Qualitative model for the insulating thermal layer formed under glow conditions.

It is thus quite obvious that the superheated insulating layer around the electrode is the governing factor responsible for the glow. It is interesting to mention here that such insulating layers have been visualized in some other branches of physics and chemistry also. This layer seems to be of particular importance in the electro-hydro-dynamic (EHD) techniques (Markels & Durfee 1968). Recently one of us (Edkie 1969) has discussed the heat transfer mechanism under the influence of applied electric fields, using the concept of such an insulating thermal layer. Mohilner (1966) has shown that electric double layer has an important role in the kinetics of the faradaic and non-faradaic processes simultaneously taking place at a charge transfer electrode. A qualitative sketch of the situation existing near the electrode in the

present experimental conditions is given in figure 6. This figure is more or less similar to the double layer picture given by Mohilner. The inner Helmholtz layer (I.H.L.), surrounding the electrode is made of a stagnant, superheated, thin layer of water molecules. The outer Helmholtz layer (O.H.L.) consists of a mixed phase of electrolytically evolved gases and steam. This layer is followed by a diffused layer consisting of excited atoms, ions and radicals. In what follows, it is shown that the results obtained in the present investigations can very well be explained with the help of figure 6.

The dimensions of the insulating layer surrounding a short and thin electrode would obviously be very small as compared to the layer surrounding a thicker electrode. When the layer is thin, the input power required for the production of the glow is small because of the ease with which the required charge across the insulating layer builds up and the discharge takes place. The effect of platinizing the electrode is to increase the effective surface area of the electrode and the corresponding input power for the production of the glow is therefore larger. If the temperature of the electrolyte is elevated, the charge build up process is further accelerated and the discharge takes place with greater ease.

The anode glow spectrum, shown in figure 4a, exhibits a continuum along with few atomic lines of the alkali metal ions present in the electrolyte but does not show the atomic lines of the anode material nor any band structure because the heat in the anode layer is primarily dissipated towards the solution side and hence the anode material and other electro-active species, surrounding the anode, are not sufficiently excited. In figures 4b to 4g the cathode glow spectra exhibit the atomic lines of the cathode material because the heat in the cathode layer is primarily dissipated on the cathode itself. The absence of atomic hydrogen lines in all the spectra shows that free hydrogen atoms do not exist in the insulating layer. This may be due to the large interaction between the hydrogen ions and the water molecules. The hydrogen atoms are probably adsorbed on the electrode surface by means of valency bonds as pointed out by Potter (1961). Since steam is invariably present in the cathode layer, the OH bands are seen in the cathode glow spectra of both NaOH and CaCl_2 solutions. Under favourable conditions, some hydride bands, as in figures 4e and 4g, and some structureless broad bands, as in figure 4f, are seen. These bands show that radical recombination processes are taking place within the insulating layer. This work thus supports the radical recombination reactions suggested by Chandross *et al* (1964, 1965). Palit

(1968) has also recently envisaged from magnetic studies of the glow the formation of ion radicals in the glow process.

The development of deformities in the A.C. wave form in figures 5a to 5c, can be attributed to the building-up of the insulating layer around the wire electrode. The layer build up process develops a sort of back e.m.f. in the cell circuit and consequently the voltage across the standard low resistance (R in figure 2) decreases. The random pulses, superimposed on the deformed A.C. wave form, shown in figures 5d and 5e represent the corona discharges of the accumulated charge through the ruptured insulating layer. Similar situation, shown in figures 5f and 5g, is also exhibited by two other wire electrodes of different materials.

CONCLUSION

Although the present study has thrown some light on the mechanism of the electrode glow, this study is by no means complete. It will be worth while to undertake theoretical as well as rigorous experimental investigations of this phenomenon which may reveal the structure of the thermal boundary layers which are encountered in many heat transfer processes. It is likely that such studies may lead to useful applications in industry and technology.

The authors wish to thank sincerely Shri P. G. Valunjkar and Smt. J.P. Hirde of the Govt. Science College, Nagpur for their help during the progress of this work.

REFERENCES

- Chandross, E. A., & Visco, R. E. 1964 *J. Am. Chem. Soc.* **86**, 5350.
Chandross, E. A., Longworth, J. W., & Visco, R. E. 1965 *J. Am. Chem. Soc.* **87**, 3259.
Eddie, R. G. 1969 *Ind. J. Pure and Appl. Phys.* **7**, 67.
Hickling, A., & Ingram, M. D. 1964 *Trans. Faraday Soc.* **60**, 783.
1964 *J. Electroanal. Chem.* **8**, 65.
Ivey, H. F. 1963 *Electroluminescence and related effects*, Academic Press, N. Y.
Kellogg. 1950 *J. Electrochem. Soc.* **97**, 133.
Kuwana, T. 1966 *Electroanalytical Chemistry*, Ed. Bard, A. J., Vol. I
Marcel—Dekker Inc., N. Y.
Mande, C. & Eddie, R. G. 1968 *Indian J. Phys.*, **42**, 271.
Markels, Michael Jr. & Durfee, Robert L. 1968 *Chem. Engr. Prog. Symposium Series*,
'Heat transfer Seattle', **64**, 67.
Mohliner, D. M. 1966 *Electroanalytical Chemistry*, Vol I., Ed. Bard, A., J. Marcel—Dekker
Inc., N. Y.
Palit, S. R. 1967 *Indian J. Phys.* **41**, 622.
1968 *Indian J. Phys.*, **42**, 414.
Potter, E. C. 1961 *Electrochemistry*, Cleaver-Hume Press Ltd., London.

On a non-homogeneous cylindrically aelotropic, magnetostrictive
rotating long cylinder

By B. CHAUDHURI

Department of Mathematics, Jadavpur University, Calcutta (India)

(Received March 31, 1969)

This article presents an analytic solution of the stresses and displacements in a long rotating cylinder of nonhomogeneous cylindrically aelotropic, magnetostrictive material of variable density.

1. INTRODUCTION

The constitutive relations of a continuous, isotropic, magnetostrictive medium have been established by Lewis (1962) from the standpoint of the theory of classical mechanics of continuous media. Thus it has been made possible to study the interaction of elastic field with magnetic field, when magnetic fields (small) are accommodated in classical problems of elasticity. The elastic problems on magnetostrictive material have been discussed in the recent papers of Sinha (1962, 1967) and of Giri (1963). In our present paper, the problem of an elastically non-homogeneous, cylindrically aelotropic, magnetostrictive, uniformly rotating, long thickwalled-hollow circular cylinder of variable density, where the elastic and the magnetostrictive constants vary radially according to power law, has been investigated. The cylindrical coordinates (r, θ, z) are used such that the z -axis coincides with the axis of the cylinder. The constitutive relations (Lewis 1952) have been modified in the present case. The problem is reduced to the solution of a second order differential equation in radial displacement.

2. PROBLEM, FUNDAMENTAL EQUATIONS AND BOUNDARY CONDITIONS

Let r_0 and r_a be the inner and outer radii respectively of the hollow thick cylinder of cylindrically aelotropic, magnetostrictive material, rotating uniformly with angular velocity Ω about its axis. The cylindrical bounding surfaces are supposed to be free from radial stress. The subsequent analysis is done under the plane strain condition. In addition to these mechanical conditions, we introduce a circumferential magnetic field produced by a constant longitudinal current density J_0 . Our object is to obtain the stresses and displacements, resulting from the interaction of mechanical and magnetic fields within the cylinder.

Evidently, the equilibrium of motion and the relation between the strain components and displacements do not depend on the type of material and as such they remain the same as in the case of isotropy. Thus for

the axially symmetric, uniformly rotating long cylinder of the material under consideration, the radial displacement u is a function of r only, the tangential displacement v is zero and the longitudinal displacement $w = e_0 z$ where e_0 is the constant extension in the axial direction. Now we take recourse to the solution of the usual stress equations of equilibrium utilising the constitutive relations.

The expressions for the strain-components are (Sokolnikoff 1956), in view of plane strain condition and symmetric displacements,

$$\left. \begin{aligned} S_{rr} &= \frac{du}{dr}, S_{\theta\theta} = \frac{u}{r}, S_{zz} = e_0 \\ S_{\theta z} &= 0, S_{zr} = 0, S_{r\theta} = 0 \end{aligned} \right\} \quad (1)$$

where S_{rr} , $S_{\theta\theta}$ and S_{zz} are respectively strain components in radial, tangential and longitudinal directions, $S_{\theta z}$, S_{zr} and $S_{r\theta}$ are the shearing strain components.

The constitutive relations, in cylindrical coordinates, as suggested by Lewis (1962) have been modified, in the present case, into

$$\left. \begin{aligned} \sigma_{rr} &= C_{11} S_{rr} + C_{12} S_{\theta\theta} + C_{13} S_{zz} + a_{11} H_r^2 + a_{12} H_\theta^2 + a_{13} H_z^2 \\ \sigma_{\theta\theta} &= C_{21} S_{rr} + C_{22} S_{\theta\theta} + C_{23} S_{zz} + a_{21} H_r^2 + a_{22} H_\theta^2 + a_{23} H_z^2 \\ \sigma_{zz} &= C_{31} S_{rr} + C_{32} S_{\theta\theta} + C_{33} S_{zz} + a_{31} H_r^2 + a_{32} H_\theta^2 + a_{33} H_z^2 \\ \sigma_{\theta z} &= C_{44} S_{\theta z} + a_{44} H_\theta H_z \\ \sigma_{zr} &= C_{55} S_{zr} + a_{55} H_z H_r \\ \sigma_{r\theta} &= C_{66} S_{r\theta} + a_{66} H_r H_\theta \end{aligned} \right\} \quad \dots (2)$$

where $C_{ij} = C_{ji}$, ($i, j=1, 2, 3$) and σ_{rr} , $\sigma_{\theta\theta}$ and σ_{zz} are radial, tangential and longitudinal stresses respectively, $\sigma_{\theta z}$, σ_{zr} and $\sigma_{r\theta}$ are the shearing stresses and C_{ij} are elastic constants. H_r , H_θ , H_z are the magnetic field components in cylindrical coordinates and a_{ij} ($i, j=1, 2, 3, 4, 5, 6$) are the magnetostrictive constants.

Now according to our previous assumption the coefficients C_{ij} and a_{ij} in (2) are taken as functions of r and let

$$\left. \begin{aligned} C_{ij} &= \mu_{ij} r^n, \\ a_{ij} &= \lambda_{ij} r^n, (\mu_{ij}, \lambda_{ij}, n \text{ are constants}). \end{aligned} \right\} \quad \dots (3)$$

Since the magnetic field originates from a longitudinal current of density J_0 , we have

$$H_r = H_z = 0; H_\theta(r) = \frac{J_0 r}{2} \quad \dots (4)$$

From the relations (1) - (4), we have

$$\left. \begin{aligned} \sigma_{rr} &= r^n \left(\mu_{11} \frac{du}{dr} + \mu_{12} \frac{u}{r} + \mu_{13} e_0 \right) + r^n \lambda_{12} \frac{J_0^2 r^2}{4} \\ \sigma_{\theta\theta} &= r^n \left(\mu_{21} \frac{du}{dr} + \mu_{22} \frac{u}{r} + \mu_{23} e_0 \right) + r^n \lambda_{22} \frac{J_0^2 r^2}{4} \\ \sigma_{zz} &= r^n \left(\mu_{31} \frac{du}{dr} + \mu_{32} \frac{u}{r} + \mu_{33} e_0 \right) + r^n \lambda_{32} \frac{J_0^2 r^2}{4} \\ \sigma_{\theta z} &= 0 \\ \sigma_{zr} &= 0 = \sigma_{r\theta} \end{aligned} \right\} \quad \dots (5)$$

where

$$\mu_{ij} = \mu_{ji}, \quad (i, j = 1, 2, 3).$$

The equilibrium equations in cylindrical coordinates are (Sokolnikoff 1956),

$$\left. \begin{aligned} \frac{\partial \sigma_{rr}}{\partial r} + \frac{1}{r} \frac{\partial \sigma_{r\theta}}{\partial \theta} + \frac{\partial \sigma_{rz}}{\partial z} + \frac{\sigma_{rr} - \sigma_{\theta\theta}}{r} + F_r &= 0 \\ \frac{\partial \sigma_{r\theta}}{\partial r} + \frac{1}{r} \frac{\partial \sigma_{\theta\theta}}{\partial \theta} + \frac{\partial \sigma_{\theta z}}{\partial z} + \frac{2\sigma_{r\theta}}{r} + F_\theta &= 0 \\ \frac{\partial \sigma_{rz}}{\partial r} + \frac{1}{r} \frac{\partial \sigma_{\theta z}}{\partial \theta} + \frac{\partial \sigma_{zz}}{\partial z} + \frac{\sigma_{rz}}{r} + F_z &= 0 \end{aligned} \right\} \quad \dots (6)$$

where F_r , F_θ and F_z are the radial, tangential and longitudinal components of the body force F per unit volume respectively.

In the case of uniformly rotating cylinder the only body force is the centrifugal force in the radial direction and this is evidently $\rho \Omega^2 r$ where ρ is the density of the material and Ω the angular velocity of the cylinder in radians per second. But conforming to our assumption ρ is taken as

$$\rho = \rho_0 \left(\frac{r}{r_0} \right)^2 \quad \text{where } \rho_0 \text{ is the density at } r = r_0.$$

The first equation of (6) reduces to

$$\frac{d\sigma_{rr}}{dr} + \frac{\sigma_{rr} - \sigma_{\theta\theta}}{r} + \rho_0 \left(\frac{r}{r_0} \right)^2 \Omega^2 r = 0 \quad \dots (7)$$

The last two equilibrium equations are identically satisfied.

Eliminating σ_{rr} and $\sigma_{\theta\theta}$ from (5) and (7), the differential equation in radial displacement is obtained as

$$r^2 \frac{d^2 u}{dr^2} + (n+1)r \frac{du}{dr} + \partial r = \phi e_0 r - \psi J_0^2 r^3 - \beta r^{3-n}, \quad \dots (8)$$

where

$$\begin{aligned}\vartheta &= \frac{n\mu_{12}-\mu_{22}}{\mu_{11}} \\ \phi &= \frac{\mu_{22}-(n+1)\mu_{12}}{\mu_{11}} \\ \psi &= \frac{(n+2)\lambda_{12}+(\lambda_{12}-\lambda_{22})}{4\mu_{11}} \\ \beta &= \frac{\rho_0\Omega^2}{\mu_{11}r_0^2}\end{aligned}$$

The boundary conditions are $(\sigma_{rr})_{r=r_0} = (\sigma_{rr})_{r=r_s} = 0$

and
$$\int_{r_0}^{r_s} \sigma_{zz} r dr = 0.$$

3. SOLUTION OF THE PROBLEM

Solving (8), we find

$$u = Ar^{\alpha_1} + Br^{\alpha_2} + \alpha_3 e_0 r - \alpha_4 J_0^2 r^3 + \alpha_5 r^{\delta-n}. \quad \dots(9)$$

where

$$\alpha_1 = \frac{-n + \sqrt{n^2 - 4\delta}}{2}.$$

$$\alpha_2 = \frac{-n - \sqrt{n^2 - 4\delta}}{2}.$$

$$\alpha_3 = \frac{\phi}{(n+\delta+1)}.$$

$$\alpha_4 = \frac{\psi}{(3n+\delta+9)}.$$

$$\alpha_5 = \frac{\beta}{(5n-\delta-25)}.$$

and A, B are constants of integration to be determined from the boundary conditions stated earlier.

The stress components in (5) thereby become

$$\begin{aligned}\sigma_{rr} &= AA_1 r^{n+\alpha_1-1} + BB_1 r^{n+\alpha_2-1} + C_1 e_0 r^n - D_1 r^{n+2} + E_1 r^4 + r^n \lambda_{12} H_0^2(r), \\ \sigma_{\theta\theta} &= AA_2 r^{n+\alpha_1-1} + BB_2 r^{n+\alpha_2-1} + C_2 e_0 r^n - D_2 r^{n+2} + E_2 r^4 + r^n \lambda_{22} H_0^2(r), \\ \sigma_{zz} &= AA_3 r^{n+\alpha_1-1} + BB_3 r^{n+\alpha_2-1} + C_3 e_0 r^n - D_3 r^{n+2} + E_3 r^4 + r^n \lambda_{32} H_0^2(r), \\ &\dots(10)\end{aligned}$$

where

$$\begin{aligned} A_i &= \alpha_1 \mu_{i1} + \mu_{i2} \\ B_i &= \alpha_2 \mu_{i1} + \mu_{i2} \\ C_i &= \alpha_3 (\mu_{i1} + \mu_{i2}) + \mu_{i3} \\ D_i &= (3\mu_{i1} + \mu_{i2}) J_0^2 \alpha_4 \\ E_i &= \{ (5-n) \mu_{i1} + \mu_{i2} \} \alpha_5 \\ (i &= 1, 2, 3) \end{aligned}$$

From the boundary condition

$$(\sigma_{rr})_{r=r_0} = (\sigma_{rr})_{r=r_a} = 0,$$

we have

$$\begin{aligned} A A_1 r_0^{n+\alpha_1-1} + B B_1 r_0^{n+\alpha_2-1} + C_1 e_0 r_0^n - D_1 r_0^{n+2} + E_1 r_0^4 + \lambda_{12} r_0^n H_2(r_0) &= 0 \\ A A_1 r_a^{n+\alpha_1-1} + B B_1 r_a^{n+\alpha_2-1} + C_1 e_0 r_a^n - D_1 r_a^{n+2} + E_1 r_a^4 &+ \lambda_{12} r_a^n H_2(r_a) = 0 \end{aligned} \quad \dots (11)$$

Now from (11) we have

$$\begin{aligned} A &= \frac{C_1 e_0 \left| \frac{r_a^{n+\alpha_1-1} r_a^n}{r_0^{n+\alpha_2-1} r_0^n} \right| - D_1 \left| \frac{r_a^{n+\alpha_2-1} r_a^{n+2}}{r_0^{n+\alpha_1-1} r_0^{n+2}} \right| + E_1 \left| \frac{r_a^{n+\alpha_2-1} r_a^4}{r_0^{n+\alpha_1-1} r_0^4} \right| + \lambda_{12} \left| \frac{r_a^{n+\alpha_2-1} r_a^n H_2(r_a)}{r_0^{n+\alpha_1-1} r_0^n H_2(r_0)} \right|}{A_1 \left| \frac{r_a^{n+\alpha_2-1} r_a^{n+\alpha_2-1}}{r_0^{n+\alpha_2-1} r_0^{n+\alpha_2-1}} \right|} \\ B &= \frac{C_1 e_0 \left| \frac{r_a^{n+\alpha_1-1} r_a^n}{r_0^{n+\alpha_1-1} r_0^n} \right| - D_1 \left| \frac{r_a^{n+\alpha_1-1} r_a^{n+2}}{r_0^{n+\alpha_1-2} r_0^{n+1}} \right| + E_1 \left| \frac{r_a^{n+\alpha_1-1} r_a^4}{r_0^{n+\alpha_1-1} r_0^4} \right| + \lambda_{12} \left| \frac{r_a^{n+\alpha_1-1} r_a^n H_2(r_a)}{r_0^{n+\alpha_1-1} r_0^n H_2(r_0)} \right|}{B_1 \left| \frac{r_a^{n+\alpha_1-1}}{r_0^{n+\alpha_1-1}} \right| \left| \frac{r_a^{n+\alpha_2-1}}{r_0^{n+\alpha_2-1}} \right|} \end{aligned}$$

As in the case of isotropy, the traction σ_{zz} at the ends of the cylinder cannot be made to vanish, but can be so adjusted that they have no static resultant.

$$\text{thus } \int_{r_0}^{r_a} \sigma_{zz} r dr = 0$$

From the last equation of (10), we have therefore,

$$\begin{aligned} & \frac{AA_3 \left(r_a^{n+\alpha_1+1} - r_o^{n+\alpha_1+1} \right)}{(n+\alpha_1+1)} + \frac{BB_3 \left(r_a^{n+\alpha_1+1} - r_o^{n+\alpha_1+1} \right)}{(n+\alpha_2+1)} \\ & + \frac{C_3 e_0 \left(r_a^{n+2} - r_o^{n+2} \right)}{(n+2)} - \frac{D_3 \left(r_a^{n+4} - r_o^{n+4} \right)}{(n+4)} \\ & + \frac{E_3 \left(r_a^6 - r_o^6 \right)}{6} + \frac{\lambda_{32} J_0^2 \left(r_a^{n+4} - r_o^{n+4} \right)}{4(n+4)} = 0. \dots(12) \end{aligned}$$

From (12) the axial extension e_0 can be determined with the help of the values of A and B . Now A and B completely determined. Thus the radial stress σ_r , can be determined.

The hoop-stresses at the inner and the outer surfaces are determined from the second relation of (10) on substituting r_o and r_a respectively for r . The longitudinal or axial stress σ_{zz} and the radial displacement u are given by the last equation of (10) and (9) respectively. And when e_0 is known, the longitudinal displacement w is known.

If now the longitudinal displacement is taken to be zero (as in the case when the ends of the cylinder are placed between two fixed planes), $e_0=0$ and the results for this case are obtained from the corresponding equations already deduced.

The the total axial pull across a normal section of the cylinder is

$$\begin{aligned} 2\pi \int_{r_o}^{r_a} \sigma_{zz} r dr &= 2\pi \left[\frac{AA_3}{(n+\alpha_1+1)} \left(r_a^{n+\alpha_1+1} - r_o^{n+\alpha_1+1} \right) \right. \\ &+ \frac{BB_3}{(n+\alpha_2+1)} \left(r_a^{n+\alpha_1+1} - r_o^{n+\alpha_1+1} \right) - \frac{D_3}{n+4} \left(r_a^{n+4} - r_o^{n+4} \right) \\ &\left. + \frac{E_3}{6} \left(r_a^6 - r_o^6 \right) + \frac{\lambda_{32} J_0^2}{4(n+4)} \left(r_a^{n+4} - r_o^{n+4} \right) \right] \dots(13) \end{aligned}$$

Therefore the mean axial stress P is

$$2 \left[\frac{AA_3}{(n+\alpha_1+1)} \left(\frac{r_a^{n+\alpha_1+1} - r_o^{n+\alpha_1+1}}{r_a^2 - r_o^2} \right) + \frac{BB_3}{(n+\alpha_2+1)} \left(\frac{r_a^{n+\alpha_2+1} - r_o^{n+\alpha_2+1}}{r_a^2 - r_o^2} \right) - \frac{D_3}{n+4} \left(\frac{r_a^{n+4} - r_o^{n+4}}{r_a^2 - r_o^2} \right) + \frac{E_3}{6} \left(r_a^4 + r_a^2 r_o^2 + r_o^4 \right) + \frac{\lambda_{33} J_o^2}{4(n+4)} \left(\frac{r_a^{n+4} - r_o^{n+4}}{r_a^2 - r_o^2} \right) \right] \quad \dots(14)$$

The above non-zero axial force must be nullified so that the longitudinal strain S_z may be zero as required under the hypothesis in this case. Thus a uniform axial compression given by (14) is to be superposed. Clearly this will not affect the radial stress σ_r , and the tangential stress σ_θ . But then the longitudinal stress becomes

$$AA_3 \left[r^{n+\alpha_1-1} - \frac{2}{(n+\alpha_1+1)} \cdot \frac{(r_a^{n+\alpha_1+1} - r_o^{n+\alpha_1+1})}{(r_a^2 - r_o^2)} \right] + BB_3 \left[r^{n+\alpha_2+1} - \frac{2}{(n+\alpha_2+1)} \cdot \frac{(r_a^{n+\alpha_2+1} - r_o^{n+\alpha_2+1})}{(r_a^2 - r_o^2)} \right] - D_3 \left[r^{n+2} - \frac{2}{n+4} \cdot \frac{(r_a^{n+4} - r_o^{n+4})}{(r_a^2 - r_o^2)} \right] + E_3 \left[r^4 - \frac{1}{3} (r_a^4 + r_a^2 r_o^2 + r_o^4) \right] + \frac{\lambda_{33} J_o^2}{4} \left[r^{n+2} - \frac{2}{(n+4)} \cdot \frac{(r_a^{n+4} - r_o^{n+4})}{(r_a^2 - r_o^2)} \right]$$

For homogeneity, $n=0$ and in the absence of magnetic field, the results agree with some standard results in purely elastic case.

I am grateful to Dr. R. R. Giri of the Department of Mathematics, Jadavpur University, Calcutta-32, for his active guidance.

REFERENCES

- Lewis, J. A. 1962, *The small-field theory of the Joule and Wiedemann*; *Quart. Appl. Math.*, 20, Nos. 1, 13.
- Sinha, D. K. 1962, *Ind. Jour. Theor. Phys.*, 10 Nos. 2 & 3, 61.
- 1967, *Rev. Roum. Sci. Techn.—Mech. Appl.*, 12, No. 2, 457, Bucarest.
- Giri, R. R. 1963, *Appl. Phys. Quart.* 8, No. 4.
- Sokolnikoff, I. S. 1956, *Mathematical Theory of Elasticity*, 2nd Ed. McGraw Hill, Inc., 183.
- Chaudhuri, B. *Gerl. Bei. Zur. Geophysik* (in the press).

Zone refining of silver iodide

By IQBAL SINGH

Defence Research Laboratory (Materials), Kanpur-4, India.

(Received March 17, 1963)

Zone refining of silver iodide has been tried under vacuum, iodine and hydriodic acid vapours. It was successful only when silver iodide precipitate was kept under hydriodic acid vapours at 150°C for considerable time. Pinholing with hydriodic acid vapours was found suitable. It was observed that Fe, Mg, Cu, Si and Al all have distribution coefficient $K < 1$. Fe was detected in the forward as well as in the rear end (both in ferric and ferrous states) of the zone refined ingot, though its concentration in the forward end was comparatively much less, thus for Fe, the K value can be taken to be close to unity, may be slightly less than unity.

INTRODUCTION

Silver chloride, bromide and iodide as such and their mixed crystals have been extensively used as photographic materials. Moser *et al* (1959) reported that one part in 10^8 of cuprous ion in silver chloride produced a readily detectable change in photolytic behaviour. Burnham *et al* (1960) studied the Hall mobility and ionic conductance of silver halides and reported that these were considerably affected by impurities. Nail *et al* (1957) prepared single crystals of silver halides. Large crystals of silver iodide have not been grown successfully apparently because of the phase transition at 146°C from the high temperature body centred cubic form to the low temperature hexagonal form. Cohen & Dobbenburgh (1928) observed that during this phase change the density of silver iodide decreased remarkably i. e. from 6.009 to 5.865. The cooling crystal thus develops strains cracks. Silver iodide is known to exist in at least six polymorphic modifications. Below 146° and at atmospheric pressure it either exists in cubic sphalerite type α -structure or hexagonal wurtzite β -structure, depending upon the details of the crystallisation process. The crystal structure of silver iodide also changes with pressure. It is also much less sensitive to light and much less transparent in the infra-red than other silver halides. Its high melting point (558.5°C) and low dissociation temperature (522°C) are probable reasons for which much work has not been done on silver iodide crystals. Recently, some heat transfer properties have been studied. Cochrane (1967) has successfully grown single crystals of silver iodide from solution to avoid phase transition. For the present work, zone refining of silver iodide has been carried out as the first step for crystal growing.

EXPERIMENTAL

The experimental operations fall into three parts : (A) preparation of silver iodide precipitate, (B) pinholing of molten silver iodide through a fine glass capillary, (C) zone refining.

A. Preparation of the precipitate

Analytical grade, (Analar) silver nitrate and potassium iodide were taken as starting materials. They were dissolved in double distilled water and recrystallised and then dried. All operations were carried out in a dark room with red light. Silver iodide, being the least soluble in water of all the silver halides, has a strong tendency to occultate impurities which are much more difficult to remove from it than other silver halides. The precipitation of silver iodide was done by slowly adding 0.1 M silver nitrate solution with stirring, to an equally dilute ammoniacal solution of potassium iodide until precipitation was complete, then adding nitric acid 1% by volume to prevent peptization. Very fine precipitate, light yellow in colour was formed. It was kept overnight to settle down and the water at the top was decanted the next day.

The precipitate settled at the bottom of the vessel was mixed with water containing 1% nitric acid by volume and kept overnight. The water at the top was again decanted. The precipitate was washed for five times in the same way. Finally the precipitate was filtered through filter paper (Whatman No.42) and washed with plain double distilled water. Water was sparingly used in the final washing as silver iodide has strong tendency to peptize. It was observed that a little part of the precipitate had gone in the colloidal form and passed through the filter paper. Light yellow precipitate in fine powder form was obtained. It was kept in a clean, dry glass dish, covered with black paper and put in an oven maintained at 70°C for drying,

B. Pinholing of molten silver halide

Melting the precipitate and then filtering the molten iodide through a fine glass capillary under some protective atmosphere and passing iodine or hydrogen iodide gas through the material has been termed as pinholing. This practice was first employed by Clark & Mitchell (1956) and later by Gunding (1960) and other workers, mainly for removing scum and water vapour. In recent years, it has become clear that silver halide crystals containing traces of silver oxide have different properties than the purest material. Stasiw & Teltow (1948) established that molten silver halides containing traces of silver oxide have strong tendency to wet glass surface. While cooling, the glass contracts but silver iodide expands, as a result the glass container invariably breaks. The pinholing

serves dual purpose, it disposes of some impurities from the melt in the form of scum, as well as renders the halide workable using glass vessels.

The procedure adopted for pinholing differed slightly from that of Clark & Mitchell (1956). Dry precipitate of silver iodide was introduced through the open end of a 10 cm long pyrex glass tube having 3 cm diameter, the other end of which was connected to a small piece of pyrex glass capillary having 0.5mm diameter. The end of the capillary was connected to another pyrex glass tube of 2.5 cm diameter and about 30 cm in length. The open end through which the precipitate was introduced inside was then sealed. The apparatus was coupled to a two stage vacuum pump. The precipitate was thoroughly outgassed and all volatile impurities and water vapour were removed. When a pressure of the order of 10^3 mm of Hg was obtained, the pinholing apparatus was filled with hydriodic acid vapour at reduced pressure and sealed. The acid vapour was introduced through a glass 'T' which had one stopcock on each side and was connected to vacuum pump, pinholing apparatus and a small glass tube containing the acid. The whole apparatus was put through coaxially in two nichrome wire heaters, fixed on some insulating sheet and kept in a vertical position. One heater covered the the upper tube while the lower tube was inside the another heater. The temperature of the upper tube containing the silver iodide precipitate was raised to 150°C and maintained for four hours. Warren (1965) adopted similar technique while zone refining alkali halides. Different workers have passed different gases such as nitrogen, helium, halogen acid vapour, or halogen through the molten silver or alkali halides during pinholing. It was observed that with silver iodide, pinholing under vacuum or iodine was not satisfactory. The apparatus broke every time during cooling. Pinholing under hydriodic acid vapour had also failed when the precipitate was melted directly. This was obviously because hydriodic acid vapour dissociated into hydrogen and iodine above 180°C .

By pointing the tip of a gas burner on the capillary, a little portion of the precipitate was melted and as soon as it flowed and entered the capillary, the flame was withdrawn. The capillary was choked. The temperature of the upper tube was then raised to about 580°C and the whole precipitate was melted. The temperature near the capillary being less, the molten halide therefore, could not flow. The halide was kept in the molten state for about 1 hour, so that all the scum could rise to the top of the molten halide. Temperature near the capillary was raised

and the molten halide was allowed to trickle down drop by drop. When some molten material came down in the lower tube, further trickling stopped, as the pressure in upper and lower tubes, became equal. The lower tube was then heated by means of the lower heater and some of the acid vapour was allowed to bubble through the molten halide. Trickling again started for a while and then stopped. By repeated heating of the lower tube, the molten halide was completely transferred to the lower tube. The scum which consisted of carbonaceous matter, hydrated silica, some unreacted silver oxide and other miscellaneous products was left behind in the upper tube. The apparatus was sealed from the lower end of the capillary. The upper tube and the capillary were discarded. The lower glass tube was employed as the container for zone refining. The pinholed silver halide when solidified was light yellow in colour and was not transparent.

C. Zone refining

Zone refining was carried out by Pfann (1952) for the first time. The subject has been extensively reviewed, by Pfann (1958) himself and Lark-Horovitz & Johnson (1959). The zone refining apparatus for silver iodide consisted of six nichrome wire heaters, made of 18 SWG wire. Each heater had twelve number of turns. They were connected in series and in a straight line and fixed on a 1.25cm thick insulating board. Each heater was provided with some insulation. Width of each heater was 1.5 cm and these were 5.5 cm apart. The glass tube containing the ingot was passed through these heaters and coupled with a slow moving device. Heaters were kept stationary while the glass container moved. The rear end (where the zones left the ingot) of the glass container was at 4–6° higher level. This type of arrangement has been employed by Moser & Burnham (1961) to avoid matter transport first observed by Pfann (1953). First ten passes were made at 3cm per hour, then the speed was reduced to 1cm per hour. Molten zones about 1.5cm in width were formed. In all 40 zone passes were made.

When zone refining was complete it was observed that colour of the silver iodide ingot varied gradually from one end to the other. This was because of the impurity gradient. The rear end of the ingot was dull yellow. The forward end was somewhat brighter yellow. The glass container was broken and the ingot readily came out, as it did not stick to glass. Silver iodide ingot was granular in nature, it could be easily broken and crushed between fingers. A little portion from each end of the zone refined ingot was taken and subjected to spectrochemical analysis.

DISCUSSION

Fe, Mg, Cu, Si and Al were all found segregated in the rear end of the ingot. The forward end was found to contain Fe, but its concentration was much less than in the rear end. No other impurities were detected in the forward end. This can happen if the distribution coefficient K for Fe is slightly less than unity. Moser *et al* (1961) who studied distribution of specific impurities by adding several ppm of the element to the starting charge of silver chloride and bromide and made 70 passes, found $K > 1$ for Mn, Cd and Ni, and $K < 1$ for Pb but no such impurities were detected in our silver iodide ingot. They also observed $K < 1$ for Cu and Fe which agreed with above observation. Under chlorine atmosphere, they reported $K < 1$, and under vacuum $K > 1$ for Fe in silver chloride. They attributed the reason to Fe being in ferric state in chlorine atmosphere and in ferrous state under vacuum. It is interesting to note that although Cu also undergoes a similar valency change, it does not show similar behaviour. However, silver iodide in which Fe and Cu have $K < 1$ under hydriodic acid vapour, agrees with their results under halogen atmosphere.

Chemical tests could not detect the presence of Fe in the forward end, but the rear end was found to have Fe in both ferrous and ferric states. It can be concluded that K is very slightly less than unity for both ferrous and ferric.

CONCLUSIONS

No quantitative measurements were carried out, However it can be concluded from the observations that distribution coefficient $K < 1$ for Fe, Mg, Cu, Si and Al. For Fe the value seems be very near to but definitely less than one. No impurity with $K > 1$ has been observed in silver iodide. The behaviour of silver iodide with respect to impurities is identical to those of silver chloride and bromide.

The author expresses his gratitude to Dr. J. N. Nanda, Director, D. R. L. (M), Kanpur for his interest in the work. Thanks are due to Shri B. K. Chaudhuri, Assistant Director (Physics), for useful discussions and encouragement at every stage of the work.

REFERENCES

- Burnham, D. C., Brown, F. C. & Knox, R. 1960 *Phys. Rev.* **119**, 1960.
Clark, P. V. Mc. D. & Mitchell, J. W. 1956 *J. Phot. Sci.*, **4**, 1.
Cochrane, G. 1967 *Brit. J. Appl. Phys.*, **18** (5) 687.
Cohen, E. & Dobbenburgh van W. J. D. 1928 *Z. Physik. Chem.* **A1**, **37**, 289,
Gründing, H. 1960 *Z. Physik.* **158**, 577,

- Lark-Horovitz, K. & Johnson, V. A. 1959 '*Methods of Experimental Physics*' *Solid State Physics*. Vol. 6, Part A, Academic Press, New York.
- Moser, F., Nail, N. R. & Urbach, F. 1959 *J. Phys. Chem. Solids*, **9**, 217.
- Moser, F. & Burnham, D. C. 1961 *J. Appl. Phys.*, **32**, 48.
- Nail N. R., Moser, F., Goddard P. E. & Urbach, F. 1957 *Rev. Sci. Instr.* **28**, 275.
- Pfann, W. G., 1952 *Trans. ME* **194** 747.
- 1953 *Trans. ME* **197** 1441.
- 1958 '*Zone Melting*', John Wiley and Sons, New York
- Stasiw, O. & Teltov, J. 1948 *Z. Anorg. Chem.*, **257** 109.
- Warren, R. W. 1965 *Rev. Sci. Instr.*, **35**, 731.

Relaxational solution of transient problem of Marx
surge generator circuit

By S. N. DUTTA

Department of Applied Physics, Calcutta University, Calcutta, India.

(Received February 17, 1969)

This paper deals with the application of relaxation method of obtaining a number of useful information at different instants during the transient period of Marx surge generator. In this connection the differential equation involved in the said circuit is solved by transforming a marching problem into a jury one. It also suggests a method to obtain the required group operation patterns to liquidate the residuals in a definite number of steps. The results thus obtained are compared with those calculated by the conventional method of solution of transient circuit problem.

INTRODUCTION

The device known as Marx surge generator is used to apply a very rapidly rising voltage similar to that arising from lightning or switching to apparatus for test purposes. The actual and its equivalent circuit diagrams of the device are shown in figure 1 and figure 2, respectively (Mem. Staff Dept. Elect. Engg., M. I. T., 1962). The differential equation that can be developed for the transient state is solved by relaxation method following the technique suggested by Allen (1954), namely, by converting the marching problem into a jury one. Thereby a number of desired quantities is found out at different instants simultaneously without much difficulty.

In order to solve the differential equation by relaxation method certain finite-difference approximations to derivatives are used. Thus the differential equation is replaced by a set of simultaneous algebraic equations to be satisfied by the values of the wanted function at the same set of points of subdivision in the range of integration, the required number of end conditions at both the ends being known. At each point of subdivision a residual is defined by a typical formula and the solution lies in the liquidation of those residuals at different points of subdivision in the range. In this connection it has been possible to develop a method of obtaining a number of group operation patterns to liquidate the residuals in a definite number of steps following the similar procedure suggested by Dutta (1966), in the case of linear simultaneous algebraic equations,

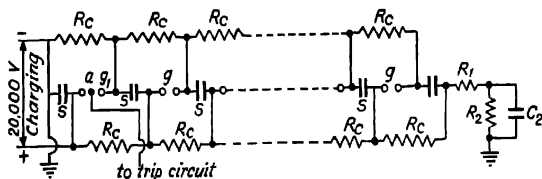


Fig. 1. Circuit diagram for a Marx surge generator.

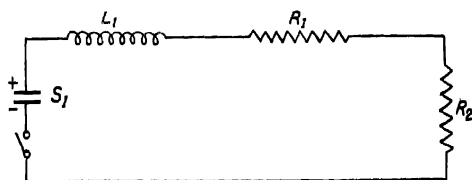


Fig. 2. Equivalent circuit diagram for a Marx surge generator.

PRINCIPLE OF THE METHOD

In order to show the applicability of relaxation method in the solution of the said problem the equivalent circuit (figure 2) is considered which is found to represent the actual circuit of the surge generator (figure 1), rather accurately. The capacitance C_2 (figure 1) of the tested apparatus significantly affects the behaviour of the surge generator-circuit. However the specimen is assumed to be of negligible capacitance and prior to breakdown, of negligible conductance. The circuit also unavoidably has a small inductance, which is sometimes increased thereby playing a significant part in the operation. In the case of electrical breakdown of the specimen the resistance R_2 (figures 1 and 2) is in effect short-circuited temporarily. Usually the voltage drop in the generator spark gaps can be neglected during condenser-discharge period as can the current in the charging resistors. Therefore the effects are not represented in the equivalent circuit. Although some of these assumptions may have to be reconsidered for accurate results in actual practice, the salient features of surge-generator behaviour are exhibited in this problem.

The problem therefore reduces to that of a simple RLS circuit where R, L and S represent the resistance, inductance, and elastance respectively. After tripping of the generator the circuit may be supposed to contain no sources and reaches a steady state with zero condenser charge and zero current, that means,

$$Q_s = 0 ; \quad I_s = 0 \quad \dots(1)$$

where Q_s and I_s are steady state charge and current respectively.

Prior to tripping of generator the resultant elastance S_1 is charged with a charge of,

$$q(0-) = a \text{ coulombs} \quad \dots (2)$$

$$\text{while,} \quad i(0-) = b = 0 \quad \dots 3)$$

where $q(0-)$ and $i(0-)$ are the respective charge and current just before tripping.

Again just after tripping of the generator,

$$q(0+) = q(0-) = a \text{ coulombs} \quad \dots (4)$$

$$\text{and,} \quad i(0+) = i(0-) = 0 \quad \dots(5)$$

where $q(0+)$ and $i(0+)$ are the respective charge and current just after tripping.

Now the differential equation of the circuit after the tripping of the generator can be written as follows :

$$\frac{d^2q}{dt^2} + \frac{R'}{L_1} \frac{dq}{dt} + \frac{S_1}{L_1} = 0 \quad \dots(6)$$

where q is the instantaneous charge of the condenser and $R' = (R_1 + R_2)$, L_1 and S_1 are as shown in the figure 2.

The above differential equation is of the form as shown below ;

$$\frac{d^2q}{dt^2} + m \frac{dq}{dt} + nq = 0 \quad \dots (7)$$

$$\text{where } m = \frac{R'}{L_1} \quad \text{and } n = \frac{S_1}{L_1}.$$

This equation is a second order differential equation and two end conditions are supplied at one end that means, at $t = 0$,

$$u = a \text{ coulombs ;} \quad i = \frac{dq}{dt} = 0 \quad \dots(8)$$

and no end condition is supplied at the other end. But this problem being of marching type cannot be solved directly by relaxation method.

In order to make the problem relaxationally solvable it has to be converted into a jury one by changing its order to four, having replaced q by a new variable u , and by imposing two extra end conditions.

The simple and sufficient substitution in this case is,

$$q = \frac{d^2 u}{dt^2} \quad \dots(9)$$

Therefore the equation (8) becomes,

$$\frac{d^4 u}{dt^4} + m \frac{d^3 u}{dt^3} + n \frac{d^2 u}{dt^2} = 0 \quad \dots(10)$$

and the end conditions (9) transforms into that at $t = 0$,

$$\frac{d^2 u}{dt^2} = a \quad \text{and} \quad \frac{d^3 u}{dt^3} = 0 \quad \dots(11)$$

As the two extra end conditions are to be chosen at the other end, that means, at $t = l$, the simple choice can be made as,

$$u = 0; \quad \frac{du}{dt} = 0 \quad \dots(12)$$

Then to have the relaxational solution of the equation (11), the derivatives are replaced by finite difference approximations holding good at a typical point of subdivision x of the range of integration as shown below,

$$\begin{aligned} \frac{1}{h^4} \left(-4u_{x+1} - 4u_{x-1} + 6u_x + u_{x+2} + u_{x-2} \right) + \frac{m}{2h^3} \left(u_{x+2} - 2u_{x+1} + 2u_{x-1} \right. \\ \left. - u_{x-2} \right) + \frac{n}{h^2} \left(u_{x+1} - 2u_x + u_{x-1} \right) = 0 \end{aligned} \quad \dots(13)$$

where h is the uniform interval between the successive points of subdivision. This expression after rearrangement and simplification can be written as,

$$\begin{aligned} u_x(12 - 4nh^2) + u_{x+1}(-8 - 2mh + 2nh^2) + u_{x-1}(-8 + 2mh + 2nh^2) \\ + u_{x+2}(2 + mh) + u_{x-2}(2 - mh) = 0 \end{aligned} \quad \dots(14)$$

At each point of subdivision x , a residual is defined by,

$$\begin{aligned} F_x = u_x(12 - 4nh^2) + u_{x+1}(-8 - 2mh + 2nh^2) + u_{x-1}(-8 + 2mh + 2nh^2) \\ + u_{x+2}(2 + mh) + u_{x-2}(2 - mh), \end{aligned}$$

$$\text{or, } F_x = Au_x + Bu_{x+1} + B'u_{x-1} + Cu_{x+2} + C'u_{x-2} \quad \dots(15)$$

where,

$$A = 12 - 4\pi h^3$$

$$B = -8 - 2mh + 2\pi h^3$$

$$B' = -8 + 2mh + 2\pi h^3$$

$$C = 2 + mh$$

$$C' = 2 - mh.$$

Therefore every residual is defined by formula (16) and hence a relaxation pattern can be constructed directly from it instead of writing operation and relaxation tables. The process of liquidation of the residuals required in connection with the solution is carried out on a relaxation diagram in place of relaxation table.

The range of integration is divided into five intervals by four points of subdivision. Then using the residual formula (16), the expressions for the residuals at different points of subdivision can be written as follows,

$$F_0 = Xu_0 + Yu_1 + Zu_2 + h^3 W \quad \dots(17)$$

$$F_1 = X_1u_0 + Y_1u_1 + Bu_2 + Cu_3 + h^3 W_1 \quad \dots(18)$$

$$F_2 = C'u_0 + B'u_1 + Au_2 + Bu_3 + Cu_4 \quad \dots(19)$$

$$F_3 = C'u_1 + B'u_2 + Au_3 + Bu_4 \quad \dots(20)$$

$$F_4 = C'u_2 + B'u_3 + Z_1u_4 \quad \dots(21)$$

where,

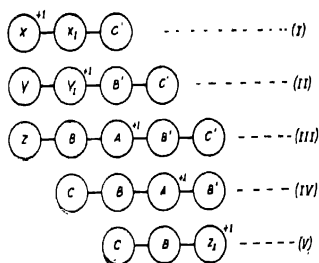
$$X = A + 2B' + 4C' \quad ; \quad X_1 = B' + 2C'$$

$$Y = B - B' - 4C' \quad ; \quad Y_1 = A - C'$$

$$Z = C + C' \quad ; \quad Z_1 = A + C$$

$$W = B'a + 2aC' \quad ; \quad W_1 = C'a.$$

From the above formulae (17 to 21) the following point relaxation patterns showing the amount of changes produced in the residuals caused by the changes in the values of the wanted function at the typical point of subdivision can be easily written.



Patterns I-V

The first three residuals can be liquidated by point relaxation pattern and the last but one residual is liquidated by block relaxation pattern which can be easily found out from the above patterns I to V. In order to liquidate the last residual a suitable group operation pattern can be found out by the method suggested here. This group operation pattern can be obtained by using the patterns I to V, the group operation and the block operation patterns (developed from those point relaxation patterns I to V), in which the first four residuals remain unchanged. Following the same procedure it is also possible to obtain the required group operation patterns to start the liquidation from the other end of the range quite quickly and systematically. Although this method suggests a general procedure to obtain the required group operation pattern it may be possible in some particular cases to find out the desired group or block operation patterns more easily depending on the type of differential equations and circuit parameters after careful study of the point relaxation pattern (Basu 1958; Joarder 1968).

ILLUSTRATION

The example that has been taken for illustration is based on the one worked out by different method (Mem. Staff Dept. Elec. Engg., M. I. T., 1962) in which,

$$R_1 = 100 \text{ ohms}, R_2 = 5000 \text{ ohms}, L_1 = 900 \times 10^{-6} \text{ henry},$$

$S_1 = 80 \times 10^{-6}$ darafs (S of 1.6×10^{-6} darafs each). The condensers are each charged to 20000 volts prior to initiating the surge.

It is desired to calculate the values of the charge of the condenser of elastance S_1 (figure 2) at different instants just after tripping of the generator.

Substituting the numerical values of different circuit constants in the differential equation (7) and performing the necessary transformations and simplifications along with the use of the conditions found out from the supplied data indicated in that connection, the residual formulae holding good at different points of subdivision can be written as follows.

$$F_0 = 36u_0 - 72u_1 + 36u_2 - 111.25 \times 10^{-15} \quad \dots (17A)$$

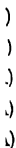
$$F_1 = -35.6u_0 + 114.7u_1 - 122.6u_2 + 43.5u_3 - 23.4375 \times 10^{-15} \quad \dots (18A)$$

$$F_2 = -7.5u_0 - 20.6u_1 + 107.2u_2 - 122.6u_3 + 43.5u_4 \quad \dots (19A)$$

$$F_3 = -7.5u_1 - 20.6u_2 + 107.2u_3 - 122.6u_4 \quad \dots (20A)$$

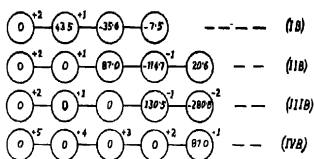
$$F_4 = -7.5u_2 - 20.6u_3 + 150.7u_4 \quad \dots (21A)$$

)
)
)
)
)



2)

pattern IB having no effect on F_0 is obtained. From this pattern IB and IVA, another group operation pattern IIB can be developed in which the residuals F_0 and F_1 remain unchanged. Next making use of this pattern IIB and VA a group operation IIIB which brings about no change in F_0 , F_1 and F_2 can be easily found out. Finally from the pattern IIIB and VIA the desired group operation pattern IVB is obtained in which F_0 , F_1 , F_2 and F_3 remain unaffected and they are shown below.



Pattern IA—IVB.

Thus the last residual F_4 can be easily liquidated by using the group operation pattern IVB, clearly indicated in figure 3. Although the calculation have been carried on upto higher place of decimal they are recorded upto fourth place in the relaxation diagram (figure 3) giving due consideration to the order of accuracy desired in this type of problem. From these values of u_0 , u_1 , u_2 , u_3 and u_4 the values of the charges of those points of subdivision corresponding to successive instants can be easily calculated. The values thus obtained are compared with those calculated by the conventional method and they are found to agree fairly well as shown in table 1 below.

TABLE 1. COMPARISON OF RESULTS

Methods	Quantity of charge in coulomb at the following instants					
	0 sec.	0.5×10^{-8} sec.	1.0×10^{-8} sec.	1.5×10^{-8} sec.	2.0×10^{-8} sec.	2.5×10^{-8} sec.
Conventional	0.125	0.01239	0.01230	0.01221	0.01211	0.01201
Relaxation	0.125	0.01236	0.01227	0.01217	0.01208	0.01198

DISCUSSION

This paper reveals clearly that relaxationally it is possible to find out the values of the desired quantities (here charges) simultaneously at different instants. Although here charges at five successive instants are found out it can be extended easily to calculate the same at larger number of instants as required in a problem at a time. By varying the value of h in the finite-difference approximation equation it is possible to attain higher accuracy.

The method developed here in order to obtain the desired group operation pattern for liquidating the residual can be used to the differential equation of any order and to keep the required number of residuals unaffected at a time. So it is possible to bring about the liquidation quickly in a definite number of steps.

The author is highly indebted to Prof. A. K. Sengupta, D.Sc. C. Eng., M.I.E.E. (Lond.), Head of the Department of Applied Physics, Calcutta University, for his guidance and help throughout the progress of this work.

REFERENCES

- Allen, D. N. de. G. 1954 *Relaxation Methods*, McGraw-Hill Book Co., Inc. New York, Pages 17, 39, 218.
- Basu, R. N. 1958 *Jour. Asson. App. Physicists* (Calcutta) 5, 55.
- Dutta, S. N. 1966 *Indian J. Phys.* 40, 581.
- Joarder, M. K. 1968 *App. Ph. Quarly. (Calcutta)* 9, No. 3, 69.
- Member of the Staff of the Department of Electrical Engineering, Massachusetts Institute of Technology, 1962 *Electric Circuits*, (The Technology Press, M.I.T.) p. 237.

On the unsteady flow of a viscous incompressible fluid
in a channel bounded by two parallel flat plates

By S. N. DUBE

Department of Mathematics, Institute of Technology, Banaras Hindu

University, Varanasi-5

(Received October 19, 1968)

In this paper an attempt is made to find the solution of the Navier-Stokes equations for the unsteady flow of a viscous incompressible fluid through a channel bounded by two parallel flat plates under the influence of pressure gradient (i) varying linearly with time, and (ii) decreasing exponentially with time. In the first case it is seen that (a) symmetrical points have the same velocity, and (b) points near the axis of the channel move faster than the points which are far from the axis of the channel.

INTRODUCTION

The present paper consists of two parts. In part A the flow through a channel bounded by two parallel flat plates under pressure gradient varying linearly with time is discussed. An expression for the velocity is obtained in dimensionless form. This consists of two parts, the one varies linearly with the parameter $T = \frac{\nu t}{y_0^2}$ and the other is the transient part of the velocity, which vanishes in the limit as t tends to infinity. It is seen that the contribution of the transient part is insignificant when $T > 1$. It is also observed that for fluid motion with small Reynolds number the transient part of the velocity dies down more quickly than in the case of fluid motion with large Reynolds number.

In part B the flow of a viscous incompressible fluid between two parallel flat plates under exponentially decreasing pressure gradient is studied. An expression for the velocity has been obtained taking

$$-\frac{1}{\rho} \frac{\partial p}{\partial x} = a_0 + \sum_{n=1}^{\infty} a_n e^{-n\pi t/l},$$

which has been compared with that of Lal's result (1964). Our expression contains some additional terms and the reason for this has been discussed. Our result is in complete agreement with similar results obtained by Ballabh (1959) and Srivastava (1963) where Ballabh has obtained the expression for the velocity by using the method of superposability and Srivastava has discussed the distribution of velocity in a circular pipe under pressure gradient decreasing exponentially with time.

1. EQUATIONS OF MOTION

Navier-Stokes equations of motion (Pai 1956) of a viscous incompressible fluid neglecting the external forces are

$$\left. \begin{aligned} \frac{Du}{Dt} &= -\frac{1}{\rho} \frac{\partial P}{\partial x} + \nu \nabla^2 u, \\ \frac{Dv}{Dt} &= -\frac{1}{\rho} \frac{\partial P}{\partial y} + \nu \nabla^2 v, \\ \frac{Dw}{Dt} &= -\frac{1}{\rho} \frac{\partial P}{\partial z} + \nu \nabla^2 w \end{aligned} \right\} \quad \dots (1.1)$$

where $\frac{D}{Dt} = \frac{\partial}{\partial t} + u \frac{\partial}{\partial x} + v \frac{\partial}{\partial y} + w \frac{\partial}{\partial z}$, and

$$\nabla^2 = \frac{\partial^2}{\partial x^2} + \frac{\partial^2}{\partial y^2} + \frac{\partial^2}{\partial z^2}.$$

The equation of continuity is

$$\frac{\partial u}{\partial x} + \frac{\partial v}{\partial y} + \frac{\partial w}{\partial z} = 0. \quad \dots (1.2)$$

For the present problem we have

$$\left. \begin{aligned} u &= u(x, y, t), \quad v = 0, \quad w = 0, \\ P &= P(x, y, t), \quad \frac{\partial}{\partial z} (\quad) = 0. \end{aligned} \right\} \quad \dots (1.3)$$

The last equation holds because the motion is two-dimensional.

Furthermore, the equation of continuity (1.2) and the conditions (1.3) give

$$\frac{\partial u}{\partial x} = 0 \text{ so that } u = u(y, t). \quad \dots (1.4)$$

Substituting equations (1.3) and (1.4) into the equations of motion (1.1), we have

$$\frac{\partial u}{\partial t} = -\frac{1}{\rho} \frac{\partial P}{\partial x} + \nu \frac{\partial^2 u}{\partial y^2}, \quad \dots (1.5)$$

and

$$\frac{\partial P}{\partial y} = 0 \text{ or } P = p(x, t). \quad \dots (1.6)$$

From equations (1.5) and (1.6) we see that $\frac{\partial P}{\partial x}$ must be a constant or a function of time only in the present problem because P is not a function of y , and u is not a function of x .

2. PART A- PRESSURE GRADIENT VARIES LINEARLY WITH TIME.

Let us assume that

$$-\frac{1}{\rho} \frac{\partial P}{\partial x} = a_0 + at, \quad \dots(2.1)$$

Equation (1.5) then becomes

$$\frac{\partial u}{\partial t} = a_0 + at + \nu \frac{\partial^2 u}{\partial y^2}. \quad \dots(2.2)$$

Let $\bar{u} = \int_0^\infty e^{-st} u dt$ be the Laplace transform of u and let u_0 be the initial value of u .

Multiplying equation (2.2) by e^{-st} and integrating between the limits 0 to ∞ , we get

$$\frac{\partial^2 \bar{u}}{\partial y^2} - P^2 \bar{u} = -\frac{1}{\nu} \left[u_0 + \frac{a_0}{s} + \frac{a}{s^2} \right], \quad \dots(2.3)$$

where $P^2 = \frac{s}{\nu}$.

We shall now find u_0 .

Initially the pressure gradient is a_0 and the motion is steady in the channel.

$$\text{Hence } \frac{\partial u_0}{\partial t} = 0 \text{ and we obtain } \frac{d^2 u_0}{dy^2} = -\frac{a_0}{\nu}. \quad \dots(2.4)$$

The boundary conditions are

$$u_0 = 0 \text{ when } y = -y_0,$$

and

$$u_0 = 0 \text{ when } y = y_0.$$

The solution of equation (2.4) under these boundary conditions is

$$u_0 = \frac{a_0}{2\nu} (y_0^2 - y^2).$$

Substituting this value of u_0 in (2.3), we get

$$\frac{\partial^2 \bar{u}}{\partial y^2} - P^2 \bar{u} = -\frac{1}{\nu} \left[\frac{a_0}{2\nu} (y_0^2 - y^2) + \frac{a_0}{s} + \frac{a}{s^2} \right]. \quad \dots(2.5)$$

The boundary conditions for \bar{u} are

$$\bar{u} = 0 \text{ when } y = -y_0,$$

and

$$\bar{u} = 0 \text{ when } y = y_0.$$

The solution of equation (2.5) under these boundary conditions is

$$u = \frac{a_0}{2\nu} \left(\frac{y_0^2 - y^2}{s} \right) + \frac{a}{s^3} \left[1 - \frac{\cosh Py}{\cosh Py_0} \right].$$

Now applying Laplace inversion theorem, we get

$$u = \frac{a_0}{2\nu} (y_0^2 - y^2) + \frac{1}{2\nu} (y_0^2 - y^2) at - \frac{a}{24\nu^2} (5y_0^2 - y^2) (y_0^2 - y^2) \\ + \frac{64ay_0^4}{\nu^3\pi^5} \sum_{n=0}^{\infty} \frac{(-1)^n}{(2n+1)^5} e^{-\frac{\nu(2n+1)^2\pi^2 t}{4y_0^2}} \cdot \cos \left[\frac{(2n+1)\pi y}{2y_0} \right]. \quad (2.6)$$

At time $t = 0$, $u = \frac{a_0}{2\nu} (y_0^2 - y^2)$. Hence from equation (2.6) by putting $t = 0$, we get

$$\sum_{n=0}^{\infty} \frac{(-1)^n}{(2n+1)^5} \cos \left[\frac{(2n+1)\pi y}{2y_0} \right] = \frac{\pi^5}{1536} \left(5 - \frac{y^2}{y_0^2} \right) \left(1 - \frac{y^2}{y_0^2} \right).$$

Writing $\frac{y}{y_0} = r$ so that $|r|$ is less than 1, we have

$$\sum_{n=0}^{\infty} \frac{(-1)^n}{(2n+1)^5} \cos \left[\frac{(2n+1)\pi}{2} r \right] = \frac{\pi}{1536} (5 - r^2) (1 - r^2).$$

Putting $r = 0$, we get

$$\sum_{n=0}^{\infty} \frac{(-1)^n}{(2n+1)^5} = \frac{5\pi^5}{1536}.$$

Now we make equation (2.6) dimensionless by introducing

$$U = \frac{u}{U_0}, \quad \frac{y}{y_0} = r, \quad T = \frac{\nu t}{y_0^2},$$

where U_0 is a characteristic velocity.

We then get

$$U = b_0(1 - r^2) + bT(1 - r^2) - \frac{b}{12} (5 - r^2) (1 - r^2)$$

$$+ \frac{128b}{\pi^5} \sum_{n=0}^{\infty} \frac{(-1)^n}{(2n+1)^5} \cdot e^{-\frac{(2n+1)^2\pi^2}{4} T} \cos \left[\frac{(n+1)\pi}{2} r \right] \quad \dots(2.7)$$

where $b_0 = \frac{a_0 y_0^2}{2\nu U_0}$ and $b = \frac{a y_0^4}{2\nu^2 U_0}$ are clearly dimensionless numbers.

We now take $U = U_1 + U_2$, where $U_1 = b_0(1 - r^2) + bT(1 - r^2)$
 $-\frac{b}{12}(5 - r^2)(1 - r^2)$; and $U_2 = \frac{128b}{\pi^5} \sum_{n=0}^{\infty} \frac{(-1)^n}{(2n+1)^5} \cdot e^{-\frac{(2n+1)^2 \pi^2}{4} T} \cdot \cos \left[\frac{(2n+1)\pi}{2} r \right]$.

The values of U for different values of r and T have been tabulated.

TABLE 1. $b_0 = 2, b = 1$

$r \backslash T$	0.01	0.1	0.2	0.3	0.4	0.8	1.0
0.0	2.0019	2.0256	2.0422	2.0874	2.1435	2.4459	2.6213
0.3	1.8220	1.8438	1.8603	1.9025	1.9544	2.2314	2.3914
0.6	1.2800	1.2979	1.3127	1.3445	1.3827	1.5813	1.6948
0.9	0.3800	0.3862	0.3921	0.4026	0.4147	0.4754	0.5096

TABLE 2. $b_0 = 1, b = 1$

$r \backslash T$	0.01	0.1	0.2	0.3	0.4	0.8	1.0
0.0	1.0019	1.0256	1.0422	1.0874	1.1435	1.4459	1.6213
0.3	0.9120	0.9338	0.9503	0.9925	1.0444	1.3214	1.4814
0.6	0.6400	0.6579	0.6727	0.7045	0.7427	0.9413	1.0548
0.9	0.1900	0.1962	0.2021	0.2126	0.2247	0.2854	0.3196

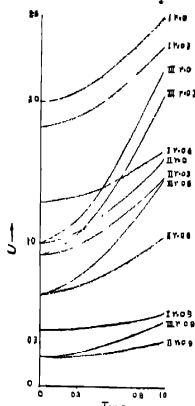
TABLE 3. $b_0 = 1, b = 2$

$r \backslash T$	0.01	0.1	0.2	0.3	0.4	-0.8	1.0
0.0	1.0038	1.0512	1.0844	1.1748	1.2870	1.8918	2.2426
0.3	0.9140	0.9576	0.9906	1.0750	1.1788	1.7328	2.0528
0.6	0.6400	0.6758	0.7054	0.7690	0.8454	1.2426	1.4696
0.9	0.1900	0.2024	0.2142	0.2352	0.2594	0.3808	0.4492

The graphs for fixed r ($r = 0, +0.3, +0.6, +0.9$) showing the variation of U with the parameter T have been drawn in three cases $b_0 = 1, b = 1$, $b_0 = 1, b = 2$, and $b_0 = 2, b = 1$ in the range $T = 0$ to $T = 1$. The graphs for negative values of r have not been drawn because of the fact that the velocity will not change whether r is negative or positive. It means that the symmetrical points have the same velocity.

Graph showing variation of U with T

Graphs marked I are for $b=10$
 " " II " " $b=6$
 " " III " " $b=2$



The graphs beyond $T=1$ have not been drawn because U_2 is very small compared to U_1 when $T>1$, hence the transient part is insignificant and U varies linearly with T in this range. From the graphs and tables of values it is observed that U increases with T for fixed r . It is also seen that for any T , U decreases with the increases of r and it is maximum when $r=0$. It means that the points near the axis of the channel move faster than the points which are far from the axis of the channel.

It can also be easily seen that for fluids with small Reynold number, the transient part of U becomes insignificant after an interval of time which is shorter than the time required in the case of fluids with large Reynold number.

3. PART B. PRESSURE GRADIENT DECREASES EXPONENTIALLY WITH TIME.

We take

$$-\frac{1}{\rho} \frac{\partial P}{\partial x} = a_0 + \sum_{m=1}^{\infty} a_m e^{-m t}, \quad \dots(3.1)$$

Equation (1.5) then becomes

$$\frac{\partial u}{\partial t} = a_0 + \sum_{m=1}^{\infty} a_m e^{-m t} + \nu \frac{\partial^2 u}{\partial y^2}. \quad \dots(3.2)$$

Let $\bar{u} = \int_0^{\infty} e^{-st} u dt$ be the Laplace transform of u and let u_0 be the initial value of u ,

Multiplying equation (3.2) by e^{-st} and integrating between the limits 0 to ∞ , we get

$$\frac{\partial^2 u}{\partial y^2} - P^2 u = -\frac{1}{\nu} \left[u_0 + \frac{a_0}{s} + \sum_{m=1}^{\infty} \frac{a_m}{s(m)} \right], \quad \dots (3.3)$$

where $P^2 = \frac{s}{\nu}$.

Here again $u_0 = \frac{a_0}{2\nu} (y_0^2 - y^2)$.

The solution of the equation (3.3) under the boundary conditions

$$u = 0 \text{ when } y = -y_0,$$

$$\text{and } \bar{u} = 0 \text{ when } y = y_0$$

is

$$\bar{u} = \frac{a_0}{2\nu} \left(\frac{y_0^2 - y^2}{s} \right) + \left[1 - \frac{\cosh Py}{\cosh Py_0} \right] \sum_{m=1}^{\infty} \frac{a_m}{s(s+m)} \quad \dots (3.4)$$

Now applying Laplace inversion theorem, we get

$$\begin{aligned} u = & \frac{a_0}{2\nu} (y_0^2 - y^2) - \sum_{m=1}^{\infty} \frac{a_m}{m} \left[1 - \frac{\cos \left\{ \left(\frac{m}{\nu} \right)^{\frac{1}{2}} y \right\}}{\cos \left\{ \left(\frac{m}{\nu} \right)^{\frac{1}{2}} y_0 \right\}} \right] e^{-mt} \\ & + \frac{4}{\pi} \sum_{n=1}^{\infty} \sum_{m=0}^{\infty} \frac{(-1)^n a_m}{(2n+1) \left[m - \frac{\nu(2n+1)^2 \pi^2}{4y_0^2} \right]} \cdot e^{-\frac{\nu(2n+1)^2 \pi^2 t}{4y_0^2}} \\ & \cos \left[\frac{(2n+1)\pi y}{2y_0} \right] = U'_1 + U'_2 + U'_3 \quad \dots (3.5) \end{aligned}$$

This expression for the velocity does not agree with Lal's result. His expression does not contain U'_3 . The difference lies in the fact that Lal has assumed the form of u as

$$u = u_0 + \sum_{m=1}^{\infty} u_m e^{-mt},$$

where u_0 and u_m are functions of τ only. Naturally then the part U'_3 will be absent in his expression. But the expression (3.5) is in full agreement with Ballabh's result where he has obtained the expression for the velocity by the method of superposability. The expression (3.5) for the velocity is also similar to an expression obtained by Srivastava where he has found the

velocity of an incompressible fluid in a circular pipe under exponentially decreasing pressure gradient.

Hence $U'_1 + U'_2 + U'_3$ is a more general solution of (3.2) and this is confirmed by Laplace Transform method used in the present paper.

The author is indebted to Dr. P. L. Bhatnagar for kind guidance in the preparation of this paper.

REFERENCES

- Lal, K. 1964 *D. Phil. Thesis*, Allahabad University.
Ballabh, R. 1959 *Proc. of 5th Congress on Theo. and Appl. Mech.*, India.
Srivastava, P. N. 1963 *The Mathematics Seminar*, 3, Nos. 1 & 2, 44.
Pai, S., 1956, *Viscous Flow Theory, I-Laminar Flow*, D. Van Nostrand Co., Inc., New York.

i)

is
al

be
th
by
is
the

On magnetic stability of some Hamiltonians

By DIPAN K. GHOSH, CHANCHAL K. MAJUMDAR AND A. K. RAJAGOPAL

Tata Institute of Fundamental Research, Colaba, Bombay 5.

(Received April 4, 1969)

We investigate the magnetic stability of certain systems with Ising & Heisenberg interactions. It is found that in general the system having more number of interacting pairs is favoured most on thermodynamic considerations.

1. INTRODUCTION

Consider a set of spins, each of spin $\frac{1}{2}$, and interacting amongst themselves with a prescribed law and arranged in various geometrical shapes. The range of interaction is restricted to the nearest neighbours; the strength is assumed to be constant. What is the most stable arrangement, in other words, which configuration will have the lowest free energy?

Questions of similar nature were raised in the past about charged particles. For instance, Coldwell-Horsfall & Maradudin (1963) found the b.c.c. electron lattice (the one considered by Wigner, 1938) has indeed the lowest energy among b. c. c., f. c. c. and s. c. arrangements. An extensive discussion of lattice stability exists for various force laws between ionic charges (Born & Huang (1966)). These results are obviously of interest in phase transitions involving crystal structure change.

The problem for spins which we consider has, however, a serious limitation as far as physics of actual magnetic solid is concerned. The actual stability of the magnetic structure is determined only partly by the Hamiltonian that we consider and the redistribution of charge is extremely important for stability considerations. One might take the spin Hamiltonian to be an effective Hamiltonian of the solid of a particular geometrical structure. When we consider different arrangement of spins, in general the exchange constant in the Hamiltonian will not be the same as before, even though the new structure may be defined by an effective spin Hamiltonian of the old type. The exchange constant may change in several ways. If we assume the charge distribution spherical (a collection of S-state ions), the distance, between nearest neighbours will change or the co-ordination number itself may change, modifying the overlap integrals. The charge distribution of most magnetic ions is not spherically symmetric, hence any rearrangement of the neighbours around one ion will modify overlap integrals. Within these limitations, however, the question of stability can be discussed for some cases. The results have certain interesting features.

2. ISING HAMILTONIAN

Take the Ising Hamiltonian first

$$H = \frac{1}{2} J \sum_{i,j} \sigma_{iz} \sigma_{jz} \quad \dots (1)$$

$J < 0$ corresponds to the ferromagnetic case. In the two dimensional situation, the free energy per spin has been rigorously evaluated for the square, triangular and hexagonal lattices (Green & Hurst 1965, Domb 1960),

$$\begin{aligned} -f_{sq}/\kappa_B T &= \frac{1}{2} \ln \sinh 2K + \frac{1}{4\pi} \int_0^{2\pi} \cosh^{-1} [\coth 2K \cosh 2K - \cos \theta] d\theta \\ -f_{tr}/\kappa_B T &= \frac{1}{2} \ln 2 + 3 \ln \cosh K + \frac{1}{4\pi} \int_0^{2\pi} \ln \left\{ A + \{A^2 - 4(1-x^2)^2 X^2(\theta)\}^{1/2} \right\} d\theta \\ -f_{h.c.}/\kappa_B T &= -f_{sq}/\kappa_B T - \ln \cosh K - \ln (1 + \tanh^3 K) + \ln 2 \quad \dots (2) \end{aligned}$$

with

$$A = (1+x^2)^3 + 8x^3 - 2x(1-x^2)^2$$

$$X(\theta) = 2x(1-x^2) \cos \frac{1}{2} \theta$$

$$x = \tanh K, K = J/\kappa_B T$$

The integrals can be numerically evaluated. We notice that for $J > 0$, the triangular lattice has the lowest free energy at all temperatures. For $J < 0$, the hexagonal configuration is the most favoured one. The free energy curves never cross, and no transformation from one type of lattice to another is possible.

No closed analytic expressions are available for 3-dimensions. However, series expansions for the partition function are available both in the high and low temperature limits. Domb & Sykes explicitly calculated the partition functions in powers of $\tanh (J/\kappa_B T)$ for both ferromagnetic and antiferromagnetic cases for different lattices. Focussing our attention on the simple cubic (s.c.), body centred cubic (b.c.c.) and the face centred cubic (f.c.c.) lattices, the high temperature expansions for $J < 0$ (Domb 1960, Domb & Sykes 1957):

$$\text{s.c. } Z = 2(\cosh K)^3 [1 + 3w^3 + 22w^6 + 192w^9 + \dots]$$

$$\text{b.c.c. } Z = 2(\cosh K)^4 [1 + 12w^4 + 148w^8 + 2568w^{12} + \dots]$$

$$\text{f.c.c. } Z = 2(\cosh K)^6 [1 + 8w^3 + 33w^6 + 168w^9 + \dots]$$

$$w = \tanh K; K = J/\kappa_B T. \quad \dots (3)$$

The f. c. c. lattice has the lowest free energy. For $J > 0$, the f.c.c. lattice cannot be decomposed into the two sublattices, as done usually in the model of an antiferromagnet. Of the remaining lattices obviously the b. c. c. is the more stable one. Note that the right hand sides of first two equations in (3) do not depend on the sign of J . In the low temperature region Sykes *et al* (1965) give expansions for free energy for both ferromagnetic and antiferromagnetic lattices in powers of $\exp(-|J|/\kappa_B T)$. The free energy of $J < 0$ is given by the formula.

$$F = -\frac{1}{2} q |J| - \kappa_B T \ln \Lambda(j, u) \quad \dots(4)$$

where \ln is given by the ferromagnetic polynomials

$$s. c. \ln \Lambda(1, u) = u^3 + 3u^5 - \frac{7}{2} u^6 + 15u^7 - 33u^8 + \dots,$$

$$b. c. c. \ln \Lambda(1, u) = u^4 + 4u^7 - \frac{9}{2} u^8 + 28u^{10} + \dots,$$

$$f. c. c. \ln \Lambda(1, u) = u^6 + 6u^{11} - \frac{13}{2} u^{12} + 8u^{15} + \dots,$$

$$u = \exp(-4|J|/\kappa_B T)$$

The dominant term at low temperatures is $-\frac{1}{2} qJ$ i.e., the free energy is asymptotically proportional to co-ordination number. Hence, the f. c. c. lattice is again the stablest configuration and the s.c. lattice has the least stability. For $J > 0$ free energy is given by a formula similar to (4) but in this case $\ln \Lambda^a(1, y)$ is given by

$$s. c. \ln \Lambda^a(1, y) = y^6 + 3y^{10} - \frac{7}{2} y^{12} + 15y^{14} + \dots$$

$$b. c. c. \ln \Lambda^a(1, y) = y^8 + 4y^{14} - \frac{9}{2} y^{16} + \dots$$

$$y = \exp(-4J/\kappa_B T) \quad \dots(5)$$

The b.c.c. lattice is stabler than the s. c. If we assume that as in the two dimensional situation, the free energy curves do not cross, no transition will occur from the f.c.c. to any other form in the $J < 0$ case, and from b.c.c. to the s. c. in the $J > 0$ case.

3. HEISENBERG HAMILTONIAN

The Hamiltonian representing the Heisenberg coupling is written as

$$H = -\frac{1}{2} J \sum_{i,j} \sigma_i \sigma_j \quad \dots(6)$$

i and j being nearest neighbours. $J > 0$ corresponds to antiferromagnetic coupling. Rigorous analytical expressions for the free energy are not known for large number of particles. We shall consider what is known as the cluster problem. Here the spins are supposed to be divided into groups which do not interact with each other. Bleaney & Bowers (1954) (see also Guha 1957, Smart 1963) have discussed the case of a compound. $\text{Cu}(\text{CH}_3\text{COO})_2 \cdot \text{H}_2\text{O}$, where a pair of Cu atoms is magnetically coupled, while different pairs are independent. We shall generalize the situation and allow each group to have 4, 6 and 8 particles, respectively. Beyond these, calculations become too involved.

Considering 4 spins first, we can arrange them at the vertices of a square (s) or a tetrahedron (t). Always allow nearest neighbour interactions. Hence the relevant Hamiltonians are

$$H_s = \frac{1}{2} J [\sigma_1\sigma_2 + \sigma_2\sigma_3 + \sigma_3\sigma_4 + \sigma_4\sigma_1]$$

$$H_t = \frac{1}{2} J [\sigma_1\sigma_2 + \sigma_2\sigma_3 + \sigma_3\sigma_4 + \sigma_4\sigma_1 + \sigma_1\sigma_3 + \sigma_2\sigma_4]. \quad \dots(7)$$

Taking 6 spins we may put them in the shape of a hexagonal ring (h) or at the vertices of an octahedron (o). The corresponding Hamiltonians are

$$H_h = \frac{1}{2} J \sum_{i=1}^6 \sigma_i \sigma_{i+1}, \quad (\sigma_7 \equiv \sigma_1)$$

$$H_o = \frac{1}{2} J \left[\sum_{i=1}^6 \sigma_i \sigma_{i+1} + \sum_{i=1}^3 \sigma_i \sigma_{i+2} \right] \quad \dots(8)$$

For 8 spins two structures of immediate interest are an eight member ring (r) or a cube (c)

$$H_r = \frac{1}{2} J \sum_{i=1}^8 \sigma_i \sigma_{i+1}; \quad (\sigma_9 \equiv \sigma_1),$$

$$H_c = \frac{1}{2} J [\sigma_1\sigma_2 + \sigma_2\sigma_3 + \sigma_3\sigma_4 + \sigma_4\sigma_1 + \sigma_1\sigma_5 + \sigma_5\sigma_6 + \sigma_6\sigma_7 + \sigma_7\sigma_8 + \sigma_8\sigma_1$$

$$+ \sigma_2\sigma_7 + \sigma_4\sigma_6 + \sigma_3\sigma_8 + \sigma_5\sigma_4 + \sigma_6\sigma_7 + \sigma_7\sigma_8 + \sigma_8\sigma_5] \quad \dots(9)$$

We want to calculate the eigenvalues of the Hamiltonians and determine their degeneracies in order to get the free energy. The eigenvalue of the Hamiltonian in equations (7) and (8) are already available from the work of Majumdar & Ghosh (1969). They studied the effect of having next nearest neighbour interaction in a linear chain represented by the Hamiltonian

$$H = \frac{1}{2} J \sum_{i=1}^N \sigma_i \sigma_{i+1} + \frac{1}{2} J' \sum_{i=1}^N \sigma_i \sigma_{i+2} \quad \dots(10)$$

($N+1 \equiv 1, N+2 \equiv 2; -1 \leq \kappa \leq 1$). An essential part of their work was devoted to the study of short chains of upto ten particles. In fact it was recognized that for $\kappa=1$, the 4 spins can be naturally arranged on a tetrahedron and six spins on an octahedron. Such arrangements could be exploited to explain the degeneracy of eigenvalues at $\kappa=1$, because these figures have simple symmetry groups associated with them. For 8 spins the results for $\kappa=0$ were known from Orbach (1959). The results for $\kappa=1$ with 8 spins do not help us as there is no simple arrangement of spins in this case. We therefore diagonalized the Hamiltonian (6) for a simple cubic arrangement of spins and obtained the free energy. The eigenvalues are listed in table 1. Dresselhaus (1962) has obtained the equations determining eigenvalues.

TABLE 1. EXCHANGE EIGENVALUES FOR A CUBIC ARRAY OF
8 ATOMS OF SPIN $\frac{1}{2}$

S_z	No. of states	Energy E/J	S_z	No. of states	Energy E/J
± 4	2	6.0000	0	2	6.0000
± 3	2	6.0000		6	4.0000
	6	4.0000		4	3.2361
	6	2.0000		2	2.5589
± 2	2	0.0000		6	2.3402
	2	6.0000		18	2.0000
	6	4.0000		6	1.2361
	4	3.2361		6	0.8284
	18	2.0000		16	0.0000
	2	0.8284		6	-0.7639
	6	0.0000		4	-1.2361
	4	-1.2361		6	-1.3778
	12	-2.0000		22	-2.0000
	2	-4.8284		2	-2.9187
± 1	2	6.0000		6	-3.2361
	6	4.0000		6	-4.0000
	4	3.2361		6	-4.8284
	6	2.3402		6	-4.9623
	18	2.0000		6	-5.2361
	6	1.2361		2	-8.0000
	2	0.8284		2	-9.6401
	14	0.0000			
	6	-0.7639			
	4	-1.2361			
	6	-1.3778			
	16	-2.0000			
	6	-3.2361			
	2	-4.8284			
	6	-4.9623			
	6	-5.2361			
	2	-8.0000			

With $J > 0$, for 4 spins, at low temperature, the square, arrangement has the lowest free energy (the ground state energy per spin is of course lower) but at high temperatures the tetrahedral arrangement lies lower. The cross over occurs at $J/\kappa_B T = 0.5785$. The change at this point is of the first order, in the sense that the slope of free energy changes discontinuously. The internal energy has a jump and the specific heat curve also has a finite jump.

For both 6 and 8 spin clusters with $J > 0$, the 3 dimensional structures—the octahedron and the cube—lie lower in free energy than the corresponding two dimensional counter parts. The results suggest the following interpretation. The three dimensional structures having more interparticle bonds are energetically favoured. The case of 4 spins is marginal; the three dimensional structure allows two extra bonds, but there is not enough gain in energy (remember the coupling is antiferromagnetic). As the 3 dimensional arrangement provides more bonds the balance is tipped in favour of stability for the 3 dimensional structure. For $J < 0$ it is found that in all these cases mentioned above the three dimensional structure is more stable for all regions of temperatures.

Though no closed expression for free energy for lattices with $N \rightarrow \infty$ in the Heisenberg Hamiltonian has been worked out so far, high temperature expansions in powers of $J/\kappa_B T$ are available from the work of Domb & Wood (1965). They express the zero field expansion of the partition function in the form

$$\ln Z_N(1/\kappa_B T, 0) = N \ln 2 + N \sum_{l=2}^{\infty} e_l (J/\kappa_B T)^{-l} 2^l / l! \quad \dots (11)$$

At sufficiently high temperatures the $l=2$ term is the leading one. The coefficient e_2 has been computed by these authors to be $3/2$ times the coordination number. It is seen that for $J < 0$, of the three lattices s.c., b. c. c. and f.c.c., the last mentioned one is the most stable and the s.c. is the least stable. For $J < 0$ clearly the f. c.c. lattice, having more bonds, will be the most stable at low temperatures. Hence this is likely to be the case at all temperatures. With antiferromagnetic coupling, $J > 0$, while the high temperature behaviour of the s.c. and b. c.c. lattices are given by (11), nothing exact is known about the ground state energy.

4. DISCUSSIONS.

The real problem of stability which includes the geometric ordering determined almost entirely by the spin independent forces between ions and the magnetic ordering controlled by the spin dependent exchange type forces is a very hard one. However, it is thought that near the magnetic transition temperature the dominant contribution to free energy determining the magnetic structure comes from the Hamiltonian of the form

discussed in this paper. Also, in complex salts with complex geometric structures, there are only a few magnetic ions and these determine the magnetic structure of the system entirely. Such systems are also described by effective spin Hamiltonians of the Heisenberg type, and our results may have relevance to them.

REFERENCES

- Bleaney, B. 1954 *Phil. Mag* [7], **43**, 372.
Born, M. & Huang, K. 1954 *Dynamics of Crystal Lattices*, Oxford University Press, p. 140.
Coldwell-Horsfall, R. A. & Maradudin, A. A. 1960 *J. Math. Phys.* **1**, 395 and Erratum, 1963, **4**, 582.
Domb, C. 1960 *Advances in Physics* **9**, 149, 245.
Domb, C. & Sykes, M. F. 1957 *Phil. Mag.* **2**, 733.
Domb, C. & Wood, D. W. 1965 *Proc. Phys. Soc.* **86**, 1.
Dresselhaus, G. 1962 *Phys. Rev.* **126**, 1664.
1962 *Lincoln Laboratory Technical Report*, No. 254.
Green, H. S. & Hurst, C. A. 1965 *Order Disorder Phenomenon*, Interscience Publishers.
Guha, B. C. 1951 *Proc. Roy. Soc. A* **206**, 353.
Majumdar, C. K. & Ghosh, D. K. 1969 *J. Math. Phys.* (to be published).
Orbach, R. 1959 *Phys. Rev.* **115**, 1181.
Smart, J. S. 1963 *Magnetism* Vol. 3, edited by G. T. Rado & H. Suhl Academic Press.
Sykes, M. F., Essam, J. W. & Gaunt, D. S. 1965 *J. Math. Phys.* **6**, 283.
Wigner, E. P. 1938 *Trans. Faraday Soc.* **34**, 678.

Letters to the Editor

Effect of lattice vibrations on the exchange-interaction in
ferro—and anti-ferro-magnetic crystals.

By A. T. MAITRA

Physics Department, Patna University.

(Received March 3, 1969)

Heisenberg (1928) for the first time gave the most successful interpretation of the origin of the apparently enormous but mysterious Weiss molecular field in a ferromagnetic in terms of exchange interaction between spins of the electrons on neighbouring atoms in a crystal lattice. According to this localized-spin model for a magnetic solid, it is well known, that the Hamiltonian of the spin system is given by $H = -2J \sum_{i,j} S_i \cdot S_j \dots (1)$, besides the zeeman energy of the spins, where S_i is the spin vector of the i th atom, measured in multiples of $\frac{1}{2}$. The term in equation (1) is the exchange energy and contains the familiar exchange integral J and the summation extends only over the neighbouring atoms. The equation (1) in the more general case takes the form $-2\sum_{i,j} J_{ij} S_i \cdot S_j$ and the sum runs over all pairs of atoms in the crystal. The magnitude of the exchange coupling constant J , between adjacent atoms, is positive for ferromagnetics and negative for antiferromagnetics. The magnitude of J , is dependent on the ratio of the radius of the atom (half the internuclear distant in the crystal) to the effective radius of the incomplete 3d or 4f shell of the atoms. The outstanding feature of the Heisenberg theory of ferromagnetism lies in showing the dependence of the Curie temperature as also of the Weiss molecular field constant on the strength of J .

Bethe (1933) showed that the exchange integral J is positive in the case of Fe, Co, and Ni (incomplete 3d shell) and Gd and Dy (incomplete 4f shell) only in the special circumstances when the ratio of the radius R of the atom to the radius γ of the incomplete 3d or 4f shell is within a certain limited range and had shown the variation of J for the ferromagnetic element, with R/γ . Néel (1936, 1946) calculated the ratio $U = \theta_C/C_A Z$ known as reduced molecular field coefficient where Z is the number of nearest neighbours of an atom C_A the usual Curie constant for a gm. atom. This reduced molecular field coefficient is also dependent on J . A more generalised curve showing the variation of U (positive for ferromagnetics and negative for antiferromagnetics with $(d-2r)$ has been drawn by Néel

(1940) and reported by Stoner (1946-47) where d is interatomic distance and r is the effective radius of the d shell.

Born (1942) in his theory of the intensity of diffuse spots due to scattered X-radiation, on the basis of lattice dynamics, has introduced the concept of a dynamic lattice constant

$$l = \frac{\hbar}{(mk\theta_D)^{1/2}} = \frac{6.96 \times 10^{-8}}{(\mu\theta_D)^{1/2}} \text{ cm.}$$

as the root mean square amplitude of a linear oscillator of frequency $W_0 = k\theta_D/\hbar$, where m = mass of the atom, k = Boltzmann constant μ = atomic mass in atomic units and θ_D = Debye temperature. As such $m l^2 \omega_0^2 = \hbar \omega_0 = k\theta_D$ (energy of lattice vibrations)

In this note some aspects of correlations due to the influence of Bohr's dynamic lattice constant in the variation of the reduced molecular field coefficient of Néel with $(d-2r)$ have been shown. Figure 1 contains two

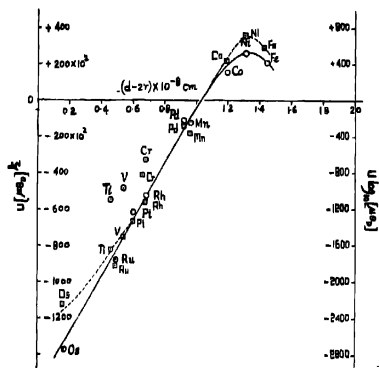


Figure 1.

- (x) Thick lined curve showing the variation of $U(\mu\theta_D)^{1/2}$ vs. $(d-2r)$.
 (b) Dotted curve showing the variation of $U \log(\mu\theta_D)$ vs. $(d-2r)$

curves, one showing the variation of $U (\mu\theta_D)^{1/2}$ (proportional to U/l) vs. $(d-2r) \times 10^{-8}$ cm. and the other showing the variation of $U \log (\mu\theta_D)$ vs. $(d-2r) \times 10^{-8}$ cm. Figure 2 shows two curves, showing the variations as noted in the captions below.

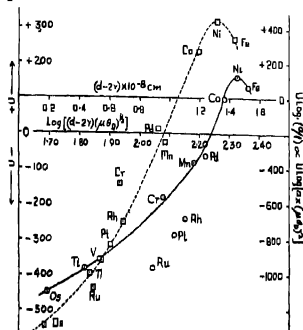


Figure 2. (a) Thick lined curve showing the variation of U vs \log

$$(d-2r)(\mu\theta_D)^{1/2}$$

(b) Dotted curve showing the variation of $U \log a, l$ or

$$U \log a (\mu\theta_D)^{1/2} \text{ vs. } (d-2r) \text{ where 'a' is the lattice constant.}$$

Figure 3 shows the variation of U vs. l^{-1} , i, e , U vs. $(\mu\theta_D)^{1/2}$. These curves bear significance and it is really interesting to find that the nature of the curves in figure 1 and 2 are very similar to that of U vs. $(d-2r)$ curve of Néel. The curve of figure 3 clearly indicates a sharp rise in the value of U for Fe, Co, Ni within a certain limited range of $(\mu\theta_D)^{1/2}$ which also means within a limited range of the dynamic lattice constant. It is very significant that l^{-1} which is proportional to $(\mu\theta_D)^{1/2}$ or some function of $(\mu\theta_D)^{1/2}$ like $\log (\mu\theta_D)^{1/2}$ is linked up with the reduced molecular field coefficient of Néel in such a way as to make it vary with $(d-2r)$ much in the same manner as the curve of Néel. Various types of interaction processes can occur involving phonons and magnons. Lattice vibrations, depending

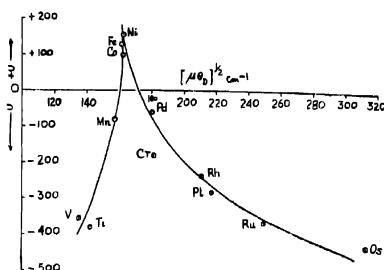


Figure 3. Showing variation of U vs. $(\mu\theta_D)^{1/2}$

on temperature, destroy perfect lattice periodicity in a crystal and produce time-dependent imperfection in the lattice. Spin waves couple first to one another and then to the lattice by the process or magnon-phonon coupling. Further Sinha & Upadhyaya (1962) and Upadhyaya & Sinha (1963) have shown the dispersion relation of magnon energy to be given by $\hbar\omega_\lambda = 2JSK_\lambda a^2$ for a ferromagnetic and $2JSK_\lambda a$ (approximately) for an antiferromagnetic crystal, where K_λ = reduced wave vector and a = lattice constant. Variation of U log as a function of $(d-2r)$ has been shown in one of the curves of figure 2. The values of U and $(d-2r)$ have been taken from Néel's work (1940) and those of θ_D from the table in Gray's book (1963).

These aspects of correlations reflect the effect of lattice vibrations on the exchange interaction constant J and provide phenomenologically an insight into the manifestation of the phonon-modified exchange which plays an important role in the mechanism of the magnon-phonon or spin-phonon interactions worked out by Sinha *et al* (1963) and Bakre, *et al* (1967). These aspects of correlations also suggest the fundamental nature of Born's dynamic lattice constant. It is apparent that there will be also a spin-phonon interaction effect on the well known Debye (1914) Waller (1923, 1925) factor modifying the intensity of X-ray diffraction maxima. Further work on these aspects in progress.

My sincere thanks are due to Professor B. N. Singh, D. Sc., Head of the Physics Department, for his kind interest in the work.

REFERENCES

- Bakre, R. V. Joshi, A. W., & Sinha, K. P., 1967 *Ind. J. P. App. Physics*, 5, No. 6, 205.
Bethe, H. 1933 *Handb. d. Physik*, 24, Part II, 595
Born, M. 1942 *Nature*, 150, 490
1942-43. *Reports. Prog. Physics*, IX, 317
Debye, P. 1914, *Annalen der Physik*, 43, 49
Gray, Dwight 18963, *American Institute of Physics Handbook*, (2nd Ed.), sec. 4, 61.
Heisenberg, W. 1928 *Z. Physik*, 24, Part II, 595.
Néel, L. 1936 *Ann. Phys.*, Paris, 5, 232.
1940, *Le Magnétisme*, Vol II, 65.
Sinha, K. P. & Upadhyaya, U. N. 1962 *Phys. Rev* 127, No 2, 432.
Stoner, E. C. 1946-47, *Reports Prog. Physics*, XI, 76.
Upadhyaya, U. N. & Sinha, K. P., 1963 *Phys. Rev.* 130, 939.
Waller, I 1923 *Z. Physik* 17 398.
1925 *Diss.* Upsala

Indian J. Phys. 43, 293-295 (1969)

Electric and thermoelectric properties of ilmenite

By A. K. MUKERJEE

Magnetism Department

Indian Association for the Cultivation of Science, Calcutta-32, India.

(Received August 2, 1969)

In an earlier observation from 300°K to about 800°K (Mukerjee 1964), the natural crystals of ilmenite (chemical composition : TiO_2 40.1%, FeO 57.4%, SiO_2 1.2% and H_2O 0.2% ; X-ray composition analysis : ilmenite—major, hemtite—minor, rutile—trace was found to be semiconducting. The recent study of its magnetic properties (Mukerjee, to be published) shows it to be weakly ferromagnetic and that its curie temperature is about 855°K. Its principal conductivities were therefore remeasured from 300°K to 1000°K to study the electrical behaviours both below and above the Curie temperature (figure 1).

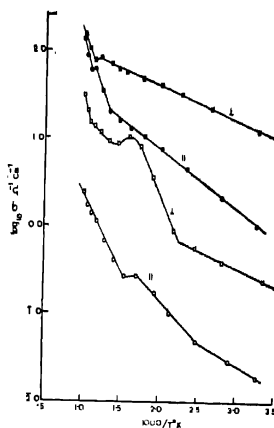


Figure 1. The conductivity of ilmenite. Open and solid points indicate measurements on fresh and heated samples.

The temperature variation of principal conductivities could be given by a formula of the type

$$\sigma = \sigma_0 \exp \frac{-\Delta E}{kT}$$

where the symbols have their usual meaning (Smith 1959) but with different sets of values for σ_0 and ΔE for different temperature ranges which are given in table 1, for different crystallographic directions i.e. \parallel and \perp to the trigonal axis, respectively. Seebeck voltage (with respect to Pt) at different temperatures was studied in order to determine the nature of the charge carrier (figure 2).

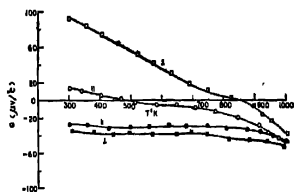


Figure 2. Seebeck effect of ilmenite. Open and solid points indicate measurements on fresh and heated samples.

TABLE 1. ΔE AND σ_0 IN DIFFERENT TEMPERATURE REGIONS

Crystal direction	Fresh (a)			Heated		
	ΔE in eV	σ_0 in $\Omega^{-1}\text{cm}^{-1}$	Temperature region °K	ΔE in eV	σ_0 in $\Omega^{-1}\text{cm}^{-1}$	Temperature region °K
Basal	.08	5.6	$T < 440$.08	2.3×10^4	$T < 820$
Plane	.42	5.2×10^4	$440 < T < 590$			
	.18	1.3×10^4	$715 < T < 925$.50	4.6×10^4	$880 < T$
	.725	1.8×10^5	$925 < T$			
C-axis	.10	1.0	$T < 400$.14	1.7×10^4	$T < 750$
	.20	12.6	$400 < T < 590$.50	5.2×10^4	$750 < T < 880$
	.36	1.5×10^4	$650 < T$.65	3.2×10^4	$910 < T$

The studies of the thermo-electric properties show that the nature of the carriers change from *p*-type to *n*-type in fresh samples at high temperatures, and that repeating measurements, the heated samples were found to be entirely *n*-type having higher conductivities. Such changes are most probably due to $\alpha\text{-Fe}_2\text{O}_3$ entering into the FeTiO_3 lattice (Ishikawa 1958), as also to a lesser degree due to changes in the other impurities present in the samples.

The author is thankful to Shri A. K. Dutta for guidance and to Prof. A. Bose for his kind interest in the work. He is also grateful to Dr. D. R. Dasgupta for helpful discussions.

REFERENCES

- Ishikawa, Y & Sawada, S 1958 *J. Phys. Soc. Japan*. 13, 37.
 Mukerjee, A. K. 1964 *Indian J. Phys.* 38, 10.
 Smith, R. A. 1959 *Semiconductors*, Cambridge University Press.

K-conversion coefficient of the 412 keV transition in Hg^{198} .

By H. S. SAHOTA AND B. S. SOOD,

Physics Department, Punjabi University, Patiala.

(Received January 28, 1969)

The internal conversion coefficient of the 412 keV transition in Hg^{198} has been determined by recording K—X-rays that follow internal conversions competing with the gamma rays, and the gamma rays with a $1'' \times 1''$ NaI (Tl) crystal scintillation spectrometer. The ratio of the effective photopeak efficiencies for 70 keV X-rays and 412 keV gamma rays has been determined by another experiment making use of Compton scattering.

662 keV gamma rays from a Cs^{137} source of nearly 200 mC strength were scattered from gold targets at an angle of 58° . The X-rays of energy 70.8 keV emerging from the target as a result of photoelectric interaction, and the Compton scattered gamma rays of energy 412 keV were recorded with the $1'' \times 1''$ NaI(Tl) detector which was later used to determine α_K in Hg^{198} . The ratio of K—X-rays and the Compton scattered gamma rays as measured under the photopeaks of the spectrum of radiation emerging from the target is given by the relation.

$$N_x/N_c = \sigma_{p, \text{eff}} / \sigma_c(\theta) \rho_{\text{eff}} / \rho_{\text{eff}_c} \epsilon_x A_x \omega_x I_x / \epsilon_\gamma A_\gamma \quad \dots (1)$$

where $\sigma_{p, \text{eff}}$ and $\sigma_c(\theta)$ are the photoelectric (K-shell) and Compton scattering cross sections for 662 keV gamma rays in gold, ρ_{eff} is the effective thickness of the target which takes into account the absorption in the target of the radiation incident on and emerging from the target. ρ_{eff_c} was determined experimentally and has been explained in an earlier paper (Ghumman 1967). The value of ρ_{eff_c} was calculated since in this case the absorption coefficients are known with an accuracy of better than two per cent. $\sigma_{p, \text{eff}}$ was extrapolated from the tables of Hubbel & Berger 1966). From a number of runs the value of the factor

$\epsilon_x A_x / \epsilon_\gamma A_\gamma \omega_x I_x$ was known from equation (1).

The target was then replaced by a weak Au^{198} source which emits K X-rays due to internal conversion in Hg^{198} and X-rays of 412 keV (~ 98 per cent) and the spectrum was taken in the same geometry. Since the energies of the Compton scattered gamma rays and K—X-rays of gold are almost the same as the energies of gamma rays and X-rays from the small source the value of the factor $\epsilon_\gamma A_\gamma / \epsilon_x A_x \omega_x I_x$ may be assumed the same in both the cases. The value of α_K is calculated from the following relation:

$$\alpha_K = \frac{N_K}{N_\gamma} \cdot \frac{\epsilon_\gamma A_\gamma}{\epsilon_K A_K I_{K\omega_K}} \quad \dots(2)$$

and comes out to be $.0311 \pm .0012$ which has been compared with the theoretical values of Rose (1958) and of Sliv & Band (1965) and experimental values of different workers using different techniques in table 1.

TABLE 1

γ -ray energy (keV)	X-ray energy (keV)	α_K	Reference	Method
411.8	70.8	$.0282 \pm .0010$	(Hamilton 1962)	PBS
		$.0285 \pm .0015$	(DeVries 1961)	IEC
		$.0305 \pm .0010$	(Pettersen 1961)	IEC
		$.03035 \pm .00045$	(Lewin 1963)	β_e
		$.0299 \pm .0005$	(Lewin 1963)†	β - γ Coinc.
		$.0308 \pm .0009$	(Pettersen 1965)	γ - γ Ang. Corr.
		$.0311 \pm .0012$	Authors.	X/ γ
		.0302	(Rose, 1958)	Theoretical.
		.0298	(Sliv and band 1965)	Theoretical.

From a study of the known experimental values of α_K for the 412 keV transition in Hg^{198} we find that the X/ γ method has not been employed to determine the value for internal conversion coefficient of this transition probably due to the presence of two more gamma rays of energies 690 keV (nearly one per cent) and 1.09 Mev (nearly 0.2 per cent). The photoelectric effect is very sensitive to energy and the intensities of these transitions are very small. The estimated contribution to K-X-rays from 690 keV γ -rays will be less than 0.7 per cent. A similar argument holds for the X-rays following internal conversions. So α_K in Hg^{198} is practically due to 412 keV transition.

REFERENCES

- Ghumman, B. S. & Sood, B. S. 1966 *Indian J. Phys.* **41**, 737.
 Hamilton, J. H., Stockendal, R. V., Camp, D. C., Langer, L. M. & Smith, D. R. 1962 *Nucl. Phys.* **36**, 567.
 De Vries, C., Blecker, E. J. & Mrs. Salomons Grobben, N. 1960 *Nucl. Phys.* **18**, 454.
 Pettersen, B. G., Thun, J. E. & Gerholm, T. R. 1961, *Nucl.* **24**, 243.
 Lewin, W. H. G., Van Nooijen, B., Van Eijk, C. W. E., & Wapstra, A. H. 1963 *Nucl. Phys.* **48**, 159.
 Pettersen, B. G., Holmberg, L. & Gerholm, T. R. 1965 *Nucl. Phys.* **65**, 454.
 Rose M. E. 1958 *Internal Conversion Coefficients*, (North Holland Publ. Co. Amsterdam).
 Sliv, L. A. & Band, I. M. 1965 *Tables of Internal Conversion Coefficients*. Alpha, Beta Gamma Ray Spectroscopy Ed. Kie Siegbahn.

Attenuation of low energy gamma rays in alloys

By J. RAMA RAO, K. PARTHASARADHI, A. LAKSHMANA RAO
AND P. V. RAMANA RAO

The Laboratories for Nuclear Research, Andhra University, Waltair, India,

(Received February 8, 1968)

With the increasing use of gamma active isotopes in industry, medicine and agriculture, it is becoming necessary to study the absorption of gamma radiation in various materials. While the absorption in elements is widely studied, very few attempts (e.g. Rama Rao *et al* (1961) seem to have been made to measure the attenuation of gamma rays in alloys and compounds. In the work by Rama Rao *et al* (1961) one of the present authors determined the total cross-sections for a few alloys and compounds at two gamma energies and compared the results with the predictions of an approximate theory based on several assumptions. No further measurements, particularly, at lower photon energies, seem to have been reported so far. Furthermore, with the availability of more accurate theoretical cross-sections it now becomes possible to make a meaningful comparison between theory and experiment. Hence the present investigations are undertaken selecting two platinum-rhodium alloys having the composition, Alloy A: Pt 80% + Rh 20%; Alloy B: Pt 60% + Rh 40%, and gamma rays of energies 84, 100 and 280 keV provided by radioactive isotopes Tm^{170} , Gm^{153} and Hg^{203} respectively.

The isotopes of strength about 10 mC each, are obtained from the Bhabha Atomic Research Centre, Bombay, India. The total gamma ray cross-sections for the two alloys are determined following the same procedure as adopted earlier on a good geometry set up by Lakshminarayana *et al* (1961). The theoretical values of the cross-section for the two alloys at the three photon energies are computed making use of the theoretical sum rule and the total gamma ray cross-section in Pt and Rh taken from the recently compiled data of Plechaty (1968). The experimental and the compiled values are given in table 1.

It can be seen from table 1 that there is excellent agreement between the compiled and experimental values at 280 keV. The agreement is not so good at 100 keV and there is definite deviation at 84 keV beyond the ascribed errors. It may be also noted that the deviation is more for alloy A which contains larger proportion of Pt. These two observations indicate that the discrepancy might be due to an overestimation of photoelectric cross-section which forms a dominant part of the total cross-section for heavy elements and low energies.

TABLE 1. TOTAL GAMMA RAY CROSS SECTIONS IN
ALLOYS BARNS PER ATOM

Energy keV	Alloy A Pt80% + Rh20%	Alloy B Pt60% + Rh40%
84 Experimental :	1580 \pm 80	1160 \pm 58
Values of Plechaty :	1785 \pm 18	1275 \pm 13
100 Experimental :	1070 \pm 54	773 \pm 36
Values of Plechaty :	1147 \pm 12	825 \pm 8
280 Experimental :	97.5 \pm 1.9	72.7 \pm 1.5
Values of Plechaty :	97.6 \pm 1.0	73.8 \pm 0.7

TABLE 2. EFFECTIVE ATOMIC NUMBERS FOR TOTAL
GAMMA RAY INTERACTION

Energy keV	Alloy A	Alloy B
84	69.5 \pm 1.0	63. \pm 1.0
100	70.0 \pm 1.0	63. \pm 1.0
280	69. \pm 1.0	62.5 \pm 1.0

The effective atomic numbers for the two alloys at each energy are deduced from plots between the total atomic cross-section versus atomic number for elements at each energy, employing the earlier results of Ramana Rao *et al* (1969), Parthasaradhi *et al* (1969) in press and Rama Rao (Ph.D. Thesis, 1964). These values are given in table 2. According to Hine (1952) the effective atomic number for total gamma ray interaction in alloys can not be represented by a single number and for each partial process the number has to be determined separately. However, from table 2 it may be noted that the number remains constant at these three energies. This may be due to the fact that the number for total interaction is mostly dominated by the number for photoelectric process in the present region of energy since most of the cross-section contribution to the total is due to that of photoelectric effect. Even though a little variation exists, it lies within the error limits of the present values.

REFERENCES

- Hine G. J. 1952, *Nuclonics* 10, 9.
 Lakshminarayana, V. & Jnanananda, S. 1961, *Proc. Phys. Soc. London* 77, 593.
 Plechaty E. L. 1968 *Photon Cross-Sections (Compilation)* Scientific Information Systems Group
 Lawrence Radiation Laboratory.
 Rama Rao, J. Lakshminarayana, V. & Jnanananda, S. 1963 *Jour. of Sci. Indus. Res.*
 20B, 587.
 Rama Rao, J. 1964, *Ph. D. Thesis*.
 Ramana Rao, P. V. Visweswara Rao, V. Rama Rao, T. & Parthasaradhi, K. 1969,
Nuovo Cimento, 1 311.
 Parthasaradhi, K., Rama Rao, J. & Ramana Rao, P. V. 1969 *Jour. of Phys. A* 2, 245

Absolute photoelectric cross sections of 800 keV gamma rays

By M. RAJA RAO, K. PARTHASARADHI AND SWAMI JNANANANDA

The Laboratories for Nuclear Research, Andhra University, Waltair, India.

(Received January 11, 1964)

The photoelectric cross-sections of 800 keV gamma rays in Au and Ta are measured by the internal external conversion technique. These values are found to be in satisfactory agreement with the recently reported theoretical values of Schmickley & Pratt (1967) within the range of errors.

Direct experimental studies on absolute photoelectric cross-sections are restricted to gamma energies below 662 keV and above 1 MeV only. Very accurate theoretical total photoelectric cross-sections are recently reported by Schmickley & Pratt (1967). In the present investigations absolute photoelectric cross-sections of 800 keV gamma rays in Au and Ta are determined for the first time utilising plastic phosphor scintillation detector and employing the internal external conversion technique.

A gamma source ^{134}Cs in liquid form is obtained from the Bhabha Atomic Research Centre, Bombay. Although the gamma ray spectrum from this source is complex, most of the gamma lines are quite weak in intensity, compared to 605 and 766 keV lines. There is another weak line of energy 802 keV very close to 796 keV line. These two lines cannot be resolved by a scintillation spectrometer and for all practical purposes a combination of these lines is treated as a gamma ray of energy 800 keV. Foils of diameter 3/8 inch and thicknesses 14.8 mg/cm² (Au) and 17.6 mg/cm² (Ta) are used. The experimental details and the method of evaluation of the photoelectron intensity and the gamma ray intensity are described in earlier publications (Raja Rao *et al* 1965, 1968). A well-type plastic phosphor of sufficient depth to detect the photoelectrons is used. The internal conversion coefficient measured by a comparison method by Trehan *et al* (1963) is employed for calculating the gamma intensity.

The obtained experimental total photoelectric cross-sections in Au and Ta are 8.3 ± 1.0 and 5.3 ± 0.6 barns per atom and the corresponding theoretical values of Schmickley & Pratt (1967) respectively are 8.3 and 5.6 barns per atom. It can be seen that there is satisfactory agreement between theory and experiment within the range of errors.

REFERENCES

- Raja Rao, M. & Jnanananda, Swami 1965 *Nuclear Instruments & Methods*, **36**, 261.
Raja Rao, M. K. Parthasaradhi & Jnanananda, Swami 1968 *Current Science* **37**, 401.
Trehan, P. N. French, J. D. & Goodich, M. 1963 *Phys. Rev.* **131**, 2625.
Schmickley R. D. & Pratt, R. H. 1967 *Phys. Rev.* **164**, 104.

BOOK REVIEWS

Directory of Scientific Instruments and Components Manufactured in India.

Published by Central Scientific Instruments Organization Sector-30, Chandigarh-20,
Price Rs. 30.00

We congratulate Dr. P. S. Gill, Director of the above Institution for bringing out this monumental work. The painstaking labour and organization behind this Directory can easily be understood on going through it. The Directory has filled a much felt need for the users of scientific and technical instruments. The compilation has been very thorough and leaves apparently very little to be desired. Indeed, it was a pleasure to find that so many things of scientific interest are obtainable in this country, only we are not sure how many of these can attain the specifications and needs of scientific research. "The proof of the pudding is in the eating" as the old adage goes, but that does not in any way reduce the credit of the compilers. We have no doubt that all scientific workers of the country will make considerable use of this Directory.

A. B.

Lectures in Theoretical High Energy Physics.

Ed. H. H. Aly John Wiley & Sons Ltd. Price \$ 17.50

This is a collection of thirteen articles by various authors on diverse aspects of Particle Physics. The articles differ vastly in their scope and content. Some of them are reviews while others present new ideas.

Sudarshan gives a brief history of Weak Interaction Theory culminating in the discovery of the V-A interaction and then discusses a theory in which the weak and electromagnetic interactions of hadrons are induced by the direct couplings of the vector and axial vector mesons. There are two articles on the P, C, T symmetries. Nilsson's article is a detailed treatment of invariance principles, especially P, C and T. Taylor deals with the problem of defining a discrete symmetry operator when it is not an exact symmetry and also discusses a magnetic monopole model for CP violation.

Pietschmann chooses two of the important results of current algebra, namely the Adler-Weissberger sum rule and the soft-pion theorem for the leptonic K decays and carries out the calculations completely for the benefit of beginners in the field. Moffat proposes a theory in which the violation of chiral $SU(3) \times SU(3)$ symmetry is due to non-Riemannian space-time geometry associated with a non-symmetrical affine connexion $\Gamma_{\mu\nu}^{\lambda}$.

Two papers deal with the quark model. Riazuddin and Sarker consider two applications of quark model, namely, the electromagnetic and strong decays of hadrons and the high energy cross section relations and then go on to discuss a theory in which the scalar and pseudoscalar densities $\bar{q} \gamma_1 q$ and $\bar{q} \gamma_5 \gamma_1 q$ determine the medium strong and electromagnetic mass differences as well as the non-leptonic weak decays. Uretsky builds up the mesons as quark-antiquark states and discusses the resulting meson spectroscopy.

The topic of composite particles in field theory is discussed in three articles. Taylor deals with bootstraps in field theory while Hagen discusses the $Z=0$ rule in various models and extends this rule to the multiparticle and virtual state situations. Lurie gives a very readable account of the Haag-Nishijima-Zimmerman analysis concerning the arbitrariness in the choice of interpolating fields and the construction of composite particle fields.

The subject of inelastic N/D equations is covered by Warnock who deals with Levinson's theorem, behaviour of partial waves at infinity in Regge theory, the Fredholm character of N/D equations etc. and then discusses a specific proposal for dynamical calculations. Potential scattering is discussed by Ali and Muller. The former considers upper bounds and analyticity properties while the latter presents a perturbation approach for any non-singular potential.

These topics were originally delivered as lectures at the American University of Beirut. Since Particle Physics is a rapidly changing field, the reader would expect to know the year in which the lectures were delivered, but the book makes no mention of that.

G. R.

Circular regions under uniform pressures in second order elasticity

By D. PANDE AND G. S. DUBE

Christ Church College and V. S. S. D College

Kanpur University, Kanpur, India,

(Received 3 January 1969)

Three problems concerning isotropic, compressible materials have been solved. These are (i) an infinite isotropic, compressible medium with a circular hole subjected to a uniform internal pressure, (ii) an isotropic, compressible finite disc subjected to uniform compression at the boundary and (iii) an elastic circular misfitting inhomogeneity in an infinite isotropic, compressible matrix. Second order elastic effects in the elastic fields for all the three cases have been evaluated in terms of complex coordinates in the initial configurations. The results obtained reveal the influence of the elastic properties of the materials to a greater extent than those obtained in the case of infinitesimal elasticity. These problems also illustrate the very important feature of second order elasticity in which the undeformed and deformed configurations are different from each other.

INTRODUCTION

The complex variable methods, as developed by Muskhelishvili (1963), and others have been usefully employed in solving problems in infinitesimal elasticity. The technique mainly consists in expressing the entire elastic field in terms of a scalar function ϕ , called the Airy's stress function. This function is expressible in terms of a set of two potential functions which are evaluated with the help of given conditions of the problem. For the second order elasticity case Airy's stress function is expanded as power series of a parameter which depends upon the physical conditions of the problem. This leads to an additional set of two potential functions. The earlier works of Adkins *et al* (1953, 1954) and more recent works of Bhargava & Pande (1964, 1966, 1967) have developed some techniques of evaluating these sets of potential function. The techniques suggested by Adkins *et al* have limited applications. Bhargava & Pande, having developed the techniques, have only concerned themselves with the deformed state of the body ignoring the undeformed state. In the present paper the problems have been solved using the configuration. The work of this paper and that of Bhargava & Pande clearly establishes the fact that in second order elasticity the initial and final configurations are distinct from each other unlike the case of infinitesimal elasticity. A brief account of the mathematical preliminaries is essential and is given below.

Let the point $P_0(x_1, x_2)$ of a body B_0 in the undeformed state be displaced to $P(y_1, y_2)$ of B , the body in the deformed state, when referred to a fixed, plane Cartesian frame of reference.

In complex coordinates let

$$\left. \begin{aligned} \zeta &= x_1 + i x_2 & \text{and } z &= y_1 + i y_2 \\ \bar{\zeta} &= x_1 - i x_2 & \text{and } \bar{z} &= y_1 - i y_2 \end{aligned} \right\} \quad (1)$$

Let the displacement vector $D(u_1, u_2)$ be the complex function

$$D = u_1 + i u_2 \quad (2)$$

$$\text{Hence,} \quad z = \zeta + D \quad \text{and} \quad \bar{z} = \bar{\zeta} + \bar{D} \quad (3)$$

In the absence of body forces the equilibrium equations are satisfied if

$$T^{11} = T^{-22} = -4 \frac{\partial^2 \phi}{\partial \zeta^2} \quad \text{and} \quad T^{12} = 4 \frac{\partial^2 \phi}{\partial \zeta \partial \bar{\zeta}} \quad (4)$$

where $T^{\alpha\beta}$ are the complex stress components in deformed state and $T^{11} = T^{-22} = p_{x_1 x_1} - p_{x_2 x_2} + 2i p_{x_1 x_2}$ and $T^{12} = p_{x_1 x_1} + p_{x_2 x_2}$ (5)

$p_{\alpha\beta}$ being the stress components in Cartesian coordinates. When the resultant force along the boundary is zero,

$$\frac{\partial \phi}{\partial \zeta} = \frac{\partial \phi}{\partial \bar{\zeta}} = 0 \quad (6)$$

The Airy's stress function ϕ and the displacement function D , being analytic functions of ζ and $\bar{\zeta}$, may be expanded in powers series of a real parameter ϵ . Thus

$$\phi(\zeta, \bar{\zeta}) = \mu \epsilon [\phi_0(\zeta, \bar{\zeta}) + \epsilon \phi_1(\zeta, \bar{\zeta}) + \epsilon^2 \phi_2(\zeta, \bar{\zeta}) + \dots] \quad (7)$$

$$D(\zeta, \bar{\zeta}) = \epsilon [D_0(\zeta, \bar{\zeta}) + \epsilon D_1(\zeta, \bar{\zeta}) + \epsilon^2 D_2(\zeta, \bar{\zeta}) + \dots] \quad (8)$$

The parameter ϵ is determined by the physical conditions of the problem. The first term of the expansions (7) and (8), namely ϕ_0 and D_0 , pertain to the infinitesimal elasticity case. These are completely determined in terms of the potential functions $\Omega(\zeta)$, $\omega(\zeta)$. The first two terms jointly give the second order effects in the elastic field. The functions ϕ_1 and D_1 are determinable in terms of two sets of potential functions $\{\Omega(\zeta), \omega(\zeta)\}$ and $\{\Delta(\zeta), \delta(\zeta)\}$.

Since only second order effects are being considered, the functions ϕ_0, D_0, ϕ_1, D_1 , alone in the expansions (7) and (8) are valid in the present case.

It is known that (Gresen & Zerna 1954),

$$\phi_0(\zeta, \bar{\zeta}) = \bar{\zeta} \Omega(\zeta) + \zeta \bar{\omega}(\bar{\zeta}) + \bar{\omega}(\bar{\zeta}) + \omega(\zeta), \quad (9)$$

$$D_0(\zeta, \bar{\zeta}) = \kappa \Omega(\zeta) - \zeta \bar{\omega}'(\bar{\zeta}) - \bar{\omega}'(\bar{\zeta}) \quad (10)$$

where $\kappa = (\lambda + 3\mu) / (\lambda + \mu)$ for the plane strain and $\kappa = (5\lambda + 6\mu) / (3\lambda + 2\mu)$ for the plane stress, λ and μ being the Lamé's constants.

The functions $\Delta(\zeta)$ and $\delta(\zeta)$ can be evaluated from the equation

$$\begin{aligned} \frac{\partial \phi_1}{\partial \bar{\zeta}} = & \Delta(\zeta) + \zeta \Delta'(\bar{\zeta}) + \bar{\delta}'(\bar{\zeta}) + (\gamma - 1) \Gamma(\zeta, \bar{\zeta}) \\ & + (B_2/\kappa) \bar{\Omega}'(\bar{\zeta}) D_0(\zeta, \bar{\zeta}) + k_1 \int_{\bar{\zeta}}^{\bar{\zeta}} \bar{\Omega}'(\bar{\zeta}) \bar{\omega}'(\bar{\zeta}) d\bar{\zeta} \\ & + \kappa_1 \int [\Omega'(\zeta)]^2 d\zeta + k_2 \zeta [\bar{\Omega}'(\bar{\zeta})]^2 \end{aligned} \quad (11)$$

The displacement function $D_1(\zeta, \bar{\zeta})$ is given by

$$\begin{aligned} D_1(\zeta, \bar{\zeta}) = & \kappa \Delta(\zeta) - \zeta \bar{\Delta}'(\bar{\zeta}) - \bar{\delta}'(\bar{\zeta}) - (\gamma - 1) \Lambda(\zeta, \bar{\zeta}) \\ & - (B_2/\kappa) \bar{\Omega}'(\bar{\zeta}) D_0(\zeta, \bar{\zeta}) + k'_1 \int_{\bar{\zeta}}^{\bar{\zeta}} \bar{\Omega}'(\bar{\zeta}) \bar{\omega}'(\bar{\zeta}) d\bar{\zeta} \\ & + k'_2 \int [\Omega'(\zeta)]^2 d\zeta + k'_3 \zeta [\bar{\Omega}'(\bar{\zeta})]^2 \end{aligned} \quad (12)$$

$$\begin{aligned} \text{where } \Gamma(\zeta, \bar{\zeta}) = & [\zeta \bar{\Omega}'(\bar{\zeta}) + \bar{\omega}'(\bar{\zeta})] [\bar{\zeta} \Omega'(\zeta) + \omega'(\zeta) - \kappa \bar{\Omega}(\bar{\zeta})] \\ & + [\Omega'(\zeta) + \bar{\Omega}'(\bar{\zeta})] [\zeta \bar{\Omega}'(\bar{\zeta}) + \bar{\omega}'(\bar{\zeta}) - \kappa \Omega(\zeta)] \end{aligned} \quad (13)$$

$$\begin{aligned} \text{and } \Lambda(\zeta, \bar{\zeta}) = & [\zeta \bar{\Omega}'(\bar{\zeta}) + \bar{\omega}'(\bar{\zeta})] [\bar{\zeta} \Omega'(\zeta) + \omega'(\zeta) - \kappa \bar{\Omega}(\bar{\zeta})] \\ & - [\kappa \Omega'(\zeta) - \bar{\Omega}'(\bar{\zeta})] [\zeta \bar{\Omega}'(\bar{\zeta}) + \bar{\omega}'(\bar{\zeta}) - \kappa \Omega(\zeta)] \end{aligned} \quad (14)$$

The constants involved in (11) and (12) have been defined in Appendix. Further, of the two sets of constants k_i and k'_i in (11) and (12) respectively, one may be taken to be zero and the other be evaluated with the help of equations given in the Appendix. For example k_i may taken to be zero in the case of first boundary value problem while in the case of the second boundary value problem it is useful to take k'_i to be zero.

To ensure uniqueness and single-valuedness of ϕ and D the functions $\Omega(\zeta)$, $\omega(\zeta)$, $\Delta(\zeta)$ and $\delta(\zeta)$ must satisfy the following conditions :

$$[\Omega'(\zeta)]_c = 0; [\bar{\omega}'(\bar{\zeta})]_c = 0; [\kappa \Omega(\zeta) - \bar{\omega}'(\bar{\zeta})]_c = 0 \quad (15)$$

$$[\Delta'(\zeta)]_c = 0; [\bar{\delta}'(\bar{\zeta})]_c = 0;$$

$$[\kappa \Delta(\zeta) - \bar{\delta}'(\bar{\zeta})]_c = -[k'_1 \int_{\bar{\zeta}}^{\bar{\zeta}} \bar{\Omega}'(\bar{\zeta}) \bar{\omega}'(\bar{\zeta}) d\bar{\zeta} + k'_2 \int [\Omega'(\zeta)]^2 d\zeta]_c = 0 \quad (16)$$

where $[]_c$ denotes the cyclic change in the function within the parenthesis while going once round the contour C lying entirely within the deformed state of the body.

With the evaluation of the functions $\Omega(\zeta)$, $\omega(\zeta)$, $\Delta(\zeta)$, $\delta(\zeta)$ and the determination of ϵ from the physical conditions the equations (7) - (12) along with (4) and (5) determine the elastic field completely in terms of Cartesian coordinates in the undeformed state of the body.

PROBLEM 1. INFINITE COMPRESSIBLE MEDIUM WITH A CIRCULAR HOLE UNDER UNIFORM RADIAL PRESSURE.

Let a homogeneous, isotropic, compressible infinite medium have a circular hole in it. Let the equation of the circular boundary in complex coordinates be

$$|\zeta| = R \quad (17)$$

Further let this circular boundary be subjected to a uniform radial pressure P . Due to the pressure, deformations would set in. It is proposed to investigate the stress and displacement fields in the medium with the help of the technique outlined above.

It is known that the transformation

$$\zeta = \frac{R}{\zeta_1} \quad (18)$$

maps the region interior to the circular hole onto the region $|\zeta_1| > 1$ and the region $|\zeta| > R$ is mapped onto the region $|\zeta_1| < 1$. The circular boundary coincides with the boundary of the unit circle $|\sigma| = 1$ where σ is the value of ζ_1 on the boundary of the unit circle. Obviously,

$$\sigma = e^{-i\theta} \quad (19)$$

θ , $Re^{i\theta}$ measured positive in the clockwise direction, maps the boundary $\zeta = Re^{i\theta}$, θ_1 measured positive in the counter clockwise direction. With the introduction of the transformation (18), the functions Ω , ω , Δ and δ will become functions of ζ_1 . Thus

$$\left. \begin{aligned} \Omega(\zeta) &= \Omega\left(\frac{R}{\zeta_1}\right) = \Omega_1(\zeta_1), \\ \omega(\zeta) &= \omega\left(\frac{R}{\zeta_1}\right) = \omega_1(\zeta_1), \\ \Delta(\zeta) &= \Delta\left(\frac{R}{\zeta_1}\right) = \Delta_1(\zeta_1), \\ \delta(\zeta) &= \delta\left(\frac{R}{\zeta_1}\right) = \delta_1(\zeta_1). \end{aligned} \right\} \quad (20)$$

The values of Ω_1 and ω_1 are known (Sokolnikoff 1956). They are

$$\left. \begin{aligned} \Omega_1(\zeta_1) &= 0 \\ \omega_1'(\zeta_1) &= -\frac{PR\zeta_1}{2} \end{aligned} \right\} \quad (21)$$

Choosing $\epsilon = -\frac{1}{\mu}$, and taking $k_1 = k_2 = 0$, the equation (11) on the boundary of the unit circle yields

$$\begin{aligned} \Delta_1(\sigma) - \frac{1}{\sigma^3} \bar{\Delta}_1'(\bar{\sigma}) + \bar{\delta}_1'(\bar{\sigma}) + (\gamma-1)I(\sigma, \bar{\sigma}) \\ + (B_3 | \kappa) \bar{\Omega}'(\bar{\sigma}) U_0(\sigma, \bar{\sigma}) + k_3 \frac{R}{\sigma} \left\{ \Omega'(\bar{\sigma}) \right\}^2 = 0 \end{aligned} \quad (22)$$

Making appropriate substitutions, the equation (22) becomes

$$\Delta_1(\sigma) - \frac{1}{\sigma^3} \bar{\Delta}_1'(\bar{\sigma}) + \bar{\delta}_1'(\bar{\sigma}) = \frac{(\gamma-1)P^2 R}{4\sigma} \quad (23)$$

On integration, the values of $\Delta_1(\xi_1)$ and $\bar{\delta}_1'(\xi_1)$ are found to be

$$\left. \begin{aligned} \Delta_1(\xi_1) &= 0. \\ \bar{\delta}_1'(\xi_1) &= \frac{(\gamma-1)P^2 R \xi_1}{4} \end{aligned} \right\} \quad (24)$$

Thus $\Omega(\xi)$, $\omega(\xi)$, $\Delta(\xi)$, $\delta(\xi)$ and ϵ being known, complete stress field is obtained from equations (4), (7), (9) and (11). Thus, making appropriate substitutions and changing into polar coordinates the stresses at any point in the medium are found to be

$$p_{rr} = \frac{-PR^2}{r^2} + \frac{(\gamma-1)P^2 R^2}{2\mu r^2} \left[\frac{R^2}{r^2} - \left(\frac{2R^2}{r^2} - 1 \right) \right] \quad (25)$$

$$p_{\theta\theta} = \frac{PR^2}{r^2} + \frac{(\gamma-1)P^2 R^2}{2\mu r^2} \left[\frac{R^2}{r^2} + \left(\frac{2R^2}{r^2} - 1 \right) \right], \quad (26)$$

$$p_{r\theta} = 0. \quad (27)$$

The displacement field is obtained directly by making proper substitutions in (8), (10), and (12). On changing into polar coordinates the displacements are

$$\left. \begin{aligned} u_r &= \frac{PR^2}{2\mu r} \left\{ 1 - \frac{(\gamma-1)P}{2\mu} \left(1 - \frac{R^2}{r^2} \right) \right\} \\ u_\theta &= 0. \end{aligned} \right\} \quad (28)$$

An examination of the above results would prove that in the case of infinitesimal elasticity stresses are free from the Poisson's ratio but in the second order case, the Poisson's ratio does affect the hoop stress as is but natural. Secondly, though the second order effects for the displacements are zero at the inner boundary but at other points they are significant.

PROBLEM 2. CIRCULAR DISC UNDER UNIFORM COMPRESSION

Let a circular disc of homogeneous, isotropic compressible material and of radius a be subjected to a uniform compressible force Q along its boundary. Let the circular edge have the equation

$$|\zeta| = R_0 \quad (29)$$

in complex coordinates in the undeformed state. Due to compression along the boundary, deformations would set in. It is proposed to obtain the stresses and displacements in the disc due to deformation.

The transformation

$$\zeta = R_0 \zeta_1 \quad (30)$$

gives an isomorphic mapping of $|\zeta| = R_0$ onto the unit circle $|\sigma| = 1$ where σ is the value of ζ_1 on the boundary of the unit circle.

It is known (Sokolnikoff 1956) that

$$\Omega(\zeta) = -\frac{Q\zeta}{4}, \quad \omega'(\zeta) = 0 \quad (31)$$

Taking $\epsilon = 1/\mu$ and following the procedure adopted in problem 1 solved above, the functions $\Delta(\zeta)$, $\delta'(\zeta)$ are found to be

$$\Delta(\zeta) = [2(\gamma-1)(\kappa-1) + (B_1-B_3)] \frac{Q^2\zeta}{32}, \quad \delta'(\zeta) = 0 \quad (32)$$

The functions $\Omega(\zeta)$, $\omega(\zeta)$, $\Delta(\zeta)$, $\delta(\zeta)$ being evaluated and ϵ being known in the medium, the stresses at any point in the medium in polar coordinates are found to be

$$\left. \begin{aligned} p_{rr} &= -Q \\ p_{\theta\theta} &= -Q \\ p_{r\theta} &= 0 \end{aligned} \right\} \quad (33)$$

Similarly the displacements are

$$\left. \begin{aligned} u_r &= -\frac{QR_0}{4\mu} \left[(\kappa-1) - \frac{(\kappa+1)QB_1}{8\mu} \right] \\ u_\theta &= 0 \end{aligned} \right\} \quad (34)$$

It will be seen that though at the boundary, for the stresses $p_{rr} = p_{\theta\theta} = -Q$, but at any point the pressures significantly differ from those in the case of classical elasticity. The same is true for displacements.

PROBLEM 3. CIRCULAR INHOMOGENEITY IN AN INFINITE ELASTIC MEDIUM

Using the results found above a very important problem obtaining in various technological and metallurgical processes can be solved. It is the problem of circular inhomogeneity in an infinite elastic matrix. Let

an isotropic, elastic circular disc of radius $a(1+\delta)$, δ being within elastic limits, be squeezed and inserted into another isotropic elastic, infinite medium with a circular hole of radius a . Let the infinite medium, called matrix, be of a different material. Due to pressure of the matrix the inserted disc, called inclusion, does not attain the free configuration and the boundaries of both the inclusion and the matrix deform. On physical grounds, the equilibrium boundary will be a concentric circle of radius, say $a(1+\epsilon_0)$, ϵ_0 also being within elastic limits. It is supposed that no relative slipping takes place along the equilibrium boundary. The whole system may be taken to be welded along the equilibrium boundary. Due to deformations, stresses and strains will develop in the bodies. Let p be the common pressure along the equilibrium interface. The solution lies in evaluating ϵ_0 which gives the equilibrium position of the system. The equilibrium pressure and the hoop stresses have been calculated.

In the case of inclusion the displacements along the equilibrium boundary are given by equation (34). They are

$$u_{r,i} = -\frac{pa(1+\epsilon_0)}{4\mu_i} \left[(\kappa_i - 1) - \frac{(\kappa_i + 1)pB_{1i}}{8\mu_i} \right], \quad u_{\theta,i} = 0. \quad (35)$$

For the matrix, equation (28) gives

$$u_{r,m} = \frac{pa(1+\epsilon_0)}{2\mu_m}, \quad u_{\theta,m} = 0. \quad (36)$$

In the present problem $u_{r,i} = -a(\delta - \epsilon_0)$ and $u_{r,m} = a\epsilon_0$.

$$\text{Hence,} \quad u_{r,i} = -a(\delta - \epsilon_0) \quad (37)$$

$$u_{r,m} = a\epsilon_0. \quad (38)$$

Eliminating p from (35) and (36), the following quadratic equation in ϵ_0 is obtained.

$$\begin{aligned} & [B_{1i}(\kappa_i + 1)\mu_m^2 - 4\mu_i\mu_m(\kappa_i - 1) - 8\mu_i^2]\epsilon_0^2 \\ & - [4\mu_i\mu_m(\kappa_i - 1) + 8\mu_i^2(1 - \delta)]\epsilon_0 + 8\mu_i^3\delta = 0 \end{aligned} \quad (39)$$

This gives two values of ϵ_0 . One of these values is inadmissible on physical grounds because it makes the value of ϵ_0 less than -1 which means that radius of the equilibrium interface is negative. Thus ϵ_0 is found to be

$$\begin{aligned} & -\{2\mu_i^2(1 - \delta) + \mu_i\mu_m(\kappa_i - 1)\} \\ & + \{[2\mu_i^3(1 - \delta) + \mu_i\mu_m(\kappa_i - 1)]^2 \\ & + 4\mu_i^2\delta\{4\mu_i^2 + 2\mu_i\mu_m(\kappa_i - 1) + \mu_m^2A\}\}^{1/2} \\ \epsilon_0 = & \frac{\quad}{4\mu_i^3 + 2\mu_i\mu_m(\kappa_i - 1) + \mu_m^2A}. \end{aligned} \quad (40)$$

where $A = -\frac{1}{2}B_{1i}(\kappa_i + 1)$

Substituting for ϵ_0 in (38), p is found to be

$$p = \frac{3\mu_m \epsilon_0}{1 + \epsilon_0}. \quad (41)$$

Further $p_{\theta\theta}$ for the inclusion and the matrix are found from equations (33), (36) after substituting for $R_{,1}$, R and $\epsilon_{,1}$. Thus

$$p_{\theta\theta 1} = -p \quad (42)$$

$$p_{\theta\theta m} = p[1 + (\gamma - 1) \frac{p}{\mu}]. \quad (43)$$

The jump in hoop stresses is found to be

$$p_{\theta\theta m} - p_{\theta\theta 1} = p \left\{ 2 + (\gamma - 1) \frac{p}{\mu} \right\}. \quad (44)$$

The case when the inclusion and the matrix are of the same material can be obtained as special case from equation (40)–(44) by putting $\mu_1 = \mu_m$.

$$\text{Thus } \epsilon_0 = \frac{-(\kappa + 1) - 2\delta + \{[(\kappa + 1) - 2\delta]^2 + 4\delta\{2(\kappa + 1) + A\}\}^{1/2}}{2(\kappa + 1) + A} \quad (45)$$

Similarly for the linear elasticity case

$$\epsilon_0 = \frac{(\lambda + \mu)}{(\lambda + 2\mu)} \delta. \quad (46)$$

It will be found that the second order effects increase the radius of the equilibrium boundary and equilibrium pressure is reduced as compared to the infinitesimal case, which is consistent on the physical grounds. Hoop stress also diminishes in the second order case. The cases of rigid inclusion in an elastic matrix and elastic inclusion in a rigid matrix can be deduced from the results obtained here. In the former case $\epsilon_0 = \delta$ and in the latter case $\epsilon_0 = 0$. Again taking λ, μ to be zero, all the stresses and displacements are found to be zero in the case of cavity.

The authors are thankful to Prof. R. D. Bhargava, Department of mathematics of the Indian Institute of Technology, Kanpur for his general advice.

APPENDIX

Elastic constants involved in the problems.

$$\left. \begin{aligned} C_1 &= -\frac{2}{\mu} \left[\frac{\partial^3 W'}{\partial J_1^3} \right]_0; C_2 = -\frac{2}{\mu} \left[\frac{\partial^3 W'}{\partial J_1 \partial J_2} \right]_0 \\ C_3 &= -\frac{2}{\mu} \left[\frac{\partial^3 W'}{\partial J_3} \right]_0; C_4 = -\frac{2}{\mu} \left[\frac{\partial^3 W'}{\partial J_1^2} \right]_0 \end{aligned} \right\} \quad (A-1)$$

where $[]_0$ indicates the values of the function within the bracket when $J_i = 0$.

$$\left. \begin{aligned} B_1 &= \frac{6C_1 - 4C_2 - 7}{2C_1 - 1} \\ B_2 &= \frac{(2C_1 - 1)(4C_2 - 8C_1 + 1) - 12C_2 - 8C_4}{(2C_1 - 1)^2} \end{aligned} \right\} \quad (\text{A-2})$$

$$\left. \begin{aligned} B_1' &= B_1 - (\kappa + 1); B_1'' = \frac{1}{2} B' + B_1 \\ B_2' &= B_2 - \frac{1}{2} (\kappa + 1)^2; B_2'' = B_1 - \frac{2B_2}{\kappa + 1} \\ B_4 &= \frac{1}{2} B' - B_2'; \gamma = \frac{B_1}{\kappa + 1} \end{aligned} \right\} \quad (\text{A-3})$$

$$\left. \begin{aligned} k_1 + k_1' &= B_1'; k_2 - k_2' = \frac{B_2}{\kappa} - B_1 \\ \kappa k_2 - k_2' &= B_4; \kappa k_3 + k_3' = \kappa B_1'' - B_2 - B_4 \end{aligned} \right\} \quad (\text{A-4})$$

REFERENCES

- Adkins, J. E., Green, A. E. & Shield, R. T. 1953 *Phil. Trans. Roy. Soc.* A246, 181.
 Adkins, J. E., G. C. Green, A. E. & G. C. Nicholas 1954 *Phil. Trans. Roy. Soc.* A247, 279.
 Bhargava, R. D. & Pande, D. 1964, *J. Sci. & Eng. Res.* 8 (Pt.2)
 1966, *J. Sci & Eng. Res.* 10 (Pt.1)
 1966 *Acta Mech.*, 2.
 1967 *Ind. Jour. of Pure. & App. Phys.* 5, 552.
 Green, A. E. & Zerna, W. 1954 *Theoretical Elasticity*, Oxford.
 Muskhelishvili, N. I. 1963 *Some Basic Problems in Mathematical Theory of Elasticity*,
 P Noordhoff, Groningen (Holland).
 Sokolnikoff, I. S. 1956, *Mathematical Theory of Elasticity*, Mc Graw Hill.

New bands in the A-X system of CaF

By K. V. SUBBARAM AND D. RAMACHANDRA RAO

Department of Physics,

Indian Institute of Technology, Kanpur.

(Received 28 November 1968, Revised 31 January 1969,
and 31 March 1969)

[PLATE-5]

The $A_2\Pi-X^2\Sigma$ system of CaF which lies in the region 6300-5830Å is reinvestigated by exciting the CaF_2 sample in a 150V d.c. carbon arc at 6-12A current. More members were observed in each of the known sequences $\Delta v = -1, 0$ and $+1$.

INTRODUCTION

The A-X system of CaF obtained in carbon arc was investigated by Datta (1921), Johnson (1929) and Harvey (1931). Mohanty & Upadhy (1967) performed a part of the rotational analysis of the (0,0) band and obtained the rotational constants.

A reinvestigation of the spectrum with high current arc discharges showed about twenty new bands in the known sequences $\Delta v = -1, 0$ and $+1$.

EXPERIMENTAL

The spectrum was excited by burning CaF_2 salt in a carbon arc at 150V d.c. and 6-12A current and was photographed on a 3.4 meter Jaco grating spectrograph. The $\Delta v = 0$ and -1 sequences were photographed at a dispersion of 2.4Å/mm and the $\Delta v = +1$ sequence at about 0.95Å/mm. The exposure times varied from 2 to 4 minutes on Ilford R-40 plates. Iron arc was used as standard.

DISCUSSION

All the newly observed bands are shown in figure 1 duly marked. The band head data and vibrational analysis are presented in table 1. Good agreement was found between the observed bands and the calculated ones with the existing formulae.

$A_2\Pi_{3/2}-X^2\Sigma$ sub-system : In the $\Delta v = -1$ sequence, eight bands belonging to P_2 series were observed out of which none were reported by earlier workers and Q_2 series consists of four new bands. In $\Delta v = 0$ sequence, one extra band in Q_2 series and two extra bands in P_2 series were recorded. However, $\Delta v = +1$ sequence shows only Q_2 heads and appears as if it has originated at 5830Å and starts diverging towards longer wavelength side and all the band heads appear to be degraded to violet. Johnson's (1929) assignment starts from (4,3) and the head lies at 17145.6 cm^{-1} . This numbering

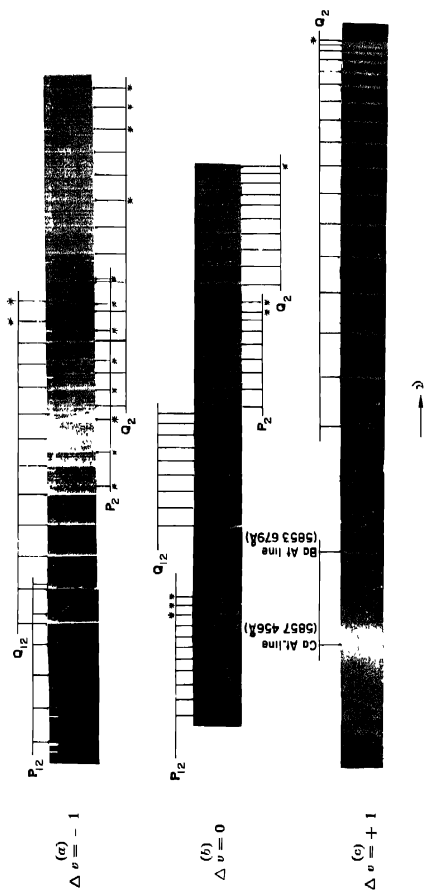


Figure 1. (a), (b), (c). Photograph showing $\Delta v = -1, 0$ and $+1$ sequences respectively of $A^2\Pi - X^2\Sigma$ system of CaF. Newly observed bands are marked *

1

100
100

TABLE 1. NEW EXPERIMENTAL DATA (IN cm^{-1}) AND VIBRATIONAL ANALYSIS

Q_1 Series	$\Delta v = -1$ $v' - v''$	Q_2 Series	$\Delta v = 0$ $v' - v''$	Q_3 Series	$\Delta v = +1$ $v' - v''$
$^2\Pi_{3/2} - ^2\Sigma$ sub-system.					
16050.0	7-8	16597.9	9-9	17146.1	1-0
75.1	10-11				
82.7	11-12				
90.2	12-13				
P_1 Series		P_2 Series			
15951.6	1-2	16552.3	7-7		
63.0	2-3	55.3	8-8		
74.0	3-4				
84.6	4-5				
96.1	5-6				
16004.3	6-7				
13.0	7-8				
21.8	8-9				
$^2\Pi_{1/2} - ^2\Sigma$ sub-system.					
Q_{12} Series		P_{12} Series			
16008.5	11-12	16457.6	8-8		
15.9	12-13	61.3	9-9		
		64.8	10-10		

was thought to be uncertain by Harvey (1931) since this end was not properly resolved and the first few Q_2 heads were supposed to be superposed. In the present work this portion of the spectrum is clearly resolved and it shows that the bands actually start from 17146.1 cm^{-1} . So, this is taken as (1,0) band of this sequence and subsequently the band at 17145.6 cm^{-1} becomes the (2,1) band and so on upto (17,16).

$^2\Pi_{1/2} - X^2\Sigma$ sub-system: The Q_{12} series in $\Delta v = -1$ sequence has two more bands and the band at 15865.6 cm^{-1} in P_{12} series is reassigned as (2,3) for consistency in the analysis. The P_{12} series in $\Delta v = 0$ sequence has three extra bands than observed by previous workers.

It has been possible to locate the new bands in the $\Delta v = 0$ sequence in the sub-systems from intensity considerations and expected positions of the band heads though they are weak and overlapped by fine structure of the preceding bands.

The red degraded bands listed in literature beyond the $\Delta v = +1$ sequence of the $^2\Pi_{3/2} - ^2\Sigma$ sub-system have not been well developed on our plates. Instead of the diffuse maximum with its centre at 5853.7\AA in the microphotometer trace given by Harvey (1931), a moderately intense sharp line at the same wavelength has been recorded on our plate 5, figure 1(c). This line is very probably due to an impurity of barium in the calcium salt.

Thanks are due to Mr. M. K. Narain who has helped during the course of investigation. Thanks are also due to Prof. Putcha Venkateswarlu for his kind interest in the work.

REFERENCES

- Datta, S. 1921 *Proc. Roy. Soc. (London)*. A. 99, 436
Harvey, A. F. 1931 *Proc. Roy. Soc. (London)*. A. 133, 336
Johnson, R. C. 1929 *Proc. Roy. Soc. (London)*. A. 122, 161
Mohanty, B. S. & Upadhyaya, K. N. 1967 *Indian Jour. of Pure and Appl. Phys.* 5, No. 11, 523

Excitation of atomic hydrogen in the Vainshtein approximation

By B. N. Roy*

Department of Mathematics, University of Durham

(Received 17 February 1969)

The post form of the Vainshtein approximation is used to calculate cross sections for the processes $H^+ + H(1s) \rightarrow H^+ + H(2s, 2p)$. It is found that the results agree with those of McCarroll & Salin (1966) who used the prior form of the Vainshtein approximation.

1. INTRODUCTION

The Born approximation gives good results at high energies of impact but its applications are limited at low and intermediate energies. The success of close coupling approximation has also been much less marked in determining inelastic cross sections. Vainshtein *et al* (1964) pointed out that the electron-electron repulsion plays a dominant role in the excitation process by electrons and they suggested to take account of this interaction explicitly. The Vainshtein approximation has been used for a large number of electron induced transitions in hydrogen and the alkali metals (Vainshtein *et al* 1964, 1965, Presnyakev 1965). McCarroll & Salin (1966) have carried out calculations of cross sections for the processes $H^+ + H(1s) \rightarrow H^+ + H(2s, 2p)$ using the prior form of the Vainshtein approximation. Here attempt has been made to carry out calculations of cross sections using the post form of the Vainshtein approximation for which the analysis is given by Coleman (1969).

2. THEORY

The cross section for direct excitation is

$$Q = \frac{1}{2\pi^2 v^3} \int_{q_{\min}}^{q_{\max}} |T_{if}|^2 q dq (\pi a_0^2) \quad \dots(1)$$

where $q = k_i - k_f$ is the momentum transfer vector and T_{if} is the transition matrix element $\langle \psi_f | V_f | \psi_i \rangle$. The limits of integration are $q_{\min} = k_i - k_f$ and $q_{\max} = k_i + k_f$ where k_f is determined by the equation $k_i^2 - k_f^2 = \mu \Delta E$

in which $\mu = \frac{M_1(M_2+1)}{M_1+M_2+1}$ is the reduced mass of the system (M_1 = mass of proton and M_2 = mass of nucleus of hydrogen atom) and ΔE the difference, in rydbergs, between the binding energies of the initial and final bound states. Vainshtein *et al* (1964) in their work on electron impact used a packing approximation and with the intention of reducing the

*Present address : Physics Department, L. S. College Muzaffarpur, Bihar, India.

error incurred in the region $s = 0$ by replacing $\phi(s)$ by $\phi(bq)$, replaced q by $-q$. For proton impact the same approximations give (Coleman 1969)

$$T_{if}^{(2)} = -Z_1 N_1(v_0) \phi(bq) I(v_0, b\mu, 0, av, q)$$

where Z_1 is the charge of the projectile,

$$|N_1(v_0)| = |\Gamma(1 + iv_0)|^2 = \frac{\pi v_0}{\sinh \pi v_0}$$

($v_0 = Z_1 v$, v = velocity of the projectile)

$$\phi(s) = \int \exp(is \cdot r) \phi_f^*(r) \phi_f(r) dr$$

$$a = \frac{M_1}{M_1 + 1}, \quad b = \frac{M_2}{M_2 + 1}$$

$$I(\nu, \kappa, 0, k, q) = \frac{4\pi}{T} \left(\frac{T - 2\alpha\delta}{T - 2\delta} \right)^{iv} {}_2F_1 \left[-iv, -iv, 1, z \right]$$

where $T = q^2$ and $\delta = -q \cdot k$.

In this case

$$z = \frac{a^2 b (q^2 + \mu \Delta E)^2}{\mu \left\{ q^2 \left(1 + \frac{a}{\mu} \right) + a \Delta E \right\} \left\{ q^2 (1 + ab) + ab \mu \Delta E \right\}} < 1$$

and

$$T_{if}^{(2)} = -\frac{4\pi}{q^2} Z_1 N_1(v_0) \phi(bq) X^{iv} {}_2F_1 \left[-iv, iv, 1, z, \right]$$

where

$$X = \frac{q^2(1 + ab) + ab\mu\Delta E}{q^2 \left(1 + \frac{a}{\mu} \right) + a\Delta E} \quad \dots(2)$$

For proton impact $a \simeq 1 \simeq b$, $\mu \gg 1$ and $z \simeq \frac{\Delta E}{q^2 + \Delta E}$, $X \simeq \mu z$.

For excitation $\Delta E > 0$ and X as defined by (2) is positive for all relevant values of q . The cross section obtained by using $T_{if}^{(2)}$ as an approximation to T_{if} in (1) is

$$Q^{(2)} = \frac{8Z_1^2}{v^2} \int_{q_{\min}}^{q_{\max}} \frac{dq}{q^3} |\phi(bq)|^2 |h(z, v_0)|^2$$

where

$$h(z, v_0) = \frac{\pi v_0}{\sinh \pi v_0} {}_2F_1 \left[-iv_0, iv_0, 1, z \right].$$

After some simplifications the cross sections for $2s$ and $2p$ excitations are

$$Q^{(1)}(s) = \frac{2^{12}\pi^2}{v^4(e^{\pi/v} - e^{-\pi/v})^2} \int_{q_{\min}}^{q_{\max}} \frac{q^2 dq}{(4q^2 + 9)^6} \left| {}_2F_1 \left[\frac{-i}{v}, \frac{i}{v}, 1, \frac{\Delta E}{q^2 + \Delta E} \right] \right|^2$$

and

$$Q^{(2)}(p) = \frac{2^{10} \times 9\pi^2}{v^4(e^{\pi/v} - e^{-\pi/v})^2} \int_{q_{\min}}^{q_{\max}} \frac{dq}{q(4q^2 + 9)^6} \left| {}_2F_1 \left[\frac{-i}{v}, \frac{i}{v}, 1, \frac{\Delta E}{q^2 + \Delta E} \right] \right|^2$$

$$\text{where } q_{\min} = k_i \left[1 - \left(1 - \frac{\mu \Delta E}{k_i^2} \right)^{1/2} \right]$$

3. RESULTS

The integration over q has been carried out numerically. In the present work z always lies in the range $0 < z < 1$. The series development of the hypergeometric function is given by

$${}_2F_1[a, b, c, x] = 1 + \frac{ab}{c}x + \frac{a(a+1)b(b+1)}{c(c+1)1 \times 2}x^2 + \dots \quad (3)$$

It has been found that convergence of this series is good for all relevant values of q and velocities of projectile used. In the present calculations the series expansion given by (3) is used and all the terms of the series are real.

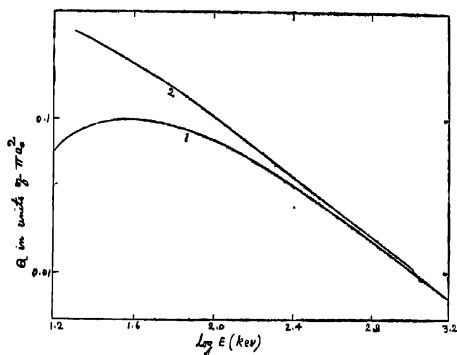
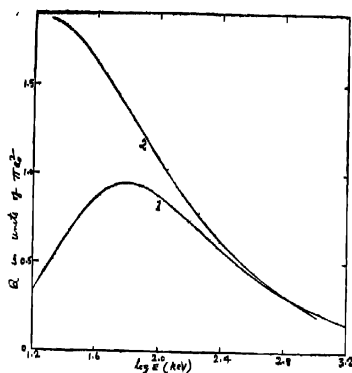


Figure 1. Cross sections for $H^+ + H(1s) \rightarrow H^+ + H(2s)$
Curve 1. Vainshtein approximation
Curve 2. Born approximation

Figure 2. Cross sections for $H^+ + H(1s) \rightarrow H^+ + H(2p)$

Curve 1. Vainshtein approximation

Curve 2. Born approximation

TABLE 1 CROSS SECTIONS FOR $H^+ + H(1s) \rightarrow H^+ + H(2s)$ EXCITATION IN UNITS OF πa_0^2

$E(\text{kev})$	Cross Section	$E(\text{kev})$	Cross section
16.0	6.26, - 2	156	5.36, - 2
25.0	9.04, - 2	225	4.05, - 2
36.0	9.92, - 2	400	2.48, - 2
42.2	9.90, - 2	624	1.65, - 2
56.2	9.36, - 2	899	1.17, - 2
63.9	8.96, - 2	1224	8.73, - 3
80.9	8.08, - 2	1599	6.74, - 3
99.9	7.20, - 2		

TABLE 2 CROSS SECTIONS FOR $H^+ + H(1s) \rightarrow H^+ + H(2p)$ EXCITATION IN UNITS OF πa_0^2

$E(\text{kev})$	Cross section	$E(\text{kev})$	Cross section
16.0	3.44, - 1	90.2	9.02, - 1
25.0	6.38, - 1	99.9	8.79, - 1
30.2	7.50, - 1	156	7.44, - 1
36.0	8.33, - 1	225	6.19, - 1
42.2	8.90, - 1	400	4.37, - 1
49.0	9.24, - 1	624	3.22, - 1
56.2	9.40, - 1	899	2.48, - 1
63.9	9.43, - 1	1224	1.96, - 1
72.2	9.36, - 1	1599	1.60, - 1
80.9	9.22, - 1		

4. DISCUSSION

It is clear from the figures that at high energies the Vainshtein approximation is in close agreement with the Born approximation. At lower energies the Vainshtein approximation cross sections are smaller than the corresponding Born approximation cross sections. The maxima are displaced considerably to higher energies as compared with the Born approximation results. It is found that the present results agree with those of McCarroll & Salin (1966) who used the prior form of the Vainshtein approximation. It is also found that in case of $1s \rightarrow 2p$ transition the Vainshtein approximation cross sections are slightly larger than the Born approximation cross sections at high energies. It is possible that the Vainshtein approximation results can be improved by introducing an effective charge (Vainshtein *et al* 1964, Crothers & McCarroll 1965).

The author wishes to express his sincere gratitude to Dr. J. P. Coleman for his valuable guidance. The author is also grateful to Bihar University for financial support.

REFERENCES

- Coleman, J. P. 1969 *Case Studies in Atomic Collision Physics*
E. W. McDaniel & M. R. C. McDowell, eds. (North Holland, Amsterdam).
Crothers, D. & McCarroll R. 1965 *Proc Phys. Soc.* **86**, 753.
McCarroll, R. & Salin, A. 1966 *Annales de Physique*, **1**, 283.
Presnyakov, L. 1965 *Soviet Physics J. E. T. P.*, **20**, 760.
Vainshtein, L., Presnyakov, L. & Sobelman, I. 1964 *Soviet Physics J. E. T. P.*, **18**, 1383.
Vainshtein, L., Opykhtin, V. & Presnyakov, L. 1965 *Soviet Physics J. E. T. P.*, **20**, 1942.

Note on the torsional vibration of a finite circular cylinder
of non-homogeneous material by a particular type of
twist on one of the plane surfaces.

By S. K. BISWAS

10, Broad Street, Calcutta-19.

(Received 19 May 1969)

In this paper the torsional vibration of a cylinder of finite length of non-homogeneous material has been considered. The rigidity and density vary exponentially with depth. One end of the cylinder is fixed while a periodic shearing force acts along the circumference of a circle on the other end.

1. INTRODUCTION

Mitra & Sen Gupta (1967) solved the problem of torsional oscillation set up in a semi-infinite circular cylinder of non-homogeneous material by a particular type of twist on the plane end. In the present paper the author considers the torsional vibration set up in a finite circular cylinder of non-homogeneous material one of whose ends is fixed, the other having prescribed twist. The cylindrical coordinates (r, θ, z) are used with the origin on the free end and the z -axis which is drawn inside the cylinder coincides with the axis of the cylinder. The length of the cylinder is assumed to be l . The end $z=l$ is fixed and at the end $z=0$, a periodic shearing force acts along the circumference of a circle of radius b where $b < a$, a being the radius of the cylinder. It is assumed that the rigidity and the density of the material of the cylinder vary exponentially with depth.

PROBLEM, FUNDAMENTAL EQUATION AND BOUNDARY CONDITIONS.

Let us assume that $u_r = u_z = 0$ and $u_\theta (= v)$ is independent of θ . The strain components are given by

$$\begin{aligned} e_{rr} &= e_{\theta\theta} = e_{zz} = e_{rz} = 0, \\ e_{r\theta} &= \frac{\partial v}{\partial r} - \frac{v}{r}, \quad e_{\theta z} = \frac{\partial v}{\partial z} \end{aligned} \quad (1)$$

and the corresponding stresses are

$$\begin{aligned} \sigma_r &= \sigma_\theta = \sigma_z = \sigma_{rz} = 0, \\ \sigma_{r\theta} &= \mu \left(\frac{\partial v}{\partial r} - \frac{v}{r} \right), \\ \sigma_{\theta z} &= \mu \frac{\partial v}{\partial z}, \end{aligned} \quad (2)$$

We suppose that the rigidity and the density of the material of the cylinder are given by

$$\begin{aligned}\mu &= \mu_0 \cdot e^{-\mu_1 z} \\ \rho &= \rho_0 \cdot e^{-\rho_1 z}\end{aligned}\quad (3)$$

where ρ_0, μ_0, μ_1 are all constants. Evidently the velocity of the torsional waves ($=\sqrt{\mu/\rho}$) remains the same for all values of z .

Then

$$\begin{aligned}\sigma_{\theta z} &= \mu_0 \cdot e^{-\mu_1 z} \cdot \frac{\partial v}{\partial z} \\ \sigma_{r\theta} &= \mu_0 \cdot e^{-\mu_1 z} \left(\frac{\partial v}{\partial r} - \frac{v}{r} \right)\end{aligned}\quad (4)$$

Two equations of motion are satisfied identically and the remaining one reduces to

$$\frac{\partial^2 v}{\partial r^2} + \frac{1}{r} \cdot \frac{\partial v}{\partial r} - \frac{v}{r^2} + \frac{\partial^2 v}{\partial z^2} - \mu_1 \frac{\partial v}{\partial z} = \frac{1}{c^2} \cdot \frac{\partial^2 v}{\partial t^2} \quad (5)$$

$$\text{where } c = \sqrt{\mu_0/\rho_0}. \quad (6)$$

Boundary conditions are given by

- i) $r\theta = 0$, when $r = a$;
- ii) $v = 0$, when $z = l$;
- iii) $(\theta z)_{z=0} = S \cdot \delta(r-b) \cdot e^{i\theta t}$, $0 < b < a$

(7)

where S is a constant and δ is the Dirac's delta function.

3. SOLUTION OF THE PROBLEM

If we take

$$v = R(r) \cdot Z(z) \cdot e^{i\theta t}, \quad (8)$$

equation (5) reduces to

$$\begin{aligned}& \frac{1}{R} \left(\frac{d^2 R}{dr^2} + \frac{1}{r} \frac{dR}{dr} - \frac{R}{r^2} \right) \\ & + \frac{1}{Z} \left(\frac{d^2 Z}{dz^2} - \mu_1 \frac{dZ}{dz} \right) \\ & = -p^2/c^2\end{aligned}$$

Hence we get

$$\frac{1}{R} \left(\frac{d^2 R}{dr^2} + \frac{1}{r} \frac{dR}{dr} - \frac{R}{r^2} \right) = -k^2, \quad (9)$$

$$\frac{1}{Z} \left(\frac{d^2 Z}{dz^2} - \mu_1 \frac{dZ}{dz} \right) = k^2 - p^2/c^2 = \alpha^2, \text{ say,} \quad (10)$$

where we assume p to be very small so that $p^3/c^2 < k^2$.

The solution of (9) is, $R = \text{const.} \times J_1(kr)$, (11)

where J_1 is the first order Bessel function.

The solution of (10) is $Z = A \cdot e^{qz} + B \cdot e^{q'z}$ (12)

where $q = \frac{\mu_1 + \sqrt{\mu_1^2 + 4\kappa^2}}{2}$, $q' = \frac{\mu_1 - \sqrt{\mu_1^2 + 4\kappa^2}}{2}$

and A, B are constants.

The first of the boundary conditions (7) gives $J_2(ka) = 0$. (13)

The roots of (13) are given by

$$k_1 a = 5.136,$$

$$k_2 a = 8.417,$$

$$k_3 a = 11.6,$$

$$\dots \dots \dots$$

and $k_n a \approx (n + 3/4)\pi$, when n is large (Jahnke & Emde 1951).

The second of the boundary conditions (7) gives

$$\sum_{n=1}^{\infty} \{A_n \cdot e^{qnl} + B_n \cdot e^{q'nl}\} \cdot J_1(k_n r) \cdot e^{i p t} = 0$$

Hence we may take

$$A_n \cdot e^{qnl} + B_n \cdot e^{q'nl} = 0 \quad (14)$$

Now, we have

$$(\theta z)_{z=0} = \mu_0 \sum_{n=1}^{\infty} (q_n A_n + q'_n B_n) \cdot J_1(k_n r) e^{i p t}$$

The third of the boundary conditions (7) gives

$$\begin{aligned} \mu_0 \sum_{n=1}^{\infty} (q_n A_n + q'_n B_n) \cdot J_1(k_n r) e^{i p t} &= S \cdot \delta(r-b) \cdot e^{i p t} \\ &= f(r) \cdot e^{i p t}, \text{ say.} \end{aligned} \quad (15)$$

$$\text{Thus } f(r) = \sum_{n=1}^{\infty} \mu_0 (q_n A_n + q'_n B_n) \cdot J_1(k_n r)$$

Therefore $\int_0^a r f(r) \cdot J_1(k_n r) dr$.

$$\begin{aligned} &= \mu_0 (q_n A_n + q'_n B_n) \int_0^a r [J_1(k_n r)]^2 dr \\ &= \mu_0 (q_n A_n + q'_n B_n) \frac{a^2}{2} \cdot [J_1(k_n a)]^2 \quad (\text{Byerly 1959}) \end{aligned}$$

$$\mu_0 (q_n A_n + q'_n B_n) = \frac{2}{a^2 [J_1(k_n a)]^2} \int_0^a r f(r) \cdot (k_n r) dr. \quad (16)$$

From (15) we have

$$f(r) = S \cdot \delta(r-b) \quad (17)$$

Using (17) in (16) and utilising the following property of Dirac delta function

$$\int_{-\infty}^{\infty} f(x) \cdot \delta(x-a) dx = f(a)$$

where $f(x)$ is continuous, we get

$$q_n A_n + q'_n B_n - \frac{2Sb \cdot J_1(k_n b)}{\mu_0 \cdot a^2 [J_1(k_n a)]^2} = 0 \quad (18)$$

From (14) and (18), we get

$$A_n = \frac{-2Sb \cdot J_1(k_n b) \cdot e^{q'_n l}}{\mu_0 \cdot a^2 \cdot [J_1(k_n a)]^2 [q'_n e^{q'_n l} - q_n e^{q_n l}]} \quad (19)$$

$$B_n = \frac{2Sb \cdot J_1(k_n b) \cdot e^{q_n l}}{\mu_0 \cdot a^2 \cdot [J_1(k_n a)]^2 [q'_n e^{q'_n l} - q_n e^{q_n l}]} \quad (20)$$

Hence from (8), (11), (12), (19), and (20) we get finally

$$v = \frac{2Sb}{\mu_0 \cdot a^2} \sum_{n=1}^{\infty} \frac{J_1(k_n b) [e^{q_n l} \cdot e^{q'_n \cdot n \cdot z} - e^{q'_n l} \cdot e^{q_n \cdot z}]}{[J_1(k_n a)]^2 [q'_n e^{q'_n l} - q_n e^{q_n l}]} \times J_1(k_n r) \cdot e^{ip t}. \quad (21)$$

The series in (21) can be verified to be a convergent series.

The author takes this opportunity to express his sincere thanks to Dr. A. K. Mitra, Reader in Mathematics, Jadavpur University for his help and guidance in the preparation of this paper.

REFERENCES

- Byerly, W. E. 1959 *An elementary treatise on Fourier series and spherical, cylindrical and ellipsoidal Harmonics*, Dover Publication.
 Jahnke, E. & Emde, F. 1951 *Tables of functions with formulas and curves*, 4th Edition, Dover Publication.
 Mitra, A. K. & Sen Gupta, A. K. 1967 *Indian Jour. of Mechanics and Math*, **5**, 43.

A note on the deformation of a rotating inhomogeneous piezoelectric thick disc

By M. BHATTACHARYA

Lake View High School, Panchuanatala Road, Calcutta-19.

(Received 11 April 1969)

The equations of elasticity, the Maxwell's electromechanical equations and the constitutive equations of piezoelectricity have been made use of in solving the problem. The results arrived at essentially agree with the results known for aeolotropic media and which are free from piezoelectric excitations.

1. INTRODUCTION

In recent years the problems of piezoelectricity have assumed importance in view of their applications in the field of ultrasonics and acoustic. Toupin (1959), Paria (1960), Paul (1961), Sinha (1962, 1963), Giri (1964), Das (1966) and Bakshi (1967) in their papers distinguished the problems of piezoelectricity as analogues of the well-known classical problems of elasticity. The present note is a piezoelectric analogue of the elastic problem concerning the determination of the deformations in a rotating thick disc with inhomogeneous material parameters. The inhomogeneities are supposed to appear due to the impurities of the crystal structure of the material.

2. THE PROBLEMS, FUNDAMENTAL EQUATIONS AND BOUNDARY CONDITIONS.

The problem, as stated above is electromechanical in character and is therefore to be solved by the equations of elasticity and electro magnetic Maxwell's equations. The problem has been considered as that of a plane strain in cylindrical co-ordinates (r, θ, z) with origin at the lower face and z -axis parallel to its thickness and direction of the electric field along z -axis. The equation of equilibrium is

$$\frac{\partial T_{rr}}{\partial r} + \frac{T_{rr} - T_{\theta\theta}}{r} + \rho \omega^2 r = 0 \quad \dots(1)$$

where T_{rr} and $T_{\theta\theta}$ are the stress components, ρ the density and ω the uniform velocity of the rotating disc. The Maxwell's equations are given by

$$\text{rot } \vec{E} = 0, \quad \text{div } \vec{D} = 0 \quad \dots(2)$$

where \vec{E} and \vec{D} are the electric intensity and electric displacement vectors, respectively.

The constitutive equations of piezoelectricity in Cartesian co-ordinates are given by Sinha (1968)

$$\begin{aligned}
 T_{xx} &= C_{11}^E S_{xx} + C_{12}^E S_{yy} + C_{13}^E S_{zz} - e_{31} E_z \\
 T_{yy} &= C_{12}^E S_{xx} + C_{11}^E S_{yy} + C_{13}^E S_{zz} - e_{31} E_z \\
 T_{zz} &= C_{13}^E (S_{xx} + S_{yy}) + C_{33}^E S_{zz} - e_{33} E_z \\
 T_{zx} &= C_{44}^E S_{zx}, \quad T_{yz} = C_{44}^E S_{yz} \\
 D_x &= e_{14} S_{yz} + e_{15} S_{zx} \\
 D_y &= e_{15} S_{yz} + e_{14} S_{zx} \\
 D_z &= e_{31}(S_{xx} + S_{yy}) + e_{33} S_{zz} + e_{33} E_z \quad \dots(3)
 \end{aligned}$$

where T —stress components, S —strain components, D —electric displacements, C —elastic compliances, e —piezoelectric constants, E —dielectric permittivities

In cylindrical co-ordinates the above equations give

$$\begin{aligned}
 T_{rr} &= \cos \theta T_{xx} + 2 \sin \theta \cos \theta T_{xy} + \sin^2 \theta T_{yy} \\
 T_{\theta\theta} &= \sin^2 \theta T_{xx} - 2 \sin \theta \cos \theta T_{xy} + \cos^2 \theta T_{yy} \\
 T_{r\theta} &= \sin \theta \cos \theta (T_{yy} - T_{xx}) + (\cos^2 \theta - \sin^2 \theta) T_{xy} \\
 T_{rz} &= \cos \theta T_{zx} + \sin \theta T_{yz} \\
 T_{\theta z} &= -\sin \theta T_{zx} + \cos \theta T_{yz} \\
 T_{zz} &= T_{zz} \\
 D_r &= D_x \cos \theta + D_y \sin \theta \\
 D_\theta &= D_y \cos \theta - D_x \sin \theta \\
 D_z &= D_z \quad \dots(4)
 \end{aligned}$$

Again the components of displacements (U, V, W) are given by

$$U = u \cos \theta, \quad V = v \sin \theta, \quad W = w \quad \dots(5)$$

whence $u(rz)$ and $w(rz)$ are the radial and axial components which are assumed to be independent of θ . The strain components are given by

$$\begin{aligned}
 S_{xx} &= \frac{u}{r} + \frac{r^2}{r} \frac{\partial}{\partial r} \left(\frac{u}{r} \right) \\
 S_{yy} &= \frac{u}{r} + \frac{y^2}{r} \frac{\partial}{\partial r} \left(\frac{u}{r} \right) \\
 S_{zz} &= \frac{\partial w}{\partial z} \\
 S_{xy} &= \frac{2xy}{r} \frac{\partial}{\partial r} \left(\frac{u}{r} \right) \\
 S_{yz} &= \frac{y}{r} \left(\frac{\partial u}{\partial z} + \frac{\partial w}{\partial r} \right) \\
 S_{zx} &= \frac{x}{r} \left(\frac{\partial u}{\partial z} + \frac{\partial w}{\partial r} \right) \quad \dots(6)
 \end{aligned}$$

Thus the simplified form of (4) gives

$$\begin{aligned}
 T_{rr} &= C_{11} \frac{\partial u}{\partial r} + C_{12} \frac{u}{r} + C_{13} \frac{\partial \omega}{\partial z} - e_{31} E_z \\
 T_{\theta\theta} &= C_{12} \frac{\partial u}{\partial r} + C_{11} \frac{u}{r} + C_{13} \frac{\partial \omega}{\partial z} - e_{31} E_z \\
 T_{rz} &= C_{44} \left(\frac{\partial u}{\partial z} + \frac{\partial \omega}{\partial r} \right) \\
 T_{zz} &= C_{13} \left(\frac{\partial u}{\partial r} + \frac{u}{r} \right) + C_{33} \frac{\partial \omega}{\partial z} - e_{33} E_z \\
 T_{r\theta} &= T_{\theta z} = 0 \\
 D_r &= e_{15} \left(\frac{\partial u}{\partial z} + \frac{\partial \omega}{\partial r} \right), \quad D_\theta = -e_{14} \left(\frac{\partial u}{\partial z} + \frac{\partial \omega}{\partial r} \right) \\
 D_z &= e_{31} \left(\frac{\partial u}{\partial r} + \frac{u}{r} \right) + e_{33} \frac{\partial \omega}{\partial z} + e_{33} E_z. \quad \dots(7)
 \end{aligned}$$

The material parameters C_{11} , C_{12} , C_{13} , e_{33} etc. are supposed to vary along the direction of the axis of the disc.

We have to solve (1) and (2) by the help of (7) and also following the boundary conditions.

(i) Electric conditions

$$\left. \begin{aligned}
 E_z &= b_1 \quad \text{at } z=l, \quad r=0 \\
 E_z &= b_2 \quad \text{at } z=l, \quad r=a \\
 E_z &= b_3 \quad \text{at } z=0, \quad r=0
 \end{aligned} \right\} \quad \dots(8)$$

(b_1, b_2, b_3 are constants)

and (ii) mechanical conditions

$$\int_0^1 T_{rr} \, dz = 0 \quad \text{at } r=a \quad \dots(9)$$

where l is the thickness of the disc.

2. SOLUTION OF THE PROBLEM

Since the problem is that of plane stress and so $T_{zz} = T_{rz} = 0$

$$C_{13} \left(\frac{\partial u}{\partial r} + \frac{u}{r} \right) + C_{33} \frac{\partial \omega}{\partial z} - e_{33} E_z = 0$$

$$\frac{\partial \omega}{\partial r} + \frac{\partial u}{\partial z} = 0 \quad \dots(10)$$

From (10) we have

$$E_z = \frac{1}{e_{33}} \left[C_{13} \left(\frac{\partial u}{\partial r} + \frac{u}{r} \right) + C_{33} \frac{\partial \omega}{\partial z} \right] \quad \dots(10a)$$

Then eliminating E_z , we have the first three equations of (7) as

$$T_{rr} = C_1 \frac{\partial u}{\partial r} + C_2 \frac{u}{r} + C_3 \frac{\partial \omega}{\partial z}$$

$$T_{\theta\theta} = C_2 \frac{\partial u}{\partial r} + C_1 \frac{u}{r} + C_3 \frac{\partial \omega}{\partial z}$$

$$D_z = e_1 \left(\frac{\partial u}{\partial r} + \frac{u}{r} \right) + e_3 \frac{\partial \omega}{\partial z} \quad \dots(11)$$

Because of our assumption of inhomogeneity of the material parameters, we have $C_{11} = C_{11}^\circ (1 + \kappa_2)$, $C_{12} = C_{12}^\circ (1 + \kappa_2)$, $e_{31} = e_{31}^\circ (1 + \kappa_2)$ etc. So that

$$C_1 = \left(C_{11} - \frac{C_{13} e_{31}}{e_{33}} \right) = C_1^\circ (1 + \kappa_2)$$

$$C_2 = \left(C_{12} - \frac{C_{13} e_{31}}{e_{33}} \right) = C_2^\circ (1 + \kappa_2)$$

$$e_1 = \left(e_{31} + \frac{C_{13} e_{33}}{e_{33}} \right) = e_1^\circ (1 + \kappa_2) \quad \dots(12)$$

etc.

whence $C_1^\circ, C_2^\circ, C_3^\circ \dots e_1^\circ, e_2^\circ, e_3^\circ$ being constants given by

$$C_1^\circ = \left(C_{11}^\circ - \frac{C_{13}^\circ e_{31}^\circ}{e_{33}^\circ} \right)$$

$$C_2^\circ = \left(C_{12}^\circ - \frac{C_{13}^\circ e_{31}^\circ}{e_{33}^\circ} \right)$$

$$e_1^\circ = \left(e_{31}^\circ + \frac{C_{13}^\circ e_{33}^\circ}{e_{33}^\circ} \right)$$

etc.

from (2)

$$\frac{\partial D_z}{\partial z} = 0$$

$$D_z = \text{a function of } r = f(r) \text{ say.} \quad \dots(13)$$

Thus the equation (1) gives

$$C_1 \frac{\partial}{\partial r} \left(\frac{\partial u}{\partial r} + \frac{u}{r} \right) + C_3 \frac{\partial^2 \omega}{\partial z \partial r} + \rho \omega^2 r = 0 \quad \dots(14)$$

The last equation of (11) reads

$$e_1 \left(\frac{\partial u}{\partial r} + \frac{u}{r} \right) + e_3 \frac{\partial \omega}{\partial z} = f(r) \quad \dots(15)$$

Eliminating u between (15) and (16)

$$-\frac{\partial^2 \omega}{\partial z \partial r} = \left(\frac{1 + \kappa z}{\kappa_1} \right) (C_1 \circ f'(r) + e_1 \circ \rho \omega^2 r) \quad \dots(16)$$

where $(C_3 e_1 - e_3 C_1) = \kappa_1$

Eliminating ω from (15) and (16) we get

$$-\frac{\partial}{\partial r} \left(\frac{\partial u}{\partial r} + \frac{u}{r} \right) + \left(\frac{1 + \kappa z}{\kappa_1} \right) (C_3 \circ f'(r) + e_3 \circ \rho \omega r)$$

Since $\frac{\partial \omega}{\partial r} + \frac{\partial u}{\partial r} = 0$,

$$\frac{\partial^2 \omega}{\partial r \partial z} = -\frac{\partial^2 u}{\partial z^2}$$

$$\text{Thus, } \frac{\partial^2 \omega}{\partial z^2} = \left(\frac{1 + \kappa z}{\kappa_1} \right) (C_1 \circ f'(r) + e_1 \circ \rho \omega^2 r)$$

Integrating,

$$u = \left(\frac{z^2}{2\kappa_1} + \frac{\kappa z^3}{6\kappa_1} \right) (C_1 \circ f'(r) + e_1 \circ \rho \omega r) + f_1(r)z + f_2(r) \quad \dots(17)$$

where $f_1(r)$ and $f_2(r)$ are arbitrary functions of r .

Putting the value of u in (14) we have

$$\begin{aligned} C_1 \circ (1 + \kappa z) \frac{\partial}{\partial r} \left\{ \left(\frac{z^2}{2\kappa_1} + \frac{\kappa z^3}{6\kappa_1} \right) (C_1 \circ f'(r) + e_1 \circ \rho \omega^2 r) + f_1'(r)z + f_2'(r) \right\} \\ + \left(\frac{z^2}{2\kappa_1} + \frac{\kappa z^3}{6\kappa_1} \right) \left(C_1 \circ \frac{f'(r)}{r} + e_1 \circ \rho \omega^2 r \right) + \frac{f_1(r)}{r} z + \frac{f_2(r)}{r} \Big\} \\ - C_3 \circ \frac{(1 + \kappa z)^2}{\kappa_1} C_1 \circ f'(r) + e_1 \circ \rho \omega^2 r + \rho \omega^2 r = 0 \quad \dots(18) \end{aligned}$$

Collecting the co-efficients of different powers of z and solving for $f(r)$, $f_1(r)$ and $f_2(r)$ we have

$$f(r) = A_1 + A_2 r^2$$

$$f_1(r) = A_3 r + \frac{B_1}{r}$$

$$f_2(r) = A_4 r + \frac{B_2}{r} + \frac{A_5}{8} \kappa_3' (A_3 + \kappa_1' \rho \omega^2) r^3 \quad \dots(19)$$

where $A_1, A_2, A_3, \dots, B_1, B_2, \dots$ are constants

$$\text{and } \kappa_2' = \frac{4C_1^0 C_2^0}{\kappa_1}, \quad \kappa_1' = \frac{e_1^0}{2C_1^0} \quad \dots(20)$$

Imposing appropriate conditions for the displacement component u we get

$$u = \frac{A_3 A_2' \kappa_2'}{8} r^3 + \frac{C_1^0}{3\kappa_1} (3\kappa^2 + \kappa z^2) A_2' r + A_3 r z + A_4 r \quad \dots(21)$$

$$\text{where } A_2' = (A_2 + \kappa' \omega^2) \quad \dots(22)$$

$$\therefore \frac{\partial u}{\partial r} + \frac{u}{r} = \frac{1}{2} A_3 A_2' \kappa_2' r^2 + \frac{2}{3} \frac{C_1^0}{\kappa_1} (3z^2 + \kappa z^3) A_2' + 2A_3 z + 2A_4$$

so that from (15)

$$\begin{aligned} \frac{\partial \omega}{\partial z} = \frac{A_1 + A_2 r^2}{e_3^0 (1 + \kappa z)} - \frac{e_1^0}{e_3^0} \left[\frac{2}{3} \frac{C_1^0}{\kappa_1} (3z^2 + \kappa z^3) A_2' + 2A_3 z \right. \\ \left. + 2A_4 + \frac{1}{2} A_2 A_2' \kappa_2' r^2 \right] \quad \dots(23) \end{aligned}$$

Thus from (10a) we can get the value of E_z and then applying the boundary conditions as stated in equations (8) and (9) we can calculate the value of all the constants and finally the values of u and ω . The constants can be expressed in terms of material parameters, radius, and prescribed electric intensity.

The author is thankful to Dr. N. C. Das of Jadavpur University for his guidance in the preparation of this paper.

REFERENCES

- Bakshi, S. K. 1967 *Jour. Sc. Engg. Res.* **11**, 167.
 Das, N. C. 1966 *Jour. Sc. Engg. Res.* **10**, 167.
 Giri, R. R. 1965 *Appl. Sci. Res. A*, **14**, 471.
 Paria, G. 1960 *Jour. Sc. Engg. Res.* **4**, 381.
 Paul, H. S. 1961 *Jour. Sc. Engg. Res.* **5**, 233.
 Sinha, D. K. 1962 *Jour. Acoust. Soc. Amer.* **34**, 1073.
 1968 *Bull. De L'academie, Polon. des. Sc.* **6**, 227.
 Toupin, R. A. 1959 *Jour. Acoust. Soc. Amer.* **31**, 315.

Thermal conductivity of CO₂-N₂ gas mixture

By R. S. GAMBHIR

Department of Physics, University of Jodhpur, India.

(Received 12 December 1968, Revised 20 March 1969)

The theory of Saxena *et al* (1965) as extended by Gambhir (1969) to those mixtures of non-polyatomic gases where each component may have more than one internal degree of freedom, has been compared with experiment in the case of CO₂-N₂ gas mixture. Also considered are the theories of Hirschfelder (1957), and Monchick *et al* (1965). No theory gives the right type of composition dependence of mixture conductivity at high temperatures. It has been concluded that the discrepancy between experiment and theory may be due to the disagreement between the two in the case of pure gases.

INTRODUCTION

Very recently Gambhir (1969) has extended the theory of heat conduction through polyatomic gas mixtures given by Saxena *et al* (1965) to those systems where each component may have more than one internal degree of freedom. The purpose of this paper is to compare these results with experiment and the theories of Hirschfelder (1957), and Monchick *et al* (1965). The system chosen for this work is CO₂-N₂ gas mixture on which extensive experimental measurements are available. This choice has been made firstly because these gases are important constituents of combustion exhaust gases, and secondly because the thermal conductivity of this system as a function of composition seems to exhibit maxima at high temperatures.

THEORY

For each of the constituents of the mixture under investigation, viz. CO₂-N₂, the number of collisions required for energy equilibration between vibrational and translational degrees, Z_{vib} , is quite large (Hertzfeld & Litovitz 1959). Therefore, under these circumstances only the contribution of rotational translational interaction is important and the expression of Gambhir (1969) reduces to

$$\lambda_{mix} = \lambda_{mon-mix} + \sum_j n \{D_j\}_{mix} X_j C_{int,j} \\ - \lambda_{mon-mix} \sum_j \frac{X_j C_{rot,j}}{C_{vtr} + X_j C_{rot,j}} \left[1 - \exp \left\{ \frac{-1}{[Z_{rot,j}]_{mix}} - \frac{C_{vtr} + X_j C_{rot,j}}{C_{vtr}} \right\} \right] \\ + C_{vtr} \sum_j \left[\frac{D_j}{C_{vtr} + X_j C_{rot,j}} \right]_{mix} \frac{X_j C_{rot,j}}{C_{vtr} + X_j C_{rot,j}} \left[1 - \exp \left\{ \frac{-1}{[Z_{rot,j}]_{mix}} - \frac{C_{vtr} + X_j C_{rot,j}}{C_{vtr}} \right\} \right] \quad \dots(1)$$

The various symbols in the above equation are the same as those of Saxena *et al* (1965), and Gambhir (1969). Further, substituting R for C_{rot} for both CO_2 and N_2 , and $3R/2$ for C_{int} due to obvious reasons, where R is the gas constant; equation (1) reduces for this binary gas mixture to :

$$\begin{aligned} \lambda_{\text{mix}} &= \lambda_{\text{mon-mix}} + n [D_1]_{\text{mix}} \frac{X_1}{1.5+X_1} C_{\text{int},1} + n [D_2]_{\text{mix}} \frac{X_2}{1.5+X_2} C_{\text{int},2} \\ &- \lambda_{\text{mon-mix}} \frac{X_1}{1.5+X_1} \left[1 - \exp \left\{ \frac{-1}{[Z_{\text{rot},1}]_{\text{mix}}} \frac{1.5+X_1}{1.5} \right\} \right] \\ &- \lambda_{\text{mon-mix}} \frac{X_2}{1.5+X_2} \left[1 - \exp \left\{ \frac{-1}{[Z_{\text{rot},2}]_{\text{mix}}} \frac{1.5+X_2}{1.5} \right\} \right] \\ &+ \frac{3R}{2} n [D_1]_{\text{mix}} \frac{X_1}{1.5+X_1} \left[1 - \exp \left\{ \frac{-1}{[Z_{\text{rot},1}]_{\text{mix}}} \frac{1.5+X_1}{1.5} \right\} \right] \\ &+ \frac{3R}{2} n [D_2]_{\text{mix}} \frac{X_2}{1.5+X_2} \left[1 - \exp \left\{ \frac{-1}{[Z_{\text{rot},2}]_{\text{mix}}} \frac{1.5+X_2}{1.5} \right\} \right] \quad \dots(2) \end{aligned}$$

Here subscript '1' refers to the heavier component, e. g., CO_2 .

COMPARISON WITH EXPERIMENT.

The values of λ_{mix} as evaluated from above expression (2) are plotted in the figure. The value of Z_{rot} for CO_2 was taken to be 1.7 at 300°K (Holmes *et al* 1965), and for N_2 it was taken to be 3.7 at 300°K (Saxena *et al* 1964). $[Z_{\text{rot},j}]_{\text{mix}}$ values were computed by procedure already explained (Saxena *et al* 1965). $Z_{\text{rot},j} = l$, the number of necessary collisions for rotational translational energy equilibration for one molecule of species 'j' when it is dispersed in otherwise pure species 'k', required for this purpose, were evaluated by fitting equation (2) in experimental λ_{mix} values at two compositions at 323°K. The various Z values were calculated at higher and lower temperatures by using for their temperature dependence the expression of Parker (1959). The calculation of λ_{mon} and $\lambda_{\text{mon-mix}}$ is based on $L-J$ (12-6) potential in conjunction with the usual combination rules for unlike interactions. For like interactions the potential parameters used are : CO_2 : $\epsilon/k = 213^\circ\text{K}$, $\sigma = 3.897\text{\AA}$; N_2 : $\epsilon/k = 91.5^\circ\text{K}$, $\sigma = 3.681\text{\AA}$ (Hirschfelder *et al* 1964). Also shown in the diagram are the λ_{mix} curves based on the theories of Hirschfelder (1957), and Monchick *et al* (1965). The latter values were calculated using Hirschfelder expression for composition dependence after evaluating the pure conductivities employing the formula of Monchick *et al* (1965) (replacing internal diffusion coefficients by ordinary self diffusion coefficients), the procedure suggested by the authors themselves. This procedure neglects inelastic effects in the mixture but includes the same in the calculations for the pure components.

Another procedure available is to employ expression (74) of Monchick *et al* (1965), using for pure conductivities the experimental data. Such calculations are available at two temperatures 273°K and 473°K (Barua *et al* 1968) considered here, and at 300°K, 500°K and 1000°K (Monchick *et al* 1965). It may be pointed out that the mixture conductivity values thus calculated will lie on, above or below the values similarly calculated (using for pure conductivities the experimental values) employing Hirschfelder expression depending upon the the values of various collision numbers (Monchick *et al* (1965). The mixture conductivity values as computed above will not be compared with other theories because these values have been forced to fit in the experiment at the end points.

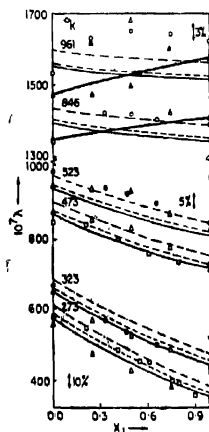


Figure 1. Dependence of thermal conductivity of $\text{CO}_2\text{-N}_2$ mixture on composition at various temperatures. Theoretical curves: - - - Hirschfelder. — — — Monchick, *et al* — present theory — — — semi-theoretical — — — Experimental points: Keyes O; Rothman & Bromley ●; Westenberg & De Haas Δ; Gambhir & Saxena ▲; Barua *et al* □.

In the diagram the experimental points at 273°K and 473°K are of Barua *et al* (1968), at 323°K and 523°K are those of Keyes (1952) and at 846°K and 961°K are the measurements of Rothman & Bromley (1955). Westenberg & DeHaas (1962) have also measured the conductivity of this system and they have presented compromise curves as a function of temperature at various compositions, using their data and data of other workers. These values have been exhibited in the figure. Recently Gambhir & Saxena (1967) have reviewed the existing experimental λ -data of non-

polar gases, including CO_2 and N_2 , and have reported compromise values. These λ -values for pure CO_2 and N_2 have also been shown in the diagram.

DISCUSSION

From the figure one can see that all the three theories give the same type of agreement with experiment at low temperatures and no theory gives the right type of composition dependence of λ_{mix} at high temperatures, where the experimental curves change curvature from convex towards the x -axis to concave. Brokaw (1959), and Westenberg & de Haas (1962) have shown that if unlike interaction parameters are found directly from the diffusion data, this trend could be explained; thus arousing a doubt about the validity of the combination rules. But this does not seem to be the final conclusion. If one has a close look on pure conductivity values recommended by Gambhir & Saxena (1967) one feels tempted to conclude that if various theories could agree at the end points, then probably the composition dependence could also be satisfied. To elaborate this point of view, λ_{mix} values have been computed at 846°K and 961°K using Hirschfelder expression (all the three theories give same type of composition dependence but this expression is simpler for calculations) with usual combination rules for $\lambda_{\text{mon-mix}}$ and D_{jk} , but for the pure conductivities for which compromise values recommended by Gambhir & Saxena (1967) have been employed. These may be called semi-theoretical curves and have been shown in the figure. These curves do exhibit change in curvature but do not show maxima. Therefore, to get a clear and final picture, accurate measurements should be performed as a function of composition at high temperatures using different techniques, preferably thick wire variant of the hot wire method which is quite sensitive to small changes in the conductivity values.

Further, the disagreement of various theories with the experiment in the case of pure gases may very well be in the calculation of translational component of thermal conductivity, λ_{mon} . To check this point, λ_{mon} values required in theoretical calculations were generated from experimental viscosity values. The various pure λ -values thus calculated may be called semi-theoretical values and these are reported in the table. Also shown in the table are the experimental λ -values recommended by Gambhir & Saxena (1967) and various purely theoretical values (within braces). From the table one can see that above suggestion is correct to some extent. From the experimental λ -values of the table one can see that at high temperatures the thermal conductivity of CO_2 is greater than that of N_2 while purely theoretical calculations show the opposite trend (see also figure). But the semi-theoretical λ -values seem to exhibit the right type of trend though not the correct magnitudes of the difference between

the λ -values of CO_2 and N_2 . Thus the cause of disagreement between theory and experiment may be attributed partly to the potential parameters of pure gases and partly to the various theories of thermal conductivity of pure gases. Therefore, more precise thermal conductivity measurements are needed in the case of pure gases also, a conclusion already reached by Gambhir (1967) in the case of CO_2 gas.

TABLE 1. EXPERIMENTAL AND VARIOUS THEORETICAL, AND SEMI-
THEORETICAL THERMAL CONDUCTIVITY VALUES IN THE
CASE OF PURE GASES.

Gas	Temperature °K	10 λ			
		Experimental (Gambhir & Saxena 1967)	Hirschfelder (1957)	Monchick, et al (1965)	Gambhir (1967)
CO_2	846	14.1	14.1*(13.9)**	13.8*(13.5)**	13.7*(13.4)**
	961	15.8	15.9 (15.6)	15.6 (15.3)	15.4 (15.2)
N_2	846	13.5	14.0 (14.4)	13.7 (14.0)	13.6 (13.9)
	961	14.8	15.5 (16.0)	15.2 (15.6)	15.0 (15.5)

* Semi-theoretical, ** Purely theoretical

REFERENCES

- Barua, A. K., Manna, A., & Mukhopadhyay, P. 1968 *J. Phys. Soc. (Japan)*, **25**, 862.
 Brokaw, R. S. 1959 *J. Chem. Phys.*, **31**, 571.
 Gambhir, R. S. 1967 *Brit. J. Appl. Phys.*, **18**, 1773.
 1969 *Brit. J. Appl. Phys.*, **2**, 463
 Gambhir, R. S. & Saxena, S. C., 1967 *Defence Sci. J. Suppl. India*, **17** (2A), 35.
 Herzfeld, K. F. & Litovitz, T. A. 1959 *Absorption and Dispersion of Ultrasonic Waves* (Academic Press, New York).
 Hirschfelder, J. O. 1957 *J. Chem. Phys.*, **26**, 282;
 1957, *Sixth International Combustion Symposium*, p.35
 (Reinhold Pub. Corp. New York)
 Hirschfelder, J. O., Curtiss, C. F. & Bird, R. B. 1964 *Molecular Theory of Gases and Liquids* (John Wiley, New York).
 Holmes, R., Jones, G. R. & Lawrence, R. 1965 *J. Chem. Phys.*, **41**, 2955.
 Keyes, P. G. 1952 *Trans ASME*, **74**, 1303.
 Monchick, L., Pereira, A. N. G. & Mason, E. A. 1965 *J. Chem. Phys.*, **42**, 3241.
 Parker, J. G. 1959 *Phys. Fluids*, **2**, 449.
 Rothman, A. J. & Bromley, L. A. 1955 *Ind. Eng. Chem.*, **47**, 899.
 Saxena, S. C., Saksena, M. P. & Gambhir, R. S. 1964 *Brit. J. Appl. Phys.*, **15**, 843.
 Saxena, S. C., Saksena, M. P., Gambhir, R. S. & Gandhi, J. M. 1965 *Physica*, **31**, 333.
 Westenberg, A. A. & de Haas, N. 1962 *Phys. Fluids*, **5**, 266,

Elastic scattering of neutrons by deuterons

By GITA PURKAYASTHA AND N. C. SIL

*Department of Theoretical Physics, Indian Association for the
Cultivation of Science, Jadavpur, Calcutta-32*

(Received 6 February 1969, Revised 13 May 1969)

The elastic scattering of neutron by deuteron has been investigated considering the exchange collision possibility. We have used a modification of the Born approximation due to Dirac which takes account of the non-orthogonality of the initial and final wave functions. The resulting integral equations have been solved by the Fredholm method. The calculations have been done for energies 60 Mev, 95 Mev. and 146 Mev of the incident neutrons. The results of our numerical calculation at 95 Mev are in good agreement with the experimental findings as well as the theoretical results of Wu & Ashkin. The non-orthogonality corrections are quite perceptible at lower energies but small at high energy.

INTRODUCTION

A number of theoretical calculations have been made by several authors (Massey & Buckingham 1941, Wu & Ashkin 1948, Chew 1948, Gammel & Christian 1953, Aron *et al* 1964, 1965) on the elastic scattering of neutrons and protons by deuterons. The Born approximation calculation which can be used for high energy of the incident particles deserves special consideration in view of its simplicity. However the exchange collision process brings in additional complications and the conventional Born-Oppenheimer approximation needs modification to take account of the lack of orthogonality of the initial and final states. Dirac (1955) has suggested a modification of Born-Oppenheimer approximation which is applicable in such cases. According to Dirac, in the transition problems for which the initial and final states belong to two different sets of orthogonal states, one has to deal with a mixture of wave functions belonging to two different orthogonal sets. It then becomes necessary to take into account the lack of orthogonality of these wave functions. In this paper we have studied the elastic scattering, including exchange, of high energy neutrons by target deuteron in ground states by taking proper account of the non-orthogonality of the wave functions as suggested by Dirac, as in this case initial and final states are non-orthogonal. In view of the fact that there is no excited bound state of deuteron, we have considered only the following two possibilities, (1) that the incident neutron is scattered leaving the target in the ground state. (2) that the neutron bound originally in the deuteron comes out and the incident neutron is captured by the proton left to form a deuteron, in the ground state. The dissociation reaction in which the deuteron breaks up into a neutron and

a proton has been neglected. By taking properly weighted symmetric and anti-symmetric combinations of the direct and exchange scattering amplitudes in the differential crosssection we make allowance for the indistinguishability of the incident neutron and the neutron in the target deuteron.

FORMULATIONS

Let 1 denote the incoming neutron, 3 and 2 are respectively the proton and the neutron originally forming the deuteron. Let us introduce the relative co-ordinate

$$r = r_1 - \frac{1}{2}(r_2 + r_3)$$

$$r' = r_2 - \frac{1}{2}(r_1 + r_3)$$

$$\rho = r_3 - r_2$$

$$\rho' = r_3 - r_1$$

We have assumed the centre of mass at rest i. e.

$$r_1 + r_2 + r_3 = 0.$$

We have considered only the following two probable reactions, (1) the incident neutron is scattered leaving the deuteron in its ground state (2) the exchange collision reaction i.e. the incident neutron is captured by the target to form a deuteron and the neutron which was originally in the target comes out. In the exchange collision process, the initial and the final wave functions are non-orthogonal as they are wave functions of two different Hamiltonians. The initial Hamiltonian is

$$H = H(D_{2,3}) + H(n_1) + V_1$$

The final Hamiltonian is

$$H = H(D_{1,3}) + H(n_2) + V_2$$

where $H(D_{2,3})$ and $H(D_{1,3})$ are the energies of the deuteron formed of particles (2,3) and (1,3) respectively $H(n_1)$ and $H(n_2)$ are energies of the neutron 1 and the neutron 2. V_1 is the interaction energy between $(D_{2,3})$ and n_1 and V_2 is the interaction energy between $(D_{1,3})$ and n_2 .

The scattering and exchange collision reaction amplitudes, denoted respectively by $a(k)$ and $b(k)$ are given by Dirac as

$$a(k) = - \int \psi_k^* | V_{12} + V_{13} | \psi_{k_0} dq - \int w(k, k') b(k') dk'$$

$$b(k) = - \int \psi_k'^* | V_{21} + V_{23} | \psi_{k_0} dq - \int w(k, k') a(k') dk'$$

where $w(\mathbf{k}, \mathbf{k}') = \int \psi_k^* \psi_{k'} d\mathbf{q}$
 $w(\mathbf{k}, \mathbf{k}') = \int \psi_k'^* \psi_k d\mathbf{q} = w(\mathbf{k}', \mathbf{k})$
 $d\mathbf{q} = r^2 \sin \theta d\theta d\phi dr \rho^2 \sin \theta' d\theta' d\phi' d\rho$

and V_{12} , V_{13} , V_{21} and V_{23} are two body interaction potentials between particles (1,2), (1,3), (2,1) and (2,3) respectively. ψ_k , ψ_k and ψ_k' are the wave functions of the system at the beginning, after elastic scattering and after exchange collision process respectively. They are the products of deuteron bound state wave function and neutron wave function in relative co-ordinate multiplied by proper normalizing constant. The calculations have been carried out omitting tensor forces. The spin-orbit effect is also neglected. We have taken the radial part of the interaction potential as well as the state functions as of Gaussian nature. This particular form of potentials and state functions are simple in nature and enables us to do the calculation analytically. Thus we have

$$V_{ij} = V_0 \exp(-\alpha^2 r_{ij}^2) \quad \dots(a)$$

$$\left. \begin{aligned} \psi_k &= A \exp(i \mathbf{k} \cdot \mathbf{r} - \lambda^2 \rho^2) \\ \psi_{k_0} &= A \exp(i \mathbf{k}_0 \cdot \mathbf{r} - \lambda^2 \rho^2) \\ \psi_{k'} &= A \exp(i \mathbf{k}' \cdot \mathbf{r}' - \lambda^2 \rho'^2) \end{aligned} \right\} \quad \dots(b)$$

where V_0 , α^2 , A and λ^2 are constant. Putting these values of V_{ij} 's and ψ 's in in (1) and (2) and integrating, we get finally

$$a(\mathbf{k}) = -f(\mathbf{k}) - \int w(\mathbf{k}, \mathbf{k}') b(\mathbf{k}') d^3 \mathbf{k}' \quad \dots(3)$$

$$b(\mathbf{k}) = -g(\mathbf{k}) - \int w(\mathbf{k}, \mathbf{k}') a(\mathbf{k}') d^3 \mathbf{k}' \quad \dots(4)$$

where

$$f(\mathbf{k}) = c \exp(-\alpha_1) (\mathbf{k}_0 - \mathbf{k})^2$$

$$g(\mathbf{k}) = d_1 \exp[-\{\beta (\mathbf{k}_0 - \mathbf{k})^2 + \gamma (\mathbf{k}_0 + \mathbf{k})^2\}]$$

$$+ d_2 \exp[-\{\delta \left(\mathbf{k} + \frac{\mathbf{k}_0}{2}\right)^2 + \mu (2\mathbf{k}_0 + \mathbf{k})^2\}]$$

with

$$c = \frac{A^2 V_0}{2^{7/2} \alpha^3 \lambda^3}, \quad \alpha_1 = \frac{8\lambda^2 + \alpha^2}{32\lambda^2 \alpha^2}$$

$$d_1 = \frac{A^2 V_0}{8\pi^2 (\lambda^2 + 2\alpha^2)^{3/2}}, \quad d_2 = \frac{A^2 V_0}{8\pi^2 (\lambda^2 + \alpha^2)^{3/2}}$$

$$\beta = \frac{1}{32\lambda^2}, \quad \gamma = \frac{9}{16(2\lambda^2 + 4\alpha^2)}, \quad \delta = \frac{1}{4\lambda^2}$$

$$\mu = 1/16 (\lambda^2 + \alpha^2)$$

$$w(\mathbf{k}, \mathbf{k}') = \frac{A^2}{8\lambda^6} \exp\left[-\frac{1}{4\lambda^2} \left\{\left(\mathbf{k} + \frac{\mathbf{k}'}{2}\right)^2 + \left(\frac{\mathbf{k}}{2} + \mathbf{k}'\right)^2\right\}\right]$$

Using equation (4) for the value of $b(k)$ in equation (3) we get

$$a(k) = F(k) + P \int W(k, k') a(k') d^3 k' \quad \dots(5)$$

Similarly equation for $b(k)$ takes the form

$$b(k) = G(k) + P \int W(k, k') b(k') d^3 k' \quad \dots(6)$$

where

$$F(k) = -f(k) + \int W(k, k') g(k') d^3 k'$$

$$G(k) = -g(k) + \int W(k, k') f(k') d^3 k'$$

$$P W(k, k') = \int W(k, k') w(k, k'') d^3 k''$$

$$\text{More explicitly } P = \frac{A^4}{\lambda^3} \left(\pi/10 \right)^{3/2}.$$

$$W(k, k') = e - \left\{ \frac{45}{272} \frac{k^2}{\lambda_0} + \frac{17}{125\lambda^3} \left(\frac{5}{4} k - \frac{10}{17} k' \right)^2 \right\}$$

$$\int w(k, k') g(k') d^3 k' = N e^{-9/80 (k/\lambda)^2} \quad \dots(7)$$

$$\text{where } N = -\frac{8d_1 A^2}{\lambda^3} \left(\frac{\pi}{5 + 16\lambda^2(\beta + \gamma)} \right)^{3/2}$$

$$\times \exp \left[- \left\{ \frac{\beta\gamma}{\beta + \gamma} 4k_0^2 + \frac{5(\beta + \gamma)}{5 + 16\lambda^2(\beta + \gamma)} \left(\frac{k_0(\beta - \gamma)}{\beta + \gamma} + \frac{4}{5} k \right)^2 \right\} \right]$$

$$+ 8 \frac{d_2 A^2}{\lambda^3} \left(\frac{\pi}{5 + 16\lambda^2(\delta + \mu)} \right)^{3/2}$$

$$\times \exp \left[- \left\{ \frac{\delta\mu}{\delta + \mu} \frac{9}{4} k_0^2 + \frac{5(\delta + \mu)}{5 + 16\lambda^2(\delta + \mu)} \left(\frac{k_0(\delta + 4\mu)}{2\delta + 2\mu} - \frac{4}{5} k \right)^2 \right\} \right]$$

$$\text{and } \int w(k, k') f(k') d^3 k' = M \exp \left[- \frac{9}{80} \left(\frac{k}{\lambda} \right)^2 \right] \quad \dots(8)$$

$$\text{where } M = \frac{C A^2}{8 \lambda^3} \left(\frac{\pi 16 \lambda^2}{5 + 16 \lambda^2 \alpha_1} \right)^{3/2}$$

$$\times \exp \left[- \frac{5\alpha_1}{5 + 16\alpha_1\lambda^2} \left(\frac{4}{5} k + k_0 \right)^2 \right]$$

The integral equations (5) and (6) cannot be solved by successive approximation method as the resulting series are not convergent. We have solved them by Fredholm method. We attempted to solve (5) and (6) by means of a power series in P

$$a(k) = \sum_{n=0}^{\infty} P^n a_n(k); \dots (9) \quad b(k) = \sum_{n=0}^{\infty} P^n b_n(k) \quad (10)$$

Substituting (9) and (10) in (5) and (6)

$$a(k) = \sum_{n=0}^{\infty} P^n a_n(k) = F(k) + P \int w(k, k') \sum_{n=0}^{\infty} P^n a_n(k') d^3 k' \quad \dots(11a)$$

$$\begin{aligned}
 b(k) &= \sum_{n=0}^{\infty} P^n b_n(k) \\
 &= G(k) + P \int W(k, k'') \sum_{n=0}^{\infty} P^n b_n(k'') d^3 k'' \quad \dots(11b)
 \end{aligned}$$

Equating coefficients of equal power of P we obtain

$$\begin{aligned}
 a_0(k) &= F(k) \\
 a_1(k) &= \int W(k, k'') a_0(k'') d^3 k'' \\
 a_2(k) &= \int W(k, k'') a_1(k'') d^3 k'' \\
 a_n(k) &= \int W(k, k'') a_{n-1}(k'') d^3 k'' \quad \dots(12)
 \end{aligned}$$

Similarly for $b(k)$'s we get

$$\begin{aligned}
 b_0(k) &= G(k) \\
 b_1(k) &= \int W(k, k'') b_0(k'') d^3 k'' \\
 b_n(k) &= \int W(k, k'') b_{n-1}(k'') d^3 k'' \quad \dots(13)
 \end{aligned}$$

In order to obtain the solution in more convenient form, we define the iterated kernels

$$\begin{aligned}
 W_1(k, k'') &= W(k, k'') \\
 W_2(k, k'') &= \int W(k, k') w(k', k'') d^3 k' \\
 W_n(k, k'') &= \int W_{n-1}(k, k') w(k', k'') d^3 k' \quad \dots(14) \\
 a_0(k) &= F(k) \\
 a_1(k) &= \int W_1(k, k'') F(k'') d^3 k'' \\
 a_2(k) &= \int W_2(k, k'') F(k'') d^3 k'' \\
 a_n(k) &= \int W_n(k, k'') F(k'') d^3 k''
 \end{aligned}$$

Also the equations for the $b(k)$'s can be obtained by writing $G(k)$ instead of $F(k)$

$$\begin{aligned}
 a(k) &= F(k) + P \int W_1(k, k'') F(k'') d^3 k'' \\
 &+ P^2 \int W_2(k, k'') F(k'') d^3 k'' + P^3 \int W_3(k, k'') F(k'') d^3 k'' + \dots \\
 &= F(k) + P \int \sum_{n=1}^{\infty} P^n W_{n+1}(k, k'') F(k'') d^3 k'' \\
 &= F(k) + P \int W(k, k'') ; P F(k'') d^3 k''
 \end{aligned}$$

$$\text{where } W(k, k'' ; P) = \sum_{n=0}^{\infty} P^n W_{n+1}(k, k'').$$

Similarly

$$b(k) = G(k) + P \int W(k, k'' ; P) G(k'') d^3 k''.$$

In Fredholm method of solution the resolvent is the ratio of two infinite series in P ,

$$W(k, k''; P) = \frac{D(k, k''; P)}{D(P)}$$

where

$$D(k, k''; P) = W(k, k'') + \sum_{n=1}^{\infty} \frac{(-1)^n}{n!} D_n(k, k'') P^n$$

$$D(P) = \sum_{n=0}^{\infty} \frac{(-1)^n}{n!} D_n P^n.$$

The coefficients D_n and the functions $D_n(k, k'')$ may be found from the following recurrence relations

$$D_m(k, k'') = W(k, k'') D_{m-m} \{ W(k, k') D_{m-1}(k', k'') dk' \}$$

where

$$D_m = \int D_{m-1}(k, k) dk \quad \text{and} \quad W(k, k'') = D_0(k, k''),$$

Using the above recurrence relation we get

$$F(k) + P \left[W(k, k'') + \sum_{n=1}^{\infty} \frac{(-1)^n}{n!} P^n \left\{ W(k, k'') D_{n-1}(k, k'') \right\} W(k, k') \right. \\ \left. D_{n-1}(k', k'') d^3 k' \right] F(k') d^3 k' \\ a(k) = - \frac{\sum_{n=0}^{\infty} \frac{(-1)^n}{n!} D_n P^n}{\sum_{n=0}^{\infty} \frac{(-1)^n}{n!} D_n P^n}$$

and a similar equation for $b(k)$'s.

We have taken upto seven order for the expansion of $a(k)$ and $b(k)$ as the seventh term is found to be sufficiently small. Making allowance for the indistinguishability we may have the differential cross-section as

$$d\sigma(\theta) = \frac{14\pi^2 \mu^2}{k^4} \left[\left\{ \frac{1}{4} \left| a_k(\theta) + b_k(\theta) \right|^2 + \frac{3}{4} \left| a_k(\theta) - b_k(\theta) \right|^2 \right\} \right]$$

where $a_k(\theta) = a(k)$ at θ ; $b_k(\theta) = b(k)$ at θ ,

Numerical calculations have been done using I.B.M. 1620 computer.

RESULTS AND DISCUSSIONS

We have calculated the differential cross section for elastic scattering at different energies of the incident neutron. The radial part of the two body interaction potentials and wave function of bound state of deuteron are taken to be of Gaussian type (cf. equations (a) and (b)). The values of the parameters used are (Wu & Ashkin 1948)

$$V_0 = 45 \text{ Mev} \quad \alpha^2 = 266 \times 10^{26} \text{ cm}^{-2}$$

$$A = 0.312 \times 10^{19} \text{ cm} \quad \lambda^2 = 0.716 \times 10^{26} \text{ cm}^{-2}.$$

The curves are drawn showing differential cross sections against scattering

angles in centre of mass system at 60 Mev, 95 Mev and 146 Mev (figures 1-3). The results at 95 Mev and 146 Mev are compared with the experimental findings of Chamberlain & Stern (1954), Cassels *et al* (1951) and with the results of theoretical calculations of Wu & Ashkin (1948). We have further added a table which gives the direct elastic and exchange collision amplitudes in Born approximation and also their modification due to the lack of orthogonality effect at those energies.

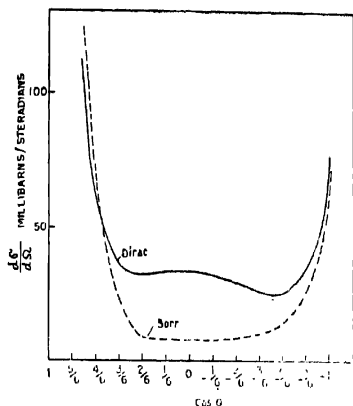


Figure 1. 60 MeV

From the nature of the curves it can be inferred that besides a sharp forward peak there is a backward peak. This backward peak is due to the exchange scattering, which decreases with the increase of energy. At 95 Mev our theoretical curve is in good agreement with the experimental curves. Here we notice that Dirac's corrected formula gives better agreement than that of Born approximation. We have not considered low energy scattering since Born approximation is not valid at low energy. At 146 Mev our results deviate from the experimental results but agree reasonably with the theoretical results of Wu & Ashkin. At this energy, experimental values are higher than the theoretical findings. However, it should be mentioned that in such range of energy the deuteron disintegration probability is quite appreciable which has not been taken into account in our formulation. It is also neglected in the formulation of Wu & Ashkin. Further in both the theoretical formulations the spin orbit forces have been neglected which may have appreciable contribution at such energies. From the curves as well as from the table it is clear that the non-

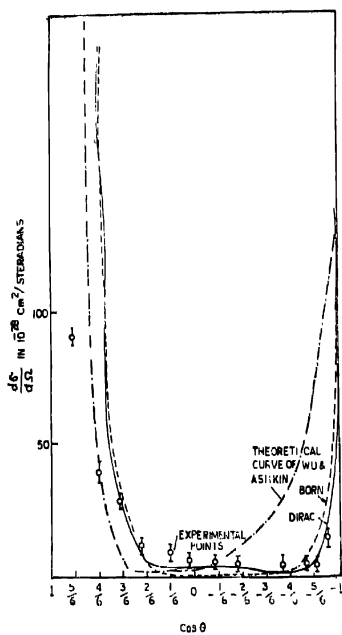


Figure 2. 95 MeV

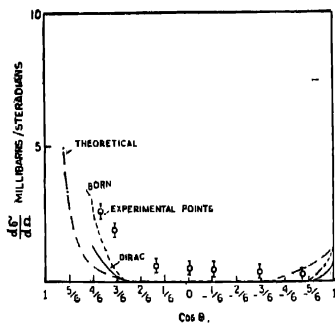


Figure 3. 146 MeV

TABLE I

Energy/Cos θ		-1	-2/3	-1/3	0	1/3	2/3	1
$a_E(\theta)$ in 10^{-14} cm	Born 60 Mev	.02037	.066	.2139	.693	2.2456	7.276	23.5765
	Dirac's correction	-.0677	-.12	-.2513	-.3738	-.353	-.4325	-.8822
$b_E(\theta)$ in 10^{-15} cm	Born	7.012	2.9789	2.639	2.482	2.436	2.2094	1.8061
	Dirac's correction	-.0587	1.0854	1.687	2.3102	2.7114	3.0113	3.8143
$a_E(\theta)$ in 10^{-14} cm	Born 95 Mev	.00033	.00214	.0137	.08856	.5697	3.665	23.5765
	Dirac's correction	-.00994	-.0136	-.0275	-.0348	-.0289	-.042	-.1688
$b_E(\theta)$ in 10^{-15} cm	Born	2.983	.4198	.265	.243	.237	.2276	.2186
	Dirac's correction	-.9008	-.087	.1997	.2467	.3266	.374	.4168
$a_E(\theta)$ in 10^{-14} cm	Born 146 Mev $.8 \times 10^{-4}$.1455 $\times 10^{-4}$.00026	.0044	.0775	1.3512	23.5765	
	Dirac's correction	-.00065	-.000734	-.001	-.00129	-.0009	-.00218	-.0209
$b_E(\theta)$ in 10^{-15} cm	Born	.8925	-.049	.0365	.0342	.0322	.0303	.0285
	Dirac's correction	-.1959	-.029	.00102	.00669	.0085	.01006	.0125

$a_E(\theta)$ = direct elastic scattering amplitude at θ

$b_E(\theta)$ = exchange elastic scattering amplitude at θ

orthogonality effect decreases the increase of energy. At 60 Mev and 90 Mev this effect is quite significant whereas at 146 Mev this effect is much less.

The authors are thankful to Prof. D. Basu for many valuable discussions. Thanks are also due to the authorities of I. I. T., Kharagpur for extending the facility of using I. B. M. 1620.

REFERENCES

- Aaron R., Amado R. D. & Yam, Y. Y. 1964 *Phys. Rev.* **136B** 650; **140B** 1965 1291.
 Buckingham, R. A. & Massey, H. S. W. 1941 *Proc. Roy. Soc.* **A179**, (123)
 Casals, J. N., Stafford, G. H., & Pickavance, T. G. 1951 *Nature*, **168**, 556.
 Chamberlain, O., & Stern, M. O., 1954 *Phys. Rev.* **94**, 666.
 Chew, G. F. 1948 *Phys. Rev.* **74**, 809.
 Christian, R. S. & Gammel, J. L. 1953 *Phys. Rev.* **91**, 100.
 Dinc, P. A. M. 1955 *Canadian Journal of Physics*, **33**, 709.
 Wu, T. Y. & Ashkin, J. 1948 *Phys. Rev.* **73**, 986.

Coherent generation and reception of frequency shift keyed signals

By A. K. DATTA

Physics Department, University of Burdwan, W. Bengal.

(Received 3 April 1969)

In this paper a few coherent systems for generation and reception of frequency shift keyed signals have been described. It is pointed out that coherent generation will ensure minimum production of transients during change over. A scheme is suggested for correcting Doppler frequency shift automatically. In the method presented, a DSB receiver is adopted for the selection of the upper and the lower sidebands of the transmitted signal. From the experimental results it becomes evident that in regard to the error rate discriminator preceded by a limiter has a decisive advantage over the one without the limiter.

INTRODUCTION

In frequency shift keying (FSK) the frequency of the transmitted signal is keyed or altered in accordance with a digital sequence obtained from the analogue message. In binary FSK, for example, this involves the transmission of energy at two slightly different frequencies for the mark and the space signalling conditions. The generally accepted convention is to transmit for the mark state a frequency slightly higher than that for the space state. Each mark and the space state has got a fixed duration. One, therefore, can write for the frequencies of these two states $f_1 = f_0 + f_d$ c/s and $f_2 = f_0 - f_d$ c/s where f_1 and f_2 correspond to the frequencies of the mark and the space signalling conditions respectively, spaced $2f_d$ cycles apart; f_d is called the deviation or shift in frequency from the centre frequency f_0 which is the arithmetic mean of the two shifted frequencies f_1 and f_2 .

A possible mathematical representation for a binary FSK signal is
$$e_k(t) = A \cos[\omega_0 \pm \omega_d] t \quad \dots \text{Type I}$$

$$\begin{aligned} \text{or } e_k(t) &= A/2 [\cos(\omega_1 t + \phi_1) - \cos(\omega_2 t + \phi_2)] \\ &+ x. A/2 [\cos(\omega_1 t + \phi_1) + \cos(\omega_2 t + \phi_2)] \end{aligned}$$

where the subscript k is either 1 or 2 and x is a random quantity which can have values either +1 or -1.

This shows that a binary FSK wave can be viewed as the sum of two steady state cosine waves given by the first term and a random component given by the second term in the above expression. The random component can be identified as a binary FSK (phase shift keying) wave at two different carrier frequencies f_1 and f_2 . So far as the intelligence

is concerned the power associated with the steady cosine waves is a waste and can be compared with the carrier power in AM. Discriminator, detection (analogous to envelope detection in AM.) is possible because of the presence of this steady component. Suppression of this power in the transmitter requires the implementation of coherent detection technique in the receiver and in such circumstances the signal can be represented simply as

$$e_k(t) = x \cdot A/2[\cos(\omega_1 t + \phi_1) + \cos(\omega_2 t + \omega_2)] \quad \dots \text{Type II}$$

FSK signal may be of two distinguishing types, (i) discontinuous phase (switching between two oscillators) and (ii) continuous phase (switching the frequency of a single oscillator). In the former, two very stable sources at frequencies f_1 and f_2 are incorporated in the transmitter and during transmission either of these sources may be selected and switched on as desired. In the latter, two state frequencies are derived from a single source. The usual technique is to use digital sequence directly for frequency modulating a voltage controlled oscillator (VCO). Whatever be the technique implemented in generating, it has to be ensured that switching ON and OFF, either from one source to the other or the same to the other or the same source between two frequencies should be instantaneous and the periods for build up and decay of oscillations should be as small as possible. Otherwise, there will be overlapping intervals within a bit period causing unwanted interference leading to misinterpretation on faulty decision of the transmitted state in the receiver.

The techniques of generation described in this paper give due consideration to the above facts and ensure a good degree of reliability in the system. The bit period is chosen so as to accommodate an integral number of rf cycles irrespective of the state of the transmitted message. Switching is done at the instants when the rf voltage passes through zero level. The keying signal is derived from the reference source itself thereby the switching instants are determined a-priori. The techniques employed in the present study may be classified as (i) sideband selection (ii) controlled scaling, (iii) feed forward, (iv) feedback and (v) phase lock type. In section 2 the proposed methods of generation of FSK signals have been dealt with in a greater detail.

With regard to reception of FSK signal emphasis in the present paper will be on semi-coherent techniques of detection rather than on incoherent (or discriminator) detection. In section 3, a scheme is described for correcting Doppler frequency shift in which a SBPL type receiver is adopted. In section 4, various aspects of receiving FSK signal have been discussed assuming the noise free received signal. In receiving FSK signal

of the type I mentioned earlier one can either make use of single CPL circuit centred at the assigned carrier frequency f_0 or two CPL circuits at the state frequencies with 'hold' in the control circuit. For FSK signal of the type II one can use a SBPL circuit centred at the state frequencies for the same. The effects of the presence of additive noise and other transmission impairment have been studied in section 5. Experimental set-up and findings have been presented in section 6.

COHERENT GENERATION OF FSK SIGNAL

Frequency shift keying of oscillator usually produces switching transients causing undesirable sideband components. Proper selection of the switching instant commensurate with the bit period, bit rate and the frequencies of the two state voltages will greatly reduce these effects thereby cross talks on other subcarrier channels will be minimised. Elimination of these transients reduces frequency transition time, permitting a high keying rate. The work of Sunde (1959) has indicated that the special case in which $2f_d = 1/T$ where T is the bit period has a theoretical advantage in that the intersymbol interference can be suppressed at the sampling instants in the output of an ideal frequency detector. According to Bennet & Rice (1963) if there is a commensurate relationship between the making, the spacing and the signalling frequencies such as to produce continuous phase at the transitions, the spectral density varies as the inverse fourth power of frequency and if in addition the derivative of the phase is also continuous, the spectral density varies as the inverse sixth power of frequencies beyond the two state frequencies.

In this section we shall describe different techniques of generating FSK signals in a coherent manner. The methods described can be classified as (i) Controlled Scaling, (ii) Sideband Selection, (iii) Feedback, (iv) Feed Forward and (v) Phase Lock type of generation.

Sideband Selection :

In the method referred to as sideband selection the system mainly consists of a carrier oscillator (a highly stable rf source), a frequency divider, a pair of balanced modulator and an adder stage. The keying signal and accordingly the shift in frequency is derived from the carrier sources (f_0) by frequency division. A reference to figure 1 will show that the output of the modulator I, may be represented by $mAcos \omega_c t. \cos \omega_d t$. The output of the modulator II may be represented by $mAsin \omega_c t. \sin \omega_d t$. This can be had by feeding the modulator II, with a quadrature carrier and a quadrature modulating signal and the polarity reversal (i.e., \pm sign) can be obtained by feeding the modulating signal either directly or a phase inverted version of it to the modulator. The term

quadrature is referred here in respect of the corresponding components in the modulator I. The modulating signal feeding the modulator II is keyed between 'directly' or 'inverted' in accordance with the message to be transmitted.

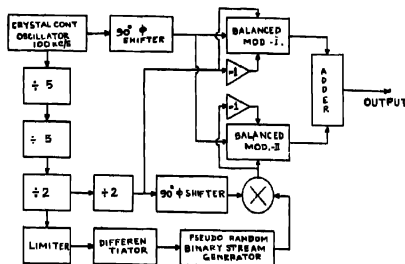


Figure 1. Block diagram of a coherent scheme of FSK generation using 'Sideband Selection' technique.

Controlled Scaling

In the method referred to as controlled scaling use is made of a highly stable rf source (X-tal controlled) to derive the mark space frequencies and the switching over signal. Thereby the time duration for the mark or space signals are clocked with the reference oscillation and change over can occur at the scheduled instants of time. The heart of this system is the controlled scaling unit. The internal logic of the scaling unit is altered to have two different counts for the mark and space states, respectively. The operation of the system is explained with a reference oscillator at 9,999 Kc/s, from which trigger pulses at the same rate are derived. The trigger pulses are fed to a selection or scaling circuit; the scaling factor by which the input pulse train are scaled down is either 99 or 101. Thus the selection circuit gives out 101,000 or 99,000 trigger pulses in a second which are ultimately converted into rectangular (or pulsed) voltage waveform. The voltages thus obtained can be given a sinusoidal shape by passing through appropriate filter networks. The selection between 99 or 101 is done in accordance with the state of the message to be transmitted. The switching over signal is also derived from the reference oscillation keeping in mind that change over is allowed at those instants of time as discussed earlier for which the generation of transients are limited to a minimum.

Feed Forward and Feed Back Techniques

In controlled scaling method of FSK signal generation the internal logic (i.e., scaling factor) of the scaling unit is changed, whereas, in these techniques the scaling factor is kept unchanged but additional pulses

generated from the input pulse train are added to the input and thus the number of pulses coming out of the scaling unit in a given time is changed. In feed forward technique the incoming pulse train is fed in parallel to a divider and the scaling unit. The other input to the scaler is the output pulses from the divider which are accepted by means of a control circuit. In feedback type, from the output of the scaler a number of pulses are generated which are fed in parallel with incoming pulse train to the scaler.

Phase Lock Type

The phase lock method of generation (figure. 2) mainly consists of an automatic phase control (APC) circuit. The VCO incorporated in the APC unit is locked in phase with either of the two reference inputs (f_1 and f_2) depending on the state of the message. The reference inputs are derived either from two very stable sources or from a single source following either of the techniques mentioned earlier. Such a system will ensure very good phase stability of the state outputs well within a bit.

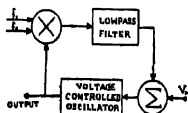


Figure 2. Block diagram of a coherent scheme of ESK generation using 'Phase Locking' technique.

ADOPTION OF A DSB RECEIVER FOR CORRECTING DOPPLER FREQUENCY SHIFT FOR SIGNAL RECEPTION

The technique of sideband phase locking has been dealt with in detail in a previous communication (Chakrabarti *et al* 1966). In this section we shall describe how a DSB receiver using sideband phase locking technique can be adopted for the reception of narrowband FS-keyed signal.

Establishing Locking of the Reference Carrier in the Receiver

It has been mentioned that a coherent receiver derives the necessary controlling voltage for establishing coherence of its local oscillator (a voltage controlled type), from the received signal itself. The received signal may be represented for FSK modulation as $A_k \cos(\omega_k t + \phi_k)$, where the subscript $k = 1$ for the mark signalling condition and $k = 2$ for the space signalling state; A_k , ω_k , and ϕ_k are the respective amplitude, angular frequency and the phase of the received signal. A reference to figure. 3 will show that incoming signal is split into two channels each of which contains

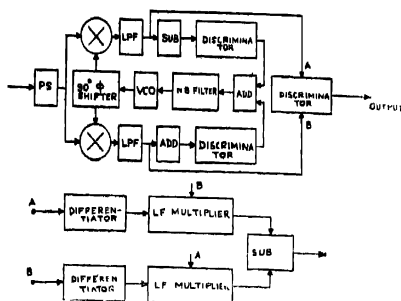


Figure 3. Block diagram of the scheme for correcting Doppler frequency shift in receiving FSK signal using a SBPL type receiver.

a product demodulator. The demodulating carriers in the demodulators are derived from the same VCO incorporated in the receiver but are in phase quadrature with each other $c_p(t) = B \cos(\omega_d t + \psi_0)$ and $c_q = B \sin(\omega_d t + \psi_0)$. The low frequency outputs accepted by means of low pass filters following the demodulators may be written as

$$P_1(t) = K \cos(\omega_d t + \phi_1 - \psi_0)$$

$$\text{and } Q_1(t) = -K \sin(\omega_d t + \phi_1 - \psi_0)$$

in the P and Q channels, respectively, for the mark signalling condition and

$$P_s(t) = K \cos(\omega_d t - \phi_s + \psi_0)$$

$$\text{and } Q_s(t) = K \sin(\omega_d t - \phi_s + \psi_0)$$

in the P and Q channels, respectively, for the space signalling conditions

The outputs $P(t)$'s and $Q(t)$'s are given phase shifts θ_P and θ_Q such that $\theta_P \sim \theta_Q = \pi/2$. The two phase shifted outputs thus obtained are then added together or subtracted from each other to make use of the discriminators following the respective adder and subtractor stages.

It is therefore clear from the above equations for $P(t)$'s and $Q(t)$'s that the existence of an output on addition shows the presence of space signalling condition at that moment. On the other hand the existence of an output on subtraction indicates the mark state of the received signal. It may further be added in this context that when an output is obtained on addition implies no output on subtraction and *vice versa*.

In the above it is tacitly assumed that the reference carrier in the receiver is in frequency synchronism with the assigned carrier in the transmitted signal. In case when there is a discrepancy between the two (i.e., $f_{ls} \neq f_o$) the frequency of the local oscillator can be supposed as $f_{ls} = f_o \pm \Delta f_o$; entailing a frequency $f_h = f_d \mp \Delta f_o$, in the mark channel output and a frequency $f_l = f_d \pm \Delta f_o$, in the space channel output. It is thus seen that a discrepancy $+\Delta f_o$ in the frequency of the injected carrier causes a decrease in frequency in the mark channel output by the same amount, whereas, the frequency of the output in the space channel is increased by the same factor. The use of a voltage controlled oscillator in the receiver enables one to circumvent the aforesaid discrepancy in frequency. The necessary controlling voltage can be obtained from a frequency discriminator operated by the outputs of the adder and subtractor stages.

It may be thought that if the outputs of the mark and space channels are applied to a discriminator of centre frequency f_d the output from the discriminator may be used to control the frequency of the local oscillator. This is not possible because of an inherent ambiguity. For one must know which channel is being received at the moment in order to fix the polarity of the controlling voltage. A little thought will show that the following conditions are to be satisfied.

Channel received		Discrepancy in frequency	Conclusion
Mark	Space		
$f_h < f_d$	$f_l > f_d$	positive ($+\Delta f_o$)	Reduce L. O. frequency
$f_h > f_d$	$f_l < f_d$	negative ($-\Delta f_o$)	Increase L. O. frequency

To get rid of the difficulty mentioned earlier it is needed to use two discriminators followed by the adder or the subtractor stages, respectively, in the mark and space channels. The characteristics of the discriminators should have the nature shown in figure 4. The outputs of these two discrimi-

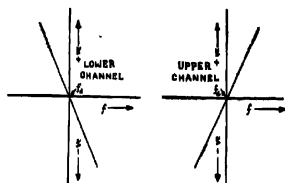


Figure 4. Shows the required characteristics for the discriminators.

minators are added and used to control the frequency of the local oscillator so as to decrease the phase discrepancy ϕ and if possible to eliminate it.

Recognition of the Mark and Space Signalling States

When locking of the demodulating carrier is established by the estimation channel in the receiving system, the low frequency outputs of the P and Q channels can be written as

$$P_1(t) = K \cos(\omega_d t + \theta)$$

$$\text{and } Q_1(t) = -K \sin(\omega_d t + \theta)$$

respectively for the mark signalling state of the received signal and that for the space state can be written as

$$P_2(t) = K \cos(\omega_d t + \theta)$$

$$\text{and } Q_2(t) = K \sin(\omega_d t + \theta).$$

The outputs of the P and Q channels are fed to a low frequency discriminator which gives at its output a dc voltage in proportion to the frequency of its inputs. The polarity of this voltage depends on the state of the incoming signal and gives the keying information. The demodulator is identified as the demodulation discriminator.

Design and Fabrication

In the following sections we shall discuss the design and fabrication of some of the important components of the reception system discussed. The most important components of such a reception system are the low frequency discriminators viz. (i) estimation discriminator and (ii) demodulation discriminator. The relevant points in fabricating the discriminators are discussed below.

Estimation Discriminator

Phase frequency characteristic of a null network may profitably be utilised in building low frequency discriminators having the desired characteristics. A reference to figure 5 will show that it consists of a LCR bridge and a product circuit. The voltage that will be developed across RC combination can be shown to be proportional to $\sin \phi$ where ϕ is the phase difference between the output voltage of the null network and its input. The parameters are to be so chosen as to have a null or zero output at a frequency equal to the shift in frequency f_d . It is known that the magnitude of the phase ϕ depends on the difference of the frequency of the input signal with that of its null frequency and the sign of the phase depends on whether the input frequency is higher or lower than the null frequency of the network. To have the desired characteristic of the second one an additional phase shift of 180° is to be introduced to the signal before it is fed to the null network.

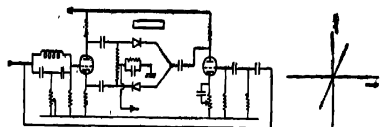


Figure 5. Circuit diagram of the discriminator unit used in the estimation channel together with its frequency-voltage characteristic.

Demodulation Discriminator

A reference to figure 6 will show that the demodulation discriminator essentially consists of differentiators, multipliers and a subtractor. The component parts are to be so designed as to give reliable performance at a frequency as low as 100 c/s. It can be shown that the discriminator output is given by $\pm D\omega_d$, where D takes account of all the constants viz, constant of the differentiator and that of the multiplier.

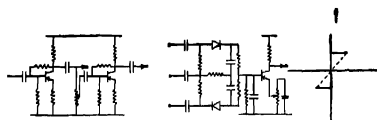


Figure 6. Circuit diagram of the discriminator unit used in the demodulation together with its frequency-voltage characteristic.

RECEPTION OF F-S KEYED SIGNALS

In this section we shall discuss various techniques of receiving FSK signals and in particular coherent scheme of detection. We consider first the case of noise free reception. The effects of noise will be dealt with in a subsequent section. The identification of the incoming state of the received signal may be carried out using (i) incoherent (or discriminator) detection and (ii) coherent detection.

In the former, the receiving system consists of two identical channels, each channel containing a bandpass filter centred at one of the state frequencies followed by an envelope detector. The outputs of the envelope detectors are subtracted from each other and the difference output is sampled. The decision of the received state is made from the polarity of this sampled output. Performance of such a receiving system becomes very unpredictable and unreliable in presence of channel perturbations caused by various transmission impairments (e. g., the Doppler shift). In such circumstances a coherent system will have a decisive advantage and may be behaving quite faithfully, of course, within certain bounds,

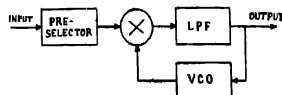


Figure 7. Block diagram of CPL type receiving unit for the reception of FSK signal.

A coherent system essentially consists of a feedback controlling loop which operates on the received signal (irrespective of the state) and derives the necessary controlling voltage for the purpose of gaining coherence and maintaining synchronism. In receiving FSK signal of the type I mentioned earlier one can make use of a single CPL circuit centred at the arithmetic mean of the two shifted frequencies for controlling the phase of the VCO automatically. But in such circumstances it is to be ensured that the loop bandwidth is so adequate that the oscillator is able to follow up the change in frequency in each bit interval and attains a steady state within a reasonable time compared to the bit interval. The input to the system is given by $A \cos (\omega_0 + x \omega_d) t$. A reference to the figure 7 will show that the output of the low pass filter is given by

$$e_d(t) = K G(s) \sin (x \omega_d t - \phi)$$

This output is used to control the frequency of the VCO and to keep the discrepancy to a minimum.

$$\frac{d\phi}{dt} = K G(s) \sin (x \omega_d t - \phi)$$

For small phase error

$$S\phi = K G(s) (x \omega_d t - \phi)$$

$$\text{or, } \phi = \frac{K G(s) x \omega_d t}{S + K G(s)}$$

$$\text{or, } (x \omega_d t - \phi) = \frac{x \omega_d}{S + K G(s)}$$

The expression for $e_d(t)$ now changes to

$$e_d(t) = \frac{x K G(s) \cdot \omega_d}{S + K G(s)}$$

While receiving FSK signal of the type II using an SBPL circuit we refer the input to the system as

$$e_i(t) = x A (\cos \omega_1 t + \cos \omega_2 t).$$

A reference to the figure 3 will show that the outputs of the P and Q

channels are given by

$$e_p(t) = x K G(s) [\cos(\omega_d t - \phi) + \cos(\omega_d t + \phi)]$$

$$\text{and } e_q(t) = x K G(s) [\sin(\omega_d t + \phi) - \sin(\omega_d t - \phi)].$$

The controlling voltage in this case is given by $e_d(t) = \langle e_p(t), e_q(t) \rangle = K_1 \sin 2\phi$. Under locked condition $\phi = 0$ which gives $e_p(t) = 0$ and $e_q(t) = K_1 G(s) x \sin \omega_d t$. This output is sampled at the bit interval where overlap is minimum. The sampled output is then tested for the polarity. Keyed integration and destructive sampling may give a still better result.

In coherent detection, the bandpass filters are followed by product demodulators with demodulating carriers in phase with either the assigned carrier or the state frequencies. The low frequency outputs of the demodulators are accepted by means of low pass filters following the demodulators. Now the decision of the received state may be made in either of the two ways (i) the outputs of the low pass filters are integrated and sampled and the decision is made from a comparison of the magnitude of the sampled output and (ii) the outputs of the low pass filters are subtracted from each other and integrated output is sampled and the decision is made from the polarity of the sampled output. Sampling should be done at the proper instants of time to achieve a maximum gain in SNR and from this consideration it is preferred to choose the sampling instant at the middle of the bit interval. At the two extremities of a bit interval there is much ambiguity in deciding exact state because of the interfering effect of the preceding and the following bits.

EFFECTS OF NOISE AND OTHER INTERFERENCES

In this section we shall consider the effects of the noise in the reception band in causing error in decision. We shall assume the noise to be additive in nature and white, gaussian in character with zero mean.

In the CPL case the input to the system in the presence of noise is given by

$$e_i(t) = A \cos(\omega_o \pm \omega_d)t + n_c \cos \omega_o t + n_q \cos \omega_o t,$$

where n_c and n_q are the in phase and quadrature components of the noise. Both n_c and n_q are white, gaussian independent variables.

The output of the VCO is given by $B \sin(\omega_c t + \phi_n)$ where the phase discrepancy ϕ_n is a slowly varying quantity. The output of the low pass filter is given by

$$e_d(t) = K [A \sin(\phi_n \mp \omega_d t) + n_c \sin \phi_n + n_q \cos \phi_n]$$

$$= K [(\mp A \sin \omega_d t + n_q) \cos \phi_n + n_c \sin \phi_n].$$

An error occurs when the sample value of $A \sin \omega_d t + n_q$ gives a polarity indication opposite to that of $A \sin \omega_d t$.

In the SBPL case the input to the system is given by
 $e_i(t) = \pm A [\cos(\omega_o + \omega_d)t + \cos(\omega_o - \omega_d)t] + n_c \cos \omega_d t + n_s \sin \omega_d t$.
 The demodulating carriers in this case are given by

$$B \cos(\omega_d t + \phi_n) \text{ and } B \sin(\omega_d t + \phi_n).$$

The P and Q channel outputs are given by

$$x AB [\cos(\omega_d t - \phi_n) + \cos(\omega_d t + \phi_n)] + n_c B \cos \phi_n - n_s B \sin \phi_n$$

$$\text{and } x AB [-\sin(\omega_d t - \phi_n) + \sin(\omega_d t + \phi_n)] + n_c B \sin \phi_n + n_s B \cos \phi_n.$$

The controlling voltage is given by

$$e_d(t) = K \sin 2\phi + n_c n_s B \cos 2\phi$$

which shows that the effect of noise in the controlling voltage is felt as a cross modulation term. The very appearance of the noise in this form will boost up low frequency spectral density, as a consequence of which the states will be held up. The bandwidth occupancy of the output noise will also increase. This high frequency boosting up of the spectral density will cause a larger number of change of states. A reference to the product output shown in figure 8 where a PR sequence of length fifteen will support the statement mentioned above.

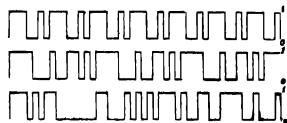


Figure 8. At the bottom is depicted the product output between two pseudo random sequences of length seven (at the top) and of length fifteen (in the middle).

EXPERIMENTAL SET-UP AND DISCUSSIONS

A laboratory model of the system (transmitter and receiver) was constructed and tested. Here we shall mainly discuss the principal features of the different component units and a few experimental findings.

A. Transmitter

It mainly consists of a modulator (FM oscillator) and a modulating source generating a random binary pattern. A pseudo-random (PR) sequence generator of length fifteen was constructed using switching transistors (type 2N404). Performance of the sequence generator was satisfactory for switching rate upto 54 Kc/s.

An rf oscillator at 2.0 Mc/s was frequency modulated using the output of the sequence generator as the keying signal. The deviation was adjusted to a proper value commensurate with the repetition rate.

B. Receiver

Discriminator detection was made to get a comparative study

with that of an APC type detection. In the discriminator detection it was tried i) with limiting and ii) without limiting cases in regard

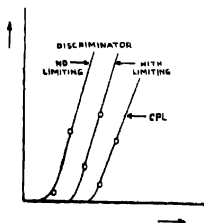


Figure 9. Shows the variation of number of errors recorded in (i) discriminator detection with and without limiting and (ii) in APC type reception.

to output SNR and error rates in presence of additive noise at the receiver. APC filter was constructed at a frequency equal to the assigned carrier i.e., at 2.0 Mc/s. Effect of filtering the output of the demodulator in regard to the output SNR and error rate was also studied.

In measuring the error rates, the transmitted sequence was first reconstructed (following filtering, amplifying and hard limiting in a Schmidt circuit) from the demodulated output and then the Mod-2 sum of the reconstructed sequence and the transmitted sequence was sampled at the middle of the bit and coincidence is detected. A counter following the AND circuit directly counts the number of erroneously received bit in a given period (present time). In respect of discriminator detection measurements of errors were made for the (i) limiting and (ii) without limiting cases with the level of the input noise and is plotted in figure 9. The figure also depicts the variation of the number of erroneously received bit with the level of the input noise for APC type detection.

CONCLUDING REMARKS

A detailed study of the experimental findings elucidating the principal objectives of the work will be presented in a future communication.

In discriminator detection it is observed that limiting, in general, improves the performance as regards the error rate and the threshold SNR. The automatic phase control type of reception using carrier and sideband phase locking techniques is particularly suitable when the received signal undergoes Doppler frequency shift. When it is not possible to achieve phase locking in the prevailing circumstances it is hoped that differentially coherent detection, where a currently received pulse may be stored and used to demodulate the pulse arriving in the next time slot, may be utilised with profit.

In recording errors there are objections to the use of non-linear processing in the Schmidt trigger. A few alternative schemes may be as follows.

(a) The received sequence is sampled (bipolar sampling) at $T/2$. The sampled pulse is multiplied with the complement of the reference sequence and pulses of only one polarity are accepted.

(b) The received sequence is sampled at $T/2$ and the sampled values are held to reconstruct the delayed sequence. The reference sequence is delayed by $T/2$ by means of a shift register. Mod-2 sum of the two sequences thus obtained is tested for the polarity.

(c) Both the received and the reference sequences are sampled. The sampled outputs are multiplied.

(d) Received sequence and the transmitted reference sequence are multiplied and integrated. The integrator output is sampled at time T_1 and tested for polarity.

(e) Mod-2 sum of the delayed received sequence and the complement of transmitted sequence is tested for polarity.

Arrangement (d) can be used for measuring both bit error and word error by adjusting the prf of the sampling pulse.

The author expresses his gratitude to Prof. N. B. Chakrabarti of I. I. T., Kharagpur for supervision of the work reported in this paper and for his valuable guidance in the preparation of the manuscript. The author wishes to thank Prof. G. S. Sanyal, Head, Department of Electronics and Electrical Communication Engineering, I. I. T., Kharagpur for his kind interest and constant encouragement also for the kind permission to work in the Department.

REFERENCES

- Bennet, W. R. & Rice, S. O. 1963 *B. S. T. J.* **42**, 2355.
Chakrabarti, N. B. & Datta, A. K. 1966 *Indian J. Phys.* **40**, 501.
Sunde, E. D. 1959 *B. S. T. J.* **38**, 1337.

Letters to the Editor

Lattice energies and thermal expansions of some heavier halides.

By M. N. SHARMA

Department of Physics, Lucknow University, Lucknow (India).

(Received 20 January 1969)

In the classical theory of ionic crystals (Born 1927, Born & Mayer 1932) it is assumed that the ions of an ionic crystal are spherically symmetrical and their interaction with each other consists of (1) an electrostatic term, (2) a repulsive interaction term, (3) multipole interactions i. e. (a) dipole-dipole interaction and (b) dipole-quadrupole interaction and (4) the zero point energy.

Taking into account all the above interactions, the energy of the crystal per unit cell may be expressed as

$$\phi(r) = -\frac{\kappa e^2}{r} + \frac{\lambda}{r^n} - \frac{C}{r^3} - \frac{D}{r^5} + \epsilon_0 \quad (1)$$

where κ is the Madelung's constant, λ is the repulsive parameter, C is the dipole-dipole interaction parameter, D is the dipole-quadrupole interaction parameter, ϵ_0 is the zero point energy, e is the electronic charge and r is the interionic distance.

We have taken the inverse power form of repulsive term because of its simplicity and also because it is justified by the fact that interionic distance between two ions remains nearly constant being near the value at the potential minimum.

The potential parameters λ and n and thence the lattice energies for some heavier halides have been calculated (table 1) using the well-known equilibrium conditions given by Hildebrand (1931).

It can be seen from table 1, that the results obtained in the present work are in as good an agreement with the experimental results as obtained by other authors employing the more cumbersome repulsive forms (Born & Mayer 1932, Huggins 1937, Cubicciotti 1959, 1961, Bleick 1934, Mayer & Levy 1933). Chatterjee (1963) using the same potential form as used here has calculated the compressibility (β) for lighter halides. However, the procedure used by him does not seem to be justified. He has used the experimental value of β to find free index n and then used value of n to find β again and

TABLE I. COMPARISON OF THEORETICAL AND EXPERIMENTAL VALUES OF LATTICE ENERGIES AND THERMAL EXPANSIONS OF HEAVIER HALIDES.

Crystal	Structure	Lattice Energy in K Cal/mole.			$\alpha_v \times 10^4$ per deg.		
		Expt.	Present work Equation(1)	Theor	Expt.	Present work (Equation(2)	Theor
NH ₄ Cl	CsCl		160.0	161.6***	142.00***	141.66	
NH ₄ Cl	CsCl		152.4	154.0***	161.00***	161.57	
CuCl	Zincblend	221.9*	213.5	216.0*	65.40*	65.76	
CuBr	Zincblend	216.0*	204.4	208.0*	62.10*	62.30	
CuI	Zincblend	213.4*	199.6	199.0*	73.50*	73.46	
AgCl	NaCl	205.7**	201.4	203.0**	98.90** 98.70+	98.73	94.44+++
AgBr	NaCl	201.8**	193.8	197.0**	104.0** 102.30+	104.38	95.53+++
AgI	Zincblend	199.0**	188.0	190.0**		113.48	
TlCl	CsCl	170.1**	164.7	167.0**	168.00**+	152.83	155.54+++
TlBr	CsCl	165.6**	161.2	164.0**		159.80	

* Mayer & Levy (1933)

** Mayer (1933)

*** Black (1934)

+ Hummel (1950)

+++ International Critical Tables (1928)

+++ Kumar (1955)

has called it β_{calc} . This is objectionable because the two equations used by him are not independent of each other and hence his procedure is of little significance.

In a crystal lattice, the ions oscillate about their equilibrium positions and their amplitudes increase with temperature. Hummel (1950), on this basis, has explained thermal expansion as being due to shifts in equilibrium positions of oscillating ions when their amplitudes become sufficiently large. In view of the effect of the ionic vibrations on thermal expansion of solids, many workers have correlated this property with vibration characteristics of ions.

In the present work, the values of the coefficient of thermal expansion (α_p) on the basis of equation (1) have been calculated by the formula

$$\alpha_p = \frac{3F_{T,p}}{T} \left\{ \frac{\frac{\alpha e^2}{r} + \frac{6c}{r^6} + \frac{8D}{r^3} - \frac{n\lambda}{r^n}}{-\frac{2\alpha e^2}{r} + n(n+1)\frac{\lambda}{r^n} - 42\frac{c}{r^6} - 72\frac{D}{r^3}} \right\} \quad (2)$$

$$\text{where } F_{T,p} = 1 + \frac{T}{\beta} \left(\frac{\partial \beta}{\partial T} \right)_p + \frac{T}{\beta^2 V} \left(\frac{\partial \beta}{\partial p} \right)_T \left(\frac{\partial V}{\partial p} \right)_T + \frac{2T}{3V} \left(\frac{\partial V}{\partial T} \right)_p$$

Calculated values of (α_p) are presented in table 1 along with the experimental values obtained by Kumar (1959) theoretically using a different potential and procedure. For salts other than NH_4Cl and NH_4Br as the data for the calculation F_p is not available we are justified in assuming $F_{T,p}=1$. Very good agreement is obtained. The calculated values of the thermal expansion seem to be in good agreement with the experimental values compared to those calculated by Kumar (1959). The cohesive energy values are, however, slightly inferior in comparison with the other values but this inferiority too does not exceed by more than 4.5% on the average. Therefore, in view of this simple procedure, which gives sufficiently satisfactory results, this simple inverse power of potential energy function may also be used for the computation of other lattice properties for heavier halides. The author anticipates that, if an accurate value of $F_{T,p}$ be used in calculating lattice energy and thermal expansion, still better agreement with experiment may be obtained.

The author is grateful to Professor B. G. Gokhale, Dr. es. Sc. (Paris) for his keen interest and encouragement throughout the present work. The author also records his thanks to the State Council of Scientific and Industrial Research, Uttar Pradesh, India, for a research grant.

REFERENCES

- Bleck, W. E. 1934 *J. Chem. Phys.*, **2**, 160.
 Born, M. 1927 *Handbuch der Physik.*, **24**, 370.
 Born, M. & Mayer J. E. 1932 *Zeit. f. Phys.* **75**, 1.
 Chatterjee, S. 1963 *Indian J. Phys.* **37**, 105.
 Cubicciotti, D. 1959 *J. Chem. Phys.* **31**, 1646.
 1961 *J. Chem. Phys.* **34**, 2189.
 Hildebrand, J. H. 1931 *Zeit. f. Phys.* **67**, 127.
 Huggins, M. L. 1937 *J. Chem. Phys.* **5**, 143.
 Hummel, F. A. 1950 *J. Amer. Ceram. Soc.* **33**, 102.
International Critical Tables, 1923 3 and 4. Mc Graw Hill, N. Y.
 Kumar. S. 1959 *Proc. Nat. Inst. Sci. India*, **25A**, 364.
 Mayer. J. E. 1933 *J. Chem. Phys.* **1**, 327.
 Mayer, J. E. & Levy R. B. 1933 *J. Chem Phys.* **1**, 647.

Indian J. Phys. **43**, 361–364 (1969)

Normal coordinate analysis of tungsten hexachloride (WCl_6)

By NITISH K. SANYAL, H. S. SINGH AND A. N. PANDEY

Department of Physics, University of Gorakhpur, Gorakhpur, India.

(Received 8 March 1969)

On the basis of available molecular dimensions and spectroscopic data, several molecules and ions of octahedral symmetry (O_h) have been subjected to normal coordinate analysis using various types of potential functions, enabling the evaluation of molecular constants like force constants, thermodynamic function, mean amplitudes of vibration etc. In continuation of the same type of work Nagarajan (1964) calculated the valence force field constants and mean amplitudes of vibration of tungsten hexachloride (WCl_6) from the estimated frequencies used in the calculation of thermodynamic functions by Stull and his associates (1962). Recently Evans & Lo (1968) have reported the assignments of all the six fundamentals frequencies of tungsten hexachloride with the help of two infrared active fundamental modes and six combination bands. The fundamental frequencies differ appreciably from the estimated frequencies used by Nagarajan (1964) in his calculations. Since we have been interested in similar work on octahedral molecules and ions (Pandey, Singh & Sanyal 1969), it was considered worthwhile to recalculate the molecular constants like force constants mean amplitudes of vibration and shrinkage effect for this molecule with the recent spectroscopic data (Evans & Lo 1968)

Valence force constants were calculated using Wilson's F - G matrix method. The general valence force field has been used and the elements of F and G matrices are taken from Kimura & Kimura (1963). The 2×2 determinant of f_{lu} species consisting of three unknown quantities was solved by a method proposed by Müller & Peacock (1968) for XY_n type molecules where $m_x > m_y$. The results of valence force field constants are presented in table 1 where the symbols have their usual significance.

TABLE 1. FORCE CONSTANTS OF TUNGSTEN HEXACHLORIDE

G. Q. P. F.	mdyne/A°	Observed frequencies cm ⁻¹	Calculated from G. Q. P. F. cm ⁻¹
$A=f_r$	2.2999	$\nu_1=408$	408
$B=f_{rr}$	0.2405	$\nu_1=312$	312
$C=f_r\alpha-f_r\alpha'$	0.0508	$\nu_1=367$	367
$D=f\alpha-f\alpha''$	0.2020	$\nu_1=165$	164.9
$E=f\alpha\alpha-f\alpha\alpha''$	-0.0097	$\nu_1=206$	206
$F=f\alpha\alpha'-f\alpha\alpha'''$	0.0519	$\nu_1=97$	97
$G=f_{rr'}$	0.2137		

TABLE 2. SHRINKAGE EFFECT IN THE CASE OF TUNGSTEN HEXACHLORIDE
(IN 10^{-2} A° UNITS)

Distance	T=0°K	T=298°K	T=500°K
ClCl (nonlinear)	-0.0275	0.0465	0.0987
ClCl (linear)	0.2550	0.8929	1.4720

Linear as well nonlinear Bastiansen-Marino shrinkages have been computed at temperatures $T=0^\circ\text{K}$, $T=298^\circ\text{K}$, and $T=500^\circ\text{K}$ using expression given by Cyvin & Meisingseth (1963). The results are presented in table 2.

The generalized mean square amplitude quantities and mean amplitude of vibration were evaluated at three temperatures $T=0^\circ\text{K}$, $T=298^\circ\text{K}$ and $T=500^\circ\text{K}$ using the method of Bye & Cyvin (1963), given in terms of symmetrized mean square amplitude matrices (\mathcal{L}). The results are presented in table 3. From the results it is concluded that the mean amplitudes of vibrations for bonded as well as non-bonded distances increase with the increase in temperature.

TABLE 3. GENERALIZED MEAN-SQUARE AND MEAN AMPLITUDE QUANTITIES IN TUNGSTEN HEXACHLORIDE.

Distance	Mean-square amplitude quantities, $10^{-4} \times \text{\AA}^2$				Mean amplitudes of vibration, $10^{-2} \times \text{\AA}$		
	Symbol	0°K	298°K	500°K	0°K	298°K	500°K
W-Cl	$\langle z^2 \rangle$	16.805	26.159	39.256			
	$\langle x^2 \rangle$	44.115	134.305	219.742	4.099	5.115	6.265
	$\langle y^2 \rangle$	44.115	134.305	219.742			
Cl.....Cl (linear)	$\langle z^2 \rangle$	28.075	42.164	62.958	5.299	6.493	7.935
	$\langle x^2 \rangle$	23.070	50.164	80.102			
	$\langle y^2 \rangle$	23.070	50.154	80.102			
Cl.....Cl (nonlinear)	$\langle z^2 \rangle$	52.415	124.380	197.789	7.240	11.153	14.064
	$\langle x^2 \rangle$	42.075	102.132	170.240			
	$\langle y^2 \rangle$	60.530	328.089	393.294			

The authors are grateful to C.S.I.R., New Delhi and State C.S.I.R., U.P. for financial assistance to two of them (A.N.P and H.S.S).

REFERENCES

- Bye, B. H. & Cyvin, S. J. 1963, *Acta Chem. Scand*, **17**, 1804.
Cyvin, S. J. and Meisingseth, E. 1963 *Acta Chem. Scand*, **17**, 1805.
Evans, J. C. and Lo, G. Y. S. 1968 *J. Mol. Spectroscopy* **26**, 147.
Kimura, M. & Kimura, K. 1963, *J. Mol. Spectroscopy*, **11**, 368.
Muller, A. & Peacock, C. J. 1968 *Molecular Phys*, **14**, 393.
Nagarajan, G. 1964 *Indian J. Pure Appl. Phys.*, **2**, 86.
Pandey, A. N., Singh, H. S. & Sanyal N. K. 1969 *Current Sci. India* **38**, 108
Prophet, H., Rizos, T. A. & Swanson, A. C. 1962 *Joint Army-Navy-Air Force Thermodynamical Tables*, The Advanced Research Projects Agency Programme US Air Force Contract No. A F 33 (616)- 6149 (The Dow Chemical Company, Midland, Michigan)
Stull, D. R., Chaio, J., Dergazarian, T. E., Hadden, S. T.,

BOOK REVIEWS

Phase-space Dynamics of Particles

by Allan J. Lichtenberg; John Wiley & Sons, Inc. New York,
Pages vii + 331, Price \$ 16.00

The book is one of the Wiley series in Plasma Physics. Recently, the idea of phase space has found very useful applications to beams and accelerators, along with plasmas. This justifies the necessity of a monograph with such an unusual title. It may be hoped that it will be welcomed by those who are in the field, particularly because of the dearth of published literature. In this monograph phase-space concepts for beams, accelerators, and confined particles are reviewed and their relations to basic theory and earlier developments are given. In the first chapter, the fundamental theories are introduced by the author. The second chapter treats adiabatic invariance. The transformations of phase space associated with a collection of particles, is first treated in the first part of the third chapter, the second part of which treats the closely related topics of beam transport systems. The remaining two chapters are devoted to accelerator applications, and confinement, trapping and heating of charged particles. The level of treatment of the book is oriented to graduate students and working technicians.

N. D. S. G.

Advances in Particle Physics Vol. 2

Edited by R. L. Cool and R. E. Marshak, John Wiley & Sons,
Inc. N. Y. Price \$ 24.95

The first half of this book deals with a status survey of our experimental knowledge about Boson resonances by Goldhabers and that of Baryon resonances by Barbaro-Galtieri. These are excellent reviews. There is however the problem that both of these subjects are rather fast changing. They are therefore generally covered at every major international conference on particle physics and are then available in their proceedings. The desirability of these reviews in the present format is therefore not clear. They both however devote some space to the general methods of resonance-analysis and this is of somewhat more permanent interest.

The rest of this book is concerned with theoretical problems. The weak interactions are covered in two articles; Application of Current algebra to weak decays by Mathur and Pandit and nonleptonic weak interactions by Rosen and Pakvasa. Their treatment is pedagogically oriented and should be found useful by research students. Lastly there is the review article on Broken Symmetries and Goldstone Theorem by Guralnik, Hagen and Kibble which is quite comprehensive.

V. S.

BOOKS RECENTLY RECEIVED FOR REVIEW

- Fundamentals of Radiation Protection*, H. F. Henry, \$ 17.50, John Wiley & Sons, N.Y.
- Semiconductor Plasma Instabilities*, Hans Hartnagel, 63sh, Heinemann Educational Books Ltd., London.
- Correlation Effects in Atoms and Molecules*, R. Lefebvre & C. Moser, \$ 29.95, John Wiley & Sons, N.Y.
- Men of Physics—L. D. Landau II*, D. ter Haar, \$ 5.50, Pergamon Press, Oxford.
- Fundamental of Quantum Electronics*, R. F. Pantell & H. E. Puthoff, \$ 15.95, John Wiley & Sons, N.Y.
- Lectures on Quantum Mechanics*, Gordon Bayn, W. A. Benjamin Inc., N.Y.
- Modern Quantum Mechanics with Applications to Elementary Particle Physics*, John A. Eisele, \$ 19.50, John Wiley & Son, N.Y.
- The World of Mars*, V. Axel Firsoff, 7/6 in U. K., Oliver & Boyd Ltd., England.
- Elektronen Mikroskopische Methodie*, G. Schimmel \$ 19.50, Springer Verlag, Berlin.
- Electrodynamics of Particles and Plasma*, Clemmow-Dougherty, \$ 17.50, Addison & Wesley, London.

Thermal expansion of some Cu-and Ag-base alloys at high temperatures.

By M. DE

*Department of General Physics & X-rays, Indian Association
for the Cultivation of Science, Calcutta-32, India.*

(Received 29 November 1968 ; Revised 28 June 1969)

Using a 19cm Unicam high temperature camera and filtered CuK_α radiation from a stabilized Philips X-ray Generator photographs were taken of powders of Cu-Ni, Ag-Mn, Cu-Sn and Cu-In alloys in the solid solution range upto 500°C . In all these cases non-linear relationships were found between lattice parameter and temperatures. The linear thermal expansion coefficients were calculated from the lattice parameter-temperature curves and compared with the previously reported results. Attempts have also been made to explain the thermal expansion behaviours qualitatively.

INTRODUCTION

Recently, Rao *et al* (1964) have reported lattice expansion of some AgPd alloys using X-ray technique. They observed some sort of structural change in some alloy compositions which they explained to be due to temperature induced electronic structure change at higher temperatures. The present investigations deal with the X-ray method of thermal expansion measurements of some Cu- and Ag- base alloys with transitional and non-transitional solutes. Of all the substances studied, the most important is the Cu-Ni alloy system which like Ag-Pd alloys forms a continuous solid solution. From the investigations of different physical properties (Koster & Schule 1957 ; Ryan *et al* 1959 ; Schroder 1961 ; Rapp *et al* 1962) the presence of a miscibility gap (or clustering) has been suggested in this system. However, work on the enthalpies of formation of the electronically similar Ag-Pd alloys (Oriani & Murphy 1962) showed negative heats of formation suggesting the presence of a positive short-range order rather than a miscibility gap. The similarity of the atomic scattering factors of the component metals Cu and Ni decreases considerably the sensitivity of both X-ray and neutron diffraction (Segre 1953) techniques to detect the presence of any such order. So it was hoped that at higher temperature the lattice parameter variation with temperature would indicate some sort of structural change present in different alloys of this system.

Besides Cu-Ni system, α - phase Ag-Mn alloys have also been investigated to study the effect of the transitional solute Mn on the thermal expansion of this system. For non-availability of any lattice parameter data at high temperatures it has also been considered desirable to extend

the work of thermal expansion to some other α -phase Cu-base alloys with non-transitional metal Sn and In as solutes.

EXPERIMENTAL PROCEDURE

Cu-Ni alloys containing 26.54, 51.97 and 76.45 atomic percent of nickel were obtained from Messrs. Goldsmith Bros. (U.S.A.) as wires of 1.5 mm. in diameter. Ag-Mn alloys with 5.54, 11.03 and 16.20 atomic percent of manganese, Cu-Sn alloys with 2.77, 5.11 and 7.98 atomic percent of tin and Cu-In alloys with 1.67, 5.16 and 6.19 atomic percent of indium were prepared from spectrographically standardized metals supplied by Messrs. Johnson, Matthey & Co., Ltd., London, following the same method as adopted previously (De 1967), the homogenization temperatures being 750-850°C. The annealing treatments were terminated by quenching in air. Weight changes during preparation being negligible no chemical analyses of the alloys were performed.

Preparations of the powder samples (about 4 mm in length and 0.5 mm in diameter) and mounting of the specimens on the specimen-holder were done in the usual way (De 1967) avoiding eccentricity. The standard 19 cm Unicam high temperature camera and filtered CuK_α radiation were used for taking the powder photographs at different temperatures lying between room temperature and 500°C. Any thermal gradient was minimised by taking very small specimens (as mentioned above) and by adjusting the controlling systems of the heating coils. Temperatures were measured within $\pm 1^\circ\text{C}$ with the help of a pair of previously calibrated Pt-PtRh thermocouples. Room temperature photographs were taken at frequent intervals to check any effect of prolonged annealing and subsequent quenching on the specimens and also to detect any significant loss of the solutes by volatilization. No such effect was observed except with Cu-In alloys where volatilization of the solute was noticed at higher temperatures. To diminish the amount of volatilization, fresh samples were taken each time at higher temperatures but even this procedure failed for the Cu-6.19% In alloy above 350°C after which considerable decrease in the lattice parameter values was observed and this was mainly due to the loss of indium as verified by the subsequent room temperature photographs. Each photograph was followed by duplicate runs to show the reproducibility of the data within the range of experimental error and the final value of the lattice parameter at any temperature given below is the mean of the results of two or more sets. The Cu-76.45% Ni alloy was studied in detail in the temperature range 70°-100°C giving temperature interval of 15°C. The lattice parameters were calculated from the line positions of the intense reflections (111), (200), (220), (311), (331)

α_1, α_2 and $(420) \alpha_1, \alpha_2$ and corrected by the standard extrapolation method of Taylor & Sinclair (1945).

RESULTS

The lattice parameter values of the alloys at different temperatures are given in table 1 and are shown in figures 1 and 2 along with those for pure Cu (figure 2) from Mitra & Mitra (1963). By extrapolating the plots of the lattice parameter values against $\frac{1}{2} \left(\frac{\cos^2 \theta}{\sin \theta} + \frac{\cos^2 \theta}{\theta} \right)$ to $\theta = 90^\circ$ (Nelson & Riley 1945) the accurate lattice parameter values at a particular temperature showed maximum deviations of $\pm 0.0003 \text{ \AA}$ for Cu-Ni and Ag-Mn alloys and $\pm 0.0004 \text{ \AA}$ for Cu-Sn and Cu-In alloys and these have been taken as the limits of accuracy. However, no correction due to refraction was applied since error due to refraction is much smaller than the experimental error.

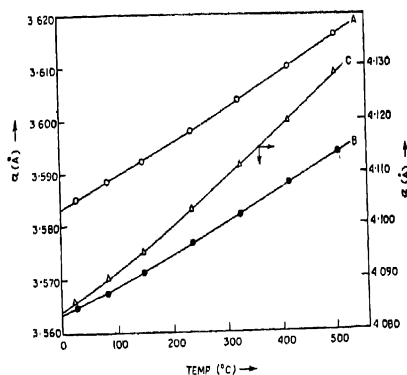


Figure 1a. Lattice parameter-temperature curves for Cu-Ni and Ag-Mn alloys. A: Cu-26.54% Ni, B: Cu-51.97% Ni; C: Ag-5.54% Mn.

From figures 1 and 2 it is found that the lattice parameter values increase with the increase of solute concentration and the lattice parameter versus temperature plots show smooth non-linear curves concave upwards. The lattice parameter-temperature curve for the Cu-76.45%Ni alloy (figure 1b), however, shows a discontinuity at about 90°C and at higher temperatures this curve is more or less linear. Some of these curves can best be represented by the following types of equations :

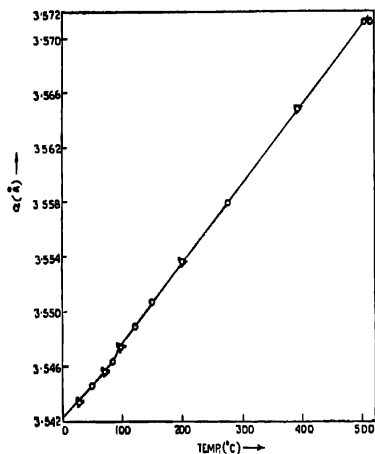


Figure 1b. Lattice parameter-temperature curve for Cu-76.45% Ni alloy.

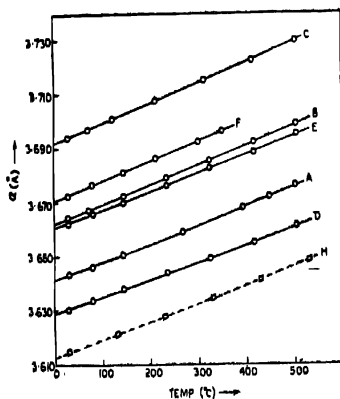


Figure 2 Lattice parameter-temperature curves for pure Cu, Cu-Sn and Cu-In alloys
 A: Cu-2.77% Sn; B: Cu-5.11% Sn; C: Cu-7.98% Sn;
 D: Cu-1.67% In; E: Cu-5.16% In; F: Cu-6.19% In;
 H: Pure Cu.

(i) For Cu-5.11% Sn :

$$a_T = 3.66232 + 6.774 \times 10^{-5}T + 1.690 \times 10^{-8}T^2 - 1.624 \times 10^{-11}T^3$$

(ii) For Cu-7.98% Sn :

$$a_T = 3.69196 + 7.393 \times 10^{-5}T + 2.866 \times 10^{-8}T^2 + 4.828 \times 10^{-12}T^3$$

(iii) For Cu-1.67% In :

$$a_T = 3.62888 + 6.068 \times 10^{-5}T + 5.473 \times 10^{-8}T^2 + 1.485 \times 10^{-12}T^3$$

(iv) For Cu-5.16% In :

$$a_T = 3.66071 + 6.323 \times 10^{-5}T + 12.302 \times 10^{-8}T^2 - 4.219 \times 10^{-12}T^3$$

(v) For Ag-5.54% Mn :

$$a_T = 4.0842 + 6.948 \times 10^{-5}T + 4.425 \times 10^{-8}T^2 - 1.357 \times 10^{-11}T^3$$

where a_T = lattice parameter at $T^\circ\text{C}$.

The room temperature lattice parameter values, measured frequently in course of the experiments, showed no changes greater than the experimental error. These values are also compared with those obtained by interpolation from the measurements of (i) Coles (1956) for Cu-Ni alloys, (ii) Raub & Engel (1946) for Ag-Mn alloys, (iii) Owen & Iball (1935), Guljaev & Trusova (1950) for Cu-Sn alloys and (iv) Jones & Owen (1954) for Cu-In alloys. The mean and maximum differences were found to be 0.0005 and 0.001 Å for Cu-Ni alloys, 0.0003 and 0.0006 Å for Ag-Mn alloys 0.0004 and 0.001 Å for Cu-Sn alloys and 0.0003 and 0.0008 Å for Cu-In alloys. However, the purity of the substances is not of the same order in all the cases and a difference of nearly 10–12°C exists between these room temperatures. Also, difference in lattice defects, if any, due to differences in residuals trains may, to some extent, change the lattice parameter values.

TABLE 1. LATTICE PARAMETER-TEMPERATURE DATA FOR Cu-Ni, Ag-Mn, Cu-Sn AND Cu-In ALLOYS.

Cu-26.54% Ni Alloy		Cu-51.97% Ni Alloy		Cu-76.45% Ni Alloy	
Temp. (°C)	Lattice parameter (Å)	Temp. (°C)	Lattice parameter (Å)	Temp. (°C)	Lattice parameter (Å)
29	3.5850	28	3.5650	27	3.5434
84	3.5885	84	3.5678	50	3.5446
148	3.5924	148	3.5714	71	3.5457
236	3.5980	236	3.5768	84	3.5464
324	3.6037	324	3.5822	97	3.5475
416	3.6098	416	3.5879	120	3.5489
505	3.6158	505	3.5935	148	3.5507
				200	3.5536
				275	3.5580
				393	3.5649
				505	3.5715

TABLE 1 (Contd.)

Ag-5.54% Mn Alloy		Ag-11.03% Mn Alloy		Ag-16.20% Mn Alloy	
Temp. (°C)	Lattice parameter (Å)	Temp. (°C)	Lattice parameter (Å)	Temp. (°C)	Lattice parameter (Å)
24	4.0860	24	4.0858	24	4.0854
84	4.0904	84	4.0903	84	4.0900
148	4.0952	148	4.0960	148	4.0962
236	4.1032	236	4.1042	236	4.1040
324	4.1112	324	4.1120	324	4.1124
416	4.1195	416	4.1204	416	4.1204
505	4.1286	505	4.1284	505	4.1288

Cu-2.77% Sn Alloy		Cu-5.11% Sn Alloy		Cu-7.98% Sn Alloy	
Temp. (°C)	Lattice parameter (Å)	Temp. (°C)	Lattice parameter (Å)	Temp. (°C)	Lattice parameter (Å)
31	3.6432	29	3.6644	30	3.6940
80	3.6463	72	3.6672	72	3.6972
144	3.6505	144	3.6724	122	3.7013
274	3.6592	236	3.6791	212	3.7082
393	3.6677	324	3.6856	312	3.7149
450	3.6718	416	3.6922	416	3.7227
505	3.6758	505	3.6986	505	3.7299

Cu-1.67% In Alloy		Cu-5.16% In Alloy		Cu-6.19% In Alloy	
Temp. (°C)	Lattice parameter (Å)	Temp. (°C)	Lattice parameter (Å)	Temp. (°C)	Lattice parameter (Å)
30	3.6306	30	3.6626	30	3.6727
80	3.6338	80	3.6658	80	3.6763
144	3.6378	144	3.6700	144	3.6809
236	3.6436	236	3.6762	212	3.6860
324	3.6492	324	3.6825	300	3.6924
416	3.6552	416	3.6888	350	3.6963
505	3.6611	505	3.6950		

From figures 1 and 2 the linear thermal expansion coefficients α were determined from the relation, $\alpha = 1/a \frac{da}{dT}$ taking different temperature intervals and are plotted in figures 3 and 4. The α values for pure Cu measured with a quartz dilatometer by Leksina & Novikova (1963) and those for Ni measured with an interferometric dilatometer by Nix & Macnair (1941) are also shown in figure 3 for comparison. In figure 4, the thermal expansion of pure Cu from Mitra & Mitra (1963) using X-ray technique has also been indicated along with the dilatometric measurements of Leksina & Novikova (1963) and it seems that at higher temperatures X-ray

method gives higher values of α than those by dilatometric method. However, the present measurements with several alloys show the consistency in the α values increasing nonlinearly with temperature. For Cu-Ni alloys this non-linearity is greater for alloys with higher nickel concentration and for Cu-76.45% Ni alloy a break occurs in the α - T curve near 90°C (figure 3). The graphical method of determining the α values by taking equal temperature intervals for some alloy compositions introduces some uncertainties in the values of da/dT and hence in α . But the smooth curves drawn through the experimental points remove these uncertainties and represent the correct temperature variation of α . The maximum fluctuation of the experimental value of α at any particular temperature from its corresponding value obtained from the smooth curve was estimated to be within 3%.

DISCUSSION

In case of alloys, Owen & Roberts (1939), Quader & Dey (1962) and Rao *et al* (1964) obtained these types of nonlinear curves from the lattice parameter-temperature plots of some other Cu-and Ag-base alloys. The interpretation for this nonlinearity, however, seems to be difficult with the present knowledge of lattice dynamics of alloys. Generally any change in the slope of the lattice parameter-temperature curves may be associated with changes in the magnetic states, short-range order and/or the electronic structure such as overlapping of Brillouin zones (Busk 1952). The vacancy concentration at higher temperatures may also cause some change in the slopes of the α - T curves. Any significant effect of the latter is, however, unlikely in these cases because the highest temperature studied is much below the melting points of the alloys. Since the room temperature lattice parameter values remained unchanged even after long annealing at higher temperatures and subsequent quenching in the camera, there is hardly any possibility of the presence of short-range order. As regards the influence of any change in the magnetic properties, all the alloy compositions, except the Cu-76.45% Ni alloy, being paramagnetic in this temperature range, may have very feeble magnetic interaction so as to produce no significant effect on the α - T curves. However, the presence of any ferromagnetic clusters in the Ni rich alloys of the Cu-Ni system (Ryan *et al* 1959; Schroder 1961) may influence the α - T curves to some extent. The discontinuity near about 90°C in the α - T curve of the Cu-76.45% Ni alloy (figure 1b) is probably related to magnetic ordering since this alloy is ferromagnetic below this temperature. Cu-Ni and Ag-Mn alloys may also have some temperature induced electronic structure change due to low degeneracy temperature of the incomplete d-shell electrons and at higher temperatures increase of holes in the d-band may change the lattice structure so as to introduce some non-linearity in the α - T curves of these alloys. Similar

behaviours were also observed in some compositions of Ag-Pd alloys (Rao *et al* 1964). In the cases of Cu-Sn and Cu-In alloys such electronic structure change is, however, unlikely.

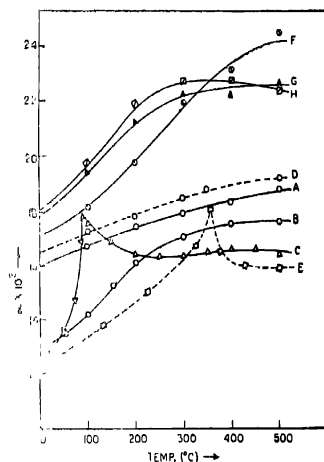


Figure 3. Linear thermal expansion coefficients α against temperature curves for Cu, Ni, Cu-Ni and Ag-Mn alloys.

A : Cu-26.54% Ni ; B : Cu-51.97% Ni ; C : Cu-76.45% Ni ;
D : Pure Cu ; L : Pure Ni ; F : Ag-5.54% Mn
G : Ag-11.03% Mn H : Ag-16.20% Mn.

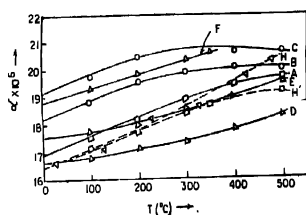


Figure 4. Linear thermal expansion coefficients α against temperature curves for Cu, Cu-Sn and Cu-In alloys

A : Cu-2.77% Sn ; B : Cu-5.11% Sn ; C : Cu-7.98% Sn ;
D : Cu-1.67% In ; E : Cu-5.16% In ; F : Cu-6.19% In ;
H : Pure Cu (X-ray method) ; H' : Pure Cu (Dilatometric method)

From figures 3 and 4 it is found that in general, the expansion coefficients α increase with the increase of temperature and concentration of the solutes—the Cu-Ni alloy system being the only exception where the α values decrease with the increase of the solute concentration (figure 3). Figure 3 also shows that in the Cu-Ni system the α - T variation for the Cu-rich alloy is similar to that for pure Cu (Leksina & Novikova 1963) whereas, the Ni-rich alloy has this variation similar to that for pure Ni (Nix & Macnair 1941). The literature (Smithells 1962) reports the room temperature α value for Cu-45 wt.% Ni to be $14.9 \times 10^{-6}/^{\circ}\text{C}$ and from the present measurements this value is $14.3 \times 10^{-6}/^{\circ}\text{C}$ for Cu-50 wt. % Ni (i.e. Cu-51.97 atomic percent Ni) alloy. The striking feature of the Cu-Ni system is the increasing nonlinearity of the α - T curves with the increase of Ni concentration which is probably due to the increasing electronic and magnetic contribution to the thermal expansion. The increasing nonlinearity in the α - T curves of Ag-Mn alloys also supports higher electronic contribution to the thermal expansion with the increase of manganese concentration. The behaviour of the thermal coefficient of expansion in the Cu-76.45% Ni is obscured by the presence of a volume change accompanying the vanishing of ferromagnetism with the result of formation of a peak at about 90°C which is the Curie point of this composition. However, the presence of small amounts of impurities in ferromagnetic substances can play a dominating role in determining the total thermal expansion near Curie point (Williams 1934; White 1961).

From figure 4 it is found that in the cases of Cu-Sn and Cu-In alloys the expansion coefficients α increase slowly with temperature and concentration of the solutes. The room temperature α value for Cu-2.77% Sn alloy is of the order of $17.4 \times 10^{-6}/^{\circ}\text{C}$. Hidnert (1943) reported a room temperature α value for Cu-1.3% Sn alloy to be $16.8 \times 10^{-6}/^{\circ}\text{C}$.

The author is grateful to Prof. B. N. Srivastava, D.Sc., F.N.I., for his continued interest in the work and to Drs. M.A. Quader and S.P. Sen Gupta for some valuable suggestions.

REFERENCES

- Busk, B. S. 1952 *J. Metals*, **4**, 207.
- Coles B. R. 1956 *J. Inst. Metals* **84**, 340.
- De, M. 1967 *Indian J. Phys.*, **41**, 79.
- Guljaev, A. P. & Trusova, E. F. 1950 *Z. Tekh. Fiz. SSSR*, **20**, 66.
- Hidnert, P. 1943 *J. Res. Nat. Bur. Stand.*, **30**, 75.
- Jones, R. O. & Owen, E. A. 1954 *J. Inst. Metals*, **82**, 445.
- Koster, W. & Schule, W. 1957 *Z. Metallk.*, **48**, 592.
- Leksina, I. E. & Novikova, S. I. 1963 *Soviet Phys. Solid State*, **5**, 798.

- Mitra, G. B. & Mitra, S. K. 1963 *Indian J. Phys.*, **37**, 462.
- Nelson, J. B. & Riley, D. P. 1945 *Proc. Phys. Soc. (London)*, **57**, 160.
- Nix, F. & Macnair D. 1941 *Phys. Rev.* **60**, 597.
- Oriani, R. & Murphy, W. K. 1962 *Acta Met.* **10**, 879.
- Owen, E. A. & Roberts, E. W. 1939 *Phil. Mag.* **27**, 294.
- Owen, E.A. & Iball, J. 1935, *J. Inst. Metals*, **57**, 267.
- Quader, M.A. & Dey, B. N. 1962 *Indian J. Phys.* **36**, 43.
- Rao, C. N. & Rao, K. K. 1964, *Canad. J. Phys.* **42** (7), 1336.
- Rapp, R. A. & Maak, F. 1962 *Acta Met.*, **10**, 63.
- Raub, E. & Engel, A. 1946, *Z. Metallk.* **37**, 62.
- Ryan, F., Pugh, E., & Smoluchowski, R. 1959 *Phys. Rev.*, **116**, 1106.
- Schroder, K. 1961 *J. Appl. Phys.* **32**, 880.
- Segre, E. 1953 *Experimental Nuclear Physics*, Vol. II, (John Wiley & Sons N.Y. U.S.A.).
- Sinclair, H. & Taylor, A. 1945 *Proc. Phys. Soc. (London)*, **57**, 108, 126.
- Smithells, C. J. 1962 *Metals Reference Hand book*, Vol II, 704, (Butterworth & Co., Ltd, London).
- White, G. K. 1961 *Aust. J. Phys.* **14**, 359.
- Williams, C. 1934 *Phys. Rev.*, **46**, 1011,

Velocity of sound and an equation of state for liquids

BY R. V. GOPALA RAO AND V. VENKATA SESHAIHAH

Department of Physical Sciences, Sree Venkateswara University College of Engineering, Tirupati, Andhra Pradesh, India.

(Received 2 February 1969)

An expression for the total pressure of liquids from the concept of sound propagation through liquids was derived. The equation connects the total pressure of the liquid to the molecular diameter d and a dimensionless parameter δ . The calculated values of the molecular diameter d agree well with those obtained by other methods. To test the validity of the pressure equation, the compressibilities and the pressure variation of bulk modulus were derived and compared with experimental value and it was found to give satisfactory agreement. It is shown that the total pressure, P , varies in a linear way with $1/\beta_T$, the isothermal bulk modulus. It was found that the attractive pressure can be better expressed as aV^{-n} and not as aV^{-3} , as in the case of Van der Waals equation especially in the liquid state of the fluid. In general, it was found that the value of n is around 2 and not exactly 2, the average value being 1.91.

INTRODUCTION

Sound propagation in a fluid is a very important illustration of compressional wave motion in a material medium. The propagation of acoustic disturbance is connected with intermolecular forces since the disturbance while being propagated has to overcome the internal forces of attraction. In the case of the gaseous phase of the fluid the forces of attraction are weak while strong forces of attraction and repulsion dominate in the liquid phase of the fluid. Hence sound velocity has to be considered as a primary property of liquids in a molecular kinetic theory and not a secondary property derived from compressibility as in normal thermodynamics.

EQUATION OF STATE FROM SOUND VELOCITY

As is well known the velocity of sound is given by (Hirschfelder 1954)

$$C^2 = (V/V_f)(\gamma RT/M)^{3/2} \quad \dots(1)$$

where, C = velocity of the sound in fluids, V = molar volume of the liquid, and V_f = molar free volume. The rest of the symbols have their usual connotation.

If a compressional wave is propagated through fluid it is easy to show that (Lindsay 1960 ; Blitz 1963),

$$C^2 = (dP/d\rho)_S = \gamma (dP/d\rho)_T \quad \dots(2)$$

From equations (1) and (2) we get

$$(dP/dV)_T = - (RT/V_f^{3/2}) (1/V^{4/3}) \quad \dots(3)$$

Along with others we assume that the molar free volume of fluids is given by (Eyring 1937 ; Hirschfelder 1954)

$$V_f = b^3 (V^{1/3} - N^{1/3}d)^3 \quad \dots(4)$$

where b is a constant depending upon the type of packing ($b = 2, 1.835$ & 1.78 for SCC, BCC. & FCC respectively) and d is the so called incompressible diameter of the molecule. In case of gases $V_f = V$, since $N^{1/3}d$ is negligible and b is unity.

From (3) and (4), we get

$$dP = - \frac{RTdV}{b^3(V^{1/3} - N^{1/3}d)^3 V^{4/3}} \quad \dots(5)$$

$$P = \frac{3RT}{b^3 A^3} \left[\frac{X}{X-A} + \frac{A}{X} - 1 + 2 \ln \left(\frac{X-A}{X} \right) \right] + K_1(T) \quad \dots(6)$$

where, $A = N^{1/3}d$, $X = V^{1/3}$, and $K_1(T)$ = a constant of integration and is independent of volume.

Thus, we have an equation of state for fluids. To evaluate the integration constant $K_1(T)$ we use the well known Maxwell theorem (De Boer 1964)

$$\int_{V_l}^V P. dV = P(V_g - V_l) \quad \dots(7)$$

If we are very much below the critical temperature which is true at room temperatures, we have $V_g \gg V_l$. Further assuming that at these low vapour pressures (~ 0.1 atm.) we can safely assume that the vapour is ideal. Hence, we have from equation (7)

$$\int_{V_l}^{V_g} P. dV = RT \quad \dots(8)$$

Using equations (6) and (8), we get

$$RT = \int_{x_l}^{x_g} \frac{9RT}{b^3 A^3} \left[\frac{x}{x-A} + \frac{A}{x} - 1 + 2 \ln \left(\frac{x-A}{x} \right) \right] x^2 dx + \int K_1(T). dV \quad \dots(9)$$

where, $x_l = V_l^{1/3}$ and $x_g = V_g^{1/3}$.

After lengthy but straightforward integration, we obtain the value of $K_1(T)$ to be

$$K_1(T) = \frac{RT}{(x_g^3 - x_l^3)} - \frac{3RT}{b^3 A^3 (x_g^3 - x_l^3)} \left\{ 2A(x_g^3 - x_l^3) + A^3(x_g - x_l) \right. \\ \left. + A^3 \ln \left(\frac{x_g - A}{x_l - A} \right) + 2x_g^3 \ln \left(\frac{x_g - A}{x_g} \right) \right. \\ \left. - 2x_l^3 \ln \left(\frac{x_l - A}{x_l} \right) \right\} \quad \dots(10)$$

from which we write after transformation into V_g and V_l

$$P = \frac{3RT}{b^3 N d^3} \left[\frac{V_l^{1/3}}{V_l^{1/3} - N^{1/3} d} - \frac{V_l^{1/3} - N^{1/3} d}{V_l^{1/3}} + 2 \ln \left(\frac{V_l^{1/3} - N^{1/3} d}{V_l^{1/3}} \right) \right. \\ \left. + \frac{b^3 N d^3}{3(V_g - V_l)} - \frac{1}{(V_g - V_l)} \left\{ 2N^{1/3} d \left(V_g^{2/3} - V_l^{2/3} \right) \right. \right. \\ \left. \left. + N^{1/3} d^2 \left(V_g^{1/3} - V_l^{1/3} \right) + N d^3 \ln \left(\frac{V_g^{1/3} - N^{1/3} d}{V_l^{1/3} - N^{1/3} d} \right) \right. \right. \\ \left. \left. + 2V_g \ln \left(\frac{V_g^{1/3} - N^{1/3} d}{V_g^{1/3}} \right) - 2V_l \ln \left(\frac{V_l^{1/3} - N^{1/3} d}{V_l^{1/3}} \right) \right\} \right] \quad \dots(11)$$

If we are far below the critical temperature $V_g \gg V_l$ and hence $V_l^{1/3} \gg V_l^{1/3}$, then the above equation (11) can be reduced to

$$P = \frac{3RT}{b^3 N d^3} \left[\frac{V_l^{1/3}}{V_l^{1/3} - N^{1/3} d} - \frac{V_l^{1/3} - N^{1/3} d}{V_l^{1/3}} \right. \\ \left. + 2 \ln \left\{ \frac{V_l^{1/3} - N^{1/3} d}{V_l^{1/3}} \right\} \right] \quad \dots(12)$$

In this connection it is found out that the contribution due to the term $b^3 N d^3 / 3(V_g - V_l)$ is also negligible since $N d^3$ itself is less than V_l .

We define now a dimensionless parameter (Gopala Rao 1967)

$$\delta \equiv \frac{3C_1 - 1}{2} \quad \dots(13)$$

and it was shown that

$$\delta = \frac{V_l^{1/3}}{V_l^{1/3} - N^{1/3} d} \quad \dots(14)$$

From equations (12) and (14) we get

$$P = \frac{3RT}{b^3 N d^3} \left[\delta - \frac{1}{\delta} - 2 \ln \delta \right] \quad \dots(15)$$

Equations (12) and (15) are surprisingly simple and are important since they give a valuable method for the evaluation of compressibilities and

other thermodynamic properties of liquids. Further (12) and (15), even though derived from velocity consideration does not contain a term involving velocity through liquids. Further equation (12) and (15) connect the pressure to a microscopic property d , the molecular diameter.

Here the pressure is the total pressure and is the sum of kinetic and static pressures, sometimes referred to as the internal pressure. It can be shown from thermodynamics that (Moelwyn-Hughes 1961)

$$P = T (dP/dT)_V - (dE/dV)_T \quad \dots(16)$$

Total pressure = Kinetic pressure + Static pressure.

The kinetic pressure is due to thermal motion and is always positive while the static pressure may be positive, negative or zero. It can be shown from elementary thermodynamics that

$$P_k = T (dP/dT)_V = \alpha_T/\beta_T \quad \dots(17)$$

$$\text{and } P_s = - (dE/dV)_T \quad \dots(18)$$

$$\text{Hence } P = \frac{\alpha_T}{\beta_T} - \frac{a}{V^2}.$$

Comparing it with Van der Waals equation we have

$$P_s = - \frac{a}{V^2} \quad \dots(19)$$

Hence we have from (15), (17), (18) and (19)

$$P = \frac{\alpha_T}{\beta_T} - \frac{a}{V^2} = \frac{3kT}{Nb^2d^3} \left[\delta - \frac{1}{\delta} - 2 \ln \delta \right] \quad \dots(20)$$

The molecular diameters were calculated from equation (20). The values so calculated are given in table 1 for various types of packing. The d values so calculated agree well with those obtained by other methods (Hirschfelder 1954 ; Handbook of Chemistry and Physics 1958 ; Gopala Rao 1969).

A further test of equation (15) is the evaluation of compressibility coefficients of the liquids. Remembering that

$$\beta_T = - \frac{1}{V} \left(\partial V / \partial P \right)_T$$

we obtain from equation (15) that

$$\begin{aligned} \frac{1}{\beta_T} = & - \frac{RT}{b^2Nd^3} \left[\frac{b^2V^{1/3}}{V_f^{2/3}} \left(\frac{2V_f^{1/3}}{b} - N^{1/3}d \right) - \frac{N^{1/3}d}{V^{1/3}} - 2 \right. \\ & \left. + \frac{1}{V_f} \left\{ \frac{bV^{1/3}}{V_f^{1/3}} Nd^3 + 6V \ln \left(\frac{V_f^{1/3}}{V^{1/3}b} \right) + \frac{2bVN^{1/3}d}{V_f^{1/3}} \right\} \right] \quad \dots(21) \end{aligned}$$

On omitting certain negligible terms we get,

$$\frac{1}{\beta_T} = \frac{RT}{\delta^2 N d^3} \left[\frac{N^{1/3} d}{V^{1/3}} \left\{ \delta^2 + 1 \right\} + 2 - 2\delta \right] \quad \dots(22)$$

Equation (22) is very simple and is important since β_T is directly connected with the liquid parameter δ and molecular diameter d . The compressibility coefficients were evaluated for some thirteen liquids (for FCC type of packing only) and compared with the experimental values. The results are given in table 1 and the agreement is found to be very good.

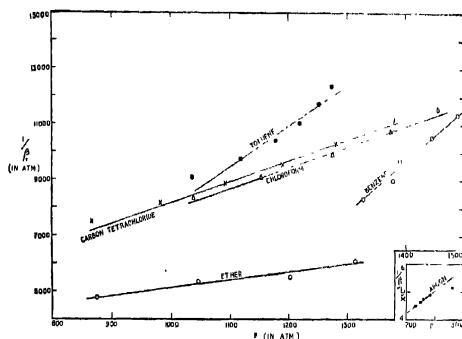


Figure 1

Remembering that (equation 14)

$$\frac{V^{1/3} - N^{1/3} d}{V^{1/3}} = \frac{1}{\delta}$$

we can rewrite equation (22) as

$$\frac{1}{\beta_T} = \frac{RT}{N d^3} \left[(\delta - 4) (\delta + 1) + 7 \right] \quad \dots(23)$$

One can therefore use the experimental compressibility coefficients and then calculate the molecular diameters d from the above equation.

Dividing equation (20) by (23) and rearranging we get

$$P = \frac{1}{\beta_T} \cdot \frac{3 \left[\delta - \frac{1}{\delta} - 2 \ln \delta \right]}{[(\delta - 4) (\delta + 1) + 7]} \quad \dots(24)$$

TABLE—I.

Sl. No.	Substance	Temp. (°Abs.)	κ ($\times 10^{-3}$)	$\left[\frac{dn}{dc}\right]_c$ [$\frac{\text{mole}}{\text{V}}$] [$\frac{\text{mole}}{\text{c.c.}}$]	P (atm.)	d (A ²) (From Eq. 20)			b (A ²) (other data)			C ₁ (From Eq. 25)		C ₁ (Exptl.)		From Eq. (22) (FCC)	From Eq. (26) (Exptl.)	
(a) Hydrocarbons :																		
1.	Hexane	296	11.1	1.352	24.39	131	1105	5.53	5.86	5.98	5.910	6.38	5.16	8.45	7.8	157	159	212
2.	Octane	296	12.5	1.377	27.32	163	1391	5.40	5.71	5.83	7.450	7.09	5.73	8.40	8.5	—	121	195
3.	Benzene	293	11.5	1.269	18.00	89	1445	5.13	5.44	5.55	5.270	6.04	4.90	9.20	8.0	104	95	187
4.	Toluene	293	11.5	1.035	24.06	106	1218	5.44	5.76	5.87	—	—	—	9.18	8.0	99	91	174
(b) Esters :																		
5.	Methyl acetate	293	11.5	1.369	15.29	79	1540	5.03	5.33	5.43	—	5.40	4.44	9.35	8.0	73	101	194
6.	Ethyl acetate	293	11.5	1.352	20.45	98	1645	4.91	5.20	5.30	—	5.85	4.80	8.50	8.0	91	105	196
7.	Ethyl propionate	293	11.5	1.273	24.39	115	1810	4.76	5.05	5.15	—	6.22	5.04	7.81	8.0	105	102	198
8.	Ethyl butyrate	293	12.3	1.201	30.07	132	1760	4.97	5.26	5.36	—	6.60	5.34	8.30	8.5	107	101	198
(c) Miscellaneous :																		
9.	Ether	283	10.8	1.693	17.38	102	1202	5.25	5.55	5.67	—	5.78	4.74	8.55	7.5	153	167	203
10.	Chloroform	293	11.8	1.248	15.17	83	1274	5.42	5.75	5.85	5.433	5.43	4.33	10.60	8.2	100	101	183
11.	Acetone	273	9.3	1.425	13.91	73	1560	4.40	4.66	4.75	—	5.06	4.28	7.02	6.5	101	93	184
12.	Carbon tetrachloride	293	12.4	1.208	20.39	97	1189	5.69	6.03	6.15	5.881	5.84	4.73	10.63	8.4	112	105	189
13.	Ethylene bromide	293	11.6	0.963	13.98	86	2895	4.09	4.33	4.42	—	5.45	4.10	7.43	8.1	65	59	191
14.	Carbon disulphide	319	10.8	1.194	11.62	59	1055	5.69	6.01	6.15	4.438	4.61	4.01	—	—	—	87	182
15.	Argon	86	9.2	4.470	1.35	29	242	4.48	4.75	4.84	3.453	3.61	2.91	—	—	—	234	177

TABLE 2.

Sl. No.	Substance	Temp. (T) (°Abs.)	Density (gm/cc)	$\frac{V}{\text{Mole}}$ (c.c.)	α ($\times 10^{-4}$)	$\beta_T \times 10^4$ (atm $^{-1}$)	$P = \frac{\alpha_T}{\beta_T} - \frac{a}{V^2}$ (atm.)	$\frac{1}{\beta_T}$ (atm.)
1.	Toluene	273	0.8848	104.0	1.035	80.8	1273	12380
		283	0.8752	105.2		85.5	1252	11700
		293	0.8657	106.3		90.6	1218	11040
		303	0.8563	107.5		96.2	1177	10390
		313	0.8470	108.7		102.7	1118	9740
		323	0.8378	109.9		110.4	1036	9091
2.	Chloroform	273	1.5264	78.21	1.248	86.6	1454	11550
		283	1.5078	79.17		93.1	1374	10740
		293	1.4888	80.19		100.7	1274	9901
		303	1.4697	81.23		109.5	1153	9091
		313	1.4505	82.30		119.5	1028	8333
		323	1.4313	83.30		129.5	903	7583
3.	Ether	273	0.7362	100.7	1.693	152.7	1314	6536
		283	0.7248	102.3		167.4	1202	5988
		293	0.7135	103.9		186.8	1046	5348
		303	0.7019	105.6		210.8	875	4739
4.	Carbon tetrachloride	273	1.6327	94.22	1.2076	89.7	1379	11150
		283	1.6134	95.35		97.0	1281	10310
		293	1.5939	96.51		104.8	1189	9524
		303	1.5748	97.68		113.3	1092	8850
		313	1.5557	98.88		123.2	982	8130
		323	1.5361	100.14		134.4	867	7463
5.	Benzene	283	0.8896	87.74	1.190	88.	1488	11360
		293	0.8790	88.79	1.209	95	1445	10530
		303	0.8684	89.88	1.230	103	1390	9709
		313	0.8576	91.01	1.259	111	1377	9009
		323	0.8467	92.18	1.280	120	1327	8333
6.	Argon	84	1.402	28.49	4.45	193	279	5181
		86	1.396	28.61	4.47	204	242	4902
		87	1.390	28.73	4.49	210	230	4762
		88	1.383	28.88	4.51	216	225	4630
		89	1.378	28.99	4.53	222	216	4505

From equation (24) we see that if we plot P versus $1/\beta_T$ we must get a straight line. The necessary data (Freyer 1929; Yosim 1964) is presented in table 2 and the plot is given in figure 1. Unfortunately the slopes obtained from the graphs are not in agreement with those calculated from equation (24).

The pressure variation of bulk modulus of liquids is an important quantity as it is related to molecular force constants (Gopala Rao 1962; Moelwyn Hughes 1951). Thus we define

$$C_1 = \left[\frac{\partial(1/\beta_T)}{\partial P} \right]_T$$

using equation (23) we get after simplification for C_1 as

$$C_1 = \frac{N^{1/2} d}{V^{1/2}} \cdot \frac{\delta^2 (2\delta - 3)}{3 [(\delta - 4)(\delta + 1) + 7]} \quad \dots (25)$$

Using equation (25) the values of C_1 were calculated and were compared with those obtained from experiment. It is very gratifying to find that the agreement is good.

The attractive internal pressure

It may be pointed out that the attractive pressure can be expressed as aV^{-n} and not as aV^{-2} as in the Van der Waals equation. Thus, n may not be exactly equal to 2 as in Van der Waals equation but may be slightly different from it. Thus, from equations (20) and (24), we have

$$\frac{\alpha_T}{\beta_T} - \frac{a}{V^n} = \frac{3 \left(\delta - \frac{1}{\delta} - 2 \ln \delta \right)}{\beta_T [(\delta - 4)(\delta + 1) + 7]} \quad \dots (26)$$

From a knowledge of α_T , β_T , δ , a and V it is possible to calculate n . Such calculations are made and given in the last column of table 1. It is observed that the value of n is slightly less than 2 in most of the cases, the average value being 1.91.

REFERENCES

- Blitz, J. 1953 *Fundamentals of Ultrasonics*, Butterworths London, P. 13.
- De Boer, J. & Uhlenbeck, G. E. 1964 *Studies in Statistical Mechanics*, Vol. II, North-Holland Publishing Co., Amsterdam, P. 76.
- Eyring, H. & Hirschfelder, J. O., 1937 *J. Phys. Chem.*, **41**, 249.
- Freyer, E. B. Hubbard, J. C. & Andrews, D. H. 1929 *J. Am. Chem. Soc.*, **51**, 759.
- Gopala Rao, R. V. 1967 *Ind. J. Pure & App. Phys.*, **5**, 357.
- Gopala Rao, R. V. & Keer, H. V. 1962 *Z. Phys. Chem.*, **219**, 321.
- Gopala Rao, R. V. & Venkata Seshalah, V. 1969 (In course of publication)
- Hand book of Chemistry and Physics*, 1957-58 Chemical Rubber Publishing Co., 39th edition, P. 2126.
- Hirschfelder, J., Curtiss, C. F. & Bird, R. B. 1954 *Molecular Theory of Gases and Liquids*, John Wiley & Sons Inc., New York, P. 280, 633 & 1110.
- Lindsay, R. B. 1960 *Mechanical Radiation*, Mc Graw Hill Book Co., Inc., New York, P. 211.
- Moelwyn-Hughes, E. A., 1951 *J. Phys. Chem.*, **55**, 1246.
- 1961 *Physical Chemistry*, Pergamon Press, Oxford, P. 583.
- Yosim, S. J. 1964 *J. Chem. Phys.*, **40**, 3069.

Acoustic amplification in semi-conductors in the presence of external electric and magnetic fields

By A. SINGH

Radio and Electronics Research Laboratory, Institute of Technology,
Banaras Hindu University, Varanasi-5., U.P.

(Received 1 January 1969, Revised 24 April 1969)

The dispersion equation is derived, on the basis of the equation of stress, taking into account the electron sound wave interaction, and the amplification of the acoustic wave, due to its interaction with the conduction electrons in the semiconductors, both piezoelectric and non-piezoelectric, in the presence of the external fields, is investigated. It is found that the amplification of the acoustic wave occurs only when the carrier drift velocity in the direction of propagation exceeds the velocity of sound. The geometric and cyclotron resonances are also found under the condition of amplification.

INTRODUCTION

A number of investigations (Hutson *et al* 1961, Pippard 1963, Solymar 1964 1966, 1967, Singh 1968, 1969 and Spector 1968) have been made of the amplification of the acoustic wave due to its interaction with the charge carriers in the semiconductors. However, there is a general agreement on the fact that the interaction becomes very much pronounced and the amplification occurs when the drift velocity, imparted to the conduction electrons in the direction of propagation of the acoustic wave by the dc fields, exceeds the velocity of sound. In this paper we undertake the study of interaction of charge carriers in the semiconductors in the presence of external dc fields, with the acoustic wave by deriving a dispersion equation for a coupled electron stream and the acoustic wave.

DISPERSION EQUATION

We consider a longitudinal acoustic wave propagating in the x-direction of the medium and define a strain S and a stress T such that

$$S = \frac{\partial u}{\partial x} \quad (1)$$

and

$$\frac{\partial T}{\partial x} = -\rho_m \frac{\partial^2 u}{\partial t^2} \quad (2)$$

where ρ_m is the mass density and u the local displacement of material in the direction of propagation of the acoustic wave. The stress tensor T can be determined from the internal energy of the medium and for an ordinary solid is given by $C.S$ where C is the elastic stiffness.

We assume that the acoustic wave interacts with conduction electrons through the deformation of the energy bands :

$$E_i = V_i S \quad (3)$$

where E_i is the interaction energy and V_i the deformation potential for the carriers of type i . In case of piezoelectric semiconductor there is an additional contribution to the internal energy from the polarisation fields which accompany the lattice displacement. Therefore the equation of stress in the presence of electron-sound interaction (Mason 1950, Weinreich 1956) is

$$T = CS - nV - dE \quad (4)$$

where d is the piezoelectric constant, n the electron density, ϵ the dielectric constant and

E = Electric field due to free charges and polarisation

$$= E_1 - (d/\epsilon) S. \quad (5)$$

The equation of continuity and Poisson's equation are

$$\epsilon \frac{\partial n}{\partial t} + \frac{\partial J}{\partial x} = 0 \quad (6)$$

$$\partial E_1 / \partial x = (ne/\epsilon) \quad (7)$$

The conductivity σ for the free electron gas (Carleton & Auer 1965) is

$$J = \sigma [E + iqeVS] \quad (8)$$

We assume that all the physical quantities can be regarded as the superposition of an unperturbed term and perturbed term, the latter varying as $\exp [i(qx - \omega t)]$. Using equation (4) together with equations (5)-(8) and neglecting the product of V and d we obtain the following dispersion equation (for details see the appendix).

$$\omega^2 - q^2 V_{s0}^2 = q^2 V_{s0}^2 (K_1 + K_2) [(\sigma / \epsilon) / (i\omega - \sigma / \epsilon)] \quad (9)$$

where q is sound wave number, V_{s0} the velocity of sound in absence of perturbation and $K_1 = \frac{d^2}{C\epsilon}$, $K_2 = q^2 V_{s0}^2 \epsilon / \rho_m V_{s0}^2$.

The RHS term in equation (9) represents the perturbation, in q , assumed to be small. We re-write therefore equation (9) as

$$q = \frac{\omega}{V_{s0}} + \frac{1}{2} \cdot \frac{\omega}{V_{s0}} \cdot (K_1 + K_2) \left(\frac{\sigma / \epsilon}{-i\omega + \sigma / \epsilon} \right) \quad \dots(10)$$

SEMICONDUCTOR IN DC ELECTRIC FIELD.

Application of the dc electric field imparts a net drift velocity (V_d) to the conduction electrons in the direction of propagation of the

acoustic wave and if the drift velocity of the charge carriers exceeds the velocity of sound, amplification occurs. This can be readily seen from the following.

Case I: $ql < 1$ where l is the electron mean free path.

Under this condition σ has the form (Spector 1962)

$$\sigma = \sigma_0 [\mu + iql V_F/3 V_{s0}] \quad \dots(11)$$

where σ_0 is the dc conductivity, V_F the Fermi velocity and $\mu = (1 - \phi)$ where $\phi = V_d/V_{s0}$. Substituting equation (11) in equation (10) and considering only the imaginary part of q , because the real part gives the acoustic velocity in semiconductor (Singh 1969), we have the following expression for the absorption coefficient.

$$\alpha(\phi) = \frac{K}{2} \cdot \frac{\omega_p^2 \tau}{V_{s0}} \left[\frac{\mu}{\mu^2 + \left(\frac{\omega_p^2 \tau}{\omega} \right)^2} \left[1 + \frac{1}{3} (\omega/\omega_p)^2 (V_F/V_{s0})^2 \right]^2 \right] \quad \dots(12)$$

where $K = (K_1 + K_2)$ and ω_p is the plasma frequency. The equation (12) agrees with that obtained by Weinreich (1956) and Spector (1962) for non-piezoelectric semiconductor. It also agrees with the result derived by Hutson *et al* (1961) for piezoelectric semiconductor provided $(\omega V_F/\omega_p V_{s0})$ is negligibly small. There is a cross over from absorption to amplification when the drift velocity exceeds the velocity of sound. The maximum in the absorption coefficient occurs at

$$\phi = 1 \pm (\omega_p^2 \tau/\omega) \left[1 + \frac{1}{3} \left(\omega V_F/\omega_p V_{s0} \right)^2 \right]. \quad \dots(13)$$

The + ve sign corresponds to the amplification and - ve sign to the absorption.

Case II.

When $ql > 1$, the conductivity σ becomes

$$\sigma = (3\sigma_0 V_{s0}/ql V_F) [(\pi\mu V_{s0}/2V_F) - i] \quad \dots(14)$$

$$\text{therefore; } \alpha(\phi) = (\pi K \omega^2 V_F/12 \omega_p^2 V_{s0}^2) [\mu / \left[1 + \frac{1}{3} (\omega V_F/\omega_p V_{s0})^2 \right]] \quad \dots(15)$$

which is in agreement with Spector's (1962) result. In this case the absorption coefficient increases linearly with drift velocity and there is no maximum in the absorption. The amplification occurs for drift velocities greater than the sound velocity.

SEMICONDUCTOR IN CROSSED ELECTRIC AND MAGNETIC FIELDS.

In the presence of crossed electric and magnetic fields (magnetic field being perpendicular to the direction of propagation) the carrier drift velocity is

$$\vec{V}_H = V_L (\vec{E} \times \vec{H})/H^2 \quad \dots(16)$$

where V_L is the velocity of light in the vacuum. The resonances in the absorption/amplification coefficient are obtained in the following two cases.

Case I : Geometric Resonance

Here the wave length (λ) of the acoustic wave is of the order of classical orbit radius. When $\omega_c \gg \omega$ and $\omega_c \tau \gg 1$ are satisfied the following expression σ is obtained (Spector 1963)

$$\sigma = \frac{3\sigma_0}{(ql)^2} \frac{(1-i\omega\tau Y) [1-g_0(X)]}{Y + (i/\omega\tau) [1-g_0(X)]} \quad \dots(17)$$

where $g_0(X)$ is oscillatory function of X and $X = (q, R)$, R is orbital radius of an electron moving perpendicular to the magnetic field with Fermi velocity and is equal to (V_F/ω_C) .

$$Y = (1 - V_H/V_{s0}) \text{ and } \phi = V_H/V_{s0}$$

Using equations (17) and (10) we obtain

$$\alpha(\phi) = \frac{3KV_{s0}Y\tau}{2V_F^2} \cdot \frac{g_0(X)[1-g_0(X)]}{\omega_c^2\tau^2 Y^2 + [1-g_0(X)]^2} \quad \dots(18)$$

which agrees with the result obtained by Spector (1963) for nonpiezoelectric semiconductor. The maxima in the absorption/amplification coefficient occur at

$$\phi = 1 \pm [1 - g_0(X)]/\omega\tau \quad \dots(19)$$

Case II : Cyclotron Resonance

In this case sound frequency is of the order of cyclotron frequency ω_c and the conductivity σ has the following form

$$\sigma = -\frac{3i\sigma_0 V_{s0}}{qlV_F} \left[1 + \frac{i\omega\tau Y}{2ql} \coth(\pi/\omega_c\tau) (1 - i\omega\tau Y) \right] \quad \dots(20)$$

Therefore the absorption coefficient in this region is

$$\alpha(\phi) = \frac{\pi\omega_K Y}{4V_F} \cdot \frac{\tanh(\pi/\omega_c\tau) \sec^2(\pi\omega Y/\omega_c)}{\tanh^2(\pi/\omega_c\tau) + \tan^2(\pi\omega Y/\omega_c)} \quad \dots(21)$$

It is quite obvious from this equation that the amplification occurs when the carrier drift velocity exceeds the velocity of sound. We have

oscillations in the amplification/absorption coefficient as long as $\omega_e \tau > 1$. The maxima in the absorption/amplification coefficient occur when

$$\omega Y = n \omega_e, (n = 1, 2, 3 \dots) \quad \dots(22)$$

This result agrees with that derived by Spector (1963) and Mikoshiba (1958) and also with that obtained by Cohen *et al* (1960) for drift velocity much less than the sound velocity *i. e.* when $Y = 1$.

DISCUSSION.

Our calculations have shown that there is a dependence of the amplification of the acoustic wave on the carrier drift velocity and the amplification of the acoustic wave occurs when the carrier drift velocity exceeds the velocity of sound. This is because maximum interaction between the charge carriers and the acoustic wave occurs when the electrons have a net drift velocity in the direction of propagation greater than the velocity of the acoustic wave. The geometric resonance in absorption/amplification coefficient is associated with the Bessel function in the conductivity tensor. This has to do with the strength of the interaction between the particular orbit and the electric field rather than the resonant absorption/amplification of energy. In quantum mechanical language geometric resonance corresponds to the variation in the matrix element, rather than in the resonance denominators also appearing in the conductivity tensor. The cyclotron resonance corresponds to the variation of the resonance denominator. *i. e.* to the resonant absorption from or transfer of energy to the sound wave.

We have also found that the amplification of the acoustic wave in both piezoelectric and non-piezoelectric semiconductors increases with frequency as shown by equations (12), (13) and (18). It is therefore possible to amplify microwave acoustic waves.

The author feels very much indebted to Prof. S. S. Banerjee for his keen interest and several helpful comments on the manuscript.

APPENDIX.

We outline here briefly the derivation of the dispersion equation (9). From equation (4), using equations (2), (5) and (7) we get

$$\rho_m \omega^2 u = C q^2 u + i q n \nabla + \frac{d^2}{\epsilon} q^2 u + \frac{n e}{\epsilon} d \quad \dots(A1)$$

substituting J from equation (6) and E from (7) into equation (8) we obtain

$$\frac{n e \omega}{q} = \sigma \left[-\frac{d}{\epsilon} i q u + \frac{n e}{i q \epsilon} - q^2 \nabla u \right] \quad \dots(A2)$$

Expressing n from equation (A2) in terms of u , substituting it into equation (A1) and assuming that $(dV) \ll 1$ and $K_1 \ll 1$, we obtain equation (9).

REFERENCES

- Carleton, H. R. & Auer, P. L. 1965 *Solid St. Electron* **8**, 285.
Cohen, M. H., Harrison, M. J. & Harrison W. A. 1960 *Phys. Rev.* **117**, 937.
Hutson, A. R., Mcfee, J. H. & White D. L. 1961 *Phys. Rev. Lett.* **7**, 237.
Mason, W. P. 1950 *Piezoelectric crystals and their applications to Ultrasonics*, Van. Nostrand, New York.
Mikoshiba, N. 1958 *J. Phys. Soc. (Japan)* **13**, 759.
Pippard, A. B. 1963 *Phil. Mag.* **8**, 161.
Singh, A. 1968 *Solid St. Electron* **11**, 1097.
1969 *Int. J. Electron*, **25**, 495.
1969 *Ind. Jr. Pure and Appl. Phys.* **7**, 456,
Solymar, L. 1964 *J. Appl. Phys.* **35**, 3420.
1966 *Solid. St. Electron* **9**, 879.
1967 *Int. J. Electron* **22**, 459.
Spector, H. N. 1962 *Phys. Rev.* **127**, 1084.
1963 *Phys. Rev.* **131**, 2512.
1968 *Phys. Rev.* **165**, 562.
Weinreich, G. 1956 *Phys. Rev.* **104**, 321.

The stability of a gravitating fluid layer of infinite extent but finite thickness with a force-free magnetic field

By K. P. Das

*Department of Mathematics, Jalpaiguri Government Engineering College
West Bengal, India*

(Received 4 June 1969)

The stability of a gravitating, homogeneous, incompressible and infinitely conducting fluid layer of infinite extent but finite thickness is investigated in presence of a force-free magnetic field. The critical wave-numbers for the onset of instability are calculated for some assigned strengths of magnetic field. It is found that stability increases with the increase of mean magnetic field. The wave-length for maximum instability and corresponding maximum growth rate of instability are calculated.

1. INTRODUCTION

Safranov (1960) pointed out the importance of the study of gravitational and magneto-gravitational stability of fluid layers in astronomical context. Oganessian (1961) studied the gravitational and magneto-gravitational stability of a fluid layer of infinite extent but finite thickness. The effect of uniform rotation on the stability of a fluid layer was studied by Chakraborty (1964) and in more details by Uberoi (1963). The effects of Hall current and finite resistance on the stability of such a layer were studied respectively by Das (1968) and Sundaran (1968). Here we study the stability of a gravitating, homogeneous, incompressible and infinitely conducting fluid layer of infinite extent but finite thickness in presence of a force-free magnetic field. The effect of a force-free magnetic field on the stability of a infinitely long gravitating cylinder was discussed by Trehan (1958). The energy method of Chandrasekhar & Fermi (1953) is applied here for examining stability. A table is given for the critical wave-number for the onset of instability for some assigned value of the mean magnetic field. The wave-length for maximum instability and the corresponding maximum growth rate of instability are calculated.

2. THE FORCE-FREE MAGNETIC FIELD IN EQUILIBRIUM CONFIGURATION

Let a uniform, homogeneous, gravitating plasma occupy the space bounded by the planes $z = h$ and $z = -h$. The remaining space is a vacuum.

Force-free magnetic field \vec{H} satisfies the equations

$$\text{rot } \vec{H} = \alpha \vec{H} \quad \dots(1)$$

$$\text{and } \text{div } \vec{H} = 0 \quad \dots(2)$$

in which κ is a constant.

The magnetic field \vec{H} can be obtained from a scalar function ψ , by the relation (Pulpton & Ferraro 1961)

$$\vec{H} = \text{rot } (a\psi) + \frac{1}{\kappa} \text{rot } (a'\psi) \quad \dots(3)$$

and ψ satisfied the equation

$$\nabla^2 \psi + \kappa^2 \psi = 0 \quad \dots(4)$$

Let us suppose that the field is independent of y coordinate and its dependence on z coordinate is periodic. Then the solution of equation 4 is

$$\psi = A \cos \gamma z \cos \beta x \quad \dots(5)$$

in which β is a constant and

$$\gamma^2 = \kappa^2 - \beta^2 \quad \dots(6)$$

Therefore by equation (3), taking $\vec{a} = \vec{x}$, a unit vector along x -axis, we have

$$\vec{H} = \vec{x} \frac{A\gamma^2}{\kappa} \cos \gamma z \cos \beta x + \vec{y} A \gamma \sin \gamma z \cos \beta x + \vec{z} \frac{\beta \gamma A}{\kappa} \sin \gamma z \sin \beta x \quad \dots(7)$$

Let at the boundary $z = \pm h$, and the magnetic field be directed along x -axis and vanish outside. Therefore we must have

$$\sin \gamma h = 0$$

$$\text{or,} \quad \gamma h = n\pi \quad \dots(8)$$

in which n is any integer.

Averaging $|\vec{H}|^2$ over x we get

$$\langle |\vec{H}|^2 \rangle = \frac{1}{2} \cdot \frac{A^2 \gamma^2}{\kappa^2} [(\beta^2 + \kappa^2) \sin^2 \gamma z + \gamma^2 \cos^2 \gamma z] \quad \dots(9)$$

The average of the square of the magnetic field per unit length along x -axis is given by,

$$\begin{aligned} \langle |\vec{H}|^2 \rangle &= \frac{1}{2} \frac{A^2 \gamma^2}{\kappa^2 h} \int_0^h [(\beta^2 + \kappa^2) \sin^2 \gamma z + \gamma^2 \cos^2 \gamma z] dz \\ &= \frac{1}{2} A^2 \gamma^2 \quad \dots(10) \end{aligned}$$

Let H_m^2 denote the average of the square of the magnetic field, then

$$H_m^2 = \langle |\vec{H}|^2 \rangle = \frac{1}{2} A^2 \gamma^2 = \frac{A^2 n^2 \pi^2}{2h^2} \quad \dots(11)$$

3. THE EXAMINATION OF STABILITY

Following Chandrasekhar & Fermi (1953), let the layer be given a small perturbation in such a way that its boundary is given by

$$z = \pm (\bar{h} + a \cos kz) \quad \dots(12)$$

in which $\frac{a}{\bar{h}} \ll 1$ and $\frac{2\pi}{k}$ is the wave-length of disturbance in z -direction.

The displacement $\vec{\xi}$ at any point is given by

$$\vec{\xi} = \text{grad } \phi \quad \dots(13)$$

in which ϕ satisfies the equation

$$\nabla^2 \phi = 0 \quad \dots(14)$$

The solution of (14) that gives displacements symmetrical about the plane $z=0$, is given by

$$\phi = B \cosh kz \cos kz \quad \dots(15)$$

The displacements are given by

$$\xi_x = -Bk \cosh kz \sin kz$$

$$\xi_z = Bk \sinh kz \cos kz$$

$$\xi_y = 0 \quad \dots(16)$$

Since at $z = \bar{h}$, ξ_z must reduce to $a \cos kz$

$$B = \frac{a}{k \sinh k\bar{h}} \quad \dots(17)$$

Now we find the change in potential energy and the change in magnetic energy due to the perturbation.

(a) *Change in potential energy*

Let U and V be the internal and external potentials respectively. These two potentials satisfy equations

$$\Delta^2 U = 0 \quad \text{and} \quad \Delta^2 V = -4\pi G\rho \quad (18)$$

in which G is gravitational constant and ρ is the density of the medium. The solution of equations (18) to the first order in a are

$$U = -4\pi G\rho \bar{h}z + aAe^{-kz} \cos kz, \quad z > \bar{h}$$

$$V = -2\pi G\rho \bar{h}^2 + aB \cosh kz \cos kz \quad \dots(19)$$

The constants A , B are obtained from the conditions that U and V and its derivatives with respect to z are continuous across $z = \bar{h} + a \cos kz$. These two conditions give

$$Ae^{-kh} = B \cosh kh$$

$$Ae^{-kh} + B \sinh kh = \frac{4\pi G\rho}{k}$$

$$\text{Solving we get } A = \frac{4\pi G\rho}{k} \cos kh, B = \frac{4\pi G\rho}{k} e^{-kh} \quad \dots(20)$$

The change in gravitational potential energy per unit length along x and y axes due to infinitesimal displacements

$$\delta\xi_x = -\frac{\delta a}{\sinh kh} \cosh kz \sin kz \quad \text{and} \quad \delta\xi_z = \frac{\delta a}{\sinh kh} \sinh kz \cos kz$$

is given by,

$$\delta(\Delta\Omega) = -2\rho \left[\int_0^{h+a\cos kx} (\delta\xi \cdot \text{grad } V) dz \right]_{\text{averaged over } x}$$

$$= -2\rho \left[\int_0^{h+a\cos kx} \left\{ \frac{\delta a}{\sinh kh} \sinh kz \cos kx (-4\pi G\rho z + 4\pi G\rho a e^{-kh} \sinh kz \cos kx) \right. \right.$$

$$\left. \left. + \frac{\delta a}{\sinh kh} \cosh kz \sin kx (4\pi G\rho a e^{-kh} \cosh kz \sin kx) \right\} dz \right]_{\text{averaged over } x}$$

$$= 4\pi G\rho^2 h a \delta a \left[1 - \frac{1}{2kh} (1 + e^{-2kh}) \right] \quad \dots(21)$$

Integrating this between the limits 0 to a , we get the change in gravitational potential energy due to displacements given by (16)

$$\Delta\Omega = H^2 \left[1 - \frac{1}{2kh} (1 + e^{-2kh}) \right] \quad \dots(22)$$

in which $H^2 = 2\pi G\rho^2 h^2$

(b) *Change in magnetic energy*

By equation (33) of Trehan (1958) we have for the change in magnetic energy per unit length along x and y axes,

$$\Delta M = \frac{1}{8\pi} \left[2 \int_0^h \left(\vec{H} \cdot \text{grad } \vec{\xi} \right)^2 dz \right]_{\text{averaged over } x}$$

$$= \frac{1}{4\pi} \left[\int_0^h \left\{ \frac{\beta^2 \gamma^2 A^2 a^2 k^2}{\alpha^2 \sinh^2 kh} \left(\sin^2 \gamma z \cosh^2 kz \sin^2 \beta x \cos^2 kx + \sin^2 \gamma z \sinh^2 kz \right. \right. \right.$$

$$\left. \left. \sin^2 \beta x \sin^2 kx \right) + \frac{\gamma^2 A^2 a^2 k^2}{\alpha^2 \sinh^2 kh} \left(\cos^2 \gamma z \sinh^2 kz \cos^2 \beta x \sin^2 kx + \cos^2 \gamma z \right. \right.$$

$$\left. \left. \cosh^2 kz \cos^2 \beta x \cos^2 kx \right) \right\} dz \right]_{\text{av. } x} = \frac{(Hm^2/8\pi) a^2 k \epsilon}{8^2 \sinh kh} \frac{\beta^2 h^2 - n^2 \pi^2}{\beta^2 h^2 + n^2 \pi^2}$$

$$\left[(1 + \delta) \frac{n^2 \pi^2 (2k^2 h^2 + \beta^2 h^2 + n^2 \pi^2)}{(k^2 h^2 + n^2 \pi^2)(\beta^2 h^2 - n^2 \pi^2)} \sinh 2kh + 2(1 - \delta)kh \right] \quad \dots(23)$$

in which the following relations have been used

$$[\sin^2 \beta x \cos^2 kx]_{av. x} = \frac{1}{4} \epsilon, \quad [\cos^2 \beta x \sin^2 kx]_{av. x} = \frac{1}{4} \epsilon$$

$$[\sin^2 \beta x \sin^2 kx]_{av. x} = \frac{1}{4} \delta, \quad [\cos^2 \beta x \cos^2 kx]_{av. x} = \frac{1}{4} \delta$$

where $\epsilon = 1$, $\delta = 1$, if $\beta \neq k$

and $\epsilon = \frac{1}{2}$, $\delta = 3$, if $\beta = k$... (24)

Thus the total change in energy is given by

$$E = \Delta Q + \Delta M = \frac{H_m^2 a^2}{h} f(kh) \quad \dots (25)$$

in which $f(kh)$ is given by

$$f(kh) = 1 - \frac{1}{2kh} (1 + e^{-2kh}) + \frac{H_m^2}{8\pi H_s^2} \cdot \frac{kh\epsilon}{8 \sinh^2 kh} \cdot \frac{\beta^2 h^2 - n^2 \pi^2}{\beta^2 h^2 + n^2 \pi^2}$$

$$[(1+\delta) \frac{n^2 \pi^2 (2k^2 h^2 + \beta^2 h^2 + n^2 \pi^2)}{(k^2 h^2 + n^2 \pi^2) (\beta^2 h^2 - n^2 \pi^2)} \sinh 2kh + 2(1-\delta)kh] \quad \dots (26)$$

To find the Lagrangian function, we shall have to find the kinetic energy of the motion resulting from the varying amplitude. Since the fluid is incompressible the velocity components can be obtained from a velocity potential ψ , through the relation.

$$\vec{u} = \text{grad } \psi \quad \dots (27)$$

and ψ satisfies the Laplace's equation. The solution for ψ that gives velocity components symmetric about the plane $z = 0$ is,

$$\psi = A \cosh kz \cos kx \quad \dots (28)$$

Therefore, $u_x = \frac{\partial \psi}{\partial x} = -Ak \cosh kz \sin kx$

$$u_z = \frac{\partial \psi}{\partial z} = Ak \sinh kz \cos kx \quad \dots (29)$$

At $z = h$ we must have

$$\frac{da}{dt} \cos kx = u_z|_{z=h} = Ak \sinh kh \cos kx$$

$$\text{or, } A = \frac{1}{k \sinh kh} \frac{da}{dt} \quad \dots (30)$$

The kinetic energy per unit length along x and y axes is thus given by

$$T = \frac{1}{2} \rho A^2 k^2 \left[2 \int_0^h \left(\sinh^2 kz \cos^2 kz + \cosh^2 kz \sin^2 kz \right) dx \right]_{\text{averaged over } x}$$

$$= \frac{\rho}{2k} \coth kh \left(\frac{da}{dt} \right)^2 \quad \dots(31)$$

Therefore the Lagrangian function L is

$$L = T - E = \frac{\rho}{2k} \coth kh \left(\frac{da}{dt} \right)^2 - \frac{H_0^2 a^2}{h} f(kh) \quad \dots(32)$$

The equation of motion derived from this Lagrangian is

$$\frac{d^2 a}{dt^2} = - \frac{4\pi G \rho kh}{\coth kh} a f(kh) \quad \dots(33)$$

Let the solution for a be

$$a = \text{constant} \cdot e^{\pm qt} \quad \dots(34)$$

then

$$q^2 = - \frac{4\pi G \rho kh}{\coth kh} f(kh) \quad \dots(35)$$

As $\coth kh > 0$, this small motion is stable if $f(kh) > 0$ and unstable if $f(kh) < 0$. As there is a single positive root X^* of the equation $f(X) = 0$ and $f(X) < 0$ when $X < X^*$; $f(X) > 0$ when $X > X^*$, all the modes of deformation with $X < X^*$, are unstable. Here $X = kh$. Thus all modes of deformation whose wave-lengths are greater than $2\pi h/X^*$ are unstable.

If $\theta = \frac{H_0^2}{8\pi H_1^2} > 1$, $X \ll 1$, in this case q^2 is given by (keeping terms up to X^2),

$$q^2 = 4\pi G \rho \left[X - 2 X^2 - \theta X^2 \left\{ \frac{\epsilon(\beta^2 h^2 - n^2 \pi^2)}{4(\beta^2 h^2 + n^2 \pi^2)} (1 - \delta) + \frac{1}{4} \epsilon(1 + \delta) \right\} \right] \quad \dots(36)$$

Let q^2 be maximum when $X = X_m = \frac{2\pi h}{\lambda_m}$ and let the corresponding value of q be q_m .

From equation (36), we get the following expressions for λ_m and q_m .

$$\lambda_m = 4\pi h \left[2 + \theta \left\{ \frac{\epsilon(\beta^2 h^2 - n^2 \pi^2)}{4(\beta^2 h^2 + n^2 \pi^2)} (1 - \delta) + \frac{1}{4} \epsilon (1 + \delta) \right\} \right] \quad \dots (37)$$

$$q_m = 2\pi G \rho X_m = \sqrt{\pi G \rho} \left[2 + \theta \left\{ \frac{\epsilon(\beta^2 h^2 - n^2 \pi^2)}{4(\beta^2 h^2 + n^2 \pi^2)} (1 - \delta) + \frac{1}{4} \epsilon \delta (1 + \delta) \right\} \right]^{1/2} \quad \dots (38)$$

This λ_m is the wave-length of disturbance, that gives maximum instability and q_m is the corresponding maximum growth rate of instability.

For non-resonance case i.e., $\beta \neq k$, $f(X)$ is given by

$$f(X) = 1 - \frac{1}{2X} (1 + e^{-2X}) + \theta \cdot \frac{n^2 \pi^2}{\beta^2 h^2 + n^2 \pi^2} \cdot \frac{X(2X^2 + \beta^2 h^2 + n^2 \pi^2)}{2(X^2 + n^2 \pi^2)} \cdot \coth X \quad \dots (39)$$

The roots X^* of the equation $f(X) = 0$, where $f(X)$ is given by the above equation (39) with $n = 1$, are given in the following table for some values of θ and βh

βh^2	θ	0.25	0.50	0.75	1.00
0.50	0.5759	0.5270	0.4874	0.4544	
0.75	0.5760	0.5271	0.4875	0.4545	
1.00	0.5761	0.5272	0.4877	0.4546	
2.00	0.5764	0.5275	0.4881	0.4550	

The author is grateful to Dr. B. Chakraborti, Department of, Mathematics, Jadavpur University, Calcutta, for helpful discussions.

REFERENCES

- Chakraborty, B.B. 1964 *Indian. J. Phys.* **38**, 490.
Chandrasekhar, S & Fermi, F. 1953 *Astrophys. J.* **118**, 116.
Das, K. P. 1968 *Canadian. J. Phys.* **46**, 2201
Oganesyan, R.S. 1961 *Soviet Astronomy*, **4**, 434, 634.
Pulpton, C & Ferraro, V.C.A. 1961 *An Introduction to Magneto-Fluid Mechanics*; Oxford University Press P. 36.
Safranov, V.S. 1960 *Ann. Astrophys* **23**, 979.
Sundaran, A.K. 1968. *Phys. Fluids* **11**, 1709.
Trehan S.K. 1958 *Astrophys. J.* **127**, 436.
Uberoi, C. 1963 *J. Indian. Inst. Sci.* **46**, 11.

Temperature distribution in generalized plane Couette
flow between two parallel flat plates

By S. N. DUBE

*Department of Mathematics, Institute of Technology,
Banaras Hindu University., Varanasi-5.*

(Received 11 September 1968)

In this paper expressions for the temperature distributions in a channel bounded by two parallel flat plates (generalized plane Couette flow) are derived when viscous incompressible fluid is flowing through it. The term for dissipation due to friction is not neglected and the rate of heat generation per unit volume (i) varies linearly with time, and (ii) decreases exponentially with time. It is seen in the first case that the temperature below the axis of the channel is more than the temperature above the axis of the channel.

INTRODUCTION

The steady flow of a viscous incompressible fluid between two parallel flat plates, one at rest and the other in uniform motion, under constant pressure gradient, is quite well known as generalized plane Couette flow. Pai (1956) has given the velocity and temperature distributions for this flow. However, he has given the solution of energy equation without considering the rate of heat generation per unit volume in the fluid (other than viscous dissipation). Bhatnagar & Tikekar (1966) have obtained the temperature distribution in a channel bounded by two co-axial circular cylinders. They assumed the rate of heat generation per unit volume as a function of time but did not include the effects of viscous dissipation. Purohit (1967) has obtained the temperature distribution in plane Couette flow between parallel flat plates. He derived the expression for the temperature by assuming the rate of heat generation per unit volume as an oscillatory function of time. Using Laplace transform technique he has obtained the solution of the energy equation which comes out in a form which exhibits the contributions of boundary conditions, dissipation due to friction and the rate of heat generation to the temperature distribution. Recently, the author (1967) has obtained the temperature distribution of a viscous incompressible fluid in a circular pipe when the rate of heat generation per unit volume (i) varies linearly with time, and (ii) decreases exponentially with time, and it has been shown that the points near the axis of the cylinder have higher temperature than those of the points which are far from the axis of the cylinder.

The present paper consists of two parts. In part A the temperature distribution in a channel bounded by two parallel flat plates when

viscous incompressible fluid is flowing through it (generalized plane Couette flow), with the rate of heat generation per unit volume varying linearly with time, is discussed. An expression for the temperature distribution is obtained in dimensionless form. This consists of two parts, the one varies linearly with dimensionless time Fourier modulus $T_1 = k't/y_0^2$ and the other is transient part of temperature, which vanishes in the limit as t tends to infinity. It is also seen that the contribution of the transient part is insignificant when $T_1 > 1$.

In part B the temperature distribution in the same channel is studied when viscous incompressible fluid is flowing through it with the rate of heat generation per unit volume decreasing exponentially with time. An expression for the temperature has been obtained taking

$$\frac{1}{\rho c_p} \frac{\partial \theta}{\partial t} = \sum_{m=1}^{\infty} a_m e^{-m^2 t},$$

The result obtained is in complete agreement with similar results obtained by Ballabh (1959) and Sneddon (1951) where Ballabh has obtained the expression for the velocity by using the method of superposability and Sneddon has discussed the heat flow under exponentially decreasing temperature gradient.

Here the expressions for the temperature distributions in both the parts are derived with the conditions that the plates situated at $y = \pm y_0$ (i) have zero initial temperatures, and (ii) are always being kept at zero temperatures.

1. FLOW DISTRIBUTION AND ENERGY EQUATION

For the case of two-dimensional flow of a viscous incompressible fluid with constant properties, the system of equations for the velocity distribution in steady flow along a xy -plane is

$$\frac{\partial u}{\partial x} + \frac{\partial v}{\partial y} = 0, \quad \dots(1.1)$$

$$u \frac{\partial u}{\partial x} + v \frac{\partial u}{\partial y} = -\frac{1}{\rho} \frac{\partial p}{\partial x} + \nu \left(\frac{\partial^2 u}{\partial x^2} + \frac{\partial^2 u}{\partial y^2} \right), \quad \dots(1.2)$$

$$u \frac{\partial v}{\partial x} + v \frac{\partial v}{\partial y} = -\frac{1}{\rho} \frac{\partial p}{\partial y} + \nu \left(\frac{\partial^2 v}{\partial x^2} + \frac{\partial^2 v}{\partial y^2} \right), \quad \dots(1.3)$$

where ρ is the density of the fluid and ν is the coefficient of kinematic viscosity.

Now let us consider the flow between two parallel flat plates at a distance $2y_0$ apart, of which one is at rest and the other is moving with constant velocity U . For this flow we have

$$u = u(y), v = 0, p = p(x).$$

Thus the equation (1.3) becomes an identity and the equations (1.1) and (1.2) assume the forms:

$$\frac{\partial u}{\partial x} = 0, \quad \dots(1.4)$$

$$\frac{\partial p}{\partial x} = \mu \frac{\partial^2 u}{\partial y^2} \quad \dots(1.5)$$

The solution of equation (1.5) under the boundary conditions

$$u = 0 \text{ when } y = -y_0; \text{ and } u = U \text{ when } y = y_0$$

is

$$u = \frac{U}{2} \left(1 + \frac{y}{y_0} \right) + u_m \left(1 - \frac{y^2}{y_0^2} \right), \quad \dots(1.6)$$

$$\text{where } u_m = - \frac{y_0^2}{2\mu} \frac{dp}{dx} =$$

The energy equation is

$$\rho c_v \left[\frac{\partial T}{\partial t} + u \frac{\partial T}{\partial x} \right] = \frac{\partial \theta}{\partial t} + k \left(\frac{\partial^2 T}{\partial x^2} + \frac{\partial^2 T}{\partial y^2} \right) + \mu \phi, \quad \dots(1.7)$$

where $\phi = (\partial u / \partial y)^2$ is the energy dissipation function; $\partial \theta / \partial t$ is the rate of heat generation per unit volume in the fluid; c_v and k are the specific heat and the coefficient of heat conductivity of the fluid respectively.

The velocity distribution is steady while the temperature is unsteady. The temperature distribution does not influence the flow field of an incompressible fluid with constant properties. We have assumed a fluid having these properties.

PART A

Rate of heat generation per unit volume varies linearly with time

If we assume that temperature is independent of its axial position,

then $\frac{\partial T}{\partial x} = 0$, and hence equation (1.7) reduces to

$$\frac{\partial T}{\partial t} = \frac{1}{\rho c_v} \frac{\partial \theta}{\partial t} + k' \frac{\partial^2 T}{\partial y^2} + A - By + Cy^2, \quad \dots(2.1)$$

where

$$A = \frac{\mu U^2}{4\rho c_v y_0^3},$$

$$B = \frac{2\mu U u_m}{\rho c_v y_0^3}$$

$$C = \frac{4\mu u_m^2}{\rho c_v y_0^4}.$$

The term $(A - By + Cy^2)$ in the equation (2.1) is dissipation due to friction and is not neglected in the present investigation.

We now assume that

$$\frac{1}{\rho c_v} \frac{\partial Q}{\partial t} = at, \quad \dots(2.2)$$

Equation (2.1) then becomes

$$\frac{\partial T}{\partial t} = at + k' \frac{\partial^2 T}{\partial y^2} + A - By + Cy^2. \quad \dots(2.3)$$

Now let $\bar{T} = \int_0^\infty e^{-st} T dt$ be the Laplace transform of T and let T_0 be the initial value of T .

Multiplying equation (2.3) by e^{-st} and integrating between the limits 0 to ∞ , we get

$$\frac{\partial^2 \bar{T}}{\partial y^2} - p^2 \bar{T} = -\frac{1}{k'} \left[T_0 + \frac{A}{s} - \frac{By}{s} + \frac{Cy^2}{s} + \frac{a}{s^2} \right], \quad (2.4)$$

where $p^2 = s/k'$.

We shall now find T_0 .

Initially the rate of heat generation is zero and the temperature is steady in the channel.

Hence $\frac{\partial T_0}{\partial t} = 0$ and we obtain $\frac{d^2 T_0}{dy^2} = -\frac{1}{k'} (A - By + Cy^2)$... (2.5)

The solution of equation (2.5) under the boundary conditions

$$T_0 = 0 \text{ when } y = -y_0; \quad T_0 = 0 \text{ when } y = y_0$$

is

$$T_0 = \frac{A}{2k'} (y_0^2 - y^2) - \frac{B}{6k'} (y_0^2 y - y^3) + \frac{C}{12k'} (y_0^4 - y^4).$$

Substituting this value T_0 in (2.4) we get

$$\begin{aligned} \frac{\partial^2 T}{\partial y^2} p^2 T = & -\frac{1}{k'} \left[\frac{A}{2k'} (y_0^2 - y^2) - \frac{B}{6k'} (y_0^2 y - y^3) \right. \\ & \left. + \frac{C}{12k'} (y_0^4 - y^4) + \frac{A}{s} - \frac{By}{s} + \frac{Cy^2}{s} + \frac{a}{s^2} \right] \end{aligned} \quad \dots(2.6)$$

The boundary conditions for T are

$$T = 0 \text{ when } y = -y_0; \text{ and } T = 0 \text{ when } y = y_0.$$

The solution of equation (2.6) under the above boundary conditions is

$$\begin{aligned} T = & \frac{A}{2k'} \left(\frac{y_0^2 - y^2}{s} \right) - \frac{B}{6k'} \left(\frac{y_0^2 y - y^3}{s} \right) + \frac{C}{12k'} \left(\frac{y_0^4 - y^4}{s} \right) \\ & + \frac{a}{s^2} \left[1 - \frac{\cosh py}{\cosh py_0} \right] \end{aligned} \quad \dots(2.7)$$

Now applying Laplace inversion theorem, we obtain

$$\begin{aligned} T = & \frac{A}{2k'} (y_0^2 - y^2) - \frac{B}{6k'} (y_0^2 y - y^3) + \frac{C}{12k'} (y_0^4 - y^4) \\ & + \frac{1}{2k'} (y_0^2 - y^2) at - \frac{a}{24k'^2} (5y_0^2 - y^2) (y_0^2 - y^2) \\ & + \frac{64ay_0^4}{k'^2 \pi^5} \sum_{n=0}^{\infty} \frac{(-1)^n}{(2n+1)^5} \cdot e^{-\frac{k'(2n+1)^2 \pi^2 t}{4y_0}} \cdot \cos \left[\frac{(2n+1)\pi y}{2y_0} \right] \end{aligned} \quad \dots(2.8)$$

$$\text{At time } t = 0, T = \frac{A}{2k'} (y_0^2 - y^2) - \frac{B}{6k'} (y_0^2 y - y^3) + \frac{C}{12k'} (y_0^4 - y^4).$$

Hence from equation (2.8) by putting $t = 0$, we get

$$\sum_{n=0}^{\infty} \frac{(-1)^n}{(2n+1)^5} \cos \left[\frac{(2n+1)\pi y}{2y_0} \right] = \frac{\pi^5}{1536} \left(5 - \frac{y^2}{y_0^2} \right) \left(1 - \frac{y^2}{y_0^2} \right).$$

Writing $\frac{y}{y_0} = r$ so that $|r|$ less than 1, we get

$$\sum_{n=0}^{\infty} \frac{(-1)^n}{(2n+1)^5} \cos \left[\frac{(2n+1)\pi}{2} r \right] = \frac{\pi^5}{1536} (5 - r^2) (1 - r^2).$$

Putting $r = 0$, we have

$$\sum_{n=0}^{\infty} \frac{(-1)^n}{(2n+1)^5} = \frac{5\pi^5}{1536}$$

Now we make equation (2.8) dimensionless by introducing

$$\tau = \frac{T}{\theta}, \quad \frac{y}{y_0} = r, \quad T_1 = \frac{k't}{y_0^2},$$

where θ is a characteristic temperature.

We then get

$$\begin{aligned} \tau &= b_1(1-r^2) - b_2r(1-r^2) + b_3(1-r^4) + bT_1(1-r^2) \\ &\quad - \frac{b}{12}(5-r^2)(1-r) \\ &\quad + \frac{128b}{\pi^5} \sum_{n=0}^{\infty} \frac{(-1)^n}{(2n+1)^5} \cdot e^{-\frac{(2n+1)^2\pi^2}{4}T_1} \cdot \cos\left[\frac{(2n+1)\pi}{2}r\right], \end{aligned} \quad \dots(2.9)$$

where $b_1 = \frac{Ay_0^3}{2k'\theta}$, $b_2 = \frac{By_0^3}{6k'\theta}$, $b_3 = \frac{Cy_0^4}{12k'\theta}$ and $b = \frac{ay_0^4}{2k'^2\theta}$ are clearly dimensionless numbers.

We now take $\tau = \tau_1 + \tau_2$, where

$$\begin{aligned} \tau_1 &= b_1(1-r^2) - b_2r(1-r^2) + b_3(1-r^4) + bT_1(1-r^2) \\ &\quad - \frac{b}{12}(5-r^2)(1-r), \end{aligned}$$

$$\text{and } \tau_2 = \frac{128b}{\pi^5} \sum_{n=0}^{\infty} \frac{(-1)^n}{(2n+1)^5} \cdot e^{-\frac{(2n+1)^2\pi^2}{4}T_1} \cdot \cos\left[\frac{(2n+1)\pi}{2}r\right].$$

The values of τ for different values of r and T_1 have been tabulated.

TABLE 1. $b_1 = 2$, $b_2 = 2$, $b_3 = 2$, $b = 1$

$T_1 \backslash r$	0.01	0.1	0.2	0.3	0.4	0.8	1.0
-0.9	3.3098	3.3160	3.3219	3.3324	3.3445	3.4052	3.4394
-0.6	3.7888	3.8067	3.8215	3.8533	3.8915	4.0901	4.2036
-0.3	4.3518	4.3736	4.3901	4.4323	4.4842	4.7612	4.9212
0.0	4.0019	4.0256	4.0422	4.0874	4.1435	4.4459	4.6213
0.3	3.2598	3.2816	3.2981	3.3403	3.3922	3.6692	3.8292
0.6	2.2528	2.2707	2.2855	2.3173	2.3645	2.5541	2.6676
0.9	0.7258	0.7320	0.7379	0.7484	0.7605	0.8212	0.8554

TABLE 2. $b_1 = 1, b_2 = 2, b_0 = 1, b = 1$

$r \backslash T_1$	0.01	0.1	0.2	0.3	0.4	0.8	1.0
-0.9	0.8759	0.8821	0.8880	0.8985	0.9106	0.9713	1.0055
-0.6	2.2784	2.2963	2.3111	2.3429	2.3811	2.5797	2.6932
-0.3	2.4499	2.4717	2.4882	2.5304	2.5823	2.8593	3.0193
0.0	2.0019	2.0256	2.0422	2.0874	2.1435	2.4459	2.6213
0.3	1.3579	1.3797	1.3962	1.4384	1.4903	1.7673	1.9273
0.6	0.7424	0.7603	0.7751	0.8069	0.8451	1.0437	1.1572
0.9	0.1919	0.1981	0.2040	0.2145	0.2266	0.2873	0.3215

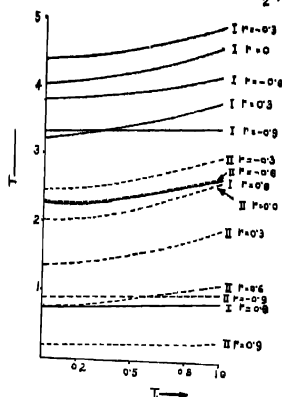
TABLE 3. $b_1 = 2, b_2 = 1, b_0 = 1, b = 2$

$r \backslash T_1$	0.01	0.1	0.2	0.3	0.4	0.8	1.0
-0.9	0.8949	0.9073	0.9191	0.9401	0.9643	1.0857	1.1541
-0.6	2.5344	2.5702	2.5998	2.6634	2.7398	3.1370	3.3640
-0.3	3.0889	3.1325	3.1655	3.2499	3.3537	3.9077	4.2277
0.0	3.0038	3.0512	3.0844	3.1748	3.2870	3.8918	4.2426
0.3	2.5429	2.5865	2.6195	2.7039	2.8077	3.3617	3.6817
0.6	1.7664	1.8022	1.8318	1.8954	1.9718	2.3690	2.5960
0.9	0.5529	0.5653	0.5771	0.5981	0.6223	0.7437	0.8121

The graphs for fixed r ($r = -0.9, -0.6, -0.3, 0.0, 0.3, 0.6, 0.9$) showing the variation of τ with the parameter T_1 have been drawn in two cases $b_1 = 2, b_2 = 2, b_0 = 2, b = 1$; $b_1 = 1, b_2 = 2, b_0 = 1, b = 1$ in the range $T_1 = 0$ to $T_1 = 1$.

The graphs beyond $T_1 = 1$ have not been drawn because τ_2 is very small compared to τ_1 when $T_1 > 1$, hence the transient part is insignificant and τ varies linearly with T_1 in this range. From the graphs and tables of values it is observed that τ increases with T_1 for fixed r . It is also seen that for any value of T_1 , the temperature of any point below the axis of the channel is more than the temperature of the point symmetrical to this above the axis of the channel and thus the temperature below the axis is more than the temperature above the axis. The present case is entirely different from that of plane Couette flow (Dube 1968a) and plane Poiseuille flow

GRAPH SHOWING VARIATION OF T WITH x
 GRAPHS MARKED I ARE FOR $b_1=b_2, b_0=2b$
 " " " " $b_1=\frac{b_2}{2}, b_0=b$



(Dube 1968b) because in the last two flows it has been shown that the temperature above and below the axis of the channel is the same.

PART B

Rate of heat generation per unit volume decreases exponentially with time

We assume that

$$\frac{1}{\rho c_v} \frac{\partial \theta}{\partial t} = \sum_{m=1}^{\infty} a_m e^{-mt}. \quad \dots(3.1)$$

Equation (2.1) then becomes

$$\frac{\partial T}{\partial t} = \sum_{m=1}^{\infty} a_m e^{-mt} + k' \frac{\partial^2 T}{\partial y^2} + A - By + Cy^3. \quad \dots(3.2)$$

Let $\bar{T} = \int_0^{\infty} e^{-st} T dt$ be the Laplace transform of T and let T_0 be the initial value of T .

Multiplying equation (3.2) by e^{-st} and integrating between the limits 0 to ∞ , we get

$$\frac{\partial^2 T}{\partial y^2} - p^2 T = -\frac{1}{k'} \left[T_0 + \frac{A}{s} - \frac{By}{s} + \frac{Cy^2}{s} + \sum_{m=1}^{\infty} \frac{a_m}{(s+m)} \right],$$

where $p^2 = \frac{s}{k'}$.

Here $T_0 = \frac{A}{2k'} (y_0^2 - y^2) - \frac{B}{6k'} (y_0^2 y - y^3) + \frac{C}{12k'} (y_0^4 - y^4)$

as obtained in part A.

The solution of equation (3.3) under the previous boundary conditions is

$$T = \frac{A}{2k'} \left(\frac{y_0^2 - y^2}{s} \right) - \frac{B}{6k'} \left(\frac{y_0^2 y - y^3}{s} \right) + \frac{C}{12k'} \left(\frac{y_0^4 - y^4}{s} \right) + \left(1 - \frac{\cosh py}{\cosh py_0} \right) \sum_{m=1}^{\infty} \frac{a_m}{s(s+m)}.$$

Now applying Laplace inversion theorem, we get

$$\begin{aligned} T = & \frac{A}{2k'} (y_0^2 - y^2) - \frac{B}{6k'} (y_0^2 y - y^3) + \frac{C}{12k'} (y_0^4 - y^4) \\ & - \sum_{m=1}^{\infty} \frac{a_m}{m} \left[1 - \frac{\cos \{ (m/k')^{1/2} y \}}{\cos \{ (m/k')^{1/2} y_0 \}} \right] e^{-mt} \\ & + \frac{4}{\pi} \sum_{n=1}^{\infty} \sum_{m=0}^{\infty} \frac{(-1)^n a_m}{(2n+1) \left[m - \frac{k'(2n+1)^2 \pi^2}{4y_0^2} \right]} \cdot e^{-\frac{k'(2n+1)^2 \pi^2}{4y_0^2} t} \\ & \times \cos \left[\frac{(2n+1) \pi y}{2y_0} \right]. \end{aligned} \quad \dots(3.4)$$

The expression (3.4) for the temperature is in complete agreement with similar results obtained by Ballabh (1959) and Sneddon (1951). Ballabh in his paper has obtained the expression for the velocity by using the method of superposability and Sneddon has discussed the heat flow under exponentially decreasing temperature gradient.

The author wishes to express his thanks to Dr. P. L. Bhatnagar for his valuable guidance in the preparation of this paper.

REFERENCES

- Fai, S., 1956 *Viscous Flow Theory, I-Laminar Flow*, D. Van Nostrand Co., Inc., New York.
- Bhatnagar, P. L. & Tikekar, V. G. 1966 *Proc. Camb. Phil. Soc.*, 62, 301.
- Purohit, G. N. 1967, *Proc. Nat. Inst. Sci. India*, 33A, 3 & 4, 142.
- Dube, S. N. 1967 *Indian J. Phys.*, 41, 433.
- Ballabh, R. 1959 *Proc. of V Congress on Theo. and Appl. Mech.* India.
- Sneddon, I. N. 1951 *Fourier Transforms*, Mc Graw-Hill Book Co., Inc., New York.
- Dube, S. N. 1968a To appear in *Journal of Technology*, India.
- 1968b To appear in *Proc. Nat. Inst. Sci. India*.

Unsteady flow through a circular tube

By KRISHNA LAL

Banaras Hindu University, Varanasi, India,

(Received 23 May 1969)

The unsteady flow of viscous laminar incompressible fluid has been discussed for the velocity and temperature distributions and expressions for the Bousinesq coefficients k and k' have been calculated. It has been shown that for steady flow the well known result $k' = 2k$ can be calculated from the present expressions. The axial pressure gradient and the external rate of heat addition are taken as linear functions of time.

1. VELOCITY DISTRIBUTION

The equation of motion is well known

$$\frac{\partial u}{\partial t} = -\frac{1}{\rho} \frac{\partial p}{\partial z} + \nu \left(\frac{\partial^2 u}{\partial r^2} + \frac{1}{r} \frac{\partial u}{\partial r} \right) \quad \dots (1)$$

where the symbols have their usual meanings.

Assuming

$$-\frac{1}{\rho} \frac{\partial p}{\partial z} = f(t) \text{ the solution of (1) may be assumed}$$

$$u(r, t) = u_0(r) f(t) + u_1(r) f'(t) \quad \dots (2)$$

where a dash denotes differentiation with respect to t .

The boundary conditions are

$$\left. \begin{array}{l} t > 0, \quad u = 0 \quad \text{On } r = a \\ t > 0, \quad u = \text{finite} \quad \text{at } r = 0 \end{array} \right\} \quad \dots (3)$$

where a is the radius of the tube.

Substituting (2) into (1), we have

$$f \left[1 + \nu \left(u_0'' + \frac{u_0'}{r} \right) \right] + f' \left[-u_0 + \nu \left(u_1'' + \frac{u_1'}{r} \right) \right] - u_1 f'' = 0 \quad \dots (4)$$

Thus for all values of t , we get one of the relations as

$$\frac{df}{dt} = \text{constant} = A \text{ (say)} \quad \dots (5)$$

$$\text{or } f = At + B$$

where A and B are certain constants.

Applying initial condition, we have

$$f(0) = B = \text{a constant.}$$

The expressions for u_0 and u_1 are obtained from (4) by equating the coefficients of $f(t)$ and $f'(t)$ to zero and solving it.

Thus

$$u_0 = \frac{1}{4\nu} (a^2 - r^2) \quad \dots (6)$$

$$u_1 = \frac{a^2 r^2}{16\nu^2} - \frac{1}{64\nu^2} (r^4 + 3a^4) \quad \dots (7)$$

$$u(r, t) = \frac{1}{4\nu} (a^2 - r^2)(At + B) + A \left[\frac{a^{2,2}}{16\nu^2} + \frac{1}{64\nu^2} (r^4 + 3a^4) \right] \dots (8)$$

DISCUSSION

The discharge of flux per second is

$$q = \int_0^a 2\pi u r dr = \frac{\pi}{8\nu} (At + B)a^4 - \frac{\pi A a^6}{48\nu^2} \quad \dots (9)$$

The axial velocity is

$$U_1 = \frac{a^2}{4\nu} (At + B) - \frac{3Aa^4}{64\nu^2} \quad \dots (10)$$

The maximum velocity, C is at $r = 0$, provided that

$$\frac{4\nu}{A} (At + B) > a^2 \quad \dots (11)$$

The expression for maximum velocity is same as U_1 . Thus using the cross-section of tube, $A_1 = \pi a^2$, we may deduce the coefficients k and k' as introduced by Boussinesq.

These are connected by

$$q = UA_1 = kKA_1^2, \quad C = k' K A_1 \quad \dots (12)$$

where U = average velocity, K = pressure gradient term $-\frac{1}{\mu} \frac{\partial p}{\partial z}$

and for the present problem, we have $K = f(t)/\nu$.

Thus we have in unsteady flow,

$$R = 0.03979 - \frac{a^2 A}{48\pi\nu (At + B)} \quad \dots (13)$$

$$k' = 0.07958 - \frac{3a^2 A}{64\pi\nu (At + B)} \quad \dots (14)$$

Hence, the well known result for steady flow

$$\frac{C}{T} = \frac{k'}{k} = 2 \quad \dots (15)$$

is obtained from (13) and (14) by putting $A = 0$.

2. TEMPERATURE DISTRIBUTION

The energy equation (Pai 1956) is

$$\rho C_s \frac{\partial T}{\partial t} = \frac{\partial Q}{\partial t} + k \left(\frac{\partial^2 T}{\partial r^2} + \frac{1}{r} \frac{\partial T}{\partial r} \right) + \phi \quad \dots (16)$$

Where the value of dissipation term, ϕ in this case is

$$\begin{aligned} \phi = \mu \left(\frac{\partial \mu}{\partial r} \right)^2 = \mu \left\{ \frac{r^6}{\nu^4} \frac{A^2}{256} + r^4 \left[\frac{A}{16\nu^3} (At+B) - \frac{A^2 a^2}{64\nu^4} \right] \right. \\ \left. + r^2 \left[\frac{(At+B)^2}{4\nu^2} - \frac{A^2 a^4}{64\nu^4} - \frac{a^2 A (At+B)}{8\nu^3} \right] \right\} \quad \dots (17) \end{aligned}$$

and $\frac{\partial Q}{\partial t}$ is the rate of external heat addition.

If we put

$$\begin{aligned} C_0 = \frac{A^2 \mu'}{256\nu^4}, \quad \psi_1(t) = \frac{\mu' A}{16\nu^3} (At+B) - \frac{A^2 \mu' a^2}{64\nu^4} \\ \psi_2(t) = \frac{\mu' (At+B)^2}{4\nu^2} + \frac{A^2 \mu' a^4}{64\nu^4} - \frac{a^2 \mu' A (At+B)}{8\nu^3} \end{aligned}$$

the equation (16) without external rate of heat addition can be written

$$\frac{\partial T}{\partial t} = k' \left(\frac{\partial^2 T}{\partial r^2} + \frac{1}{r} \frac{\partial T}{\partial r} \right) + [C_0 r^6 - \psi_1(t) r^4 + \psi_2(t) r^2] \quad \dots (18)$$

where

$$k' = \frac{k}{\rho C_s}, \quad \mu' = \frac{\mu}{\rho C_s}.$$

To solve equation (18), we assume

$$T(r, t) = r^0 \phi_1(t) + r^2 \phi_2(t) + r^4 \phi_3(t) + \phi_4(t) \quad \dots (19)$$

Substituting (19) into (18) and equating the coefficients of various powers of r and constant term to zero, we have the following simple differential equations

$$\left. \begin{aligned} \phi_1' - C_0 &= 0 \\ \phi_2' - 36k' \phi_1 - \psi_1 &= 0 \\ \phi_3' - 16k' \phi_2 - \psi_2 &= 0 \\ \phi_4' - 4k' \phi_3 &= 0 \end{aligned} \right\} \quad \dots (20)$$

Initially $t = 0$ and $T = 0$ for all values of r .

Thus

$$\phi_1(0) = \phi_2(0) = \phi_3(0) = \phi_4(0) = 0 \quad \dots(21)$$

Solving the equations of set (20) with boundary conditions of (21), we have

$$\phi_1 = \frac{A^2 \mu'}{256 \nu^4} t \quad \dots(22a)$$

$$\phi_2 = t^2 \left[\frac{9A^2 k' \mu'}{128 \nu^4} + \frac{\mu' A^2}{32 \nu^3} \right] + t \left[\frac{\mu' AB}{16 \nu^3} - \frac{A^2 \mu' a^2}{64 \nu^4} \right] \quad \dots(22b)$$

$$\begin{aligned} \phi_3 = t^3 \left[\frac{3A^2 k'^2 \mu'}{8 \nu^4} + \frac{\mu' k' A^2}{6 \nu^3} + \frac{\mu' A^2}{12 \nu^2} \right] \\ + t^2 \left[\frac{\mu' k' AB}{2 \nu^3} - \frac{A^2 k' \mu' a^2}{8 \nu^4} + \frac{\mu' AB}{4 \nu^2} - \frac{a^2 \mu' A^2}{16 \nu^3} \right] \\ + t \left[\frac{\mu' B^2}{4 \nu^3} + \frac{A^2 \mu' a^4}{64 \nu^3} - \frac{a^2 \mu' AB}{8 \nu^3} \right] \quad \dots(22c) \end{aligned}$$

$$\begin{aligned} \phi_4 = t^4 \left[\frac{3A^2 k'^3 \mu'}{8 \nu^4} + \frac{\mu' k'^2 A^2}{6 \nu^3} + \frac{\mu' k' A^2}{12 \nu^2} \right] \\ + t^3 \left[\frac{2\mu' k'^2 AB}{3 \nu^3} - \frac{A^2 k'^2 \mu a^2}{6 \nu^4} + \frac{\mu' k' AB}{3 \nu^2} - \frac{a^2 \mu' k' A^2}{12 \nu^3} \right] \\ + t^2 \left[\frac{\mu' k' B^2}{2 \nu^3} + \frac{A^2 \mu' k' a^4}{32 \nu^3} - \frac{a^2 \mu' k' AB}{4 \nu^3} \right] \quad \dots(22d) \end{aligned}$$

Thus the temperature distribution comes out to be in the form of

$$\begin{aligned} T(r, t) = r^0(a_1 t) + r^4(a_2 t^2 + a_3 t) + r^2(a_4 t^3 + a_5 t^2 + a_6 t) \\ + (a_7 t^4 + a_8 t^3 + a_9 t^2) \quad \dots(23) \end{aligned}$$

where $a_1 = 1, 2, 9$ are certain constants and are known from equations (22).

However, if the dissipation term is neglected as a small quantity, the energy equation is reduced to the form of equation of motion (Lahiri 1965) and can be easily solved. If the rate of external heat addition be taken in the form

$$\frac{1}{\rho c_p} \frac{\partial Q}{\partial t} = \phi_1(t), \text{ say} \quad \dots(24)$$

the fourth equation of the set (20) with the form of $T(r, t)$ given by (19) is replaced by

$$\phi_4' - 4k' \phi_3 - \phi_1 = 0 \quad \dots(25)$$

solution of which is

$$\phi_4(t) = a_7 t^4 + a_8 t^3 + \left(a_9 + \frac{a_1}{2} \right) t^2 \quad \dots(26)$$

It is easily seen that the axial temperature is given by $\phi_4(t)$.

Further, if in equation (21), we assume the initial boundary condition as $t = 0$, $T = f_1(r)$, we may write from (19)

$$\left. \begin{aligned} T(0,0) &= \phi_4(0) \\ T(a,0) &= a^6 \phi_1(0) + a^4 \phi_2(0) + (a^2 \phi_3(0) + T(0,0)) \\ T(a/2, 0) &= \frac{a^6}{64} \phi_1(0) + \frac{a^4}{16} \phi_2(0) + \frac{a^2}{4} \phi_3(0) + T(0,0) \\ T(a/3, 0) &= \frac{a^6}{729} \phi_1(0) + \frac{a^4}{81} \phi_2(0) + \frac{a^2}{9} \phi_3(0) + T(0,0) \end{aligned} \right\} \dots(27)$$

where $T(0,0)$ = initial axial temperature, $T(a,0)$ = initial boundary temperature, $T(a/2,0)$ = initial temperature at $r=a/2$, $T(a/3,0)$ = initial temperature at $r=a/3$.

Solving the equation of set (27), we have for $\phi_1(0)$ as

$$\phi_1(0) = \frac{1}{a^6} \left[36T(0,0) - \frac{3}{2} T(a,0) - \frac{69}{2} T\left(\frac{a}{3}, 0\right) \right] \dots(28)$$

and similarly $\phi_2(0)$, $\phi_3(0)$ may easily be calculated.

Using $\phi_1(0)$ in (21) and (22 a), we have

$$\phi_1(t) = \frac{A^2 \mu' t}{256 \nu^4} + \frac{1}{a^6} \left[36T(0,0) - \frac{3}{2} T(a,0) - \frac{69}{2} T\left(\frac{a}{3}, 0\right) \right] \dots(29)$$

and thus from (20), we see that the calculations of ϕ_2 , ϕ_3 , ϕ_4 become more complicated. To avoid it, we have assumed the boundary conditions of (21).

If we assume in (19) that

$$T(r,t) = T_0(r) \psi_1(t) + T_1(r) \psi_2(t) + T_2(r) \psi_3(t) \quad \dots(30)$$

then substituting in (18) and solving the equations obtained by equating to zero the coefficients of ψ_1 , ψ_2 , ψ_3 , we have

$$\left. \begin{aligned} T_0(r) &= T_0(a) + \frac{1}{36k'} (a^6 - r^6) \\ T_1(r) &= T_1(a) + \frac{1}{16k'} (a^4 - r^4) \\ T_2(r) &= T_2(a) - \frac{T_1(a)}{4k'} (a^2 - r^2) - \frac{a^4(a^2 - r^2)}{64k'^2} \\ &\quad + \frac{1}{576k'^3} (a^6 - r^6) \end{aligned} \right\} \dots(31)$$

where $T_0(a)$, $T_1(a)$, $T_2(a)$ are the values of $T_0(r)$, $T_1(r)$, $T_2(r)$ at $r = a$ i. e. boundary of the pipe.

From above calculations it is clear that $T(r, t)$ in both the cases is of the form $r^2 f_1(t) + r^4 f_2(t) + r^2 f_3(t) + f_4(t)$ where f_i i.e. are certain functions of time.

REFERENCES

- Bateman & al 1932 *Hydrodynamics*, Dover Publications 172.
 Lahiri, S. 1965 *Rev. Roum. Sci. Techn. Mec Appl.* **10**, 1329.
 Pai, S. I. 1956 *Viscous Flow Theory I—Laminar Flow* (INC) New York, 41.

Field theoretic treatment of Ionization of H-atom by protons

By A. ROY CHOWDHURY

Physics Department, Jadavpur University.

(Received 9 November 1968 ; Revised on 27 January 1969)

In this paper attempt is made to obtain the effect of statistics on the ionization crosssection of hydrogen like atoms by the proton impact. An exchange term is obtained, whose evaluation is really difficult. Its effect has been estimated to show a reduction in the value of the differential crosssection.

INTRODUCTION

The problem of ionization of hydrogenlike atoms by proton impact has been of considerable interest from a long time. Mott & Massey (1949) have treated it with the help of usual non-relativistic Born approximation. And almost the same line of thinking has been followed by Bates & Griffing (1993) in re-evaluation of the same. But an important feature namely, the identity of the two protons has been overlooked in both the treatments. In the computations mentioned above there is no way to take into account this identity, not even with the help of usual antisymmetrization technique. This is where statistics comes into play. We have tried to show the effect of this identity on the cross-section for the above mentioned process. Quantum field theory takes care of this identity, with the aid of the anticommutation rules for the field operators for the protons.

FORMULATION OF THE PROBLEM

The initial and final state vectors and the interaction Hamiltonian of the whole system is written (Roy 1960) as

$$H' = \bar{\psi} \gamma_{\mu} A_{\mu} (x) \psi (x) + \bar{\phi} (x') \gamma_{\nu} A_{\nu} (x') \phi (x') \quad (1)$$

$$| \psi_i \rangle = \int dk dk' g(k, k') a^{\dagger} (k) A^{\dagger} (k') A^{\dagger} (p_1) | 0 \rangle$$

and

$$| \psi_f \rangle = a^{\dagger} (p_f) A^{\dagger} (p_1') A^{\dagger} (p_2') | 0 \rangle \quad (2)$$

where ψ is the electron field operator and ϕ is the same for proton. $g(k, k')$ being the fourier transform of the bound state wave function.

The matrix element of the process is given by :

$$M_{fi} = \frac{e^2}{2i} \langle \psi_f | \int \int H'(x) H'(x') dx dx' | \psi_i \rangle \quad (3)$$

Equation (3) with the help of (1) & (2) gives the following expression for M_{fi} ,

$$M_{fi} = M_{fi}(PP) + M_{fi}(Pe) \quad (4)$$

where,

$$\begin{aligned} \text{a) } M_{fi}(Pe) &= \left[1 + \frac{(p_1 - p_2')^2}{M^2 c^2} \right] \frac{g(p_f + p_2' - p_1, p_1')}{(p_1 - p_2')^2} \\ &\quad - \left[1 + \frac{(p_1 - p_1')^2}{M^2 c^2} \right] \times g(p_f + p_1' - p_1, p_2') \times \frac{1}{(p_1 - p_1')^2} \end{aligned} \quad (5)$$

coming from proton-electron interaction term.

$$\begin{aligned} \text{b) } M_{fi}(PP) &= \left[1 + \frac{(p_1 - p_2')^2}{M^2 c^2} \right] \frac{g(p_f, p_1' + p_2' - p_1)}{(p_1 - p_2')^2} \\ &\quad - \left[1 + \frac{(p_1 - p_1')^2}{M^2 c^2} \right] \frac{g(p_f, p_1' + p_2' - p_1)}{(p_1 - p_1')^2} \end{aligned} \quad (6)$$

which is due to proton-proton term.

In these equations P_1', P_2' are the outgoing momenta of the two protons and P_1 that of incoming proton. These are the relativistic generalisation of those of Bates & Griffing (1963). It can be easily seen that equation (6) is zero in non-relativistic limit due to orthogonality of the wave functions.

TRANSFORMATION TO CENTRE OF MASS SYSTEM

Due to the energy range covered by the experiments (upto 50 Kev) we usually deal with the NR limit of equation (5). In NR limit it reduces to the familiar expression of Mott & Massey (1949), with the exception of the exchange term. When transformed to cm system first term becomes,

$$\frac{1}{4\pi} \int dx d\vec{r} \exp \left(\frac{-iXm}{\hbar} (\vec{v}_1' - \vec{v}_f) + \frac{i\vec{r}M}{\hbar} (v_q - v_q) \right) \frac{\phi(X)}{|\vec{r} - \vec{X}|} \quad (7)$$

where \vec{v}_1, \vec{v}_2 etc. are velocities corresponding to moments P_1, P_2 . \vec{v}_p, \vec{v}_q being the relative velocities corresponding to the initial and final state of the system. Equation (7) is then seen to be equal to

$$\frac{1}{(\vec{K}_q - \vec{K}_q)^2 \{ 1 + a_0^2 (\vec{K}_p - \vec{K}_q + \vec{K}_1)^2 \}} \quad (8)$$

when $\phi(X)$ is taken to be the 1S-state, while the exchange term

reduces to

$$\frac{1}{(\vec{K}_p + \vec{K}_q + \vec{K}_1)^2 \{1 + a_0^2(\vec{K}_p + \vec{K}_p)^2\}^2}$$

in which \vec{K}_p and \vec{K}_q are defined by

$$\vec{K}_p = \frac{2\pi M}{h} \vec{p}, \quad \vec{K}_q = \frac{2\pi M}{h} \vec{v}_q \quad (9)$$

EVALUATION OF CROSSSECTION

For the ejected electron to be in solid angle $d\sigma$, the proton in $d\omega$ and electron momenta within K_1 and $K_1 + dK_1$, the crosssection of the process is then given by,

$$Id\sigma d\omega dK_1 = \frac{4\pi^2 M^2}{h^4} \cdot \frac{K_q}{K_p} \cdot |M_{fi}|^2 d\sigma d\omega dK_1 \quad \dots(10)$$

which with the above expression for M_{fi} gives, after adjustment of proper normalising factors,

$$Id\sigma d\omega dK_1 = \{f(K_p, K_q, K_1) d\sigma d\omega dK_1\} \pi a_0^2 \quad \dots(11)$$

where,

$$f(K_p, K_q, K_1) = \frac{2^{12} \pi^4 M^2 e^4}{h^4} a_0 \cdot \frac{K_q}{K_p} K_1^2 \times \left[\frac{1}{(K_p - K_q)^4 \{1 + a_0^2(K_p - K_p + K_1)^2\}^4} + \frac{1}{(K_p + K_q + K_1)^4 \{1 + a_0^2(K_p + K_q)^2\}^4} - \frac{2}{(K_p - K_q)^2(K_p + K_q + K_1)^2 \{1 + a_0(K_p + K_q)^2\}^2 \{1 + a_0^2(K_p - K_q + K_1)^2\}^2} \right] \quad \dots(12)$$

First term in equation (12) is the result of usual non-relativistic calculation, while the 2nd and 3rd terms are the results of the exchange effect due to statistics.

For the total crosssection we are to integrate over the angular distributions of the ejected electrons and protons. First term in equation (12) gives

$$\theta_{tot} = \pi a_0^2 \left[\frac{29\pi^4}{h^2 v_p^2} \int_0^{x_{max}} \int_{t_1}^{t_2} \frac{d\omega d\chi x^2 dt}{t^3 \{1 + (\chi + t)^2\}^4} \right] \quad \dots(13)$$

where

$$x = a_0 \vec{K}_1; \vec{t} = a_0(\vec{K}_p - \vec{K}_q) \\ t_{1,2} = a_0(\vec{K}_p \mp \vec{K}_q); x_{max} = a_0 \left[\frac{m}{M} K_p^2 - \frac{2m}{h^2} |E_b| \right]^{1/2} \quad \dots(14)$$

Equation (13) gives exactly the same expression for crosssection as that of Mott & Massey (1949) if we neglect the distortion of the ejected electron.

CONCLUSION

In our treatment, the differential cross-section for the process is given by equations (11) & (12).

In equation (12) a feature which deserves special mention is that the computation of Bates & Griffing and our computed result lead essentially to the same result so long as we neglect the exchange interaction. The square of the matrix element (which is proportional to the cross-section) is in powers of K_p as K_p^{-12} , however the appearance of exchange interaction as shown by expression (12) cancels this K_p^{-12} term and thus the leading term becomes higher than K_p^{-12} (the inverse power is enhanced). As energy E is proportional to K_p^2 , it is proportional to E^{-6} .

Thus $d \log I / d \log E$ must be < -6 . Looking back to the experimental result by Bates & Griffing, we see from the diagram (Fite *et al* 1960) that the experimental curve falls more sharply than the curve of Bates & Griffing for high values of K_p , which means $d \log I / d \log E$ is of the order of $-\mu$ where $\mu > 6$. Thus the result of present calculation seems to favour the experimental results rather than those of Bates & Griffing.

The reason why we have estimated the nature of the curve rather than fully computing it, is due to difficulty in the numerical computation, which can only be done by a high speed computer. The results of such computation will be communicated elsewhere.

The author is grateful to Prof. T. Roy of Physics Department, Jadavpur University for suggesting the problem and for many helpful discussion. He also wishes to thank the Council of Scientific and Industrial Researches, for a fellowship.

REFERENCES

- Bates D. H. & Griffing G. 1953 *Proc. Phys. Soc.* 66, 961.
 Fite *et al* 1960 *Phys. Rev.* 119, 663.
 Mott N.F. & Massey H.S. 1949 *Theory of Atomic Collision*, Clarendon Press, Oxford.
 Roy, T. 1960 *Zeit. für Physik.* 158, 142.

Letters to the Editor

Angular distributions of K shell photoelectrons

K. PARTHASARADHI AND J. RAMA RAO

The Laboratories For Nuclear Research, Andhra University,
 Waltair, India.

(Received 21 May 1969)

Of all the theories on the K-shell photoelectric effect Nagel's (1960) theory is the first one, which gives satisfactory results at all the energies and in all the elements. The results of theories later developed (Pratt 1964 ; Rakavy & Ron 1967 ; Schmickley & Pratt 1967) are found to be in satisfactory agreement with that of Nagel (1960). In the present investigations a study of the angular distributions of K-shell photoelectric cross-sections based on Nagel's (1960) theory with energy and atomic number is made.

The study of angular distributions of photoelectric cross-sections is rather interesting as the intensity of photoelectrons varies with angle and energy. Hultberg *et al* (1961) made numerical calculations utilising the expressions of Nagel (1960) at 662, 412, 279, 208 and 140 keV in U, verified experimentally at 662 keV and found a satisfactory agreement within the limits of the experimental accuracy and difficulty. Measurements of Sujkowiskis' (1961) and Bergkvist *et al* (1965) on the angular distribution

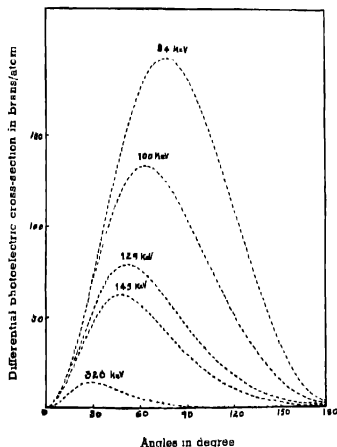


Figure 1. Plot between photoelectric cross-sections Vs angle at various gamma energies in tantalum.

are found to be in agreement with Nagel's (1960) calculations at 279 and 412 keV gamma energies. In view of these agreements with the experimental results systematic theoretical studies are made on the angular distributions of K-shell photoelectrons in Pb, Pt, Ta, Sn, Rh and Cu at gamma energies 84, 100, 129, 145 and 320 keV. The necessary calculations utilising Nagel's (1960) expressions are made on computer.

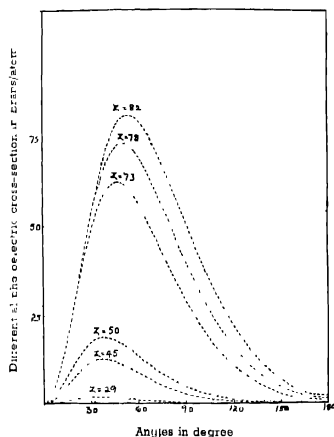


Figure 2. Plot between photoelectric cross-section vs angle in various elements at gamma energy 145 keV.

In figures 1 and 2 typical distributions with energy and atomic number are shown. It can be seen from these figures that photoelectrons will be emitted from 0° to 180° . As the angle increases the intensity increases, reaches a maximum and decreases gradually. The intensity also increases as the gamma energy decreases and as the atomic number increases. In table 1 the angle at which the intensity of the K-shell photoelectrons is maximum for each element at each energy is given. It can be seen from the table that the angle of maximum intensity emission increases as the atomic number increases and gamma energy decreases.

TABLE 1. ANGLE OF MAXIMUM PHOTOELECTRON EMISSION (IN DEGREES)

Energy keV	Pb	Pt	Ta	Sn	Rh	Cu
84	77	...	48	...
100	...	73	63	...	45	...
129	62	56	51	...	39	...
145	54	51	48	39	...	34
320	31	29	28	26	...	24

It is hoped that these findings are useful for experimental verification, especially at low gamma energies, where no experimental data are available.

The authors are thankful to Dr. S. Hultberg for kindly arranging the computations of differential K-shell photoelectric cross-sections at Sweden, and also to the Swedish Government for sparing free machine time.

REFERENCES

- Bergkvist, K. & Hultberg, S. 1965 *Arkiv For Fysik*, **27**, 326.
 Hultberg, S., Nagel, B. & P. Olsson, 1961 *Arkiv For Fysik*, **20**, 555.
 Nagel, C. H. 1960 *Arkiv For Fysik*, **18**, 1.
 Pratt, R. H. Levee, R. D. Pexton, R. H. & Aron W. *Phys. Rev.*, **134A**, 898.
 Rakavy, G. & Ron, A. 1967 *Phys. Rev.*, **159**, 50.
 Schmickley, R. D. & Pratt, R. H. 1967 *Phys. Rev.*, **163**, 104.
 Sujkowski, Z. 1961 *Arkiv For Fysik*, **20**, 269.

Indian J. Phys. **43**, 421—361 (1969)

A furnace with uniform temperature region for a horizontal X-ray diffractometer

P. D. PATHAK AND N. G. VASAVADA

Physics Department, Gujarat University, Ahmedabad-9,

(Received 1968, Revised 28 August 1969)

In this paper a simple diffractometer furnace assembly is described which can be built from materials available in ordinary laboratories. The sample holder can be detached at will. The heater can also be removed with the sample holder in position. Complete range of 2θ angles (0° to 180°) can be investigated. The furnace, using nichrome wire, is used upto 800°C but with Pt-10% Rh winding the range can be extended to 1200°C . The furnace assembly is designed to fit the horizontal diffractometer made by Rich. Seifert, Germany.

The heater is shown in figure 1. A porous pot used in Daniel Cells was cut from both sides so as to obtain a cylinder of about 8.5 cm. in length and 5 cm. in diameter. A slot was cut along its length, as shown in the figure, for X-rays to enter and leave. The heating element consists of nichrome wire of S. W. G. 26. The element is in the coiled coil form inside the furnace and straight outside. The distance between two consecutive coils and the pitch of the coil were so adjusted, especially near the slot as to obtain a region of as uniform a temperature inside the furnace as possible.

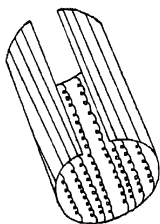


Figure 1

The heater is placed on an asbestos cement disc E (figure 2) of about 15 cm. diameter. Four pegs A B C D (C D not shown) are screwed on the disc to fix the position of the heater (shown dotted). The asbestos disc is placed on a hollow metal disc M of the same diameter and height about 1 cm. During the experiment cold water is continually circulated through this disc in order to prevent the heat of the furnace from reaching the main body of the diffractometer. Two pillars P_1P_2 carry the specimen holder as shown. The fused silica rods R_1R_2 rest in specially designed grooves in the pillars.

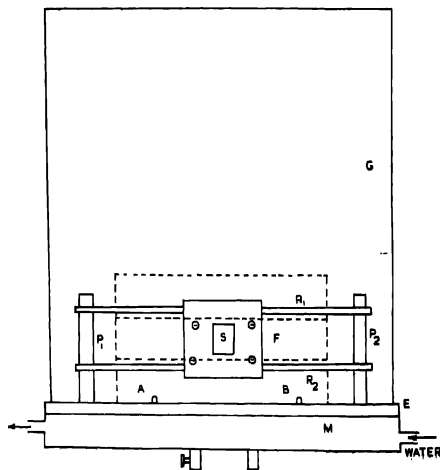


Figure 2

The specimen holder F consists of a slice of size about 3.5 cm. \times 3 cm. \times 0.3 cm. cut from an insulation brick of a burnt out muffle furnace. A hole S of size 1.0 cm. \times 1.3 cm. was cut through it. On its back side grooves are made to carry the fused silica rods R_1R_2 . The back side is then covered by a thin sheet of platinum. The specimen in the form of powder is filled in the groove S. The thermocouple consisting of Pt-Pt 10% Rh is placed in contact with the front surface of the specimen. The pillar P_2 can be moved perpendicular to the plane of the paper by about 0.5 cm. by a screw adjustment in order to bring the front surface of the specimen along the central vertical axis of the diffractometer.

The whole furnace assembly was covered with a copper cylinder G. A slot about 2 cm. wide and 180° in circumference was cut in the cylinder and covered with aluminium foil.

The inside region of the furnace was investigated with a Pt-Pt 10% Rh thermocouple at different temperatures. Typical results of such an investigation are shown in figure 3.

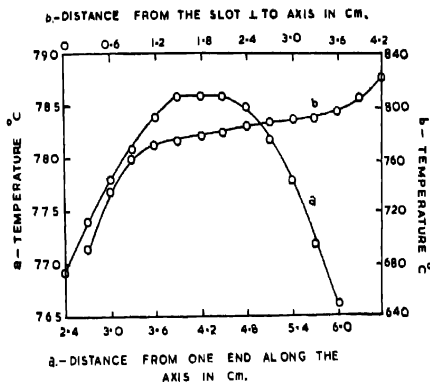


Figure 3

It is seen from figure 3 that between 3.5 cm. and 4.9 cm. a region of fairly uniform temperature is obtained. The variation of temperature between these extreme points is about 3°C . From the same figure it is seen that the region between 2.1 cm. and 2.7 cm. (depth of 0.6 cm.) is again of fairly uniform temperature, the difference of temperature being only 4°C . In view of the fact that the specimen thickness is about 0.3 cm. and X-rays normally penetrate only through about 0.01 cm. of the specimen, the design of the furnace was considered quite satisfactory.

The δ -parameter of liquid state and evaluation of molecular diameter

By R. V. GOPALA RAO AND V. VENKATA SESHIAH

Department of Physical Sciences, Sree Venkateswara University
College of Engineering, Tirupati A.P., India.

(Received 9 January 1969; Revised 24 April 1969)

From the concept of free volume of liquids, the molecular diameters d are evaluated from the δ -parameter defined by

$$\delta = \frac{3C_1 - 1}{2} \quad \dots(1)$$

where $C_1 = \frac{\partial}{\partial P} \left[\frac{1}{\beta} \right]_T$ is the pressure variation of bulk modulus (Gopala Rao 1967).

Assuming a cubic type of packing it is well known (Eyring 1937; Hirschfelder 1954) that the free volume

$$V_f = N v_f = b^3 (V^{1/3} - N^{1/3} d)^3 \quad \dots(3)$$

where V is the volume and b depends on the type of packing and may vary with temperature. Thus for an fcc packing, $b = 4.78$ (Hirschfelder 1954). Remembering that $v = (V/N)$ and with the assumption that γ , the ratio of specific heats, does not vary with temperature, it can be easily shown (Gopala Rao 1967) that

$$\left[\frac{\partial \ln V_f}{\partial V} \right]_T = b V_f^{-1/3} V^{-2/3} = \frac{3C_1 - 1}{2V} = \frac{\delta}{V} \quad \dots(4)$$

$$\text{or } \delta = b V^{1/3} V_f^{-1/3} \quad \dots(5)$$

From (3) and (5), it can be shown that

$$\delta = V^{1/3} [V^{1/3} - N^{1/3} d]^{-1} \quad \dots(6)$$

and

$$d = (\delta - 1) \delta^{-1} V^{1/3} N^{-1/3} \quad \dots(7)$$

Equation (7) is important since δ can be evaluated (Gopala Rao 1967) by a number of methods.

The molecular diameters d are calculated from the knowledge of δ and V for a number of liquids using equation (7). The values of d calculated are given in the table along with those obtained from viscosity data. The necessary data was collected from literature (International Critical Tables 1928; Gopala Rao 1962).

TABLE I MOLECULAR DIAMETER d

Sl. No.	Liquid	Temp. T (in °abs)	Vol V (in c.c)	δ	(d in Å)	
					Present work from equation (7)	From viscosity
1.	Pentane	293	112	9.6	5.10	5.769
2.	Hexane	296	131	11.1	5.47	5.910
3.	Benzene	293	89	11.5	4.82	5.270
4.	Ethyl alcohol	273	57	10.0	4.10	4.455
5.	Methyl alcohol	273	40	12.7	3.73	3.585
6.	Chloroform	293	80	11.8	4.67	5.430
7.	Carbon Tetra- chloride	293	97	12.4	5.00	5.881
8.	Carbon disulphide	319	59	10.8	4.18	4.438
9.	Hydrogen	16	27	6.13	2.97	2.968
10.	Nitrogen	74	34	8.32	3.37	3.681
11.	Oxygen	80	26	7.90	3.06	3.433
12.	Argon	86	28	9.16	3.22	3.400

As seen from the table the agreement is very good considering the simplicity of the equation and the methods (Gopala Rao 1962) available for the evaluation of C_1 , and hence δ .

REFERENCES

- Eyring, H. & Hirschelder. J.O. 1937, *J. Phys. Chem.*, **41**, 249.
 Gopala Rao, R.V. 1967 *Indian J. Pure Appl. Phys.* **5**, 357.
 Gopala Rao, R.V. & Keer, H.V. 1962. *Z. Phys. Chem.*, **219**, 321.
 Hirschelder, J. Curtiss, C.F. & Bird, R.B., 1954 *Molecular theory of Gases and Liquids*, John Wiley & Sons Inc., New York, 280.
International Critical Tables, 1928 Vol. III., Mc Graw Hill Book Co. Inc., New York.

X-ray study of the orthorhombic modification of the para-acetotoluidide crystals

By S. N. MITRA

Indian School of Mines, Dhanbad, India.

(Received 20 June 1969)

Crystals of para-acetotoluidide (CH_3 , CONH , C_6H_4 , CH_3) (Beilstein 1929) are grown out of saturated solution of alcohol by rapid evaporation. These crystals appear as thin prisms with a (100), b (010) and m (110) faces bounded by r (101) and c (001) faces. They are examined with the help of a Fuess horizontal circle goniometer and the interfacial angles thus measured are found in good agreement with those recorded in Groth (1917). The crystals belong to the orthorhombic system.

The crystals are first studied by the rotation method in a camera of 10 cm. diameter as well as by the powder method in a Unicam camera of 19 cm. diameter, with $\text{Cu-K}\alpha$ radiation.

The axial lengths are thus obtained as :

$$a=12.98\text{\AA}, b=9.82\text{\AA} \text{ and } c=6.52\text{\AA}.$$

The specific gravity of the crystals is found by the floatation method in a solution of ZnSO_4 in water, as 1.19. The number of molecules in the unit cell of the crystal comes out to be four only.

The axial ratio of $a : b : c$ is thus found to be 1.322 : 1 : 0.6639 as against 0.6515 : 1 : 0.3289 given by Groth (1917).

Several zero layer-line and first layer line Weissenberg photographs are taken about the a , b and c axes respectively and the reflexions are analysed. From the reflexions in the photographs as analysed, it is concluded that :

For $h00$ reflexions $h = 2n$		For $h0l$ reflexions-no condition.
For $0k0$ „ $k = 2n$	and	For $0kl$ „ „ „
For $00l$ „ $l = 2n$		For hkl „ „ „
		For hkl „ „ „

The orthorhombic crystals of the para-aceto-toluidide are thus assigned the space-group $P2_12_12_1$

Structural analysis is in progress.

The author expresses his grateful thanks to Prof. J. Dhar for suggesting the problem and taking keen interest in the work.

REFERENCES

- Beilstein 1929, *Handbuch der Organische Chemie*, 920.
Groth, P. 1917 *Chemische Kristallographie*, 4, 400.

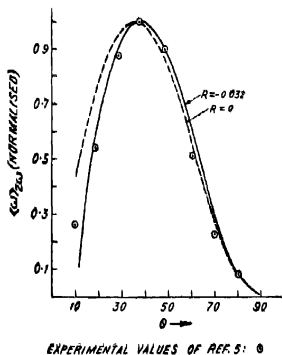
On second harmonic generation in a two level system

By B. K. MOHANTY AND G. P. SASTRI

Department of Physics, Indian Institute of Technology, Kharagpur

(Received 17 January 1969)

Recently one of the authors (Mohanty 1967, henceforth referred to as I; Mohanty 1968) had discussed certain aspects of second harmonic processes in a two level system. Using a general treatment valid for any dipole type of interaction (Feynman *et al* 1957) the angular dependence of the second harmonic dipole moment $\langle \mu \rangle_{2\omega}$ was shown to be $\sim \cos^2 \theta \sin \theta$, θ being the angle between the direction of the permanent dipole moment (electric or magnetic) and the applied oscillating field. The experimental results of Voskonyan *et al* (1964) are in excellent agreement with the conclusions of I for large θ , but are lower in value for small θ . This note aims to show that the higher order calculations with the model of I tend to remove this disagreement. This establishes the validity of the model and throws some light on the relative magnitudes of successive orders of expansion in calculating $\langle \mu \rangle_{2\omega}$.



Graph 1

The model and the mathematical methods are discussed in detail in I. The expectation value of the dipole moment operator μ is :

$$\langle \mu \rangle = \mu_{12} r_1 \quad (1)$$

where $\mu_{12} = \int \psi_1^* \mu \psi_2 dv$ and r_1 is defined by the geometrical picture of the Schrodinger equation

$$\frac{d\mathbf{r}}{dt} = \omega \times \mathbf{r} \quad (2)$$

ω and r defined in I.

Under an interaction of the type $V = -Re. (\mu.E_0 e^{-i\omega t})$ and a rotating coordinate approximation equation 2 reduces to (details are given in I) :

$$\begin{aligned} -\frac{i\hbar\omega}{\gamma} u_{n,v} + S u_{n,v} + \frac{1}{2} (v_{n-1,v-1} + v_{n+1,v-1}) &= 0 \\ -\frac{i\hbar\omega}{\gamma} v_{n,v} - S v_{n,v} - \frac{1}{2} (u_{n-1,v-1} + u_{n+1,v-1}) r_{n,v} &= 0 \\ -\frac{i\hbar\omega}{\gamma} r_{n,v} - u_{n,v} &= 0 \end{aligned} \quad (3)$$

The quantities involved are $\gamma = 2\mu_{12}.E_0/\hbar$ and $S = \frac{\omega_{21} - \omega}{\hbar}$ where

ω_{12} is the transition frequency between the two levels defined in I. $u_{n,v}$, $v_{n,v}$ and $r_{n,v}$ are defined by,

$$\begin{aligned} r_1 \cos \omega t + r_2 \sin \omega t &= r'_1 = \sum_{n=-\infty}^{\infty} \sum_{v=0}^{\infty} u_{n,v} q^v e^{-in\omega t} \\ r_2 \cos \omega t - r_1 \sin \omega t &= r'_2 = \sum_{n=-\infty}^{\infty} \sum_{v=0}^{\infty} v_{n,v} q^v e^{-in\omega t} \\ r_3 &= r'_3 = \sum_{n=-\infty}^{\infty} \sum_{v=0}^{\infty} r_{n,v} q^v e^{-in\omega t} \end{aligned} \quad (4)$$

where $q = \frac{\delta}{\gamma}$, $\delta = \frac{(\mu_{11} - \mu_{22}).E}{\hbar}$

Further calculations, under the same conditions as I (also see Sengupta 1967) and in the neighbourhood of $2\omega \approx \omega_{12}$ yield for high $\omega (\omega \gg \gamma^2)$,

$$r_1(2\omega) = \frac{\gamma^2 \omega_{12}}{2K} \left(r_{00} + r_{02} \frac{\delta^2}{\gamma^2} \right) \cos 2\omega t. \quad (5)$$

with $K = -(\omega_{12} - \omega)^2 + \omega^2 - \gamma^2$.

Hence,

$$\langle \mu \rangle_{2\omega} = \mu_{12} \frac{\omega_{12} \gamma^2 \delta}{2K} r_{00} \left(1 + \frac{r_{02}}{r_{00}} \frac{\delta^2}{\gamma^2} \right) \cos 2\omega t.$$

The dependence of $\langle \mu \rangle_{2\omega}$ (observed perpendicular to E_0) on θ is

$$\langle \mu \rangle_{2\omega} \approx \cos^2 \theta \sin \theta (1 + R \cot^2 \theta) \quad (6)$$

where $R = (r_{02}/r_{00}) (|\delta^2|/|\gamma^2|)$

A comparison of the experimental values for normalised $\langle \mu \rangle_{2\omega}$ (Voskonyan *et al* 1964) with the results of I and that given by equation 6 shows

an excellent agreement at all θ for $R = -0.032$ (the weighted mean of R calculated assuming an identity of experimental and theoretical values at $\theta = 90^\circ$ and at the experimental maximum). The negative sign of R may be interpreted as the effective decrease of $\langle \mu \rangle_{2\omega}$ as energy of second harmonic must be shared by other harmonics also. It may be pointed out that the result gives a general idea about the relative magnitudes in the expansion of r_3 (equation 4). This calculation also shows that all other contributions to $\langle \mu \rangle_{2\omega}$ (near $\omega_{12} \approx 2\omega$) upto this order vanish. The conclusions seem to establish the validity of the model for frequency conversion processes, which have been under investigation by the authors for some time (Mohanty 1968)

The authors are indebted to Prof H.N. Bose for his kind interest in the work.

REFERENCES

- Feynman, R. P. Vernon F. L. & R.W. Hellwarth 1957 *J. Appl. Phys.* **28**, 49
Mohanty, B. K. 1967 *Indian J. Phys.*, **41**, 60.
1968 Ph. D. thesis, I.I.T., Kharagpur, Chapter III.
Sengupta, N. D. 1967 *Z. Physik*, **200**, 13.
Voskonyan, A. V., Klyshko, D. & Vusmanov, V. 1964 *Soviet Phys. JETP*, **18**, 967.

BOOK REVIEWS

Algebra of Vectors (with Applications to Geometry and Mechanics) and

An Introduction to Vector Calculus

by Shanti Kumar M. Sc., Published by S. K. Lahiri & Co. (P) Ltd.,
Calcutta-12 Price Rs. 7.00

This is one more of the many textbooks in Vector Algebra. The description in the fairly long title of the book is accurate. The coverage of the book in the algebra of vectors is adequate. Chapter I deals with fundamental definitions and operation in algebra of vectors with elementary physical applications. Chapter II deals with scalar product and its application to mechanics. In the same way the subsequent chapters deal with vector product, scalar and vector triple products and reciprocal systems of three vectors respectively. Geometrical and mechanical applications are adequately treated. The chapter on trigonometrical applications is welcome.

The appendices on vector calculus and orthogonal curvilinear co-ordinate systems are meant for application only.

R. N. B.

Solid State Physics-An Introduction to its Theory

by H. Clark ; Macmillan, London. Mellourne. Toronto and St. Martin's Press,
New York ; 1968 ; Price 40 sh.

The book is meant for students, who have got some preliminary idea about the theories of solid physics and want to study the more advanced theories in the line. Author has therefore tried to explain the physical conceptions behind all those theories.

The author has explained and illustrated in a simple manner the application of group theory in Solid State Physics. Problems are included at the end of each chapter and these are helpful in making the theories clearer. The book will therefore be helpful to students of degree and M. Sc. classes as also to research workers in the line.

A. K. D.

BOOKS RECENTLY RECEIVED FOR REVIEW

Le Renoncement Scientifique de Notre Epoque, Ed. Jean Rigaud, 12, Boulevard Pasteur,
63-Clermont Ferranal.

Elementary Calculation in Biochemistry and Physiology, J. A. Barclay and K. White,
20sh, J. A. Churchill Ltd., London.

Transfer and Storage of Energy by Molecules, Ed. G. M. Burnett & A. M. North,
Wiley Interscience, London.

Physics of the Solid State, Ed. S. Balakrishna, \$ 24.00, Academic Press London

Rotational Structure in the Spectra of Diatomic Molecules, Istvan Kovacs, Adam Hilger
Ltd, London.

Transistor, E. J. M. Kendall, \$ 5.50, Pergamon Press, London.

Voyage to the Moon, Rossote Krishna Pillai, Rs. 5.50, Orient Longman, New Delhi.

The Indian Ephemeris & Nautical Almanac for the year 1970, Rs. 14.00, Director General
of Observatories, New Delhi-3.

Studies on some microstructures on octahedral faces
of natural diamonds

By A. R. PATEL AND M. K. AGARWAL

*Department of Physics, Sardar Patel University, Vallabh Vidyanaagar
Gujarat State*

(Received 16 August 1969)

Diamond octahedra having large steps on their faces have been examined by keeping the axis of the microscope equally inclined to all the four $\{111\}$ faces meeting at one corner. Some of the steps show 'quadrons' similar to such features on $\{100\}$ natural faces. Further tilt revealed other steps on which trigons similar to those observed on natural $\{111\}$ faces have been found. It is conjectured that growth on different forms of diamond takes place by the depositions of layers parallel to the faces of the form of the crystal.

INTRODUCTION

Since growth and dissolution of crystals proceed on the faces of a crystal, the crystal surfaces are the right places at which the phenomena concerning crystal growth and dissolution are most vividly reflected. It is therefore likely that the study of the structure of crystal faces, may be able to predict the mechanism, process and history of crystal growth and dissolution. It is probably with this view in mind, that a number of investigators have carried out the studies on the microstructures of natural diamonds. Chief amongst these are, Fersmann and Goldschmidt (1911), Vanderveen (1913), Sutton (1928), Williams (1932) and Tolansky and his school 1955, 1960). Recently Varma (1967a, 1967b, 1967c) has made a critical study of all the different forms of diamonds. He has conjectured from his studies that growth in all forms of diamond occurs by the deposition of layers parallel to $\{111\}$ planes irrespective of whether the crystal is an octahedron, a cube or a dodecahedron. According to him even the possibility of growth to occur on $\{100\}$ and $\{110\}$ planes to form the cube or the dodecahedron is not considered. It is rather difficult for the authors to conceive why growth should not have taken place on $\{100\}$ and $\{110\}$ planes at least in those crystals which are of the cubic and dodecahedron form.

While examining natural diamonds, quite often one observes several steps of quite large step heights on their finished surfaces. It appears that none of the previous workers was interested in the studies of such steps. It is well known according to the theory of crystal growth (Volmer 1939, Kossel 1927, Stranskii 1928, 1949 and Becker & Doring 1935) that growth preferentially takes place along the surface steps and kinks. It

was therefore considered that a critical study of these steps and kinks on the surfaces of natural diamonds should be very interesting and encouraging since such studies might reveal a great deal of information about the mechanism of growth of the crystal which is technically a very important substance. It is with this aim that the present work on the studies of steps on octahedral faces of diamonds was undertaken.

EXPERIMENTAL

In order to examine the surface of the steps on [111] faces of diamond the crystal was set such that the (111), ($\bar{1}\bar{1}1$), ($\bar{1}\bar{1}\bar{1}$) and ($1\bar{1}\bar{1}$) faces were equally inclined to the axis of the microscope i. e. an imaginary (100) plane of the crystal was normal to the axis of the microscope, as shown schematically in figure 1(a). For observing those steps

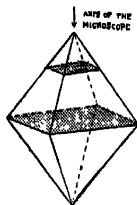


Figure 1(a). Schematic diagram showing an imaginary (100) plane normal to the axis of the microscope.

whose surfaces were (111) (schematic diagram of figure 1(c)) the axis of the microscope was further tilted and made perpendicular to them.

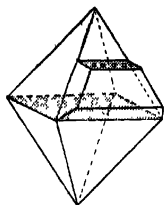


Figure 1(b). Schematic diagram showing (100) step.

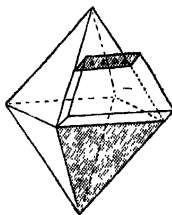


Figure 1(c). Schematic diagram showing (111) step.

Epignost and Vickers's projection microscopes were used for the investigations and about 160 natural octahedral faces were studied. The

diamond octahedra were all obtained on request from the Diamond Research Laboratory, South Africa. Out of all the surfaces of the steps examined, twenty four steps showed the quadrilateral pits known as 'quadrons' (Tolansky & Sunagawa 1959) and an equal number showed the triangular pits known as 'trigons'. In some cases the pits were numerous and in others only few. It was found that on one crystal the surfaces of all the steps showed quadrons, while on other either trigons or quadrons were observed. Out of number of observations made we describe here only few of them which are typical.

OBSERVATION

1. *Quadrons*

It may be pointed out that all the steps whose surfaces were examined were lying in $\langle 110 \rangle$ direction. When the crystals were examined with the axis of the microscope perpendicular to (100) planes, number of quadrons were seen at some places as shown in figures 2 ($\times 800$) and 3 ($\times 1000$), which are the photomicrographs of surfaces of two different steps on an octahedral face of a crystal and are representative of all such features on the remaining twenty two faces. In order to resolve the pits better, some of the steps showing such features were examined by electron microscopy by preparing a single stage carbon replica as reported by Patel & Patel (1968). In fact it was very difficult to prepare the replicas from such steps because of uneven surface but with repeated efforts the authors were successful in getting the replicas of the surfaces of the steps. Thus figure 4 ($\times 8500$) is the electron micrograph of the surface of a step on the octahedral face. Quadrons similar to those observed on natural (100) faces are



Figure 2. ($\times 800$) quadrons in (100) steps.

very clearly seen in the picture. These features are observed on the two steps seen crossing the face shown in figure 5 ($\times 55$). The steps are marked as AB and CD in the figure. The steps were measured and found to be $55\ \mu$ and $22\ \mu$ respectively.



Figure 3. ($\times 100$) quadrans in (100) steps



Figure 4. ($\times 8500$) Electron micrograph showing quadrans in a (100) step.

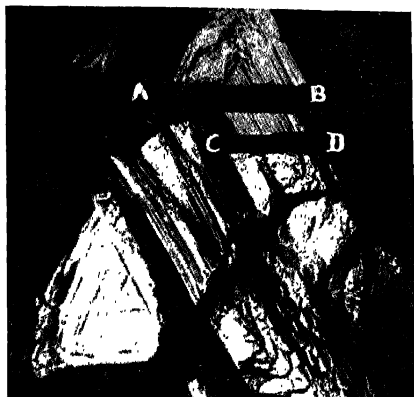


Figure 5. ($\times 55$) Octahedral face showing the steps in which quadrons are observed.

2. *Trigons*

During the examination it was found that in some cases the axis of the microscope was required to be tilted more to make it perpendicular to the surface of the step. On these steps trigons similar to those observed on natural (111) faces were observed. Figure 6 ($\times 55$) represents the photomicrograph of a surface of a step on which the trigons are observed. In order to see these trigons more clearly a picture was taken at a higher magnification. Thus figure 7 ($\times 450$) is a magnified photograph of a region shown in figure 6 in which the trigons are very distinctly seen. The octahedral face on which a step having the surface markings described above is shown in figure 8 ($\times 55$). It is only in such steps that the trigons mentioned above have been observed.



Figure 6. ($\times 55$) Trigons in (111) step.



Figure 7. ($\times 450$) Trigons in (111) step at a higher magnification.

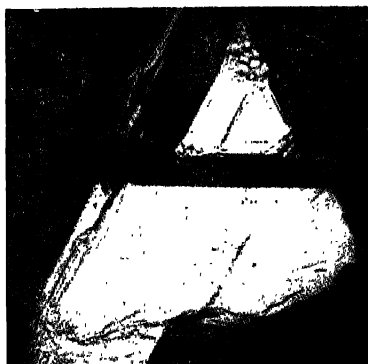


Figure 8. ($\times 55$) Octahedral face showing steps in which trigons are seen.

DISCUSSION

That the steps observed on (111) faces of diamond all lie in $\langle 110 \rangle$ direction suggests that they might have been formed due to the termination of either (100) or (111) faces on the (111) planes of observation. According to theory of crystal growth (Stranskii 1928, 1949) for growth to take place on flat crystal faces the probability for the growth to proceed is more at

the kinks or steps upon them. It is therefore more likely for the growth to proceed on the surfaces of the step rather than elsewhere on the surface on which these steps are observed. The mechanism of growth of the crystal will therefore be revealed by the microstructures on the surfaces of the steps.

Despite existing differences in the interpretation of trigons and quadrons i. e. whether they are formed due to growth or by dissolution there is agreement that trigons are seen only on the (111) plane and quadrons only on the (100) planes in diamond. That the microstructures on the surfaces of the steps examined in the present work show trigons similar to those observed on (111) natural faces and quadrons similar to those observed on (100) natural faces suggests that before the growth ceased (111) and (100) planes might also be the surfaces on which the growth might be taking place. The fact that a large number of steps have been found to have 'quadrons' on their surfaces suggests that growth might also proceed by deposition of layers along (100) planes just as it could take place by deposition of layers parallel to (111) faces. In fact, it is difficult to conceive how growth can proceed by depositing (111) layers in the case of a cube. The answer is, as in the case of an octahedron growth proceeds by deposition of layers parallel to (111) planes, the growth in the cube form of the crystal might also proceed by depositing layers parallel to (100) planes. It seems to us more logical and appropriate to think on these lines rather than to say that growth in all forms of diamond proceeds by the deposition of (111) layers. In fact the present work has clearly shown that even in the octahedron form of diamond at some place the growth in all forms of diamond proceeds by the deposition of (111) layers. In fact the present work has clearly shown that even in the octahedron form of diamond at some place the growth proceeds by depositing layers parallel to (100) planes while at others it might proceed by depositing layers parallel to (111) planes. This view is supported by the existence of trigons on the surfaces of the steps of some crystals and quadrons on the remaining ones.

Thus the authors are of the view that growth will proceed on different forms of the crystals in different manner depending upon the form of the crystal. According to this view in the case of dodecahedron the growth might proceed by depositing layers parallel to (110) planes.

REFERENCES

- Becker, Von R., & Döring, W. 1935 *Ann. Physik. Leipzig*, **24**, 719.
Fersmann, A., & Goldschmidt, V. 1911 *Der Diamant* (Heidelberg : Winter).
Kossel, W. 1927 *Nachr. Ges. Wiss., Göttingen Math. Physik K. 1* IIa, 135.
Patel, A. R., & Patel, S. M. 1968 *Rev. Sci. Instruments*, **39**, 409.

- Stranskii, I. N., 1928 *Z. Phys. Chem.* **136**, 259.
1949 *Disc. Faraday Soc.* **5**, 13.
- Sutton, J. R. 1928 *Diamond* (London : Murby & Co.)
- Tolansky, S. & Sunagawa, I. 1959 *Ind. Diamond Rev.*, **20**, 7.
- Tolansky, S. 1955 *The Microstructures of Diamond Surfaces* (London : N. A. G. Press) :
1960 *Surface Microtopography* (London : Longmans, Green & Co.)
- Van der Veen, 1913 *Z. Kristallogra. Miner.*, **51**, 545.
- Varma, C. K. R. 1967 a, *Phil. Mag.* **16**, 611.
1967 b, *Phil. Mag.* **16**, 621.
1967 c, *Phil. Mag.* **16**, 657.
- Volmer, M. 1939 *Kinetik der Phasenbildung* (Steinkopf, Dresden & Leipzig).
- Williams, A. F. 1932 *The Genesis of Diamond* (London, Benn)

Reduction of wavefunction which transforms as complex
antisymmetric tensor to irreducible representation
of Lorentz group (zero mass system)

By B. S. RAJPUT

Department of Physics, Kurukshetra University

(Received 1 April 1969)

The reduction of the wavefunction which transforms as a complex antisymmetric tensor to the irreducible representation of proper, orthochronous, inhomogeneous Lorentz group for zero mass system has been discussed by giving the proofs of the essential theorems. The change of gauge is discussed as the unphysical change in the wavefunction under the pure Lorentz transformation. The effects of reality condition, wave equation and the canonical formalism as well as the second quantizations also have been discussed. By assuming the total energy to be positive the constants of the expansion of wavefunction which satisfies wave-equation, have been calculated to give the energies for four modes corresponding to positive and negative values of Hamiltonian density.

INTRODUCTION

The general ways of reduction of any unitary ray representation of the proper, orthochronous, inhomogeneous Lorentz group have been discussed by Lomont & Moses (1967) for both non-zero and zero mass systems where for the former one obtains the Foldy (1956)-Shirokov (1958, 1959) relations and for the latter one is led to the Lomont-Mose (1964) realization. These results were used by Moses (1967) to reduce the wavefunction which transforms as an antisymmetric (real) tensors for non-zero mass system to the irreducible representation of the proper orthochronous, inhomogeneous Lorentz group. We (Rajput 1969) extended this reduction for of the wavefunction which transforms as complex-antisymmetric tensor. Moses (1968) discussed the reduction of the wavefunction which transforms as real antisymmetric tensor for zero mass system. In the present paper we discuss the reduction of wavefunction which transforms as a complex anti-symmetric tensor for zero mass system to the irreducible representation of the inhomogeneous Lorentz group by giving the proofs of essential theorems which are used in this case. Here we calculate the change of gauge as the inessential change in the wavefunction due to the operations of three generators (corresponding to space time relations) of proper, orthochronous, inhomogeneous Lorentz group. We have also discussed the effect of reality condition and wave equation on the wavefunction and the second quantization in connection to canonical formalism. It is noted in these calculations that to reduce the wavefunction, only the transformation properties are necessary while the requirements of the wave equation and reality condition restrict the

number of independent irreducible representations. The results of the present paper can be used to reduce the electromagnetic field wavefunction to the irreducible representations.

TRANSFORMATION OF THE WAVEFUNCTION

The components of a complex anti-symmetric tensor is given by

$$\begin{aligned} F^{ij} &= F_R^{ij} + F_I^{ij} \\ F^{ij} &= -F^{ji} \end{aligned} \quad \dots (1)$$

Where R denotes real part and I the imaginary part. To give the wavefunction field description of this tensor we define

$$\left. \begin{aligned} E_{iR} &= F_R^{0i}, \\ E_{iI} &= F_I^{0i}, \\ H_{iR} &= \epsilon_{ijk} F_R^{jk}, \\ H_{iI} &= \epsilon_{ijk} F_I^{jk} \end{aligned} \right\} \quad \dots (2)$$

Then the wave function ψ , which transforms as a complex anti-symmetric tensor, is the six components column vector given by

$$\psi = \begin{bmatrix} \psi_R \\ \psi_I \end{bmatrix} \quad \dots (3)$$

where ψ_R and ψ_I are three components column vectors given by

$$\begin{aligned} \psi_R(\vec{x}, t, r) &= E_{rR}(\vec{x}, t) - i H_{rR}(\vec{x}, t) \\ \psi_I(\vec{x}, t, r) &= E_{rI}(\vec{x}, t) - i H_{rI}(\vec{x}, t), \quad r = 1, 2, 3. \end{aligned} \quad (4)$$

In terms of infinitesimal generators of proper, orthochronous, inhomogeneous Lorentz group the wave function ψ transforms as (Rajput 1969)

$$\left. \begin{aligned} \psi'(x) &= \exp \left[i \sum_j a^j P_j \right] \psi(x) \\ \psi'(x) &= \exp \left[i \vec{\theta} \cdot \vec{K} \right] \psi(x) \\ \psi'(x) &= \exp \left[i \vec{\beta} \cdot \vec{Z} \right] \psi(x) \end{aligned} \right\} \quad \dots (5)$$

where

$$\left. \begin{aligned} P_j &= P^j = -i \nabla_j I \quad (j = 1, 2, 3) \\ P^0 &= -P_0 = H = -i \frac{\partial}{\partial t} I, \quad i = (-1)^{1/2} \\ K_j &= M_j - i (x \times \nabla)_j I, \\ Z_j &= N_j + i \left(x_j \frac{\partial}{\partial t} + t \nabla_j \right) I \end{aligned} \right\} \quad (6)$$

For tensor field we have

$$M_1 = \begin{pmatrix} 0 & 0 & 0 \\ 0 & 0 & -i \\ 0 & i & 0 \end{pmatrix}, \quad M_2 = \begin{pmatrix} 0 & 0 & i \\ 0 & 0 & 0 \\ -i & 0 & 0 \end{pmatrix}, \quad M_3 = \begin{pmatrix} 0 & -i & 0 \\ i & 0 & 0 \\ 0 & 0 & 0 \end{pmatrix},$$

$$N_1 = \begin{pmatrix} 0 & 0 & 0 \\ 0 & 0 & -1 \\ 0 & 1 & 0 \end{pmatrix}, \quad N_2 = \begin{pmatrix} 0 & 0 & 1 \\ 0 & 0 & 0 \\ -1 & 0 & 0 \end{pmatrix}, \quad N_3 = \begin{pmatrix} 0 & -1 & 0 \\ -1 & 0 & 0 \\ 0 & 0 & 0 \end{pmatrix}.$$

Thus M_i are Hermitian matrices while N_i are not so. The massless representation of the infinitesimal generators of the inhomogeneous Lorentz group is given in terms of the representation of the infinitesimal generators of the two dimensional Euclidean group. For this we consider the three operators T_1, T_2, J which satisfy the commutation rules for the infinitesimal generators of the two dimensional Euclidean group given by

$$\begin{aligned} [T_1, T_2] &= 0, \\ [T_1, J] &= -iT_2, \\ [T_2, J] &= iT_1 \end{aligned}$$

The matrices or kernels: $T_1(\lambda | \lambda')$, $T_2(\lambda | \lambda')$ and $J(\lambda | \lambda')$ defined as :

$$\begin{aligned} T_1 F(\lambda) &= \sum_{\lambda'} T_1(\lambda | \lambda') F(\lambda') \\ T_2 F(\lambda) &= \sum_{\lambda'} T_2(\lambda | \lambda') F(\lambda') \\ J F(\lambda) &= \sum_{\lambda'} J(\lambda | \lambda') F(\lambda') \end{aligned}$$

Constitute a representation of the infinitesimal generator of two dimensional Euclidean group. $F(\lambda)$ here is the function of the real variable λ which can be continuous, discrete or finite dimensional and represents the eigen values of the matrix J . The operators T_1, T_2 and J are given in terms of M_i and N_i as follows

$$\left. \begin{aligned} T_1 &= -M_2 - \epsilon N_1 \\ T_2 &= M_1 - \epsilon N_2 \\ J &= M_3 \end{aligned} \right\} \quad \dots(6)$$

Then the realization of the infinitesimal generators of inhomogeneous Lorentz group given by Lomont & Moses (1967) can be taken as

$$\begin{aligned}
\hat{P}_0 f(\vec{p}) &= H f(\vec{p}) = \epsilon p f(\vec{p}) \\
\hat{P}_i f(\vec{p}) &= p_i f(\vec{p}) \\
\hat{K}_1 f(\vec{p}) &= \left[L_1 + \frac{p_1 J}{p + p_3} \right] f(\vec{p}) \\
\hat{K}_2 f(\vec{p}) &= \left[L_2 + \frac{p_2 J}{p + p_3} \right] f(\vec{p}) \\
\hat{K}_3 f(\vec{p}) &= [L_3 + J] f(\vec{p}) \\
\hat{\mathcal{L}}_1 f(\vec{p}) &= \epsilon \left\{ i p \frac{\partial}{\partial p_1} + \frac{p_2}{p + p_3} J + \left[\frac{p_1^2}{p^2(p + p_3)} - \frac{1}{p} \right] T_1 \right. \\
&\quad \left. + \frac{p_1 p_2}{p^2(p + p_3)} T_2 \right\} f(\vec{p}) \\
\hat{\mathcal{L}}_2 f(\vec{p}) &= \epsilon \left\{ i p \frac{\partial}{\partial p_2} - \frac{p_1}{p + p_3} J + \frac{p_1 p_2}{p^2(p + p_3)} T_1 \right. \\
&\quad \left. + \left[\frac{p_2^2}{p^2(p + p_3)} - \frac{1}{p} \right] T_2 \right\} f(\vec{p}) \\
\hat{\mathcal{L}}_3 f(\vec{p}) &= \epsilon \left\{ i p \frac{\partial}{\partial p_3} + \frac{1}{p^2} [p_1 T_1 + p_2 T_2] \right\} f(\vec{p}) \quad (7)
\end{aligned}$$

Where L_1 , L_2 and L_3 are the components of orbital angular momentum given by

$$L_i f(\vec{p}) = -i \sum_{ij} \epsilon_{ijk} p_j \frac{\partial}{\partial p_k} f(\vec{p}) \quad \dots (8)$$

and

$$\epsilon = \pm 1.$$

Here \hat{P}^a , \hat{K} , and $\hat{\mathcal{L}}$ are the infinitesimal generators of the unitary ray representation of Lorentz group. They satisfy the same commutation rules as those of the generators P^a , K and Z . Hence the required reduction requires the expression of the wavefunction $\psi(x)$ in terms of $f(\vec{p})$.

REDUCTION OF THE WAVEFUNCTION

In equations (6) the matrix M_3 is Hermitian and hence diagonalised by a unitary matrix U :

$$U^{-1} M_3 U = d$$

where d is diagonal matrix. Then λ , the eigenvalues of M_3 are given by :

$$| M_3 - \lambda I | = 0$$

which gives

$$\lambda = 1, 0, -1.$$

$$\text{Hence, } d = \begin{bmatrix} 1 & 0 & 0 \\ 0 & 0 & 0 \\ 0 & 0 & -1 \end{bmatrix} \quad \dots(10)$$

By equations (9) and (10) we get

$$U = \begin{bmatrix} -(2)^{-1/2} & 0 & (2)^{-1/2} \\ -i(2)^{-1/2} & 0 & -i(2)^{-1/2} \\ 0 & 1 & 0 \end{bmatrix} \quad \dots(11)$$

Let us define the column vector $\chi(\epsilon, p, \lambda)$ as

$$\chi(\epsilon, p, \lambda) = [\exp(i\vec{\omega} \cdot \vec{M}) \exp(i\nu N_3) U]_{r,\lambda} \quad (12)$$

where \vec{p} is in one to one correspondence with $\vec{\omega}$ and scalar ν through the expressions

$$p = e^{i\omega},$$

$$p_1 = -p \left(\frac{\sin \omega}{\omega} \right) \omega_2$$

$$p_2 = p \left(\frac{\sin \omega}{\omega} \right) \omega_1 \quad \dots(13)$$

$$p_3 = \cos \omega, \quad \omega_3 = 0, \quad \omega = |\vec{\omega}|$$

Using the values of $\exp(i\vec{\omega} \cdot \vec{M})$ and $\exp(i\nu N_3)$ from our previous paper (Rajput 1969) the vector $\chi(\epsilon, p, \lambda)$ is written as follows

$$\chi(\epsilon, p, 0) = \begin{bmatrix} p_1 | p \\ p_2 | p \\ p_3 | p \end{bmatrix} \text{ for } \lambda = 0 \quad \dots(14)$$

$$\chi(\epsilon, p, \lambda) = [\lambda p^{-\epsilon\lambda} (2)^{1/2}] \sigma(\epsilon, p, \lambda)$$

$$= [\lambda p^{-\epsilon\lambda} (2)^{1/2}] \begin{bmatrix} \frac{p_1 (p_1 + i\lambda p_2)}{p(p + p_3)} - 1 \\ \frac{p_2 (p_1 + i\lambda p_3)}{p(p + p_3)} - i\lambda \\ \frac{p_1 + i\lambda p_3}{p} \end{bmatrix} \text{ for } \lambda = \pm 1 \quad \dots(15)$$

Now we consider the function $f(\xi)$ as the representation of the vector ψ in the basis which is characterised by the space of wavefunctions in Hilbert space upon which the generators of Lorentz group operate. ξ

collectively denotes all the variables upon which the function in the given representation depends. Then as the result of Lomont & Moses (1967) we have

$$f(\xi) = \sum_{\mu} \sum_{\lambda} \left\{ \frac{d\mu}{\omega(\mu, p)} \right\} \times \langle \xi | \mu, \epsilon, p, \lambda \rangle > f(\mu, \epsilon, p, \lambda) \dots (16)$$

In our case $\mu = 0$, $\lambda = 0$ or ± 1 and hence equation (16) reduces to :

$$f(\xi) = \sum_{\epsilon=\pm 1} \sum_{\lambda=0, \pm 1} \left\{ \frac{dp}{p} \right\} \times \langle \xi | 0, \epsilon, p, \lambda \rangle > f(\epsilon, p, \lambda) \dots (17)$$

with the assumption that all the generators of the inhomogeneous Lorentz group are Hermitian. The value of the transformation function $\langle \xi | 0, \epsilon, p, \lambda \rangle$ for the present case is given by

$$\begin{aligned} \langle \xi | 0, \epsilon, p, \lambda \rangle &= \langle x, t, r, | \epsilon, p, \lambda \rangle \\ &= \{ \exp [i \vec{\omega} \cdot \vec{K}] \} \cdot \exp. [i \nu Z_3] U \{ f(x, t, r; \epsilon, \lambda) \\ &= \{ \exp [i \vec{\omega} \cdot \vec{M}] \} \cdot \exp [i \nu N_3] U \{ \exp [\vec{\omega} \cdot (\vec{x} \times \nabla)] I \} \\ &\times \exp \left[\left[i \nu \left(x_3 \frac{\partial}{\partial t} + t \frac{\partial}{\partial x_3} \right) I \right] \right] f(x, t, r; \epsilon, \lambda) \dots (18) \end{aligned}$$

The function $f(x, t, r; \epsilon, \lambda)$ satisfies the following equation

$$\begin{aligned} P_1 f(x, t, r; \epsilon, \lambda) &= P_2 f(x, t, r; \epsilon, \lambda) = 0 \\ P_3 f(x, t, r; \epsilon, \lambda) &= f(x, t, r; \epsilon, \lambda) \dots (19) \\ P^0 f(x, t, r; \epsilon, \lambda) &= H f(x, t, r; \epsilon, \lambda) = \epsilon f(x, t, r; \epsilon, \lambda). \end{aligned}$$

Using equations (5) in (19) we get

$$\begin{aligned} \frac{\partial}{\partial x_1} f(x, t, r; \epsilon, \lambda) &= - \frac{\partial}{\partial x_2} f(x, t, r; \epsilon, \lambda) = 0 \\ \frac{\partial}{\partial x_3} f(x, t, r; \epsilon, \lambda) &= i f(x, t, r; \epsilon, \lambda) \\ - \frac{\partial}{\partial t} f(x, t, r; \epsilon, \lambda) &= - i \epsilon f(x, t, r; \epsilon, \lambda) \end{aligned}$$

the general solution of which is given by

$$f(x, t, r; \epsilon, \lambda) = \exp [i(x_3 - \epsilon t)] C(\epsilon, \lambda) \dots (20)$$

where $C(\epsilon, \lambda)$ is the constant of integration. Using equation (20), (5) and (12) in equation (18) we get

$$\langle x, t, r; \epsilon, \lambda \rangle = \text{Exp} [i(x_3 - et)] \chi(r | \epsilon, p, \lambda).$$

$$\begin{aligned} \psi(x) = & \sum_{\epsilon} \sum_{\lambda} \left[C(\epsilon, \lambda) \int \frac{d\vec{p}}{p} \chi(\epsilon, p, \lambda) f(\epsilon, p, \lambda) \right. \\ & \left. \exp \{i(\vec{p}, \vec{x} - \epsilon pt)\} \right. \\ & \left. + C'(\epsilon, \lambda) \int \frac{d\vec{p}}{p} \chi'(\epsilon, p, \lambda) f'(\epsilon, p, \lambda) \exp \{i(\vec{p}, \vec{x} - \epsilon pt)\} \right] \\ = & \sum_{\epsilon} C(\epsilon, 0) \int \frac{d\vec{p}}{p} \chi(\epsilon, p, 0) f(\epsilon, p, 0) \exp \{i(\vec{p}, \vec{x} - \epsilon pt)\} \\ & + C'(\epsilon, 0) \int \frac{d\vec{p}}{p} \chi'(\epsilon, p, 0) f'(\epsilon, p, 0) \exp \{i(\vec{p}, \vec{x} - \epsilon pt)\} \\ & + \sum_{\lambda=\pm 1} \frac{\lambda}{(2)^{1/2}} \left\{ C(\epsilon, \lambda) \int \frac{d\vec{p}}{p} p^{-\epsilon \lambda \sigma(p, \lambda)} f(\epsilon, p, \lambda) \exp \{i(\vec{p}, \vec{x} - \epsilon pt)\} \right\} \\ & + C'(\epsilon, \lambda) \int \frac{d\vec{p}}{p} p^{-\epsilon \lambda \sigma'}(p, \lambda) f'(\epsilon, p, \lambda) \exp \{i(\vec{p}, \vec{x} - \epsilon pt)\} \dots (21) \end{aligned}$$

where unprimed functions represent ψ_R and primed functions represent ω_T . No. let,

$$h(\epsilon, p, \lambda) = \exp(-2i\lambda\phi) f^*(-\epsilon, -p, \lambda)$$

where, $\tan\phi = p_0/p_1$

$$C(\lambda) = C(+1, \lambda), D(\lambda) = C(-1, \lambda)$$

$$f(p, \lambda) = f(+1, p, \lambda).$$

then

$$\begin{aligned} \psi(x) = & \int \frac{d\vec{p}}{p} \chi(p, 0) [C(0) f(\vec{p}, 0) \exp \{i(\vec{p}, \vec{x} - pt)\} \\ & - D(0) h^*(\vec{p}, 0) \exp \{-i(\vec{p}, \vec{x} - pt)\} \\ & + \int \frac{d\vec{p}}{p} \chi'(\vec{p}, 0) [C'(0) f'(\vec{p}, 0) \exp \{i(\vec{p}, \vec{x} - pt)\} \\ & - D'(0) h^{*'}(\vec{p}, 0) \exp \{-i(\vec{p}, \vec{x} - pt)\}] \\ & + \sum_{\lambda=\pm 1} \frac{\lambda}{(2)^{1/2}} \left[C(\lambda) \int \frac{d\vec{p}}{p} p^{-\lambda \sigma}(\vec{p}, \lambda) f(\vec{p}, \lambda) \exp \{i(\vec{p}, \vec{x} - pt)\} \right. \\ & \left. - D(\lambda) \int \frac{d\vec{p}}{p} p^{\lambda \sigma^*}(\vec{p}, \lambda) h^*(\vec{p}, \lambda) \exp \{-i(\vec{p}, \vec{x} - pt)\} \right] \end{aligned}$$

$$\begin{aligned}
& + O'(\lambda) \left\{ \frac{d\vec{p}}{p} p^{-\lambda} \sigma'(\vec{p}, \vec{\lambda}) f'(\vec{p}, \vec{\lambda}) \exp \{i(\vec{p}, \vec{x} - p\ell)\} \right. \\
& \left. - D'(\lambda) \left\{ \frac{d\vec{p}}{p} p^{\lambda} \sigma^{*'}(\vec{p}, \vec{\lambda}) h^{*'}(\vec{p}, \vec{\lambda}) \exp \{-i(\vec{p}, \vec{x} - p\ell)\} \right\} \right\} \\
& \dots(22)
\end{aligned}$$

GAUGE CHANGE

If A is any of the infinitesimal generators P_i, H, J_i then $A \psi(x)$ has the same expansion (22) on replacing $f(\epsilon, \vec{p}, \lambda)$ by $\hat{A} f(\epsilon, \vec{p}, \lambda)$, where \hat{A} is the corresponding finite spin generator given by equation (7). If A stands for any of Z_i , then \hat{A} is not Hermitian operator and $\hat{A} f(\epsilon, \vec{p}, \lambda)$ consists of two parts, one of which corresponds to a true physical change of wavefunction and other gives unphysical change (change of gauge)

$$\hat{Z}_i f(\vec{p}) = g_i(\vec{p}) + \hat{Z}'_i f(\vec{p}) \quad \dots(23)$$

where \hat{Z}'_i is finits spin operator for which $T_i = 0$, and $g_i(\vec{p})$ is the nonessential change in the wavefunction or the gauge change given by

$$\begin{aligned}
g_1(\vec{p}) &= \epsilon \left[\left\{ \frac{p_1^2}{p^2(p + p_3)} - \frac{1}{p} \right\} T_1 \right. \\
& \left. + \frac{p_1 p_2}{p^2(p + p_3)} T_2 \right] f(\vec{p}) = \epsilon B_1 f(\vec{p}), \\
g_2(\vec{p}) &= \epsilon \left[\frac{p_1 p_2}{p^2(p + p_3)} T_1 \right. \\
& \left. + \left\{ \frac{p_2^2}{p^2(p + p_3)} - \frac{1}{p} \right\} T_2 \right] f(\vec{p}) = \epsilon B_2 f(\vec{p}), \\
g_3(\vec{p}) &= \epsilon \left[\frac{p_1 T_1 + p_2 T_2}{p^2} \right] f(\vec{p}) = \epsilon B_3 f(\vec{p}) \quad \dots(24)
\end{aligned}$$

Hence,

$$\begin{aligned}
Z_i \psi(x) &= \sum_{\epsilon} \sum_{\lambda} \left[O(\epsilon, \lambda) \left\{ \frac{d\vec{p}}{p} \chi(\epsilon, \vec{p}, \lambda) \hat{Z}_i f(\epsilon, \vec{p}, \lambda) \right. \right. \\
& \times \exp \left\{ i(\vec{p}, \vec{x} - \epsilon p\ell) \right\} \left. \right] \\
& + \sum_{\epsilon} \sum_{\lambda} \left[O'(\epsilon, \lambda) \left\{ \frac{d\vec{p}}{p} \chi'(\epsilon, \vec{p}, \lambda) \hat{Z}_i f'(\epsilon, \vec{p}, \lambda) \right. \right. \\
& \times \exp \left\{ i(\vec{p}, \vec{x} - \epsilon p\ell) \right\} \left. \right] + G_i(x) \quad \dots(25)
\end{aligned}$$

where $G_i(x)$ is the gauge change and should be added to ψ when the frame of reference is changed by an infinitesimal space time transformation. Hence,

$$\begin{aligned}
 G_i &= \sum_{\epsilon} \sum_{\lambda} \left[C(\epsilon, \lambda) \int \frac{d\vec{p}}{p} \chi(\epsilon, \vec{p}, \lambda) g_i(\vec{p}) \exp \left\{ i(\vec{p}, x - \epsilon p t) \right\} \right] \\
 &\quad + \sum_{\epsilon} \sum_{\lambda} \left[C'(\epsilon, \lambda) \int \frac{d\vec{p}}{p} \chi'(\epsilon, \vec{p}, \lambda) g'_i(\vec{p}) \right. \\
 &\quad \quad \quad \left. \times \exp \left\{ i(\vec{p}, x - \epsilon p t) \right\} \right] \\
 &= \sum_{\epsilon} \sum_{\lambda} \left[C(\epsilon, \lambda) \int \frac{d\vec{p}}{p} \chi(\epsilon, \vec{p}, \lambda) \epsilon B_i f(\epsilon, \vec{p}, \lambda) \exp \right. \\
 &\quad \quad \quad \left. \left\{ i(\vec{p}, x - \epsilon p t) \right\} \right] \\
 &\quad + \sum_{\epsilon} \sum_{\lambda} \left[C'(\epsilon, \lambda) \int \frac{d\vec{p}}{p} \chi'(\epsilon, \vec{p}, \lambda) \epsilon B_i f'(\epsilon, \vec{p}, \lambda) \right. \\
 &\quad \quad \quad \left. \times \exp \left\{ i(\vec{p}, x - \epsilon p t) \right\} \right] \\
 &= \sum_{\epsilon} \sum_{\lambda} \left[C(\epsilon, \lambda) \epsilon \int \frac{d\vec{p}}{p} \Gamma_i(\epsilon, \vec{p}, \lambda) f(\epsilon, \vec{p}, \lambda) \right. \\
 &\quad \quad \quad \left. \times \exp \left\{ i(\vec{p}, x - \epsilon p t) \right\} \right] \\
 &\quad + \sum_{\epsilon} \sum_{\lambda} \left[C'(\epsilon, \lambda) \epsilon \int \frac{d\vec{p}}{p} \Gamma_i(\epsilon, \vec{p}, \lambda) f'(\epsilon, \vec{p}, \lambda) \right. \\
 &\quad \quad \quad \left. \times \exp \left\{ i(\vec{p}, x - \epsilon p t) \right\} \right] \dots (26)
 \end{aligned}$$

where the column vector $\Gamma_i(\epsilon, \vec{p}, \lambda)$ is given by

$$\Gamma_i(r | \epsilon, \vec{p}, \lambda) = \left\{ \exp(i\omega M) \exp(i\nu N_3) B_i U \right\}_{r, \lambda} \dots (27)$$

If we define a matrix A_i as

$$A_i = \exp \left[i\omega M \right] \exp \left[i\nu N_3 \right] B_i \dots (28)$$

then as discussed by Moses (1967) we have

$$e^{-A} B e^A = \sum_n \left\{ B, A \right\}^n \frac{1}{n!} \dots (29)$$

Using equations (29) and (6) and commutation rules for M_i and N_i we get
 $\exp(i\nu N_3) T_i \exp(-i\nu N_3) = p T_i$

or

$$\exp(i\nu N_3) T_i = p T_i \exp(i\nu N_3) \quad \dots(30)$$

Using equations (24) in (30) we have

$$\exp(i\nu N_3) B_i = p B_i \exp(i\nu N_3)$$

Similarly,

$$\begin{aligned} \exp\left[i\omega \cdot \vec{M}\right] B_i &= \frac{1}{p^3} \left[-(\vec{p} \times \vec{M})_i - \epsilon \left(\frac{p_i}{p} \right) (\vec{p} \cdot \vec{N}) \right. \\ &\quad \left. + \epsilon p N_i \right] \times \exp\left[i\omega \cdot \vec{M}\right] \end{aligned}$$

Hence equations (28) reduces to

$$\begin{aligned} A_i &= \frac{1}{p} \left[-(\vec{p} \times \vec{M})_i - \epsilon \left(\frac{p_i}{p} \right) (\vec{p} \cdot \vec{N}) + \epsilon p N_i \right] \\ &\quad \times \exp\left[i\omega \cdot \vec{M}\right] \exp(i\nu N_3) \quad (31) \end{aligned}$$

If we define a column vector $\phi_n(x)$ as

$$\begin{aligned} \phi_n(x) &= \sum_n \sum_\lambda \left[C(\epsilon, \lambda) \int \frac{d\vec{p}}{p^{n+1}} x(\epsilon, \vec{p}, \lambda) f(\epsilon, \vec{p}, \lambda) \right. \\ &\quad \left. \exp\left\{i\left(\vec{p} \cdot \vec{x} - \epsilon p t\right)\right\} \right. \\ &\quad \left. + C'(\epsilon, \lambda) \int \frac{d\vec{p}}{p^{n+1}} x'(\epsilon, \vec{p}, \lambda) f'(\epsilon, \vec{p}, \lambda) \right. \\ &\quad \left. \exp\left\{i\left(\vec{p} \cdot \vec{x} - \epsilon p t\right)\right\} \right] \quad \dots(32) \end{aligned}$$

such that,

$$\frac{\partial^2}{\partial t^2} \phi_n(x) = -\phi_n(x).$$

Then putting $\nabla_i = \partial/\partial x_i$ and using the equations (27), (26), (32) and (31) we get

$$\begin{aligned} G_j(x) &= i \left[-i \left(\vec{M} \times \vec{\nabla} \right)_j + \frac{\partial}{\partial t} N_j \right] \phi_1(x) \\ &\quad + i \left(\vec{N} \cdot \vec{\nabla} \right) \nabla_j \frac{\partial}{\partial t} \phi_0(x) \quad \dots(33) \end{aligned}$$

If the unit vector in the direction of the i^{th} space axis is given by

$$\vec{e}_1 = (1, 0, 0).$$

$$G_i(x) = -\nabla \phi_{1,i}(x) + \vec{e}_i [\vec{\nabla} \cdot \vec{\phi}_1(x)] - i \frac{\partial}{\partial t} [\vec{e}_i \times \vec{\phi}_1(x)] \\ - i \frac{\partial^2}{\partial x_i \partial t} [\vec{\nabla} \times \vec{\phi}_2(x)] \quad \dots (34)$$

where $\phi_{1,i}$, denotes the component of the vector.

REALITY CONDITION

If ψ transforms as a real antisymmetric tensor then we have

$$C'(0) = C'(\lambda) = D'(\lambda) = 0$$

and hence the equation (22) reduces to :

$$\psi(x) = \int \frac{d\vec{p}}{p} x(\vec{p}, 0) [C(0)f(\vec{p}, 0) \exp \{i(\vec{p} \cdot \vec{x} - pt)\} - D(0)h^*(\vec{p}, 0) \\ \exp \{-i(\vec{p} \cdot \vec{x} - pt)\}] \\ + \sum_{\lambda=\pm 1} \frac{\lambda}{(2)^{1/2}} \left[C(\lambda) \int \frac{d\vec{p}}{p} p^{-\lambda} \sigma(\vec{p}, \lambda) f(\vec{p}, \lambda) \exp \{i(\vec{p} \cdot \vec{x} - pt)\} - D(\lambda) \right. \\ \left. \int \frac{d\vec{p}}{p} p^{\lambda} \sigma^*(\vec{p}, \lambda) h^*(\vec{p}, \lambda) \exp \{i(\vec{p} \cdot \vec{x} - pt)\} \right] \quad \dots (35)$$

which is similar to the equation as derived by Moses (1968). If $\psi(x)$ given by equation (35) is real then,

$$\psi(x) = \psi^*(x) \quad \dots (36)$$

so,

$$C(0)f(\vec{p}, 0) = -D(0)h(\vec{p}, 0).$$

and,

$$p^{-\lambda} C(\lambda)f(\vec{p}, \lambda) = p^{\lambda} D(\lambda)h(\vec{p}, \lambda)$$

then,

$$\psi(x) = A \int \frac{d\vec{p}}{p} x(\vec{p}, 0) f(\vec{p}, 0) \exp \{i(\vec{p} \cdot \vec{x} - pt)\} \\ + \sum_{\lambda=\pm 1} \frac{\lambda}{(2)^{1/2}} B(\lambda) \int \frac{d\vec{p}}{p} p^{-\lambda} \sigma(\vec{p}, \lambda) \exp \{i(\vec{p} \cdot \vec{x} - pt)\} \quad \dots (37)$$

where A and $B(\lambda)$ are constants.

MAXWELL'S EQUATION

Using equations (2), (3) and (4) Maxwell's equations in vacuum for

\vec{E} and \vec{H} become

$$\nabla \cdot \psi = 0 \quad \dots (38)$$

$$\nabla \times \psi = -i \frac{\partial}{\partial t} \psi \quad \dots(39)$$

From the equations (14), (15) we can prove that

$$\left. \begin{aligned} \nabla \cdot \chi(\vec{p}, 0) \exp \{ i(\vec{p}, \vec{x}) \} &= i p \\ \nabla \cdot \sigma(\vec{p}, \lambda) \exp \{ i(\vec{p}, \vec{x}) \} &= 0 \end{aligned} \right\} \quad \dots(40)$$

Using equations (22) and (40) in (38) we get

$$C(0)f(\vec{p}, 0) + C'(0)f'(\vec{p}, 0) = 0$$

$$D(0)h(\vec{p}, 0) + D'(0)h'(\vec{p}, 0) = 0$$

The constants $C(0)$, $C'(0)$, $D(0)$ and $D'(0)$ are arbitrary, so

$$f(\vec{p}, 0) = f'(\vec{p}, 0) = h(\vec{p}, 0) = h'(\vec{p}, 0) = 0 \quad \dots(41)$$

Similarly,

$$\left. \begin{aligned} \nabla \times \chi(\vec{p}, 0) \exp \{ i(\vec{p}, \vec{x}) \} &= 0 \\ \nabla \times \sigma(\vec{p}, \lambda) \exp \{ i(\vec{p}, \vec{x}) \} &= p\lambda\sigma(\vec{p}, \lambda) \end{aligned} \right\} \quad \dots(42)$$

Using equations (22) and (42) in (39) we get

$$\left. \begin{aligned} \sum_{\lambda=\pm 1} \lambda(\lambda-1) [C(\lambda)f(\vec{p}, \lambda) + C'(\lambda)f'(\vec{p}, \lambda)] &= 0 \\ \text{and,} \\ \sum_{\lambda=\pm 1} \lambda(1-\lambda) [D(\lambda)h(\vec{p}, \lambda) + D'(\lambda)h'(\vec{p}, \lambda)] &= 0 \end{aligned} \right\} \quad \dots(43)$$

first of equations (43) results into the following equations

$$C(+1)f(\vec{p}, +1) + C'(+1)f'(\vec{p}, +1) = 0$$

which gives

$$f(\vec{p}, +1) = f'(\vec{p}, +1) = 0 \quad \dots(44)$$

while second of equations (43) gives

$$h(\vec{p}, -1) = h'(\vec{p}, -1) = 0 \quad \dots(45)$$

Thus in the expansion (22) only the wavefunction $f(\vec{p}, -1)$ and $h(\vec{p}, -1)$ need not be identically zero for ψ to satisfy Maxwell's equation (38) and (39). Hence the wavefunction which transforms as a complex antisymmetric tensor and satisfies Maxwell's equation, is given by

$$\begin{aligned}
\psi(x) = & \frac{-1}{(2)^{1/2}} [D(+1) \int d\vec{p} \sigma^* (\vec{p}, +1) h^* (\vec{p}, +1) \\
& \exp \{ -i (\vec{p} \cdot \vec{x} - pt) \} \\
& + D'(+1) \int d\vec{p} \sigma^* (\vec{p}, +1) h^* (\vec{p}, +1) \\
& \exp \{ -i (\vec{p} \cdot \vec{x} - pt) \} \\
& + C(-1) \int d\vec{p} \sigma' (\vec{p}, -1) f' (\vec{p}, -1) \exp \{ i (\vec{p} \cdot \vec{x} - pt) \} \\
& + C'(-1) \int d\vec{p} \sigma' (\vec{p}, -1) f' (\vec{p}, -1) \exp \{ i (\vec{p} \cdot \vec{x} - pt) \}] \\
= & C \int d\vec{p} \sigma (\vec{p}, -1) f (\vec{p}) \exp \{ i (\vec{p} \cdot \vec{x} - pt) \} \\
& + C' \int d\vec{p} \sigma' (\vec{p}, -1) f' (\vec{p}) \exp \{ i (\vec{p} \cdot \vec{x} - pt) \} \\
& + D \int d\vec{p} \sigma^* (\vec{p}, +1) h^* (\vec{p}) \exp \{ -i (\vec{p} \cdot \vec{x} - pt) \} \\
& + D' \int d\vec{p} \sigma^* (\vec{p}, +1) h^* (\vec{p}) \exp \{ -i (\vec{p} \cdot \vec{x} - pt) \} \dots (46)
\end{aligned}$$

where,

$$C = \frac{-1}{(2)^{1/2}}, C(-1), C' = \frac{-1}{(2)^{1/2}}, C'(-1)$$

$$D = \frac{-1}{(2)^{1/2}}, D(+1), D' = \frac{-1}{(2)^{1/2}}, D'(+1)$$

and

$$f(\vec{p}) = f(\vec{p}, -1), f'(\vec{p}) = f'(\vec{p}, -1),$$

$$h(\vec{p}) = h(\vec{p}, +1), h'(\vec{p}) = h'(\vec{p}, +1).$$

CANONICAL FORMALISM

We choose the values of the constants O_s and D_s so that the usual canonical formalism in terms of Hamiltonian density agrees with the particle interpretation. Hamiltonian density of the field in the present case given by

$$H(x) = (8\pi)^{-1} \psi^* \cdot \psi \quad \dots (47)$$

and the energy of the field is given by

$$E = \int_{-\infty}^{\infty} H(x) dx \quad \dots (48)$$

Now we consider following four modes

$$(i) \quad f'(\vec{p}) = h(\vec{p}) = h'(\vec{p}) = 0, f(\vec{p}) \neq 0$$

$$\text{then,} \quad \psi = C \int d\vec{p} \sigma (\vec{p}, -1) f (\vec{p}) \exp \{ i (\vec{p} \cdot \vec{x} - pt) \} \quad \dots (49)$$

The expectation energy for this mode is given by

$$\int_{-\infty}^{\infty} \frac{d\vec{p}}{p} f^*(\vec{p}) \vec{p} f(\vec{p}) = \int_{-\infty}^{\infty} d\vec{p} |f(\vec{p})|^2 \quad \dots(50)$$

Comparing equation (5) with (48) for ψ given by (49) we have

$$C = \frac{-1}{\pi(2)^{1/2}}.$$

$$(ii) \quad f(\vec{p}) = h(\vec{p}) = h'(\vec{p}) = 0, f'(\vec{p}) \neq 0.$$

$$\text{then,} \quad \psi = C' \int \frac{d\vec{p}}{p} \sigma^*(\vec{p}, -1) f'(\vec{p}) \exp \{i(\vec{p} \cdot \vec{x} - pt)\}.$$

and the expectation energy is

$$E_f = \int_{-\infty}^{\infty} d\vec{p} |f'(\vec{p})|^2 \quad \dots(51)$$

which leads to

$$C' = \frac{-1}{\pi(2)^{1/2}}$$

$$(iii) \quad f'(\vec{p}) = f(\vec{p}) = h'(\vec{p}) = 0, h(\vec{p}) \neq 0,$$

then, $\psi(x) = hD \int d\vec{p} \sigma^*(\vec{p}, -1) h^*(\vec{p}) \exp \{-i(\vec{p} \cdot \vec{x} - pt)\}$
and the expectation energy is

$$E_h = \int_{-\infty}^{\infty} d\vec{p} |h(\vec{p})|^2 \quad \dots(52)$$

which leads to, $D = -1/\pi(2)^{1/2}$

$$(iv) \quad f'(\vec{p}) = f(\vec{p}) = h(\vec{p}) = 0, h'(\vec{p}) \neq 0$$

Then, $\psi(x) = D' \int d\vec{p} \sigma^{*'}(\vec{p}, -1) h^{*'}(\vec{p}) \exp \{-i(\vec{p} \cdot \vec{x} - pt)\}$

$$\text{and,} \quad E_{h'} = \int_{-\infty}^{\infty} d\vec{p} |h'(\vec{p})|^2 \quad \dots(53)$$

which leads to $D' = \frac{-1}{\pi(2)^{1/2}}$

The expectation value of the total energy when the state is the superposition of all the modes is given by

$$E = E_f + E_{f'} + E_h + E_{h'} \quad \dots(54)$$

SECOND QUANTIZATIONS

To second quantize the theory, we consider $f(\vec{p}), f'(\vec{p}), h(\vec{p})$ and $h'(\vec{p})$ as creation operators and $f^*(\vec{p}), f'^*(\vec{p}), h^*(\vec{p})$ and $h'^*(\vec{p})$ as

destruction operators. They satisfy the well known Boson-commutation rules. The operator $\psi(x)$ is then defined by replacing the amplitudes in the expansion (46) by these operators. Then for any operator \hat{A} , we define a second quantized operator $[A]$ by

$$\begin{aligned}
 [A] = & \int \frac{d\vec{p}}{p} f^*(\vec{p}, \lambda) \hat{A} f(\vec{p}, \lambda) \\
 & + \int \frac{d\vec{p}}{p} f^{*'}(\vec{p}, \lambda) \hat{A} f'(\vec{p}, \lambda) + \int \frac{d\vec{p}}{p} h^*(\vec{p}, \lambda) \hat{A} h(\vec{p}, \lambda) \\
 & + \int \frac{d\vec{p}}{p} h^{*'}(\vec{p}, \lambda) \hat{A} h'(\vec{p}, \lambda) \quad . \quad (55)
 \end{aligned}$$

The operators $[A]$ are the infinitesimal generators for the second quantized theory. Under the translation $T(\vec{a})$, rotation $R(\vec{\theta})$ and pure Lorentz transformation $L(\vec{\beta})$ the set of operators $\psi(x)$ transforms to $\psi'(x)$ by

$$\begin{aligned}
 \psi'(x) &= \psi(x + \vec{a}) = \exp \{-i \Sigma_a^a [P_a]\} \psi(x) \exp \{i \Sigma_a^a [P_a]\} \\
 \psi'(x) &= \exp \{-i \vec{\theta} \cdot [\vec{K}]\} \psi(x) \exp \{i \vec{\theta} \cdot [\vec{K}]\} \quad .. \quad (56) \\
 \psi'(x) &= \exp \{-i \vec{\beta} \cdot [\vec{Z}]\} \psi(x) \exp \{i \vec{\beta} \cdot [\vec{Z}]\}.
 \end{aligned}$$

REFERENCES

- Foldy, L. 1956 *Phys Rev.*, **102**, 568.
 Lomont, J. S. & Moses, H. E. 1964 *Journ. Math. Phys.*, **5**, 294.
 1967 *Journ. Math. Phys.*, **8**, 837.
 Moses, H. E. 1967 *Journ. Math. Phys.*, **8**, 1134.
 1968 *Journ. Math. Phys.*, **5**, 16.
 Rajput, B. S. 1969 *Indian J. Phys.* **43** 135.
 Shrokov, I.U.M. 1958 *Soviet Phys., JETP* **6**, 919.
 1959, *Soviet Phys. JETP* **8**, 703.

Molecular force fields for germanium compounds

By K. RAMASWAMY AND V. BALASUBRAMANIAN

Department of Physics, Annamalai University, Annamalainagar P.O.

Tamil Nadu, S. India

(Received 8 June 1969)

Molecular force fields of GeH_3F , GeH_2Cl , GeH_2Br and GeH_3I were calculated using the kinematic methods suggested by Torkington, Herranz and Castano & Biles. It was found that the method suggested by Herranz & Castano gives satisfactory force fields for the lighter molecules GeH_3F and GeH_2Cl while the method suggested by Torkington leads to satisfactory force fields for the heavier molecules GeH_2Br and GeH_3I .

INTRODUCTION

The solution to the force constant problem is not unique and for an n th order secular equation, we obtain $n!$ solutions for the $1/2 n(n+1)$ potential energy constants, corresponding to the $n!$ different ways of assignments. Solutions nearer to the correct one are obtained by using additional data like the isotopic vibrational frequencies, mean amplitudes, coriolis coupling coefficients and rotational distortion constants. Especially attempts by Duncan & Mills (1964a, 1964b), Aldous & Mills (1962, 1963) and Mirri (1967) using the coriolis coefficients and rotational distortion constants as additional data have yielded most satisfactory results. But for a majority of molecules all these constants are not available with great accuracy. Hence approximate solutions for the force fields are obtained using the simplified force fields like the Urey-Bradley force field (1931), the orbital valence force field (Heath & Linnet 1948) and the hybrid orbital force field (Mills 1963). Another way of obtaining a reasonable force field for any molecule is the use of kinematic methods suggested by Torkington (1949), Biles (1966) and Herranz & Castano (1966a & 1966b). These methods use exclusively the geometry and the vibrational frequencies to fix the force field. The applicability of these kinematic methods to the XY_2 non-linear symmetric molecules was examined by Freeman (1968). In this paper the molecular force fields of the germynl halides were calculated using these kinematic methods and their relative merits discussed.

POTENTIAL ENERGY CONSTANTS

The characteristic features of these three kinematic methods are given below :

The method of 'progressive rigidity' suggested by Torkington (1949) consists in reducing the determinant product $|GF|$ in the secular determinantal equation $|GF - \lambda E| = 0$ to the product of its diagonal elements.

Here G is the Wilson's inverse symmetric (kinetic energy matrix, F is the force constant matrix, Λ a diagonal matrix with its element $\lambda_k = 4\pi^2\nu_k^2 c^2$ where ν_k is the k^{th} vibrational wavenumber, and c is the velocity of light in cm sec^{-1} and E is the unit matrix. The conditions for the above mentioned reduction were given by Torkington (1949).

The symmetry coordinates used to construct G are arranged in the decreasing order of frequencies. The calculation of force constants becomes easy by defining two subsidiary matrices e and h obtained from the various minors of the G matrix. The general solution for the force constants is given by

$$F_{ij} = \sum_{k=1}^n (e_{ik} e_{jk} / e_{kk} h_{kk}) \lambda_k \quad (i > j) \quad \dots(1)$$

The matrix L which relates the set of symmetry coordinates S to the vibrational normal coordinates Q and given by $S = LQ$, is triangular in this method. Further the frequencies factor out in the decreasing order of magnitude and the molecule increases in rigidity as factorization proceeds.

In the method suggested by Biles (1966) the normal coordinate transformation matrix L is given as,

$$L = B \Gamma^{-1} \quad \dots(2)$$

and the solution for the force field is given as

$$F = B \Gamma^{-1} \Lambda B^* \quad \dots(3)$$

where B is an orthogonal matrix which diagonalises G and Γ is a diagonal matrix having the eigenvalues of G as its elements, and Λ a diagonal matrix with the element $\lambda_k = 4\pi^2\nu_k^2 c^2$. The asterisk denotes transposition of the matrix. Here the matrix product GF is symmetric.

In the method of 'characteristic set of valence coordinates' suggested by Herranz and Castano (1966a, 1966b) the normal coordinate transformation matrix L is symmetric. This method has been extensively used for fixing the force fields of some highly conjugated acetylenes (Ramaswamy & Srinivasan 1967, 1968). The present work deals with applicability of the above methods to a series of germanium compounds.

The germyl halides discussed here belong to the C_{3v} point group and each has six fundamental vibrational frequencies of which three belong to the totally symmetric (a_1) species and three belong to doubly degenerate (e) species. The symmetry coordinates used are the same as those given by Meister & Cleveland (1946). The structural parameters used in the calculations are those given by Freeman *et al* (1963). The valence force constants calculated by the three methods are given in table 1,

TABLE I VALENCE FORCE CONSTANTS IN MDYNES/Å² OF THE GERMYL HALIDES BY THE KINEMATIC METHODS

Valence force constants	GeH ₃ F Methods			GeH ₃ Cl Method			GeH ₃ Br Methods			GeH ₃ I Methods		
	I	II	III	I	II	III	I	II	III	I	II	III
f_D^1	4.2488* (4.2130)*	4.2511	6.6055	2.5458 (2.5620)*	2.5504	10.2317	2.1290 (2.1180)*	2.1387	15.8820	1.7166 (1.7456)*	1.7285	18.4046
f_a^2	2.6548 (2.6660)*	2.6563	0.2747	2.6509 (2.6670)*	2.6570	0.5845	2.6404 (2.6560)*	2.6418	0.1712	2.6272 (2.6360)*	2.6285	0.1558
f_a^3	0.1597	0.1626	0.8559	0.1557	0.1602	0.7350	0.1549	0.1583	0.8578	0.1484	0.1518	0.5395
f_β^4	0.1742	0.1759	0.4901	0.1300	0.1324	0.3531	0.1159	0.1177	0.3844	0.0990	0.1003	0.3414
$f_{\alpha\alpha}$	-0.0259	-0.0273	-0.1032	-0.0296	-0.0315	-0.1576	-0.0246	-0.0261	-0.0893	-0.0240	-0.0254	-0.0876
$f_{\beta\beta}$	-0.0397	-0.0405	0.0403	-0.0310	-0.0318	-0.0280	-0.0228	-0.0234	0.0345	-0.0191	-0.0197	0.0340
$f_{\alpha\alpha}$	0.0028	0.0101	0.0062	0.0091	0.0330	0.1045	0.0026	0.0095	-0.0201	0.0025	0.0393	-0.0194
$f_{\alpha\beta}$	0.0050	0.0180	-0.0084	0.0010	0.0112	-0.1092	0.0020	0.0131	0.0365	0.0017	0.0117	0.0051
$f_{\alpha\alpha}$	0.0185	0.0554	0.0360	0.0105	0.0501	0.0546	0.0087	0.0548	0.0684	0.0970	0.0577	0.0760
$f_{\alpha\alpha}$	0.0032	0.0031	0.0169	0.0048	0.0052	0.2410	0.0072	0.0339	-0.0518	0.0055	0.0055	-0.0533

*This number of significant figures is retained to secure internal consistency in the calculations.

Method I—Method of progressive rigidity; Method II—Method of characteristic set of coordinates; Method III—Method suggested by Biles

 $f_D^1 = f_{Ge-X}$ ($X = F, Cl, Br, I$); $f_a^2 = f_{Ge-H}$; $f_a^3 = f_{HG-H}$; $f_\beta^4 = f_{HG-X}$; $f_{\alpha\alpha} = f_{HG-X}$.Freeman *et al* (1963)

TABLE 2 MEAN AMPLITUDES OF THE GERMYL HALIDES AT $T = 298.16^\circ\text{K}$

Mean amplitudes in Å ^a	GeH ₄ F		GeH ₃ Cl		GeH ₂ Br		GeH ₃ I	
	Method I	Method II	Method I	Method II	Method I	Method II	Method I	Method II
Ge-X	0.0418* (0.039)*	0.0418	0.0464 (0.045)*	0.0465	0.0477 (0.048)*	0.0478	0.0518 (0.054)*	0.0519
Ge-H	0.0893	0.0893	0.0893	0.0894	0.0894	0.0894	0.0895	0.0895
H...H	0.1532	0.1540	0.1530	0.1518	0.1543	0.1541	0.1553	0.1552
H...X	0.1241	0.1267	0.1350	0.1355	0.1390	0.1406	0.1448	0.1443

^aMuller and Cyvin (1968).^{*}This number of significant figures is retained to secure internal consistency in the calculations.TABLE 3 VALUES OF ROTATIONAL DISTORTION CONSTANTS D_j , D_{jk} AND D_k IN KC/SEC.

Rotational distortion constants in kc/sec.	GeH ₄ F		GeH ₃ Cl		GeH ₂ Br		GeH ₃ I	
	Method I	Method II	Method I	Method II	Method I	Method II	Method I	Method II
D_j	8.9500*	8.9323	1.9232	1.9124	0.6140	0.6123	0.2910	0.2903
D_{jk}	127.6549	130.3529	27.2071	27.1186	8.8245	8.8957	4.3968	4.1298
D_k	684.7540	671.6973	925.3866	866.1315	706.1169	697.4949	731.7817	723.0498

^{*}This number of significant figures is retained to secure internal consistency in the calculations.

TABLE 4 CORIOLIS COUPLING CONSTANTS OF THE GERMYL HALIDES

Coriolis coupling constants	GeH ₄ F		GeH ₃ Cl		GeH ₃ Br		GeH ₃ I	
	Methods		Methods		Methods		Methods	
	I	II	I	II	I	II	I	II
ζ_a	0.0183*	-0.0019	0.0179	-0.0319	0.0185	-0.0013	0.0185	-0.0011
ζ_b	-0.2046	-0.1283	-0.2366	-0.1192	-0.1859	-0.1131	-0.1854	-0.1123
ζ_c	0.2483	0.1923	0.2447	0.1771	0.1826	0.1295	0.1771	0.1237
$\sum \zeta_i$	0.0620	0.0621	0.0259	0.0260	0.0152	0.0152	0.0103	0.0103
$I_A/2I_B$	0.0620	0.0620	0.0259	0.0259	0.0152	0.0152	0.0103	0.0103

*Rhee and Wilson (1965).

*This number of significant figures is retained to secure internal consistency in the calculations.

MEAN AMPLITUDES

The symmetric mean square amplitude matrix Σ for both the species were evaluated using the relation given by Cyvin (1959),

$$\Sigma = L \Delta L^* \quad \dots (4)$$

where Δ is a diagonal matrix whose elements are given by

$$\Delta_{ii} = \frac{\hbar}{8\pi^2 c \nu_i} \coth \left(\frac{\hbar c \nu_i}{2kT} \right) \quad \dots (5)$$

where \hbar is the Planck's constant, k the Boltzmann's constant, T the absolute temperature, ν_i the i^{th} vibrational wavenumber.

The various bonded and non-bonded mean square amplitudes can be obtained as the linear combinations of the Σ matrix elements. The non-bonded mean square amplitudes were obtained by the method of Ramaswamy *et al* (1962). The mean square amplitudes were evaluated for all the four molecules using the L matrices obtained in the method of progressive rigidity and the method of characteristic set of coordinates. The computed mean amplitudes at $T = 298.16^\circ\text{K}$ are presented in table 2.

ROTATIONAL DISTORTION CONSTANTS

For calculating the rotational distortion constants the rigid rotor harmonic oscillator approximation as suggested by Nielsen (1951) was assumed and the theory of Kivelson & Wilson (1952, 1953) was applied. For a molecule belonging to the C_{3v} point group, the rotational distortion constants D_{11} , D_{12} and D_{22} alone exist and these can be expressed as linear combinations of certain elements denoted by τ . These constants can be evaluated from a knowledge of the principal components of the moment of inertia tensor, the vibrational wavenumbers and the 'I' matrix which relates the vibrational normal coordinates to the mass weighted Cartesian coordinates. The explicit relations are given in the paper by De Alti *et al* (1965).

The principal axis of the molecule is taken as the Z axis with one Ge-H bond lying in the XZ plane. The rotational distortion constants evaluated in the first two methods are given in table 3.

CORIOLIS COUPLING CONSTANTS

The coriolis coupling constants were evaluated using the relation given by Meal & Polo (1956)

$$\zeta^{\alpha} = |M^{\alpha}|^*$$

where $\alpha = (x, y, z)$ denotes the axis of rotation and M^{α} is a block diagonal supermatrix made up of n identical (3×3) submatrices one for each atom. The L matrices obtained in the first two methods were used

to calculate the ζ^2 values for the coupling between the components of the degenerate vibrations. They are presented in table 4.

The ζ sum rule for these symmetric top molecules is given by

$$\sum_i \zeta_i = I_A/2 I_B$$

where I_A and I_B are the principal moments of inertia of the molecule.

DISCUSSION

Barring the small interaction force constants the values of the stretching and bending force constants are very nearly the same in the first two methods. The values compare well with those given by Krishnamachari (1955), Pillai & Perumal (1964) and Freeman *et al* (1963). Going through the series some systematic trends are observed with the values of the force constants. The Ge-H stretching force constant in GeH_3F is about 2.7% greater than that in GeH_3I . The Ge-X stretching force constant markedly decreases with decreasing electronegativity of the substituted halogen. The value of the bending constant f_β decreases with decreasing electronegativity of the halogen while f_α is practically unaffected. These trends were also observed by Freeman *et al* (1963). The method of progressive rigidity gives smaller values for the interaction force constants. The values of the various force constants obtained by the method of Biles are in poor agreement with the reported values. Further they do not show any of the systematic trends noted above.

To see which of the first two methods gives a better approximation to the true force field in these molecules, other molecular constants like the mean amplitudes, rotational distortion constants and coriolis coupling constants were evaluated.

From table 2 it is clear that the values of the various mean amplitudes are the same in the two methods. The values obtained for the Ge-H and the H...H mean amplitudes are comparable to the corresponding values of 0.0895 \AA° and 0.1525 \AA° obtained by Cyvin (1968) for GeH_4 . Also the calculated mean amplitudes for the Ge-X bonds can be compared to the values of Muller & Cyvin (1968) for the same bonds in GeX_4 molecules.

The values of the rotational distortion constants D_j , D_{jk} and D_k obtained in the two methods are also the same. Both D_j and D_{jk} markedly decrease with increasing mass of the substituted halogen. As seen from figures 1 and 2 the plots of $\log D_j$ and $\log D_{jk}$ against $\log m_x$ where m_x is the mass of the substituted halogen give straight lines. Similar results were obtained by Rao & Rao (1968) for XY_3 type molecules belonging to the C_{3v} point group. This shows that the values of D_j and D_{jk} obtained are reasonable. Since no experimentally observed values of these

constants are available no comparison of the calculated values can be made.

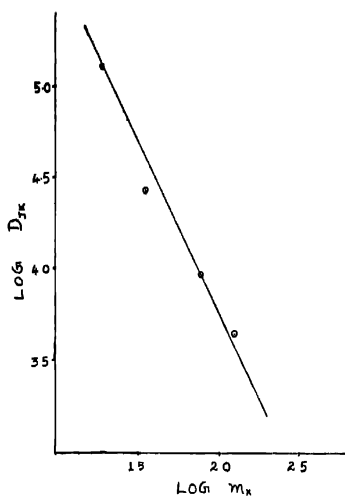


Figure 1

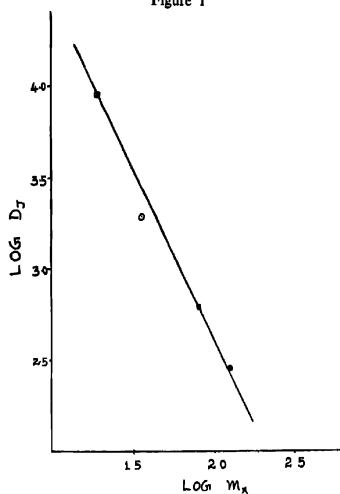


Figure 2

The coriolis coupling constants obtained in the two methods are different for all the four molecules. The ζ sum rule is perfectly verified in both the methods though agreement with the observed values is unsatisfactory. For GeH_3F and GeH_3Cl the value of ζ_5 and ζ_6 are closer to the observed values while they deviate more and more from the observed values as the mass of the substituted halogen increases, in the method suggested by Herranz & Castano. In the method suggested by Torkington the ζ values approach the observed values as the mass of the halogen increases.

From a study of these four molecules by the kinematic methods, it may be concluded that the method of 'Characteristic set of valence coordinates' suggested by Herranz & Castano gives a better approximation to the true force field, for the lighter molecules GeH_3F and GeH_3Cl while the method of 'progressive rigidity' suggested by Torkington seems to give a better approximation to the correct force field for the heavier molecules GeH_3Br and GeH_3I . The method suggested by Biles gives quite unsatisfactory force fields for these molecules. To fix exactly the proper force field for germanium compounds, further work along these lines with different germanium compounds is in progress.

One of the authors (V.B) is grateful to the Council of Scientific and Industrial Research, New Delhi, for financial assistance by the award of a Junior Research Fellowship.

REFERENCE

- Aldous, J. & Mills, I.M., 1962 *Spectrochim. Acta*, **18**, 1073.
1963 *Spectrochim. Acta*, **19**, 1567.
Biles, F. 1966 *Acta. Chim. Acad. Sci. Hung.*, **47**, 53.
Cyvin, S.J. 1959 *Acta. Chem. Scand.*, **13**, 2135.
1968, *Molecular Vibrations and Mean Square Amplitudes*, Universitet for laget, Oslo.
Duncan, J.L., & Mills, I.M. 1964a *Spectrochim. Acta*, **20**, 523.
1964b *Spectrochim. Acta*, **20**, 1089.
Freeman, D.E., 1968 *J. Mol. Spectry.*, **27**, 27.
Freeman, D.E., Rhee, K.H., & Wilson, M.K. 1963 *J. Chem. Phys.*, **39**, 2908.
De Altì, G. C. Galasso, V. & Costa, G. 1965 *Spectrochim. Acta*, **21**, 649.
Heath, D.F., & Linnet, J.W. 1948 *Trans. Farad. Soc.*, **44**, 873.
Herranz, J. & Castano, F., 1966a *Anales Real Soc. Espan. Fis. Quim.* (Madrid) Ser. A **62** 199.
1966b *Spectrochim. Acta*, **22**, 1965.
Rao, K. P. & Rao, B. P. 1968 *Spectroscopia Molecular*, **17**, 8.
Krishnamachari, S.L.N.G., 1955 *Indian J. Phys.*, **29**, 147.
Pillai, M. G. K., & Perumal, A. 1964 *Bull. Soc. Chim. Belg*, **73**, 641.

- Meal, J. H. & Polo, S.R. 1956 *J. Chem. Phys.*, **24**, 1119.
- Melster, A.G. & Cleveland, F.F. 1946 *Am. J. Physics*, **14**, 13.
- Mills, I.M. 1963 *Spectrochim. Acta*, **19**, 1585.
- Mirri, A.M., 1967 *J. Chem. Phys.* **47**, 2823.
- Muller, A., & Cyvin, S.J. 1968. *J. Mol. Spectry.*, **26**, 315.
- Nielsen, H.H; 1951, *Rev. Modern Phys.*, **23**, 90.
- Ramaswamy, K. & Srinivasan, K. 1967 *Aust. J. Chem.*, **21**, 575.
1969 *Aust. J. Chem.* **22**, 1/23.
- Ramaswamy, K., Sathianandam, K., & Cleveland, F. F., 1962 *J. Mol. Spectry.*, **9**, 107.
- Rhee, K.H. & Wilson, M.K. 1965 *J. Chem. Phys.*, **43**, 333.
- Torkington, P. 1949 *J. Chem. Phys.*, **17**, 1026.
- Urey, H.C. & Bradley C.A. 1931. *Phys. Rev.*, **38**, 1969.
- Wilson, E. B., Decius, J.C., & Cross, P.C. 1955 *Molecular Vibrations*, McGraw Hill, New York.
- Wilson, E.B. & Kivelson, D., 1952, *J. Chem. Phys.*, **20**, 1575.
1953, *J. Chem. Phys.*, **21**, 1229,

A field theoretic view of atom-atom collision

By A. ROY CHOWDHURY

Physics Department, Jadavpur University

(Received 9 November 1968, Revised 27 January 1969)

The process of atom-atom collision is treated in a field theoretic way. The non-relativistic interaction potential is shown to be consequence of the field interaction.

INTRODUCTION

Excitation or ionization of an atom by the impact of another atom is a phenomenon on which has a basic importance in many physical processes. There are usually two kinds of such processes, (1) when the striking atom does not change the state, called a collision of the first kind, and (2) when the initial state of the striking atom also gets changed, called a collision of the second kind. Theoretical explanation of these processes are usually given by the help of usual Born approximation. Bates & Griffing (1953) has made an exhaustive treatment of these kind of events. The main defect of their treatment is that they cannot justify the use of the interaction potential which is written in a phenomenological way. Our field theoretic treatment of the bound state gives rise to these interactions, from the usual interaction between, electron-proton field and electromagnetic field in the form $J_p A_p$, J_p being the current corresponding to the nucleon.

PROCESS OF THE FIRST KIND

We consider the collision of two atoms consisting of two nuclei of charges Z_1, Z_2 respectively (being considered as Fermions) each surrounded by a single electron. The interaction Hamiltonian for the whole system is written as.

$$H_{int} = J_p^1 A_p + J_p^2 A_p + J_p^e A_p \quad (1)$$

where $J_p^{1,2,e}$ are the currents due to the two nuclei and an electron. The initial and final state vectors are written (Roy-1960) as

$$|\psi_i\rangle = \int g_1^i(\mu, \mu') a^*(\mu) A^+(\mu') g_2^0(\sigma, \sigma') a^*(\sigma) B^+(\sigma') |0\rangle$$

$$d\mu d\mu' d\sigma d\sigma' \quad (2)$$

$$|\psi_f\rangle = \int g_1^f(\tau, \tau') a^*(\tau) A^+(\tau') g_2^f(\lambda, \lambda') a^*(\lambda) B^+(\lambda') |0\rangle$$

$$d\tau d\tau' d\lambda d\lambda'$$

where a^+, A^+, B^+ are creation operators for the electron and the two nuclei. The matrix element of the process is given by (Schweber 1964).

$$M_{fi} = \frac{1}{2!} \int \langle \psi_f | H_{int} H_{int} | \psi_i \rangle \quad (3)$$

$H_{int}H_{int}$ contains different combinations of the 3 terms in (1), one of which is seen to be $e^2(\bar{\psi}\nu_\mu A_\mu \psi \bar{\psi}\nu_\nu A_\nu \psi)$

(4)

Here ψ , have the usual expansion, $\psi(x) = \int a(p)e^{ip \cdot x} d^3p$

(5)

Spin of the particle being neglected, substituting for $|\psi_i\rangle$, $|\psi_f\rangle$ we have the following form of M_{fi} ,

$$M_{fi} = \frac{e^2}{2!} \int <0| B(\lambda') a(\lambda) g_2^{0*}(\lambda, \lambda') A(\tau') a(\tau) g_1^i(\tau, \tau') \\ a^+(p) a(p') a^+(q) a(q) g_1^i(\mu, \mu') a^+(\mu) A^+(\mu') g_2^i(\sigma, \sigma') \\ a^+(\sigma) B^+(\sigma') |0> \frac{\delta(p' - p + q' - q)}{(q' - q)^2} \quad (6)$$

Since we are interested only in the non-relativistic region, we have separated out the retarded interaction from the Coloumb by an extension of the technique of Feynmann (1949) which is due to Intemann & Pollock (1967) and the Coloumb part only remains in the NR limit.

The vacuum expectation in (6) gives different combinations of delta functions, one such term is

$$\delta(p' - \mu)\delta(p - \lambda)\delta(\tau - \sigma)\delta(q' - \sigma')\delta(q - \tau')\delta(\lambda' - \mu') \quad (7)$$

This when combined with, the $g(k, k')$'s occuring in (6) and integrated over the arguments of delta functions gives one term of M_{fi} , which is

$$M_{fi}(ee) = \frac{1}{(Q - P)^2} \int d\lambda \phi_1^i(\lambda, P - \lambda) \phi_1^i(\lambda - P + \theta, P - \lambda) \\ \int \phi_2^i(\sigma, P' - \sigma) \times \phi_2^0(\sigma, Q' - \sigma) d\sigma \quad (8)$$

where we have used the following expression for (gk, k) expressing the breaking up of the centre of mass and relative motion,

$$g(k, k') = \phi(k, k') \delta(k + k' - P) \quad (9)$$

If we now use the inverse Fourier transforms of the ϕ 's (the bound state wave functions) it can be easily seen that (8) boils down to the following form

$$M_{fi}(ee) = \int \phi_2^{*0}(r_b) V \phi_2^i(r_b) \quad (10)$$

$$\text{where, } V = \int \phi_1^i(r_a) \left| \frac{e^2}{R + \bar{r}_b - \bar{r}_a} \right| \phi_1^{*i}(r_a) dr_a. \quad (11)$$

When, all the terms of $H_{int} H_{int}$ are treated in the same manner, then total matrix element of the process is seen to be,

$$M_{fi} = M_{fi}(ee) + M_{fi}(P_1, P_2) M_{fi}(eP_1) - M_{fi}(eP_2) \quad (12)$$

where

$$M_{fi}(P_1, P_2) = \frac{1}{(P-Q)^2} \int \phi_1'(\mu, P-\mu) \phi_1'(\mu, Q-\mu) d\mu \times \int \phi_2^0(\sigma, Q'-\sigma) \phi_2^0(\sigma, P'-\sigma) d\sigma \quad (13)$$

$$M_{fi}(eP_1) = \frac{1}{(P-Q)^2} \int eP_1 \phi_1'(\lambda, P-\mu) \phi_1'(\lambda, Q-\lambda) d\lambda \times \int \phi_2^0(\sigma, Q'-\sigma) \phi_2^0(P'-Q'+\sigma, Q'-\sigma) d\sigma \quad (14)$$

$$M_{fi}(eP_2) = \frac{1}{(P-Q)^2} \int \phi_1'(\lambda, P-\lambda) \phi_1'(\lambda-P+Q, P-\lambda) d\lambda \times \int d\sigma \phi_2^0(\sigma, P'-\sigma) \phi_2^0(\sigma, Q'-\sigma) d\sigma \quad (15)$$

where \vec{Q}, \vec{Q}' are the incoming and \vec{P}, \vec{P}' are the outgoing momenta of the two atoms. Then the inverse Fourier transform of (12) can be written as

$$M_{fi} = \phi_1^0(r_b) \nabla \phi_2^0(r_b) dr_b dR \quad (16)$$

where V stands for the interaction potential, given by

$$V = \phi_1^0(r_a) \left[\frac{Z_1 Z_2 e^2}{R} + \frac{e^2}{|R + \vec{r}_a - \vec{r}_b|} - \frac{Z_1 e^2}{|\vec{r}_a - R|} - \frac{Z_2 e^2}{|\vec{r}_b - R|} \right] \phi_1'(r_a) \quad (17)$$

where \vec{r}_a, \vec{r}_b etc. stand for same distances and co-ordinates as in BG.

PROCESS OF SECOND KIND

Following the same procedure as above we obtain the matrix element in the form as (17) except that $\phi_1'(r_a)$ is replaced by $\phi_1'(r_a)$, where superscript s denotes 1S state of the atom and 'e' any other excited state.

CONCLUSIONS

Our mode of approach is quite general and does not involve any type of ad-hoc assumption, so it seems that it can be applied to evaluate the interaction potential and cross-section for more complex systems.

The author is grateful to Prof. T. Roy of Physics Department for suggesting the problem and for many helpful discussions. He also wishes to thank the Council of Scientific and Industrial Research for a fellowship.

REFERENCES

- Bates, D.R. & Grifing, G. 1953 *Proc. of Phys. Soc.* 66, 961.
Feynmann, R.P. 1949 *Phys. Rev.* 74, 769.
Intemann, R.L. & Pollock, F. 1967, *Phys. Rev.* 157, 41.
Roy, T. 1960 *Zeit. fur Physik.* 142, 162.
Schweber, S. 1964 *Relativistic Quantum Field Theory*, Harper & Row, New York.

Variation of modulus of elasticity with frequency of vibration

By B. R. PRADHAN, S. S. KAKKAR AND A. P. SAXENA

Department of Physics, Govt. College of Engg. &

Tech., Raipur, M. P., (India)

(Received 22 August 1969)

Young's modulus of various species of wood at different frequencies have been determined experimentally by Kakkar (1969). It has been found that there is a gradual increase of Young's Modulus for a particular species with increase in frequency leading to a constant value at high frequency. The variation has been explained on the assumption that the state of vibration of the specimen gradually changes from isothermal to adiabatic condition. An expression has been derived which agrees fairly well with experimentally observed variation in the case of wood and perspex.

INTRODUCTION

Experimental beam was placed horizontally on two knife edges separated by a known distance in such a way that their positions formed the nodes of the vibrating beam (Free-Free bar method). By changing the length of the specimen it was made to vibrate at different resonant frequencies with the help of an audio oscillator feeding a dc energised electro-magnet (Kakkar 1969). From the knowledge of the resonant frequency the dynamic Young's modulus was calculated, taking a small depth span ratio. (Lord Rayleigh 1926, Timoshenko 1921, 1922).

It was found that the value of dynamic Young's modulus for wooden species continually rises with frequency of vibration to a limiting value, which is 20 to 25% higher than the static value.

THEORETICAL

The higher value of dynamic modulus of elasticity under vibrating condition has been accounted for as due to the thermal effect in the filament.

When a solid is compressed, mechanical energy is partly converted into thermal energy and the compressed parts become warmer than the extended parts. Energy transfer between elements with a temperature difference results in a different elastic constant for adiabatic conditions (no heat lost from the compressed region) than for isothermal conditions (temperature equilibrium obtains between all the stressed parts).

From Maxwell's second relation of thermodynamics, if an element is suddenly stretched (extended) or compressed by applying a force ΔF , ΔT a cooling or heating effect takes place in the element given by the formula (Saha & Srivastava 1950)

$$\Delta T = \frac{T\alpha}{WC} \Delta F \quad \dots(1)$$

where α = Positive coefficient of linear expansion.
 W = mass per unit length of the element
 C = Specific heat
 T = room temperature in absolute degrees.

Since in the case of a vibrating beam extensions and compressions take place in quick succession, equation (1) may usefully be applied to evaluate the heating or cooling produced in the case of a vibrating beam and hence to explain the frequency dependence of modulus of elasticity.

Let us consider the instantaneous case of the compressed filament of a vibrating beam. The heat produced in a filament is used up in two ways :-

...(1) a part of heat produced is conducted away to the neighbouring cooler filaments.

(2) the remaining part is confined to the filament and raises its temperature. The rise of temperature will depend on the thermal capacity of the filament.

The increased rate of vibration of a beam decreases the probability of equalisation of temperature of different filaments of the specimen because of the reduced time for conduction of heat. Progressively larger part of the heat, produced during compression, is retained by the filament itself. This state of vibration of the beam represents the gradual transition from isothermal (Static) to the adiabatic state of vibration. After a certain frequency of vibration, characteristic of the specimen and above; the loading and unloading rate is high enough to be substantially adiabatic, hence no energy is lost. This represents the state of equilibrium of the vibrating bar with the ambient medium. For a bad conductor the perfect adiabatic state of vibration would approach comparatively at low frequency than for a good conductor. If T_m represents the steady temperature of the filament (adiabatic state) and T' the temperature at any lower frequency n , then we have the relation

$$\frac{dT'}{dn} \propto \frac{T_m - T'}{KS} = \frac{\lambda}{KS} (T_m - T') = \mu (T_m - T') \quad \dots(2)$$

embodying that the rate of rise of temperature of a filament with frequency is directly proportional to the difference of maximum temperature (T_m corresponding to steady state) and the temperature of the filament T' corresponding to the frequency of vibration n and inversely proportion to the thermal conductivity (K) and thermal capacity (S) of the filament.

Here λ the constant of proportionality is independent of the nature of the material of the vibrating beam, and μ is a constant depending upon the nature of the material of the vibrating beam.

Integrating (2) and evaluating the constant of integration by applying the limiting condition $n \rightarrow 0$, $T' \rightarrow T_i$; where T_i is the instantaneous temperature of the filament in the static compressed state, we get

$$T' = T_i + (T_m - T_i)(1 - e^{-\mu n}) \quad \dots(3)$$

Putting $T_m - T_i = T_d$ (difference of maximum and minimum temperature) we get

$$T' = T_i + T_d(1 - e^{-\mu n}) \quad \dots(4)$$

Making use of equation (1) and considering the case of an element of unit length and unit cross section corresponding to a frequency of vibration n , the equation (4) reduces to

$$\frac{T_d}{\rho c} F = T_i + T_d(1 - e^{-\mu n}) \quad \dots(5)$$

where ρ = density of the material.

Even at low rates of loading there are important time effects (Richards 1961). The first is the elastic after effect, or delayed elasticity, a transient variation of strain with time. One of the simpler elastic after effects is thermoelastic action. When a member is compressed, its volume decreases accompanied by a rise in its temperature. If compression takes place slowly enough so that thermal equilibrium is maintained, dissipation of heat to its surroundings holds the temperature of the member constant and the process is isothermal. If, on the other hand, compression is rapid and there is insufficient time for heat transfer, the process is adiabatic, and the temperature of the member is raised. If, after a member is loaded adiabatically to certain stress, the stress is held constant while the member is allowed to dissipate heat, a further contraction takes place until the total contraction is the same as in the isothermal process. It will be clear from the foregoing that for the same stress, the strain will be different at different rates of vibration of the beam. Isothermal strain will be larger than the adiabatic strain. Strain will be smaller at higher rates of vibration and vice versa.

If l_0 is the maximum strain for a given stress at $n = 0$, then the strain at a frequency of vibration n will be $(l_0 - \Delta l_n)$ where Δl_n represents the small decrease in the strain. Hence the dynamic Young's modulus at the frequency of vibration n will be given by

$$Y_n = \frac{F}{(l_0 - \Delta l_n)} \quad \dots(6)$$

From (5) and (6), we get

$$\frac{T_d}{\rho c} Y_n = \frac{1}{(l_0 - \Delta l_n)} \left[T_i - T + T_d (1 - e^{-\rho n}) \right]$$

Since $\Delta l_n \ll l_0$, neglecting higher powers of Δl_n we have

$$\begin{aligned} Y_n &= \frac{\rho c}{T_d} \left(\frac{l_0 + \Delta l_n}{l_0^2} \right) [T_i - T + T_d (1 - e^{-\rho n})] \\ &= \frac{\rho c}{T_d l_0} T_i - \frac{\rho c}{\alpha l_0} + \frac{\rho c}{T_d \alpha l_0^2} \Delta l_n T_i - \frac{\rho c}{\alpha l_0^2} \Delta l_n \\ &\quad + \frac{\rho c}{T_d} \left(\frac{l_0 + \Delta l_n}{l_0^2} \right) T_d (1 - e^{-\rho n}) \end{aligned} \quad \dots(7)$$

Since T_i is very nearly equal to T , we may take

$$\frac{\rho c}{\alpha l_0^2} \Delta l_n \frac{T_i}{T} = \frac{\rho c}{\alpha l_0^2} \Delta l_n$$

Then equation (7) reduces to

$$Y_n = \frac{\rho c}{\alpha l_0} \frac{T_i}{T} - \frac{\rho c}{\alpha l_0} + \frac{\rho c T_d}{T_d} \left(\frac{l_0 + \Delta l_n}{l_0^2} \right) (1 - e^{-\rho n}) \quad (8)$$

From equation (7), when $n \rightarrow 0$, $Y_n \rightarrow Y_0$, hence we get

$$Y_0 = \frac{\rho c}{T_d} (T_i - T) \quad \dots(9)$$

Here Y_0 represents the static value of Young's modulus.

Again from equation (7), when $n \rightarrow \infty$, $Y_n = Y_m$ where Y_m represents the max. value of dynamic modulus of elasticity.

$$Y_m = \frac{\rho c}{T_d} \left(\frac{l_0 + \Delta l_m}{l_0^2} \right) [T_i - T + T_d] \quad \dots(10)$$

Here Δl_m represents the maximum decrease in strain corresponding to adiabatic state of vibration.

Let $Y_m - Y_0 = Y_d$ (the difference between the maximum value of the dynamic Young's modulus and static Young's modulus).

From (9) and (10), we get

$$\begin{aligned} Y_m - Y_0 = Y_d &= \frac{\rho c}{T_d} \frac{l_0}{l_0} T_i + \frac{\rho c \Delta l_m T_i}{T_d \alpha l_0^2} - \frac{\rho c}{T_d} \frac{l_0}{l_0} - \frac{\Delta l_m \rho c}{\alpha l_0^2} \\ &\quad + \frac{\rho c}{T_d} \frac{l_0}{l_0} T_d + \frac{\Delta l_m \rho c T_d}{T_d \alpha l_0^2} - \frac{\rho c}{T_d} \frac{l_0}{l_0} T_i + \frac{\rho c}{\alpha l_0^2} \end{aligned}$$

Since $\frac{T_d}{T}$ is very nearly equal to unity, the above equation reduces to

$$Y_d = \frac{\rho c}{T \alpha l_0^2} [l_0 T_d + \Delta l_m T_d] \quad \dots(11)$$

From (8), (9) and (11) and taking $\Delta l_m T_d = \Delta l_n T_d$ for various values of n , we get

$$Y_n = Y_0 + Y_d (1 - e^{-P^n}) \quad \dots(12)$$

DISCUSSIONS

By substituting the values of Y_m , Y_d and n in equation (12) from the experimentally observed data in the case of wood (Kakker 1969) the value

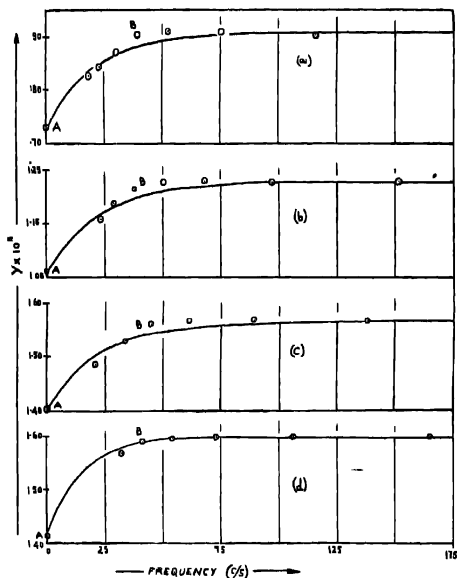


Figure 1. Variation of dynamic Young's modulus with frequency

(a) *Petrocarpus Marsupium* (Bija)

(b) *Tectona grandis* (Teak)

(c) *Shorea robusta* (Sal).

(d) *Terminalia* (Saja)

A static Young's modulus

AB transition region

○ observed results.

Variation of modulus of elasticity with frequency of vibration 473

of μ calculated in the transition region AB, (figure 1) for different species of wood, has been shown in column 4 of table 1.

TABLE 1

Sl. No.	Name of species	Frequency	Value of μ	Mean value of μ
1	2	3	4	5
1.	Petrocarpus Marsupium (Bija)	18 22-23 29	0.0450 0.0488 0.0518	0.049
2.	Tectonagrandis (Teak)	23 29	0.0385 0.0498	0.0442
3.	Shoresrobusta (Sal)	27 34-35	0.0422 0.0419	0.0421
4.	Terminalia (Saja)	32-33 41-42	0.0561 0.0703	0.0632

The value of μ for a particular species at various frequencies of vibration in the transition region comes out to be nearly constant (column 4, table 1) and this is in accordance with the theoretical consideration.

Taking the average value (Kaye & Laby) of K , ρ and $C : 0.5 \times 10^{-9}$ cal. $\text{cm}^{-1} \text{sec}^{-1} \text{ } ^\circ\text{C}^{-1}$, 0.701 gm/cc and 0.5 cal. $\text{gm}^{-1} \text{ } ^\circ\text{C}^{-1}$ respectively and average value of μ (table 1) for the tested wooden species, λ comes out to be 8.67×10^{-6} . According to theoretical considerations as outlined above, λ should be the same for all materials. Later work carried out in these laboratories on perspex shows that value of λ for perspex is of the same order as for wood. This gives additional support to the correctness of underlying physical considerations in the derivation of the formula. Work with other bad and good conductors is in progress.

We are indebted to Principal V.V. Sarvate for encouragement.

REFERENCES

- Kakkar, S.S. 1969 *Indian Forester*, 95, 418.
 Kaye, G. W. C. & Laby, T. H *Tables of Physical and Chemical Constants and Some Mathematical Functions* III Ed. Longman Green & Co., London, 1911-68.
 Lord Rayleigh 1926 *Theory of Sound* II Ed. Vol. I, Macmillan & Co., London, 242-306
 Richards Cedie, W. 1961 *Engg. Materials Science*, Wardsworth Publishing Co. Inc., San Francisco 243-246
 Saha, M.N. & Srivastava, B.N. 1950 *A Treatise on Heat* III Ed. The Indian Press Ltd., Allahabad and Calcutta, 328-330.
 Timoshenko, S. 1921 *Phil. Mag. Series 6*, 41, 744.
 1922 *Phil. Mag. Series 6*, 43, 125.

On the vibrational spectra of benzyl benzoate

By S. CHATTOPADHYAY

Optics Department, Indian Association for the Cultivation of Science,
Calcutta-32

(Received 2 July 1969)

[PLATE 6]

Raman and infrared spectra of benzyl benzoate have been studied and the observed results have been compared to those reported for similar double molecules by previous authors. The results indicate that the two phenyl rings may be reasonably assumed to be only weakly coupled and their vibrations may be treated separately. In characterizing the phenyl ring vibrational frequencies, assignments reported for suitable monosubstituted benzene molecules have been duly considered for comparison. Tentative assignments for vibrations of the substituent group have also been made.

INTRODUCTION

In recent times several authors have reported analysis of vibrational spectra of a class of molecules containing two benzene rings connected through a weakly conjugated linkage, some times called "double-molecules". From a study of the infrared spectra of diphenyl and its derivatives Cannon & Sutherland (1951) concluded that in such molecules the two benzene rings vibrate independently. Steele & Lippincott (1961) discussed the close resemblance of the vibrational spectra of diphenyl and deca-deutero-diphenyl with the spectra of monosubstituted benzenes and assigned the frequencies of these compounds to different modes by comparing the data with those of fluoro-benzene. Katon *et al* (1964) observed that the two benzene rings of diphenyl ether are not equivalent and the benzene like vibrations of the molecule could be treated in terms of a monosubstituted benzene. In their infrared absorption study, some of the bands due to phenyl ring vibrations were found to occur in pairs. Recently, Green (1968) reported vibrational assignments for the 'double-molecules' diphenyl ether and diphenyl sulphide.

The molecule of benzyl benzoate may also be treated as a 'double molecule' in which the two benzene rings are connected through the

$$\begin{array}{c} \text{O} \\ || \\ -\text{C}-\text{O}-\text{CH}_2 \text{ group.} \end{array}$$

The vibrational spectrum of this molecule has not been analysed before and it would be of interest to find out whether the spectrum exhibits the characteristics of a double-molecule. For this purpose a study of the Raman spectrum of benzyl benzoate in the liquid state and the infrared spectra of the compound in the liquid state and in solutions was made. In this paper the results and their analysis have been presented.

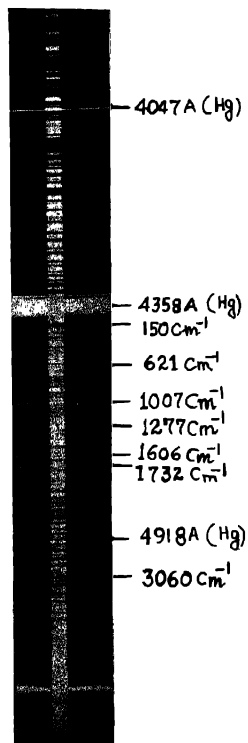
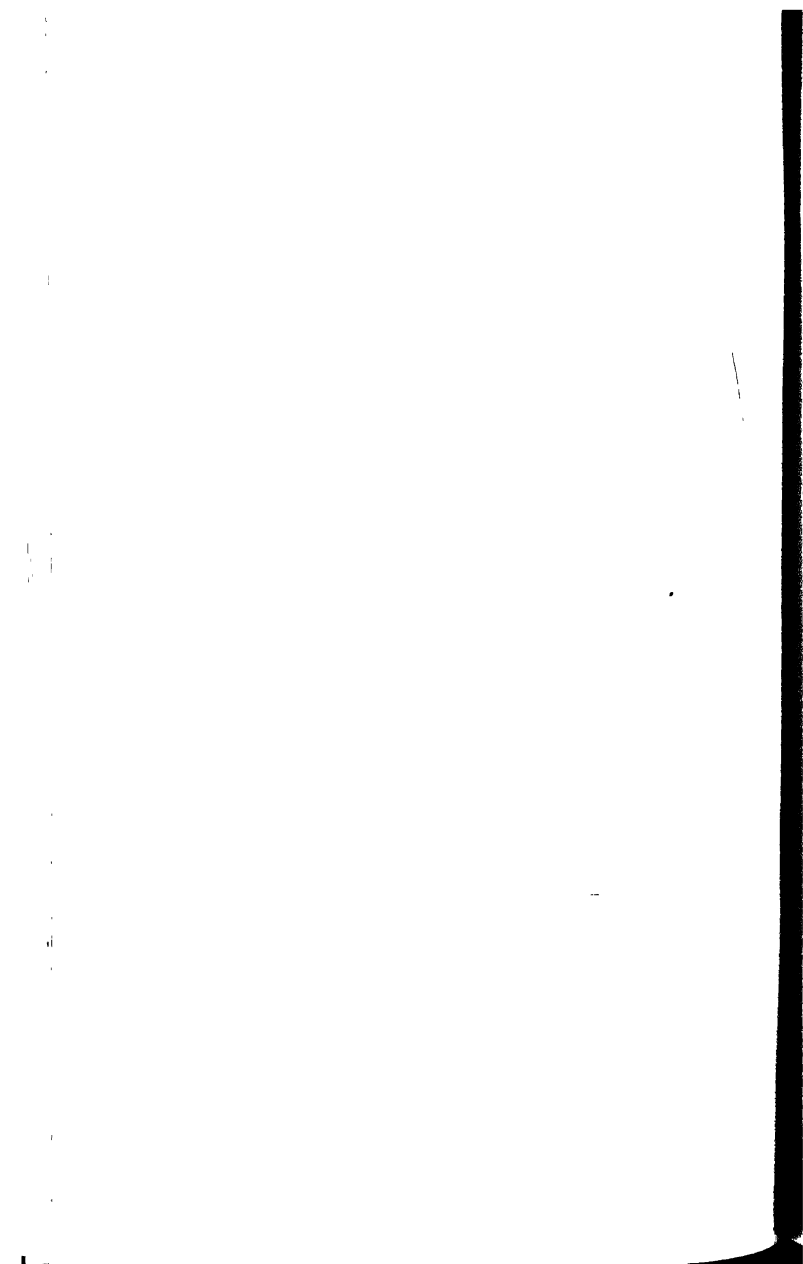


Figure 1. Raman spectra of benzyl benzoate (Pure liquid at 28°C)



EXPERIMENTAL

Sample of pure benzyl benzoate was supplied by Rhodia (France) and was first fractionally distilled and the proper fraction thus collected was repeatedly distilled under reduced pressure before use.

The Raman spectrum and the state of polarisation of the Raman lines were recorded in a manner described in a previous paper (Chattopadhyay & Mukherjee 1967). The infrared spectra of the sample in the liquid state and in solutions in different solvents were recorded in the usual way with a Perkin-Elmer Model 21 spectrophotometer fitted with NaCl optics. The measured frequencies are accurate within $\pm 5 \text{ cm}^{-1}$ for broad band near 3000 cm^{-1} region below which the accuracy is still higher ($\sim \pm 2 \text{ cm}^{-1}$). All measurements were made at 26°C .

RESULTS

The Raman spectrum and the infrared absorption curves of the sample are reproduced in figures 1 (plate 6) and 2 respectively. The Raman shifts ($\Delta\nu \text{ cm}^{-1}$) and infrared absorption frequencies ($\nu \text{ cm}^{-1}$) of benzyl benzoate in liquid state and in solutions in CCl_4 and CHCl_3 together with their intensities and observed state of polarisation of the Raman lines are included in table 1. The assignments of the frequencies to vibrational modes of the ring and the internal vibrations of the substituent group are summarised in tables 2 and 3 respectively.

DISCUSSION

The molecule of benzyl benzoate should normally belong to the point group C_1 and its seventy eight normal vibrations should all be active both in Raman effect and in infrared absorption. These will include eighteen vibrational modes of the substituent group some of which may be identified with some certainty while the remaining sixty vibrations should be characteristic of the two benzene rings. But it can be seen from table 1 that the number of observed frequencies in the vibrational spectrum of benzyl benzoate is much smaller than the total number of sixty expected ring vibrations even though some of the vibrational bands in the infrared absorption spectrum (figure 2) are found to occur in pairs. These results are similar to those observed for diphenyl ether (Katon *et al* 1964) and diphenyl sulphide (Green 1968). Assignment of the observed vibrational frequencies to different modes of vibration of the molecules has been proposed and an attempt has been made to understand the characteristic feature of the infrared spectrum. Discussions have been presented in the following paragraphs.

TABLE 1

Raman shifts ($\Delta\nu$ cm ⁻¹) Liquid at 28°C	Infrared frequencies (ν cm ⁻¹)		
	Pure liquid at 26°C (Thin film)	Solution in	
		CCl ₄	CHCl ₃
150 (1) D			
205 (3b) D ?			
249 (2)			
621 (5) D	628 sh		625 vw
680 (1)	675 s	676 m	674 s
	686 sh	686 vs	685 sh
	705 vsb		710 sh
	720 sh	720 s	725 sh
	735 vs		
	745 vs		
807 (3)	804 s		798 sh
825 (1)	825 m	830 vw	832 sh
	845 m	850 sh	850 m
901 (2) P	888 m	885 m	
	916 vs	912 m	915 m
964 (0)	962 vsb	958 wb	963 w
1007 (10) P	1003 s	1006 vw	1005 sh
1034 (4) P	1026 vs	1030 vs	1030 vs
	1070 vs	1072 vs	1072 vs
	1106 vsb	1112 vs	1115 vs
1162 (4) D	1160 s	1162 vvw	
1182 (2) P	1179 vs	1178 s	1180 s
1216 (3) P	1216 vs	1216 w	1220 vsb
	1254 vs	1255 sh	1255 sh
1277 (4b) D	1265 vs	1272 vsb	1275 vs
1320 (0)	1316 vs	1318 s	1318 s
1385 (3) P	1380 vs	1382 m	1382 m
	1430 sh	1426 w	1428 mb
1459 (1)	1455 vs	1458 s	1456 s
	1500 vs	1502 w	1504 m
1606 (8b) D	1606 vs	1606 m	1605 m
1732 (6b) P	1720 vsb	1725 vs	1720 vs
	2880 mb	2900 w	
	2966 s	2970 wb	2970 sh
	3030 sh		3045 s
	3058 vs		
3060 (6b) P	3063 vsb	3060 m	

TABLE 2. ASSIGNMENTS OF THE PHENYL RING VIBRATIONS

Nature of the mode	Correspondence with vibration no. in benzene (Pitzer & Scott, 1943)	Ring I	Ring II	Methyl benzoate	Benzyl acetate
(Vibrational frequencies in cm ⁻¹)					
a [*]					
$\nu(\text{CH})$	20A	3063	3063		3080
$\nu(\text{CH})$	20B	3063	3063		3080
$\nu(\text{CH})$	7B	3058	3058	3073	3067
$\nu(\text{CH})$	2	3030	3030	3073	3037
$\nu(\text{CH})$	13	3030	3030	3073	3045
$\nu(\text{CC})$	8B	1606	1606	1603	1605
$\nu(\text{CC})$	8A	1606	1606	1591	1590
$\nu(\text{CC})$	19A	1500	1500	1495	1499
$\nu(\text{CC})$	19B	1455	1455	1452	1485
$\nu(\text{CC})$	14	1380	1380	1376	1380
$\beta(\text{CH})$	3	1316	1316	1311	1362
$\beta(\text{CH})$	9A	1179	1179	1183	1180
$\beta(\text{CH})$	9B	1160	1160	1160	1160
$\beta(\text{CH})$	15	1106	1070	1064	1040
$\beta(\text{CH})$	18A	1034	1026	1028	1025
Ring breathing	1	1003	1003	1003	1000
$\omega(\text{CCC})$	6B	621	628	621	620
X-sensitive	7A	1216	1216	1111	1214
X-sensitive	12	825	845	826	830
X-sensitive	6A	249	249	360	482
X-sensitive	18B	205	205	218	367
a [*]					
$\gamma(\text{CH})$	5	962	962	969	960
$\gamma(\text{CH})$	17A	916	888	938	915
$\gamma(\text{CH})$	10A	804	804	850	830
$\gamma(\text{CH})$	11	735	745	710	740
$\gamma(\text{CH})$	17B	705	720	686	692
$\phi(\text{CC})$	4	686	675	679	640
$\phi(\text{CC})$	16A				400
X-sensitive	16B				254
X-sensitive	10B	150	150	134	178

TABLE 3. ASSIGNMENTS OF INTERNAL VIBRATIONS
OF SUBSTITUENT GROUP

Approximate nature of the modes	Vibrational frequencies (in cm^{-1})
CH_3 asymmetric stretching	2966
CH_3 symmetric stretching	2880
$\text{C}=\text{O}$ stretching	1720
CH_3 scissoring	1430
$\text{C}-\text{O}$ stretching	1265
CH_3 wagging	1254

(a) *Vibrations of the phenyl ring*

It can be seen from table 1 that the observed vibrational spectra of benzyl benzoate contain a large number of frequencies whose values are almost identical with those of many monosubstituted benzene compounds. So, for the purpose of assignment of these vibrational frequencies the molecule of benzyl benzoate ($\phi_1 \text{COOCH}_2 \phi_{11}$) has been treated as monosubstituted benzene in two different ways. In one case the molecule is

looked upon as a benzoic acid ester $\phi_1 \begin{array}{c} \text{O} \\ \parallel \\ \text{C} \\ \diagup \quad \diagdown \\ \quad \quad \text{OX} \end{array}$ where X represents $\text{CH}_2 \phi_{11}$

and in the other, it is treated as a benzyl derivative $\phi_{11} \text{CH}_2 \text{X}$, X represent-

ing the group $\phi_1 \begin{array}{c} \text{O} \\ \parallel \\ \text{C} \\ \diagup \quad \diagdown \\ \quad \quad \text{O} \end{array}$. With these assumptions, qualitative comparison of

the frequencies of vibrations involving mainly the ring ϕ_1 of benzyl benzoate molecule has been made with those of methyl benzoate, while in the case of the ring ϕ_{11} comparison with benzyl derivative like benzyl acetate has been made. The frequencies due to methyl benzoate (Chattopadhyay 1968) and benzyl acetate have been included in table 2 for this purpose. In view of some recent work it was found necessary to revise the assignments of some of the frequencies for benzyl acetate reported earlier by Chattopadhyay *et al* (1967) and for the sake of consistency the revised assignments have been included in the table. In analysing the observed vibrational bands of benzyl benzoate molecule, it has been found convenient to assume the symmetry of the molecule to be at least approximately C, with the two rings either in the same plane or oriented through an angle of 90° with respect to each other. Moreover, in order to account for the intensities of some of the bands in the Raman and in infrared

spectra and the polarisation of Raman lines, the local symmetry of each ring, which is C_{2v} , was found to be an important determining factor.

The assumption that the molecule of benzyl benzoate may be treated as a monosubstituted benzene in two ways is equivalent to assuming that the two rings may be treated independently. Since this implies that they may be considered to be only weakly coupled such that the corresponding vibrations of the two rings are almost noninteracting some of the modes of vibrations of one ring, especially those not sensitive to substitution should be expected to have frequencies only slightly different from the frequencies due to corresponding modes of the other ring. But it is seen from table 1 that such doubling of vibrational frequencies does not occur in most cases which leads to the conclusion that the vibrational frequencies due to many of the modes of one ring are identical with those of the corresponding modes of the other ring. On the basis of the assignments proposed in table 2 it is seen that these frequencies correspond to the modes which are least affected by substitution. Similar conclusions were previously arrived at by Katon *et al* (1964) for diphenyl ether molecule. It is, however, seen (figure 2) that some of the vibrational frequencies arising from such modes appear as pairs of infrared bands and according to the assignments given in table 2, most of these correspond to the modes of benzene which involve in-plane and out-of-plane bending vibrations. Due to limitation of the rock salt optics in the infrared spectrophotometer used, only two modes among the six substituent-sensitive low frequency vibrational modes which are expected to exhibit more pronounced doublet character, could be studied in the infrared. Of these two modes, one mode corresponding to the substituent-sensitive mode 12 (Pitzer & Scott 1943) is observed to give two distinct frequencies at 825 and 845 cm^{-1} (figure 2, table 2).

(b) Internal vibrations in the substituent group

Of the frequencies originating from the internal vibrations of the substituent group, the infrared absorption bands at 1720, 2880 and 2966 cm^{-1} may be readily assigned to C=O stretching, CH_2 symmetric stretching and CH_2 asymmetric stretching modes respectively. There is a broad and strong Raman line at 1277 cm^{-1} , whereas the infrared absorption curves clearly show two resolved bands at 1254 and 1265 cm^{-1} . These two infrared bands have been assigned to CH_2 wagging and C—O stretching modes respectively. The frequency due to CH_2 scissoring mode is generally expected in the 1450 cm^{-1} region. As such, the band at 1430 cm^{-1} which appears as a shoulder in the infrared spectrum is tentatively assigned to this mode.

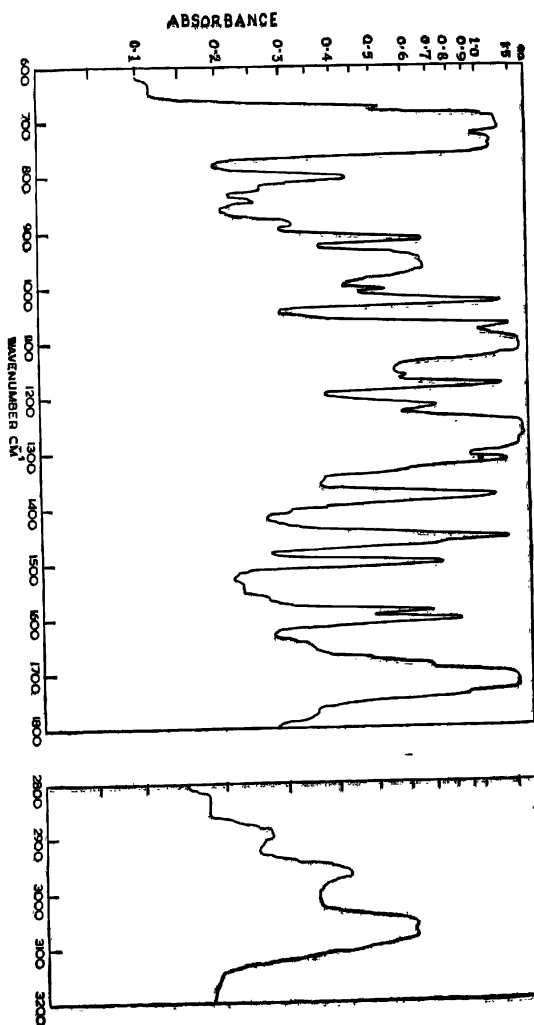


Figure 2. Infrared spectra of benzyl benzoate (liquid, thin film, at 25°C).

The author expresses his sincerest thanks to Professor G. S. Kastha, D. Sc. and Dr. S. B. Benerjee for their kind interest in the present work.

REFERENCES

- Cannon, C. G. & Sutherland, G. B. B. M. 1951 *Spectrochim Acta*, 4, 373.
Chattopadhyay, S. & Mukherjee, D. K. 1967 *Indian J. Phys.*, 40, 409.
Green, J. H. S., 1968 *Spectrochim Acta*, 24A, 1627.
Katon, J. E. Fairheller, W. R. Jr., & Lippincott, E. R. 1964 *J. Mol. Spect.*, 13, 72.
Pitzer, K. S. & Scott, D. W. 1943 *J. Amer. Chem. Soc.*, 65, 803.
Steele, D. & Lippincott, E. R., 1961 *J. Mol. Spect.*, 6, 238.

Setting up of a double beam recording spectrophotometer

By R. K. MUKHERJEE, S. C. BERA AND M. CHOUDHURY

Magnetism Department,

Indian Association for the Cultivation of Science Calcutta-32

(Received 14 July 1969)

A double-beam recording spectrophotometer has been constructed with commercially available monochromator and recorder. Its merits and demerits have been discussed. The instrument is easy to handle, fairly quick-recording, flexible and capable of recording polarised single crystal spectra at low temperature.

INTRODUCTION

In the past, electronic structure of the paramagnetic complexes in crystals, have been extensively studied in our laboratory employing magnetic balances. In order to interpret these results unambiguously, it is of great value to find out directly by spectroscopic methods the energy level schemes in these substances.

It was, therefore, intended to set up a quick recording spectrophotometer to record the polarised absorption at temperatures upto 20°K for studying the degeneracies and symmetries of electronic levels.

Conventional recording double beam spectrophotometers may be classified into groups on the basis of

- (1) the number of detectors,
- (2) how the absorption ratio I/I_0 is measured and
- (3) how the two beams are optically separated and the voltage signals demodulated.

(1) Spectrophotometer may use two detectors, one for each beam (Cook & Smith 1947) or may use one detector which receives the two beams alternately (Savitzky & Halford 1950). In the case of double detector instruments, the response vs. wavelength character of the two detectors should be matched. In our case we have used one detector for recording both the beams, so that the question of matching does not arise.

(2) Spectrophotometers may measure I/I_0 by two different methods. One is the null method (Baird, *et al* 1947) and the other is the voltage comparison method (Horning *et al* 1950). In the null method, the two signals corresponding to I and I_0 are led to a servo-motor which drives a calibrated comb placed in the path of the reference beam to reduce its intensity until the two signals are equal. In the voltage comparison method, the two voltages corresponding to crystal and reference beam are compared potentiometrically, the advantage of which is obvious. We have used the latter method.

(3) To separate the two beams, some spectrophotometers use rotating or vibrating mirrors, while some others use only a light chopper (Kaye & Davancy 1952; Kaye *et al* 1951; Yang & Legallais 1954). In instruments using mirrors, the mirror rotates or vibrates to allow the same beam of light to pass through the crystal and the blank alternately. The optical paths are not the same in the two cases and the instrument uses optical parts in motion which introduces complications apart from polarising the beam. But as the instrument uses essentially the same beam of light, the spectral distributions in the crystal beam and the blank beam are identical. We have avoided rotating optical parts. The two beams are placed very close to each other and a vibrator alternately allows the beams to pass. To avoid a difference in the spectral distribution of the two beams, we have taken the image of the central portion of the source after making it sufficiently magnified.

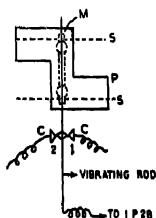


Figure 1. Vibrator. P-plastic piece, M-monochromator slit, S-auxiliary slit, C1, C2—two contact points.

CONSTRUCTION OF THE SPECTRO-PHOTOMETER

In our instrument light from a point source is focussed by an achromat on two tiny holes in a metal sheet very close to each other, one of them containing the crystal. The images of the two holes are then focussed on the monochromator slit. In front of the slit, a 100 cps vibrator (Phillips Triller) is placed. A light thin rigid rod about 2 cm. long is attached to the vibrating rod to increase the amplitude of vibration. The rod carries an opaque piece of plastic cut as shown in figure 1 which at each extreme point allows one of the beams and stops the other. The photomultiplier RCA IP28 is placed at the exit slit of the monochromator (Zeiss SPM2). The signal is separated by the vibrator itself. The output of the photomultiplier is connected to the vibrating rod. When the prong moves to the right, the lower beam is allowed to the monochromator and the contact C1 (figure 1) receives the corresponding signal. Similarly the the contact C2 receives the signal corresponding to the upper beam. Thus the two signals of the two beams are separated. The sig-

nals are of pulsating dc type and one is separated by a phase of 180° from the other as shown in figure 2.

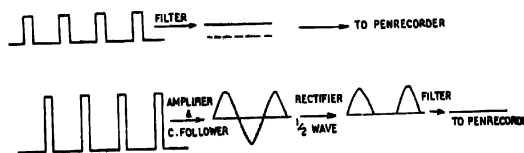


Figure 2. Upper one corresponds to the crystal beam, lower one to the reference beam.

The signal corresponding to the blank is fed to a 3 stage amplifier and a rectifier. The last stage of the amplifier is of cathode follower type as is necessary for impedance matching. This amplified dc signal is fed into the pen-recorder across the two ends of the potentiometer wire. The signal corresponding to the crystal beam is directly fed into the high impedance input of (the sliding contact of the potentiometer) the pen-recorder, after filtering out the ripples. The two signals, one from the direct beam and another from the crystal beam are then compared in the recorder. The circuit of the pen-recorder is modified to change it from a direct voltage recorder to a ratio recorder.

In the original circuit of the pen-recorder, as shown in figure 3 the voltage source U of internal resistance R_i which is under examination is applied to contact 1 and the comparison voltage $X.U_k$ ($X < 1$)

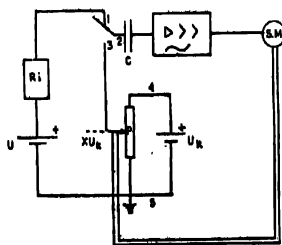


Figure 3. Circuit diagram of pen-recorder.

to contact 3 of a vibrating contactor, which changes the middle contact 2 at a frequency of 50 c/s. If the voltage at 1 and 3 are different, an alternating voltage is generated of corresponding amplitude and phase and this is transferred through the capacitor C to an ac voltage which drives the synchronomotor varying the position of the sliding contact of the precision potentiometer (P) until the ac voltage $V_e = U - X.U_k = 0$ so

that $X = U/U_k$. We have disconnected U_k and connected the dc voltage corresponding to the reference beam across the precision potentiometer (P) through the wires 4 and 5. The potentiometer has got a resistance of 1 K . A cathode follower is used in the last stage of the amplifier for impedance matching. The dc voltage corresponding to the crystal beam is connected to the contact point 1 directly.

The modified circuit now acts as a ratio recorder. The U_k is proportional to I_0 and U is proportional to I and hence it measures I/I_0 . The chart drive is coupled with the wavelength drive of the monochromator and the recorder automatically plots X or I/I_0 against wavelength. If there is a change in lamp intensity or detector intensity or detector sensitivity both U_k and U change simultaneously and the sliding contact remains stationary. Also the deflection in the penrecorder is independent of the slit width of the monochromator within a certain limit. The limiting value depends on the linearity of the amplifier that we use. The slit is manually adjusted to keep the direct beam signal within this linear region of the amplifier.

At wavelength where the crystal absorption is very large, the direct beam should also be reduced in intensity to have a comparable value. This is achieved by another slit, slit length mounted horizontally before the monochromator slit, as shown in the figure 1 by the dotted line. If the intensities of both the beams become large they are simultaneously controlled by the monochromator slit and individual intensity can be varied by the horizontal slit.

The chief advantage of our double beam recording spectrophotometer is its flexibility. We can use it for crystals, solutions and for gases, for various pathlengths with only slight modification. In the case of highly absorbing crystals, the source intensity can be increased and the direct beam I_0 may be arbitrarily cut down to bring the ratio within proper limits. The scattered light is reduced to a minimum by appropriate Corning filters, the 'cross talk' between the beams is small ($<1\%$). In those cases, where I_0 is arbitrarily reduced, the absolute value of the optical density is not very accurate. Nevertheless, the relative values at different wavelengths are accurate and the spectrum gives clearly the wavelength position of peaks and humps which is our main point of interest. In the case of solution spectrum, the optical densities can be obtained accurately by using a parallel beam and making the direct beam and sample beam equal in intensity with a blank. The spectrophotometer provides enough space for inserting the liquid H_2 dewar and Wollaston quartz prism and

the ratio of the intensities in the two polarisations can be compared. The recording can be done swiftly and the spectrophotometer is useful for measuring the variation of optical density with time. The same spectrophotometer can be used to record emission spectrum of solution at the room temperature and of glassy solution at the liquid N_2 temperature.

To test the performance of our instrument we have recorded the solution spectra of benzoquinone in isopentane (figure 4) and a comparison with the spectrum taken with other spectrophotometers is made.

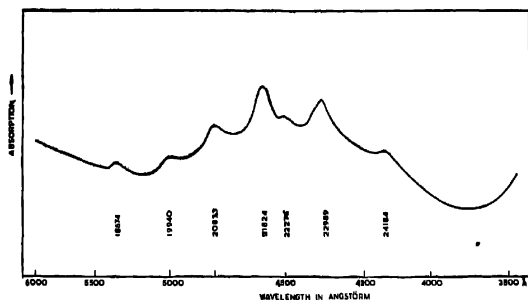


Figure 4. Spectrum of benzoquinone in isopentane.

The authors wish to thank Prof. A. Bose for constant help and guidance. One of the authors, R. K. Mukherjee is grateful to Patna University for granting him leave for doing the work. Thanks are due to C. S. I. R. for granting a Jr. Fellowship to one of us (S.C.B.)

REFERENCES

- Baird, W. S. O' Bryan, H. M., Ogden, George & Lee, Dorothy, 1947 *J. Opt. Soc. Am.*, **37**, 754
- Coor, Jr. T. & Smith, D. C. 1947 *Rev. of Sc. Inst.*, **18**, 173.
- Horning, D. F. Hyde, G. F. & Adococh, W. A. 1950 *J. Opt. Soc. Am.*, **40**, 497
- Kaye, W. & Devancy, R. G. 1952 *J. Opt. Soc. Am.*, **42**, 569.
- Kaye, W. Canon, C. & Devancy, R. G. 1951 *J. Opt. Soc. Am.*, **41**, 658.
- Lehrer, E. 1942 *Zeits und Tech. Physik*, **23**, 169.
- Savitzky, A. & Halford, R. S. 1950 *Rev. of Sc. Inst.* **21**, 203.
- Wright, N. & Herscher, I. H. 1947 *J. Opt. Soc. Am.*, **37**, 211.
- Yang, C. C. & Legallais, V. 1954 *Rev. Sc. Inst.* **35**, 801.

Letters to the Editor

The crystal structure of calcium fumarate, trihydrate
 $\text{CaC}_4\text{H}_2\text{O}_4 \cdot 3\text{H}_2\text{O}$

By M. P. GUPTA AND B. N. SAHU

Department of Physics, University of Ranchi, Ranchi-8.

(Received 1 December 1969)

We have, for sometime, been investigating the crystal structures of simple dicarboxylic organic acids and their salts (hydrated or otherwise). In course of this programme, we have studied calcium fumarate, trihydrate $\text{CaC}_4\text{H}_2\text{O}_4 \cdot 3\text{H}_2\text{O}$. There is a previous mention by Wherry and Hann (1954) of a so-called calcium salt of fumaric acid ($\text{C}_4\text{H}_4\text{O}_4$) which is erroneously reported to be a dihydrate, $\text{Ca} \cdot \text{C}_4\text{H}_4\text{O}_4 \cdot 2\text{H}_2\text{O}$.

The crystal structure is of unusual interest from the point of view of stereochemistry of the fumarate groups themselves. Calcium is divalent and one calcium atom is expected to ionize both the carboxyl groups in the fumaric acid molecule ($\text{COOH} \cdot \text{CH} : \text{CHCOOH}$). However, the two carboxyl groups are at the opposite ends of the centrosymmetric molecule and the relative disposition of the Ca^{++} ions, simultaneously linked to two carboxyl groups of the acid molecules in the structure is of unusual interest. The role of as many as three water molecules in the crystal structure, from the point of view of packing, is also of great significance.

X-ray data :

Single crystals with a platy habit, (010) being the platy face, give on X-ray examination, the following data. Orthorhombic, $a = 6.57\text{\AA}$, $b = 17.66\text{\AA}$, $c = 7.00\text{\AA}$. This agrees with the value quoted, from morphological studies, by Wherry & Hann (1954) ($a : b : c = 0.397 : 1 : 0.377$). $\rho_{\text{meas}} = 1.71 \text{ gm/ml}$, $V = 812\text{\AA}^3$, $Z = 4$ (number of asymmetric units in the unit cell). Unit cell content = 836.64 (amu). This gives the formula as $\text{C}_4\text{H}_2\text{O}_4 \cdot \text{Ca} \cdot 3\text{H}_2\text{O}$ (theoretical value 832 (amu). Thus the correct formula is established as a trihydrate.

Space group :

The following systematic absences were observed. ($0k1$, $k+1 = 2n+1$; $h01$, $h = 2n+1$; $00l$, $l = 2n+1$, $h00$, $h = 2n+1$; $0k0$, $k = 2n+1$). This leads to the choice of space group as $Pna2_1$ or $Pnam$. However, as there are eight general positions in the space group $Pnam$ and only four asymmetric units are present in the unit cell and none conforming to the symmetries of the special positions in the space group $Pnam$, the latter is ruled out. Statistical intensity tests (Howells *et al* 1950)

for the *okl* data, which is a non-centrosymmetric projection, supports the case for the space group to be the non-centrosymmetric one, $Pna2_1$.

Intensity data :

Complete zonal data and three dimensional X-ray diffraction data were collected using single crystals and normal (for the zonal reflexions) and equi-inclination (for the upper layers) Weissenberg photography. They were corrected for the usual geometrical factors (LPF, Spot-shape and size).

Crystal structure :

Patterson projections failed to give any clue for the calcium atom. Patterson-Harker Sections were computed ($Z = 0$, $Z = \frac{1}{4}$) as also some other sections ($Z = 1/8$, $\frac{1}{2}$, $3/8$) using complete three-dimensional intensity data. A systematic study of the Patterson-Harker peaks gave values for Ca, $x/a = \pm 0.058$, $y/b = \pm 0.10$ or ± 0.20 . Fourier analysis and trial and error methods, left us with only one choice $x/a = +0.06$, $y/b = +0.20$. A Fourier projection down the $[001]$ axis (which is centrosymmetric), with calcium based signs, failed to reveal either the organic part of the molecule or the water molecules. However, a re-examination of the Harker sections for the Ca—O and Ca—C vectors corresponding to the "intramolecular" vectors (i.e. Ca — light atom vectors for the same molecule) revealed a possible gross position for the organic molecule. New signs were derived on this model and the list of signs was

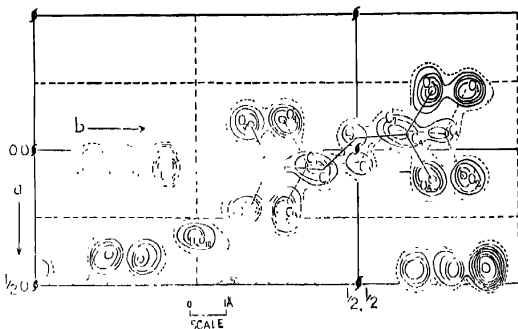


Figure # 1. Electron density map projected down the $[001]$ axis.

expanded using sign relations of the type $S_H S_K = S_{H+K}$ ($H = h_1, k_1, l_1$, $K = h_2, k_2, l_2$) using such terms as had large unitary structure factors. This gave a reasonable Fourier map which could be readily interpreted. The final Fourier down the [001] axis is shown in figure 1 below. The present co-ordinates presented in table 1 give $R(hk0) = 0.210$, with only an overall isotropic temperature factor of $B = 1.1 \text{ \AA}^2$ for all atoms. The structure has been confirmed by the other projections which are, however, suffering from serious overlap and are non-centrosymmetric and less sensitive to parameter changes.

TABLE 1

Atoms	x/a	y/b	Atoms	x/a	y/b
C ₁	0.063	0.367	O ₃	0.225	0.613
C ₂	0.092	0.450	O ₄	0.100	0.611
C ₃	-0.050	0.497	(H ₂ O)I	0.054	0.090
C ₄	-0.058	0.574	(H ₂ O)II	0.053	0.148
O ₁	0.231	0.333	(H ₂ O)III	0.316	0.249
O ₂	-0.097	0.330	Ca	0.062	0.203

In the crystal, the three water molecules play decisive roles in binding together, short H-bonds, chains of fumarate groups which are all aligned roughly parallel to the [010] axis of the crystal. The $\text{Ca}^{++} - \text{O}$ distances are all normal (2.4 \AA upwards) with a eight-fold co-ordination. The geometry of the fumarate group is normal.

The structure is being subjected to a full matrix three-dimensional least squares refinement, the results of which will be reported later but the salient features of the crystal structure are not likely to change from what is being reported here.

REFERENCES

- Howells, E. R., Phillips, D. C. & Rogers D., 1950. *Acta Cryst.* 3, 210.
 Wherry, A & Hann, P (*J. Wash. Acad. Sci.* 2, 286 Quoted in Winchell, A. N. (1954):
The Optical Properties of Organic Compounds, Academic Press Inc., New York.

1S - 2S excitation in e-H collision by Glauber approximation

By A. S. GHOSH AND N. C. SIL

Department of Theoretical Physics, Indian Association for the
Cultivation of Science, Jadavpur, Calcutta-32

(Received 15 October 1969)

In this note we apply Glauber approximation (1959) to inelastic $1s-2s$ electron hydrogen scattering. This approximation has been extensively used in nuclear and particle physics (Franco & Glauber 1966, Harrington 1968 and others). In atomic Physics, it has been applied to electron hydrogen scattering problems (Franco 1968, Tai *et al* 1968).

We consider the target proton to be infinitely heavy and the origin of the co-ordinates to be placed at the proton. Let r denote the position vector of the atomic electron and b be the impact parameter vector relative to the origin. The amplitude for scattering $f_{fi}(\theta)$ in which the hydrogen atom undergoes a transition from an initial state i with wave function ϕ_i to a final state f with wave function ϕ_f , is given by (Franco 1968)

$$f_{fi}(\theta) = \frac{i\pi}{2\pi} \int \phi_f^*(r) \Gamma(b, r) \phi_i(r) \exp(iq \cdot b) d^3b dr$$

with $\Gamma(b, r) = 1 - (|b - s|/|b|)^{2in}$

where s is the projection of r onto the plane of impact parameters and $n = e/\hbar v$, v being the velocity of the incident particle. Here the initial and final states are, respectively, the $1s$ and $2s$ of the hydrogen atom.

Thus we have

$$\phi_i = (\pi a_0^3)^{-1/2} \exp(-r/a_0)$$

and

$$\phi_f = (2^3 a_0^3 \pi)^{-1/2} (1 - r/2a_0) \exp(-r/2a_0)$$

where, a_0 is the first Bohr radius. Substituting for ϕ_i , ϕ_f and $\Gamma(b, r)$ we get after some calculations (Franco 1968) the scattering amplitude as

$$\begin{aligned} f_{fi}(\theta) = & -\frac{2^{11} i k_0 a_0^3}{3^2 \sqrt{2}} \int_0^{\pi/2} \sin^2 \theta \cos \theta \left((\sin^4 \theta - \frac{28}{9} (a_0 q)^2 \cos^2 \theta \sin^2 \theta \right. \\ & \left. + \frac{64}{81} (a_0 q)^4 \cos^4 \theta \right) \\ & \times (\sin^2 \theta + \frac{4}{9} (a_0 q)^2 \cos^2 \theta)^{-5} \times [1 - (|\cos 2\theta|/|\cos \theta|)^{2in} |\cos 2\theta| \\ & \times {}_2F_1(5 + .5 in, 1 + .5 in, 1; \sin^2 \theta)] d\theta \end{aligned}$$

The integration is done numerically by Gaussian quadrature of 16 point, The differential cross-section for 1s-2s excitation is obtained by means of the relation

$$I(\theta) = \frac{k_1}{k_0} |F_{s1}(\theta)|^2,$$

where k_0 , k_1 are respectively, the momenta of the incident and the scattered electron.

The total cross section for the process is given by

$$Q = 2\pi \int_0^\pi I(\theta) \sin\theta d\theta.$$

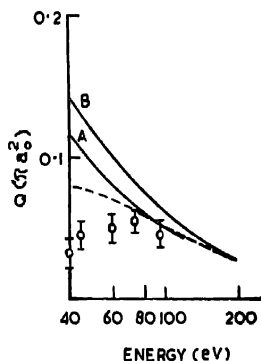


Figure 1: Total inelastic (1s-2s) cross section. Q , is plotted against energy.

Curve B — Born approximation; Curve A — Ochkur approximation
(Banerjee *et al* 1966) Present calculation; Experimental points — Stebbins *et al* 1960.

We note that the cross-sections obtained by Born and Glauber approximations are nearly identical for $E > 200$ eV and in this region these are in good agreement with the experimental findings. Below 100 eV our curve (figure 1) lies below Ochkur, (Banerjee *et al* 1966) and Born curves. Detailed calculations of total and differential cross sections for wider energy region will be published soon.

REFERENCES

- Banerjee, S. N. 1966 *Indian J. Phys.* **40**, 491.
 Franco, V. & Glauber, R. J. 1966 *Phys. Rev.* **142**, 1195.
 Franco, V. 1968 *Phys. Rev. Letters*, **20**, 700.
 Glauber, R. J. 1959 *Lectures in Theoretical Physics*. Edited by Wesley, E. Brittin, *et al* (Inter Science Publishers, Inc. New York), Vol. I. p. 315.
 Harrington, D. R. 1968 *Phys. Rev.* **176**, 1982.
 Stebbins, R.F. 1960 *Phys. Rev.* **129**, 1939.
 Tai, H., Teubner, P. J. & Bessel, R.H. 1969. *Phys. Rev., Letters* **22**, 1415.

Incoherent scattering of gamma rays by K-shell electrons

By SURYA N. CHINTALAPUDI AND K. PARTHASARADHI

*The Laboratories for Nuclear Research,
Andhra University, Waltair, India*

(Received 26 August 1969, Revised 21 November 1969)

Incoherent scattering is one of the major processes by which gamma rays interact with matter in large energy range. In a discription of this process it is usual to assume that the scattering electrons are free and stationary. This assumption is valid for outer electrons in an atom for which the momentum transfer in the collision greatly exceeds the momentum of the electron in its motion. However, the effects of atomic binding have to be considered in dealing with the interior electrons. To account for this the so called incoherent scattering function is introduced as a correction factor for the Klein-Nishina cross-section. Theoretical approaches for the calculation of this function are already available (Grodstein 1957 ; Jauch *et al* 1955). Shimuju *et al* (1965) evolved a new expression for the calculation of incoherent scattering function.

TABLE 1. INCOHERENT SCATTERING FUNCTION OF GAMMA RAYS

Angle of scattering		Pb	Ta	Sm
Energy 320 KeV				
45°	Experimental	0.50±0.08	0.53±0.08	0.65±0.10
	Theoretical	0.18	0.23	0.30
60°	Experimental	0.60±0.10	0.66±0.10	0.75±0.11
	Theoretical	0.25	0.31	0.42
90°	Experimental	0.70±0.11	0.75±0.11	0.83±0.13
	Theoretical	0.36	0.45	0.63
110°	Experimental	0.84±0.13	0.85±0.13	0.91±0.14
	Theoretical	0.41	0.52	0.73
Energy 662 KeV				
30°	Experimental	0.52±0.06	0.49±0.05	0.63±0.09
	Theoretical	0.30	0.38	0.52
45°	Experimental	0.72±0.08	0.73±0.08	0.76±0.12
	Theoretical	0.49	0.64	0.89
60°	Experimental	0.86±0.09	0.92±0.10	0.92±0.14
	Theoretical	0.68	0.88	0.99
90°	Experimental	1.29±0.14	1.13±0.12	
	Theoretical	0.94	1.22	
130°	Experimental	1.54±0.17	1.36±0.14	
	Theoretical	1.12	1.46	

(all the values are corrected to the second decimal place)

Incoherent scattering of gamma rays by K-shell electrons 493

In the present investigations, calculations are made using this expression of Shimuju *et al* for 662 and 320 KeV gamma energies in elements Pb, Ta and Sm at various scattering angles and these are compared with the experimental results reported from these laboratories by Reddy (1965). All these results are given in table 1.

It can be seen from the table that at both energies in all elements the calculated values are following the same trend as that of the experimental values. However, for both the energies the theoretical values are smaller than those of the experimental values except at 662 KeV and above 30° in Sm and at 130° in Ta. But the agreement is better as the energy, angle and the atomic number increases.

REFERENCES

- Grodstein, G. W. 1957 *NBS Circular* 583 (Various approaches are summarised)
Jauch, J. M. & Rohrlich, F. 1955 *The Theory of Photons and Electrons* (Addison-Wesley Publishing Company, Cambridge, Massachusetts, USA)
Reddy, Ramalinga A. 1965 *Studies on Incoherent Scattering of Gamma Rays by K-shell Electrons, Ph. D. Thesis* (Andhra University), unpublished.
Shimuju, S., Nakayama, Y. & Mukoyama, T. 1965 *Phys. Rev.* **140**, A 806.

BOOK REVIEWS

SUPERNOVAE, by I. S. Shklovsky, John Wiley and Sons, London, 1968.

Volume XXI in the series Interscience Monographs and Texts in Physics and Astronomy.

Price \$ 20.20

This publication is an authoritative monograph on supernovae, the various problems connected with the causes of supernova explosions, their evolution and physical understanding of the complex processes occurring in the nebula. This information is now obtained through optical, radio and X-ray astronomy. The frequency of the occurrence of supernovae in a galaxy is a debatable point but roughly it can be taken to be about one in 300 years. In the monograph a description of all the supernovae which have been recorded so far is given. These supernovae can be divided into various types depending upon the shape of their photographic light curves. In supernovae of type I, there is a sudden increase in the luminosity followed by a gradual decrease. In supernovae of type II, the curve has a broader maximum than that of type I.

The supernovae of the type II are relatively young objects with sufficiently large masses and during explosion the ejected shells may be of mass greater than $100 M_{\odot}$. The fine-fibred nebula in Cygnus is an example. A detailed discussion of all the known supernovae of type II is given. Their optical characteristics, radio-frequency emission and the decrease in flux and intensity, shock waves in interstellar medium caused by the outbursts and the influence of the magnetic fields on the characteristics of remnants are described.

The Crab nebula belongs to remnant of type I supernova. This nebula has been studied most carefully due to its relative proximity and also due to the presence of the powerful synchrotron radiation. The flux density and polarisation of the radiofrequency radiation have been studied and various interpretations given. The Crab nebula consists of thin filaments arranged in the form of a shell surrounding the central part of the nebula. An analysis of the emission from this part shows that the emission is thirty times brighter than the emission from the filament and has a purely continuous spectrum. The analysis of the photographs shows that it has not been possible, so far, to explain the structure and the characteristic rates of change. From the study of the spectrum in the entire frequency range, attempts have been made to discuss problems like the age and the magnetic field strength. The most important result is the proof that relativistic electrons of high and super-high energies are still being produced at present in Crab nebula.

The study of supernovae is also connected with the problem of the origin of primary cosmic rays, that is the source of the relativistic protons and heavy nuclei. The author also discusses various theories which have been advanced to explain the causes of supernova explosion. This problem is also connected with the evolution of stars and their catastrophic collapse. Much work is being done on these problems. In this respect the book will prove to be very valuable to the students of modern astrophysics.

F. C. A.

"DIFFUSE MATTER IN SPACE", by L. Spitzer, Jr., Interscience Publishers,
John Wiley & Sons, New York, 1968. Pp 212 + XIII, Price \$ 11.50

The interstellar material plays a major role in the evolution of stars and the galaxies. It is known that new clusters are born within the interstellar clouds, and ejection of matter from old stars, especially from supernovae, enriches the interstellar gas with atoms of heavy elements. Here various physical processes occur which are not encountered in stellar atmospheres. There are enormous deviations from thermal equilibrium and the time scales for dynamical processes are much longer than the time scale for radiation cooling. The interaction between the energetic ions and the magnetic field pose interesting and difficult problems.

The book gives an introduction to this subject of interstellar material. The first three chapters provide the necessary observational data obtained with optical or radio telescopes and these data are interpreted in terms of the density and velocity distribution of the absorbing or emitting atoms, ions, molecules or solid grains. A number of major features in the interstellar emission or absorption spectra are due to hydrogen. The 21 cm line of neutral hydrogen is emitted primarily from H I region. In H II region collisions between electrons and protons lead to emission of continuous radiation and recombination both in visual and radio regions. The information from absorption lines complements that obtained from the emission lines. The non-thermal emission given by relativistic electrons provides the interstellar magnetic field. As radiation passes through a region of space containing solid particles, or grains, the radiant energy is scattered or converted into heat by absorption. This extinction process of scattering and absorption depends on the geometrical shape of the grains, the simplest shapes being spheres, cylinders and spheroids. Polarisation has been measured for a number of stars, and its dependence on wavelength, Galactic longitude observed. The spectral distribution of interstellar matter shows non-uniformity in the solar neighbourhood.

The physical processes which are associated with encounters between various types of interstellar particles and which determine ionization level, and the velocity distribution of the atoms, and the size, composition and orientation of the grains are the subject matter of chapter four. The dynamics of the interstellar gas like appearance of shock fronts and ionization fronts expansion of H II regions, the explosion of supernova and the interaction between clouds and stars are discussed in chapter five. The last chapter deals with the problem of formation of stars in galaxies, gravitational instability, fragmentation of a collapsing cloud and physical properties of the stellar material as its density increases.

The book will be found invaluable for students of astro-physics interested in the subject of interstellar matter.

F. C. A.

LECTURES ON THE THEORY OF NORMAL METALS DELIVERED AT THE CENTRE
FOR ADVANCED STUDY IN PHYSICS, DELHI UNIVERSITY, DELHI (INDIA).

by Acad. A. A. Abrikosov, Institute of Theoretical Physics,
Academy of Science, U. S. S. R. ;

Hindustan Publishing Corporation (India), Delhi-7,
India. 1968. Price Rs. 35.00.

The book is based on a course of lectures which the distinguished author delivered at the Department of Physics and Astrophysics of the Delhi University. The usually important topics like the electronic spectra of metals, conductivity (thermal and electrical), galvanomagnetic effects, behaviour of metals in high frequency fields and absorption of sound are dealt with. The approach to the different topics are fundamental and rigorous and many of the treatments are novel. Further he has discussed many newly discovered phenomena to show how these can be utilised for obtaining the electronic spectra of metals. This book, inspite of the presence of some good works on the subject in the field, will be very useful to both theoretical and experimental workers on metal physics and allied lines.

The reference system of the book needs improvement.

A. K. D.

ERRATA

Effect of lattice vibrations on the exchange-interaction in
ferro and antiferromagnetic crystals.

By A. T. MAITRA.

Vol. 43, No. 5, May, 1969.

Page 289.

- 2nd para, Line 4, *Read* radius r *Instead of* radius γ
Line 6, *Read* elements *Instead of* element
Line 8, *Read* and C_A *Instead of* C_A

Page 290.

- Line 11, *Read* influence of Born's *Instead of* Bohr's
Figure I, *Read* (a) *Instead of* (x)

Page 291.

- Line 1, *Read* (proportional to (U/l) *Instead of* U/l .
Figure 2(b), *read* $U \log (a/l)$ *Instead of* $U \log a$

Page 292.

- Line 2, *Read* imperfections *Instead of* imperfection.
Line 3, *Read* by the process of magnon-phonon coupling
Instead of by the process or magnon-phonon coupling.
Line 8, *Read* Variation of $U \log (a/l)$ *Instead of* $U \log$.
Last but two lines, *Read* these aspects is in progress *Instead*
of in progress.

INDIAN JOURNAL OF PHYSICS, VOL. 43, 1969

Statement about ownership and other particulars about newspaper
Indian Journal of Physics Vol. 43, 1969

FORM IV

(See Rule 8)

1. Place of publication ... Indian Association for the Cultivation of Science, 2 & 3, Raja Subodh Mallick Road, Calcutta-32
2. Periodicity of its publication ... Monthly
3. Printer's Name ... Sri Subir Bose,
Nationality ... Indian
(Address) ... 2/B, Garcha Ist Lane, Calcutta-19
4. Publisher's Name ... Sri Samarendranath Sen
Nationality ... Indian
Address ... Registrar, I. A. C. S. Calcutta-32
5. Editors' Name ...
Nationality ... As below
Address ...
6. Prof. F. C. Auluck
Indian
Department of Physics
University of Delhi
Delhi-7
7. Prof. D. S. Kothari
Indian
Department of Physics
Delhi University
Delhi
8. Prof. D. N. Kundu
Indian
Director
Saha Institute of Nuclear Physics
92, Acharya Prafulla Ch. Road Calcutta-9.
9. Dr. B. D. Nag Choudhuri
Indian
Member, Planning Commission Yojana Bhavan
New Delhi
10. Prof. K. R. Rao
Indian
Department of Physics
Andhra University
Waltair
11. Dr. R. Ramanna
Indian
Director, Physical Wing
Bhabha Atomic Research Centre
Apollo Pier Road
Bombay
12. Prof. S. C. Sirkar
Indian
22/1B, South Sinthi Road
Calcutta-30
13. Prof. B. N. Srivastava
Indian
Dept. of General Physics
and X-ray. I. A. C. S.
Calcutta-32
14. Prof. A. R. Verma
Indian
Director, National Physical Laboratory
New Delhi
15. Prof. A. Bose (Hon. Secretary)
Indian
Dept. of Magnetism
I. A. C. S.
Calcutta-32
6. Names and addresses of individuals who own the newspaper and partners or shareholders holding more than one percent of the total capital.

I, Sri Samarendranath Sen, hereby declare that the particulars given above are true to the best of my knowledge and belief.

Dated : 20-2-70

Sd- Samarendranath Sen
Signature of Publisher

Theoretical design of the experiment to study scattering of electrons and positrons by electrons

By M. R. BHIDAY, V. M. BHISE AND A. G. SHASTRI

G. S. Institute of Technology and Science, Indore.

(Received 24 July 1969)

Experiments to measure the electron-electron and positron-electron scattering cross-sections using a transverse magnetic field are in progress in this laboratory. The theoretical design study of these experiments is discussed in this paper. Monoenergetic beams of electrons or positrons are incident nearly normally to the scattering foil placed in the plane of the magnetic field. It is shown that the scattered and recoil particles due to electron-electron or positron-electron collisions with energy transfer q are focussed on two lines along the magnetic field. Relations between the x and z coordinates of the scattered particles, when focussed on the lines and the angles of scattering, are derived enabling the design and exact positioning of the scintillators in order to achieve a high collection efficiency and good resolution.

INTRODUCTION

A direct check on the Dirac theory of the electron is provided by the comparison of experimental results on electron-electron scattering as per the predictions of quantum-electrodynamics. When the incident electron has energies in the relativistic region, the problem becomes one of quantum-electrodynamics, an exact solution of which cannot be obtained directly but must be approached through an expansion in terms of the

interaction constant $\frac{e^2}{\hbar v}$.

The Moller formula (1932) for the relativistic electron-electron scattering cross-section may be written very conveniently in terms of the energy transfer occurring in the collision rather than in terms of the scattering angle. If the fractional kinetic energy transfer is denoted by q , the differential scattering cross-section becomes (Mott & Massey 1949)

$$\sigma(q)dq = 2\pi \left(\frac{e^2}{mv^2} \right)^2 \left(\frac{1}{\gamma-1} \right) \left[X^2 - 3X + \left(\frac{\gamma+1}{\gamma} \right)^2 (1+X) \right] dq$$

where,

$$X = [q(1-q)]^{-1}.$$

We have done experiments to verify the above formula by measuring the cross-section for electron-electron scattering accurately to 5%. Results of this accuracy have not been reported so far by earlier workers (Ashkin *et al* 1954). Movable pairs of scintillation counters have been used for the first time in our experiments, the results of which will be published separately. The purpose of this paper

is to report on the theoretical design of the experiment to measure the electron-electron scattering cross-section, in which the line focussing property (Bhiday & Tripathi 1962), for the scattered electrons in a transverse magnetic field has been brought out clearly and used in the design (Bhatnagar *et al* 1965) of the scintillator shape.

THEORETICAL DESIGN OF THE EXPERIMENT

In our experimental set up a beam of electrons, energy selected by a 60° sector magnet (Bhattacharya & Bhiday 1967), is directed on to a thin scattering foil with its plane parallel to a uniform magnetic field. Any electron-electron scatter in the foil gives rise to the scattered and the recoil electrons. These were detected in coincidence by two long scintillators placed in a plane parallel to the field and containing the foil. By measurements of the coincidence counting rate, the foil thickness and the incident beam intensity, the scattering cross-section was deduced. In order to measure the scattering occurring in a particular angular range, the two scintillators must be placed so that only for scatters occurring within this range can both scattered and recoil electrons be detected simultaneously. To position these scintillators correctly, it was necessary to know the relationship between the points where the scattered electrons cross the scintillator plane and the scattering angle (figure 1).

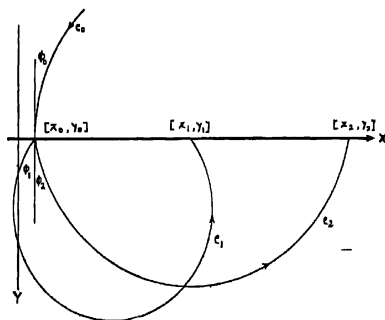


Figure 1. Projection on the XY plane.

This relationship can most conveniently be derived using a set of Cartesian axes defined so that the Z direction was that of the magnetic field and the XZ plane contained the scattering foil and the scintillator surfaces.

Figures 1 and 2 show the projections on to the XY and XZ planes, respectively, of the electron orbits occurring due to an electron-electron collision in the foil. The particle e_0 represents an electron of total energy γ_0 rest

masses incident upon the foil at a point (x_0, z_0) . After collision the scattered and recoil electrons e_1 and e_2 travel in helices in the uniform magnetic field and recross the XZ plane at (x_1, z_1) and (x_2, z_2) respectively.

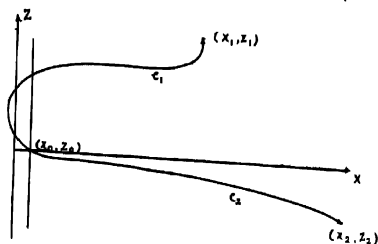


Figure 2. Projection on the XZ plane.

The electron paths at the point of collision are shown in more detail in figures 3 and 4.

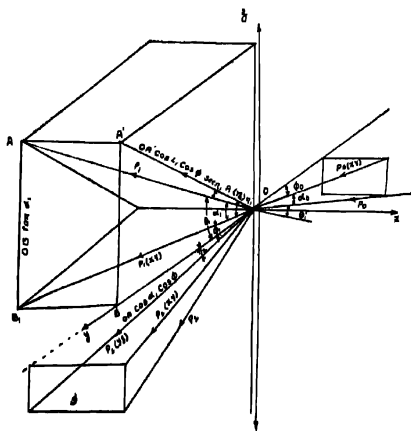


Figure 3. Electron trajectories at the point of collision

Let $P_r, r=0, 1, 2$ represent the momenta in directions $(l_r, m_r, n_r), r=0, 1, 2$ carried by $e_r, r=0, 1, 2$ and let $P_{r(x,y)}, r=0, 1, 2$ denote projections of P_r in XY plane having direction cosines $(l_r', m_r', 0)$. Similarly $P_{r(y,z)}$ denote the projection of P_r in YZ plane. If the pitch angle of helix in which the electron travels be denoted by α_r ,

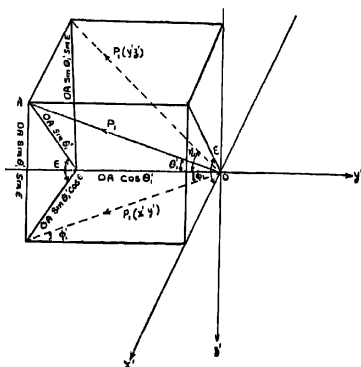


Figure 4. Electron trajectories at the point of collision

$$\alpha_r = \widehat{P_r, P_{r(x,y)}} \text{ and } \theta_r = \widehat{P_r, OY}, \phi_r = \widehat{P_{r(x,y)}, OY} \\ \theta'_r = \widehat{P_{0r}, P_r} = \text{Scattering angle and } \eta_r = \widehat{P_{r(y,z)}, OY}.$$

From figure (3) we obtain

$$\cos \alpha_1 \cos \phi_1 = \cos \theta_1 \text{ or } l_1 l'_1 + m_1 m'_1 \quad m'_1 = m_1. \quad \dots (1)$$

and $\tan \alpha_1 = \cos \phi_1 \tan \eta_1$.

As $P_1, P_1(YZ)$ and OX are coplanar, projecting OA along OA_1 gives $\dots (2)$

$$\cos \alpha_1 \cos \phi_1 \sec \eta_1 = m_1 \sec \eta_1 = (1 - l_1^2)^{\frac{1}{2}}, \quad \dots (3)$$

where $l_1 = \cos \alpha_1 \sin \phi_1$.

From figure (1), it can be seen that,

$$x_1 - x_0 = 2\rho_1 m'_1 \quad \dots (4)$$

and

$$2\rho_1 = \beta_1 \gamma_1 (l_1 l'_1 + m_1 m'_1) \bar{M}, \quad \dots (5)$$

where

$$\bar{M} = \frac{2M_0 c}{eH}.$$

Herein ρ_1 is the radius of helix in which e_1 is travelling, H = magnetic field, β_1 = velocity of e_1 relative to that of light. Substituting for ρ_1 from (5) and using (1) we get,

$$x_1 - x_0 = \bar{M} \beta_1 \gamma_1 m_1 \quad (6)$$

Theoretical design of the experiment to study scattering etc. 503

To obtain m_1 in terms of θ_1 —the scattering angle—consider a new set of orthogonal axes where OY' lies along P_0 , OX' lies in the XY plane and OZ' in the direction perpendicular to OX' and OY' .

From figure 4,

$$\phi'_r = P_r(x'y'), OY \quad r = 1, 2$$

and ϵ = angle between the planes of P_0P_1 and $X'Y'$.

$$\text{Hence } \tan \phi'_1 = \tan \theta'_1 \cos \epsilon. \quad \dots(7)$$

Some direct relations are :

$$\left. \begin{aligned} \cos \phi_0 &= m'_0, \sin \phi_0 = l'_0; \\ \cos \alpha_0 &= (l'_0 l'_0 + m'_0 m'_0) = N_1 \text{ say and} \\ \sin^2 \alpha_0 &= n_0^2 + (l'_0 m'_0 - m'_0 l'_0)^2 = N_2^2 \text{ say.} \end{aligned} \right\} \quad \dots(8)$$

$$\left. \begin{aligned} \sin^2 \theta'_1 &= \Sigma (m_0 n_1 - m_1 n_0)^2 = \frac{2(1-q)}{2 + q(\gamma_0 - 1)} = A^2 \text{ say,} \\ \cos^2 \theta'_1 &= (\Sigma l_0 l_1)^2 = \frac{q(\gamma_0 + 1)}{2 + q(\gamma_0 - 1)} = B^2 \text{ say} \end{aligned} \right\} \quad \dots(9)$$

and

$$\beta_1^2 \gamma_1^2 = [2 + q(\gamma_0 - 1)] q (\gamma_0 - 1)$$

where q is the fractional kinetic energy transfer occurring in the collision, since it is found more useful to put θ_1 in terms of q by equating moments and energies before and after the collision. As the direction cosines of OX' and OY' are $m'_0, l'_0, 0$ and l_0, m_0, n_0 respectively, therefore, the direction cosines of OZ' are

$$(l'_0 n_0 - m'_0 n_0, m'_0 m_0 - l'_0 l_0)/D \quad \dots(10)$$

$$\text{where } D^2 = n_0^2 + (m'_0 m'_0 - l'_0 l'_0)^2.$$

We wish to obtain m_1 in terms of ϵ and the direction cosines of P_0, P_1 .

Using (10) the direction cosines of OY with respect to new axes are :

$$-l'_0, N_1 m'_0, N_2 m'_0 \quad \dots(11)$$

The direction cosines of P_1 with respect to new axes are :

$$\left. \begin{aligned} l'_1 m'_0 + m'_1 l'_0, \Sigma l'_0 l_1, [l'_1 l'_0 n_0 - m'_1 m'_0 n_0 - n_1 (m'_0 m'_0 - l'_0 l'_0)]/D \end{aligned} \right\} \quad \dots(12)$$

and also

$$\sin \theta'_1 \cos \epsilon, \quad \cos \theta'_1, \quad \sin \theta'_1 \sin \epsilon$$

From (12) using (9) we obtain,

$$\left. \begin{aligned} \cos \epsilon &= (l'_1 m'_0 + m'_1 l'_0)/A \\ \text{and } \sin \epsilon &= [l'_1 l'_0 n_0 - m'_1 m'_0 n_0 + n_1 (m'_0 m'_0 - l'_0 l'_0)]/DA \end{aligned} \right\} \quad \dots(13)$$

From (11) and (12) and substituting in terms of ϵ from (13) we have,

$$m_1 = A[m'_0 N_2 \sin \epsilon - l'_0 \cos \epsilon] + B m'_0 N_1 \quad \dots(14)$$

Substituting in (6) for m_1 from (14) and for $\beta_1 \gamma_1$ from (9) we get,

$$x_1 - x_0 = \bar{M} (\gamma_0^2 - 1)^{\frac{1}{2}} (m'_0 N_1) \left[q + \frac{A}{N_1} \left(N_2 \sin \epsilon + \frac{l'_0}{m'_0} \cos \epsilon \right) \right] \quad \dots(15)$$

where \bar{M} , N_1 , N_2 and A are defined in (5), (8) and (9). Similarly it can be shown that,

$$x_2 - x_0 = \bar{M} (\gamma_0^2 - 1)^{\frac{1}{2}} (m'_0 N_1) \left[(1 - q) - \frac{A}{N_1} \left(N_2 \sin \epsilon - \frac{l'_0}{m'_0} \cos \epsilon \right) \right] \quad \dots(16)$$

From the equation to the helix, the z coordinate of the point where the scattered electron e_1 will cross the XZ plane is given by,

$$z_1 - z_0 = 2\rho_1 \left(\frac{\pi}{2} - \phi_1 \right) \tan \alpha_1 \quad \dots(17)$$

taking ϕ_1 as positive if the scatter is into the x positive quadrant and negative if the scatter is into the x negative quadrant.

Substituting for $\tan \alpha_1$ from (2) and using (6),

$$z_1 - z_0 = \left(\frac{\pi}{2} - \phi_1 \right) \bar{M} \beta_1 \gamma_1 (1 - l_1^2 - m_1^2)^{\frac{1}{2}} \quad \dots(18)$$

Now we wish to obtain m_1 and ϕ_1 in terms of q and ϵ . For m_1 equating the values of $(x_1 - x_0)$ from (6) and (15) we get,

$$m_1 \left[\frac{\beta_1 \gamma_1}{m'_0 N_1^2 (\gamma_0^2 - 1)} \right] = q + \left[\frac{2q(1-q)}{\gamma_0 + 1} \right]^{\frac{1}{2}} \times \frac{1}{N_1} \left(N_2 \sin \epsilon - \frac{l'_0}{m'_0} \cos \epsilon \right) \quad \dots(19)$$

The coordinates of any point $P(-r \sin \phi_1, r \cos \phi_1, \theta)$ on $P_1(xy)$ using (10) become

$$\left. \begin{aligned} & -r \sin \phi_1 m'_0 + r \cos \phi_1 l'_0, \quad -r \sin \phi_1 l'_0 + r \cos \phi_1 m'_0, \\ & (-r \sin \phi_1 l'_0 m'_0 - r \cos \phi_1 m'_0 n'_0) / D \end{aligned} \right\} \quad \dots(20)$$

and also,

$$r \cos \alpha_0 \sin \phi'_1, -r \cos \alpha_0 \cos \phi'_1, r \sin \alpha_0$$

as the $X'Y'$ plane is inclined at α_0 with XY plane. From (20) by equating x and y coordinates we get,

$$-\tan \phi'_1 = \frac{\sin \phi_0 - \cos \phi_0 \tan \phi_1}{m_0 - l_0 \tan \phi_1} \quad \dots(21)$$

From (21) and (7) we get,

$$\tan \phi_1 = \frac{l'_0 + \frac{A}{B} m_0 \cos \epsilon}{m'_0 + \frac{A}{B} l_0 \cos \epsilon} \quad \dots(22)$$

Substituting in (18) the value of $\left(\frac{\pi}{2} - \phi_1\right)$ from (22),

$$(z_1 - z_0) = \cot^{-1} \left[\frac{l'_0 + \frac{A}{B} m_0 \cos \epsilon}{m'_0 + \frac{A}{B} l_0 \cos \epsilon} \right] \bar{M} \beta_1 \gamma_1 (1 - l_1^2 - m_1^2)^{\frac{1}{2}} \dots (23)$$

where m_1 is given by (19).

Similarly it can be shown that $(z_2 - z_0)$ is obtained by replacing l_1 by l_2 and q by $(1 - q)$.

From equations (15) and (16) it can be seen that when α_0 and ϕ_0 are small, the x coordinates of the points where e_1 and e_2 cross the counter plane are independent of the azimuth of the plane of scattering. For a monoenergetic electron beam incident on a line $x = x_0$ on the scattering foil, all scattered and recoil electrons due to electron-electron collisions with energy transfer q will cross the counter plane as two lines given by

$$x_1 - x_0 = \bar{M} q (\gamma_0^2 - 1)^{\frac{1}{2}} \quad \dots(24)$$

and

$$x_2 - x_0 = \bar{M} (1 - q) (\gamma_0^2 - 1)^{\frac{1}{2}} \quad \dots (25)$$

This is the line focussing property of the uniform transverse magnetic field used in the present experiment. This magnetic field was obtained between pole pieces 13 inches in diameter with a gap of 6 inches in which a scattering chamber containing the foil and the scintillators with the light guides could be inserted.

When $\alpha_0 \rightarrow 0$, $\phi_0 \rightarrow 0$, we have $l_0 = n_0 = 0$ and $m_0 = 1$ then (23) becomes

$$z_1 - z_0 = \cot^{-1} \left(\frac{A}{B} \cos \epsilon \right) \bar{M} \beta_1 \gamma_1 (1 - l_1^2 - B^2)^{\frac{1}{2}} \quad \dots(26)$$

The last bracket has a maximum value when $l_1 \rightarrow 0$ with $l_1 \rightarrow 0$, $\cos \epsilon \rightarrow 0$ and the first bracket reduces to $\frac{\pi}{2}$.

Then the maximum positive value of z shift is given by

$$(z_1 - z_0)_{\max} = \frac{\pi}{2} \bar{M} \beta_1 \gamma_1 (1 - B^2)^{\frac{1}{2}} \quad \dots(27)$$

and the maximum negative value is given when $\epsilon \rightarrow \frac{3\pi}{2}$. For ϵ_2 the position is reversed, the maximum positive and negative values of z_2 being when ϵ is near $\frac{3\pi}{2}$ and $\frac{\pi}{2}$ respectively. The mathematical treatment is true for positron-electron scattering also except that the positrons and electrons will be bent in opposite directions with the positron carrying away a kinetic energy denoted by factor $(1 - q)$.

The line focussing property mentioned above was used with advantage by making the detecting scintillators long in the Z direction and placing them on the focus lines corresponding to the scattering angle for which it is desired to make measurements. The scintillators were mounted on cylindrical light guides so that these could be moved along the X axis. In this way good collection efficiency was obtained without loss of angular resolution. Because of this efficiency, scattering measurements of good accuracy and resolution have been made using the relatively weak particle beams obtainable from radioactive sources. In addition to the economic considerations, the use of a radioactive source of particles has the advantage that, an apparatus of this type can be used either for electron-electron scattering measurements or for positron-electron scattering measurements. Both are under investigation in this laboratory using pairs of movable scintillation counters which enable scattering measurements to be done for continuously variable values of q , the kinetic energy transfer.

Thanks are due to Dr. S. M. Das Gupta, Director, G. S. Institute of Technology and Science.

REFERENCES :

- Aahkin, A., Page, L. A. & Woodward, W. M. 1954 *Phys. Rev.* **94**, 357.
 Bhatnagar, K. G., Bhawalkar, D. V., Bhiday, M. R. 1965 *Ind. J. Pure & Appl. Phys.* **3**, 500.
 Bhattacharya, P. K. & Bhiday, M. R. 1967 *Ind. J. Pure & Appl. Phys.* **5**, 386.
 Bhiday, M. R. & Tripathi, R. N. 1962 *Nucl. Phys. Symp. Madras*, 193.
 Moller C., 1932 *Ann. Physik.*, **14**, 531.
 Mott, N. F. & Massey, H. S. W., 1949 *Theory of Atomic Collisions*, Oxford.

Flow of a viscous incompressible fluid between two co-axial
unsteadily rotating porous cylinders

By S. N. DUBE AND S. R. MUKHERJEE

*Department of Mathematics, Institute of Technology,
Banaras Hindu University, Varanasi-5*

(Received 3 January 1969)

In the present paper an attempt is made to find the solution of the Navier-Stokes equations for the unsteady flow of a viscous incompressible fluid between two co-axial porous cylinders rotating with angular velocities varying periodically with time. A solution has been obtained under the assumption of uniform conditions along the axis of the cylinders. The cylinders being porous, a time-independent hyperbolic cross-flow velocity distribution is superimposed over the circumferential velocity produced due to rotation. It is seen that there is a Bernoulli-type pressure variation in the radial direction. The results are obtained for a particular value of the cross-flow Reynolds number R ($R = -2$). It is observed that in the case of very large frequencies the maxima of circumferential velocity distribution exist in the neighbourhood of the walls. The results transform to the known ones for Couette flow between uniformly rotating co-axial cylinders when $R = 0$ and frequencies are very small.

INTRODUCTION

Couette first obtained the exact solution of the Navier-Stokes equations for steady laminar flow of a viscous incompressible fluid between two co-axial rotating cylinders. The solution proved is of importance as it has been used to determine the coefficient of viscosity of a fluid. In a recent paper Sinha & Choudhary (1966) have studied the laminar flow of a viscous incompressible fluid between two co-axial rotating cylinders with uniform radial velocity imposed at the surfaces. They have assumed that the pressure is uniform along the axis of the cylinders.

In this paper we have discussed the unsteady flow of a viscous liquid between two co-axial porous cylinders rotating with angular velocities varying periodically with time. We have also assumed that pressure is uniform along the axis of the cylinders. The cylinders being porous, a time-independent hyperbolic cross-flow velocity distribution is superimposed over the circumferential velocity produced due to rotation. The results are obtained when the cross-flow Reynolds number R is -2 and we see that they are all finite whereas in the case of Sinha & Choudhary all the results are indeterminate when $R = -2$. The solutions are also obtained in the two extreme cases of small and large frequencies and it is seen that in the case of very large frequencies the maxima of circumferential velocity distribution exist in the neighbourhood of the

walls. When $R = 0$ and frequencies are very small, the results transform to the known ones for Couette flow between two uniformly rotating coaxial cylinders.

NOTATIONS

- ρ = density of the fluid
 x = axial coordinate
 r = radial coordinate
 ϕ = azimuthal coordinate
 u = axial velocity
 v = cross-flow velocity
 w = azimuthal velocity
 P = pressure
 μ = coefficient of viscosity
 ν = kinematic viscosity
 r_1 = radius of the inner cylinder
 r_2 = radius of the outer cylinder
 v_1 = cross-flow velocity at the wall of the inner cylinder
 v_2 = cross-flow velocity at the wall of the outer cylinder

1. Equations of Motion and their Solution

The Navier-Stokes equations of motion of a viscous incompressible fluid in cylindrical polar coordinates are (Pai 1956)

$$\begin{aligned} \frac{\partial v}{\partial t} + v \frac{\partial v}{\partial r} + \frac{w}{r} \frac{\partial v}{\partial \phi} - \frac{w^2}{r} + u \frac{\partial v}{\partial x} \\ = -\frac{1}{\rho} \frac{\partial P}{\partial r} + \nu \left[\frac{\partial^2 v}{\partial r^2} + \frac{1}{r} \frac{\partial v}{\partial r} - \frac{v}{r^2} + \frac{1}{r^2} \frac{\partial^2 v}{\partial \phi^2} \right. \\ \left. - \frac{2}{r^2} \frac{\partial w}{\partial \phi} + \frac{\partial^2 v}{\partial x^2} \right] \end{aligned} \quad \dots(1.1)$$

$$\begin{aligned} \frac{\partial w}{\partial t} + v \frac{\partial w}{\partial r} + \frac{w}{r} \frac{\partial w}{\partial \phi} + \frac{vw}{r} + u \frac{\partial w}{\partial x} \\ = -\frac{1}{\rho} \frac{1}{r} \frac{\partial P}{\partial \phi} + \nu \left[\frac{\partial^2 w}{\partial r^2} + \frac{1}{r} \frac{\partial w}{\partial r} - \frac{w}{r^2} + \frac{1}{r^2} \frac{\partial^2 w}{\partial \phi^2} \right. \\ \left. + \frac{2}{r^2} \frac{\partial v}{\partial \phi} + \frac{\partial^2 w}{\partial x^2} \right], \end{aligned} \quad \dots(1.2)$$

$$\begin{aligned} \frac{\partial u}{\partial t} + v \frac{\partial u}{\partial r} + \frac{w}{r} \frac{\partial u}{\partial \phi} + u \frac{\partial u}{\partial x} \\ = -\frac{1}{\rho} \frac{\partial P}{\partial x} + \nu \left[\frac{\partial^2 u}{\partial r^2} + \frac{1}{r} \frac{\partial u}{\partial r} + \frac{1}{r^2} \frac{\partial^2 u}{\partial \phi^2} + \frac{\partial^2 u}{\partial x^2} \right], \end{aligned} \quad \dots(1.3)$$

and the equation of continuity is

$$\frac{\partial v}{\partial r} + \frac{v}{r} + \frac{1}{r} \frac{\partial w}{\partial \phi} + \frac{\partial u}{\partial x} = 0. \quad \dots(1.4)$$

For flow between two rotating porous cylinders

$$\frac{\partial}{\partial \phi} \left(\right) = 0, \text{ for axial symmetry;}$$

$$u = 0, \text{ for motion due to rotation only.}$$

Under these conditions, equations (1.1), (1.2), (1.3) and (1.4) reduce to

$$\begin{aligned} \frac{\partial v}{\partial t} + v \frac{\partial v}{\partial r} - \frac{w^2}{r} = - \frac{1}{\rho} \frac{\partial P}{\partial r} + \nu \left[\frac{\partial^2 v}{\partial r^2} + \frac{1}{r} \frac{\partial v}{\partial r} \right. \\ \left. - \frac{v}{r^2} + \frac{\partial^2 v}{\partial x^2} \right], \end{aligned} \quad \dots(1.5)$$

$$\frac{\partial w}{\partial t} + v \frac{\partial w}{\partial r} + \frac{vw}{r} = \nu \left[\frac{\partial^2 w}{\partial r^2} + \frac{1}{r} \frac{\partial w}{\partial r} - \frac{w}{r^2} + \frac{\partial^2 w}{\partial x^2} \right], \quad \dots(1.6)$$

$$\frac{\partial P}{\partial x} = 0, \quad \dots(1.7)$$

and

$$\frac{\partial v}{\partial r} + \frac{v}{r} = 0. \quad \dots(1.8)$$

Equation (1.7) states the condition of uniform pressure distribution along the axis of the cylinders.

Assuming $\frac{\partial v}{\partial x} = 0$, for uniform suction and injection throughout the

whole length and $\frac{\partial w}{\partial x} = 0$, for circumferential velocity produced due to rotation only, equations (1.5), (1.6) and (1.8) reduce to

$$\frac{\partial v}{\partial t} + v \frac{\partial v}{\partial r} - \frac{w^2}{r} = - \frac{1}{\rho} \frac{\partial P}{\partial r} + \nu \left[\frac{\partial^2 v}{\partial r^2} + \frac{1}{r} \frac{\partial v}{\partial r} - \frac{v}{r} \right] \quad \dots(1.9)$$

$$\frac{\partial w}{\partial t} + v \frac{\partial w}{\partial r} + \frac{vw}{r} = \nu \left[\frac{\partial^2 w}{\partial r^2} + \frac{1}{r} \frac{\partial w}{\partial r} - \frac{w}{r^2} \right], \quad \dots(1.10)$$

and

$$\frac{\partial v}{\partial r} + \frac{v}{r} = 0. \quad \dots(1.11)$$

We now assume that the suction rate at one wall is equal to the injection rate at the other wall. Therefore

$$r_2 v_2 = r_1 v_1, \quad \dots (1.12)$$

where v_1, v_2 are the cross-flow velocities at the walls of the smaller and larger tubes, respectively. Then from equations (1.11) and (1.12), we get

$$vr = v_1 r_1 = v_2 r_2. \quad \dots (1.13)$$

From equations (1.9) and (1.11), assuming cross-flow velocity to be independent of time, we get

$$\rho \left(\frac{v^2 + w^2}{r} \right) = \frac{\partial P}{\partial r}. \quad \dots (1.14)$$

Equation (1.14) states Bernoulli-type pressure variation in the radial direction. Now equation (1.10) becomes

$$\frac{\partial^2 w}{\partial r^2} + \frac{(1-R)}{r} \frac{\partial w}{\partial r} - \frac{(1+R)}{r^2} w = \frac{1}{\nu} \frac{\partial w}{\partial t}, \quad \dots (1.15)$$

where $R = \frac{r_1 v_1}{\nu}$ is cross-flow Reynolds number.

We now put $w = f(r)e^{int}$ (1.16)

into (1.15) and take the real part of the final solution as the required result. Substituting equation (1.16) into equation (1.15), we have

$$\frac{d^2 f}{dr^2} + \frac{(1-R)}{r} \frac{df}{dr} - \left[\frac{in}{\nu} + \frac{(1+R)}{r^2} \right] f = 0. \quad \dots (1.17)$$

The boundary conditions for w are

$w = \Omega_1 r_1 e^{int}$ when $r = r_1$, and $w = \Omega_2 r_2 e^{int}$ when $r = r_2$, where only the real parts are taken.

Therefore the boundary conditions for f are

$$\left. \begin{aligned} f &= \Omega_1 r_1 \text{ when } r = r_1, \\ \text{and} \\ f &= \Omega_2 r_2 \text{ when } r = r_2. \end{aligned} \right\} \quad \dots (1.18)$$

The general solution of equation (1.17) under the boundary conditions (1.18) is

$$\begin{aligned} f = r^{R/2} & \left[\Omega_1 r_1^{(2-R)/2} \frac{\{J_m(r_2 p_i^{3/2}) Y_m(r_2 p_i^{3/2}) - J_m(r_2 p_i^{3/2}) Y_m(r_1 p_i^{3/2})\}}{J_m(r_1 p_i^{3/2}) Y_m(r_2 p_i^{3/2}) - J_m(r_2 p_i^{3/2}) Y_m(r_1 p_i^{3/2})} \right. \\ & \left. + \Omega_2 r_2^{(2-R)/2} \frac{\{J_m(r_1 p_i^{3/2}) Y_m(r_2 p_i^{3/2}) - J_m(r_2 p_i^{3/2}) Y_m(r_1 p_i^{3/2})\}}{J_m(r_1 p_i^{3/2}) Y_m(r_2 p_i^{3/2}) - J_m(r_2 p_i^{3/2}) Y_m(r_1 p_i^{3/2})} \right] \end{aligned}$$

Or

$$f = r^{R/2} \left[\Omega_1 r_1^{(2-R)/2} \left\{ \frac{J_m(r p i^{3/2}) J_{-m}(r_2 p i^{3/2}) - J_m^*(r_2 p i^{3/2}) J_{-m}(r p i^{3/2})}{J_m(r_1 p i^{3/2}) J_{-m}(r_2 p i^{3/2}) - J_m(r_2 p i^{3/2}) J_{-m}(r_1 p i^{3/2})} \right\} \right. \\ \left. + \Omega_2 r_2^{(2-R)/2} \left\{ \frac{J_m(r_1 p i^{3/2}) J_{-m}(r p i^{3/2}) - J_m(r p i^{3/2}) J_{-m}(r_1 p i^{3/2})}{J_m(r_1 p i^{3/2}) J_{-m}(r_2 p i^{3/2}) - J_m(r_2 p i^{3/2}) J_{-m}(r_1 p i^{3/2})} \right\} \right]$$

according as m is an integer or not, where $m = \pm \frac{R+2}{2}$ and $p = (n/\nu)^{1/2}$.

Therefore the circumferential velocity is

$$w = R_c(r)^{R/2} \left[\Omega_1 r_1^{(2-R)/2} \left\{ \frac{J_m(r p i^{3/2}) Y_m(r_2 p i^{3/2}) - J_m(r_2 p i^{3/2}) Y_m(r p i^{3/2})}{J_m(r_1 p i^{3/2}) Y_m(r_2 p i^{3/2}) - J_m(r_2 p i^{3/2}) Y_m(r_1 p i^{3/2})} \right\} \right. \\ \left. + \Omega_2 r_2^{(2-R)/2} \left\{ \frac{J_m(r_1 p i^{3/2}) Y_m(r p i^{3/2}) - J_m(r p i^{3/2}) Y_m(r_1 p i^{3/2})}{J_m(r_1 p i^{3/2}) Y_m(r_2 p i^{3/2}) - J_m(r_2 p i^{3/2}) Y_m(r_1 p i^{3/2})} \right\} \right] e^{int},$$

Or

$$w = R_c(r)^{R/2} \left[\Omega_1 r_1^{(2-R)/2} \left\{ \frac{J_m(r p i^{3/2}) J_{-m}(r_2 p i^{3/2}) - J_m(r_2 p i^{3/2}) J_{-m}(r p i^{3/2})}{J_m(r_1 p i^{3/2}) J_{-m}(r_2 p i^{3/2}) - J_m(r_2 p i^{3/2}) J_{-m}(r_1 p i^{3/2})} \right\} \right. \\ \left. + \Omega_2 r_2^{(2-R)/2} \left\{ \frac{J_m(r_1 p i^{3/2}) J_{-m}(r p i^{3/2}) - J_m(r p i^{3/2}) J_{-m}(r_1 p i^{3/2})}{J_m(r_1 p i^{3/2}) J_{-m}(r_2 p i^{3/2}) - J_m(r_2 p i^{3/2}) J_{-m}(r_1 p i^{3/2})} \right\} \right] e^{int}$$

according as m is an integer or not. In the above expressions R_c denotes the real part.

Now the circumferential velocity when $R = -2$ is

$$w = R_c \left[\Omega_1 r_1^2 \left\{ \frac{J_0(r p i^{3/2}) Y_0(r_2 p i^{3/2}) - J_0(r_2 p i^{3/2}) Y_0(r p i^{3/2})}{J_0(r_1 p i^{3/2}) Y_0(r_2 p i^{3/2}) - J_0(r_2 p i^{3/2}) Y_0(r_1 p i^{3/2})} \right\} \right. \\ \left. + \Omega_2 r_2^2 \left\{ \frac{J_0(r_1 p i^{3/2}) Y_0(r p i^{3/2}) - J_0(r p i^{3/2}) Y_0(r_1 p i^{3/2})}{J_0(r_1 p i^{3/2}) Y_0(r_2 p i^{3/2}) - J_0(r_2 p i^{3/2}) Y_0(r_1 p i^{3/2})} \right\} \right] e^{int} \quad \dots (1.19)$$

The expression (1.19) is finite whereas the expression for the circumferential velocity obtained by Sinha & Choudhury takes indeterminate form for $R = -2$.

2 Velocity Distribution for Small Frequencies

For small frequencies, that is n is small, we have

$$J_0(r p i^{3/2}) \simeq 1 + \frac{i r^2 p^2}{4}$$

and

$$Y_0(r p i^{3/2}) \simeq \frac{2}{\pi} \left[\left(\gamma + \log \frac{r p i^{3/2}}{2} \right) \left(1 + \frac{i r^2 p^2}{2} \right) - \frac{i r^2 p^2}{4} \right],$$

where γ is Euler's constant.

Hence

$$\begin{aligned} & J_0(r_1 p i^{3/2}) Y_0(r_2 p i^{3/2}) - J_0(r_2 p i^{3/2}) Y_0(r_1 p i^{3/2}) \\ &= \frac{2}{\pi} \left[\log \left(\frac{r_2}{r_1} \right) + \frac{i p^2}{4} \left\{ (r_1^2 + r_2^2) \log \left(\frac{r_2}{r_1} \right) - (r_2^3 - r_1^3) \right\} \right] \end{aligned}$$

Substituting these values in (1.19), we get

$$w r = \frac{\Omega_1 r_1^3 \log \left(\frac{r_2}{r_1} \right) + \Omega_2 r_2^3 \log \left(\frac{r_1}{r_2} \right)}{\log \left(\frac{r_2}{r_1} \right)} \cos n t. \quad \dots (2.1)$$

3. Velocity Distribution for Large Frequencies

When n is large, taking asymptotic expansions of Bessel functions, $r p > 10$ and $-\frac{\pi}{2} \leq \text{phase } (r p i^{3/2}) \leq \frac{\pi}{2}$, we have

$$J_0(r p i^{3/2}) \simeq \left(-\frac{2}{\pi r p i^{3/2}} \right)^{1/2} \cos \left(r p i^{3/2} - \frac{\pi}{4} \right)$$

and

$$Y_0(r p i^{3/2}) \simeq \left(-\frac{2}{\pi r p i^{3/2}} \right)^{1/2} \sin \left(r p i^{3/2} - \frac{\pi}{4} \right).$$

Substituting these values in (1.19), we have

$$\begin{aligned} w r &= \Omega_1 r_1^3 \left(\frac{r_1}{r} \right)^{1/2} e^{-(r-r_1)p/\sqrt{2}} \cos \left\{ (r-r_1)p/\sqrt{2} - n t \right\} \\ &+ \Omega_2 r_2^3 \left(\frac{r_2}{r} \right)^{1/2} e^{-(r_2-r)p/\sqrt{2}} \cos \left\{ (r_2-r)p/\sqrt{2} - n t \right\} \quad \dots (3.1) \end{aligned}$$

Hence when n is large, it is found that maxima of circumferential velocity distribution exist in the neighbourhood of the walls.

4. Results When the Inner Cylinder is at Rest

The case, when the inner cylinder is at rest and the outer rotates, has some practical importance. The circumferential velocity when the inner cylinder is at rest and $R = -2$

$$w r = R \left[\frac{\Omega_2 r_2^3 \{ J_0(r_1 p i^{3/2}) Y_0(r p i^{3/2}) - J_0(r p i^{3/2}) Y_0(r_1 p i^{3/2}) \}}{J_0(r_1 p i^{3/2}) Y_0(r_2 p i^{3/2}) - J_0(r_2 p i^{3/2}) Y_0(r_1 p i^{3/2})} \right] e^{i n t} \quad \dots (4.1)$$

Now from (4.1) the expressions for the circumferential velocity for small and large frequencies can easily be obtained.

Using the recurrence relation

$$-J_0(z) Y_1(z) + J_1(z) Y_0(z) = \frac{2}{\pi z}$$

we get the shearing stress at the inner cylinder from (4.1) as

$$\tau = \mu \left(\frac{\partial w}{\partial r} \right)_{r=r_1} = R_0 \left[\frac{2\mu}{\pi} \cdot \frac{\Omega_0 r_0^2}{r_1^3} \cdot \frac{1}{J_0(r_1 p i^{3/2}) Y_0(r_2 p i^{3/2}) - J_0(r_2 p i^{3/2}) Y_0(r_1 p i^{3/2})} \right] e^{int}. \quad \dots (4.2)$$

The shearing stress for small frequencies is

$$\tau = \frac{\mu \Omega_0 r_0^2}{r_1^3 \log \left(\frac{r_2}{r_1} \right)} \cos nt. \quad \dots (4.3)$$

For large frequencies the shearing stress is

$$\tau = \mu \Omega_0 \left(\frac{2 r_0^2}{r_1^3} \right)^{1/2} e^{-(r_2 - r_1) p / \sqrt{2} - nt} [\cos \{(r_2 - r_1) p / \sqrt{2} - nt\} + \sin \{(r_2 - r_1) p / \sqrt{2} - nt\}] \quad \dots (4.4)$$

From (4.4) it is clear that the shearing stress at the inner cylinder will be very small in the case of very large frequencies.

The torque transmitted by the fluid to unit length of the inner cylinder is

$$M = R_0 \left[\frac{4\mu \Omega_0 r_0^2}{J_0(r_1 p i^{3/2}) Y_0(r_2 p i^{3/2}) - J_0(r_2 p i^{3/2}) Y_0(r_1 p i^{3/2})} \right] e^{int}. \quad \dots (4.5)$$

From (4.5) the expressions for the torque transmitted by the fluid to unit length of the inner cylinder for small and large frequencies can be easily derived.

5. Solutions for the case $R = 0$

The circumferential velocity when $R = 0$ is

$$w_0 = R_0 \left[\Omega_1 r_1 \frac{\{J_1(r_1 p i^{3/2}) Y_1(r_2 p i^{3/2}) - J_1(r_2 p i^{3/2}) Y_1(r_1 p i^{3/2})\}}{J_1(r_1 p i^{3/2}) Y_1(r_2 p i^{3/2}) - J_1(r_2 p i^{3/2}) Y_1(r_1 p i^{3/2})} + \Omega_2 r_2 \frac{\{J_1(r_1 p i^{3/2}) Y_1(r_2 p i^{3/2}) - J_1(r_2 p i^{3/2}) Y_1(r_1 p i^{3/2})\}}{J_1(r_1 p i^{3/2}) Y_1(r_2 p i^{3/2}) - J_1(r_2 p i^{3/2}) Y_1(r_1 p i^{3/2})} \right] e^{int}. \quad \dots (5.1)$$

For small frequencies

$$J_1(r_1 p i^{3/2}) Y_1(r_2 p i^{3/2}) - J_1(r_2 p i^{3/2}) Y_1(r_1 p i^{3/2}) = \frac{(r_0^2 - r_1^2)}{\pi r_1^2},$$

Therefore the circumferential velocity for small frequencies is

$$w_0 = \frac{1}{(r_2^2 - r_1^2)} \left[r (\Omega_2 r_2^2 - \Omega_1 r_1^2) - \frac{r_1^2 r_2^2}{r} (\Omega_2 - \Omega_1) \right] \cos nt, \quad \dots (5.2)$$

The expression (5.2) is as in the Couette flow between two uniformly rotating cylinders with solid surfaces ($R = 0$).

For large frequencies we have

$$J_1(rp_i^{3/2}) \simeq \left(\frac{2}{\pi r p_i^{3/2}} \right)^{1/2} \cdot \cos \left(r p_i^{3/2} - \frac{3\pi}{4} \right)$$

and

$$Y_1(rp_i^{3/2}) \simeq \left(\frac{2}{\pi r p_i^{3/2}} \right)^{1/2} \cdot \sin \left(r p_i^{3/2} - \frac{3\pi}{4} \right).$$

Substituting these values in (5.1), we obtain

$$w_0 = \Omega_1 \left(\frac{r_1^3}{r} \right)^{1/2} e^{-(r-r_1)p/\sqrt{2}} \cdot \cos \left\{ (r-r_1)p/\sqrt{2} - nt \right\} \\ + \Omega_2 \left(\frac{r_2^3}{r} \right)^{1/2} e^{-(r_2-r)p/\sqrt{2}} \cdot \cos \left\{ (r_2-r)p/\sqrt{2} - nt \right\}. \quad \dots (5.3)$$

Hence when n is large, it is again found that maxima of circumferential velocity distribution exist in the neighbourhood of the walls.

Now the circumferential velocity when the inner cylinder is at rest and $R = 0$ is

$$w_1 = R_1 \left[\Omega_2 r_2 \frac{J_1(r_1 p_i^{3/2}) Y_1(r_2 p_i^{3/2}) - J_1(r_2 p_i^{3/2}) Y_1(r_1 p_i^{3/2})}{J_1(r_1 p_i^{3/2}) Y_1(r_2 p_i^{3/2}) - J_1(r_2 p_i^{3/2}) Y_1(r_1 p_i^{3/2})} \right] e^{int}. \quad \dots (5.4)$$

Using the recurrence relation

$$-J_1(z) Y_2(z) + J_2(z) Y_1(z) = \frac{2}{\pi z}$$

we get the shearing stress at the inner cylinder from (5.4) as

$$\tau_0 = R_1 \left[\frac{2\mu}{\pi} \cdot \frac{\Omega_2 r_2}{r_1} \frac{1}{J_1(r_1 p_i^{3/2}) Y_1(r_2 p_i^{3/2}) - J_1(r_2 p_i^{3/2}) Y_1(r_1 p_i^{3/2})} \right] e^{int}. \quad \dots (5.5)$$

The shearing stress for small frequencies is

$$\tau_0 = \frac{2\mu\Omega_2 r_2^2}{(r_2^2 - r_1^2)} \cos nt, \quad \dots (5.6)$$

The expression (5.6) for shearing stress is as in the Couette flow between two uniformly rotating cylinders with solid surfaces.

For large frequencies the shearing stress is

$$\tau_{\theta} = \mu p \Omega_0 \left(\frac{2r_2^3}{r_1} \right)^{1/2} e^{-(r_2 - r_1)p/\sqrt{2}} \cdot \left[\cos \left\{ (r_2 - r_1)p/\sqrt{2} - nt \right\} + \sin \left\{ (r_2 - r_1)p/\sqrt{2} - nt \right\} \right] \quad \dots(5.7)$$

From (5.7) it is obvious that the shearing stress at the inner cylinder will be very small in the case of very large frequencies.

Now the torque transmitted by the fluid to unit length of the inner cylinder is

$$M_0 = R_0 \left[\frac{4\mu\Omega_0 r_1^2 r_2}{J_1(r_1 p i^{3/2}) Y_1(r_2 p i^{3/2}) - J_1(r_2 p i^{3/2}) Y_1(r_1 p i^{3/2})} \right] e^{int} \quad \dots(5.8)$$

For small frequencies the above expression gives

$$M_0 = \frac{4\mu\pi\Omega_0 r_1^2 r_2^2}{(r_2^3 - r_1^3)} \cos nt.$$

The expression (5.8) for large frequencies is

$$M_0 = 2\sqrt{2}\mu\pi p \Omega_0 r_1^{3/2} r_2^{3/2} e^{-(r_2 - r_1)p/\sqrt{2}} \left[\cos \left\{ (r_2 - r_1)p/\sqrt{2} - nt \right\} + \sin \left\{ (r_2 - r_1)p/\sqrt{2} - nt \right\} \right],$$

which will also be very small for very large frequencies

CONCLUSIONS

Sinha & Choudhary have made the calculations for small values of R ($-1 \leq R \leq 1$) and results obtained by them become indeterminate when $R = -2$, but in the present paper we have not imposed any restriction upon R and it is also seen that the results can be obtained for all possible values of R including $R = -2$.

The authors are extremely grateful to Prof. P. L. Bhatnagar Vice-Chancellor for his constant encouragement in the preparation of this paper.

REFERENCES

- Sinha, K. D. & Choudhary, R. C. 1966 *Proc Nat. Inst Sci. India*, **32A**, No. 1, 81.
 Pau, S. 1956 *Viscous Flow Theory, I-Laminar Flow*, D. Van Nostrand Co., Inc., Princeton, p.38.

Mechanical response of a free piezoelectric plate

By D. K. SINHA

Department of Mathematics, Jadavpur University, Calcutta-32

(Received 4 May 1968, Revised 4 April 1969)

The paper uses the constitutive equations of a piezoelectric (monoclinic) material, the equations of electricity and the equations of mechanical motion to determine the mechanical response of a free piezoelectric plate.

1. INTRODUCTION

The problem of evaluating responses-mechanical or electrical-in piezoelectric transducers owing to prescribed inputs (mechanical or electrical) is an important electromechanical problem from the standpoint of ultrasonic and acoustic engineering, (Mason 1948, Cady 1946). The studies of such problems have long been undertaken from the point of view of circuit theory, (Mason 1948) and it is only in recent years such problems are being tackled by applying the techniques of mechanics of continuous media and of electricity. The efforts in this direction are due to Redwood (1961), Sinha (1962, 1965, 1968, 1966a, 1967a), Giri (1966b), (1967b), Roy (1967c), Das (1967d). The present paper is an analogous attempt and it seeks to investigate the responses in a free piezoelectric plate (unlike those considered in the papers cited above) characterized by a time-decaying polarization gradient, a fact supported by experiments as referred to in Mason (1948b), and Swann (1950). The electrically excited free plate, as observed by Sruetzer (1967), is a useful arrangement for the dynamic measurements of material parameters. The paper makes use of the methods of Laplace transform to facilitate the solution of the problem.

2. PROBLEM, FUNDAMENTAL EQUATIONS AND BOUNDARY CONDITIONS.

As our object is to obtain the mechanical response owing to an electrical input, we shall first evolve a relation connecting the two variables representing the two fields-mechanical and electrical. The constitutive relations for the piezoelectric material (for a monoclinic crystal) in the direction of the x -axis are given by

$$T_1 = c_{11} S_1 + e_{11} E_1 \quad \dots (1)$$

$$P_1 = e_{11} S_1 + K_{11} E_1 \quad \dots (2)$$

where T_1 , S_1 , E_1 and P_1 are the components of stress, strain, electric intensity and polarization, respectively, and c_{11} , e_{11} , K_{11} are the elastic, piezoelectric and dielectric susceptibility co-efficients.

If ξ be the mechanical displacement in the x -direction, the equation of motion is given by

$$\frac{\partial T_1}{\partial x} = \rho \frac{\partial^2 \xi}{\partial t^2} \quad \dots(3)$$

ρ being the density of the material. Since $S_1 = \frac{\partial \xi}{\partial x}$ we have from (1), (2), (3)

$$\rho \frac{\partial^2 \xi}{\partial t^2} = \left(c_{11} - \frac{e_{11}^2}{K_{11}} \right) \frac{\partial^2 \xi}{\partial x^2} - \frac{e_{11}}{K_{11}} \frac{\partial P_1}{\partial x} \quad \dots(4)$$

As assumed earlier, we take the polarization gradient $\frac{\partial P_1}{\partial x}$ to be equal to $P_0 e^{-\alpha x}$ where P_0 is a constant and $\alpha > 0$. Substituting this value of $\frac{\partial P_1}{\partial x}$ and taking the Laplace transform (of parameter p) of both sides of the resulting equation, we get

$$\frac{\partial^2 \bar{\xi}}{\partial x^2} - \frac{p^2}{v^2} \bar{\xi} = - \frac{P_0 e_{11}}{(c_{11} K_{11} - e_{11}^2)} \cdot \frac{1}{p + \alpha} \quad \dots (5)$$

$$\text{where } v^2 = \left(c_{11} - \frac{e_{11}^2}{K_{11}} \right) / \rho$$

The equation (4) with the assumed value of $\frac{\partial P_1}{\partial x}$ is the fundamental equation of the problem and it is to be solved subject to the condition that the extremities $x = 0$ and $x = X$ to be stress-free i.e. $T'(0) = 0$ and $T'(X) = 0$. Solving (5), we have

$$\bar{\xi} = A e^{\frac{px}{v}} + B e^{-\frac{px}{v}} + \frac{\rho e_{11}}{p} \cdot \frac{1}{p^2 (p + \alpha)} \quad \dots (6)$$

Using (5) and (6) in the boundary conditions as well as the relevant expression for T (from which E_{11} has been eliminated by means of (1) and (2)) we get

$$\left. \begin{aligned} A - B &= 0 \\ A e^{\frac{pX}{v}} - B e^{-\frac{pX}{v}} + \frac{P_0 e_{11} K_{11} v X}{(c_{11} K_{11} - e_{11}^2) p (p + \alpha)} &= 0 \end{aligned} \right\} \quad \dots(7)$$

Solving for A and B and substituting in (6) we find $\bar{\xi}$. This, when inversely transformed, gives ξ for any value of x and t . In particular,

$$\begin{aligned} (\bar{\xi})_{x=0} &= A + B - \frac{P_0 e_{11}}{\rho} \cdot \frac{1}{p^2 (p + \alpha)} \\ &= - \left(\frac{2 P_0 e_{11} K_{11} v X}{(c_{11} K_{11} - e_{11}^2) p (p + \alpha)} \right) \left(e^{-\frac{pX}{v}} - e^{-\frac{pX}{v}} \right) \\ &\quad + \frac{P_0 e_{11}}{\rho} \cdot \frac{1}{p^2 (p + \alpha)} \end{aligned}$$

Expanding the first term on the righthand side binomially, as in Redwood (1961), and retaining the first order terms we have

$$(\bar{\xi})_{s=0} = - \frac{2 P_0 e_{11} K_{11} v \times e^{-\frac{px}{v}}}{(c_{11} K_{11} \rho_{11}^2) p (p + \alpha)} - \frac{P_0 e_{11}}{\rho} \cdot \frac{1}{p^2 (p + \alpha)}$$

Taking the inverse transform, we have

$$\begin{aligned} (\xi)_{s=0} &= \frac{P_0 e_{11}}{\rho \alpha^2} (1 - e^{-\alpha t} - \alpha t), \quad 0 < t < \frac{X}{v} \\ &= - \frac{2 P_0 e_{11} K_{11} v X}{(c_{11} k_{11} - e_{11}^2) \alpha} (1 - e^{-\alpha t}) \\ &\quad + \frac{P_0 e_{11}}{\rho \alpha^2} (-1 + e^{-\alpha t} + \alpha t), \quad t > \frac{X}{v}. \end{aligned}$$

Thus the response by the plate is partly transient, partly linear in time and partly independent of time, similar to what we observe for a plate with rigidly backed extremities.

REFERENCES

- Cady, W. 1946 *Piezoelectricity*, Mc. Graw Hill Book Co.
- Das, N. C. 1967 *Indian Jour. Phys.* **41**, 611.
- Giri, R. R. 1966 *Rev. Roum. Techn. Sc.* **11**, 253.
- 1967 *Proc. Nat. Inst. Sc. India A*, **33**, 325.
- Mason, W. P. 1948 *Electromechanical transducers and wave filters*, D. Van Nostrand Co.
- 1960 *Piezoelectric crystals and their applications to ultrasonics*, D. Van Nostrand Co. New Jersey.
- Redwood, M. 1961 *Jour. Acoust. Soc. Amer.* **33**, 527.
- Roy, P. 1967c *Indian Jour. Pure & Appl. Phys.* **5**, 152.
- Sinha, D. K. 1962 *Indian Jour. Theor. Phys.* **10**, 21.
- 1965 *Proc. Nat. Inst. Sc. Indian A*, **31**, 395.
- 1966 *Bull. Cal. Math. Soc.* **58**, 15.
- 1967 *Indian Jour. Phys.* **41**, 925.
- 1968 *Proc. Indian Jour. Pure & Appl. Phys.* **5**, 611.
- Stuetzer, O. M. 1967 *Jour. Acoust. Soc. Amer.* **42**, 502.
- Swann, W. F. G. 1950 *Jour. Frank. Inst.* **250**, 219.

Propagation of shock waves in earth's atmosphere

By V. P. SINGH

Defence Science Laboratory, Delhi†

(Received 28 July 1969)

A plane shock wave as it propagates vertically upward in the static atmosphere of earth is studied. Variation of Mach number and velocity of the shock is obtained analytically by using Whitham's Rule. It is found that shock velocity increases as the shock propagates in an atmosphere with decreasing density normal to the plane of the shock front.

INTRODUCTION

Problem of propagation of shock waves in non-uniform medium with various density distributions has been discussed by different authors, such as, Kopal (1956), Carrus *et al* (1951), Grover & Hardy (1966). These authors have used the technique of similarity solutions and have found the behaviour of the fluid flow in the presence of shock waves.

Applying Whitham's method (1958) to the propagation of shock waves in a non-homogeneous medium, Bhatnagar & Sachdev (1966) have obtained the differential relation between the Mach number, pressure and density. This differential equation was integrated numerically for different stellar models.

In the present paper we have also used the Whitham's rule and discussed the problem of propagation of shock waves in the earth's atmosphere. With minor changes the experimental data for temperature distribution given by Mitra (1952) has been used. It is assumed that the gravity is varying as

$$g_0 = g_1 \left(\frac{R_0}{R_0 + x_0} \right)^2 \quad \dots(1)$$

where g_1 is the value of g_0 at the surface of the earth, R_0 is the radius of the earth and x_0 is the vertical distance from the surface of the earth. Using different temperature distributions of the earth's atmosphere, the variation of the Mach number of the shock is obtained. In the latter part, the results are combined to find the variation of shock velocity as the shock propagates in the atmosphere. Variation of shock velocity is shown in figure 1. It is found that the shock velocity increases as the shock propagates into the medium which becomes rarer and rarer with the distance measured from the surface of the earth.

As the shock velocity increases with the distance, high velocity of the shock causes the fluid velocity to be greater than the escape velocity in

† Present address : Terminal Ballistic Research Laboratory, Chandigarh.

the upper atmosphere. But at such a height, the density of the fluid is so small that very small quantity of the fluid escapes from the earth's gravity.

This study of the atmosphere is somewhat approximate, partly because the temperature variations in the atmosphere are not exactly what we have considered, partly because the method used is approximate. Moreover the effects of magnetic field, turbulent motion of gases in the atmosphere and solar radiations, which have not been taken into account, are disturbing the atmosphere. But in all, this study leads us to a physical picture of the shock wave propagation in the atmosphere of the earth.

FORMULATION OF THE PROBLEM

We assume that there is an intense explosion at the surface of the earth, due to which a strong shock wave propagates in the atmosphere. As the radius of the earth is very large in comparison to the height of the atmosphere, therefore it can be assumed that the layers of the atmosphere are planar and the path of shock wave is one dimensional. Taking x -axis to be normal to the surface of the earth, let p_1, ρ_1, T_1, g_1 and p_0, ρ_0, T_0, g_0 be pressure, density, absolute temperature and acceleration due to gravity at the surface of the earth and at a distance x_0 from the surface. The gravity g_0 at a distance x_0 is assumed (Mitra 1952) to be as given in equation. The pressure variations in equilibrium conditions is given by,

$$\frac{dp_0}{p_0} = - \frac{g_0}{RT_0} dx_0 \quad \dots (2)$$

where R is the gas constant. We take α a standard constant, having dimensions as inverse of a distance, as

$$\alpha = \frac{g_1}{RT_1} \quad \dots (3)$$

and u, p, ρ, x, t , and g as the dimensionless fluid velocity, pressure, density, distance, time and acceleration due to gravity, as

$$u = \sqrt{\gamma u_0 c_1}, \bar{p} = p_0/p_1, \bar{\rho} = \rho_0/\rho_1, x = \alpha x_0, \\ \bar{R} = \alpha R_0, t = \frac{\alpha c_1 t_0}{\sqrt{\gamma}} \text{ and } g = g_0/g_1 \quad \dots (4)$$

where $c_1^2 = \gamma p_1/\rho_1$

The equations of motion in dimensionless parameters can be written as

$$\begin{aligned}\frac{\partial \rho}{\partial t} + u \frac{\partial \rho}{\partial x} + \rho \frac{\partial u}{\partial x} &= 0 \\ \frac{\partial u}{\partial t} + u \frac{\partial u}{\partial x} + \frac{1}{\rho} \frac{\partial p}{\partial x} + \left(\frac{\bar{R}}{\bar{R} + x} \right)^2 &= 0 \\ \frac{\partial}{\partial t} (p \rho^{-\gamma}) + u \frac{\partial}{\partial x} (p \rho^{-\gamma}) &= 0.\end{aligned}\quad \dots (5)$$

When the shock produced on the earth reaches a distance $x = r$ where u, p, ρ , are the fluid velocity, pressure and density and if u_s, p_s, ρ_s , are the values of u, p, ρ , behind the shock front, Rankine-Hugoniot relations are given by,

$$\begin{aligned}u_s(r, t) &= \frac{2c}{(\gamma+1)} \{M - M^{-1}\} \\ p_s(r, t) &= \frac{\gamma p}{(\gamma+1)} f(M)\end{aligned}\quad \dots (6)$$

$$\rho_s(r, t) = \frac{(\gamma+1)\rho M^2}{g(M)}$$

where

$$f(M) = \left\{ 2M^2 - \frac{\gamma-1}{\gamma} \right\}$$

$$g(M) = \{2 + (\gamma-1)M^2\} \quad \dots (7)$$

and

$$c^2 = \gamma p / \rho.$$

We apply Whitham's Rule to the flow parameters behind the shock front. Equation of motion along the positive characteristic axis, just behind the shock front is,

$$dp_s + \rho_s c_s du_s + \frac{\rho_s c_s}{u_s^2 + c_s^2} \left(\frac{\bar{R}}{\bar{R} + r} \right)^2 dr = 0 \quad \dots (8)$$

Substituting values of parameters u_s, ρ_s and c_s from relations (6) and (7) in relation (8), we get after some simplifications,

$$\begin{aligned}2\{(M^2 + 1)h(M) + 2M^2\} \frac{dM}{M} + f(M) \frac{dp}{p} + 2(M^2 - 1)h(M) \frac{dc}{c} \\ + \left(\frac{\bar{R}}{\bar{R} + r} \right)^2 \frac{(\gamma+1)^2 M^2 h(M) dr}{c^2 \{2(M^2 - 1) + 1/r + g\}} = 0\end{aligned}\quad \dots (9)$$

where c is the dimensionless sound velocity and r is the distance of the shock front from the surface of the earth. The equation (9) gives the relation between M, p and c . If the absolute temperature is given, one

can find pressure from equation (2) and M can be calculated from the relation (9).

Now the atmosphere can be adiabatic or isothermal or the temperature may be monotonically increasing or decreasing in it. Therefore, the relation (9) has been discussed for different cases.

ADIABATIC ATMOSPHERE

The atmosphere of the earth is extremely transparent to the radiations from the sun, and is hardly heated by it. Thus almost all the radiation from the sun falls on the surface of the earth. The radiation falling on the surface of the earth is reflected back to the atmosphere in the form of infrared rays. The infrared rays are absorbed by the carbon dioxide and water vapour in the lower part of the atmosphere. Thus near the surface of the earth, the temperature falls rapidly with the height. This rapid fall produces instability in the density of the atmosphere and thus there are strong air currents in this region. They stabilize the fluctuations in the temperature. As the rate of conduction of heat in the gases is very small, therefore an adiabatic equilibrium condition is set up. This state occurs in the troposphere. For adiabatic atmosphere the dimensionless pressure, density, temperature and sound velocity are given as,

$$\begin{aligned} p &= \left[1 - \frac{\gamma-1}{\gamma} \frac{\bar{R}x}{\bar{R}+x} \right]^{\frac{\gamma}{(\gamma-1)}} \\ \rho &= \left[1 - \frac{\gamma-1}{\gamma} \frac{\bar{R}x}{\bar{R}+x} \right]^{\frac{1}{(\gamma-1)}} \quad \dots(10) \\ T &= \left[1 - \frac{\gamma-1}{\gamma} \frac{\bar{R}x}{\bar{R}+x} \right] \\ c^2 &= \gamma p / \rho, \end{aligned}$$

Substituting the value of p and c from (10) into (9), one gets after some simplifications at $x = r$,

$$\frac{2}{M} \frac{dM}{dr} = K_s(M) \frac{(\bar{R}/(\bar{R}+r))^2}{\left[1 - \frac{\gamma-1}{\gamma} \frac{\bar{R}r}{\bar{R}+r} \right]} \quad \dots(11)$$

where,

$$K_s(M) = K_1(M) + \frac{\gamma-1}{\gamma} K_2(M) \quad \dots(12)$$

$$K_1(M) = \frac{\left\{ f(M) - \frac{(\gamma+1)^2 \gamma M^2 h(M)}{2(M^2-1) + \sqrt{\gamma+g}} \right\}}{\{(M^2+1)h(M) + 2M^2\}} \quad \dots(13)$$

$$K_2(M) = \frac{2(M^2-1)h(M)}{\{(M^2+1)h(M) + 2M^2\}}$$

From the numerical computations it is found that variation in $K_1(M)$ and $K_2(M)$ and therefore in $K_3(M)$ is small for values of M greater than 3. Therefore for the purpose of integration, we can take $K_3(M)$ outside the integral sign while integrating equation (11).

Integrating relation (11) between $r = 0$ to $r = r$ one gets,

$$M = M_i \left[1 - \frac{\gamma-1}{\gamma} \frac{Rr}{R+r} \right]^{-\frac{\gamma K_3(M)}{2(\gamma-1)}} \quad \dots(14)$$

and hence the shock velocity U can be obtained as,

$$U = \sqrt{\gamma} M_i \left[1 - \frac{\gamma-1}{\gamma} \frac{Rr}{R+r} \right]^{-\left(\frac{\gamma K_3}{\gamma-1} - 1 \right)/2} \quad \dots(15)$$

The relations (14) and (15) give variation of Mach number and shock velocity in an adiabatic atmosphere. It is observed from these expressions that the adiabatic atmosphere is monotonically decreasing only for

$$r < \frac{\gamma R}{(\gamma-1)R-\gamma} \quad \text{or} \quad \frac{\gamma}{\gamma-1} = 3.5, \quad \text{for } \gamma = 1.4.$$

It is also observed that

Mach number and shock velocity increase as r increases from zero to 3.5. At $r = 3.5$, there is discontinuity, meaning that the atmosphere is unstable.

ISOTHERMAL ATMOSPHERE

In case there are no external forces acting on the atmosphere, there will be no motion of the air. Since conduction of heat from one part of the atmosphere to the other is slow, in the absence of the external forces the atmosphere will attain uniform temperature after sufficient length of time. If T_1 be uniform dimensionless temperature, p_1 the pressure at $x = x_1$, the pressure at a distance $x, x \gg x_1$, is given by,

$$p = p_1 \exp \left\{ -R^2(x - x_1)/T_1(R + x_1)(R + x) \right\} \quad \dots(16)$$

substituting the value of p in equation (9), one gets at $x = r$,

$$\frac{2}{M} \frac{dM}{dr} = \left(\frac{R}{R+r} \right)^2 \frac{K_1(M)}{T_1} \quad \dots(17)$$

Integrating (17) taking $K_1(M)$ to be constant for the purpose of integrating, it is easy to get,

$$M = M_1 \exp \left\{ \frac{\bar{R}^2 K_1(M) (r - r_1)}{2T_1 (\bar{R} + r_1) (\bar{R} + r)} \right\} \quad \dots(18)$$

and the shock velocity as,

$$U = U_1 \exp \left\{ \frac{\bar{R}^2 K_1(M) (r - r_1)}{2T_1 (\bar{R} + r_1) (\bar{R} + r)} \right\} \quad \dots(19)$$

where M_1 , U_1 are the Mach number and the shock velocity at $r = r_1$.

MEDIUM WITH MONOTONICALLY INCREASING TEMPERATURE

In the upper atmosphere, ultraviolet rays of the sun cause some of the air to ionise, which combines with oxygen and forms ozone. Ozone is found at the height of 10 km to 15 km from the surface of the earth. It absorbs the heat of the sun and thus the atmosphere is heated by it. The heat absorbed up to the height of 30 km is negligible, but beyond 30 km the temperature of the atmosphere starts increasing. Here gas is much rarefied. If β is the rate of increase of temperature per kilometer, T_2 the temperature at a distance x_2 , the beginning of the hot layer, we have

$$T = T_2 + \frac{\beta}{\alpha T_2} (x - x_2) \quad \dots(20)$$

The dimensionless pressure at a distance x_2 from the surface of the earth is,

$$p = p_2 \left\{ \frac{T_2 (\bar{R} + \bar{x})}{\bar{R}_1 (T_2 + \delta \bar{x})} \right\}^{\frac{\bar{R}^2 \delta}{(\bar{R}_1 \delta - T_2)^2}} \exp \left\{ \frac{-\bar{x} \bar{R}_1}{(\bar{R}_1 + \bar{x})(T_2 - \bar{R}_1 \delta)} \right\} \quad (21)$$

where, $\delta = \frac{\beta}{\alpha T_2}$, $\bar{R}_1 = \bar{R} + x_2$, $\bar{x} = x - x_2$, -

Substituting $\frac{dp}{p}$ and $\frac{dc}{c}$ from (21) and (20) respectively, into (9) we get,

$$\frac{2}{M} \frac{dM}{dr} = \frac{\bar{R}^2 K_1(M)}{(T_2 + \delta \bar{r})(\bar{R}_1 + \bar{r})^2} + \frac{\delta K_2(M)}{2(T_2 + \delta \bar{r})} \quad \dots(22)$$

integrating (22) between $r = r_0$ to $r = r$, we get,

$$M = M_0 \left\{ \frac{\bar{R}_1(T_2 + \delta\bar{r})}{T_2(\bar{R}_1 + \bar{r})} \right\}^{\frac{\bar{R}_0 K_1}{2(\bar{R}_1 \delta - T_0)^2}} \left\{ \frac{T_2 + \delta\bar{r}}{T_2} \right\}^{-K_1/4} \\ \times \exp \left\{ \frac{\bar{R}^2 K_1 \bar{r}}{2\bar{R}_1(R_1 + \bar{r})(T_2 - \bar{R}_1 \delta)} \right\} \quad \dots(23)$$

The relation (23) gives the variation of Mach number in hot layer. The shock velocity is obtained as,

$$U = \sqrt{\gamma} M (T_2 + \delta\bar{r})^{1/2} \quad \dots (24)$$

The hot layer extends from 30 to 50 km from the surface of the earth.

THE GENERAL PROBLEM

From the results so far discussed, one can find the variation of the Mach number and the shock velocity, when the shock propagates in the atmosphere of earth. We have considered a model in which the temperature decreases adiabatically from $x_0 = 0$ to $x_0 = 10$ km. Then it becomes constant until the height of 30 km is attained. Between 30 km to 50 km the temperature increases with gradient 5.5°K per km, K being the absolute temperature. From 50 to 55 km, temperature again remains constant and then upto 78 km it decreases with temperature gradient 9°K per km. Beyond this height it is assumed that the temperature increases continuously with temperature gradient 3.25°K per km. (Kolobkov 1960).

We assume that the shock wave propagates in the above mentioned atmosphere with initial Mach number 4 at the surface of the earth. The variation of shock velocity is computed from relation (15) for adiabatic atmosphere, from (19) for isothermal atmosphere and from (23) and (24) for atmosphere with increasing temperature and is shown in figure 1. It can be seen that the shock velocity increases as the shock propagates in the decreasing density medium. The variation of shock velocity is slower in isothermal medium, but is sharp in the rest of the medium. It is concluded that the variation of shock velocity mainly depends on the density of the medium and increases as the density decreases, and is not much effected by the variation of the temperature.

ESCAPE OF GASES FROM ATMOSPHERE

When the shock moves in the gaseous medium, the fluid behind the shock is also set in motion. If the fluid velocity is greater than the escape

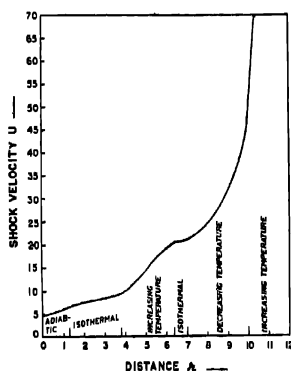


Figure 1. Variation of the shock velocity in the atmosphere.

velocity of the gas particles, the particles will escape the earth's gravitation and go into space. The escape velocity of the fluid particles is given by,

$$v_E^2 = \frac{2g\bar{R}^2}{(\bar{R} + r)}$$

In figure 2 we have drawn the fluid velocity behind the shock and escape velocity versus distance from the surface of the earth. It is found that the fluid velocity is greater than the escape velocity at a distance $r = 10$. But at such a height the density of the air is very small and the amount

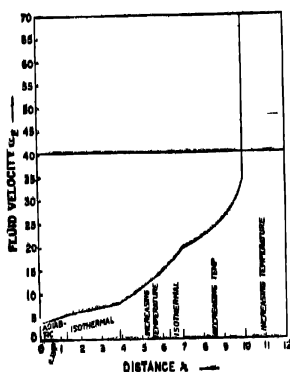


Figure 2. Variation of the fluid velocity behind the shock front in the atmosphere.

of the gas escaping in the space is negligible as compared to the huge mass of the atmosphere.

CONCLUSION

Although the model considered is idealized yet it leads us to some significant results. It is found that the strength of the shock goes on increasing as the atmosphere becomes rarefied. In isothermal part, the increase in shock velocity is small but is large in layers in which the temperature decreases. Above 78 km of height, we have assumed temperature to be increasing. In this region the shock becomes stronger and stronger as it propagates upwards. In ionosphere the gas is much rarefied and is ionized too. Is this region fluid velocity becomes greater than the escape velocity, so that some of the gas escapes from the earth's gravitation, though the amount of the gas escaped is very small as compared to the whole mass of the atmosphere.

Beauty of the method considered in this investigation is that it can be applied to the more complex problems of the earth's atmosphere. The method used is simple, although a bit approximate. By this method it is possible to get analytic relations for the Mach number and the shock velocity, which was not so easy by the earlier methods. It can be directly seen that Mach number and the shock velocity are variables, not constant as shown in references. (Bhatnagar & Sachdev 1966 ; Carrus 1951 ; Kopal 1956).

The author is thankful to Dr. Prem Kumar, for his sincere guidance and to Dr. R. S. Srivastava and Dr. R. R. Agarwal, for their interest in the work. Thanks are also due to Dr. Kartar Singh, Director, D.S.L. Delhi, for his kind permission to publish the work.

REFERENCES

- Bhatnagar, P. L. & Sachdev, P. L. 1966 *Nuovo Cimento*, **44**, 15.
Carrus, P. A., Fox, P. A., Kopal, Z. & Haas, F 1951 *Ap. J.*, **113**,
Grover, R. & Hardy, J. W. 1966 *Ap. J.*, **143** 193, 496, 48.
Kopal, Z. 1956 *Ap. J.*, **120**, 159.
Kolobkov, N., 1960 *Our Atmospheric Ocean*, Foreign Language Publishing House, Moscow, **41**.
Mitra, S. K. 1952, *Upper Atmosphere*, Asiatic Society, Calcutta.
Whitham, G. B., 1958 *J. Fluid Mech.*, **4**, 337.

Free convection oscillatory flow along an infinite vertical plate with constant suction

By KRISHNA LAL

Banaras Hindu University, Varanasi-5, India

(Received 5 July 1969)

Similarity solution using spiral group transformations has been obtained. For constant suction at the wall, the velocity and temperature of the wall have been found to vary according to $\exp(p\bar{t})$, p being certain constant. The equations of motion and energy have been linearized and solved. For small frequency of oscillation, the skin friction is found to be constant after some time. The rate of heat transfer from the plate to the fluid has a phase lead over the surface temperature fluctuations for small and large frequency of oscillations.

BASIC EQUATIONS

Taking \bar{x} axis vertically along the plate and \bar{y} axis perpendicular to it, the basic equations which describe the unsteady free convection flow of a viscous incompressible fluid of density ρ past an infinite flat plate are

$$\frac{\partial \bar{v}}{\partial \bar{t}} = 0 \quad \dots (1.1)$$

$$\frac{\partial \bar{u}}{\partial \bar{t}} + \bar{v} \frac{\partial \bar{u}}{\partial \bar{y}} = g\beta (\bar{T} - \bar{T}_\infty) + \nu \frac{\partial^2 \bar{u}}{\partial \bar{y}^2} \quad \dots (1.2)$$

$$\frac{\partial \bar{v}}{\partial \bar{t}} = -\frac{1}{\rho} \frac{\partial \bar{p}}{\partial \bar{y}} \quad \dots (1.3)$$

$$\frac{\partial \bar{T}}{\partial \bar{t}} + \bar{v} \frac{\partial \bar{T}}{\partial \bar{y}} = k \frac{\partial^2 \bar{T}}{\partial \bar{y}^2} \quad \dots (1.4)$$

where \bar{u} , \bar{v} are the velocity components, \bar{T} is the temperature, g the acceleration due to gravity, β is the coefficient of volume expansion, k is the thermal diffusivity, \bar{p} is the pressure, \bar{T}_∞ is the equilibrium temperature.

We introduce dimensionless quantities

$$\left. \begin{aligned} y &= \bar{y}/L, \quad t = \nu \bar{t}/L^2, \quad u = \frac{\bar{u}L}{\nu}, \quad v = \frac{\bar{v}L}{\nu} \\ T &= g\beta L^3 (\bar{T} - \bar{T}_\infty)/\nu^2, \quad p = \bar{p}L^3/\rho\nu^2 \end{aligned} \right\} \quad \dots (1.5)$$

where L is the characteristic length. Thus we have from above equations

$$\frac{\partial v}{\partial y} = 0 \quad \dots (1.6)$$

$$\frac{\partial u}{\partial t} + v \frac{\partial u}{\partial y} = T + \frac{\partial^2 u}{\partial y^2} \quad \dots(1.7)$$

$$\frac{\partial v}{\partial t} = - \frac{\partial p}{\partial y} \quad \dots(1.8)$$

$$\frac{\partial T}{\partial t} + v \frac{\partial T}{\partial y} = \frac{1}{\sigma} \frac{\partial^2 T}{\partial y^2} \quad \dots(1.9)$$

where σ is the Prandtl number.

The boundary conditions are

$$\left. \begin{aligned} y = 0, u = 0, v = v_0 f(t), T = 1 + \epsilon \cos \omega t, \epsilon \ll 1 \\ y = \infty, u = 0, T = 0 \end{aligned} \right\} \quad \dots(1.10)$$

SIMILARITY SOLUTIONS BY SPIRAL TRANSFORMATIONS

To get the similar solutions of the equations (1.7) and (1.9), we introduce

$$t = \bar{t} + \beta_1 b, u = e^{\beta_2 b} \bar{u}, v = e^{\beta_3 b} \bar{v}, y = e^{\beta_4 b} \bar{y}, T = e^{\beta_5 b} \bar{T} \quad \dots(1.11)$$

into above equations, where $\beta_1, \beta_2, \beta_3, \beta_4, \beta_5$ and b are certain constants.

Thus we have following relations between the constants

$$\left. \begin{aligned} \beta_2 = \beta_2 + \beta_3 - \beta_4 = \beta_5 = \beta_2 - 2\beta_4 \\ \beta_5 = \beta_3 + \beta_5 - \beta_4 = \beta_5 - 2\beta_4 \end{aligned} \right\} \quad \dots(1.12)$$

which give

$$\beta_2 = \beta_5, \beta_3 = \beta_4 = 0 \quad \dots(1.13)$$

Substituting from equations (1.13) into (1.11), we see that

$$\left. \begin{aligned} \frac{u}{e^{pt}} &= \frac{\bar{u}}{e^{p\bar{t}}} \\ v &= v_0 \text{ (constant)} \\ y &= \bar{y} \\ \frac{T}{e^{pt}} &= \frac{\bar{T}}{e^{p\bar{t}}} \end{aligned} \right\} \quad \dots(1.14)$$

where $p = \beta_4/\beta_1 = \text{constant}$.

And the absolute invariants are

$$\left. \begin{aligned} u &= F(y)e^{pt} \\ T &= \theta(y)e^{pt} \\ v &= -v_0 \text{ (for suction)} \end{aligned} \right\} \quad \dots(1.15)$$

for similarity solutions

METHOD OF SOLUTION

In solving equations (1.7) and (1.9) for constant suction at the wall, we replace the first boundary condition for T as

$$T = 1 + \epsilon e^{i\omega t} \quad \dots(2.1)$$

and replace u , v and T by

$$\left. \begin{aligned} u &= u_s + \epsilon u_1 e^{i\omega t} \\ v &= -v_0 \text{ (constant)} \\ T &= T_s + \epsilon T_1 e^{i\omega t} \end{aligned} \right\} \quad \dots(2.2)$$

in above equations where u_s , T_s the steady mean flow satisfy

$$\left. \begin{aligned} -v_0 \frac{du_s}{dy} &= T_s + \frac{d^2 u_s}{dy^2} \\ -v_0 \frac{dT_s}{dy} &= \frac{1}{\sigma} \frac{d^2 T_s}{dy^2} \end{aligned} \right\} \quad \dots(2.3)$$

with boundary conditions

$$\left. \begin{aligned} y=0 : u_s &= 0, T_s = 1 \\ y=\infty : u_s &= 0, T_s = 0 \end{aligned} \right\}$$

and equating the coefficient of $\epsilon e^{i\omega t}$, we find that u_1 and T_1 satisfy

$$\left. \begin{aligned} i\omega u_1 - v_0 \frac{du_1}{dy} &= T_1 + \frac{d^2 u_1}{dy^2} \\ i\omega T_1 - v_0 \frac{dT_1}{dy} &= \frac{1}{\sigma} \frac{d^2 T_1}{dy^2} \end{aligned} \right\} \quad \dots(2.5)$$

With the boundary conditions

$$\left. \begin{aligned} y=0 : u_1 &= 0, T_1 = 1 \\ y=\infty : u_1 &= 0, T_1 = 0 \end{aligned} \right\} \quad \dots(2.6)$$

Solving above equations we have

$$u_s = \frac{1}{v_0^2(\sigma - \sigma^2)} [\exp(-\sigma v_0 y) - \exp(-v_0 y)] \quad \dots(2.7)$$

$$T_s = e^{-\sigma v_0 y} \quad \dots(2.8)$$

$$T_1 = e^{-h y} \quad \dots(2.9)$$

$$u_1 = \frac{1}{h^2 - v_0 h - i\omega} [\exp(-S y) - \exp(-h y)] \quad \dots(2.10)$$

$$\text{where } h = \frac{v_0 \sigma}{2} \left[1 + \left(1 + \frac{4i\omega}{v_0^2 \sigma} \right)^{1/2} \right] \quad \dots(2.11)$$

$$\text{and } S = \frac{v_0}{2} \left[1 + \left(1 + \frac{4i\omega}{v_0^2 \sigma} \right)^{1/2} \right] \quad \dots(2.12)$$

DISCUSSIONS

(i) When frequency is small

Expanding for h and S , in powers of ω , we find that

$$h \simeq \sigma v_0 + \frac{i\omega}{v_0} + \frac{\omega^2}{v_0^3 \sigma} + O(\omega^3) \quad \dots(3.1)$$

$$S \simeq v_0 + \frac{i\omega}{v_0} + \frac{\omega^2}{v_0^3} + O(\omega^3) \quad \dots(3.2)$$

Thus, we get for u_1 and T_1

$$\begin{aligned} u_1 = & \frac{1}{v_0^2(\sigma^2 - \sigma)} \left\{ \left(e^{-v_0 y} - e^{-v_0 \sigma} \right) + \frac{i\omega}{v_0} \left[y \left(e^{-v_0 \sigma y} - e^{-v_0 y} \right) \right. \right. \\ & + \left. \frac{2(\sigma - v_0)}{v_0^2(\sigma^2 - \sigma)} \left(e^{-v_0 \sigma y} - e^{-v_0 y} \right) \right] + \frac{\omega^2}{v_0^2} \left[\frac{(e^{-v_0 y} - e^{-v_0 \sigma})}{v_0^2 \sigma^2} \right. \\ & + \frac{4(\sigma - v_0)^2}{v_0^2(\sigma^2 - \sigma)^2} \left(e^{-v_0 \sigma y} - e^{-v_0 y} \right) + \frac{2y(\sigma - v_0)}{v_0^2(\sigma^2 - \sigma)} \\ & + \left(e^{-v_0 \sigma y} - e^{-v_0 y} \right) + \frac{y}{\sigma v_0} \left(e^{-v_0 \sigma y} - e^{-v_0 y} \right) \\ & \left. \left. + \frac{y^2}{2} \left(e^{-v_0 \sigma y} - e^{-v_0 y} \right) \right] \right\} \quad \dots(3.3) \end{aligned}$$

$$T_1 = e^{-v_0 \sigma y} \left\{ 1 - \frac{i\omega y}{v_0} - \frac{\omega^2}{v_0^2} \left(\frac{y}{v_0 \sigma} + \frac{y^2}{2} \right) + \dots \right\} \quad \dots(3.4)$$

From above expressions (3.3) and (3.4) we see that the solutions for u_1 and T_1 as given by the equations (2.7) and (2.8) are obtained by putting $\omega = 0$.

The velocity field in the boundary layer is given by

$$v(y, t) = \frac{1}{v_0^2(\sigma - \sigma^2)} \left[e^{-\sigma v_0 y} - e^{-v_0 y} \right] + \frac{\epsilon e^{i\omega t} [e^{-S y} - e^{-h y}]}{h^2 - v_0 h - i\omega} \quad \dots(3.5)$$

The skin friction τ_0 is given by

$$\begin{aligned} \tau_0 = & \mu \left(\frac{\partial u}{\partial y} \right)_{y=0} \\ = & \frac{\mu v}{L^2} \left[\frac{1}{\sigma v_0} + \frac{h - S}{h^2 - h v_0 - i\omega} \epsilon e^{i\omega t} \right] \quad \dots(3.6) \end{aligned}$$

Thus the non-dimensional form of τ_0 defined by τ'_0 is given by

$$\tau'_0 = \frac{\tau_0 L^2}{\mu v} = \frac{1}{\sigma v_0} + \epsilon |\beta| \cos(\omega t + \alpha) \quad \dots(3.7)$$

$$\left. \begin{aligned} \text{where } B &= B_r + i B_i = \frac{h - S}{h^2 - v_0 h - i \omega} \\ \text{and } \alpha &= \tan^{-1} \frac{B_i}{B_r} \end{aligned} \right\} \quad \dots(3.8)$$

For small value of ω , we see that

$$\begin{aligned} \frac{h - S}{h^2 - v_0 h - i \omega} &= \left\{ \frac{1}{\sigma v_0} - \frac{\omega^2}{\sigma^2 v_0^3} \left[1 + \frac{4(\sigma - v_0)^2}{\sigma(\sigma - 1)^2 v_0^2} \right] \right\} \\ &+ i \left\{ -\frac{2\omega(\sigma - v_0)}{v_0^4 \sigma^2 (\sigma - 1)} \right\} \end{aligned} \quad \dots(3.9)$$

Thus for $\sigma > v_0$, we see that

$$\tau'_0 = \frac{1}{\sigma v_0} + \epsilon |B| \cos(\omega t - \alpha) \quad \dots(3.10)$$

and for

$$\omega t - \alpha = \pi(n + \frac{1}{2}), \quad n = 0, 1, 2, \quad \dots(3.11)$$

the skin-friction becomes independent of time.

Hence after time t , given by

$$\frac{1}{\omega} [\alpha + \pi(n + \frac{1}{2})]$$

the skin friction is independent of time and remains a constant quantity.

The rate of heat transfer from the wall to the fluid is

$$q = -k \left(\frac{dT}{dy} \right)_{y=0} = \frac{k\nu^2}{L^2 \eta \beta} (\sigma v_0 + h \epsilon e^{i\omega t}) \quad \dots(3.12)$$

Defining non-dimensional quantity q' by

$$q' = q L^2 \eta \beta / k \nu^2,$$

$$\text{we have } q' = \sigma v_0 + \epsilon e^{i\omega t} (h_r + i h_i) \quad \dots(3.13)$$

where

$$h = h_r + i h_i = \left(v_0 \sigma + \frac{\omega^2}{v_0^3 \sigma} \right) + i \left(\frac{\omega}{v_0} \right) -$$

for small frequency of oscillations.

Thus

$$q' = \sigma v_0 + \epsilon |h| \cos(\omega t + \beta) \quad \dots(3.14)$$

$$\text{where } \beta = \tan^{-1} \frac{h_i}{h_r}$$

and the rate of heat transfer from the plate to the fluid has a phase lead over the surface temperature fluctuations. This phase lead, β increases as ω decreases for given v_0 and σ .

(ii) When ω is large

In this case we may write

$$\left. \begin{aligned} h &\approx \sqrt{\frac{i\omega}{\sigma}} \\ s &\approx \sqrt{i\omega} \end{aligned} \right\} \quad \dots 3.15$$

and thus

$$T_1 = e^{-y\sqrt{i\omega/\sigma}} \quad \dots 3.16$$

$$u_1 = \frac{1}{i\omega \left(\frac{1-\sigma}{\sigma} \right) - v_0 \sqrt{\frac{i\omega}{\sigma}}} \left[e^{-y\sqrt{i\omega}} - e^{-y\sqrt{i\omega/\sigma}} \right] \quad \dots 3.17$$

$$\tau_0' = \frac{1}{\sigma v_0} + E |A| \cos(\omega t + \gamma) \quad \dots 3.18$$

$$\left. \begin{aligned} \text{where } A = A_r + i A_i = \frac{\sqrt{\sigma} - \sigma}{\sqrt{i\omega(1-\sigma)} - v_0 \sqrt{\sigma}} \\ r = \tan^{-1} \frac{A_i}{A_r} \end{aligned} \right\} \quad \dots 3.19$$

We find that γ is a positive quantity and thus τ_0' decreases as γ increases. Similarly, we see that

$$q' = \sigma v_0 + \epsilon h e^{i\omega t} = \sigma v_0 + \epsilon |l| \cos(\omega t + \delta) \quad \dots 3.20$$

where

$$l = l_r + i l_i + \sqrt{\frac{i\omega}{\sigma}}, \quad \delta = \tan^{-1} \frac{l_i}{l_r}$$

$$\text{Thus } \delta = \pi/u, \quad |l| = \sqrt{\omega/\sigma}$$

In this case the rate of heat transfer from the plate to the fluid has a phase lead over the surface temperature fluctuations by an angle $\frac{\pi}{4}$

CONCLUSION

For small frequency of oscillations, the skin friction lags behind by a certain angle while for large frequency of oscillations, it leads by the same angle over the wall temperature. For large value of ω , we see that the rate of heat transfer from the wall to the fluid leads by an angle 45° .

REFERENCES

- Messiha, S.A.S. 1966 *Proc. Camb. Phil. Soc.* **62** 329.
 Na, T. Y. 1964 *AIAA Jour.* **3**, No. 2 (Tech. notes), 378.

Waves in metals at low temperatures

By P. MISRA*

Department of Physics, Ravenshaw College, Cuttack.

AND

S. K. RAY,

Department of Physics, B. J. B. College, Bhubaneswar

(Received 27 July 1969)

From the explicit expressions of response function, obtained by Misra (1966), the nature of waves that can propagate inside metals at extremely low temperatures can be analysed in presence of a steady magnetic field. The results so obtained are similar to the experimental results of Bowers *et al* (1961). They reported that at 4°K in presence of a magnetic field of 10,000 gauss waves of frequency 32 cycles/sec. can propagate inside sodium in the direction of the field with a phase velocity of 0.68 cm./sec.

INTRODUCTION

Inside metals, there are positive ions and free electrons. It can be considered that these free electrons are moving on a positive background. Hence these can be treated as electron gas. The density of these electrons is very high i.e., 10^{23} per c.c. Therefore, at low temperature the free electrons inside metals are degenerate in the statistical sense, and the thermal velocity of electrons obey Fermi-Dirac distribution law. Misra (1966) obtained expressions for the response function of an electron gas using Fermi-Dirac statistics. Therefore, his results can be used to study the nature of wave propagation inside metals.

Refractive Index from Response Function :

In the presence of a magnetic field the dielectric function is an unsymmetric tensor and not real even in the absence of absorption. In this case displacement vector is parallel to the electric field only when they are in the direction of the magnetic field, i.e.

$$D_3 = \epsilon_{33} E_3 \quad \dots(1)$$

But for other components

$$D_1 \pm iD_2 = (\epsilon_{11} \pm i\epsilon_{12}) (E_1 \pm iE_2) \quad \dots(2)$$

From this it is clear that the displacement vector in the XY plane is proportional to the electric field that rotates clockwise or counter-clockwise. Therefore we can write from equation (2)

$$D_{1r} = \epsilon_{1r} E_{1r} \quad \dots(3)$$

*Present Address : Reader in Physics, S. C. S. College, Puri.

Hence ϵ_{lr} can be expressed in terms of the response function as follows :

$$\epsilon_{lr} = 1 - \frac{4\pi i K_{lr}(\vec{R}, \omega)}{\omega} \quad \dots(4)$$

where $K_{lr} = K_{11} \pm iK_{12}$

Using the expressions for response function, obtained by Misra (1966) in equation (4), we get assuming the absorption to be small,

$$\begin{aligned} n_{lr}^2 = 1 - & \frac{3\omega_0^2 c}{4\omega^2 n_{lr}^3 v_0^3} \left[\frac{2cn_{lr}v_0(\omega \pm \Omega)}{\omega} \right. \\ & + \left\{ n_{lr}^2 v_0^2 - \frac{c^2(\omega \pm \Omega)^2}{\omega^2} \right\} \ln \left[\frac{c(\omega \pm \Omega) + v_0 n_{lr} \omega}{c(\omega \pm \Omega) - v_0 n_{lr} \omega} \right] \\ & - \frac{\pi^2 \omega_0^2 c}{8m^2 \beta^2 \omega^2 n_{lr} v_0^4} \left[\frac{4cn_{lr}\omega(\omega \pm \Omega)}{c^2(\omega \pm \Omega)^2 - v_0^2 n_{lr}^2 \omega^2} \right. \\ & \left. \left. + \frac{1}{v_0} \ln \left\{ \frac{c(\omega \pm \Omega) + v_0 n_{lr} \omega}{c(\omega \pm \Omega) - v_0 n_{lr} \omega} \right\} \right] \quad \dots(5) \end{aligned}$$

where we have taken $k = \frac{n_{lr} \omega}{c}$

Propagation of electromagnetic waves in a metal can be analysed with the aid of equation (5). But this expression is very lengthy and complicated. However, for the two following special cases, the wave propagation can easily be analysed,

$$\text{Case I} \quad \frac{v_0 \omega n_{lr}}{c(\omega \pm \Omega)} < 1,$$

$$\text{Case II} \quad \frac{c(\omega \pm \Omega)}{v_0 \omega n_{lr}} < 1.$$

The first case is satisfied for $n_{lr} < 1$ and $\omega > \Omega$. Under this approximation we can expand

$$\ln \left| \frac{1 + \frac{v_0 n_{lr} \omega}{c(\omega \pm \Omega)}}{1 - \frac{v_0 n_{lr} \omega}{c(\omega \pm \Omega)}} \right| \quad \text{and} \quad \left[1 - \frac{v_0^2 n_{lr}^2 \omega^2}{c^2(\omega \pm \Omega)^2} \right]^{-1}$$

in a power series of $\frac{v_0 n_{lr} \omega}{c(\omega \pm \Omega)}$ and neglect terms much less than one.

After simple calculation we get

$$n_{ir}^2 = \frac{1 - \frac{\omega_0^2}{\omega(\omega \pm \Omega)} \left[1 + \frac{3\pi^2}{4m^2\beta^2v_0^4} \right]}{1 + \frac{\omega_0^2 v_0^2 \omega}{5c^2(\omega \pm \Omega)^3} \left[1 + \frac{35\pi^2}{12m^2\beta^2v_0^4} \right]} \quad \dots(6)$$

The second case is satisfied for $\omega \sim \Omega$ as well as for ω , for which $n_{ir}^2 \gg 1$. Under this approximation we get,

$$n_{ir}^2 = 1 - \frac{3\omega_0^2 c^2 (\omega \pm \Omega)}{\omega^3 v_0^2 n_{ir}^2} \left[1 - \frac{\pi^2}{12m^2\beta^2v_0^4} \right] \quad \dots (7)$$

DISCUSSION OF THE RESULTS

From equation (6) it is clear that for $\omega_0^2 > \frac{1 + \frac{3\pi^2}{4m^2\beta^2v_0^4}}{\omega(\omega \pm \Omega)}$ refractive index is imaginary. So the wave cannot propagate through the medium. For $\omega > \omega_0$ equation (6) becomes

$$n_{ir}^2 = 1 - \frac{\omega_0^2}{\omega(\omega \pm \Omega)} \left[1 + \frac{3\pi^2}{4m^2\beta^2v_0^4} \right]$$

Further if we neglect the effect of temperature the above equation reduces to AH equation, when the wave is propagating in the direction of the magnetic field.

Equation (7) shows that n_{ir} is always imaginary for the ordinary wave. Hence the ordinary wave cannot propagate through the medium for $n_{ir} > 1$, whereas, the extra-ordinary wave can propagate through the medium for values of ω less than Ω . To get a clear picture of electromagnetic waves that can propagate through sodium at 4°K, the calculated values of n_{ir}^2 for different values of ω are given in the table. In the calculation, the magnitude of the steady magnetic field is taken to be 10^4 gauss and density of free electrons to be 2.6×10^{23} .

TABLE

ω	n_{ir}^2	ω	n_{ir}^2 imaginary
10	1.3×10^{22}	1.8×10^{11}	
60	8.3×10^{20}	9.12×10^{15}	0
192	1.14×10^{20}	1×10^{16}	0.27
10^3	1.3×10^{16}	1.5×10^{16}	0.63
10^7	13×10^{12}	2×10^{16}	0.8
10^9	6×10^9	3×10^{16}	0.91
1.5×10^{11}	8×10^8	4×10^{16}	0.95
1.75×10^{11}	4×10^8	1×10^{17}	0.99
Ω	1		

From the table it is clear that in case of sodium, electromagnetic waves, for which, $9.12 \times 10^{13} > \omega > 1.76 \times 10^{11}$, can not propagate through. But it is interesting to note that even waves of frequency of the order 10 cycles/sec. can penetrate through sodium in the direction of the magnetic field. The phase velocity of the wave is of the order of 1 cm. Similar qualitative experimental results were obtained by Bowers *et al* (1961). From their results it comes out that electromagnetic waves of 32 cycles per second can penetrate through sodium in the direction of the magnetic field of magnitude 10^4 gauss at 4°K. And the refractive index is found to be 1.5×10^9 .

The authors are grateful to Prof. Pradhan for his valuable suggestions and guidance and want to express their thanks to B. C. Ray.

REFERENCES

- Bowers, R., Legendy, C. & Rose, F. 1961 *Phys. Rev. Letters* **7**, 339.
Mishra P., 1966 *Indian J. Phys.*, **40**, 253.

Temperature effect on resistance of Tl_2Se and Tl_2Te films*

By A. M. DIOHE AND A. GOSWAMI

National Chemical Laboratory, Poona-8, India.

(Received 5 September 1969)

The variation of $\log R$ vs $1/T$ curve due to the maximum temperature of heating has been observed for Tl_2Se and Tl_2Te film and the reason for it remains unexplained.

During our recent studies of electrical properties of vacuum deposited films, it was observed that $\log R$ vs $1/T$ curves were mostly independent of the maximum temperature of heating (T_m) provided it was below the temperature of discontinuity, T_d (Goswami & Jog 1964, 1968; Goswami & Koli 1966a, b). Only recently, however, a few exceptions have been noted for Bi-Se, Sn-S and Sn-Se systems where the above curves are also dependent on T_m (Goswami & Koli 1969; Goswami & Jog 1969). A similar behaviour has also been observed in the case of Tl_2Se and Tl_2Te films and the results are reported below.

Bulk Tl_2Se and Tl_2Te compounds were prepared in the manner described previously (Barua & Goswami 1969) and deposition on glass substrate (size about 4 cm \times 0.4 cm) at room temperature in vacuo ($\approx 10^{-4}$ mm Hg). Film thickness was estimated from the difference in weight of deposits and the knowledge of deposit area assuming, however, that the density of the films was the same as that of the bulk material.

Figure 1 shows a typical $\log R$ vs $1/T$ curve for Tl_2Se films when heated continuously even beyond T_d region. Similar was also the nature

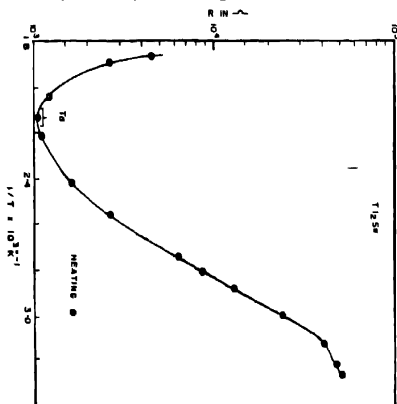


Figure 1. Variation of $\log R$ vs $1/T$ curve for continuous heating (Tl_2Se films)

*Communication No. 992 from National Chemical Laboratory, Poona-8, India.

of the curve for Tl_2Te films (figure 2). Since T_m had considerable effects on the actual heating and cooling paths as reported for Bi-Se, Sn-Se

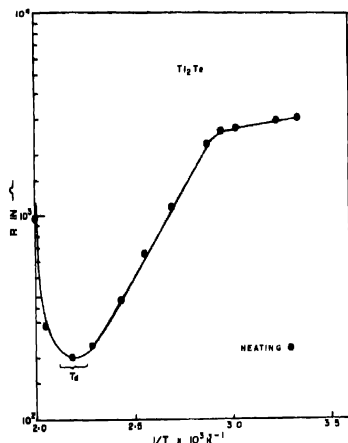
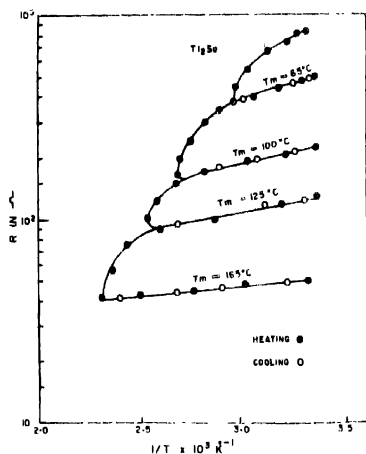
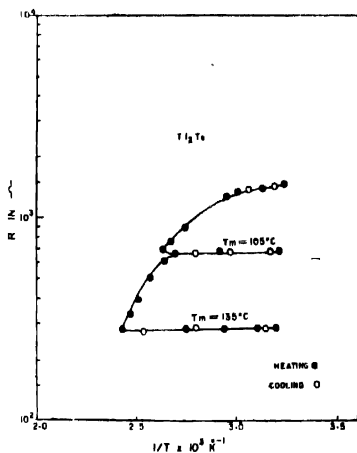


Figure 2. Variation of $\log R$ vs $1/T$ curve for continuous heating (Tl_2Te films)

systems (loc.cit.), the resistance of these were measured in the following conditions without exceeding T_d viz. (i) during heat to any T_m followed by cooling and repeating the heating and cooling cycles keeping T_m constant, (ii) raising the temperature to a new T_m followed by cooling and heating cycles as in (i) and finally (iii) increasing to new T_m in each case and followed by repeated cycles.

Figures 3 and 4 show the results of measurements for Tl_2Se and Tl_2Te film. It is seen that reaching the first T_m say $65^\circ C$ (cf figure 3) cooling curve takes a new path different from the initial heating curve. During the subsequent heating and cooling cycles the path remains the same so long as T_m ($\approx 65^\circ C$) is not exceeded. On raising T_m to a new value ($\approx 110^\circ C$), cooling path again changes and the subsequent path follows exactly the same so long maximum temperature does not exceed the above.

Figure 3. Effect of T_m on $\log R$ vs. $1/T$ curves (Ti_2Se)Figure 4. Effect of T_m on $\log R$ vs. $1/T$ curves (Ti_2Te)

Similar is the case for other new T_m say 125° and $165^\circ C$, etc. Similar has been the case for Ti_2Tc films (cf figure 4).

For a comparison of activation energy (ΔE), films of different thicknesses were arbitrarily annealed to about 125°C and results are shown in figure 5.

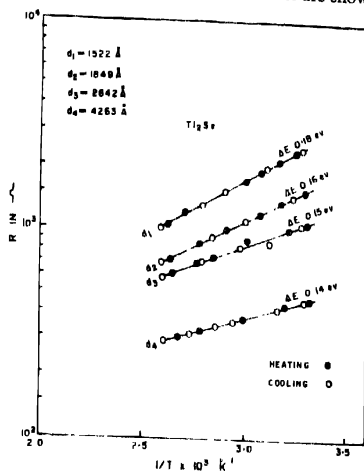


Figure 5. Variation of activation energy with film-thickness (Tl_2Se)

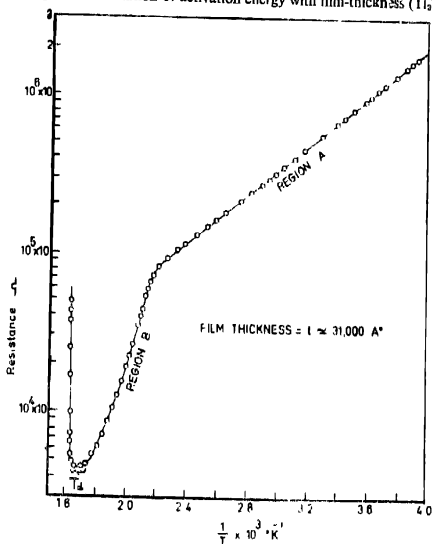


Figure 6. Variation of c.m.f. and α with film thickness (Tl_2Se)

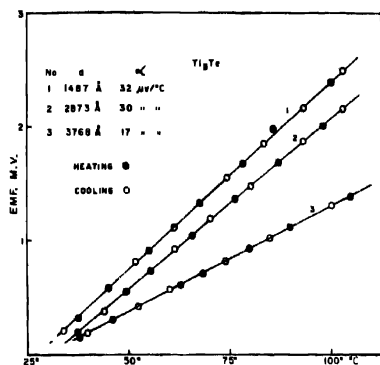


Figure 7. Variation of e.m.f. and α with film thickness (Ti_2Te).

The variation of ΔE ranges from 0.18 eV to 0.14 eV, thinner films having higher values. Figures 6 and 7 show the measurement of thermoelectric power (α) for selenide and telluride films of different thicknesses.

The above study reveals that not only the path but also the absolute resistance are dependent on the T_m which also affects the slope but only to a small extent. Similar characteristic features observed in the case of Bi-Se and Sn-S system appeared to be associated with new phase-formation (loc. cit.). In the case selenide and telluride of thallium, however, no new phase could so far be detected by electron diffraction studies (Barua & Goswami 1969) and hence these features still remain unexplained from the structural consideration.

REFERENCES.

- Barua, K. C. & Goswami, A. 1969, *Surface Science*, **14**, 415.
 Goswami, A. & Jog, R. H., 1964 *Indian J. Pure Appl. Phys.* **2**, 403.
 Goswami, A. & Jog, R. H., 1968 *Indian J. Pure Appl. Phys.* **6**, 416.
 Goswami, A. & Jog, R. H., 1968 *Indian J. Phys.* (Communicated).
 Goswami, A. & Koh, S. S. 1966, *Z. Naturforsch.* **21a**, 1462; 1966, *Proc. Int. Symp. on Basic Problem in Thin Film Physics*, 646, (Published by Van den hoeck and Ruprecht, Gottingen)

Diffusion of macromolecules by high frequency technique

By J. N. CHAKRAVORTY AND K. SENGUPTA*

Research Laboratory, Physics Department, Ramkrishna Mission

Residential College, Narendrapur, 24 Parganas (West Bengal.)

(Received 16 August 1969)

The diffusion of acacia catechuic acid molecules has been studied by high frequency oscillatory circuit operating on 8 Mc/s at a constant temperature. The graph of l vs. \sqrt{t} yields a straight line where l is the length of the column and t the time of diffusion.

INTRODUCTION

Acacia catechuic acid is a gum acid derived from the electro dialysis of acacia catechu. It has been found (Hulyalkar *et al* 1956) the gum, on acid hydrolysis yields *d*-galactose, *l*-arabinose, *d*-rhamnose and *d*-glyceronic acid. Its average molecular weight was found to be 4.8×10^6 and the root mean square end to end distance to be $327 \text{ m}\mu$ in aqueous solution (Chakravorty *et al* 1963). From viscometric and light scattering studies, (Chakravorty *et al* 1963, Kulshrestha *et al* 1962) it was established that the molecule belonged to randomly coiled type and was endowed with typical polyelectrolyte behaviour. In order to study its diffusion with distilled water the high frequency method has been adopted.

The chief advantage of the method lies in the fact that the relaxation effect of the ions has been eliminated and the measurement is followed in an "electrode free" manner i. e. without any galvanic contact with the solution. This method of measurement was used by G. G. Blake (1947) to study the diffusion of electrolyte solutions like potassium bromide with respect to water. The method has been extended here for the case of acacia catechuic acid, a typical polyelectrolyte.

EXPERIMENTAL

A glass tube of about 50 cm. in length and 1.8 cm. in diameter was filled with distilled water and was inverted vertically over a glass vessel containing a solution of 1% acacia catechuic acid. The output terminals of the oscillometer was connected to the electrode fitted outside the glass

*Physics Department, D. A. College, Garia.

tube. The electrodes were kept at a distance of 3 cm from each other (figure 1). The oscilloscope used in the present investigation was of capacitative type (Mukherjee *et al* 1963) and its operating frequency was 8 Mc/s.

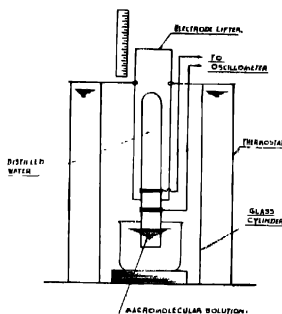


Figure 1. High frequency diffusion in cell.

To start with, the average height of the electrodes was made equal to 3 cms from the surface of ACA solution. The arrangement was left in this condition for about 24 hours. Certain amount of ACA had diffused into the water of the glass tube by this time and the electrical resistance of the liquid was changed. The condenser dial was adjusted so as to obtain a resonance. The vernier dial reading pertaining to this resonance condition was noted. With time, more and more ACA would diffuse into water, thereby changing the electrical resistance as well as the capacitance of the liquid enclosed between the electrodes. Hence in order to restore the original resonance condition, either the condenser dial reading has to be altered or the electrode system has to be lifted up along the experimental glass tube. In this experiment, we did not disturb the setting of the condenser dial but moved the electrodes up the tube till the resonance was obtained keeping, of course, the interelectrode distance constant which was 3 cms. Thus by gradually raising the electrode system the process of diffusion was followed. The temperature of the whole arrangement was maintained constant by a thermostat. The experiment was performed at two different temperatures viz. 22°C and 37°C.

DISCUSSION

The length l of the diffusing column in mm of the liquid was noted at various intervals and a graph was plotted against \sqrt{t} where t is the

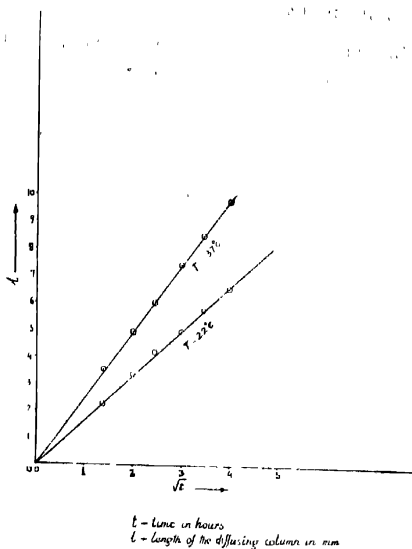


Figure 2

time in hours. It was found that the graph yielded a straight line for each temperature as shown in the figure 2. Thus Fick's law is obeyed by the macromolecular solution of ACA in course of its diffusion through distilled water.

Further work in this line is in progress.

REFERENCES

- Blake, G. G. 1947 *Jour. Sci. Instruments*, **24**, 77.
 Chakravorty, J. N. & Mukherjee, S. N. 1963 *Jour. Ind. Chem. Soc.* **40**, 812.
 Hulyalkar, R. K., Ingle, T. R. & Bhide, B. V. 1956, *Jour. Ind. Chem. Soc.* **33**, 861.
 Kulshrestha, V. K., Chatterjee, A.C., and Mukherjee, S. N. 1962
Makromol. Chem. 1962, **54**, 205.
 Mukherjee, S. N. & Chakravorty, J. N. 1963 *Jour. Ind. Chem. Soc.* **40**, 643.

Note on the pure bending of thin non-isotropic plates in the presence of couple stresses.

By RATHINDRA NATH DAS

Department of Mathematics, Krishnagar Government College,
Krishnagar, Nadia, India.

(Received August, 1969)

Effects of couple stresses on the pure bending of plates in some simple cases of isotropic material have recently been discussed by Koiter (1964) and Hoffman (1964). The object of this note is to prove that simple expressions for the displacements and bending moments can also be obtained when the material of the plate has either orthogonal elastic symmetry or is cylindrically anisotropic.

INTRODUCTION

In a Cosserat continuum we have not only the small strain tensor

$$\epsilon_{ij} = \frac{1}{2} (u_{ij} + u_{ji}) \text{ (cf. Koiter 1964, equation 31)} \quad (1)$$

but also the twist curvature tensor

$$k_{ij} = \omega_{ji} \quad (2)$$

corresponding to the deformation. Components of K_{ij} with $i=j$ are twists and those with $i \neq j$ are curvatures. u_i is the displacement vector and,

$$\omega_i = \frac{1}{2} \epsilon_{ijk} u_{kj}$$

is the small rotation vector. The couple stress tensor μ_{ij} is given by the equations

$$\mu_{ij} = B_1 k_{ij} + B_2 k_{ji}$$

where B_1 and B_2 are moduli of curvatures.

Equations of equilibrium in the absence of body forces and body couples reduce to

$$\sigma_{jkj} = 0. \quad \dots (3) \quad \text{and} \quad \mu_{ijj} = l_{ijk} \sigma_{jk} = 0 \quad \dots (4)$$

MATERIAL WITH ORTHOGONAL SYMMETRY

Solution of the problem: The stress strain relations in the case of material with three orthogonal planes of elastic symmetry are given by (cf. Love p. 161)

$$\begin{pmatrix} \tau_{xx} \\ \tau_{yy} \\ \tau_{zz} \end{pmatrix} = \begin{pmatrix} A & H & G \\ H & B & F \\ G & F & C \end{pmatrix} \begin{pmatrix} l_{xx} \\ l_{yy} \\ l_{zz} \end{pmatrix} \quad \dots (5)$$

$$\begin{pmatrix} \tau_{yz} \\ \tau_{zx} \\ \tau_{xy} \end{pmatrix} = \begin{pmatrix} L \\ M \\ N \end{pmatrix} \begin{pmatrix} l_{yx} \\ l_{zx} \\ l_{xy} \end{pmatrix} \quad \dots(6)$$

We assume the displacements to be given by

$$\left. \begin{aligned} u &= k_1 xz \\ v &= k_2 yz \\ w &= -\frac{k_1}{2}x^2 + \frac{k_2}{2}y^2 + \frac{P}{2}z^2 \end{aligned} \right\} \quad \dots(7)$$

where k_1 and k_2 are components of curvatures and P is a constant to be determined. By equation (1) the non-zero stress components are $\epsilon_{11} = k_1 z$, $\epsilon_{22} = -k_2 z$, $\epsilon_{33} = Pz$. From equation (2) the non-zero twist curvature components are obtained as $k_{12} = k_1$, $k_{21} = k_2$.. (8)

Values assumed for the displacements make

$$\tau_{xx} = \tau_{yy} = \tau_{xy} = \tau_{yz} = \tau_{zx} = 0;$$

τ_{xz} will also be zero if

$$CP = Fk_2 - Gk_1 \quad \dots(9)$$

It is also found that the stress equations of equilibrium are satisfied. The statistically equivalent stress couples per unit width of section for a plate of thickness h are

$$\begin{aligned} M_{xy} &= \int_{-h/2}^{h/2} (z \tau_{xx} + \mu_{xy}) dz \\ &= (Ak_1 - Hk_2 + GP) \frac{h^3}{12} + h (B_1 k_1 + B_2 k_2) \quad \dots(10) \end{aligned}$$

$$\begin{aligned} M_{yx} &= \int_{-h/2}^{h/2} (-z \tau_{yy} + \mu_{yx}) dz \\ &= - (Hk_1 - Bk_2 + FP) \frac{h^3}{12} + (B_1 k_1 + B_2 k_2) \quad \dots(11) \end{aligned}$$

where B_1 and B_2 are the moduli of curvatures characteristic of the material. The Curvatures in terms of the stress couples are given by

$$k_1 = \frac{\left(M_{xy} - \frac{PGh^3}{12} \right) \left(hB_1 + \frac{Bh^3}{12} \right) - \left(hB_2 - \frac{Hh^3}{12} \right) \left(M_{yx} + \frac{PFh^3}{12} \right)}{\left(\frac{Ah^3}{12} + hB_1 \right) \left(hB_1 + \frac{Bh^3}{12} \right) - \left(hB_2 - \frac{Bh^3}{12} \right)^2} \quad \dots(12)$$

$$k_2 = \frac{\left(M_{yx} + \frac{PFh^3}{12}\right)\left(\frac{Ah^3}{12} + hB_1\right) - \left(hB_2 - \frac{Hh^3}{12}\right)\left(M_{xx} - \frac{GPh^3}{12}\right)}{\left(\frac{Ah^3}{12} + hB_1\right)\left(hB_1 + \frac{Bh^3}{12}\right) - \left(hB_2 - \frac{Bh^3}{12}\right)^2} \quad \dots(13)$$

Special case (I) : Uniaxial bending.

With $M_{yx} = 0$

$$k_1 = \frac{\left(M_{xx} - \frac{PGh^3}{12}\right)\left(hB_1 + \frac{Bh^3}{12}\right) - \frac{PFh^3}{12}\left(hB_2 - \frac{Hh^3}{12}\right)}{\left(\frac{Ah^3}{12} + hB_1\right)\left(hB_1 + \frac{Bh^3}{12}\right) - \left(hB_2 - \frac{Bh^3}{12}\right)^2}$$

$$k_2 = \frac{\frac{PFh^3}{12}\left(\frac{Ah^3}{12} + B_1 h\right) - \left(hB_2 - \frac{Hh^3}{12}\right)\left(M_{xx} - \frac{GPh^3}{12}\right)}{\left(\frac{Ah^3}{12} + B_1 h\right)\left(B_1 h + \frac{Bh^3}{12}\right) - \left(hB_2 - \frac{Bh^3}{12}\right)^2}.$$

Special case (II) : Cylindrical bending.

The moment curvature relations corresponding to those derived by Koiter and Hoffman may be obtained by putting $k_2 = 0$

$$M_{xx} = (Ak_1 + GP) \frac{h^3}{12} + hB_1 k_1$$

$$M_{yx} = k_1 \left(hB_2 - \frac{Hh^3}{12}\right) \frac{PFh^3}{12}$$

Special case : (III) Pure twist.

when $M_{xx} = M_{yy}$,

$$k_2 = \frac{M_{xx} \left[h(B_1 - B_2) + \frac{h^3}{12}(B + H) \right] - \frac{Ph^4}{12}(GB_1 + FB_2) - \frac{Ph^4}{144}(BG - FH)}{\left(\frac{Ah^3}{12} + hB_1\right)\left(hB_1 + \frac{Bh^3}{12}\right) - \left(hB_2 - \frac{Bh^3}{12}\right)^2}$$

$$k_1 = \frac{M_{xx} \left[h(B_1 - B_2) + \frac{h^3}{12}(B + H) \right] + \frac{Ph^4}{12}(FB_1 + GB_2) + \frac{Ph^4}{144}(AF - GH)}{\left(\frac{Ah^3}{12} + hB_1\right)\left(hB_1 + \frac{Bh^3}{12}\right) - \left(hB_2 - \frac{Bh^3}{12}\right)^2}$$

CYLINDRICAL AEOLOTROPY

In the case of cylindrical aeolotropy we have the stress strain relations

$$\begin{pmatrix} \tau_{xx} \\ \tau_{yy} \\ \tau_{zz} \end{pmatrix} = \begin{pmatrix} c_{11} & c_{12} & c_{13} \\ c_{12} & c_{11} & c_{13} \\ c_{13} & c_{13} & c_{33} \end{pmatrix} \begin{pmatrix} e_{xx} \\ e_{yy} \\ e_{zz} \end{pmatrix}, \quad c_{ij} = c_{ji} \quad \dots(1)$$

$$\tau_{\theta z} = c_{44} e_{\theta z} \tau_{zr} = c_{44} e_{zr}, \tau_{r\theta} = c_{08} e_{r\theta} \quad \dots (2)$$

For the uniform bending of a circular plate we assume in this case

$$\left. \begin{aligned} u_r &= k_{rz} \\ u_\theta &= 0 \\ u_z &= -\frac{k}{2} r^2 + \frac{P}{2} z^2 \end{aligned} \right\} \quad \dots (3)$$

where P is a constant to be determined. Here (r, θ, z) are the cylindrical coordinates with the origin at the centre of the plate and the axis of z perpendicular to it.

With the above components of displacement the stress components become

$$\left. \begin{aligned} \tau_{rr} &= z (kc_{11} + kc_{12} + Pc_{13}) \\ \tau_{\theta\theta} &= z (kc_{12} + kc_{11} + Pc_{13}) \\ \tau_{zz} &= z (kc_{13} + kc_{13} + Pc_{33}) \end{aligned} \right\} \quad \dots (4)$$

$$\tau_{\theta z} = \tau_{zr} = \tau_{r\theta} = 0. \quad \dots (5)$$

It is found that the stress equations of equilibrium are satisfied.

$$\text{The rotation component } \omega_\theta = \frac{1}{2} \left(-\frac{\partial u_r}{\partial z} - \frac{\partial u_z}{\partial r} \right) = k, \quad \dots (6)$$

and the couple stress component μ_r is given by

$$\mu_r = B \frac{\partial}{\partial r} \omega_\theta = B_k \quad \dots (7)$$

The statically equivalent stress couple M_r is given by

$$\begin{aligned} M_r &= \int_{-h/2}^{h/2} (z\tau_{rr} + \mu_r) dz \\ &= \frac{h^3}{12} (kc_{11} + kc_{12} + Pc_{13}) + Bkh. \end{aligned}$$

REFERENCES :

- Hoffman. 1964 *Jour. of Appld Mechanics*, vol. 706.
 Koiter. w. T. 1964 *Proceedings Koninkl. Nederl. Academie van Wetenschappen*
Amsterdam series B, 67, No. 1.
 Love. A. E. H. *A treatise on the mathematical theory of elasticity*, 4th edition,
 page 161.

A note on the linear flow of a viscous incompressible conducting
fluid past an infinite flat plate with constant suction
in the presence of a transverse magnetic field

By S. N. DUBE

*Department of Mathematics, Institute of Technology, Banaras Hindu
University, Varanasi-5, India*

(Received 7 July 1969)

Analytical solution has been obtained for the momentum equations of the linear flow of a viscous incompressible electrically conducting fluid past an infinite porous flat plate in the presence of a transverse magnetic field when the suction velocity normal to the plate is constant. It is observed that the velocity in the boundary layer increases with the increase of the intensity of the magnetic field.

INTRODUCTION

The study of the response of laminar two-dimensional boundary layers to the fluctuations in the oncoming stream, initiated by Lighthill (1954), attracted the attention of many research workers in the past few years. Stuart (1955) investigated the flow of a viscous incompressible fluid past an infinite flat plate with constant suction at the surface when the free-stream velocity fluctuates about a mean value. Reddy (1964) extended the work of Stuart to the case when the fluid is moderately rarefied by introducing the slip boundary conditions. Pandey (1968) studied the same problem when the free-stream velocity varies exponentially with time. The corresponding magneto-hydrodynamic problem, when the fluid is electrically conducting and a transverse magnetic field is present, has been studied by Suryaprakaso Rao (1962, 1963). Kelly (1965) and Messiha (1966) have investigated the problem with an incompressible non-conducting fluid when the suction velocity is oscillatory. Recently Mehta & Radha Krishna (1968) studied the corresponding magnetohydrodynamic problem with a viscous incompressible electrically conducting fluid in the presence of a transverse magnetic field.

In the present note an attempt has been made to study the effects of the magnetic field and constant suction on the flow of an incompressible electrically conducting fluid when the free-stream velocity varies linearly with time. The magnetic field of strength B_0 is imposed normal to the plate.

BASIC EQUATIONS

We consider a two-dimensional viscous incompressible electrically conducting fluid flow along an infinite porous flat plate in the presence of a transverse magnetic field. The flow is independent of the distance

parallel to the plate and the suction velocity normal to the plate is directed towards it and is constant. The x' -axis is taken along the plate, y' -axis normal to the plate. Dashes denote dimensional quantities. Neglecting the induced magnetic field which is usually small and assuming the electric field \vec{E} to be equal to zero, the equations of motion and continuity (Pai 1962) are

$$\frac{\partial u'}{\partial t'} + v' \frac{\partial u'}{\partial y'} = -\frac{1}{\rho'} \frac{\partial p'}{\partial x'} + \nu' \frac{\partial^2 u'}{\partial y'^2} - \frac{\sigma_e'}{\rho'} B_0'^2 u', \quad \dots (1)$$

$$\frac{\partial v'}{\partial t'} = -\frac{1}{\rho'} \frac{\partial p'}{\partial y'}, \quad (2)$$

$$\frac{\partial v'}{\partial y'} = 0, \quad \dots (3)$$

where σ_e' is the electrical conductivity of the fluid.

The boundary and initial conditions are

$$\left. \begin{aligned} t' = 0, \quad u' = 0 \quad \text{for all } y' \\ t' > 0 : \quad u' = 0 \text{ at } y' = 0 \text{ and } u' \rightarrow U'(t') \text{ at } y' \rightarrow \infty \end{aligned} \right\}, \quad \dots (4)$$

where $U' = u'_{t'}$ is the velocity at a large distance from the wall.

Although the equation (3) shows that v' is a function of time only, we now further restrict consideration to the case of v' equal to a negative constant ($-v_0'$), from which it follows that p' is independent of y' . Now outside the boundary layer equation (1) gives

$$\frac{dU'}{dt'} = -\frac{1}{\rho'} \frac{\partial p'}{\partial x'} - \frac{\sigma_e'}{\rho'} B_0'^2 U'. \quad (5)$$

Substituting for the pressure term in equation (1) from (5), we get

$$\frac{\partial u'}{\partial t'} - v_0' \frac{\partial u'}{\partial y'} = \nu' \frac{\partial^2 u'}{\partial y'^2} + \frac{dU'}{dt'} + \frac{\sigma_e'^2}{\rho'} B_0'^2 (U' - u'). \quad \dots (6)$$

We now introduce the non-dimensional quantities defined by

$$y = \frac{y' v_0'}{U_0'}, \quad t = \frac{v_0'^2 t'}{4\nu'}, \quad u = \frac{u'}{U_0'}, \quad U = \frac{U'}{U_0'}, \quad M = \frac{B_0'^2}{U_0'} \sqrt{\frac{\nu' \sigma_e'}{\rho'}}, \quad (7)$$

where U_0' is a reference velocity and M is the Hartmann number.

Equation (6) takes the non-dimensional form as

$$\frac{\partial^2 u}{\partial y^2} + \frac{\partial u}{\partial y} - \frac{1}{4} \frac{\partial u}{\partial t} = -\frac{1}{4} \frac{dU}{dt} - M^2 (U - u), \quad \dots (8)$$

subject to the boundary conditions

$$\left. \begin{aligned} t = 0, u = 0 \text{ for all } y \\ t > 0 : u = 0 \text{ at } y = 0 \text{ and } u \rightarrow U(t) \text{ at } y \rightarrow \infty \end{aligned} \right\} \quad \dots(9)$$

The dimensionless form of the free-stream velocity is

$$U = ct,$$

where $c = \frac{4a'v'}{U_0'v_0'^2}$ is clearly a dimensionless constant. Substituting the above value of U in (8), we get

$$\frac{\partial^2 u}{\partial y^2} + \frac{\partial u}{\partial y} - \frac{1}{4} \frac{\partial u}{\partial t} = -\frac{c}{4} - M^2(ct - u). \quad \dots(10)$$

Multiplying equation (10) by e^{-st} and then integrating the resulting equation with respect to t between the limits 0 to ∞ , we get

$$\frac{\partial^2 \bar{u}}{\partial y^2} + \frac{\partial \bar{u}}{\partial y} - \left(M^2 + \frac{s}{4} \right) \bar{u} = -c \left[\frac{1}{4s} + \frac{M^2}{s^2} \right], \quad \dots(11)$$

where \bar{u} is the Laplace transform of u defined by

$$\bar{u} = \int_0^\infty e^{-st} u \, dt.$$

The boundary conditions (9) reduce to

$$\bar{u} = 0 \text{ at } y = 0 \text{ and } \bar{u} \rightarrow \frac{c}{s^2} \text{ at } y \rightarrow \infty. \quad (12)$$

The solution of equation (11) under the conditions (12) is

$$\bar{u} = \frac{c}{s^2} \left[1 - e^{-\frac{1 + \sqrt{1 + s + 4M^2}}{2} y} \right]. \quad \dots(13)$$

Now applying Laplace inversion theorem, we get

$$\begin{aligned} u = ct \left[1 - e^{-\frac{1 + \sqrt{1 + 4M^2}}{2} y} \right] \\ + \frac{c}{4\sqrt{1 + 4M^2}} y \cdot e^{-\frac{1 + \sqrt{1 + 4M^2}}{2} y} \end{aligned} \quad \dots(14)$$

The non-dimensional skin-friction τ_0 is given by

$$\tau_0 = \left(\frac{\partial u}{\partial y} \right)_{y=0} = \frac{1 + \sqrt{1 + 4M^2}}{2} \cdot ct + \frac{c}{4\sqrt{1 + 4M^2}} \quad \dots(15)$$

Figure 1 has been obtained by plotting the velocity distribution u against y for $c = 4$, $t = 1$ and $M = 0, \frac{1}{2}, 1$. From the figure it is clear that initially u increases with the increase of y upto about $y = 3.5$, but beyond $y = 3.5$, u is constant. This means that the velocity profiles beyond $y = 3.5$ are straight lines normal to the plate. This graph also indicates that the velocity in the boundary layer increases with the increase of the intensity of the magnetic field.

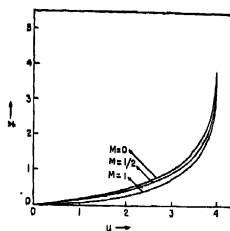


Figure 1

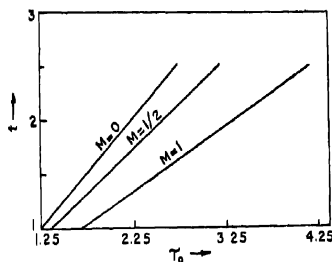


Figure 2

Figure 2 has been obtained by plotting τ_0 against t for $c = 1$ and $M = 0, \frac{1}{2}, 1$. The expression (15) and the figure 2 show that the skin-friction τ_0 varies linearly with time. From this figure it is also evident that the skin-friction τ_0 increases with the increase of the intensity of the magnetic field.

For $M = 0$, the results transform to the results obtained by the author (1969) for the two-dimensional viscous incompressible non-conducting fluid flow past an infinite flat plate with constant suction at the surface when the free-stream velocity varies linearly with time.

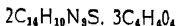
The author wishes to express his gratitude to Professor P. L. Bhatnagar Vice-Chancellor, Rajasthan University, for his kind guidance in the preparation of this note.

REFERENCES

- Dube, S. N. 1969 (*Accepted for publication in J. Indian Math. Soc.*)
Kelly, R. E., 1965 *Quart. J. Mech. Appl. Math.*, **18**, 287.
Lighthill, M. J. 1954 *Proc. Roy. Soc. A*, **224**, 1.
Mehta, K. N. & Radha Krishna, C. V. 1968 *Proc. Nat. Inst. Sci. India, A*, **34**, 28.
Messiha, S. A. S. 1966 *Proc. Cumb. Phil. Soc.*, **62**, 329.
Pai, S. 1962 *Magneto gas-dynamics and Plasma Dynamics*, Springer-Verlag Berlin
Pandey, K. S. 1968 *Indian J. Phys.*, **42**, 213.
Reddy, K. C. 1964 *Quart. J. Mech. Appl. Math.*, **17**, 381.
Stuart, J. T. 1955 *Proc. Roy. Soc., A*, **231**, 116.
Suryaprakaso Rao, U. 1962 *Z. Angew. Math. Mech.*, **42**, 133.
1963 *Z. Angew. Math. Mech.*, **43**, 127.

Letters to the Editor

X-ray crystallographic data on metha pyrilene fumarate



By M. P. GUPTA & S. M. PRASAD

Department of Physics, University of Ranchi,

Received 22 November 1969

Metha pyrilene fumarate with the empirical formula $2C_{14}H_{19}N_3S, 3C_4H_4O_4$ was made available to us through the courtesy of M/S Pharmed Private Ltd., Chembur, Bombay-71 and was investigated by us, using X-ray diffraction technique, because of the complex it forms with the fumaric acid whose salts [Gupta & Roy 1967, Gupta & Sahu 1968, Gupta & Roy 1969, Gupta & Sahu (Communicated)] have been extensively investigated in this laboratory. The material was obtained in a powder form but was re-crystallized from a solution in water, giving single crystals as elongated plates. Examined under the polarizing microscope with the platy face horizontal, the crystals give oblique extinction of 38° with the long edge. The platy face is the (110) face on the basis of the unit cell chosen.

X-ray data :

Rotation and Weissenberg photographs (normal and equi-inclination) show that the crystals are monoclinic with

$$a = 11.35\text{\AA}, b = 22.94\text{\AA}, c = 8.63\text{\AA}, \beta = 105^\circ 37'$$

ρ_{calc} with 2 molecules in the unit cell = 1.35, gm/ml. As high density of 2.71 gm/ml is unlikely for an organic molecule containing only light atoms, one must assume only two formula units of $2C_{14}H_{19}N_3S, 3C_4H_4O_4$ present in the unit cell i. e. there are four metha pyrilene groups ($C_{14}H_{19}N_3S$) and six fumarate groups ($C_4H_4O_4$) in one unit cell of the crystal.

Space group :

The only absences which were noticed are :

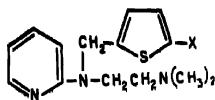
$$h0l, h \neq 2n,$$

$$0k0, k \neq 2n,$$

$$hkl, \text{ no condition.}$$

This fixes the space group uniquely a $P2_1/a$. As only two asymmetric units of $2C_{14}H_{19}N_3S, 3C_4H_4O_4$ are present, one must infer that each is occupying a special position of centre of symmetry. No other symmetry or special position is possible in the molecule. Since the metha

pyriline (MP) group cannot be centrosymmetric with the stereochemical formula



and the fumaric acid molecule is definitely centrosymmetric [Brown 1966, Post *et. al* 1966, Gupta & Sahu, communicated] one must infer the follow-

TABLE 1 X-ray powder diffraction data for metha pyriline fumarate
 $2C_{14}H_{10}N_8S \cdot 3C_4H_4O_4$

I/I ₀	d (Å)		hkl	I/I ₀	d (Å)		hkl
	obs.	calc.			obs.	calc.	
15	11.48	11.47	020	50	3.03	3.03	17 $\bar{1}$
30	9.88	9.87	110			3.02	311
20	7.95	7.91	120			3.02	14 $\bar{2}$
5	7.27	7.24	11 $\bar{1}$	15	2.89	2.89	35 $\bar{1}$
40	6.31	6.35	12 $\bar{1}$	18	2.80	2.80	062
90	5.44	5.40	13 $\bar{1}$			2.80	152
		5.45	200	18	2.69	2.69	341
10	5.19	5.21	121			2.70	26 $\bar{2}$
25	4.95	4.95	220	17	2.62	2.62	402
70	4.60	4.59	14 $\bar{1}$			2.61	242
		4.65	131	17	2.55	2.54	280
						2.54	351
35	4.34	4.33	23 $\bar{1}$			2.54	44 $\bar{1}$
55	4.05	4.04	012	18	2.49	2.48	32 $\bar{3}$
		4.01	21 $\bar{1}$	17	2.43	2.41	401
55	3.95	3.93	15 $\bar{1}$			2.42	163
15	3.84	3.82	060	5	2.37	2.38	361
		3.81	20 $\bar{2}$			2.37	322
						2.38	133
65	3.61	3.61	151	5	2.33	2.31	290
		3.61	333			2.33	262
		3.60	310	20	2.24	2.23	460
		3.62	032			2.22	203
		3.62	22 $\bar{2}$	20	2.19	2.18	510
100	3.43	3.42	16 $\bar{1}$	7	2.06	2.05	362
		3.45	25 $\bar{1}$			2.04	402
15	3.33	3.35	33 $\bar{1}$			2.04	461
15	3.23	3.22	132				
40	3.13	3.13	260				
		3.11	15 $\bar{2}$				

ing spatial geometry for the asymmetric unit of metha pyrilene fumarate in the crystal :



In this arrangement, the central fumaric acid molecule must be so located that the centre of its central C = C bond occupies a special position of symmetry. There is nothing surprising in linkages of fumarate groups in this fashion, as already shown by the results of many workers (Brown 1966, Post *et al* 1966, Gupta & Sahu 1968). In the metha pyrilene fumarate group itself, the molecular complex will be built up through associations of the acid molecules, via hydrogen bonds of the carboxyl groups of the acid molecules, the end acid molecules themselves going to the X-position as shown in the stereochemical formula above.

A complete structure determination of the compound is in progress in this laboratory. Indexed powder data for the compound (taken with filtered Cu radiation, 57.3 mm radius powder camera) will be found in table-1 below.

REFERENCES

- Brown, C. J. 1966 *Acta Cryst.* **21**, 1.
Gupta, M. P. & Roy, P. K. 1967 *Indian J. Phys.* **41**, 787.
Gupta, M. P. & Roy, P. K. 1969 *Zett. fur Krist.* **129**, 203.
Gupta, M. P. & Sahu, R. G. 1968 *Curr. Sci.* **37**, 195.
Acta Cryst. (In Press)
Post *et al* 1966 *Acta Cryst.* **21**, 566.

Indian J. Phys. **43**, 557—559 (1969)

Electron Paramagnetic Study Resonance of calcium copper acetate, hexahydrate

By D. MAJUMDAR AND P. K. BISWAS

*Magnetism Department, Indian Association for the Cultivation of Science
Jadavpur, Calcutta-32, India.*

(Received 26 March 1970)

The measurement of g-values and location of g-axis in crystals by electron paramagnetic resonance method is the most fruitful complement to magnetic susceptibility data. In continuation of the magnetic studies on calcium copper acetate hexahydrate (Biswas & Sengupta 1970) e. p. r. experiment has been carried out by us on this complex.

The spectrometer used is a transmission type with a 2K33 klystron as the microwave (1.28 cm) source set up in our laboratory by Bose, Ghosh, Bagchi & Pal (1964).

The x-ray studies of Lang & Hare (1967) indicate that single crystal of calcium copper acetate hexahydrate belongs to tetragonal class with four ions in the unit cell (ions being all parallel). The variation of g^2 -values with ϕ -axis horizontal are plotted in figure 1. The value of g in the symmetry plane was separately measured and as expected is found to be isotropic

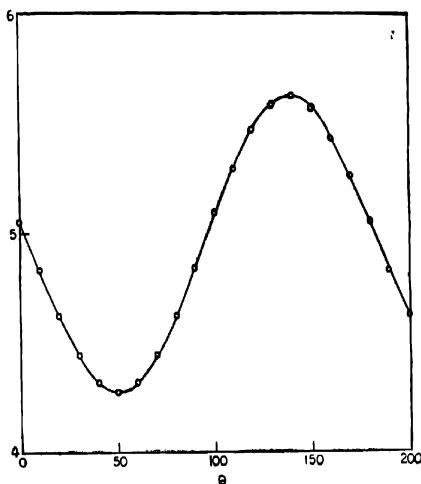


Figure 1

in this plane. The minimum g -value of the above plot corresponds to the value in the symmetry plane and hence this gives g_{\perp} . The maximum g -value of the above plot thus gives g_{\parallel} . The experimental values $g_{\perp} = 2.066$ and $g_{\parallel} = 2.371$, thus obtained agree well with $g_{\perp} = 2.068$ and $g_{\parallel} = 2.40$ calculated from magnetic susceptibility and anisotropy measurements by Biswas & Sengupta (1970).

The line width in this complex is found to be similar in magnitude to that of copper tutton salts although in some of the directions it is quite narrow unlike the latter salts. The case bears some analogy in this respect to copper sulphate pentahydrate except that in the latter, the

line becomes too wide in certain directions to be detected by resonance experiment. X-ray data show that in the single crystal all ions are parallel and two neighbouring copper ions are at a distance of about $\frac{1}{2}\text{\AA}$, similar to that of copper tutton salt. Hence there should be a fair amount of isotropic exchange interaction between "similar" ions precessing about parallel axes in the magnetic field, and super-exchange through intervening atoms between two neighbouring copper atoms will also be appreciable. The spin-spin interaction is probably responsible for the angular variation of the line width and the general narrowness of the resonance line is attributed to the strong isotropic exchange. The resonance spectrum of calcium copper acetate hexahydrate corresponding to $S = \frac{1}{2}$ is evidently fundamentally different from that of copper acetate monohydrate, in which the spectrum corresponds to $S = 1$ arising from a strong direct exchange coupling between a dimeric Cu^{2+} complex. This is in complete agreement with the magnetic susceptibility and anisotropy measurements. Thus the presence of Ca^{2+} ion between two copper atoms in the former case as compared to the latter drastically changes the magnetic and e. p. r. behaviours.

The authors express their gratefulness to Prof. A. Bose, D.Sc., F.N.I., for his guidance. They also thankfully acknowledge the co-operation of Dr. U. S. Ghosh and Mr. A. K. Pal.

REFERENCES

- BINWAS P. K. and SENGUPTA P. 1970 In Press
BOSE A., GHOSH U. S., BAGCHI R. N. and PAL A. K. 1964 Indian J. Physics. 38, 36,
LANGE D. A. and HARE C. R. 1967 Chem. Comm. 890.

Indian J. Phys. 43, 562-560 (1969)

Comment on the results on ultraviolet absorption spectra of ortho -and meta-bromoanilines

G. N. R. TRIPATHI

Department of Physics, University of Gorakhpur, Gorakhpur.

(Received 29 December 1969)

The ultraviolet absorption spectra of ortho- and meta-bromoaniline molecules in vapour phase have been reported recently by Tripathi (present author 1968) and Rama Rao (1968) independently. The experimental results of the two authors do not agree on some points. This communication aims at finding out the probable impurity which would account for the difference in published spectra by the two authors.

Rama Rao has measured a good number of sharp and discrete bands in o-bromoaniline, while Tripathi has reported only a few broad and diffuse bands in this isomer. The 0,0 bands determined by the two authors differ by 510 cm^{-1} in position and there is no common band reported. Though Rama Rao has reported only a few bands compared to Tripathi for m-bromoaniline, the 0,0 band and other intense bands are common within a variation of $\pm 10\text{ cm}^{-1}$. These considerations lead one to conclude that the o-bromoaniline sample used by one of the authors was contaminated.

The electronic spectra of isomeric fluoro-, chloro- and bromoanilines are expected to exhibit a close similarity. The order of the red shifts in the 0,0 bands of the three isomers, relative to benzene or aniline is para > ortho > meta for fluoroanilines (Murthy *et al* 1965) and chloroanilines (Harnath *et al* 1957) and so it should be for isomeric bromoanilines. This supports the results of Tripathi. If Rama Rao's data be accepted, the order of the 0,0 band shifts in bromoaniline becomes $p > m > o$. Besides, the 0,0 band shifts in the ortho- and meta- isomers of most of the disubstituted benzenes are very close which is consistent with the data given by Tripathi but inconsistent with that reported by Rama Rao.

In order to identify the spectrum of o-bromoaniline reported by Rama Rao, with some probable impurity, the spectrogram was compared with that reported by Ginsburg and Matsen (1945) for aniline vapours and it was established that the two spectra coincide. The positions of the prominent bands also agree if error of measurement for some bands be taken as high as $\pm 20\text{ cm}^{-1}$. The presence of aniline impurity is very probable in a sample of o-bromoaniline, which may decompose, when exposed to light.

REFERENCES

- Ginsburg, N. & Matsen, F. A. 1945 *J. Chem. Phys.* **13**, 167.
Haranath, P.B.V. & Sreerama Murty, K. 1957, *Indian J. Phys.* **40** 577.
Murty, D. S. N. & Santhamma, C. 1965 *Ind. J. Pure. Appl. Phys.* **3** 495.
Rama Rao, C. G., 1968 *Indian J. Phys.* **42** 354.
Tripathi, G. N. R. 1968 *Ind. J. Pure Appl. Phys.* **6** 25.

BOOK REVIEW

High-speed photography: Proceedings of the 8th International Congress on High-speed Photography.

By N. ROBERT,

John Wiley, New York

High-speed photography affords a glimpse of the world that is normally beyond our power of observation by virtue of its speed and/or transient character. Just as microscopy helps us to overcome our limitation of observation in space, high-speed photograph helps to remove the limitation upon observation in TIME that nature has imposed upon us. It reveals to us the most amazing, interesting and important details of these innumerable varieties of fleeting phenomena.

The photography of rapid events—instrumentation as well as its application to a very diverse field—has seen phenomenal development all over the world in the past two decades. The International Congress on High-speed Photography, which since 1952 has been meeting every time in a different country, has provided a purposeful exchange of information, ideas and know-how amongst workers who otherwise might not have met. It has afforded a unique forum for assessment of achievements and trends. The proceedings of these conferences therefore have been amongst the most valuable publications in this field.

The 8th International Congress on High-speed Photography was held in Stockholm, Sweden in June 1968. It was attended by some 480 participants from 22 countries. The proceedings of this Congress, published in a creditably short time after the Congress, is a welcome addition to the series. It contains 122 lectures on various topics in the field, three addresses of welcome, indexing material, a lecture on Prof. Hubert Schardin and a list of his publications, on 503 pages of 296 × 210 mm of art paper.

Of the 122 papers, eighteen are devoted to techniques and cameras based on the use of image converter tubes and electronic shutters. These clearly show the importance gained by the image converter tubes for applications to high-speed photography in recent years and consequent achievements. An image converter framing camera with time resolution upto 10^{-12} sec. has also been reported from USSR.

There are six papers in the section on mechanical shutters. A study of dichroitic, exploding wire, carbon injection and collapsing foil shutters has been reported from Germany while an American paper also discusses the collapsing foils.

An invited lecture on fibre optics, while reviewing the status, informs that during the last fifteen years since the fibre optics was first developed as a laboratory curiosity, the development has been such that, at present, the commercial sales on fibre optics amount to more than 50 million dollars per year in USA alone.

The chapter on streak cameras includes three papers and that on framing cameras twelve. Then there are four papers on image dissection cameras. A camera having framing rates upto 5×10^6 per sec., using velocity doubler, has been reported from USA and another in the same speed range utilizing multiple sparks on Cranz Schardin principle from France. Russian report describes a camera using lenticular plates, capable of speeds upto two million frames per second.

There are seven papers describing the excellent work on time resolved spectroscopy, ten on various aspects of flash light sources, nine papers on x-ray flash systems and four on highspeed photography using laser beams. The progress in the new field of holography

is specially noticeable from the ten papers on this subject. These are followed by seven papers under the title—Schlieren Techniques. One of these describing a three dimensional Schlieren system is from USA and another describing a simple coloured Schlieren system is from Czechoslovakia. There are five papers on the application of high-speed photography to problems involving interferometry.

One paper informs about the International Dictionary on High Speed Photography and Cinematography containing 4000 terms in English, French, German and Russian. Suggestions are invited.

Then follow six papers on general photographic techniques and seventeen papers on various applications of high-speed photography varying from gas dynamics through flame propagation, detonation, laser damage in glass, fractures, photoelasticity etc. to the forming of cavities in liquids. Last of all there are seven papers on various topics of analysis, data recording and photographic materials etc., mostly theoretical.

On page 386 is an invited paper in memory of Prof. Hubert Schardin who was a pioneer worker in this field and on page 497 is given a list of his publications. Mention must also be made of two addresses of welcome which are very informative and thought provoking.

The Proceedings thus is a kaleidoscopic window on a great variety of work which is going on all over the world in this fast growing and poignant field. The papers' committee deserves congratulations on the technique adopted by it in requesting the participants to submit their manuscripts in a predecided format. The authors' adherence to the specified pattern while keeping their individuality of typing and diagrams etc. has resulted in a pleasant setting of diversity in conformity,

In our country little is being done to promote the development of high-speed photographic cameras and their application in spite of their established usefulness not only in purely scientific investigations in the laboratories but also in many of our technological and industrial problems.

H. V.

Electrical properties of tin-chalcogenide films*

By A. GOSWAMI AND R. H. JOG

National Chemical Laboratory, Poona-8, India.

(Received September 5, 1969)

A study has been made on some electrical properties such as resistivity (ρ), activation energy (ΔE), thermoelectric power (ϵ), temperature coefficient of resistance (TCR) etc., of vacuum deposited films of SnSe , Sn_2Se_3 , SnS and SnTe . While the selenides and sulphide in film-state behaved as semiconductors, the telluride had a semi-metal character. The decrease of resistance of SnSe , Sn_2Se_3 and SnS films with an increase of T_{max} appears to be associated with the gradual phase change occurring in them.

INTRODUCTION

In a series of papers, Goswami and his coworkers (1962, 1964, 1966) have shown that vacuum deposited films of semiconducting materials behave often in a different manner from the bulk and also that some of the semiconducting properties are considerably affected by variables such as rate of deposition, substrate temperature, thickness, annealing etc. The following is a report of our study on vacuum deposited films of SnSe , Sn_2Se_3 , SnS and SnTe .

EXPERIMENTAL

The selenides and telluride of tin were prepared by mixing the constituent elements in their stoichiometric proportions and melting the mixture after sealing them in vacuo ($\approx 10^{-5}$ mm of Hg) in silica tubes in a furnace. The heating of the samples was carried out in stages and the final temperature was about 50°C above the melting point of the individual compounds. The molten samples were kept at these temperatures for about 4-6 hours while the contents were mixed by occasional shaking. These were then removed and suddenly plunged into water. Solid compounds thus obtained were then used for evaporation in vacuo ($\approx 10^{-5}$ mm of Hg).

SnS powder was, however, prepared by passing a stream of H_2S gas through a solution of stannous chloride obtained by warming in HCl (A.R.) containing a small amount of metallic tin, as described previously (Badachhape & Goswami 1964). The precipitate thus formed was then washed with distilled water till free from chloride, then with alcohol and finally dried in vacuo.

The chalcogenides of tin thus prepared were evaporated from micro-conical silica baskets and deposited on glass substrates of dimensions $4\text{ cm} \times 0.5\text{ cm}$ in the usual way. Specimens of different thicknesses were obtained not only from the same set of evaporation, but also from

*Communication No. 1189 from the National Chemical Laboratory, Poona-8, India.

different sets. The thickness of each film was estimated from the difference in weight before and after deposition and from the known area of deposit, assuming that the density of deposited film is the same as that of the bulk material.

The experimental set-up and techniques for measuring resistivity (ρ), thermoelectric power (τ) etc., was similar to those described previously (Goswami & Jog 1964). Resistance measurements were carried out both by ac and dc methods with the help of suitable bridges during heating and cooling cycles. Heating of specimens was made by an external heater provided with a control. Thermoelectric power was determined from the potential difference due to the thermal gradient, created with the help of two micro-heaters attached at the two ends of the experimental film. The emf developed was measured by a vernier potentiometer and temperatures at different positions of film by chromel-p-alumel thermocouples. In the case of high resistance films, ambient temperature was also raised

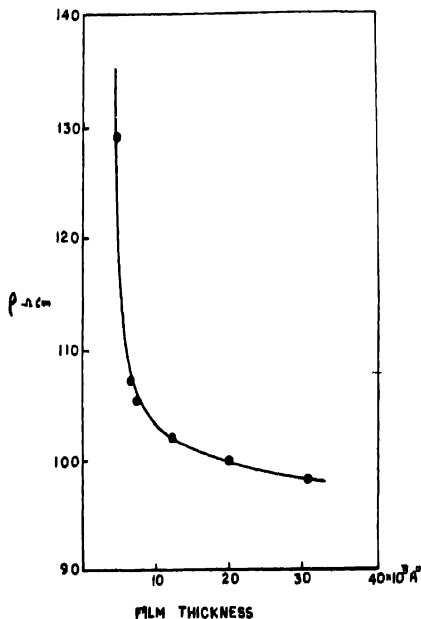


Figure 1. Variation of resistivity with film-thickness.

by an external heater to a measurable emf. All measurements of resistance, thermoelectric power etc., were carried out in vacuo ($\approx 10^{-5}$ mm of Hg) to minimise the oxidation or adsorption of gases.

RESULTS

(a) Resistivity (ρ) and film thickness (t)

The variation of ρ with T was measured for all the above chalcogenide films and figure 1 shows a typical graph for SnSe films. Similar was also the nature of Sn_2Se_3 , SnS and SnTe films. It is seen that ρ is very much dependent on film thickness.

(b) Temperature effect on Resistance (R) and activation energy (ΔE)

(i) SnSe films

A typical $\log R$ vs $1/T$ graph for the first heating cycle of an unannealed film ($\approx 31000 \text{ \AA}$) beyond the range of discontinuity temperature T_d , (Goswami & Jog 1964) is shown in figure 2. It is seen that the curve has two distinct slopes in two regions of temperatures, A and B, while an additional

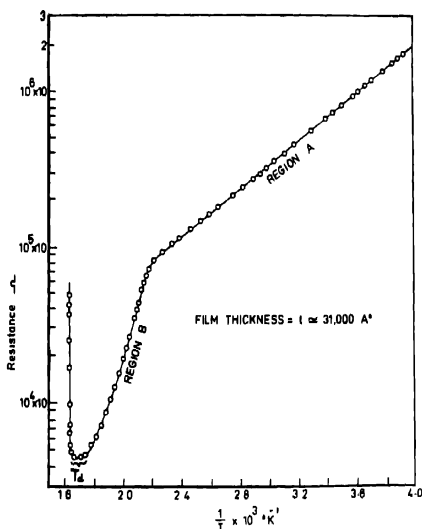


Figure 2. Variation of $\log R$ vs $1/T$ for an unannealed SnSe film ($t \approx 31,000 \text{ \AA}$)

change occurs at the T_d region, the last being no doubt due to a break in the continuity of the film. The change of slope of the graph from A to B

region occurred between 150°C to $\simeq 180^{\circ}\text{C}$, depending upon the film-thickness, T_d being $\simeq 310^{\circ}\text{C}$.

In some preliminary experiments, contrary to our general expectation, resistance of any film during heating and cooling cycles was considerably dependent on the temperature of annealing. Even simply heating specimens in vacuo to any temperature beyond the region A, caused a significant change in the cooling path, which was quite different from the heating one. Subsequent heating and cooling paths followed the initial cooling path provided the temperature did not exceed the maximum temperature (hereafter called T_{max}) reached in the first heating cycle. These features of $\log R$ vs $1/T$ curves are quite in contrast with those of other vacuum deposited films previously reported (Goswami & Jog 1964, Goswami & Koli 1966, Deokar & Goswami 1966). The temperature effect was there-

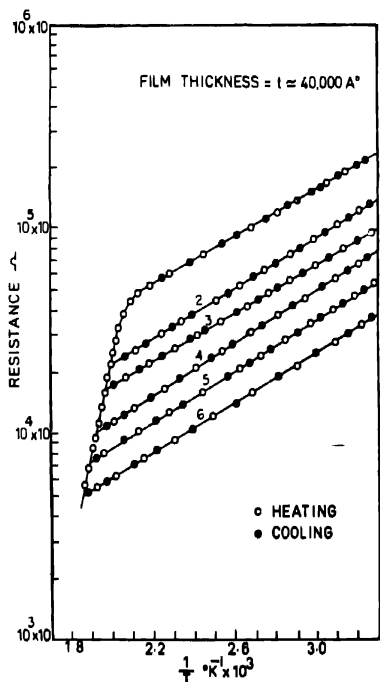


Figure 3. Variation of resistance with T_{max} of Sn_3Se_8 films.

fore studied by measuring film resistance under the following conditions viz. (i) in the temperature region A, during both the heating and cooling cycles repeating several times with varying T_{max} upto the upper limit of region A; (ii) raising T_{max} to any temperature beyond the region A and continuing the measurements as in (i); (iii) increasing T_{max} after measurements as in (ii) in the region B and continuing the process.

The results of the above measurements are shown in figure 3. Under the condition (i), the curve follows the path 1, for all repeated heating and cooling cycles, even when T_{max} varies from room temperature to the maximum temperature of the range A thus suggesting that heating and cooling paths in this region were more or less the same and independent of T_{max} . For the condition (ii), on the other hand, the cooling path differed considerably from the first heating one. Subsequent heating and cooling paths were the same as the initial cooling path and it was characteristic of T_{max} as shown by curves 2, 3, 4, 5 or 6 (figure 3). With increasing T_{max} as in (iii) the cooling paths changed from 2 to 5, each time resistance of the film decreasing with the rise of T_{max} . It is also seen that

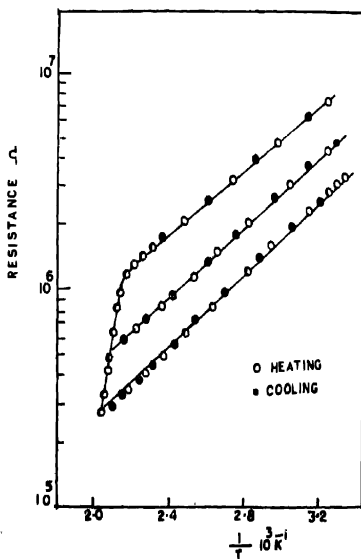


Figure 4. Variation of resistance with T_{max} of Sn_3Se_3 films.

the effect of increasing T_{max} was a new $\log R$ vs $1/T$ curve independent of the previous history of heating of the sample. Even a slight variation of T_{max} by 5-7°C was sufficient to show a significant change in the above curve. It is interesting to mention that any change in T_{max} or time of heating in the region A had no effect on the path.

Similar results were also observed for different film thicknesses, though the value of the slope slightly differed, thinner films having higher values. The activation energy thus observed for SnSe films varied from 0.30 eV to 0.23 eV for film thicknesses ranging between 15,000 Å to $\approx 40,000$ Å.

(ii) Sn_2Se_3 film

Figure 4 shows $\log R$ vs $1/T$ curves for a film ($\approx 32,000$ Å), for different T_{max} . Here also it is seen that paths changed considerably with T_{max} . Similar results were also obtained for other film-thicknesses. T_d and the change of slope were found to occur in the same range as for SnSe films.

(iii) SnS films

These films had higher resistances compared to selenide films of corresponding thicknesses. Figure 5 shows the variation of $\log R$ vs $1/T$

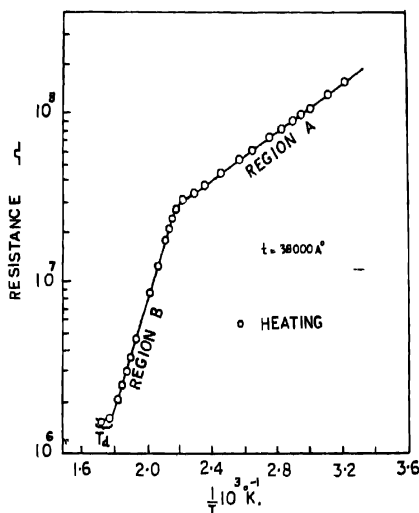


Figure 5. Variation of $\log R$ vs $1/T$ of SnS films (unannealed).

for a film of thickness $\approx 38,000 \text{ \AA}$. The change of paths with T_{max} was also observed for these films.

(iv) *SnTe films*

Unlike the selenides and sulphide, resistance of these films increased, though slightly, with the rise of temperature. Figure 6 shows the variation

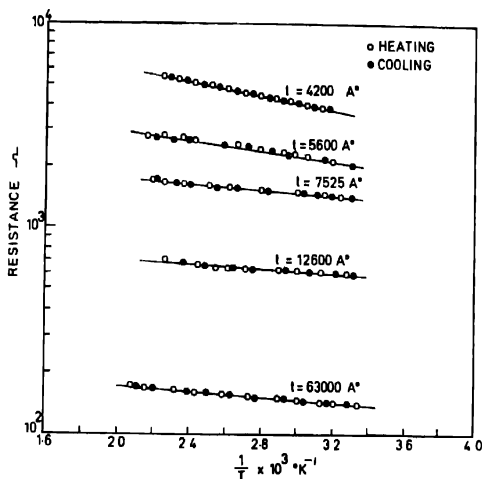


Figure 6. Variation of R vs $1/T$ of SnTe films.

of $\log R$ vs $1/T$ for different film thicknesses. It is interesting to note that T_{max} had no effect at all on the heating or cooling paths.

(c) *Thermoelectric power (α)*

For selenides and sulphide films ambient temperature was raised to 150°C and the thermoelectric power was measured in the usual way. Figure 7 shows a typical emf vs temperature difference curve. Similar graphs were also obtained for different film-thicknesses. For SnTe films also similar graphs were obtained even when the ambient temperature was the same as the room temperature. It may be mentioned here that α remained more or less constant for each of the compounds even

though the thickness range varied from $15,000 \text{ \AA}$ to $\approx 40,000 \text{ \AA}$ and the values were found to be about 160, 150 and $42 \mu\text{V}/^\circ\text{C}$ respectively, for SnS , Sn_2Se_3 , SnS and SnTe films.

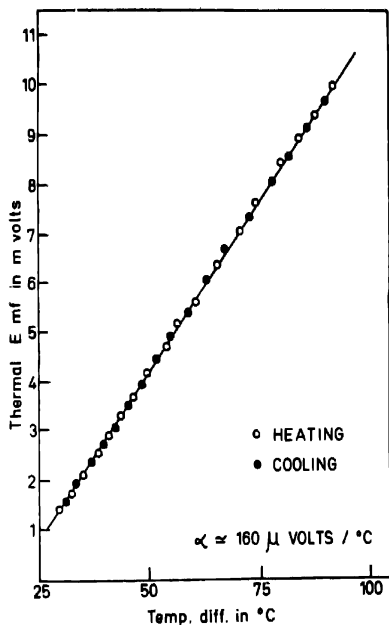


Figure 7. Thermal emf vs temperature difference between two ends of SnSe film.

(d) *Temperature coefficient of resistance (TCR)*

TCR given by $\left(\frac{1}{R} \cdot \frac{dR}{dT} \right)$ was calculated at different temperatures from the graph of resistance vs temperature. Figures 8–10 show the variation of TCR with temperature for selenides and sulphide films. It will be seen that TCR was negative in all cases. Another feature of above graphs is that, the magnitude of TCR decreased with the increase of temperature

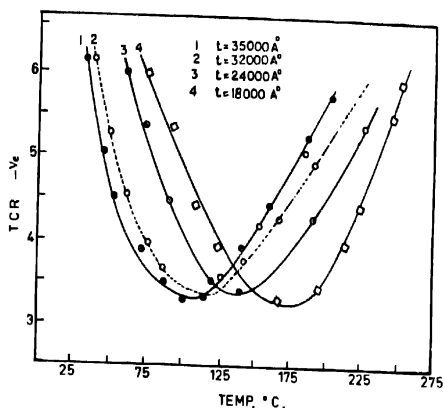


Figure 8. Variation of TCR with temperature of SnSe films,

upto a minimum value and again increased with a further rise of temperature, the exact temperature region for this change, however, depended on the film-thickness. TCR for SnTe films was found to be positive.

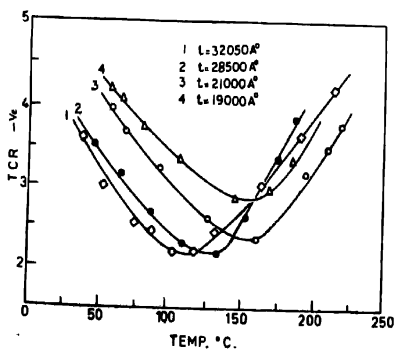


Figure 9. Variation of TCR with temperature of $SnTeSe_3$ films,

(e) *Electron diffraction study*

The deposit films were also examined by electron diffraction methods. It was observed that similar to SnS (Badacchape & Goswami 1964), the

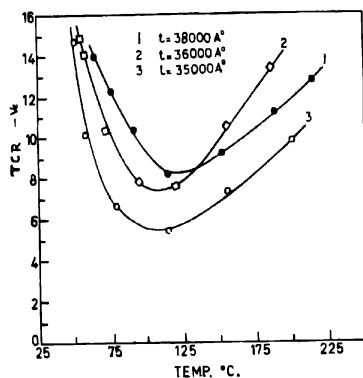


Figure 10. Variation of TCR with temperature of SnS films.

selenide SnSe developed an orthorhombic structure (figure 11) when deposited at room temperature. But at a higher substrate temperature say about 300°C and above, a cubic phase along with the orthorhombic

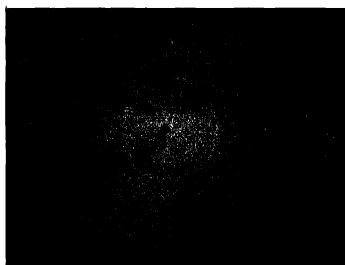


Figure 11. Polycrystalline SnSe (orthorhombic).

was formed (figure 12). This transformation was found to be irreversible as was the case for SnS.



Figure 12. Single crystal SnSe (cubic & orthorhombic)

DISCUSSION

From the above study it is seen that films of SnSe, Sn_2Se_3 and SnS are semiconducting in nature as shown by the decrease of resistance with the increase of temperature and by the high value of negative TCR. But the reverse is the case for SnTe films, showing a semi-metallic behaviour. The distinguishing feature of selenides and sulphide films in contrast with telluride is the dependence of the heating and cooling paths on T_{max} beyond the region A. This effect does not seem to be related to the annealing of defects such as dislocations, microtwins etc., which are invariably present in evaporated films, since in that case heating to any T_{max} such as 2 or 3 in the region B would not affect the heating as well as the cooling paths, as shown in curves 4, 5 or 6 when T_{max} was further raised (cf. figure 3). The temperature effects observed for SnSe, Sn_2Se_3 and SnS appear to be associated with a phase change occurring during the heating of deposits. Our observation of transformation of orthorhombic SnSe to a cubic phase at higher temperature and also of SnS (Badacchape & Goswami 1964) lends support to this view. Since the phase change was an irreversible process and dependent on temperature, the shift of $\log R$ vs $1/T$ curve with T_{max} can easily be understood. It seems likely that similar process may also take place for Sn_2Se_3 films. It may be mentioned here that no new phase could be observed for SnTe films even though the deposition was made at various substrate temperatures.

There is no satisfactory theory as yet to explain the various semiconducting behaviours of vacuum deposited films having thicknesses in the ranges studied in this paper. Island structure theory (Naugebauer 1962, 1964) proposed for very thin films, takes into account the growth process leading to the formation of discrete islands of average radius (r) separated by a mean distance (d). With the increase of film thickness there will be an increase in island size r and a corresponding decrease of d . The expression for conductivity (σ) takes these into account. During our studies of resistance of many vacuum deposited films of low thicknesses it was observed that the activation energy changed with film thickness, thinner films having higher values (Goswami & Jog 1964). Surprisingly enough similar trend was also observed in the present cases, where island structure theory is not valid as these films are no longer discontinuous. The variation of TCR with temperature in thicker films is similar to those of very thin films.

REFERENCES

- Badachhape S. B. & Goswami A. 1964 *Indian J. Pure & Appl. Phys.* **2**, 250.
Deokar V.D. & Goswami A. 1966 *Indian J. Pure & Appl. Phys.* **4**, 288, 653.
Goswami A. & Jog R. H. 1964 *Indian J. Pure & Appl. Phys.* **2**, 407.
Goswami A. & Koli S. S. 1966 *Z. Naturforsch.* **21A**, 1462.
1966 *Proc. Int. Symp. on Basic Problems in Thin Film Physics*,
Clausthal, Gottingen, 646.
Naugebauer C.A. 1962 *Z. Angew. Phys.* **14**, 182.
1964 *Physics of Thin Films*, Academic Press, New York, **2**, 7.

A fast high voltage spark gap pulser

By GURMEJ SINGH

Central Scientific Instruments Organisation, Chandigarh (India)

(Received 24 December 1968, Revised 24 July 1969)

A fast high voltage pulse generator built around an EFP-60, 4C35 hydrogen thyatron and a three electrode spark gap is described. The performance of the pulser and the construction of the spark gap are given.

A high voltage spark gap pulser shown in figure 1 has been developed for firing a Marx Voltage Multiplier circuit which supplies high voltage trigger

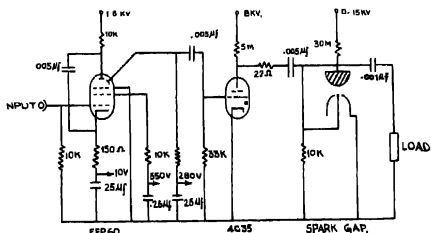


Figure 1. High voltage spark gap pulser.

pulses to a wide gap spark chamber. The input stage of the pulser consists of an EFP-60 secondary emission sharp cut-off pentode which is commonly used for its high power output and excellent pulse characteristics.

The EFP-60 tube, working here as a univibrator due to its capacitive coupling between anode and the cathode, is normally cut-off and triggers on receiving pulses of amplitude greater than 15 volts. The dynode output is a pulse of large amplitude and of sharp rise time. The oscilloscope (Tektronix 585A) record of the waveform is shown in figure 2, where the vertical sensitivity and the sweep speed used are indicated in the caption of the figure. The pulse amplitude as seen in the figure is about 800 volts and its rise time (10% to 90% rise) is about 30 nanoseconds. The pulse power is sufficient to switch the extinguished thyatron 4C35. The large pulse power is mainly due to 1.6KV applied to the plate of the tube and to rather generous cathode emission characteristics of EFP-60. The

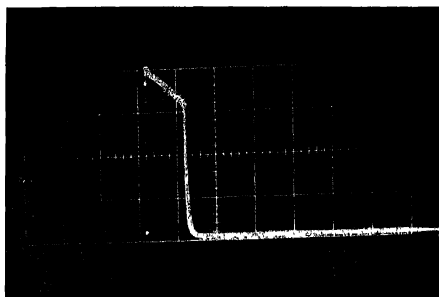
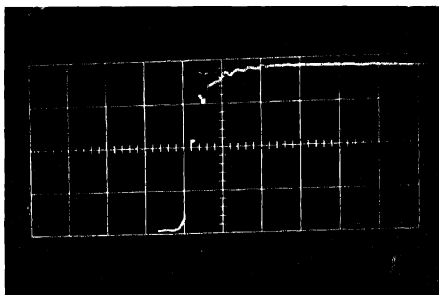


Figure 2. (a) Oscillogram showing the EFP-60 dynode output (full wave form).
Vertical sensitivity—200 volts/cm
Sweep speed—5 microsec/cm



(b) Oscillogram showing the EFP 60 dynode output leading edge of the waveform).
Vertical sensitivity—200 volts cm
Sweep speed—50 nanosec/cm

emission of secondary electrons from the sensitive surface of the dynode also contributes significantly to the pulse power.

The large grid drive used to switch the thyatron tends to decrease its switching delay which is mainly due to the firing time of the grid cathode gap of the thyatron. The overall delay of the circuit in this case is about 100 nanoseconds. This is clearly seen in the oscilloscope record of the output waveform (figure 3, upper trace), measured after attenuating the

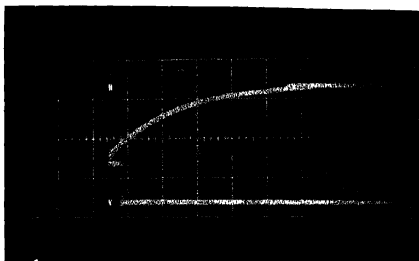
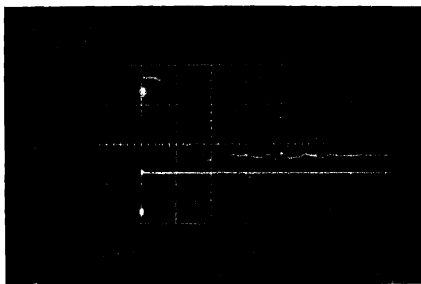


Figure 3. (a) Oscillogram showing the complete waveform.
Vertical sensitivity—5 KV/cm
(upper trace-negative output) and 20 volts/cm (lower trace positive input).
Sweep speed—10 microsec/cm.



(b) Oscillogram showing the delay time. Vertical sensitivity—as in 3 (a)
Sweep speed—100 nanoseconds/cm

pulse amplitude to 1/25th of its value by using resistance voltage divider network. The rectangular input trigger pulse is seen in the lower trace.

Other methods to reduce this delay include the increase of heater voltage (Burgov *et al* 1964) of the thyatron and the application of a positive grid bias (Korenchenko *et al* 1965). Increasing the heater voltage, however, affects the life of the thyatron adversely and positive grid bias increases the danger of accidental sparking in the thyatron due to any unknown voltage fluctuation.

The spark gap, which fires on receiving trigger pulses of 3 KV and more from the thyatron 4C35, when the spark gap high voltage electrode

is set about 500 volts below the spontaneous sparking voltage, is described below.

The Spark Gap

The spark gap of the three electrode type which is easy to fabricate and requires only normal machining tolerances is shown in figure 4.

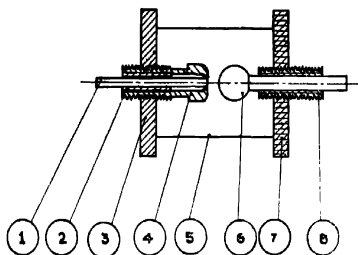


Figure 4. Sectional view of the spark gap (diagram not to scale)

- (1) Trigger electrode (2) Perspex insert (3) Metal support (4) Adjustable ground electrode (5) Brass case (6) High voltage electrode (7) Perspex support (8) Perspex screw for adjusting the distance of the high voltage electrode from the ground electrode.

The trigger electrode is insulated from the ground electrode by using perspex insert. The air gap between the trigger and the ground electrode is of the order of 0.05 mm. For reliable triggering it is only necessary that the air gap at some point be less than 0.002 mm/100V of trigger pulse height. This value is 1/4th that given by Lavoie *et al* (1964) who used a barium titanate covered trigger electrode. The low value of the triggering electric field in the case of Lavoie *et al* is obviously due to the dielectric effect of barium titanate, which on account of its high dielectric constant (over 1000), increases the effect of the electric-field in the adjacent air gap.

While studying the operation of the spark gap pulser it is observed that if the trigger electrode is kept flush with the ground electrode as done by Lavoie *et al* direct sparking takes place between the high voltage electrode and the trigger electrode. This leads to frequent failures of the pulser due to shorting of the air gap between the trigger electrode and the ground electrode by metal deposits produced in the sparking. The difficulty can be removed by blowing an air stream between the two electrodes. This has, however, been overcome simply by setting the trigger electrode a little below the upper surface of the ground electrode so that there is no

direct sparking between the trigger and the high voltage electrode. The pulser works satisfactorily in this setting and there are no frequent failures.

The author wishes to express his gratitude to Dr. P. S. Gill, Director, CSIO, Chandigarh, for his kind interest in this work. Thanks are also due to Shri N. G. Srivatsan for useful discussions, to Shri Gian Singh for fabrication of spark gap, to Shri Gurdev Singh and Shri I. P. S. Bajwa for the help in setting the high voltage power supply. The award of a Research Fellowship by the CSIR is gratefully acknowledged.

REFERENCES

- Burgov N. A. Kiselev Yu. T. & Ushakov V. I. 1964 *Pril. Tekhn. Eksp.* EN2, 104.
Lavoie L., Parker S., Rey C. & Schwartz D. 1964 *Rev. Sci. Instr.* 35, 1567.
Kotenchenko S. M. & Nekrasov K. G. 1965 *Pril. Tekhn. Eksp.* N4, 120.

Laminar flow of two incompressible immiscible fluids between two parallel plates with suction and injection.

By D. S. RAWAT

Mathematics Department, College of Basic Sciences & Humanities

U. P. Agricultural University, Pantnagar Nainital.

(Received 8 September 1969)

The paper is devoted to a study of laminar flow of two viscous incompressible immiscible fluids occupying equal heights between two parallel porous plates with suction at the upper plate and an equal injection at the lower plate under the action of constant pressure gradient. The effects of suction and injection on flow field have been investigated and compared with those cases where no suction and injection are present. A critical value of the ratio of suction/injection Reynold's numbers of the two fluids for which there is no shifting of the position of interface has also been determined in terms of fluid viscosities. The velocity distribution and dependence of interface position on suction/injection are also represented graphically and results have been discussed critically.

1. INTRODUCTION

Flow through channels with porous walls in presence of suction/injection has been studied by Berman (1958) and others. Bird *et al* (1960) have considered adjacent flows of two immiscible liquids in a horizontal thin slit and Rawat (1968) has discussed the corresponding steady flow problem for power law fluids. We propose to study the laminar flow problem of two incompressible immiscible viscous fluids between two infinite parallel porous plates with suction/injection under the influence of constant pressure gradient.

2. FORMULATION OF THE PROBLEM

Consider two incompressible immiscible fluids of densities ρ_i ($\rho_1 > \rho_2$) and viscosities μ_i ($i = 1, 2$) each occupying a height h , flowing in the x - direction between two flat porous plates, at $y = 0$, $y = 2h$ under the action of a constant pressure gradient, $-\partial p/\partial y$.

A constant uniform suction at the upper plate and an equal injection at the lower plate are applied; the position of the interface in steady state is $y = h^*$ ($h^* > h$) and we assume that the components u , v , in the direction of x and y are independent of x . Hence, from the equation of continuity, viz.,

$$\frac{\partial u}{\partial x} + \frac{\partial v}{\partial y} = 0 \quad \dots(1)$$

$$\text{we get} \quad v(x, y) = \text{constant} = v_0 \text{ (say),} \quad \dots(2)$$

where v_0 is positive for both injection/suction.

Also, the equations governing the steady flow of two incompressible fluids are

$$v_0 \frac{\partial u_i}{\partial y} = -\frac{1}{\rho_i} \frac{\partial p}{\partial x} + \frac{\mu_i}{\rho_i} \frac{\partial}{\partial y} \left(\frac{\partial u_i}{\partial y} \right), \quad (i = 1, 2), \quad \dots(3)$$

$$\text{or } \frac{\partial^2 u_i}{\partial y^2} - \frac{R_i}{h} \frac{\partial u_i}{\partial y} = -\frac{P}{\mu_i}, \quad (4)$$

$$\text{where } \frac{\partial p}{\partial x} = -P \text{ and } R_i = \frac{v_0 h \rho_i}{\mu_i}, \quad \dots(5)$$

are the suction/injection parameters called Reynold's numbers and $u_i(y)$ are the velocities of the two fluids.

The boundary conditions are

$$\left. \begin{aligned} [u_1]_{y=0} &= [u_2]_{y=h} = 0 \\ [u_1]_{y=h^*} &= [u_2]_{y=h^*} = U_I \quad (\text{say}), \end{aligned} \right\} \quad \dots(6)$$

and assuming the continuity of shear stress at the interface, we have

$$\left[\mu_1 \frac{\partial u_1}{\partial y} \right]_{y=h^*} = \left[\mu_2 \frac{\partial u_2}{\partial y} \right]_{y=h^*}, \quad \dots(7)$$

where U_I is the common interface velocity. Suffix 1 refers to the lower fluid and 2 to the upper fluid.

Also, the velocities obtained in (2) are given by

$$\left. \begin{aligned} u_{10} &= \frac{Ph^2}{2\mu_1} \left[-\frac{2\mu_1}{\mu_1 + \mu_2} + \frac{\mu_1 - \mu_2}{\mu_1 + \mu_2} \left(\frac{y}{h} \right) - \left(\frac{y}{h} \right)^2 \right], \\ u_{20} &= \frac{Ph^2}{2\mu_2} \left[\frac{2\mu_2}{\mu_1 + \mu_2} + \frac{\mu_1 - \mu_2}{\mu_1 + \mu_2} \left(\frac{y}{h} \right) - \left(\frac{y}{h} \right)^2 \right], \\ \text{and } U_0 &= \frac{Ph^2}{\mu_1 + \mu_2}, \end{aligned} \right\} \quad \dots(8)$$

where, in this case, y is measured from the interface position taken as x -axis and U_0 is the interface velocity.

3. SOLUTION OF THE EQUATIONS

Solving (4), subject to (6), we get.

$$\frac{u_i \mu_i}{Ph^2} = -\frac{1}{R_i} \left[\bar{y} - \lambda \frac{e^{\frac{R_i \bar{y}}{R_i \lambda} - 1}}{e^{\frac{R_i \bar{y}}{R_i \lambda} - 1}} \right] + \frac{U_I \mu_1}{Ph^2} \frac{e^{\frac{R_i \bar{y}}{R_i \lambda} - 1}}{e^{\frac{R_i \bar{y}}{R_i \lambda} - 1}}, \quad \dots(9)$$

$$\begin{aligned} \frac{u_2 \mu_2}{Ph^2} &= \frac{1}{R_2} \left[(\bar{y} - 2) + (2 - \lambda) \frac{1 - e^{-(2-\bar{y})R_2}}{1 - e^{-(2-\lambda)R_2}} \right] \\ &+ \frac{U_1 \mu_2}{Ph^2} \frac{1 - e^{-(2-\bar{y})R_2}}{1 - e^{-(2-\lambda)R_2}}, \end{aligned} \quad \dots(10)$$

and on using (7), (9) and (10), we get

$$\frac{U_1 \mu_1}{Ph^2} = \frac{\frac{1}{R_2} - \frac{1}{R_1} + \frac{2-\lambda}{1-e^{-(2-\lambda)R_2}} + \frac{\lambda}{1-e^{-\lambda R_1}}}{\frac{\mu R_2}{e^{-(2-\lambda)R_2}} - 1 + \frac{R_1}{1-e^{-\lambda R_1}}} \quad \dots(11)$$

$$= \Phi(R_1, R_2, \lambda, \bar{\mu}), \quad (\text{say}), \quad \dots(11a)$$

where $\bar{\mu} = \frac{\mu_2}{\mu_1}$, $\bar{y} = \frac{y}{h}$ and $\lambda = \frac{h^*}{h}$ ($1 \leq \lambda \leq 2$).

Total flux is given by

$$Q = \int_0^{h^*} u_1 dy + \int_{h^*}^{2h} u_2 dy = Q_1 + Q_2 \quad (\text{say}),$$

where from (9) and (10) respectively, we have

$$\frac{Q_1 \mu_1}{Ph^2} = \frac{\lambda}{R_2^2} \left[\frac{R_1}{2} \coth \frac{\lambda R_1}{2} - 1 \right] + \frac{U_1 \mu_1}{Ph^2} \frac{1}{R_1} \left[1 + \frac{\lambda R_1}{1 - e^{-\lambda R_1}} \right], \quad \dots(13)$$

and

$$\begin{aligned} \frac{Q_2 \mu_2}{Ph^2} &= \frac{2-\lambda}{R_2^2} \left[\frac{2-\lambda}{2} R_2 \coth \frac{2-\lambda}{2} R_2 - 1 \right] \\ &+ \frac{U_1 \mu_2}{Ph^2} \frac{1}{R_2} \left[\frac{(2-\lambda) R_2}{1 - e^{-(2-\lambda)R_2}} - 1 \right] \end{aligned} \quad \dots(14)$$

The skin frictions at the lower and upper plates are respectively, given by

$$\begin{aligned} \tau_1 &= \left[\mu_1 \frac{\partial u_1}{\partial y} \right]_{y=0} \\ &= Ph \left[\frac{1}{R_1} + \frac{\lambda}{1 - e^{-\lambda R_1}} + \frac{U_1 \mu_1}{Ph^2} \frac{R_1}{e^{-\lambda R_1} - 1} \right], \end{aligned} \quad \dots(15)$$

$$\text{and } \tau_2 = \left[-\mu_2 \frac{\partial u_2}{\partial y} \right]_{y=2h}$$

$$= -Ph \left[\frac{1}{R_2} - \frac{2-\lambda}{1-e^{-(2-\lambda)R_2}} - \frac{U_1 \mu_2}{Ph^2} - \frac{R_2}{1-e^{-(2-\lambda)R_2}} \right]$$

...(16).

We introduce the following dimensionless variables

$$\bar{u}_i = \frac{u_i}{U_1}, \quad P_m = \frac{Ph^2}{U_1 \mu_1} = \frac{1}{\phi(R_1, R_2, \lambda, \bar{\mu})} \quad \dots (17).$$

Equations (9) and (10), on using (17), transform to the dimensionless form

$$\bar{u}_1 = \frac{e^{R_1 \bar{y}} - 1}{e^{R_1 \lambda} - 1} + \frac{P_m}{R_1} \left[\bar{y} - \lambda \frac{e^{R_1 \bar{y}} - 1}{e^{R_1 \lambda} - 1} \right], \quad \dots (18)$$

$$\bar{u}_2 = \frac{1 - e^{-(2-\bar{y})R_2}}{1 - e^{-(2-\lambda)R_2}} + \frac{P_m}{R_2} \left[(\bar{y} - 2) + (2 - \lambda) \frac{1 - e^{-(2-\bar{y})R_2}}{1 - e^{-(2-\lambda)R_2}} \right].$$

...(19)

If λ is fixed, P_m , U_1 , \bar{u}_1 , \bar{u}_2 can be determined for given R_1 , R_2 and $\bar{\mu}$. Further we assume that the interface velocity remains the same as in ordinary flow (Bird *et al* 1960) i. e.,

$$U_1 = U_0 = Ph^2/(\mu_1 + \mu_2),$$

then from (11) we get

$$\frac{1}{R_1} - \left(\lambda - \frac{R_1}{1+\bar{\mu}} \right) \frac{1}{1 - e^{-\lambda R_1}} = \frac{1}{R_2}$$

$$+ \left[(2-\lambda) + \frac{\bar{\mu}}{1+\bar{\mu}} R_2 \right] \frac{1}{1 - e^{-(2-\lambda)R_2}} \quad \dots (20)$$

which determines λ , the position of interface, and the corresponding velocity distribution can be easily obtained from (9) and (11).

4. APPROXIMATE SOLUTION FOR SMALL SUCTION-INJECTION PARAMETERS

Considering only first power of R_1 and R_2 , neglecting the terms of the order of R_1^2 , R_2^2 and also assuming $\lambda R_1 < 1$ and $(2 - \lambda) R_2 < 1$ from (13), (19) and (11), respectively, we get

$$\bar{u}_1 = \frac{\bar{y}}{\lambda} + \frac{\bar{y}(\lambda - \bar{y})}{2} P_m \left[1 + \frac{R_1}{6} \left\{ \frac{6}{\lambda P_m} - (2\bar{y} - \lambda) \right\} \right], \quad (21)$$

$$\bar{u}_2 = \frac{2 - \bar{y}}{2 - \lambda} + \frac{(2 - \bar{y})(\lambda - \bar{y})}{2} P_m \left[1 + \frac{R_2}{6} \left\{ \frac{6}{(2 - \lambda) P_m} + 2\bar{y} - \lambda - 2 \right\} \right] \quad \dots(22)$$

$$\text{and } \frac{U_I \mu_1}{P h^2} = \frac{1 + \frac{1}{12} [\lambda^2 R_1 - (2 - \lambda)^2 R_2]}{2 - \lambda \left[1 - \frac{1}{2} (2 - \lambda) R_2 \right] + \frac{1}{\lambda} \left[1 + \frac{\lambda R_1}{2} \right]} \quad \dots(23)$$

TABLE 1. VALUES OF $\frac{U_I \mu_1}{P h^2}$

$R_1 = .1 \text{ fixed}$							
$\bar{\mu} \downarrow R_2 =$.2	.3	.4	.5	.6	.7	.8
.5	.6528	.6637	.6706	.6799	.6896	.6997	.7100
1	.4334	.4416	.4501	.4594	.4685	.4783	.4886
1.5	.3244	.3314	.3389	.3468	.3547	.3634	.3724
$R_2 = .1 \text{ fixed}$							
$\bar{\mu} \downarrow R_1 =$.2	.3	.4	.5	.6	.7	.8
.5	.6345	.6236	.6170	.6085	.6024	.5935	.5865
1	.4235	.4204	.4187	.4179	.4160	.4141	.4130
1.5	.3178	.3180	.3182	.3183	.3183	.3183	.3183
$R_1 = R_2$							
$\bar{\mu} \downarrow$.1	.2	.3	.5			
.5	.6443	.6426	.6415	.6392			
1	.4268	.4312	.4376	.4423			
1.5	.3177	.3178	.3316	.3382			

Table 1 exhibits clearly the behaviour of the interface velocity at $\lambda = 1.4$ for different values of R_1 , R_2 and $\bar{\mu}$. It indicates that U_I increases with

R_2 for all $\bar{\mu}$ but as R_1 increases it decreases when $\bar{\mu} \leq 1$ and increases very slowly to a constant value when $\bar{\mu} > 1$.

Again, putting $U_I = U_0$ and $\lambda = 1 + I$, $\left(I = \frac{h^* - h}{h} \right)$, in (21) and (24), we get

$$(R_2 - R_1) I^4 - 2(R_1 + R_2) I^3 - 6 \left(2 + \frac{\bar{\mu} R_2 - R_1}{1 + \bar{\mu}} \right) I^2 - 2 I \left[6 \frac{\bar{\mu} - 1}{\bar{\mu} + 1} - R_1 - R_2 \right] - \frac{R_1(5 - \bar{\mu}) - R_2(5\bar{\mu} - 1)}{1 + \bar{\mu}} = 0 \quad \dots(24)$$

from which I , (or λ) can be determined.

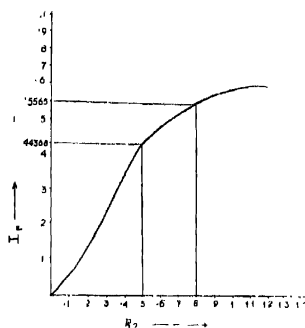


Figure 1. Shifting of common interface with increasing R_2 ($R_1=1$)

Equation (24) shows that in the presence of small suction/injection the interface will not shift from the ordinary state position $y = h$, if

$$\frac{R_2}{R_1} = \frac{5 - \bar{\mu}}{5\bar{\mu} - 1}, \quad (2 < \bar{\mu} < 5), \quad \dots(25)$$

The plot of I , against R_2 (figure 1) at fixed R_1 shows that as R_2 increases the common interface shifts towards the less viscous second fluid but never approaches the plate.

5. RESULTS AND DISCUSSION

- (i) When we take the limit of (9), (10), (11), (12), (13), (14), (15) and (16) as R_1 and R_2 tend to zero (i.e., v_0 is zero) we get the results obtained by Bird *et al* (1960).

(ii) If $\mu_1, \bar{y}, \lambda, R_1$ are interchanged with $\mu_2, \bar{y} - 2, \lambda - 2, R_2$ respectively, then u_1 is interchanged with u_2, Q_1 with Q_2 and τ_1 with τ_2 . This is the result expected from symmetry also.

(iii) Putting $R_i = \frac{v_0 h \rho_i}{\mu_i}$ and keeping ρ_i fixed, (9), (10) and (11) show that u_1, u_2, U_I decrease as μ_1, μ_2 increase.

(iv) For fixed $\bar{\mu}, \lambda$ equations (9), (10) and (11) show that the velocities u_1, u_2, U_I increase with increasing suction parameter R_2 and decrease with increasing injection parameter R_1 .

(v) (a) Comparing the fluid velocities in (21) and (22) with those in ordinary state flow (8) (Bird *et al* 1960) a little consideration shows that $\frac{u_1}{U_0} >, = \text{ or } < \frac{u_{10}}{U_0}$ when $\bar{y} <, = \text{ or } > \frac{\lambda}{2}$, which is also evident from graph (figure 2), which represents the velocity profiles of the two types of flows (with or without suction/injection) at $\lambda = 1.4368$ and $\lambda = 1.2329$ for $\bar{\mu} \leq 1$.

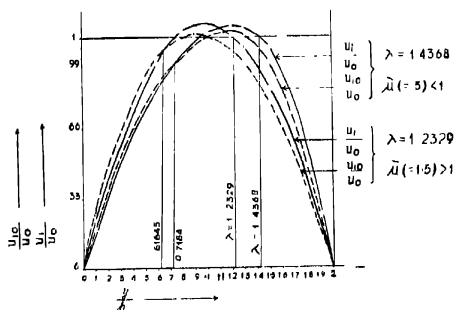


Figure 2. Velocity profiles with or without suction and injection

(b) Comparing interface velocities of the two kinds of flows, we have $U_I >, = \text{ or } < U_0$ according as

$$\Phi(R_1, R_2, \lambda, \bar{\mu}) >, = \text{ or } < \frac{1}{1 + \bar{\mu}} \quad \dots(26)$$

and for small R_1, R_2

$$\frac{\bar{\mu}R_2 - R_1}{1 + \bar{\mu}} + \frac{R_1\lambda^2 - R_2(2 - \lambda)^2}{6} >, = \text{or} < \frac{2(\lambda - 1)}{\lambda(2 - \lambda)} \cdot \frac{(1 + \bar{\mu})\lambda - 2}{1 + \bar{\mu}} \quad \dots(27)$$

$$\text{and } \frac{R_2}{R_1} >, = \text{or} < \frac{5 - \bar{\mu}}{5\bar{\mu} - 1} \quad (\text{when } \lambda = 1, .2 < \bar{\mu} < 5) \quad \dots(28)$$

(vi) τ_1 decreases with increasing R_1 and τ_2 numerically increases with increasing R_2 . Q_1 and Q_2 also behave in a similar manner.

6. UNIQUENESS OF VELOCITY MAXIMUM

To find velocity maximum, we have

$$\frac{\partial u_i}{\partial y} = 0, (i = 1, 2), \quad \dots(29)$$

which on using (9) and (10), give

$$\frac{y_1}{h} = \lambda + \frac{1}{R_1} \log \frac{1 - e^{\lambda R_1}}{\lambda R_1 - \Phi(R_1, R_2, \lambda, \bar{\mu}) R_1^2} \quad \dots(30)$$

$$= \lambda + \frac{1}{R_1} \log \frac{f_1}{f_2} \quad (\text{say}), \quad \dots(30a)$$

and

$$\frac{y_2}{h} = \lambda + \frac{1}{R_2} \log \frac{e^{(2-\lambda)R_2} - 1}{(2 - \lambda) R_2 + \bar{\mu} R_2^2 \phi(R_1, R_2, \lambda, \bar{\mu})} \quad \dots(31)$$

$$= \lambda + \frac{1}{R_2} \log \frac{F_1}{F_2} \quad (\text{say}), \quad \dots(31a)$$

where $\Phi(R_1, R_2, \lambda, \bar{\mu})$ is defined in (11a).

The velocity maximum will occur in the first or second fluid according as $0 < \frac{y_1}{h} < \lambda$ or $\lambda < \frac{y_2}{h} < 2$. The velocity maximum will be at the common interface (i. e., at $y = h^*$) if $f_1 = f_2$, $F_1 = F_2$ or $\bar{\mu} = \mu^*$,

$$\text{where, } \mu^* = \frac{e^{(2-\lambda)R_1} - (2 - \lambda) R_2 - 1}{R_1^2} \bigg/ \frac{e^{-\lambda R_1} + R_1 \lambda - 1}{R_1^2}, \quad \dots(32)$$

which is the critical value of the ratio of the viscosity coefficients of the two fluids.

Also, we observe the following facts :

- (i) If $\bar{\mu} > \mu^*$, we have $F_1/F_2 < 1$ so that $y_2/h < \lambda$ and $f_1/f_2 < 1$ so that $y_1/h < \lambda$, which shows that the maximum velocity will occur in the first fluid and not in the second fluid.
- (ii) If $\bar{\mu} < \mu^*$, we have $f_1/f_2 > 1$ so that $y_1/h > \lambda$ and also $F_1/F_2 > 1$ so that $y_2/h > \lambda$ showing that the maximum velocity will occur in the second fluid and not in the first fluid.

Besides this the velocity as well as its derivatives are continuous at all points except at the interface where the derivative can change only in magnitude but not in sign and velocity vanishes at the plates. Hence, from these considerations, we conclude that there is a unique velocity maximum and it occurs in the lower fluid, interface or upper fluid according as $\bar{\mu} >$, = or $< \mu^*$ and its position is given by (30) or (31).

Author is very grateful to Shri D. P. Singh, Vice-chancellor and Dr. K. G. Gollakata, Director, for their encouragement during this investigation.

REFERENCES

- Berman A. S. 1958 *J. Appl. Phys.* **29**, 71
 Bird R. S., Stewart W. E. & Lightfoot E. N. 1960 *Transport Phenomenon*, John Wiley and Sons, New York.
 Rawat D. S. 1968 *Appl. Phys. Quarterly*, **10**, No. 2, 43
 Schlichting H. *Boundary Layer Theory*, Fourth Edition.

$1^1S \rightarrow 2^1P$ excitation of helium-like ions by electron impact

By D. P. SURAL

Department of Physics, Jadavpur University,

AND

N. C. SIL

*Department of Theoretical Physics, Indian Association for the
Cultivation of Science,*

Calcutta-32,

(Received 8 September 1969)

The $1^1S \rightarrow 2^1P$ excitation of helium-like ions by electron impact is studied in the Coulomb-Born approximation. The total crosssections for this process are computed at threshold and higher energies for the particular ion Li^+ . Results of calculation using the Coulomb-Bethe approximation are found to differ considerably from that using the Coulomb-Born method.

INTRODUCTION

A knowledge of the crosssections for excitation of ions by electron impact is often required for explaining the intensities of certain spectral lines occurring in stellar radiations as also for determining the electron temperatures in high temperature plasma. The use of helium-like ions for the latter purpose has been found to be particularly suitable (Williams & Kaufman 1960). However, direct experimental measurements of such crosssections have been made only in a few cases as the technique involved is rather complicated (Dance *et al* 1966). In a previous paper (Sural & Sil 1966) we have studied the problem of $1^1S \rightarrow 2^1S$ excitation of helium-like ions by electron impact using the Coulomb-Born approximation method and have obtained the scattering amplitude in a closed form. The dominating nature of the Coulomb field of the ion makes the approximation reliable even when the energy of the incident electron is not high. In this paper we have considered collisions between electrons and helium-like ions resulting in the excitation of the ions from their ground to the 2^1P state and have calculated, for the particular ion Li^+ , the cross sections at different incident energies. The Coulomb-Born approximation has again been used, but because of the nature of certain integrals, it has not been possible to obtain a closed expression for the scattering amplitude. The Coulomb waves representing the incident and scattered electrons occurring in the expression for the scattering amplitude have therefore been expanded into partial waves in the manner described in the next section. Similar procedures used for other types of ions have been reviewed by Moisewitsch and Smith (1968).

THEORY

The scattering amplitude for the process of excitation of helium-like ions by electron impact in the Coulomb-Born approximation (using atomic units) is given by

$$f = -\frac{1}{2\pi} \int \psi_n^*(\mathbf{r}_2, \mathbf{r}_3) \chi(Z-2, -\mathbf{k}_n, \mathbf{r}_1) \left(-\frac{2}{r_1} + \frac{1}{r_{12}} + \frac{1}{r_{13}} \right) \psi_0(\mathbf{r}_2, \mathbf{r}_3) \chi(Z-2, \mathbf{k}_0, \mathbf{r}_1) d\mathbf{r}_1 d\mathbf{r}_2 d\mathbf{r}_3 \quad \dots (1)$$

where ψ_0 and ψ_n are, respectively, the wave functions of the ion in its ground state and excited state and the χ 's are the Coulomb wave functions corresponding to charge, $Z-2$ and momentum vectors, \mathbf{k}_n and \mathbf{k}_0 . Introducing the symbols

$$\alpha_0 = \frac{Z-2}{k_0} \quad \text{and} \quad \alpha_n = \frac{Z-2}{k_n}, \quad \dots (2)$$

$$\chi(z-2, \mathbf{k}_0, \mathbf{r}) = \exp(i\pi\alpha_0) \Gamma(1-i\alpha_0) \exp(i\mathbf{k}_0 \cdot \mathbf{r}) F_1(i\alpha_0; 1; i(k_0 r - \mathbf{k}_0 \cdot \mathbf{r})) \quad \dots (3)$$

and a similar expression for $\chi(Z-2, -\mathbf{k}_n, \mathbf{r})$. F_1 is a confluent hypergeometric function.

For the 1^1S and 2^1P states of the helium-like ions we have used the wave functions proposed by Morse *et al* (1935). One can then show that

$$\int \psi_n^*(\mathbf{r}_2, \mathbf{r}_3) \left(-\frac{2}{r_1} + \frac{1}{r_{12}} + \frac{1}{r_{13}} \right) \psi_0(\mathbf{r}_2, \mathbf{r}_3) d\mathbf{r}_2 d\mathbf{r}_3 = \begin{cases} 2^{1/2} \cos \theta_1 & (\text{for } m=0) \\ C_3 g(r_1) \sin \theta_1 \exp(-i\phi_1) & (\text{for } m=+1) \\ \sin \theta_1 \exp(+i\phi_1) & (\text{for } m=-1) \end{cases} \quad (4)$$

where θ_1 and ϕ_1 are, respectively, the polar and azimuthal angle of \mathbf{r}_1 and

$$g(r) = \frac{1}{r^2} \left[1 - (1 + \nu r + \frac{1}{2} \nu^2 r^2 + \frac{1}{6} \nu^3 r^3) \exp(-\nu r) \right],$$

$$C_3 = 256 \left(\frac{\mu a}{\lambda} \right)^3 \left(\frac{\mu'' c''}{\gamma^2} \right)^{5/2} (\mu' a')^{3/2} \quad (5)$$

with $\lambda = \mu'' a'' + \mu a$, $\nu = \mu'' c' + \mu a$.

Numerical values of the parameters μa , $\mu'' c''$ and $\mu'' a''$ for several helium-like ions are given by Morse *et al* (1935).

A final integration over r_1 is to be performed to get the scattering amplitude from (1). For the case of $1^1S \rightarrow 2^1S$ excitation the integral can

be worked out and the scattering amplitude has been obtained in a closed form. However, for excitation to the 2^1P state with the form of $g(r)$ given by (5) it has not been possible to perform the integration analytically and consequently we expand the Coulomb wave functions in terms of the Legendre polynomials,

$$\chi(Z-2, \mathbf{k}_0, \mathbf{r}) = \sum_{l=0}^{\infty} (2l+1) i^l \exp(i\eta_{0l}) \frac{F_{\kappa_{0l}}(r)}{k_0^{1/2} r} P_l(\cos \theta_0) \quad \dots (6)$$

where θ_0 is the angle between \mathbf{k}_0 and \mathbf{r}

$$\eta_{0l} = \arg \Gamma(l+1 - i\kappa_{0l}).$$

The radial functions $F_{\kappa_{0l}}$ satisfy

$$\frac{d^2 F_{\kappa_{0l}}}{dr^2} + \left[k_0^2 + \frac{2(Z-2)}{r} - \frac{l(l+1)}{r^2} \right] F_{\kappa_{0l}} = 0 \quad (7)$$

With the asymptotic form

$$F_{\kappa_{0l}}(r) \sim \frac{1}{k_0^{1/2}} \sin [k_0 r - \frac{1}{2}l\pi + \eta_{0l} + \kappa_{0l} \ln(2k_0 r)] \quad \dots (1)$$

Expansion for $\chi(Z-2, -\mathbf{k}_n, \mathbf{r})$ will similarly involve the radial function $F_{\kappa_{nl}}$.

Substituting these expansions in (1), using the formula for the total cross-section for the process

$$Q = 2\pi \int_0^\pi |f|^2 \sin \theta d\theta \quad \dots (9)$$

and taking the sum of the contributions for the states with $m = 0, \pm 1$ we get, after some calculation, the total cross-section for $1^1S \rightarrow 2^1P$ excitation of helium-like ions by electron impact :

$$Q = 32\pi \frac{C_1^2}{k_0^3} \left[\sum_{l=0}^{\infty} \left\{ (l+1) \left| \int_0^\infty F_{\kappa_{nl}}(r_1) F_{\kappa_{0l+1}}(r_1) g(r_1) dr_1 \right|^2 \right\} + \sum_{l=1}^{\infty} \left\{ l \left| \int_0^\infty F_{\kappa_{nl}}(r_1) F_{\kappa_{0l-1}}(r_1) g(r_1) dr_1 \right|^2 \right\} \right] \quad \dots (10)$$

The radial integrals occurring in (10) can be expressed in terms of one of the Appel functions, a type of generalized hypergeometric function of two variables. These functions, however, are not of much use for computational purposes. We have therefore, separated each of the radial integrals in (10) into two parts, one containing the asymptotic part

$\frac{1}{r_1^2}$ of $g(r_1)$ and the other containing the rest of $g(r_1)$. To be specific we have taken the case of $1^1S \rightarrow 2^1P$ excitation of the ion Li^+ for which the relevant parameters are

$$\mu a = 2.69, \mu' c'' = 0.98, \mu' a' = 3.00, Z = 3, k_0^2 - k_n^2 = 4.573. \dots (11)$$

The integrals containing the asymptotic part of $g(r_1)$ can be expressed in terms of the integrals of the type

$$I_l = \int_0^\infty F_{\alpha n l}(r) F_{\alpha_0 l}(r) \frac{dr}{r}. \quad \dots (12)$$

The I_l 's can be analytically evaluated. It can be shown that they satisfy the recursion relation

$$\begin{aligned} & 2l(l+1)^2 + \alpha_n^2 \{ (l+1)^2 + \alpha_0^2 \} I_{l+1} \\ & - (2l+1) \left\{ \frac{\alpha_n^2 + \alpha_0^2}{\alpha_n \alpha_0} l(l+1) + 2\alpha_n \alpha_0 \right\} I_l \\ & + (2l+2)(l^2 + \alpha_n^2)^{1/2} (l^2 + \alpha_0^2)^{1/2} I_{l-1} = 0 \end{aligned} \quad \dots (13)$$

so that, for a given pair of values of k_0 and k_n , a computation of I_0 and I_1 enables one to find out the values of I_l for other values of l .

To evaluate the integrals

$$\int_0^\infty F_{\alpha n l}(r) F_{\alpha_0 l \pm 1}(r) \left[g(r) - \frac{1}{r^2} \right] dr \quad \dots (14)$$

we have first computed the functions $F_{\alpha l}(r)$ for the required values of k and different values of l and r . The known series expansion of $F_{\alpha l}(r)$ has been used for the range $r = 0$ to $r = 1$. For higher values of r we have numerically solved the differential equation (7). The evaluation of (14) becomes simplified as, with increase in r , the integrand rapidly converges to zero because of the exponential term $\exp(-vr)$ with $v = 3.67$.

After the numerical determination of the radial integrals these are substituted in (10) to calculate the cross-sections for the excitation process.

RESULTS

Table 1 shows the values obtained by us for the $1^1S \rightarrow 2^1P$ excitation cross-section for the particular helium like ion Li^+ . The cross-sections are given in units of πa_0^2 where a_0 is the Bohr radius. The energies E of the incident electrons are expressed in units of ΔE , the threshold

energy for the particular process. It is seen that in the energy range considered the cross section varies only slightly from the value obtained at threshold. The behaviour is very similar to that obtained by Burgess (1961) for the crosssection for excitation $2P$ state from the ground state of the hydrogenic ion He^+ . At higher energies the crosssections will surely decrease but then the Coulomb waves will approximate to plane waves. The finite value of the crosssection at threshold is a characteristic property for ion-excitation process, not to be found for excitation of neutral atoms except perhaps for the hydrogen atom whose excited states are degenerate (Celtman 1969). At present there is no experimental results for Li^+ excitation, but Dance *et al* (1966) have measured a finite crosssection at the threshold energy for $1S \rightarrow 2S$ excitation of He^+ by electron impact.

TABLE 1. Total cross section for $1^1S \rightarrow 2^1P$ excitation of Li^+ by electron impact

Incident Energy $E/\Delta B$	Cross section in units of πa_0^2	
	Coulomb - Born	Coulomb - Bethe
1	0.035	0.268
1.5	0.037	0.197
2	0.036	0.161
3	0.032	0.126

We have also included in table 1 the results of our calculation using the so-called Coulomb-Bethe approximation which amounts to a replacement of $g(r_1)$ in (6) by its asymptotic value $\frac{1}{r_1}$. This type of approximation is often used to get a quick estimate of excitation crosssections but is seen to be not very reliable in this particular case, within the energy considered.

The authors are thankful to Prof. D. Basu, Director, Indian Association for the Cultivation of Science for his kind interest in the work.

REFERENCES.

- Burgess A. 1961 *Mem. Soc. Roy. Sci. Liege* **4**, 299.
- Dance D.F., Harrison M.F.A. & Smith A.C.H. 1966 *Proc. Roy. Soc.* **A290**, 74.
- Geltman S. 1969 *Topics in Atomic Collision Theory*, Academic Press, New York and London, 153.
- Moiseiwitsch B.L. & Smith S.J. 1968 *Rev. Mod. Phys.* **40**, 238.
- Morse P.M., Young L.A. & Haurwitz E.S. 1935 *Phys. Rev.* **48**, 948.
- Sural D.P. & Sil N.C. 1966 *Proc. Phys. Soc.* **87**, 201.
- Williams R.V. & Kaufman S. 1960 *Proc. Phys. Soc.* **56**, 329.

A note on the molecular and intramolecular relaxation times of anisole and phenetole in carbon tetrachloride solution

By B. DUTTA (NÉE SINHA)

Optics Department,

Indian Association for the Cultivation of Science, Calcutta-32.

(Received 15 October 1969)

From the study of the absorption of microwaves of wavelength 1.64 cm, 0.83 and 0.77 cm in the case of dilute solutions of phenetole and anisole in carbon tetrachloride at different temperatures the values of loss tangent ($\tan \delta$) have been measured and these have been used to the values of molecular relaxation time (τ_1), intramolecular relaxation time (τ_2) and the relative contribution factors C_1 and C_2 of the two processes to the overall dielectric losses

From the analysis of these results it has been pointed out that the relaxation time τ_2 is probably an intramolecular characteristic but the quantity C_2 is dependent on the nature of the medium. In phenetole the intramolecular rotation appears to be hindered to a greater extent than that of the methoxy group in anisole.

INTRODUCTION

The results on the measurements of the loss tangent ($\tan \delta$) values of anisole in dilute solutions of a number of non-polar solvents at different temperatures in the microwave frequency region of 38.8 KMc/s were reported earlier (Kastha *et al* 1967) and the relaxation times τ_1 and τ_2 respectively for molecular and intramolecular orientation together with the relative contribution factors C_1 and C_2 were determined in the case of solutions in hexane and paraffin. But it was not then possible to analyse the loss tangent values in the case of CCl_4 solution to obtain these parameters. In order to determine these quantities measurements of the loss tangent values of anisole in dilute CCl_4 solution due to absorption of microwaves of wavelength 1.64 cm at different temperatures have been made. Also similar measurements in the case of dilute solutions of phenetole in CCl_4 solution at different temperatures and at two microwave frequencies of wavelengths 0.83 cm and 1.64 cm have been carried out. The analysis of all these results for the determination of τ_1 and τ_2 and C_2 values of these two molecules is presented in this paper.

EXPERIMENTAL

Chemically pure anisole and phenetole were first subjected to fractional distillation and the proper fractions were distilled under reduced pressure and dried before being used in the investigation. The solvent carbon tetrachloride was dried by the usual method. The experimental arrangement for measuring loss tangent values in the case of 0.83 cm and 1.64 cm microwaves was the same as described earlier (Bhattacharjee *et al*

1964) except that the microwave generators were modulated by square waves of frequency 1000 c/sec and the transmitted microwave power was measured after detection by a tuned detector amplified in conjunction with an amplifier. The values of loss tangent factor were calculated in the same way as described in the above paper.

RESULTS

The value of $\tan \delta$ (loss tangent) at different temperatures at different microwave frequencies in anisole and phenetole are given in tables 1, 2 and 3 respectively. The results also contain the values of the parameter $\xi(T)$

TABLE 1. VARIATION OF LOSS TANGENT WITH TEMPERATURE AT TWO FREQUENCIES OF ANISOLE AND PHENETOLE IN CARBON TETRACHLORIDE SOLUTION

2.73 $\times 10^{-4}$ moles/cc of anisole in CCl ₄		6.42 $\times 10^{-4}$ moles/cc of anisole in CCl ₄		4.71 $\times 10^{-4}$ moles/cc of phenetole in CCl ₄		5.49 $\times 10^{-4}$ moles/cc of phenetole in CCl ₄	
$\lambda = 0.77$ cm		$\lambda = 1.64$ cm		$\lambda = 0.83$ cm		$\lambda = 1.64$ cm	
Temp °K	$\tan \delta$ $\times 10$	Temp °K	$\tan \delta$ $\times 10$	Temp °K	$\tan \delta \times 10$	Temp °K	$\tan \delta$ $\times 10$
285	.0747	283	.211	287	.105	287	.160
295	.0767	293	.207	295	.101	294	.159
305	.0788	305	.197	304	.114	303	.156
311	.0809	315	.187	323	.101	313	.150
319	.0830	325.5	.174	335	.108	323	.143
329	.0788	335	.158	344	.103	333	.135
339	.0747	343	.145			343	.125

TABLE 2 ANISOLE IN CCl₄

$\lambda = 0.77$ cm					$\lambda = 1.64$		
Temp °K	τ_1 per sec	τ_2 per sec	C_1/C_2	$\xi(\tau)^*$ observed	$\xi(\tau)$ calculated from eqn. (2) with pre- sent values of τ_1, τ_2 & C_2	$\xi(\tau)^*$ observed	$\xi(\tau)$ calculated from eqn. (2) with pre- sent values of τ_1, τ_2 & C_2
285	17.0	3.0	.6/4	.311	.320	.367	.364
295	14.0	2.5	.6/4	.332	.340	.373	.375
305	11.5	2.1	.5/5	.360	.358	.368	.358
315	9.5	1.9	.5/5	.384	.370	.360	.355
325	8.2	1.7	.5/5	.386	.378	.346	.344
335	7.1	1.4	.5/5	.375	.369	.323	.324

*calculated from $\tan \delta$ values in table 1 with $\mu = 1.25 D$

TABLE 3. PHENETOLE IN CCl_4

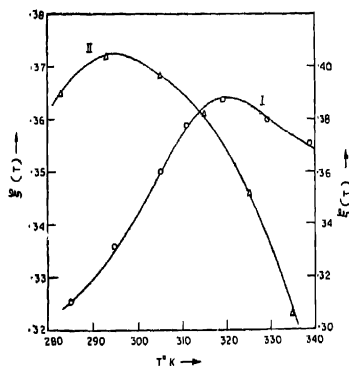
Temp. °K	τ_1 per sec.	τ_2 per sec.	C_1/C_2	$\lambda = .83 \text{ cm.}$		$\lambda = 1.64 \text{ cm.}$	
				$\xi(T)^*$ observed	$\xi(T)^*$ calculated from eqn. (2) with the present τ_1, τ_2, C_1 values	$\xi(T)^*$ observed	$\xi(T)^*$ calculated from eqn. (2) with the present τ_1, τ_2 and C_2 values.
285	18.0	4.5	.5/.5	322	339	420	.398
295	15.0	3.6	.5/.5	349	.358	.433	.402
305	11.0	3.0	.5/.5	.374	.393	.436	.415
315	9.0	2.4	.5/.5	383	.405	.433	.403
325	7.8	2.2	.5/.5	388	417	425	.394
345	6.5	1.5	.5/.5	.381	.401	392	.355

*Calculated from $\tan \delta$ values in of table 1 with $\mu = 1.1D$

obtained from the measured $\tan \delta$ values with the help of the following expression (Kastha *et al* 1967)

$$\frac{T \tan \delta}{c} \left/ \frac{4\pi N \mu^2}{27k} \cdot \frac{(\epsilon_0 + 2)^2}{\epsilon_0} \right. = \xi(T) \quad \dots (1)$$

The graphs depicting the variation of $\xi(T)$ with temperature for the two compounds at the different microwave frequencies are shown in figures 1 and 2.

Figure 1. Plots of $\xi(T)$ vs T for solutions of anisole at two frequencies.I. $\lambda = 0.77 \text{ cm.}$ (Right hand side ordinate values)II. $\lambda = 1.64 \text{ cm.}$ (Left hand side ordinate values)

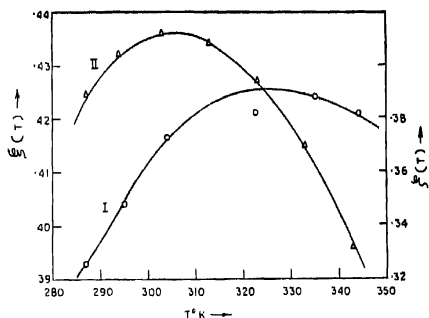


Figure 2. Plots of $\xi(T)$ vs T for solutions of phepetole at two frequencies.

I. $\lambda = 0.83$ cm. (Right hand side ordinate values)

II. $\lambda = 1.64$ cm. (Left hand side ordinate values)

The values of τ_1 , τ_2 and C_2 have been calculated from the measured $\xi(T)$ values with the help of the following equation. (Kastha *et al* 1967)

$$\xi(T) = \frac{C_1 \omega \tau_1}{1 + \omega^2 \tau_1^2} + \frac{C_2 \omega \tau_2}{1 + \omega^2 \tau_2^2} \quad \dots (2)$$

by a trial and error method. It was shown earlier (Kastha *et al* 1967) that for microwaves having the angular frequency ω the value of τ_2 at the temperature at which $\xi(T)$ is maximum is less than $1/\omega$ while that of τ_1 at the corresponding temperature is greater than $1/\omega$.

It is seen from the figure 1 that in case of the solution of anisole in CCl_4 the values of $\xi(T)$ is maximum at about 315°K for microwaves of 0.77 cm wavelength while for microwaves of wavelength 1.64 cms the maximum of $\xi(T)$ occurs at about 295°K. Hence it is concluded that the values of τ_2 at 315°K is less than 4.1 per sec and that of τ_1 at 295°K is greater than 8.7 per sec. With these limits for τ_1 and τ_2 sets of values of τ_1 , τ_2 and C_2 were assumed for each temperature and the values of $\xi(T)$ for the two frequencies at each temperature were calculated from equation (2). The agreement between the calculated and experimental values was then studied. In this way the values of τ_1 , τ_2 and C_2 which produced the studied maximum agreement were found out. These values of τ_1 , τ_2 , C_2 and the values of $\xi(T)$ calculated with these parameters are shown in table 2. It is seen that the agreement between the two values in most cases lies within 4% and is therefore quite satisfactory.

The plots of $\log(\tau_1 T)$ vs $1/T$ and $\log(\tau_2 T)$ vs $1/T$ for anisole are shown in figure 3. The graphs are found to be reasonably straight lines and the activation energies calculated from these slopes are found to be about 2.6 and 2.7 KCal/mole, respectively, for processes of molecular and intramolecular orientations.

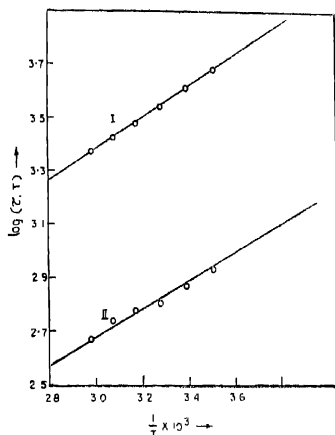


Figure 3. Plot of $\log(\tau T)$ vs $1/T$ for solutions of anisole (τ in pico-secs)

I. $\log(\tau_1 T)$ vs $1/T$

II. $\log(\tau_2 T)$ vs $1/T$

The values of τ_1 , τ_2 and C_2 for phenetole have similarly been determined. The values of these quantities together with the calculated values of $\xi^{(m)}$ are shown in table 3. The agreement in this case is not as good as in anisole. However, the discrepancies in most cases do not exceed 7%. The graphs of $\log(\tau_1 T)$ vs $1/T$ and $\log(\tau_2 T)$ vs $1/T$ have been shown in figure 4. The activation energies obtained are 3.3 and 3.0 K Cal/mole for the two processes of relaxation.

DISCUSSION

It can be seen from tables 2 and 3 that the τ_1 values of anisole and phenetole are almost equal while the τ_2 values of phenetole is slightly greater than that of anisole. This fact is consistent with the larger size of the ethoxy group of phenetole in comparison with the methoxy group in anisole. Moreover, the activation energy for intramolecular relaxation in phenetole is found to be somewhat greater than that in anisole and also

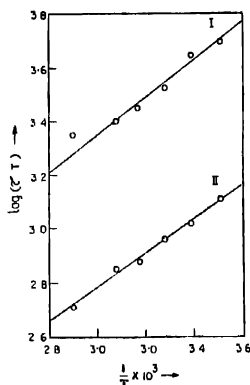


Figure 4. Plot of $\log(\tau T)$ vs $1/T$ for solutions of phenetole (τ in pico-secs)

I. $\log(\tau_1 T)$ vs $1/T$

II $\log(\tau_2 T)$ vs $1/T$

the percentage contribution of the intramolecular relaxation process to overall loss values in the former case is slightly less than that in the latter. These results indicate that the rotation of the ethoxy group is hindered to a greater extent than that of the methoxy group.

In order to find out how far the values of τ_2 is an intramolecular characteristic quantity, the values of τ_2 in anisole for different solvents and the pure liquid together with the corresponding C_2 values are shown in table 4. It is seen from the table that the τ_2 values in different media are almost the same but the values of C_2 are different and depend on the nature of the medium.

TABLE 4 ANISOLE : DEPENDENCE OF τ_2 AND C_2 VALUES IN DIFFERENT MEDIA

Medium	Temp. °K	τ_2 per sec.	C_2	Reference
Hexane	296	2.2	0.30	Kastha <i>et al</i> (1967)
Paraffin	296	2.2	0.10	Kastha <i>et al</i> (1967)
CCl_4	295	2.5	0.50	Present work
Liquid	293	2.2	0.49	Kastha <i>et al</i> (1969)

From this it may be concluded that the relaxation time for the orientation of the methoxy group is an intramolecular characteristic, but the contribution of the relaxation process is conditioned by the nature of the surrounding medium.

The author is grateful to Professor G. S. Kastha, D.Sc., for his help and guidance throughout the progress of this work.

REFERENCES

- Bhattacharyya J., Sinha B., Roy S. B. & Kastha G. S. 1964 *Indian J. Phys.* **38**, 413.
Kastha G. S., Dutta B. & Roy S. B. 1967 *Indian J. Phys.* **41**, 725
Kastha G. S., Dutt B., Bhattacharyya J. & Roy S. B. 1969 *Indian J. Phys.* **43**, 14

Reduction of three-dimensional vector fields to the irreducible representation of inhomogeneous Lorentz group

By B. S. RAJPUT

Department of Physics, Kurukshetra University, Kurukshetra

(Received 21 August 1969)

The reduction of wavefunction which transforms as a three dimensional space-vector for non-zero and zero mass systems, to the irreducible representation of the proper, orthochronous, inhomogeneous Lorentz group has been discussed. The results are used to derive the reduction of electromagnetic fields for nonzero and zero mass systems. For the second case the reduction and the second quantization of the fields have been discussed for linear as well as angular momentum basis. In the solution of Maxwell's equations for free-space the reduced expansion of electric and magnetic fields have been obtained as the components of an electromagnetic wave which is circularly polarised in opposite directions.

INTRODUCTION

The reduction of electromagnetic potential to the photon wavefunction in linear momentum basis according to the Wigner's classification (1939) of the relativistic particles corresponding to the irreducible representation of the proper, orthochronous, inhomogeneous Lorentz group, has been discussed by H. E. Moses (1966). This representation in linear momentum basis was transformed, (Moses 1967a) to the angular momentum basis using the general ways discussed by H. E. Moses (1965). The recipe of the discussion of H. E. Moses & J. S. Lomont (1967) enables one to reduce any unitary ray representation of the proper, orthochronous, inhomogeneous Lorentz group for both non-zero and zero mass systems (Moses 1967b, 1968), where for the former, one obtains the Foldy (1956)-Shirokov (1958) relations and for the latter, one is led to the Lomont-Moses realization (1964). Using these techniques we discussed the reduction of wavefunctions which transforms as complex antisymmetric tensor (Rajput 1969a, 1969b) and scalar (Rajput 1969c) fields. We extended these reductions for complex electromagnetic fields (Rajput 1969d) to discuss the group-theoretical nature of these fields.

In the present paper the reduction of wavefunction, which transforms as a three-dimensional space-vector for nonzero mass systems, to the irreducible representation of the inhomogeneous Lorentz group has been discussed. The results are used to derive the reduction of electromagnetic fields for nonzero and zero mass cases. We have also discussed the reduction and second quantization of these fields in angular momentum basis. In the solution of Maxwell's equation in free-space without source

we obtain the reduced expansions of electric and magnetic fields of electromagnetic wave which is proved to be circularly polarized in opposite directions for $\lambda = +1$ and $\lambda = -1$.

TRANSFORMATION OF THE VECTORS.

In terms of components of antisymmetric tensors the components of electromagnetic fields are given by :

$$\begin{aligned} E_i(x,t) &= F^{0i}(x,t) \\ H_i(x,t) &= \epsilon_{ijk} F^{jk}, \quad i, j, k = 1, 2, 3. \end{aligned} \quad \dots (1)$$

The components of antisymmetric tensors can be expressed in terms of three-dimensional space vector $\vec{A}(x)$ as follows :

$$F_{ij} = \frac{\partial}{\partial x_j} A_i - \frac{\partial}{\partial x_i} A_j \quad \dots (2)$$

where,

$$\vec{A}(x) = \begin{bmatrix} A_1(x) \\ A_2(x) \\ A_3(x) \end{bmatrix} \quad \dots (3)$$

Combining equations (1) and (2) we get :

$$\begin{aligned} \vec{E}(x,t) &= - \frac{\partial}{\partial t} \vec{A}(x) \\ \vec{H}(x,t) &= \text{Curl } \vec{A}(x). \end{aligned} \quad \dots (4)$$

Under the Lorentz transformations the vector $\vec{A}(x)$ transforms as follows :

$$\begin{aligned} A'(\vec{x}) &= A[T(\vec{a})\vec{x}] = \text{Exp} \left[\sum a^i P_i \right] A(\vec{x}) \\ A'(\vec{x}) &= \text{Exp}(i\vec{\theta} \cdot \vec{M}) A[R(-\vec{\theta})\vec{x}] = \text{Exp}[i\vec{\theta} \cdot \vec{K}] A(\vec{x}) \\ A'(\vec{x}) &= \text{Exp}(i\vec{\beta} \cdot \vec{N}) A[L(-\vec{\beta})\vec{x}] = \text{Exp}[i\vec{\beta} \cdot \vec{Z}] A(\vec{x}) \end{aligned} \quad \dots (5)$$

where $T(\vec{a})$, $R(\vec{\theta})$ and $L(\vec{\beta})$ are Lorentz transformations corresponding to translation, rotation and pure Lorentz transformations, respectively. Matrices M and N are given by :

$$\begin{aligned} M_1 &= \begin{pmatrix} 0 & 0 & 0 & 0 \\ 0 & 0 & 0 & 0 \\ 0 & 0 & 0 & -i \\ 0 & 0 & i & 0 \end{pmatrix}, M_2 = \begin{pmatrix} 0 & 0 & 0 & 0 \\ 0 & 0 & 0 & i \\ 0 & 0 & 0 & 0 \\ 0 & -i & 0 & 0 \end{pmatrix}, M_3 = \begin{pmatrix} 0 & 0 & 0 & 0 \\ 0 & 0 & -i & 0 \\ 0 & i & 0 & 0 \\ 0 & 0 & 0 & 0 \end{pmatrix}, \dots (6) \\ N_1 &= \begin{pmatrix} 0 & -i & 0 & 0 \\ -i & 0 & 0 & 0 \\ 0 & 0 & 0 & 0 \\ 0 & 0 & 0 & 0 \end{pmatrix}, N_2 = \begin{pmatrix} 0 & 0 & -i & 0 \\ 0 & 0 & 0 & 0 \\ -i & 0 & 0 & 0 \\ 0 & 0 & 0 & 0 \end{pmatrix}, N_3 = \begin{pmatrix} 0 & 0 & 0 & -i \\ 0 & 0 & 0 & 0 \\ 0 & 0 & 0 & 0 \\ -i & 0 & 0 & 0 \end{pmatrix}, \end{aligned}$$

They satisfy the commutation rules of the infinitesimal generators of the proper, orthochronous, homogeneous Lorentz group. In the reduced form we can write M_i as :

$$M'_i = \begin{bmatrix} 0 & 0 \\ 0 & S' \end{bmatrix} \quad \dots(7)$$

where S' , constitute the irreducible representation of the generators of the rotation group corresponding to the vector rotations such that :

$$\text{Exp} (i\vec{\theta}.S') = I + i (\vec{\theta}.S') \frac{\sin\theta}{\theta} + (\vec{\theta}.S')^2 \frac{\cos\theta - 1}{\theta^2} = R(\vec{\theta})$$

Hence,

$$[\hat{R}(\vec{\theta})]_{\alpha\beta} = \delta_{\alpha\beta} \cos\theta - \frac{\theta_\alpha\theta_\beta}{\theta^2} (\cos\theta - 1) + \sum_\gamma \epsilon_{\alpha\beta\gamma} \theta_\gamma \frac{\sin\theta}{\theta} \quad \dots(8)$$

Similarly for $L(\vec{\beta})$ we have :

$$\begin{aligned} [L(\vec{\beta})]_{\alpha\beta} &= [\text{Exp}(i\vec{\beta}.N)]_{\alpha\beta} \\ &= \delta_{\alpha\beta} \cosh\beta - \frac{\beta_\alpha\beta_\beta}{\beta^2} (\cosh\beta - 1) + i \sum_\gamma \epsilon_{\alpha\beta\gamma} \beta_\gamma \frac{\sinh\beta}{\beta} \quad \dots(9) \end{aligned}$$

The infinitesimal generators $P^0 = H$, P_j , K_j and Z_j of equation (5) constitute the proper, orthochronous, inhomogeneous Lorentz group and satisfy the following commutation rules :

$$\begin{aligned} [P^\alpha, P^\beta] &= 0, [K_\alpha, K_\beta] = i \sum_\gamma \epsilon_{\alpha\beta\gamma} K_\gamma, \\ [K_\alpha, P_\beta] &= i \sum_\gamma \epsilon_{\alpha\beta\gamma} P_\gamma, [Z_\alpha, Z_\beta] = -i \sum_\gamma \epsilon_{\alpha\beta\gamma} K_\gamma. \quad \dots(10) \end{aligned}$$

REDUCTION OF VECTORS FOR NON-ZERO MASS SYSTEM.

Under the infinitesimal generators \hat{P}_α , \hat{K}_i , \hat{Z}_i of the unitary ray representation of Lorentz group, the complex function $f(\mu, \epsilon, \vec{p}, \lambda)$ transforms in the following manner (Moses & Lomont 1967) :

$$\begin{aligned} \hat{P}_0 f(\mu, \epsilon, \vec{p}, \lambda) &= \hat{H} f(\mu, \epsilon, \vec{p}, \lambda) = \epsilon \omega(\mu, p) f(\mu, \epsilon, \vec{p}, \lambda), \\ \hat{P}_i f(\mu, \epsilon, \vec{p}, \lambda) &= p_i f(\mu, \epsilon, \vec{p}, \lambda), \\ \hat{K}_i f(\mu, \epsilon, \vec{p}, \lambda) &= \left[- \sum_{jk} \epsilon_{ijk} p_j \frac{\partial}{\partial p_k} + S_i \right] f(\mu, \epsilon, \vec{p}, \lambda), \quad \dots(11) \end{aligned}$$

$$\hat{Z}_i f(\mu, \epsilon, \vec{p}, \lambda) = \epsilon \left[i\omega(\mu, \vec{p}) \frac{\partial}{\partial p_i} + \frac{1}{\omega(\mu, \vec{p}) + \mu} \sum_{j,k} \epsilon_{ijk} p_j S_k \right] f(\mu, \epsilon, \vec{p}, \lambda),$$

where \vec{p} has the components p_i ($i = 1, 2, 3$), μ is the eigen value of the mass operator, $M = (H^2 - P^2)^{1/2}$, ϵ gives the sign of the energy (± 1) and λ may have any value from 1 to $2s + 1$, where s is the spin corresponding to matrices S_i . $\omega(\mu, \vec{p})$ is given by:

$$\omega(\mu, \vec{p}) = [\mu^2 + p^2]^{1/2}.$$

These generators satisfy the commutation rules of the generators of Lorentz group. Hence for the required reduction we express $\hat{A}(x)$ in terms of $f(\mu, \epsilon, \vec{p}, \lambda)$. For this we consider the function $f(\xi)$ as the representation of $\vec{A}(x)$ in the basis being characterised by the space of wavefunction in Hilbert space upon which the generators operate. ξ , collectively denote all the variables upon which the function depends in this basis. Then we have (Moses & Lomont 1967),

$$f(\xi) = A(x) = \sum_{\epsilon} \int d\mu \sum_{\lambda} \frac{dp}{\omega(\mu, \vec{p}) + \mu} \times \langle \epsilon | \mu, \epsilon, \vec{p}, \lambda \rangle f(\mu, \epsilon, \vec{p}, \lambda) \dots (12)$$

where,

$$\begin{aligned} \langle \xi | \mu, \epsilon, \vec{p}, \lambda \rangle &= \langle x, t, \gamma | \mu, \epsilon, \vec{p}, \lambda \rangle \\ &= \text{Exp} [-i\vec{\beta} \cdot \vec{Z}] g(\xi, \mu, \epsilon, \lambda). \end{aligned} \dots (13)$$

$g(\xi, \mu, \epsilon, \lambda)$ satisfies following equations:

$$P_i g(x, t, \gamma; \mu, \epsilon, \lambda) = 0$$

$$H g(x, t, \gamma; \mu, \epsilon, \lambda) = \epsilon \mu g(x, t, \gamma; \mu, \epsilon, \lambda)$$

Using the values of operators P_i , H we have Rajput (1969a):

$$\begin{aligned} \frac{\partial}{\partial x_i} g(x, t, \gamma; \mu, \epsilon, \lambda) &= 0 \\ i \frac{\partial}{\partial t} g(x, t, \gamma; \mu, \epsilon, \lambda) &= \epsilon \mu g(x, t, \gamma; \mu, \epsilon, \lambda) \end{aligned} \dots (14)$$

solution of which may be written as:

$$g(x, t, \gamma; \mu, \epsilon, \lambda) = C(\gamma | \mu, \epsilon, \lambda) \exp(-i\epsilon\mu t) \dots (15)$$

where $C(\gamma | \mu, \epsilon, \lambda)$ is the constant of integration in which for convenience λ is chosen to go through the same range of values as γ ,

$$\text{so, } C(\gamma | \mu, \epsilon, \lambda) = C(\mu, \epsilon) \delta_{\gamma, \lambda} \dots (16)$$

Using equations (5) and (16) in (15) we have :

$$\begin{aligned} \langle \xi | \mu, \epsilon, \vec{p}, \lambda \rangle &= C(\mu, \epsilon) \exp [i\{\vec{p}, \vec{x} - \epsilon \omega(\mu, \vec{p})t\}] \\ &\times \exp [-i\vec{\beta}, \vec{N}]_{\gamma\lambda} \end{aligned} \quad \dots(17)$$

Now for each set of the elements along the principal diagonal of M_i given by equation (7) we define the column vector $\chi^a(\mu, \epsilon, \vec{p}, \lambda)$ with components :

$$\chi^a(\gamma | \mu, \epsilon, \vec{p}, \lambda) = \{\exp(-i\vec{\beta}, \vec{N})\}_{\gamma\lambda} \quad \dots(18)$$

where α for null-matrix on principal diagonal of M_i is zero and hence the variable λ takes only one value and it need not be indicated, while for S' , (the second elements on the principal diagonal of M_i) α is 1 for which $\lambda = 1, 2, 3$.

Using equations (9) and (18) we have :

$$\begin{aligned} \chi^0(0 | \mu, \epsilon, \vec{p}) &= \frac{\omega(\mu, \vec{p})}{\mu}, \\ \chi^0(\gamma | \mu, \epsilon, \vec{p}) &= \frac{\epsilon}{\mu} p_\gamma, \\ \chi^1(0 | \mu, \epsilon, \vec{p}, \lambda) &= \left(\frac{\epsilon}{\mu}\right) p_\lambda \\ \chi^1(\gamma | \mu, \epsilon, \vec{p}, \lambda) &= \frac{1}{\mu} \left[\mu \delta_{\gamma\lambda} + \frac{p_\gamma p_\lambda}{\omega(\mu, \vec{p}) + \mu} \right], \quad \lambda, \gamma = 1, 2, 3. \dots(19) \end{aligned}$$

The function $f(\mu, \epsilon, \vec{p}, \lambda)$ in equation (12) represents $f^0(\mu, \vec{p})$ for $\gamma = 0$ and $f(\mu, \vec{p})$ for $\gamma = 1$.

Using equation (17) and (19) the equation (12) reduces to :

$$\begin{aligned} A(\vec{x}) &= \sum_{\epsilon=\pm 1} \int dM^0(\mu, \epsilon) \int \frac{d\vec{p}}{\omega(\mu, \vec{p})} \vec{p} f^0(\mu, \epsilon, \vec{p}) \\ &\quad \times \exp [i\{\vec{p}, \vec{x} - \epsilon \omega(\mu, \vec{p})t\}] \\ &+ \sum_{\epsilon=\pm 1} \int dM^1(\mu, \epsilon) \int \frac{d\vec{p}}{\omega(\mu, \vec{p})} \left[\mu f(\epsilon, \mu, \vec{p}) + \frac{\vec{p} \cdot \vec{f}(\epsilon, \mu, \vec{p})}{\omega(\mu, \vec{p}) + \mu} \right] \\ &\quad \times \exp [i\{\vec{p}, \vec{x} - \epsilon \omega(\mu, \vec{p})t\}] \end{aligned} \quad \dots(20)$$

where $dM(\mu, \epsilon) = C(\mu, \epsilon) d\mu$ (measure function).

Equation (20) may be written as :

$$\begin{aligned}
A(\vec{x}) = & \int dM^0(\mu) \left\{ \frac{d\vec{p}}{\omega(\mu, \vec{p})} \vec{p} f^0(\mu, \vec{p}) \exp [i\{\vec{p} \cdot \vec{x} - \omega(\mu, \vec{p})t\}] \right. \\
& + \int dN^0(\mu) \left\{ \frac{d\vec{p}}{\omega(\mu, \vec{p})} \vec{p} h^{0*}(\mu, \vec{p}) \exp [-i\{\vec{p} \cdot \vec{x} - \omega(\mu, \vec{p})t\}] \right. \\
& + \int dM^1(\mu) \left\{ \frac{d\vec{p}}{\omega(\mu, \vec{p})} [\mu f(\mu, \vec{p}) + \frac{\vec{p} \cdot \vec{p} f(\mu, \vec{p})}{\omega(\mu, \vec{p}) + \mu}] \exp [i\{\vec{p} \cdot \vec{x} - \omega(\mu, \vec{p})t\}] \right. \\
& + \left. \int dN^1(\mu) \left\{ \frac{d\vec{p}}{\omega(\mu, \vec{p})} [\mu h^*(\mu, \vec{p}) + \frac{\vec{p} \cdot \vec{p} h^*(\mu, \vec{p})}{\omega(\mu, \vec{p}) + \mu}] \right. \right. \\
& \quad \times \exp [-i\{\vec{p} \cdot \vec{x} - \omega(\mu, \vec{p})t\}] \quad \dots (21)
\end{aligned}$$

where,

$$M^*(\mu) = M^*(\mu, +1), \quad N^*(\mu) = M^*(\mu, -1)$$

$$f^*(\mu, \vec{p}) = f^*(\mu, +1, \vec{p})$$

and,

$$h^*(\mu, \vec{p}) = f^{**}(\mu, -1, -\vec{p})$$

Applying reality condition, Lorentz condition and the requirement that

$A(\vec{x})$ satisfies wave equation, the expression (21) reduces to :

$$\begin{aligned}
A(\vec{x}) = & C \int \frac{d\vec{p}}{\omega(\vec{p})} \exp [i\{\vec{p} \cdot \vec{x} - \omega(\vec{p})t\}] \times [mf(\vec{p}) \frac{\vec{p} \cdot \vec{p} f(\vec{p})}{\omega(\vec{p}) + m} \\
& + D \int \frac{d\vec{p}}{\omega(\vec{p})} \exp [-i\{\vec{p} \cdot \vec{x} + \omega(\vec{p})t\}] \\
& \quad \times [mh^*(\vec{p}) + \frac{\vec{p} \cdot \vec{p} h(\vec{p})}{\omega(\vec{p}) + m}] \quad \dots (22)
\end{aligned}$$

where C and D are positive real constants and,

$$f(\vec{p}) = f(m, \vec{p}), \quad h(\vec{p}) = h(m, \vec{p})$$

$$\omega(\vec{p}) = \omega(m, \vec{p})$$

Using canonical formalism (Rajput 1969a) the constants C and D are calculated to have the following values :

$$C = D = (2)^{-1/2} (2\pi)^{-3/2}.$$

Hence,

$$\begin{aligned}
 A(\vec{x}) = & \frac{1}{4\pi^{3/2}} \int \frac{d\vec{p}}{\omega(\vec{p})} [m f(\vec{p}) + \frac{\vec{p} \cdot \vec{p} \cdot f(\vec{p})}{\omega(\vec{p}) + \mu}] \\
 & \times \exp [i\{\vec{p} \cdot \vec{x} - \omega(\vec{p})t\}] \\
 & + \frac{1}{4\pi^{3/2}} \int \frac{d\vec{p}}{\omega(\vec{p})} [m h^*(\vec{p}) + \frac{\vec{p} \cdot \vec{p} \cdot h^*(\vec{p})}{\omega(\vec{p}) + \mu}] \\
 & \times \exp [-i\{\vec{p} \cdot \vec{x} - \omega(\vec{p})t\}] \quad \dots (23)
 \end{aligned}$$

The inner product of two vectors $A(\vec{x})$ and $A_1(\vec{x})$ in configuration space is defined as :

$$(A_1, A) = \int \frac{d\vec{p}}{\omega(\vec{p})} f_1^*(\vec{p}) \cdot f(\vec{p}) + \int \frac{d\vec{p}}{\omega(\vec{p})} h^*(\vec{p}) \cdot h_1(\vec{p}).$$

Using equations (23) and (4) we can now reduce the electromagnetic fields to the irreducible representation of inhomogenous Lorentz group for non-zero mass system. We get :

$$\vec{E} = \frac{i}{4\pi^{3/2}} \sum_{\epsilon=\pm 1} \epsilon \left\{ \frac{d\vec{p}}{\omega(\vec{p})} [m f(\epsilon, \vec{p}) + \frac{\vec{p} \cdot \vec{p} \cdot f(\epsilon, \vec{p})}{\omega(\vec{p}) + \mu}] \times \exp [i\{\vec{p} \cdot \vec{x} - \epsilon \omega(\vec{p})t\}] \right\} \quad \dots (24)$$

and,

$$\begin{aligned}
 \vec{H} &= \frac{i}{4\pi^{3/2}} \sum_{\epsilon=\pm 1} \int m \frac{d\vec{p}}{\omega(\vec{p})} \{ \vec{p} \times f(\epsilon, \vec{p}) \} \times \exp [i\{\vec{p} \cdot \vec{x} - \epsilon \omega(\vec{p})t\}] \\
 &= \frac{i}{4\pi^{3/2}} \int m \frac{d\vec{p}}{\omega(\vec{p})} \left[\{ \vec{p} \times f(\vec{p}) \} \exp [i\{\vec{p} \cdot \vec{x} - \omega(\vec{p})t\}] \right. \\
 &\quad \left. - \{ \vec{p} \times h^*(\vec{p}) \} \exp [-i\{\vec{p} \cdot \vec{x} - \omega(\vec{p})t\}] \right] \quad \dots (25)
 \end{aligned}$$

Using Maxwell's equation :

$$\text{Curl } H = 4\pi j + \frac{\partial \epsilon}{\partial t}, \quad \text{and} \quad \text{div } E = 4\pi \rho \quad \dots (26)$$

we may find ρ and j for the required field. The second of equation (26) gives :

$$\begin{aligned}
 4\pi \rho = & - \frac{1}{4\pi^{3/2}} \int \frac{d\vec{p}}{\omega(\vec{p})} [\vec{p} \cdot f(\vec{p}) \exp i\{\vec{p} \cdot \vec{x} - \omega(\vec{p})t\}] \\
 & + \vec{p} \cdot h^*(\vec{p}) \exp -i\{\vec{p} \cdot \vec{x} - \omega(\vec{p})t\}] \quad \dots (27)
 \end{aligned}$$

Current density \vec{j} can be reduced into similar expression to (23) in terms of $j(\epsilon, \vec{p})$ as follows :

$$\vec{j}(\vec{x}) = \frac{1}{4\pi^{3/2}} \sum_{\epsilon=\pm 1} \int \frac{d\vec{p}}{\omega(\vec{p})} \left[m j(\epsilon, \vec{p}) + \frac{\vec{p} \{ \vec{p}, j(\epsilon, \vec{p}) \}}{\omega(\vec{p}) + m} \right] \\ \times \exp \{ i \{ \vec{p}, \vec{x} - \epsilon \omega(\vec{p}) t \} \}$$

Then first of equation (26) gives the following result :

$$4\pi \left[m j(\epsilon, \vec{p}) + \frac{\vec{p} \{ \vec{p}, j(\epsilon, \vec{p}) \}}{\omega(\vec{p}) + m} \right] = m [\vec{p}^2 f(\epsilon, \vec{p}) - \vec{p} \{ \vec{p}, f(\epsilon, \vec{p}) \}] \\ - \omega^2(\vec{p}) \left[m f(\epsilon, \vec{p}) - \frac{\vec{p} \{ \vec{p}, f(\epsilon, \vec{p}) \}}{\omega(\vec{p}) + m} \right] \quad \dots (28)$$

SECOND QUANTIZATION OF ELECTROMAGNETIC FIELDS FOR NON-ZERO MASS SYSTEM

To second quantize the electromagnetic field in the basis the components $f(\vec{p})$ and $h(\vec{p})$ are considered as destruction and creation operators, respectively. Assuming Bose-statistics we require that all the commutators vanish except the following :

$$[f(\vec{p}, \lambda), f^*(\vec{p}', \lambda')] = \omega(\vec{p}) \delta(\vec{p} - \vec{p}') \delta_{\lambda, \lambda'} \\ [h(\vec{p}, \lambda), h^*(\vec{p}', \lambda')] = \omega(\vec{p}) \delta(\vec{p} - \vec{p}') \delta_{\lambda, \lambda'} \quad \dots (29)$$

We thus regard the components of electric and magnetic fields as operators.

If \hat{A} is any of the operators $\hat{H}, \hat{P}_i, \hat{K}_i, \hat{Z}_i$ and if $\hat{A} f(\vec{p})$, $\hat{A} h(\vec{p})$ are the operators formed when \hat{A} acts on \vec{p} and λ , as though $f(\vec{p})$ and $h(\vec{p})$ were representatives instead of destruction operators, then for each operator \hat{A} we define a second quantized operator :

$$[A] = \sum_{\lambda} \int \frac{d\vec{p}}{\omega(\vec{p})} f^*(\vec{p}, \lambda) \hat{A} f(\vec{p}, \lambda) + \sum_{\lambda} \int \frac{d\vec{p}}{\omega(\vec{p})} h^*(\vec{p}, \lambda) \hat{A} h(\vec{p}, \lambda) \quad \dots (30)$$

The operator E transforms under translation, rotation and pure Lorentz transformation as follows ;

$$E'(x) = \text{Exp} \left\{ -i \sum_j a^j [P_j] \right\} E(x) \exp \left\{ i \sum_j a^j [P_j] \right\}$$

$$E'(x) = \text{Exp} \left\{ -i \vec{\theta} \cdot [K] \right\} E(x) \exp \left\{ i \vec{\theta} \cdot [K] \right\}$$

$$E'(x) = \text{Exp} \left\{ -i \vec{\beta} \cdot [Z] \right\} E(x) \exp \left\{ i \vec{\beta} \cdot [Z] \right\}$$

The similar transformation can be derived for magnetic field operator $H(x)$

REDUCTION FOR ZERO MASS SYSTEM

The mass-less representation of the infinitesimal generators of inhomogeneous Lorentz group is given in terms of the representation of infinitesimal generators (T_1, T_2, J) of two dimensional Euclidean group,

$$T_1 = -M_2 - N_1$$

$$T_2 = M_1 - N_2$$

$$J = M_3 \quad \dots(32)$$

For a real function $f(\lambda)$ of real variable λ (the eigenvalues of matrix M_3) the realization of the infinitesimal generators of inhomogeneous Lorentz group discussed by Lomont & Moses (1967) can be taken as :

$$\hat{P}_0 f(\vec{p}) = H f(\vec{p}) = \epsilon p f(\vec{p})$$

$$P_i f(\vec{p}) = p_i f(\vec{p})$$

$$\hat{K}_1 f(\vec{p}) = \left[L_1 + \frac{p_1}{p+p_3} J \right] f(\vec{p})$$

$$\hat{K}_2 f(\vec{p}) = \left[L_2 + \frac{p_2}{p+p_3} J \right] f(\vec{p})$$

$$\hat{K}_3 f(\vec{p}) = [L_3 + J] f(\vec{p})$$

$$\hat{Z}_1 f(\vec{p}) = \epsilon \left\{ i p \frac{\partial}{\partial p_1} + \frac{p_2}{p+p_3} J + \left[\frac{p_1^2}{p^2(p+p_3)} - \frac{1}{p} \right] T_1 + \frac{p_1 p_2 T_2}{p^2(p+p_3)} \right\} f(\vec{p})$$

$$\hat{Z}_2 f(\vec{p}) = \epsilon \left\{ i p \frac{\partial}{\partial p_2} - \frac{p_1 J}{p+p_3} + \frac{p_1 p_2}{p^2(p+p_3)} T_1 + \left[\frac{p_2^2}{p^2(p+p_3)} - \frac{1}{p} \right] T_2 \right\} f(\vec{p})$$

$$\hat{Z}_3 f(\vec{p}) = \epsilon \left\{ i p \frac{\partial}{\partial p_3} + \frac{1}{p^2} \left[p_1 T_1 + p_2 T_2 \right] \right\} f(\vec{p}) \quad \dots(33)$$

where

$$L_i f(\vec{p}) = -i \sum_{jk} \epsilon_{ijk} p_j \frac{\partial}{\partial p_k}$$

The required reduction requires the expression of the vector $A(\vec{x})$ in terms of $f(\vec{p})$. The matrix M_3 defined in equation (6) is Hermitian which can be diagonalized by a unitary matrix U :

$$U^{-1} M_3 U = d, \quad (\text{diagonal matrix})$$

λ , the eigen values of M_3 are give by :

$$| M_3 - \lambda I | = 0$$

which gives $\lambda = 1, 0, 0, -1$.

So,

$$d = \begin{bmatrix} -1 & 0 & 0 & 0 \\ 0 & 0 & 0 & 0 \\ 0 & 0 & 0 & 0 \\ 0 & 0 & 0 & -1 \end{bmatrix}$$

Hence,

$$U = \begin{bmatrix} 1 & 0 & 0 & 0 \\ 0 & -(2)^{-1/2} & 0 & (2)^{-1/2} \\ 0 & -i(2)^{-1/2} & 0 & -i(2)^{-1/2} \\ 0 & 0 & 1 & 0 \end{bmatrix} \quad \dots (34)$$

Now we define a column vector $\chi(\epsilon, p, \lambda)$ components of which are given as :

$$\chi(\gamma | \epsilon, p, \lambda) = [\exp(i\omega \cdot M) \exp(i\nu N_3)]_{\gamma\lambda} \quad (35)$$

where the correspondence of \vec{p} with $\vec{\omega}$ and ν is given by the following expressions :

$$p = \text{Exp}(\epsilon\nu)$$

$$p_1 = -p \left(\frac{\sin \omega}{\omega} \right) \omega_1$$

$$p_2 = p \left(\frac{\sin \omega}{\omega} \right) \omega_1$$

$$p_3 = \cos \omega$$

$$\omega_3 = 0$$

...(36)

Using equation (8) and (9) in equation (35) we have :

$$\begin{aligned} x(\epsilon, p, 0) &= \frac{1}{p} \begin{bmatrix} 0 \\ p_1 \\ p_2 \\ p_3 \end{bmatrix} \\ \chi(\epsilon, p, \lambda) &= \frac{\lambda}{(2)^{1/2}} \begin{bmatrix} \frac{p_1(p_1 + i\lambda p_3)}{p(p + p_3)} - 1 \\ \frac{p_2(p_1 + i\lambda p_3)}{p(p + p_3)} - i\lambda \\ \frac{p_1 + i\lambda p_3}{p} \end{bmatrix} \\ &\quad \frac{\lambda}{(2)^{1/2}} \begin{bmatrix} 0 \\ \sigma(p) \end{bmatrix} \end{aligned} \quad \dots(37)$$

Now equation (12) for this case reduces to :

$$f(\xi) = A(\vec{x}) = \sum_{\epsilon, \pm 1} \sum_{\lambda=0, \pm 1} \int \frac{d\vec{p}}{p} \langle \xi | \epsilon, p, \lambda \rangle f(\epsilon, p, \lambda) \quad (38)$$

where (Rajput 1969b),

$$\begin{aligned} \langle \xi | \epsilon, p, \lambda \rangle &= \langle x, t, \gamma | \epsilon, p, \lambda \rangle \\ &= \text{Exp} [i(x_3 - \epsilon t)] \chi(\gamma | \epsilon, p, \lambda) \end{aligned}$$

Hence equation (38) reduces to :

$$\begin{aligned} A(\vec{x}) &= \sum_{\epsilon} \sum_{\lambda} C(\epsilon, \lambda) \int \frac{d\vec{p}}{p} \chi(\epsilon, p, \lambda) f(\epsilon, p, \lambda) \exp [i\{\vec{p} \cdot \vec{x} - \epsilon p t\}] \\ &= \sum_{\epsilon} [C(\epsilon, 0) \int \frac{d\vec{p}}{p} \chi(\epsilon, p, 0) f(\epsilon, p, 0) \exp \{i(\vec{p} \cdot \vec{x} - \epsilon p t)\} \\ &\quad + \sum_{\lambda=\pm 1} C(\epsilon, \lambda) \int \frac{d\vec{p}}{p} \sigma(\epsilon, p, \lambda) f(\epsilon, p, \lambda) \exp \{i(\vec{p} \cdot \vec{x} - \epsilon p t)\}] \end{aligned} \quad \dots(39)$$

Now let,

$$h(\epsilon, p, \lambda) = \text{Exp} (-2i\lambda\phi) f^*(-\epsilon, -\vec{p}, \lambda)$$

where,

$$\tan \phi = p_3 / p_1$$

$$C(0) = C(+1, 0), \quad D(0) = C(-1, 0)$$

$$C(\lambda) = C(+1, \lambda), \quad D(\lambda) = D(-1, \lambda)$$

$$f(\vec{p}, \lambda) = f(+1, \vec{p}, \lambda)$$

$$\chi(\vec{p}, 0) = \chi(+1, \vec{p}, 0)$$

$$\chi(\vec{p}, 0) = \chi(-1, \vec{p}, 0) = -\chi(\vec{p}, 0)$$

$$\chi(\vec{p}, \lambda) = \chi(+1, \vec{p}, \lambda) = \frac{\lambda}{(2)^{1/2}} \begin{bmatrix} 0 \\ \sigma(\vec{p}) \end{bmatrix}$$

$$\eta(\vec{p}, \lambda) = \chi(-1, \vec{p}, \lambda) = -\chi^*(\vec{p}, \lambda)$$

Then,

$$\begin{aligned} A(\vec{x}) = C(0) & \int \frac{d\vec{p}}{p} \chi(\vec{p}, 0) f(\vec{p}, 0) \exp \{i(\vec{p} \cdot \vec{x} - pt)\} \\ & - D(0) \int \frac{d\vec{p}}{p} \chi(\vec{p}, 0) h^*(\vec{p}, 0) \exp \{-i(\vec{p} \cdot \vec{x} - pt)\} \\ & + \sum_{\lambda} \left[C(\lambda) \int \frac{d\vec{p}}{p} \sigma(\vec{p}, \lambda) f(\vec{p}, \lambda) \exp \{i(\vec{p} \cdot \vec{x} - pt)\} \right. \\ & \left. - D(\lambda) \int \frac{d\vec{p}}{p} \sigma^*(\vec{p}, \lambda) h^*(\vec{p}, \lambda) \exp \{-i(\vec{p} \cdot \vec{x} - pt)\} \right] \dots (40) \end{aligned}$$

For Γ any of the infinitesimal generators $P_i, H, J_i, \Gamma A(x)$ has the same expression (40) on replacing $f(\epsilon, \vec{p}, \lambda)$ by $\hat{\Gamma} f(\epsilon, \vec{p}, \lambda)$.

But for $\hat{\Gamma}$ one of the $Z_i, \hat{\Gamma}$ will not be Hermitian and $\hat{\Gamma} A(x)$ consists of two parts one of which corresponds to a true physical change called change of gauge :

$$\begin{aligned} Z_i A(x) = \sum_{\epsilon} \sum_{\lambda} C(\epsilon, \lambda) & \int \frac{d\vec{p}}{p} \chi(\epsilon, \vec{p}, \lambda) \hat{Z}_i f(\epsilon, \vec{p}, \lambda) \\ & \times \exp \{i(\vec{p} \cdot \vec{x} - \epsilon pt)\} + G_i(x) \dots (41) \end{aligned}$$

where $G_i(x)$ is the gauge change given by (Rajput 1969b) :

$$\begin{aligned} G_j(x) = i & \left[(m \times \nabla)_j + \frac{\partial}{\partial t} N_j \right] \phi_1(x) + i(N \cdot \nabla)_j \frac{\partial}{\partial t} \phi_2(x) \\ & = -\nabla \alpha_{1,j}(x) + e_j [\nabla \cdot \phi_1(x)] - i \frac{\partial}{\partial t} [e_j \times \phi_1(x)] \\ & \quad - i \frac{\partial^2}{\partial x_j \partial t} [\nabla \times \phi_2(x)] \end{aligned}$$

where,

$$\phi_n(x) = \sum_{\epsilon} \sum_{\lambda} C(\epsilon, \lambda) \int \frac{d\vec{p}}{p^{n+1}} \chi(\epsilon, \vec{p}, \lambda) f(\epsilon, \vec{p}, \lambda) \exp \{i(\vec{p} \cdot \vec{x} - \epsilon pt)\} \dots (42)$$

\vec{e}_j is the unit vector in the direction of j -th space axis and $\phi_{1,j}$ denotes the j -th component of the vector $\phi_1(x)$

If $A(x)$ is a real vector,

$$A(x) = \bar{A}(x)$$

$$\text{then,} \quad C(0) f(\vec{p}, 0) = -D(0) h(\vec{p}, 0)$$

$$\text{and,} \quad C(\lambda) f(\vec{p}, \lambda) = -D(\lambda) h(\vec{p}, \lambda).$$

Hence the real vector is expressed as :

$$\begin{aligned} A(x) = C(0) \int \frac{d\vec{p}}{p} \chi(\vec{p}, 0) [f(\vec{p}, 0) \exp \{i(\vec{p}, \vec{x} - p\ell)\} \\ + f^*(\vec{p}, 0) \exp \{-i(\vec{p}, \vec{x} - p\ell)\}] \\ + \sum_{\lambda=\pm 1} C(\lambda) \int \frac{d\vec{p}}{p} [\sigma(\vec{p}, \lambda) f(\vec{p}, \lambda) \exp \{i(\vec{p}, \vec{x} - p\ell)\} \\ + \sigma^*(\vec{p}, \lambda) f^*(\vec{p}, \lambda) \exp \{-i(\vec{p}, \vec{x} - p\ell)\}] \quad \dots(43) \end{aligned}$$

Using equation (4) and (43) we can reduce the electromagnetic fields to the irreducible representation of inhomogeneous Lorentz group for zero mass system. Thus we get :

$$\begin{aligned} E(\vec{x}) = iC(0) \int d\vec{p} \chi(\vec{p}, 0) [f(\vec{p}, 0) \exp \{i(\vec{p}, \vec{x} - p\ell)\} \\ - f^*(\vec{p}, 0) \exp \{-i(\vec{p}, \vec{x} - p\ell)\}] \\ + i \sum_{\lambda=\pm 1} C(\lambda) \int d\vec{p} [\sigma(\vec{p}, \lambda) f(\vec{p}, \lambda) \exp \{i(\vec{p}, \vec{x} - p\ell)\} \\ - \sigma^*(\vec{p}, \lambda) f^*(\vec{p}, \lambda) \exp \{-i(\vec{p}, \vec{x} - p\ell)\}] \quad \dots(44) \end{aligned}$$

$$\begin{aligned} H(\vec{x}) = \sum_{\lambda=\pm 1} \lambda C(\lambda) \int d\vec{p} [\sigma(\vec{p}, \lambda) f(\vec{p}, \lambda) \exp \{i(\vec{p}, \vec{x} - p\ell)\} \\ + \sigma^*(\vec{p}, \lambda) f^*(\vec{p}, \lambda) \exp \{-i(\vec{p}, \vec{x} - p\ell)\}] \quad \dots(45) \end{aligned}$$

We can write equations (44) and (45) as :

$$E(x) = E^L + E^T$$

$$H(x) = H^L + H^T$$

where E^L and E^T are longitudinal and transverse parts of electric field given by :

$$\begin{aligned} E^L = iC(0) \int d\vec{p} \chi(\vec{p}, 0) [f(\vec{p}, 0) \exp \{i(\vec{p}, \vec{x} - p\ell)\} \\ + f^*(\vec{p}, 0) \exp \{-i(\vec{p}, \vec{x} - p\ell)\}] \quad \dots(46) \end{aligned}$$

$$\begin{aligned} E^T = \sum_{\lambda=\pm 1} iC(\lambda) \int d\vec{p} [\sigma(\vec{p}, \lambda) f(\vec{p}, \lambda) \exp \{i(\vec{p}, \vec{x} - p\ell)\} \\ - \sigma^*(\vec{p}, \lambda) f^*(\vec{p}, \lambda) \exp \{-i(\vec{p}, \vec{x} - p\ell)\}] \quad \dots(47) \end{aligned}$$

Similarly the transverse part of magnetic fields is given by equation (45) :

$$H^T = H(x), \quad \text{while,} \quad H^L = 0.$$

Thus the longitudinal part of magnetic field in electro-magnetic wave is always zero.

In the free space Maxwell's equations lead to :

$$f(\vec{p}, 0) = 0$$

Hence equation (44) reduces to :

$$E(\vec{x}) = i \sum_{\lambda=+1} C(\lambda) \int d\vec{p} [\sigma(\vec{p}, \lambda) f(\vec{p}, \lambda) \exp \{i(\vec{p} \cdot \vec{x} - pt)\} \\ - \sigma^*(\vec{p}, \lambda) f^*(\vec{p}, \lambda) \exp \{-i(\vec{p} \cdot \vec{x} - pt)\}] \quad \dots (48)$$

It is clear at this stage that $\phi_n(x)$ given by equation (42) satisfies Maxwell's equation when \vec{E} and \vec{H} do. Hence the gauge changes are identically zero.

So \vec{E} and \vec{H} transform without the necessity of introducing the gauge changes.

We choose the value of the constant such that the usual canonical formalism in terms of Hamiltonian density agrees with the particle interpretation. Hamiltonian density of the electromagnetic fields is defined as :

$$H(x) = \frac{1}{8\pi} (E^2 + H^2) \quad \dots (49)$$

The energy of the field is :

$$T = \int_{-\infty}^{\infty} H(x) dx \\ = (8\pi)^{-1} \int_{-\infty}^{\infty} (E^2 + H^2) dx$$

while the expectation energy is given by :

$$T_f = \int_{-\infty}^{\infty} \frac{dp}{p} f^*(\vec{p}, +1) \vec{p} f(\vec{p}, +1) \\ \int_{-\infty}^{\infty} dp |f(\vec{p}, +1)|^2 \quad \dots (50)$$

Equations (49) and (50) lead to :

$$C(\lambda) = (8\pi^2)^{-1/2}$$

Hence,

$$E(x) = i(8\pi^2)^{1/2} \sum_{\lambda} \int d\vec{p} [\sigma(\vec{p}, \lambda) f(\vec{p}, \lambda) \exp \{i(\vec{p} \cdot \vec{x} - pt)\} \\ - \sigma^*(\vec{p}, \lambda) f^*(\vec{p}, \lambda) \exp \{-i(\vec{p} \cdot \vec{x} - pt)\}] \quad \dots (51)$$

$$H(x) = (8\pi^3)^{-1/2} \sum_{\lambda=\pm 1} \lambda \int d\vec{p} \left\{ \sigma(\vec{p}, \lambda) f(\vec{p}, \lambda) \exp \{i(\vec{p} \cdot \vec{x} - pt)\} + \sigma^*(\vec{p}, \lambda) f^*(\vec{p}, \lambda) \exp \{-i(\vec{p} \cdot \vec{x} - pt)\} \right\} \quad \dots(52)$$

Equations (51) and (52) can be written as follows :

$$E(x) = E_1(x, t) + E_1^*(x, t), \quad \dots(51a)$$

where,

$$E_1(x, t) = \frac{1}{(8\pi^3)^{1/2}} \sum_{\lambda=\pm 1} \int d\vec{p} f(\vec{p}, \lambda) \sigma(\vec{p}, \lambda) \exp \{i(\vec{p} \cdot \vec{x} - pt)\}$$

and

$$H(x) = H_1(x, t) + H_1^*(x, t) \quad \dots(52a)$$

where,

$$H_1(x, t) = \frac{1}{(8\pi^3)^{1/2}} \sum_{\lambda=\pm 1} \lambda \int d\vec{p} f(\vec{p}, \lambda) \sigma(\vec{p}, \lambda) \exp \{i(\vec{p} \cdot \vec{x} - pt)\}$$

In equation (51) if we take :

$$f(\vec{p}, \lambda) = \delta_{\lambda, 1} \delta(p_1 - k) \delta(p_2) \delta(p_3) \quad \dots(53)$$

then the function $f(\vec{p}, \lambda)$ represents in the limiting case a wave function of photon of momentum k moving in the positive x -direction for $\lambda = +1$.

For this value of $f(\vec{p}, \lambda)$ we have :

$$\sigma(\vec{p}, \lambda) f(\vec{p}, \lambda) = \begin{bmatrix} 0 \\ -i \\ 1 \end{bmatrix}$$

and hence equation (51) gives :

$$E_1 = 0$$

$$E_2 \sim \cos k(t - x)$$

$$E_3 \sim \sin k(t - x) \quad \dots(54)$$

The wave represented by equation (54) is circularly polarized in the positive x -direction. Similarly we can show that $\lambda = -1$ gives circular polarization in the opposite direction. The x -component of the Poynting vector is given by :

$$\frac{1}{4\pi} [\vec{E} \times \vec{H}]_x = \frac{1}{8\pi^3} \quad \dots(55)$$

while the other components are zero,

To second quantize the electromagnetic fields given by equations (55) and (52) the function $f(\vec{p}, \lambda)$ and its complex conjugate are considered as destruction and creation operators, respectively. Using Bose-statistics we get the following commutation relations for these operators :

$$\begin{aligned} [f(\vec{p}, \lambda), f(\vec{p}', \lambda')] &= [f^*(\vec{p}, \lambda), f^*(\vec{p}', \lambda')] = 0 \\ [f(\vec{p}, \lambda), f^*(\vec{p}', \lambda')] &= p\delta_{\lambda, \lambda'} \delta(\vec{p} - \vec{p}') \end{aligned} \quad \dots (56)$$

For these operators electric and magnetic fields are also considered as operators which satisfy usual commutation rules. For every infinitesimal generator \hat{A} we can define a second quantized operator $[A]$ by :

$$[A] = \sum_{\lambda} \left[\int \frac{d^3p}{p} f^*(\vec{p}, \lambda) \hat{A} f(\vec{p}, \lambda) \right] \quad \dots (57)$$

Under the Lorentz transformations the electric and magnetic fields transform according to the equations (31) where second quantized operator is given by equation (57)

REDUCTION OF ELECTROMAGNETIC FIELDS IN ANGULAR MOMENTUM BASIS

In angular momentum basis wave function depends on the energy, the total angular momentum quantum number k , the quantum number m for J_z (z -component of angular momentum) and the helicity λ . In this case let this function be $F(p, k, m, \lambda)$ then we have (Moses 1965, Lomont & Moses 1967)

$$\begin{aligned} f(\vec{p}, \lambda) &= \frac{1}{p} \sum_{k=1}^{\infty} \sum_{m=-k}^{k} \text{Exp} \left\{ i\pi \left(\lambda - \frac{m}{2} \right) \right\} \\ &\quad Y_k^{m\lambda}(\theta, \phi) F(p, k, m, \lambda) \end{aligned} \quad \dots (58)$$

where $Y_k^{m\lambda}(\theta, \phi)$ are generalised spherical harmonics defined as :

$$\begin{aligned} Y_k^{m\lambda}(\theta, \phi) &= (-1)^{m-\lambda} \left(\frac{1}{2} \right)^{m+1} \\ &\quad \left[\frac{(2k+1)}{\pi} \right]^{1/2} \left[\frac{(k-m)! (k+\lambda)!}{(k-\lambda)! (k+m)!} \right]^{1/2} \end{aligned} \quad \dots (59)$$

$$\times \exp [i(m-\lambda)\phi] (\sin \theta)^{m-\lambda} (1 + \cos \theta)^{\lambda} P_{k-\lambda}^{m-\lambda, m+\lambda}(\cos \theta)$$

$$\vec{p} = p(\sin \theta \cos \phi, \sin \theta \sin \phi, \cos \theta).$$

θ and ϕ vary in the ranges 0 to π and 0 to 2π , respectively, and

$$P_{k-\lambda}^{m-\lambda, m+\lambda}(\cos \theta) \text{ is a Jacobi polynomial.}$$

The expression for $\sigma(\vec{p}, \lambda)$ in terms of angular momentum basis is given by (Lomont & Moses 1967) :

$$\sigma(\vec{p}, \lambda) = - \left(\frac{8\pi}{3} \right)^{1/2} \sum_{\beta=0, \pm 1} (i)^{\beta-\lambda} \chi(\beta) Y_1^{\beta\lambda*}(\theta, \phi) \quad \dots (60)$$

where,

$$\chi(\beta) = (2)^{-1/2} (1, i\beta, 0) \quad \text{for } \beta = \pm 1$$

$$\chi(\beta) = -i(0, 0, 1) \quad \text{for } \beta = 0.$$

and,

$$Y_1^{\beta\lambda*}(\theta, \phi) = (-1)^{\lambda-\beta} Y_1^{\lambda\beta}(\theta, \phi) \quad \dots (61)$$

The expansion for $\exp(i\vec{p} \cdot \vec{x})$ in terms of angular momentum basis can be written as :

$$\text{Exp. } (i\vec{p} \cdot \vec{x}) = 4\pi \sum_{k=1}^{\infty} \sum_{m=-k}^k (i)^k j_k(pr) Y_k^{m0}(\theta, \phi) Y_k^{m0*}(\theta, \phi) \quad \dots (62)$$

where $r = |\vec{x}|$, j_k is the spherical Bessel's function of order k and θ, ϕ are the polar angles which describe the direction of \vec{x} . Now using the equations (58), (60) and (62) in the equation (51a) we get the reductions of electric fields to the inhomogeneous Lorentz group in angular momentum basis :

$$\begin{aligned} E_1 = 4\sqrt{\pi/3} \sum_{\lambda=\pm 1} \sum_{\beta=0, \pm 1} \sum_{k=1}^{\infty} \sum_{m=k}^k (i)^{k+1+\beta-\lambda} \\ \chi(\beta) \exp \left[i\pi \left(\lambda - \frac{m}{2} \right) \right] \\ \times Y_k^{m\lambda}(\theta, \phi) Y_1^{\beta\lambda*}(\theta, \phi) Y_k^{m0}(\theta, \phi) Y_k^{m0*}(\theta, \phi) \\ \times \int \frac{dp}{p} j_k(pr) F(p, k, m, \lambda) \exp \{ipt\} \quad \dots (63) \end{aligned}$$

Equation (63) can further be simplified using Clebsch-Gordan coefficients. Similarly magnetic field may also be expressed as :

$$\begin{aligned}
H_1(x) = & -4\sqrt{\pi/3} \sum_{\lambda=\pm 1} \sum_{\beta=\alpha_j \pm 1} \sum_{k=1}^{\infty} \sum_{m=-k}^k \lambda [(i)^{k+\beta-\lambda}] \chi(\beta) \exp \left\{ i\pi \left(\lambda - \frac{m}{2} \right) \right\} \\
& \times Y_k^{m\lambda}(\theta, \phi) Y_1^{\beta\lambda*}(\theta, \phi) Y_k^{m\alpha}(\hat{\theta}, \hat{\phi}) Y_k^{m\alpha*}(\theta, \phi) \\
& \times \int \frac{dp}{p} j_k(pr) F(p, j, m, \lambda) \exp \{-ip t\} \quad \dots (64)
\end{aligned}$$

The plane electromagnetic wave is regular everywhere, including the point $r = 0$. Therefore, only the regular spherical Bessel's function occurs in the expansions (63) and (64).

Hence,

$$j_k(pr) = (pr)^{-1} F_k(r) \quad \dots (65)$$

$F_k(r)$ in equation (65) is regular function defined as :

$$F_k(r) = \left(\frac{\pi pr}{2} \right)^{1/2} J_{k+1/2}(pr)$$

where $J_{k+1/2}(pr)$ is the regular Bessel's function.

We can also second-quantize the electro-magnetic fields in the angular momentum representation. For this we introduce the annihilation and creation operators, respectively, as :

$$F(p, k, m, \lambda) = a(s)$$

$$F^*(p, k, m, \lambda) = a^*(s)$$

They satisfy the commutation relations :

$$[a(s), a(s')] = [a^*(s), a^*(s')] = 0$$

$$[a(s), a^*(s')] = p\delta(s - s').$$

The annihilation operator in the angular momentum basis is related to annihilation operator in linear momentum basis according to the equation (58). The creation operators are related in complex conjugate manner. The quantized electric field is treated as the sum of operators E_1 and E_1^* , which are obtained by substituting annihilation and creation operator for $F(\vec{p}, k, m, \lambda)$ and $F^*(\vec{p}, k, m, \lambda)$, respectively, in equation (63) and the similar equation for $E_1^*(x)$. In a similar manner magnetic field is quantized in the angular momentum representation.

REFERENCES

- Foldy, L.L. 1956 *Phys. Rev.* **102**, 568.
- Lomont, J. S. & Moses, H. E. 1964 *Journ. Math. Phys.*, **5**, 294.
1967 *Journ. Math. Phys.*, **8**, 837.
- Moses, H. E. 1965 *Journ. Math. Phys.* **6**, 1928.
1966 *Nuovo Cimento*, **42**, 757.
1967a *Nuovo Cimento*, **48**, 43.
1967b *Journ. Math. Phys.* **8**, 1134.
1967c *Ann. Phys.*, **41**, 166.
1968 *Journ. Math. Phys.*, **9**, 16.
- Rajput, B.S. 1969a *Indian. J. Phys.*, **43**, 135
1969b *Indian. J. Phys.* (In press)
1969c, *Ind. J. Pure Appl. Phys.* **7**, 720
1969d *Nuovo Cimento* **66A**, 517
- Shirokov, Iu. M. 1958 *Soviet Phys. JETP* **6**, 919.
- Wigner, E.P., 1939 *Ann. Math.* **40**, 149

Letters to the Editor

Excited state Zeeman splitting of $K_3Cr(CN)_6$

By R. MUKHERJEE, S. C. BERA, A. ROSE

Indian Association for the Cultivation of Science Calcutta.

AND

M. CHOUDHURY

Presidency College, Calcutta.

(Received 1 January 1970)

In the octahedral complexes of Cr^{3+} , the ground state ${}^4A_2(t_g^3)$ has a nearly spin-only value of the g-factor, which is practically isotropic and fairly insensitive to small distortions in the surrounding ligand field. We have, therefore, focussed our attention on the doublet excited states 2E , 2T_1 and 2T_2 arising out of the same (t_g^3) configuration, since their magnetic behaviour, containing a fair amount of orbital contribution, depend more sensitively on the combined effect of the spin-orbit coupling and the ligand field of lower symmetry.

Potassium chromicyanide was prepared in the laboratory and purified by recrystallizing several times from dilute KCN solution. The single crystal was prepared by slow evaporation and oriented under the polarising microscope. The oriented single crystal was mounted on a coldfinger type dewar containing liquid hydrogen and the polarised spectrum was recorded photographically with the help of a high-dispersion grating spectrograph PGS-2 (dispersion $3\text{\AA}/\text{mm}$) and quartz Wollaston prism polariser. Kodak I-N and 103 a - E films were used.

For Zeeman experiments high magnetic field is necessary to make the splitting larger than the bandwidth. The transitory high magnetic field was generated by Kapitza's capacitor discharged technique. A bank of capacitors (460 μF) charged to 2.5 KV is suddenly discharged through an air-core coil with the help of an electronic key ignitron. The current increases rapidly to a maximum and then decays down. The spectrum was taken at the peak of the magnetic field, generated in the air-core coil, by synchronising a high voltage Xenon flash lamp with the magnetic field with the help of a variable delay circuit. The magnetic field lasts for several milliseconds while the lifetime of the flash is several microseconds. The synchronisation is monitored with the help of an oscilloscope, and the field remains effectively constant during the period for which the flash works. About 200 flashes are necessary for 8000 \AA transition and 50 for the 5400 \AA transition. The fields are reproducible within the limits of the experiment.

The ground state of the complex has an isotropic g -value of nearly 2 as determined by ESR experiments (Bowers, 1952). In case of trigonal distortion the combined action of the spin-orbit coupling and the trigonal field splits the 2E state, which exhibits large anisotropic g -value, as shown in the case of ruby (Tanabe & Sugano 1956). If the upper state has $g = 0$, each line should split into four components under the magnetic field, while a three line pattern will mean that $g = 2$ nearly. We observe a three line pattern with the magnetic field applied in any of the three directions a, b, c (when the field is applied along c -direction, the number of lines observed is two, but this is probably due to the vanishing intensity of the middle component). A tetragonal field will split the doubly degenerate 2E level and will give rise to two spin doublets with isotropic g -value. Our observations, therefore, agree with a tetragonal or orthorhombic distortion. The intensities of the lines depend on the direction of the magnetic field. We are now looking into the spin-orbit coupling mechanism through which the components borrow their intensities. Forster (1968) suggested that the ${}^4A_2 - {}^2E$ transition is a magnetic dipole allowed one. Our spectrum does not support this view.

We have been able to study the Zeeman splitting of the group of first four vibrational bands.

We are now trying to locate the missing 2T_1 state in the large number of lines observed along with the main bands. The nature of the transition (magnetic or electric dipole allowed) and the g -values are to be looked into more closely. More details of the work are in progress and will be communicated shortly.

We are also studying the same transitions of Cr^{3+} in an environment of perfect O_h symmetry to further confirm the nature of the transition. The Cr^{3+} doped in $\text{Cs}_2\text{LiCo}(\text{CN})_6$ offers an ideal condition (Wolberg, 1969) and we are using this crystal for our purpose.

REFERENCES.

- Bowers K. D. *Proc. Phys. Soc.* **A65**, 860.
Forster L.S. & Conrade R.E, 1968 *J. Chem. Phys.* **48**, 151.
Tanabe & Sugano 1956 *J. Phys. Soc. Japan* **11**, 864.
Wolberg A. 1969 *Acta Cryst.* **25 B**, 161.

Internal conversion coefficients

By M. RAJA RAO AND K. PARTHASARADHI

The Laboratories for Nuclear Research, Andhra University, Waltair, India

(Received 28 July 1969. Revised 17 February, 1970)

Studies on the Internal Conversion Coefficients (ICC) are useful for an understanding of nuclear structure. One of the accurate methods for the determination of these coefficients is the Internal External Conversion (IEC) technique. In this method the conversion electron intensity and the gamma ray intensity are measured separately. For the measurement of gamma ray intensity the photoelectron intensity is measured using an external converter. Assuming the theoretical photoelectric cross-section, the gamma ray intensity is determined from the measured photoelectron intensity.

In previous investigations by Raja Rao (1965) and Raja Rao & Jnanananda (1965, 1966, 1967) conversion coefficients for a few transitions are measured utilising scintillation technique and the IEC method. However, the theoretical photoelectric cross-sections are taken from the data of Grodstein (1957). These values are within an accuracy ranging from 5 to 15%. However, very recently accurate theoretical total photoelectric cross-sections of 0.5% accuracy are reported by Schmickley & Pratt (1967). So it is of interest to improve the accuracy of the ICC by using the new theoretical photoelectric cross-sections.

In the mentioned investigations of Raja Rao and Raja Rao & Jnanananda various external converters are used. So these values are corrected using the recent and accurate theoretical photoelectric cross-sections of Schmickley & Pratt (1967). In the cases where there are no reported cross-sections, the values are obtained by interpolations. The mean value of the ICC's obtained from various converters are estimated and from these the K-conversion coefficients are deduced using the available ratios of the conversion coefficients among different shells (Raja Rao 1965; Raja Rao & Jnanananda 1965, 1966, 1967). These values along with the theoretical values of Rose (1958) and with other experimental data are given in table 1. It can be seen from the table that the accuracy in the measured ICC's is greatly improved.

It can be seen from table 1 that there is satisfactory agreement between the present values and those of Rose (1958) except in the case of ^{134}Ba where the experimental value is a little bit higher. However, in all the

cases, there is agreement at least with some of the available experimental data.

TABLE 1. K-INTERNAL CONVERSION COEFFICIENTS

Present	Theoretical (Rose 1958)	Other experimental
I. ^{137}Ba (Gamma energy 662 keV) converters: Pb, Au, Sn, Ag and Cu		
0.096 ± 0.005	0.090	0.0920 (Wapstra 1954)
$(0.0925 \pm 10\%)$		0.0976 (Yoshizawa 1958)
		0.0930 (Hultberg 1959)
		0.0930 (Daniel 1962)
		0.0894 (Hamilton 1965)
		0.0940 (Hamilton 1965)
II. ^{204}Tl (Gamma energy 279 keV) converters: Pb, Sn and Cu		
0.160 ± 0.008	0.160	0.163 (Nijgh <i>et al</i> 1959)
$(0.154 \pm 15\%)$		0.164 (Wapstra <i>et al</i> 1956)
		0.150 (O'Friel <i>et al</i> 1956)
		0.160 (Stockendal 1956)
		0.162 (Croft 1965)
		0.163 (Hamilton 1965)
III. ^{114}In (Gamma energy 192 keV) converters: Ta, Cd		
2.00 ± 0.16	2.18	2.16 (Steffen 1951)
$(1.95 \pm 15\%)$		2.15 (Boehm <i>et al</i> 1959)
		2.17 (Hoffman 1957)
IV. ^{134}Ba (Gamma energy 800 keV) converters: Au, Ta		
0.0030 ± 0.0002	0.0026	0.0026 (Trehan <i>et al</i> 1963)
$(0.00285 \pm 10\%)$		0.0030 (Keister <i>et al</i> 1955)
		0.0021 (Schmidt <i>et al</i> 1952)

The values in the brackets are of Raja Rao (1965) and Raja Rao & Juanananda (1965, 1966, 1967)

REFERENCES

- Boehm F. & Preisswerk P. 1949 *Hel. Phys. Acta* **22**, 321.
 Croft W. L. Pettersson B. G. & Hamilton J. H. 1963 *Nuclear Physics* **48**, 267.
 Daniel H. & Schmitt H. 1962 *Z. Phys.* **168**, 292.
 Grodstein G. W. 1957 *NBS Circular* 583.
 Hamilton J. H. 1966 *Internal Conversion Process*, Academic Press, 643.
 Hoffman K. W. 1957 *Z. Phys.* **148**, 298.

- Hultberg S., Wapstra A. H., Ornstein L. T. M., Salomons-Grobbe N. & Huizenga J. R. 1959 *Arkiv fur Fysik*, **14**, 565.
- Keister G., Wapstra A. H., Ornstein L. T. M., Salomons-Grobbe N. & Huizenga, J. R. 1955 *Phys. Rev.*, **97**, 451.
- Nijgh G. J., Wapstra A. H., Ornstein L. T. M., Salomons-Grobbe N. & Huizenga J. R. 1959 *Nuclear Physics* **9**, 528.
- O'Friel Z. & Weber A. H. 1950 *Phys. Rev.*, **101**, 1076
- Rose M. E. 1958 *Internal Conversion Coefficients*, NRP-1, Amsterdam
- Rao Raja, 1965 *Experimental Studies on Internal Conversion Coefficients*, Ph.D. Thesis, Andhra University
- Rao Raja & Jnanananda Swami 1965 *Nuclear Instruments and Methods* **36**, 261.
1966 *Current Science* **35**, 435.
1967 *Indian J. Phys.* **41**, 55.
- Schmickley R. D. & Pratt R. H. 1967 *Phys. Rev.* **163**, 104.
- Schmidt F. H. & Keister G. L. 1952 *Phys. Rev.* **86**, 63
- Steffen R. M. 1951 *Phys. Rev.* **83**, 166
- Stockendal R. V. 1956 *Arkiv Fur Fysik* **17**, 579
- Tielens P. M., French J. D. & Goodrich M. 1963 *Phys. Rev.*, **131**, 2625
- Wapstra A. H. 1954 *Arkiv for Fysik* **7**, 275
- Yoshizawa Y. 1958 *Nuclear Physics*, **5**, 122.

Indian J. Phys. **43**, 625—627 (1969)

Radiation damping of electromagnetic waves in plasmas

By R. BURMAN

Department of Physics, University of Western Australia

(Received 18 November 1969)

The non-relativistic equation of motion of a point electron, with radiation damping included is $-m\ddot{\mathbf{r}} + m\dot{\mathbf{r}} = \mathbf{F}$. The electron is at \mathbf{r} at time t , and is acted on by an external force \mathbf{F} ; in MKS units, $\tau = (1/4\pi\epsilon_0) (2e^2/3mc^3)$ in standard notation.

With collisions neglected, the electron distribution function $f(\mathbf{r}, \mathbf{v}, t)$, where $\mathbf{v} \propto \dot{\mathbf{r}}$, is described by the Vlasov equation

$$\frac{\partial f}{\partial t} + \mathbf{v} \cdot \frac{\partial f}{\partial \mathbf{r}} + \frac{\partial \mathbf{v}}{\partial t} \cdot \frac{\partial f}{\partial \mathbf{v}} = 0. \quad \dots(1)$$

The electric and magnetic fields are written $\mathbf{E}_1 \exp(ikx - i\omega t)$ and $\mathbf{B}_1 \exp(ikx - i\omega t)$; there are no static fields present. Also, f is written $f_0(v) + f_1(v) \exp(ikx - i\omega t)$, f_0 being a function of only the magnitude v of \mathbf{v} . The equation of motion gives $\mathbf{v} = (1 + i\omega\tau)^{-1} (\mathbf{F}/m)$. Substituting into (1) and linearizing gives (with e , the electron charge, a negative quantity)

$$f_1 = \frac{-ie/m}{1 + i\omega\tau} \frac{\mathbf{E}_1 \cdot \partial f_0 / \partial \mathbf{v}}{\omega - k v_x} \quad \dots (2)$$

It is found from Maxwell's equations that $(n^2 - 1) \mathbf{E}_t = i\mathbf{J}_t / \omega \epsilon_0$, where n is the refractive index kc/ω , while \mathbf{E}_t and \mathbf{J}_t are the transverse parts of the electric field and current density \mathbf{J} . Taking \mathbf{E}_1 and \mathbf{B}_1 to be transverse with \mathbf{E}_1 in the y direction, and using $\mathbf{J} = e \int f_1 \mathbf{v} d^3v$ with f_1 given by (2), leads to the dispersion relation

$$n^2 - 1 = \frac{\omega_p^2 / N_0 \omega}{1 + i\omega\tau} \int \frac{v_y \partial f_0 / \partial v_y}{\omega - k v_x} d^3v \quad \dots (3)$$

Here ω_p is the electron plasma frequency and N_0 is the equilibrium electron number density. Integrating by parts gives

$$n^2 = 1 - \frac{\omega_p^2 / N_0 \omega}{1 + i\omega\tau} \int \frac{f_0 d^2v}{\omega - k v_x} \quad \dots (4)$$

For longitudinal waves, a dispersion relation including radiation damping has been given recently (Burman, 1969).

For large ω/k , expanding the integrand in (4) and integrating term by term (ignoring the singularity) gives

$$n^2 = 1 - \frac{\omega_p^2 / \omega^2}{1 + i\omega\tau} \left(1 + n^2 \frac{\overline{v_x^2}}{c^2} + \dots \right) \quad \dots (5)$$

For a cold plasma, (5) reduces to $n^2 = 1 - (\omega_p^2 / \omega^2) (1 + i\omega\tau)^{-1}$; for small $\omega\tau$, this gives a formula which has been used in cosmological calculations (Hoyle & Narlikar 1964).

Using the Maxwellian distribution $f_0 = (N_0 / \pi^{3/2} a^3) \exp(-v^2/a^2)$ and following calculations (Tanenbaum 1967) for the case in which $\tau = 0$, (4) leads to

$$n^2 = 1 - \frac{\omega_p^2 / \omega^2}{1 + i\omega\tau} \left(2C \int_0^C e^{z^2 - C^2} dz - i\pi^{1/2} C e^{-C^2} \right) \quad \dots (6)$$

where $C = \omega/ka$; for large C

$$n^2 = 1 - \frac{\omega_p^2 / \omega^2}{1 + i\omega\tau} \left(1 + n^2 \frac{a^2}{2c^2} + \dots - i\pi^{1/2} C e^{-C^2} \right) \quad \dots (7)$$

This shows the exponential term (leading to Landau-type damping) which is omitted in the expansion used to obtain (5). Relativistic considerations suggest omitting this term (Tanenbaum 1967).

REFERENCES

- Burman R. 1969 *Physics Letters* **30A**, 431.
Hoyle F. & Narlikar J. V. 1964 *Proc. Roy. Soc.* **A277**, 1.
Tanenbaum B. S. 1967 *Plasma physics* Mc Graw-Hill, New York, section 4.6.

BOOK REVIEWS

Photoemissive Materials-Preparation, properties and uses

by A. H. Sommer, John Wiley & Sons, Inc, 1968, \$ 12.95

This is probably the first book on the subject after the well known work by Hughes and DuBridge. The author a well known worker in the field has collected in a single volume all relevant informations on photoemissive materials which have so long been scattered in different journals. The book is mainly devoted to the technology of the subject though theoretical aspects have also been qualitatively discussed. Finally the book contains an excellent up-to-date bibliography on photoemissive materials. It will be an useful reference book for all workers in the field.

A. K. D.

A First Course In Vector Analysis

by Maity and Ghosh, New Central Book Agency, Calcutta-9

Fourth Edition, March 1969, pp. 284, Rs. 5/-

The earlier editions of Maity and Ghosh's "A First Course in Vector Analysis" are well known to the undergraduate students of Indian Universities for whom the treatise is intended. In this new edition the authors have preserved the excellent balance between the mathematical treatment of the fundamentals and their interesting applications that characterized the earlier volumes. They have now added new materials in the form of differential operators.

The basic principles of vectors are presented in the first four chapters of the book. The subject has been developed logically, approaching from algebraic as well as geometric points of view. Applications to numerous examples have made the subject illustrative. The fifth chapter presents a short course of vector calculus in which the concepts of limit and continuity of vector differentiation and integration have been introduced. Chapters six and seven involve the application of vectors to differential geometry and elementary mechanics dealing with the motion of particles. The last chapter is a new addition which introduces, in a concise form, the differential operators giving the idea of gradient, divergence and curl.

The book is written for the undergraduate students at the Pass and Honours level, presuming only an elementary knowledge of algebra and geometry. The latter part of the text presents materials suitable for post graduate students. The book is written in an interesting and logical style, reflecting extensive experience of the authors as teachers.

J. G. C.

BOOKS RECENTLY RECEIVED FOR REVIEW.

- The Structure and Chemistry of Solid Surfaces*. Ed. Gabor A. Somorjai, \$ 37.50, John Wiley & Sons, New York.
- Mathematics of Classical and Quantum Physics*, Vol. 1, Byron-Fuller, Addison-Wesley, London.
- Advances in Plasma Physics*, Vol. 2, Ed. A. Simon & W. B. Thompson, \$ 13.50, John Wiley & Sons, New York.
- Physics of the Earth*, F. D. Stacey, \$ 11.95, John Wiley & Sons, New York.
- Springer Tracts in Modern Physics (51) Synchron Radiation as a Light Source* Ed. G. Hofter, Springer-Verlag, Berlin.
- Mathematics of Classical & Quantum Physics*, Vol. 2, Byron-Fuller, Addison-Wesley, London.
- Thermal Physics*, G. Kittel \$ 10.95, John Wiley & Sons, New York.
- Codata International Compendium of Numerical Data Project DM 48*, Springer-Verlag, Berlin.
- Vth International Congress on X-ray Optics and Microanalysis* Ed. G. Mollenstedt & K. H. Gaukler, DM 198, Springer-Verlag, Berlin.
- Daylight and its Spectrum*, S. T. Henderson, \$ 5.20, Adam Hilger Ltd, London.
- Elements of Statistical Mechanics*, B. K. Agarwal, Pothishala (P) Ltd, Allahabad.
- Conference Booklet on High Magnetic Fields and Their Application*, 30sh, Brian W. Berry, The Institute of Physics and Physical Science, London.
- Quantum Mechanics*, Ed. Merbacher, \$ 13.93, John Wiley & Sons, New York.



1

1

Chemiluminescent reaction between sodium and oxygen atoms

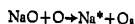
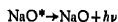
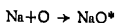
By S. N. GHOSH, A. N. SRIVASTAVA AND R. V. SHUKLA

*J. K. Institute of Applied Physics and Technology, University of Allahabad,
Allahabad, India.*

(Received 2 July 1969—Revised 7 November 1969)

PLATES 7A, 7B, 8A, 8B

The chemiluminescent glow produced by the reaction between sodium and oxygen atoms has been investigated spectroscopically, photometrically and microphotometrically. In addition to sodium *D* lines, 5685.44 Å, 5672.90 Å and certain other lines of Na and a band of Na₂ were observed. The relative intensity of *D* lines with respect to 3302 Å line has been obtained. The excitation mechanism of sodium *D* line has been proposed as follows :



The quenching coefficients of *D* lines by O₂, A, and N₂ gases at room temperature were found to be 1.9×10^{-7} cm³/sec mole, 1.1×10^{-9} cm³/sec mole and 3.8×10^{-10} cm³/sec mole, respectively. These coefficients indicate that the emitting layer of *D* lines in the night airglow should be situated at a height of about 100 Km.

1. INTRODUCTION

To understand the reaction responsible for the emission of sodium line in the upper atmosphere, it is necessary to consider laboratory investigation of reactions between sodium, oxygen and ozone. Tanaka (1951) and Tanaka & Ogawa (1954) produced sodium glow in the laboratory by reaction between ozone and sodium vapour and concluded the following :

- (1) Compared to atomic sodium, molecular sodium plays a more important role in the reaction.
- (2) The sodium glow is produced mainly by reaction between molecular sodium and ozone and not between molecular sodium and oxygen*.

To have more information of the reaction responsible for the excitation of sodium *D* line, the present investigation of the reaction between sodium and oxygen atoms was undertaken.

* It will be shown subsequently in this paper that oxygen quenches the sodium glow to a great extent. Hence the glow produced by reaction between sodium and oxygen may be subsequently quenched.

2. EXPERIMENTAL ARRANGEMENTS

The reaction chamber R which was made of pyrex tube, was about 25 cm in length and 2.5 cm in internal diameter and was closed at one end (figure 1). Sodium vapour was produced in a chamber below the reaction chamber by heating solid sodium in an atmosphere of N_2 or argon

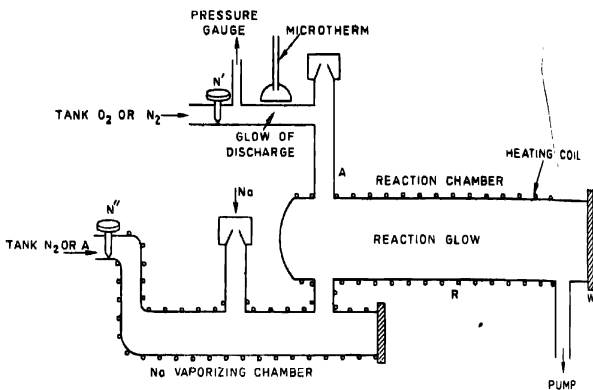


Figure 1. Experimental arrangement for producing chemiluminescent reaction between sodium and oxygen atoms.

(these gases prevented burning of sodium in the residual oxygen present in the system). The vapour was carried to the reaction chamber by N_2 or argon gas. The wall of the reaction chamber was heated to prevent condensation of sodium vapour on it. The O_2 gas (tank O_2 or O_3 containing about 0.5 per cent of tank N_2 as impurity) was dissociated by a discharge and was introduced into the reaction chamber opposite to the inlet of sodium vapour. The discharge was initiated by a Raytheon microtherm (magnetron oscillator), type CMD-4. It has a maximum output power of 100 watts, generating microwave at a frequency of 2450 Mc/sec. The flow rates of O_2 and carrier N_2 or argon gas were controlled by Hoke needle valves N' and N'' . A pressure of the order of 10^{-2} mm was maintained in the reaction chamber and was measured by a NRC thermocouple gauge. The sodium glow was observed through the quartz window W.

Tank O_2 and argon were introduced into the system directly without purification. Tank N_2 was at first used without purification. Afterwards it was made nearly free from oxygen content by passing it through a solution of alkaline pyrogallol and an aqueous solution of vanadium sulphate,

respectively. It was then dried by passing it through concentrated sulphuric acid.

The spectra of the luminescent glow were photographed against copper arc spectrum on Kodak 103-F(3) and Ilford HP (3) plates by a baby quartz and a Hilger's medium quartz spectrograph.

The photometric studies were carried out with a RCA 1P21 photomultiplier tube operated by a highly stabilized Baird atomic power supply. The photo-electric current was measured with a RCA ultrasensitive dc microammeter, type WV-84B. The spectral lines from the glow were picked by a Bausch and Lomb monochromator, type 33-86-40, using a grating of 250 mm focal length, 600 lines per mm and having a dispersion of 66 Å/mm.

3. PRODUCTION OF SODIUM GLOW

After running the pump for several hours, the vacuum system was flushed with tank N₂. The reaction chamber and sodium vapourizing chambers were heated slowly. When sufficient amount of sodium vapour was produced, it was carried to the reaction chamber by the carrier gas where it met atomized oxygen by dissociation of O₂ by the microtherm discharge. The following observations were made.

1. The flow of tank O₂ and/or N₂ were varied but no glow was observed.
2. After stopping the flow of tank O₂, tank N₂ flow was varied. It was observed that when the flow rate of N₂ was very small the whole of the reaction chamber was full of a strong yellow-orange glow.
3. When tank N₂ was made nearly free from oxygen impurity by passing through solutions mentioned above, the intensity of the glow was considerably decreased. When it was completely free from it, practically no glow was observed.
4. The glow was also produced when instead of tank N₂, argon as the carrier and tank O₂ as the reacting gas were used. At a small flow rate of O₂, a faint glow was observed which disappeared when the flow of O₂ gas was slightly increased.
5. If instead of tank O₂, the reacting gas is tank N₂ and the carrier gas argon, a very strong glow was obtained. The intensity of the glow decreased if the tank N₂ was made nearly free from O₂ content.

4. SPECTROSCOPIC AND PHOTOMETRIC STUDIES OF SODIUM GLOW

The spectroscopic and photometric and microphotometric observations of the glow are as follows :

A. Spectroscopic Observations : Six spectra for observation 2 of section 3 were taken—four by the baby quartz spectrograph and two by the medium quartz spectrograph. Of the four spectra taken by the baby quartz spectrograph two were of sodium glow—one taken at the position A near the discharge at right angle to the reaction chamber (Plate 7A.1) and another through the window W (Plate 7A.2). The other two spectra

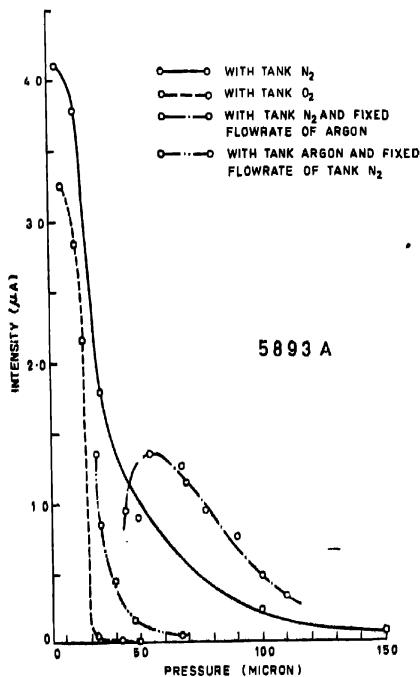
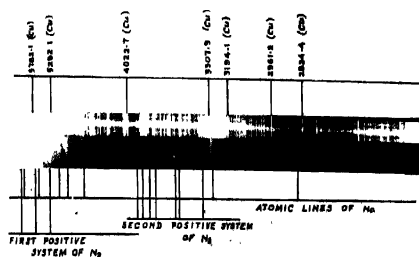
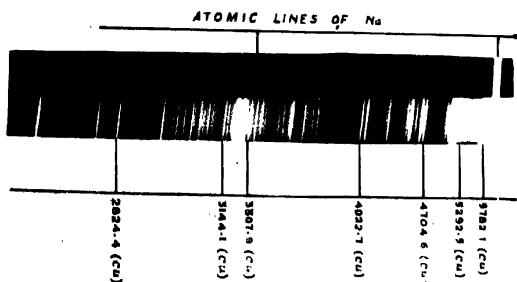


Figure 2. Variation of intensity of 5893 Å line with pressure of (a) tank N_2 , (b) tank O_2 , (c) tank N_2 at a fixed flow rate of argon and (d) argon at a fixed flow rate of tank N_2 .



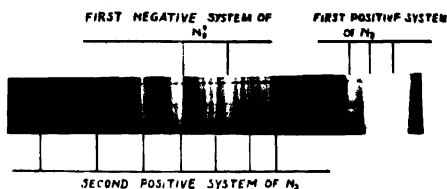
Figure—1



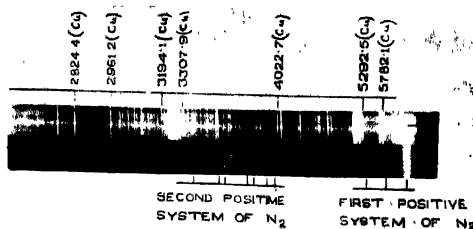
Figure—2

Plate 7A. Figure 1. Spectrum of the sodium glow at the position A (see figure 1) taken with a baby quartz spectrograph on Kodak 103 — F(3) plate in the range 2800-7000Å. The presence of first positive and second positive systems of N₂ due to discharge. Exposure time : 3 hrs.

Plate 7A. Figure 2. Spectrum of the sodium glow in the range 3000-7000Å taken with a baby quartz spectrograph through the quartz window W. Exposure time : 6 hrs.



Figure—3



Figure—4

Plate 7B. Figure 3 Spectrum of N_2 discharge taken with a baby quartz spectrograph in the range 3000-7000 \AA when the sodium glow was maintained in the reaction chamber. Exposure time : 60 minutes.

Plate 7B. Figure 4 Spectrum of N_2 discharge in the absence of sodium glow in the range 2800-7000 \AA taken with a baby quartz spectrograph. Exposure time : 3 hrs

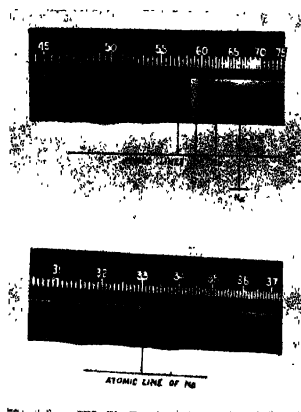
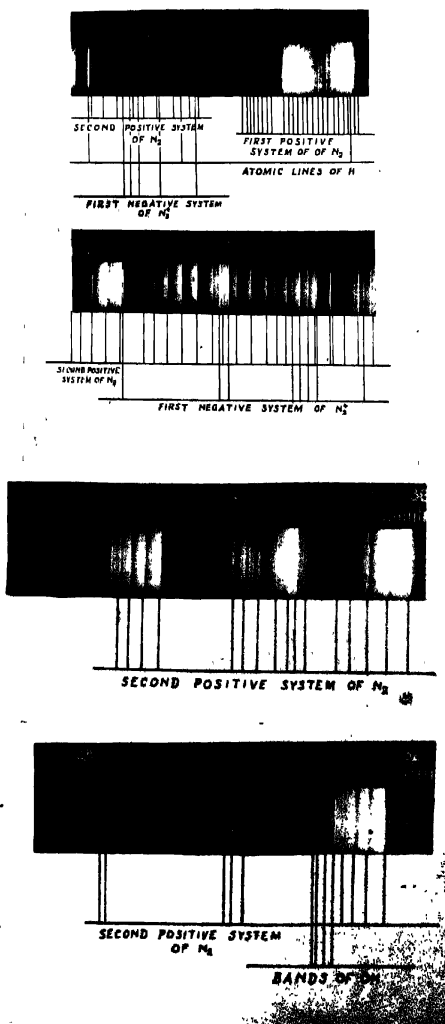


Figure 5.

Plate 8A. Figure 5. Spectrum of the sodium glow taken with a medium quartz spectrograph through the window W in the range 3000-7000Å. Exposure time : 12 hrs.



Figure—6

Plate 8B. Figure 6. Spectrum of N_2 discharge with a medium quartz spectrograph in the range $3000 - 7000\text{\AA}$. Exposure time : 45 minutes.

taken with the baby quartz spectrograph at the position A (figure 1) were of N_2 discharges—one of them was taken when the glow was maintained (Plate 7B.1) and the other when there was no glow in the reaction chamber (Plate 7B.2). Of the two spectra taken by the Hilger medium quartz spectrograph one was of the glow through the window W (Plate 8A) and the other of the N_2 discharge (Plate 8B).

Since the sodium glow (observation 2 of section 3) was weak, it was photographed with wide slits of spectrographs. Kodak 103-F(3) plates were used. For plates 7A.1 and 7A.2 exposures of 3 and 6 hours were given. The contribution of light (table 4) from the discharge to the glow in Plate 7A.1 were noted from Plate 7B.2.

For Plate 7B.1 an exposure of 60 minutes was given. No sodium feature was observed in the N_2 discharge indicating that the sodium did not diffuse in sufficient quantity into the region where discharge was maintained. For plates 8A and 8B exposures of 12 hours and 45 minutes, respectively, were given.

B Photometric Observations: Photometric studies of the sodium glow were carried out for observations 2 to 5 of section 3.

For observation 2, sodium lines 5893\AA and 3302\AA were selected by the monochromator described before and their intensities were measured

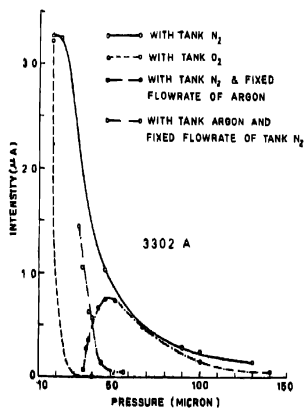


Figure 3. Variation of the intensity of 3302\AA line with pressure of (a) tank N_2 , (b) tank O_2 , (c) tank N_2 at a fixed flow rate of argon and (d) argon at a fixed flow rate of tank N_2 .

at different pressures of N_2 (18–150 microns; figures 2 and 3). To determine the quenching of 5893Å and 3302Å by oxygen; tank O_2 was introduced and the intensities of these lines were noted at different partial pressures of tank O_2 in the range 18–50 microns. These are shown in figures 2 and 3. The variation of intensities of these lines with tank argon partial pressure in the range 30–70 microns (figure 2) and 30–60 microns (figure 3) was also studied. Keeping a constant flow rate of argon, intensities of 5893Å and 3302Å lines were varied with tank N_2 pressure in the range 45–110 microns (figure 2) and 35–140 microns (figure 3), respectively.

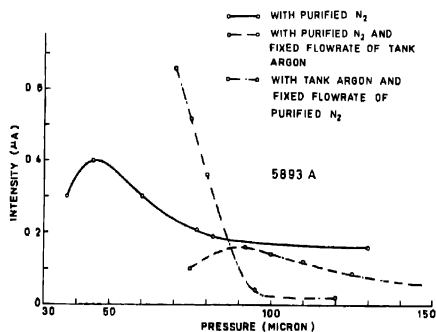


Figure 4. Variation of intensity of 5893Å line with pressure of (a) purified tank N_2 , (b) purified tank N_2 at a fixed flow rate of argon and (c) argon at a fixed flow rate of purified tank N_2 .

For observation 3, photometric studies of 5893Å and 3302Å were made by varying N_2 (purified by the method already described in section 2) in the pressure range 35–130 microns (figure 4) and 25–110 microns (figure 5), respectively. For observation 5, section 3, the variation of intensities of these sodium lines was studied in the pressure range 75–150 microns (figure 4) and 35–110 microns (figure 5) keeping the flow rate of tank argon constant and varying the flow rate of purified N_2 . By keeping the flow rate of purified N_2 constant and varying tank argon in the range 75–120 microns (figure 4) and 50–110 microns (figure 5), the variation of sodium line intensities was also studied.

For observation 4, due to small intensities of sodium lines, the photometric studies were not carried out.

C. Microphotometric Analysis: The intensities of sodium lines and of the microtherm discharge of tank N_2 (Plates 7A.1, 7B2 and 8B) were

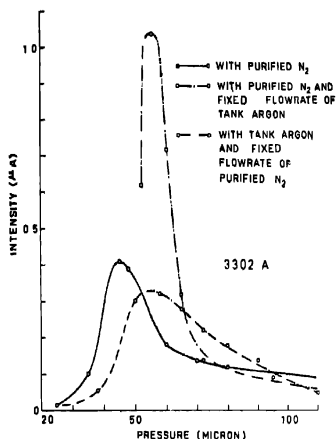


Figure 5. Variation of the intensity of 3302 Å line with pressure of (a) purified tank N_2 , (b) purified tank N_2 at a fixed flow rate of argon and (c) argon at a fixed flow rate of purified tank N_2 .

recorded by a Hilger and Watts (London) microphotometer (No. L459.301/57) utilising RCA 931A photomultiplier tube coupled to a Minneapolis Honeywell recorder (Model 153 \times 17V - X - 30R). The photomultiplier tube was supplied with a voltage of 800V by a series of dry batteries. To account for the drift in the coupling and dc amplifiers, the dark current signal was recorded at regular intervals. The plates were scanned from 2800 Å to 7000 Å with the help of a servomotor rated for a speed of 0.75 mm/minute.

Figure 8 shows the microphotometer records of the spectra of sodium glow taken at the position A at right angles to the reaction chamber (curve (a)) and at the window W (curve (b)). Curve (c) shows the record of the microtherm discharge of tank N_2 taken at the position A. The areas covered by 5893 Å and 3302 Å lines in curve (b) are measured with the help of a planimeter and their ratio is found to be 2.03.

5. RESULTS

After analysing the spectroscopic and photometric observations the following results were obtained :

(1) *Spectroscopic* : Spectroscopic studies were only carried for observation 2. Atomic sodium lines (table 1), molecular band of sodium (table 2)

TABLE 1 OBSERVED SODIUM LINES IN
THE SODIUM GLOW

Observed lines (Å)	Standard wavelength (Å)	Intensity (visual)
6157.5*	6157.50	VS
5892.9*	5862.94	VVS
5685.4*	5685.44	VS
5672.9*	5672.94	VS
5151.4*	5151.37	S
4980.7	4982.84	S
4667.8	4666.73	W
4490.4	4496.00	VW
3534.9	3533.01	W
3302.7	3302.66	VS
2852.5	2852.93	W

* These lines were identified from Plate

TABLE 2 OBSERVED Na₂ BAND IN
THE SODIUM GLOW

Band Head (Å)	Standard wavelength (Å)	Transition	Intensity (visual)
3364.6	3369.2	4.1	S

TABLE 3 UNIDENTIFIED FEATURES
IN SODIUM GLOW

Unidentified lines (Å)	Intensity (visual)
5162.4	W
4863.3	S
4759.6	W
4411.1	W
4332.4	VW
3925.4	VW
3549.2	W

Chemiluminescent reaction between sodium and oxygen atoms 639

TABLE 4 OBSERVED FEATURES OF DISCHARGE
IN THE GLOW

Emission	Band Head (Å)	Standard wavelength (Å)	Intensity (visual)
N ₂ second Positive System	4257.4	4269.7	VVW
"	4196.6	4200.5	VVW
"	3989.2	3998.4	VVW
"	3899.6	3894.6	VVW
"	3797.1	3804.9	VW
"	3756.5	3755.4	VW
"	3574.3	3576.9	W
"	3533.7	3536.7	VW
"	3367.8	3371.3	W
"	3154.9	3159.3	VVW

and seven unidentified features (table 3) were obtained when the spectrum of the sodium glow was taken at the position A (Plate 7A.1). On the other hand, when the spectrum was taken through the window W (Plates 7A.2 and 8A), sodium lines 5893Å, 3303Å, and 5679Å, and hydrogen line H_{α} were obtained in addition to the very weak sodium line 6157.5Å. In the first case certain features of the discharge are superimposed on the sodium glow (table 4), whereas, in the later case no such feature is observed (Plates 7B.2 & 8A)

(2) *Photometric* : When tank N₂ was used as the reacting gas (observation 2 of Sec. 3), intensities of 5893Å and 3302Å attain maximum values at about 18 microns and then decrease exponentially with the increase of tank N₂ pressure (figure 2 and 3). When, however, tank argon is mixed with tank N₂, their intensities attain maximum values at about 55 and 50 microns, respectively and then decrease exponentially with the increase of tank N₂ pressure (figure 2 and 3). When the glow was obtained with purified N₂ as the reacting gas (observation 3 of Sec. 3), the intensities of 5893Å and 3302Å attain maximum values at about 45 microns. The decrease of intensities of these lines with pure N₂ pressure is exponential (figure 4 and 5). The intensity of the glow obtained with N₂ (observations 2 of Sec. 3) is nearly 10 times the intensity obtained with pure N₂ (observations 3 of Sec. 3). When tank argon was mixed with purified N₂, the intensities of 5893Å and 3302Å attain maximum values at 90 and 55 microns, respectively (figures 4 and 5). The intensities of these lines decrease exponentially with increase of pressure.

In all the above figures, the increase of intensities of 5893Å and 3302Å with pressure before reaching the maximum values can be represented by $I = Cp^2$, where I is the intensity at a pressure p and C is a constant. From figures 2 and 3, it follows that 5893Å and 3302Å lines are quenched in decreasing order by tank O_2 , tank argon, tank N_2 and a mixture of tank N_2 and argon. The quenching of these lines (when the glow was produced by N_2 nearly free from O_2) by tank argon is large compared to the quenching by pure N_2 and a mixture of pure N_2 and tank argon (figures 4 and 5).

When the ratio I_0/I for 5893Å line is plotted against the particle concentrations of tank O_2 , tank argon and purified N_2 , the curves are straight lines (figures 6 and 7), where I_0 and I are the intensities of 5893Å

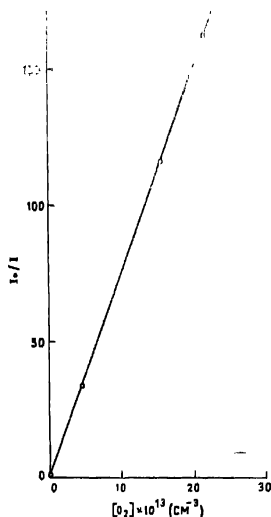


Figure 6. I_0/I for 5893Å is plotted against the concentration of O_2 molecules.

line without and with the quenching gas, respectively. By calculating slopes of these lines, the values of quenching coefficients for tank O_2 , tank argon and pure N_2 are obtained at the temperature of the system i. e. 550°K. Ghosh *et al* (1963) observed that in the case of quenching of CN bands by CH_2Cl_2 , the quenching coefficient is directly proportional to temperature,

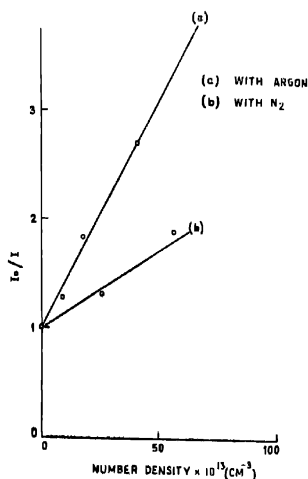


Figure 7 (a). I_0/I for 5893 Å line is plotted against the concentration of argon.

(b). I_0/I for 5893 Å line is plotted against $[N_2]$.

Assuming the same for 5893 Å sodium line, the quenching coefficient can be represented as follows :

$$K_T = K_R (1 + \delta T)$$

where, K_R , K_T , are the quenching coefficients at room temperature and at $T^\circ K$, respectively, $\delta T = (T - t)/t$, where t is the room temperature.

From the above equation, one obtains the quenching coefficients at room temperature which are given in table 5.

TABLE 5 QUENCHING RATES AND
QUENCHING CROSS-SECTIONS
AT 300°K

Gas	Quenching Rate (cm ³ /sec mole)	Quenching cross-section (cm ²)
O ₂	1.9×10^{-7}	7.7×10^{-13}
A	1.1×10^{-9}	3.9×10^{-15}
N ₂	3.8×10^{-10}	1.30×10^{-16}

The quenching cross-section for tank O_2 , tank argon and pure N_2 have been calculated by using the following formula,

$$\sigma^2 = K_T \left[8\pi kT \left\{ \frac{1}{m_{Na}} + \frac{1}{m_M} \right\} \right]^{-1/2}$$

where, k = Boltzmann constant

T = absolute temperature of the reaction chamber

m_{Na} = atomic mass of sodium

m_M = molecular mass of the quenching gas

The calculated quenching cross-sections for O_2 , N_2 and argon are given in table 5.

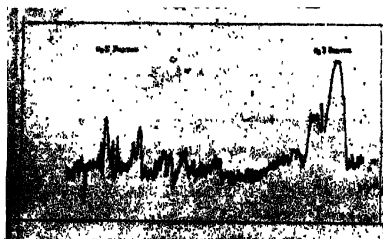
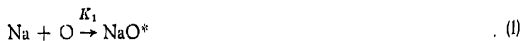


Figure 8. The microphotometer traces of the sodium glow taken at the position A figure 1. (curve a), at the window W (curve b), and of the N_2 discharge (curve c).

6. DISCUSSION

In the present investigation, lines of Na atoms which are observed with sufficient intensity are 5893\AA and 3302\AA lines. From the investigation described before, the following mechanism for excitation of 5893\AA and 3302\AA lines may be proposed.



where A is the transition probability corresponding to the emission from NaO ,

The NaO^* molecule (Baun & Evans 1937, Chapman 1939) comes down to the ground state as follows :



The excited sodium atoms may be lost as follows :



where M' , O'_2 , N'_2 are vibrationally or electronically excited particles. It was also found that argon atoms quench the sodium glow (see section 5(2)).



The intensity of the sodium line after attaining the maximum value may be represented by

$$I = \frac{K_1 K_2 [\text{Na}] [\text{O}]^2}{1 + \frac{K}{A} [\text{M}]} \quad \dots(9)$$

where K is the quenching coefficient of 5893\AA line by $\text{M} = \text{O}_2$, N_2 or A . The values of quenching coefficients of 5893\AA by O_2 , A and N_2 at room temperature are given in table 5. Carrington (1959) determined the value of quenching cross-section for electronically excited OH bands by H_2O molecules to be $3.5 \times 10^{-15} \text{ cm}^2$. Ghosh *et al* (1963) obtained $1.8 \times 10^{-14} \text{ cm}^2$ as the quenching cross-section for CN bands by CH_2Cl_2 molecules. In a private communication, Sharma (1965) informed that the quenching cross-section of sodium D line by N_2 is of the order 10^{-15} cm^2 . The value of $\sigma^2(\text{O}_2)$ is nearly hundred times larger compared to that of $\sigma^2(\text{N}_2)$ and $\sigma^2(\text{A})$. It may be noted that Young and Black (1966) obtained that the quenching coefficient of $\text{O}^1(\text{SO})$ state by O_2 molecules is very large.

From the equation (9), it is seen that for constant $[\text{Na}]$, the intensity of sodium D lines should at first vary as $[\text{O}_2]^2$ or as p^2 with the increase of the pressure p . On further increase of p , it should attain a maximum value and then decrease. This agrees well with the observations made in the present investigation.

Heppner & Meredith (1958) and Tousey (1958) obtained from rocket borne experiments that the 5893\AA line is emitted from the earth's atmosphere in the altitude range 85 — 110 Km. From the 'Atlas of the Airglow Spectrum' compiled by Krassovsky *et al* (1962) the intensity of sodium D line in the night airglow is $30R$ in summer and $200R$ in winter.

In the laboratory excitation, the intensity of the 5893\AA line is given by equation (9). Since for this line $A = 6.29 \times 10^7 \text{ sec}^{-1}$. (Demtroder,

1962), K/A for O_2 , N_2 , and argon are, respectively, 7.53×10^{-18} cm³/molecule, 1.50×10^{-15} cm³/molecule and 4.25×10^{-16} cm³/molecule at 220°K which is the mean temperature at the altitude range 80-115 Km (Champion, 1965). The particle concentration in this altitude range varies from 3.251×10^{13} to 3.492×10^{11} for O_2 , 1.212×10^{14} to 1.620×10^{12} for N_2 and 1.450×10^{12} to 1.938×10^{10} for argon (Champion 1965). Using these

data, one obtains that the quenching term $\frac{K}{A} [M]$ Equation (9) is negligibly small in the range 80 – 115 Km. The intensity of 5893Å line in this altitude range is therefore given by

$$I = K_1 K_3 [Na] [O]^2 = K_e [Na] [O]^2, \quad \dots (11)$$

where $K_e = K_1 K_3$. The concentrations of O_2 , N_2 , A and O given by Champion (1965) and that of sodium by Bullock & Hunten (1961) were used. From the I/K_e versus altitude curve (figure 9), it is observed that the emission of 5893Å line is maximum at about 100 Km.

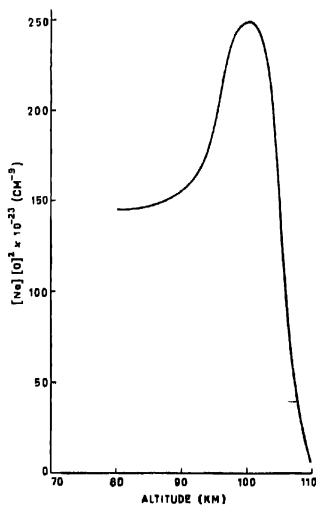


Figure 9. The calculated I/K_e of 5893Å sodium line at different altitudes. From the curve, it is clear that the maximum emission occurs at about 100 Km.

7. CONCLUSION

For the present investigation the following conclusions may be drawn :

- (1) The sodium glow does not appear with N_2 free from O_2 (observations 3 and 5 of Section 3)

- (2) The glow is produced by Na — O reaction (Sections 5(2) and 6).
- (3) The amount of oxygen required to produce the glow is small (about 0.5 per cent) (observations 2 and 5 of Section 3.)
- (4) Compared to N₂ and A the O₂ quenches the sodium glow very strongly (table 5)
- (5) The maximum emission of 5893Å line occurs at about 80 — 110 Km (figure 9).

REFERENCES

- Bates D. R. & Nicolet M. 1950 *J. Geophys. Res.* **55**, 235.
Baun C. E. H. & Evens A. G. 1937 *Trans. Faraday. Soc.* **33**, 1571.
Bullock W. R. & Huntten D. M. 1961 *Canad. J. Phys.* **39**, 976.
Carrington T. 1959 *J. Chem. Phys.* **30**, 1087.
Champion K. S. W. 1965 Report No. AFCLR-65-443, Airforce Cambridge Research Laboratories, L. G. Hanscom Field, Bedford, Mass. (U. S. A.)
Chapman S. 1939 *Astrophys. J.* **90**, 309.
Demtroder W. 1962 *Zeits. f. Phys.* **166**, 42.
Ghosh S. N., Sharda Nand & Sharma A. 1963 *Proc. Phys. Soc.* **81**, 713.
Heppner J. P. & Meredith L. H. 1958 *J. Geophys. Res.* **63**, 51.
Krassovsky V. I., Shefov N. N. & Yarin V. I. 1962 *Planet. Space. Sci.* **9**, 883.
Miller L. E. 1957 *J. Geophys. Res.* **62**, 351.
Sharma A. 1965 *Private Communication*
Tanaka Y. 1951 *Science of Light* (Tokyo) **1**, 61.
Tanaka Y. & Ogawa, M. 1954 *Science of Light* (Tokyo) **3**, 47.
Tousey R. 1958 *Ann. Geophys.* **14**, 186.
Young R. A. & Black G. 1966 *J. Chem. Phys.* **44**, 3741.

The study of magnetic anisotropy and susceptibility of
ruthenium acetylacetonate

By MADHUSUDAN SAHA

Department of Magnetism, Indian Association for the Cultivation
of Science, Jadavpur, Calcutta-32

(Received 30 July 1969)

Magnetic anisotropy and susceptibility of Ru^{3+} ion in ruthenium acetylacetonate crystal in the temperature range from 300°K to 90°K are reported in this communication. Both the results show marked deviation from the Curie law. The anisotropy is very large varying from 60% to 125% of the mean susceptibility in the above temperature range. The effective moment is nearly 1.9 BM near room temperature. All these results clearly indicate that the usual weak field scheme completely fails in this case. A strong ligand field treatment must have to be invoked to interpret the present findings in terms of anisotropic ligand field theory. In particular, the present anisotropy data together with the mean susceptibility results will be most fruitful for accurate evaluation of anisotropic ligand field and covalency parameters and also for obtaining a knowledge about the expected variation of anisotropic part of the ligand field with temperature as observed in the salts so far investigated in our laboratory.

INTRODUCTION

Very little work on the magnetic behaviour of single crystals of paramagnetic complexes belonging to the palladium (4d) and platinum (5d) groups of elements has yet been done. Moreover, the present theories were found to be inadequate to explain the observed experimental data. The complexes of palladium and platinum groups of elements differ from those of the first transition (3d) elements mainly because of four factors—(a) stronger crystal field (b) stronger spin-orbit coupling (c) interelectronic repulsion comparable to spin-orbit coupling (d) larger overlap of charge clouds of 4d or 5d electrons with the ligands. A study of magnetic anisotropy as well as mean susceptibility and their variations with temperature should provide useful informations on the relative contributions of the factors involved and enable us to extend the ligand field theory in these cases also.

The case of ruthenium acetylacetonate belonging to the palladium group is interesting in the sense that electronic configuration of the ground state of the free ion Ru^{3+} being $4d^5 \ ^6S_{5/2}$ in the Russel-Saunders Scheme, a weak field treatment would lead to a very feeble magnetic anisotropy of the ion, the spin moment would correspond to an effective Bohr magneton 5.9 and the mean susceptibility should follow a Curie law very accurately. Figgis *et al* (1966) have measured the mean susceptibility indicating a value of effective moment 1.9 BM at room temperature. There is also appreciable deviation from the Curie law. Weak field procedure therefore is

obviously not apt in this case. Figgis *et al* (1966) from their above data have evaluated the axial field splitting Δ of the lowest degenerate state, a triplet under strong field scheme. Evaluation of Δ from mean susceptibility alone is not considered to be very accurate since unlike the magnetic anisotropy the mean susceptibility is not very sensitive to the axial field. Moreover, the axial field may change appreciably with temperature, which will be hard to detect from mean susceptibility alone, so that the above mentioned calculation of Δ is not very significant. Again the calculation of the covalency factor (Figgis *et al* 1966) from mean susceptibility does not take into account the anisotropy in the delocalization of the ligand and central ion electrons. All these informations can be obtained much more precisely from anisotropy and mean susceptibility results when considered together.

In view of these, a detailed experimental investigation of the magnetic anisotropy and susceptibility of ruthenium acetylacetonate has been undertaken and the experimental values are reported in this communication.

Preparation of the crystal

Ruthenium acetylacetonate was prepared by treating aqueous ruthenium trichloride and acetylacetone solution with potassium bicarbonate solution and than refluxing the mixture (Wilkinson 1952, Hartmann & Buschbeck 1957, Grobelyny *et al* 1966). The red precipitate of the compound was washed repeatedly, filtered and dried. The single crystals were grown from benzene solution by very slow evaporation.

Structural data

No detailed crystal structure has yet been investigated. Jarrett (1957) has reported preliminary measurements on aluminium-, chromium-, cobalt-, and ruthenium acetylacetonates and found them to be isomorphous. Dingle (1965) from a study of external morphology and X-ray powder pattern has also substantiated the isomorphism and concluded that they should belong to the monoclinic space group C_2^2 with four molecules in the unit cell. Three acetylacetonate groups surround the metal ion to form an octahedron of three pairs of chelating oxygen atoms. Thus it may be presumed from the stereo-chemical considerations that the crystalline field has a trigonal symmetry analogous to some of the other isomorphous compounds as observed by Singer (1955).

EXPERIMENTAL TECHNIQUE

(a) Mean susceptibility

The mean susceptibility was measured with the help of a very sensitive Curie type balance but of robust construction designed by Bose *et al* (1963). Suspension of the balance beam was of moderately thick phosphor-bronze

strip and the deflectional sensitivity was made very high by using a balanced pair of photo-electric cells connected across a galvanometer and actuated by a light spot reflected from a mirror at the centre of the balance beam. The sample is suspended vertically from one arm of the beam in the central part of a Sucksmith type of inhomogeneous horizontal magnetic field with a small gradient at right angles to the field in the same plane. The translational magnetic force on the sample is balanced electro-dynamically by the force exerted on a small current bearing coil attached rigidly to the other arm of the balance beam and placed in the field of a small permanent magnet.

The sample hangs freely within the experimental chamber of a new type of liquid oxygen cryostat (Bose *et al* 1963) placed between the poles of the electromagnet in which any desired temperature between 400°K to 65°K may be reached and kept automatically constant within 0.01°K. The temperature at the crystal is measured with a calibrated Cu-constantan thermocouple. The mass susceptibility of the sample at room temperature is calculated from the expression,

$$\chi = \frac{i}{i_s} \left(\chi_s - \frac{k_s}{\rho_s} \right) \frac{m_s}{m_i} + \frac{k_a}{\rho}$$

in which χ , i , m and ρ are the mass susceptibility, balancing electric current, mass and density of the sample; χ_s , i_s , m_s and ρ_s are those of the standard chromium potassium alum, k_s being the volume susceptibility of the surrounding air.

Although the mean susceptibility results have already been reported by Figgis *et al* (1966) we have measured it again with our very accurate susceptibility balance and the cryostatic device mentioned earlier. The measurements are shown graphically side by side (figure 1) with those given Figgis *et al* (1966) showing an appreciable difference except at very low temperatures.

(b) Anisotropy

The magnetic anisotropy is measured by the null deflection method developed here (Dutta 1956). The crystal specimen is attached to the lower end of a thin glass rod with a known plane or axis horizontal or vertical with the help of a two-circle goniometer. The glass rod in turn is suspended from an accurate vernier torsion head reading to 0.1°, by means of a fine quartz fibre. The image of an illuminated scale, from one or the other of a hexagonal set of vertical mirrors attached to the upper end of the glass rod, can always be observed as the crystal is rotated. The crystal is suspended inside the experimental chamber of a liquid oxygen cryostat placed between the poles of a strong electromagnet.

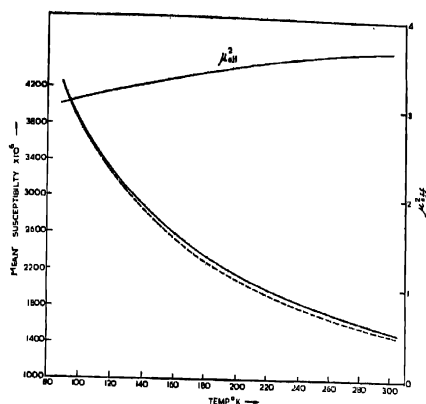


Figure 1. Showing curves for μ_{eff} vs. T (right-hand scale) and χ vs T (left-hand scale). The dotted line is due to Figgis *et al* (1966)

The position of the crystal for zero couple in the magnetic field, corresponding to setting of the crystal with its maximum susceptibility direction in the horizontal plane along the lines of forces, was obtained by rotating the torsion head till the twist in the fibre was nil. The crystal is then turned through in the absence of the field to the maximum couple position i. e. at 45° to the initial setting position. The magnetic field is now switched on again, which causes the crystal to rotate, towards zero setting position and it is brought back to the 45° position by rotating the torsion head. The gram-molecular anisotropy $\Delta\chi$ in the horizontal plane of the crystal is given by

$$\Delta\chi = \frac{2\alpha MC}{180mH^2}$$

where α is the angle through which the torsion head is rotated from 45° position. C , the torsion constant of the fibre, H , the magnetic field, M and m , the molecular weight and mass of the crystal respectively.

The constant C/H^2 is determined with the help of a standard nickel sulphate hexahydrate crystal whose anisotropy is accurately known (Dutta 1956).

For anisotropy measurement at any desired temperature in the range 300° to 90°K , the automatic gas flow-type cryostat (Bose 1947) was used. The

liquid oxygen kept in a separate reservoir, was pumped into the cryostatic chamber, evaporated and made to flow round the experimental chamber, the control of temperature being effected partly by adjusting the flow of liquid and partly by a gas thermometer relay device. Any desired temperature can be maintained steady to better than 0.1°K and measured accurately with a calibrated Cu-constantan thermocouple.

For a monoclinic crystal the anisotropy in the horizontal plane measured, where the crystal is suspended with b axis vertical, is given by

$\Delta\chi = (\chi_1 - \chi_2)$. It is assumed as usual that one of the principal susceptibility axes, say χ_3 , is along the b axis by symmetry requirements, and of the two principal susceptibilities in the (ac) plane χ_1 is greater than χ_2 . Also χ_1 and χ_2 make angles of ψ and θ with c and a axes of the crystal respectively.

With a axis vertical the anisotropy is

$$\Delta\chi = \pm \{ (\chi_1 - \chi_2) \sin^2\theta - (\chi_1 - \chi_3) \}$$

and with (001) plane horizontal

$$\Delta\chi = \pm \{ (\chi_1 - \chi_2) \cos^2\theta - (\chi_1 - \chi_3) \}$$

The + ve or - ve sign is chosen according as the b axis lies along or normal to the field, in the present case the former sign is the correct one. Using the above formula the values of $(\chi_1 - \chi_2)$, $(\chi_1 - \chi_3)$ and θ are obtained at different temperatures. The value of θ can also be obtained by finding the orientation of two $h0l$ planes in the magnetic field with b axis vertical (Datta 1956).

Since from the structural data we have assumed a trigonal symmetry of the ligand complex, the principal ionic susceptibilities are $K_z = K_{||}$ along the trigonal axis and $K_x = K_y = K_{\perp}$ perpendicular to this axis. Then the ionic anisotropy is calculated from the expressions

$$K_{||} - K_{\perp} = 2(\chi_1 - \chi_2) - (\chi_1 - \chi_3), \text{ when } K_{||} > K_{\perp}$$

$$K_{\perp} - K_{||} = (\chi_1 - \chi_2) + (\chi_1 - \chi_3), \text{ when } K_{\perp} > K_{||}$$

The expressions for the angle between the symmetry axes of the two magnetically inequivalent ions, one derived from the other by reflection in the (ac) plane are given in the two cases by

$$\cos 2\phi = \frac{\chi_1 - \chi_3}{K_{||} - K_{\perp}}, \text{ when } K_{||} > K_{\perp}$$

$$\cos 2\phi = \frac{(\chi_1 - \chi_2) - (\chi_1 - \chi_3)}{K_{\perp} - K_{||}}, \text{ when } K_{\perp} > K_{||}$$

The ambiguity in the sign of $|K_{\parallel} - K_{\perp}|$ can be removed if epr values on g_{\parallel} and g_{\perp} are available, or in some special cases from the magnetic anisotropy data itself leading to $\cos 2\phi > 1$, or inconsistent and unreasonable fitting of the data with the theory. In our present case epr data give $g_{\parallel} = 2.82$ and $g_{\perp} = 1.52$ so that we may take $K_{\parallel} > K_{\perp}$ and used the proper formulae for calculating $K_{\parallel} - K_{\perp}$ and $\cos 2\phi$ at different temperatures. It can be mentioned that our magnetic investigation alone unambiguously shows that $K_{\parallel} > K_{\perp}$ which is supported also by the epr data. The other alternative $K_{\perp} > K_{\parallel}$ leads to an absurd value of $\cos 2\phi > 1$.

EXPERIMENTAL RESULTS.

The results of principal crystalline anisotropies $\chi_1 - \chi_2$, $\chi_1 - \chi_3$ at 20° interval from smoothed out graphs are shown between 300°K and 90°K in table 1. The table includes values of θ at different temperatures and the values of ϕ and $K_{\parallel} - K_{\perp}$ calculated at these temperatures using formulae mentioned earlier are also given. The results of mean susceptibility at the same temperatures are shown in figure 1 together with those of squares of effective moments.

TABLE 1

T°K	$(\chi_1 - \chi_2) \times 10^6$	$(\chi_3 - \chi_1) \times 10^6$	θ	ϕ	$K_{\parallel} - K_{\perp}$
300	296	319.7	56.4	53°14'	911.7
280	330	357.1	56.2	53°13'	1017
260	378	406.5	56.2	53°10'	1162
240	435	449.6	56.2	54°57'	1319
220	510	497.0	56.0	54°33'	1517
200	600	562.5	56.0	54°16'	1762
180	723	650.1	56.0	53°58'	2096
160	880	767.6	56.0	53°51'	2527
140	1080	922.7	56.0	53°42'	3082
120	1317	1127	56.0	53°41'	3761
100	1623	1404	56.0	53°43'	4650
90	1820	1599	56.0	54°6'	5239

DISCUSSIONS

We have seen that the electronic structure of Ru^{3+} free ion is $4d^5$ $^6S_{5/2}$. But under the strong field scheme as it appears to hold in the present

case the effect of the strong octahedral ligand field on the d -orbitals is manifested by the fact that $R-S$ coupling is broken and the single electron d orbitals break up into a ground triplet t_{2g} , with a wide separation from the upper doublet e_g . The available electrons completely fill up two of the t_{2g} orbitals leaving one unpaired electron in the third orbital. The ground state of the system will be ${}^2T_{2g}$ (t_{2g}^5). The Coulomb repulsion cannot split this orbital triplet. Thus the magnetism of the compound corresponds roughly to spin quantum number $S = 1/2$ (equivalent to magnetic moment $\mu = 1.73 BM$) as is to be expected for the configuration t_{2g}^5 . However the observed room temperature moment $\mu = 1.91 BM$ is appreciably higher than the spin only value. This shows that the orbital moment has not been fully quenched as is to be expected for the case of a T_{2g} state lying lowest under the cubic field. As opposed to the weak field scheme in which case the magnetic anisotropy should be very feeble, our measurements show the magnetic anisotropy of the complex to be very high, about 60% at 300°K and it increases to 125% at 90°K. This is indeed to be expected in the case of an orbital triplet lying lowest in the cubic field stark pattern and further split up (to the order of kT) by the axial field. This large anisotropy is confirmed from *esr* measurement which shows the g factors ($g_{||} = 2.82$, $g_{\perp} = 1.52$) are highly anisotropic. Thus the case resembles Ti^{3+} ion under a predominant octahedral field with a small trigonal component except for conditions mentioned earlier. Perhaps an even better analogy is the case of potassium ferricyanide with some modifications as required by the said conditions.

Table 1 shows that ionic anisotropy of trivalent ruthenium in ruthenium acetylacetonate is about 60% and 125% of the mean susceptibility values at 300° and 90°K respectively. The crystalline anisotropy depends in a complicated manner on temperature, increasing by about 5 times when the temperature is reduced from 300°K to 100°K. It should be noted here the mean susceptibility increases by only 2.6 times in the same range of temperature. This shows that neither the mean value nor the anisotropy obeys the Curie law, though the deviation is less marked in the former (see graph). This is again to be expected for a triplet orbital state lying lowest.

The table shows that both θ and ϕ change very little with temperature, in the range of temperature from 300°K to 90°K they change only by 0.4° and 1°33' respectively. However the negligible changes of θ and ϕ should not be considered as conclusive indication of absence of any orientational change of the ion. In $Cu(NH_4SeO_4)_2 \cdot 6H_2O$ crystal (Bose *et al* 1957) although ϕ and θ are found to vary very little with temperature (about 1°), the recent *esr* experiments (Ghosh *et al* 1967) which offer a direct probe into the ion,

shows that the ion rotates appreciably in its own symmetry plane keeping the symmetry axis fixed. The rotation of the ion about its symmetry axis will not be reflected in the values of θ and ϕ which will therefore remain unchanged. Thus even though θ and ϕ do not change appreciably with temperature, the ion may undergo appreciable orientational changes which affect the packing of the lattice with consequent changes in the anisotropic part of the ligand field with temperature. Thus, apart from normal deviation from the Curie law we may expect further deviations from even the Curie-Weiss Law owing to thermal dependence of the ligand field.

Detailed theory for this complex will be shortly reported interpreting the above experimental results.

The author expresses his sincerest thanks to Dr. B.C. Guha for suggesting the problem and constant guidance during the pursuance of the work. He is deeply grateful to Prof. A. Bose for his keen interest in the work. He is also indebted to Dr. U. S. Ghosh and Mrs. D. Ghosh for their valuable suggestions. Finally the author expresses his thanks to the C. S. I. R. for the grant of a research fellowship.

REFERENCES

- Bose A. 1947 *Indian J. Phys.* **21**, 275.
Bose A., Dutta Roy S. K., Ghosh P. K. & Mitra S. 1963 *Indian J. Phys.* **38**, 505.
Bose A., Mitra S. C. & Dutta S. K. 1957 *Proc. Roy. Soc. A* **239**, 165.
Dingle R. 1965 *J. Molec. Spectros.* **28**, 276.
Datta S. K. 1956 *D. Phil. Thesis*, Calcutta University.
Figgis B. N., Lewis J., Mabbs F. E. & Webb G. A. 1966 *J. Chem. Soc. A* **422**, 442.
Ghosh U. S., Bagchi R. N., Pal A. K. & Mitra S. N. 1967 *Indian J. Phys.* **41**, 286.
Grabelny R., Jezowska-Trebatowska B. & Wojciechowski W. 1966 *J. Inorg Nucl. Chem.* **28**, 2715.
Hartmann H. & Buschbeck C. 1957 *Z. Phys. Chem.* **11** 120.
Jarrett H. S. 1957 *J. Chem. Phys.* **27**, 1298.
Scha M. 1968 *J. Pure & Appl. Phys.* **6**, 596.
Singer L. S. 1955 *J. Chem. Phys.* **23**, 379.
Wilkinson G. J. 1952 *J. Am. Chem. Soc.* **74**, 6146.

Properties of ionic crystals on Born-Mayer theory

By C. M. KACHHAVA

Physics Department, University of Rajasthan, Jaipur, India

AND

S. C. SAXENA

Department of Energy Engineering, University of Illinois, Chicago, U.S.A.

(Received 24 May 1967—Revised 12 November 1969)

This paper considers a number of crystal properties around room temperature in the spirit of Born-Mayer lattice theory. Specifically, the properties calculated are: thermal expansion, Gruneisen constant, reststrahlen frequency, dielectric and elastic constants. The potential, used explicitly includes the three types of interactions between the positive and negative ions, present in the lattice. A comparison of the results is made with the experimental data as well as with another form of interaction potential, which may be treated as a simplified form of the present one. The results are reasonably satisfactory in view of the employment of approximate theories.

INTRODUCTION

One of the most complete forms for the effective interaction potential per ion pair is:

$$\Phi(r) = -\frac{\alpha e^2}{r} - \frac{C}{r^8} - \frac{D}{r^9} + Mbc + -e^{(r_+ + r_- - r)/\rho} \\ + M' \frac{b}{2} \left[c_- - e^{(2r_- - ar)/\rho} + c_+ + e^{(2r_+ - ar)/\rho} \right] \quad \dots (1)$$

The various symbols have meanings as given in the papers of Born & Mayer (1932) and Huggins & Mayer (1933). In the evaluation of the potential parameter ρ , use has been made of the Born-Mayer thermodynamical condition. The choice of b is completely arbitrary and it has the value 10^{-12} erg per molecule. These authors exposed the above potential to test by calculating interionic distances, cohesive energy, compressibility and characteristic frequency. The computations were later on repeated by Cubicciotti (1959) using the newly available data. He was successful in achieving a certain amount of improvement in the results.

However, the arbitrariness in the choice of ionic radii and potential parameter gave ample scope for Fumi & Tosi (1964) and Tosi & Fumi (1964) to further improve the results. They adopted a very elaborate procedure to compute the values of b , ρ and the ionic radii. These authors have confined themselves to the calculations of only cohesive energy of alkali

halides The present work endeavours to extend the ideology of Fumi and Tosi for the calculations of other crystal properties.

CALCULATION OF PROPERTIES.

One of the thermodynamical relations due to Born and Mayer (1932) is

$$\beta = 9vF_T, r r_0^{-2} \left[\frac{d^2 \phi(r)}{dr^2} \right]_{r=r_0}^{-1} \quad \dots(2)$$

with

$$F_{T,P} = 1 + \frac{T}{\beta} \left(\frac{\partial \beta}{\partial T} \right) + \frac{T}{\beta^2 v} \left(\frac{\partial V}{\partial T} \right)_P \left(\frac{\partial \beta}{\partial P} \right)_T + \frac{2T}{3V} \left(\frac{\partial V}{\partial T} \right)_P \quad \dots (3)$$

Huggins (1937) and Cubicciotti (1959) have calculated β for the two cases. In one case $F_{T,P} = 1$, while in the other it is not so. These lead to crude estimates only. We do not expect any appreciable improvement by employing the newly determined parameters. As such the calculations are not proposed to be repeated.

Kachhava & Saxena (1966a) have shown that the coefficient of thermal expansion is expressed reasonably well by the relation,

$$\alpha = -C_v \phi'''(r_0) [\phi''(r_0)]^{-1} (2r_0 N)^{-1}. \quad \dots(4)$$

Here C_v is the molar specific heat at constant volume and the primes indicate the order of differentiation with respect to interatomic distance. The results are displayed in table 1.

Gruneisen constant γ is another property for which accurate experimental data are available. A simple approach for its theoretical estimation was advanced by Kachhava & Saxena (1966a), according to which

$$\gamma = -r_0 [6\phi''(r_0)]^{-1} \phi'''(r_0). \quad \dots(5)$$

Table 1 also lists the theoretical values of γ obtained from equation (5) on the basis of the potential of equation (1).

The characteristic reststrahlen frequency ω_0 of an ionic crystal is also related to $\phi(r)$, as is evident from the work of Kellermann (1940), and Krishnan & Roy (1952). For NaCl-type crystals, we have

$$\omega_0^2 = \left[(B + 2A) - \frac{4\pi}{3} \right] (\mu v)^{-1} e^2, \quad \dots(6)$$

in which μ is the reduced mass and

$$A = e^{-2} r_0^{-1} v v'(r_0),$$

and

$$B = 2e^{-2} v v''(r_0).$$

Here $M\rho(r)$ is the contribution of overlap to $\phi(r)$, where M is the coordination number. Computed values of the frequencies according to

equation (6) in conjunction with equation (1) are cited in table 1 along with the experimental values.

An alternative procedure has been adopted by Huggins (1937). It can be best summarized by quoting the general expression for the force constant k applicable to all classes of structures given by Born & Huang (1956). It is

$$k = \frac{M}{3} \left[v''(r_0) + \frac{2v'(r_0)}{r_0} \right] \quad (7)$$

The values of ω_0 computed through the relation,

$$\omega_0^2 = \mu^{-1} k \quad \dots (8)$$

are recorded in the last column of table 1.

TABLE 1. COMPARISON OF EXPERIMENTAL AND VARIOUS CALCULATED VALUES OF α , γ and ω_0

Crystal	$\alpha(10^{-5}/^{\circ}\text{C})$		γ		$\omega_0(10^{12}\text{ s}^{-1})$		
	Exptl. ^a	Cal. Eqn. (1)	Exptl. ^b	Cal. Eqn. (1)	Exptl. ^c		Cal. Eqn. (8)
					Eqn. (6)		
LiF	34.0	37.1	1.64	1.37	5.73	...	10.3
LiCl	44.0	62.2	1.69	1.84	3.84	2.76	4.40
LiBr	50.0	56.5	1.88	1.99	3.26	3.81	5.24
LiI	59.0	60.1	2.03	1.67	2.71	2.74	4.12
NaF	36.0	57.8	1.83	1.64	4.63	2.99	5.16
NaCl	40.0	35.4	1.64	1.88	3.09	3.33	4.17
NaBr	43.0	53.2	1.72	1.91	2.54	2.57	2.96
NaI	48.3	65.8	1.66	1.91	2.20	1.99	2.72
KF	36.7	47.3	1.58	1.74	3.62	3.15	4.09
KCl	38.3	50.0	1.49	1.83	2.71	2.69	3.21
KBr	40.0	54.9	1.46	2.05	2.18	2.29	2.67
KI	45.0	62.8	1.45	2.11	1.94	1.93	2.20
RbF	31.67	47.7	1.37	1.95	3.01	3.64	3.70
RbCl	36.0	52.5	1.57	2.14	2.24	2.51	2.80
RbBr	38.0	43.7	1.43	1.81	1.69	1.80	2.04
RbI	43.0	61.5	1.51	2.30	1.41	1.57	1.72
CsF	1.49	2.35	2.39	3.66	3.80

a. Kachhava C. M. & Saxena S. C. 1965 *Indian J. Phys.* 39, 145.

b. Kachhava C. M. 1966 *Ph. D. Thesis: Certain Problems of Solid State Physics*, Rajasthan University,

c. Kachhava C. M. & Saxena S. C. 1966 *Indian J. Phys.* 40, 567.

The appropriateness of the two theories is to be judged on the basis of the fact that both neglect the electronic polarizabilities of the ions. Further, the relative assessment of the two must be made by keeping in view the inclusion and exclusion of the Lorentz field correction effect associated with ionic displacements in equations (6) and (8), respectively.

The classical theory of dielectric constant (Mott & Gurney 1948) and its relationship with interaction potential is elaborated by Kachhava & Saxena (1966b). Here we quote only the final result which connects ϵ_0 (the low frequency dielectric constant) with the high frequency constant $\epsilon \propto$ the effective charge s and δ . The relation and defining equations are

$$\frac{\epsilon_0 - 1}{3 + (\epsilon_0 - 1)s} = \frac{\epsilon \propto - 1}{3 + (\epsilon \propto - 1)s} + \frac{(4/3)\pi \delta}{1 - (4/3)\pi \delta (1 - s)}, \quad \dots (9)$$

$$\delta = Ne^2 k^{-1} \quad \text{and} \quad s = 1 + e^{-2} r_0^3 v'(r_0)$$

Employing the observed values of $\epsilon \propto$ as given by Born & Huang (1956), we have calculated ϵ_0 and these results are contained in table 2.

TABLE 2. THE EXPERIMENTAL AND VARIOUS CALCULATED VALUES OF ϵ_0 AND THOSE OF C_{11} , C_{12} AND C_{44} IN UNITS OF 10^{11} erg/cm²

Crystal	ϵ_0		C_{11}		Exptl. ^b		Cal. $C_{11} = C_{44}$
	Exptl. ^a	Eqn. (9)	Exptl. ^b	Cal	C_{11}	C_{44}	
LiF	8.96	...	11.35	7.17	4.80	6.35	5.27
LiCl	11.95	...	4.94	3.28	2.26	2.49	3.05
LiBr	13.25	...	3.94	4.02	1.88	1.91	2.52
LiI	16.85	...	2.85	2.40	1.40	1.35	1.96
NaF	5.10	58.9	9.71	6.04	2.43	2.80	3.66
NaCl	5.91	9.51	4.93	5.76	1.31	1.275	1.67
NaBr	6.38	11.3	4.02	4.23	1.15	0.99	1.41
NaI	7.26	19.5	3.035	2.62	0.90	0.72	1.14
KF	5.46	18.9	6.58	5.42	1.49	1.28	2.23
KCl	4.87	7.74	4.08	4.34	0.69	0.635	0.98
KBr	4.91	7.37	3.49	4.14	0.58	0.51	0.80
KI	5.10	8.81	2.775	3.12	0.47	0.38	0.64
RbF	6.48	11.3	5.7	6.11	1.25	0.91	1.86
RbCl	4.92	1.34	3.645	4.65	0.61	0.475	0.78
RbBr	4.87	6.55	3.185	3.79	0.48	0.385	0.65
RbI	4.94	6.99	2.585	3.30	0.375	0.281	0.51
CsF	7.09	1.53

a. Martin D. H. 1965 *Advances in Phys.* 14, 39.

b. Spangenberg K. & Haussuhl S. 1957 *Z. Krist.* 109, 422.

Lastly, we consider the elastic constants. The general expressions for the elastic constants have been given by Cowley (1962) and they depend on the crystal structure. Thus, for the NaCl-type crystals,

$$C_{11} = \frac{e^2}{v r_0} \left[\frac{1}{2} (A + A' + A'' + B' + B'') - 2.55604 \right] \quad (10)$$

and

$$C_{12} = C_{44} = \frac{e^2}{v r_0} \left[\frac{1}{4} (A' + A'' - B' - B'') + 0.6955 \right] \quad (11)$$

in which

$$\left. \begin{aligned} A &= \frac{2v}{e^2} v_{12}''(r_0), \quad B = \frac{2v}{e^2 r_0} v_{12}'(r_0), \quad A' = \frac{2v}{e^2} v_{11}' 2^{1/2}(r_0) \\ B' &= \frac{2^{1/2}}{e^2 r_0} v_{11}' 2^{1/2}(r_0), \quad A'' = \frac{2v}{e^2} v_{22}'' 2^{1/2}(r_0) \\ \text{and } B'' &= \dots \dots \dots \frac{2^{1/2} v}{e^2 r_0} v_{22}' 2^{1/2}(r_0). \end{aligned} \right\} \quad (12)$$

The application of these equations to the potential of equation (1) is straightforward. Calculated values of C_{11} , C_{12} and C_{44} are to be found in table 2 together with experimental data.

DISCUSSION

We now critically examine the different calculated properties reported in tables 1 and 2 with reference to corresponding experimental data. The reproduction of ϵ is in general not very satisfactory. The calculated values of γ exhibit the same trend as ϵ , in accordance with our expectation.

It may be noted that the method based on equation (8) leads to values which are always greater than those obtained on the basis of equation (6). The relative superiority of the simple equation (6) can be gauged from the fact that it yields theoretical values which agree within the average absolute deviation of 10.5% only in contrast to 30.5% for equation (8).

The method suggested here for the calculation of dielectric constant is rather discouraging. In particular, the values for lithium halides are negative. This failure is to be ascribed to the crude nature of the dielectric theory employed, rather than to the form of the interaction potential given by equation (1). It is therefore desirable to employ more advanced formulations of dielectric theories such as of Szigeti (1949, 50) and of Dick & Overhauser (1958). We have worked on these theories and the results are published elsewhere.

The reproduction of elastic constants from equation (11), though not excellent, may be reasonably well. Indeed any simpler theory of this type is not likely to succeed satisfactorily for the description of elastic constants, for it has to predict the non-equivalence of C_{12} and C_{44} and then explain the difference quantitatively. It may be pointed out that this inequality in the elastic constants results from the assumption of non-central forces (Cowley 1962). Woods *et al* (1960), and Cowley *et al* (1963) have achieved good success by adopting such an approach for NaI and KBr. Considerable success has also been achieved by Dick (1963) to explain the difference between C_{12} and C_{44} by the shell model due to Dick & Overhauser (1958).

REFERENCES

- Born M. & Huang K. 1956 *Dynamical Theory of Crystal Lattices*, Clarendon Press, Oxford.
- Born M. & Mayer J. E. 1932 *Z. Physik* **75**, 1.
- Cowley R. A. 1962 *Proc. Roy. Soc. (London)* **A268**, 121.
- Cowley R. A. Cochran W. Brockhouse B. N. & Woods A. D. B. 1963 *Phys. Rev.* **131**, 1030.
- Cubicciotti D. 1959 *J. Chem. Phys.* **31**, 1646.
- Dick B. G. 1963 *Phys. Rev.* **129**, 1583.
- Dick B. G. & Overhauser A. W. 1958 *Phys. Rev.* **112**, 90.
- Fumi F. G. & Tosi M. P. 1964 *J. Phys. Chem. Solids* **25**, 31.
- Huggins M. L. 1937 *J. Chem. Phys.* **5**, 143.
- Huggins M. L. & Mayer J. E. 1933 *J. Chem. Phys.* **1**, 643.
- Kachhava C. M. & Saxena S. C. 1966a *Indian J. Phys.* **40**, 273.
- 1966b *Indian J. Phys.* **40**, 225.
- Kellermann E. W. 1940 *Phil. Trans. Roy. Soc.* **238**, 513.
- Krishnan K. S. & Roy S. K. 1952 *Proc. Roy. Soc. A* **210**, 481.
- Mott N. F. & Gurney R. W. 1948 *Electronic Processes in Ionic Crystals*, Clarendon Press, Oxford.
- Szigeti B. 1949 *Trans. Faraday Soc.* **45**, 155.
- Szigeti B. 1950 *Proc. Roy. Soc. A* **204**, 51.
- Tosi M. P. & Fumi F. G. 1964 *J. Phys. Chem. Solids* **25**, 45.
- Woods A. D. B., Cochran W. & Brockhouse B. N. 1960 *Phys. Rev.* **119**, 980.

Surface conductivity of freshly cleaved mica

By R. N. DHAR

National Physical Laboratory, New Delhi-12

(Received 18 March 1969 — Revised 7 November 1969)

The surface conductivity of freshly cleaved muscovite and phlogopite micas has been determined at room temperature. It has been observed that freshly cleaved mica has higher conductivity than unsplit mica.

INTRODUCTION

From their crystallographic study Metsik & Zhidikhanov (1958) have shown the presence of partly bound water molecules in the interblock layer of muscovite crystal through which contact between individual blocks is established at a number of points. On splitting the mica crystals along their cleavage planes, separation of heterogeneous particles occur, and the surfaces become electrified (Metsik 1959-60). The freshly split mica specimen may thus be regarded as a composite dielectric consisting of the mica specimen and a charged layer of partly bound water molecules. In an earlier communication (Dhar 1966) it has been reported that the presence of partly bound layer of water molecules on the surface of freshly split muscovite mica was responsible for the increase of its dissipation factor over that of unsplit muscovite mica.

When a solid insulating material is stressed by a steady electrical potential, there is flow of leakage conduction current not only throughout its volume but also along its surfaces. Semenov & Chirkov (1946) and Chirkov (1947) have observed that the surface conduction in mica is due to flow of current through a film of moisture adsorbed or other conducting material present on the surface of mica. Presence of layer of partly bound water molecules on the surface of freshly split mica may be expected to have some effect on the surface conduction in mica. This communication reports the finding of some observations on the surface conductivity of freshly cleaved muscovite and phlogopite micas.

EXPERIMENTAL

Megohmmeter (Model RM 160) of British Physical Laboratories was used for measurement of surface conductivity of mica. Accuracy of measurement was within 6%. Electrode system employed was similar to that described by Lacoste (1965). Highly polished brass electrodes were used to ensure intimate contact with test specimen. The surface conductance was measured between two parallel blocks of brass

electrodes placed on the surface of the test specimen at a gap of 25 mm. The low potential electrode was the guarded electrode. In order to concentrate the field near the surface, we placed an electrode on the other side of the sample and it was connected with the guard electrode. The electric stress applied was 500 volts d.c. All measurements were made at room temperature, $30 \pm 1^\circ\text{C}$, and relative humidity 25 to 30%.

After the electrical measurement was over, the thickness of the sample was determined with a micrometer correct to ± 0.001 mm.

The surface conductivity was calculated from the following formula

$$\sigma_s = G_s \cdot \frac{g}{b}$$

where

σ_s is the surface conductivity in mho, G_s conductance in mho, g the distance between electrodes is in cm and b the breadth of the electrode is also in cm.

RESULTS AND DISCUSSION

The surface conductivities of a few unsplit mica samples have been presented in table 1. (These samples were dried in a desiccator for 48 hours before any measurement taken on them). This shows that in the experimental technique adopted the thickness of the test specimen had but little effect on the surface conductivity. In table 2 are given the results of the surface conductivity of muscovite and phlogopite mica immediately after splitting to different thicknesses. It is observed that the surface conductivity of the split mica is much greater than unsplit mica. The systematic variation in surface conductivity with thickness indicates that the contribution of volume effect could not be totally eliminated. From table 1 it is seen, however, that the effect of thickness is not

TABLE 1. SURFACE CONDUCTIVITY OF
UNPLIT MICA

Sample	Thickness mm	Surface conductivity mho
Muscovite	0.958	8.00×10^{-14}
Mica	0.432	8.00×10^{-14}
	0.216	8.70×10^{-14}
	0.178	9.00×10^{-14}
Phlogopite	0.889	4.00×10^{-13}
Mica	0.140	5.97×10^{-13}

TABLE 2. SURFACE CONDUCTIVITY OF
FRESHLY SPLIT MICA

Sample	Thickness mm	Surface conductivity mho
Ruby Muscovite		
Before splitting	0.254	8.00×10^{-14}
After splitting	0.165	1.00×10^{-11}
	0.102	4.76×10^{-11}
	0.076	6.70×10^{-11}
	0.051	8.33×10^{-11}
Phlogopite Mica		
Before splitting	0.148	5.97×10^{-13}
After splitting	0.089	1.40×10^{-12}
	0.076	1.30×10^{-12}
	0.061	4.24×10^{-11}

so much as to decrease surface conductivity by decades as observed for freshly split mica specimens.

The increase in surface conductivity of mica on splitting indicates the presence of some conducting layer on their surface. From Metšik's (1959-60) observation we know that partly bound water molecules are present on the surface of freshly split mica. These water molecules might be responsible for the increase in surface conductivity. They have also been found earlier (Dhar 1966) to increase the dissipation factor of freshly split muscovite mica.

Table 3 shows the results of the surface conductivity of a few mica immediately after splitting and drying for 24 hours in a desiccator.

TABLE 3. EFFECT OF STORING ON SURFACE
CONDUCTIVITY OF FRESHLY SPLIT MICA

Sample	Surface conductivity mho		
	Before splitting	Immediately after splitting	24 hours after splitting
Ruby Muscovite	8.70×10^{-14} (0.216)	1.56×10^{-11} (0.076)	1.56×10^{-12} (0.076)
Green Muscovite	8.00×10^{-14} (0.432)	2.86×10^{-11} (0.089)	1.12×10^{-11} (0.089)
Phlogopite	6.00×10^{-11} (0.140)	1.37×10^{-10} (0.064)	2.30×10^{-12} (0.064)

Figures within brackets in tables 3 and 5 indicate thickness of the sample in mm.

It is observed that drying in a desiccator decreases the surface conductivity. Similar decrease in dissipation factor on storing as well as drying freshly split muscovite mica has been observed earlier (Dhar 1966). As explained earlier evaporation of the surface moisture during storage as well as leakage of charge over the surfaces might be responsible for the change.

The presence of a fluid medium on the surface of a freshly split mica is corroborated from the results reported in table 4, which des-

TABLE 4. FLASHOVER VOLTAGE OF
FRESHLY SPLIT MICA

Sample	Thickness mm	Flashover voltage kv
Ruby Muscovite		
Before splitting	0.700	9.5
After splitting	0.140	6.1
Green Ruscovite		
Before splitting	0.597	8.0
After splitting	0.127	6.0

cribes the average voltage flashover at 50 cps of freshly split mica for a surface spacing gap of 25 mm. The flashover voltage is affected by the nature of the solid surface ; particularly the presence of moisture on the surface decreases the flashover voltage.

A few mica samples were heated at 130°C for 24 hours, dried in a desiccator for the same period and then the surface conductivity was determined. The mica sample was then split and the surface conductivity redetermined. The results reported in table 5 show that the

TABLE 5. EFFECT OF INITIAL HEATING
ON SURFACE CONDUCTIVITY OF
FRESHLY SPLIT MICA

Sample	Surface conductivity mho	
	Before splitting	After splitting
Ruby Muscovite	9.04×10^{-14} (0.292)	3.89×10^{-11} (0.102)
Green Muscovite	1.72×10^{-12} (0.798)	1.34×10^{-11} (0.190)
Phlogopite	1.80×10^{-12} (0.535)	1.15×10^{-11} (0.064)

initial heating of mica before splitting did not affect the surface conductivity on splitting. In other words, interlaminar moisture could not be expelled on heating the mica sample at 130°C.

The surface conductivity, σ_s , is related to the volume conductivity, σ_v , of the surface layer by the relation

$$\sigma_s = \sigma_v \cdot t \text{ (McIlhagger \& Salthouse 1965).}$$

Where t is the thickness of the layer. The volume conductivity of water is about 10^{-8} mho cm^{-1} and the surface conductivity of freshly split mica is of the order of 10^{-11} mho. This gives a layer thickness of the order of 1000 Å or about 350 molecular layer of water on the surface of freshly split mica. But a film of this thickness is unreasonable (Yager & Morgan 1931). To bring the film thickness to a reasonable level, the volume conductivity of film should be much higher than 10^{-8} mho cm^{-1} . This is possible if the film is charged and it is then compatible with the observation of Metsik that there are electrically charged areas on the surface of a freshly cleaved mica.

The author expresses his grateful thanks to Shri R. K. Tandan, Scientist-In-Charge, Division of Electricity, National Physical Laboratory, New Delhi, for keen interest and helpful discussion.

REFERENCES

- Chirkov N. M. 1947 *Zh. Fiz. Khim.* **21**, 1303.
Dhar R. N. 1966 *Nature* **210** (5041), 1144.
Lacoste R. 1959 *C. R. Acad. Sci.* **248**, 655.
McIlhagger D. S. & Salthouse E. C. 1965 *Proc. I.E.E.* **112**, 1468.
Metsik M. S. & Zhudikhanov R. A. 1958 *Kristallografiya* **3**, 9995.
Metsik M. S. 1959-50 *Sov. Phys. Sol. State* **1**, 9910.
Semenov N. N. & Chirkov N. M. 1946 *CR Acad. Sci. URSS* **51**, 39.
Yager W. A. & Morgan S. O. 1931 *J. Phys. Chem.* **35**, 2026.

On the ultraviolet band system of silicon monoxide

By JAGADISH SINGH, K. N. UPADHYA AND K. P. R. NAIR

Department of Spectroscopy, Banaras Hindu University, Varanasi. 5

(Received 9 August 1968—Revised 24 July, 23 September

and 20 November 1969)

PLATE 9

The ultraviolet bands of SiO have been obtained in transformer discharge and the rotational analyses of (0,0), (2,0), (3,0), (4,0), (4,1) and (5,1) bands have been done from plates taken on the third order of a 10.6 meter concave grating spectrograph. The molecular constants derived are as follows :

$$B_e'' = 0.7271 \text{ cm}^{-1}$$

$$B_e' = 0.6305 \text{ cm}^{-1}$$

$$r_e'' = 1.508 \text{ \AA}$$

$$r_e' = 1.619 \text{ \AA}$$

In addition several perturbations have been obtained in the upper state.

INTRODUCTION

The rotational analysis of the ultraviolet band system of silicon monoxide lying in the region $2000\text{\AA} - 3000\text{\AA}$ was done by Saper (1932) and the transition involved was found to be a ${}^2\Pi - {}^1\Sigma^+$ type transition analogous to the fourth positive system in CO molecule. He had also observed perturbations in the upper state, but his analysis was limited only to $v' = 0$ and 1 levels. Later Lagerqvist & Uhler (1953) analysed seven bands and obtained perturbations in the $v' = 2$ level also. However, they did not analyse bands involving higher vibrational levels in the upper state. Hence it was thought desirable to extend the analysis to bands involving higher vibrational levels in the upper state and to investigate the perturbations in those levels. Previous workers obtained the spectrum from an arc source and photographed the spectra on a 21 ft concave grating spectro-graph. They have also discussed in detail the nature of perturbing states and their constants. We have now succeeded in getting the bands with higher vibrational levels in the upper state and a number of perturbations in the different vibrational levels of the upper electronic states have been detected.

EXPERIMENTAL

The bands were obtained in a π -type discharge tube through the flowing vapour of SiCl_4 . Under this condition the bands due to SiO molecule are developed well and hence other possible sources were not attempted. The bands were photographed in the third order of the 10.6 meter concave grating spectrograph with a disperson of 0.23 \AA/mm . Iron arc spectrum was used as the comparison spectrum. A chlorine gas filter

was used to cut off the second order spectra. Exposure of nearly 10 hours was sufficient to photograph the spectra with good intensity. The (0,0), (2,0), (3,0), (4,0), (4,1) and (5,1) bands were measured and analysed. The (2,0) band was included since new perturbations were detected.

ROTATIONAL ANALYSIS

The bands show three series of lines with an intense Q branch showing a transition of the type ${}^1\Sigma^+ - {}^1\Sigma^+$ (figure 1). In (4,1) band only two series of lines are observed in which the series are supposed to be Q and R branch. Such cases are also observed by Lagerqvist in the cases of (1,1) and (0,4) bands. Combination differences were obtained with bands having common lower vibrational levels. The rotational constants for these levels were obtained by plotting $\Delta_2 F(J)/(J + \frac{1}{2})$ versus $(J + \frac{1}{2})^2$ as given by Herzberg (1950). For common levels mean $\Delta_2 F(J)$ values were taken. The constants for the upper perturbed levels were determined from the ΔB values obtained from the graphs,

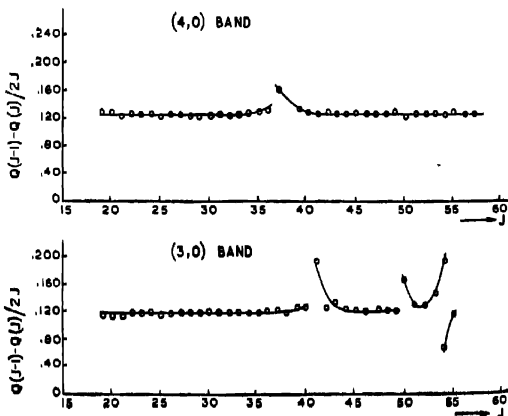
$$Q(J) = \nu_0 + (B_v' - B_v'')J(J+1) \quad (1)$$

$$\text{and} \quad R(J-1) + P(J) = 2\nu_0 + 2(B_v' - B_v'')J^2 \quad (2)$$

ΔB values were also obtained from the graphical relations

$$\frac{R(J-2) - R(J-1) + P(J) - P(J+1)}{4J} = B'' - B_v'' + 6D'' - 2J^2(D'' - D') \quad (3)$$

$$\text{and} \quad \frac{Q(J-1) - Q(J)}{2J} = B'' - B_v'' - 2J^2(D'' - D'), \quad (4)$$



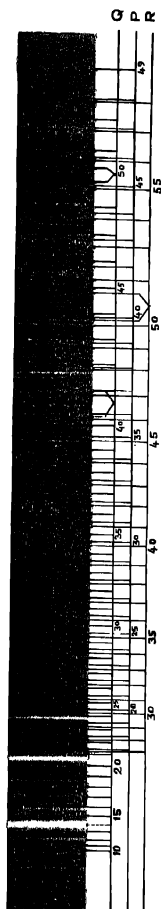


Figure 1. 3.0 Band



the intercept of the graph at $J = 0$ giving the ΔB value (Gerö 1935). The analysis and the J assignments of the individual lines are given in table 1.

TABLE 1.
(2,0) band

J	$Q(J)$	$P(J)$	$R(J)$	J	$Q(J)$	$P(J)$	$R(J)$
5	44306.19			36	60.57	14.92	06.81
6	04.19			37	52.22	10.24 } 03.73 }	199.0
7	02.54	44292.71		38	43.59	098.40	91.32
8	00.34	89.94		39	34.86	87.74	83.62
9	297.67	86.51		40	25.92	77.75	76.92
10	95.42	83.09		41	16.69	67.42	68.24
11	92.71	79.37		42	07.33	56.87	59.79
12	89.94	75.33		43	097.60	45.92	51.31
13	87.37	71.09		44	87.74	34.85	42.65
14	84.15	66.88		45	77.75	23.39	33.71
15	80.92	62.33		46	67.42	11.87	24.73
16	77.24	57.61	44298.14	47	56.87	00.02	14.92
17	73.57	52.72	95.42	48	45.92	43988.00	05.63
18	69.59	47.76	92.71	49	34.85	75.61	095.93
19	65.33	42.47	89.94	50	23.39	63.32	85.64
20	60.94	36.67	86.51	51	11.87	50.52	75.65
21	56.26	30.67	83.09	52	00.02	37.64	64.94
22	51.34	24.41	79.37	53	43988.02	24.49	55.10
23	46.29	17.88	75.33	54	75.61	11.24	43.19
24	40.88	11.38	71.09	55	61.62	97.49	32.02
25	35.12	04.41	69.59 } 66.88 }	56	56.05 } 43.80 }	83.72	20.36
26	29.41	197.21	63.86	57	40.84	69.74	08.87
27	23.25	91.33 } 89.19 }	58.85	58	26.88	54.86	43996.82
28	17.02	83.62	53.61	59	13.23	41.11	84.71
29	10.09	76.10	47.76	60	899.40	25.85	—
30	03.92	63.24	42.47	61	85.97	10.87	59.35
31	197.21	59.79	36.57	62	71.33	—	46.16
32	94.26	51.10	36.37	63	56.77		32.64
33	85.12	42.65	24.41	64	41.11		
34	76.17	33.71	17.88	65	25.85		
35	68.76	24.76	15.78 } 09.23 }				

TABLE 1. (Continued)
(3,0) band

J	$Q(J)$	$P(J)$	$R(J)$	J	$Q(J)$	$P(J)$	$R(J)$
9	45112.2			38	47.82	02.71	44995.58
10	09.94			39	37.98	892.20	87.36
11	07.20			40	27.83	81.56	79.02
12	04.86			41	21.97 } 12.67 }	70.76	70.65
13	01.17		45119.12	42	12.67	59.57	61.97
14	—	45080.98	17.05	43	01.33	47.94	52.92
15	094.68	76.61	14.14	44	890.61	36.59	43.52
16	90.76	—	—	45	79.69	24.80	34.09
17	86.75	66.10	08.58	46	68.69	12.54	25.16
18	82.42	59.69	04.50	47	57.42	00.31	14.87
19	78.01	54.91	02.37	48	45.86	787.53	03.76
20	73.04	49.29	098.84	49	34.04	74.75	894.20
21	68.56	43.14	94.78	50	23.16 } 17.16 }	61.36	85.37
22	63.28	36.65	90.76	51	09.69	48.35	82.47 } 70.76 }
23	57.82	30.02	86.85	52	796.44	34.50	53.51
24	52.05	23.30	82.42	53	94.51 } 81.01 }	32.66 } 19.83 }	41.42
25	46.37	16.33	78.01	54	73.73	698.58	26.46
26	40.24	08.87	73.40	55	61.36	83.70	14.35
27	33.89	01.09	68.56	56		66.81	01.62
28	27.26	44993.76	63.28	57		52.00	789.51
29	20.48	85.50	56.72	58		36.01	75.77
30	13.39	77.20	50.81	59			63.88
31	05.99	68.87	44.73				
32	44998.42	60.13	38.60				
33	90.68	51.00	31.72				
34	82.75	41.82	25.01				
35	74.39	32.57	18.07				
36	65.75	22.98	10.72				
37	56.78	13.67	03.06				

TABLE 1 (Continued)
(4,0) band

<i>J</i>	<i>Q(J)</i>	<i>P(J)</i>	<i>R(J)</i>	<i>J</i>	<i>Q(J)</i>	<i>P(J)</i>	<i>R(J)</i>
3		45919.63		34	76.95	36.27	18.26
4		17.81		35	67.86	26.24	11.05
5	45921.00	15.25		36	58.24	15.77	03.28
6	19.63	12.53	45928.16	37	50.43 } 46.33 }	04.67	795.26
7	17.81	09.44	27.61	38	42.46	695.41	86.98
8	15.83	06.41	26.82	39	31.95	84.45	78.45
9	13.60	03.20	25.77	40	21.62	74.46	68.84
10	11.43	899.24	24.61	41	11.19	62.52	61.74
11	08.33	95.34	22.64	42	01.37	51.37	51.39
12	05.16	91.11	21.00	43	690.55	39.41	41.45
13	01.85	86.77	19.10	44	79.38	26.60	32.42
14	898.27	81.78	16.82	45	67.85	14.28	22.92
15	94.08	77.19	14.34	46	56.44	02.56	12.09
16	90.77	71.99	11.43	47	44.58	588.90	01.37
17	86.50	66.46	08.33	48	32.54	75.97	690.55
18	82.11	60.71	05.85	49	19.88	63.08	79.38
19	78.26	55.01	01.85	50	07.64	48.07	68.00
20	73.15	49.14	898.27	51	594.81	32.87	56.44
21	68.01	42.25	94.82	52	81.63	19.93	44.58
22	62.46	35.61	89.51	53	68.35		32.54
23	56.70	28.74	84.82	54	54.84		19.88
24	50.64	21.68	80.24	55	40.79		07.64
25	44.46	14.27	75.28	56	26.77	594.81	
26	37.94	06.76	70.14	57	12.45		81.63
27	31.24	798.07	64.56	58			68.35
28	24.29	90.35	58.66	59			54.84
29	17.13	81.75	52.62	60			40.79
30	09.65	73.23	46.41	61			26.77
31	01.82	64.46	39.83	62			12.45
32	793.92	55.40	32.90				
33	85.59	46.33	25.53				

TABLE 1. (continued)

(4,1) band			(5,1) band			
<i>J</i>	<i>Q</i> (<i>J</i>)	<i>R</i> (<i>J</i>)	<i>J</i>	<i>Q</i> (<i>J</i>)	<i>P</i> (<i>J</i>)	<i>R</i> (<i>J</i>)
18	44656.98		16		45432.74	
19	50.97		17		27.45	
20	46.16	44670.50	18		21.59	
21	41.10	66.30	19		15.59	
22	35.86	62.95	20		08.97	45458.00
23	30.38	58.77	21	45428.49	03.34	54.04
24	24.60	54.06	22	22.46	396.38	49.63
25	18.56	49.23	23	16.72	89.61	44.49
26	12.37	44.17	24	09.96	82.33	40.22
27	06.00	38.93	25	04.48	74.22	34.93
28	599.04	33.67	26	397.84	66.94	29.40
29	92.24	27.79	27	90.87	58.85	23.89
30	85.04	21.99	28	83.84	50.51	18.00
31	77.57	15.60	29	70.47	41.73	11.77
32	70.03	09.13	30	68.75	33.36	05.69
33	61.97	02.28	31	61.13	24.38	398.95
34	53.61	595.24	32	53.29	15.16	92.04
35	44.99	88.26	33	44.61	05.61	85.12
36	35.65	81.09	34	36.20	295.82	77.43
37	31.62 } 22.18 }	73.15	35	27.42	85.93	69.86
			36	18.34	75.55	62.13
38	20.40	65.54	37	08.81	65.00	53.29
39	10.31	57.44	38	299.14	54.32	44.81
40	00.26	48.88	39	88.80	43.10	36.20
41	493.03 } 90.16 }	40.21	40	79.29	31.63	27.42
			41	68.95	20.65	18.34
42	80.98	31.62	42	58.21	08.49	08.81
43	70.35	28.32 } 25.65 }	43	47.38	196.69	299.14
			44	36.26	84.07	88.80
44	59.56	14.94	45	24.62	71.76	78.57
45	49.86	04.74	46	12.96	58.64	68.07
46	37.78	494.89	47	01.07	45.47	57.25
47	26.29	84.50	48	188.75	31.89	46.25
48	14.90		49	76.27		35.38
			50	63.29		23.80
			51	49.83		
			52	35.89		

The equality of combination differences $\Delta_2 F''(J)$ obtained for $v' = 0$ level from different bands are collected in table 2 and the rotational constants

TABLE 2

Combination differences for bands having the same lower state $v'' = 0$

$$\Delta_2 F''(J) = R(J-1) - P(J+1)$$

J	(0,0) band	(2,0) band	(3,0) band	(4,0) band	J	(0,0) band	(2,0) band	(3,0) band	(4,0) band
7				21.75	36	105.52	105.52	104.40	106.38
8				24.59	37	108.44	108.41	108.01	107.87
9				27.48	38	111.57	111.27	110.86	110.86
10				30.43	39	113.70	113.57	114.02	112.52
11	33.35			33.50	40	116.40	116.20	116.60	115.93
12	36.80			35.87	41	119.93	119.23	119.45	119.47
13	39.69			39.22	42	122.75	122.32	122.71	122.33
14	41.75			42.00	43	125.28	124.94	125.38	124.70*
15	44.58			44.83	44	128.34	127.92	128.12	127.17*
16	47.94			47.88	45	131.46	130.78	130.98	129.86*
17	50.34	50.38		50.72	46	134.11	133.69	133.78	130.17*
18	53.66	52.95	53.67	53.32	47	136.83	136.71	137.63	135.67*
19	56.19	56.04		56.02	48	139.92	139.31	140.12	138.29*
20	58.48	59.27	59.23	59.60	49	142.17	142.31	142.40	142.48*
21	62.19	62.10		62.66	50	145.34	145.41	145.85	146.51
22	65.16	66.21	64.66	66.08	51	147.97	148.00	147.97	148.07
23	68.01	67.91	67.46	67.83	52	150.83	151.16	150.76	
24	70.86	70.92	70.42	70.55	53	153.87	153.70	154.93	
25	73.64	73.88	73.55	73.48	54		157.61		
26	76.79	76.48	76.92	77.21	55		159.47		
27	79.59	80.24	79.64	79.79	56		162.28		
28	82.33	82.75	83.06	82.81	57		165.50		
29	85.65	85.37	86.08	85.43					
30	88.06	87.97	87.85	88.16					
31	90.86	91.16	90.68	91.01					
32	93.91	93.92	93.73	93.50					
33	96.68	96.96	96.78	96.63					
34	99.78	99.68	99.15	99.29					
35	102.57	102.96	102.03	102.49					

* Corresponding lines are very much diffused.

are collected in table 3. In the case of (4,1) band where only two series are detected the constant for the upper state was obtained by drawing $Q(J)$

TABLE 3. ROTATIONAL CONTENTS FOR THE
ULTRAVIOLET BANDS OF
SiO (in cm^{-1})

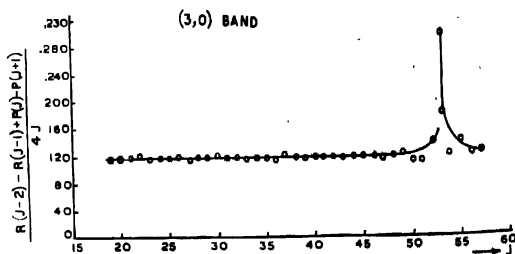
Band	$B''v$	$D''v \times 10^6$	$B'v$	v_0
0,0	0.7246	1.02	0.6271	42640.75
2,0	0.7246	1.02	0.6122	44308.75
3,0	0.7246	1.02	0.6062	45124.00
4,0	0.7246	1.02	0.6002	45925.00
4,1	0.7195	1.00	0.6002	44696.75
5,1	0.7195	1.00	0.5925	45487.50
$B''_e = 0.7271 \text{ cm}^{-1}$				$r''_e = 1.508 \text{ \AA}$
$B'_e = 0.6305 \text{ cm}^{-1}$				$r'_e = 1.619 \text{ \AA}$

against $J(J+1)$ the slope of which gives the ΔB value. The B'_e value was obtained from the B''_e value obtained from the analysis of (5,1) band. The Δ -type doubling in the upper $^1\pi$ state was obtained from the relation

$$[R(J - Q(J)) - [Q(J + 1) - P(J + 1)]] = 2p(J + 1)^2 \quad (5)$$

and the value obtained is $B^d - B^e = p = -7 \times 10^{-5} \text{ cm}^{-1}$.

A large number of perturbations in Q , R and P branches are observed. Perturbations were detected by using equations (3) and (4) and plotting the expressions on the left hand side against J (Lagerqvist & Uhler 1953, Lagerqvist *et al* 1958). The interesting feature is that perturbations are observed in Q as well as R and P branches at different J values which indicates that both the Δ levels of $^1\pi$ state are perturbed. The perturbation in some of the bands are represented in figure 2.



The authors wish to thank Prof. N L. Singh for his interest in the work and to Dr. D. K. Rai for valuable discussion. They are grateful to the National Bureau of Standards, U.S.A., and to the Council of Scientific and Industrial Research, India, for financial assistance.

REFERENCES

- Gerö, L. 1935 *Z. Physik* **93**, 669.
Herzberg, G. 1950 *Spectra of Diatomic Molecules*, D. Von Nostrand & Co. Inc., New York.
Lagerqvist, A. & Uhler, U. 1953 *Ark. For Fysik* **6**, 95.
Lagerqvist, A., Westerlund, H., Wright, C. V. & Burrow, R. F. 1958 *Ark. For. Fysik* **14**, 387.
Saper, P. 1932 *Phys. Rev.* **42**, 498.
Verma, R. D. 1961 *Can. J. Phys.* **39**, 908.

On the variational states and the ground state energy

By N. D. SEN GUPTA

Tata Institute of Fundamental Research, Bombay 5

(Received 8 October 1969)

The object of this paper is to show that the estimate of the ground state energy may be considerably improved with the help of another variational state. In addition to that used for the estimation of the ground state energy.

INTRODUCTION

In many applications of quantum mechanics to problems in physics and physical chemistry, use is made of variational states to determine approximately the ground state energy, as well as those of the neighbouring excited states; the corresponding expectation values, which are extremized, are taken as approximate eigen-values. A little critical examination reveals that if two or more variational states and the corresponding estimates of the eigen-values are known, in general, it is possible to obtain a much better estimate of the ground state energy. This is possible only because of the absolute minimum character of the ground state energy, which is the lowest eigen-value. The object of this paper is to show explicitly, how this can be done with the knowledge of two variational states and respective expectation values of the energy. This is accomplished by finding new variational states from the two known variational states which minimizes the expectation value of energy. As it is expected, in general, this further lowers the expectation value. The method can be easily extended to the case where more than two variational states are known.

In the following section the new variational states with a real parameter and the improved estimates of the expectation values are worked out. The next section is devoted to the algebraic significance of the method. It contains further discussions on the practical use and the possible generalization of the method. The paper is supplemented by an appendix in which the parameter introduced for the formation of the new variational state is no longer real. This does not change the basic nature of the result which is obtained with a real parameter, but further improves the estimate.

In short, it is shown here that in addition to the determination of the mutually orthogonal variational states for obtaining the ground state energy, a further restriction should be imposed that the Hamiltonian must be diagonalized in this subspace of the variational states. Since one of

the diagonal element is less than the previous determination of the ground state energy, it is a better estimate of the latter, because of the absolute minimum property of the ground state energy.

THE VARIATIONAL STATES AND THE ESTIMATE OF THE EIGEN-VALUES.

Let H be the total Hamiltonian of the system and let ϕ_1 be the solution of the variation problem

$$\text{with } \left. \begin{aligned} \tilde{(\phi, H\phi)} &= 0 \\ \tilde{(\phi, \phi)} &= 1, \end{aligned} \right\} \quad \dots(1)$$

$$\text{and let } \tilde{(\phi_1, H\phi_1)} = E_1 \quad \dots(2)$$

So that E_1 may be taken as an estimate of the ground state energy. Further, let ϕ_2 be another solution of equation (1) such that

$$\tilde{(\phi_2, \phi_1)} = 0 \quad \dots(3)$$

$$\text{and let } \tilde{(\phi_2, H\phi_2)} = E_2 \quad \dots(4)$$

Thus E_2 which is greater than E_1 may be taken as an estimate of the energy of some neighbouring state (not necessarily the adjacent one).

Let us consider the new variational state

$$\psi = (\phi_1 + \epsilon \phi_2) (1 + \epsilon^2)^{-\frac{1}{2}} \quad \dots(5)$$

which is a linear combination of ϕ_1 and ϕ_2 ; it is normalized to unity. In order to avoid unnecessary complications we take ϵ to be a real parameter. In the appendix it is shown that the estimate of energy is further improved by taking ϵ complex. Now

$$\tilde{(\psi, H\psi)} = (E_1 + 2\epsilon k + \epsilon^2 E_2) (1 + \epsilon^2)^{-1} \quad \dots(6)$$

$$\text{where } 2k = \tilde{(\phi_1, H\phi_2)} + \tilde{(\phi_2, H\phi_1)}. \quad \dots(7)$$

Since H is hermitian k is real, in general k is different from zero. In that case the expression (6), *qua* a function of ϵ , say $f(\epsilon)$, can be extremized. Since

$$\frac{df(\epsilon)}{d\epsilon} = \frac{2}{(1 + \epsilon^2)^2} \left\{ k(1 - \epsilon^2) + \epsilon(E_2 - E_1) \right\} \quad \dots(8)$$

the two extrema are given by

$$\epsilon_{\pm} = (E_2 - E_1 \pm \bar{E}) / 2k \quad \dots(9)$$

where

$$\bar{E} = | (E_2 - E_1)^2 + 4k^2 |^{\frac{1}{2}} \quad \dots(10)$$

$$\frac{d^2 f(\epsilon)}{d\epsilon^2} = \mp 2\bar{E} (1 + \epsilon_{\pm}^2)^{-\frac{3}{2}} \quad \dots(11)$$

Hence, at ϵ_+ it is maximum and at ϵ_- it is minimum. It is important to note that these extremum properties are independent of the sign of k . From the expression (6), the nature of $f(\epsilon)$ is now quite clear. Equations (9) and (10) show that $\epsilon_+ > 0$ and $\epsilon_- < 0$ when $k > 0$, otherwise when $k < 0$. So that when $k > 0$ as ϵ increases from $-\infty$, $f(\epsilon)$ decreases gradually from E_2 to a minimum at ϵ_- , then increases (passing through E_1 at $\epsilon = 0$) upto a maximum at ϵ_+ , further, it gradually decreases to E_2 as $\epsilon \rightarrow +\infty$. Hence, the minimum is less than E_1 . The nature of variation of $f(\epsilon)$ for $k < 0$ may be easily inferred from the fact that the expression (6) is invariant with simultaneous change of sign of k and ϵ . The expressions for f_{min} and f_{max} may be obtained easily as

$$f_{min} \equiv f(\epsilon_-) = E_1 - \frac{1}{2} \{ \bar{E} - (E_2 - E_1) \}, \quad \dots(12)$$

and

$$f_{max} \equiv f(\epsilon_+) = \bar{E}_2 + \frac{1}{2} \{ \bar{E} + (E_2 - E_1) \}. \quad \dots(13)$$

From expression (10) $\bar{E} > (E_2 - E_1)$, hence

$$f_{min} < E_1 \quad \text{and} \quad f_{max} > E_2. \quad \dots(14, 15)$$

The corresponding variational states are

for

$$f_{min} : \psi_- = (\phi_1 + \epsilon_- \phi_2)(1 + \epsilon_-^2)^{-\frac{1}{2}} \quad \dots(16)$$

for

$$f_{max} : \psi_+ = (\phi_1 + \epsilon_+ \phi_2)(1 + \epsilon_+^2)^{-\frac{1}{2}}. \quad \dots(17)$$

Further, they are again orthogonal, i.e.

$$(\psi_+ \cdot \psi_-) = 0. \quad \dots(18)$$

This follows from equations (9) and (10) in virtue of

$$\epsilon_+ \epsilon_- = -1. \quad \dots(19)$$

DISCUSSION

The expression (11) for f_{min} shows that the estimate of ground state energy is further lowered with the help of variational states ψ_- . Since the ground state energy is an absolute minimum this is a better estimation of the latter and from the expressions (10) and (12) this difference

increases with k . It is of interest to note that the method can not be repeated further with the new variational state ψ_- and ψ_+ , as

$$(\tilde{\psi}_+ \cdot H\psi_-) + (\tilde{\psi}_- \cdot H\psi_+) = 0. \quad \dots(20)$$

This follows from the fact that

$$(\tilde{\psi}_+ \cdot H\psi_-) = \frac{\hbar^2}{2k} \{(\tilde{\phi}_+ \cdot H\tilde{\phi}_-) - (\phi_+ H\phi_-)\} \quad \dots(21)$$

is purely imaginary and

$$(\tilde{\psi}_- \cdot H\psi_+) = (\tilde{\psi}_+ \cdot H\psi_-)^* \quad \dots(22)$$

It has already been indicated that the method is not useful when $k = 0$, as in this case the only solutions of equation (8) are $\epsilon = 0$ and $|\epsilon| \rightarrow \infty$, which lead to ϕ_1 and ϕ_2 for ψ_{\mp} .

As a matter of fact, in case of real variational states the method is equivalent to the diagonalization of H operator in the subspace of these two states. From this point of view the initial variational problem may be reformulated, such that in addition to equations (2) and (3),

$$(\tilde{\phi}_2 H \phi_1) = 0, \quad \dots(23)$$

i. e. the variational states should diagonalize H in this two-dimensional subspace of real ϕ 's. In general for complex ϕ 's, it is shown in the appendix that working with ϵ as a complex number equation (23) is still valid. The choice of new variation states in equation (5) is nothing other than to satisfy equation (20) or (24); hence, it cannot be further iterated.

Finally, the usefulness of the method in improving the estimates of the ground state energy is quite clear when one more variational state, in addition to that for the estimation of the ground state energy, is known. However, once the variational state for a tolerable estimate of the ground state energy is known, one can suitably choose another variational state in the usual manner, which satisfies equation (3). If this new state does not satisfy equation (24), ($k \neq 0$), i. e. H is not diagonalized in this two dimensional subspace, then the above method immediately yields an improved estimate of the ground state energy. It is evident from expression (12) that the magnitude of the extent of lowering of the ground state energy increase with k , i. e. the more the magnitude of the real part of the non-diagonal elements of H , in this subspace, in comparison to the difference of the diagonal elements, the better is the improvement for the estimation state energy.

Further, the method in principle may be extended to the case when more than two variational states are known initially. However, this will introduce complication in the computations. We refrain from doing that at this stage.

APPENDIX

As stated in section 2, let us consider the new variational state to be formed with a complex parameter. Thus, the new normalized variational state is

$$\psi = (\phi_1 + \epsilon \phi_2) (1 + \epsilon_0^2)^{-1/2} \quad \dots(A1)$$

$$\text{and } \langle \psi, H \psi \rangle = \{E_1 + \epsilon_0^2 E_2 + 2\epsilon_0 k_0 \cos(\theta + \eta)\} (1 + \epsilon_0^2)^{-1} \quad \dots(A2)$$

where $\epsilon = \epsilon_0 e^{i\theta}$ and $k_0 e^{i\eta} = \langle \tilde{\phi}_1, H \phi_2 \rangle$

$$\text{and } \epsilon \langle \tilde{\phi}_1, H \phi_2 \rangle + \epsilon^* \langle \tilde{\phi}_2, H \phi_1 \rangle = 2\epsilon_0 k_0 \cos(\theta + \eta). \quad \dots(A3)$$

The extrema of the expression (A2) *qua* a function $f(\epsilon, \theta)$ of two variables are obtained from the conditions

$$\frac{\partial f(\epsilon, \theta)}{\partial \epsilon} = 0, \quad \frac{\partial f(\epsilon, \theta)}{\partial \theta} = 0 \quad \dots(A4)$$

The extremum positions are given by the roots of the simultaneous equations

$$\left. \begin{aligned} & \{ \epsilon_0 (E_2 - E_1) + (1 - \epsilon_0^2) k_0 \cos(\theta + \eta) \} (1 + \epsilon_0^2)^{-2} = 0 \\ \text{and } & \epsilon_0 k_0 \sin(\theta + \eta) / (1 + \epsilon_0^2) = 0 \end{aligned} \right\} \quad \dots(A5)$$

The only solutions which are relevant to the problem are

$$\left. \begin{aligned} & \sin(\theta + \eta) = 0, \text{ i. e., } \cos(\theta + \eta) = \pm 1 \\ \text{and } & (1 - \epsilon_0^2) k_0 + \sigma \epsilon_{\pm} (E_2 - E_1) = 0 \end{aligned} \right\} \quad \dots(A6)$$

with $\sigma = \pm 1$, the roots of which are

$$\epsilon_{\pm} = \{ \sigma (E_2 - E_1) \pm \bar{E}_0 \} / 2k_0 \quad \dots(A8)$$

where $\bar{E}_0 = [\{ (E_2 - E_1)^2 + 4k_0^2 \}^{1/2}]$.

The other roots of equation (A5), namely (i) $\epsilon_0 = 0$ and $\cos(\theta_0 + \eta) = 0$ and (ii) $\epsilon_0 \rightarrow \infty$ leads asymptotically to values E_1 and E_2 respectively. for $f(\epsilon, \theta)$ as discussed in section 2.

In order that the extremum may be a minimum or a maximum, the quadratic form

$$\frac{\partial^2 f}{\partial \epsilon^2} (\Delta \epsilon)^2 + 2 \frac{\partial^2 f}{\partial \epsilon \partial \theta} \Delta \epsilon \Delta \theta + \frac{\partial^2 f}{\partial \theta^2} (\Delta \theta)^2$$

should be positive definite or negative definite at these points. Since

$$\left(\frac{\partial^2 f}{\partial \epsilon^2}\right)_{\theta_0, \epsilon_{\pm}} = -\frac{\sigma \bar{E}_0}{(1 + \epsilon_{\pm}^2)^2}, \quad \left(\frac{\partial^2 f}{\partial \epsilon \partial \theta}\right)_{\theta_0, \epsilon_{\pm}} = 0$$

$$\text{and} \quad \left(\frac{\partial^2 f}{\partial \theta^2}\right)_{\theta_0, \epsilon_{\pm}} = -\frac{2\sigma \epsilon_{\pm} k_0}{1 + \epsilon_{\pm}^2} \quad (\text{A } 9)$$

It follows that f is minimum at $\sigma = -1$, ϵ_+ and f is maximum at $\sigma = +1$, ϵ_+ . These values of f are given by

$$f_{min} = E_1 - \frac{1}{2}\{\bar{E}_0 - (E_0 - E_1)\} \quad \dots(\text{A}10)$$

$$f_{max} = E_2 - \frac{1}{2}\{\bar{E}_0 + (E_2 - E_1)\}. \quad \dots(\text{A}11)$$

Though they are exactly of the same form as given by equation (12) and (13), f_{min} in equation (A10) is in general less than f_{min} in equation (12). This is because in the expression (A8) for \bar{E}_0 , $k_0 \geq k$ as $k = k_0 \cos \eta$, from equation (7) and (A3). In this case also the two variational states corresponding to these extrema are orthogonal,

$$\langle \tilde{\psi}_+ \cdot \psi_- \rangle = 0 \quad \dots (12)$$

As before this is due to $\epsilon_+ \epsilon_- = -1$, which follows from the equation (A7). Thus the method of forming the new variational states is equivalent to the construction of states such that the Hamiltonian is diagonalized in this two dimensional subspace.

On Initial development of axisymmetric waves due to sources

By L. DEBNATH*

Department of Mathematics, Imperial College, University of London.

Received 3, October, 1969,

An initial value investigation into the linearised problem of axisymmetric wave motions in a fluid of finite and infinite depth generated by a harmonically oscillating three dimensional source is made in this paper. An asymptotic analysis of the problem is carried out in some detail for a clear understanding of the steady state and transient solutions. The limiting behaviour of the asymptotic solution as time tends to infinity is given due attention.

1. INTRODUCTION

In recent years, an initial value investigation into the linearised wave problems dealing with the generation of surface waves in a fluid with a free surface by harmonically oscillating pressure distributions on the free surface and sources beneath the free surface of the fluid, has received considerable attention by Stokes (1957), Miles (1962), Debnath (1967, 1969) and others. Debnath has explained the difficulties of the several methods developed independently by Lamb (1905, 1923, 1932), Lighthill (1960, 1964) and Thorne (1953) in connection with the steady state wave problems. He suggested various reasons in favour of the initial value approach with a special emphasis that the most rigorous way of deriving the unique solution of wave problems, without the need for any of the essentially physical assumptions of this methods stated above.

The primary aim of this paper is to investigate an initial value approach to the linearised problem of axisymmetric wave motions in a fluid of limited and unlimited depth produced by a harmonically oscillating point source situated at a finite depth below the undisturbed free surface of the fluid. An asymptotic analysis of the problem is carried out in some detail for a clear understanding of the steady state and transient solutions. The limiting behaviour of the asymptotic solution as time tends to infinity has also been examined.

Thorne has considered the corresponding steady state problem and obtained a solution of physical interest by imposing the radiation condition at infinity. This solution is obtained as a limiting case of the initial value problem considered here.

2. MATHEMATICAL FORMULATION OF THE PROBLEM

We consider linearised problem of axisymmetric wave propagation in inviscid, incompressible and homogeneous fluid with a free surface

*Present Address—Department of Mathematics, East Carolina University, Greenville, North Carolina, USA.

(initially at rest) due to a harmonically oscillating point source of fixed frequency ω .

We fix the origin of co-ordinates at the source at a depth \bar{D} , below the undisturbed free surface of the fluid and take $X-Z$ plane to be horizontal passing through the origin and Y -axis vertical positive upward. We choose the cylindrical polar co-ordinates (R, θ, Y) and assume the cylindrical symmetry about the Y -axis such that R is equal to $\sqrt{X^2 + Z^2}$.

As the motion is irrotational, there exists a wave potential $\Phi(R, Y, T)$ which satisfies the Laplace equation

$$\Phi_{RR} + \frac{1}{R} \Phi_R + \Phi_{YY} = 0 \quad \dots (2.1)$$

$$0 \leq R < \infty, \quad \bar{D} \leq Y \leq \bar{D} + h$$

everywhere within the fluid of depth h except at the source at $(0, 0)$.

At $R = 0, Y = 0$, Φ has the form

$$\left. \begin{aligned} &= m M(R_1) e^{i\omega T} \\ &= m M(R, Y) e^{i\omega T} \end{aligned} \right\} T \geq 0, \quad \dots (2.2)$$

where m denotes the strength of the source with the frequency ω and $R_1^2 = R^2 + Y^2$.

The boundary conditions are given by

$$\Phi_T + gE = 0 \quad (2.3) \quad \left. \vphantom{\begin{matrix} \Phi_T + gE = 0 \\ \Phi_T = E_T \end{matrix}} \right\} Y = \bar{D}$$

$$\Phi_T = E_T \quad (2.4) \quad \left. \vphantom{\begin{matrix} \Phi_T + gE = 0 \\ \Phi_T = E_T \end{matrix}} \right\} T > 0$$

where, $E = E(R, T)$ represents the free surface elevation at a distance R and at time T , and g the gravitational acceleration.

The condition at the bottom boundary is given by

$$\Phi_T = 0 \quad \text{at} \quad Y = -(\bar{D} + h) \quad \dots (2.5)$$

The initial conditions are given by

$$E(R, T) = 0, \quad \text{everywhere at} \quad T = 0 \quad \dots (2.6)$$

$$\left. \begin{aligned} &\Phi = 0, \quad \text{everywhere except at} \quad (0, 0) \\ &\quad \quad \quad \text{at time} \quad T = 0 \\ &\Phi = m M(R_1) e^{i\omega T} \quad \text{at} \quad (0, 0), T \geq 0 \end{aligned} \right\} \quad \dots (2.7)$$

which are equivalent to

$$\Phi = m M(R_1) \delta(R) e^{i\omega T}, \quad T \geq 0 \quad \dots (2.7)$$

We complete the formulation of the initial value problem with a three dimensional source together with the further assumption that the functions Φ and E possess the Hankel transform with respect to R .

Remarks. The formulation of the corresponding axisymmetric wave problem as a steady state considered by Thorne can be obtained from that of the initial value problem stated above, just by omitting the initial conditions (2.6) – (2.7). Thorne investigated the steady state problem and obtained a solution of physical interest by imposing the radiation condition at infinity

3. FORMAL SOLUTION OF THE PROBLEM

For simplicity, we introduce non-dimensional variables $r, y, \bar{d}, t, r_1, \eta$ and $\tilde{\phi}$ defined by the relations

$$(r, y, \bar{d}, r_1) = \frac{\omega^3}{g} (R, Y, \bar{D}, R_1)$$

$$t = \omega T, \quad \phi = \frac{g}{m\omega^3} \Phi, \quad \eta = \frac{g^2 E}{m\omega^3},$$

and we introduce a non-dimensional parameter D by the relation.

$$D = \frac{\omega^3 h}{g}.$$

These relations enable us to rewrite the fundamental equations (2.1)–(2.7) into the form

$$\tilde{\phi}_{,rr} + \frac{1}{r} \tilde{\phi}_{,r} + \tilde{\phi}_{,yy} = 0 \quad \dots(3.1)$$

$$0 \leq r < \infty, \quad (\bar{d} - D) \leq y \leq \bar{d}$$

everywhere within the fluid except at $(0, 0)$. At $r = 0, y = 0, \tilde{\phi}$ has the form

$$\tilde{\phi} = M(r_1)e^{it} \quad t \geq 0 \quad \dots(3.2)$$

The boundary conditions reduce to

$$\left. \begin{aligned} \tilde{\phi}_r + \eta &= 0 & (3.3) \\ \tilde{\phi}_y &= \eta_1 & (3.4) \end{aligned} \right\} \quad y = \bar{d}, \quad t > 0$$

The condition at the bottom is then

$$\tilde{\phi}_y = 0 \quad \text{at} \quad y = \bar{d} - D \quad \dots(3.3)$$

The initial conditions are given by

$$\eta(r, t) = 0, \quad \text{everywhere at} \quad t = 0 \quad \dots(3.6)$$

$$\left. \begin{aligned} \tilde{\phi} &= 0 && \text{everywhere except at } (0, 0) \\ \tilde{\phi} &= e^{iu} M(r_1) && \text{at time } t = 0 \\ \tilde{\phi} &= e^{iu} M(r_1) && \text{at } (0, 0), t \geq 0 \end{aligned} \right\} \quad \dots(3.7)$$

which are equivalent to

$$\tilde{\phi} = M(r_1) \delta(r) e^{iu} \quad \text{at } t \geq 0 \quad \dots(3.8)$$

Now we introduce a bounded expression

$$\phi = \tilde{\phi} - e^{iu} M(r_1) \quad \dots(3.9)$$

for all r, y and t .

Making reference to this relation (3.9), equations (3.1) – (3.7) can further be put into the form

$$\phi_{,rr} + \frac{1}{r} \phi_{,r} + \phi_{,yy} = 0 \quad 0 \leq r < \alpha, \bar{d} - D \leq y \leq \bar{d} \quad \dots(3.10)$$

$$\phi_t + \eta = -ie^{iu} M(r_1) \quad (3.11) \quad y = \bar{d}$$

$$\phi_{,y} - \eta_t = -e^{iu} \frac{\partial}{\partial y} M(r_1) \quad (3.12) \quad t \geq 0$$

$$\phi_{,y} = -e^{iu} \frac{\partial}{\partial y} M(r_1) \quad \text{at } y = (\bar{d} - D) \quad \dots(3.13)$$

$$\eta = 0 \quad \text{everywhere at } t = 0 \quad \dots(3.14)$$

$$\left. \begin{aligned} \phi &= -e^{iu} M(r_1) && \text{everywhere except} \\ \phi &= 0 && \text{at } (0, 0) \text{ at } t = 0 \\ &&& \text{at } (0, 0) \quad t \geq 0 \end{aligned} \right\} \quad \dots(3.15)$$

We introduce the Laplace transforms $\bar{\phi}$, $\bar{\eta}$ of ϕ , η , respectively, with respect to t by the integral like

$$\bar{\phi} = \bar{\phi}(r, y; s) = \int_0^\infty e^{-st} \phi(r, y; t) dt$$

We next introduce the Hankel transforms $\bar{\bar{\phi}}$, $\bar{\bar{\eta}}$ of functions $\bar{\phi}$, $\bar{\eta}$, respectively, with respect to r by the integral like

$$\bar{\bar{\phi}} = \bar{\bar{\phi}}(k, y; s) = \int_0^\infty r J_0(kr) \bar{\phi}(r, y; s) dr$$

The joint Laplace and Hankel transforms enable us to transform equations (3.10)–(3.15) into their equivalent forms as

$$\bar{\bar{\phi}}_{,yy} = k^2 \bar{\bar{\phi}}; \quad 0 \leq k < \alpha, (\bar{d} - D) \leq y \leq \bar{d} \quad \dots(3.16)$$

$$\left. \begin{aligned} s \bar{\phi} + \bar{\eta} + \frac{s}{s-i} M_1 &= 0 & \dots (3.17) \\ \bar{\phi} y - s \bar{\eta} + \frac{M_2}{s-i} &= 0 & \dots (3.18) \end{aligned} \right\} \begin{aligned} y &= \bar{d} \\ s &> 0 \end{aligned}$$

where M_1, M_2 are given by the integrals

$$\left. \begin{aligned} M_1 &= M_1(k, \bar{d}) = \int_0^\infty r J_0(kr) M(r, \bar{d}) dr \\ M_2 &= M_2(k, \bar{d}) = \int_0^\infty r J_0(kr) \frac{\partial M}{\partial y}(r, \bar{d}) dr \end{aligned} \right\} \dots (3.19)$$

$$\bar{\phi}_y = -\frac{M_2(k, -y)}{(s-i)} \quad \text{at } y = (\bar{d} - D) \quad (3.20)$$

$$\bar{\eta} = 0 \text{ everywhere at } s = 0 \quad \dots (3.21)$$

$$\left. \begin{aligned} \bar{\phi} &= -\frac{M_1}{(s-i)} \text{ except at } k=0, y=0, s=0 \\ \bar{\phi} &= 0 \quad \text{at } (0, 0) \quad s \geq 0 \end{aligned} \right\} \dots (3.22)$$

The solution of equation (3.16) with the boundary conditions (3.17), (3.18) and (3.20) can be obtained in the form

$$\begin{aligned} \bar{\phi}(k, y; s) &= \frac{M_2(k, D - \bar{d})}{k(s-i)} e^{k(\bar{d}-y-D)} \\ &+ \left[M_2(k, D - \bar{d}) e^{-kD} \left(1 - \frac{s^2}{k} \right) - \left\{ M_2(k, \bar{d}) + s^2 M_1(k, \bar{d}) \right\} \right] \\ &+ \frac{\cosh k(y - \bar{d} + D)}{(s-i)(s^2 + \alpha^2) \cosh kD} \end{aligned} \quad \dots (3.23)$$

And the expression for $\bar{\eta}(k, s)$ is given by

$$\bar{\eta}(k, s) = \frac{s \left[M_2(k, \bar{d}) - \alpha^2 M_1(k, \bar{d}) - \left(1 + \frac{\alpha^2}{k} \right) M_2(k, D - \bar{d}) e^{-kD} \right]}{(s-i)(s + \alpha^2)} \quad \dots (3.24)$$

$$\alpha^2 = \alpha^2(k) = k \tanh kD \quad \dots (3.25)$$

Using the inversion theorem for the Laplace and Hankel transforms combined with the convolution theorem for the Laplace transform, we obtain the wave potential $\phi(r, y; t)$ in the form

$$\begin{aligned}
\phi(r, y; t) = & \int_0^{\infty} \left[M_2(k, D - \bar{d}) e^{k(D - y - D) + it} \right. \\
& + \frac{\cosh k(y - \bar{d} + D)}{(a^2 - 1) \cosh kD} \left\{ (k + a^2) \frac{e^{-kD}}{k} M_2(k, D - \bar{d}) \right. \\
& + \alpha^2 M_1(k, \bar{d}) - M_2(k, \bar{d}) \left. \right\} k e^{it} \\
& - \frac{\cosh k(y - \bar{d} + D)}{\cosh kD} \left\{ \frac{e^{-kD}}{k} M_2(k, D + \bar{d}) + M_1(k, \bar{d}) \right\} k e^{it} \\
& + \frac{\cosh k(y - \bar{d} + D)}{(a^2 - 1) \cosh kD} \left\{ \left(\frac{1}{a} + \frac{a}{k} \right) e^{-kD} M_2(k, D - \bar{d}) \right. \\
& + a M_1(k, \bar{d}) - \frac{M_2(k, \bar{d})}{a} \left. \right\} (i \sin at + a \cos at) \left. \right] J_0(kr) dk \quad \dots (3.26)
\end{aligned}$$

This is a general expression for the wave potential $\phi(r, y; t)$.

Similarly, we can derive the expression for the surface elevation $\eta(r, t)$ as

$$\begin{aligned}
\eta(r, t) = & \int_0^{\infty} \left[\left\{ M_2(k, \bar{d}) - \alpha^2 M_1(k, \bar{d}) \right. \right. \\
& - \left(1 + \frac{a^2}{k} \right) e^{-kD} M_2(k, D - \bar{d}) \left. \right\} i e^{it} \\
& + \left\{ M_2(k, \bar{d}) - \alpha^2 M_1(k, \bar{d}) - \left(1 + \frac{a^2}{k} \right) e^{-kD} M_2(k, D - \bar{d}) \right\} \\
& \left. (a \sin at - i \cos at) \right] k (a^2 - 1)^{-1} J_0(kr) dk \quad \dots (3.27)
\end{aligned}$$

This is a general integral representation for the surface elevation $\eta(r, t)$.

We next derive the integral form of the wave potential $\phi(r, y; t)$ as well as the surface elevation $\eta(r, t)$ in case of a fluid of infinite depth (i.e. when $D \rightarrow \infty$) as

$$\begin{aligned}
\phi(r, y; t) = & \int_0^{\infty} k (k - 1)^{-1} e^{k(y - t)} J_0(kr) \\
& (M_1 - M_2) e^{it} + (M_2 - k M_1) (\cos \sqrt{k} t + \frac{1}{\sqrt{k}} \sin \sqrt{k} t) \quad \dots (3.28)
\end{aligned}$$

$$\begin{aligned}
\eta(r, t) = & \int_0^{\infty} (M_2 - k M_1) (i e^{it} - i \cos \sqrt{k} t + \sqrt{k} \sin \sqrt{k} t) \\
& \times k (k - 1)^{-1} J_0(kr) dk \quad \dots (3.29)
\end{aligned}$$

Remarks : The integral representation of the solution for the wave potential $\phi(r, y; t)$ and the surface elevation $\eta(r, t)$ in a fluid of finite and infinite depth cannot, in general, be worked out exactly except for simple cases of interest. Hence one needs asymptotic methods (Copson 1965) to evaluate them for a clear understanding of the wave motions. We propose to do it in the next section.

4. ASYMPTOTIC TREATMENT OF THE PROBLEM FOR SOURCES OF PHYSICAL INTEREST.

An important three dimensional source of independent interest related to a particular form $M(r_1)$ as

$$M(r_1) = M(r, y) = \frac{1}{r_1} = \frac{1}{\sqrt{r^2 + y^2}}$$

would be considered.

Then

$$M_1 = \int_0^\infty \frac{J_0(kr) dr}{1 + \frac{r^2 + d^2}{d^2}} = \frac{e^{-k\bar{d}}}{k}$$

$$M_2 = - \int_0^\infty r J_0(kr) \frac{d}{(r^2 + d^2)^{3/2}} dr = -e^{-k\bar{d}}$$

where $\bar{d} > 0$.

These lead us to obtain the wave potential $\phi(r, y; t)$ in the form

$$\begin{aligned} \phi(r, y; t) = & \int_0^\infty e^{it} e^{k(2\bar{d} - 2D - y)} \\ & + \frac{\cosh k(y - \bar{d} + D)}{\cosh kD} \left\{ e^{-k\bar{d}} - e^{-k(2D - \bar{d})} \right\} \left(\frac{k+1}{a^2-1} \right) e^{it} \\ & + \frac{k \cosh k(y - \bar{d} + D)}{(a^2-1) \cosh kD} \left\{ e^{-k(2D - \bar{d})} - e^{-k\bar{d}} \right\} \left(\frac{1}{a} + \frac{a}{k} \right) \\ & \times k (i \sin at + a \cos at) \Big] J_0(kr) dk \end{aligned} \quad \dots(4.1)$$

Similarly, we find

$$\begin{aligned} \eta(r, t) = & \int_0^\infty \left\{ e^{-k(2D - \bar{d})} - e^{-k\bar{d}} \right\} \\ & \times \{ i e^{it} + (a \sin at - i \cos at) \} (a^2 + k)(a^2 - 1)^{-1} J_0(kr) dk \end{aligned} \quad \dots(4.2)$$

Making $D \rightarrow \infty$, the corresponding result for $\phi(r, y; t)$ and $\eta(r, t)$ in the case of infinite depth can be obtained as

$$\phi(r, y; t) = \int_0^{\infty} e^{k(y-z)} \left[(1+k)e^{it} - 2(k \cos \sqrt{kt} + i\sqrt{k} \sin \sqrt{kt}) \right] \times (k-1)^{-1} J_0(kr) dk \quad \dots (4.3)$$

$$\eta(r, t) = 2 \int_0^{\infty} k e^{-kz} (i e^{it} - i \cos \sqrt{kt} + \sqrt{k} \sin \sqrt{kt}) \times (1-k)^{-1} J_0(kr) dk \quad \dots (4.4)$$

Remarks: We thus obtain

$$\tilde{\phi}(r, y; t) = M(r) e^{it} + \phi(r, y; t) \quad (4.5)$$

where $\phi(r, y; t)$ is given by the integral (4.1) or (4.3) according as the depth of the fluid is finite or infinite.

This integral expression for $\phi(r, y; t)$ contains a transient term in addition to a steady state term which is the solution of the corresponding stationary problem considered by Thorne. In order to compare Thorne's steady state solution, one has to treat the integral for $\phi(r, y; t)$ as the Cauchy principal value, which is permissible.

It may be noticed that the integral for $\phi(r, y; t)$ has no singularities in $(0, \infty)$. Hence the path of integration can be deformed into a path M (say) in the $s = k + i\mu$ plane, which coincides with the range $(0, \infty)$ except that it is diverted round the zero of the denominator. We then break up the integral into a sum of components where the integrals do become singular at the zero of the denominator.

Then it is possible to work out each component asymptotically by asymptotic methods combined with calculus of residues. Unfortunately, Thorne did not evaluate the steady state wave integral obtained as a solution. We propose to evaluate the solution for $\eta(r, t)$ asymptotically in a considerable detail.

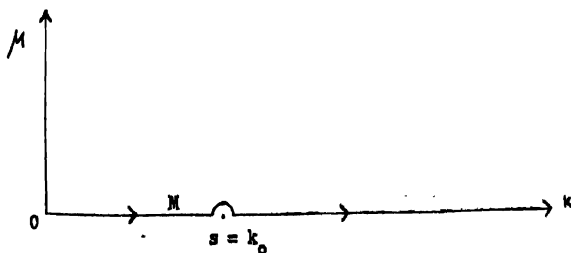


Figure 1. The $s = k + i$ plane.

An argument similar to the wave potential $\phi(r, y; t)$ enables us to obtain $\eta(x, t)$ in the form

$$\eta(r, t) = I_1 + I_2$$

where I_1 and I_2 are given by the integrals

$$I_1 = ie^{it} \int_M \left\{ e^{-i(2D-\bar{d})} - e^{-i\bar{d}} \right\} \left(\frac{\alpha^2 + s}{\alpha^2 - 1} \right) J_0(sr) ds$$

$$I_2 = \int_M \left\{ e^{-i(2D-\bar{d})} - e^{-i\bar{d}} \right\} (a \sin \alpha t - i \cos \alpha t) \\ \times \left(\frac{\alpha^2 + s}{\alpha^2 - 1} \right) J_0(sr) ds.$$

With $\alpha = \alpha(s) = \sqrt{s \tanh sD}$, $s = k_0$ is the only real root of the equation

$$\alpha^2(s) = 1$$

in $(0, \infty)$ and $-\pi < \arg s \leq \pi$.

To evaluate the steady state integral I_1 , we replace $J_0(sr)$ by a pair of Hankel functions (Whittaker & Watson 1920), $H_0^{(1)}(sr)$ and $H_0^{(2)}(sr)$. As a consequence, we obtain

$$I_1 = \frac{1}{2} e^{it} (I_1' + I_1'')$$

where I_1' and I_1'' are given by

$$I_1' = \int_M \left\{ e^{-s(2D-\bar{d})} - e^{-s\bar{d}} \right\} \left(\frac{\alpha^2 + s}{\alpha^2 - 1} \right) H_0^{(1)}(sr) ds$$

$$I_1'' = \int_M \left\{ e^{-s(2D-\bar{d})} - e^{-s\bar{d}} \right\} \left(\frac{\alpha^2 + s}{\alpha^2 - 1} \right) H_0^{(2)}(sr) ds$$

We take contours Γ_1 and Γ_2 for the integrals I_1' and I_1'' , respectively. They are bounded by the path M , μ -axis and the circular arcs C_1, C_2 lying in the first and the fourth quadrants, respectively. We then make reference to Cauchy's theorem of residues, and it follows from partial integration

that the integrals along the μ axis are $O\left(\frac{1}{r}\right)$

For evaluating the integrals along the arcs C_1, C_2 , we replace the Hankel functions by their asymptotic value for large sr and it can be shown easily that the value of the integrals tend to zero as the radii of the arcs tend to infinity.

Thus, it turns out that

$$I_1 \sim \frac{\{k_0 + \alpha^2(k_0)\}}{W'(k_0)} \left\{ e^{-k_0(2D-\bar{d})} - e^{-k_0\bar{d}} \right\} \left(\frac{2\pi}{rk_0} \right)^{\frac{1}{2}} \\ \times e^{i(\epsilon - r k_0 + \frac{\pi}{2})} + O\left(-\frac{1}{r}\right) \quad \dots (4.6)$$

where the function $W(s)$ is given by

$$W(s) \equiv \alpha^2(s) - 1. \quad \dots (4.7)$$

In order to perform evaluation of the integral I_2 , we first replace the Bessel function $J_0(sr)$ by its integral formula (Whittaker & Watson, 1920).

$$J_0(sr) = \frac{2}{\pi} \int_0^{\pi/2} \cos(sr \cos \theta) d\theta.$$

Then it follows, by a simple rearrangement of the integrand, that

$$I_2 = \frac{i}{2\pi} \int_0^{\pi/2} (I_1 + I_2 + I_3 + I_4) d\theta, \quad \dots (4.8)$$

where I_1 , I_2 , I_3 and I_4 are given by the integrals

$$I_1 = \int_M \left\{ e^{-i(zD-\bar{d})} - e^{-i\bar{d}} \right\} \left(\frac{\alpha^2 + s}{\alpha - 1} \right) e^{-i(\alpha t - sr \cos \theta)} ds \\ I_2 = \int_M \left\{ e^{-i\bar{d}} - e^{-i(zD-\bar{d})} \right\} \left(\frac{\alpha^2 + s}{\alpha - 1} \right) e^{i(\alpha t + sr \cos \theta)} ds \\ I_3 = \int_M \left\{ e^{-i\bar{d}} - e^{-i(zD-\bar{d})} \right\} \left(\frac{\alpha^2 + s}{\alpha - 1} \right) e^{i(\alpha t + sr \cos \theta)} ds \\ I_4 = \int_M \left\{ e^{-i(zD-\bar{d})} - e^{-i\bar{d}} \right\} \left(\frac{\alpha^2 + s}{\alpha + 1} \right) e^{-i(\alpha t + sr \cos \theta)} ds$$

It may be observed that these transient integrals are very much similar to those already encountered before in Debnath (1967) and Debnath & Rosenblatt (1969). Hence a similar asymptotic technique can be applied to evaluate them. Having done this, we work out the θ -integral involved in the integral I_2 by the method of stationary phase (Copson 1965) for large values of t .

Finally, we obtain the following asymptotic representation of the surface elevation $\eta(r, t)$

$$\begin{aligned}
\eta(r, t) \sim & \left(\frac{2\pi}{rk_0} \right)^{\frac{1}{2}} \frac{\{\alpha^2(k_0) + k_0\}}{W'(k_0)} \left\{ e^{-k_0(2D - \bar{d})} - e^{-k_0 \bar{d}} \right\} \\
\times & \left[e^{i(t - rk_0 + \frac{\pi}{4})} - \frac{1}{2} \left\{ 1 + \alpha(k_0) \right\} e^{i\{ \alpha(k_0) - rk_0 + \frac{\pi}{4} \}} \right] \\
& \quad , k_1 > k_0 \\
& \quad , k_1 < k_0 \\
+ & \frac{\{\alpha^2(k_1) + k_1\} \left\{ e^{-k_1 \bar{d}} - e^{-k_1(2D - \bar{d})} \right\}}{\{4 r t k_1 |f''(k_1)|\}^{\frac{1}{2}}} \\
\times & \frac{e^{-\{rk_1 - \alpha(k_1)\}}}{\alpha(k_1) - 1} - \frac{e^{i\{rk_1 - \alpha(k_1)\}}}{\alpha(k_1) + 1} \quad \dots(4.9)
\end{aligned}$$

In the case of a fluid of *unlimited* depth (i. e. when $D \rightarrow \infty$), the asymptotic representation of the surface elevation is given by

$$\begin{aligned}
\eta(r, t) \sim & \begin{cases} -2 \frac{2\pi}{r} e^{i(t - r + \frac{\pi}{4})}, & t \gg 2r \\ 0, & t \ll 2r \end{cases} \\
- & \frac{t^{\frac{3}{2}} e^{-\frac{\bar{d} t^2}{4r^2}}}{\sqrt{2} r^{\frac{3}{2}} \left(\frac{t^2}{4r^2} - 1 \right)} \left[\frac{t}{2r} \sin \left(\frac{t^2}{4r} \right) - i \cos \left(\frac{t^2}{4r} \right) \right] \quad (4.10)
\end{aligned}$$

Remarks : It may be remarked that the solutions (4.9) and (4.10) become invalid at $k_1 = k_0$ and $t = 2r$, respectively. We are particularly interested in the asymptotic solution for large values of $k_1 > k_0$ and $t \gg 2r$. So it appears to us that the computation of the solution for $\eta(r, t)$ valid at $k_1 = k_0$ and $t = 2r$ is not so important in the present analysis. However, it can be done by a method similar to Wurtele (1955).

5. DISCUSSION OF THE WAVE MOTIONS

The above asymptotic analysis reveals an interesting conclusion that the transient term involved in the asymptotic solution for the surface elevation $\eta(r, t)$ does tend to zero as t tends to infinity for fixed values of r and $\bar{d} (\neq 0)$. As a consequence, an ultimate steady state is set up. In fact, the asymptotic value of $\eta(r, t)$ assumes the form

$$\eta(r, t) \sim -2 \sqrt{\frac{2\pi}{r}} e^{i \left(t - r + \frac{\pi}{4} \right) - \bar{d}}$$

This corresponds to progressive circular waves advancing with the phase velocity $\frac{\omega}{k}$ and the group velocity $\frac{g}{2\omega}$, and the amplitude of the waves decays like r^{-1} .

On the other hand, when the source is on the free surface of the fluid (i.e. when $d \rightarrow 0$), the asymptotic solution for $\eta(r, t)$ has the form

$$\eta(r, t) \sim \begin{cases} -2 \sqrt{\frac{2\pi}{r}} e^{i(\omega t - r + \frac{\pi}{4})}, & t \gg 2r \\ 0, & t \ll 2r \end{cases} \\ - \frac{t^2 \left[\frac{t}{2r} \sin\left(\frac{t^2}{4r}\right) - i \cos\left(\frac{t^2}{4r}\right) \right]}{\sqrt{2} r^3 \left(\frac{t^2}{4r} - 1 \right)} + O\left(\frac{1}{t^3}\right)$$

This solution suggests that the transient term is now free from the exponential factor $e^{-\sqrt{2}t/4r^3}$ and hence it does not tend to zero in the limit $t \rightarrow \infty$ for fixed r . In other words, the solution does not tend to the steady state in the limit when the source is situated on the undisturbed free surface of the fluid.

Furthermore, it may be observed that the nature of this asymptotic solution has a similarity with that obtained in Debnath (1967a) and Debnath (1967b) due to a harmonically oscillating pressure distribution with the forcing frequency ω in the form

$$P(R, T) = P \frac{\delta(R)}{R} e^{i\omega T} H(T)$$

acting on the undisturbed free surface of the fluid. To explain the strange character of the solution, physical and mathematical arguments similar to those suggested by Debnath (1968, 1967) in detail can also be advanced here. To avoid duplication of similar discussion, reference may be made to the above works of the author.

Next, proceeding to the limit $r \rightarrow \infty$, for fixed t , the solution for $\eta(r, t)$ given in (4.10) behaves as

$$\eta(r, t) \sim - \frac{t^2 e^{-\sqrt{2}t/4r^3}}{\sqrt{2} r^3 \left(\frac{t^2}{4r} - 1 \right)} \left[\frac{t}{2r} \sin\left(\frac{t^2}{4r}\right) - i \cos\left(\frac{t^2}{4r}\right) \right]$$

Finally, if the source is situated at an infinite depth (i.e. when $d \rightarrow \infty$) in an infinitely deep fluid, the solution for the surface elevation $\eta(r, t)$ becomes exponentially small as really expected,

The author wishes to express his grateful thanks and deep gratitude to Dr. S. Rosenblat of Imperial College of Science and Technology, London, for his active guidance and encouragement during the preparation of the work.

REFERENCE

- Copson, E. T. 1965 *Asymptotic Expansions* Cambridge University Press.
- Debnath, L. 1967a *Ph. D. Thesis* (University of London).
- Debnath, L. 1967b *Proc. Nat. Inst. Sci India (In Press)*.
- Debnath, L. 1968 *Zeit. Ange. Math. & phys. (ZAMP)* **19** p948—961.
- Debnath, L. & Rosenblat, S. 1969, *Quant. J. Mech. and Applied Math.* **22**, 221—233.
- Lamb, H. 1905 *Proc. Lond. Math. Soc.* **2**, 271—400
- 1923 *Proc. Lond. Math. Soc.* **21**, 356—372
- 1932 *Hydrodynamics*, Cambridge University Press.
- Lighthill, M. J. 1960 *Phil. Trans. Roy. Soc.* **A252**, 397—430.
- Lighthill, M. J. *J. Inst. Math. Applic.* **1**, 1—28.
- Miles, J. W. 1962 *J. Fluid Mech.* **13**, 145—150.
- Stoker, J. J. 1957 *Water Waves* (Interscience).
- Thorne, R. C. 1953 *Proc. Camb. Phil.* **49**, 707—716.
- Whittaker E. T. & Watson, G. K. 1920 *A Course of Modern Analysis* Cambridge University Press.
- Wurtele, M. G. 1955 *J. Mar. Res.* **14**, 1—13.

Green's function analysis of NF_3 and NCl_3

K. RAMASWAMY AND N. MOHAN

Department of Physics, Annamalai University, Annamalai Nagar, S, India

(Received 7 November 1969)

The molecular constants of $^{14}\text{NF}_3$ and $^{14}\text{NCl}_3$ were evaluated using the Green's function analysis. In the case of $^{14}\text{NF}_3$, the values of the potential energy constants were found to be in good agreement with the values of Anna Mirri determined by least square fit using the experimental values of other molecular constants. The treatment of central atom substitution was found to give accurate values of the individual Coriolis coupling constants in consistency with the earlier results.

INTRODUCTION

The determination of a unique set of symmetry force constants occurring in general force field calculations often becomes difficult when the number of independent force constants exceeds the number of vibrational frequencies. To circumvent this difficulty, simplified force fields such as UBFF (Urey & Bradley 1931), OVFF (King 1962) and HBFF (Heath & Linnett, 1948) have been formulated. Additional molecular constants like the mean amplitudes of vibration, rotational distortion constants, Coriolis coupling constants and the vibrational frequency shifts for isotopically substituted molecules are often used in getting a unique set of force constants. Such attempts have been made earlier by several authors like Duncan & Mills (1964), Anna mirri (1967) and Levin & Abramowitz (1966) using the rotational distortion constants and the Coriolis coupling constants and Iwasaki & Hedberg (1962) using the mean amplitudes of vibration from electron diffraction data.

The Green's function analysis of substituted and perturbed molecules developed by Dewames, Wolfram & coworkers (1964, 1966) comes in handy to determine the force constants from the vibrational spectra of the parent and the perturbed molecules. Wherever isotopic data are available, this approach helps to determine other molecular constants without assuming a force field mode. Using this method, isotopic rules similar to the Teller-Redlich product rule (Herzberg, 1945), which do not involve the moments of inertia explicitly were obtained for XY_3 , XY_2 , X_2Y_4 and XY_4 (Ramaswamy & coworkers, 1968, 1969) types of molecules. This formalism also leads to the evaluation of the vibrational frequencies of related molecules from a knowledge of the nature of vibrations of the parent molecule. In the present paper, Green's function analysis of $^{14}\text{NF}_3$ and $^{14}\text{NCl}_3$ belonging to the C_{3v} point group is made to obtain the molecular constants. The molecular constants of NF_3 have been earlier determined

from experimental data by Anna Mirri (1967), Popplewell *et al* (1967) and Otake *et al* (1968) so that direct comparison of the results is possible to fix the force field for the molecule.

ISOTOPIC RULES FOR $XY_3 \rightarrow X^iY_3$

The dynamics of the parent molecule in Green's function analysis is studied through the secular determinant, (1964)

$$|\epsilon \omega^2 G(\omega^2) - I| = 0 \quad \dots(1)$$

for isotopic substitution. For the substitution $XY_3 \rightarrow X^iY_3$, $\epsilon = \frac{m_x}{m_x^i} - 1$

where m_x and m_x^i are masses of the X atom and $G(\omega^2)$ is the Green's function for the unperturbed molecule. The Green's function is constructed from the normal coordinate representation, using the matrix of transformation (U) from the normal to the mass weighted Cartesian coordinates. The product rule obtained for the two vibrational species of the XY_3 pyramidal type molecules are.

$$\omega_1^i{}^3 \omega_2^i{}^3 = \frac{\omega_1^2 \omega_2^2 A^2 (m_x + B^2)}{A^2 B^2 + A^2 m_x \epsilon + 3m_y \epsilon (B^2 \cos^2 \beta + m_x \sin^2 \beta)} \quad \dots(2)$$

$$\omega_3^i{}^3 \omega_4^i{}^3 = \frac{\omega_3^2 \omega_4^2 C^2 \left[D^2 + \epsilon \frac{m_x}{B^2} (D^2 + 6m_y \cos^2 \beta) \right]}{3m_y \sin^2 \beta \epsilon (D^2 + m_x \sin^2 \beta) + C^2 \left[D^2 + \frac{m_x}{B^2} (D^2 + 6m_y \cos^2 \beta) \right]} \quad \dots(3)$$

where ω_k 's are the frequencies of the parent molecule ($^{14}\text{NF}_3$ or $^{14}\text{NCl}_3$) and ω_k^i 's are the frequencies of the isotopically substituted molecules ($^{15}\text{NF}_3$ or $^{15}\text{NCl}_3$), $A^2 = m_x + 3m_y \cos^2 \beta$; $B^2 = m_x + 3m_y$; $C^2 = 2m_x + 3m_y \sin^2 \beta$; $D^2 = C^2 - m_x \sin^2 \beta$ and $\sin \beta = 2/\sqrt{3} \sin \alpha/2$ where α is the angle between the XY bonds. The frequency sum rule is obtained in terms of the elements of the mixing parameter matrix (A), which is starting matrix for the evaluation of the molecular constants, without assuming a force field model. It can be seen from equations (2) and (3) that if the vibrational frequencies of any set of isotopic species are known the molecular parameters (in this case bond angle α) can be obtained. Using the spectral data for $^{14}\text{NCl}_3$ and $^{15}\text{NCl}_3$ a value of bond angle of 106° for $^{14}\text{NCl}_3$ have been obtained. This value of α was used in the present calculations along with an assumed value of 1.7 \AA for the N-Cl bond length. The vibrational frequencies for $^{14}\text{NF}_3$, $^{15}\text{NF}_3$, $^{14}\text{NCl}_3$, $^{15}\text{NCl}_3$ along with the molecular

parameters are given in table 1. The vibrational assignment for NF_3 and NCl_3 are those given by Otake *et al* (1968) and Bayersdorfer *et al* (1968)

TABLE 1. MOLECULAR PARAMETERS AND THE VIBRATIONAL FREQUENCIES
IN cm^{-1} FOR NF_3 AND NCl_3 .
(O take *et al* 1968 and Bayersdorfer *et al* 1968)

Molecular parameters	Vibrational frequencies	
	$^{14}\text{NF}_3$	$^{14}\text{NCl}_3$
$d_{\text{N-F}} = d = 1.371 \text{ \AA}$	1032	1009
	647	643
$\text{F-N-F} = \alpha = 120^\circ 10'$	907	886
	493	492
$d_{\text{N-Cl}} = d = 1.7 \text{ \AA}$	$^{14}\text{NCl}_3$	$^{14}\text{NCl}_3$
	540.5	528.0
	349.0	348.0
$\text{Cl-N-Cl} = \alpha = 106^\circ$	643	628
	257	257

POTENTIAL ENERGY CONSTANTS

The symmetry force constant matrix (F) for NF_3 and NCl_3 were generated from the relation,

$$F = \bar{B}^{-1} A A A \bar{B}^{-1} \quad \dots(4)$$

where $B = T M^{-1} S$ (Wolfram *et al* 1966) T , being the transformation matrix between the internal symmetry coordinates and the Cartesian coordinates, M being the mass matrix and S being the transformation matrix between the external symmetry coordinates and the mass weighted cartesian coordinates. A is a diagonal matrix containing the squares of the observed vibrational frequencies. The elements of the (F) matrix along with the valence force constants are given in table 2.

MEAN AMPLITUDES OF VIBRATION

The symmetrized (Z) matrix containing the mean square amplitudes for the various bonded and non-bonded atom pairs was constructed from the relation (Cyvin 1959)

$$Z = L \Delta L = B A \Delta A B \quad \dots(5)$$

TABLE 2. ELEMENTS OF THE SYMMETRIZED F MATRIX AND VALENCE FORCE CONSTANTS IN M. DYNES/Å FOR NF₃ AND NCl₃

F elements	Valence force constants.	Otake <i>et al</i> (1968)	Anna Mirri (1967)
NF ₃			
F_{11} 7.4189*	$f_d = 4.7915$	4.3	4.24
F_{10} 2.1468	$f_{dd} = 1.3136$	0.91	1.02
F_{12} 1.3447	$f = 0.9708$	1.02	1.04
F_{20} 3.4779	$f_{\alpha\alpha} = 0.0857$	0.13	0.11
F_{22} 1.6638	$f_{d\alpha} = 0.4501$	0.31	0.30
F_{24} -0.5057	$f'_{d\alpha} = 0.0812$	-0.02	0.04
NCl ₃			
F_{11} 4.1076	$f_d = 2.5888$		
F_{10} 1.4868	$f_{dd} = 0.7594$		
F_{12} 1.3767	$f_{\alpha} = 0.4533$		
F_{20} 1.8294	$f_{\alpha\alpha} = 0.0306$		
F_{22} 1.2218	$f_{d\alpha} = 0.3140$		
F_{24} -0.2249	$f'_{d\alpha} = -0.1817$		

* This number of significant figures is retained for internal consistency in calculations.

where Δ is a diagonal matrix with elements

$$\Delta_{ii} = \frac{\hbar}{8\pi^2 c \omega_i} \coth \left(\frac{\hbar c \omega_i}{2kT} \right) \quad \dots(6)$$

where \hbar is the Planck's constant, k the Boltzmann constant, T the absolute temperature and c the velocity of light. The mean square amplitudes for non-bonded atom pairs were calculated using the method of Ramaswamy *et al* (1962). The calculated values of the (Σ) matrix elements along with the values of the mean amplitudes of vibration for bonded and non-bonded atom pairs are given in table 3.

ROTATIONAL DISTORTION CONSTANTS AND CORIOLIS COUPLING CONSTANTS

The rotational distortion constants (D_J , D_K and D_{JK}) were evaluated from the elements of the (1) matrix of transformation between the normal and the mass weighed Cartesian coordinates determined using the relations suggested by Oka & Morino (1961) and Alti *et al* (1965). The

TABLE 3. ELEMENTS OF THE SYMMETRIZED Σ MATRIX AND MEAN AMPLITUDES OF VIBRATION IN \AA AT 298.16°K FOR NF_3 AND NCI_3

Σ Matrix elements	Mean amplitudes of vibration	Bakken, (1958)
NF_3		
Σ_{11} 0.001567*		
Σ_{22} 0.004098		
Σ_{12} -0.001121	N-F 0.04828	0.0535
Σ_{33} 0.002713	F..F 0.07208	0.0786
Σ_{44} 0.004143		
Σ_{54} -0.001174		
NCI_3		
Σ_{11} 0.003347		
Σ_{22} 0.008254		
Σ_{12} -0.003024	N-Cl 0.06939	—
Σ_{33} 0.005548	Cl...Cl 0.10688	—
Σ_{44} 0.007041		
Σ_{54} 0.001644		

* This number of significant figures is retained for internal consistency in calculations.

theory of Wilson and Kivelson (1952, 1953) was used to evaluate the rotational distortion constants. The Coriolis coupling constants were evaluated from the (1) matrix using the relation suggested by Meal & Polo (1956). The calculated values of the rotational distortion constants and the Coriolis constants are given in table 4.

DISCUSSION

The value of N-F stretching force constant (4.79 mdynes/ \AA) obtained from Green's function analysis agrees well with the value of 4.24 mdynes/ \AA calculated by Anna Mirri (1967) from least square method, utilising all the available molecular constants such as the rotational distortion constants and the value of 4.3 mdynes \AA /reported by Otake *et al* (1968). The application of Badger's rule (Badger 1934) yields a value of 5.6 mdynes/ \AA for the N-F stretching force constant and 3.6 mdynes/ \AA for the N-Cl stretching force constant. The mean amplitudes of vibration calculated for NF_3 (N-F = 0.04828 \AA , F..F = 0.07208 \AA) are in agreement

TABLE 4. ROTATIONAL DISTORTION CONSTANTS IN Kc/SEC. AND CORIOLIS COUPLING CONSTANTS FOR NF_3 AND NCl_3 .

Present study		Anna Mirri (1967)	Otake <i>et al</i> (1968)	Popplewell <i>et al</i> (1967)
NF_3				
D_J	13.57	14.53	14.85	13.5
D_K	10.20		10.30	
D_{JK}	-22.11	-22.80	-23.21	-25.71
ζ_3	0.768			0.81
ζ_3	-0.875	-0.965	-0.895	-0.90
NCl_3				
D_J	2.26			
D_K	1.73			
D_{JK}	-3.78			
ζ_3	0.912			
ζ_4	-0.951			

with the reported values of Bakken (1958). (Mean amplitudes $\text{N-F} = 0.05350 \text{ \AA}$, $\text{F-F} = 0.07860 \text{ \AA}$).

The values of D_J (13.57 Kc/sec) and D_{JK} (-22.11 Kc/sec) calculated by Green's function analysis for $^{14}\text{NF}_3$ are close to the values obtained by Popplewell *et al* (1967) ($D_J = 13.5$ Kc/sec, $D_{JK} = -25.71$ Kc/sec) and Otake *et al* (1968) ($D_J = 14.85$ Kc/sec, $D_K = 10.3$ Kc/sec and $D_{JK} = -23.21$ Kc/sec) from infrared spectral data. The values of the Coriolis coupling constants, determined for $^{14}\text{NF}_3$ (0.788 and -0.875) are in good agreement with the values of (-0.895) and (-0.90, 0.81) reported by earlier authors (Popplewell *et al* 1967 and Otake *et al* 1968). It is found, in comparison with the individual values of the Coriolis constants, obtained earlier by Green's function analysis of pyramidal XY_3 type molecules (Ramaswamy & Swaminathan, 1968), that central atom substitution gives a better value of the individual Coriolis coupling constants than the ones obtained for end atom substitution, though the sum rule is verified accurately in both the cases. Since molecular data for $^{14}\text{NCl}_3$ are lacking no direct comparison is possible.

ACKNOWLEDGEMENT

One of the authors (N. M.) is grateful to the Council of Scientific and Industrial Research, Government of India for the award of a Junior Research Fellowship.

REFERENCES

- Alti G. D., Galasso V. & Giacomocosta, 1965, *Spectrochim. Acta*, **21**, 649.
Anna Mirri, M. 1967, *J. Chem. Phys.*, **47**, 2823.
Badger R. M. 1934 *J. Chem. Phys.*, **2**, 128.
Bakken J. 1958 *Acta Chem. Scand.*, **12**, 594.
Bass C. D., Lynds L., & Wolfram T., 1964, *J. Chem. Phys.*, **40**, 3611.
Bayersdorfer L. Engelhardt U., Hohne, K. Fischer, J. & Jander, J. 1968 *Z. Naturforsch* **23b**, 1602.
Cyvin S. J. 1959 *Spectrochim. Acta*, **15**, 828.
Dewames R. E. & Wolfram, T. 1964 *J. Chem. Phys.*, **40**, 853.
Duncan J. L. & Mills I. M. 1964 *Spectrochim. Acta*, **20**, 522.
Heath D. F. & Linnett J. W. 1948, *Trans. Faraday Soc.*, **44**, 873.
Herzberg G. 1945 *Infrared and Raman Spectra of Polyatomic Molecules*, D. Van Nostrand Co. Inc. New York 231.
Iwasaki M. & Hedberg, K. 1962 *J. Chem. Phys.*, **36**, 594.
King, W. T. 1962 *J. Chem. Phys.*, **36**, 165.
Levin I. W. & Abramowitz S. 1966 *J. Chem. Phys.*, **44**, 2562.
Meal J. H. & Pole S. R. 1956 *J. Chem. Phys.*, **24**, 1119.
Oka J. & Morino U. 1961 *J. Molec. Spectrosc.*, **6**, 472.
Otake M., Hirose E. & Morino Y. 1968 *J. Molec. Spectrosc.*, **28**, 316, 325.
Poppellwell R. J. L., Masri F. N. & Thompson, H. W. 1967 *Spectrochim. Acta*, **23A**, 2797.
Ramaswamy K., Sathianandan K., & Cleveland F. F. 1962 *J. Molec Spectrosc.*, **9**, 107.
Ramaswamy K. & Devarajan. V. 1968a *Acta. Phys. Polonica*, **XXXIV**, 985.
Ramaswamy K. & Ranganathan, V. 1968b *Indian J. Pure Appl. Phys.*, **6**, 657.
Ramaswamy K. & Swaminathan S. 1969 *Aust. J. Chem.*, **22**, 291.
Ramaswamy K. & Srinivasan K. *J. Mole. Struc.* (In press.)
Urey H. C. & Bradley C. A. 1931 *Phys. Rev.*, **38**, 1969.
Wilson E. B. & Kivelson D. 1952 *J. Chem. Phys.*, **20**, 1575.
Wilson E. B. & Kivelson D. 1953 *J. Chem. Phys.*, **21**, 1229.
Wolfram T., Bass C. D. Dewames R. E. & Lynds L. 1966 *Bull. Chem. Soc. Japan*, **39**, 201.
Wolfram T. & Dewames R. E. 1966 *Bull. Chem Soc. Japan*, **39**, 207.

Letters to the Editor

Probability-operator of a quantum system for thermodynamics.*

By M. DUTTA

Centre of Advanced Studies in Applied Mathematics, University of

Calcutta, Calcutta-9, India.

(Received 28 August 1969)

Essentially statistical investigations of a physical system with two fundamental entities, which are additive, numerically measurable, but random in nature were made by Dutta (1953, '55, '59, '60, '65, '66) for solving the main problem of (equilibrium) thermodynamics. The probability distribution for the measured values of the fundamental entities were written by arguments similar to those used for Bayes' rule or for writing the likelihood-function after Fisher and then parameters were estimated by the method of maximum likelihood. From the equation for conservation of any one of the fundamental entities, the known results of statistical thermodynamics were deduced. Afterwards it was shown (Dutta 1966) that additivity of fundamental entities leads to an exponential (a canonical or a grand canonical) law for distributions in statistical physics. The entire discussion may be equally applicable to a system, composed of a large number of constituent microscopic parts or to a single macroscopic system with some entities of which the total measure may fluctuate at random. A purely probabilistic treatment of thermodynamic problems is also due to Jaynes (1957).

A system like quantum liquid (viz. liquid helium) is essentially a quantum (macro-) system (Landau & Lifshitz 1969). Also, a system with strong interactions amongst its constituent parts is usually considered as a single quantum system. So, it is necessary as well as interesting to see how to modify the discussions of essentially statistical theory of thermodynamics, consistently with the usual formalism of quantum mechanics, i.e. in terms of Hilbert space and linear operators on it, so that an essentially quantum system may be duly investigated. The present note is an attempt in that direction.

For a quantum system, the states are represented by points of a Hilbert space, H , and any physical (dynamical) variable is a Hermitean linear operator on H into H (Dirac 1936, von Neumann 1955). Measured values of a physical variable are eigen-values of the corresponding linear operator.

*A brief synopsis of this note was accepted by the International Conference on Statistical Mechanics held at Kyoto (Japan) in September 1968.

Now, in statistical investigations, to a set of measured values of fundamental physical entities, a probability-distribution is associated. If the probability is also taken as a measurable physical quantity, a linear operator P on H is to be associated with it. To take account of the statistical distribution associated with a thermodynamic system, von Neumann (1955) also introduced a linear operator U on H , named by him as the statistical operator.

As the probability is a function of the measured values of fundamental entities like energy etc., so P is a function of operators corresponding to them, viz., Hamiltonian etc. The product rule of probabilities of independent random variables implies multiplicative property of P and operators like Hamiltonian etc., representing fundamental physical quantities for independent systems are commutative in the cartesian product of Hilbert spaces of states of those independent systems and the total Hamiltonian is the sum of two Hamiltonians of constituent parts. Now, P is an operator valued function of the Hamiltonians, H 's, and is multiplicative for the statistically independent systems. As statistical independence implies absence of interactions, so for the statistically independent systems, H 's are evidently commutative and the total Hamiltonian is the sum.

Now, Hilbert space is also a Banach space and a space of linear operators on a Banach space to a Banach space is also a Banach space. Moreover, as linear operators representing physical (dynamical) variable are endomorphisms of H , so they form a Banach algebra. It is well-known that in a Banach algebra B , the functional equation

$$P(H_1 + H_2) = P(H_1) + P(H_2), H_1, H_2, P(H_1), P(H_2) \in B$$

is satisfied by

$$P(H) = j \exp(L(H))$$

where j is an idempotent, $L(H)$ is a linear on B , to itself and j , $L(H_1)$, $L(H_2)$ commute for all $H_1, H_2 \in B$. Now, the simplest form of $L(H)$ is taken as αH where due to the Hermiticity of the operators, α is real. If j be taken as the unit element e one gets

$$P(H) = \exp(\alpha H)$$

This expression agrees with that for the statistical operator of von Neumann obtained for a system composed of a large number of simple quantum constituents by methods partly quantum mechanical and partly thermodynamic. In this case, the conditions of statistical (thermodynamic) equilibrium will yield as a function of temperature etc., characteristics of thermodynamic equilibrium. If j be taken as the null element θ , $P(H) = \theta$ and this solution appears to be physically untenable. If B contains idempotent

elements other than θ and ϵ and j represent one of them (not θ nor ϵ) one gets,

$$P(H)=j \exp (\alpha H)=j \exp (\alpha j H), (\alpha \text{ real})$$

as j also commutes with H . This result appears to be new and interesting and the investigation of its full significance will be the subject matter of a future work. Here, it may only be pointed that as j , $L(H)$ etc. commute with H 's, so the argument of exponential must be some constant of motion associated with the system ; in this respect the result appears to be similar to the general probability distribution proposed by Gibbs (1902) for the classical cases.

In order that the above theorem is applicable, H_1 and H_2 should have values in a closed subset of the Banach space formed by the linear operators on H . This will be realisable if the systems (1) and (2), of which one is a system under consideration and the other is the surroundings, be looked upon like heat-bath and matter-bath which can interchange their constituents freely within a suitable range as in the corresponding cases, discussed earlier (Dutta, 1965). The assumption of the existence of a set of values of H_1 and H_2 leads to the hypothesis of the resolution of the Hilbert space, the direct sum of the Hilbert spaces of the systems (1), (2) in a large number of different ways. This point requires a careful mathematical scrutiny which will be investigated later.

REFERENCES

- Dirac, P.A.M. 1947 *The Principles of Quantum Mechanics*, 3rd edition, Oxford University Press.
- Dutta M. 1953a *Bulletin of Int. Stat. Inst.* **32**, 268.
 1953b *Proc. Nat. Inst. Sc. (Ind)* **19**, 109.
 1955 *Proc. Nat. Inst. Sc. (Ind.)* **21**, 373.
 1960 Gnan O Bignan (in Bengali) **13**, 737.
 1965 *Zeit. f. Phys. Chemie* **228**, 380.
 1966 *Indian J. Phys.* **40**, 85.
 1969a *Proc. Sum. Inst. of Theor. Physics at Missouri (India)* 231.
 1969b *Statistical Physics (Foundation)*, World Press (India), (in Press).
- Gibbs, J. W. 1902 *Elementary Principles of Statistical Mechanics*, Yale University Press, New Haven, USA.
- Hille, E. 1957 *Functional Analysis and Semigroups*, Amer. Math. Soc. Publications (1957).
- Jaynes, E. T. 1957 *Phys. Rev.*, **106**, 620, and **107**, 171.
- Landau, L. D. & Lifshitz, E. M. 1959 *Statistical Physics*, Pergamon Press., U. K.
- Von Neumann, John 1955 *Mathematical Foundation of Quantum Mechanics*, Princeton University Press, U.S.A.,

Some observations on dynamic vibrations of homogeneous incompressible elastic shells,

By M. DUTTA

Advanced Centre of Applied Mathematics, Calcutta University.

(Received 8 September 1969 — Revised 30 December 1969)

By Cinelli's method (1965, 1966), a suitable alternative form of the method of Hankel's transform Chatterjee (1968), claimed to find the transient displacements and stressed for 'dynamic' (?) vibrations of homogeneous incompressible elastic spherical and cylindrical shells as a series of Cinelli's functions which are a linear combination of two Bessel functions of the same order. Due to incompressibility, i.e. the vanishing of volume dilatation, the only non-zero displacement, $u(r, t)$, satisfies a partial differential equation of the first order involving $\frac{\partial u}{\partial r}$ and so $\frac{\partial^2 u}{\partial r^2}$ and $\frac{\partial u}{\partial r}$ in

the equation of motion are replaceable by expressions involving $u(r, t)$ only. In some recent general discussions of solutions of differential equations by methods of integral transforms (Dutta & Debnath 1965, 1967), it was explained clearly that a differential equation involving some differential operator L can be solved by an integral transform associated with an irreducible differential operator L (if $L = f(L)$) where, $f(z)$ is a polynomial (or an integral function) of z with constant coefficients. Then, a differential equation is solvable by Cinelli's method if its differential operator is at least of the second order. But in the case of incompressible elastic shells, the equation of motion is reducible to one of order less than two regarding the partial derivative with respect to r and is not solvable by Cinelli's method. The expression for displacement in terms of Cinelli's functions (Chatterjee, 1968) does not satisfy the differential relation signifying the incompressibility. This point has been clarified by some easy discussions from the theory of operators. Straight calculation implies the impossibility of time-dependent radial displacements for the problems discussed.

In the case of incompressible spherical shells for radial displacements in polar coordinates

$$u_r = u(r, t), u_\theta = 0, u_\phi = 0 \quad \dots (1)$$

due to incompressibility, one gets

$$\frac{\partial u}{\partial r} + \frac{2u}{r} = 0 \quad \dots (2)$$

After proper choice of elastic constants the equation of motion is (Love 1944)

$$\frac{\partial^2 u}{\partial r^2} + \frac{2}{r} \frac{\partial u}{\partial r} - \frac{2u}{r^2} = \frac{1}{c^2} \frac{\partial^2 u}{\partial t^2} \quad (c \text{ being a constitutive constant}) \quad \dots(3)$$

with initial condition,

$$\frac{\partial u}{\partial t} = 0 \quad \text{at} \quad t = 0. \quad \dots(4)$$

Due to the equation (2), the equation (3) reduces to the equation,

$$0 = \frac{1}{c^2} \frac{\partial^2 u}{\partial t^2}, \quad \text{or} \quad u(r, t) = A(r)t + B(r) \quad \dots(5)$$

$$\text{By (3), } A(r) \equiv 0 \quad \text{and} \quad u(r, t) = B(r) \quad \dots(6)$$

Even if the initial condition is not used, the fact that the linear theory of elasticity is a theory of small displacements leads to (5).

Then from (1) and (4)

$$\frac{B'(r)}{B(r)} = -\frac{2}{r} \quad \text{or} \quad u(r, t) = B(r) = Cr^{-2} \quad (C \text{ being a constant}) \quad \dots(7)$$

Thus, the loads in the outer and the inner surfaces must be in a ratio $a^2 : b^2$, a and b being the inner and the outer radii. The equation (7) shows that there cannot be a radial vibration and the loads on the boundary surfaces cannot be arbitrary as asserted by Chatterjee (1968).

In case of incompressible cylindrical shells for displacements in cylindrical coordinates,

$$u_r = u(r, t), \quad u_\theta = 0, \quad u_z = 0 \quad (1)$$

the equation of motion after proper choice of elastic constants (Love, 1944) is

$$\frac{\partial^2 u}{\partial r^2} + \frac{1}{r} \frac{\partial u}{\partial r} - \frac{u}{r^2} = \frac{1}{c^2} \frac{\partial^2 u}{\partial t^2} \quad \dots(3)$$

with the initial condition,

$$\frac{\partial u}{\partial t} = 0, \quad \text{at} \quad t = 0 \quad (4)$$

Proceeding as in the previous case, one gets

$$u(r, t) = C'r^{-1} \quad (C' \text{ being a constant}) \quad \dots(7)$$

The loads on the boundary surfaces are in the ratio $a^2 : b^2$, a and b being the outer and the inner radii. The concluding comments are the same as in the previous case.

To get a clear idea about the nature of errors, let us denote

$$l_{1r} \equiv \frac{\partial}{\partial r} + \frac{2}{r}, \quad l'_{1r} \equiv \frac{\partial}{\partial r} + \frac{1}{r}, \quad \dots(8)$$

$$l_{2r} \equiv \frac{\partial^2}{\partial r^2} + \frac{1}{r} \frac{\partial}{\partial r} - \frac{4}{r^2}, \quad l'_{2r} \equiv \frac{\partial^2}{\partial r^2} + \frac{1}{r} \frac{\partial}{\partial r} - \frac{1}{r^2}. \quad \dots(9)$$

The linear operators are defined on a set of functions having continuous derivative of the second order in $[a, b]$ which, after topologising in the usual way, is denoted by $D_2[a, b]$ (Shilov, 1965). It is easy to see that

$$l_{2r} \equiv \left(l_{1r} - \frac{3}{r} \right), \quad l'_{2r} \equiv \left(l'_{1r} - \frac{1}{r} \right) l'_{1r}, \quad \dots(10)$$

Relations (10) show that the solutions of $l_{1r} u = 0$ and $l'_{1r} u = 0$ are solutions of $l_{2r} u = 0$ and $l'_{2r} u = 0$, respectively. But the converse is not true. Nonnull images of the set points in $D_2[a, b]$ for which $\left(l_{1r} - \frac{3}{r} \right) u = 0$ and $\left(l'_{1r} - \frac{1}{r} \right) u = 0$, respectively, with respect to $(l_{1r})^{-1}$ and $(l'_{1r})^{-1}$ are solutions of $l_{2r} u = 0$, and $l'_{2r} u = 0$, respectively, but evidently $l_{1r} u \neq 0$ and $l'_{1r} u \neq 0$.

REFERENCES

- Chatterjee, D. 1968 *Indian J. Phys.* **42**, 539.
Cinelli, G. 1965 *Intern Jour. Eng. Sciences* **3**, 539.
Cinelli, G. 1966 *Jour. Appl. Math.*, 825.
Dutta, M. & Debnath, L. 1965 *Stud. Univ. Bab.* **33**, 37.
Love, A.R.H. 1944 *On the Mathematical Theory of Elasticity*, Dover Publication, N.Y.
Shilov, G. Ye. 1965 *Mathematical Analysis*, Pergamon Press, Oxford

Indian J. Phys. **34**, 705—707 (1969)

Decay characteristics of CaS (Zr, Di) phosphors

By B. R. MALHOTRA

Central Road Research Institut^e, New Delhi.

(Received 22 August—Revised 23 December 1969)

Phosphorescence decay characteristics of CaS phosphors activated with Zr and Di (Pr+Nd) impurities have been studied to gather information about the type of phosphorescence decay, value of time constant of decay and the effective trap depths contributing to the phosphorescence in this system of phosphors.

Experimental results reveal that decay of phosphorescence follows the hyperbolic relation $I = I_0 t^{-b}$ with b varying from 0.77 to 0.92 and the kinetics being monomolecular. The value of decay constant b increases with the increase in concentration of Di impurity implying thereby that Di atoms introduce shallow traps which get emptied soon. Group of traps with trap depth 0.7 eV contribute most effectively to the phosphorescence. The close agreement between two values of trap depths E as obtained from phosphorescence decay and thermoluminescence justifies the validity of the fundamental equation $p = a \cdot e^{-E/kT}$ in this system of phosphors.

Blokhinsev (1937) and De Groot (1939) were the first among early workers who derived a theoretical time dependence of the decay of phosphorescence from considerations of electron transitions between various energy levels. Lord *et al* (1947) identified these energy states as arising activators which have lost their electrons. The decay of phosphorescence is distinguished to be of two types depending on whether the kinetics involved in the luminescence process are of the first order or of the second order. Radiative transitions which are monomolecular in character, result in exponential decay of the form $I = I_0 \cdot \exp(-pt)$, while in the case of bimolecular mechanism involving recombination of the free electrons and holes, the decay obeys the inverse square law, $I = I_0/(1 + at)^2$.

Phosphorescence decay characteristics of CaS phosphors activated with zirconium and rare earth didymium (praesodymium+neodymium) have been studied to gather information on the type of decay and trap depths contributing to phosphorescence. Phosphors were prepared by heating an intimate mixture of CaSO_4 , a triple flux, activators zirconium and didymium in suitable proportions at 950°C for two hours in a reducing atmosphere of carbon. Four series of phosphors with different constant concentrations of Zr in respective series were prepared and didymium content was varied from .001 to 0.4 percent by weight of CaSO_4 in each series.

Decay characteristics were studied by plotting intensity measured in arbitrary units against time on logarithmic scale. The deviation of the curve from the straight line eliminates the possibility of exponential decay. However the $\log I - \log t$ curve shows a linear relationship signifying a hyperbolic decay of the $I = I_0 t^{-b}$ where b is known as decay constant. The hyperbolic decay is supposed to result from the superposition of intensities, each of which is varying exponentially with time, when different trap depths are involved in contributing to phosphorescence. The decay constant b has been calculated by introducing new variables to get a more workable relationship. So taking the logarithm of the above expression,

$$\log I = \log I_0 + b \log t$$

and putting $y = \log I$, $x = \log t$ and $c = \log I_0$,

we get, $y = bx + c$

The problem is simplified to, fitting a straight line to a set of points in the xy plane and thus to a simple problem of least squares. b and c can be calculated from the following expressions :

$$b = \frac{\Sigma x_i y_i - n \Sigma x \Sigma y}{(\Sigma x)^2 - n \Sigma x^2}$$

$$c = \frac{\Sigma y_i \Sigma x^2 - \Sigma x_i \Sigma y}{n \Sigma x^2 - (\Sigma x)^2}$$

Value of b has been calculated for all the samples in the time interval from 5 seconds after excitation to the time when the intensity decayed to a negligibly small value. As b turns out to be a negative quantity, the equation becomes $I = I_0 \cdot t^{-b}$.

As shown by data collected for all the samples, value of decay constant varies from 0.77 to 0.92 with the increase in concentration of Di which implies that Di introduces shallow traps which get emptied soon, thus giving a higher value of the decay constant. Hyperbolic decay is considered to be the result of superposition of exponentials corresponding to different trap depths. To determine the different traps contributing to phosphorescence, the decay curves were broken into three exponentials and trap depths corresponding to these were determined. Trap depths as calculated from the three exponentials for most of the phosphors are 0.61, 0.65 and 0.69 eV. From the limited number of exponentials it is reasonable to assume the distribution to be Gaussian. Thus the group of traps contributing predominantly to phosphorescence may be assigned the value of trap depth corresponding to that of its maximum, i.e. 0.69. This value of trap depth is in close agreement with that determined from glow-curve experiment implying thereby that the kinetics involved are mono-molecular and the validity of the equation $p = s \cdot e^{-E/kT}$ holds good.

REFERENCES

- Blokhinsev D. 1937 *J. Exptl. Theor Physics, U.S.S.R.* 7, 1242.
 De Groot W. 1949 *Phys.* 6, 275.
 Lord, Rees & Wise 1947 *Proc. Phys Soc.* 59, 488.

BOOK REVIEWS

Voyage to the Moon, The Epic of Man in Space ;

By Rosskote Krishna Pillai, 1969, pp 156, Price Rs. 6. 50 ; Orient Longmans,

Bombay, Madras, Calcutta, New Delhi.

It is a quite readable little book, written in epic style, rather than scientific, and gives in a collected form practically all information on space-flight and Moon-travel published from time to time in news letters and information circulars. A large number of well reproduced illustrations doubles the pleasure of reading. Without reducing in any way the credit of the author in giving the lay public a nice book of very topical interest, we may make a few remarks for consideration in future editions of the book.

On page 19, 3rd para the last sentence : "But this duration varies because the moon, like all the planets, is constantly under the influence of other planets, the earth and the sun" is not happy.

Popular writers are surely permitted to use approximate numbers in giving data but it appears to be stretching the point too far when in 6th and 7th para of page 19, the volume of the moon is given as 1/50th that of the earth, whereas, the diameter is given as 1/4. Also the mass of the moon is given as 1/80th that of the earth, and the gravity is given as 1/6, which latter is then too small if the diameter is taken as 1/4. On page 21 last paragraph, the readers might be interested to know the cause of difference in *sideral* month and *synodic* month. Some information on the lunar tidal effects on earth would complete the information on "Our Inseparable Companion". Page 33, para 1 : Surely the author can feel gravity, can he not ? para 2 : "Life on earth without gravity would be miserable, walking would be difficult, we would have to leap from place to place. Rain would not fall, there would be no water falls. We would be weightless, everything would be weightless". We should be thankful if this is the utmost that could happen to us in the absence of gravity !

Page 33. 1st para, last sentence : "Thus when we weigh ourselves we are in fact measuring our mass plus the pull of gravity" is too loose a statement even for school children. 2nd para 2nd sentence : "...had thought of an invisible force". Is it possible to think of a visible force ? 4th para : It would be better to speak of "acceleration" rather than "velocity" unless we qualify it by stating "at the same height".

Page 35 last para : It is never possible to "..... go away from the gravitational pull" altogether. Page 37, para 4 : The explanation of reaction is very loosely stated and would create wrong impression of Newton's 3rd law in the minds of school children or lay public. Same applies to page 37 last sentence, which is quite wrong.

On page 86 1st para, "The first to circle round and land on Moon was not man but a vehicle made by man". The expression is very loose ; can a man go round and land on Moon without a vehicle ?

On page 100, the correct temperature of liquid oxygen at normal atmospheric pressure should be -183°C .

On the same page and the next, 2nd stage is stated to lift the vehicle to "a height of 182 km" and 3rd stage to an "altitude of 184 km"; both cannot be correct. Page 102, 4th para: "The module is coated with a special material which burns off when it reenters the atmosphere at 2760°C " How could it get so heated outside the atmosphere? What is the temperature thereafter and what protects the module during the rest of the journey through atmosphere, if the coating has already burnt off?

It would be very useful if in going to the next edition, the author gets the book revised by a scientist. Otherwise, the initial success in presenting a book of this nature to the public may be more than counterbalanced by the doubts arising in the minds of logical readers.

A. B.

The World of Mars

By V.A. Firsoff, 1969, pp 128, Price 7sh 6d, Oliver & Boyd, Edinburgh.

This little book covers practically the entire information available on the planet Mars up-to-date. The author is himself a well known worker in Areology and speaks with authority and conviction on the subject. The writing is informative, instructive and intriguing. The confrontation between telescopic and other earthbound instrumental observations and the close range but limited observations by Mariner 4 probe, has been critically discussed to show the pitfalls in arriving at conclusions on Martian geography, geology, meteorology and ecology derived from either class of data. The mysteries of Schiaparelli's "Canals", the seasonal color and topological variations constituting some of the most intriguing and controversial subjects on Mars, have been given as logical an explanation as to be expected, considering all the conflicting data. A layman to fully appreciate the book would be expected to have a fairly good knowledge of several associated subjects, but for the specialist it should be a source of pleasure to go through the book and ruminate over the many problems of Mars, only the fringe of which appears to have been touched as yet. There seems to be now little logical doubt that Mars mostprobably contains plant and bacterial life and the necessary factors for their sustenance. Whether the "Canals" of Mars are really subterranean aqueducts, whether some of the observed mushrooming clouds on Mars are from nuclear explosions or whether the mysterious twin satellites of Mars are really huge spacecrafts indicating the existence and activities of superhuman Martians, a positive answer to such speculations, according to the author, are improbable but not impossible. Without more unambiguous data it is still premature to build up a theory of the Martian World, but the day is perhaps not very far off when manned earth spacecrafts going round or landing on Mars itself will settle all controversy. Till then most of the theories on Mars are to remain "not proven for the time being" as the author very cautiously asserts.

A.B.

BOOKS RECENTLY RECEIVED FOR REVIEW

- Gallium Arsenide Lasers*, Ed. C. H. Gooch, John Wiley & Sons, New York
- Nuclear Electronics*, by E. Kowalski, \$26.40, Springer-Verlag, Berlin
- Photoelectronic Devices*, by J. B. Dance, \$2-10-0, ILIFFE Books Ltd, London
- University Optics. Vol. 1*, by D. W. Tenquist, R. M. Whittle, & J. Yarwood, £3-50-0
ILIFFE Books Ltd, London
- Topics in Interval Analysis*, Ed. E. R. Hansen, \$2-50-0, Oxford University Press
- Cosmic Ray Physics*, S. Hayakawa, £39.50, John Wiley Sons, New York
- Atomic Spectra*, by H. G. Kuhn, 105s net, Longman, Green & Co. Ltd. England
- NMR, Basic Principle and Progress*, Vol. 1, Ed. P. Deihl, E. Fluck, R. Koseld, \$10.80,
Springer-Verlag, Berlin
- Advances in Plasma Physics, Vol. 3*, Ed. Simon and Thompson, \$14.95, John Wiley &
Sons, New York,
- Cosmic Electrodynamics*, John Hobart Piddington, John Wiley & Sons, New York
- Physics of Hot Plasma*, Ed. B. J. Rye, T. C. Taylor, £8-0-0. Oliver & Boyd, England
- Geometrical Optics*, by H. G. Zimmer, \$9.40, Springer-Verlag, Berlin,

Angular correlation studies in Tc^{99}

By P. JAGAM AND V. LAKSHMINARAYANA

The Laboratories For Nuclear Research, Andhra University, Waltair, India.

(Received 28 July 1967—Revised 22 January and 20 December 1968)

The combined angular correlation pattern of the cascades 740-180 and 740-(40)-140 keV is studied by the sum-peak-coincidence technique using a fast-slow coincidence scintillation spectrometer and a 100 channel analyser. Assuming equal admixture of the cascades and the spins of the ground 140 and 180 keV states in Tc^{99} to be $9/2+$, $7/2+$ and $5/2+$ respectively, the observed correlation pattern indicated a spin assignment of $1/2+$ for the 920 keV state.

INTRODUCTION

Cappeller & Klingelhofer (1954), Raboy & Krohn (1958), Estulin *et al* (1958), Bodenstedt *et al* (1959), and Andrade *et al* (1965) carried out investigations on angular correlations of the cascades connecting the excited state at 920 keV and the ground in Tc^{99} . The 920 keV state decays to the ground state through two prompt cascades 740-180 keV and 740-(40)-140 keV. The transitions 140 and 180 keV could not be completely separated by scintillation spectrometers. As a result, the angular correlation studies are beset with the difficulty of interference between the two cascades. All the investigators tried to separate these cascades. The result of the study of Andrade *et al* (1965) in which sufficient precautions are reported to have been adopted to minimise the admixture of the cascades, differs from the theoretical value by as much as 20%, although the error in estimation is much smaller. It thus appears that instead of attempting to separate out the contributions of the 140 and 180 keV transitions, it is proper to accept them collectively and separate the effect of one of them estimated theoretically. Studies on angular correlations are therefore undertaken with a sum-peak-coincidence scintillation spectrometer.

EXPERIMENTAL DETAILS

The sum-peak-coincidence technique was first described by Kantele & Fink (1962), the characteristics of the high efficiency 4π sum-peak-coincidence arrangement being studied in detail by Kantele (1962). In this work he gave a detailed account of the methods of sum-peak-coincidence spectrometry. They also referred to the possibilities of angular correlation studies using this technique. In the present investigation, the detectors are symmetrically situated at a distance of 7 cms from the central source. The detectors are enclosed in anti-Compton shields, the radiations from the source being accepted via a narrow conical opening. In this arrangement, the attenuation factor, defined by Kantele, for

monochromatic gamma rays is found to be zero. This proves that 'the cross-talk' (Kantele) is completely eliminated. As such this arrangement is extremely useful for studying weak cascades in the presence of intense singles radiations.

The block diagram of the experimental arrangement is shown in figure 1. The scintillation heads consists of two well matched hermetically sealed Harshaw Type $1\frac{3}{4}$ " dia x 2" thick NaI(Tl) crystals attached to two DuMont 6292 photomultipliers. The heads contain the lead shielding and the electrical connections. The heads are fixed to wooden V-grooves by aluminium collars and mounted on a circular glass plate such that they could be rotated about one another in the horizontal plane with respect to a vertical pivot fixed at the centre of the glass plate. The circumference of the glass plate is divided into 5° intervals to facilitate the measurement of the angle between the axes of the two detectors. A 20° interval is also divided into unit angular intervals for angular resolution experiments. The central pivot about which the detectors rotate, supports a perspex block for holding the source containers. The source container is a thin walled perspex tube of internal dimensions 4 mm diam x 10 mm high. The two scintillation detectors are connected in a fast-slow type of electronic summing arrangement (figure 1). This arrangement

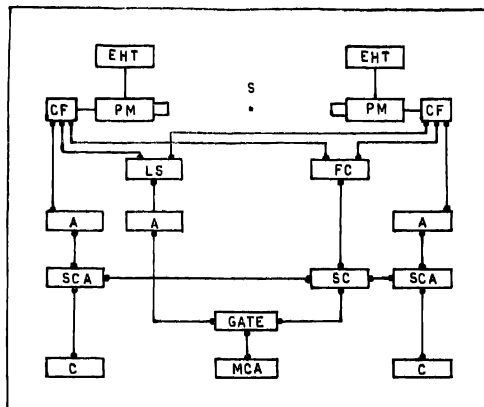


Figure 1. Block diagram of the experimental arrangement: *S*: Source, *PM*: Photomultiplier, *EHT*: High Tension Unit, *CF*: Cathode Follower, *LS*: Linear Summing Network, *A*: Amplifier, *FC*: Fast Coincidence Unit, *SCA*: Single Channel Analyser, *SC*: Slow Coincidence Unit, *C*: Counter, *MCA*: 100 Channel Analyser.

is similar to that of Kantale & Fink except for the inclusion of the fast channel. The fast channel of the present arrangement is based on blocking oscillators and the effective resolving time of the arrangement is experimentally determined to be 100 ± 10 ns. The sum peak-coincidence spectra are recorded on a 100 channel analyser (Type 2A/NISS/ED) supplied by Bhaba Atomic Research Centre, India.

RESULTS

Scintillation Spectrometer Characteristics : The performance of the electronic summing scintillation spectrometer thus assembled is tested with a Co^{60} source. A few drops of the source are placed in the source container. The position of the source container is adjusted such that the count rate in the movable counter situated in different angular positions is constant to within 0.5%. The sum spectrum is recorded and is shown in figure 2. It can be seen from the figure that

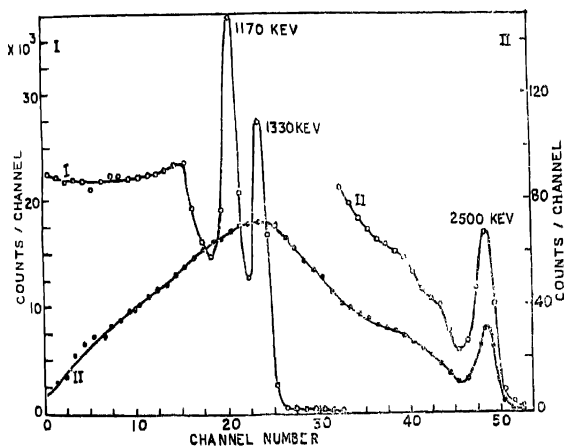


Figure 2. The Sum and Sum-peak Coincidence Spectra for Co^{60} . The curve with O (open circles) represents the sum spectrum and the curve with \bullet (full circles) represents the zero-bias sum-peak coincidence spectrum.

peaks appear at energies 1.17, 1.33 and 2.5 MeV corresponding to single gamma components and the coincident sum energy. The zero-bias sum-peak-coincidence spectrum is recorded by setting the side channels integrally at zero-bias (approximately 80 keV in the present work). This spectrum is also shown in figure 2 for comparison. It can be seen

from this figure that the sum-peak-coincidence spectrum consists of the sum energy peak at 2.5 MeV, the singles peaks being completely attenuated. The area above the continuous distribution under the peak at 2.5 MeV is representative of the coincidence count rate. The coincidence counting efficiency is thus double that of an identical conventional set up in which narrow differential channels select 1.17 and 1.33 MeV for coincidence counting. The background is also completely eliminated from the coincidence spectrum.

The sum-peak-coincidence spectrum is recorded on the 100 channel analyser for angles 90° , 135° , 180° , 225° and 270° between the detectors. These angular positions are changed once in every fifteen minutes to smooth out time dependent fluctuations. A pooled total of 30,000 counts are collected at each angle under the peak at 2.5 MeV. The correlation coefficients are obtained employing White's (1963) method. The values of the coefficients thus obtained are

$$A'_2 = 0.099 \pm 0.006$$

$$A'_4 = 0.008 \pm 0.006$$

These are to be corrected for the angular resolution of the detectors as suggested by Frackel (1951) while neglecting the source size effects. The attenuation factor is given by

$$S_{2\nu} = J_{2\nu}/J_0 \quad \dots(1)$$

where

$$J_{2\nu} = \int_0^{\theta_{max}} P_{2\nu}(\cos\theta) \epsilon(\theta) \sin\theta d\theta \quad \dots(2)$$

J_0 is the value of $J_{2\nu}$ for $\nu = 0$

$P_{2\nu}(\cos\theta)$ is the Legendre Polynomial

$\epsilon(\theta)$ is the relative efficiency

θ_{max} is the angle of the conical opening in the shielding of the detector.

The relative efficiencies $\epsilon(\theta)$ are obtained from the angular resolution curves plotted for different energies (In^{114m} : 192 keV, Cs^{137} : 662 keV, Co^{60} : 1170 keV and 1330 keV, Sb^{124} : 1690 keV) by the method of Lawson & Frauenfelder (1953). The correction factors S_2 and S_4 for the experimental arrangement in the present work are shown in figure 3. For the case of Co^{60} , the attenuation factors for the 1.17 and 1.33 MeV energies are employed to obtain the corrected coefficients $A_{2\nu}$. The corrected coefficients are obtained from the experimental coefficients $A'_{2\nu}$ from the relation

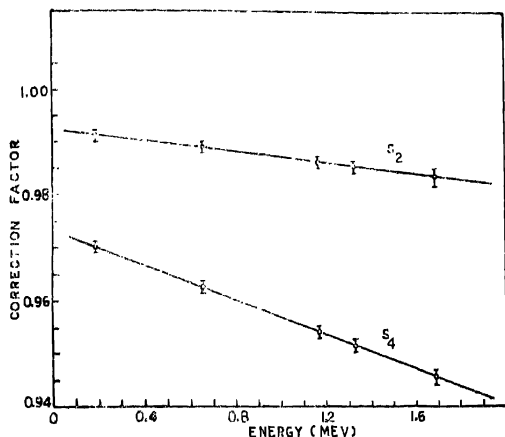


Figure 3. Plots of the attenuation factors S_2 (Upper line) and S_4 (lower line) as functions of energy. They are experimentally determined for the present arrangement.

$$A_{2v} = \frac{A'_{2v}}{S_{2v}(\gamma_1) \cdot S_{2v}(\gamma_2)} \quad \dots(3)$$

where $S_{2v}(\gamma_1)$ and $S_{2v}(\gamma_2)$ are the attenuation factors for the coincident gamma rays γ_1 and γ_2 of the cascade under investigation. In the present case of Co^{60} , the corrected coefficients are obtained to be

$$A_2 = 0.101 \pm 0.006$$

$$A_4 = 0.008 \pm 0.006$$

The value of A_2 and A_4 thus obtained to fit the correlation pattern expected for a $E2 - E2$ cascade in the spin sequence $4 \rightarrow 2 \rightarrow 0 \rightarrow$ thereby showing the suitability of the present arrangement for undertaking angular correlation studies.

Note on figure 3 for the correction factors : It is mentioned in the experimental details that the scintillation detectors are enclosed in lead shielding, the radiations from the source being accepted *via* an axial conical opening in the front, which is contrary to normal practice. However, the lead shields are essential because of the sum-peak-coincidence technique in the present investigation. The reason is that, because of the summation, the single gamma rays also appear in the coincidence spectrum of crystal to crystal scattering (referred to as "cross-talk" by Kantele 1962). The lead

shielding is designed to avoid all the cross-talk and to provide good geometry with maximum efficiency as illustrated in figure 2 with a Co^{60} source. The absence of the well resolved peaks at 1170 and 1330 keV in the coincidence spectrum proves that the cross-talk is completely by eliminated.

Because of the shielding of the crystals, the correction to be applied for the finite size of the detectors with the shielded crystal geometry is not the same as that with open crystal geometry. Hence, the correction factors quoted in literature for the open crystal geometries are not valid in the present case. As in the case of open crystal geometries, the angular resolution corrections must be determined by the method of Lawson & Frauenfelder (1953) for the particular shielded crystal geometry.

In the present investigation, the $1\frac{3}{4}'' \times 2''$ detectors are provided with lead shields with a frontal thickness of 1.6 cm. The axial conical opening has an opening diameter of 1.4 cm and a base diameter of 2 cm in the lead shield. The detector almost touches the lead shield when assembled in the detector head. For a source situated at the apex of the cone, i.e. at 7 cm from the face of the crystal along the axis, the detector has an acceptance angle of approximately 15° . Because of the conical opening in the front the effective acceptance angle of the detector is not the same at all the energies. Due to the penetration of the higher energy gamma rays, the detector has a larger opening angle at higher energies than at lower energies. In the angular resolution experiment performed with these detectors, on the lines of Lawson & Frauenfelder (Jagam), it is found that the acceptance angle increases from 15° at 192 keV to 19° at 1690 keV. As a result of the increase in the opening angle of the detector, the value of the correction factor decreases with the increase of energy. As such the attenuation for the angular correlation coefficients increases at higher energies contrary to the trend observed with open crystal geometries as reported in the literature. It is therefore evident that one has to be careful in applying the angular resolution corrections with shielded crystal geometries.

Study of Angular Correlations in Tc^{99} : The radioactive source Mo^{99} is obtained from the Isotope Division of Bhabha Atomic Research Centre, India. It is produced by the fission of uranium with neutrons from the reactor. The Mo^{99} fraction is separated from the fission fragments by alumina-gel chromatography. Carrier free Mo^{99} is finally obtained as ammonium molybdate in dilute ammonium hydroxide solution the activity being 3mC/ml. The decay scheme of Mo^{99} is well established (Cretzu & Hohmuth 1965, Jagam & Lakshminarayana 1967) and is shown in figure 4.

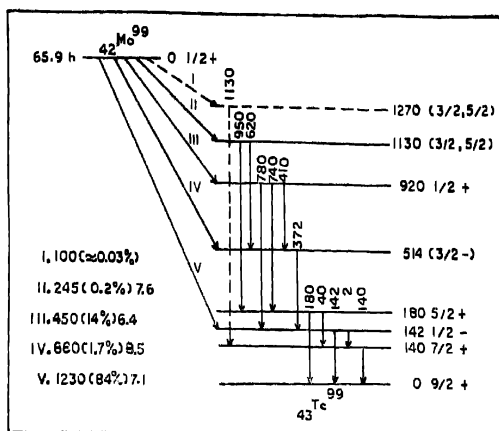


Figure 4. The decay scheme of Mo^{99} . The dashed lines represent the transitions and levels introduced from the work of Jngam & Lakshminarayana.

A few drops of the source sample are placed in the source container. After making the usual adjustments, the zero-bias sum-peak-coincidence spectrum is recorded for fifteen minutes and shown in figure 5. The peak at 920 keV contains predominant contributions from the two prompt cascades 740-180 and 740-(40)-140 keV. A small amount of contribution from the 620-370 keV cascade on the high energy side of the 920 keV peak can be neglected. It can be seen from the figure that the intensity of the peak at 920 keV above the continuous distribution is large and can be measured accurately. The angular correlation studies are carried out by recording the coincidence spectrum at angles 90° , 135° , 180° , 225° and 270° between the detectors. The position of detectors is changed every fifteen minutes and a pooled total of about 30,000 counts is collected at each angular position under the peak at 920 keV. The counts are fitted by White's analysis to the standard polynomial.

$$W(\theta) = 1 + A'_2 P_2(\cos \theta) + A'_4 P_4(\cos \theta)$$

where

$$A'_2 = -0.030 \pm 0.006$$

$$A'_4 = +0.009 \pm 0.004$$

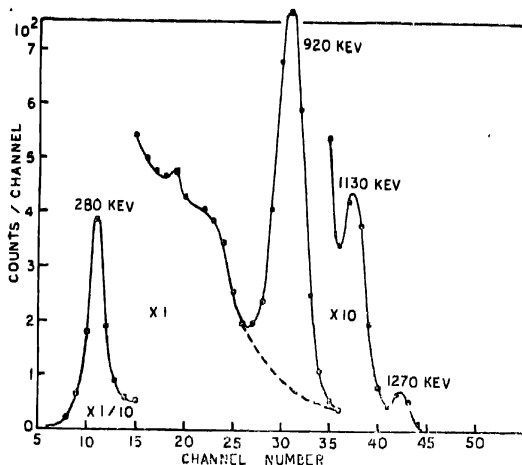


Figure 5. The zero-bias sum-peak-coincidence spectrum recorded for 15 minutes. It can be seen that the 920 keV peak can be well resolved from the distribution.

are the correlation coefficients determined experimentally. These are to be corrected for the angular resolution of the detectors. For this purpose, the correction factors for energies 140, 180, and 740 keV are obtained from the figure 3 by interpolation. The angular resolution correction is effected by employing equation (3). The corrected values of the correlation coefficients are given by

$$A_2 = -0.031 \pm 0.006$$

$$A_4 = +0.009 \pm 0.004$$

The peak at 920 keV occurring in the sum-peak-coincidence spectrum accepts both the cascades 740-180 and 740-(40)-140 keV. The 180 keV state decays in equal proportions (after allowing for internal conversion) via the two branches. Thus the observed correlation is the result of admixture of the two cascades in equal proportions. However, the first one is a double cascade and the second one is a triple cascade with the intermediate gamma (40 keV) unobserved. Thus the correlation patterns are given by

$$W(\theta)_{740-180} = 1 + A_2 P_2(\cos \theta) + A_4 P_4(\cos \theta)$$

$$W(\theta)_{740-(40)-140} = 1 + U_2 A_2 P_2(\cos \theta) + U_4 A_4 P_4(\cos \theta)$$

The factor U_{2k} is given by

$$U_{2k} = \frac{- \left\{ \begin{smallmatrix} I_a & I & 2k \\ I_b & I_b & 1 \end{smallmatrix} \right\} + \delta^2 \left\{ \begin{smallmatrix} I_a & I_a & 2k \\ I_b & I_b & 2 \end{smallmatrix} \right\}}{1 + \delta^2} \times \\ (-1)^{I_a + I_b} [(2I_a + 1)(2I_b + 1)]^{\frac{1}{2}}$$

where I_a and I_b are the initial and final spins connected by the unobserved gamma-ray and δ^2 is the mixing ratio of the transition. In the present case, since equal admixture of the two cascades are involved, the final values of A_2 and A_4 are given by

$$A_2 = \frac{1}{2} [A_2 (740-180) + U_2 A_2 (740-140)]$$

$$A_4 = \frac{1}{2} [A_4 (740-180) + U_4 A_4 (740-140)]$$

The theoretical values of A_2 and A_4 are estimated using the above relations for accepted spins of the ground, 140 and 180 keV states (viz. $9/2+$, $7/2+$, and $5/2+$ respectively) and possible spin values of $1/2+$ and $3/2+$ for the 920 keV state. In this estimation, however, there is an uncertainty arising out of the errors in the relative intensity estimates of the cross-over and the cascade from the 180 keV state. These errors are also estimated for an assumed 10% deviation in the relative intensity of the cascade and cross-over transitions (i.e. 40-140 and 180 keV). If the spin of the 920 keV state is assumed to be $1/2+$, the 740 keV transition is pure $E2$. The 40 and 140 keV transitions may be of $M1 + E2$ types, while the 180 keV transition is pure $E2$. From the experimental evidence (Estulin *et al* 1958, Ravier *et al* 1961) the 40 keV transition is assumed to be pure $M1$ and the correlation coefficients are estimated using the relations given above, for various values of the mixing amplitude δ in the 140 keV transition. The total values of the correlation coefficients for the two cascades weighted as detailed above, are given in table 1. It can be seen from table 1 that the present experimental value of A_2 falls in between the theoretical values for quadrupole contents between 1.2% and 5.9% or above 98.8% for the 140 keV transition. However, the latter value for the quadrupole content requires a large negative A_4 coefficient. The present experimental value for A_4 , however, is small and positive. It therefore appears reasonable to accept the first possibility (quadrupole content in the 140 keV transition between 1.2 and 5.9% with δ positive). The result is also in agreement with the experimental value of Ravier *et al* (1961) (2% for the quadrupole content in the 140 keV transition). A spin assignment of $1/2+$ for the 920 keV state therefore seems appropriate.

However, in order to find out whether other possible spin assignments can be made, theoretical values of the correlation coefficients are estimated

TABLE 1. THEORETICAL VALUES OF THE TOTAL CORRELATION COEFFICIENTS FOR THE 740-(40)-140 KEV TRANSITIONS. A SPIN SEQUENCE OF $1/2+ \rightarrow 5/2+ \rightarrow 7/2+ \rightarrow 9/2+$ IS ASSUMED. THE 40 KEV TRANSITION IS ASSUMED TO BE PURE $M1$. THE VALUES AND SIGNS OF δ GIVEN IN THE TABLE REFER TO THE 140 KEV TRANSITION

No	δ	A_2 (total) for		A_4 (total)	Quadrupole content % $\delta^2/1+\delta^2$
		δ positive	δ negative		
1	0	$+0.015 \pm 0.006$	$+0.015 \pm 0.006$	$+0.0046 \pm 0.0005$	0.00
2	1/9	-0.024 ± 0.009	$+0.053 \pm 0.005$	$+0.0043 \pm 0.0005$	1.22
3	1/4	-0.068 ± 0.013	$+0.095 \pm 0.006$	$+0.0028 \pm 0.0005$	5.88
4	3/7	-0.116 ± 0.018	$+0.135 \pm 0.009$	-0.0003 ± 0.0007	15.51
5	2/3	-0.156 ± 0.020	$+0.165 \pm 0.012$	-0.0050 ± 0.0011	30.75
6	1	-0.176 ± 0.023	$+0.172 \pm 0.013$	-0.0110 ± 0.0016	50.00
7	3/2	-0.169 ± 0.023	$+0.153 \pm 0.011$	-0.0169 ± 0.0021	69.23
8	7/3	-0.139 ± 0.020	$+0.113 \pm 0.008$	-0.0217 ± 0.0027	84.48
9	4	-0.098 ± 0.016	$+0.066 \pm 0.005$	-0.0247 ± 0.0029	94.14
10	9	-0.056 ± 0.011	$+0.020 \pm 0.006$	-0.0261 ± 0.0031	98.77
11	∞	-0.019 ± 0.009	-0.019 ± 0.009	-0.0265 ± 0.0031	100.00

for a spin assignment of $3/2+$ for the 920 keV state. In this estimation, as in the previous case, the 40 keV transition is assumed to be pure $M1$. In addition, the 140 keV transition is assumed to be $M1$ with 2% $E2$ admixture; but both signs of δ are considered in the estimates. Assuming at first the sign of δ in the 140 keV transition to be positive the correlation coefficients are estimated for different values of δ (as well as the two signs) in the 740 keV transition ($920 \text{ keV } 3/2+ \rightarrow 180 \text{ keV } 5/2+$). The procedure is repeated for the negative sign of δ in the 140 keV transition. As in the previous case, the two cascades are weighted together with an error of 10% in their admixtures. The values of the total correlation coefficients are given in tables 2 and 3. It can be seen from tables 2 and 3 that there are four cases of agreement between the theoretical and experimental values of the A_2 coefficients. However, in none of these cases the theoretical values of A_4 is of correct sign. In all these cases the theoretical values for the A_4 coefficients are negative, while the experimental value is positive. It appears unlikely that the spin of 920 keV state is

TABLE 2. THEORETICAL VALUES OF THE TOTAL CORRELATION COEFFICIENTS FOR THE 740-(40)-140 + 740-180 KEV TRANSITIONS. A SPIN SEQUENCE OF $3/2+ \rightarrow 5/2+ \rightarrow 7/2+ \rightarrow 9/2+$ IS ASSUMED. THE 40 KEV TRANSITION IS ASSUMED TO BE PURE $M1$. THE 140 KEV TRANSITION IS ASSUMED TO BE $M1+2\% E2$ WITH δ POSITIVE. THE VALUES AND SIGNS OF δ GIVEN IN THE TABLE REFER TO THE 740 KEV TRANSITION.

No.	δ	A_2 (total) for		A_1 (total)	Quadrupole content % $\delta^2/1+\delta^2$
		δ positive	δ negative		
1	0	+ 0.024 \pm 0.007	+ 0.024 \pm 0.007	- 0.00000 \pm 0.00000	0.00
2	1/9	+ 0.011 \pm 0.004	+ 0.037 \pm 0.011	- 0.00006 \pm 0.00001	1.22
3	1/4	- 0.007 \pm 0.002	+ 0.050 \pm 0.015	- 0.00030 \pm 0.00002	5.88
4	3/7	- 0.025 \pm 0.008	+ 0.062 \pm 0.018	- 0.00070 \pm 0.00008	15.51
5	2/3	- 0.043 \pm 0.013	+ 0.069 \pm 0.020	- 0.00140 \pm 0.00020	30.75
6	1	- 0.055 \pm 0.016	+ 0.066 \pm 0.020	- 0.00230 \pm 0.00030	50.00
7	3/2	- 0.057 \pm 0.017	+ 0.055 \pm 0.016	- 0.00320 \pm 0.00040	69.23
8	7/3	- 0.050 \pm 0.015	+ 0.037 \pm 0.011	- 0.00390 \pm 0.00050	84.48
9	4	- 0.038 \pm 0.012	+ 0.019 \pm 0.006	- 0.00440 \pm 0.00050	94.14
10	9	- 0.025 \pm 0.007	+ 0.002 \pm 0.001	- 0.00450 \pm 0.00050	98.77
11	∞	- 0.012 \pm 0.004	- 0.012 \pm 0.004	- 0.00460 \pm 0.00050	100.00

TABLE 3. THEORETICAL VALUES OF TOTAL CORRELATION COEFFICIENTS FOR THE 740-(40)-140 + 730-180 KEV TRANSITIONS. A SPIN SEQUENCE OF $3/2+ \rightarrow 5/2+ \rightarrow 7/2+ \rightarrow 9/2+$ IS ASSUMED. THE 40 KEV TRANSITION IS ASSUMED TO BE PURE $M1$. THE 140 KEV TRANSITION IS ASSUMED TO BE $M1 + 2\% E2$ WITH δ NEGATIVE. THE VALUES AND SIGNS OF δ GIVEN IN THE TABLE REFER TO THE 740 KEV TRANSITION.

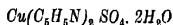
No.	δ	A_2 (total) for		A_1 (total)	Quadrupole content % $\delta^2/1+\delta^2$
		δ positive	δ negative		
1	0	- 0.044 \pm 0.004	- 0.044 \pm 0.004	- 0.00000 \pm 0.00000	0.00
2	1/9	- 0.019 \pm 0.002	- 0.068 \pm 0.005	- 0.00006 \pm 0.00001	1.22
3	1/4	+ 0.013 \pm 0.001	- 0.093 \pm 0.008	- 0.00030 \pm 0.00002	5.88
4	3/7	+ 0.048 \pm 0.004	- 0.115 \pm 0.009	- 0.00070 \pm 0.00008	15.51
5	2/3	+ 0.080 \pm 0.006	- 0.127 \pm 0.010	- 0.00140 \pm 0.00020	30.25
6	1	+ 0.102 \pm 0.008	- 0.123 \pm 0.010	- 0.00230 \pm 0.00030	50.00
7	3/2	+ 0.106 \pm 0.009	- 0.102 \pm 0.008	- 0.00320 \pm 0.00040	69.23
8	7/3	+ 0.092 \pm 0.008	- 0.068 \pm 0.005	- 0.00390 \pm 0.00050	84.48
9	4	+ 0.067 \pm 0.006	- 0.034 \pm 0.003	- 0.00440 \pm 0.00050	94.14
10	9	+ 0.047 \pm 0.004	- 0.003 \pm 0.001	- 0.00450 \pm 0.00050	98.77
11	∞	+ 0.023 \pm 0.002	+ 0.023 \pm 0.002	- 0.00460 \pm 0.00050	100.00

$3/2 +$. The present experimental results therefore favour a unique assignment of $1/2 +$ for the spin of 920 keV state.

REFERENCES

- Andrade, P. Da R., Maciel, A., Muller, C. S., Wirth, J. & Zawislak, F. C. 1965
Nucl. Phys. **66**, 545.
- Bodenstedt, E., Matthias, E. & Korner, H. J. 1959 *Z. Phys.*, **153**, 423.
- Cappelier, U. & Klingelhoff, R. 1954 *Z. Phys.*, **139**, 402.
- Cretzu, T. & Hohmuth, K. 1965 *Nucl. Phys.* **66**, 391.
- Estulin, I. S., Cherov, G. M. & Pastukhov, Z. N. 1958 *Soviet Physics JETP*, **35**, 71.
- Frankel, S. 1951 *Phys. Rev.*, **83**, 673.
- Jagam, P. 19 Ph. D. thesis, Andhra University, 95, 67, Andhra.
- Jagam, & P. Lakshminarayana, V. 1967 *Proceedings of the Nuclear Physics
and Solid State Physics Symposium*, Kanpur, 477.
- Kantele, J. & Fink, R. W. 1962 *Nucl. Instr. and Meth.*, **15**, 69.
- Kantele, J. 1962 *Nucl. Instr. and Meth.* **17**, 33.
- Lawson, J. S. & Frauenfelder, H. 1953 *Phys. Rev.*, **91** 649.
- Raboy, S. & Krohn, V. E. 1958 *Phys. Rev.*, **111**, 579.
- Ravier, J., Marguin, P. & Moussa, A. 1961 *J. Phys. Rad.*, **22**, 249.
- White, D. H. 1963 *Nucl. Instr. and Meth.*, **21**, 209.

E. S. R. study of copper dipyrindine sulphate dihydrate



By P. V. GOPALAKRISHNA MURTHY

Department of Physics, Andhra University, Waltair, India.

(Received 1 November 1968—Revised 22 September and 7 November 1969)

Electron spin resonance spectra have been obtained on the (a) the powder specimen and (b) single crystals of copper dipyrindine sulphate using an X-band ESR spectrograph. Variation of g^2 and of line widths ΔH are measured from derivative tracings. The principal g -values are obtained in each case. The data are briefly discussed in the light of known crystal structure.

INTRODUCTION

Electron spin resonance (ESR) studies on the pyridine complexes of Cu^{++} are meagre. Gresmann (1962) has made investigations on CuCl_2 pyridine in solutions, the solvent being 40 percent pyridine and 60 percent chloroform. ESR investigations have also been made on polycrystalline samples of $\text{Cu}(\text{Py})_2 \cdot \text{S}_2\text{O}_8$ etc. by Smaller (1961) at 77°K and by Abe & Ono (1956) on a number of copper complexes including copper hexapyridine nitrate and copper pyridine sulphate $\text{Cu}(\text{Py})_6 \cdot \text{SO}_4 \cdot n\text{H}_2\text{O}$. But there has been no work so far reported on copper dipyrindine sulphate dihydrate. The purpose of this paper is to present the results on the determination of the principal g -factors of this particular complex from ESR studies on line shapes of the signal for the polycrystalline powder adopting Kneübuhr's (1961) method, as well as on single crystals of the substance. The results are discussed in the light of known crystal structure of the substance.

EXPERIMENTAL

Experiments have been carried out at room temperature using the ESR spectrometer described earlier (Narasimhamurthy 1963) operating in the X-band region with crystal detection. The modulation employed is 50 CPS.

The crystals are grown according to the method described by Cannillo & Giuseppetti (1964) from an aqueous solution of copper sulphate and pyridine. The density and water of hydration are checked from preliminary experiments. The crystals are orthrhombic and of density 1.54.

The derivative tracings are recorded for both the powder specimen and single crystals. In the latter case, measurements have been taken in the three crystallographic planes ab , bc and ac rotating the crystal in each in steps of 10° with respect to the external magnetic field. In this process a series of experiments have been carried out on a number of

crystals taking particular care that the planes are properly cut in each crystal. Both the g -value and linewidth anisotropy are studied.

RESULTS ON POWDER SAMPLE

The derivative trace for the powder specimen is shown in figure 1. It is similar to that in polycrystalline copper sulphate and has a line shape corresponding to that with five points of inflection and two g -values, g_{max} and g_{min} . The g -values obtained are given in table 1.

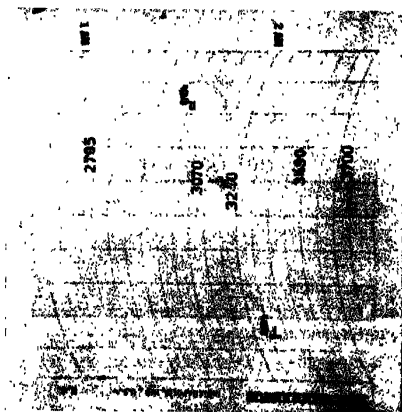


Figure 1. Derivative trace for powder specimen.

The error involved ($\delta g_{max}/g_{max}$) in this determination as calculated from the positions of the peaks of the derivatives using equation (9) of Kneübuhl's paper is found to be 0.53×10^{-3} which is well within the order of experimental error found even on measurements on single crystals.

RESULTS ON SINGLE CRYSTALS

As reported by Cannillo & Giuseppetti (1964) the copper dipyrindine sulphate dihydrate crystal belongs to the orthorhombic class of space group $Pbcn$, the lattice constants being

$$a = 15.43 \text{ \AA} \quad b = 14.34 \text{ \AA} \quad c = 6.85 \text{ \AA}$$

The unit cell contains four molecules. According to this structure, the inequivalent copper ions are adjacent to two water molecules and to two nitrogen atoms of the pyridine ring occupying the corners of a square

and presenting two longer bonds with two oxygens of the SO_4 tetrahedron, to form a slightly distorted octahedron.

At first Schonland's (1959) method of calculation of principal g -values has been attempted, since this may be applicable to a general case where no obvious axis or plane of symmetry can be distinctly defined. The difficulty however in applying this method in the present case is that there are two magnetically inequivalent sites in the lattice and these are not distinctly resolvable in the present ESR spectrum. Hence the following procedure is adopted in the interpretation of the results.

From the above description of the copper environment, it has been first assumed that the paramagnetic ion might possess a rhombic crystalline electric field symmetry. But the experiments gave g -variation in three planes contrary to the above expectation, unlike in the case of copper ammonium chloride and isomorphous salts (Narasimhamurthy & Premswarup 1964).

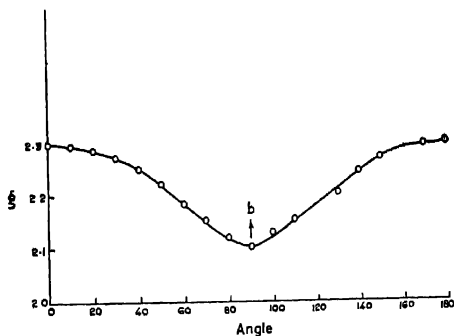


Figure 2. Angular variation of g -value in bc plane,

A scrutiny of the g -variation in the three plane in figure 2 (showing the variation in the bc plane) has suggested a tetragonal symmetry of the crystalline electric field; the tetragonal axis is the line $\text{O}_1-\text{Cu}-\text{O}_1$ in the ac plane and makes about 11° with the c -axis according to the crystal structure. This leads to a tetragonal symmetry in g -tensor. The g^2 value at any angle is then given by the equation

$$g^2 = g_{\parallel}^2 \cos^2 \theta + g_{\perp}^2 \sin^2 \theta$$

Where θ is the angle between the applied magnetic field and the tetragonal axis. This holds good for each of the ions. Then the principal g -values for unresolved peak are,

$$g_a = (g_{\parallel}^2 \sin^2 \alpha + g_{\perp}^2 \cos^2 \alpha)^{1/2}$$

$$g_b = g_{\perp}$$

$$g_c = (g_{\parallel}^2 \cos^2 \alpha + g_{\perp}^2 \sin^2 \alpha)^{1/2}$$

where g_a , g_b , and g_c are the ionic g -values along the three crystallographic axes, because all the paramagnetic ions are magnetically equivalent along the crystallographic axes.

Because the crystallographic b -axis is perpendicular to the tetragonal axis, the g -value along this axis has been taken as g_{\perp} value and from the above equations the g_{\parallel} and α have been obtained and presented in table 1 along with the values of the powder sample.

TABLE 1. PRINCIPAL g -VALUES IN COPPER DIPYRIDINE SULPHATE DIHYDRATE

Results from single crystal	Results from powder
$g_a = 2.115$	
$g_b = 2.100$	$g_{\max} = 2.30$
$g_c = 2.295$	$g_{\min} = 2.08$
$g_{\parallel} = 2.31$	
$g_{\perp} = 2.10$	
$\alpha = 11^\circ$ from crystal structure.	
$\alpha = 15^\circ$ from experiments.	

VARIATION OF LINEWIDTH

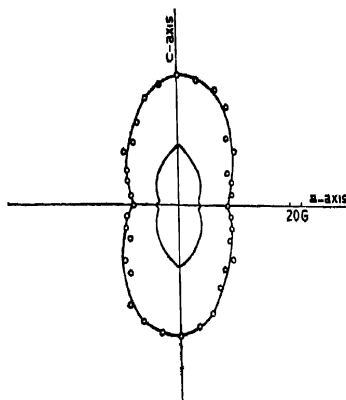
The linewidth ΔH has shown anisotropy with orientation as indicated in figure (3). An approximate estimate of the variation of the linewidth is made, using Van Vleck's (1948) formula, including the term for unlike spins.

$$(\Delta H^2)_{ss} = 3/4 g^2 \beta^2 S(S+1) \sum_j (1 - 3 \cos^2 \theta_{ij})^2 r_{ij}^{-6} \\ + 1/3 g'^2 \beta'^2 S'(S'+1) \sum_k (1 - 3 \cos^2 \theta_{ik})^2 r_{ik}^{-6}$$

Contributions both from equivalent and non-equivalent ions have been estimated. The calculated variation is shown in figure 3, together with the observed variation. A fair agreement is clearly seen.

Assuming a simple cubic lattice and neglecting the spin-lattice interaction contribution, the exchange frequency is estimated. (Anderson & Weiss 1953 and Locher & Gorter 1962). The full linewidth is given by

$$\Delta H = 2 \left[\frac{10 H_p^2}{3 H_c} \right]$$



ΔH. VARIATION IN ac-PLANE.

Figure 3. Linewidth variation in ac plane.

where the contributions due to dipolar and exchange interactions respectively are given by

$$H_p^2 = 5.1 \left(g\beta \frac{N\rho}{M} \right) S(S+1)$$

$$H_e = [2.83 S(S+1)]^{1/2} J/g\beta$$

Substituting the values along the crystallographic *b*-axis, $g=2.10$, $\Delta H=120$, the value of exchange frequency is obtained as 0.07 cm^{-1} ; this is less than 0.15 cm^{-1} found for copper sulphate pentahydrate (Bagguley & Griffiths 1950).

ACKNOWLEDGEMENT

The author is deeply indebted to Prof. K. R. Rao for his constant guidance throughout the work.

REFERENCE

- Abe, H. & Ono, K. 1956 *J. Phys. Soc. Japan* **11**, 949, 896.
- Anderson, P. W. & Weiss, P. R. 1953 *Rev. Mod. Phys.* **25**, 269.
- Bagguley, D. M. S. & Griffiths, J. H. E. 1950 *Proc. Roy. Soc.* **201**, 366.
- Cannillo, E. & Giuseppetti, G. 1964 *Lineari Rend. Sci. Fis. Matnat*, **36**, 878.
- Geramann, H. R. & Swalen, J. D. 1962 *J. Chem. Phys.* **36**, 3221.
- Kneubuhl, F. K. 1960 *J. Chem. Phys.* **33**, 1074.
- Locher, P. R. & Gorter, C. J. 1962 *Physica* **28**, 797.
- Narsimhamurthy, A. 1963 *Ind. J. Pure and Appl. Phys.* **1**, 140.
- Narsimhamurthy, A. & Premwarup, D. 1964 *Proc. Phys. Soc.* **83**, 199.
- Schonland, D. C. 1959 *Proc. Phys. Soc.* **73**, 788.
- Van Vleck, J. H. 1948 *Phys. Rev.* **74**, 1168.

Mean scattering cross-section of radiation during diffusion

By R. C. MOHANTY

Ulrica College of Arts and Science, Syracuse University, U. S. A.

(Received 20 November 1969)

In this paper, a general discussion for mean scattering cross-section for radiation during diffusion is presented. Necessary general formulas are derived for mean number of scatterings and application is made to one dimensional medium in which radiation of constant frequency undergoes diffusion.

INTRODUCTION

A knowledge of the mean time for which radiation is present in a medium is needed to determine the time for the establishment of radiative equilibrium in the medium. Determination of this mean time depends on a knowledge of the mean number of scatterings of the radiations in the medium. No work has been done towards the determination of the mean number of radiation scattered in a homogeneous medium during their diffusion. For this purpose in this paper necessary general formulae have been derived and application has been made to a one dimensional medium in which monoenergetic radiation undergo diffusion.

Let us consider (Sobolev 1956) a homogeneous medium which can absorb a radiation incident at any point on it and can scatter the incident radiation with a probability p , which is a constant throughout the medium under consideration, filling a volume v .

If Q is taken as the probability that the radiation absorbed at a particular point during diffusion will leave the medium. Then $1-Q$ is the probability that it will be absorbed. This probability Q is a function of the shape, optical dimension of the given volume v , parameter p , and of the coordinates of the point at which the original radiation-absorption took place. Let the mean number of scatterings of a radiation coming out of the medium be denoted by 0p_1 and let the mean number of scatterings of an annihilated radiation during diffusion be denoted by 0p_2 .

Then the mean number of scatterings of radiation ${}^0p = {}^0p_1 Q + {}^0p_2 (1-Q)$
...(1)

An expansion of Q as a power series in p yields :

$$Q = pQ_1 + p^2Q_2 + p^3Q_3 + \dots \quad \dots(2)$$

These terms on the right hand side successively give the probability of a radiation going out of the medium after first, second, third scatterings, etc. We can then write

$${}^0p_1 = \frac{1}{Q} (pQ_1 + 2p^2Q_2 + 3p^3Q_3 + 4p^4Q_4 + \dots) \quad \dots(3)$$

$$\text{Equation (2) gives us } {}^0p_1 = p \frac{\partial \ln Q}{\partial p}. \quad \dots(4)$$

Writing ${}^0p = 1 + p(1 - Q_1) + p^2(1 - Q_1 - Q_2) + \dots$, \dots (5)
we get mathematical expectation of first, second, third scatterings, etc., given successively by the first, second, third, etc., terms on the right hand side of equation (5).

$$\text{But } Q_1 + Q_2 + Q_3 + \dots = 1$$

Combining this with equation (2) we can write

$$\begin{aligned} 1 - Q &= (1-p)Q_1 + (1-p)^2Q_2 + (1-p)^3Q_3 + (1-p)^4Q_4 + \dots \\ \text{or } 1 - Q &= (1-p) \{Q_1 + (1+p)Q_2 + (1+p+p^2)Q_3 + \dots\} \\ &= (1-p) \{1 + p(1 - Q_1) + p^2(1 - Q_1 - Q_2) + \dots\} \end{aligned} \quad (6)$$

A comparison between (5) and (6) gives

$$1 - Q = {}^0p(1 - p)$$

Therefore

$${}^0p = \frac{1 - Q}{1 - p} \quad \dots(7)$$

Substituting (7) and (4) in (1) we have

$${}^0p_1 = \frac{1}{1 - p} + p \frac{\partial \ln(1 - Q)}{\partial p} \quad \dots(8)$$

Using (4), (7), and (8) we have

$${}^0p_1 = \frac{P^0p}{1 - (1 - p)^0p} \left[1 - (1 - p) \frac{\partial \ln {}^0p}{\partial p} \right] \quad \dots(9)$$

and

$${}^0p_1 = 1 + p \frac{\partial \ln {}^0p}{\partial p} \quad \dots(10)$$

Equation (9) and (10) show that a knowledge of 0p gives us 0p_1 and 0p_2 . An examination of (7) shows that for pure scattering 0p is indeterminate for pure scattering $p = 1$; expansion gives therefore ${}^0p = \frac{\partial Q}{\partial p}$,

To consider various sources of radiation, let Q^* stand for number of scatterings of photons in the entire medium due to any radiation source. Let β be the volume absorption co-efficient in the medium and $f\beta dv$ be the number of photons from the sources of radiation absorbed in the volume dv , f , here can be due to radiation sources outside and inside the medium.

Then total number of radiation absorbed in the medium = $\int f \beta dv$ and the fraction coming out of the medium is given by

$$\frac{\int Q f \beta dv}{\int f \beta dv} \quad \dots(11)$$

Let ${}^o p_1^+$ and ${}^o p_2^+$ stand for mean number of scatterings experienced by photons which came out and those which are annihilated, respectively. Then the mean number of scatterings undergone by all the photons absorbed in the medium

$${}^o p^+ = \frac{\int (1-Q) f \beta dv}{(1-p) \int f \beta dv} \quad \dots(12)$$

or

$${}^o p^+ = \frac{1}{1-p} [1 - \int Q f \beta dv / \int f \beta dv]$$

Using

$$\frac{Q f \beta dv}{\int f \beta dv} = Q^+$$

we can write

$${}^o p^+ = \frac{1-Q^+}{1-p} \quad \dots(13)$$

Then

$${}^o p_1^+ = \frac{p \partial \ln Q^+}{\partial p} \quad \dots(14)$$

$${}^o p_2^+ = \frac{1}{1-p} + p \frac{\partial \ln (1-Q^+)}{\partial p} \quad \dots(15)$$

f , in equation (11) can be simply written as $\frac{P}{4\pi} f = F$, if the sources

of radiation are situated inside the medium and if these sources radiate isotropically, then $F \beta dv$ gives the number of photons emitted by the element of volume dv per unit solid angle. So we can write

$$Q^+ = \frac{\int Q F \beta dv}{\int F \beta dv} \quad \dots(16)$$

Here we have this equation in place of equation (11). Q^+ is the fraction of photons which emerge from the medium for the stipulated radiation sources.

APPLICATION TO ONE DIMENSIONAL SEMI-INFINITE MEDIUM

During an elementary event, let us assume that the radiation, are emitted with equal probability in either direction with constant frequency.

*The function Q was used before to express number of scatterings of radiation absorbed at a particular point in the medium.

Let $Q(h)$ be the probability of emergence of a radiation absorbed in the medium at the depth h .

$$\text{Then } Q(h) = \frac{p}{2} \int_0^\infty -e^{(h-t)} Q(t) dt + \frac{p}{2} e^{-h} \quad \dots (17)$$

$$\text{Solution to equation (17) takes the form : } Q(h) = (1-k)e^{-kh} \quad \dots (18)$$

where $k = \sqrt{1-p}$

Substituting (18) into (7), (4), and (8) we have

$${}^0p(h) = 1 - (1-k)e^{-kh} \quad \dots (19)$$

$${}^0p_1(h) = \frac{1}{2k} (1+k+p h) \quad \dots (20)$$

and

$${}^0p_2(h) = \frac{1}{1-p} - \frac{p}{2k} [1 + (1-k)h] \frac{e^{-kh}}{1-(1-k)e^{-kh}} \quad \dots (21)$$

When radiation absorption takes place at the boundary of the medium we have for $h = 0$,

$${}^0p(0) = \frac{1}{(1-p)1/2} \quad \dots (22)$$

$${}^0p_1(0) = \frac{1}{2} \left(\frac{1}{(1-p)^{1/2}} + 1 \right) \quad \dots (23)$$

$${}^0p_2(0) = \frac{1}{1-p} \left(1 - \frac{p}{2} \right) \quad \dots (24)$$

We have for $p < 1$ and h quite large from equations (19) and (21),

$${}^0p(h) \simeq {}^0p_1(h) \simeq \frac{1}{1-p} \quad \dots (25)$$

$$\text{and equation (20) gives } {}^0p_1(h) \simeq \frac{ph}{2\sqrt{1-p}} \quad \dots (26)$$

Substitution of numerical values for p in equations (22), (23), and (24) will produce considerably different values for ${}^0p_1(0)$, the mean number of scatterings for radiation going out of the medium, for ${}^0p_2(0)$ the mean number of annihilated photons, and for ${}^0p(0)$ the total number of photons in question. Again the last equation shows that the mean number of scatterings of radiation which undergoes absorption at large h and which emerges from the medium is proportional to the depth h . Again the mean number of scatterings for radiation which emerges from the medium will be much greater than the annihilated radiation for extremely large values of h .

For any source of radiation : Let the sources of radiation be located outside the medium and let radiation of intensity I_0 be incident on the boundary of this medium. We can write $f(h) = I_0 e^{-h}$ and

$$Q^* = \int_0^{\infty} Q(h) e^{-h} dh = \frac{1-k}{1+k} \quad \dots(27)$$

Substitution of (27) into (13), (14), and (15) gives

$$\sigma_{p^+} = \frac{2}{p} \left(\frac{1}{(1-p)^{1/2}} - 1 \right) \quad \dots(28)$$

$$\sigma_{p^+} = \frac{1}{(1-p)^{1/2}} \quad \dots(29)$$

and

$$\sigma_{p^+} = \frac{1+(1-p)^{1/2}}{2(1-p)} \quad \dots(30)$$

These equations show that for pure scattering, i.e. for $p = 1$, the mean number of scatterings for radiation or for photons in general in a semi-infinite medium is very great. This is true for any radiation sources.

REFERENCE

Sobolev V. V. 1956 *Radiative Transfer in Stellar and Planetary Atmospheres*, Moscow.

Force field for germylacetylene

By K. RAMASWAMY AND V. BALASUBRAMANIAN

Department of Physics, Annamalai University, Annamalai Nagar

(Received 7 November 1969.)

Approximate force field for germylacetylene was attempted using the kinematic methods suggested by Torkington (1949) and Herranz & Castano (1966). The former method was found to give a satisfactory force field for this molecule.

INTRODUCTION

The well known basic equations (Wilson, 1955) in molecular force field calculations are,

$$L \tilde{L} = G \quad \dots(1)$$

$$\tilde{L} FL = A \quad \dots(2)$$

and

$$GFL = LA \quad \dots(3)$$

where L is the transformation matrix between the set of symmetry coordinates and the normal coordinates, F and G refer to the potential and inverse kinetic energy matrices and A a diagonal matrix with the element $A_k = 4\pi^2\nu_k^2 c^4$, where ν_k is the k^{th} vibrational wavenumber and c is the velocity of light in cm sec^{-1} . It is seen from the above equations that the matrix L assumes importance in the determination of a unique set of force constants. The kinematic methods (Torkington 1949, Herranz & Castano 1966 and Biles 1966) are those which give the values of the L matrix elements consistent with the equations (1) to (3), purely from the geometry of the molecule without any assumptions regarding the force constants. In a previous paper (Ramaswamy & Balasubramanian 1969) approximate force fields for the germyl halides using the above kinematic methods were attempted and Torkington's method was found to give a better approximation to the correct force field for the two heavier molecules GeH_3Br and GeH_3I while the method suggested by Herranz & Castano gave a close approximation to the correct force field for the two lighter molecules GeH_3Cl and GeH_3F . This paper deals with the force field for germylacetylene by the first two methods.

POTENTIAL ENERGY CONSTANTS

In the method suggested by Torkington (1949) the product of the matrices G and F is triangular and the L matrix obtained as the eigen

vector of GF is also triangular. In the method suggested by Herranz & Castano (1966) the L matrix is defined as,

$$L = BM^{1/2} \tilde{B} \quad \dots(4)$$

where B is an orthogonal matrix which diagonalises G and M is a diagonal matrix with the reciprocals of the eigen values of G as its elements.

Germylacetylene belongs to the C_{3v} point group and its infrared spectrum was reported by Lovejoy & Baker (1967). Its microwave spectrum was given by Thomas & Laurie (1966). The structural data and the vibrational frequencies used in the calculations are given in table 1. The symmetry coordinates used are the same as those of Sathianandan & Margrave (1963). The values of important valence force constants obtained in the two methods are presented in table 2.

TABLE 1. OBSERVED FREQUENCIES IN WAVE NUMBERS AND STRUCTURAL PARAMETERS FOR GeH_3CCH

Observed frequencies in cm^{-1} (Lovejoy & Baker, 1967)		Structural data (Thomas & Laurie, 1966)
α_1 species	e species	
ν_1 3313.5	ν_6 2117.2	$d(\text{Ge-H}) = 1.521 \text{ \AA}$
ν_2 2120.0	ν_7 886.0	$r_1(\text{Ge-C}) = 1.896 \text{ \AA}$
ν_3 2060.0	ν_8 673.0	$r_2(\text{C-C}) = 1.208 \text{ \AA}$
ν_4 843.8	ν_9 643.8	$r_3(\text{C-H}) = 1.056 \text{ \AA}$
ν_5 530.0	ν_{10} 216.4	$\angle(\text{H-Ge-H}) = 109^\circ 54'$
		$\beta(\text{H-Ge-C}) = 109^\circ 2'$
		$\phi(\text{Ge-C-C}) = 180^\circ$
		$\theta(\text{C-C-H}) = 180^\circ$

MEAN AMPLITUDES

The various bonded mean amplitudes were calculated by the method of Cyvin (1959) and the nonbonded ones by the method of Ramaswamy *et al* (1962). The important mean amplitudes obtained in the first method are given in table 3.

TABLE 2. VALENCE FORCE CONSTANTS
IN MDYN FOR/Å GeH_9CCH

Valence force constant	Method I ^a	Method II ^b
f_{r_1}	6.1161*	6.2609
f_{r_2}	16.4557	24.1624
f_{r_3}	3.1112	7.4759
f_d	2.6276	2.6286
$f_{r_1 r_2}$	1.2742	2.5875
$f_{r_1 r_3}$	1.6183	11.4762
$f_{r_2 d}$	0.0135	0.0964
f_{dd}	0.0146	0.0156
$f_{\alpha} - f_{\alpha\alpha}$	0.1905	0.1957
$f_{\beta} - f_{\beta\beta}$	0.1951	0.2050
f_{θ}	0.1775	0.1939
f_{ϕ}	0.0739	0.0906
$f_{d\alpha}$	0.0059	0.0181
$f_{d\beta}$	0.0056	0.0264

^aMethod of 'Progressive rigidity' suggested by Torkington^bMethod of 'characteristic set of valence coordinates' suggested by Herranz and Castano.

*As under table 3

TABLE 3. VIBRATIONAL MEAN AMPLITUDES OF
 GeH_9CCH AT 298.16°K.

Pair	Mean amplitudes (Å)	Mean amplitudes for similar types of bonds in different molecules.		
		Mean amplitudes (Å)	Molecule	Reference
C-H	0.0740*	0.0743	C_2H_2	Bakken (1958)
$\text{C}\equiv\text{H}$	0.0366	0.0357	C_2H_2	Bakken (1958)
Ge-C	0.0484	—	—	—
Ge-H	0.0895	0.0895	GeH_4	Cyvin (1968)
H...H.	0.1540	0.1525	GeH_4	Cyvin (1968)
H...C	0.1318	—	—	—

*This number of significant figures is retained to secure internal consistency in the calculations.

ROTATIONAL DISTORTION CONSTANTS

The centrifugal stretching constants D_J , D_{JK} and D_K were calculated using the relations given by De Alti *et al* (1965). The values are presented in table 4.

TABLE 4. ROTATIONAL
DISTORTION CONSTANTS
IN KC/SEC. FOR GeH_3CCH

Quantity	Calculated	Observed
D_J	0.6565*	—
D_{JK}	26.6906	38
D_K	802.9760	—

CORIOLIS COUPLING CONSTANTS

The ζ^t values for the perpendicular modes of vibration were calculated using the relations given by Meal & Polo (1965). The values are presented along with the experimentally observed values. The ζ sum rule for this molecule is,

$$\sum_i \zeta_i = \frac{I_A}{2I_B} + 2 \quad \dots(5)$$

where, I_A and I_B are the principal components of the moment of inertia tensor.

TABLE 5. CORIOLIS COUPLING
CONSTANTS ζ FOR GERMYLACETYLENE

	Calculated	Observed
ζ_6	0.0183*	-0.052
ζ_7	-0.2043	-0.266
ζ_8	1.0000	—
ζ_9	0.2579	0.364
ζ_{10}	0.9503	—
$\sum_i \zeta_i$	2.0222	
$(I_A/2I_B) + 2$	2.0222	

*As under table 3

DISCUSSION

The method of Torkington (1949) gives for the $\text{C}\equiv\text{C}$ stretching and $\text{C}-\text{H}$ stretching force constant values of 16.4557 mdyn/ \AA and 6.1161 mdyn/ \AA while the method given by Herranz & Castano (1966) gives the values of 24.1624 mdyn/ \AA and 6.2609 mdyn/ \AA , respectively. The first set is comparable with the values of 15.80 mdyn/ \AA and 6.442 mdyn/ \AA obtained by Daykin *et al* (1962) for methylacetylene and 15.59 mdyn/ \AA and 5.87 mdyn/ \AA of Duncan (1964) for silylacetylene. For $\text{Ge}-\text{C}$ bond stretching we obtain values of 3.1112 mdyn/ \AA and 7.4759 mdyn/ \AA in the two methods, respectively. The first value is closer to the value of 2.87 mdyn/ \AA obtained by Clark & Weber (1966) for methylgermane. The second method gives an abnormally high value of 11.4762 mdyn/ \AA for the interaction force constant $f_{r_1 r_2}$. The other bending, stretching and interaction force constants are of comparable magnitude in both the methods as seen from table 2. They are also consistent with the values obtained for germylhalides in our previous study. The second method gives quite large values for the various force constants of the linear skeleton $\text{Ge}-\text{C}\equiv\text{C}-\text{H}$, barring the $\text{C}-\text{H}$ stretching. High values for interaction force constants were also obtained by Ramaswamy & Srinivasan (1967, 1969) for the linear molecules like cyanoacetylene, diacetylene and dicyanoacetylene. They attributed these high values to the high degree of conjugation, and electron transfer in those molecules. Here the linear skeleton $\text{Ge}-\text{C}\equiv\text{C}-\text{H}$ is not a conjugated system and hence the second method is quite unsatisfactory in describing the force field for this molecule. So the other molecular constants were found using only the L matrix obtained in the first method.

From table 3 it is seen that the mean amplitudes of vibration for the bonds $\text{C}-\text{H}$ (0.0740 \AA) and $\text{C}\equiv\text{C}$ (0.0366 \AA) are comparable with the values of 0.0743 \AA and 0.0357 \AA obtained by Bakken (1958) for C_2H_2 . The bonded $\text{Ge}-\text{H}$ (0.0895 \AA) and the nonbonded $\text{H}\cdots\text{H}$ (0.1540 \AA) mean amplitudes are also comparable to the values of (0.0895 \AA) and (0.1525 \AA) for GeH_4 obtained by Cyvin (1968). These values are also consistent with the values obtained for germylhalides in our earlier study.

The value of the centrifugal stretching constant D_{JK} (26.6906 kc/sec) is low compared to the value of 38 kc/sec obtained by Thomas & Laurie (1966) from microwave studies of germylacetylene. The difference might be due to the approximate description of the normal modes.

Lovejoy & Baker (1967) from the analysis of perpendicular band contours of the infrared spectrum of germylacetylene reported the values of ζ_6 , ζ_7 and ζ_9 . From the sum rule, $\zeta_8 + \zeta_{10}$ was calculated to be 1.975.

Further, they predicted ζ_8 and ζ_{10} to be approximately equal and slightly less than one. In similar molecules like silylacetylene (Reeves *et al* 1964) and methylacetylene (Thomas & Thompson 1968) the sum of the above two corresponding ζ elements is 1.89. For methylacetylene the two ζ 's have the values of 1 and 0.89 respectively. The values ζ_8 (1) and ζ_{10} (0.95) of the present study are close to those predicted by Lovejoy & Baker (1967). The value of ζ_6 (0.0183) and ζ_7 (-0.2043) are consistent with the values obtained for similar motions in the germylhalides. As for the germylhalides, here also the individual ζ values differ from the observed values. The ζ sum rule is thus verified.

CONCLUSION

Of the two kinematic methods the above study shows the method of 'Progressive rigidity' suggested by Torkington as the most satisfactory in describing the force field for this molecule. However, as shown by the values of the ζ elements and the centrifugal stretching constant, the solution to the force field is only an approximate one. This may be due to the approximate L matrix which is derived entirely from the geometry of the molecule.

ACKNOWLEDGEMENT

One of the authors (V. B.) is grateful to the Council of Scientific and Industrial Research, New Delhi, for financial assistance by the award of a Junior Research Fellowship.

REFERENCES

- Bakken J. 1958 *Acta Chem. Scand.*, **12**, 594.
Biles F. 1966 *Acta. Chim. Acad. Sci. Hung.*, **47**, 53.
Cyvin S. J. 1959 *Acta. Chem. Scand.*, **13**, 2135.
1968 *Molecular vibrations and Mean square amplitudes*, Universitiet forlaget, Oslo.
Clark A. & Alfons Weber. 1966 *J. Chem. Phys.*, **45**, 1759.
Daykin P. N., Sundaram, S. & Cleveland F. F. 1962, *J. Chem. Phys.*, **37**, 1087.
Duncan J. L. 1964 *Spectrochim. Acta*, **20**, 1807.
Gian Carlo De Altì Vinicio Galasso & Giacomo Costa 1965 *Spectrochim Acta* **21**, 649.
Herranz J. & Castano F. 1966 *Spectrochim. Acta*, **22**, 1965.
Lovejoy, R. W. & Baker D. R. 1967 *J. Chem. Phys.*, **46**, 658.
Meal J. H. & Polo S. R. 1956 *J. Chem. Phys.*, **24**, 1119.
Ramaswamy K. & Balasubramanian V. *Ind. J. Phys.* (In press)

- Ramaswamy K. Sathianandan K. & Cleveland F. F. 1962 *J. Mol. Spectry.*, **9**, 107.
- Ramaswamy K. & Srinivasan K. 1967 *Aust. J. Chem.*, **21**, 575.
1969 *Aust. J. Chem.*, **22**, 1123
- Sathianandan K. & Margrave J. L. 1963 *J. Mol. Spectry.*, **10**, 442.
- Thomas E. C. & Laurie W. 1966 *J. Chem. Phys.*, **44** 2602
- Thomas R. K. & Thompson H. W. 1968 *Spectrochim. Acta*, **24A**, 1337.
- Torkington P. 1949 *J. Chem. Phys.*, **17**, 1026.
- Wilson E. B. Jr., Decius J. C. & Cross P. C. 1955 *Molecular Vibrations*, McGraw Hill,
New York.

Vibrational transition probabilities of the bands of BO - α System.

By A. P. WALVEKAR

Department of Physics, Bangalore University, Bangalore.

(Received 3 October 1969—Revised 28 November 1969)

Franck-Condon factors have been computed by Bates' method (1949). These results have been used along with the already available experimental data from the work of Elliot (1933) to evaluate a relation between R_e , the electronic transition moment and r , the internuclear separation, in the form.

$$R_e(r) = \text{Constant} (1 - 0.4584r)$$

This relation has been used to obtain improved Franck-Condon factors.

Robinson & Nicholls (1960) have reported the value of coefficient p as 1.66. A check has been made on this value by using their data and we obtained the result as 0.3954 instead. It is shown that the coefficient 0.4584 gives a better approach towards theoretical values.

INTRODUCTION

The study of molecular spectra has been a powerful tool in the investigation of astrophysical problems. The recent improvements in the basic theoretical concepts have enhanced its importance.

The BO molecule is an astral molecule. The quantitative experimental data available from the old work of Elliot (1933) reproduced in table 1, is subjected to verification by theoretical study. The accuracy in the measurement of intensities as stated by Elliot is $\pm 5\%$. Intensity values of Robinson & Nicholls (1960) and of Elliot (1933) are nearly identical.

THEORETICAL COMPUTATIONS

Anharmonic wave-functions have been computed by treating the diatom as anharmonic oscillator. These in turn are used to evaluate the Franck-Condon factors. The numerical integration method of Bates (1949) is used for this purpose. The results of these calculations are provided in table 1. The constants from Herzberg's compilation are used in the computations.

TABLE 1

Band	Intensity	F.C. Factors	r-centroids
0,0	4.6	0.0386	1.275
0,1	9.2	0.1427	1.301
0,2	8.5	0.2443	1.328
0,3	6.0	—	1.357
1,0	9.5	0.1015	1.257
1,1	10.0	0.1683	1.241
1,2	3.8	0.1007	1.310
2,0	8.9	0.1586	1.241
2,1	4.4	0.1103	1.266
2,2	—	—	1.294
2,3	—	—	1.319

r-centroids

The r -centroids are essential for the study of variation of electronic transition moment. As it is the object of this work to take into account the contribution of electronic transition moment to the vibrational transition probability, r -centroids have been evaluated by the quadratic equation method of Nicholls & Jarman (1956). The results are reproduced in table 1.

R_s — r RELATION

r -centroids so obtained have been used along with the experimental intensity measures, to obtain the following relation between R_s and r . In the absence of theoretical method of obtaining a relation between R_s and r , the semi-empirical method due to Nicholls & Jarman (1956) is used.

$$R_s(r) = \text{const.} (1 - 0.4584r)$$

Using the relation the Franck-Condon factors have been smoothed out. These results are listed in column 4 of table 2.

Table 2 shows the comparison of Franck-Condon factors with the experimental (I/ν^4) values, where I is the intensity and ν the band frequency. These quantities have been expressed in terms of the values for the first band in each progression. The ratios of I/ν^4 values with the Franck-Condon

factors for anharmonic oscillator are designated as δ_{AH} and those for the smoothed values as δ smoothed.

TABLE 2. TRANSITION PROBABILITIES BO - π SYSTEM

Progression	V''	δ_{AM}	δ smoothed ($\rho=0.4583$)	δ smoothed ($\rho=0.3954$)
$V'=0$	0	1	1	1
	1	0.9241	0.939	0.918
	2	0.6708	0.76	0.733
	3	0.7375	0.894	0.845
	4	0.775	1.01	0.928
$V'=1$	0	1	1	1
	1	0.8704	0.91	0.903
	2	1.184	1.32	1.291
$V'=2$	0	1	1	1
	0	1.198	1.28	1.251
	3	1.769	1.699	2.026
	4	2.925	3.756	3.487

DISCUSSION

The introduction of electronic transition moment factor has improved the agreement between theory and experiment, the nearer also is the approach of ratio δ smoothed to unity.

Robinson & Nicholls (1960) have obtained from their observations the relation

$$R_e(r) = \text{const.} (1 - 1.66r).$$

The value 1.66 of ρ , the coefficient in $R_e - r$ relation, is significantly different from the present value of 0.4584. A check was made on their value by using their data. This gave the result as

$$R_e(r) = \text{const.} (1 - 0.3954r)$$

This value of ρ is very close to the value derived by the author. To have a further check on these ρ - values the smoothed transition probabilities using this coefficient in $R_e(r)$ variation are reduced and entered in table 2, column 5. The results show a better approach towards theoretical values by the use of coefficient 0.4583 than by the use of constant 0.3954.

Re-checking was made on Robinson & Nicholls value a number of times. It gave the same result for ρ , i.e. 0.3954. But it was difficult to trace the point at which the mistake has occurred.

REFERENCES

- Bates, 1949 *Proc. Roy. Soc. A* **196**, 217.
Elliot 1933 *Proc. Phys. Soc.* **45**, 627.
Nicholls & Jarman, 1956 *Proc. Phys. Soc. A* **69**, 253.
Robinson & Nicholls, 1960 *Proc. Phys. Soc. A* **75**, 486.

Negative pion capture in closed shell nuclei

By B. BANERJEE

Tata Institute of Fundamental Research, Bombay, India.

(Received 28 November 1969)

The capture of bound π^- mesons by closed shell nuclei is calculated using the phenomenological Hamiltonian of Eckstein. Numerical calculations are carried out for ^{16}O and the results compared with experiments.

INTRODUCTION

The two-nucleon process from nuclei as a result of absorption of a bound π^- meson has recently attracted considerable experimental (Ozaki *et al* 1960, Fedotov 1966, Demidov *et al* 1963, Zaimidarogo 1967, Nordberg *et al* 1968) and theoretical (Ericson 1966, Jibuti & Kopaleishvili 1964, Cheon 1966, 1967, Nguyen-Truong & Sakamoto, 1967, Koltun & Reitan 1966, 1967, Spector 1964, Eisenberg & Letourneux 1967, Brueckner *et al* 1951, Eckstein, 1963, Divakaran 1965) attention. This has been prompted by the hope that this process may give information about the short-range correlation between the nucleons, since at least two nucleons must participate in the process to conserve energy and momentum. Most calculations proceed by assuming the pion-nuclear interaction to be

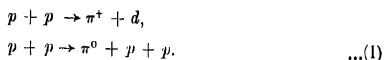
the sum of the one-body pion nucleon interaction
$$\frac{f\pi}{\mu c} \bar{\psi}_N \gamma_5 \gamma_\mu \tau \psi_N \frac{\partial \phi}{\partial x_\mu}.$$

The matrix element of the capture process is then calculated assuming a pair-correlation of the two nucleons.

This approach assumes the pion absorption to be a *two-step* process, in which nucleon 1 absorbs the pion then collides with nucleon 2 to share the momentum and since the probability of finding two nucleons close together is higher than finding more than two, the nucleons 1 and 2 leave the region of interaction without any further collisions. The difficulty in this approach is that the two steps are arbitrarily selected out of the many possible way a meson can be absorbed by the two nucleons. Moreover, even if it is allowed that it is the dominant process, we would not know how to calculate the second step since the meson physics involved is extremely complicated. In other words the conventional approach presents an oversimplified picture of the *two-body* character of the meson-nuclear interaction.

Recently Eckstein (1963) following Brueckner *et al* (1951) has proposed an alternative approach. Here the Hamiltonian describing the interaction of the π^- meson with the capturing nucleons is treated as a two-body operator and is constructed phenomenologically. The pion is assumed

to be in a relative s -state with respect to the pair of nucleons. The nucleons themselves are also in a relative s -state. The Hamiltonian contains two amplitudes corresponding to captures in 3S_1 and 1S_0 states (see sec. 2). These amplitudes are determined from the following elementary processes :



Eckstein has used this effective Hamiltonian to calculate the branching ratios of the various modes of capture in ^4He , while Divakaran (1965) has calculated the absolute capture rate in ^4He . Ericson (1963, 1964) has calculated the imaginary part of the pion-nuclear optical potential using these two-body amplitudes. This calculation has been greatly extended and generalised by Ericson & Ericson (1966) and the optical potential obtained is in very good agreement with experiments (Sens, 1968).

In this paper we calculate the ratio R of the number of neutron pairs emitted to the number of neutron-proton pairs and the angular distribution as a function of the opening angle θ between the nucleons using Eckstein's Hamiltonian and shell-model wave functions. The specific examples chosen are closed shell nuclei since the wave function for these nuclei are relatively simple. Numerical calculations are carried out for ^{16}O . We make several approximations to keep the treatment simple. These and other details of the calculation are described in the next section. It should be mentioned that Ericson (1963) has also calculated the ratio R for carbon and aluminium without, however, making any specific assumption about the nuclear wave-function. In concluding this section we would like to point out that in this approach we need assume a wave-function which describes the behaviour of the nucleons only at large separations. The correlations at short distances are taken care of by the effective Hamiltonian. Therefore, the usual harmonic oscillator wave-functions should be adequate. It is also appropriate to emphasize that since the constants of the Hamiltonian are already determined there are no free parameters in this approach. In the calculations of Jibuti & Kopaleishvili (1964), Cheon (1966, 1967), Nguyen-Truong & Sakamoto (1967) and Eisenberg & Letourneux (1967) there is usually an adjustable parameter in the correlation function.

THEORY

1. The Hamiltonian,

The two-body Hamiltonian described in the previous section has the form

$$H_{12} = \int d^3r_1 d^3r_2 \psi^\dagger(\vec{r}_1) \psi^\dagger(\vec{r}_2) M_{12} \psi(\vec{r}_1) \psi(\vec{r}_2) \quad \dots(2)$$

where $\psi^*(r)$ and $\psi(r)$ create and annihilate a nucleon at the point r and M_{12} is an operator involving the momenta, spin and isospin of particles 1 2. The form M_{12} has been extensively discussed by Eckstein (1963) and Divakaran (1965), so we shall merely state it here :

$$M_{12} = [g_0 \{ \frac{1}{2} (\vec{\tau}_1 - \vec{\tau}_2) \cdot \vec{\phi}(\vec{r}) \} \frac{1}{2} (\vec{\sigma}_1 + \vec{\sigma}_2) \cdot \vec{k} \\ + g_1 \{ \frac{1}{2} (\vec{\tau}_1 + \vec{\tau}_2) \cdot \vec{\phi}(\vec{r}) \} \frac{1}{2} (\vec{\sigma}_1 - \vec{\sigma}_2) \cdot \vec{k} \mid T_{12}^{\sigma} T_{12}^{\tau} \delta(\vec{r}_1 - \vec{r}_2) \dots (3)$$

Here $\vec{\phi}$ is the pion field operator. $\vec{\tau}_1, \vec{\tau}_2$ and $\vec{\sigma}_1, \vec{\sigma}_2$ are the isospin and spin operators respectively, of the two nucleons and \vec{k} is the relative momentum of the outgoing nucleons ; $T_{12}^{\sigma}, T_{12}^{\tau}$ are the spin, isospin triplet projection operators. The first term in equation (3) describes the transition from 3S_1 state of the two nucleons to 3P_1 state, while the second term describes the transition from 1S_0 to 3P_0 state. The amplitudes of these transitions, g_0 and g_1 , are determined from the reactions of equation (1).

2. The Absorption Rate.

Let $|i\rangle, |\psi_f\rangle, |\psi_n\rangle$ be, respectively, the initial state consisting of the pion and the ground-state of the target nucleus of A nucleons described by the wave-function $|\psi_i\rangle$, the wave-function of the two outgoing nucleons and the wave-function of the residual nucleons. The matrix element for pion capture is given by

$$T_f = \sqrt{\frac{1}{2} A(A-1)} \langle \psi_n \psi_f | H_{12} | i \rangle \dots (4)$$

Here we have neglected the antisymmetry of the emitted nucleons with the residual nucleons. This should be a good approximation considering the high momenta of the outgoing nucleons. We also neglect the interaction of the nucleons with the residual nucleons. The absorption rate is given by

$$dW = 2\pi \delta(E_n + E_f - E_i) \frac{1}{2} A(A-1) |\langle \psi_n \psi_f | H_{12} | i \rangle|^2 \\ \times \frac{\Omega d^3 k_1}{(2\pi)^3} \frac{\Omega d^3 k_2}{(2\pi)^3} \dots (5)$$

\vec{k}_1 and \vec{k}_2 are the momenta of the outgoing nucleons and Ω is the quantization volume. The energies occurring in the δ -function are

$$E_i = m_\pi + B_i \\ E_n + E_f = E_1 + E_2 - B_r + E_n + E_f,$$

where m_π is the rest mass of the pion ($\hbar = c = 1$). E_1, E_2 and E_r are, respectively, the kinetic energy of the emitted nucleons, and the residual nucleus. B_i and B_r are the binding energies of the target and residual

nuclei while E_n is the excitation energy of the latter. We have now to sum over the states n of the residual system. To do this we follow Brueckner *et al* (1951) and invoke the closure approximation, that is, assume that the states of the residual nucleus belong to a narrow range of energy defined by an average

$$\bar{E} = \langle E_n + E_r + B_i - B_f \rangle_{AV} \ll m_\pi. \quad \text{Carrying out the sum over } n$$

in (4) with this assumption we get

$$dW = 2\pi\delta(E - \bar{E}) \frac{\Omega d^3k_i}{(2\pi)^3} \frac{\Omega d^3k_f}{(2\pi)^3} u \quad \dots(6)$$

where

$$E = E_1 + E_2 - m_\pi$$

and

$$u = \frac{1}{2} A (A-1) \int dx_1' dx_2' \int dx_1 dx_2 \int dx_3 \dots dx_A \phi_\pi^* (x_1) \phi_\pi (x_1') \\ \times \psi_{if}^* (x_1, x_2) M_{12} \psi_i (x_1, x_2, x_3, \dots, x_A) \psi_f^* (x_1', x_2', x_3, \dots, x_A) \\ M_{12}^+ \psi_f (x_1', x_2') \quad \dots(7)$$

Here x_i stands for the discrete and the continuous variables and the integration sign includes the summation over the discrete variables. ϕ_π is the wave-function of the bound pion.

We shall now specialize to the case of a closed shell nucleus. We can therefore choose for ψ_i a single determinant constructed with harmonic oscillator functions $\phi_\alpha(\vec{r})$ where α stands for (nlm) which specify the orbit and τ , the charge of the particle. Then the two-particle density matrix ρ given by

$$\rho(x_1', x_2', x_1, x_2) = \frac{1}{2} A (A-1) \int dx_3 \dots dx_A \psi_i(x_1, x_2, x_3, \dots, x_A) \\ \psi_i^*(x_1', x_2', x_3, \dots, x_A) \\ = \frac{1}{2} \sum_{\alpha\beta} \phi_\alpha^*(\vec{r}_1') \phi_\beta^*(\vec{r}_2') \{ \phi_\alpha(\vec{r}_1) \phi_\beta(\vec{r}_2) - \phi_\alpha(\vec{r}_2) \phi_\beta(\vec{r}_1) \} \\ \dots(8)$$

The final-state wave function ψ_f of the outgoing nucleons is given

$$\psi_f(12) = \frac{1}{\Omega} \exp i(\vec{K} \cdot \vec{R} + \vec{k} \cdot \vec{r}) \chi_{S_f M_f} \xi_{T_f \lambda_f} \quad \dots(9)$$

where $\chi_{S_f M_f}$ and $\xi_{T_f \lambda_f}$ are, respectively, the spin and isospin functions of the two particles. Here

$$\vec{K} = \vec{k}_1 + \vec{k}_2, \quad \vec{k} = \frac{1}{2}(\vec{k}_1 - \vec{k}_2) \\ \vec{R} = \frac{1}{2}(\vec{r}_1 + \vec{r}_2), \quad \vec{r} = \vec{r}_1 - \vec{r}_2$$

Substituting equation (9) in (7) and carrying out the sums over the isospin quantum numbers we obtain for the capture in 3S_1 and 1S_0 states of the pair, respectively,

$$u_0 = \frac{1}{2\Omega^2} g_0^2 F_1(\vec{k}, \vec{K}) \quad \dots(10a)$$

$$u_1 = \frac{1}{2\Omega^2} g_1^2 F_2(\vec{k}, \vec{K}) \quad \dots(10b)$$

where,

$$F_1(\vec{k}, \vec{K}) = \sum_{\alpha\beta} \int d^3r d^3r' e^{i\vec{k} \cdot (\vec{r}-\vec{r}') + i\vec{K} \cdot \vec{r}} \phi_{\alpha}^*(\vec{r}') \phi_{\beta}^*(\vec{r}) \phi_{\pi}^*(\vec{r}) \times \left\{ \frac{1}{2} (\vec{\sigma}_1 + \vec{\sigma}_2) \cdot \vec{k} \right\} \phi_{\alpha}(\vec{r}) \phi_{\beta}(\vec{r}) \phi_{\pi}(\vec{r}) \quad \dots(11)$$

and

$$F_2(\vec{k}, \vec{K}) = \sum_{\alpha\beta} \int d^3r d^3r' e^{i\vec{k} \cdot (\vec{r}-\vec{r}') + i\vec{K} \cdot \vec{r}} \phi_{\alpha}^*(\vec{r}') \phi_{\beta}^*(\vec{r}) \phi_{\pi}^*(\vec{r}) \times \left(\frac{1}{2} (\vec{\sigma}_1 - \vec{\sigma}_2) \cdot \vec{k} \right) \phi_{\alpha}(\vec{r}) \phi_{\beta}(\vec{r}) \phi_{\pi}(\vec{r}) \quad \dots(12)$$

The integral over the space coordinates can be carried out by expanding the exponential in spherical harmonics and integrating over the angles. Substituting equations (10a) and (10b) in (6) we obtain the absorption rates,

$$dW_0 = 2\pi\delta(E - \bar{E}) g_0^2 F_1(k, K) \frac{d^3k_1}{(2\pi)^3} \frac{d^3k_2}{(2\pi)^3} \quad \dots(13a)$$

$$dW_1 = 2\pi\delta(E - \bar{E}) g_1^2 F_2(k, K) \frac{d^3k_1}{(2\pi)^3} \frac{d^3k_2}{(2\pi)^3} \quad \dots(13b)$$

The expression for the capture rate is thus given simply as product of three factors : phase-space, the probability of transition of the capturing nucleons from S to P states and the probability of finding them with a total momentum \vec{K} . Since we consider the capture of π^- by the two nucleons at zero separation only these two probabilities appear as product.

We now apply the above formulae to ^{16}O . The summations in (11) and (12) range over the levels os and op only. Also for comparing with experimental results we have to integrate the expressions (13a) and (13b) over E_1 and E_2 , since they are not measured. Carrying out the summations and integrations we get, for capture from $1S$ orbit

$$d\sigma_0^S = \frac{g_0^2}{2\pi^4} \frac{m_p}{m_\pi} \left(\frac{Z}{a_0} \right)^3 \left(4I_0 + \frac{1}{4\nu^2} I_2 \right) \quad \dots(14a)$$

$$d\sigma_1^S = \frac{g_1^2}{2\pi^4} \frac{m_p}{m_\pi} \left(\frac{Z}{a_0} \right)^3 \left(4I_0 + \frac{1}{4\nu^2} I_2 \right) \quad \dots(14b)$$

for capture from $2P$ orbit

$$d\sigma_0^P = \frac{g_0^2}{64\pi^4} \frac{m_p}{m_\pi} \left(\frac{Z}{a_0} \right)^5 \frac{1}{\nu} \left(18I_0 - \frac{2}{\nu} \cdot I_1 + \frac{3}{4\nu^2} \cdot I_2 + \frac{1}{16\nu^3} \cdot I_3 \right) \quad \dots(15a)$$

$$d\sigma_1^P = \frac{g_1^2}{128\pi^4} \frac{m_p}{m_\pi} \left(\frac{Z}{a_0} \right)^5 \frac{1}{\nu} \left(18I_0 - \frac{2}{\nu} \cdot I_1 + \frac{3}{4\nu^2} \cdot I_2 + \frac{1}{16\nu^3} \cdot I_3 \right) \quad \dots(15b)$$

where

$$I_n = \int k_1^2 dk_1 \int k_2^2 dk_2 \delta(a^2 - k_1^2 - k_2^2) k_1^{2n} \exp\left(-\frac{K^2}{2\nu}\right)$$

and

$$a^2 = 2m_p \bar{E}$$

Here $\nu = 0.323 f_m^{-2}$, the oscillator constant as determined from electron scattering. The wave-functions of the bound pions have been approximated as follows

$$\phi_{\pi^S}^S(r) \approx \phi_{\pi^S}^S(0) = \frac{1}{\sqrt{\pi}} \left(\frac{Z}{a_0} \right)^{3/2}$$

$$\phi_{2\pi}^{2P}(r) \approx \left(\frac{Z}{2a_0} \right)^{3/2} \frac{Z}{a_0\sqrt{3}} r Y_{1m}(\theta, \psi)$$

where a_0 is the Bohr radius of the pionic atom.

RESULTS AND DISCUSSION

(i) We first calculate the total capture rate. To do this we have to estimate the value of \bar{E} which is the average of the difference in energy between the outgoing nucleons and the rest mass of the pion. The difference of the binding energies $B, -B_i$ is 23 MeV. The recoil energy varies from 0 to 15 MeV depending on the angle θ . Therefore \bar{E} will depend on θ . The value of \bar{E} has been fixed at 35 MeV in our calculations. We have verified that our results are not very sensitive to small changes in \bar{E} .

The total capture rate is obtained by integrating the expressions (14a) (15b) over θ . The values of the constants g_0^2 and g_1^2 are

$$g_0^2 = 0.60 \pm 0.05 f_m^2$$

$$g_1^2 = 0.29 \pm 0.15 f_m^2$$

The value of g_0^2 differs from that of Eckstein (1963) because we have used the more recent experimental results of Rose (1967) for $p + p \rightarrow \pi^+ + d$ cross section. Using these values for the amplitudes one obtains

$$\sigma_{\text{tot}}^{1S} = (1.42 \pm 0.32) \times 10^{18} \text{ sec}^{-1}.$$

The experimental value as measured by Backenstoss *et al* (1967) is $(11.1 \pm 0.1) \times 10^{18} \text{ sec}^{-1}$.

The calculated absorption rate from $2P$ orbit is $\sigma_{10},^{2P} = 2 \times 10^{15} \text{ sec}^{-1}$. This is 3–4 times larger than the $2P \rightarrow 1S$ radiative transition rate. This is in accord with the experimental observation that most absorptions take place from $2P$ orbit.

(ii) The angular distribution for absorption from $2P$ orbit (since most absorptions take place from this orbit) is plotted in figure 1. The experimental points and the theoretical curve are normalized to unity at $\theta = 180^\circ$. With this normalization the theoretical curve does not distinguish between the emission of (nn) and (np) pairs [see equations (15a) and (15b)].

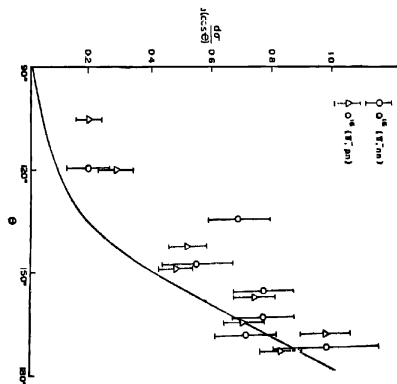


Figure 1. Angular distribution of nucleon-pairs emitted following pion absorption from $2P$ orbit. The experimental points and the theoretical curve are normalized to unity at $\theta = 180^\circ$. The experimental points are taken from Nordberg *et al* (1968)

(iii) The ratio $R = \frac{\sigma_{np \rightarrow nn}}{\sigma_{p \rightarrow np}} = 1 + \frac{2g_0^2}{g_1^2} = 5.14 \pm 2.20$, which is in agreement with the value 3.4 ± 1.1 measured by Nordberg *et al* (1968).

We see from the above calculations that the phenomenological model gives a reasonable result for the angular distribution and the ratio R . The total absorption rate from $1S$ orbit is, however, smaller than the experimental value. This disagreement may be due to the presence of the δ -function form factor in the Hamiltonian M_{12} (equation 3). The δ -function allows only relative angular momentum $l = 0$ states for the nucleons, whereas, in ^{16}O , l can have values upto 2. It should be pointed

out that the neglect of absorption of p -wave pions is not likely to affect our results, since it has been shown by Ericson & Ericson (1966) that the $1S$ level width is not affected by the p -wave pion. Lastly, the assumption of a single determinant of harmonic oscillator wave-functions for ^{16}O is not a limitation as far as this calculation is concerned. Because it describes the behaviour of nucleons at large distances correctly, as is known from electron scattering data (Ehrenberg *et al* 1959). A modification of the form factor in the effective Hamiltonian may therefore be necessary to achieve a better agreement of the absorption rate with the experimental value.

ACKNOWLEDGEMENT

Many helpful discussions with Dr. P. P. Divakaran and computational help from Mr. A. S. Anikhindi are gratefully acknowledged.

REFERENCES

- Baekenstose G., Charalumbus S., Daniel H., Koch H., Poelz G., Schmitt H. & Tanscher L. 1967 *Phys. Lett.*, **25B**, 365.
- Brueckner K. A., Serber R. & Watson K. M. 1951 *Phys. Rev.* **84**, 258.
- Cheon Il-Tong. 1966 *Phys. Rev.* **145**, 794.
- 1967 *Phys. Rev.* **158**, 900.
- Demodov V. S., Kirillov-Ugrumov V. G., Ponomov A. K., Protosov V. P. & Sergeev F. M. 1963 *Sov. Phys. JETP*, **17**, 773.
- Divakaran P. P. 1965 *Phys. Rev.* **139B**, 387.
- Eckstein S. C. 1963 *Phys. Rev.*, **129**, 413.
- Ehrenberg H. F., Hofstadter R., Mayer-Berkhout U., Ravenhall D. G. & Sobottka S. E. 1959 *Phys. Rev.* **113**, 666.
- Eisenberg J. M. & Letourneux J. 1967 *Nucl. Phys.*, **B3**, 47.
- Ericson T. E. O. 1966 *Proc. Int. Conf. on Nuclear Physics, Gatlinberg (Academic Press)*.
- Ericson M. 1963 *Compt. Rend.*, **257**, 3831.
- 1964 *Compt. Rend.*, **258**, 1471.
- Ericson M. & Ericson T. E. O. 1966 *Ann. Phys.*, **36**, 323.
- Fedotov P. 1966 *Sov. J. Nuclear Physics*, **2**, 335.
- Jibuti R. I. & Kopaleishvili T. I. 1964 *Nucl. Phys.* **55**, 337.
- Koltun D. S. & Reitan A. 1966 *Phys. Rev.*, **141**, 1413.
- 1967 *Phys. Rev.*, **155**, 1139.
- Nguyen-Truong C. & Sakamoto Y. 1967 *Nucl. Phys.*, **B1**, 139.
- Nordberg M., Kinsey K. F. & Burman R. L. 1968 *Phys. Rev.*, **165**, 1096.
- Oraki S., Weinstein R., Glass G., Loh E. & Wattenberg A. 1960 *Phys. Rev. Lett.*, **4**, 533.
- Rose C. M., 1967 *Phys. Rev.*, **154**, 1305.
- Sens J. C. 1967 *Second Int. Conf. on High Energy Physics and Nuclear Structure, Rehovoth (North-Holland)*.
- Spector R. M. 1964 *Phys. Rev.*, **134B**, 101.
- Zaimidaro O. A., 1967 *Sov. Phys. JETP*, **24**, 1111.

Fluid flow through a channel bounded by parallel flat walls

By RAM CHARITRA TRIPATHI

Department of Mathematics, Banaras Hindu University, Varanasi-5.

(Received 9 April 1969—Revised 7 November 1969)

In this paper, we have considered the unsteady laminar flow of a viscous incompressible fluid through a channel bounded by two parallel flat walls. In section 1, the basic equations are given and the velocity distribution for the oscillatory flow calculated, which has been utilized to find the expression for the flux flow, drag, work-expended, energy-utilized and the efficiency. In section 2, temperature field has been discussed for the oscillatory motion when (i) the walls are kept at a constant temperature (ii) the wall temperature varies as an oscillatory function of time.

FORMULATION OF THE PROBLEM

The equations of conservation of mass, momentum and energy for two dimensional flow are (Lal, in press)

$$\frac{\delta u}{\delta x} + \frac{\delta v}{\delta y} = 0 \quad \dots(1.1)$$

$$\rho \left(\frac{\delta u}{\delta t} + u \frac{\delta u}{\delta x} + v \frac{\delta u}{\delta y} \right) = - \frac{\delta p}{\delta x} + \mu \left(\frac{\delta^2 u}{\delta x^2} + \frac{\delta^2 u}{\delta y^2} \right) \quad \dots(1.2)$$

$$\rho \left(\frac{\delta v}{\delta t} + u \frac{\delta v}{\delta x} + v \frac{\delta v}{\delta y} \right) = - \frac{\delta p}{\delta y} + \mu \left(\frac{\delta^2 v}{\delta x^2} + \frac{\delta^2 v}{\delta y^2} \right) \quad \dots(1.3)$$

$$g\rho c \left(\frac{\delta T}{\delta t} + u \frac{\delta T}{\delta x} + v \frac{\delta T}{\delta y} \right) = k \left(\frac{\delta^2 T}{\delta x^2} + \frac{\delta^2 T}{\delta y^2} \right) + 2\mu\phi \quad \dots(1.4)$$

where

$$\phi = \left(\frac{\delta u}{\delta x} \right)^2 + \left(\frac{\delta v}{\delta y} \right)^2 + \frac{1}{2} \left(\frac{\delta v}{\delta x} + \frac{\delta u}{\delta y} \right)^2 \quad \dots(1.5)$$

Let the flow be along the x -axis so that $v = 0$ and consequently $\frac{\delta u}{\delta x} = 0$

from equation (1.1). The equation (1.2) together with equation (1.1) reduces to

$$\frac{\delta u}{\delta t} = - \frac{1}{\rho} \frac{\delta p}{\delta x} + \nu \frac{\delta^2 u}{\delta y^2} \quad \dots(1.6)$$

The equation (1.6) has been solved elsewhere (Lal, in press) by taking the following forms for the pressure gradient and consequently velocity distribution. He has calculated the velocity distribution which is given below for further use in the paper.

Let

$$\left. \begin{aligned} & - \frac{1}{\rho} \frac{\delta p}{\delta x} = K e^{i\omega t} \\ \text{and} \quad & u(y, t) = f(y) e^{i\omega t} \end{aligned} \right\} \quad \dots(1.7)$$

Fluid flow through a channel bounded by parallel flat walls 755

where real part of both equations are to be considered and making substitutions from equation (1.7) into (1.6), we have after some simplifications

$$\frac{d^2 f}{dy^2} + A^2 f = B \quad \dots (1.8)$$

where

$$A^2 = -\frac{i\omega}{\nu} \text{ and } B = -\frac{K}{\nu} \quad \dots (1.9)$$

Solution of equation (1.8) is

$$f = c_1 \sin Ay + c_2 \cos Ay + \frac{B}{A^2} \quad \dots (1.10)$$

where c_1 and c_2 are arbitrary constants of integration. Now, using the boundary conditions as

$$u = 0 \text{ at } y = \pm y_0 \text{ (on the walls for all values of } t) \quad \dots (1.11)$$

and consequently

$$f = 0 \text{ at } y = \pm y_0 \quad \dots (1.12)$$

Equation (1.10) gives

$$\left. \begin{aligned} f &= \frac{B}{A^2} \left(1 - \frac{\cos Ay}{\cos Ay_0} \right) \\ \text{and} \quad u(y, t) &= \frac{B}{A^2} \left(1 - \frac{\cos Ay}{\cos Ay_0} \right) e^{i\omega t} \end{aligned} \right\} \quad \dots (1.13)$$

where the real part of the equation gives the required expression for u . The discharge of flux per second as given earlier (1) is

$$Q = B \int_{-y_0}^{y_0} u dy = Re \{ e^{i\omega t} \int_{-y_0}^{y_0} \frac{B}{A^2} \left(1 - \frac{\cos Ay}{\cos Ay_0} \right) dy \} \quad \dots (1.14)$$

The above expression has not been separated earlier into the real and imaginary parts. We have made such calculations and the result is given below. From equation (1.14), we get

$$\begin{aligned} Q &= \frac{2K}{\omega} y_0 \sin \omega t + \frac{(2\nu)^{1/2} K}{\omega^{3/2}} \frac{\{ \sinh(2\sqrt{\omega/2\nu} y_0) - \sin(2\sqrt{\omega/2\nu} y_0) \cos \omega t \}}{\cos(2\sqrt{\omega/2\nu} y_0) + \cosh(2\sqrt{\omega/2\nu} y_0)} \\ &\quad - \frac{(2\nu)^{1/2} K}{\omega^{3/2}} \frac{\{ \sin(2\sqrt{\omega/2\nu} y_0) + \sinh(2\sqrt{\omega/2\nu} y_0) \sin \omega t \}}{\cos(2\sqrt{\omega/2\nu} y_0) + \cosh(2\sqrt{\omega/2\nu} y_0)} \quad \dots (1.15) \end{aligned}$$

and for small ω , we have

$$Q_1 = \frac{2Ky_0^3}{3\nu} - \frac{K\omega^{1/2} y_0^3}{3\nu} \quad \dots (1.16)$$

Certain calculations for discharge of flux, drag, work-expended, energy-utilized and efficiency have been deduced for the oscillatory flow which has not been discussed earlier by Lal (In Press).

For the boundary conditions

$$\left. \begin{array}{l} u = U = f_1 e^{i\omega t} (f = f_1) \text{ at } y = y_0 \\ \text{and} \\ f = 0 \text{ at } y = -y_0 \end{array} \right\} \quad \dots(1.17)$$

for all time $t > 0$ we get

$$f = \frac{f_1}{2} \left(\frac{\sin Ay}{\sin Ay_0} + \frac{\cos Ay}{\cos Ay_0} \right) + \frac{B}{A^2} \quad \dots(1.18)$$

and thus considering the real part in (1.18) the discharge of flux becomes

$$\begin{aligned} Q_2 = & \frac{f_1 \sqrt{\nu}}{\sqrt{2\omega}} \frac{\{\sinh 2\sqrt{\omega/2\nu}y_0 + \sin(2\sqrt{\omega/2\nu}y_0)\} \cos \omega t}{\cos(2\sqrt{\omega/2\nu}y_0) + \cosh(2\sqrt{\omega/2\nu}y_0)} \\ & - \frac{f_1 \sqrt{\nu}}{\sqrt{2\omega}} \frac{\{\sin(2\sqrt{\omega/2\nu}y_0) - \sinh(2\sqrt{\omega/2\nu}y_0)\} \sin \omega t}{\cos(2\sqrt{\omega/2\nu}y_0) + \cosh(2\sqrt{\omega/2\nu}y_0)} \\ & + \frac{2Ky_0 \sin \omega t}{\omega} + \frac{(2\nu)^{1/2}K}{\omega^{3/2}} \frac{\{\sinh(2\sqrt{\omega/2\nu}y_0) - \sin(2\sqrt{\omega/2\nu}y_0)\} \cos \omega t}{\cos(2\sqrt{\omega/2\nu}y_0) + \cosh(2\sqrt{\omega/2\nu}y_0)} \\ & - \frac{(2\nu)^{1/2}K}{\omega^{3/2}} \frac{\{\sin(2\sqrt{\omega/2\nu}y_0) + \sinh(2\sqrt{\omega/2\nu}y_0)\} \sin \omega t}{\cos(2\sqrt{\omega/2\nu}y_0) + \cosh(2\sqrt{\omega/2\nu}y_0)} \quad \dots(1.19) \end{aligned}$$

For small ω , we have

$$\begin{aligned} Q_3 = & f_1 y_0 + \frac{2}{3\nu} Ky_0^3 + \omega^2 \left(-\frac{f_1 t^2 y_0}{2} + \frac{f_1 y_0^3 t}{3\nu} - \frac{K t^2 y_0^3}{3\nu} \right) \\ & + \omega^4 \left(\frac{-f_1 t^2 y_0^3}{18\nu} \right) \quad (1.20) \end{aligned}$$

The traction per unit width and along the length l , of the upper wall (Dryden *et al* 1932) is

$$l\mu \left(\frac{\partial u}{\partial y} \right)_{y=y_0} = \frac{l\mu f_1}{2} A (\cot Ay_0 - \tan Ay_0) e^{i\omega t} + \frac{\mu l B}{A} \tan Ay_0 e^{i\omega t} \quad \dots(1.21)$$

Considering real part of the above equation, we get for drag

$$\begin{aligned} D = & -\frac{\mu l f_1 \sqrt{\omega}}{2\sqrt{2\nu}} \frac{\{\sin(4\sqrt{\omega/2\nu}y_0) + \sinh(4\sqrt{\omega/2\nu}y_0)\} \cos \omega t}{\cos^2(2\sqrt{\omega/2\nu}y_0) - \cosh^2(2\sqrt{\omega/2\nu}y_0)} \\ & - \frac{\mu l f_1 \sqrt{\omega}}{2\sqrt{2\nu}} \frac{\{\sin(4\sqrt{\omega/2\nu}y_0) - \sinh(4\sqrt{\omega/2\nu}y_0)\} \sin \omega t}{\cos^2(2\sqrt{\omega/2\nu}y_0) - \cosh^2(2\sqrt{\omega/2\nu}y_0)} \\ & - \frac{K\mu l}{\sqrt{2\nu\omega}} \frac{(\cos \omega t - \sin \omega t) \cdot \sin(\sqrt{\omega/2\nu}y_0)}{(\cos 2\sqrt{\omega/2\nu}y_0) + \cosh(2\sqrt{\omega/2\nu}y_0)} \\ & - \frac{K\mu l}{\sqrt{2\nu\omega}} \frac{(\cos \omega t + \sin \omega t) \cdot \sinh(2\sqrt{\omega/2\nu}y_0)}{\cos(2\sqrt{\omega/2\nu}y_0) + \cosh(2\sqrt{\omega/2\nu}y_0)} \quad \dots(1.22) \end{aligned}$$

The work-expended is

$$\begin{aligned}
 U_1 &= R \left\{ \frac{f_1 \mu l A U}{2} (\cos Ay_0 - \tan Ay_0) e^{i\omega t} + \frac{\mu l B U}{2} \tan Ay_0 e^{i\omega t} \right\} \\
 &= - \frac{\mu l f_1^2 \sqrt{\omega}}{2\sqrt{2\nu}} \frac{\{\sin(4\sqrt{\omega/2\nu}y_0) + \sinh(4\sqrt{\omega/2\nu}y_0)\} \cos 2\omega t}{\cos^2(2\sqrt{\omega/2\nu}y_0) - \cosh^2(2\sqrt{\omega/2\nu}y_0)} \\
 &\quad - \frac{\mu l f_1^2 \sqrt{\omega}}{2\sqrt{2\nu}} \frac{\{\sin(4\sqrt{\omega/2\nu}y_0) - \sinh(4\sqrt{\omega/2\nu}y_0)\} \sin 2\omega t}{\cos^2(2\sqrt{\omega/2\nu}y_0) - \cosh^2(2\sqrt{\omega/2\nu}y_0)} \\
 &\quad - \frac{K f_1 \mu l}{\sqrt{2\nu\omega}} \frac{(\cos 2\omega t - \sin 2\omega t) \sin(2\sqrt{\omega/2\nu}y_0)}{\cos(2\sqrt{\omega/2\nu}y_0) + \cosh(2\sqrt{\omega/2\nu}y_0)} \\
 &\quad - \frac{K f_1 \mu l}{\sqrt{2\nu\omega}} \frac{(\cos 2\omega t + \sin 2\omega t) \sinh(2\sqrt{\omega/2\nu}y_0)}{\cos(2\sqrt{\omega/2\nu}y_0) + \cosh(2\sqrt{\omega/2\nu}y_0)} \quad \dots (1.22)
 \end{aligned}$$

While the energy-utilized is

$$E = \mu l Q_0 \left(-\frac{1}{\rho} \frac{\partial p}{\partial x} \right) = \mu l Q_0 (K e^{i\omega t}) \quad \dots (1.23)$$

Considering the real part of the equation (1.24) we get for E_1 as

$$\begin{aligned}
 E_1 &= \frac{K \mu l f_1 \sqrt{\nu}}{\sqrt{2\omega}} \frac{\{\sin(2\sqrt{\omega/2\nu}y_0) + \sinh(2\sqrt{\omega/2\nu}y_0)\} \cos 2\omega t}{\cos(2\sqrt{\omega/2\nu}y_0) + \cosh(2\sqrt{\omega/2\nu}y_0)} \\
 &\quad - \frac{K \mu l f_1 \sqrt{\nu}}{\sqrt{2\omega}} \frac{\{\sin(2\sqrt{\omega/2\nu}y_0) - \sinh(2\sqrt{\omega/2\nu}y_0)\} \sin 2\omega t}{\cos(2\sqrt{\omega/2\nu}y_0) + \cosh(2\sqrt{\omega/2\nu}y_0)} \\
 &\quad + \frac{2K^2 \mu l y_0}{\omega} \sin 2\omega t \\
 &\quad + \frac{(2\nu)^{1/2} K^2 \mu l}{\omega^{3/2}} \frac{\{\sinh(2\sqrt{\omega/2\nu}y_0) - \sin(2\sqrt{\omega/2\nu}y_0)\} \cos 2\omega t}{\cos(2\sqrt{\omega/2\nu}y_0) + \cosh(2\sqrt{\omega/2\nu}y_0)} \\
 &\quad - \frac{(2\nu)^{1/2} K^2 \mu l}{\omega^{3/2}} \frac{\{\sin(2\sqrt{\omega/2\nu}y_0) + \sinh(2\sqrt{\omega/2\nu}y_0)\} \sin 2\omega t}{\cos(2\sqrt{\omega/2\nu}y_0) + \cosh(2\sqrt{\omega/2\nu}y_0)} \quad \dots (1.25)
 \end{aligned}$$

The efficiency η is given by

$$\eta = \frac{E_1}{U_1} \quad \dots (1.26)$$

where E_1 and U_1 are as in equations (1.23) and (1.25)

TEMPERATURE DISTRIBUTION

Lal (In Press) has studied the temperature field for exponential flow. Oscillatory flow has more important application in engineering problems and hence we have considered the energy equation when the wall temperature varies as an oscillatory function of time. The basic energy equation (3) is

$$\frac{\partial T}{\partial t} = k' \frac{\partial^2 T}{\partial y^2} + k'' \left(\frac{\partial u}{\partial y} \right)^2 \quad \dots(2.1)$$

where

$$k' = \frac{k}{\rho c} \text{ and } k'' = \frac{\mu}{\rho c} \quad \dots(2.2)$$

Substituting for $\frac{\partial u}{\partial y}$ from equation (1.13) into (2.1), we have

$$\frac{\partial T}{\partial t} = k' \frac{\partial^2 T}{\partial y^2} + k'' \frac{B^2}{A^2} \left(\frac{\sin^2 A y}{\cos^2 A y_0} \right) e^{2t\omega} \quad \dots(2.3)$$

To solve the equation (2.3), we take

$$T = f(y) e^{2t\omega} \quad \dots(2.4)$$

Substituting from equation (2.4) into (2.3), we have

$$-\frac{d^2 f}{dy^2} + A_1^2 f = A_2 \sin^2 A y \quad \dots(2.5)$$

where

$$A_1^2 = -\frac{2t\omega}{k'} \text{ and } A_2 = \frac{k''}{k'} \times \frac{-B^2}{A^2} \cdot \frac{1}{\cos^2 A y_0} = \text{const.} \dots(2.6)$$

The solution of equation (2.5) is

$$f = c_1 \cos A_1 y + c_2 \sin A_1 y - \frac{A_2}{2A_1^2} - \frac{A_2 \cos 2Ay}{2(A_1^2 - 4A^2)} \quad \dots(2.7)$$

where c_1 and c_2 are constants of integration. Assuming the boundary conditions as

$$\left. \begin{array}{l} T = T_1 \text{ at } y = 0 \\ T = T_0 \text{ at } y = \pm y_0 \end{array} \right\} \begin{array}{l} \text{when } t \text{ is} \\ \text{finite, say, } t > 0 \end{array} \quad \dots(2.8)$$

and consequently

$$\left. \begin{array}{l} T_1 = f_1 e^{2t\omega} (f = f_1) \text{ at } y = 0 \\ T_0 = f_0 e^{2t\omega} (f = f_0) \text{ at } y = \pm y_0 \end{array} \right\} \begin{array}{l} \text{when } t \text{ is} \\ \text{finite, say, } t > 0 \end{array} \quad \dots(2.9)$$

($f_0 = 0$, if the walls are kept at constant temperature for all time $t > 0$)

From the first boundary condition, we get

$$c_2 = 0, c = f_1 + \frac{2 A_2 A^2}{A_1^2 (A_1^2 - 4A^2)} \quad \dots(2.10)$$

Thus, we get

$$f = \left\{ f_1 + \frac{2 A_2 A^2}{A_1^2 (A_1^2 - 4A^2)} \right\} \cos A_1 y + \frac{A_2}{2} \left\{ \frac{1}{A_1^2} - \frac{\cos 2Ay}{A_1^2 - 4A^2} \right\} \quad \dots(2.11)$$

So that

$$T = \left\{ f_1 + \frac{2 A_2 A^2}{A_1^2 (A_1^2 - 4A^2)} \right\} \cos A_1 y e^{2i\omega t} + \frac{A_2}{2} \left\{ \frac{1}{A_1^2} - \frac{\cos 2Ay}{A_1^2 - 4A^2} \right\} e^{2i\omega t} \quad \dots(2.12)$$

From the second boundary conditions, we have

$$\begin{aligned} f_0 &= c_1 \cos A_1 y_0 - c_2 \sin A_1 y_0 + \frac{A_2}{2 A_1^2} - \frac{A_2}{2} \frac{\cos 2A y_0}{A_1^2 - 4A^2} \\ f_0 &= c_1 \cos A_1 y_0 + c_2 \sin A_1 y_0 + \frac{A_2}{2 A_1^2} - \frac{A_2}{2} \frac{\cos 2A y_0}{A_1^2 - 4A^2} \end{aligned} \quad \dots(2.13)$$

We find that

$$c_2 = 0 \text{ and } c_1 = \left\{ f_0 - \frac{A_2}{2} \left(\frac{1}{A_1^2} - \frac{\cos 2A y_0}{A_1^2 - 4A^2} \right) \right\} \cdot \frac{1}{\cos A_1 y_0} \quad \dots (2.14)$$

and thus we get

$$\begin{aligned} T &= \left\{ f_0 + \frac{A_2}{2} \cdot \frac{\cos 2A y_0}{A_1^2 - 4A^2} - \frac{A_2}{2 A_1^2} \right\} \frac{\cos A_1 y}{\cos A_1 y_0} e^{2i\omega t} \\ &+ \frac{A_2}{2} \left\{ \frac{1}{A_1^2} - \frac{\cos 2Ay}{A_1^2 - 4A^2} \right\} e^{2i\omega t} \quad \dots (2.15) \end{aligned}$$

Temperature field T_1 , when the walls are at a constant temperature is

$$\begin{aligned} T_1 &= \left\{ \frac{A_2}{2} \cdot \frac{\cos 2A y_0}{A_1^2 - 4A^2} - \frac{A_2}{2 A_1^2} \right\} \frac{\cos A_1 y}{\cos A_1 y_0} e^{2i\omega t} \\ &+ \frac{A_2}{2} \left\{ \frac{1}{A_1^2} - \frac{\cos 2Ay}{A_1^2 - 4A^2} \right\} e^{2i\omega t} \quad \dots (2.16) \end{aligned}$$

The equation (2. 16) can be put as

$$\begin{aligned} T_1 &= \frac{(pP - qQ + MN(P_1 - P_2) \cos 2\omega t + MN(Q_1 - Q_2) \sin 2\omega t)}{MN} \\ &+ i \frac{(pQ - qP + MN(Q_1 - Q_2) \cos 2\omega t + MN(P_1 - P_2) \sin 2\omega t)}{MN} \\ &= P_r + iP_i \quad \dots(2.17) \end{aligned}$$

where P_r stands for the real part in equation (2.17) and P_i the imaginary part.

Thus, we get the real part as

$$P_r = \frac{pP - qQ + MN(P_1 - P_2) \cos 2\omega t + MN(Q_1 - Q_2) \sin 2\omega t}{MN} \quad \dots(2.18)$$

where

$$K^2 \mu k' \left\{ \nu \cosh 2\phi \cos 2\phi (\sinh^2 \phi \sin^2 \phi - \cosh^2 \phi \cos^2 \phi) + \sinh^2 \phi \sin^2 2\phi \sinh \phi \cosh \phi + \{(2k' - \nu)(\sinh^2 \phi \sin^2 \phi - \cosh^2 \phi \cos^2 \phi)\} \right\}$$

$$P = \frac{4k\omega^2 \nu (2k' - \nu)(\cosh^2 \phi \cos^2 \phi + \sinh^2 \phi \sin^2 \phi)^2}{\dots} \quad (2.19)$$

$$K^2 \mu k' \{ \nu \sinh 2\phi \sin 2\phi (\sinh^2 \phi \sin^2 \phi - \cosh^2 \phi \cos^2 \phi) + \cosh \phi \sinh \phi \cosh 2\phi \cos 2\phi \sin 2\phi + \{(2k' - \nu)(\sinh \phi \cosh \phi \cos \phi \sin \phi)\} \}$$

$$Q = \frac{4k\omega^2 \nu (2k' - \nu)(\cosh^2 \phi \cos^2 \phi + \sinh^2 \phi \sin^2 \phi)^2}{\dots} \quad (2.20)$$

$$p = X \cos 2\omega t - Y \sin 2\omega t \quad (2.21)$$

$$q = X \sin 2\omega t + Y \cos 2\omega t \quad (2.22)$$

$$P_1 = \frac{K^2 \mu k' \left[\cosh^2 \phi \cos^2 \phi - \sinh^2 \phi \sin^2 \phi \right]}{4k\omega^2 \nu (\cosh^2 \phi \cos^2 \phi + \sinh^2 \phi \sin^2 \phi)^2} \quad (2.23)$$

$$K^2 \mu k' [\cosh 2\phi_1 \cos 2\phi_1 (\cosh^2 \phi \cos^2 \phi - \sinh^2 \phi \sin^2 \phi) + \sinh 2\phi_1 \sin 2\phi_1 \sinh \phi \cosh \phi]$$

$$P_2 = \frac{4k\omega^2 (\nu - 2k') (\cosh^2 \phi \cos^2 \phi + \sinh^2 \phi \sin^2 \phi)^2}{\dots} \quad (2.24)$$

$$Q_1 = -\frac{K^2 \mu k' \cosh \phi \cos \phi \sin \phi \sinh \phi}{2k\omega^2 \nu (\cosh^2 \phi \cos^2 \phi + \sinh^2 \phi \sin^2 \phi)^2} \quad (2.25)$$

$$K^2 \mu k' \{ \sinh 2\phi_1 \sin 2\phi_1 (\cosh^2 \phi \cos^2 \phi - \sinh^2 \phi \sin^2 \phi) - 2 \cosh 2\phi_1 \cos 2\phi_1 \cosh \phi \sinh \phi \cos \phi \sin \phi \}$$

$$Q_2 = \frac{4k\omega^2 (\nu - 2k') (\cosh^2 \phi \cos^2 \phi + \sinh^2 \phi \sin^2 \phi)^2}{\dots} \quad (2.26)$$

$$M = \cosh^2 \alpha \cos^2 \alpha + \sinh^2 \alpha \sin^2 \alpha \quad (2.27)$$

$$N = (\cosh^2 \phi \cos^2 \phi + \sinh^2 \phi \sin^2 \phi)^2 \quad (2.28)$$

$$X = \cosh^{\Psi} \cosh^{\Psi} \cos^{\alpha} \cosh^{\alpha} + \sinh^{\Psi} \sinh^{\Psi} \sin^{\alpha} \sinh^{\alpha} \quad (2.29)$$

$$Y = \sinh^{\Psi} \sinh^{\Psi} \cos^{\alpha} \cosh^{\alpha} - \cosh^{\Psi} \cosh^{\Psi} \sin^{\alpha} \sinh^{\alpha} \quad (2.30)$$

$$\text{and} \quad \phi = \sqrt{\omega/2\nu} y_0, \phi_1 = \sqrt{\omega/2\nu} y, \Psi = \sqrt{\omega/k'} y, \alpha = \sqrt{\omega/k'} y_0 \quad (2.31)$$

To calculate the phase angle, we put equation (2.16) such as

$$T = \left\{ \frac{PX - QY + MN(P_1 - P_2)}{MN} + i \frac{PY + QX + MN(Q_1 - Q_2)}{MN} \right\} e^{i\omega t}$$

Considering real part in (2.32), we may write it as (2.32)

$$T_0 = |Z| \cos(2\omega t + \beta) \quad (2.33)$$

where $Z = s_r + is_i$

$$= \frac{1}{MN} [PX - QY + MN(P_1 - P_2) + i(PY + QX + MN(Q_1 - Q_2))] \quad \dots(2.34)$$

and

$$\beta = \tan^{-1} \frac{s_i}{s_r} \text{ is the phase angle}$$

The wall temperature leads or lags behind the fluid temperature by a phase angle and the phase angle is zero if $s_i = 0$ and it is $\frac{\pi}{2}$ if $s_r = 0$.

ACKNOWLEDGEMENT

Thanks are due to Dr. Krishna Lal, D.Sc., Department of Mathematics, for valuable guidance and to the reference for his helpful comments.

REFERENCES

- Dryden H. L., Murnaghan F. P. & Bateman H. 1932 *Hydrodynamics*,
Dover Publication, 184.
Lal K. *Science Research Journal*, B.H.U. In Press.
Pal S. I. 1956 *Viscous flow theory, Laminar flow* (INO, Vol. I. 43-52.)

On Kelvin-Helmholtz Instability In the presence
of a uniform electric field

By S. NARASIMHA MURTHY

Department of Applied Mathematics, Indian Institute of Science,
Bangalore-12

(Received 6 June 1969).

The interfacial instability arising due to relative motion of two fluids in the presence of a uniform electric field is studied. The parameters involved are a , b , c which denote the relative velocities, the electric part of the Maxwellian stress and the surface tension, respectively. It is shown that in the absence of surface tension and if $a+b>1$ the system is unstable for all wave numbers. Moreover, if $a+b<1$ the system is stable for wave numbers less than the critical wave number α_0 beyond which the system is unstable. Further, we note that in the presence of surface tension when $a+b>1$ the system is unstable below the critical wave number α'_0 above which the system is stable. It has been found that the increase in surface tension decreases the wave number band. On the other hand, if $a+b<1$ the system is always stable for all permissible C .

INTRODUCTION

The stability of a horizontal fluid interface between a conducting and a non-conducting fluid in the presence of transverse dc electric field has been studied experimentally by Taylor & McEwan (1965). It has been shown that the interface becomes unstable under the action of a sufficiently great electric field. Yih (1968) extended the investigation to ac electric fields and showed that the interface can be unstable even if the electric field is at all times weaker than that needed for stability in the case of a steady field, and that when instability occurs the waves may either be synchronous with the electric field or have twice its frequency. The purpose of this note is to study the stability of the interface when the fluids are in relative horizontal motion. The analysis takes into account the hydrodynamics and electrodynamics through the continuum picture.

We consider incompressible inviscid fluids. The upper fluid with constant density ρ_1 is taken to be nonconducting and the lower with density ρ_2 a perfect conductor. The XOY plane is taken to coincide with the unperturbed middle level of the layer and the positive Z -axis in the upward direction normal to the unperturbed fluid surfaces. The upper fluid is bounded above by an electrode at $z=h_1$ with potential ϕ_{10} and below by the interface, and the lower fluid is bounded below by an electrode at $z=-h_2$ with potential ϕ_{20} . Further, we assume that initially the non-conducting and conducting fluids are moving with velocities \vec{V}_1 and \vec{V}_2 , respectively, in the X -direction.

BASIC EQUATIONS AND EQUILIBRIUM STATE

The basic equations of the problem for the non-conducting and conducting fluids are as follows

Non-conducting :

$$\operatorname{div} \vec{v}_1 = 0, \quad \dots (2.1)$$

$$\rho_1 \left[\frac{\delta \vec{v}_1}{\delta t} + (\vec{v}_1 \nabla) \vec{v}_1 \right] = -\operatorname{grad} P_1 + \frac{K}{8\pi} \operatorname{grad} E_1^2 - \rho_1 g, \quad \dots (2.2)$$

$$\nabla^2 \phi_1 = 0 \quad \dots (2.3)$$

$$\vec{g} = (0, 0, g)$$

where $\vec{E}_1 = -\operatorname{grad} \phi_1$, is the electric field and K is the dielectric constant.

Conducting :

$$\operatorname{div} \vec{v}_2 = 0, \quad \dots (2.4)$$

$$\rho_2 \left[\frac{\delta \vec{v}_2}{\delta t} + (\vec{v}_2 \nabla) \vec{v}_2 \right] = -\operatorname{grad} P_2 - \rho_2 g, \quad \dots (2.5)$$

$$\vec{g} = (0, 0, g).$$

In the equilibrium state

$$\vec{v}_1 = (v_1, 0, 0) \text{ and } \vec{v}_2 = (v_2, 0, 0) \quad \dots (2.6)$$

The pressure distributions in the two fluids are given as

$$P_{10} = P_0 - \rho_1 g z, \quad \dots (2.7)$$

$$P_{20} = P_0 - \frac{K E_0^2}{8\pi} - \rho_2 g z, \quad \dots (2.8)$$

where, P_0 is the hydrostatic pressure at the interface $z=0$.

The electric potential ϕ_0 is ϕ_{20} in the conducting fluid so that the electric field in the fluid is zero. In the non-conducting fluid

$$\phi_0 = \phi_{20} + \frac{\phi_{10} - \phi_{20}}{h_1} z \quad \dots (2.9)$$

so the vertical electric field in that fluid is

$$\vec{E}_g = \frac{\phi_{20} - \phi_{10}}{h_1} \quad \dots (2.10)$$

LINEARIZED EQUATIONS AND BOUNDARY CONDITIONS

Assuming that the perturbed quantities depend on time t and spatial co-ordinates x and y on $\exp i(\omega t + kx + ly)$, the linearized equations for the non-conducting and conducting fluids are as follows

$$\nabla \cdot \vec{v}_{11} = 0, \quad \dots(3.1)$$

$$\rho_{11} \cdot i(\omega + kV_1) \vec{v}_{11} = -\nabla \left(P_{11} - \frac{K}{4\pi} \vec{E}_1 \cdot \vec{E}_0 \right), \quad \dots(3.2)$$

$$\nabla^2 \phi_{11} = 0, \quad \dots(3.3)$$

$$\nabla \cdot \vec{v}_{21} = 0, \quad \dots(3.4)$$

$$\rho_{21} \cdot i(\omega + kV_2) \vec{v}_{21} = -\nabla P_{21} \quad \dots(3.5)$$

Let $z = \delta z e^{i(\omega t + kx + ly)}$ be the equation of the perturbed surface. The boundary conditions satisfied by the electric potential are

$$\phi_1 = \phi_0 \quad \text{at } z = h_1$$

$$\phi_1 = \phi_2 \quad \text{at } z = \delta z, \text{ perturbed surface}$$

$$\left. \begin{array}{l} \text{i.e.} \quad \phi_{11} = 0 \quad \text{at } z = h_1 \\ \text{and} \quad \phi_{11} = -\delta z \left(\frac{\phi_{10} - \phi_{20}}{h_1} \right) \text{ at } z = 0, \text{ the unperturbed surface} \end{array} \right\} \dots(3.6)$$

The kinematic boundary conditions are

$$\frac{v_{z11}}{i(\omega + kV_1)} = \frac{v_{z21}}{i(\omega + kV_2)} \text{ at } z = 0, \quad \dots(3.7)$$

$$v_{z11} = 0 \quad \text{at } z = h_1 \quad \dots(3.8)$$

$$v_{z21} = 0 \quad \text{at } z = -h_2 \quad \dots(3.9)$$

The dynamic boundary condition is

$$P_{11} - P_{21} + \delta z(\rho_2 - \rho_1)g - \frac{K}{4\pi} \vec{E}_1 \cdot \vec{E}_0 = T \nabla^2 \delta z, \text{ at } z = 0, \quad \dots(3.10)$$

T being the surface tension.

DISPERSION RELATION

From equation (3.1) — (3.5) on solving we get

$$v_{z11, 21} = \alpha(C_{11, 21} e^{\alpha z} - C_{21, 22} e^{-\alpha z}), \quad \dots(4.1)$$

$$P_{11, 21} = -i\rho_{1, 2}(\omega + kV_{1, 2})(C_{11, 21} e^{\alpha z} + C_{21, 22} e^{-\alpha z}), \quad \dots(4.2)$$

$$\phi_{11} = (A_1 e^{\alpha z} + B_1 e^{-\alpha z}), \quad \dots(4.3)$$

where $\alpha = \sqrt{k^2 + l^2}$, C_{11} , C_{21} , C_{22} , A_1 , B_1 are arbitrary constants.

The six boundary conditions (3.6) — (3.10) give six homogeneous equations for the six arbitrary constants. The eliminant of these gives the following dispersion relation

$$(\omega + kV_1)^2 \rho_1 \coth \alpha h_1 + (\omega + kV_2)^2 \rho_2 \coth \alpha h_2 + \alpha \left\{ \frac{K}{4\pi} \left(\frac{\phi_{10} - \phi_{20}}{h_1} \right)^2 \coth \alpha h_1 - (\rho_2 - \rho_1)g - \alpha^2 T \right\} = 0 \quad \dots(4.4)$$

which gives

$$\omega(\rho_1 \coth \alpha h_1 + \rho_2 \coth \alpha h_2) + k(\rho_1 V_1 \coth \alpha h_1 + \rho_2 V_2 \coth \alpha h_2) = \pm i [X]^{\frac{1}{2}} \quad \dots (4.5)$$

$$\text{where } X = \frac{k^2 \rho_1 \cdot \rho_2 \coth \alpha h_1 \coth \alpha h_2 (V_1 - V_2)^2}{\alpha(\rho_1 \coth \alpha h_1 + \rho_2 \coth \alpha h_2)} + \frac{K}{4\pi} \left(\frac{\phi_{10} - \phi_{20}}{h_1} \right)^2 \coth \alpha h_1 - (\rho_2 - \rho_1) g - \alpha^2 T. \quad \dots (4.6)$$

Considering the wave motion in X -direction only, i.e. putting $l=0$ and $h_1=h_2$, X can be put in the following form

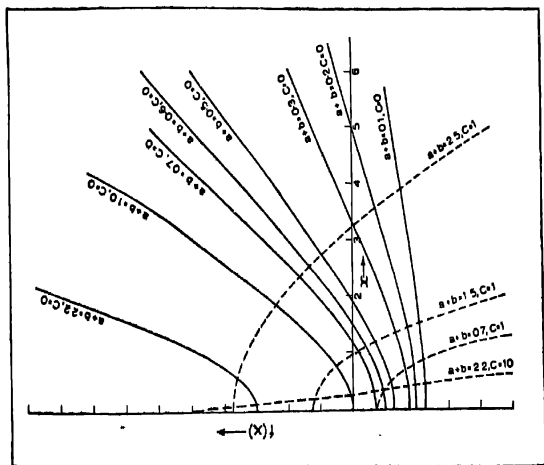
$$X = (a+b) x \coth x - (1+cx^2), \quad \dots (4.7)$$

where

$$\left. \begin{aligned} a &= \frac{\rho_1 (V_1 - V_2)^2}{h_1 \left(1 + \frac{\rho_1}{\rho_2} \right) (\rho_2 - \rho_1) g}, \\ b &= \frac{K}{4\pi h_1 (\rho_2 - \rho_1) g} \cdot \left(\frac{\phi_{10} - \phi_{20}}{h_1} \right)^2, \\ c &= \frac{T}{h_1^2 (\rho_2 - \rho_1) g} \end{aligned} \right\} \quad \dots (4.8)$$

As $\rho_2 > \rho_1$, we note that from (4.7) and (4.5) the interface will be unstable if the function

$$f(x) = (a+b) x \coth x - (1+cx^2), \text{ is positive and stable when it is negative.} \quad \dots (4.9)$$



The function $f(x)$ is plotted in figure 1 for various values of a, b and c . From the analytic behaviour of $f(x)$ and that shown in the figure we make the important conclusions in the following section.

CONCLUSIONS

Case I $c=0$.

$$f(x) = (a+b)x \coth x - 1$$

From the numerical work done we conclude that if $(a+b) > 1$ the system is unstable for all wave numbers. If $(a+b) < 1$ the system is stable for wave numbers less than the critical wave number x_0 , beyond which the system is unstable. We know the relative streaming between two fluids destabilizes short wave-length perturbations (3). The above results show that this is the case even when the electric part of the Maxwellian stress is present and further that this short wavelength instability is enhanced by the presence of Maxwellian stresses.

Case II *Effect of surface tension*

In this case we have

$$f(x) = (a+b)x \coth x - (1+cx^2),$$

For $(a+b) > 1$ and for small values of c the system is unstable for $x < x'_0$ and then it is stable for $x > x'_0$. As we decrease the surface tension parameter c it appears that the unstable wave number band is increased. For large c the wave number band is decreased.

When $(a+b) < 1$ and whatever may be the value of c , the surface tension parameter, the system is always stable. Thus we conclude that for $(a+b) > 1$, and for any value of c the system has a stabilizing effect due to the presence of surface tension. In this case we may say that the surface tension inhibits the Kelvin-Helmholtz instability.

ACKNOWLEDGEMENT

The author is grateful to Dr. C. Uberoi for suggesting the problem and her constant guidance during the preparation of this note. He is also grateful to Prof. P. L. Bhatnagar for his keen interest and kind encouragement.

REFERENCES

- Taylor G. I. & McEwan A. D. 1965 *J. Fluid Mech.* **22**, 1
- Yih 1968 *Phys. of Fluids* **11**, No. 7, 1447.
- Chandrasekhar S. 1961 '*Hydrodynamic and Hydromagnetic Stability*', Oxford University Press.

Note on the longitudinal vibration in a thin visco-elastic rod of variable cross-section,

By SATYANARAYAN MANDAL

Hatugunj M. N. K. High School P.O. Hatugunj, Dist. 24-Parganas,
West Bengal,

(Received 12 December, 1969)

In this note, the longitudinal stress in a thin visco-elastic rod of variable cross-section has been obtained in the presence of a body force. The medium has been taken of the type considered by Achenbach & Chao (1962). The approximate result of the longitudinal stress has been obtained for small values of time. The convolution theorem and Laplace transform have been found suitable.

INTRODUCTION

In this paper, the longitudinal stress in a thin visco-elastic rod of variable cross-section, has been worked out in the presence of a body force in the medium of the type considered by Achenbach & Chao (1962). This stress-strain relation considered by them is given by

$$\left(D + \frac{m^{1/2}}{T}\right)^2 \sigma = E_1 \left(D + \frac{m}{T}\right)^2 \epsilon, \quad \dots(1)$$

where D is the differential operator $\frac{d}{dt}$ and E_1, m, T are material constants σ and ϵ are the stress and strain, respectively. The body force has been considered as $\rho A e^{-kx} \delta(t)$ where ρ is the density of the medium, A , the variable cross-section of the rod and $\delta(t)$, the Dirac delta function. Because of the complication in taking inverse transforms of $\bar{\sigma}$, approximate results of the longitudinal stress have been obtained for small values of time. The use of the convolution theorem and Laplace transform have been found suitable to solve the problem.

EQUATIONS

The stress-strain relation is taken in the form (1). The rod is supposed to be bounded by the sections $x = a$ and $x = b$, its axis being the x - axis.

The equation of motion is given by

$$\frac{\partial}{\partial x}(A\sigma) + \rho A e^{-kx} \delta(t) = \rho A \frac{\partial^2 u}{\partial t^2} \quad \dots(2)$$

where u is the displacement along the x - axis, of a section whose undisturbed position is at a distance x from the origin, A being the area

of this section, ρ , the density of the medium. The body force is given by equation (2)

$$\text{The strain is given by } \epsilon = \frac{\partial u}{\partial x} \quad \dots(3)$$

For linear variation of the cross-section, we write

$$A = A_0 x \quad \dots(4)$$

where A_0 is constant.

End conditions are assumed to be

$$\left. \begin{aligned} \sigma(x, t) &= -P e^{-\omega_1 t} \text{ at } x = a \\ \text{and,} \quad &= 0 \text{ at } x = b \end{aligned} \right\} \quad \dots(5)$$

METHOD OF SOLUTION

Using (5), equation (3) becomes

$$\rho x e^{-kx} \cdot \delta(t) + \sigma + x \frac{\partial \sigma}{\partial x} = \rho x \frac{\partial^2 u}{\partial t^2} \quad \dots(6)$$

Writing $\frac{m^{1/2}}{T} = R$, $\frac{m}{T} = S$ and using equations (1), (4), (7)

we get

$$\begin{aligned} \frac{\partial^4 \sigma}{\partial t^4} + 2R \frac{\partial^3 \sigma}{\partial t^3} + R^2 \frac{\partial^2 \sigma}{\partial t^2} &= \frac{E_1}{\rho} \left(-\frac{\partial^4 \sigma}{\partial t^2 \partial x^2} + 2S \frac{\partial^3 \sigma}{\partial t \partial x^2} + S^2 \frac{\partial^2 \sigma}{\partial x^2} \right) \\ &+ \frac{E_1}{\rho x} \left(\frac{\partial^3 \sigma}{\partial t^2 \partial x} + 2S \frac{\partial^2 \sigma}{\partial t \partial x} + S^2 \frac{\partial \sigma}{\partial x} \right) \\ &- \frac{E_1}{\rho x^2} \left(\frac{\partial^2 \sigma}{\partial t^2} + 2S \frac{\partial \sigma}{\partial t} + S^2 \sigma \right) \\ &- E_1 k e^{-kx} \left\{ \frac{\partial^2}{\partial t^2} \delta(t) + 2S \frac{\partial}{\partial t} \delta(t) + S^2 \delta(t) \right\} \quad \dots(7) \end{aligned}$$

Applying the Laplace transform given by

$$\bar{f}(x, p) = \int_0^{\infty} e^{-pt} \cdot f(x, t) dt$$

to equation (8), with the initial conditions,

$$\sigma(x, 0) = 0 \text{ and } \frac{\partial}{\partial t} \sigma(x, 0) = 0, \quad a \leq x \leq b. \quad \dots(8)$$

and writing $D \equiv \frac{\partial}{\partial x}$, $D^2 \equiv \frac{\partial^2}{\partial x^2}$, etc.

$$\text{we get } D^2 \bar{\sigma} + \frac{1}{x} D \bar{\sigma} - \left\{ \frac{1}{x^2} + q^2 \right\} \bar{\sigma} = A_1 e^{-kx} \quad \dots(9)$$

$$\text{Where } A_1 = \rho k, \quad q^2 = \frac{E_1}{\rho} \quad \text{and} \quad q^2 = \frac{(p^2 + Ep)^2}{c^2(p + S)^2} \quad (10)$$

The solution of equation (9) is given by (Inche 1956)

$$\bar{\sigma}_1(qx) v_1(x) + k_1(qx) v_2(x)$$

where $I_1(qx)$ and $k_1(qx)$ are two fundamental solutions of the reduced

$$\text{equation } D^2 \bar{\sigma} + \frac{1}{x} D \bar{\sigma} - \left\{ \frac{1}{x^2} + q^2 \right\} \bar{\sigma} = 0$$

and $v_1(x)$, $v_2(x)$ are given by

$$\begin{aligned} v_1(x) &= V_1(x) + c_1 = -A_1 \left\{ \frac{k_1(qx)}{\Delta(I_1(qx), k_1(qx))} \cdot e^{-kx} dx + c_1 \right\} \\ v_2(x) &= V_2(x) + c_2 = A_1 \left\{ \frac{I_1(qx)}{\Delta(I_1(qx), k_1(qx))} \cdot e^{-kx} dx + c_2 \right\} \end{aligned} \quad \dots(11)$$

where $\Delta(I_1, k_1)$ is the Wronskian of $I_1(qx)$ and $k_1(qx)$ and c_1 , c_2 are the integration constants. Hence,

$$\bar{\sigma} = c_1 I_1(qx) + c_2 k_1(qx) + I_1(qx) V_1(x) k_1(qx) V_2(x) \quad \dots(12)$$

Now, Laplace transform of (6) is given by

$$\bar{\sigma} = - \frac{P}{p + \omega_1} \text{ at } x = a \quad \dots(13)$$

and,

$$= 0 \text{ at } x = b$$

From equations (12) and (13) we get

$$\begin{aligned} & [-k_1(qa) I_1(qb) V_1(b) - k_1(qa) k_1(qb) V_2(b) + k_1(qb)] \\ c_1 &= \frac{k_1(qa) V_2(a) + k_1(qa) I_1(qa) V_1(a) + \frac{P}{p + \omega_1} \cdot k_1(qb)}{I_1(qb) k_1(qa) - I_1(qa) k_1(qb)} \\ & [-I_1(qb) I_1(qa) V_1(a) - I_1(qb) k_1(qa) \\ c_2 &= \frac{V_2(a) + I_1(qa) k_1(qb) V_2(b) + I_1(qa) I_1(qb) V_1(b) - \frac{P}{p + \omega_1} \cdot I_1(qb)}{I_1(qb) k_1(qa) - I_1(qa) k_1(qb)} \end{aligned} \quad \dots(14)$$

From (14) and (12) we observe that the form of $\bar{\sigma}$ is very complicated. Therefore, the approximate results for small values of time t have been evaluated.

We proceed as follows :

$$\Delta[I_1(qx), k_1(qx)] = \left| \frac{I_1(qx), k_1(qx)}{I'_1(qx), k'_1(qx)} \right|, \text{ where the prime denotes differentiation with respect to } x.$$

$$\cong \left| \frac{1}{(2\pi q)^{1/2}} \left(\frac{e^{qx}}{x^{1/2}} - \frac{3e^{qx}}{8qx^{3/2}} + \dots \right), \left(\frac{\pi}{2q} \right)^{1/2} \left(\frac{e^{-qx}}{x^{1/2}} + \frac{3e^{-qx}}{8qx^{3/2}} - \dots \right) \right|$$

$$\cong \left| \frac{1}{(2\pi q)^{1/2}} \left(\frac{qe^{qx}}{x^{1/2}} - \frac{7e^{qx}}{8x^{3/2}} + \dots \right), \left(\frac{\pi}{2q} \right)^{1/2} \left(-\frac{qe^{-qx}}{x^{1/2}} - \frac{7e^{-qx}}{8x^{3/2}} - \dots \right) \right|$$

$$\cong -\frac{1}{x}. \quad \dots(15)$$

$$\text{Again } v_1(x) = V_1(x) + c_1 \cong A_1 \int \left(\frac{\pi}{2q} \right)^{1/2} \cdot \frac{x}{x^{1/2}} \cdot e^{-kx} \cdot e^{-qx} \cdot \left(1 + \frac{3}{8qx} + \dots \right) dx + c_1$$

$$\cong -A_1 \left(\frac{\pi}{2q} \right)^{1/2} \cdot \frac{e^{-(k+q)x}}{k+q} \cdot x^{1/2} + c_1 \quad \dots(16)$$

$$v_2(x) = V_2(x) + c_2 \cong -A_1 \int \frac{1}{(2\pi q)^{1/2}} \cdot \frac{e^{qx}}{x^{1/2}} \cdot x \cdot e^{-kx} \cdot \left(1 - \frac{3}{8qx} + \dots \right) dx + c_2$$

$$\cong -A_1 \cdot \frac{1}{(2\pi q)^{1/2}} \cdot \frac{e^{(q-k)x}}{q-k} \cdot x^{1/2} + c_2. \quad \dots(17)$$

$$-k_1(qa)I_1(qb)V_1(b)I_1(qx) \cong \frac{A_1}{4q^3} \cdot \frac{1}{(x,a)^{1/2}} \cdot \frac{1}{q+k} \cdot e^{qx-q a-k b}$$

$$-I_1(qx)k_1(qa)k_1(qb)V_2(b) \cong \frac{A_1}{4q^3} \cdot \frac{1}{(x,a)^{1/2}} \cdot \frac{1}{q-k} \cdot e^{qx-q a-k b}$$

$$k_1(qb)k_1(qa)V_2(a)I_1(qx) \cong -\frac{A_1}{4q^3} \cdot \frac{1}{(x,b)^{1/2}} \cdot \frac{1}{q-k} \cdot e^{qx-q b-k a}$$

$$k_1(qb)I_1(qa)V_1(a)I_1(qx) \cong -\frac{A_1}{4q^3} \cdot \frac{1}{(x,b)^{1/2}} \cdot \frac{1}{q+k} \cdot e^{qx-q b-k a}$$

$$-I_1(qb)I_1(qa)V_1(a)k_1(qx) \cong \frac{A_1}{4q^3} \cdot \frac{1}{(x,b)^{1/2}} \cdot \frac{1}{q+k} \cdot e^{qx-q b-k a}$$

$$-k_1(qx)I_1(qb)k_1(qa)V_2(a) \cong \frac{A_1}{4q^3} \cdot \frac{1}{(x,b)^{1/2}} \cdot \frac{1}{q-k} \cdot e^{qx-q b-k a}$$

$$I_1(qa)I_1(qb)V_1(b)k_1(qx) \cong -\frac{A_1}{4q^3} \cdot \frac{1}{(x,a)^{1/2}} \cdot \frac{1}{q+k} \cdot e^{qa-q x-k b}$$

$$I_1(qb)V_2(b) \cong -\frac{A_1}{4q^3} \cdot \frac{1}{(x,a)^{1/2}} \cdot \frac{1}{q-k} \cdot e^{qa-q x-k b} \quad \dots(18)$$

$$-\frac{P}{p + \omega_1} [I_1(qb)k_1(qx) - k_1(qb)I_1(qx)] \cong -\frac{P}{p + \omega_1} \cdot \frac{e^{q(b-x)}}{2q(bx)^{1/2}} \left[1 + \frac{3}{8q} \cdot \frac{b-x}{bx} - e^{-2q(b-x)} \cdot \left(1 - \frac{b-x}{bx} \cdot \frac{3}{8q} \right) \right]$$

Similarly (Sarkar 1967) (Sarkar 1967)...(19)

$$k_1(qa)I_1(qb) - k_1(qb)I_1(qa) \cong \frac{e^{q(b-a)}}{2q(ba)^{1/2}} \left[1 + \frac{3}{8q} \cdot \frac{b-a}{ba} - e^{-2q(b-a)} \left\{ 1 - \frac{(b-a)}{ba} \cdot \frac{3}{8q} \right\} \right] \quad \dots(20)$$

Hence, neglecting the terms containing $\frac{1}{q^2}$ and its higher powers from (18), (19) and (20) we get

$$-\frac{P}{p + \omega_1} \cdot \frac{[I_1(qb)k_1(qx) - k_1(qb)I_1(qx)]}{[k_1(qa)I_1(qb) - k_1(qb)I_1(qa)]} \cong -\frac{P}{p + \omega_1} \cdot \left(\frac{a}{x} \right)^{1/2} \cdot e^{q(a-x)} \cdot \left[1 + \frac{1}{q} \left\{ \frac{3(b-x)}{8bx} - \frac{3(b-a)}{8ab} \right\} \right] \cong -\frac{P}{p + \omega_1} \left(\frac{a}{x} \right)^{1/2} \cdot e^{q(a-x)}, \quad \dots(21)$$

and

$$I_1(qx)V_1(x) + k_1(qx)V_2(x) \cong -A_1 \frac{e^{-kx}}{(2k)} \left[\frac{1}{q-k} - \frac{1}{q+k} \right] \quad \dots(22)$$

From equations (12), (14), (21) and (22) we get

$$\bar{\sigma} \cong -P \cdot \left(\frac{a}{x} \right)^{1/2} \cdot \frac{1}{p + \omega_1} \cdot e^{q(a-x)} - A_1 e^{-kx} \cdot \frac{1}{(2k)} \left[\frac{1}{q-k} - \frac{1}{q+k} \right] \quad \dots(23)$$

Putting $a - x = -h_1$ in (23) we get

$$\bar{\sigma} = P \cdot \left(\frac{a}{x} \right)^{1/2} \left[\frac{1}{p + \omega_1} \cdot e^{-h_1 q} \right] - \frac{A_1}{2k} \cdot e^{-kx} \left[\frac{1}{q-k} - \frac{1}{q+k} \right] \quad \dots(24)$$

Now, putting the value of $q^2 = \frac{(p^2 + R\rho)^2}{c^2(p+S)^2}$ we have

$$\frac{1}{q-k} = \frac{C(p+S)}{\left(p + \frac{R-kc}{2} \right)^2 - N^2}$$

and

$$\frac{1}{q+k} \cong \frac{c(p+S)}{\left(p + \frac{R+kc}{2} \right)^2 - N_1^2} \quad \dots(25)$$

$$\text{where } N^2 = \left(\frac{R - kc}{2} \right)^2 + kcS \quad \text{and} \quad N_1^2 = \left(\frac{R + kc}{2} \right)^2 - kcS$$

Using the notation of Van der Pol & Bremmer in (25) we have

$$x(t) \cdot e^{c_3 t} = \frac{c}{2N} \left[\frac{N - S_1}{p + N} + \frac{N + S_1}{p - N} \right]$$

and $x_1(t) \cdot e^{c_4 t} = \frac{c}{2N_1} \left[\frac{N_1 - S_2}{p + N_1} + \frac{N_1 + S_2}{p - N_1} \right] \quad \dots(26)$

$$\text{where } c_3 = \frac{R - kc}{2}, \quad c_4 = \frac{R + kc}{2}, \quad S_1 = S - \frac{R - kc}{2},$$

$$S_2 = S - \frac{R + kc}{2}.$$

Again, using the value of q^2 we have

$$\frac{1}{p + \omega_1} \cdot e^{-\frac{h_1}{c} q} = \frac{e^{-\frac{h_1}{c} [p - (S - R)]}}{p + \omega_1} - \frac{e^{-\frac{h_1}{c} [p - (S - R)]}}{p + \omega_1} \cdot \left[1 + e^{-\frac{c_3}{p + S}} \right] \quad \dots(27)$$

$$\text{where } c_3 = \frac{h_1}{\sigma} S(S - R).$$

Using the notation of Van der Pol & Bremmer, we write

$$x_2(t) = \frac{e^{-\frac{h_1}{c} [p - (S - R)]}}{p + \omega_1} \quad \text{and} \quad x_3(t) = \left[1 - e^{-\frac{c_3}{p + S}} \right]$$

$$\left. \begin{aligned} \text{Hence, } x_2(t) \cdot e^{(R-S)t} &= 0, \quad 0 < t < \frac{h_1}{c} \\ &= e^{-\alpha \left(t - \frac{h_1}{c} \right)}, \quad t > \frac{h_1}{c} \end{aligned} \right\} \quad \dots(28)$$

(Erdelyi)

$$\text{where } \alpha = \omega_1 + S - R,$$

$$\text{and } x_3(t) \cdot e^{St} = c_s^{1/2} \cdot t^{-1/2} \cdot J_1(2c_s^{1/2} t^{1/2}) \quad \dots(29)$$

(Erdelyi)

Using (24), (26), (28) and (29) we get

$$v \cong -e^{-kx} \left[B e^{-\frac{h_1}{c} t} F e^{-\frac{t}{\sigma}} G e^{-\frac{t}{\sigma}} H e^{-\frac{t}{\sigma}} \right], \quad 0 < t < \frac{h_1}{c} \quad \dots(30)$$

$$\begin{aligned}
 \text{and } \sigma &\cong -P\left(\frac{a}{x}\right)^{1/2} \left[e^{-\omega_1 t} \cdot e^{\frac{h_1 c}{c}} - e^{-\omega_2 t} \cdot e^{\frac{h_2 c}{c}} \right. \\
 &\quad \left. {}^*c_5^{1/2} \cdot e^{-S_1 t} \cdot t^{-1/2} \cdot J_1 \left(2c_5^{1/2} t^{1/2} \right) \right] \\
 &\quad - e^{-kx} [E e^{-\xi_1 t} + F e^{\xi_2 t} - G e^{-\xi_3 t} - H e^{-\xi_4 t}], \quad t > \frac{h_1}{c} \\
 &= -P\left(\frac{a}{x}\right)^{1/2} \cdot e^{\frac{h_1 c}{c}} \cdot e^{-\omega_1 t} \left[1 + c_5^{1/2} \right. \\
 &\quad \left. \int_0^t e^{(\omega_1 - S)\tau} \cdot \tau^{-1/2} \cdot J_1 \left(2c_5^{1/2} \tau^{1/2} \right) d\tau \right] \\
 &\quad - e^{-kx} \left(E e^{-\xi_1 t} + F e^{\xi_2 t} - G e^{-\xi_3 t} - H e^{-\xi_4 t} \right), \quad t > \frac{h_1}{c}.
 \end{aligned}$$

(Churchill 1958) ..(31)

where $E = \frac{A_1}{2k} \cdot \frac{c}{2N} (N - S_1)$, $F = \frac{A_1}{2K} \cdot \frac{c}{2N} (N + S_1)$,

$G = \frac{A_1}{2k} \cdot \frac{c}{2N_1} (N_1 - S_2)$

$H = \frac{A_1}{2k} \cdot \frac{c}{2N_1} \cdot (N_1 + S_2)$, $\xi_1 = (c_3 + N)$,

$\xi_2 = (N - c_3)$, $\xi_3 = (c_4 + N_1)$, $\xi_4 = (c_4 - N_1)$.

Now, $J_1(x) = \sum_{r=0}^{\infty} \frac{(-1)^r \cdot \left(\frac{x}{2}\right)^{1+2r}}{r! \Gamma(r+2)}$, $e^{Q\tau} = \sum_{n=0}^{\infty} \frac{(Q\tau)^n}{n!}$

if $\omega_1 - S = Q > 0$

if $\omega_1 - S = -Q < 0$ } ... (32)

and $e^{-Q\tau} = \sum_{n=0}^{\infty} \frac{(-1)^n (Q\tau)^n}{n!}$

Therefore, using (32) we get

$$\begin{aligned}
 &\int_0^t e^{(\omega_1 - S)\tau} \cdot \tau^{-1/2} \cdot J_1 \left(2c_5^{1/2} \tau^{1/2} \right) d\tau \\
 &= \sum_{r,n=0}^{\infty} \frac{(-1)^r \cdot c_5^{\frac{1+2r}{2}} \cdot Q^n}{r! n! \Gamma(r+2) \cdot (r+n+1)} t^{r+n+1}, \quad \text{if } \omega_1 - S > 0 \\
 &\text{and} \\
 &\int_0^t e^{(\omega_1 - S)\tau} \cdot \tau^{-1/2} \cdot J_1 \left(2c_5^{1/2} \tau^{1/2} \right) d\tau \\
 &= \sum_{r,n=0}^{\infty} \frac{(-1)^{r+n} \cdot c_5^{\frac{1+2r}{2}} \cdot Q^n}{r! n! \Gamma(r+2) \cdot (r+n+1)} t^{r+n+1}, \quad \text{if } \omega_1 - S < 0
 \end{aligned}$$

(33)

Substituting the value of h_1 in (29), (31) and using (33) we get

$$\sigma \cong -e^{-kx} \left[Ee^{-\zeta_1 t} + Fe^{-\zeta_2 t} - Ge^{-\zeta_3 t} - He^{-\zeta_4 t} \right], \quad 0 < t < \frac{x-a}{c} \quad \dots(34)$$

$$\sigma \cong -P \left(\frac{a}{x} \right)^{1/2} \cdot e^{\left(\frac{x-a}{c} \right) \alpha} \cdot e^{-\omega_1 t} \left[1 - \right.$$

$$\left. c_5 \sum_{r,n=0}^{\infty} \frac{(-1)^{r+n} \cdot c_5^r \cdot Q^n}{r! n! (r+n+1) \Gamma(r+2)}, t^{r+n+1} \right]$$

$$- e^{-kx} \left[Ee^{-\zeta_1 t} + Fe^{\zeta_2 t} - Ge^{-\zeta_3 t} - He^{-\zeta_4 t} \right],$$

$$\omega_1 - S < 0 \text{ and } t > \frac{x-a}{c}$$

$$\sigma \cong -P \left(\frac{a}{x} \right)^{1/2} \cdot e^{\left(\frac{x-a}{c} \right) \alpha} \cdot e^{-\omega_1 t} \left[1 - \right.$$

$$\left. c_5 \sum_{r,n=0}^{\infty} \frac{(-1)^{r+n} \cdot c_5^r \cdot Q^n}{r! n! (r+n+1) \Gamma(r+2)}, t^{r+n+1} \right]$$

$$+ e^{-kx} \left[Ee^{-\zeta_1 t} + Fe^{\zeta_2 t} - Ge^{-\zeta_3 t} - He^{-\zeta_4 t} \right],$$

$$\omega_1 - S < 0 \text{ and } t > \frac{x-a}{c} \dots(35)$$

The author expresses his sincere gratitude to Dr. S. K. Sarkar, Jadavpur University, for his kind help and guidance in this work.

REFERENCES

- Churchill, R. V. 1958 *Operational Mathematics*, 2nd ed.
 Erdelyi—*Tables of Integral Transforms*, 242 and 245.
 Inche E. L. 1956 *Ordinary differential equation*—Dover Publication, Inc. 122
 Sarkar, S. K. 1967 Note on the vibration of visco-elastic rod of variable cross section—*Tomul. XIII (XVII), Fasc. 1-2*,
Bulletin of the Calcutta Mathematical Society 1965, 57

Letters to the Editor

Polarised absorption spectrum of Co^{2+} doped in CsCdCl_3 at 77°K and 20°K .

By RANAJIT KR. SHAHA, RANAJIT KR. MUKHERJEE AND A. BOSE
Indian Association for the Cultivation of Science, Calcutta-32

AND

MIHIR CHOWDHURY

Presidency College, Calcutta

(Received 3 March 1970.)

The energy levels of Co^{2+} have been studied extensively in octahedral field of oxides, (Low 1959) in tetrahedral fields of oxides, sulfides and halides (McLure 1957, Pappalardo & Dietz 1961, Cotton *et al* 1961) and also in cubic field of fluorides (Stahl-Brada & Low 1959). In order to study the ligand field provided by a distorted octahedron of Cl^- we have grown single crystals of CsCdCl_3 doped with Co^{2+} from the melt at about 485°C in an inert atmosphere by the Stock-Berger method and recorded the polarised spectrum at 77°K and 20°K . (Gruen & McBeth 1963)

Crystals of CsCdCl_3 are hexagonal as grown from melt. The structure has been reported by Siegel & Gebert (1964) (Space Group C_6/mmm C_6 , $Z = 6$). Six Cl^- ions form a trigonally distorted octahedron around the central metal ion.

Figure 1 shows the low resolution spectrum at 77°K . A high resolution polarised spectrum for the visible region at the liquid hydrogen temperature was photographed in a Zeiss PGS 2 grating spectrograph with Kodak

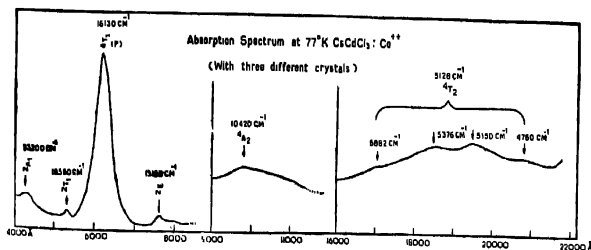


Figure 1

103 A-E film. Figures 2a and 2b reproduce the microphotometer tracing of the photographs taken at 20°K .

The ground term 4F of Co^{2+} splits in the octahedral field into 4T_1 , 4T_2 and 4A_2 with 4T_1 lying lowest. We have assigned the band at 5128 cm^{-1} to the ${}^4T_1 \rightarrow {}^4T_2$ transition and calculated D_q to be $\sim 640\text{ cm}^{-1}$. This low value of D_q is presumably due to the large Cd-Cl distance (2.59 \AA average) and the large difference in ionic radii of Cd^{2+} (1.03 \AA) and of Co^{2+} (0.80 \AA).

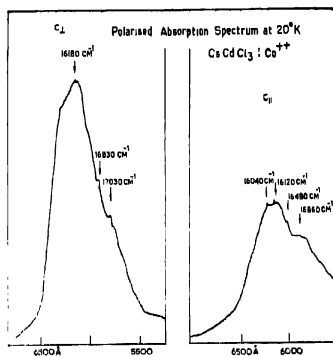


Figure 2a

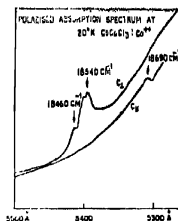


Figure 2b

The observed band at 10420 cm^{-1} is ascribed to ${}^4T_1 \rightarrow {}^4A_1$ transition. The band is weak compared to the ${}^4T_1 \rightarrow {}^4T_2$ transition, for it corresponds to a two electron jump. The observed band at 16130 cm^{-1} is ascribed to the ${}^4T_1 \rightarrow {}^4T_1$ (4P) transition. The energy separation between 4F and 4P is calculated to be 12410 cm^{-1} which is less than the free ion value 14500 cm^{-1} . The sharp band at 18550 cm^{-1} is assigned to a spin forbidden transition to the doublet state (2T_1) arising from the 2G state. The high intensity is presumably due to the mixing with the 4P quartet state. The 2T_2 term may be somewhere around the 2T_1 term. The band

at 23200 cm^{-1} may be identified as the ${}^4T_1({}^4F) \rightarrow {}^3A_1({}^3G)$ transition. The ${}^2E({}^2G)$ term has been located at 13160 cm^{-1}

The observed humps at 5376 cm^{-1} , 5150 cm^{-1} and 4760 cm^{-1} probably correspond to the components of the 4T_2 state split by the spin-orbit and the trigonal field interactions. From the observed fine structure at 17030 cm^{-1} , 16830 cm^{-1} and 16180 cm^{-1} in $C \perp$ spectrum and at 16480 cm^{-1} , 16120 cm^{-1} and 16180 cm^{-1} at $C \parallel$ spectrum (figure 2a) at 20°K we calculated λ_s (spin-orbit coupling for 4P) to be 120 cm^{-1} and Δ (trigonal field splitting) $\sim 140\text{ cm}^{-1}$. The observed fine structure at 18540 cm^{-1} and 18460 cm^{-1} in $C \perp$ spectrum and at 18690 cm^{-1} in $C \parallel$ spectrum at 20°K gives the value of $\lambda_G \sim 105\text{ cm}^{-1}$ and Δ to be $\sim 150\text{ cm}^{-1}$ (corresponding values for 3G state)

Theoretical and experimental details of the energy level pattern along with the magnetic susceptibility and anisotropy of the crystal will be reported shortly in details.

REFERENCES

- Cotton F. A., Goodgame D. M. L. & Goodgame M. 1961 *J. Am. Chem. Soc.* **83**, 4690.
 Gruen D. M. & McBeath R. 1963 *Pure and Applied Chemistry*, **6** No. 1, 23.
 Low W. 1959 *Phys. Rev.* **109**, 256
 McClure D. S. 1957 *J. Phys. Chem. Solids* **3**, 311.
 Pappalardo R. & Dietz R. E. 1961 *Phys. Rev.*, **123**, 1188.
 Siegel S. & Gebert E. 1964, *Acta Cryst.* **17**, 790.
 Stahl-Brada R. & Low W.: 1959 *Phys. Rev.* **113**, 775

Indian Phys. **43**, 777—778 (1969)

The crystal structure of potassium salt of homophthalic acid

By M. P. GUPTA AND D. S. DUBEY

Department of Physics, University of Ranchi, Ranchi-8

(Received 20 January 1970)

As part of a programme for studying the structures of simple organic acids and their salts and the scheme of hydrogen bonding in these structures, we have been studying for sometime homophthalic (α -2-toluene dicarboxylic) acid $\text{C}_9\text{H}_8\text{O}_4$ (Gupta & Bose 1969). We thought it worthwhile to get the skeletal arrangement of the homophthalate group itself by the well-known heavy atom technique in crystallography. Our preliminary results are interesting and are being reported here.

There are two carboxyl groups in this molecule and depending upon the pH values of the solutions, one would expect for a dicarboxylic acid, either an acid salt or a neutral salt of the acid. However, reactions with stoichiometric amounts of reacting substances do not yield the desired compounds. This has been reported by Gupta & Barnes (1956, 1961) for other dicarboxylic acids also.

In this particular case, chemical considerations favour simultaneous ionization of both the COOH groups leading to the formation of a neutral salt. But we find that stoichiometric proportions of the reacting substances (acid + potassium hydroxide) in a water solution, yield crystals, the chemical composition of which could be written down only as $C_6H_7O_4 \cdot \frac{1}{2}K$ i.e. per homophthalic acid molecule, there is associated only half a potassium atom.

As this raised interesting points of structural arrangement (viz., whether both the COOH groups are ionized or only one, and the function and disposition of the heavy atom relative to the carboxyl groups), we have completed an X-ray examination of these crystals.

X-ray data :

X-ray diffraction data with single crystals show them to be monoclinic with, $a = 32.35\text{\AA}$, $b = 5.43\text{\AA}$, $c = 9.96\text{\AA}$, $\beta = 95^\circ 54'$, ρ obs. = 1.51 gm/ml. With the above value of observed density, the total unit cell content is 1583 (amu). For the empirical formula $C_6H_7O_4 \cdot \frac{1}{2}K$ and eight such asymmetric units in the cell the expected value is 1588 (amu). We have ruled out completely the possibility of water of crystallization in the structure from a structure determination.

Space group absences: hkl , when $h + k = 2n + 1$, $h0l$ when $l = 2n + 1$, $0k0$ when $k = 2n + 1$, $h00$ when $h = 2n + 1$. This fixes the space group uniquely as $C_{2/c}$ with eight general positions. As the asymmetric unit formula is $C_6H_7O_4 \cdot \frac{1}{2}K$ and there are eight general positions, there would be only four heavy atoms in the structure and these must occupy special positions. We have completed a Fourier analysis of the zonal data $h0l$, $hk0$, the Fourier looking down the $[010]$ axis being shown in figure 1 below. The orientation of the molecule and the positions of the heavy atoms have been confirmed again by the other projection. The least-squares refined data, with only overall isotropic temperature factor, for the projections gives $R(h0l) = 0.18$, $R(hk0) = 0.21$.

As there is considerable overlap in the other two projections and the interesting points of structural chemistry cannot be settled without a complete three-dimensional analysis leading to accurate values of the bond

The crystal structure of potassium salt of homophthalic acid 779

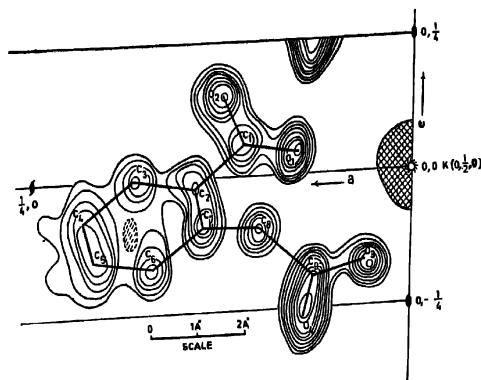


Figure 1

lengths and angles, we are doing a three-dimensional least-squares refinement of the X-ray data, the results of which will be published later.

REFERENCES

- Gupta M. P. & Bose S. 1969 *Indian J. Phys.* **43**, 45.
 Gupta M. P. & Barnes W. H. 1956 *Can. J. Chem.* **34**, 563.
 Gupta M. P. & Barnes W. H. 1961 *Can. J. Chem.* **39**, 1739

BOOKS RECENTLY RECEIVED FOR REVIEW

- Springer Tracts in Modern Physics (52) Weak Interactions*—Ed. G. Hohlar, \$16.00
Springer-Verlag, Berlin.
- The Indian Ephemeris and Nautical Almanac for the Year 1971*—Director, Regional,
Meteorological Centre, Rs. 17.00 or \$6.12.
- National Physical Laboratory Report for 1969-70*, Her Majesty's Stationery Office
£1-8-0, England.
- Nuclear Magnetic Resonance Spectroscopy*, Ruth M. Lynden Bell and Robin K.
Harris, £3-10-0, Thomas Nelson & Son Ltd., London.
- Handbook of Gas Laser Experiments*, G. L. Rogers, 30S, Butterworth & Co. Ltd., London.
- High temperature information Bulletin*, British Council, London.
- High temperature Reaction Rate Data*, British Council, London.
- Operational Calculus*, Gregers Grabbe, \$14.45, Springer-Verlag, Berlin.
- Lectures in theoretical Physics* Mathematical methods in theoretical Physics V. XI D K. T.
Mahantappa and W. E. Brittin, \$20 40, Gordon & Breach Science Publishing Ltd. London.
- Proceedings of the International Conference on Organic Superconductor*, Ed. William
A. Little, Interscience Publisher a division of John Wiley & Sons. New York.
- Atomic Spectra (Second Edn.)*, H. G. Kuhn, 105.00 Longman, Green & Co. Ltd. London.
- Lectures on symmetric*, J. Leite Lopes Pub. £6-5-0, Gordon & Breach Science
Publishing Co. London.
- Phase transformation*, H. I. Aaronson, Seminar Coordinator, 247, Chapman Hall Ltd, London.
- Plane elastic deformation*, R. Tiffen, 40sh, Longman, London.
- The application of Holography*, H. J. Caulfieldt and S. Lu \$9.95, John Wiley & Son, New York.
- Direct nuclear reaction theories*, Norman Austern, \$19.95, John Wiley & Son, New York.
- Elementary Particle Physics and Scattering Theory*, Vol. 1 and Vol. 2, Ed. M. Chretien and
S. S. Schweber, £14-15 0 and £13-15.0, Gordon & Breach Science Publishers, London.
- Lectures on Electrodynamics*, J. R. Oppenheimer, £7-5-0, Gordon & Breach Science
Publisher, London.
- Nuclear Reactions*, D. F. Jackson, 65sh, Methuen & Co. Ltd., Eondon.

PROCEEDINGS
OF THE
INDIAN ASSOCIATION FOR THE CULTIVATION OF SCIENCE

(Edited in Collaboration with the Indian Physical Society).

Vol 52

No. 12

MAHENDRA LAL SIRCAR MEMORIAL LECTURE, 1969

Delivered on 22 September, 1969

By

J. C. Roy

PUBLISHED BY THE
INDIAN ASSOCIATION FOR THE CULTIVATION OF SCIENCE
JADAVPUR, CALCUTTA-32



Mahendralal Sircar Memorial Lecture, 1969

By Dr. J. C. Roy D.Sc. F.N.A.

Indian Institute for Biochemistry and Experimental Medicine

Calcutta-32

(Delivered on 22 September, 1969)

Fellow Scientists, Ladies and Gentlemen,

I am deeply sensible of the honour of being invited to deliver Mahendralal Sircar Memorial Lecture for 1969. A pioneer of rare quality, Dr. Mahendralal Sircar was endowed with unequalled imaginative richness and scientific perception. The Indian Association for the Cultivation of Science is his monumental work, an imperishable legacy of a great endeavour.

To-day we really celebrate the centenary of Dr. Sircar's endeavour to establish the originality and identity of Indian science. Writing in 1869 in the Calcutta Journal of Medicine he gave us the first steps we should take in formulating any national plan for the development of science and technology in the country. Dr. Mahendralal Sircar was a medical man and medicine was then wrapped in an atmosphere of empiricism. It is really amazing that from wayside he could watch the triumphant march of the quickening spirit of physical sciences and rapid advances which brought wealth and prosperity to Europe as a whole. A magnificent man as he was, his vision transcended the barriers of confused thinking. It is to the undying credit of Dr. Sircar that he managed to instil a perception of science at a time when thinking was clouded by medievalism.

In order that a proper climate could be had for pursuit of research, Dr. Sircar thought boldly of an institution dedicated to science for the Indians, of the Indians and by the Indians.

Science is international but scientists are national. This was true as much for Mahendralal Sircar as for Louis Pasteur. And in adhering to this truth unflinchingly he faced many difficulties and privations but the challenge was accepted and the response, as you see it to-day, was a national laboratory of international fame, the product of his singular effort and neverceasing pursuit of uncompromising idealism.

It does give me much pain to note that even after independence the Indian Association for the Cultivation of Science remained a Cinderella while the Government could be Prince Charming to so many institutions.

This institution carrying as it did a rich legacy deserved very special attention. Yet it lacks equipments of modern specialized variety even to-day. Much remains to be done in this regard. This is hardly a fitting

tribute to the pioneer of pure science in India who laid such enduring foundations for scientific research.

When I took the decision of locating the Indian Institute for Biochemistry & Experimental Medicine at the adjacent building which was then a marshy low land with tanks and gulleys, I had faced criticism but was not deterred as I had felt somewhat thrilled by sheer historicity of the site. I was clear in my mind that I was taking the Institute into a scientific colony amidst which stood with passionless grandeur the epitome of pure scientific endeavour : the Indian Association for the Cultivation of Science. To be anywhere near it is to breathe in an atmosphere of research.

Such has been the lure of heritage of the Indian Association for the Cultivation of Science, yet the institution itself suffered gross neglect. The Government grants are woefully inadequate. So are the equipment and personnel as a result. The remedy lies in the Central Government stepping in and helping the Institute to expand on modern lines.

With the above observations, I would like to pass on to the theme of my lecture *viz.* the tools and techniques of microbiological research.

TOOLS AND TECHNIQUES OF MICROBIOLOGICAL RESEARCH

In all branches of biological research to-day, new techniques and instrumentation have opened out vast areas for investigation and provided the means for the rapid advancement of knowledge. This has come about mainly as a result of development in applied physics—optics, electronics and electrical technology—and the intensive application of physico-chemical concepts and techniques in biological research. We have in fact reached a stage when it is necessary sometimes to guard against the tendency to exaggerate the importance of instrumentation and techniques and to consider them an end in themselves. However powerful and versatile the tools available to the research worker, he can get little out of them unless he uses them purposefully and for fruitfully conceived ends—the scientific objective of his study. In this sense, the human brain retains, as it will always retain, its unchallenged pre-eminence as the means to the acquisition and extension of scientific knowledge.

Nevertheless, it is important for the working scientist to keep abreast of advances in techniques and instrumentation in his field, for they are the tools of his trade and the quality of his work will be determined by his expertise in their use. The development of science is conditioned not only by the social milieu in which the scientist works, but also by the tools and techniques available to him for his work. Thus, the classical investigations on X-rays and elementary particles followed from the

development of techniques for producing high vacua, and the discovery of the rare gases from accurate techniques of quantitative chemical analysis. In this sense techniques and instrumentation set not only the pace of progress in science but also the directions of that progress.

The role of instrumentation and techniques in the advancement of science is most aptly illustrated in the history of microbiology. Microbiology as a science was born with the invention of the microscope. The use of the microscope, in combination probably with the method of dark ground illumination enabled Leeuwenhoek to discover bacteria and describe practically all the morphological types of them known today. The technique of cultivation of bacteria in pure culture which Koch established opened up inexhaustible fields of research and influenced the whole subsequent history of bacteriology; this, in spite of the fact that the method was simplicity itself. In Koch's own words "the peculiarity of my method is that it supplies a firm, and where possible, a transparent pabulum; that its composition can be varied to any extent suited to the organism under observation; that all precautions against the possibility of after-contamination are rendered superfluous; that subsequent cultivation can be carried out by a larger number of single cultures of which, of course, only those cultures which remain pure are employed for further cultivation; and that, finally, a constant control over the state of the culture can be obtained by the use of microscope".

Next only in order of importance to the development of the science of bacteriology was the establishment of techniques for staining bacteria. The employment of stains for bacteria followed from their earlier use in ordinary histological work. This started with carmine preparations which were originally employed by Goeppert and Cohn but came into prominence through the work of Hartig and later, Gerlach. The preparation of dyes from aniline and coal tar took place about this time and greatly influenced staining techniques in bacteriology. Weigert showed that methyl violet can be successfully used to reveal cocci in tissues, and other workers stained bacteria in an aqueous solution of fuchsin. But again, it was Koch who laid the foundation of the technical procedures employed today for staining. Realizing the importance of getting the bacteria into a non-motile state, he prepared thin films on cover glasses and dried them. He then fixed the preparations with alcohol and applied various stains, and finally mounted the preparations in Canada balsam. From then onwards staining methods were rapidly perfected, much of it on the basis of the epoch-making work of Ehrlich on the staining of specific granulations in white blood corpuscles.

Proceeding from these three basic techniques—microscopy, pure cultivation and staining—I shall rapidly review recent developments which have augmented and diversified their scope and application in bacteriological research and consider their impact on current objectives of microbiological study. For the examination of living cells, phase contrast microscopy has become the method of choice. This method, first described by Zernike in 1942 has been in general use for over fifteen years and I need not describe it at length. In conventional microscopy a transparent object remains invisible, because it has no effect on the intensity of light while the eye or the photographic plate are only sensitive to variations in light intensity. Nevertheless, a transparent objective influences light passing through it by delaying or altering the phase or optical path to an extent determined by its thickness and refractive index. In a heterogeneous transparent object such as a living cell there are regions of different thickness and refractive index. Each such region will therefore introduce a phase change in a light wave passing through it. These invisible phase changes are converted into intensity changes and a transparent object made to appear as if it were an absorbing object in the phase contrast microscope by separating the original and the diffracted wave and altering their relative phase contrast before recombining them. Briefly, the practical achievement of phase contrast depends on the ability to separate the original and diffracted waves.

It will be evident that the development of the phase contrast microscope represents a dual advance in technique ; it not only extends the scope of microscopic observation but provides at the same time what may be described as an optical equivalent to chemical staining techniques. Staining procedures designed to reveal details of sub-cellular structure reduce the dynamic morphological features of the living cell to a static condition, and destroy or distort the vital activity of the features under observation. The phase contrast microscope enables structures to be observed without chemical interference with normal cellular activity.

However the phase contrast microscope suffers from certain shortcomings, chiefly the appearance of a halo around every object-detail and the non-uniformity of the phase contrast effect which tends to fall off towards the centre of large uniform objects. The halo effect is reduced or eliminated in some forms of interference microscopes, which are thus more suitable for quantitative work. The basic theory underlying the operation of the interference microscope, is that a transparent object can be made to appear like an absorbing one by adding a suitable wave, instead of as in phase contrast, by altering the phase relationship between the direct and diffracted waves.

An important application of both the phase contrast and interference microscopes is in the measurement of the concentration of solids and the mass of cells. In both types of microscopy image contrast depends upon the optical path difference or phase change induced by the object, which in turn is a function of its refractive index. It is thus possible to determine the refractive index of the object under observation, from known mathematical relationships. The technique of cell refractometry consists essentially in varying the refractive index of the immersing medium until those parts of the cell in contact with the medium disappear. Since many careful measurements have shown that the relationship between refractive index and the concentration of dissolved substances is linear, it becomes a simple matter to calculate the concentration of solids (and dry mass of the cell) from the observed value for refractive index. The dry mass may also be calculated from direct measurement of the phase change using the interference microscope. However, there is no simple method at present of determining the total dry mass of an entire cell, although it is comparatively easy to determine the dry mass per unit area of any region of a cell.

Cell refractometry, applied to large populations of cells, has already yielded valuable information about the solid concentration in many species of bacteria grown on solid and liquid media. Refractometry has also been used for the study of fungal growth. Mitchinson used interference microscopy to show that the increase in the dry mass of a single yeast cell was approximately linear upto the stage of division, whereas the solid concentration was fluctuating.

Another important advance in the employment of special types of microscope has been the development of the ultraviolet microscope. It gives photographic records indicating difference in absorption of short wave ultraviolet light by particular substances, especially nucleic acids. Fluorescence microscopy has found even wider application; although the first fluorescence microscope was constructed by Kohler more than fifty years ago, it is only during the last ten years that the instrument has become prominent in research, notably in the fields of immunology and virology. In it the specimen itself is rendered luminous and emits light to form the observed image. The high pressure mercury vapour lamp is now used in most laboratories as the most convenient source for excitation of the specimen and this is combined with a collecting lens, and an appropriate long wave ultraviolet or blue glass filter.

The prevailing interest in fluorescence microscopy is due largely to the fluorescent antibody technique, which originated with the discovery of Coons & Kaplan in 1950 that antibody globulins from the blood of

immunized animals could be linked to a fluorescent compound, fluorescein isocyanate, without loss of their capacity to combine with their specific antigens. Owing to the characteristic pale green fluorescence of the fluorescein-treated antibody, it was possible, with a fluorescence microscope, to detect for the first time in tissues the exact sites of interaction between the antibody and the antigen. The technique may be modified for locating the site of antibody production in immunized animals and for detecting antibody protein deposited in abnormal situations.

One of the most rewarding applications of the fluorescent antibody technique has been in the study of various phases of virus growth in cell cultures or in sections of infected tissue. Some components of viral protein at an early stage of synthesis, as well as aggregations of the fully formed virus particles can thus be located. In certain instances different viral components are seen to be synthesized in separate parts of the host cell and to be combined later in the assembly of the mature virus.

Fluorescent antibody reagents are also finding increasing application in the study of auto-immune diseases, in which antibodies are formed against certain elements of the patient's own tissues. Thus in Hashimoto's disease, an antigen-antibody reaction has been observed in the thyroid colloid and thyroid cells of the patient from whom the fluorescein-antibody complex had been prepared. More recently, a positive reaction of this kind has been observed in heart muscle with fluorescent antibody prepared from the serum of patients with rheumatic heart disease.

The development of fluorescence microscopy has in turn led to important advances in staining technology. Highly fluorescent substances, the fluorochromes are being used as direct stains for fixed tissue preparations. The use of the fluorescent stain auramine for the quick identification of tubercle bacilli in sputum and other specimen is now common practice. The compound acridine orange is a fluorochrome of special interest, as under controlled conditions it is selectively bound to cell components containing nucleic acids. This method has proved particularly useful in virus research owing to its sensitivity and the invariable presence of nucleic acid, either DNA or RNA as an essential part of all viruses. The normal nucleic acid pattern of the host cell is profoundly altered in virus infections and significant changes of this kind have been demonstrated microscopically, using acridine orange, during the growth of influenza virus, adenovirus, polyoma virus and others.

The special types of microscopes so far considered share the same fundamental basis, the use of light to illuminate the specimen and of a series of lenses operating on and magnifying the object itself as well as

the images produced of it. They share a common limitation also, for the detail that can be observed in the image produced by them is limited to structures larger than about one-fourth of a micron. This limit is the wave-length of light and a permanent restriction to the resolution of such detail. Some thirty five years ago research on the properties of electron beams led to the idea of a microscope in which electron beams and magnetic fields replaced visible light and glass lenses. The extremely short wave-length of an electron beam suggested that an image might ultimately be obtained with such an instrument showing detail even below one-thousandth of a micron (or one-millionth of a millimetre) which is roughly the size of the diameter of the polypeptide chain in a protein molecule. The electron image itself is not visible but like X-rays, electrons can excite a fluorescent screen or darken a photographic film so that the image may be viewed and recorded.

The first attempt to build an electron microscope was made by Knoll & Ruska in 1932. This eventually led to the production of the first commercial electron microscope by von Borries & Ruska about 1938. The instrument utilized magnetic lenses entirely and its resolution approached 2 millimicrons. In the last 25 years the performance of the electron microscope as an instrument has been improved by a factor of only 2 or 3, but the limit in the resolution of objects now reached is not far short of the size of the atom. The detail seen in practice is however much more seriously limited by the conditions under which the enlarged electron image has to be obtained. Advances in technique have now overcome many of the limitations set by these requirements, but the full theoretical potentialities of the instrument have not even yet been completely realized. Electron microscopes are being applied to biological problems at resolutions representing again of over 100 times beyond the light microscope. A further increase by a factor of 10 is theoretically possible.

The essential requirement for electron microscope specimens is extreme thinness, and for obtaining sufficient contrast in the picture, density approaching that of a metal. The difficulties of maintaining the architecture of biological material so thinly sliced have been largely solved. A satisfactory cutting edge was found in broken pieces of ordinary plate glass. A widely used method for increasing the contrast of direct specimens is that of metal shadow casting. More recently a technique has been developed for the deposition of viruses on support films in which virus particles are deposited from an extremely strong solution of phosphotungstic acid. After evaporation of the liquid vehicle and examination in the electron microscope, the phosphotungstic acid is seen to surround

the virus particles as a dense background matrix which allows the virus to be observed as a negative image. By this technique many surface details of the virus are preserved, which are lost if the virus is examined directly.

The impact of the electron microscope on microbiological research, especially the study of viruses, can only be described as revolutionary. With few exceptions, viruses are of a size well below that of objects visible under a light microscope, but are ideal objects for study by the electron microscope as they do not require to be sectioned. The electron microscope has in fact already yielded exact and detailed knowledge of the structure of viruses, and shown up almost every surface feature of many of them. It provides the only exact method of estimating the number of virus particles in a suspension and of measuring the rate at which viruses arrive at a surface such as that of a cell, which they are going to infect. This rate of arrival at a surface has been shown to depend on random Brownian movement.

The electron microscope proves potentially useful in the classification and identification of bacteria. Previously and even now morphology and chemical activities are being used only as criteria for the purpose. Electron microscope has revealed much greater details in the structure and morphology of bacterial cells. Recently attempts are therefore being made for classification and identification of bacteria purely on electron-micrographs. Host-virus interrelationships form the basis of viral classification and identification. Now electron-microscope has revealed much finer details in viral surface structures. Hence work is now in progress to classify and identify viruses purely on the basis of morphological details. Electron microscopy coupled with staining has demonstrated the existence of cell wall and protoplasmic membrane in bacterial cells. That the membrane is constituted of three distinct layers is another advance in the study of the structure of bacterial cells.

Electron microscope has proved to be of invaluable help in the study of sub-cellular particles not only of bacterial but also of mammalian cells. Electron-micrographs of sub-cellular particles like mitochondria, microsome, nucleus, chromosome etc., have revealed much valuable informations not only as to their structures and dimensions but also to their function in the biology of the cell. Recently electron microscopy has revealed the existence of another class of sub-cellular particles called polyribosome which is essentially a polymer of ribosome. Its discovery has brought us one step forward in our understanding of the genetic transcription and translation process and hence protein synthesis,

Genetic exchange by way of mating has been demonstrated first by Lederberg in *E. Coli* K12 with the help of auxotrophic mutants. Reversion to prototrophy over the spontaneous mutation rate has been taken as one of the criteria of genetic exchange or sexuality. This is further confirmed by electron microscopic observations which has revealed the presence of a clearly visible transparent bridge between conjugating pairs in a bacterial population.

Clearly, the results so far obtained mark only the beginning of the contributions of electron microscopy to microbiological research. An instrument that places in our hands the means to see, and count, and measure objects such as viruses, which formerly could be detected only by indirect methods, has almost limitless potency as an aid and indeed a stimulus to research.

Among advances that bear on the technique of cultivation in pure culture, recent developments relating to the continuous culture of micro-organisms merit special notice. The evolution of devices for maintaining cell suspensions in continuous growth originated in efforts to provide growing micro-organisms with frequent replenishments of nutrients, preferably with an apparatus into which the food supply could be introduced mechanically. Two classes of instrument allow automatic addition of nutrient and the attainment of a steady state at a relatively uniform population density of growth rate. The first class add nutrient in response to increased turbidity of the culture, thus maintaining a uniform density through dilution and wash-out of cells. In the second category, exemplified by the chemostat of Novick and Szilard, and the bactogen of Monod, growth is kept at a constant level by a growth limiting factor supplied at a fixed rate of input. A modification of the chemostat also enables its use as an instrument working by turbidity control.

The maintenance of a uniform level of turbidity of the culture is achieved through control devices generally known as turbidostats, operated by a system of photocells. Dispersion is provided by a magnetic stirrer, and various adjustments control the time of operation of the pump delivering nutrient to the culture volume on actuation by the photo-electric device, volume of fluid delivered per stroke of the pump, heating rate of the culture, rotational velocity of the stirrer and other parameters. Sterile air is continuously provided under pressure to the air space above the culture, escaping to the atmosphere by exit at the top of the growth tube. The turbidostat has been mainly used for growing bacteria.

In the chemostat, the bacterial suspension contained in a growth tube is fed fresh nutrient at a rate set by the experimenter. The contents

of the tube are mixed and aerated by bubbling air. The bacterial suspension is removed from the tube at the same rate at which fresh nutrient enters it, and for this reason the volume of suspension in the growth tube remains constant. The rate at which the contents of the tube are diluted by the flow of liquid through it is kept less than the maximum rate of growth exhibited by the bacteria in the entering medium.

Mass propagation of micro-organisms is the most direct application of continuous culture methods and naturally it is in fermentation technology that prominent use has been made of the method. In the manufacture of yeast as well as alcohol by yeast fermentation, continuous culture techniques have been found to be specially advantageous. They have also found application in the large scale production of algae as a potential source of food, and as a source of oxygen for the continuous treatment of sewage.

Pilot plant experiments are under way for fermentative production of enzymes. Work on steroid, transformation synthesis of dextran and antibiotics like penicillin, streptomycin, chloro-tetracycline, novobiocin, chloramphenicol, studies on production of B_{12} from wastes, proteins from hydrocarbons, acetone-butanol, citric acid, glycogen etc., are however, confined as yet to academic research.

However, continuous culture methods are readily applicable on the laboratory scale also, and ideally suited for the study of important aspects of the biology of micro-organisms, such as the influence of environmental conditions on growth and biosynthetic activities of growing cells. For yield measurements, production of antigenic components and studies of population genetics and interaction of mixed bacterial populations, continuous cultivation is obviously the method of choice, and has already yielded results of fundamental interest.

Besides the instrumentation techniques as referred to above, recent years have seen tremendous progress in microbial genetics and biochemical genetics in particular due to the development of some biological techniques like mutation, conjugation, transformation, transduction, radiobiological techniques etc.

After the discovery of mutation in *Drosophila*, by Muller, the method has been successfully applied by Beadle in an ingenious way to *Neurospora* in which gene changes have been in the ultimate analysis equated to biochemical alterations. This leads to the postulation of one gene one enzyme theory. Recent researches of Jacob and Monod further modified one gene one enzyme theory and established multi-genetic control of protein synthesis. Mutation technique has another

useful application in the development of potent strains in fermentation technology. As a matter of fact the tremendous reduction in the production cost of penicillin is primarily because of two reasons, firstly development of potent strains and secondly the quick separation of penicillin by centrifugation technique. Auxotrophic mutants as isolated by classical method of Beadle have been in use for the bioassay of vitamins and aminoacids. Mutation production in TMV coupled with amino-acid analysis of coat proteins by finger print method has also greatly helped in establishing the genetic code.

In recent years mutation technique itself has been much simplified. The isolation of mutants by total isolation method of Beadle is an extremely painstaking and laborious task. Penicillin enrichment technique discovered independently by Lederberg and Davis, coupled with Replica plating has tremendously simplified the isolation procedure. The method is however applicable only to penicillin sensitive gram positive organisms. Penicillin may be replaced by azaguanine in case of penicillinase producing or penicillin insensitive organisms. Filamentous fung may be tackled by filtration technique for the isolation of auxotrophic mutants.

Transformation, another important biological technique, has identified "genes" of biologists with "DNA" of chemists. It will pave the way for our understanding of the sexual mating process on a molecular plane. Genetic homology may be a convenient method of testing sexual compatibility. Transduction, another method of genetic exchange, also discovered by Lederberg *et al*, has proved extremely useful in the analysis of fine genetic structure.

The cultivation of mammalian cell culture is another method that has been steadily gaining in prominence in microbiological research. The technique of tissue culture had been standardized at far back as 1923, and from the beginning its incalculable value in virological research was fully realized. Cell culture methods have now been developed for quantitative assay of viruses, for diagnosis and for the production of vaccines. However, the potentialities of tissue culture in other areas of microbiological study have not been as yet fully exploited. It is only recently that tissue culture has begun to be used in the study of intracellular organisms like the Rickettsiae, the myco-bacteria and the pleuropneumonia organisms. The results so far obtained clearly indicate how fruitful the technique can be in such work. *Lepraemurium* has been successfully grown, for example, in the strain L cell and detailed information obtained about the growth, life-cycle and metabolism of Rickettsiae. These organisms are all either slow-growing or else dependent on the

presence of living cells and tissue culture is the logical method for their investigation. But of equal promise is work, that is only beginning, on more rapidly growing pathogenic organisms using the fast-growing cells strains that have been recently introduced. These investigations should advance knowledge of host-parasite relationships at the cellular level, especially the biochemical bases of pathogenicity which are apparent only in organisms grown *in vivo* or in the cellular environment necessary for the full induction of their pathogenic capacity.

Cell culture technique has neen of great use in the study of mammalian biochemistry on a cellular level. Its importance in immunological research can hardly be described. Some of the important questions of immunology *e.g.*, active site of antigens, biogenesis of antibodies *etc.*, which have been a puzzling block for a pretty long time may now be successfully tackled on a cellular level. The biochemistry of many genetic and metabolic diseases can be more conveniently studied with the help of cell-culture technique. The technique may be used for fermentative production of many animal products, *viz.*, insulin, antibodies *etc.* Organ culture, although not a microbiological but definitely a mammalian cell culture technique, has immense future possibilities.

Amongst important advances in techniques of characterization I have already referred to fluorescence microscopy and the fluorochrome stains. Mention should be made of two other methods which have recently become available, cell electrophoresis and the partition of cells in aqueous polymer two-phase systems, which are applicable to the characterization as well as isolation of micro-organisms. Both these techniques originated from work on the fractionation of proteins and other macro-molecules at the Institute of Biochemistry in Uppsala. The theoretical basis of cell electrophoresis is the uniform and characteristic electrical charge of cells in a population deriving from the same strain and grown under identical cultural conditions. The cells therefore possess a uniform and characteristic electrophoretic mobility. The method involves direct microscopic observation of the cells as they migrate in the electric field. The cells are suspended in a suitable buffer solution and placed in a small flat or cylindrical transparent cell through which an electric current is passed. The time for a cell to cover a given distance as measured with a micrometer eyepiece is determined and from this the mobility or velocity per unit field strength may be calculated. For preparative purposes a different design is necessary, but a fully satisfactory arrangement has still to be evolved. Cell electrophoresis has been applied in the measurement of the mobilities of viruses absorbed on collodion particles, and the effect thereon of strain differences and

chemical treatment. It has been shown that the mobility of a given strain of bacteria is characteristic of that strain and remains constant through many sub-cultures. The method has also been found useful for distinguishing between sub-groups within a species, especially variants of the rough-smooth type and for studying the action of detergents and antibiotics on bacterial surfaces.

The partition of cells and cell particles by distribution in liquid-liquid two-phase systems is also based on the specificity of their surface properties. Separation of substances by partition is a classical and perhaps the most widely used method in organic chemistry. In biochemistry most of the partition methods were originally developed for low-molecular substances like peptides, hormones and vitamins and subsequently modified, as in partition chromatography, for the separation of proteins, enzymes and nucleic acids. Special problems which arise when a phase system has to be applied to particles of biological origin have been solved by Albertsson through the use of an aqueous polymer two-phase system yielding phases rich in water and allowing a reproducible partition of even fragile particles and macromolecules under mild conditions. The method has not been fully explored in microbiological research, but offers important possibilities, in the concentration and purification of viruses and antigen-antibody complexes, and the differentiation of bacterial strains.

Early fifties have seen tremendous advance in the study of the chemistry of bacterial cell walls, when the mode of action of penicillin has been fairly worked out. In the preparation of pure cell walls free from cytoplasmic contaminants low speed differential centrifugation has been of great use. The preparation of pure cytoplasmic membranes may be conveniently achieved with the help of differential centrifugation technique.

To this must be added ultracentrifugation the importance of which in separation technique needs no exaggeration. The separation of sub-cellular particles like mitochondria, microsome, chromosome etc., depends entirely upon the use of ultracentrifugation. Further fractionation of sub-cellular particles, *e.g.*, microsomes into ribosomes, its constituent 70S, 30S or 50S particles *etc.*, depends upon successful application of differential ultracentrifugation. The usefulness of the separation of sub-cellular particles in developing our present concept of protein synthesis and in establishing the universal genetic code and also its degeneration, can hardly be described,

The application of biochemical methods in the study of microbial metabolism, particularly paper chromatography, and radio-isotope technique has extended the horizon of knowledge in sciences, and provides a spectacular example of the cross-fertilization of ideas in sciences. In fact biochemical techniques have been assimilated as an essential and integral part of microbiological methodology.

I have attempted in this review to give only a bird's eye view of the present state of micro-biological methodology. I have perforce had to take a selective view, largely based on my own particular scientific interests, in choosing the development I have discussed as typical of the historic growth of microbiology and exemplifying the present status of its techniques and instrumentation. But I believe there can be no disagreement over the conclusion I would put before you, that the techniques we have now available have opened out vast new areas for investigation and provide a most potent stimulus to research in all the separate and specialist disciplines of study which the science of micro-biology now comprehends.